



# VIDYA BHARATI MAHAVIDYALAYA AMRAVATI

NAAC Re-accredited with Grade "A" (CGPA 3.23-Third Cycle) | CPE Status (Thrice) by UGC

Mentor College under Paramarsh Scheme by UGC

'Lead College' by S.G.B. Amravati University, Amravati.

## **3.3.2. Number of research papers per teachers in the Journals notified on UGC website during the year**



# VIDYA BHARATI MAHAVIDYALAYA AMRAVATI

NAAC Re-accredited with Grade "A" (CGPA 3.23-Third Cycle) | CPE Status (Thrice) by UGC  
Mentor College under Paramarsh Scheme by UGC  
'Lead College' by S.G.B. Amravati University, Amravati.

## INDEX

### 3.3.2. Number of research papers per teachers in the Journals notified on UGC website during the year

Sr. No	Title of paper	Name of the author/s	Department of the teacher	Name of journal	Year of publication	ISSN number	Link to the recognition in UGC enlistment of the Journal
1	In-vitro ANTI-INFLAMMATORY AND ANTIOXIDANT ACTIVITY OF NOVEL 1-SUBSTITUTED-3-SUBSTITUTED PROPANE-1,3-DIONES ( $\beta$ -DIKETONES) DERIVED FROM VANILLIN	Dr Pravin S Bodkhe	Chemistry	RASAYN J. Chem.	2022-2023	0974-1496	<a href="http://www.rasayanjournal.com">http://www.rasayanjournal.com</a>
2	Study of Pharmacophoric Consensus Pattern for Benzoic Acid Derivatives of 1,3,4-	Dr Pravin S Bodkhe	Chemistry	International Journal of Scientific Research in Science and Technology	2022-2023	2395-6011	www.ijsrst.com

	Thiadiazole As Antibacterial Agent						
3	Effect of Solvent Polarity on Viscosity of 2-Hydroxy Substituted 1, 3-Dipropenone	Dr Pravin S Bodkhe	Chemistry	Asian Journal of Organic & Medicinal Chemistry, Vol. 7 No. 2 (April - June, Special Issue - V 2022)	2022-2023	2456-893	<a href="http://ajomc.asianpubs.org">http://ajomc.asianpubs.org</a>
4	Mechanistic Analysis of Chemically Diverse Bromodomain-4 Inhibitors Using Balanced QSAR Analysis and Supported by X-ray Resolved Crystal Structures	Magdi E. A. Zaki, Sami A. Al-Hussain, Aamal A. Al-Mutairi, Vijay H. Masand, Abdul Samad, and Rahul D. Jawarkar	Chemistry	Pharmaceuticals	2022-2023	1424-8247	doi:10.3390/ph15060745
5	Perceiving the Concealed and Unreported Pharmacophoric Features of the 5-Hydroxytryptamine Receptor Using Balanced QSAR Analysis	Syed Nasir Abbas Bukhari, Mervat Abdelaziz Elsherif, Kashaf Junaid, Hasan Ejaz, Pravej Alam, Abdul Samad, Rahul D. Jawarkar, Vijay H. Masand	Chemistry	Pharmaceuticals	2022-2023	1424-8247	doi:10.3390/ph15070834
6	Synthesis and Evaluation of Some New 4H-Pyran Derivatives as Antioxidant, Antibacterial and Anti-HCT-116 Cells of CRC, with Molecular Docking, Antiproliferative, Apoptotic and ADME Investigations	Nahed N. E. El-Sayed, Magdi E. A. Zaki, Sami A. Al-Hussain, Abir Ben Bacha, Malika Berredjem, Vijay H. Masand, Zainab M. Almarhoon, Hanaa S. Omar	Chemistry	Pharmaceuticals	2022-2023	1424-8247	doi:10.3390/ph15070891

7	QSAR, Molecular Docking, MD Simulation and MMGBSA Calculations Approaches to Recognize Concealed Pharmacophoric Features Requisite for the Optimization of ALK Tyrosine Kinase Inhibitors as Anticancer Leads	Rahul D. Jawarkar, Praveen Sharma, Neetesh Jain, Ajaykumar Gandhi, Nobendu Mukerjee, Aamal A. Al-Mutairi, Magdi E. A. Zaki, Sami A. Al-Hussain, Abdul Samad, Vijay H. Masand, Arabinda Ghosh, Ravindra L. Bakal	Chemistry	Molecules	2022-2023	1420-3049	doi:10.3390/molecules27154951
8	QSAR Evaluations to Unravel the Structural Features in Lysine-Specific Histone Demethylase 1A Inhibitors for Novel Anticancer Lead Development Supported by Molecular Docking, MD Simulation and MMGBSA	Rahul D. Jawarkar, Ravindra L. Bakal, Nobendu Mukherjee, Arabinda Ghosh, Magdi E. A. Zaki, Sami A. Al-Hussain, Aamal A. Al-Mutairi, Abdul Samad, Ajaykumar Gandhi, Vijay H. Masand	Chemistry	Molecules	2022-2023	1420-3049	doi:10.3390/molecules27154758
9	Repurposing food molecules as a potential BACE1 inhibitor for Alzheimer's disease	Nobendu Mukerjee, Anubhab Das, Rahul D. Jawarkar, Swastika Maitra, Padmashree Das, Melvin A. Castrosanto, Soumyadip Paul, Abdul Samad, Magdi E. A. Zaki, Sami A. Al-Hussain, Vijay H. Masand, Mohammad Mehedi Hasan, Syed Nasir Abbas Bukhari, Asma Perveen, Badrah S. Alghamdi, Athanasios	Chemistry	Frontiers in Aging Neuroscience	2022-2023	1663-4365	doi:10.3389/fnagi.2022.878276

		Alexiou, Mohammad Amjad Kamal, Abhijit Dey, Sumira Malik, Ravindra L. Bakal, Adel Mohammad Abuzenadah, Arabinda Ghosh, Ghulam Md Ashraf					
10	Quinoline Derivatives with Different Functional Groups: Evaluation of Their Catecholase Activity	Mohamed Moutaouakil, Said Tighadouini, Zainab M. Almarhoon, Maha I. Al-Zaben, Abir Ben Bacha, Vijay H. Masand, Jamal Jamaledine, Rafik Saddik	Chemistry	Catalysts	2022- 2023	2073- 4344	doi:10.3390/catal12111468
11	Pharmacophore Synergism in Diverse Scaffold Clinches in Aurora Kinase B,	Vijay H. Masand, Sami A. Al-Hussain, Mithilesh M. Rathore, Sumer D. Thakur, Siddhartha Akasapu, Abdul Samad, Aamal A. Al-Mutairi, Magdi E. A. Zaki	Chemistry	International journal of molecular sciences	2022- 2023	1422- 0067	doi:10.3390/ijms232314527
12	Magnetic solid phase extraction of Sunitinib malate in urine samples assisted with mixed hemimicelle and spectrophotometric detection	E. Pourbasheer, L. Malekpour, Z. Azari, V.H. Masand, M.R. Ganjali,	Chemistry	Scientific Reports	2022- 2023	2045- 2322	doi: 10.1038/s41598-023- 30404-6
13	QSAR modeling approaches to identify a novel ACE2 inhibitor that selectively	Rahul D. Jawarkar, Magdi E. A. Zaki, Sami A. Al- Hussain, Aamal A. Al- Mutairi, Abdul Samad,	Chemistry	JOURNAL OF BIOMOLECULAR STRUCTURE AND DYNAMICS	2022- 2023	0739- 1102	doi: 10.1080/07391102.2023.22 05948

	bind with the C and N terminals of the ectodomain	Nobendu Mukerjee, Arabinda Ghosh, Vijay H. Masand, Long Chiau Ming & Summya Rashid					
14	Synthesis and Biological Evaluation of Some New 3-Aryl-2-thioxo-2,3-dihydroquinazolin-4(1H)-ones and 3-Aryl-2-(benzylthio)quinazolin-4(3H)-ones as Antioxidants; COX-2, LDHA, -Glucosidase and -Amylase Inhibitors; and Anti-Colon Carcinoma and Apoptosis-Inducing Agents	Nahed Nasser Eid El-Sayed, Taghreed M. Al-Otaibi, Assem Barakat, Zainab M. Almarhoon, Mohd. Zaheen Hassan, Maha I. Al-Zaben, Najeh Krayem, Vijay H. Masand and Abir Ben Bacha	Chemistry	Pharmaceuticals	2022-2023	1424-8247	doi: 10.3390/ph16101392
15	In silico study to recognize novel angiotensin-converting-enzyme-I inhibitors by 2D-QSAR and constraint-based molecular simulations	Sapan Shah, Dinesh Chaple, Vijay H. Masand, Magdi E.A Zaki, Sami A. Al-Hussain, Ashish Shah, Sumit Arora, Rahul Jawarkar & Mohammad Tauqeer	Chemistry	JOURNAL OF BIOMOLECULAR STRUCTURE AND DYNAMICS	2022-2023	0739-1102	doi: 10.1080/07391102.2023.2203261
16	Leveraging nitrogen occurrence in approved drugs to identify structural patterns	Vijay H. Masand, Sami Al-Hussain, Abdullah Y. Alzahrani, Nahed N. E. El-Sayed, Chien Ing Yeo, Yee Seng Tan & Magdi E.A. Zaki	Chemistry	Expert Opinion on Drug Discovery	2022-2023	1746-045X	doi: 10.1080/17460441.2023.2266990
17	The impact of Financial Constraint on student enrollment in higher	Dr. S. B. Kadu	Commerce	B. Aadhar	2022-2023	2278-9308	www.aadharsocial.com

	education: a major challenge in higher education						
18	Innovation in EdTech: Improving Access and outcome for Learners	Dr. P.B. Upase	Commerce	B. Aadhar	2022-2023	2278-9308	www.aadharsocial.com
19	Use of Technology In education During pandemic	Dr. S.K. Rodde	Commerce	B. Aadhar	2022-2023	2278-9308	www.aadharsocial.com
20	THE ROLE OF OPEN EDUCATIONAL RESOURCES (OERS) IN PROMOTING AFFORDABLE AND ACCESSIBLE HIGHER EDUCATION	Dr. P.B. Upase	Commerce	Tojdel (Care Listed)	2022-2023	2147-6454	www.tojdel.net
21	Transition from IPv4 to IPv6 Network in IoT Security Based upon Transition Methods	Prof. S.B.Sarvaiya	Computer Science	International Journal on Orange Technology(IJOT)	2022-2023	2615-8140	<a href="https://journals.researchparks.org/index.php/IJOT">https://journals.researchparks.org/index.php/IJOT</a>
22	Analysis of IoT Data Transfer Messaging Protocols on Application Layer	Prof. S.B.Sarvaiya	Computer Science	International Journal for Research in Applied Science and Engineering Technology(IJRASET)	2022-2023	2321-9653	<a href="http://www.ijraset.com">www.ijraset.com</a>
23	Trustworthy IoT Traditional Network Security to Authentication and Access Control Model for Heterogeneous Devices	Prof. S.B.Sarvaiya	Computer Science	International Journal of Innovative Research in Technology	2022-2023	2349-6002	<a href="http://www.ijirt.org">www.ijirt.org</a>
24	Misconceptions of Covid-19 among College Students	Dr. S. D. Wakode	Psychology	Printing Area	2022-2023	23945303	<a href="https://www.vidyawarta.com/03/">https://www.vidyawarta.com/03/</a>

25	The Effect of Job Vulnerability on Pandemic Prevalent Concern: Lonliness	Dr. S. D. Wakode	Psychology	B. Aadhar	2022-2023	22789308	<a href="https://www.aadharsocial.com/index.aspx#">https://www.aadharsocial.com/index.aspx#</a>
26	A Study of Coping Strategies of Frontline And Nonfrontline Workers	Dr. S. D. Wakode	Psychology	B. Aadhar	2022-2023	22789308	<a href="https://www.aadharsocial.com/index.aspx#">https://www.aadharsocial.com/index.aspx#</a>
27	Sthanik swarajya sanstha aani Mahila Netrutv	Mr. A.P. Ingole	Political Science	Srujan Bharat	2022-2023	22491171	
28	Covid-19 Aani Sdhyache Badlte jagtik Rajkaran	Mr. A.P. Ingole	Political Science	B. Aadhar	2022-2023	22789308	<a href="https://www.aadharsocial.com/index.aspx#">https://www.aadharsocial.com/index.aspx#</a>
29	Covid-19 Challenges and Opportunities in Indian Economy	Dr. D.S. Rangacharya	Economics	B. Aadhar	2022-2023	22789308	<a href="https://www.aadharsocial.com/index.aspx#">https://www.aadharsocial.com/index.aspx#</a>
30	Dalit Aatmkathnatil Stri Purush Smbandh	Dr. G.D. Bansod	Marathi	B. Aadhar	2022-2023	22789308	<a href="https://www.aadharsocial.com/index.aspx#">https://www.aadharsocial.com/index.aspx#</a>
31	Samkalin Lekhikechya Kadmbaritil Stri Nayika aani Jivanchitran	Dr. G.D. Bansod	Marathi	B. Aadhar	2022-2023	22789308	<a href="https://www.aadharsocial.com/index.aspx#">https://www.aadharsocial.com/index.aspx#</a>
32	Arjun Dangle Yanchya Nile Adhorekhit Madhil Nikhl Aani Prakhar Nondi	Dr. G.D. Bansod	Marathi	Aksharvaidrbhi	2022-2023	0776-0296	
33	Smrutishesh Ganesh Tale Yanchya Surkala Nantrchya Kavita	Dr. G.D. Bansod	Marathi	Sarvdhara	2022-2023	2249-3034	
34	Impact Of Covid-19 And Lockdown On Mental Health Of Various Sections	Dr. D.S. Ramteke	Psychology	B. Aadhar	2022-2023	22789308	<a href="https://www.aadharsocial.com/index.aspx#">https://www.aadharsocial.com/index.aspx#</a>
35	Vakatakkalin Vishnushilp	Dr. M. M. Kherde	History	B. Aadhar	2022-2023	22789308	<a href="https://www.aadharsocial.com/index.aspx#">https://www.aadharsocial.com/index.aspx#</a>




36	Covid-19 impacts on woman with Poly Cystic Ovary Syndrome on their pre-existing Mental Health Issues in Vidrbha : Thamatic Study	Dr. D.S. Ramteke	Psychology	B. Aadhar	2022-2023	22789308	<a href="https://www.aadharsocial.com/index.aspx#">https://www.aadharsocial.com/index.aspx#</a>
37	Biometric Authentication & It's Security Purposes	Prof. S.B. Bele	MCA	International Research Journal of Innovations in Engineering and Technology (IRJIET)	2022-2023	2581-3048	<a href="https://irjiet.com">https://irjiet.com</a>
38	Comparative Analysis of Robotic Operating Systems	Prof. S.B. Bele	MCA	(IRJIET)	2022-2023	2581-3048	<a href="https://irjiet.com">https://irjiet.com</a>
39	Data Mining Techniques: A Review Literture	Prof. S.B. Bele	MCA	International Journal of Scientific Research & Engineering Trends	2022-2023	2395-566X	<a href="https://ijsret.com/">https://ijsret.com/</a>
40	Mobile Broadband Networking	Prof. S.B. Bele	MCA	(IRJIET)	2022-2023	2581-3048	<a href="https://irjiet.com">https://irjiet.com</a>
41	Methods in Cryptography	Prof. S. K. Totade	MCA	(IRJIET)	2022-2023	2581-3048	<a href="https://irjiet.com">https://irjiet.com</a>
42	Challenges of Digital Forensic in Cloud Computing	Prof. S. K. Totade	MCA	(IRJIET)	2022-2023	2581-3048	<a href="https://irjiet.com">https://irjiet.com</a>
43	Cloud Computing Security	Prof. S. K. Totade	MCA	(IRJIET)	2022-2023	2581-3048	<a href="https://irjiet.com">https://irjiet.com</a>
44	Natural Language Processing (NLP): A Review	Prof. S. K. Totade	MCA	(IRJIET)	2022-2023	2581-3048	<a href="https://irjiet.com">https://irjiet.com</a>

45	Advancements in 5G and Beyond Networks: Enabling the Fourth and Sixth Industrial Revolutions	Prof K P. Raghuwanshi	MCA	(IRJIET)	2022-2023	2581-3048	<a href="https://irjiet.com">https://irjiet.com</a>
46	AI in Healthcare	Prof K P. Raghuwanshi	MCA	(IRJIET)	2022-2023	2581-3048	<a href="https://irjiet.com">https://irjiet.com</a>
47	Cloud Computing for Big Data Analytics: A Comparative Evaluation	Prof K P. Raghuwanshi	MCA	(IRJIET)	2022-2023	2581-3048	<a href="https://irjiet.com">https://irjiet.com</a>
48	Generalization of Data Mining with Cloud Computing	Prof K P. Raghuwanshi	MCA	(IRJIET)	2022-2023	2581-3048	<a href="https://irjiet.com">https://irjiet.com</a>
49	Transparent Supply Chains with Blockchain	Dr. S. R. Thakare	MCA	(IRJIET)	2022-2023	2581-3048	<a href="https://irjiet.com">https://irjiet.com</a>
50	Impact of Machine Learning in Natural Language Processing (NLP)	Dr. S. R. Thakare	MCA	(IRJIET)	2022-2023	2581-3048	<a href="https://irjiet.com">https://irjiet.com</a>
51	Artificial Intelligence in E-commerce	Prof. Rana Afreen Sheikh,	MCA	JETIR	2022-2023	2349-5162	<a href="http://JETIR.ORG">http://JETIR.ORG</a>
52	BLOCKCHAIN & CRYPTOCURRENCY	Prof. Rana Afreen Sheikh,	MCA	JETIR	2022-2023	2349-5162	<a href="http://JETIR.ORG">http://JETIR.ORG</a>
53	Chat GPT Curse or Blessing	Prof. Rana Afreen Sheikh,	MCA	(IRJIET)	2022-2023	2581-3048	<a href="https://irjiet.com">https://irjiet.com</a>
54	Cloud Computing & It's Security	Prof. Rana Afreen Sheikh,	MCA	(IRJIET)	2022-2023	2581-3048	<a href="https://irjiet.com">https://irjiet.com</a>
55	Impact of Garlic (Allium sativum) on Glycogen Level of Fresh Water Fish Channa Striatus (Bloch, 1793)	Dr. N.R. Thorat	Zoology	Journal of Scientific Research in Science and Technology	2022-2023	2395-602X	<a href="https://ijsrst.com/IJSRST229172">https://ijsrst.com/IJSRST229172</a>
56	Impact of Garlic (Allium sativum) on Glycogen Level	Dr. S. H. Rathod	Zoology	Journal of Scientific Research	2022-2023	2395-602X	<a href="https://ijsrst.com/IJSRST229173">https://ijsrst.com/IJSRST229173</a>

	of Fresh Water Fish Channa Striatus (Bloch, 1793)			in Science and Technology			
57	Toxic effect of Parthenium hysterophorus on muscle of freshwater fish Labeo rohita	Dr. A. M. Vikhar (Khedkar)	Zoology	Journal of Scientific Research in Science and Technology	2022-2023	2395-602X	<a href="https://ijsrst.com/IJSRST2296113">https://ijsrst.com/IJSRST2296113</a>
58	Effect of Zingiber officinale and Tinospora cordifolia on Freshwater Fish Ophocephalus striatus (Bloch 1973)	Dr. S. H. Rathod	Zoology	Research Journal for Agricultural Science	2022-2023	0976-1675	<a href="https://ugccare.unipune.ac.in/Apps1/User/WebA/SearchList">https://ugccare.unipune.ac.in/Apps1/User/WebA/SearchList</a>
59	Behaviour of Bianchi Type V model In Modified Theory of Gravity With specific Form of Hubble Parameter	Dr. P. P. Khade	Mathematics	Jordan Journal of Physics	2022-2023	1994-7607	<a href="https://scopus.com/sourceid/21100871853">https://scopus.com/sourceid/21100871853</a>
60	Electrical Response of PVC-PMMA Thin Films: A Comprehensive Investigation into the Effects of Frequency, Temperature, and Salicylic Acid Dopant	A.B.More, G.T.Lamdhade, K.B. Raulkar	Physics	International Journal of Professional Studies	2022-2023	2455-6270	<a href="http://www.ijps.in">http://www.ijps.in</a>
61	Nanocrystalline Titanium Dioxide Dipped with AlCl <sub>3</sub> as a Humidity Sensors	R B Butley, R V Joat, G T Lamdhade, K B Raulkar, A O Chauhan	Physics	International Journal of Research in Science and Technology	2022-2023	2395 - 602X	<a href="https://www.ijrst.com/index.php">https://www.ijrst.com/index.php</a>
62	Preparation and Characterization of 4:1 (ECPVC) Ethyl Cellulose - Polyvinyl Chloride Polyblends Thin Films	Welekar N.R., Wasnik T.S., Lamdhade G. T.	Physics	International Journal of Research in Science and Technology	2022-2023	2249-0604	<a href="https://www.ijrst.com/index.php">https://www.ijrst.com/index.php</a>

63	To Study the Effect of Solvent on AC Conductivity and Dielectric Constant on Blend Formation of Poly (Styrene): Poly (Vinyl Acetate)	H.G. Pande, G. T. Lamdhade	Physics	International Journal of Research in Science and Technology	2022-2023	2249-0604	<a href="https://www.ijrst.com/index.php">https://www.ijrst.com/index.php</a>
64	Nonlinear I–V Characteristics and Thermal Stability of Nanocrystalline Titanium Oxide	Balkhade V.M., Lamdhade G.T.	Physics	International Journal of Research in Science and Technology	2022-2023	2249-0604	<a href="https://www.ijrst.com/index.php">https://www.ijrst.com/index.php</a>
65	Synthesis and Characterisation of Cupric Oxide (CuO) Doped Tungsten Oxide (WO <sub>3</sub> ) Multilayer Thick Films	Mankar S.S, Lamdhade G.T, Raulkar K.B	Physics	Multidisciplinary International Journal	2022-2023	2454-924X	<a href="http://www.themijournal.com">http://www.themijournal.com</a>
66	Investigation of Dielectric Constant of PVC-PMMA Thin Films Doped with Salicylic Acid at Different Frequency, Dopant and Temperature	A.B.More, G.T.Lamdhade, K.B. Raulkar	Physics	Multidisciplinary International Journal	2022-2023	2454-924X	<a href="http://www.themijournal.com">http://www.themijournal.com</a>
67	Cupric Oxide (CuO) Doped Tin Oxide (SnO <sub>2</sub> ) MOS Multilayer CO <sub>2</sub> Gas Sensor	Mankar S.S, Lamdhade G.T, Raulkar K.B	Physics	International Journal of Research in Science and Technology	2022-2023	2249-0604	<a href="https://www.ijrst.com/index.php">https://www.ijrst.com/index.php</a>
68	Exploitation of Nano-Crystalline Cupric Oxide (CuO) Doped Zinc Oxide (ZnO) Multilayer Thick Film as a CO <sub>2</sub> Gas Sensor	Mankar S.S, Lamdhade G.T, Raulkar K.B	Physics	International Journal of Research in Science and Technology	2022-2023	2249-0604	<a href="https://www.ijrst.com/index.php">https://www.ijrst.com/index.php</a>

69	Exploitation of PANI based Metal Oxide (ZnO-SnO <sub>2</sub> ) Thick Films Humidity Sensor	T.R. Ingle, G.T. Lamdhade	Physics	International Journal of Scientific Research in Science and Technology	2022-2023	2395 - 602X	<a href="https://www.ijrst.com/index.php">https://www.ijrst.com/index.php</a>
70	Investigation of Frequency and Temperature Dependent Electrical and Structural Characterization of PVC-PMMA Thin Films with Salicylic Acid Doping	A.B.More, G.T.Lamdhade	Physics	International Journal of Research in Science and Technology	2022-2023	2249-0604	<a href="https://www.ijrst.com/index.php">https://www.ijrst.com/index.php</a>

  
**Prof. P. G. BANSOD**  
 Co-ordinator  
 IQAC Quality Assurance Cell  
 Vidya Bharati Mahavidyalaya  
 Camp, Amravati-427602 (M.S.)



  
 SIGNATURE  
 PRINCIPAL  
**Principal**  
 Vidya Bharati Mahavidyalaya  
 Amravati.

## ***In-vitro* ANTI-INFLAMMATORY AND ANTIOXIDANT ACTIVITY OF NOVEL 1-SUBSTITUTED-3-SUBSTITUTED PROPANE-1,3-DIONES ( $\beta$ -DIKETONES) DERIVED FROM VANILLIN**

**Pravin S. Bodkhe<sup>1</sup>, Sushil K. Pagariya<sup>2</sup> and Prafulla P. Chaudhari<sup>3,✉</sup>**

<sup>1</sup>Department of Chemistry, Vidyabharati Mahavidyalaya, Amravati-444602, Maharashtra, India

<sup>2</sup>Department of Chemistry, Government Vidarbha Institute of Science and Humanities,  
Amravati-444604, Maharashtra, India

<sup>3</sup>Department of Chemistry, G.S. Tompe Arts, Commerce and Science College,  
Chandur Bazar-444704, Maharashtra, India

✉Corresponding Author: [prafullc76@gmail.com](mailto:prafullc76@gmail.com)

### ABSTRACT

In synthetic chemistry, propane-1,3-diones or  $\beta$ -diketones act as significant intermediates for the synthesis of core heterocycles due to their specific chemoselectivity properties as well as provide convenient building blocks to biologically active substituents. In the present work, a new series of  $\beta$ -diketones namely 1-(5'-Formyl-2'-hydroxy-3'-methoxyphenyl)-3-(substitutedphenyl) propane-1,3-diones 4(a-e) have been synthesized from versatile 4-hydroxy-3-methoxybenzaldehyde viz. vanillin and studied their invitro anti-inflammatory and antioxidant potential by performing inhibition of protein denaturation assay and reducing power assay method respectively. All the newly synthesized compounds exhibit notable and satisfactory anti-inflammatory potential as well as potent antioxidant activity due to the presence of vanillin moiety in their molecular structures.

**Keywords:**  $\beta$ -diketones, Propane-1,3-diones, Vanillin, Anti-Inflammatory, Antioxidant.

RASĀYAN *J. Chem.*, Vol. 16, No.1, 2023

### INTRODUCTION

The property of substances that reduce inflammation is termed anti-inflammatory and substances as anti-inflammatory drugs. Diseases or medical conditions that cause inflammation have a name ending in '-itis' such as Bronchitis (an inflammation of the bronchi), Cystitis (an inflammation of the bladder), Dermatitis (a disease where the skin is inflamed), Uveitis (an inflammation inside the eye), etc. Usually, non-steroidal anti-inflammatory drugs (NSAIDs) are one of the most common therapeutic groups of agents used worldwide for the treatment of pain, inflammation, and fever.<sup>1</sup> Most frequently used NSAIDs drugs are salicylates (such as Aspirin), paraaminophenol derivatives (such as Paracetamol), pyrrole derivatives (such as Ketorolac), indole derivatives (such as Ibuprofen), propionic acid derivatives (such as ibuprofen, Ibuprofen and Paracetamol combination, Flurbiprofen, Ketoprofen, Naproxen, Fenamates, and Mefenamic acid), aryl acetic acid derivatives (such as Diclofenac sodium, Diclofenac potassium, Diclofenac and paracetamol combination, Diclofenac and Serratiopeptidase combination), pyrazolones (such as Phenylbutazone and Oxyphenbutazone), others (such as Celecoxib, Rofecoxib, Valdecoxib, and Nimesulide), etc. Nowadays, both steroidal and non-steroidal anti-inflammatory drugs are used extensively for the relief of inflammatory pain because inflammatory diseases are becoming very common in society throughout the world. Steroids have an obvious role in the treatment of inflammatory diseases, but due to their toxicity, their long-term use causes serious adverse effects. Prolonged use of NSAIDs is also associated with gastric irritation, nausea, vomiting, peptic ulcers, gastric ulcers, and gastric bleeding. Owing to a wide assortment of side effects of NSAIDs, an alternative anti-inflammatory drug with the least side effects is needed for an hour. In recent years, the population in rural areas uses many alternative drugs such as substances produced from medicinal plants (ayurveda) for the treatment of inflammation, because the management of inflammation-related diseases is a real and challenging issue in rural communities still today. Hence, the search for natural remedies and phytochemicals with anti-inflammatory properties has significantly increased. For example, curcumin, a bioactive compound



containing bis- $\alpha$ ,  $\beta$ -unsaturated 1,3-diketone moiety, is found mainly in the turmeric plant rhizome (*Curcuma longa*) has a wide range of beneficial activities such as anti-inflammatory, antitumor, antioxidative, cardiovascular protective effects.<sup>2</sup> A survey of the literature reveals that compounds containing  $\beta$ -diketones moiety unit exhibit good anti-inflammatory as well as anti-mitotic activities.<sup>3</sup> Ramaa and More reported the synthesis and anti-inflammatory activity of fluorinated propanedione derivatives ( $\beta$ -diketones) which possessed good anti-inflammatory activity against carrageenan-induced edema in the rat paw.<sup>3</sup> Also,  $\beta$ -diketone ligand prepared by Baker-Venkataraman transformation and its complexes shows antioxidant and anti-inflammatory action.<sup>4-5</sup> Antioxidants are also significant compounds that reduce or neutralize free radicals, thus protecting the cells from oxidative injury because the high level of free radicals can cause damage to biomolecules such as enzymes, proteins, lipids, nucleic acids in the cells membrane which may result in many diseases such as cancer, diabetes, cardiomyopathy and autoimmune diseases, and neurodegenerative disorders.<sup>6</sup> Examples of common antioxidants include vitamins A, C, and E, selenium, and carotenoids such as  $\beta$ -carotene, lycopene, lutein, and zeaxanthin. Vegetables and fruit-rich diets which are good sources of antioxidants have been found to be healthy, however, research has not shown antioxidant dietary supplements to be beneficial in improving health in humans, or to be effective in preventing diseases. Hence, considerable research has been directed toward the identification of new antioxidant molecules to prevent radical-induced damage. Various methods are reported in the literature for determining antioxidant activity but DPPH (Diphenylpicryl hydrazine) free radical scavenging assay is one of the widely accepted methods for screening antioxidant activity.<sup>7</sup> Also, the protein denaturation inhibition assay suggested by Mizushima and Kobayashi and Sakat *et al.* is widely used for the determination of anti-inflammatory activities. A careful review of the literature indicates that very little work has been reported on the anti-inflammatory and antioxidant activities of  $\beta$ -diketones or their derivative. The literature survey also surprised that, no approach has been made to evaluate the in vitro anti-inflammatory and antioxidant potential of  $\beta$ -diketones comprising a moiety of phenolic aldehyde vanillin. In our previous work, we have synthesized 1-(5'-Formyl-2'-hydroxy-3'-methoxyphenyl)-3-(4'-nitrophenyl) propane-1, 3-dione (4a), 1-(5'-Formyl-2'-hydroxy-3'-methoxyphenyl)-3-(4'-methoxyphenyl) propane-1, 3-dione (4b), 1-(5'-Formyl-2'-hydroxy-3'-methoxyphenyl)-3-(2'-chlorophenyl) propane-1, 3-dione (4c), 1-(5'-Formyl-2'-hydroxy-3'-methoxyphenyl)-3-(4'-chlorophenyl) propane-1, 3-dione (4d), 1-(5'-Formyl-2'-hydroxy-3'-methoxyphenyl)-3-(2',4'-dichlorophenyl) propane-1,3-dione (4e) from vanillin by using Fries rearrangement and Baker-Venkataraman transformation, characterized them by IR and <sup>1</sup>H NMR spectra and studied their antimicrobial activities.<sup>8</sup> In continuation of our previous work, we have carried out the invitro anti-inflammatory and antioxidant activity of these novel compounds 4(a-e).

## EXPERIMENTAL

### Material and Methods

All the reagents used for the analysis of anti-inflammatory and antioxidant studies were of higher analytical grade. The anti-inflammatory activity was carried out in vitro by inhibition of protein denaturation assay reported by Mizushima and Kobayashi<sup>9</sup> and Sakat *et al.*<sup>10-11</sup> In-vitro antioxidant activity was performed by reducing power assay method.<sup>12-13</sup>

### General Procedure

#### Determination of Anti-Inflammatory Activity

Initially, 500  $\mu$ L of 1% albumin was added to 100  $\mu$ L of the test sample. This mixture was kept at room temperature for 10 min, followed by heating at 51°C for 20 min. The resulting solution was cooled down to room temperature and absorbance was recorded at 660 nm. Standard Diclofenac was taken as a positive control. The experiment was carried out in triplicates and percent inhibition for protein denaturation was calculated using the following formula:

$$\% \text{ Inhibition} = 100 - ((A1 - A2) / A0) \times 100 \quad (1)$$

Where A1 is the absorbance of the sample, A2 is the absorbance of the product control and A0 is the absorbance of the positive control.

### Determination of Antioxidant Activity

Different concentrations of the drug (10-50 $\mu$ g/mL) were added to 2.5 mL of 0.2 M sodium phosphate buffer (pH 6.6) and 2.5 mL of 1% potassium ferricyanide [ $K_3Fe(CN)_6$ ] solution. The reaction mixture was vortexed well and then incubated at 50°C for 20 min using a vortex shaker. At the end of the incubation, 2.5 mL of 10% trichloroacetic acid was added to the mixture and centrifuged at 3000 rpm for 10 min. The supernatant (2.5 mL) was mixed with 2.5 mL of deionized water and 0.5 mL of 0.1% ferric chloride ( $FeCl_3$ ). The colored solution was read at 700 nm against the blank with reference to the standard using a UV spectrophotometer. Here, Ascorbic acid (Vitamin C) was used as a reference standard or positive control at the same selected concentrations and in the same operating conditions as the sample, and reducing the power of the sample was compared with the reference standard.

### RESULTS AND DISCUSSION

The results on anti-inflammatory activities of 1-(5'-Formyl-2'-hydroxy-3'-methoxyphenyl)-3-(substituted phenyl) propane-1,3-diones compounds 4(a-e) are depicted in Table-1 to 6. As well the results of antioxidant studies of these compounds are depicted in Table-7 to 8 and shown in Fig.s-1 to 3.

Table-1: Anti-Inflammatory Activity of Standard Diclofenac

Concentration ( $\mu$ g/mL)	% Inhibition of Denaturation of Protein					
	4a	4b	4c	4d	4e	Standard Diclofenac
50 $\mu$ g/mL	42.85	28.57	39.63	60.71	64.28	71
100 $\mu$ g/mL	46.42	39.28	50.00	60.71	60.71	78
200 $\mu$ g/mL	50.00	42.85	53.57	64.28	64.71	85
400 $\mu$ g/mL	53.57	46.42	57.14	67.85	67.85	89

Table-2: Anti-Inflammatory Activity of Newly Synthesized Compound (4a)

Concentration ( $\mu$ g/mL)	The absorbance of the test sample	% of protein inhibition	Absorbance of Std drug (Diclofenac)	% of protein inhibition
50 $\mu$ g/mL	0.016	42.85	0.008	71.42
100 $\mu$ g/mL	0.015	46.42	0.006	78.57
200 $\mu$ g/mL	0.014	50.00	0.004	85.71
400 $\mu$ g/mL	0.013	53.57	0.003	89.28

Table-3: Anti-Inflammatory Activity of the Newly Synthesized Compound (4b)

Concentration ( $\mu$ g/mL)	The absorbance of the test sample	% of protein inhibition	Absorbance of Std drug (Diclofenac)	% of protein inhibition
50 $\mu$ g/mL	0.020	28.57	0.008	71.42
100 $\mu$ g/mL	0.017	39.28	0.006	78.57
200 $\mu$ g/mL	0.016	42.85	0.004	85.71
400 $\mu$ g/mL	0.015	46.42	0.003	89.28

Table-4: Anti-Inflammatory Activity of the Newly Synthesized Compound (4c)

Concentration ( $\mu$ g/mL)	The absorbance of the test sample	% of protein inhibition	Absorbance of Std drug (Diclofenac)	% of protein inhibition
50 $\mu$ g/mL	0.017	39.63	0.008	71.42
100 $\mu$ g/mL	0.014	50.00	0.006	78.57



200 µg/mL	0.013	53.57	0.004	85.71
400 µg/mL	0.012	57.14	0.003	89.28

Table-5: Anti-Inflammatory Activity of Newly Synthesized Compound (4d)

Concentration (µg/mL)	The absorbance of the test sample	% of protein inhibition	Absorbance of Std drug (Diclofenac)	% of protein inhibition
50 µg/mL	0.011	60.71	0.008	71.42
100 µg/mL	0.011	60.71	0.006	78.57
200 µg/mL	0.010	64.28	0.004	85.71
400 µg/mL	0.009	67.85	0.003	89.28

Table-6: Anti-Inflammatory Activity of the Newly Synthesized Compound (4e)

Concentration (µg/mL)	The absorbance of the test sample	% of protein inhibition	Absorbance of Std drug (Diclofenac)	% of protein inhibition
50 µg/mL	0.010	64.28	0.008	71.42
100 µg/mL	0.011	60.71	0.006	78.57
200 µg/mL	0.010	64.71	0.004	85.71
400 µg/mL	0.009	67.85	0.003	89.28

Table-7: Antioxidant Activity of Standard Ascorbic Acid

Sr. No.	Concentration (µg/mL)	Absorbance (A)
1	10	0.251
2	20	0.499
3	30	0.775
4	40	0.943
5	50	1.240

Table-8: Antioxidant Activity of Newly Synthesized Compounds 4(a-e)

Sr. No.	Sample	Concentration (µg/mL)	Absorbance (A)	Sr. No.	Sample	Concentration (µg/mL)	Absorbance (A)
1	4a	30	0.689	6	4c	50	0.874
2	4a	50	0.755	7	4d	30	0.806
3	4b	30	0.507	8	4d	50	0.831
4	4b	50	0.667	9	4e	30	0.721
5	4c	30	0.852	10	4e	50	0.794

The results on anti-inflammatory activity reveal that all the newly synthesized compounds 4(a-e) has shown good inhibition of denaturation of protein at all the tested concentration, however as compared to other compounds, compound 4d and 4e exhibit notable inhibition at all the tested concentrations when compared with standard Diclofenac. From the results on antioxidant activity, it was observed that all the samples showed 4c > 4d > 4e > 4a > 4b order of reducing power and their reducing strength was increased with increasing concentration. The high value of absorbance of the reaction mixture clearly indicated greater reducing power. By comparing their reducing strength with standard reference, it was observed that the reducing power of all the synthesized compounds was found to be in good agreement with the standard ascorbic acid as well as their values were found to be comparable with it.



Fig.-1: 1-(5'-Formyl-2'-hydroxy-3'-methoxyphenyl)-3-(substituted phenyl) propane-1,3-diones Compounds 4(a-e) Before Centrifugation



Fig.-2: 1-(5'-Formyl-2'-hydroxy-3'-methoxyphenyl)-3-(substituted phenyl) propane-1,3-diones Compounds 4(a-e) After Centrifugation



Fig.-3: 1-(5'-Formyl-2'-hydroxy-3'-methoxyphenyl)-3-(substituted phenyl) propane-1,3-diones compounds 4(a-e) With Colour Changes After Addition of  $\text{FeCl}_3$  Solution

## CONCLUSION

In conclusion, from the results on anti-inflammatory activities presented in Table-1 to 6, it is concluded that all these newly synthesized  $\beta$ -diketones 4(a-e) comprising moiety of vanillin were found to possess satisfactory anti-inflammatory potential when equated with the reference Diclofenac. The screening results on antioxidant studies (Table-7 to 8) indicate that all five compounds exhibited potent antioxidant activities due to the presence of vanillin moiety in the molecular structure of synthesized compounds.

After comparing the results of antioxidant activities with standard Ascorbic acid, it is confirmed that the reducing power (as indicated by absorbance at 700 nm) of all samples increased with increasing their concentrations. As well, experimental findings on anti-inflammatory and antioxidant studies may be implicated as an informative resource for pharmaceutical industries engaged in the manufacturing of drugs and medicines not only for human beings but also for veterinary sciences.

## ACKNOWLEDGMENTS

All the authors are grateful to the Director, Government Vidarbha Institute of Science and Humanities, Amravati for providing a laboratory facility and Dr. S. L. Deore, Associate Professor, Government

College of Pharmacy, Amravati for her cooperation in carrying out anti-inflammatory and antioxidant activity.

### CONFLICT OF INTERESTS

The authors declare that there is no conflict of interest.

### AUTHOR CONTRIBUTIONS

All the authors contributed significantly to this manuscript, participated in reviewing/editing, and approved the final draft for publication. The research profile of the authors can be verified from their ORCID ids, given below:

P. S. Bodkhe  <https://orcid.org/0009-0008-8690-3230>

S.K. Pagariya  <https://orcid.org/0000-0001-6110-213X>

P.P. Chaudhari  <https://orcid.org/0000-0001-8372-9742>

**Open Access:** This article is distributed under the terms of the Creative Commons Attribution 4.0 International License (<http://creativecommons.org/licenses/by/4.0/>), which permits unrestricted use, distribution, and reproduction in any medium, provided you give appropriate credit to the original author(s) and the source, provide a link to the Creative Commons license, and indicate if changes were made.

### REFERENCES

1. I. Alkabodi, S. Almekhlafi and D.A. Ibrahim, *Journal of Chemical and Pharmaceutical Research*, **8(3)**, 307(2016).
2. H. Hatcher, R. Planalp, J. Cho, F.M. Torti and S.V. Torti, *Cellular and Molecular Life Sciences*, **65(11)**, 1631(2008), <http://doi.org/10.1007/s00018-008-7452-4>
3. A.H. More, C.S. Ramaa, *Indian Journal of Chemistry*, **49B (3)**, 364(2010).
4. S.G. Bibave, A.E. Athare, *Oriental Journal of Chemistry*, **35(6)**, 1799(2019), <http://dx.doi.org/10.13005/ojc/350624>
5. S.G. Bibave, S.J. Takate and A.E. Athare, *Oriental Journal of Chemistry*, **37(2)**, 413(2021), <http://dx.doi.org/10.13005/ojc/370221>
6. F. Alam, B.K. Dey, *Der Pharma Chemica*, **7(1)**, 230(2015).
7. A.S. Shawali, *Journal of Advanced Research*, **5**, 1(2014), <http://doi.org/10.1016/j.jare.2013.01.004>
8. S. Pagariya, R. Pathade, R. Isankar, P. Bodkhe, In Proceedings of International Conference on Innovative Trends in Natural and Applied Sciences-2021, Gadchandur, Maharashtra, *Journal of Advanced Scientific Research*, **ICITNAS**, 312-317 (2021).
9. Y. Mizushima, M. Kobayashi, *Journal of Pharmacy and Pharmacology*, **20(3)**, 169(1968), <http://doi.org/10.1111/j.2042-7158.1968.tb09718x>
10. S.S.Sakat, A.R. Juvekar, M.N. Gambhire, *International Journal of Pharmacy Pharmaceutical Sciences*, **2(1)**, 146(2010).
11. S.S.Sakat, P.N. Tupe, A.R. Juvekar, *Pharmacologyonline*, **3**, 221(2009).
12. S. Ismahene, S. Ratiba, C.M.D. Miguel and C. Nuria, *Pharmacognosy Journal*, **10(1)**, 64(2018), <http://doi.org/10.5530/pj.2018.1.13>
13. M. Oyaizu, *Japanese Journal of Nutrition*, **44(6)**, 307(1986), <http://doi.org/10.5264/eiyogakuzoshi.44.307>

[RJC-8193/2022]

# Study of Pharmacophoric Consensus Pattern for Benzoic Acid Derivatives of 1,3,4-Thiadiazole As Antibacterial Agent

C. N. Jadhav<sup>1</sup>, M. M. Rathore<sup>2</sup>, V. H. Masand<sup>3</sup>, P. S. Bodkhe<sup>4</sup>

<sup>1</sup>Research Scholar, Vidya Bharati Mahavidyalaya, Amravati, Maharashtra, India

<sup>2</sup>Professor & Head, Department of Chemistry, Vidya Bharati Mahavidyalaya, Amravati, Maharashtra, India

<sup>3</sup>Professor, Department of Chemistry, Vidya Bharati Mahavidyalaya, Amravati, Maharashtra, India

<sup>4</sup>Associate Professor, Department of Chemistry, Vidya Bharati Mahavidyalaya, Amravati, Maharashtra, India

## ABSTRACT

### Article Info

### Publication Issue

Volume 10, Issue 1  
January-February-2023

### Page Number

167-174

### Article History

Accepted: 10 Jan 2023  
Published: 27 Jan 2023

Microbial infections have targeted millions of victims in human history. In spite of the great efforts that are being continuously made to find effective medication, still no drug exists that can truly cure and have no side effects for the said infections. Amongst the drugs that are available in the market for microbial infections, 1,3,4-thiadiazole derivatives have found to have extensive pharmacological activities and further optimized for other diseases [1,2]. Efforts are done to synthesize various carboxylic acid derivatives of 1,3,4 thiadiazol and to study their pharmacological activities [1,2]. In this research article, comparative study of various previously synthesized carboxylic acid derivatives of 1,3,4 thiadiazol is done using their pharmacophore modeling to identify the prominent structural features [1]. The analysis indicates that the synthesized molecules have specific hydrogen acceptor, hydrogen donor and lipophilic centers with some variations.

**Keywords** : 1,3,4-Thiadiazole, Pharmacophore Modeling, Antifungal, Antibacterial, Lipophilic, H-Bond Acceptor, H-Bond Donor.

## I. INTRODUCTION

Heterocyclic compounds have found to persist considerable importance in the field of pharmacology and drug design. Consequently, noticeable increase in research interest of synthesis and pharmacological applications of heterocyclic compounds is observed. Substituted five membered heterocyclic compounds thiazole, oxazole, imidazole, oxadiazole and thiadiazol

have demonstrated significance pharmacological activities [1-5]. Amongst all the five membered heterocycles, thiadiazols have shown potent pharmacological activities [6-8]. There is total four positional isomers of thiadiazol viz. 1,2,3-thiadiazole, 1,2,4-thiadiazole, 1,2,5- thiadiazol and 1,3,4-thiadiazole. 1,3,4-thiadiazole, a fascinating pharmacophore, is a weak base because of the inductive effect exerted by the Sulphur atom and

possess relatively high aromaticity. Of these four isomeric forms 1,3,4-thiadiazole have displayed a broad spectrum of biological activities such as antimicrobial, anticancer, diuretic, antioxidant, anticonvulsant and anti-inflammatory activity. Many 1,3,4-thiadiazole derivatives have been synthesized which are found to have various pharmacological activities.

Various benzoic acid derivatives of 1,3,4-thiadiazole were synthesized [10]. The synthesis was done by reaction of an aromatic carboxylic acid with thiosemicarbazide in the presence of POCl<sub>3</sub> to obtain 1,3,4-thiadiazole. which was further reacted with an aromatic aldehyde in the presence of methanol to obtain a Schiff's base derivative of 1,3,4-thiadiazole. These 1,3,4-thiadiazoles were further reacted with thioglycolic acid to obtain 1,3,4-thiadiazole derivatives. [10]. These 1,3,4-thiadiazoles were found to have antifungal and antibacterial activities [10].

The synthesized derivatives of 1,3,4-thiadiazole derivatives shows variations in their pharmacological

activities [10]. These molecules contain specific hydrogen donor, hydrogen acceptor and lipophilic centers with some variations. The present work is done on purpose to develop pharmacophore models of the synthesized molecules and to explain the variation in pharmacological activities due to structural variations of molecules.

## II. EXPERIMENTAL METHODOLOGY

### 1. Database selection:

The pharmacophore models were developed using a database of 11 molecules [10]. All the selected molecules were screened for their antibacterial and antifungal activity [10]. The MIC values of the molecules with respect to antibacterial activity and antifungal activity were considered. These MIC values of molecules with similar types of substitution with variation in the position of the substituents were compared with each other. Table-1 contains the molecules that are used.

**Table-1:** Labels and SMILES notations of molecules used

Sr. No.	Label	SMILES	MIC values
1	A1	<chem>O=C(CSC3C4=CC=CC=C4)N3C2=NN=C(S2)C1=CC=CC=C1</chem>	1.838
2	A2	<chem>O=C(CSC3C4=CC=C(Cl)C=C4)N3C2=NN=C(S2)C1=CC=CC=C1</chem>	0.835
3	A3	<chem>O=C(CSC3C4=C(Cl)C=C(Cl)C=C4)N3C2=NN=C(S2)C1=CC=CC=C1</chem>	0.765
4	A4	<chem>O=C(CSC3C4=C(F)C=CC=C4)N3C2=NN=C(S2)C1=CC=CC=C1</chem>	0.890
5	A5	<chem>O=C(CSC3C4=C(Br)C=CC=C4)N3C2=NN=C(S2)C1=CC=CC=C1</chem>	0.747
6	A6	<chem>O=C(CSC3C4=CC(O)=CC=C4)N3C2=NN=C(S2)C1=CC=CC=C1</chem>	1.760
7	A7	<chem>O=C(CSC3C4=CC=C(O)C=C4)N3C2=NN=C(S2)C1=CC=CC=C1</chem>	1.760
8	A8	<chem>O=C(CSC3C4=C(OC)C=CC=C4)N3C2=NN=C(S2)C1=CC=CC=C1</chem>	1.689
9	A9	<chem>O=C(CSC3C4=CC=C(OC)C=C4)N3C2=NN=C(S2)C1=CC=CC=C1</chem>	1.689
10	A10	<chem>O=C(CSC3C4=CC=C([N+])([O-])=O)C=C4)N3C2=NN=C(S2)C1=CC=CC=C1</chem>	1.623
11	A11	<chem>O=C(CSC3C4=C([N+])([O-])=O)C=CC=C4)N3C2=NN=C(S2)C1=CC=CC=C1</chem>	1.627

## 2. Development of pharmacophore model: [12-14]

All the pharmacophore models are built using the steps given below

- Structure drawing: ChemSketch 12 freeware was used to draw structures of the molecules.
- Structure optimization: Avogadro 2 was employed to optimize the 3D- structure of 11 benzoic acid derivatives of 1,3,4-thiadiazol.
- Alignment of molecules: This step was accomplished using Open3Dalign.
- Model generation: Lastly, top five active aligned molecules were introduced in PyMOL 2.0. Then, PyMOL plugin 'LIQUID' was employed to generate consensus model using default settings.

### III. RESULTS AND DISCUSSION

All the molecules considered for the study are classified into four groups (Group 1 to 4) with respect to the similarity in the type of substitution (Table 2). Few molecules which are compared are positional

isomers of each other. The pharmacophore-based analysis of all these molecules reveals that these molecules show relation between their antibacterial activities and H-bond donor, H-bond acceptor and lipophilic regions. All the molecules have three lipophilic regions and one H-bond acceptor region as shows in the fig. 1. The substituents on the ring gives variation in the type of the region (H-bond acceptor, H-bond donor or lipophilic) which results in the differentiation in the antibacterial activity of these molecules. These variations are discussed below.

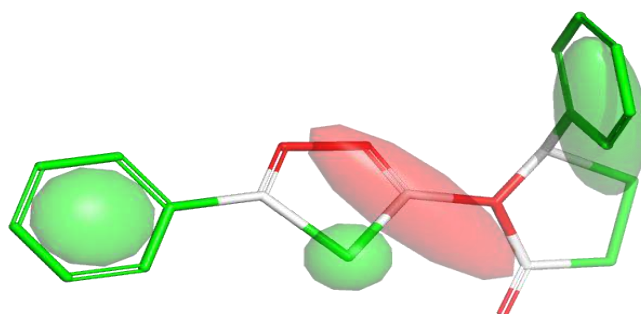


Fig 1: Pharmacophore model of A1 molecule

Table 2 : Classification of molecules

Sr. No.	Group	Label	Substitution
-	-	A1	-
1	Group 1	A2	p-Chloro
		A3	o,p-di-Chloro
		A4	o-Fluro
		A5	o-Bromo
2	Group 2	A6	m-hydroxy
		A7	p-hydroxy
3	Group 3	A8	o-methoxy
		A9	p-methoxy
4	Group 4	A10	p-nitro
		A11	o-nitro

Table 2: Classification of molecules

**Group 1:**

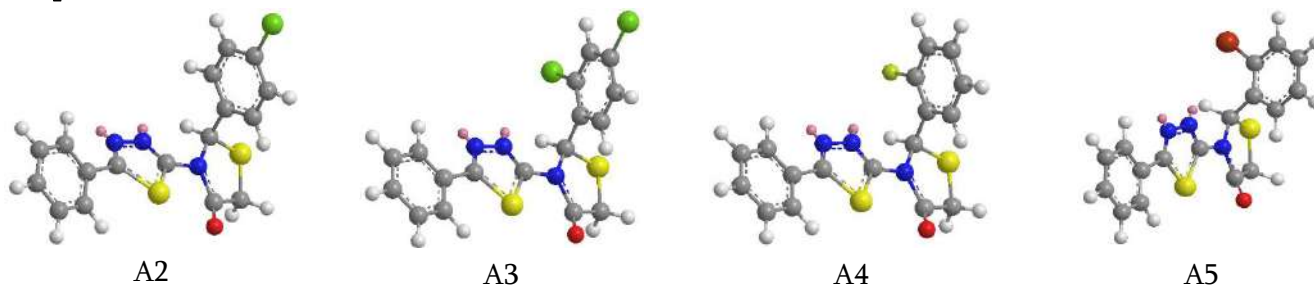


Fig 2: 3D structure of molecules A2, A3, A4 and A5

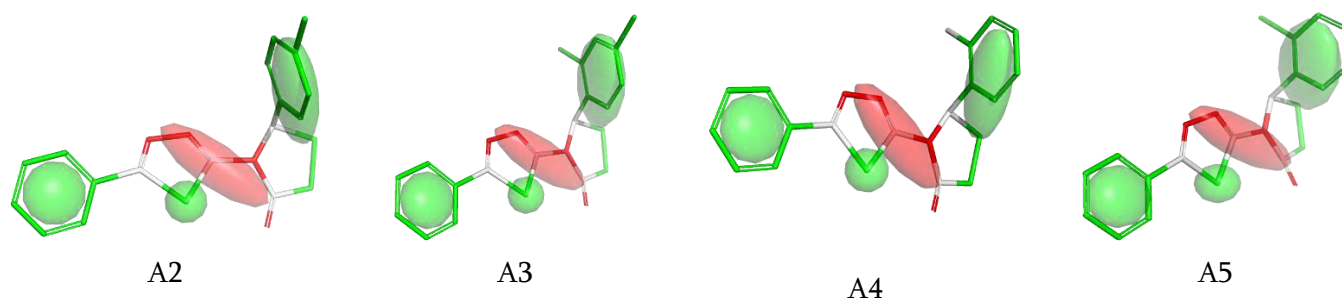


Fig 3: Pharmacophore models of A2, A3, A4 and A5

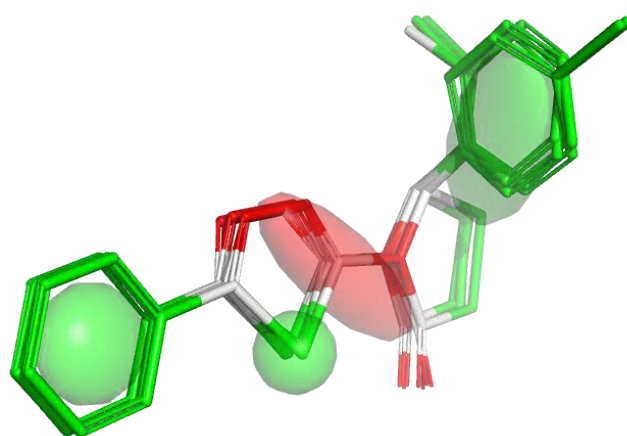


Fig 4: Consensus pharmacophore model of molecules A2, A3, A4 and A5 representing various regions (Green: Lipophilic, Red: H-Bond acceptor region)

The antibacterial activities of the molecules are due to presence of lipophilic and H-bond acceptor regions in the A2, A3, A4 and A5 molecules. These molecules are the most active with respect to antibacterial activities amongst all the selected molecules. This increased activity is due to the electron withdrawing groups (F, Cl and Br). The lipophilic regions of these molecules are increased due to the presence of halogen substituents as the non-substituted molecules are found to be least potent against the bacterial strain.

**Group 2:**

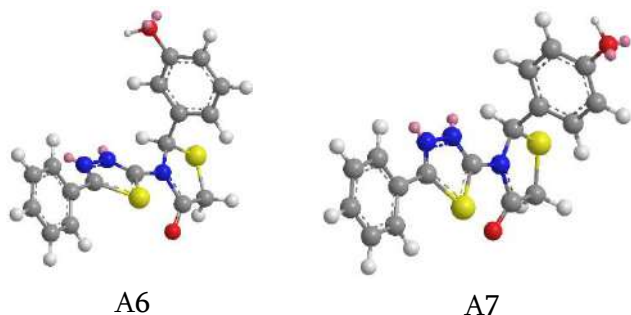


Fig 5: 3D structure of molecules A6 and A7

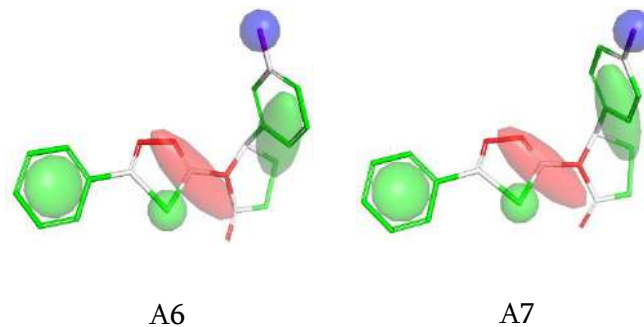


Fig 6: Pharmacophore models of A6 and A7

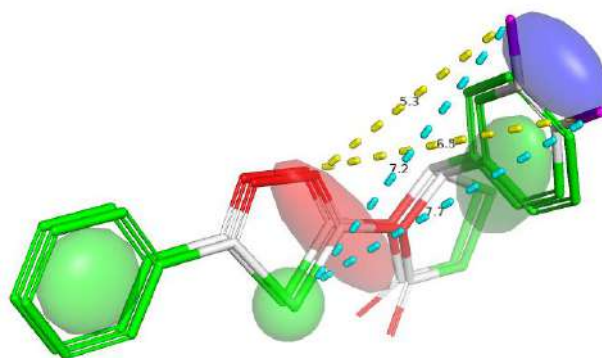


Fig 7: Consensus pharmacophore model of molecules A6, and A7 representing various regions  
(Green: Lipophilic, Red: H-Bond acceptor region, Blue:H-Bond Acceptor)

Molecules A6 and A7 are positional isomers of each other. These molecules have found to have similar activity against bacterial strain. The presence of the H-bond acceptor region of -OH group decreases the strength of the molecules as compared to the molecules with halogen substituents.

**Group 3**

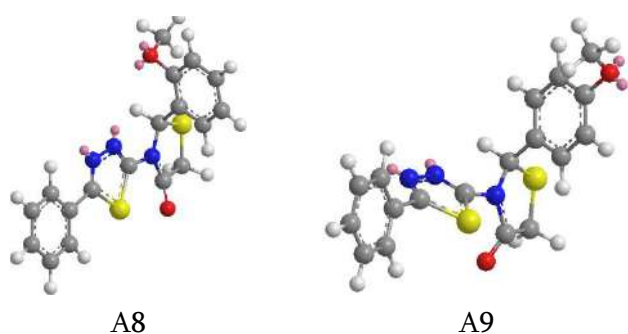


Fig 8: 3D structure of molecules A8 and A9

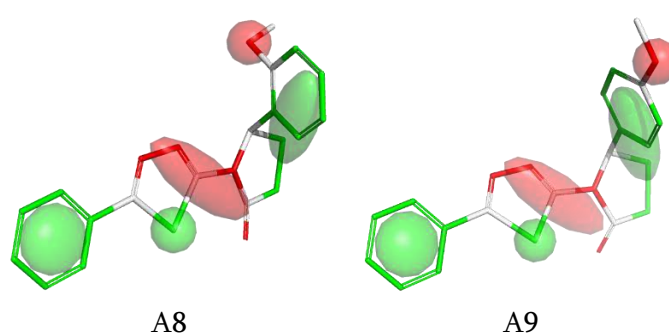


Fig 9: Pharmacophore models of A8 and A9



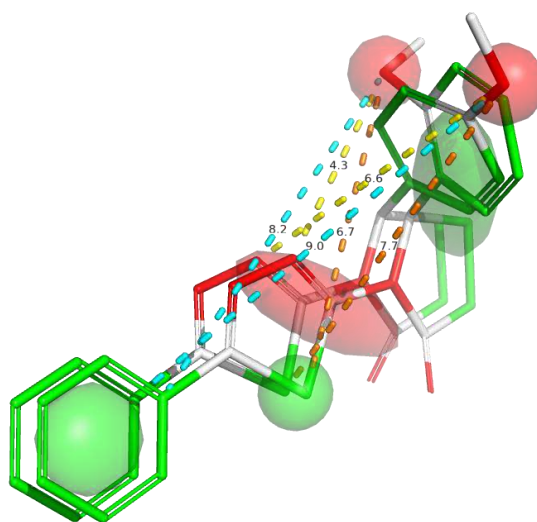


Fig 10: Consensus pharmacophore model of molecules A8, and A9 representing various regions (Green: Lipophilic, Red: H-Bond acceptor region,)

Molecules A8 and A9 have similar  $-OCH_3$  substituents but with varying position hence these molecules have similar strength against bacterial strain. The increased H-Bond-Acceptor region of  $-OCH_3$  groups of these molecules decreases the antibacterial activities of the molecules.

**Group 4:**

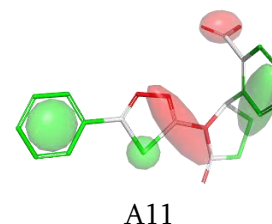
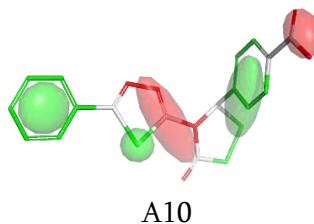
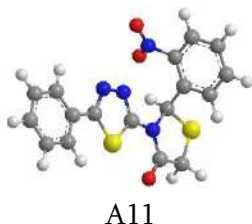
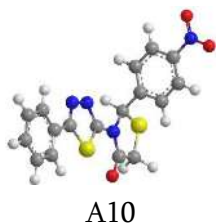


Fig 11: 3D structure of molecules A10 and A11

Fig 12: Pharmacophore models of A10 and A11

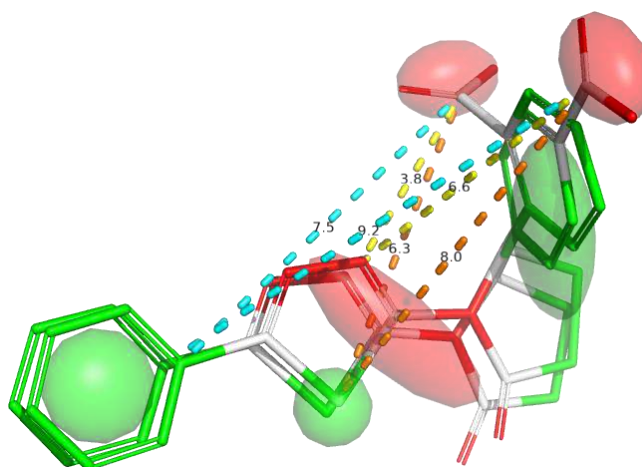


Fig 13: Consensus pharmacophore model of molecules A10, and A11 representing various regions (Green: Lipophilic, Red: H-Bond acceptor region,)

These molecules have similar antibacterial strength since they have similar molecular formula. The presence of the -NO<sub>2</sub> region increases one H-Bond-Acceptor region which decreases the antibacterial activity of these molecules as compared to the molecules with halogen substituents.

A closer inspection of the pharmacophore models of all the molecules unveils that the antibacterial activity of these molecules is closely related to the H-bond donor, H-bond acceptor and lipophilic regions present in the molecules. When the antibacterial activity of the molecule (A1) which has non-substituted benzene ring is compared with remaining molecules (A2 to A11) which have substituted benzene ring, a deviation in the antibacterial activities is observed.

In case with the halogen substituents (A2, A3, A4 and A5) the molecules are found to be more active against bacterial strain. This is because of the increased lipophilic region due to the presence of halogen substituents. Whereas in the molecules with -OH substituent (A6 and A7), microbial activity is decreased. This decreased activity is because of the H-bond acceptor region that raised due to -OH group. But in the molecules A8 and A9 with -OCH<sub>3</sub> substitution and A10 and A11 with -NO<sub>2</sub> substitution H-bond acceptor region increases that decreases the strength of the molecules against bacterial strain.

#### IV. CONCLUSION

The antibacterial activity of the molecules is associated with the type of the substitution on benzene ring. From the above discussion it can be concluded that the increased lipophilic region increases the antibacterial activity of the molecules while increase in the H-bond donor and H-bond acceptor regions decreases it. Hence the halogen substituents must be retained to have molecules with good antibacterial activity. The present study has

helped to discover useful structural features of the molecules for future optimization.

#### V. REFERENCES

- [1]. A. Pandey, R. Rajavel, S. Chandraker, D. Dash; E-Journal of Chemistry; 9(2012), 2524
- [2]. Kai Zhang, Peng Wang, Li-Na Xuan, Xiao-Yun Fu, Fen Jing, Sha Li, Yu-Ming Liu, Bao-Quan Chen, Bioorganic & Medicinal Chemistry Letters, 24 (2014) 5154-5156
- [3]. M. M. Raj, H. V. Patel, L. M. Raj, N. K. Patel; IJPCBS, 3(2013), 814-819
- [4]. Husam A. Ameen, Ahlam J. Qasir; Iraqi J Pharm Sci, 21(2012), 98-104
- [5]. T. Ahmad, A. K. Singh, N. Jaiswal, D. Singh; IRJP, 3(2012), 70-82
- [6]. W. Płonka, A. Paneth, P. Paneth; Molecules, 25(2020), 4645
- [7]. Ming Chen, Wen-Gui Duan, Gui-Shan Lin, Zhong-Tian Fan, Xiu Wang; Molecules, 26(2021), 1708.
- [8]. Georgeta Serban; Molecules, 25(2020), 942
- [9]. P. A. Datar, T. A. Deokule; Medicinal Chemistry; DOI: 10.4172/2161-0444.1000170
- [10]. B. Shrivastava, O. Sharma, P. Sharma, J. Singh; Asian Journal of Pharmacy and Pharmacology; 5(2019): 368-372
- [11]. O. Sharma, P. Sharma, B. Shrivastava, J. Singh; Asian Pac. J. Health Sci.; 5(2018):325-330
- [12]. Masand, V. H., & Rastija, V. (2017). PyDescriptor : A new PyMOL plugin for calculating thousands of easily understandable molecular descriptors. Chemometrics and Intelligent Laboratory Systems, 169, 12-18.
- [13]. Masand, V. H., El-Sayed, N. N. E., Mahajan, D. T., & Rastija, V. (2017). QSAR analysis for 6-arylpyrazine-2-carboxamides as Trypanosoma brucei inhibitors. SAR and QSAR in Environmental Research, 28(2), 165-177.
- [14]. Masand, V. H., El-Sayed, N. N. E., Mahajan, D. T., Mercader, A. G., Alafeefy, A. M., & Shibi, I.

G. (2017). QSAR modeling for anti-human African trypanosomiasis activity of substituted 2-Phenylimidazopyridines. Journal of Molecular Structure, 1130, 711-718.

**Cite this article as :**

C. N. Jadhav, M. M. Rathore, V. H. Masand, P. S. Bodkhe, "Study of Pharmacophoric Consensus Pattern for Benzoic Acid Derivatives of 1,3,4-Thiadiazole As Antibacterial Agent", International Journal of Scientific Research in Science and Technology (IJSRST), Online ISSN : 2395-602X, Print ISSN : 2395-6011, Volume 10 Issue 1, pp. 167-174, January-February 2023. Available at doi : <https://doi.org/10.32628/IJSRST1231011>  
Journal URL : <https://ijsrst.com/IJSRST1231011>

## Effect of Solvent Polarity on Viscosity of 2-Hydroxy Substituted 1, 3- Dipropanone

Dongapure A. C<sup>1</sup>, Bodkhe P. S<sup>2</sup> and Choudhari P. P<sup>3\*</sup>

<sup>1</sup>Department of Chemistry, Shankarlal Agarwal Science College Salekasa, Gondia, Maharashtra, India

<sup>2</sup>Government Vidarbha Institute of Science and Humanities, Amravati, Maharashtra- 444604, India

<sup>3</sup>Department of Chemistry, G.S Tompe College, Amravati, Maharashtra- 444704, India

### ABSTRACT

We are going to report the observed measurements of the viscosity and density of two binary mixtures comprising various molar concentrations of 1-(5-Bromo-2-hydroxyphenyl)-3-p-tolylpropane-1,3-dione with Dimethyl sulfoxide (DMSO) and water at three different percentage (60%, 70%, and 80%). The measurements were conducted at various molar concentration C as follows: C = (0.01, 0.005, 0.0025, 0.00125, and 0.000625). The viscosity and density measurements were carried out using Ostwald's viscometer and pycnometer. The results were correlated using the graph of  $(\eta_r - 1)/\sqrt{C}$  versus  $\sqrt{C}$  relations that express density and viscosity as functions of the Falkenhagen coefficient and Jones-Dole coefficient, which explain the solvent - solvent, and solute - solvent interaction. To study the viscosity of the binary mixtures as a function of density, and composition, we have applied several polarities mixing DMSO in water.

Keywords: Viscosity, density, relative viscosity, 2-hydroxy Substituted 1,3- Dipropanone containing phenol, Ligand, DMSO

### INTRODUCTION

1-(5-Bromo-2-hydroxyphenyl)-3-p-tolylpropane-1,3-dione is a  $\beta$ -diketone more important because it is a key intermediates synthesis of Carbon-Carbon bonds in a vast quantity of biologically and pharmaceutically products (1). The compounds having a 1,2 diketone functional group with phenyl ring have been reported to possess various biological activities such as anti-inflammatory, antimicrobial (2), antioxidant (3) (4), anti-malarials (5), anti-tuberculosis (6), anti-HIV and antitumor (7). Viscometric studies have found a wide range of applications in various fields. Density and viscosity are significant factors employed for equipment design, solution theory, process simulation, and molecular dynamics (8) (9). Viscosity is a play important role in physical property for calculations related to fluid flow. Thermophysical parameters have been explain intermolecular interactions in liquids over the past several years (10) (11). Several researchers reported the thermoacoustical parameters in polymers, liquefied gases, organic liquids, and binary liquid mixtures (12) (13). Viscosity measurement is helpful to understand the type of molecular interactions and this helps to examine the solvent-solvent interaction and solute-solvent interaction occurring in solutions (14). The literature reveals that work on acoustical properties of solutions of organic compounds was carried out by using viscometric techniques (15).

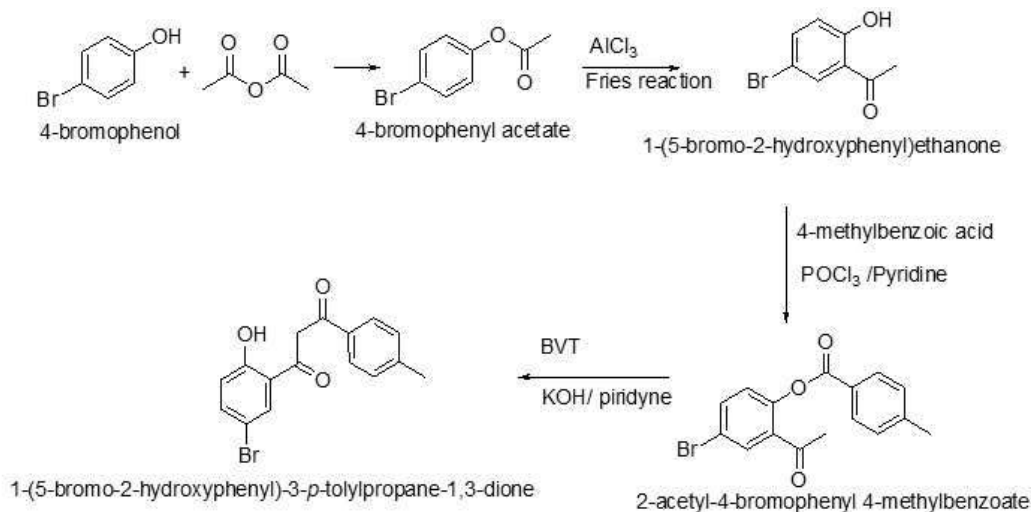
The DMSO was chosen as a solvent because of its broad applicability in chemical, and biological processes (16) (17), pharmacy, and medicine (18). The essential pharmacological use of DMSO in drugs idoxuridine is to upturn the dispersion of the drug into the skin (19). The structure of DMSO contains hydrophobic methyl groups bonded to a greatly polar sulfoxide group. DMSO molecules show association due to the dipole-dipole interactions among the sulfur and oxygen (20). DMSO contains hydrogen acceptor oxygen atom; hence it can form Hydrogen-bonds with hydroxyl (OH) groups (21).

Because of the above-mentioned consequence of DMSO and  $\beta$ -diketone in medicinal and pharmaceutical chemistry, we aim to synthesize  $\beta$ -diketone (22) and to study the effect of the concentration of this  $\beta$ -diketone on the different percentage of solvent mixtures. Water and DMSO (60%, 70%, and 80%) were used as a solvent. The density  $\rho$ , viscosity  $\eta$ , the Falkenhagen coefficient A and Jones-Dole coefficient B of solutions of these compounds were experimentally observed at different molar concentrations of 1-(5-Bromo-2-hydroxyphenyl)-3-p-tolylpropane-1,3-dione. These experimentally calculated results help to study molecular interactions.

### EXPERIMENTAL

In this present investigation, the attempt is made to understand the behaviour of  $\beta$ -diketone ligands namely 1-(5-Bromo-2-hydroxyphenyl)-3-p-tolylpropane-1,3-dione have been carried out in organic solvents Dimethyl sulfoxide (DMSO). The ligand 1-(5-Bromo-2-hydroxyphenyl)-3-p-tolylpropane-1,3-dione was already prepared by using a very common synthetic method (23). Then the viscosity and density measurements of a diverse molar solution of ligand at room temperature were calculated. All chemicals used to synthesise substituted  $\beta$ -

diketone ligand were of A.R. grade. DMSO was purified by described method (24). The reaction scheme for the synthesis of 1-(5-Bromo-2-hydroxyphenyl)-3-p-tolylpropane-1,3-dione from 4-Bromophenol is shown below



**Figure 1:** Reaction scheme for the synthesis of Ligand

Solutions of 1-(5-Bromo-2-hydroxyphenyl)-3-p-tolylpropane-1,3-dione as a function of molality  $0.01 \text{ mol kg}^{-1}$  were prepared in pure DMSO and varied concentration 0.005, 0.0025, 0.00125, and 0.00062 was prepared by using  $0.01 \text{ mol kg}^{-1}$  solution. The weighing of 1-(5-Bromo-2-hydroxyphenyl)-3-p-tolylpropane-1,3-dione was done on an electronic single pan five digit Balance with a precision of  $\pm 0.0001 \text{ mg}$ . Before every measurement, calibrated and standardized at  $25^\circ\text{C}$  with triply distilled water and dry air at normal atmospheric pressure. Using Ostwald's viscometer method viscosity was measured with a common relative uncertainty of  $\pm 1 \times 10^{-6} \text{ Pa s}$ . The stopwatch was used to observe the efflux time of solutions with an precision of  $\pm 0.01 \text{ s}$ . The mean of at least three readings was taken as the final efflux time for every sample for the calculation of the viscosity of the solution.

## RESULTS AND DISCUSSION

The relative viscosity and density of these compounds increase with an increase in concentration. The increase in viscosity with an increase in concentration is credited to the increase in the solute-solvent interactions due to the intermolecular hydrogen bonding between  $\text{-S=O}$  group of DMSO and  $\text{-OH}$  group of 2-Hydroxy substituted 1,3-Dipropenone containing phenol group. The experimentally determined values of density  $\rho$ , viscosity  $\eta$ , relative viscosity  $\eta_r$ , specific viscosity  $\eta_{sp}$ , Falkenhagen coefficient-A and Jones-Dole coefficient-B, in DMSO water mixture at room temperatures, are listed in tables no.1 to 3.

The relation between viscosity ( $\eta_{sp}/\sqrt{C}$ ) and concentration of the solution ( $\sqrt{C}$ ) is represented by plotting the graph (Fig. no.2 to 4). The graph for each system shows a linear straight line recognizing the validity of the Jones-Dole equation. The value of the Jones-Dole coefficients-B is the slope of the graph ( $\eta_{sp}/\sqrt{C}$ ) versus ( $\sqrt{C}$ ), while the value of Falkenhagen coefficient-A is the intercept of the graph of ( $\eta_{sp}/\sqrt{C}$ ) versus ( $\sqrt{C}$ ).

From table 4, the B-coefficient is found to be negative values for all the systems, and is a measure of disorder introduced by the solute into the solvent in all the systems. The Falkenhagen coefficient-A is a positive value in all the systems, and this coefficient reflects strong solute-solute interaction.

**Table 1**

Temp:  $(305 \pm 0.1) \text{ K}$

Medium: 60% DMSO-Water

Conc. (C) (mol/lit)	$\sqrt{C}$ ( $\text{mol}^{1/2}\text{lit}^{-1/2}$ )	Density (gm/cc)	Time Flow (s)	Relative Viscosity $\eta_r = \eta/\eta_0$	Specific Viscosity $\eta_{sp} = \eta_r - 1$	$\eta_{sp}/\sqrt{C}$
0.01	0.1000	1.1263	22.123	1.1944	0.19442	12.2826
0.005	0.0707	1.1253	22.098	1.1920	0.1920	15.1137
0.0025	0.0500	1.1243	21.123	1.1384	0.1384	22.7918
0.00125	0.0354	1.1232	20.478	1.1025	0.1025	27.9003
0.000625	0.0250	1.1220	19.854	1.0678	0.0678	33.4475

**Table 2**

Temp: (305 ± 0.1) K

Medium: 70% DMSO-Water

Conc. (C) (mol/lit)	$\sqrt{C}$ (mol <sup>1/2</sup> lit <sup>-1/2</sup> )	Density (gm/cc)	Time Flow (s)	Relative Viscosity $\eta_r = \eta / \eta_0$	Specific Viscosity $\eta_{sp} = \eta_r - 1$	$\eta_{sp}/\sqrt{C}$
0.01	0.1000	1.1258	24.509	1.88439	0.88439	8.8439
0.005	0.0707	1.1236	23.675	1.88059	0.88059	12.4534
0.0025	0.0500	1.1220	22.864	1.7395	0.7395	14.79
0.00125	0.0354	1.1208	21.156	1.79603	0.79603	22.5151
0.000625	0.0250	1.1198	20.987	1.68473	0.68473	27.3892

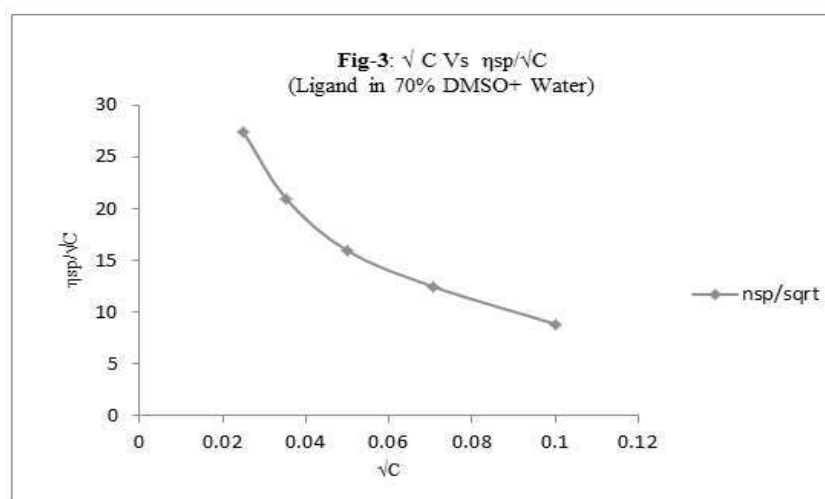
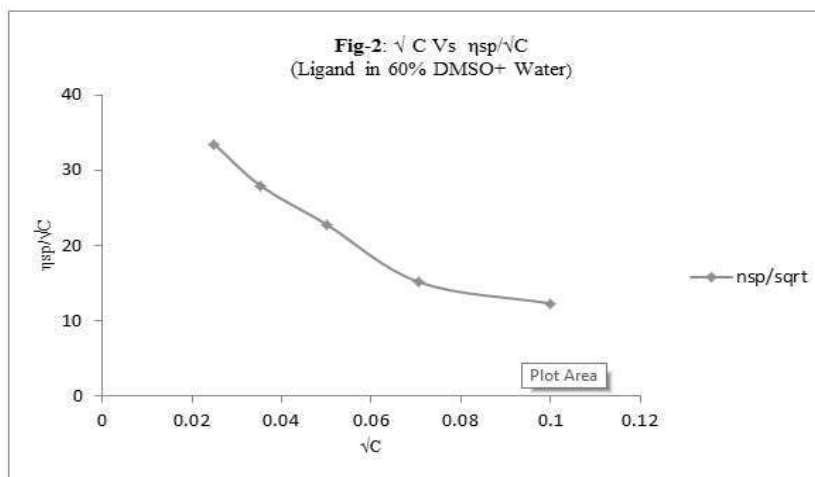
**Table 3**

Temp: (305 ± 0.1) K

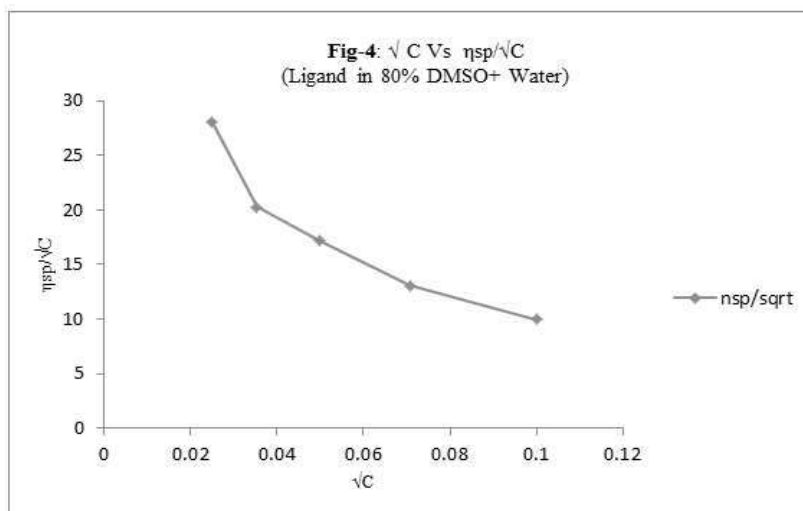
Medium: 80% DMSO-Water

Conc. (C) (mol/lit)	$\sqrt{C}$ (mol <sup>1/2</sup> lit <sup>-1/2</sup> )	Density (gm/cc)	Time Flow (s)	Relative Viscosity $\eta_r = \eta / \eta_0$	Specific Viscosity $\eta_{sp} = \eta_r - 1$	$\eta_{sp}/\sqrt{C}$
0.01	0.1000	1.0756	30	1.99721	0.99721	9.9721
0.005	0.0707	1.0700	28	1.92538	0.92538	13.0868
0.0025	0.0500	1.0685	29	1.85674	0.85674	17.1348
0.00125	0.0354	1.0655	27	1.71624	0.71624	20.2583
0.000625	0.0250	1.0637	25	1.70102	0.70102	28.0408

The drop in viscosity concerning an increase in the concentration of ligand may be credited to the decline in solute-solvent interactions. From the graph of  $(\eta_r - 1) / \sqrt{C}$  versus  $\sqrt{C}$ . 'A' which shows the solute-solute interactions and 'B' which then shows solute-solvent interactions have been calculated. The large and small values of 'A' show the stronger and weaker solute-solute interactions.



For 60% DMSO, 70% DMSO, and 80% DMSO in water, at various molar concentrations of 1-(5-Bromo-2-hydroxyphenyl)-3-p-tolylpropane-1,3-dione, the value of relative viscosity, specific Viscosity,  $\eta_{sp}/\sqrt{C}$  increases. This increase is due to strong solute-solvent interactions due to the increasing strength of the bond between the (-OH) group of water and the (-C=O) group of the ligand as well as the interactions between the (-OH) group of ligand and (-C=O) group DMSO.



**Table 4:** A and B Coefficient values

	A	B
Ligand in 60% DMSO+ Water	38.191	-282.6
Ligand in 70% DMSO+ Water	30.541	-237.35
Ligand in 80% DMSO+ Water	29.929	-217.57

## CONCLUSIONS

In this article, Density  $\rho$ , viscosity  $\eta$ , relative viscosity  $\eta_r$ , specific viscosity  $\eta_{sp}$ , Falkenhagen coefficient-A, and Jones-Dole coefficient-B explained the solvent-solvent, solute-solvent and molecular interactions for different concentrations of 1-(5-Bromo-2-hydroxyphenyl)-3-p-tolylpropane-1,3-dione in various solvent mixtures.

## ACKNOWLEDGEMENT

The authors are thankful to Principal, G.S Tompe College, Amravati for the necessary facilities.

## REFERENCES

1. Kharat, Pandharinath S. Nikam and Sanjeevan J. s.l. : J. Pharm. Pharmacol. 46 (1994) pp. 1291–1295.
2. Tahereh Sedaghat, Marjan Monajjemzadeh and Hossein Motamedi. s.l.: Coord Chem Rev., 64, 18 (2011), pp. 3169-3179.
3. Galano, Annia. s.l. : Chemical Physics 363 (2009) pp. 13-23.
4. N. Sreejayan, K.I. Priyadarsini, T.P.A. Devasagayam, M.N.A. Rao., s.l. : Int. J.Pharmacol. 151 (1997) pp. 127-130.
5. Jakob Kljun, Iztok Turel. s.l. : Org. Biomol. Chem., 12, (2014) pp. 1655–1666.
6. A.J. Ruby, G. Kuttan, K.D. Babu., s.l. : Cancer Lett. 94 (1995) pp. 79-83.
7. Abbas, H. s.l. : DRUG DELIVERY 29,1, (2022) pp. 714-727.
8. D. Venkatesan, Joshua Amarnath D, T. Srinivasa Krishna, P. Biswas, R. Dey. s.l. : J.Mol. Liq. 299 (2020) pp. 112221.
9. J.V. Srinivasu, T.S. Krishna, K. Narendra, G. SrinivasaRao, B. SubbaRao. s.l. : J. Mol. Liq.236 (2017) pp. 27-37
10. TA. Saini, A. Harshavardhan, R. Dey, Indian Journal of Chemistry Section a 56(1), pp. 21-35.
11. S. K. Lomesh, D. Kumar,. Journal of Molecular Liquids, 241, pp. 764-771.
12. K. Narendra, Ch. Kavitha, T. S. Krishna,. International Journal of Ambient Energy, 43 (1), pp. 1113-1119.



13. J. Jugan, M. Abdulkhadar,. *Journal of Molecular Liquids*, 100 (3), pp. 217-227.
14. Sain, Akanksha,. *Journal of Molecular Liquids*, 323, pp. 114593.
15. Abbas Mehrdad, Mohsen Hajikarimi. s.l. : *The Journal of Chemical Thermodynamics*, 139 (2019), pp. 105880.
16. Raj Chakrabarti, Clarence E.Schutt. *Gene*, 274 (1–2) (2001), pp. 293-298.
17. Masaji Sawai, Kozo Takase, Hirobumi Teraoka, Kinji Tsukada. *Experimental Cell Research*, 187(1), (1990), pp. 4-10.
18. Capriotti K, Capriotti J., *International Medical Case Reports Journal*, 8, (2015) pp. 231—233.
19. L.Spotswood. s.l. : *J. Chem. Eng. Data* 50 (2005) 1161 (2), pp. 191–197.
20. J. Catalan, C. Diaz, F. Garcia-Blanco. s.l. : *J. Org. Chem.* 66 (2001) pp. 5846–5852.
21. Kristina Noack, Johannes Kiefer, Alfred Leipert. s.l. : *J. Chem. Eng. Data* 48 (2003) pp. 630-637.
22. Dongapure A.C, Choudhari P.P. s.l. : *Der Pharma Chemica*, 14 (2022) pp. 24-27.
23. S Bodkhe, Pathade R. M.and. s.l. : *IJCESR*, 6 (2019), pp. 84-87.
24. Furniss B.S., Hannaford A.J. A.R. *Vogel’s Text Book of Practical Organic Chemistry*. s.l. : Fifth Edition, 2007.
25. M.J.W. Povey, S.A. Hindle, J.D.Kennedy, Z. Stec,. s.l. : *Chem.Phys.* 5 (2003) pp. 73-78.
26. C.D. Eads. s.l. : *J. Phys. Chem. B* 104 (2000) pp. 6653–6661.
27. J.N. Nayak, M.I. Aralaguppi, T.M. Aminabhavi. s.l. : *J. Chem. Eng. Data* 48 (2003) 628.
28. Dongapure A.C, Choudhari P.P. s.l. : *Der Pharma Chemica*, 2022, 14(5): 24-27.
29. S, Pathade R. M.and Bodkhe P. s.l. : *IJCESRE*, 6, (2019), pp. 84-87,.





## Article

# Mechanistic Analysis of Chemically Diverse Bromodomain-4 Inhibitors Using Balanced QSAR Analysis and Supported by X-ray Resolved Crystal Structures

Magdi E. A. Zaki<sup>1,\*</sup>, Sami A. Al-Hussain<sup>1</sup>, Aamal A. Al-Mutairi<sup>1</sup>, Vijay H. Masand<sup>2,\*</sup>, Abdul Samad<sup>3</sup>   
and Rahul D. Jawarkar<sup>4</sup> 

- <sup>1</sup> Department of Chemistry, Faculty of Science, Imam Mohammad Ibn Saud Islamic University, Riyadh 13318, Saudi Arabia; sahusain@imamu.edu.sa (S.A.A.-H.); aamutairi@imamu.edu.sa (A.A.A.-M.)  
<sup>2</sup> Department of Chemistry, Vidya Bharati Mahavidyalaya, Amravati 444602, India  
<sup>3</sup> Department of Pharmaceutical Chemistry, Faculty of Pharmacy, Tishk International University, Erbil 44001, Iraq; abdul.samad@tiu.edu.iq  
<sup>4</sup> Department of Medicinal Chemistry, Dr. Rajendra Gode Institute of Pharmacy, University-Mardi Road, Amravati 444901, India; rahuljawarkar@gmail.com  
\* Correspondence: mezaki@imamu.edu.sa (M.E.A.Z.); vijaymasand@gmail.com (V.H.M.)

**Abstract:** Bromodomain-4 (BRD-4) is a key enzyme in post-translational modifications, transcriptional activation, and many other cellular processes. Its inhibitors find their therapeutic usage in cancer, acute heart failure, and inflammation to name a few. In the present study, a dataset of 980 molecules with a significant diversity of structural scaffolds and composition was selected to develop a balanced QSAR model possessing high predictive capability and mechanistic interpretation. The model was built as per the OECD (Organisation for Economic Co-operation and Development) guidelines and fulfills the endorsed threshold values for different validation parameters ( $R^2_{tr} = 0.76$ ,  $Q^2_{LMO} = 0.76$ , and  $R^2_{ex} = 0.76$ ). The present QSAR analysis identified that anti-BRD-4 activity is associated with structural characters such as the presence of saturated carbocyclic rings, the occurrence of carbon atoms near the center of mass of a molecule, and a specific combination of planer or aromatic nitrogen with ring carbon, donor, and acceptor atoms. The outcomes of the present analysis are also supported by X-ray-resolved crystal structures of compounds with BRD-4. Thus, the QSAR model effectively captured salient as well as unreported hidden pharmacophoric features. Therefore, the present study successfully identified valuable novel pharmacophoric features, which could be beneficial for the future optimization of lead/hit compounds for anti-BRD-4 activity.

**Keywords:** QSAR; BRD-4; pharmacophoric features; X-ray



**Citation:** Zaki, M.E.A.; Al-Hussain, S.A.; Al-Mutairi, A.A.; Masand, V.H.; Samad, A.; Jawarkar, R.D. Mechanistic Analysis of Chemically Diverse Bromodomain-4 Inhibitors Using Balanced QSAR Analysis and Supported by X-ray Resolved Crystal Structures. *Pharmaceuticals* **2022**, *15*, 745. <https://doi.org/10.3390/ph15060745>

Academic Editors: Jun Qi and Adam David Durbin

Received: 16 May 2022

Accepted: 7 June 2022

Published: 14 June 2022

**Publisher's Note:** MDPI stays neutral with regard to jurisdictional claims in published maps and institutional affiliations.



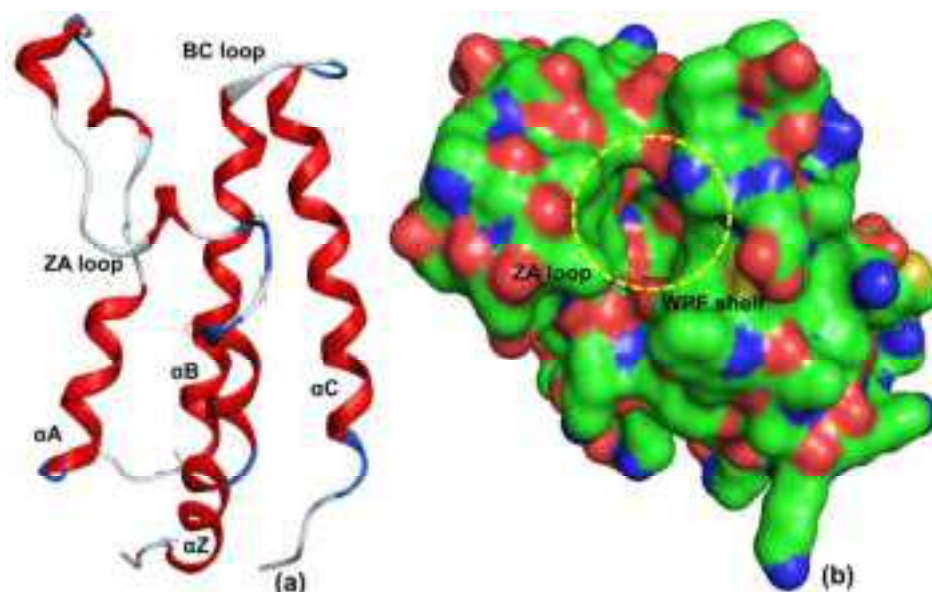
**Copyright:** © 2022 by the authors. Licensee MDPI, Basel, Switzerland. This article is an open access article distributed under the terms and conditions of the Creative Commons Attribution (CC BY) license (<https://creativecommons.org/licenses/by/4.0/>).

## 1. Introduction

Cancer and heart failure are major causes of mortality [1], health complications, and social and economic problems for millions of people around the globe. Researchers have identified different chemotherapeutic methods to minimise heart failure as well as the onset, growth, and survival of cancer cells [1]. However, different serious health issues initiated or echoed by different anti-cancer and cardiac drugs are of great concerns. Therefore, the quest for a harmless and effective anti-cancer and cardiac drug is an important goal for the research and development laboratories of pharmaceutical companies and academic institutions. For this, researchers generally prefer to inhibit any irregularity occurring during a vital cellular process. A good number of recent studies have confirmed that reversible lysine acetylation (RAL) is a dynamic process responsible for protein post-translational modifications, transcriptional activation, and other cellular processes [2–11]. Therefore, any anomaly with RAL could lead to the initiation of malignancy or its survival [7,12]. RAL is regulated by three types of epigenetic regulatory proteins [12,13]: (1) histone acetyltransferases (HATs) acetylate lysine, (2) Histone deacetylases (HDACs), and (3) bromodomain

(BRD) family of proteins. HATs are responsible for acetylation of lysine residues on histone tails and thereby behave as “writers”, whereas the reverse is true for HDACs and sirtuins, which work as “erasers” that are accountable for the elimination of the acetyl group from acetylated lysine (KAc) [14]. The Bromodomain and Extra-terminal (BET) family selectively recognises and links with acetylated lysine residues in histones H3 and H4 [15–17]; thus, they function as “readers”. The BET proteins, viz., BRD2, BRD3, and BRD-4, and bromodomain testis-specific protein (BRDT) are widely recognised as druggable target proteins for regulating cellular epigenetics [15]. Therefore, intruding interactions between BET proteins and acetylated lysine have attracted many researchers to develop better therapeutics for various human diseases including cancer, acute heart failure, and inflammation [2–11].

BRD-4, also called mitotic chromosomal-associated protein (MCAP), Fshrg4, or Hunk1, is ubiquitously expressed and plays a crucial role in a number of DNA-centered processes [15]. It is generally localised in the nucleus and regulates transcription by RNA polymerase II through a positive transcriptional elongation factor complex [15]. Structurally, it comprises two highly conserved N-terminal bromodomains (BD1 and BD2), an ET domain, and a C-terminal domain (CTD) [7]. Furthermore, BRD-4 contains a set of four helices:  $\alpha Z$ ,  $\alpha A$ ,  $\alpha B$ , and  $\alpha C$ .  $\alpha Z$  and  $\alpha A$  helices are connected through the ZA loop, whereas the BC loop connects the  $\alpha B$  and  $\alpha C$  helices [11,18]. Together, the four helices and the two loops create an active acetyl-lysine binding pocket (see Figure 1) [11,18]. The active site also consists of a hydrophobic WPF shelf (Trp81, Pro82, and Phe83), ZA loop, Tyr97, Asn140, and Met149 [11,18]. The majority of BRD-4 inhibitors compete with histone H4 to imitate the interactions with Tyr97 and Asn140 [3]. The WPF shelf is believed to play an important role in deciding the selectivity for BET bromodomains [6].

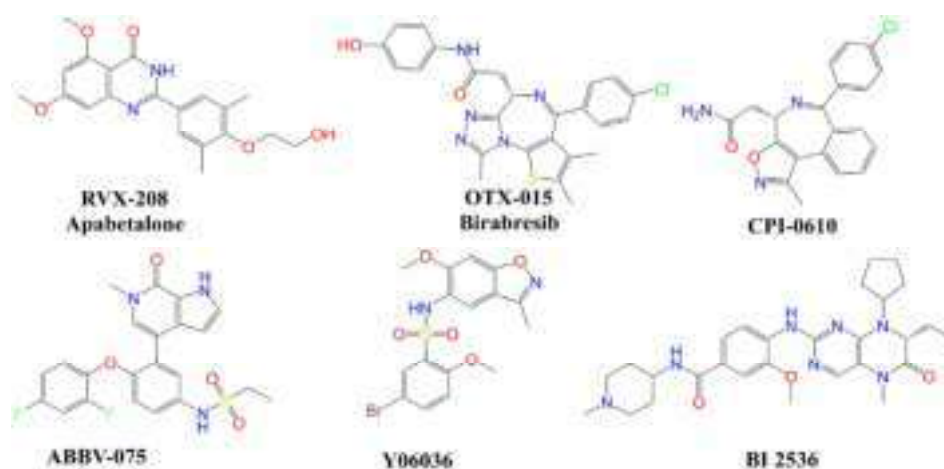


**Figure 1.** X-ray resolved structure of BRD-4 using pdb 5UVT (a) without molecular surface and (b) with molecular surface (green: carbon; red: oxygen; blue: nitrogen).

Recent studies indicate that the inhibition of BRD-4 is a good strategy, and a good number of BRD-4 inhibitors are in clinical or pre-clinical trials (see Figure 2) [2,19,20].

However, the quest for a safer and effective BRD-4 inhibitor with an optimum ADMET (Absorption, Distribution, Metabolism, Excretion, and Toxicity) profile with a retention of potency is still in progress. For this, it is essential to know the prominent and concealed pharmacophoric features associated with BRD-4 inhibitors. To achieve this goal, a good number of researchers have reported SAR (Structure Activity Relationships) and QSAR (Quantitative SAR) analyses of BRD-4 inhibitors. Tahir et al. [21] developed a CoMSIA (3D-QSAR) model with an  $R^2_{tr}$  (coefficient of determination) = 0.982 and  $R^2_{cv}$  (or  $Q^2_{loo}$ ) (cross-validated coefficient of determination for leave-one-out) = 0.500 for a dataset of

60 quinolinone and quinazolinone derivatives as BRD-4 inhibitors. Tong et al. [22] reported four 3D-QSAR models possessing  $R^2_{tr} = 0.912$  to  $0.963$  and  $R^2_{cv} = 0.574$  to  $0.759$  for the BRD-4 inhibitory activity of 4,5-dihydro-[1,2,4]triazolo[4,3-f]pteridine derivatives. Obadawo and co-workers [23] performed QSAR modelling ( $R^2_{tr} = 0.93$  and  $R^2_{cv} = 0.70$ ) for 40 different substituted 4-Phenylisoquinolinones as potent BET bromodomain (BRD-4-BD1) inhibitors. Speck-Planche and Scotti [6] performed multi-target QSAR for bromodomain inhibitors using linear discriminant analysis and artificial neural networks. Their binary classification (active/inactive), which is based on a fragment-based topological approach, and analysis led to the identification of a good number of pharmacophoric features. However, the fragment-based topological approach involved the use of SMILES of molecules and thereby lacks the inclusion of 3D information. Thus, even though these studies are successful in identifying easily visible pharmacophoric features, they are based on small datasets with limited variations in structures, binary classification, lack thorough validation and general applicability, and provide partial mechanistic interpretations.



**Figure 2.** Chemical structures of selected BRD-4 inhibitors.

A literature survey reveals that BRD-4 inhibitors possess structural isomerism (positional, chain, etc.), variations in central scaffolds, and their chemical space is very broad [6,7]; therefore, many concealed or hidden correlations of pharmacophoric features cannot be identified by visual inspection [24]. In such a situation, there is a need to accomplish thorough QSAR analysis using a larger dataset of BRD-4 inhibitors. In the present work, we have performed QSAR analysis of 980 structurally diverse BRD-4 inhibitors. The developed QSAR model possesses a balance of excellent predictive ability with in-depth mechanistic interpretations, which are reinforced by reported X-ray-resolved structures of BRD-4 inhibitors with the target enzyme.

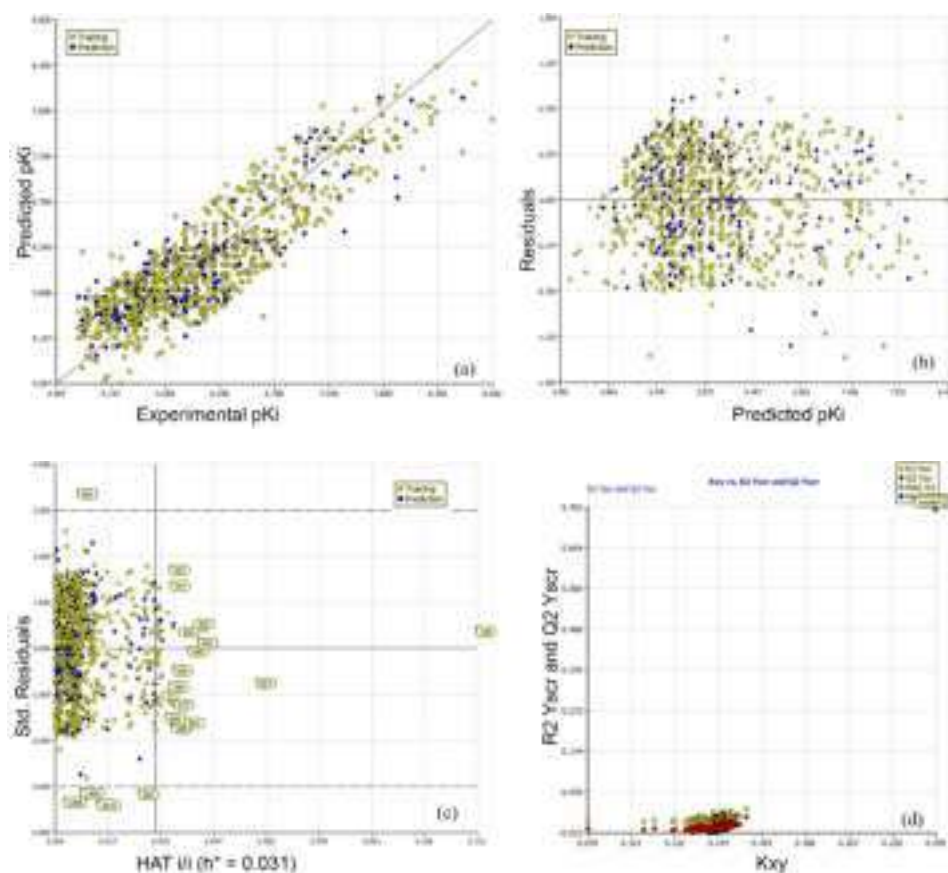
## 2. Results

The present QSAR analysis is based on a dataset covering a broad chemical space and data range owing to the inclusion of structurally diverse compounds with experimentally measured  $IC_{50}$  in the range of 1 nM to 15  $\mu$ M. Consequently, this helped us in developing an appropriately validated genetic algorithm multi-linear regression (GA-MLR) model for gathering or extending exhaustive information about the pharmacophoric traits that govern the desired bio-activity (Descriptive QSAR) and also possessing acceptable external predictive capability (Predictive QSAR) [25–27]. The seven variable-based GA-MLR QSAR model (see model-A), along with selected internal and external validation parameters (see Supplementary Material for additional parameters), is as follows.

**Model-A:**  $pIC_{50} = 4.27 (\pm 0.156) + 0.093 (\pm 0.017) * fsp3CringC2B + 0.108 (\pm 0.014) * com\_C\_4A + 0.391 (\pm 0.066) * Saturated\_Carbo\_Rings + 0.428 (\pm 0.036) * fsulfonSaroC8B + 0.625 (\pm 0.059) * flipoacc3B + 0.921 (\pm 0.067) * fsp3OaroN6B - 0.367 (\pm 0.063) * fpIaNN4B$ .

**Validation of Model-A:** Method of splitting = Random, No. of descriptors = 7,  $N_{\text{training}} = 785$ ,  $N_{\text{test}} = 195$ ,  $R^2_{\text{tr}} = 0.762$ ,  $R^2_{\text{adj.}} = 0.760$ ,  $\text{RMSE}_{\text{tr}} = 0.389$ ,  $\text{MAE}_{\text{tr}} = 0.326$ ,  $\text{CCC}_{\text{tr}} = 0.865$ ,  $s = 0.391$ ,  $F = 355.446$ ,  $R^2_{\text{cv}} (Q^2_{\text{loo}}) = 0.757$ ,  $\text{RMSE}_{\text{cv}} = 0.393$ ,  $\text{MAE}_{\text{cv}} = 0.329$ ,  $\text{CCC}_{\text{cv}} = 0.862$ ,  $Q^2_{\text{LMO}} = 0.756$ ,  $R^2_{\text{Yscr}} = 0.009$ ,  $Q^2_{\text{Yscr}} = -0.012$ ,  $\text{RMSE}_{\text{ex}} = 0.392$ ,  $\text{MAE}_{\text{ex}} = 0.323$ ,  $R^2_{\text{ex}} = 0.762$ ,  $Q^2\text{-F}^1 = 0.762$ ,  $Q^2\text{-F}^2 = 0.760$ ,  $Q^2\text{-F}^3 = 0.758$ ,  $\text{CCC}_{\text{ex}} = 0.860$ .

A multitude of statistical validation parameters and analysis of associated graphs has been recommended by different researchers to confirm the statistical robustness and external prediction ability of a QSAR model [28–39]. The same approach has been followed in the present work. A high value of  $R^2_{\text{tr}}$ ,  $R^2_{\text{adj.}}$ ,  $R^2_{\text{cv}} (Q^2_{\text{loo}})$ ,  $R^2_{\text{ex}}$ ,  $Q^2\text{-F}^n$ ,  $\text{CCC}_{\text{ex}}$ , etc., and a small value of LOF (lack-of-fit),  $\text{RMSE}_{\text{tr}}$ ,  $\text{MAE}_{\text{tr}}$ ,  $R^2_{\text{Yscr}}$  ( $R^2$  for Y-scrambling), etc., along with different graphs (Figure 3a–d) related to model-A support the external predictive ability, statistical robustness, and point out the lack of chancy correlation for model-A [28–38]. Moreover, the Williams plot [40–44] point out that the majority of molecules (929 molecules) are within the applicability domain; thus, the model is statistically acceptable (see Figure 3b). The outliers with high leverage have been labeled in Figure 3b. Therefore, it fulfills all the Organisation for Economic Co-operation and Development (OECD) endorsed guidelines for generating a thriving QSAR model.



**Figure 3.** Different graphs associated with the model: (a) experimental vs. predicted  $\text{pIC}_{50}$  (the solid line represents the regression line); (b) experimental vs. residuals values; (c) Williams plot for applicability domain (the vertical solid line represents  $h^* = 0.031$  and horizontal dashed lines represent the upper and lower boundaries for standard residuals); (d) Y-randomization.

The descriptions of seven molecular descriptors constituting model-A have been tabulated in Table 1.

**Table 1.** Details of molecular descriptors present in model-A.

Variable	Description	Software Used for Calculation
fsp3CringC2B	Frequency of occurrence of ring carbon atoms exactly at 2 bonds from sp <sup>3</sup> -hybridised carbon atoms	PyDescriptor [45]
com_C_4A	Total number of carbon atoms within 4 Å from centre of mass (com) of molecule	PyDescriptor
Saturated_Carbo_Rings	Total number of saturated rings containing carbon atoms only	DataWarrior [46]
fsulfonSaroC8B	Frequency of occurrence of aromatic carbon atoms exactly at 8 bonds from sulphur atoms of Sulfone group	PyDescriptor
fsp3OaroN6B	Frequency of occurrence of aromatic nitrogen atoms exactly at 6 bonds from sp <sup>3</sup> -hybridised oxygen atoms	PyDescriptor
flipoacc3B	Frequency of occurrence of H-bond acceptor atoms exactly at 3 bonds from lipophilic atoms	PyDescriptor
fplaNN4B	Frequency of occurrence of nitrogen atoms exactly at 4 bonds from planer nitrogen atoms	PyDescriptor

Interestingly, five molecular descriptors, viz., com\_C\_4A, fsp3CringC2B, flipoacc3B, fsulfonSaroC8B, and Saturated\_Carbo\_Rings, comprise the presence of different types of carbon atoms, which indicates the importance of carbon atoms in deciding BRD-4 inhibitory activity. The same is true for nitrogen, which is a part of three molecular descriptors, viz., flipoacc3B, fplaNN4B, and fsp3OaroN6B. Since, in general, the presence of carbon increases lipophilicity whereas nitrogen is attributed to significantly influence the pharmacological and hydrophilic profile, therefore, a balance of an appropriate number of carbons for lipophilicity and nitrogen is necessary to obtain adequate BRD-4 inhibitory activity. Of the seven descriptors in model-A, six have positive coefficients and only one has a negative coefficient. The effects of descriptors and their role in deciding the BRD-4 inhibitory profile have been discussed in more detail with relevant examples in the Discussion section.

### 3. Discussion

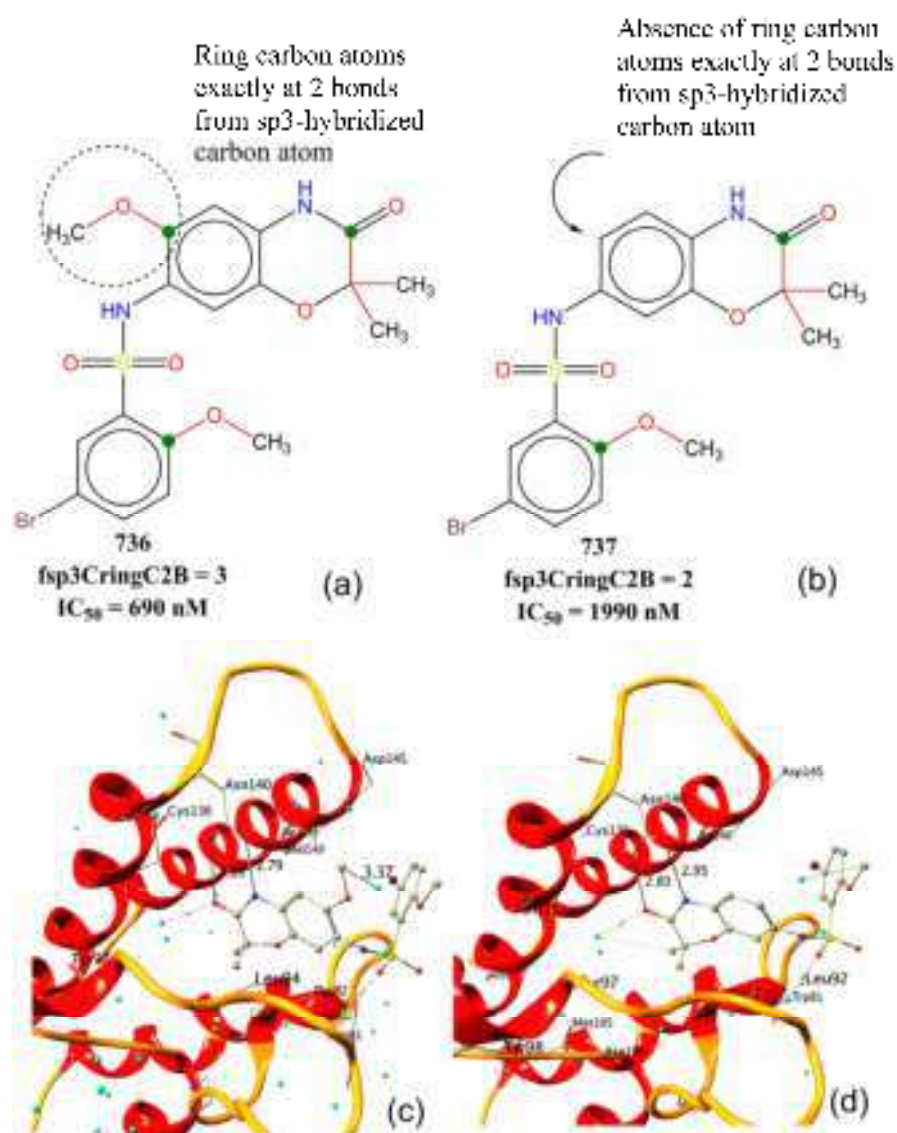
#### *Mechanistic Interpretation of QSAR Model*

An appropriately validated relationship between prominent structural features or molecular descriptors of the molecules with the bioactivity enlarges knowledge about mechanism of action of molecules, reasons for their specificity, and pharmacophoric atoms/groups accountable for the desired bioactivity [20,26,39]. In the present analysis, although we have equated the IC<sub>50</sub> values of different molecules in a relationship with a specific molecular descriptor (or feature), a synergistic or reverse effect of other molecular descriptors or unknown factors having a superseding influence in deciding the overall IC<sub>50</sub> value of a molecule cannot be ignored. That is, a single molecular descriptor or feature neither decides nor completely explains the experimental IC<sub>50</sub> value for such a large and structurally diverse set of molecules. In other words, the effective use of a validated QSAR model depends on the synergetic consideration of constituent molecular descriptors. The newly developed QSAR model-A comprises seven descriptors.

The molecular descriptor fsp3CringC2B represents the frequency of occurrence of ring carbon atoms exactly at two bonds from sp<sup>3</sup>-hybridised carbon atoms. If the same ring carbon atom was also present at less than two bonds from any other sp<sup>3</sup>-hybridised carbon atoms, then it was excluded while calculating fsp3CringC2B. Its positive coefficient in model-A and also a correlation of 0.30 with pIC<sub>50</sub> indicate that increasing such a combination of ring and sp<sup>3</sup>-hybridised carbon atoms could lead to better inhibitory activities for BRD-4. For example, a comparison of molecule 736 with 737 indicates the significant influence of ring carbon atoms (shown using green dots in Figure 4a,b) at exactly two bonds from sp<sup>3</sup>-hybridised carbon atoms. This is further supported by their reported

X-ray resolved structures with BRD-4. Molecule 736 (pdb: 5z1s [47]) has an additional water-mediated interaction with receptors with a distance of 3.37 Å (see Figure 4c) due to the  $-OCH_3$  group present in the benzoxazinone ring. The same  $-OCH_3$  group is responsible for increasing the value of  $fsp3CringC2B$  for 736, but it is absent in 737 (pdb: 5z1r [47]). The difference in  $IC_{50}$  for the following pairs of molecules further support the influence of  $fsp3CringC2B$  on the activity profile: 255 with 499, 725 with 716, 231 with 240, and 89 with 105, to mention a few.

From this discussion, it appears that ring carbon atoms alone are important. However, replacing  $fsp3CringC2B$  by number of ring carbon atoms as a descriptor in model-A reduced the statistical performance from  $R^2_{tr} = 0.76$  to 0.73. In addition, the number of ring carbon atoms has a correlation of 0.27 with  $pIC_{50}$ . Therefore,  $fsp3CringC2B$  is a better descriptor than the number of ring carbon atoms.

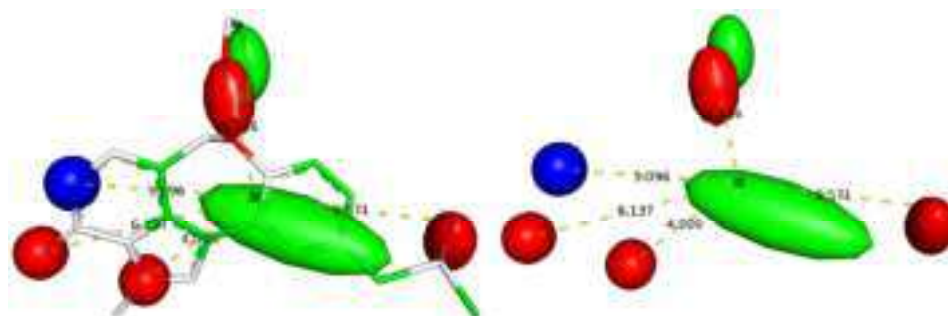


**Figure 4.** Comparison of BRD-4 inhibitory activity of molecule 736 with 737 with respect to  $fsp3CringC2B$ : (a,b) 2D representation of 736 and 737; (c,d) X-ray-resolved structures of 737 (pdb: 5z1r) and 736 (pdb: 5z1s). Cyan coloured spheres represent water molecules, and dashed lines signify interactions and distances in Å.

$com\_C\_4A$ , which stands for total number of carbon atoms within 4 Å from centre of mass (com) of molecule, has a positive coefficient in model-A. Therefore, increasing the value of  $com\_C\_4A$  leads to better inhibitory activities. This observation is supported

by the fact that it has a correlation of 0.404 with  $\text{pIC}_{50}$ , and molecules with  $\text{IC}_{50} < 10$  nM (29 molecules) possess a high value of  $\text{com\_C\_4A}$ . In addition, a simple comparison of the following pairs of the molecules strengthens this observation: 620 with 621, 720 with 710, 724 with 717, 526 with 518, and 691 with 692, and 595 with 596. At first glance, it looks as if  $\text{com\_C\_4A}$  is pointing out the importance of the number of carbon atoms. However,  $\text{nC}$  (number of carbon atoms) has a correlation of 0.29 with  $\text{pIC}_{50}$  and substituting  $\text{com\_C\_4A}$  by  $\text{nC}$  led to a decrease in statistical performance of model-A from  $R^2_{\text{tr}} = 0.76$  to 0.69. Therefore,  $\text{com\_C\_4A}$  is a better choice as a variable for model-A.

As the presence of carbon is generally associated with the increased lipophilicity of a molecule, therefore,  $\text{com\_C\_4A}$  indicates that the lipophilic part must be concentrated near the com of the molecule for better activities. This in turn provides a crucial hint about the active site of BRD-4. It appears that a significant portion of the active site of BRD-4 is reasonably lipophilic in nature. This is supported by the fact that the active site of BRD-4 consists of a hydrophobic WPF shelf (see Figure 1) [11,18]. Thus, the findings of the present QSAR analysis are supported by the reported X-ray-resolved structure of BRD-4 enzyme. In addition, the pharmacophore model, depicted in Figure 5, generated using most active molecule 297, again points out the presence of a lipophilic region near the com of the molecule.



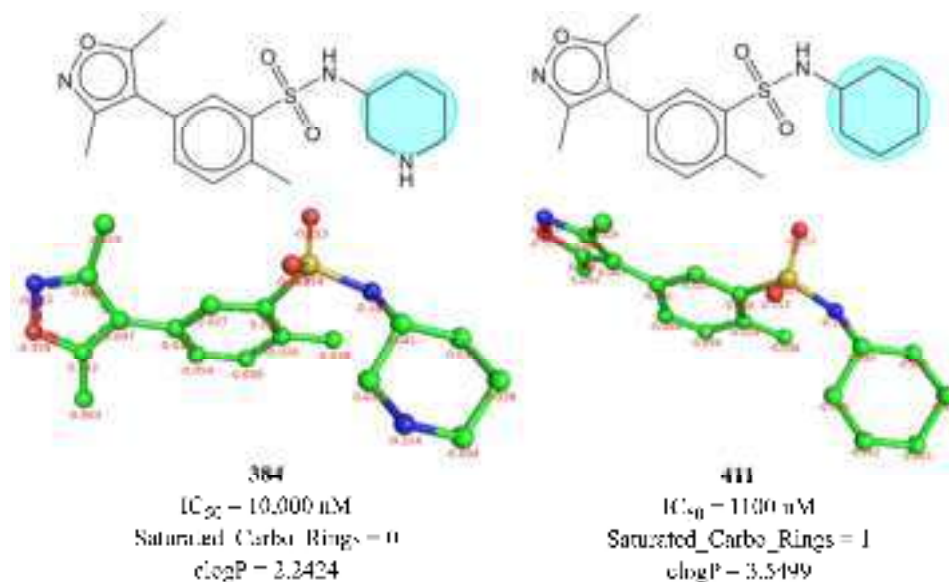
**Figure 5.** Pharmacophore model using most active molecule 207 (red: H-bond acceptor; blue: H-bond donor; green: hydrophobic region). Distances are shown using yellow dashed lines and figures indicate the distances in Å for different regions from center of mass. The black sphere represents the position of the center of mass of molecule.

Another descriptor that also point outs the importance of lipophilicity of a molecule is  $\text{flipoacc3B}$ , which represents the frequency of occurrence of H-bond acceptor atoms exactly at three bonds from lipophilic atoms. However, an acceptor atom was excluded while calculating  $\text{flipoacc3B}$  if it is also present within two or less bonds from same or any other lipophilic atom. Evidently, the lipophilic part of a molecule close to H-bond acceptor moiety (O or N atoms) plays a crucial role in deciding the inhibitory effect for BRD-4. This is once again visible in the pharmacophore model depicted in Figure 6. A simple comparison of the following pairs of molecules supports this observation: 812 with 823, 7 with 8, and 4 with 10.

An easily interpretable and influential molecular descriptor is  $\text{Saturated\_Carbo\_Rings}$ , which corresponds to total number of saturated carbocyclic rings. It has positive coefficient in model-A; therefore, increasing such rings is beneficial. A comparison of  $\text{IC}_{50}$  for 411 with 384 (see Figure 6), 137 with 127, 73 with 67, 131 with 124, 60 with 61, 570 with 573, and 572, 230 with 247 is in favour of this observation.

The importance of  $\text{Saturated\_Carbo\_Rings}$  in model-A indicates that the lipophilicity and flexibility of a molecule are the actual factors governing an activity profile. It is noteworthy that  $\text{clogP}$ , which represents molecular lipophilicity, has a correlation of 0.193 with  $\text{pIC}_{50}$ , whereas  $\text{Saturated\_Carbo\_Rings}$  has 0.240. Thus,  $\text{Saturated\_Carbo\_Rings}$  is a better choice, as it pinpoints the specific feature or part of the molecule (saturated carbocyclic rings), which is correlated with the activity due to its lipophilic nature, whereas  $\text{clogP}$  is a molecular property. A plausible reason could be the crucial role played by hydrophobic zones such as saturated carbocyclic rings at the periphery or outer part of

molecule as a proxy for BRD4 selectivity through their interaction with the WPF shelf [6]. Therefore, saturated carbocyclic rings should be retained in future optimizations for better activity profiles. Thus, the present work is successful in identifying the significance of saturated carbocyclic rings as a novel unreported pharmacophore feature associated with BRD-4 inhibitory activity.

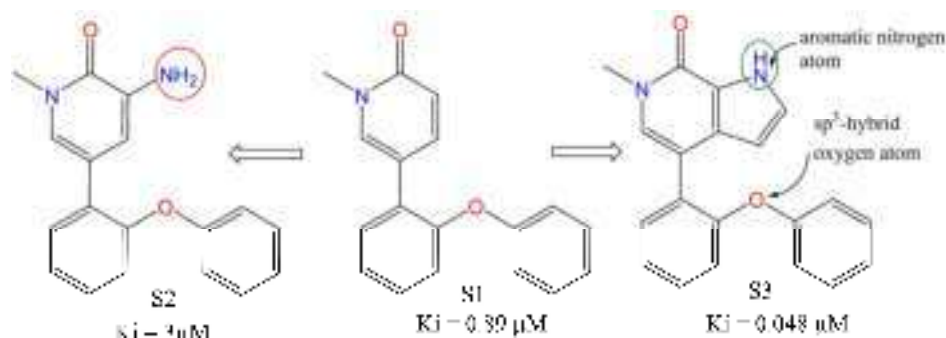


**Figure 6.** Depiction of influence of Saturated\_Carbo\_Rings on  $IC_{50}$  using molecule 384 and 411 as representative examples (2D and 3D representations with partial charges).

The molecular descriptor *fsulfonSaroC8B* (frequency of occurrence of aromatic carbon atoms exactly at eight bonds from sulphur atoms of Sulfone ( $-SO_2-$ ) group) has a positive coefficient in model-A. Consequently, increasing the value of *fsulfonSaroC8B*, favours binding with BRD-4. It is to be noted that if the same aromatic carbon atom is also present at  $\leq 7$  bonds from a sulphur atom of same or different Sulfone group through any path, then it was excluded while calculating *fsulfonSaroC8B*. Obviously, this descriptor signifies the importance of the Sulfone group (a highly polar group) and its correlation with aromatic rings (a lipophilic moiety) in deciding the binding with BRD-4. This is clearly reflected in the difference in the activity of the following pairs of molecules: 715 with 718, 723 with 724, 714 with 715, 707 with 716, 936 with 941, and 942 with 943. Recent studies indicate that Sulfone moiety is present in a cleft near the ZA-loop and establishes an H-bond with the  $-CONH-$  (amide) of backbone [19].

*fsp3OaroN6B* stands for the frequency of occurrence of aromatic nitrogen atoms exactly at six bonds from  $sp^3$ -hybridised oxygen atom. If the same aromatic nitrogen atom is also present at  $\leq 5$  bonds from the same or any other  $sp^3$ -hybridised oxygen atom through any path, then it was excluded while calculating *fsp3OaroN6B*. For example, 79 with 609, 81 with 620, and 614 with 615, to mention a few. In our previous study [20], we identified a similar descriptor *notringO\_acc\_6B* (total number of all non-ring Oxygen atoms present within a distance of six bonds from H-bond acceptor atoms) as an important pharmacophoric feature that governs the binding affinity ( $K_i$ ) of a molecule for BRD-4. Thus, a consensus between the previous and the present study indicates that a molecule must have an H-bond acceptor (preferably aromatic nitrogen) at a distance of six bonds from a  $sp^3$ -hybridised oxygen atom (non-ring oxygen favoured). This observation is supported by the difference in the activity of molecule S1, S2, and S3 [48] (see Figure 7). To add further, the  $sp^3$ -hybridised oxygen atom is present as a linker between two aromatic rings or as an  $-OR$  (alkoxy) group in a good number of molecules [20].





**Figure 7.** Effect of fsp3OaroN6B on BRD-4 inhibitory activity.

The only descriptor with a negative coefficient in model-A is fplaNN4B, which corresponds to frequency of occurrence of nitrogen atoms exactly at 4 bonds from planer nitrogen atoms. If the same nitrogen atom is also present at  $\leq 3$  bonds from the same or any other planer nitrogen atom through any path, then it was excluded while calculating fplaNN4B. The following pairs of molecules have a significant difference in their activities, which could be attributed to the presence of fplaNN4B as a structural feature: 945 with 954, 936 with 944, 411 with 385, 170 with 171, 722 with 714, 563 with 577, 737 with 734, 239 with 240. Therefore, such a combination of nitrogen atoms should be avoided to have better inhibition of BRD-4.

#### 4. Materials and Methods

The present work follows the standard procedure recommended by OECD and different researchers to perform QSAR analysis [49–51]. All the software were used with default settings to obtain a QSAR model possessing a balance of predictive ability and mechanistic interpretation; however, some settings were changed, which have been reported at appropriate places. The different steps are as follows.

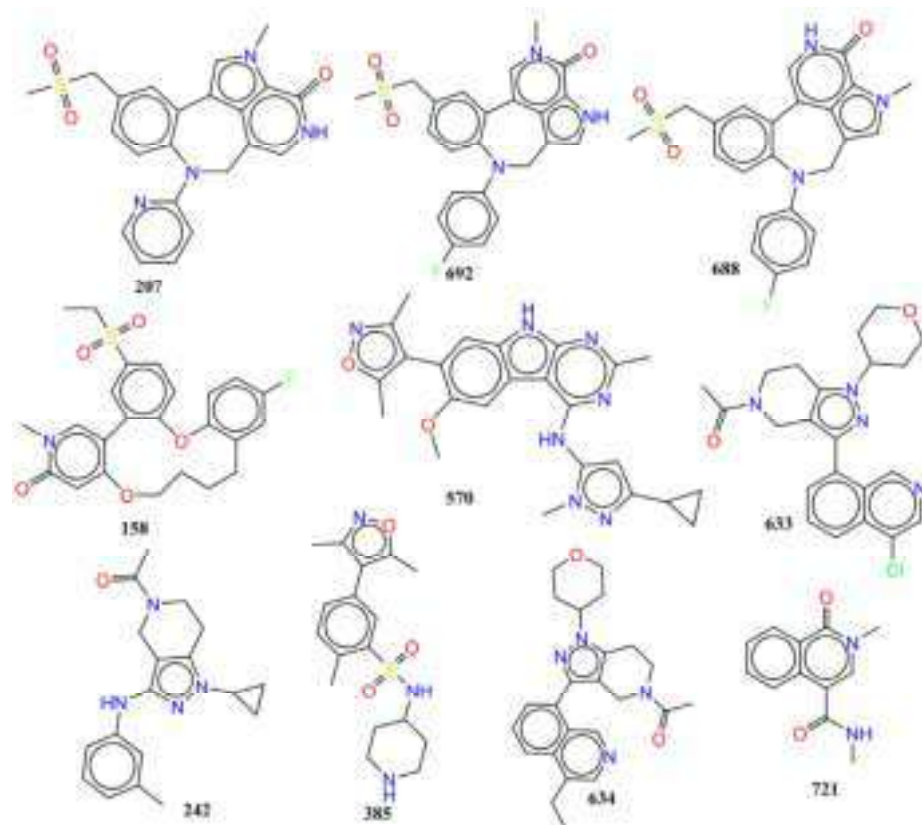
**Step-1:** Collection of data and curation: The present work commenced with the collection of a large dataset of 2026 experimentally tested BRD-4 inhibitors from a free and publicly available database BindingDB (<https://www.bindingdb.org/bind/index.jsp>, accessed on 16 March 2022). A QSAR analysis is significantly influenced by the quality of data, its composition, and its appropriate curation before further processing [50,52–54]. Therefore, in the next step, data curation was performed [55], which involved the removal of duplicate entries, organometallic compounds, salts, molecules with ambiguous IC<sub>50</sub> values, etc. This reduced the dataset to 980 molecules only. The reduced dataset still consists of molecules with experimental IC<sub>50</sub> (nM) in the range 1 nM to 15 μM and the presence of diverse scaffolds such as heterocyclic rings, positional isomers, stereoisomers, etc., enhancing the chemical space and consequently widening the applicability of the newly developed model. The SMILES (Simplified Molecular Input Line Entry System) notations, including experimental IC<sub>50</sub> and pIC<sub>50</sub> ( $= -\log_{10}IC_{50}$ ) of all the molecules used in the present work, are available in Supplementary Materials. For the sake of convenience, representative examples have been presented in Figure 8 to depict the structural diversity of the current dataset.

In Table 2, five most and least active molecules have been included as examples only along with their SMILES notation: IC<sub>50</sub> (nM) and pIC<sub>50</sub> (M).

**Step-2:** In the next step, SMILES notations were used to develop the optimised 3D structures (semi-empirical PM3 method) of the molecules, accomplished using OpenBabel 2.4 [56] and MOPAC 2012 (openmopac.net) using default settings.

**Step-3:** A QSAR model achieves a balance of mechanistic interpretation and predictive ability if a good number of diverse molecular descriptors are calculated, followed by adequate pruning to reduce the chances of overfitting from noisy redundant descriptors [57]. The next step involved the calculation of myriad number of 1D- to 3D-molecular descriptors for all molecules. For this, *PyDescriptor* [45] and *DataWarrior* [46] were used, which

generated more than 40,000 molecular descriptors for a single molecule. Obviously, the descriptor pool contained a good number of redundant molecular descriptors; therefore, highly correlated ( $|R| > 0.95$ ) and nearly constant (>98%) variables were removed using QSARINS 2.2.4 [58]. This considerably decreased the size of set of molecular descriptor pool from 30,000 to 4326, which still contained a variety of molecular descriptors.



**Figure 8.** Representative examples to indicate the structural scaffold diversity in the present dataset.

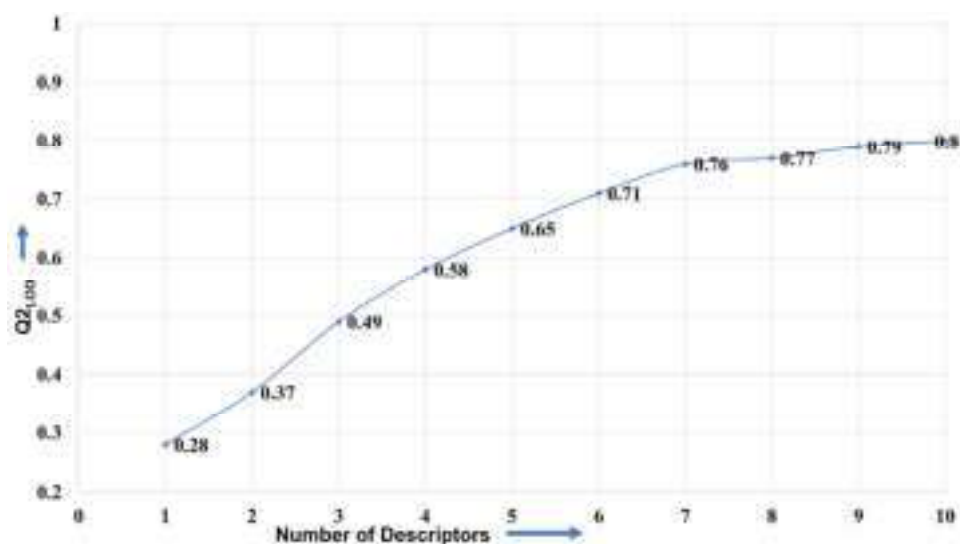
**Table 2.** SMILES notation and  $IC_{50}$  (nM) and  $pIC_{50}$  (M) of five most and least active molecules of the selected data set.

SN	Ligand SMILES	$IC_{50}$ (nM)	$pIC_{50}$ (M)
207	<chem>Cn1cc2-c3cc(CS(C)(=O)=O)ccc3N(Cc3c[nH]c(=O)c1c23)c1cccn1</chem>	1	9
692	<chem>Cn1cc2-c3cc(CS(C)(=O)=O)ccc3N(Cc3c[nH]c(=O)c1c23)c1cc(F)cc1</chem>	1.5	8.824
158	<chem>CCS(=O)(=O)c1ccc2Oc3ccc(F)cc3CCCCOc3cc(=O)n(C)cc3-c2c1</chem>	2	8.699
570	<chem>COc1cc2c(cc1-c1c(C)noc1C)[nH]c1nc(C)nc(Nc3cc(nn3C)C3CC3)c21</chem>	2	8.699
688	<chem>Cn1cc2CN(c3ccc(F)cc3)c3ccc(CS(C)(=O)=O)cc3-c3c[nH]c(=O)c1c23</chem>	2.5	8.602
633	<chem>CC(=O)N1CCc2c(C1)c(nn2C1CCOCC1)-c1cccc2c(Cl)cncc12</chem>	14,000	4.854
242	<chem>CC(=O)N1CCc2c(C1)c(Nc1cccc(C)c1)nn2C1CC1</chem>	15,000	4.824
385	<chem>Cc1noc(C)c1-c1ccc(C)c(c1)S(=O)(=O)NC1CCNCC1</chem>	15,000	4.824
634	<chem>CCc1cncc2c(cccc12)-c1nn(C2CCOCC2)c2CCN(Cc12)C(C)=O</chem>	15,000	4.824
721	<chem>CNC(=O)c1cn(C)c(=O)c2cccc12</chem>	15,000	4.824

#### 4.1. Splitting the Data Set into Training and External Sets and Subjective Feature Selection (SFS)

For developing a useful QSAR model and its appropriate validation, it is essential to divide the dataset into training and external (also called as prediction or test set) sets [50,52–54,59]. Consequently, in the present work, the dataset was randomly divided into training (80% = 785 molecules) and external (20% = 195 molecules) sets to minimise any bias. The only purpose of the training set was to choose suitable number of variables

(molecular descriptors), whereas the external set was employed only for validation purpose, i.e., external validation of the model (Predictive QSAR). Genetic Algorithm (GA) and multi-linear regression (MLR) available in QSARINS 2.2.4 were used for model building. For this,  $Q^2_{LOO}$  was used as a fitness function, and the number of generations was set to 10,000. A decisive step in QSAR modelling is to select the optimum number of molecular descriptors for model building to avoid over-fitting and to obtain acceptable interpretability. Consequently, the heuristic search involved building multiple models from univariate to multivariate with the successive addition of molecular descriptors until there was an increase in the value of  $Q^2_{LOO}$ , which is called the breaking point [39,60]. A 2D graph between the number of molecular descriptors involved in the models and  $Q^2_{LOO}$  values has been depicted in Figure 9. The number of variables matching with the breaking point was considered optimal for model building as there was no improvement in the statistical performance of model upon the inclusion of additional molecular descriptors. The analysis led to the matching of breaking points with seven variables. Therefore, QSAR models with more than seven descriptors were excluded.



**Figure 9.** Graph between number of descriptors against leave-one-out coefficient of determination  $Q^2_{LOO}$  to identify the optimum number of descriptors.

#### 4.2. Building Regression Model and Its Validation

Appropriate validations involving cross/inter validation, external validation, Y-randomization analysis, and applicability domain (Williams plot) are necessary to estimate the reliability and general applicability of a QSAR model [25,31,33,50,61]. A properly validated QSAR model finds its usage for QSAR-based virtual screening, lead/hit optimization, decision making, etc. The following validation parameters and their recommended threshold values are usually used to assess a model [39,60]:  $R^2_{tr}$  (coefficient of determination)  $\geq 0.6$ ;  $Q^2_{100}$  (cross-validated coefficient of determination for leave-one-out)  $\geq 0.5$ ;  $Q^2_{LMO}$  (cross-validated coefficient of determination for leave-many-out)  $\geq 0.6$ ;  $R^2 > Q^2$ ;  $R^2_{ex}$  (external coefficient of determination)  $\geq 0.6$ ; CCC (Concordance Correlation Coefficient)  $\geq 0.80$ ;  $Q^2-F^n \geq 0.60$ ; high values of external validation parameters  $R^2_{ex}$ ,  $Q^2_{F1}$ ,  $Q^2_{F2}$ , and  $Q^2_{F3}$ , with low values of  $R^2_{Yscr}$  (coefficient of determination for Y-randomization); RMSE (Root mean square error); MAE (Mean absolute error);  $RMSE_{tr} < RMSE_{cv}$ . The formulae for calculating these statistical parameters are available in Supplementary Materials. In the present analysis, a Williams plot was used to assess the applicability domain of the newly developed QSAR model.

#### 4.3. Pharmacophore Model

For pharmacophore modelling, the 3D-optimised structure of the most active molecule, 207, was selected. The model was generated using LIQUID [62,63], a free and easy to use PyMOL plugin, using default settings, except that the contour region was set to 3 for H-bond donor/acceptor and hydrophobic regions.

#### 4.4. Other Experimental Details

The reported X-ray resolved structures (pdb 5z1r and 5z1s) were downloaded from Protein Data Bank ([www.rcsb.org](http://www.rcsb.org) accessed on 13 April 2022). PyMOL version 2.4 has been used for the depiction of molecular interactions between the compounds and the protein.

### 5. Conclusions

In the present study, a seven-descriptor-based and rigorously validated GA-MLR QSAR model with  $R^2_{tr} = 0.79$ ,  $Q^2_{LMO} = 0.79$ , and  $R^2_{ex} = 0.78$  was derived to identify the significant pharmacophoric features that influence BRD-4 inhibitory activity. As mentioned earlier, it is essential to perceive salient and visually unrecognizable pharmacophoric features linked with BRD-4 inhibitory activity for different chemical scaffolds. The analysis indicates that the presence of ring carbon and nitrogen atoms, occurrence of carbon atoms near the center of mass of a molecule, specific combination of planer nitrogen with ring carbon, donor and acceptor atoms, etc., are prominent features to be retained in future optimizations. On the other hand, a combination of nitrogen atoms with planer nitrogen atoms exactly at four bonds should be avoided for better BRD-4 inhibitory activity. The reported crystal structures of BRD-4 inhibitors strengthen these observations. The present study efficaciously captured and reported novel pharmacophoric features and has a good balance of predictive ability and mechanistic interpretations.

**Supplementary Materials:** The following supporting information can be downloaded at: <https://www.mdpi.com/article/10.3390/ph15060745/s1>.

**Author Contributions:** Conceptualization, V.H.M., M.E.A.Z. and A.S.; formal analysis and data curation: V.H.M., R.D.J. and S.A.A.-H.; writing, M.E.A.Z., V.H.M. and A.A.A.-M.; revisions, M.E.A.Z., V.H.M. and A.S.; editing and proofreading, V.H.M., M.E.A.Z., R.D.J. and A.A.A.-M.; funding and resources, S.A.A.-H. and M.E.A.Z. All authors have read and agreed to the published version of the manuscript.

**Funding:** The authors acknowledge the Deanship of Scientific Research at Imam Mohammad Ibn Saud Islamic University, Riyadh, Saudi Arabia, for its support of this research through research group number RG-21-09-77.

**Institutional Review Board Statement:** Not applicable.

**Informed Consent Statement:** Not applicable.

**Data Availability Statement:** Data is contained within the article and Supplementary Material.

**Acknowledgments:** V. H. Masand is thankful to Paola Gramatica (Italy) and her team for providing the free copy of QSARINS 2.2.4.

**Conflicts of Interest:** The authors declare no conflict of interest.

#### Abbreviations

SMILES	Simplified molecular-input line-entry system
GA	Genetic algorithm
MLR	Multiple linear regression
QSAR	Quantitative structure–activity relationship
WHO	World Health Organization
OLS	Ordinary least square
QSARINS	QSAR Insubria
OECD	Organisation for Economic Co-operation and Development

## References

1. Boer, R.A.; Meijers, W.C.; Meer, P.; Veldhuisen, D.J. Cancer and heart disease: Associations and relations. *Eur. J. Heart Fail.* **2019**, *21*, 1515–1525. [[CrossRef](#)] [[PubMed](#)]
2. Fidanze, S.D.; Liu, D.; Mantei, R.A.; Hasvold, L.A.; Pratt, J.K.; Sheppard, G.S.; Wang, L.; Holms, J.H.; Dai, Y.; Aguirre, A.; et al. Discovery and optimization of novel constrained pyrrolopyridone BET family inhibitors. *Bioorg. Med. Chem. Lett.* **2018**, *28*, 1804–1810. [[CrossRef](#)] [[PubMed](#)]
3. Guest, E.E.; Pickett, S.D.; Hirst, J.D. Structural variation of protein–ligand complexes of the first bromodomain of BRD4. *Org. Biomol. Chem.* **2021**, *19*, 5632–5641. [[CrossRef](#)] [[PubMed](#)]
4. Liu, Z.; Chen, H.; Wang, P.; Li, Y.; Wold, E.A.; Leonard, P.G.; Joseph, S.; Brasier, A.R.; Tian, B.; Zhou, J. Discovery of Orally Bioavailable Chromone Derivatives as Potent and Selective BRD4 Inhibitors: Scaffold Hopping, Optimization, and Pharmacological Evaluation. *J. Med. Chem.* **2020**, *63*, 5242–5256. [[CrossRef](#)] [[PubMed](#)]
5. Alqahtani, A.; Choucair, K.; Ashraf, M.; Hammouda, D.M.; Alloghbi, A.; Khan, T.; Senzer, N.; Nemunaitis, J. Bromodomain and extra-terminal motif inhibitors: A review of preclinical and clinical advances in cancer therapy. *Future Sci. OA* **2019**, *5*, FSO372. [[CrossRef](#)] [[PubMed](#)]
6. Speck-Planche, A.; Scotti, M.T. BET bromodomain inhibitors: Fragment-based in silico design using multi-target QSAR models. *Mol. Divers* **2018**, *23*, 555–572. [[CrossRef](#)] [[PubMed](#)]
7. Duan, Y.; Guan, Y.; Qin, W.; Zhai, X.; Yu, B.; Liu, H. Targeting Brd4 for cancer therapy: Inhibitors and degraders. *MedChemComm* **2018**, *9*, 1779–1802. [[CrossRef](#)]
8. Zhao, Y.; Bai, L.; Liu, L.; McEachern, D.; Stuckey, J.A.; Meagher, J.L.; Yang, C.-Y.; Ran, X.; Zhou, B.; Hu, Y.; et al. Structure-Based Discovery of 4-(6-Methoxy-2-methyl-4-(quinolin-4-yl)-9H-pyrimido[4,5-b]indol-7-yl)-3,5-dimethylisoxazole (CD161) as a Potent and Orally Bioavailable BET Bromodomain Inhibitor. *J. Med. Chem.* **2017**, *60*, 3887–3901. [[CrossRef](#)]
9. Xing, J.; Lu, W.; Liu, R.; Wang, Y.; Xie, Y.; Zhang, H.; Shi, Z.; Jiang, H.; Liu, Y.-C.; Chen, K.; et al. Machine-Learning-Assisted Approach for Discovering Novel Inhibitors Targeting Bromodomain-Containing Protein 4. *J. Chem. Inf. Model.* **2017**, *57*, 1677–1690. [[CrossRef](#)]
10. Kuang, M.; Zhou, J.; Wang, L.; Liu, Z.; Guo, J.; Wu, R. Binding Kinetics versus Affinities in BRD4 Inhibition. *J. Chem. Inf. Model.* **2015**, *55*, 1926–1935. [[CrossRef](#)]
11. Ember, S.W.J.; Zhu, J.-Y.; Olesen, S.H.; Martin, M.P.; Becker, A.; Berndt, N.; Georg, G.I.; Schönbrunn, E. Acetyl-lysine Binding Site of Bromodomain-Containing Protein 4 (BRD4) Interacts with Diverse Kinase Inhibitors. *ACS Chem. Biol.* **2014**, *9*, 1160–1171. [[CrossRef](#)] [[PubMed](#)]
12. Shorstova, T.; Foulkes, W.D.; Witcher, M. Achieving clinical success with BET inhibitors as anti-cancer agents. *Br. J. Cancer* **2021**, *124*, 1478–1490. [[CrossRef](#)] [[PubMed](#)]
13. Wang, L.; Pratt, J.K.; Soltwedel, T.; Sheppard, G.S.; Fidanze, S.D.; Liu, D.; Hasvold, L.A.; Mantei, R.A.; Holms, J.H.; McClellan, W.J.; et al. Fragment-Based, Structure-Enabled Discovery of Novel Pyridones and Pyridone Macrocycles as Potent Bromodomain and Extra-Terminal Domain (BET) Family Bromodomain Inhibitors. *J. Med. Chem.* **2017**, *60*, 3828–3850. [[CrossRef](#)] [[PubMed](#)]
14. Filippakopoulos, P.; Qi, J.; Picaud, S.; Shen, Y.; Smith, W.B.; Fedorov, O.; Morse, E.M.; Keates, T.; Hickman, T.T.; Felletar, I.; et al. Selective inhibition of BET bromodomains. *Nature* **2010**, *468*, 1067–1073. [[CrossRef](#)] [[PubMed](#)]
15. Liu, Z.; Wang, P.; Chen, H.; Wold, E.A.; Tian, B.; Brasier, A.R.; Zhou, J. Drug Discovery Targeting Bromodomain-Containing Protein 4. *J. Med. Chem.* **2017**, *60*, 4533–4558. [[CrossRef](#)]
16. Filippakopoulos, P.; Picaud, S.; Mangos, M.; Keates, T.; Lambert, J.-P.; Barseyte-Lovejoy, D.; Felletar, I.; Volkmer, R.; Müller, S.; Pawson, T.; et al. Histone Recognition and Large-Scale Structural Analysis of the Human Bromodomain Family. *Cell* **2012**, *149*, 214–231. [[CrossRef](#)]
17. Donati, B.; Lorenzini, E.; Ciarrocchi, A. BRD4 and Cancer: Going beyond transcriptional regulation. *Mol. Cancer* **2018**, *17*, 164. [[CrossRef](#)]
18. Zaware, N.; Zhou, M.-M. Bromodomain biology and drug discovery. *Nat. Struct. Mol. Biol.* **2019**, *26*, 870–879. [[CrossRef](#)]
19. Sheppard, G.S.; Wang, L.; Fidanze, S.D.; Hasvold, L.A.; Liu, D.; Pratt, J.K.; Park, C.H.; Longenecker, K.; Qiu, W.; Torrent, M.; et al. Discovery of N-Ethyl-4-[2-(4-fluoro-2,6-dimethyl-phenoxy)-5-(1-hydroxy-1-methyl-ethyl)phenyl]-6-methyl-7-oxo-1H-pyrrolo[2,3-c]pyridine-2-carboxamide (ABBV-744), a BET Bromodomain Inhibitor with Selectivity for the Second Bromodomain. *J. Med. Chem.* **2020**, *63*, 5585–5623. [[CrossRef](#)]
20. Masand, V.H.; Patil, M.K.; El-Sayed, N.N.E.; Zaki, M.E.A.; Almarhoon, Z.; Al-Hussain, S.A. Balanced QSAR analysis to identify the structural requirements of ABBV-075 (Mivebresib) analogues as bromodomain and extraterminal domain (BET) family bromodomain inhibitor. *J. Mol. Struct.* **2021**, *1229*, 129597. [[CrossRef](#)]
21. Tahir, A.; Alharthy, R.D.; Naseem, S.; Mahmood, N.; Ahmed, M.; Shahzad, K.; Akhtar, M.N.; Hameed, A.; Sadiq, I.; Nawaz, H.; et al. Investigations of Structural Requirements for BRD4 Inhibitors through Ligand- and Structure-Based 3D QSAR Approaches. *Molecules* **2018**, *23*, 1527. [[CrossRef](#)] [[PubMed](#)]
22. Tong, J.-B.; Luo, D.; Feng, Y.; Bian, S.; Zhang, X.; Wang, T.-H. Structural modification of 4, 5-dihydro-[1, 2, 4] triazolo [4, 3-f] pteridine derivatives as BRD4 inhibitors using 2D/3D-QSAR and molecular docking analysis. *Mol. Divers.* **2021**, *25*, 1855–1872. [[CrossRef](#)] [[PubMed](#)]

23. Babatunde Samuel Obadawo, O.E.O. Mayowa Monday Anifowose, Kehinde Henry Fagbohunge, Justinah Solayide Amoko, QSAR modeling of novel substituted 4-Phenylisoquinolinones as potent BET bromodomain (BRD4-BD1) inhibitors. *Biomed. Lett.* **2019**, *5*, 69–78.
24. Zaki, M.E.A.; Al-Hussain, S.A.; Masand, V.H.; Akasapu, S.; Lewaa, I. QSAR and Pharmacophore Modeling of Nitrogen Heterocycles as Potent Human N-Myristoyltransferase (Hs-NMT) Inhibitors. *Molecules* **2021**, *26*, 1834. [[CrossRef](#)]
25. Gramatica, P. Principles of QSAR Modeling. *Int. J. Quant. Struct. Prop. Relatsh.* **2020**, *5*, 61–97. [[CrossRef](#)]
26. Polishchuk, P. Interpretation of Quantitative Structure–Activity Relationship Models: Past, Present, and Future. *J. Chem. Inf. Model.* **2017**, *57*, 2618–2639. [[CrossRef](#)]
27. Fujita, T.; Winkler, D.A. Understanding the Roles of the “Two QSARs”. *J. Chem. Inf. Model.* **2016**, *56*, 269–274. [[CrossRef](#)]
28. Krstajic, D.; Buturovic, L.J.; Leahy, D.E.; Thomas, S. Cross-validation pitfalls when selecting and assessing regression and classification models. *J. Cheminform.* **2014**, *6*, 10. [[CrossRef](#)]
29. Gramatica, P. External Evaluation of QSAR Models, in Addition to Cross-Validation Verification of Predictive Capability on Totally New Chemicals. *Mol. Inf.* **2014**, *33*, 311–314. [[CrossRef](#)]
30. Gütlein, M.; Helma, C.; Karwath, A.; Kramer, S. A Large-Scale Empirical Evaluation of Cross-Validation and External Test Set Validation in (Q)SAR. *Mol. Inf.* **2013**, *32*, 516–528. [[CrossRef](#)]
31. Gramatica, P. On the development and validation of QSAR models. *Methods Mol. Biol.* **2013**, *930*, 499–526. [[CrossRef](#)] [[PubMed](#)]
32. Chirico, N.; Gramatica, P. Real external predictivity of QSAR models. Part 2. New intercomparable thresholds for different validation criteria and the need for scatter plot inspection. *J. Chem. Inf. Model.* **2012**, *52*, 2044–2058. [[CrossRef](#)] [[PubMed](#)]
33. Chirico, N.; Gramatica, P. Real external predictivity of QSAR models: How to evaluate it? Comparison of different validation criteria and proposal of using the concordance correlation coefficient. *J. Chem. Inf. Model.* **2011**, *51*, 2320–2335. [[CrossRef](#)] [[PubMed](#)]
34. Consonni, V.; Ballabio, D.; Todeschini, R. Comments on the definition of the Q<sub>2</sub> parameter for QSAR validation. *J. Chem. Inf. Model.* **2009**, *49*, 1669–1678. [[CrossRef](#)]
35. Rao, R.B.; Fung, G.; Rosales, R. *On the Dangers of Cross-Validation. An Experimental Evaluation*; SIAM: Philadelphia, PA, USA, 2008; pp. 588–596. [[CrossRef](#)]
36. Gramatica, P.; Giani, E.; Papa, E. Statistical external validation and consensus modeling: A QSPR case study for Koc prediction. *J. Mol. Graph. Model.* **2007**, *25*, 755–766. [[CrossRef](#)]
37. Hawkins, D.M.; Basak, S.C.; Mills, D. Assessing model fit by cross-validation. *J. Chem. Inf. Comput. Sci.* **2003**, *43*, 579–586. [[CrossRef](#)]
38. Masand, V.H.; Mahajan, D.T.; Nazeruddin, G.M.; Hadda, T.B.; Rastija, V.; Alfeefy, A.M. Effect of information leakage and method of splitting (rational and random) on external predictive ability and behavior of different statistical parameters of QSAR model. *Med. Chem. Res.* **2015**, *24*, 1241–1264. [[CrossRef](#)]
39. Zaki, M.E.A.; Al-Hussain, S.A.; Bukhari, S.N.A.; Masand, V.H.; Rathore, M.M.; Thakur, S.D.; Patil, V.M. Exploring the Prominent and Concealed Inhibitory Features for Cytoplasmic Isoforms of Hsp90 Using QSAR Analysis. *Pharmaceuticals* **2022**, *15*, 303. [[CrossRef](#)]
40. Kar, S.; Roy, K.; Leszczynski, J. Applicability Domain: A Step Toward Confident Predictions and Decidability for QSAR Modeling. In *Computational Toxicology*; Humana Press: New York, NY, USA, 2018; pp. 141–169.
41. Gramatica, P.; Kovarich, S.; Roy, P.P. Reply to the comment of S. Rayne on “QSAR model reproducibility and applicability: A case study of rate constants of hydroxyl radical reaction models applied to polybrominated diphenyl ethers and (benzo-)triazoles”. *J. Comput. Chem.* **2013**, *34*, 1796. [[CrossRef](#)]
42. Roy, P.P.; Kovarich, S.; Gramatica, P. QSAR model reproducibility and applicability: A case study of rate constants of hydroxyl radical reaction models applied to polybrominated diphenyl ethers and (benzo-)triazoles. *J. Comput. Chem.* **2011**, *32*, 2386–2396. [[CrossRef](#)]
43. Gadaleta, D.; Mangiatordi, G.F.; Catto, M.; Carotti, A.; Nicolotti, O. Applicability Domain for QSAR Models. *Int. J. Quant. Struct. Prop. Relatsh.* **2016**, *1*, 45–63. [[CrossRef](#)]
44. Tropsha, A.; Golbraikh, A. Predictive QSAR modeling workflow, model applicability domains, and virtual screening. *Curr. Pharm. Des.* **2007**, *13*, 3494–3504. [[CrossRef](#)] [[PubMed](#)]
45. Masand, V.H.; Rastija, V. PyDescriptor: A new PyMOL plugin for calculating thousands of easily understandable molecular descriptors. *Chemom. Intell. Lab. Syst.* **2017**, *169*, 12–18. [[CrossRef](#)]
46. Sander, T.; Freyss, J.; von Korff, M.; Rufener, C. DataWarrior: An Open-Source Program For Chemistry Aware Data Visualization And Analysis. *J. Chem. Inf. Model.* **2015**, *55*, 460–473. [[CrossRef](#)] [[PubMed](#)]
47. Xiang, Q.; Zhang, Y.; Li, J.; Xue, X.; Wang, C.; Song, M.; Zhang, C.; Wang, R.; Li, C.; Wu, C.; et al. Y08060: A Selective BET Inhibitor for Treatment of Prostate Cancer. *ACS Med. Chem. Lett.* **2018**, *9*, 262–267. [[CrossRef](#)]
48. McDaniel, K.F.; Wang, L.; Soltwedel, T.; Fidanze, S.D.; Hasvold, L.A.; Liu, D.; Mantei, R.A.; Pratt, J.K.; Sheppard, G.S.; Bui, M.H.; et al. Discovery of N-(4-(2,4-Difluorophenoxy)-3-(6-methyl-7-oxo-6,7-dihydro-1H-pyrrolo[2,3-c]pyridin-4-yl)phenyl)ethanesulfonamide (ABBV-075/Mivebresib), a Potent and Orally Available Bromodomain and Extraterminal Domain (BET) Family Bromodomain Inhibitor. *J. Med. Chem.* **2017**, *60*, 8369–8384. [[CrossRef](#)]
49. Dearden, J.C.; Cronin, M.T.; Kaiser, K.L. How not to develop a quantitative structure-activity or structure-property relationship (QSAR/QSPR). *SAR QSAR Environ. Res.* **2009**, *20*, 241–266. [[CrossRef](#)]

50. Cherkasov, A.; Muratov, E.N.; Fourches, D.; Varnek, A.; Baskin, I.I.; Cronin, M.; Dearden, J.; Gramatica, P.; Martin, Y.C.; Todeschini, R.; et al. QSAR modeling: Where have you been? Where are you going to? *J. Med. Chem.* **2014**, *57*, 4977–5010. [[CrossRef](#)]
51. Huang, J.; Fan, X. Why QSAR fails: An empirical evaluation using conventional computational approach. *Mol. Pharm.* **2011**, *8*, 600–608. [[CrossRef](#)]
52. Muratov, E.N.; Bajorath, J.; Sheridan, R.P.; Tetko, I.V.; Filimonov, D.; Poroikov, V.; Oprea, T.I.; Baskin, I.I.; Varnek, A.; Roitberg, A.; et al. QSAR without borders. *Chem. Soc. Rev.* **2020**, *49*, 3525–3564. [[CrossRef](#)]
53. Golbraikh, A.; Muratov, E.; Fourches, D.; Tropsha, A. Data set modelability by QSAR. *J. Chem. Inf. Model.* **2014**, *54*, 1–4. [[CrossRef](#)] [[PubMed](#)]
54. Martin, T.M.; Harten, P.; Young, D.M.; Muratov, E.N.; Golbraikh, A.; Zhu, H.; Tropsha, A. Does rational selection of training and test sets improve the outcome of QSAR modeling? *J. Chem. Inf. Model.* **2012**, *52*, 2570–2578. [[CrossRef](#)] [[PubMed](#)]
55. Fourches, D.; Muratov, E.; Tropsha, A. Trust, but verify: On the importance of chemical structure curation in cheminformatics and QSAR modeling research. *J. Chem. Inf. Model.* **2010**, *50*, 1189–1204. [[CrossRef](#)] [[PubMed](#)]
56. O’Boyle, N.M.; Banck, M.; James, C.A.; Morley, C.; Vandermeersch, T.; Hutchison, G.R. Open Babel: An open chemical toolbox. *J. Cheminform.* **2011**, *3*, 33. [[CrossRef](#)]
57. Tetko, I.V.; Sushko, I.; Pandey, A.K.; Zhu, H.; Tropsha, A.; Papa, E.; Oberg, T.; Todeschini, R.; Fourches, D.; Varnek, A. Critical assessment of QSAR models of environmental toxicity against *Tetrahymena pyriformis*: Focusing on applicability domain and overfitting by variable selection. *J. Chem. Inf. Model.* **2008**, *48*, 1733–1746. [[CrossRef](#)]
58. Gramatica, P.; Chirico, N.; Papa, E.; Cassani, S.; Kovarich, S. QSARINS: A new software for the development, analysis, and validation of QSAR MLR models. *J. Comput. Chem.* **2013**, *34*, 2121–2132. [[CrossRef](#)]
59. Tropsha, A.; Gramatica, P.; Gombar, V.K. The Importance of Being Earnest Validation is the Absolute Essential for Successful Application and Interpretation of QSPR Models. *QSAR Comb. Sci.* **2003**, *22*, 69–77. [[CrossRef](#)]
60. Zaki, M.E.A.; Al-Hussain, S.A.; Masand, V.H.; Sabnani, M.K.; Samad, A. Mechanistic and Predictive QSAR Analysis of Diverse Molecules to Capture Salient and Hidden Pharmacophores for Anti-Thrombotic Activity. *Int. J. Mol. Sci.* **2021**, *22*, 8352. [[CrossRef](#)]
61. Gramatica, P. Principles of QSAR models validation internal and external. *QSAR Comb. Sci.* **2007**, *26*, 694–701. [[CrossRef](#)]
62. Yuan, S.; Chan, H.C.S.; Hu, Z. Using PyMOL as a platform for computational drug design. *WIREs Comput. Mol. Sci.* **2017**, *7*, e1298. [[CrossRef](#)]
63. Tanrikulu, Y.; Nietert, M.; Scheffer, U.; Proschak, E.; Grabowski, K.; Schneider, P.; Weidlich, M.; Karas, M.; Gobel, M.; Schneider, G. Scaffold hopping by “fuzzy” pharmacophores and its application to RNA targets. *Chembiochem* **2007**, *8*, 1932–1936. [[CrossRef](#)] [[PubMed](#)]



## Article

# Perceiving the Concealed and Unreported Pharmacophoric Features of the 5-Hydroxytryptamine Receptor Using Balanced QSAR Analysis

Syed Nasir Abbas Bukhari <sup>1,\*</sup>, Mervat Abdelaziz Elsherif <sup>2</sup>, Kashaf Junaid <sup>3</sup>, Hasan Ejaz <sup>3</sup>, Pravej Alam <sup>4</sup>, Abdul Samad <sup>5</sup>, Rahul D. Jawarkar <sup>6</sup> and Vijay H. Masand <sup>7,\*</sup>

<sup>1</sup> Department of Pharmaceutical Chemistry, College of Pharmacy, Jouf University, Sakaka 72388, Saudi Arabia

<sup>2</sup> Chemistry Department, College of Science, Jouf University, Sakaka 72388, Saudi Arabia; maelsherif@ju.edu.sa

<sup>3</sup> Department of Clinical Laboratory Sciences, College of Applied Medical Sciences, Jouf University, Sakaka 72388, Saudi Arabia; kjunaid@ju.edu.sa (K.J.); hetariq@ju.edu.sa (H.E.)

<sup>4</sup> Department of Biology, College of Science and Humanities, Prince Sattam Bin Abdulaziz University, Al-Kharj 11942, Saudi Arabia; alamprez@gmail.com

<sup>5</sup> Department of Pharmaceutical Chemistry, Faculty of Pharmacy, Tishk International University, Erbil 44001, Iraq; abdul.samad@tiu.edu.iq

<sup>6</sup> Department of Medicinal Chemistry, Dr. Rajendra Gode Institute of Pharmacy, University-Mardi Road, Amravati 444603, Maharashtra, India; rahuljawarkar@gmail.com

<sup>7</sup> Department of Chemistry, Vidya Bharati Mahavidyalaya, Amravati 444602, Maharashtra, India

\* Correspondence: sbukhari@ju.edu.sa (S.N.A.B.); vijaymasand@gmail.com (V.H.M.)



**Citation:** Bukhari, S.N.A.; Elsherif, M.A.; Junaid, K.; Ejaz, H.; Alam, P.; Samad, A.; Jawarkar, R.D.; Masand, V.H. Perceiving the Concealed and Unreported Pharmacophoric Features of the 5-Hydroxytryptamine Receptor Using Balanced QSAR Analysis. *Pharmaceuticals* **2022**, *15*, 834. <https://doi.org/10.3390/ph15070834>

Academic Editors: Dongsheng Cao and Daniela Catarzi

Received: 23 May 2022

Accepted: 25 June 2022

Published: 5 July 2022

**Publisher's Note:** MDPI stays neutral with regard to jurisdictional claims in published maps and institutional affiliations.



**Copyright:** © 2022 by the authors. Licensee MDPI, Basel, Switzerland. This article is an open access article distributed under the terms and conditions of the Creative Commons Attribution (CC BY) license (<https://creativecommons.org/licenses/by/4.0/>).

**Abstract:** The 5-hydroxytryptamine receptor 6 (5-HT<sub>6</sub>) has gained attention as a target for developing therapeutics for Alzheimer's disease, schizophrenia, cognitive dysfunctions, anxiety, and depression, to list a few. In the present analysis, a larger and diverse dataset of 1278 molecules covering a broad chemical and activity space was used to identify visual and concealed structural features associated with binding affinity for 5-HT<sub>6</sub>. For this, quantitative structure–activity relationships (QSAR) and molecular docking analyses were executed. This led to the development of a statistically robust QSAR model with a balance of excellent predictivity ( $R^2_{tr} = 0.78$ ,  $R^2_{ex} = 0.77$ ), the identification of unreported aspects of known features, and also novel mechanistic interpretations. Molecular docking and QSAR provided similar as well as complementary results. The present analysis indicates that the partial charges on ring carbons present within four bonds from a sulfur atom, the occurrence of sp<sup>3</sup>-hybridized carbon atoms bonded with donor atoms, and a conditional occurrence of lipophilic atoms/groups from nitrogen atoms, which are prominent but unreported pharmacophores that should be considered while optimizing a molecule for 5-HT<sub>6</sub>. Thus, the present analysis led to identification of some novel unreported structural features that govern the binding affinity of a molecule. The results could be beneficial in optimizing the molecules for 5-HT<sub>6</sub>.

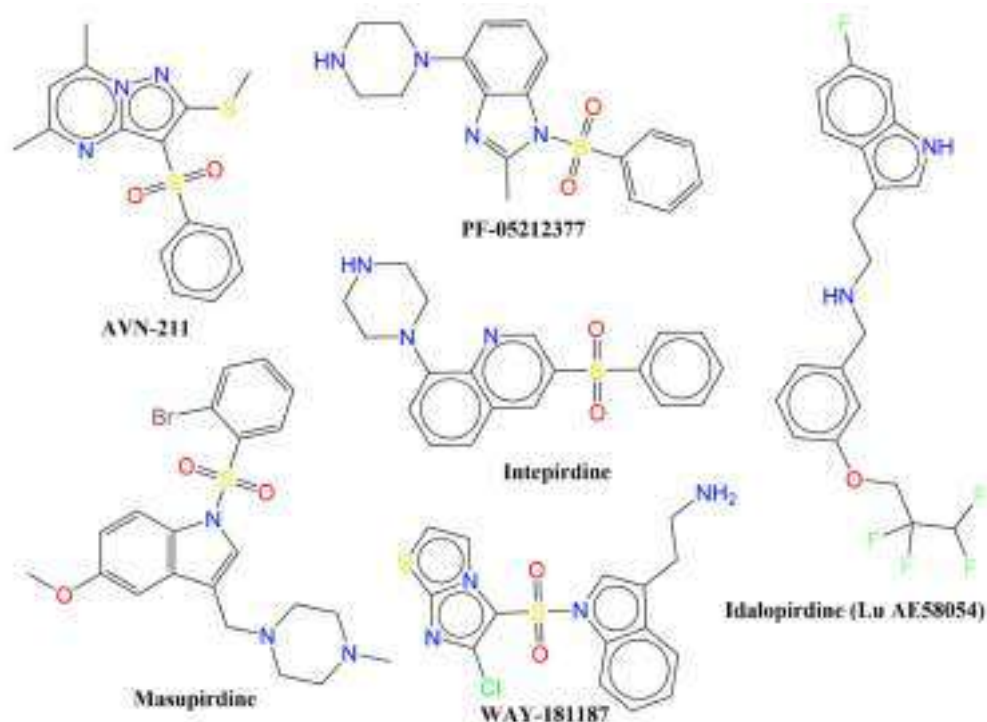
**Keywords:** 5-hydroxytryptamine receptor 6; neurodegeneration; QSAR; molecular docking; pharmacophoric features

## 1. Introduction

Millions of people are suffering from central nervous system (CNS)-related diseases, such as Alzheimer's disease, schizophrenia, cognitive dysfunctions, anxiety, depression, etc. [1–4], and are facing diverse health and social challenges. Though therapeutic agents are available for the treatment of these diseases, they lack the ability to reduce the continuous loss of cognitive function, as most of them target only the acetylcholine deficit [2,3,5–9]. Therefore, there is a need to develop a therapeutic agent with a different mechanism of action and bio-activity profile to support the existing drug space. Recently, G-protein-coupled receptors (GPCRs), viz., the serotonergic system of serotonin (5-hydroxytryptamine) receptors, have received greater attention due to their vital role in signal transduction pathways



and numerous neurological functions [2,4,7–10]. To add further, 5-hydroxytryptamine receptors (5-HT<sub>1–7</sub>) play vital roles in many cognitive dysfunctions such as memory loss, reduced learning ability, etc. [4,5,8,9]. Among them, the 5-HT<sub>6</sub> receptor has emerged as a promising target due to its crucial role in the onset of Alzheimer's disease, cognitive processes, mood control, depression, and anxiety [4,5,8,9], to name a few. It is believed that blocking the 5-HT<sub>6</sub> receptor significantly improves learning and memory processes [4,5,8,9]. In addition, it has also emerged as a molecular target for the treatment of obesity and the related metabolic syndrome [11]. An additional advantage associated with 5-HT<sub>6</sub> is its restricted and exclusive occurrence within the CNS, which implies that compounds acting through this receptor could have minimal peripheral side effects [2,3,6,10,12]. Even though several molecules have been identified as promising ligands with high binding affinities for 5-HT<sub>6</sub> (see Figure 1), none of them has cleared the clinical stages or been approved as a drug [1,7–10,12].



**Figure 1.** Chemical structures of representative examples of clinically tested 5-HT<sub>6</sub> ligands.

Therefore, there is a need to develop a novel therapeutic agent with a better ADMET (absorption, distribution, metabolism, excretion, and toxicity) profile and the retention of a high binding affinity for 5-HT<sub>6</sub>. For this, it is essential to know the prominent and concealed pharmacophoric features associated with binding affinities for 5-HT<sub>6</sub> using a broad, structurally diverse dataset with adequate variations in activity space. To achieve these targets, computer-aided drug designing (CADD) is a contemporary and feasible solution due to its low cost and time efficacy [13,14]. Ligand-based drug designing (LBDD) is a thriving and widely accepted branch of CADD with a higher success rate of identification of key pharmacophoric features. It is the method of choice if the 3D structure of a target protein is not available [14]. Under the terrain of LBDD, the quantitative structure–activity relationship (QSAR) is an effective and multidisciplinary approach that is useful to identify salient and hidden pharmacophoric features [15–18].

Though different types of ligands encompassing diverse scaffolds are known for 5-HT<sub>6</sub>, the lack of an X-ray-resolved 3D structure restricts the use of structure-based drug designing (SBDD) approaches. Consequently, many researchers have performed QSAR analysis for 5-HT<sub>6</sub> using different types of scaffolds. Doddareddy and co-workers [1] accomplished a 3D QSAR analysis using a small dataset of 33 N1-arylsulfonylindole

compounds as 5-HT6 antagonists. The analysis reinforced the pharmacophoric features reported by López-Rodríguez et al. [4,19]. Later in 2011, Hao et al. [3] studied relatively a larger dataset of 223 ligands reported for 5-HT6 for QSAR, homology-based molecular docking, and molecular dynamics simulations for 5 ns. Their analysis pointed out that the interaction with the residue Asp106 is important. A 2D and 3D QSAR analysis of arylsulfonamide-derived 5-HT6 receptor antagonists [12] highlighted the importance of the pharmacophore model reported by López-Rodríguez et al. [4,19]. Though these studies contributed to the identification of some important structural features, the developed QSAR models were either based on smaller datasets or specific scaffolds only, thereby lacking general applicability. In addition, poor external predictive ability restricts their usage for a lead optimization pipeline. A QSAR analysis based on a large and diverse set of molecules, with a balance of predictive ability (predictive QSAR) and mechanistic interpretation (mechanistic QSAR) provides an in-depth understanding of the correlation between the structural features and the desired bio-activity [15,20,21]. Therefore, QSAR analysis has been executed in the present work using a large and diverse dataset that covers a broad chemical and activity space to find out the structural features of high importance for 5-HT6 ligands. Molecular docking has been carried out to support and complement the QSAR analysis. Further, an in-depth analysis of a larger dataset comprising diverse scaffolds led to the identification of reported as well as unreported pharmacophoric features, which could be useful in the optimization of molecules during a drug discovery pipeline.

## 2. Results

In the present work, we have identified reported as well as unreported structural features of 5-HT6 ligands. As stated in the introduction section, the emphasis was on building a genetic algorithm–multilinear regression (GA-MLR) model with a balance of predictive ability and mechanistic interpretations. The newly built six-parametric model is as follows:

$$\text{Model-1: } pK_i = 6.754 (\pm 0.091) - 0.109 (\pm 0.014) * \text{com\_Hhyd\_3A} - 0.700 (\pm 0.043) * \text{ringC\_S\_4Bc} - 0.604 (\pm 0.104) * \text{flipo\&S\_ringN3B} - 0.528 (\pm 0.075) * \text{KRFPc620} - 0.339 (\pm 0.053) * \text{sp3N\_sp2O\_8B} + 0.545 (\pm 0.067) * \text{fsp3Cdon1B}$$

The details of the molecular descriptors present in Model-1 have been tabulated in Table 1 and are discussed in detail in the discussion section. Table 2 contains selected validation parameters associated with Model-1.

**Table 1.** Some details of constituent molecular descriptors present in Model-1.

Molecular Descriptor	Description	Software Used for Calculation	Correlation with pKi
com_Hhyd_3A	Total number of hydrogen atoms with partial charge in the range of $\pm 0.2$ within 3 Å from center of mass of molecule	PyDescriptor	−0.625
ringC_S_4Bc	Sum of partial charges on ring carbon atoms present within four bonds from sulfur atom	PyDescriptor	−0.696
flipo&S_ringN3B	Frequency of occurrence of ring nitrogen atom present exactly at three bonds from lipophilic atom	PyDescriptor	−0.248
sp3N_sp2O_8B	Total number of sp <sup>3</sup> -hybridized nitrogen atoms present within eight bonds from sp <sup>2</sup> -hybridized oxygen atoms	PyDescriptor	−0.133
KRFPc620	Nitrogen attached to three CH <sub>3</sub> CH <sub>2</sub> - groups	PaDEL	−0.444
fsp3Cdon1B	Frequency of occurrence of H-bond donor atom bonded with sp <sup>3</sup> -hybridized carbon atom	PyDescriptor	0.026

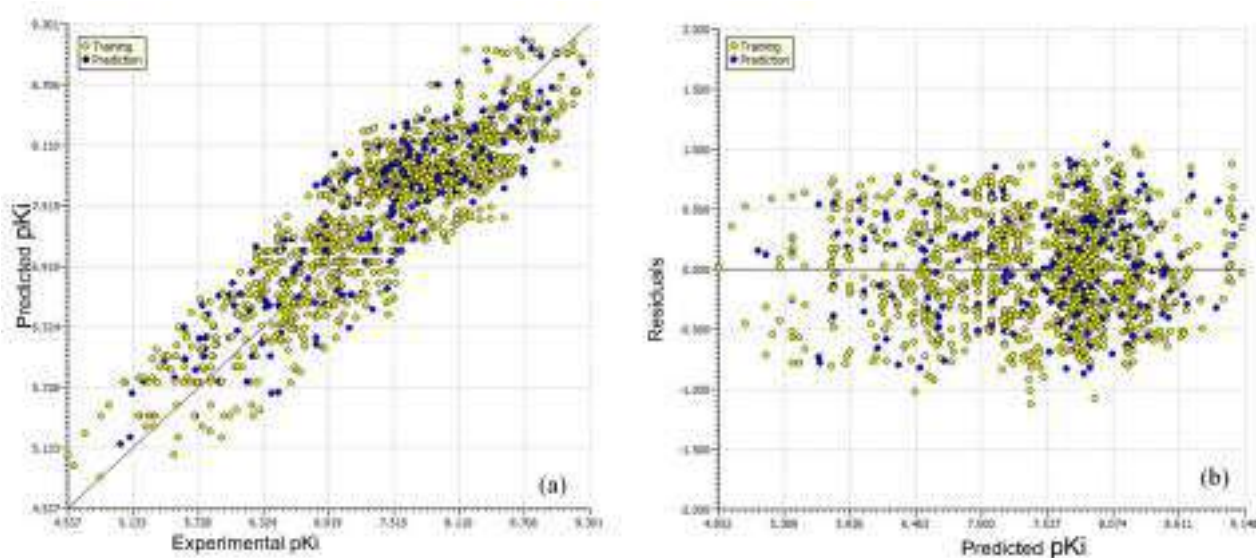
**Table 2.** Selected statistical validation parameters for Model-1.

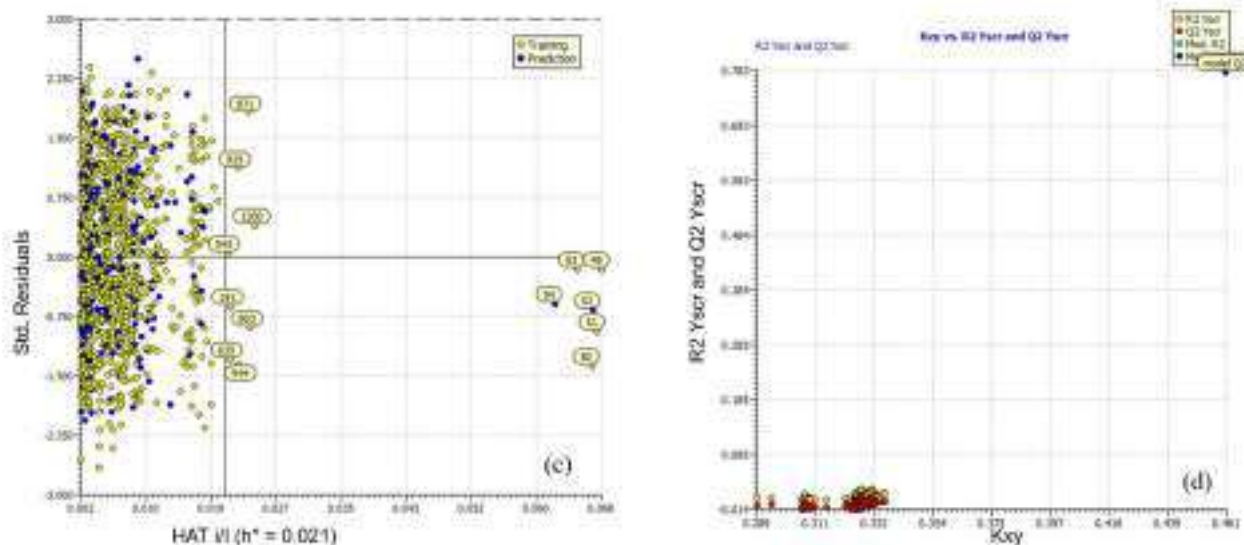
Parameter	Value	Parameter	Value
$R^2_{tr}$	0.783	$Q^2_{LMO}$	0.779
$R^2_{adj.}$	0.781	$R^2_{Yscr}$	0.006
$RMSE_{tr}$	0.419	$RMSE_{ex}$	0.425
$MAE_{tr}$	0.350	$MAE_{ex}$	0.357
$CCC_{tr}$	0.878	$R^2_{ex}$	0.772
$R^2_{cv}$ ( $Q^2_{loo}$ )	0.780	$Q^2-F^1$	0.768
$RMSE_{cv}$	0.422	$Q^2-F^2$	0.768
$MAE_{cv}$	0.352	$Q^2-F^3$	0.777
$CCC_{cv}$	0.876	$CCC_{ex}$	0.871

Note: tr—Training, cv—Cross-validation, ex—External.

It is evident from above statistical parameters that the model is statistically predictive, with high values of different parameters such as  $R^2_{tr}$  (coefficient of determination),  $R^2_{adj.}$  (adjusted coefficient of determination), and  $R^2_{cv}$  ( $Q^2_{LOO}$ ) (cross-validated coefficient of determination for leave-one-out),  $R^2_{ex}$  (external coefficient of determination),  $Q^2-F^n$ , and  $CCC_{ex}$  (concordance correlation coefficient for external set), etc., and low values of LOF (lack-of-fit), RMSE (root-mean-square error), MAE (mean absolute error),  $R^2_{Yscr}$  ( $R^2$  for Y-scrambling), etc. Thus, the model possesses high external predictive ability, is free from chance correlations, and satisfies the recommended threshold values for various validation parameters [16,22–29]. All validation parameters associated with Model-1 and their formulae are available in the Supplementary Materials.

Figure 2 contains the different graphs associated with Model-1, viz., the experimental vs. predicted pKi (Figure 2a), experimental vs. residuals (Figure 2b), and the Y-randomization plot (Figure 2d). We used a Williams plot to judge the applicability domain of the model (see Figure 2c). Thus, it satisfies all the OECD-endorsed guidelines and criteria for creating a useful QSAR model.

**Figure 2.** Cont.



**Figure 2.** Different graphs associated with the Model-1. (a) Experimental vs. predicted pKi (the solid line represents the regression line); (b) experimental vs. residuals; (c) Williams plot for applicability domain (the vertical solid line represents  $h^* = 0.021$  and the horizontal dashed lines represent the upper and lower boundaries of the applicability domain); (d) Y-randomization plot.

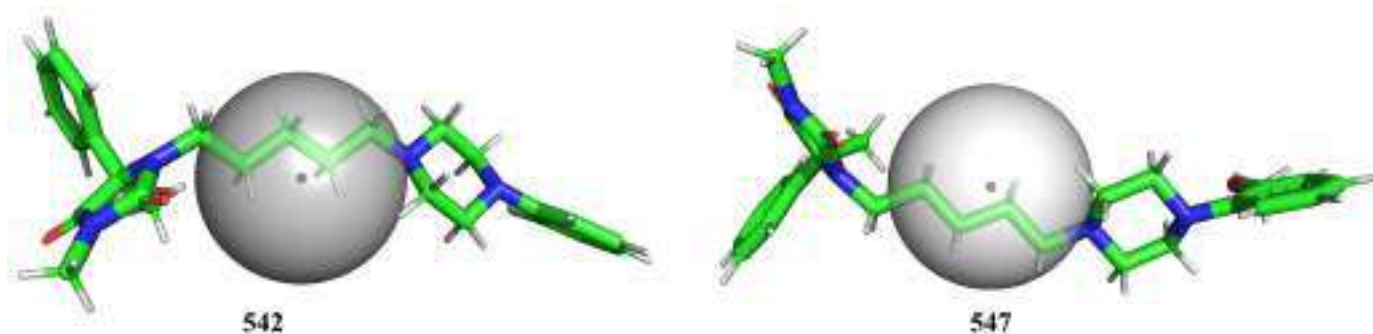
The docking scores for all the molecules are incorporated in the Supplementary Materials (see Excel file ‘SupplementaryMaterial-Final.xls’, available in the Supplementary Materials).

### 3. Discussion

The interpretation of a QSAR model using molecular descriptors, also known as mechanistic interpretation, is a crucial aspect to highlight and link various structural features with significant influence in deciding the bio-activity of molecules [15,21]. It is also one of the requirements suggested by the OECD for developing a thriving QSAR model. In the present work, we used a simple approach in which the pKi values of different molecules were compared using a specific molecular descriptor. Nonetheless, we make clear that the final experimental pKi value of a molecule cannot be governed by just a single structural feature (molecular descriptor). To add further, the extending or reverse effect of other molecular descriptors and unknown factors play crucial roles in deciding the pKi value of a molecule. Therefore, a concomitant consideration of all molecular descriptors and their associated structural features is a better strategy for the effective use of a QSAR model. Model-1 encompasses six molecular descriptors.

The molecular descriptor `com_Hhyd_3A` represents the total number of hydrogen atoms with a partial charge in the range of  $\pm 0.200$  and also present within  $3 \text{ \AA}$  from the center of mass (com) of the molecule. As the partial charge must be within the range  $\pm 0.200$ , this descriptor expresses the role played by non-polar hydrogens [30] when present within  $3 \text{ \AA}$  from the center of mass of the molecule. The descriptor `com_Hhyd_3A` has a negative coefficient in Model-1, which indicates that the lower the value, the better the binding affinity. This could be achieved by replacing non-polar hydrogen atoms with suitable atoms/groups. This indirectly points out that the presence of polar hydrogens, in turn, polar groups nearer to center of mass of a molecule, are beneficial for escalating the pKi value. In addition, hydrogen is smaller than other elements, and replacing it with any other element will increase the steric bulk. Therefore, bulkiness near the center of mass of the molecule is highly favorable for increasing the pKi value. To add further, `com_Hhyd_3A` depends on the location of the center of mass, which changes with the positions of groups/atoms (positional isomers). Therefore, the value of `com_Hhyd_3A` varies for positional isomers, for example, molecules number 331 and 332. Hence, the descriptor effortlessly captures the importance of positional isomerism in deciding the

pKi value. Thus, the descriptor *com\_Hhyd\_3A* and its negative correlation (correlation coefficient  $R = -0.63$ ) with pKi highlighted the crucial role played by the presence of polar groups and steric bulkiness near the center of mass of a molecule as well as the positional isomerism. This observation was further confirmed by comparing following pairs of molecules: 542 ( $K_i = 25520$  nM, *com\_Hhyd\_3A* = 8) with 547 ( $K_i = 2506$  nM, *com\_Hhyd\_3A* = 6) (depicted in Figure 3), 543 ( $K_i = 14650$  nM, *com\_Hhyd\_3A* = 9) with 545 ( $K_i = 8611$  nM, *com\_Hhyd\_3A* = 6), 1011 ( $K_i = 91$  nM, *com\_Hhyd\_3A* = 6) with 1082 ( $K_i = 419$  nM, *com\_Hhyd\_3A* = 7), 935 ( $K_i = 2843$  nM, *com\_Hhyd\_3A* = 8) vs. 937 ( $K_i = 2005$  nM, *com\_Hhyd\_3A* = 6), and 929 ( $K_i = 2427$  nM, *com\_Hhyd\_3A* = 7) vs. 938 ( $K_i = 1540$  nM, *com\_Hhyd\_3A* = 5), to list a few. Thus, for the first time, *com* has been used as a useful approach to explain the differences in the binding affinities of ligands for 5-HT6. In addition, this novel approach provides a novel justification for the differences in the activity of positional isomers.

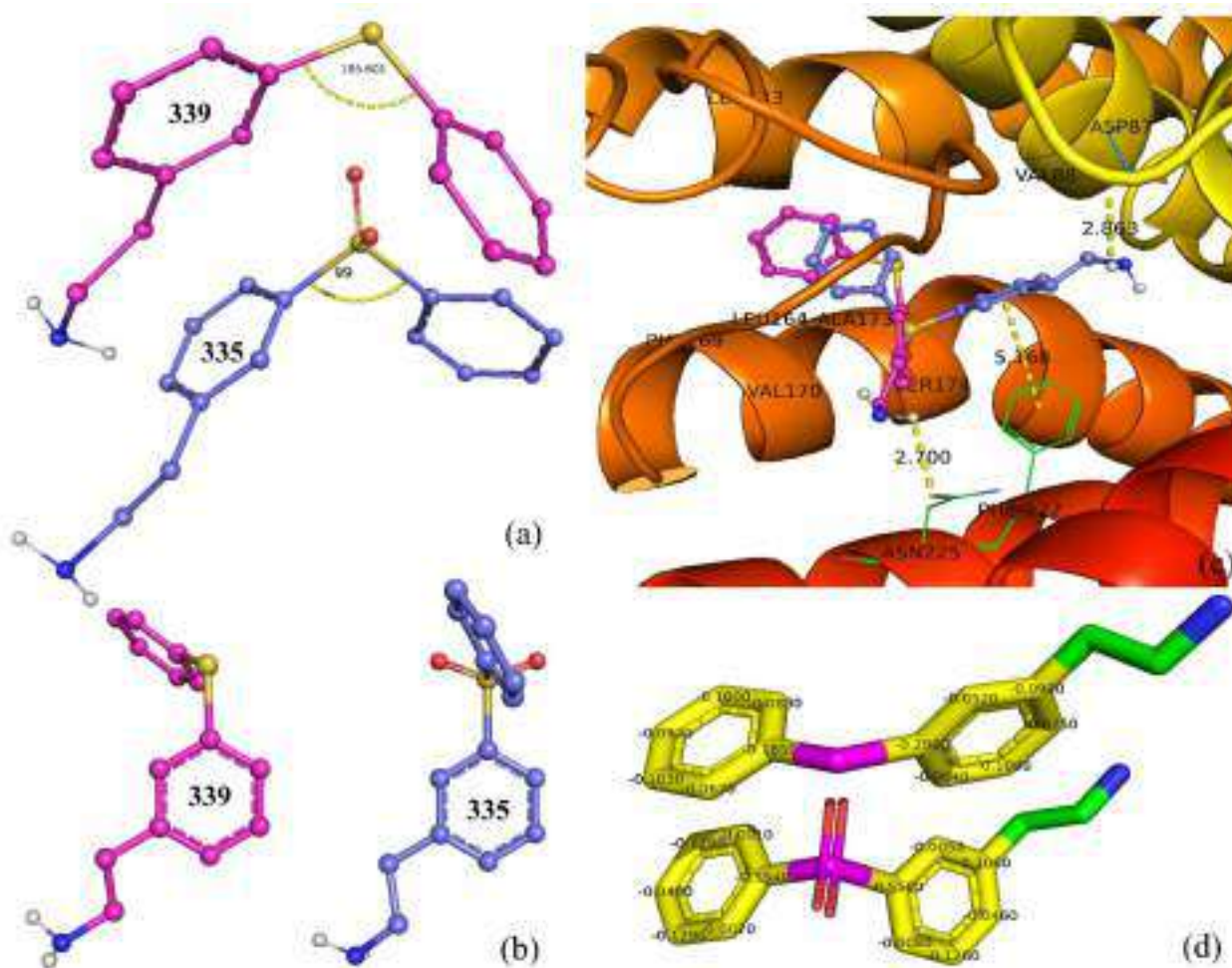


**Figure 3.** Depiction of *com\_Hhyd\_3A* using molecules 542 and 547 as representative examples (radius of gray sphere is 3 Å).

*ringC\_S\_4Bc*, which signifies the sum of partial charges on ring carbon atoms present within four bonds from a sulfur atom, has a negative coefficient in Model-1. In addition, it has a correlation coefficient of  $-0.696$  with pKi. Therefore, decreasing the value of *ringC\_S\_4Bc* could lead to a higher pKi value, i.e., a better binding affinity. The descriptor highlights the importance of ring carbon and sulfur atoms; therefore, it looks as if merely ring carbon or sulfur atoms are enough to control the binding affinity. Replacing it with *nringC* (the total number of ring carbon atoms) or *nS* (the total number of sulfur atoms) reduced the statistical performance of Model-1 ( $R^2 = 0.74$  and  $0.73$ ). Therefore, a combined presence of ring carbons and sulfur atoms within four bonds from each other has more influence. The descriptor is shown using molecules 335 and 339 as representative examples in Figure 4. A comparison of the following pairs of molecules confirmed the observation: 335 with 339, 952 with 953, 954 with 955, 248 with 249, 762 with 763, 221 with 260, 175 with 650, 1089 with 1101, 989 with 1030, etc.

A literature survey revealed that a combination of a H-bond acceptor, such as a sulfonamide or sulfone moiety, along with fused rings such as naphthalene, benzothiophene, or indole, is highly suitable for augmenting the pKi values of 5-HT6 ligands [6] due to their hydrophobic character [5]. Interestingly, the sulfone or sulfonamide groups are directly attached to fused rings in many compounds of the present dataset. In addition, in the present work, we found that the partial charges on the ring carbons of fused rings also influenced the binding affinity of a molecule for 5-HT6. Therefore, the hydrophobic character of fused rings and the partial charges on a ring carbon are equally important. This observation is further supported by the molecular docking analysis. The molecular docking analysis revealed that molecules number 335 and 339 have different poses and types of interactions. Molecule 335 has an established H-bond with Asp87 (distance 2.86 Å) and a pi-pi interaction with Phe-222 (distance 5.17 Å), whereas molecule 339 has only a H-bond formation with Asn225 (distance 2.70 Å) and lacks any pi-pi interactions. Molecule 335 was able to establish a pi-pi interaction due to the presence of a sulfone group, which caused substantial changes in the partial charges of ring carbon atoms and the C-S-C bond

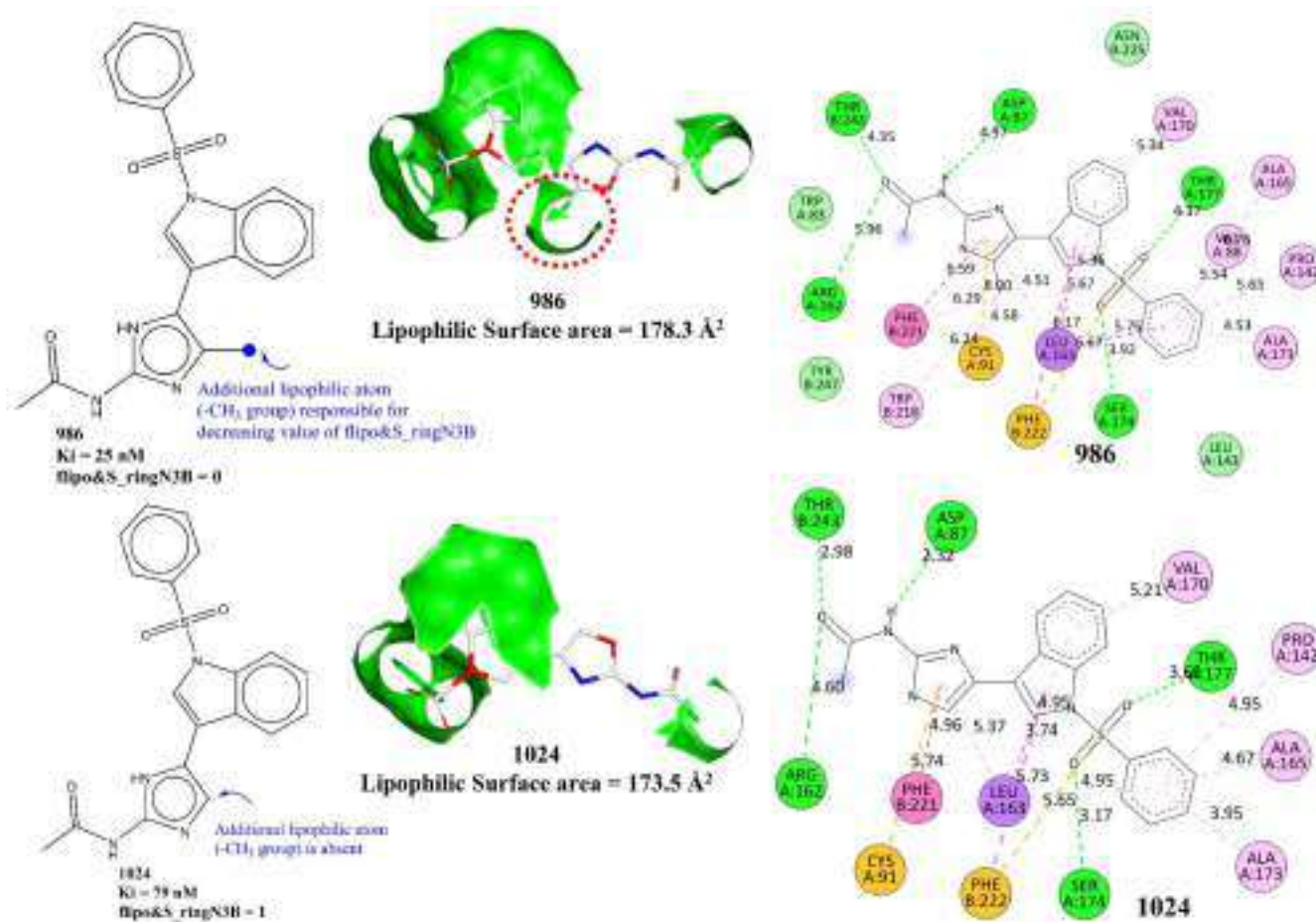
angle ( $99.8^\circ$  in 335 and  $105.6^\circ$  in 339) and also changed the solvent-accessible surface areas ( $2312.8 \text{ \AA}^2$  for 335 and  $2098.4 \text{ \AA}^2$  for 339). The docking poses for molecules number 335 and 339 are shown in Figure 4c. The yellow dotted line represents the prominent interaction with distances in Angstrom units. It is clear from the present analysis that not only lipophilic factors but electronic factors associated with ring carbon atoms vicinal to sulfur, in turn aromatic/aliphatic rings, are an important parameter in deciding the inhibitory activity for 5-HT<sub>6</sub>. Thus, the present work is successful in identifying novel unreported crucial aspects of a previously known pharmacophoric feature required for better activity for 5-HT<sub>6</sub>.



**Figure 4.** Molecules 335 and 339 as representative examples to depict the effect of descriptor ringC\_S\_4Bc. (a) Comparison of docking pose of 335 (pink) and 339 (blue), (b) C-S-C bond angle shown using yellow dotted lines, (c) docking pose for 335 (pink) and 339 (blue), (d) carbon atoms (yellow) within four bonds of sulfur (magenta) with respective partial charges.

The molecular descriptor  $\text{flipo}\&\text{S\_ringN3B}$  represents the frequency of occurrence of a ring nitrogen atom exactly three bonds from a lipophilic atom or sulfur atom. If the same ring nitrogen atom is also present at two or less bonds from any other lipophilic atom or sulfur atom, then it is neglected while calculating  $\text{flipo}\&\text{S\_ringN3B}$ . It has a negative coefficient in Model-1, which suggests that lowering the value of  $\text{flipo}\&\text{S\_ringN3B}$  could lead to a better binding profile. This observation is justified by the fact that there are 383 molecules with  $K_i \leq 10 \text{ nM}$ , but only one of them has  $\text{flipo}\&\text{S\_ringN3B} = 2$  (molecule number 50). Only two molecules (molecules number 569 and 978) possess  $\text{flipo}\&\text{S\_ringN3B} = 1$ , and the remaining 380 molecules have  $\text{flipo}\&\text{S\_ringN3B} = 0$ . A comparison of molecules 870 with 871, 896 with 903, and 892 with 897 and 898 further strengthens the observation. For example, consider molecules 986 and 1024. In the case of

molecule 986, the presence of an additional  $-CH_3$  group on the imidazole ring increased the number of lipophilic atoms within three bonds of the ring nitrogen as well as the lipophilic surface area ( $178.3 \text{ \AA}^2$ ), thereby having  $\text{flipo}\&\text{S\_ringN3B} = 0$ , while molecule 1024 lacks such a substituent and consequently has  $\text{flipo}\&\text{S\_ringN3B} = 1$  and a lower lipophilic surface area of  $173.5 \text{ \AA}^2$  (See Figure 5).

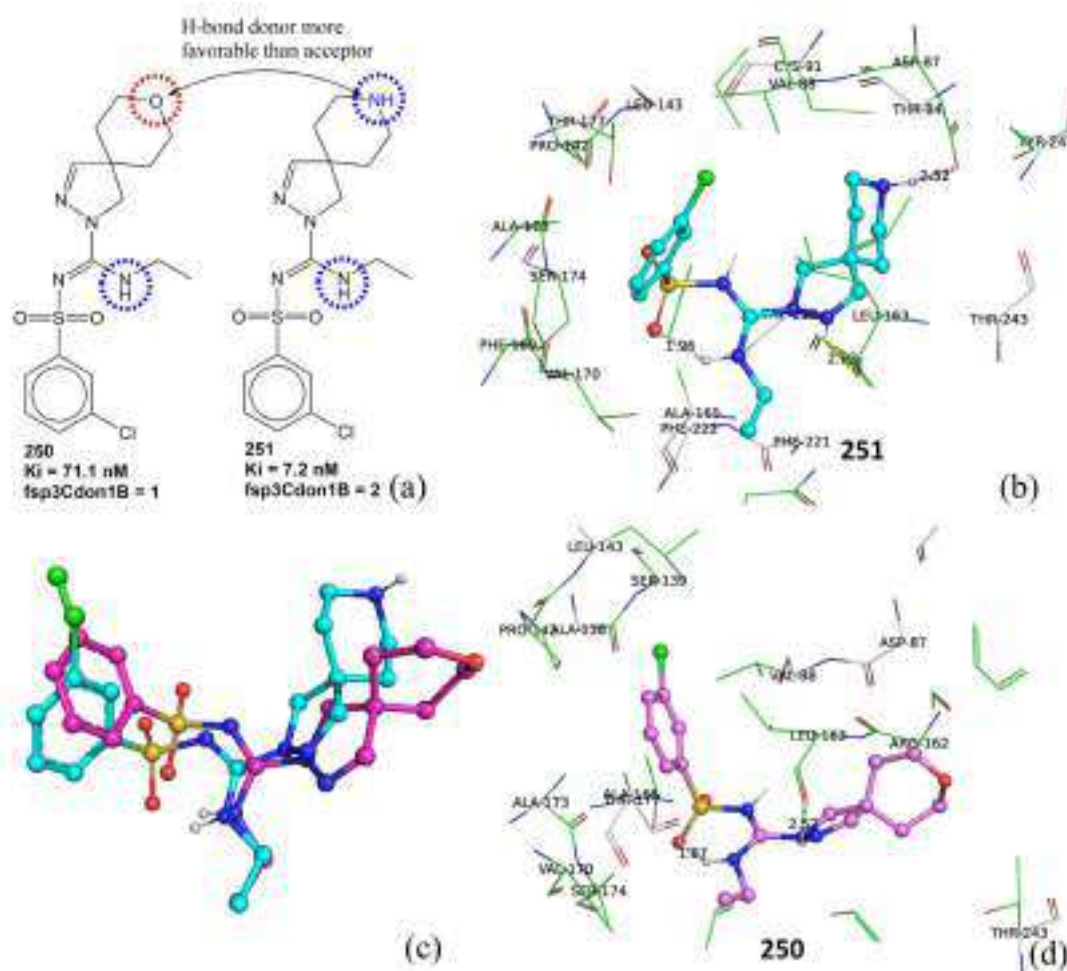


**Figure 5.** Representation of  $\text{flipo}\&\text{S\_ringN3B}$  using molecules 986 and 1024 as examples. The green contour in the middle figures depicts the lipophilic surface area.

Likewise, in the case of highly active molecules, a lower value of  $\text{flipo}\&\text{S\_ringN3B}$  is possible due to a lower number of ring nitrogen (for example molecule 681) or due to the presence of lipophilic atoms within three bonds of a ring nitrogen. Thus, this descriptor signifies that the presence of lipophilic atoms near ring nitrogen atoms decreases the value of  $\text{flipo}\&\text{S\_ringN3B}$ , which in turn increases the  $\text{pK}_i$  value. In other words, it points out an unreported structural feature of conditional importance of lipophilic atoms as well as ring nitrogen atoms in deciding the binding affinity profile. A plausible reason could be attributed to the fact that increasing the lipophilic environment around a ring nitrogen balances the polarity induced by the highly electronegative nature of nitrogen, which ultimately leads to improved brain penetration [4] due to the better lipophilic characters of the molecule. The molecular docking poses for molecules number 986 and 1024 (see Figure 5) indicate that the additional  $-CH_3$  group is responsible for pi-alkyl hydrophobic interactions with the active site residues of 5-HT<sub>6</sub> for molecule number 986. In the case of molecule number 986, the additional  $-CH_3$  group interacts with Phe221, Cys91, and Trp218. The interaction with Trp218 is absent in case of molecule number 1024.

The molecular descriptor  $\text{fsp3Cdon1B}$ , which signifies the frequency of occurrence of a H-bond donor atom directly bonded with an  $\text{sp}^3$ -hybridized carbon atom, has a positive coefficient in Model-1. Therefore, increasing such a combination of carbon and H-bond

donor atoms could lead to a higher pKi value. An inspection of molecules with  $K_i \leq 10$  nM (383 molecules) reveals that only 16 molecules lack such a combination of donor and carbon, 286 molecules have one such combination, and 82 molecules possess  $\text{fsp3Cdon1B} = 2$ . A comparison of molecules number 250 ( $K_i = 71.1$  nM,  $\text{fsp3Cdon1B} = 0$ ) and 251 ( $K_i = 7.2$  nM,  $\text{fsp3Cdon1B} = 1$ ) further supports the positive effect of the presence of  $\text{fsp3Cdon1B}$  on the pKi value (see Figure 6). The molecular docking poses for molecules number 250 and 251 support this observation (see Figure 6b–d). Both molecules interact with similar residues such as Leu163 (H-bond). However, a prominent difference in the docking poses of molecules number 251 and 250 is the H-bond formation with a distance of 2.52 Å by the -NH of the piperidine ring with Asp87, which is absent in the case of 250. This is due to the fact that the pyran ring of molecule 250 is oriented away from Asp87, whereas the piperidine ring of 251 is close enough to establish a H-bond with Asp87. Thus, it highlights the importance of the presence of a donor atom in the 5-HT<sub>6</sub> ligand. The -NH of the piperidine ring is responsible for  $\text{fsp3Cdon1B} = 1$  for molecule number 250. Thus, the molecular docking and QSAR provided similar and complementary results.

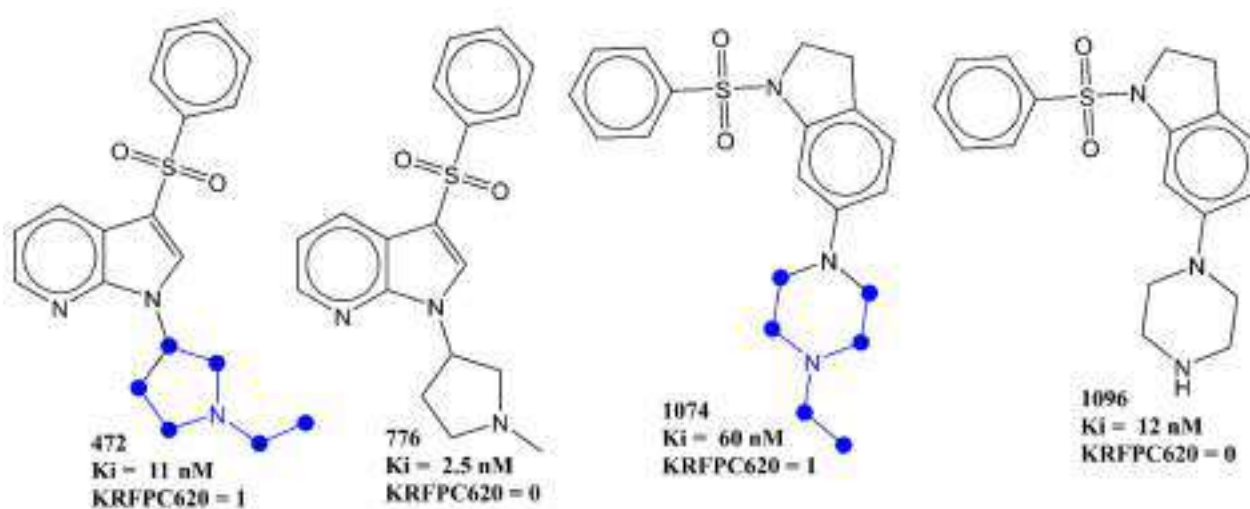


**Figure 6.** (a) Representation of  $\text{fsp3Cdon1B}$  using molecules number 250 and 251 as examples, (b) docking pose for molecule number 251 (dotted line represents H-bond formation), (c) overlap of docking pose of 250 (cyan) and 251 (pink), (d) docking pose for 250.

Another molecular descriptor which highlights the importance of nitrogen atoms and their local environment is KRFPC620. The molecular descriptor KRFPC620 considers the count of a fragment that encompasses a planer nitrogen atom attached to three  $\text{CH}_3\text{-CH}_2\text{-}$  groups. For better clarification, it is depicted in Figure 7 using representative examples only. The negative coefficient for the descriptor indicates that the pKi value increases with



a decrease in the value of KRFPC620. A comparative analysis of the following pairs of molecules supports this trend: 472 with 776, 748 with 749, 757 with 761, 1074 with 1096, 1068 with 1075, 1100 with 1116, 1094 with 1058, etc. To add further, of the 383 molecules with  $K_i \leq 10$  nM, 37 molecules have KRFPC620 = 1, whereas 346 molecules lack the presence of KRFPC620. Therefore, such a combination of nitrogen with  $\text{CH}_3\text{-CH}_2\text{-}$  must be avoided for a better pK<sub>i</sub> value.



**Figure 7.** Pictorial representation of KRFPC660 (blue colored) using representative examples.

Many researchers have highlighted the importance of the presence of a positive ionizable atom or group such as the nitrogen in piperazine or in a (dimethylamino)ethyl fragment for a better binding affinity for 5-HT<sub>6</sub> [4]. The present work also successfully highlighted the negative impact of a third ethyl group on ionizable nitrogen on binding affinity. Therefore, in agreement with previous studies [4,12], a methyl substituted piperazine, non-substituted piperazine, or a (dimethylamino)ethyl fragment is a better choice to act as a positive ionizable moiety.

Another descriptor whose value must be lowered due to its negative coefficient in Model-1 to have a better pK<sub>i</sub> value is sp<sup>3</sup>N\_sp<sup>2</sup>O\_8B. It counts the total number of sp<sup>3</sup>-hybridized nitrogen atoms present within eight bonds of sp<sup>2</sup>-hybridized oxygen atoms. Of the 383 molecules with  $K_i \leq 10$  nM, 181 molecules lack such a combination of nitrogen and oxygen atoms, whereas the remaining 201 molecules possess only one such combination. In addition, the following pairs of molecules, on comparison, support the observation: 624 with 627 (see Figure 8), 557 with 556 and 555, 271 with 274, 116 with 120, and 117 with 123, to mention a few.

To summarize the prominent structural features and the pharmacophoric model, we used the two most active molecules, 681 and 271, as representative examples (see Figure 9). The pharmacophoric pattern consists of two hydrophobic regions (green contour), two H-bond acceptor regions (red contour), and one H-bond acceptor region (blue contour), as depicted in Figure 9a using molecule 681. Thus, the pharmacophoric pattern agrees with previous studies [4,12]. Figure 9b depicts the molecular descriptor ringC\_S\_4Bc in molecule 271. Figure 9c represents the descriptors fliporingN3B and fsp3Cdon1B. The three hydrophobic  $\text{-CH}_3$  groups shown by green dots are responsible for balancing the hydrophilic effect of ring nitrogen atoms, thus enhancing the CNS penetration ability of a molecule. Moreover, the  $\text{-CH}_3$  groups labelled as A and B enhance the value of fsp3Cdon1B, as they are directly attached to donor atoms. Thus, the present work not only captured the pharmacophoric features reported by López-Rodríguez et al. [4,12] but also successfully extended it.

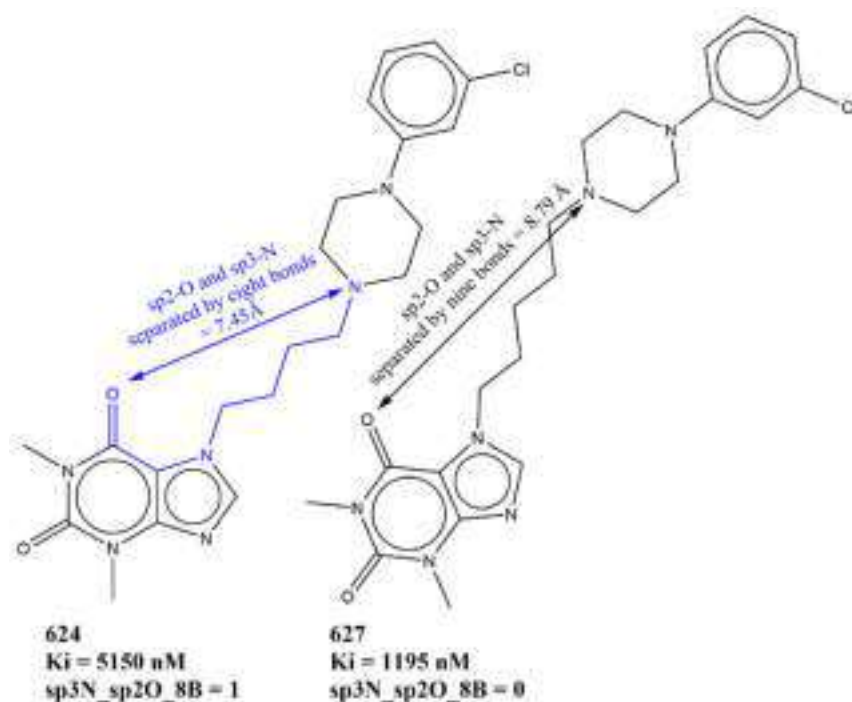


Figure 8. Illustrative examples for representation of sp3N\_sp2O\_8B.

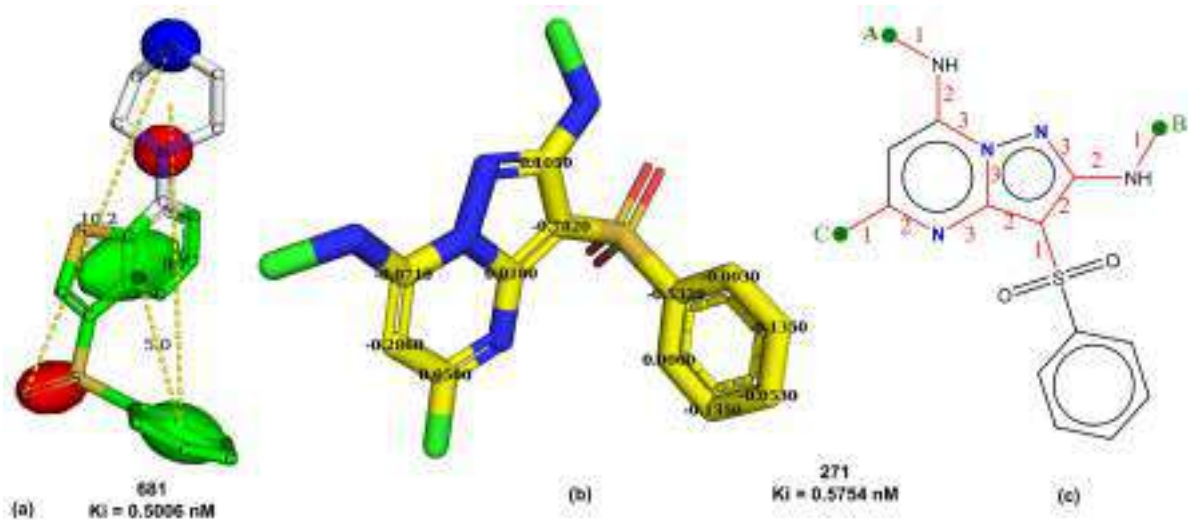
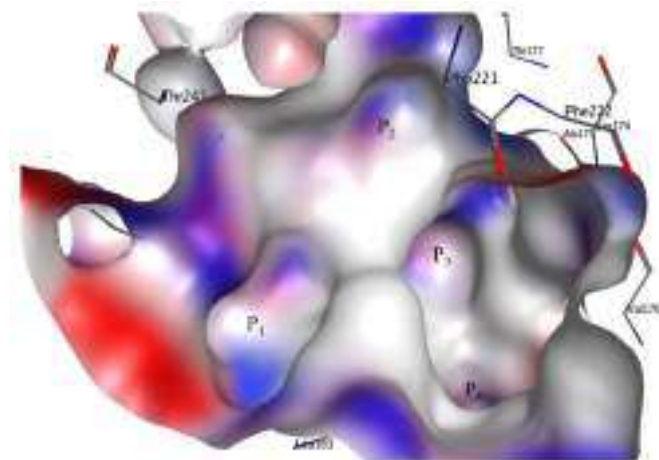


Figure 9. Depiction of (a) pharmacophoric feature using molecule 681 (green: hydrophobic, red: H-bond acceptor, blue: H-bond donor regions, dotted lines show distances in Angstrom units), (b) yellow atoms represent ringC\_S\_4Bc in molecule 271, (c) fliporingN3B represented by red-colored bonds with numbering using molecule 271.

The molecular docking score spans from  $-5.7$  to  $-12.2$  for molecules in the current dataset (see Supplementary Materials). For the sake of convenience, twenty molecules with the highest and lowest molecular docking scores are tabulated in Table 3. Surprisingly, not only the molecular docking score has a weak correlation of 0.10 with pKi but also many molecules with lower binding affinity values have better docking scores (see Tables 3 and 4). This could be attributed to the large size of the active site of 5-HT<sub>6</sub> (see Figure 10), which allows the adoption of different conformations for molecules. Moreover, recent studies point out that current docking software such as AutoDock, Dock, etc., and respective algorithms for docking scores are inclined toward the flexibility of ligands, which in turn, is associated with the loss of ligand conformational entropy on binding [31]. The molecules

with lower binding affinity for 5-HT<sub>6</sub> have a high degree of flexibility. Thus, all these factors together resulted in an artificially more favorable binding score for the more flexible decoys than for actives.



**Figure 10.** Binding site of 5-HT<sub>6</sub> used in the present work.

**Table 3.** The molecular docking score and K<sub>i</sub> (nM) for ten molecules with the highest and lowest molecular docking scores.

Molecule Number	SMILES	K <sub>i</sub> (nM)	Affinity-Docking Score (Kcal/mol)
741	<chem>CC(=O)Nc(cc1)ccc1CCNICC2Cc(c23)ccc4c3ccn4S(=O)(=O)c5ccccc5</chem>	79.43	−12.2
134	<chem>C1NCCCC1C(=O)Nc(ccc2)c(c23)[nH]nc3S(=O)(=O)c4cccc(c45)cccc5</chem>	9.8	−12
489	<chem>c1cccc(c12)[nH]cc2C(C3=O)CC(=O)N3CCCN(CC4)CCC4c5c[nH]c(c56)ccc(c6)OC</chem>	264	−11.9
490	<chem>c1cccc(c12)[nH]cc2C(C3=O)CC(=O)N3CCCN(CC4)CCC4c5c[nH]c(c56)ccc(F)c6</chem>	1146	−11.8
1093	<chem>CC(=O)Nc(n1)[nH]c(c1C)-c2cn(c(c23)cccc3)S(=O)(=O)c4cccc(c45)cccc5</chem>	13	−11.7
668	<chem>Cl(C)CCC1c2c[nH]c(c23)ccc(c3)NS(=O)(=O)c(ccc4)c(c45)nccc5</chem>	21.2	−11.7
133	<chem>C1CCCN1CCC(=O)Nc(ccc2)c(c23)[nH]nc3S(=O)(=O)c4cccc(c45)cccc5</chem>	24	−11.7
381	<chem>FC(F)(F)c1cc(ccc1)S(=O)(=O)n(c(c2c34)CCC(C2)N)c3ccc(c4)OC</chem>	39.1	−11.7
805	<chem>c1cccc(c12)ccc(c2)S(=O)(=O)NCCN(CC3)CC=C3c4c[nH]c(c45)ccc(F)c5</chem>	67	−11.7
628	<chem>c1cccc(c12)CN([C@@H](C2)C(=O)N)C(=O)CCCCN3CCN(CC3)c(cccc4)c4-c5ccccc5</chem>	594	−11.7
1086	<chem>CCn1cncc1-c2c[nH]c(c23)ccc(Br)c3</chem>	1349	−7.3
1016	<chem>CCn1cncc1-c2c[nH]c(c23)cccc3</chem>	3020	−7.3
1203	<chem>N1CCC[C@@H]1Cc2c[nH]c(c23)cccc3</chem>	60	−7.2
1202	<chem>c1cccc(c12)n(cc2)C[C@H]3CCCN3C</chem>	550	−7.2
339	<chem>NCCc1cc(ccc1)Sc2ccccc2</chem>	115	−7.1
93	<chem>CCN(CC)CCc1c[nH]c(c12)cccc2</chem>	575	−6.4
738	<chem>NCCc1c[nH]c(c12)ccc(c2)O</chem>	42.333	−6.2
534	<chem>CC(N)Cc1c[nH]c(c12)cccc2</chem>	910.505	−6.2
444	<chem>NCCc1c[nH]c(c12)ccnc2</chem>	64	−5.7
445	<chem>CN(C)CCc1c[nH]c(c12)ccnc2</chem>	100	−5.7

**Table 4.** SMILES (simplified molecular input line entry system) notation, Ki (nM), pKi (M), and molecular docking score for the five most and five least active molecules of the selected dataset.

Molecule Number	SMILES (Simplified Molecular Input Line Entry System) Notation	Ki(nM)	pKi(M)	Docking Score (Kcal/mol)
681	<chem>C1CNCCN1c(ccc2)c(c23)sc3S(=O)(=O)c4cccc4</chem>	0.5006	9.301	−9
271	<chem>Cc(n1)cc(NC)n(c12)nc(NC)c2S(=O)(=O)c3cccc3</chem>	0.5754	9.24	−8.3
142	<chem>C1CNCCC1Nc(c2)ccc(c23)[nH]nc3S(=O)(=O)c(c4)ccc(c45)cccc5</chem>	0.6	9.222	−10.8
279	<chem>Cc(n1)IN)c(C)n(c12)nc(NC)c2S(=O)(=O)c3cccc3</chem>	0.6457	9.19	−8.4
428	<chem>CN(C1)CIn2)c1c(C)n(c23)nc(NC)c3S(=O)(=O)c4cccc4</chem>	0.66	9.18	−9.1
622	<chem>O=I(C)c(=O)n(C)c(c12)ncn2CCCCN3CCN(CC3)c4cccc4</chem>	14210	4.847	−9.6
543	<chem>c1cccc(OC)c1N(CC2)CCICCCCI(=O)N(C)C(=O)C3(C)c4cccc4</chem>	14650	4.834	−10.1
267	<chem>c1cccc1N(CICCN2CC(O)CN3C(=O)N(C)C(=O)C3(c4cccc4)c5cccc5</chem>	20410	4.69	−9.7
542	<chem>c1cccc(F)c1CC2)I2CCCCCN3C(=O)N(C)C(=O)C3(C)c4cccc4</chem>	25520	4.593	−10.1
266	<chem>c1cI(OC)c1N(CC2)CCN2CCCN3C(=O)N(C)C(=O)C3(c4cccc4)c5cccc5</chem>	29070	4.537	−10.8

#### 4. Materials and Methods

In the present study, we have followed the OECD (Organization for Economic Co-operation and Development) guidelines and standard protocol, which has been endorsed by different researchers, for an effective QSAR analysis [15,17,18,21,29,32–35]. The different steps for developing a model involved a careful selection of a dataset and data curation, followed by 3D structure generation for all molecules, molecular descriptor calculations and their pruning, model development and its thorough validation (internal and external), and mechanistic interpretation [20,36,37]. These steps were executed sequentially to avoid errors and human bias and to ensure the appropriate validation of the model.

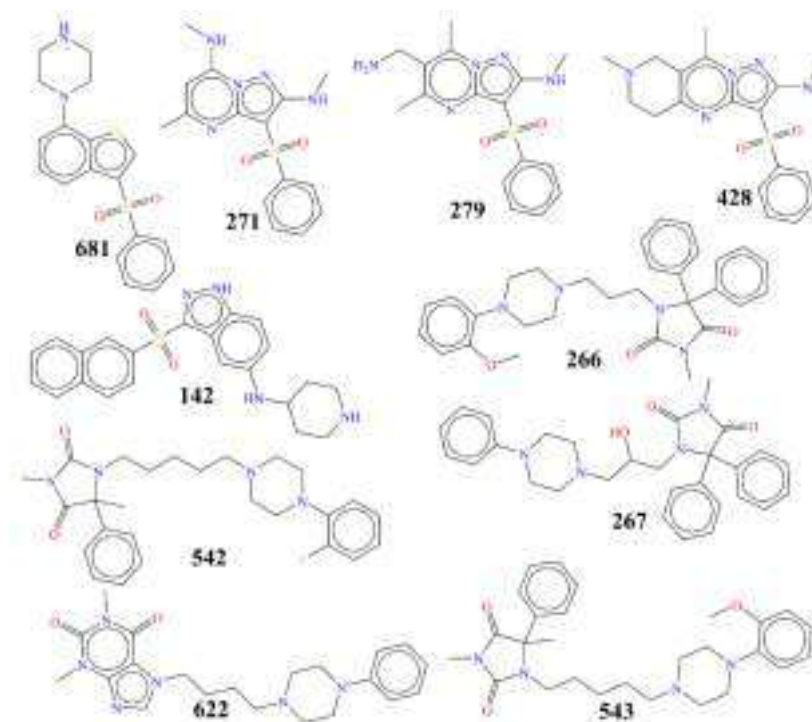
##### 4.1. Selection of Dataset

The size, composition, and structural diversity of the dataset are important characteristics that decide the success and utility of QSAR and molecular docking analysis throughout the pipeline of drug discovery [15–17,21,29,32,34,38–41]. Therefore, a large dataset of 3398 reported ligands for 5-HT<sub>6</sub> was downloaded from BindingDB (<https://www.bindingdb.org/bind/index.jsp>, accessed on 14 January 2022). Then, duplicates, salts, metal derivatives, rule-of-five violators, and molecules with undefined Ki values were removed as a part of data curation [42], which reduced the size of the dataset to only 1278 molecules. The reduced dataset was still diverse enough, with the presence of positional and chain isomers, different heterocyclic and aromatic scaffolds, stereoisomers, etc. The experimental Ki spanned five orders of magnitude (0.5006 nM to 29.07 μM). For a better QSAR analysis, the experimental Ki values were converted to pKi (pKi = −lgKi). To understand the structural variation possessed by the dataset, some highly active and least active molecules are depicted in Figure 11, and their other details are presented in Table 4.

##### 4.2. Calculation of Molecular Descriptors and Objective Feature Selection (OFS)

The next step involved the conversion of all SMILES notations to respective 3D-optimized structures using the appropriate method. For this, OpenBabel 3.1 [43] was used to convert SMILES to SDF (structure data file). After that, MOPAC2016 [44] was used to convert SDF to MOL2 using PM3, a semi-empirical method based on the same formalism and equations as the Austin Model-1 (AM1) method, for structure optimization and partial charge assignment. Then, molecular descriptor calculations were accomplished using PyDescriptor [45] and PaDEL [46], which together provided more than 42,000 molecular descriptors for each molecule. Though the myriad numbers of molecular descriptors increase the possibility of achieving a successful QSAR analysis, they also increase the risk of chance correlations or overfitting from noisy redundant descriptors. Therefore,

OFS was performed using QSARINS 2.2.4 [47], which eliminated near constant (for 90% molecules) and highly intercorrelated ( $|R| > 0.90$ ) molecular descriptors. After OFS, the reduced set of molecular descriptors encompassed only 4186 descriptors, which still covered a broad descriptor space due to the presence of 1D to 3D descriptors, fingerprint, and charged-based descriptors as well as atom-pair descriptors. The remaining descriptors were easily interpretable in terms of structural features, thereby increasing the possibility of mechanistic interpretation of the model.



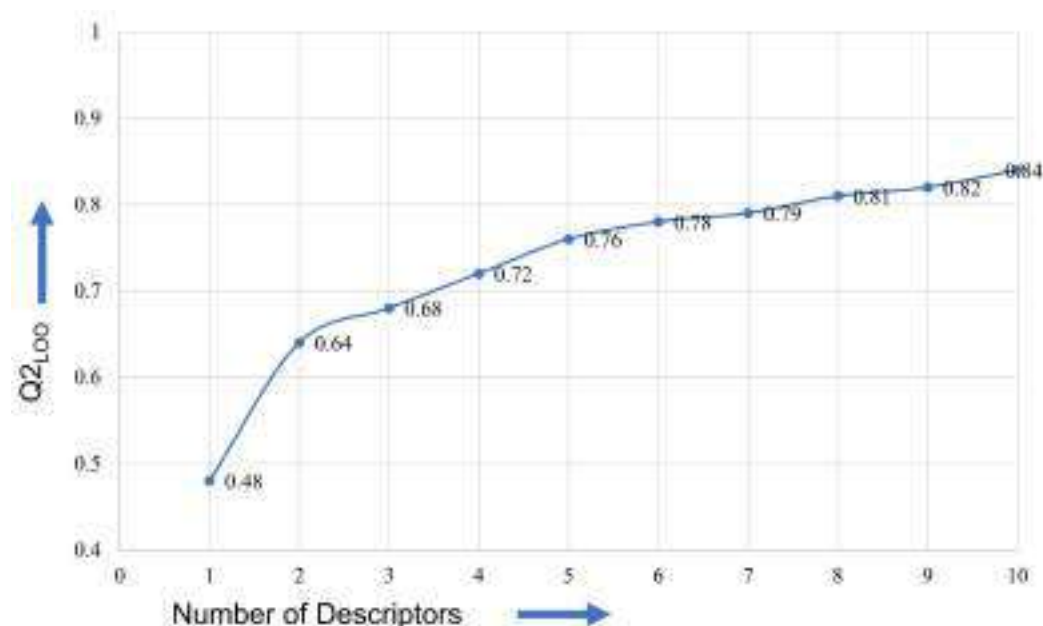
**Figure 11.** Representative examples from the selected dataset (five most active and five least active molecules) of 5-HT<sub>6</sub> ligands.

#### 4.3. Splitting the Dataset and Subjective Feature Selection (SFS)

SFS is a crucial step during model building to select a suitable number and set of molecular descriptors using a suitable feature selection algorithm such as stepwise regression, genetic algorithm, etc. For the appropriate training and validation of the model, before actual model building, the dataset was randomly divided into a training set (80%, i.e., 1024 molecules) and a prediction set (20%, i.e., 254 molecules). The random division of a dataset into an 80:20 proportion was performed to avoid any bias and minimize information leakage [32,48], to confirm the external predictive ability of the model, and to achieve a better composition of the training and prediction sets [29,34]. The training set was used only for the selection of the appropriate number and set of molecular descriptors. The prediction set, also termed the external validation set, was used only for the validation of the newly developed model.

It is essential to include the optimum number of molecular descriptors in the model to avoid over- and underfitting. Consequently, a simple graphical method was used to identify the optimum number of descriptors for a model. Usually, the successive addition of a variable (molecular descriptor) in a multilinear regression (MLR) model augments the value of  $Q^2_{LOO}$  until the final elevation point is achieved [25,29]. After that, there is little or poor augmentation to the value of  $Q^2_{LOO}$ . Hence, the number of molecular descriptors matching the elevation point were considered optimum for model building [36]. This is depicted in Figure 12 as a graph. From Figure 12, the final elevation point is matched to six molecular descriptors. Therefore, the heuristic search was confined to including only six molecular descriptors in the QSAR model using a multi-regression analysis. The set

of molecular descriptors were selected using a genetic algorithm as a feature selection algorithm and using  $Q^2_{LOO}$  as the fitness parameter along with the genetic algorithm–multilinear regression (GA-MLR) method using QSARINS-2.2.4 [47].



**Figure 12.** Plot of number of descriptors against leave-one-out coefficient of determination,  $Q^2_{LOO}$ , to identify the optimum number of descriptors.

#### 4.4. Building Regression Model and Its Validation

The search for six molecular descriptors for the development model ultimately provided different combinations of different molecular descriptors. However, only one combination of molecular descriptors was selected due to the statistical performance and the satisfaction of the following stringent parameters and criteria, which have been suggested by other researchers [16,22–29]:

$R^2_{tr} \geq 0.6$ ;  $Q^2_{LOO} \geq 0.5$ ;  $Q^2_{LMO}$  (cross-validated coefficient of determination for leave-many-out)  $\geq 0.6$ ;  $R^2_{tr} > Q^2_{LOO}$ ;  $R^2_{ex} \geq 0.6$ , CCC (concordance correlation coefficient)  $\geq 0.80$ ;  $Q^2_{F^n} \geq 0.60$ ; high values of the external validation parameters  $R^2_{ex}$ ,  $Q^2_{F1}$ ,  $Q^2_{F2}$ , and  $Q^2_{F3}$ ; and low values of  $R^2_{Yscr}$  (coefficient of determination for Y-randomization), RMSE (root-mean-square error), and MAE (mean absolute error), with  $RMSE_{tr} < RMSE_{cv}$ .

The formulae and other details of these statistical parameters are available in the Supplementary Materials. For further validation, it was essential to determine the applicability domain of the QSAR model [49,50]. For this, we used a Williams plot (standardized residuals vs. hat values) to evaluate the applicability domain of the QSAR model [47].

#### 4.5. Molecular Docking

Since the X-ray-resolved structure of 5-HT6 is not available, an appropriately validated and reported homology model built using a  $\beta_2$  receptor template (PDB ID: 4LDE) by Vanda et al. [8] was used for molecular docking [6,7] in the present work. 4LDE (selected template) and 5-HT6 (modelled receptor) possess equivalent positions for the most conserved amino acid in each helix and motifs characteristic for class A GPCRs [6–8]. The sequences of 5-HT6 and 4LDE were retrieved from the UniProtKB/Swiss-Prot database [8]. The protein was prepared using Chimera ([www.cgl.ucsf.edu/chimera/](http://www.cgl.ucsf.edu/chimera/), accessed on 14 January 2022) with default settings. Then, for the execution of molecular docking, AutoDock Vina [51], available in DockingApp [52], which allows users to select flexible residues of the input receptor, was used with flexible docking for virtual screening with default settings. The binding site of 5-HT6, which consists of four major grooves, P1-P4, used in the present work, is depicted in Figure 10. The binding site was used for automated

molecular docking for all the molecules. Further details of molecular docking are available in the Supplementary Materials.

## 5. Conclusions

The present work has resulted in the development of a statistically predictive GA-MLR model with a balance of excellent predictive ability ( $R^2_{tr} = 0.78$ ,  $R^2_{ex} = 0.77$ ) and novel mechanistic interpretations. The present QSAR and molecular docking analysis has successfully identified the importance of steric bulkiness, polar groups, and substitution with respect to the center of mass. It also highlighted the role played by partial charges on ring C atoms present near sulfur atoms. Further, Model-1 successfully identified that a conditional occurrence of lipophilic atoms/groups with respect to nitrogen atoms is better for having a higher pKi value. The crucial role played by the interrelationships between specific types of atoms, such as sp<sup>3</sup>-hybridized carbon/nitrogen atoms, ring nitrogen atoms, etc., further escalated the expediency of Model-1. The model possesses high external predictive ability, which is evident from its statistical performance. In conclusion, the present work not only effectively identified reported and novel unreported pharmacophoric features associated with 5-HT<sub>6</sub> but also offers a highly predictive QSAR model. It could be beneficial throughout the drug discovery pipeline to optimize the lead compounds to develop a better therapeutic for 5-HT<sub>6</sub>.

**Supplementary Materials:** The following supporting information can be downloaded at: <https://www.mdpi.com/article/10.3390/ph15070834/s1>: Additional statistical parameters for model-1, Additional details of experimental procedure for molecular docking, Statistical symbols with names and explanations, Molecular descriptors for all molecules used in model-1, their correlation matrix and molecular docking score.

**Author Contributions:** Conceptualization, V.H.M., S.N.A.B. and M.A.E.; formal analysis and data curation, V.H.M., K.J. and P.A.; writing, V.H.M., H.E., S.N.A.B., R.D.J. and A.S.; editing and proofreading, V.H.M., S.N.A.B., H.E. and M.A.E. All authors have read and agreed to the published version of the manuscript.

**Funding:** The authors' work was supported through grant number "375213500" from the Deputyship for Research and Innovation, Ministry of Education, in Saudi Arabia.

**Institutional Review Board Statement:** Not applicable.

**Informed Consent Statement:** Not applicable.

**Data Availability Statement:** The data is contained within the article and Supplementary Materials.

**Acknowledgments:** The authors extend their appreciation to the Deputyship for Research and Innovation, Ministry of Education, in Saudi Arabia, and the central laboratory at Jouf University for supporting this study. V.H.M. is thankful to Paola Gramatica and her team for providing a free copy of QSARINS 2.2.4.

**Conflicts of Interest:** The authors declare no conflict of interest.

## Abbreviations

SMILES	Simplified molecular-input line-entry system
GA	Genetic algorithm
MLR	Multiple linear regression
QSAR	Quantitative structure–activity relationship
WHO	World Health Organization
ADMET	Absorption, distribution, metabolism, excretion, and toxicity
OLS	Ordinary least square
QSARINS	QSAR Insubria
OECD	Organisation for Economic Co-operation and Development

## References

1. Doddareddy, M.R.; Cho, Y.S.; Koh, H.Y.; Pae, A.N. CoMFA and CoMSIA 3D QSAR analysis on N1-arylsulfonylindole compounds as 5-HT6 antagonists. *Bioorganic Med. Chem.* **2004**, *12*, 3977–3985. [[CrossRef](#)] [[PubMed](#)]
2. Codony, X.; Burgueño, J.; Ramírez, M.J.; Vela, J.M. 5-HT6 Receptor Signal Transduction. In *Pharmacology of 5-HT6 Receptors—Part 1*; Academic Press: Cambridge, MA, USA, 2010; pp. 89–110.
3. Hao, M.; Li, Y.; Li, H.; Zhang, S. Investigation of the Structure Requirement for 5-HT6 Binding Affinity of Arylsulfonyl Derivatives: A Computational Study. *Int. J. Mol. Sci.* **2011**, *12*, 5011–5030. [[CrossRef](#)] [[PubMed](#)]
4. Benhamú, B.; Martín-Fontecha, M.; Vázquez-Villa, H.; Pardo, L.; López-Rodríguez, M.L. Serotonin 5-HT6 Receptor Antagonists for the Treatment of Cognitive Deficiency in Alzheimer's Disease. *J. Med. Chem.* **2014**, *57*, 7160–7181. [[CrossRef](#)]
5. Karila, D.; Freret, T.; Bouet, V.; Boulouard, M.; Dallemagne, P.; Rochais, C. Therapeutic Potential of 5-HT6 Receptor Agonists. *J. Med. Chem.* **2015**, *58*, 7901–7912. [[CrossRef](#)] [[PubMed](#)]
6. Łażewska, D.; Kurczab, R.; Wićcek, M.; Kamińska, K.; Satała, G.; Jastrzebska-Więsek, M.; Partyka, A.; Bojarski, A.J.; Wesolowska, A.; Kieć-Kononowicz, K.; et al. The computer-aided discovery of novel family of the 5-HT 6 serotonin receptor ligands among derivatives of 4-benzyl-1,3,5-triazine. *Eur. J. Med. Chem.* **2017**, *135*, 117–124. [[CrossRef](#)] [[PubMed](#)]
7. Kucwaj-Brysz, K.; Baltrukevich, H.; Czarnota, K.; Handzlik, J. Chemical update on the potential for serotonin 5-HT6 and 5-HT7 receptor agents in the treatment of Alzheimer's disease. *Bioorganic Med. Chem. Lett.* **2021**, *49*, 128275. [[CrossRef](#)] [[PubMed](#)]
8. Vanda, D.; Canale, V.; Chaumont-Dubel, S.; Kurczab, R.; Satała, G.; Koczurkiewicz-Adamczyk, P.; Krawczyk, M.; Pietruś, W.; Blicharz, K.; Pękała, E.; et al. Imidazopyridine-Based 5-HT6 Receptor Neutral Antagonists: Impact of N1-Benzyl and N1-Phenylsulfonyl Fragments on Different Receptor Conformational States. *J. Med. Chem.* **2021**, *64*, 1180–1196. [[CrossRef](#)] [[PubMed](#)]
9. Zajdel, P.; Grychowska, K.; Mogilski, S.; Kurczab, R.; Satała, G.; Bugno, R.; Kos, T.; Gołębiowska, J.; Malikowska-Racia, N.; Nikiforuk, A.; et al. Structure-Based Design and Optimization of FPPQ, a Dual-Acting 5-HT3 and 5-HT6 Receptor Antagonist with Antipsychotic and Pro-cognitive Properties. *J. Med. Chem.* **2021**, *64*, 13279–13298. [[CrossRef](#)]
10. Staroń, J.; Kurczab, R.; Warszycki, D.; Satała, G.; Krawczyk, M.; Bugno, R.; Lenda, T.; Popik, P.; Hogendorf, A.S.; Hogendorf, A.; et al. Virtual screening-driven discovery of dual 5-HT6/5-HT2A receptor ligands with pro-cognitive properties. *Eur. J. Med. Chem.* **2020**, *185*, 111857. [[CrossRef](#)]
11. Heal, D.J.; Smith, S.L.; Fisas, A.; Codony, X.; Buschmann, H. Selective 5-HT6 receptor ligands: Progress in the development of a novel pharmacological approach to the treatment of obesity and related metabolic disorders. *Pharmacol. Ther.* **2008**, *117*, 207–231. [[CrossRef](#)]
12. Da Silva, A.P.; de Angelo, R.M.; de Paula, H.; Honório, K.M.; da Silva, A.B.F. Drug design of new 5-HT6 antagonists: A QSAR study of arylsulfonamide derivatives. *Struct. Chem.* **2020**, *31*, 1585–1597. [[CrossRef](#)]
13. Imam, S.S.; Gilani, S.J. Computer Aided Drug Design: A Novel Loom to Drug Discovery. *Org. Med. Chem.* **2017**, *1*, 113–118. [[CrossRef](#)]
14. Baig, M.H.; Ahmad, K.; Roy, S.; Ashraf, J.M.; Adil, M.; Siddiqui, M.H.; Khan, S.; Kamal, M.A.; Provaznik, I.; Choi, I. Computer Aided Drug Design: Success and Limitations. *Curr. Pharm. Des.* **2016**, *22*, 572–581. [[CrossRef](#)]
15. Gramatica, P. Principles of QSAR Modeling. *Int. J. Quant. Struct. Prop. Relatsh.* **2020**, *5*, 61–97. [[CrossRef](#)]
16. Gramatica, P. On the development and validation of QSAR models. *Methods Mol. Biol.* **2013**, *930*, 499–526. [[CrossRef](#)]
17. Gramatica, P.; Cassani, S.; Roy, P.P.; Kovarich, S.; Yap, C.W.; Papa, E. QSAR Modeling is not Push a Button and Find a Correlation: A Case Study of Toxicity of (Benzo-)triazoles on Algae. *Mol. Inform.* **2012**, *31*, 817–835. [[CrossRef](#)]
18. Huang, J.; Fan, X. Why QSAR fails: An empirical evaluation using conventional computational approach. *Mol. Pharm.* **2011**, *8*, 600–608. [[CrossRef](#)]
19. López-Rodríguez, M.L.; Benhamú, B.; de la Fuente, T.; Sanz, A.; Pardo, L.; Campillo, M. A Three-Dimensional Pharmacophore Model for 5-Hydroxytryptamine6 (5-HT6) Receptor Antagonists. *J. Med. Chem.* **2005**, *48*, 4216–4219. [[CrossRef](#)]
20. Masand, V.H.; Patil, M.K.; El-Sayed, N.N.E.; Zaki, M.E.A.; Almarhoon, Z.; Al-Hussain, S.A. Balanced QSAR analysis to identify the structural requirements of ABBV-075 (Mivebresib) analogues as bromodomain and extraterminal domain (BET) family bromodomain inhibitor. *J. Mol. Struct.* **2021**, *1229*, 129597. [[CrossRef](#)]
21. Fujita, T.; Winkler, D.A. Understanding the Roles of the “Two QSARs”. *J. Chem. Inf. Model.* **2016**, *56*, 269–274. [[CrossRef](#)]
22. Krstajic, D.; Buturovic, L.J.; Leahy, D.E.; Thomas, S. Cross-validation pitfalls when selecting and assessing regression and classification models. *J. Cheminform.* **2014**, *6*, 10. [[CrossRef](#)]
23. Chirico, N.; Gramatica, P. Real external predictivity of QSAR models. Part 2. New intercomparable thresholds for different validation criteria and the need for scatter plot inspection. *J. Chem. Inf. Model.* **2012**, *52*, 2044–2058. [[CrossRef](#)]
24. Chirico, N.; Gramatica, P. Real external predictivity of QSAR models: How to evaluate it? Comparison of different validation criteria and proposal of using the concordance correlation coefficient. *J. Chem. Inf. Model.* **2011**, *51*, 2320–2335. [[CrossRef](#)]
25. Consonni, V.; Ballabio, D.; Todeschini, R. Comments on the definition of the Q2 parameter for QSAR validation. *J. Chem. Inf. Model.* **2009**, *49*, 1669–1678. [[CrossRef](#)]
26. Rao, R.B.; Fung, G.; Rosales, R. On the Dangers of Cross-Validation. An Experimental Evaluation. In Proceedings of the 2008 SIAM International Conference on Data Mining (SDM), Atlanta, GA, USA, 24–26 April 2008; pp. 588–596; ISBN 978-0-89871-654-2. [[CrossRef](#)]
27. Gramatica, P.; Giani, E.; Papa, E. Statistical external validation and consensus modeling: A QSPR case study for Koc prediction. *J. Mol. Graph. Model.* **2007**, *25*, 755–766. [[CrossRef](#)]



28. Tropsha, A.; Gramatica, P.; Gombar, V.K. The Importance of Being Earnest Validation is the Absolute Essential for Successful Application and Interpretation of QSPR Models. *QSAR Comb. Sci.* **2003**, *22*, 69–77. [[CrossRef](#)]
29. Cherkasov, A.; Muratov, E.N.; Fourches, D.; Varnek, A.; Baskin, I.I.; Cronin, M.; Dearden, J.; Gramatica, P.; Martin, Y.C.; Todeschini, R.; et al. QSAR modeling: Where have you been? Where are you going to? *J. Med. Chem.* **2014**, *57*, 4977–5010. [[CrossRef](#)]
30. Todeschini, R.; Consonni, V. *Molecular Descriptors for Chemoinformatics*; Wiley-VCH: Weinheim, Germany, 2009; Volumes I and II.
31. Huang, S.-Y. Comprehensive assessment of flexible-ligand docking algorithms: Current effectiveness and challenges. *Brief. Bioinform.* **2018**, *19*, 982–994. [[CrossRef](#)]
32. Masand, V.H.; Mahajan, D.T.; Nazeruddin, G.M.; Hadda, T.B.; Rastija, V.; Alfeefy, A.M. Effect of information leakage and method of splitting (rational and random) on external predictive ability and behavior of different statistical parameters of QSAR model. *Med. Chem. Res.* **2015**, *24*, 1241–1264. [[CrossRef](#)]
33. Polishchuk, P. Interpretation of Quantitative Structure–Activity Relationship Models: Past, Present, and Future. *J. Chem. Inf. Model.* **2017**, *57*, 2618–2639. [[CrossRef](#)]
34. Golbraikh, A.; Muratov, E.; Fourches, D.; Tropsha, A. Data set modelability by QSAR. *J. Chem. Inf. Model.* **2014**, *54*, 1–4. [[CrossRef](#)] [[PubMed](#)]
35. Li, J.; Gramatica, P. The importance of molecular structures, endpoints' values, and predictivity parameters in QSAR research: QSAR analysis of a series of estrogen receptor binders. *Mol. Divers* **2010**, *14*, 687–696. [[CrossRef](#)] [[PubMed](#)]
36. Zaki, M.E.A.; Al-Hussain, S.A.; Masand, V.H.; Akasapu, S.; Lewaa, I. QSAR and Pharmacophore Modeling of Nitrogen Heterocycles as Potent Human N-Myristoyltransferase (Hs-NMT) Inhibitors. *Molecules* **2021**, *26*, 1834. [[CrossRef](#)] [[PubMed](#)]
37. Zaki, M.E.A.; Al-Hussain, S.A.; Masand, V.H.; Akasapu, S.; Bajaj, S.O.; El-Sayed, N.N.E.; Ghosh, A.; Lewaa, I. Identification of Anti-SARS-CoV-2 Compounds from Food Using QSAR-Based Virtual Screening, Molecular Docking, and Molecular Dynamics Simulation Analysis. *Pharmaceuticals* **2021**, *14*, 357. [[CrossRef](#)]
38. Masand, V.H.; Mahajan, D.T.; Hadda, T.B.; Jawarkar, R.D.; Alafeefy, A.M.; Rastija, V.; Ali, M.A. Does tautomerism influence the outcome of QSAR modeling? *Med. Chem. Res.* **2014**, *23*, 1742–1757. [[CrossRef](#)]
39. Masand, V.H.; Mahajan, D.T.; Gramatica, P.; Barlow, J. Tautomerism and multiple modelling enhance the efficacy of QSAR: Antimalarial activity of phosphoramidate and phosphorothioamidate analogues of amiprofos methyl. *Med. Chem. Res.* **2014**, *23*, 4825–4835. [[CrossRef](#)]
40. Gramatica, P. External Evaluation of QSAR Models, in Addition to Cross-Validation Verification of Predictive Capability on Totally New Chemicals. *Mol. Inform.* **2014**, *33*, 311–314. [[CrossRef](#)]
41. Tropsha, A. Recent trends in statistical QSAR modeling of environmental chemical toxicity. In *Molecular, Clinical and Environmental Toxicology*; Springer: Berlin/Heidelberg, Germany, 2012; Volume 101, pp. 381–411. [[CrossRef](#)]
42. Fourches, D.; Muratov, E.; Tropsha, A. Trust, but verify: On the importance of chemical structure curation in cheminformatics and QSAR modeling research. *J. Chem. Inf. Model.* **2010**, *50*, 1189–1204. [[CrossRef](#)]
43. O'Boyle, N.M.; Banck, M.; James, C.A.; Morley, C.; Vandermeersch, T.; Hutchison, G.R. Open Babel: An open chemical toolbox. *J. Cheminform.* **2011**, *3*, 33. [[CrossRef](#)]
44. Stewart, J.J.P. MOPAC: A semiempirical molecular orbital program. *J. Comput. Aided Mol. Des.* **1990**, *4*, 1–103. [[CrossRef](#)]
45. Masand, V.H.; Rastija, V. PyDescriptor: A new PyMOL plugin for calculating thousands of easily understandable molecular descriptors. *Chemom. Intell. Lab. Syst.* **2017**, *169*, 12–18. [[CrossRef](#)]
46. Yap, C.W. PaDEL-descriptor: An open source software to calculate molecular descriptors and fingerprints. *J. Comput. Chem.* **2011**, *32*, 1466–1474. [[CrossRef](#)]
47. Gramatica, P.; Chirico, N.; Papa, E.; Cassani, S.; Kovarich, S. QSARINS: A new software for the development, analysis, and validation of QSAR MLR models. *J. Comput. Chem.* **2013**, *34*, 2121–2132. [[CrossRef](#)]
48. Martin, T.M.; Harten, P.; Young, D.M.; Muratov, E.N.; Golbraikh, A.; Zhu, H.; Tropsha, A. Does rational selection of training and test sets improve the outcome of QSAR modeling? *J. Chem. Inf. Model.* **2012**, *52*, 2570–2578. [[CrossRef](#)]
49. Kar, S.; Roy, K.; Leszczynski, J. Applicability Domain: A Step Toward Confident Predictions and Decidability for QSAR Modeling. In *Computational Toxicology*; Humana Press: New York, NY, USA, 2018; pp. 141–169.
50. Netzeva, T.I.; Worth, A.; Aldenberg, T.; Benigni, R.; Cronin, M.T.; Gramatica, P.; Jaworska, J.S.; Kahn, S.; Klopman, G.; Marchant, C.A.; et al. Current status of methods for defining the applicability domain of (quantitative) structure-activity relationships. The report and recommendations of ECVAM Workshop 52. *Altern. Lab. Anim. ATLA* **2005**, *33*, 155–173. [[CrossRef](#)]
51. Trott, O.; Olson, A.J. AutoDock Vina: Improving the speed and accuracy of docking with a new scoring function, efficient optimization, and multithreading. *J. Comput. Chem.* **2009**, *31*, 455–461. [[CrossRef](#)]
52. Di Muzio, E.; Toti, D.; Polticelli, F. DockingApp: A user friendly interface for facilitated docking simulations with AutoDock Vina. *J. Comput. Aided Mol. Des.* **2017**, *31*, 213–218. [[CrossRef](#)]



## Article

# Synthesis and Evaluation of Some New 4H-Pyran Derivatives as Antioxidant, Antibacterial and Anti-HCT-116 Cells of CRC, with Molecular Docking, Antiproliferative, Apoptotic and ADME Investigations

Nahed N. E. El-Sayed <sup>1,\*</sup>, Magdi E. A. Zaki <sup>2,\*</sup>, Sami A. Al-Hussain <sup>2</sup>, Abir Ben Bacha <sup>3,4</sup>, Malika Berredjem <sup>5</sup>, Vijay H. Masand <sup>6</sup>, Zainab M. Almarhoon <sup>7</sup> and Hanaa S. Omar <sup>8,9</sup>

- <sup>1</sup> National Organization for Drug Control and Research, Egyptian Drug Authority (EDA), 51 Wezaret El-Zeraa St., Giza 35521, Egypt
  - <sup>2</sup> Department of Chemistry, Faculty of Sciences, Imam Mohammad Ibn Saud Islamic University, Riyadh 13318, Saudi Arabia; sahusain@imamu.edu.sa
  - <sup>3</sup> Biochemistry Department, College of Sciences, King Saud University, Riyadh 11495, Saudi Arabia; aalghanouchi@ksu.edu.sa
  - <sup>4</sup> Laboratory of Plant Biotechnology Applied to Crop Improvement, Faculty of Science of Sfax, University of Sfax, Sfax 3038, Tunisia
  - <sup>5</sup> Laboratory of Applied Organic Chemistry LCOA, Synthesis of Biomolecules and Molecular Modeling Group, Badji-Mokhtar-Annaba University, Annaba 23000, Algeria; mberredjem@yahoo.fr
  - <sup>6</sup> Department of Chemistry, Vidya Bharati College, Amravati 444602, Maharashtra, India; vijaymasand@gmail.com
  - <sup>7</sup> Department of Chemistry, College of Science, King Saud University, Riyadh 11451, Saudi Arabia; zalmarhoon@ksu.edu.sa
  - <sup>8</sup> Department of Genetics, Faculty of Agriculture, Cairo University, Giza 12613, Egypt; hanaa.omar@agr.cu.edu.eg
  - <sup>9</sup> GMO Laboratory, Faculty of Agriculture, Cairo University, Research Park, Giza 12613, Egypt
- \* Correspondence: nnelsayed@gmail.com or nahed.elsayed@edaegypt.gov.eg (N.N.E.E.-S.); mezzaki@imamu.edu.sa (M.E.A.Z.)



**Citation:** El-Sayed, N.N.E.; Zaki, M.E.A.; Al-Hussain, S.A.; Ben Bacha, A.; Berredjem, M.; Masand, V.H.; Almarhoon, Z.M.; Omar, H.S. Synthesis and Evaluation of Some New 4H-Pyran Derivatives as Antioxidant, Antibacterial and Anti-HCT-116 Cells of CRC, with Molecular Docking, Antiproliferative, Apoptotic and ADME Investigations. *Pharmaceuticals* **2022**, *15*, 891. <https://doi.org/10.3390/ph15070891>

Academic Editor: Luis M. T. Frijia

Received: 20 May 2022

Accepted: 2 July 2022

Published: 19 July 2022

**Publisher's Note:** MDPI stays neutral with regard to jurisdictional claims in published maps and institutional affiliations.



**Copyright:** © 2022 by the authors. Licensee MDPI, Basel, Switzerland. This article is an open access article distributed under the terms and conditions of the Creative Commons Attribution (CC BY) license (<https://creativecommons.org/licenses/by/4.0/>).

**Abstract:** Colorectal cancer oncogenesis is linked to dysbiosis, oxidative stress and overexpression of CDK2. The 4H-pyran scaffold is considered an antitumoral, antibacterial and antioxidant lead as well as a CDK2 inhibitor. Herein, certain 4H-pyran derivatives were evaluated as antibacterial, antioxidant and cytotoxic agents against HCT-116 cells. Derivatives **4g** and **4j** inhibited all the tested Gram-positive isolates, except for *B. cereus* (ATCC 14579), with lower IC<sub>50</sub> values (μM) than ampicillin. In addition, **4g** and **4j** demonstrated the strongest DPPH scavenging and reducing potencies, with **4j** being more efficient than BHT. In cell viability assays, **4d** and **4k** suppressed the proliferation of HCT-116 cells, with the lowest IC<sub>50</sub> values being 75.1 and 85.88 μM, respectively. The results of molecular docking simulations of **4d** and **4k**, inhibitory kinase assays against CDK2, along with determination of CDK2 protein concentration and the expression level of CDK2 gene in the lysates of HCT-116 treated cells, suggested that these analogues blocked the proliferation of HCT-116 cells by inhibiting kinase activity and downregulating expression levels of CDK2 protein and gene. Moreover, **4d** and **4k** were found to induce apoptosis in HCT-116 cells via activation of the caspase-3 gene. Lastly, compounds **4g**, **4j**, **4d** and **4k** were predicted to comply with Lipinski's rule of five, and they are expected to possess excellent physicochemical and pharmacokinetic properties suitable for in vivo bioavailability, as predicted by the SwissADME web tool.

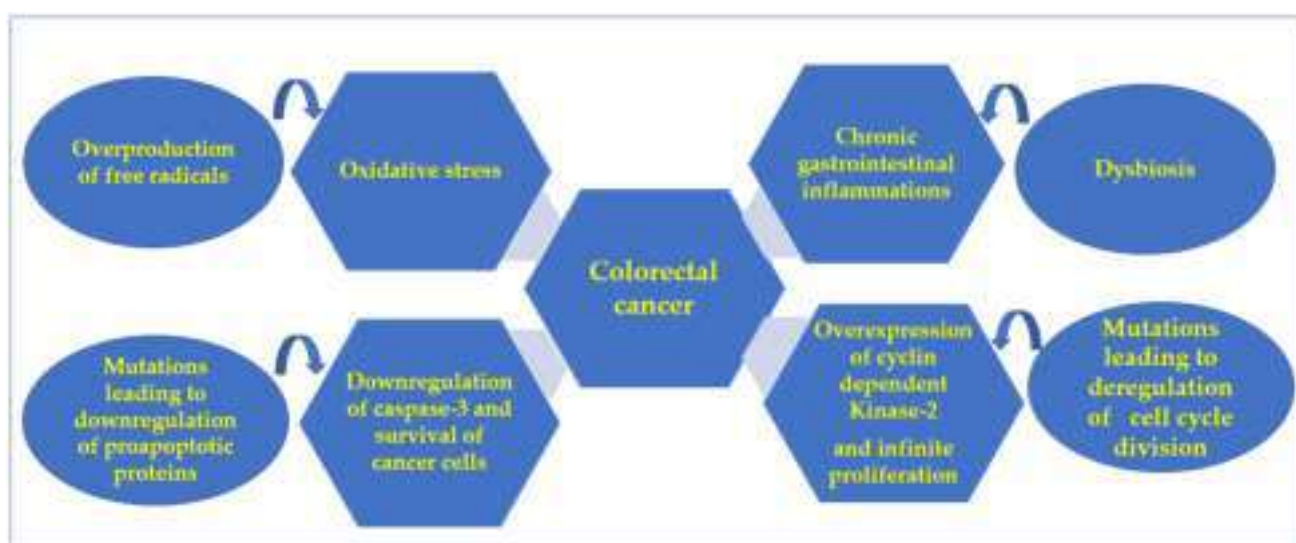
**Keywords:** colorectal cancer; dysbiosis; oxidative stress; 4H-pyran; CDK2; caspases; ADME

## 1. Introduction

Colorectal cancer (CRC) is a huge international health burden. It is currently ranked as the third most common cancer and the fourth most common cause of cancer-related death

globally [1]. According to estimates from GLOBOCAN, in 2020 there were 1.9 million new CRC incident cases and 0.9 million deaths worldwide. The global projections for 2040 of new CRC cases are estimated to reach approximately 3.2 million [2].

Colorectal tumorigenesis is a highly complex process (Figure 1). Although little is known about the exact causes of sporadic cancer (with no family history of genetic predisposition), it is initiated by a number of carcinogenic events, which lead to the accumulation of genetic mutations in oncogenes and tumor suppressor genes, in addition to epigenetic modifications. These events drive the transformation of normal cells into uncontrolled adenomas and eventually to malignant carcinomas [3]. A good understanding of the factors promoting or accompanying these carcinogenic events would enable better policies for prevention and targeted therapy. Oxidative stress and dysbiosis of colon microflora constitute risk factors that drive these carcinogenic events, while deregulation of cell-cycle related proteins is a key feature of all cancer cells [4].



**Figure 1.** Background of this work.

Oxidative stress is caused by an overwhelming production of reactive oxygen species (ROS) accompanied by the downregulation of antioxidant enzymes within the cell. These reactive molecular species may be generated from endogenous sources (intrinsic), including mitochondria, inflammatory cells and several enzymatic cellular complexes. In addition, they can originate from external sources (extrinsic), such as toxins, certain drugs, radiation and tobacco smoking. It is now well established that uncontrolled increased levels of reactive oxygen species contribute to the etiology of CRC via different mechanisms. One mechanism involves lipid peroxidation via attacking polyunsaturated fatty acids, which lead to the production of malonaldehyde, hexanal, acrolein and 4-hydroxy-2-nonenal, all of which are known mutagenic products capable of inducing persistent destabilization of chromosomes [5]. A second mechanism involves DAN modification, which results in mutations particularly in the p53 gene and mitochondrial DNA [5]. A third mechanism comprises induction of chronic inflammatory bowel diseases (IBDs), including, Crohn's disease (CD) and ulcerative colitis (UC) [6]. Moreover, deregulation of ROS is accompanied by the generation of an inflammatory environment, which suppresses apoptosis and activates proliferation and angiogenesis, thus eventually leading to the initiation of neoplastic transformation [7]. In addition, several studies have also proved the involvement of ROS in the migration and invasion of cancerous cells [8]. Furthermore, ROS play a prominent role in chemotherapy resistance toward drugs, such as 5-fluorouracil, vinblastine, doxorubicin and tamoxifen [8]. Consequently, trapping free radicals with antioxidants seems to be a possible approach to prevent inflammation and cancer. Additionally, antioxidants are reported to exhibit anticancer activities through activating immune response, inhibiting angiogenesis, downregulating oncogenes and stimulating tumor suppressor genes [9].

Experimental evidence has established that dysbiosis of certain intestinal bacterial strains can promote chronic gastrointestinal inflammations, which eventually will lead to the development and spread of CRC [10,11]. The Gram-negative strains, *Escherichia coli* [12] and *Klebsiella pneumonia* belong to this class of virulent pathogens [13]. Additionally, certain studies have hypothesized that *Pseudomonas* bacteria are directly pro-oncogenic and promoters for CRC [14].

Additionally, animal model studies have shown that *Enterococcus faecalis* caused colon inflammation after infection, which promoted CRC occurrence [15]. In addition to this, some case studies indicated that the mean copy number of *Enterococcus faecalis* in people with colorectal cancer was significantly higher than in those with polyps and healthy people, which implies the ability of this strain to induce colorectal carcinogenesis [16].

Despite the recent advances in novel chemotherapy, such as immune checkpoint inhibitors, limitations due to chemotherapeutic resistance remain. Many preclinical and clinical studies have shown that microbiota modulate cancer treatment responses via influencing pharmacokinetic properties, such as metabolism, enzymatic degradation and pharmacodynamics (i.e., immunomodulation), in cancer therapy. Therefore, some new insights into cancer treatment are proposed based on manipulating the gut microbiota to augment cancer therapeutic responses [17].

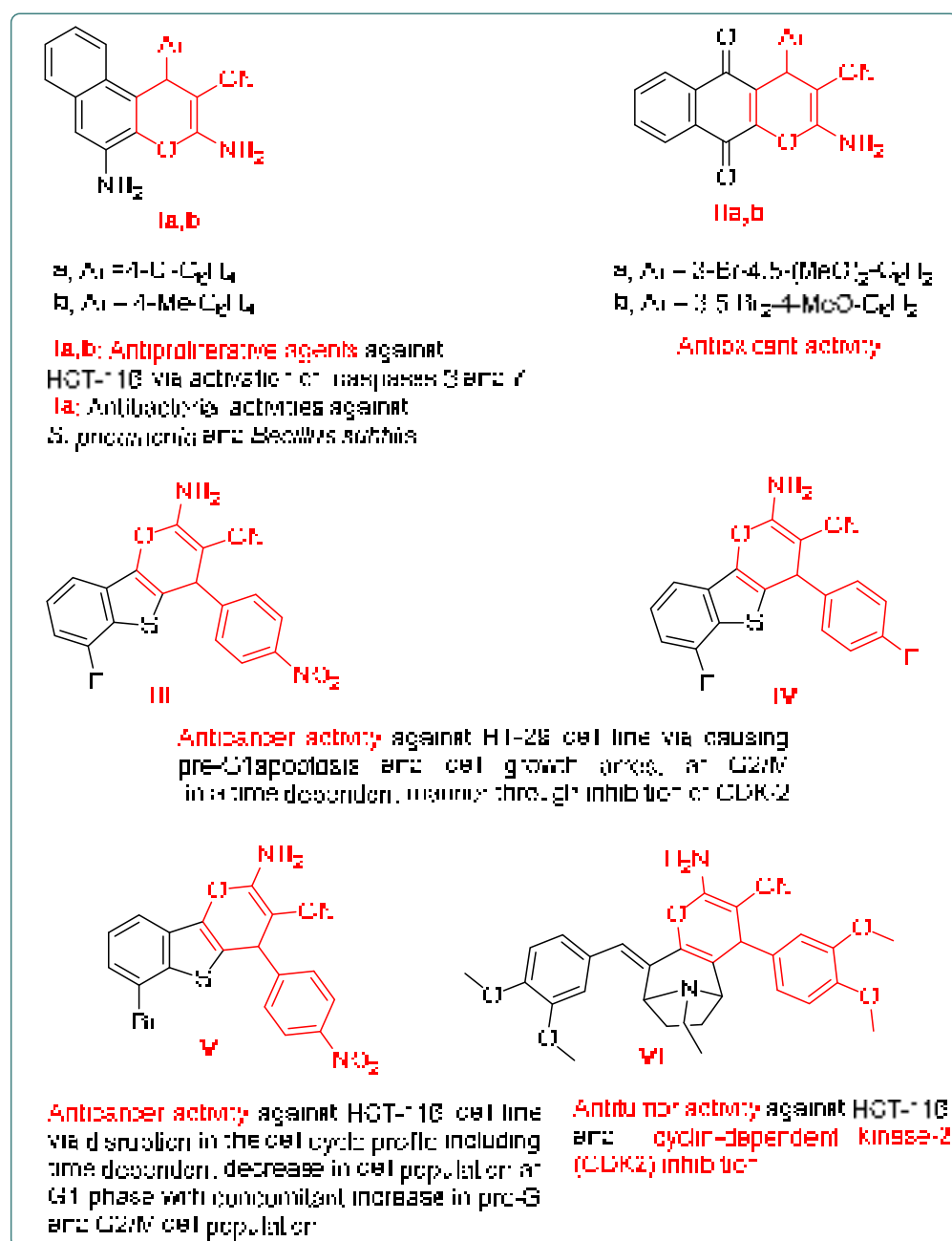
Cancer patients who are undergoing anticancer treatment have severely weakened immune systems; thus, they are more vulnerable to bacterial infections and their life-threatening complications. A previous retrospective surveillance study revealed that the most common associated bacterial pathogens were *Klebsiella pneumonia* and *Enterococcus faecium* (bloodstream), *Pseudomonas aeruginosa* (respiratory tract), *Escherichia coli* (in urinary tract), *Staphylococcus aureus* and *S. epidermidis* (skin and soft tissues) [18]. It is worth noting that some of these microbes are rather difficult to treat, as they are considered to be drug-resistant isolates [19]. Furthermore, several reports have associated antibiotic resistance with oxidative stress [20]. Therefore, molecules exerting antioxidant [21] and/or antibacterial [22] effects would be considered as attractive candidates that could provide protection against the development of CRC and its complications.

Up to 85% of CRC cases exhibit chromosomal instability (CIN), featuring changes in chromosome numbers and structure. CIN affects the expression of tumor-associated genes and/or genes regulating cell-cycle division [23]. Decades of research in diverse fields, including cell biology, yeast genetics, biochemistry and genetic engineering, have identified the regulators of the cell division cycle [24]. Normally, the transitions of the cell cycle of the mammalian cell are strictly mediated by many cyclins and their effectors, cyclin dependent kinases (CDKs), which are a group of conserved serine/threonine protein kinases, each of which regulates a specific stage of the cell cycle [25]. In human cells, 20 CDKs and 29 cyclins have been identified. The CDK family is comprised of CDK1–7 and CDK14–18, which mediate cell-cycle transitions and cell division, whereas CDK8–13 and CDK19–20 regulate gene transcription [26]. Thus, any deregulation in the function or change in the level of these enzymes can result in the induction of tumorigenesis, including CRC [27]. In fact, previous reports have confirmed that the expression of CDK2 is dramatically increased in various colon cancer cell lines [28], including HCT-116, HCT-15 [29], LoVo and DLD-1 [30], compared with “normal” human colon epithelial cells (HCECs). Thus, targeting CDK2 has been recognized as a potential therapeutic approach for colon cancer treatment [31]. In addition, CDK2 inhibitors are likewise expected to have effectiveness in combination with other drugs or where synthetic lethality can be identified [32].

Taken together, the discovery, design and development of novel effective molecules for neutralizing free radicals and eradicating virulent bacterial strains and inhibiting CKD2 are to be considered as preventive and therapeutic approaches against CRC.

Consequently, in a quest to design new chemical compounds to meet all these health needs, the pyran scaffold can be considered a potential synthetic target. The 4*H*-Pyran motif is embedded in bioactive 4*H*-chromene derivatives which display antitumoral and antibacterial effects, such as compounds **Ia,b** [33], and antioxidant activities, such as

derivatives **IIa,b** [34]. Moreover, compelling evidence has indicated that CDK2 is a valid anticancer target of pyran-containing compounds **III–VI**, as shown in Figure 2 [35–37], due to its pro-tumorigenic role via interference with cell division cycle.



**Figure 2.** Examples of pyran-containing compounds with antibacterial [33], antioxidant [34] and anticancer activities via inhibition of CDK2 [35–37].

Synthetically, 4*H*-pyrans and pyrano[2,3-*c*]pyrazoles derivatives are easily accessible, using a variety of catalysts [38,39] at ambient temperature, or under microwave or ultrasound irradiations [40–42]. These compounds are proven to display antibacterial [43–45], antitumoral [46–48] and antioxidant activities [49].

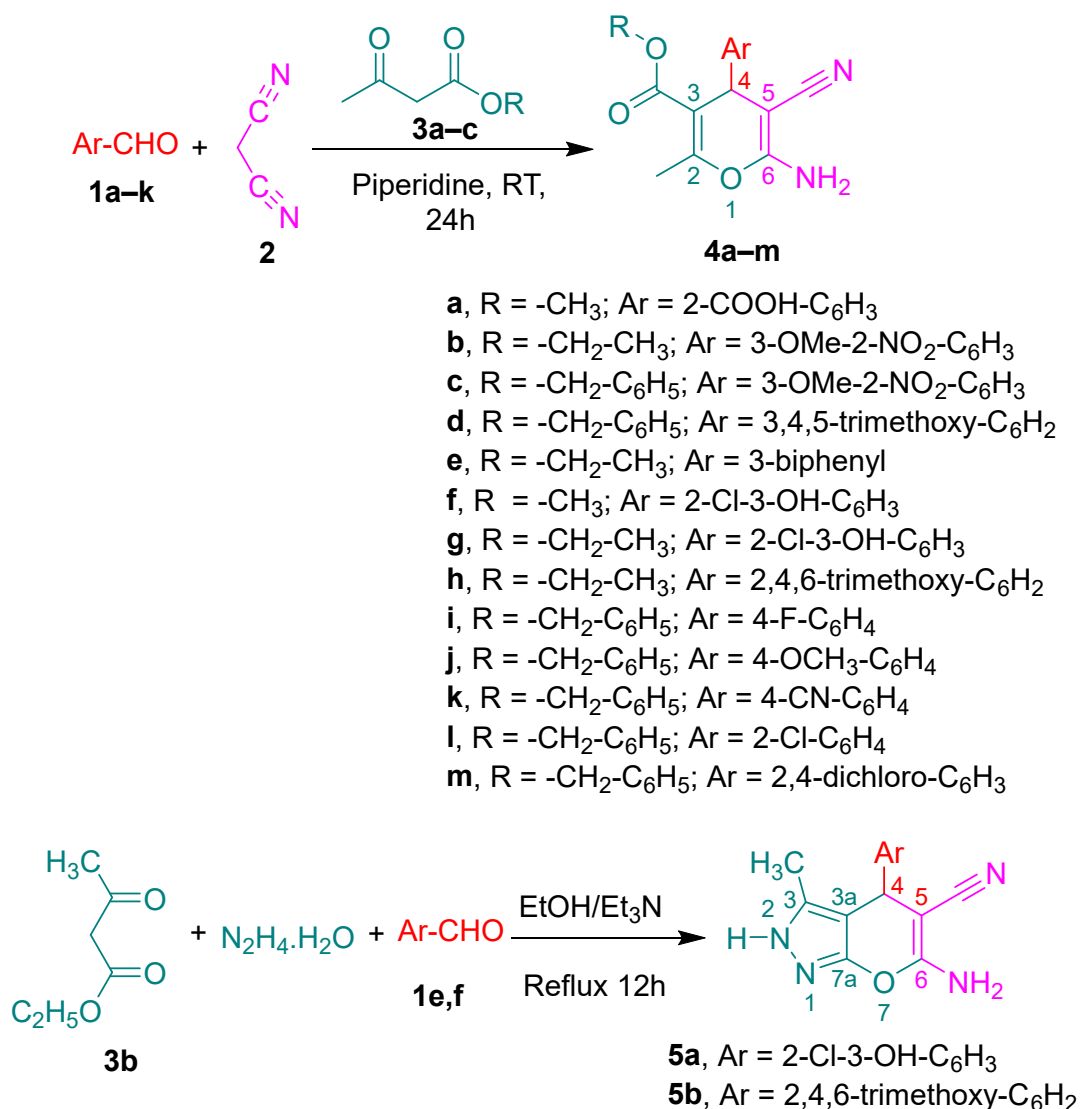
Based on the above-stated facts and in continuation of our research program of anticancer drug discovery, we designed and synthesized some new 4*H*-pyran and pyrano[2,3-*c*]pyrazole derivatives for in vitro biological screening as antioxidant, antibacterial and antiproliferative agents against HCT-116 cells of human colorectal cancer [50,51]. The underlying mechanism of the antiproliferative actions of the promising cytotoxic 4*H*-

pyran derivatives was studied using molecular docking simulations in the ATP binding pocket of CDK2 and through the performance of a CDK2 inhibitory assay. Moreover, the concentration of CDK2 protein and the expression level of CDK2 gene in the lysates of HCT-116 cells treated with the cytotoxic candidates were measured and compared with positive and negative control experiments. Furthermore, quantitative real time PCR experiments for the caspase-3 gene were carried out to investigate the apoptotic activity of these candidates. Lastly, the expected physiochemical and pharmacokinetic properties of the active candidates were predicted using a Lipinski's rule of five filter and BOILED-EGG and bioavailability radar charts.

## 2. Results and Discussion

### 2.1. Chemistry

Initially, the 4*H*-pyran templates **4a–m** were prepared using one-pot, tandem cascade Knoevenagel condensation/Michael addition and cyclization reactions of diverse aryl aldehydes **1a–k**, malononitrile **2** and various  $\beta$ -ketoesters **3a–c** in ethanolic piperidine solutions at room temperature. Similarly, the synthesis of pyrano[2,3-*c*]pyrazole derivatives **5a,b** was efficiently achieved via one-pot, four-component reactions of ethyl acetoacetate **3b**, hydrazine hydrate, aromatic aldehydes **1e,f** and malononitrile **2** under thermal heating and in the presence of ethanol as a solvent and triethyl amine as a catalyst (Scheme 1).



**Scheme 1.** Synthesis of 4*H*-pyrans and 4*H*-pyrano[2,3-*c*]pyrazole derivatives.

The structures of all synthesized compounds were confirmed by their spectroscopic data, in addition to the results of elemental analyses. Thus, the IR spectra of derivatives **4a–m** showed the characteristic stretching absorption bands in the frequency range of  $\nu_{\max}$  (KBr)/ $\text{cm}^{-1}$  3478~3416 (asymmetric vibration— $\text{NH}_2$ ) and 3349~3197 (symmetric vibration— $\text{NH}_2$ ), 2203~2188 ( $\text{C}\equiv\text{N}$ ) and 1724~1689 ( $\text{C}=\text{O}$ ); whereas the IR spectra of **5a,b** indicated the presence of the stretching absorption bands at  $\nu_{\max}$  (KBr)/ $\text{cm}^{-1}$  3377 and 3309 (asymmetric vibration— $\text{NH}_2$ ), 3381 and 3357 (symmetric vibration— $\text{NH}_2$ ), 3159 and 3183 (NH) and 2170 and 2183 ( $\text{C}\equiv\text{N}$ ).

The detailed  $^1\text{H}$ NMR and  $^{13}\text{C}$ NMR analytical data for derivatives **4a–m** and **5a,b** are presented in the experimental section. In addition, the mass spectrum (EI) of each compound displayed the anticipated molecular ion peak. The spectra of some representative examples are provided in the Supplementary Materials.

Finally, the results of the elemental analyses for C, H and N of all the synthesized compounds were found to be within the permissible limits.

## 2.2. Biological Screening

### 2.2.1. Antioxidant Assays

Antioxidants are substances capable of free radical scavenging, quenching singlet oxygen, inactivating peroxides and other reactive oxygen species (ROS), chelating metal ions, quenching secondary oxidation products and inhibiting pro-oxidative enzymes. Therefore, the antioxidant potential of a compound can be evaluated using a variety of chemical assays with different mechanisms [52]. Since the synthesized compounds are electron-rich, with substituents capable of electron donation and H-bond donation as well, in this study, two radical scavenging methods were employed, including the 1,1 diphenyl-2-picrylhydrazyl (DPPH) assay and the ferrous-reducing antioxidant capacity (FRAC) assay.

Initially, the DPPH radical scavenging potency assay was performed at various concentrations of the studied compounds ranging from 0.03 to 1 mg/mL. The  $\text{IC}_{50}$  values for DPPH were calculated from the plot of the scavenging effect against the compound concentration.

The obtained results (Table 1) showed that the compounds **4g**, **4j**, **4l**, **4m** and **4d** exhibited the highest scavenging activity at 1 mg/mL, with scavenging potencies of 90.50, 88.00, 70.20, 69.00 and 65.25 %, respectively, as compared to 95.30 % for BHT. At the same concentration, the remaining compounds demonstrated poor to moderate DPPH radical scavenging activities ranging from 23.25 to 57.10%. Determination of the half-maximal inhibitory concentrations indicated that compounds **4g** and **4j** displayed the most promising free radical scavenging activities, with the lowest  $\text{IC}_{50}$  values of 0.329 and 0.1941 mM, respectively, as compared to BHT, which exhibited 0.245 mM.

Secondly, FRAC was determined over the concentration range of 0.0–1 mg/mL via monitoring  $\text{Fe}^{3+}$ – $\text{Fe}^{2+}$  transformation in the presence of the studied compounds and the reference antioxidant BHT to estimate the values of efficient concentration ( $\text{EC}_{50}$ ), expressed in mM. As depicted in Table 1, the pyrans **4g**, **4j** and BHT exhibited comparable tendencies with respect to their reducing power, with  $\text{EC}_{50}$  values of 0.072, 0.074 and 0.089 mM, respectively, whereas the rest of the tested compounds were less effective, with  $\text{EC}_{50}$  values in the range of 0.149–1.562 mM.

**Table 1.** Antioxidant activities of the studied 4*H*-pyran and 4*H*-pyrano[2,3-*c*]pyrazole derivatives as determined by calculation of IC<sub>50</sub> (mM) and EC<sub>50</sub> (mM) values. Experiments were performed in triplicate and are reported as the means ± standard deviations.

Comp. No.	IC <sub>50</sub> (mM) for DPPH Scavenging Potency	DPPH Radical Scavenging Efficiency (%) at 1 mg/mL	Reducing Power EC <sub>50</sub> (mM)
4a	2.291 ± 0.134	24.15 ± 1.62	0.827 ± 0.045
4b	2.560 ± 0.117	23.25 ± 1.06	1.197 ± 0.079
4c	2.243 ± 0.050	57.10 ± 1.56	1.234 ± 0.067
4d	0.504 ± 0.032	65.25 ± 1.77	0.149 ± 0.016
4e	1.651 ± 0.097	39.25 ± 1.06	0.305 ± 0.039
4f	3.336 ± 0.131	43.75 ± 1.77	0.398 ± 0.045
4g	0.329 ± 0.042	90.50 ± 2.12	0.072 ± 0.004
4h	1.309 ± 0.075	33.50 ± 2.12	0.221 ± 0.011
4i	1.784 ± 0.115	26.05 ± 1.06	0.274 ± 0.039
4j	0.194 ± 0.011	88.00 ± 1.41	0.074 ± 0.004
4k	1.050 ± 0.075	40.55 ± 2.19	1.562 ± 0.102
4l	0.919 ± 0.026	70.20 ± 1.70	0.801 ± 0.019
4m	0.421 ± 0.017	69.0 ± 2.83	0.506 ± 0.034
5a	0.826 ± 0.092	45.50 ± 2.12	0.363 ± 0.047
5b	1.781 ± 0.082	37.50 ± 2.12	0.467 ± 0.041
BHT	0.245 ± 0.027	95.30 ± 0.42	0.089 ± 0.003

### 2.2.2. Antibacterial Assays

The results for the *in vitro* antibacterial properties of the synthesized compounds against five Gram-positive and four Gram-negative human-pathogenic strains, which were assessed by both the agar diffusion method (based on inhibition zone (IZ)) and the broth dilution bioassay (for the determination of the half-maximal inhibitory concentration (IC<sub>50</sub>) values), using ampicillin as the reference antibiotic drug, are shown in Tables 2 and 3.

Some of the tested compounds were found to be more effective against Gram-positive bacteria than Gram-negative isolates by producing larger IZs and lowering IC<sub>50</sub> against certain strains. Reduced sensitivity against Gram-negative pathogens can be attributed to the restricted permeability of the chemical inhibitors across their cell walls due to the existence of an outer cell envelope, which acts as a selective barrier [53].

The results against Gram-positive strains identified compound 4g as the most active agent against *B. subtilis* (ATCC 6633), with a lowered IC<sub>50</sub> value (25.69 μM) and a bigger inhibition zone of 28.00 mm, compared to the results obtained for ampicillin: IC<sub>50</sub> = 37.20 μM, IZ = 25.50 mm. Despite pyrans 4f, 4i, 4j, 4l and 4m displaying lower IC<sub>50</sub> values (ranging from 36.79 to 23.64 μM), their IZs were bigger, in the range of 21.50 (4j) to 9.50 mm (4i).

Considering *S. aureus* (ATCC 25923) and *S. epidermidis* (ATCC 14990), bigger IZs (mm) were displayed by 4g (27.50, 29.75) and 4j (25.25, 26.65) as compared to the results of 21.50, 22.50 obtained for ampicillin, respectively. In addition, these derivatives exhibited lowered IC<sub>50</sub> (μM) values (4g: 27.78, 30.32) and (4j: 33.34, 33.34) as compared to 38.64 and 50.09 produced by ampicillin against these isolates, respectively.



**Table 2.** Antibacterial evaluation of the studied compounds against some Gram-positive bacterial strains by measurement of the diameters of the inhibition zones (IZs, mm) and determination of the half-maximal inhibitory concentrations (IC<sub>50</sub>s, µM). Ampicillin was used as the reference antibiotic. Results were obtained from three independent experiments.

Comp. No.	<i>B. cereus</i> (ATCC 14579)		<i>B. subtilis</i> (ATCC 6633)		<i>E. faecalis</i> (ATCC 29122)		<i>S. aureus</i> (ATCC 25923)		<i>S. epidermidis</i> (ATCC 14990)	
	IZ (mm)	IC <sub>50</sub> (µM)	IZ (mm)	IC <sub>50</sub> (µM)	IZ (mm)	IC <sub>50</sub> (µM)	IZ (mm)	IC <sub>50</sub> (µM)	IZ (mm)	IC <sub>50</sub> (µM)
4a	7.50 ± 0.71	71.75 ± 2.04	5.20 ± 0.28	64.43 ± 3.37	9.00 ± 1.41	49.64 ± 1.81	8.00 ± 1.41	41.20 ± 2.48	9.50 ± 0.71	42.32 ± 1.33
4b	16.50 ± 0.71	43.14 ± 1.98	19.50 ± 0.71	49.12 ± 1.39	15.50 ± 0.71	56.77 ± 1.59	20.50 ± 0.71	50.23 ± 1.39	23.50 ± 0.71	32.42 ± 1.39
4c	14.00 ± 1.41	44.50 ± 0.83	11.00 ± 1.41	46.27 ± 1.68	10.00 ± 1.41	41.05 ± 2.18	15.50 ± 0.71	37.01 ± 2.02	16.65 ± 0.50	30.37 ± 1.00
4d	9.50 ± 0.71	39.52 ± 0.80	12.00 ± 1.41	40.32 ± 1.95	14.50 ± 0.71	29.10 ± 2.27	9.00 ± 1.41	24.40 ± 1.15	8.50 ± 0.71	26.69 ± 1.15
4e	23.00 ± 1.41	33.57 ± 1.58	20.50 ± 0.71	37.73 ± 1.58	15.50 ± 0.71	37.32 ± 2.16	16.50 ± 2.10	34.82 ± 2.16	20.50 ± 2.12	30.80 ± 1.58
4f	22.50 ± 0.71	42.40 ± 2.65	19.50 ± 0.71	36.79 ± 0.87	19.00 ± 1.41	34.61 ± 0.59	16.50 ± 0.71	38.35 ± 1.31	14.50 ± 0.71	33.05 ± 2.65
4g	29.00 ± 1.41	29.42 ± 1.49	28.00 ± 1.41	25.69 ± 1.70	24.50 ± 0.71	31.82 ± 1.49	27.50 ± 0.71	27.78 ± 1.25	29.75 ± 0.35	30.32 ± 1.49
4h	4.50 ± 0.71	46.48 ± 1.52	6.00 ± 1.41	50.08 ± 2.83	8.00 ± 1.41	45.94 ± 0.75	17.50 ± 0.71	32.72 ± 0.93	16.50 ± 0.71	35.79 ± 1.52
4i	14.50 ± 0.71	38.01 ± 1.37	9.50 ± 0.71	31.56 ± 1.95	6.50 ± 0.71	37.46 ± 1.37	9.50 ± 2.12	40.21 ± 1.37	11.50 ± 0.71	45.97 ± 0.96
4j	24.50 ± 0.71	27.63 ± 1.51	21.50 ± 0.71	23.64 ± 0.37	23.20 ± 0.57	28.16 ± 1.51	25.25 ± 1.06	33.34 ± 1.70	26.65 ± 0.92	33.34 ± 1.70
4k	7.00 ± 1.41	48.06 ± 1.35	4.50 ± 0.71	42.14 ± 2.48	5.50 ± 0.71	45.37 ± 0.57	5.75 ± 0.35	43.89 ± 0.57	4.50 ± 0.71	50.22 ± 2.48
4l	10.00 ± 1.41	33.22 ± 2.42	11.50 ± 0.71	32.56 ± 1.50	6.00 ± 1.41	37.81 ± 1.50	9.00 ± 1.41	31.12 ± 0.55	10.50 ± 0.71	33.35 ± 1.10
4m	18.50 ± 0.71	35.76 ± 1.20	21.50 ± 0.71	32.75 ± 2.05	20.50 ± 0.71	35.28 ± 2.22	17.50 ± 0.71	33.23 ± 1.01	18.50 ± 0.71	35.04 ± 1.88
5a	12.50 ± 0.71	62.43 ± 0.46	12.50 ± 0.71	62.43 ± 0.46	10.50 ± 0.71	51.86 ± 1.39	14.00 ± 1.40	43.93 ± 1.39	13.50 ± 0.71	54.84 ± 1.88
5b	8.00 ± 1.41	42.65 ± 1.66	8.50 ± 0.71	41.77 ± 1.23	9.75 ± 1.06	45.13 ± 1.87	5.50 ± 0.71	39.14 ± 1.66	6.60 ± 0.57	50.05 ± 0.61
<b>Ampicillin</b>	23.50 ± 0.71	25.76 ± 0.57	25.50 ± 0.71	37.20 ± 1.43	24.50 ± 0.71	36.49 ± 3.03	21.50 ± 0.71	38.64 ± 2.00	22.50 ± 0.71	50.09 ± 3.43

**Table 3.** Antibacterial evaluation for the studied compounds against some Gram-negative bacterial strains by measurement of the diameters of the inhibition zones (IZs, mm) and determination of the half-maximal inhibitory concentrations (IC<sub>50</sub>s, µM). Ampicillin was used as the reference antibiotic. Results were obtained from three independent experiments.

Comp. No.	<i>E. coli</i> (ATCC 25966)		<i>K. pneumonia</i> (ATCC 700603)		<i>P. aeruginosa</i> (ATCC 27853)		<i>S. enteric</i> (ATCC 43972)	
	IZ (mm)	IC <sub>50</sub> (µM)	IZ (mm)	IC <sub>50</sub> (µM)	IZ (mm)	IC <sub>50</sub> (µM)	IZ (mm)	IC <sub>50</sub> (µM)
4a	4.5 ± 0.71	138.41 ± 6.68	2.5 ± 0.7	131.09 ± 3.50	5.5 ± 0.7	37.6 ± 0.5	4.5 ± 0.7	119.63 ± 1.91
4b	2.5 ± 0.71	100.19 ± 3.90	1.5 ± 0.7	99.07 ± 2.50	2.5 ± 0.7	84.05 ± 5.01	1.5 ± 0.7	118.14 ± 3.34
4c	2.5 ± 0.71	93.74 ± 4.98	3.5 ± 0.7	112.25 ± 1.42	7.5 ± 0.7	85.90 ± 2.61	8.5 ± 0.7	100.26 ± 2.61
4d	3.5 ± 0.71	88.67 ± 2.52	4.5 ± 0.7	72.63 ± 0.69	6.5 ± 0.7	67.36 ± 1.37	7.0 ± 0.0	65.77 ± 2.29
4e	2.7 ± 0.35	103.22 ± 3.05	2.5 ± 0.7	90.73 ± 2.78	4.5 ± 0.7	87.96 ± 2.78	3.5 ± 0.7	96.14 ± 2.50
4f	7.5 ± 0.71	95.72 ± 5.61	4.5 ± 0.7	82.00 ± 3.43	6.0 ± 1.4	104.76 ± 2.81	6.5 ± 0.7	94.16 ± 3.43
4g	11.0 ± 1.41	61.84 ± 5.38	11.5 ± 0.7	61.84 ± 2.99	13.5 ± 0.7	54.07 ± 4.48	11.5 ± 0.7	53.02 ± 3.29
4h	1.5 ± 0.71	114.05 ± 0.80	3.5 ± 0.7	118.33 ± 2.67	4.5 ± 0.7	89.48 ± 2.94	5.5 ± 0.7	111.65 ± 2.94
4i	5.5 ± 0.71	82.57 ± 1.65	6.5 ± 0.7	79.86 ± 3.02	8.5 ± 0.7	62.02 ± 2.20	8.0 ± 1.4	91.52 ± 2.74
4j	10.5 ± 0.71	57.12 ± 0.80	12.0 ± 1.4	48.35 ± 3.99	14.5 ± 0.7	49.68 ± 4.78	14.5 ± 0.7	51.81 ± 2.92
4k	4.5 ± 0.71	80.24 ± 4.31	2.5 ± 0.7	77.82 ± 2.96	3.5 ± 0.7	73.24 ± 3.50	2.5 ± 0.7	75.53 ± 2.42
4l	3.5 ± 0.7	90.07 ± 2.63	2.5 ± 0.7	77.46 ± 7.08	4.5 ± 0.7	72.74 ± 2.63	4.0 ± 0.0	77.60 ± 1.58
4m	5.5 ± 0.71	69.35 ± 2.89	6.5 ± 0.7	66.70 ± 2.41	9.5 ± 0.7	60.92 ± 2.17	8.5 ± 0.7	61.77 ± 2.17
5a	2.8 ± 0.21	109.67 ± 5.95	6.0 ± 1.4	96.46 ± 4.96	5.5 ± 0.7	85.89 ± 3.30	4.5 ± 0.7	104.72 ± 1.32
5b	3.5 ± 0.71	116.84 ± 4.09	4.5 ± 0.7	109.54 ± 1.75	6.5 ± 0.7	92.30 ± 1.46	7.5 ± 0.7	106.03 ± 2.92
Ampicillin	23.5 ± 0.71	57.96 ± 4.87	21.0 ± 1.4	32.91 ± 2.29	21.5 ± 0.7	41.50 ± 1.72	19.5 ± 0.7	14.88 ± 0.34

Moreover, derivative **4b** selectively exerted a larger IZ (23.50 mm) and a lower IC<sub>50</sub> value (32.42 µM) against *S. epidermidis*, whereas compounds **4a**, **4c**, **4d**, **4e**, **4f**, **4l**, **4m** and **5b** inhibited it, with lowered IC<sub>50</sub> values (µM) spanning from 50.05 (**5b**) to 26.69 (**4d**), though they displayed smaller inhibition zones than the reference, ranging from 6.60 (**5b**) to 20.50 (**4e**). Therefore, *S. epidermidis* can be considered the most sensible strain to the synthesized compounds. Similarly, compounds **4c**, **4d**, **4e**, **4f**, **4h**, **4l** and **4m** suppressed the growth of *S. aureus*, with lowered IC<sub>50</sub> values spanning from 24.40 (**4d**) to 38.35 (**4f**) and smaller IZs ranging from 9.00 (**4d** and **4l**) to 17.50 (**4m** and **4h**).

With regard to *E. faecalis* (ATCC 29122), pyran **4g** and the standard drug produced equal inhibition zones of 24.50 mm; however, **4g** was capable of exhibiting a lowered IC<sub>50</sub> value of 31.82 µM in comparison with that of 36.49 µM for ampicillin.

Contrarily, pyrans **4d**, **4f**, **4j** and **4m** showed lower inhibition zones, ranging from 14.50 (**4d**) to 23.20 mm (**4j**), and lower IC<sub>50</sub> values, ranging from 28.16 (**4j**) to 35.28 µM (**4m**), than ampicillin.

Lastly, although the same compounds **4g** and **4j** exerted the biggest inhibition zones of 29.00 and 24.50 mm relative to that of 23.50 mm exerted by ampicillin against *B. cereus*, they exhibited higher IC<sub>50</sub> values (29.42 and 27.63 µM, respectively) as compared to ampicillin (25.76 µM).

Collectively, **4g** showed promising antibacterial efficiency (lower IC<sub>50</sub> values and bigger IZs) against all of the tested isolates as compared to the reference antibiotic, except for *B. cereus*, which was the microbe least sensitive to the synthesized compounds. Similarly, **4j** was very effective against *S. aureus* (ATCC 25923) and *S. epidermidis* (ATCC 14990).

Contrarily, the anti-Gram-negative evaluation revealed that none of the studied compounds was capable of inhibiting the microbes with bigger IZs or lower IC<sub>50</sub> values, except for **4a**, which inhibited *P. aeruginosa* (ATCC 27853), with an IC<sub>50</sub> of 37.6 µM, which is lower than those of ampicillin (41.50 µM) and **4j**, which suppressed *E. coli* (ATCC 25966) by a comparable concentration of 57.12 µM to that of ampicillin (57.96 µM).

Furthermore, the lowest IC<sub>50</sub> values against *K. pneumonia* (ATCC 700603) and *S. enteric* (ATCC 43972) were displayed by the derivatives **4g** (61.84 and 54.07 µM) and **4j** (48.35 and 49.68 µM) as compared to 32.91 and 41.50 µM, respectively, for ampicillin.

In summary, although none of the tested compounds showed significant activities against Gram-negative microbes, the observed anti-Gram-positive potential of compounds **4g** and **4j** is of great significance. This is due to the fact that Gram-positive strains are reported to be common causes of bloodstream, skin, soft-tissue and intra-abdominal in-

fections [54], which result in severe manifestations, such as sepsis [55] and/or endocarditis [56], especially in immunosuppressed cancer patients. Furthermore, recent reports have indicated that some of these bacterial isolates showed multidrug-resistant profiles [57], particularly *E. faecalis* and *S. aureus*, which amplify their serious complications and increase health care expenditures.

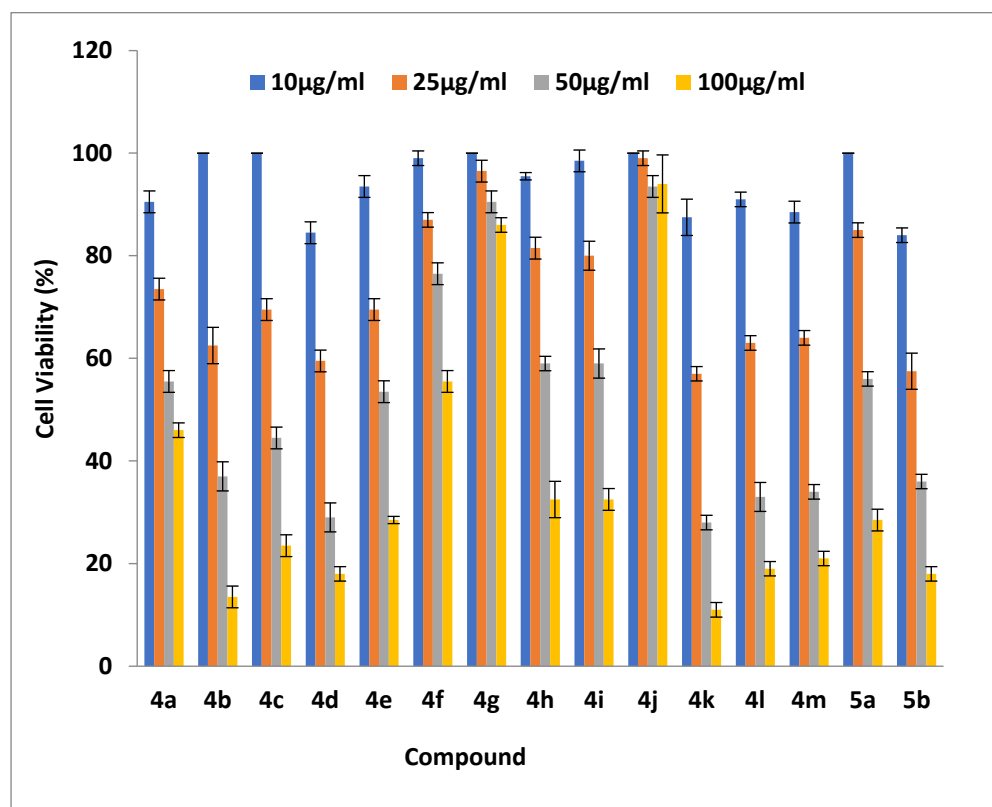
The observed broad-spectrum anti-Gram-positive profiles of **4g** and **4j** as compared to the other analogues can be attributed to their improved antioxidant capabilities. Indeed, the positive correlation between these two activities is well-documented. Catechin, which is a well-known potent free radical scavenger, has been reported to display anti-Gram positive and anti-Gram negative activities as well. Several mechanisms have been reported to account for the toxicity of catechin towards bacteria. Oxidative damage through membrane permeabilization was found to be the inhibitory mechanism of catechin against *B. subtilis* [58]. In addition, some experimental data showed a significant decrease in superoxide dismutase (SOD) and catalase (CAT) activity after treatment of the Gram-positive *S. aureus* strain with catechin at its minimum inhibitory concentration (MIC). These inhibitions could be attributed to the capability of catechin as an antioxidant agent to chelate the metal cofactors (Zn, Fe and Mn) at SOD catalytic sites [59]. Inhibiting superoxide dismutase would increase the bacterial sensitivity to the reactive oxygen species, resulting in inhibition of bacterial growth [60]. Other alternative proposals for the bactericidal actions of catechin include its ability to generate hydrogen peroxide, which causes cell membrane damage [61]. Hydrogen peroxide generation by antioxidants was reportedly attributable to antioxidant autoxidation in culture media [62]. In the view of the aforementioned facts, it can be suggested that the antibacterial effects of the antioxidant candidates **4g** and **4j** might be attributed to one or more of the indicated mechanisms, which could be investigated in future.

### 2.2.3. Cell Viability Assays

The synthesized compounds were also examined at four concentrations (10, 25, 50 and 100 µg/mL) for their cytotoxic effects on human colorectal cancer HCT-116 cells after their incubation together for 24 h. The results, which were expressed in terms of percent of viable cells at each concentration as plotted in Figure 3, revealed that analogs **4g** and **4j** were not able to inhibit the growth of the cancerous cells, even at the highest used concentration (100 µg/mL). Conversely, they displayed the highest detectable percentages of viable cells: 86.0 and 94.0% at 100 µg/mL, respectively. Meanwhile, eleven compounds, namely, **4k**, **4b**, **4d**, **6b**, **4l**, **4m**, **4c**, **4e**, **5a**, **4h** and **4i**, exhibited potent cytotoxic activity at a concentration of 100 µg/mL by reducing cells viability to the extent of 11.0–32.5. The remaining compounds in this series, namely, **4a** and **4f**, displayed the least cytotoxic effects with percent cell viability measures of 46.0 and 55.5, respectively.

Based on these results, the IC<sub>50</sub> values for the promising cytotoxic candidates were determined, as shown in Table 4.

The calculated IC<sub>50</sub> values (µM) ranged from 75.10 (**4d**) to 332.59. The smallest median concentrations were exhibited by compounds **4d** (75.10), **4k** (85.88), **4m** (89.33), **4l** (93.35) and **5b** (97.91).



**Figure 3.** Cytotoxic potency of the studied compounds on HCT-116 cells expressed as percentages of viable cells at 10, 25, 50 and 100 µg/mL concentrations. Results were obtained from three independent experiments.

**Table 4.** IC<sub>50</sub> values of cytotoxicity for the studied 4*H*-pyran and pyrano[2,3-*c*]pyrazole derivatives on HCT-116 cells expressed in µg/mL and µM. Experiments were performed in triplicate and are reported as the means ± standard deviations.

Comp. No.	Mean IC <sub>50</sub> (µg/mL)	Mean IC <sub>50</sub> (µM)
4a	51.99 ± 4.54	165.43 ± 14.44
4b	36.51 ± 3.18	101.60 ± 8.83
4c	43.01 ± 2.03	102.07 ± 4.82
4d	32.78 ± 2.22	75.10 ± 5.09
4e	49.71 ± 3.53	137.92 ± 9.78
4f	106.67 ± 4.29	332.59 ± 13.38
4g	ND <sup>1</sup>	ND <sup>1</sup>
4h	69.21 ± 4.29	184.89 ± 11.46
4i	65.95 ± 4.53	180.99 ± 12.42
4j	ND <sup>1</sup>	ND <sup>1</sup>
4k	31.90 ± 2.83	85.88 ± 7.61
4l	35.55 ± 1.77	93.35 ± 4.63
4m	37.10 ± 2.10	89.33 ± 5.05
5a	60.00 ± 3.28	189.21 ± 10.84
5b	33.52 ± 2.42	97.91 ± 7.06

<sup>1</sup> ND: Not determined.

#### 2.2.4. Investigation of the Underlying Mechanism of Action for the Antiproliferative Candidates

##### 2.2.4.1. Molecular Docking Simulations against CDK2 as a Potential Molecular Target

The molecular docking approach has become a powerful tool for identifying compounds showing potential anticancer activity against a specific target and with a selective

inhibition mechanism [63]. Cancer is increasingly viewed as a cell-cycle disease. Cyclin-dependent kinases (CDKs) are a crucial protein family involved in cell proliferation through regulating the progression of the cell cycle and transcription. Animal model studies and molecular analyses of human tumors have indicated that many of these regulators are altered in cancer, particularly, CDK4, CDK6 and CDK2 and their substrates, which control progression through the G1/S phases of cell-cycle division. A literature survey confirmed that CDK2 is a valid target for 4*H*-pyran derivatives (Figure 2) with anticancer activities [33–37]. Therefore, to investigate whether or not the cellular mechanism by which the most active cytotoxic derivatives **4d** and **4k** suppressed the proliferation of HCT-116 cells is related to the inhibition of CDK2, the induced-fit docking approach in the ATP active site of the enzyme using the Glide program of Schrodinger-Maestro 11.2 was employed prior to the in vitro inhibitory kinase assays. The ATP-binding pocket of CDK2 is considered to be the site most commonly targeted by the kinase inhibitors. They compete with ATP to bind at the kinase site by forming hydrogen bonds with backbone amino acid residues and by establishing hydrophobic interactions with side chains of surrounding residues [64], leading to the inhibition of kinase phosphorylation and suppression of CDK2 hyperactivation, thus, holding back infinite cell proliferation [65].

In this study, the docking procedures were initially validated using redocking approach. Thus, the CDK2-inhibitor 4-[3-hydroxyanilino]-6,7-dimethoxyquinazoline (co-crystallized ligand, **DTQ**) was removed, after which it was redocked to reproduce the reported complex (PDB code: 1DI8). The significant residues in the active site of the protein are Lys33, Glu51 and Asp145. Figure 4 shows the superimposition of the predicted and the co-crystal structure of the reference inhibitor in the ATP active site of the protein. Moreover, the value of the root-mean-square deviation (RMSD) between the redocked conformation of **DTQ** and that observed in the X-ray crystallographic complex was found to be 0.34 Å, which is less than the cutoff value (2 Å) for the correct docking procedures. These observations confirmed that the redocked ligand was closely bound to the true conformation, indicating the reliability of the docking protocols.

Afterwards, a comparative in silico molecular modeling study using the most active cytotoxic derivatives **4d** and **4k**, along with the least active analogue, **4f**, and the well-known CDK2 inhibitor **BMS-265246**, which was used in the in vitro inhibitory kinase assays, as well as the co-crystallized ligand (**DTQ**), was performed. Upon completion of each docking calculation, a maximum of 100 poses per ligand were generated and the final best-docked conformations were ranked using an XP Glide score function and Glide energy.

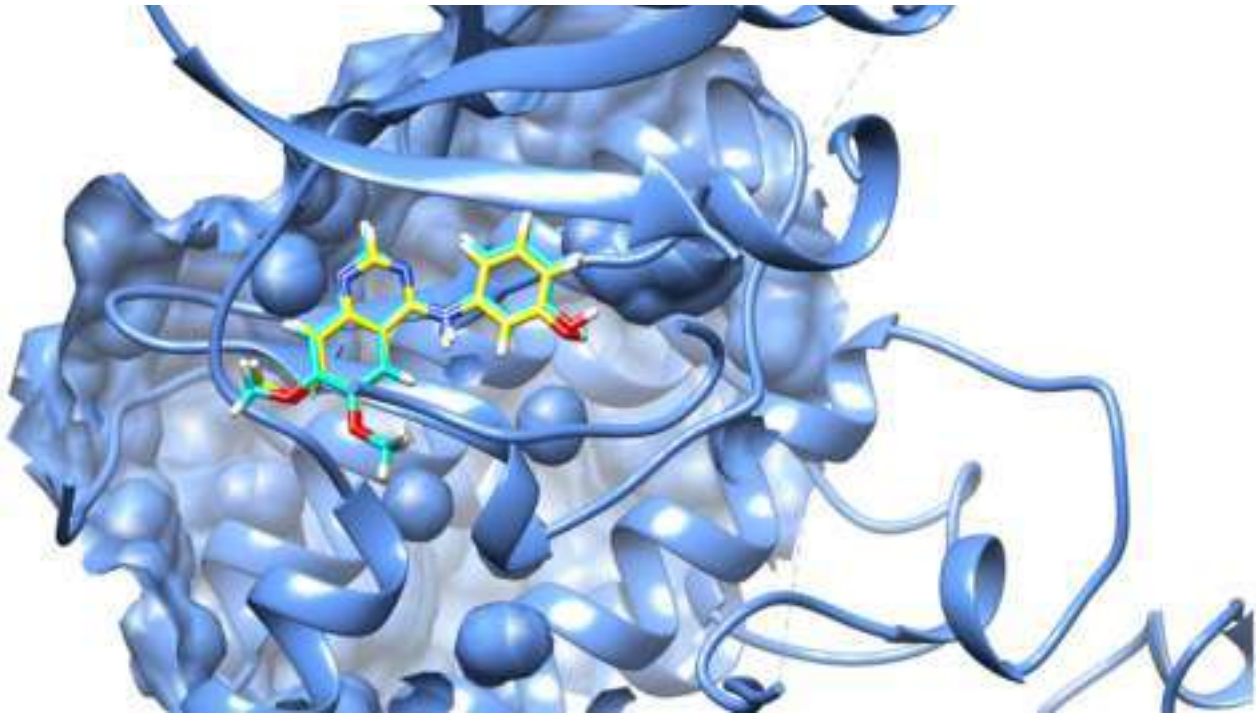
According to the data presented in Table 5, the cocrystal ligand **DTQ** and **BMS-265246** showed better scoring functions than the synthesized compounds. Both **4d** and **4k** showed high affinity to the target protein, with **4d** demonstrating comparable binding strength (Glide energy = −48.700 Kcal/mol) to the co-crystal ligand (Glide energy = −49.122 Kcal/mol) and **BMS-265246** (Glide energy = −47.340 Kcal/mol), whereas the inactive analog **4f** exhibited the lowest affinity to the enzyme with the highest Glide energy value (−30.726 Kcal/mol).

Lastly, the lowest-energy docked complexes of the co-crystallized ligand **DTQ**, the reference inhibitor **BMS-265246**, **4d**, **4k** and **4f** with the protein were used to identify the crucial interactions for inhibition of CDK2. The ligand–protein interactions (hydrogen bonds, as well as hydrophobic interactions) are shown in Figures 5–14.

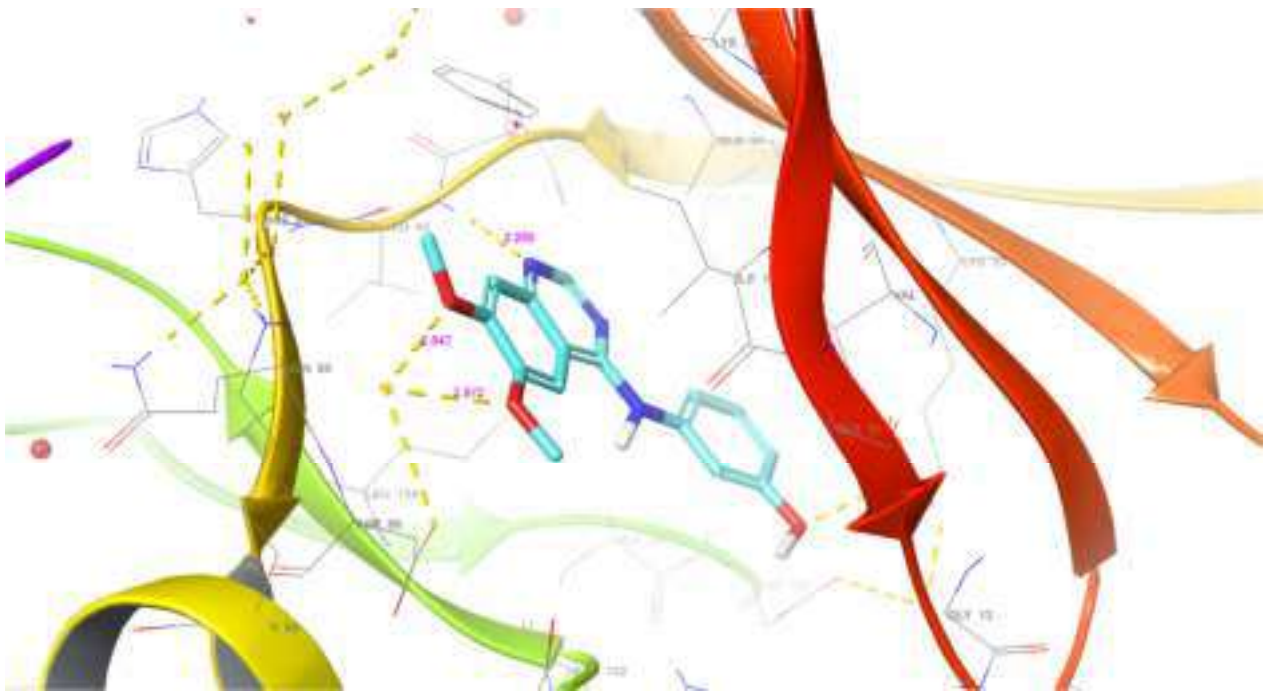
**Table 5.** Binding free energy of **4d**, **4k**, **4f**, **BMS-265246** and **DTQ** at the active site of CDK2.

Ligands	Glide Score XP	Glide Energy Kcal/mol
<b>4k</b>	−6.383	−43.311
<b>4d</b>	−6.224	−48.700
<b>4f</b>	−4.160	−30.726
<b>Co-crystallized ligand (DTQ<sup>1</sup>)</b>	−9.649	−49.122
<b>BMS-265246</b>	−7.187	−47.340

<sup>1</sup> **DTQ**: 4-[3-hydroxyanilino]-6,7-dimethoxyquinazoline.



**Figure 4.** Redocked (yellow) and co-crystallized (baby blue) ligand (DTQ) in the ATP binding pocket of CDK2 after self-docking calculations.



**Figure 5.** Three-dimensional binding interactions of DTQ within the ATP binding pocket of CDK2. Hydrogen bonds (yellow dotted lines), hydrogen atoms (white), nitrogen atoms (blue), and oxygen atoms (red).

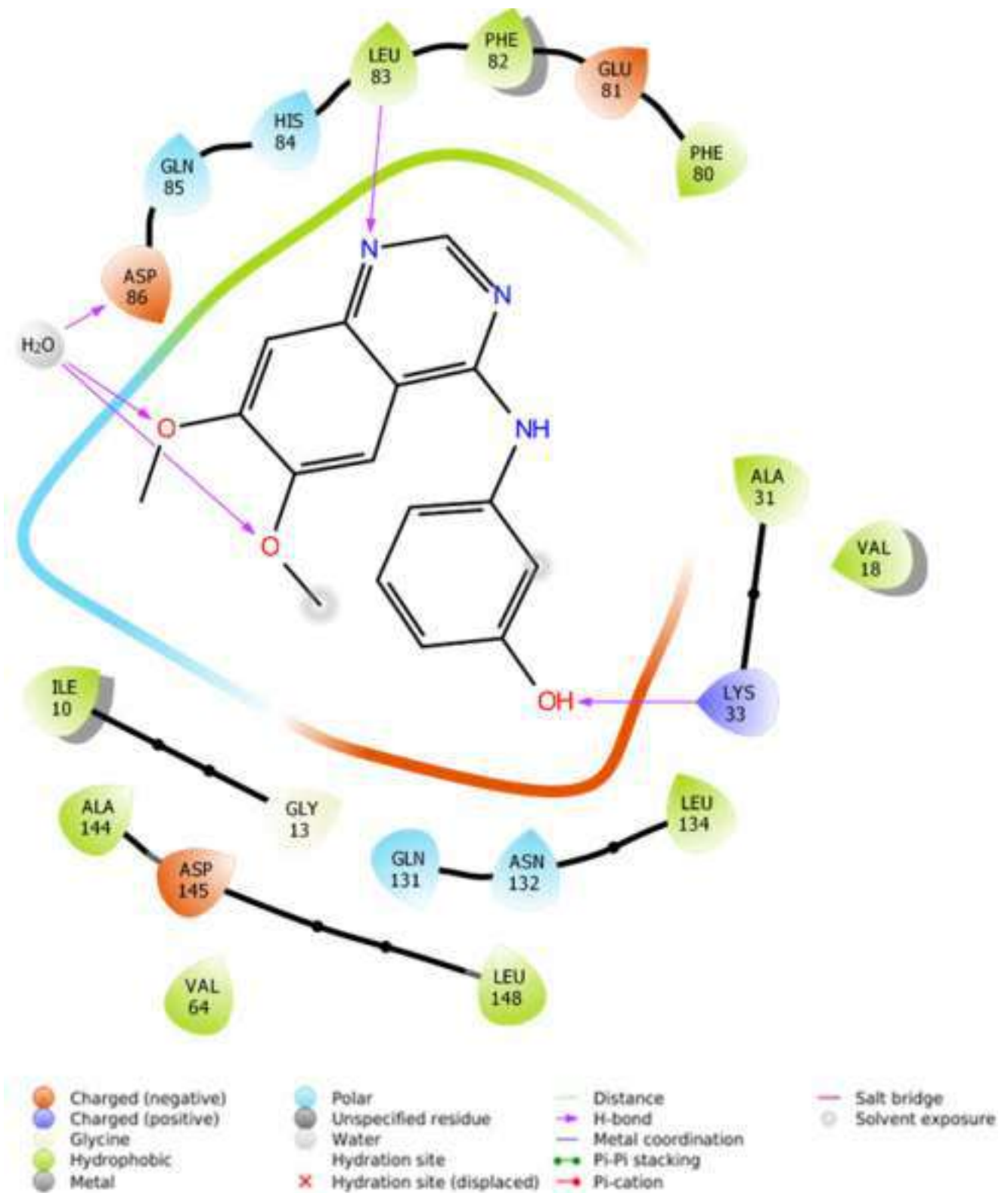
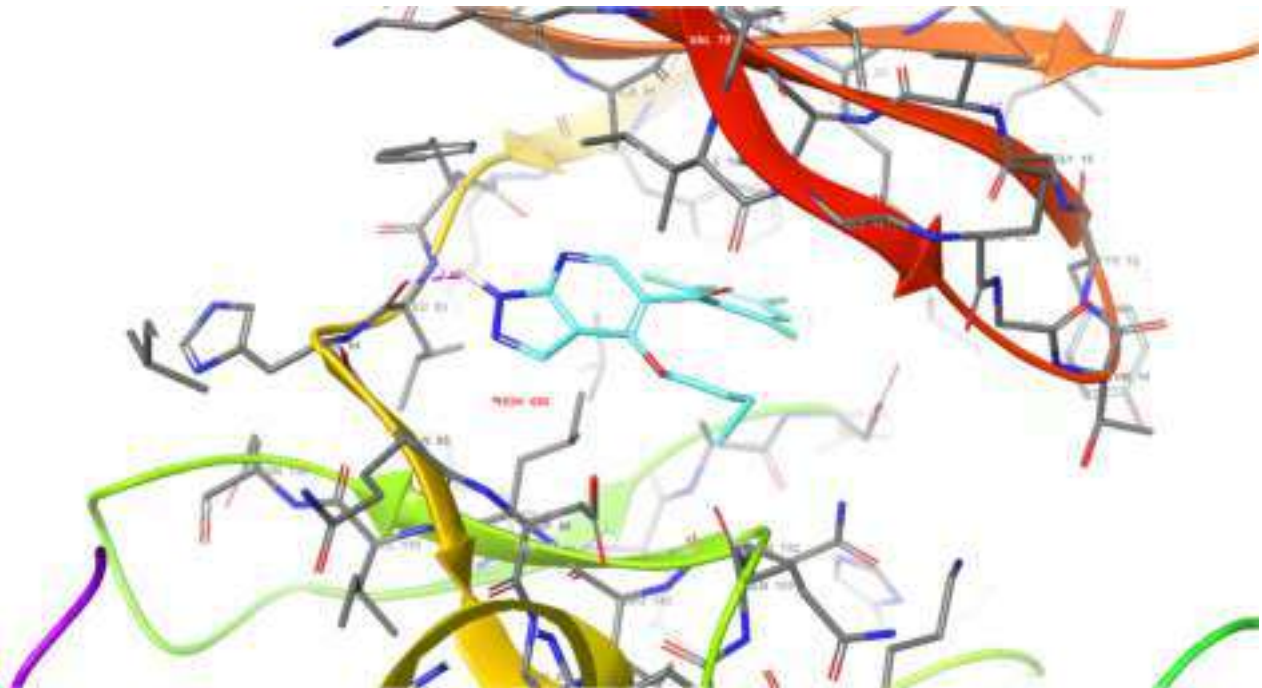
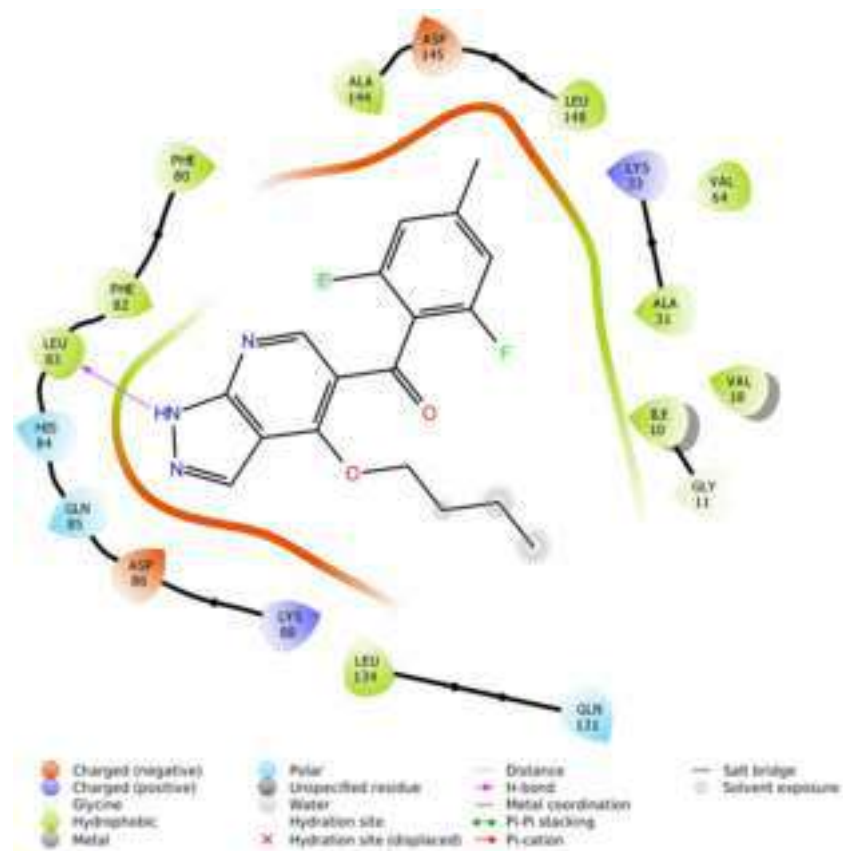


Figure 6. Two-dimensional binding interactions of DTQ within the ATP binding pocket of CDK2.



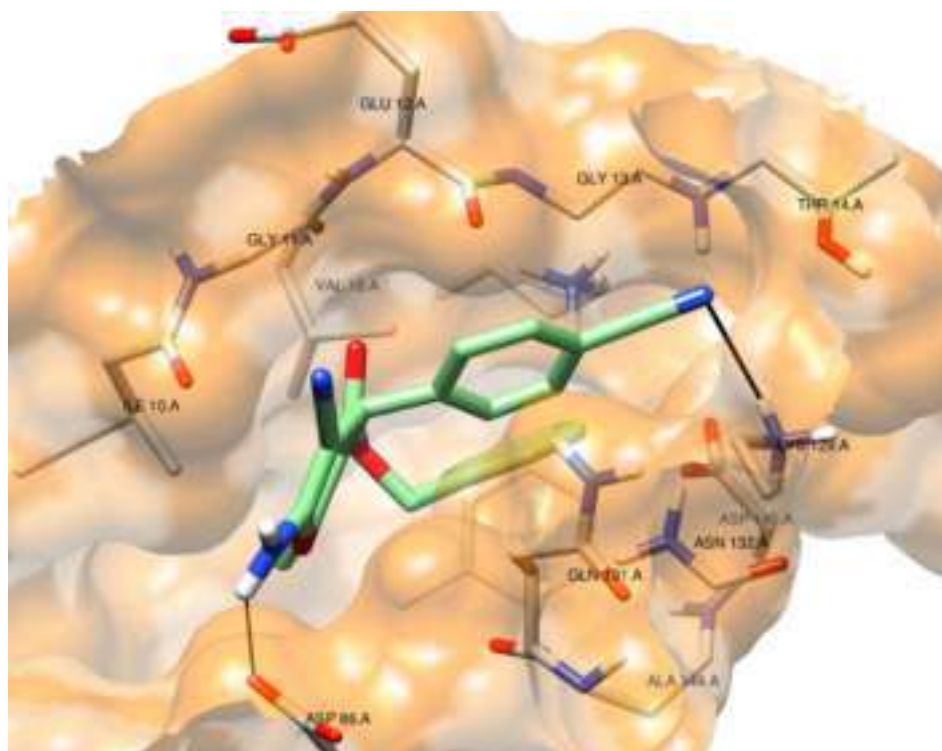
**Figure 7.** Three-dimensional binding interactions of **BMS-265246** within the ATP binding pocket of CDK2. Hydrogen bond (purple dotted line), hydrogen atoms (white), nitrogen atoms (blue), fluorine atoms (light green), and oxygen atoms (red).



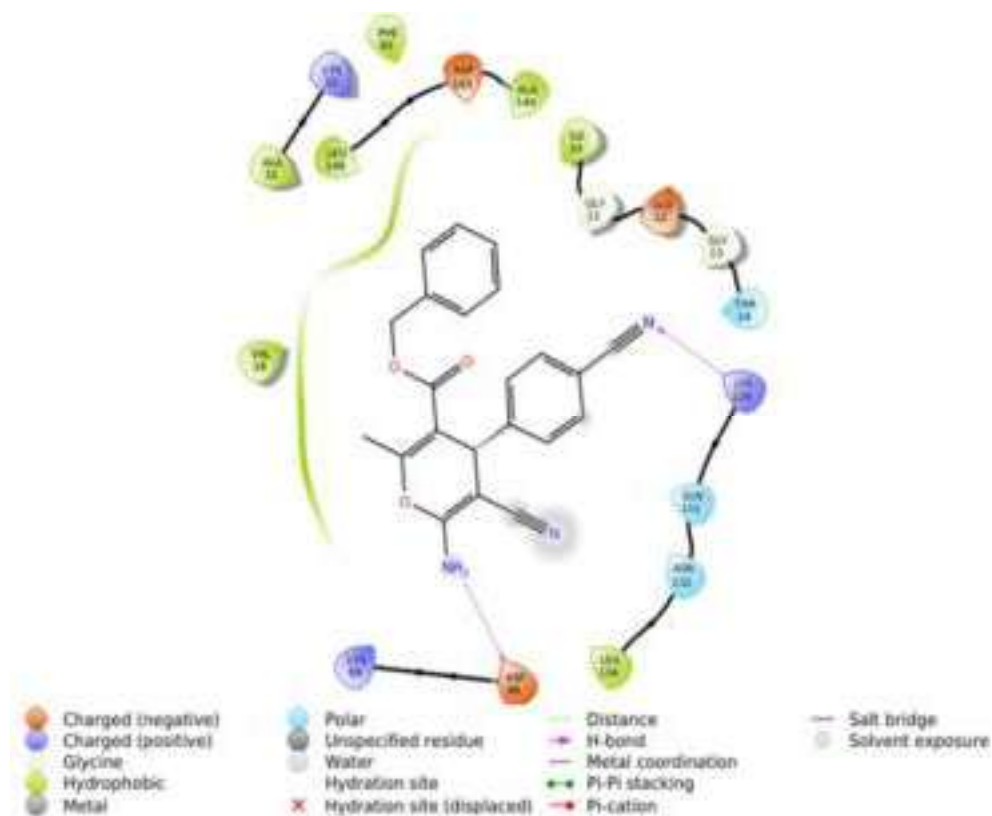
**Figure 8.** Two-dimensional interactions of **BMS-265246** within the ATP binding pocket of CDK2 kinase.



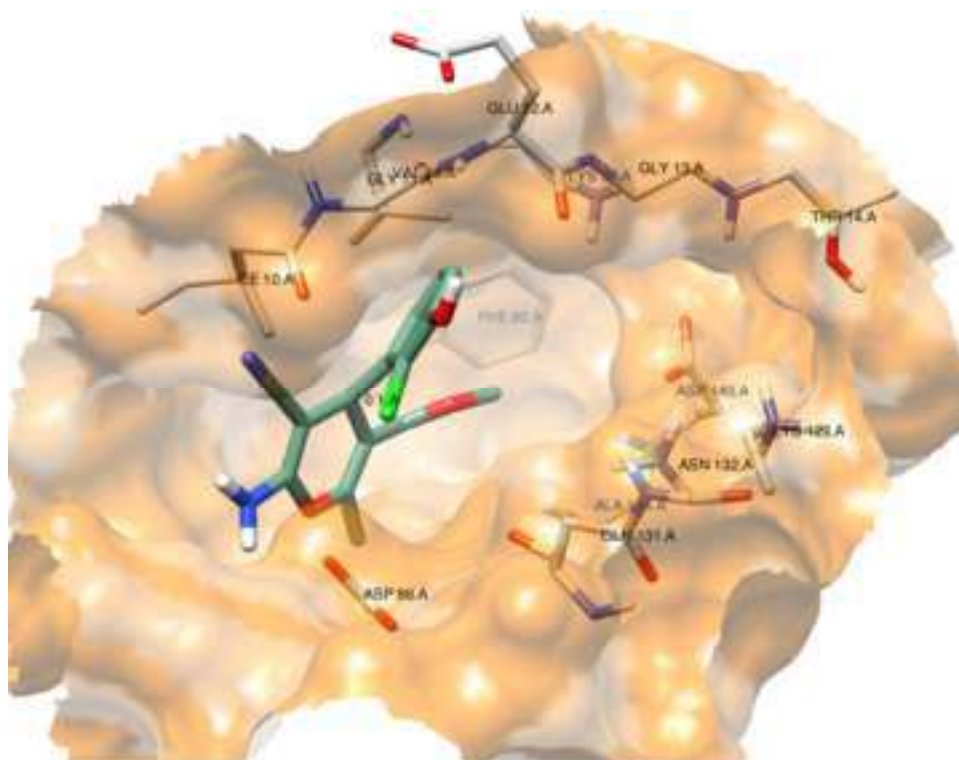




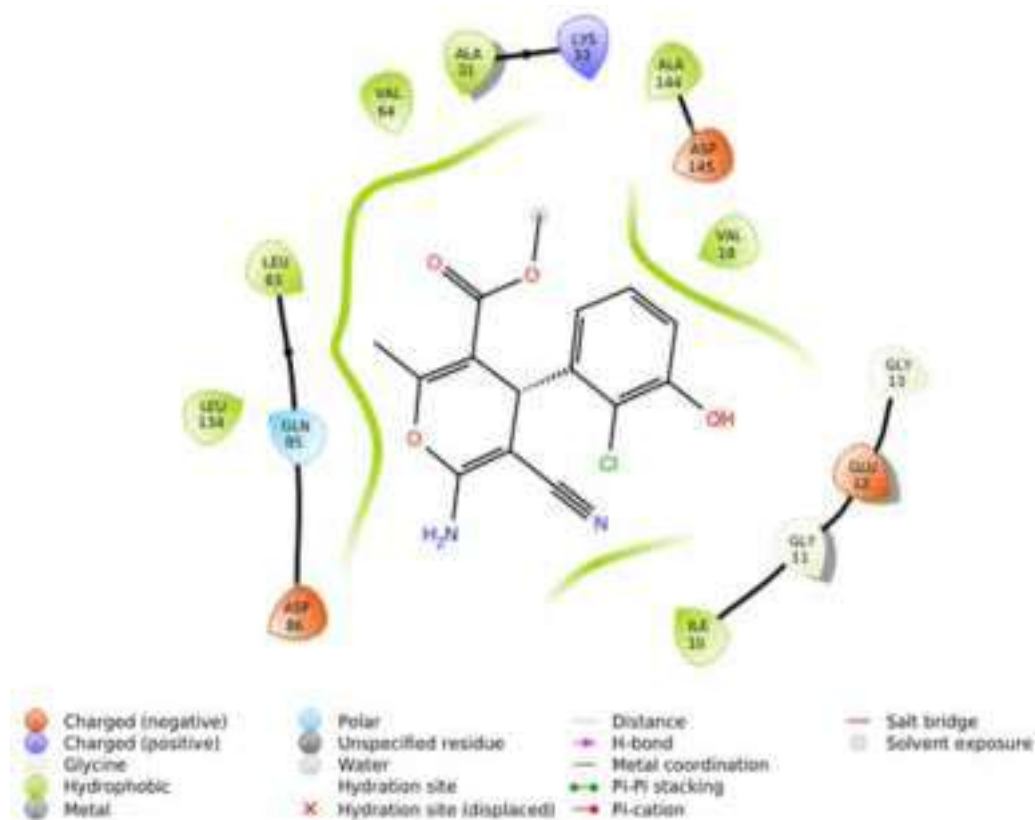
**Figure 11.** Three-dimensional model of binding interactions of compound **4K** after docking calculations in the ATP binding pocket of CDK2. Hydrogen bond (black lines), hydrogen atoms (white), nitrogen atoms (blue), and oxygen atoms (red).



**Figure 12.** Two-dimensional model of binding interactions of compound **4K** after docking calculations in the ATP binding pocket of CDK2.



**Figure 13.** Three-dimensional model of binding interactions of compound **4f** after docking calculations in the ATP binding pocket of CDK2. Hydrogen atoms (white), nitrogen atoms (blue), chlorine atom (green), and oxygen atoms (red).



**Figure 14.** Two-dimensional model of binding interactions of compound **4f** after docking calculations in the ATP binding pocket of CDK2.

#### Docking pose for DTQ:

Through examination of molecular docking, the pose of **DTQ** is shown to be very interesting, as it involves an active site water molecule as a bridge for H-bond establishment [66]. In addition to this, the phenolic OH and N-1 of the pyrimidine ring of **DTQ** are responsible for H-bond formation with Lys33 and Leu83, respectively (Figures 5 and 6).

It is noteworthy that the H-bonding interactions with Lys33 and Leu83 on the protein backbone are important for potent inhibitory activity [67].

#### Docking pose for BMS-265246:

The docking pose for **BMS-265246** indicates that it coordinated different residues of the enzyme due to hydrophobic and polar interactions.. The Leu83 residue and the NH of the pyrazole ring of **BMS-265246** are responsible for a strong H-bond formation with a distance of 2.15 Å. The N-2 atom of the same pyrazole ring interacted with Asp86 due to mild polar interactions. The 2,6-difluoro-4-methyl phenyl moiety established hydrophobic interactions with the nearby residues, viz. Ala144, Asp145 and Leu148 (Figures 7 and 8). From these docking results, the obtained pose of **BMS-265246** established similar important molecular interactions, in particular, H-bonding with Leu83, as documented before [68].

#### Docking pose for 4d:

This pyran derivative formed three hydrogen bonds—with amino acid residue ASP86 through its amino group as a donor, with amino acid GLN131 through the 3-methoxyl group as an acceptor and the last with ASN132 as an acceptor through the 5-methoxyl group. These binding interactions confirmed the importance of the methoxy groups at the *m*-positions (3,5-positions) as well as the amino group for further optimization. Additionally, this ligand showed lipophilic interactions with ILE10, VAL18, ILE10, PHE80 and LEU148. Moreover, the phenyl ring was involved in pi–pi stacking interactions with PHE80 (Figures 9 and 10)

#### Docking pose for 4k:

Likewise, the analysis of the binding interactions between CDK2 and compound **4k** (Figures 11 and 12) revealed the formation of two hydrogen bonds between the amino acid residues ASP86 and LYS129 in the active pocket and amino (as a donor) and nitrile (as an acceptor) substituents of **4k**. Additionally, the phenyl ring of the benzyl moiety showed lipophilic interactions with ILE10, VAL18, ILE10, PHE80, LEU148, LEU134 and VAL64.

#### Docking pose for 4f:

Contrarily, the inactive derivative **4f** did not form any hydrogen bonds inside the active site of CDK2. However, it showed lipophilic interactions with ILE10, VAL18, LEU83 and Val64, as shown in Figures 13 and 14.

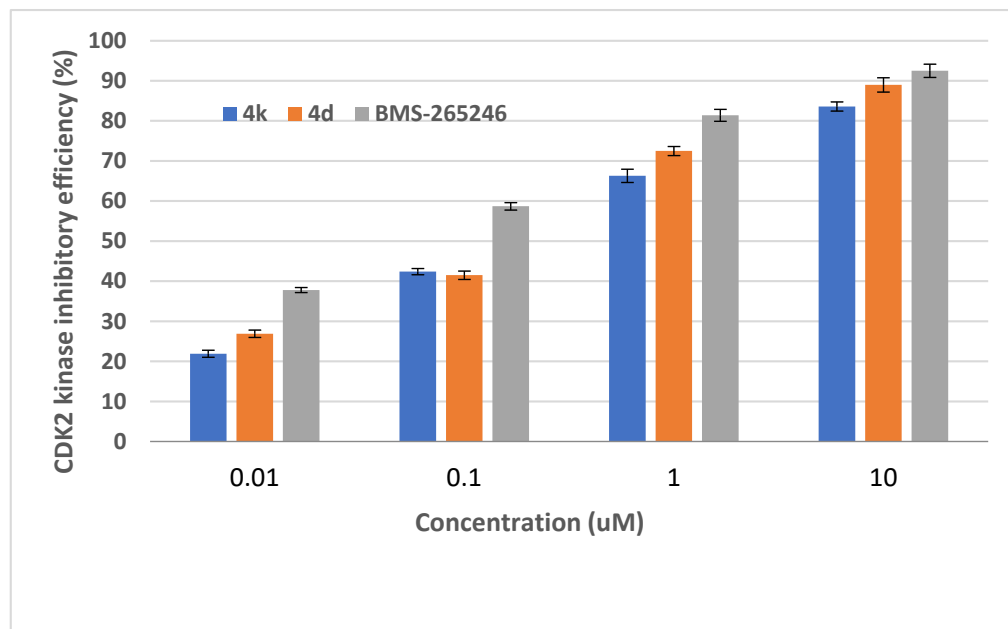
Overall, it can be concluded that there is a positive correlation between the docking simulations and the results of the cell viability assays, which support our claim that CDK2 is a potential target which could be responsible for the observed antiproliferative activities of compounds **4d** and **4k**.

Moreover, the docking analyses of **4d**, **4k** and **4f** successfully provided information on possible structural modifications to improve kinase inhibitory efficiency. These analyses highlighted that an inhibitor for CDK2 requires a bulkier ring to be attached to the main scaffold (the pyran ring in the present case) through a flexible chain of two to three atoms. Furthermore, it should be present at the periphery of the molecule to penetrate well inside the ATP binding site to establish lipophilic and mild polar interactions [69]. In addition, docking analyses indicated that H-bond donors or acceptors on the central scaffold could substantially enhance binding with the receptor.

#### 2.2.4.2. In Vitro CDK2 Inhibitory Assays

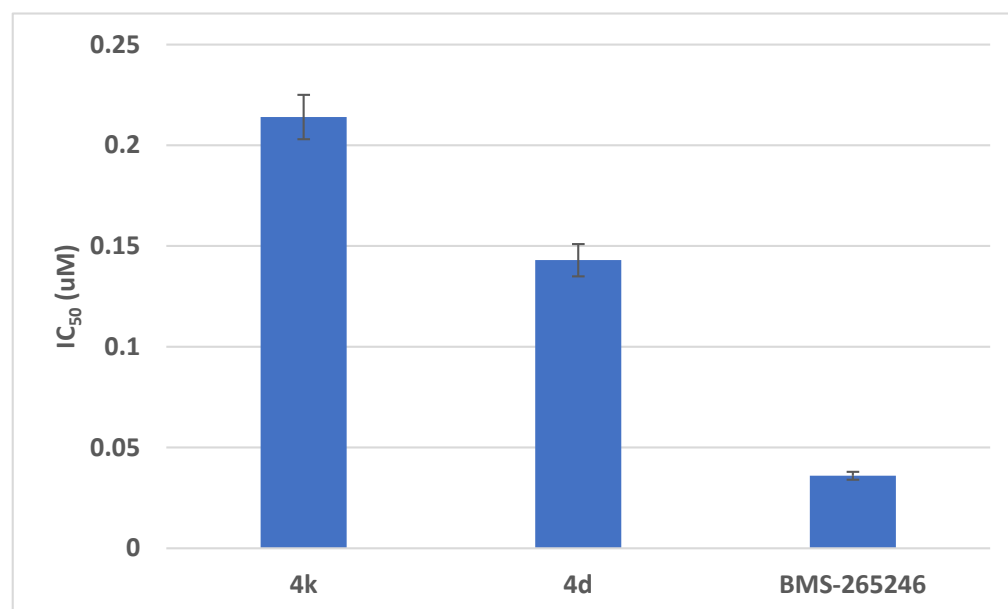
To further substantiate the promising results of the docking analyses of pyrans **4d** and **4K** in the ATP active site of CDK2, their in vitro potencies to inhibit the enzyme activity were evaluated over a concentration range of 0.01–10 µM. The results of kinase assays (Figure 15) revealed that both pyrans strongly affected CDK2 activity in a dose-dependent manner. Thus, compound **4d**, at 0.01, 0.1, 1, or 10 µM, decreased CDK2 activity by 26.9, 41.5,

72.5 and 89%, respectively, while compound **4k** inhibited kinase efficiency by 21.9, 42.4, 66.3 and 83.6%, respectively, at the same concentrations. On the other hand, the positive control **BMS-265246** was found to be more effective and reduced CDK2 activity by 92.3% at the highest concentration used (10  $\mu$ M).



**Figure 15.** In vitro evaluation of the CDK2 inhibitory efficiency of pyrans **4d** and **4K** as compared to the reference inhibitor **BMS-265246** over a concentration range of 0.01–10  $\mu$ M. Results were obtained from three independent experiments.

Moreover, the  $IC_{50}$  values for **4k**, **4d** and **BMS-265246** were deduced (Figure 16) and they were found to be 0.214, 0.143 and 0.036  $\mu$ M, respectively.



**Figure 16.**  $IC_{50}$  values of **4d**, **4K** and **BMS-265246** against CDK2.

Thus, our results for the kinase inhibitory assays are in agreement with the previously reported studies, which indicated that tropane–pyran hybrid structures could be considered as promising core scaffolds for developing new anticancer agents acting as CDK2 inhibitors [37].

It is worth noting that inhibition of CDK2 activity is considered to be a good approach for preventing chemotherapy-induced alopecia (CIA) by arresting the cell cycle without sensitization of the epithelium [70].

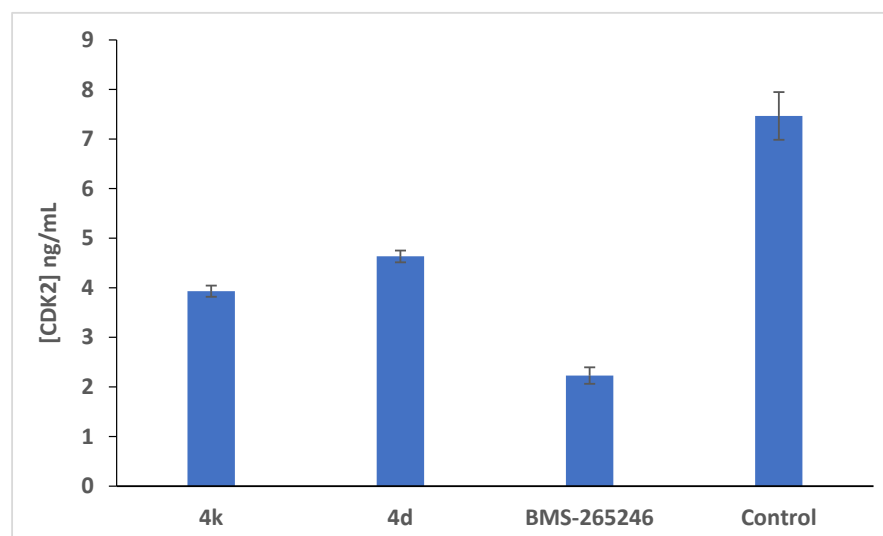
Collectively, the results of the docking simulations, the cell viability inhibition assays in HCT-116 colon cancer cells and the *in vitro* CDK2 inhibitory assays confirmed the potential of pyrans **4k** and **4d** as antiproliferative agents via the induction of cell-cycle arrest through CDK-2 inhibition.

#### 2.2.4.3. Further Mechanistic Studies via Quantitative Determination of the Concentration of CDK2 Protein and the Expression Profile of the CDK2 Gene in HCT-116 Cells Treated with the Cytotoxic Candidates

During the pathogenesis of cancer in humans, the enzymatic machinery, including human cyclins and their kinase (CDK) partners, which control the decisions to progress from a resting state (G0) to the cell cycle (G0-to-G1 transition) and/or to progress from the G1 (Gap-1) phase (in which the cell prepares for DNA synthesis) to the S phase (DNA synthesis phase), was found to be dysregulated, resulting in unrestrained proliferation. Furthermore, mutations have been observed in genes encoding CDKs; thus, the growth promoter and activator of G1 phase progression (the CDK2 gene) has been reported to be overexpressed in some human cancer subtypes, including colorectal, leukemia, pancreatic and renal carcinomas [24,71]. Moreover, overexpression of CDK2 in primary CRC tumors is linked to lymph node metastasis [72]. Therefore, different strategies for therapeutic intervention have been proposed based on inhibiting CDK activity and silencing the co-expressed genes in colon cancer cells to prevent them from proliferating and to induce their death [73].

Based on these facts, the effects of **4d** and **4k** on the expression levels of the CDK2 protein as well as the CDK2 gene were studied in a two-step protocol.

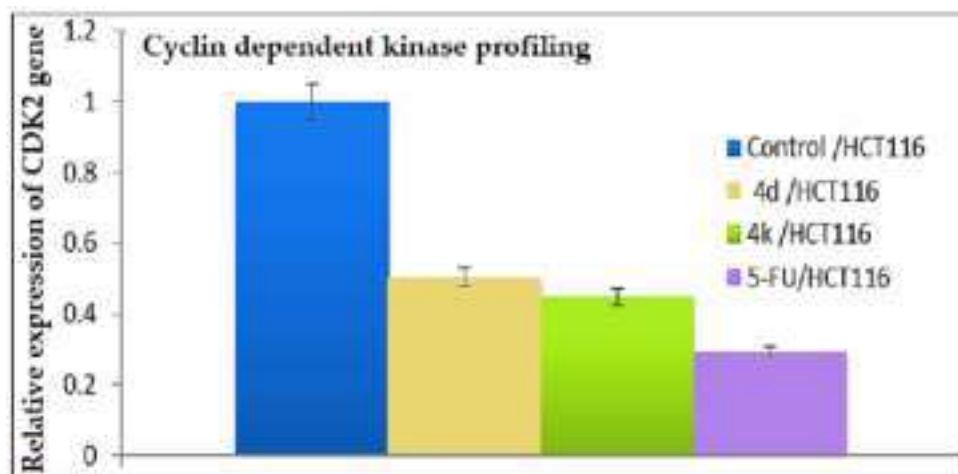
First, the commercial Human CDK2 ELISA Kit was used to estimate concentrations of the protein in the lysate of HCT-116 cells treated with **4d** and **4k**. The results were compared with the positive (cells treated with the reference CDK inhibitor, **BMS-265246**) and negative control experiments. The data presented in Figure 17 show that the concentration of CDK2 was estimated to be 7.466 ng/mL in the negative control experiment, while it was reduced to 2.229, 3.932 and 4.634 ng/mL in the positive control, **4k**- and **4d**-treated samples, respectively. These results implied that compounds **4d** and **4k** downregulated the expression of the CDK2 protein 1.9- and 1.6-fold, respectively, as compared to the negative control.



**Figure 17.** *In vitro* quantitative determination of the concentrations of CDK2 (ng/mL) in HCT116 cells treated with pyrans **4d** and **4k** compared with the positive control **BMS-265246** and the negative control samples.

Second, the expression profiles of the CDK2 gene in HCT-116 cells treated with compounds **4d** and **4k** were determined. The results were compared with the positive control (cells treated with the well-known cytotoxic drug 5-fluorouracil) and the negative control (untreated cells).

As shown in Figure 18, the CDK2 transcript levels were decreased significantly, 0.29-, 0.45- and 0.50-fold, by 5-FU, **4K** and **4d**, respectively, as compared to the untreated cells after 24 h of the treatment.



**Figure 18.** The expression profiles of the CDK2 gene in the lysate of HCT-116 cancer cells treated with compounds **4d** and **4k**.

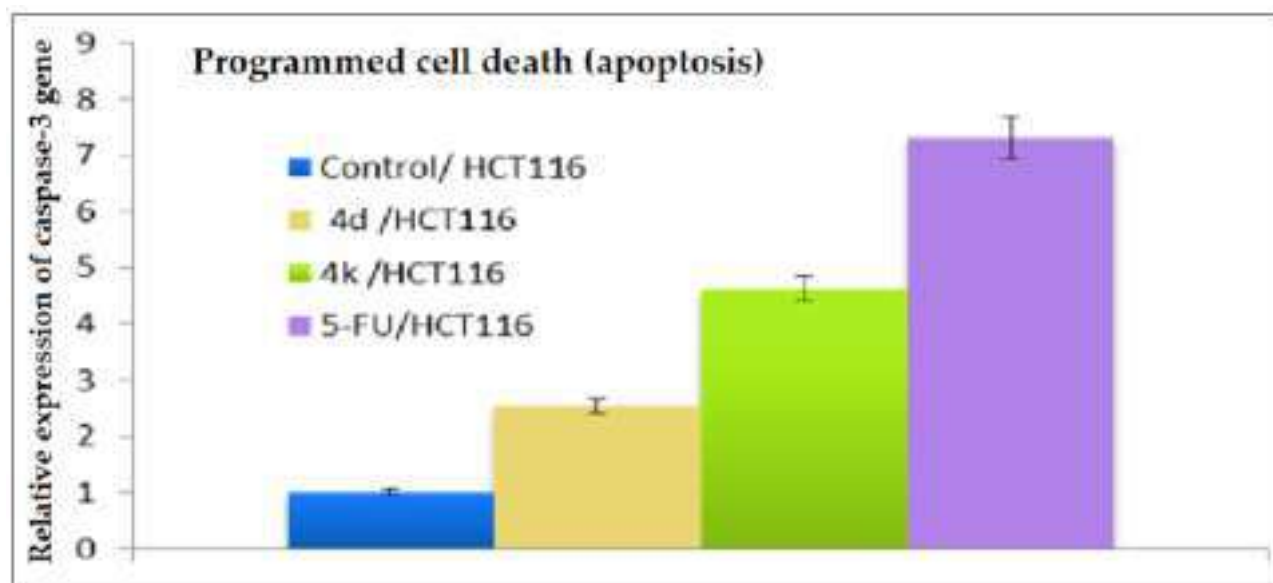
Accordingly, our results imply that pyrans **4K** and **4d** might cause growth arrest in HCT-116 cancer cells via downregulation of CDK2 gene and protein as well.

#### 2.2.5. Investigation of the Apoptotic Potential via Real-Time PCR Determination of the Expression Profile of the Caspase-3 Gene in HCT-116 Cells Treated with Pyrans **4d** and **4k**

Normally, apoptosis, or programmed cell death, is considered as a safeguard mechanism for managing stress and maintaining tissue homeostasis. It proceeds through a series of well-ordered biochemical cascades of events, which are regulated by a network of proteins. However, due to genetic and epigenetic mutations, deregulation of these proteins occurs, which results in evasion of apoptosis. This oncogenic transformation is a hallmark of human cancer, and it contributes to other tumorigenic events, including uncontrolled growth, accumulation of further genetic mutations, tumor angiogenesis and metastasis and chemotherapeutic resistance [74]. Therefore, reinitiating selective cancer cell death is a fundamental goal in anticancer drug development. Research in cancer biology has provided fundamental insights into the apoptotic pathways and their deregulation in colon cancer. Moreover, it has identified the molecular targets for reinitiating selective tumor cell death, including antiapoptotic Bcl-2 family proteins, apoptosis inhibitors and activators of the TRAIL death receptor signaling pathway, as well as other apoptotic markers, such as caspases. Among the caspases, which play critical roles in apoptosis, are the initiators, including caspases-8 or 9, and the effectors, including caspase-3 and caspase-7. After being activated by the initiators, the executioner caspases cleave numerous vital structural and regulatory proteins, leading to cell death [75]. Previous studies have demonstrated that expression level of caspase-3 is downregulated in cancer; therefore, enhancing its activity with natural and synthetic compounds was suggested as a possible strategy for cancer therapy [76,77]. In fact, pyran-containing, 4*H*-chromene derivatives, such as 3-amino-1-(4-fluorophenyl)-1*H*-benzo[*f*]chromene-2-carbonitrile [78] and 3-amino-1-(4-iodophenyl)-8-methoxy-1*H*-benzo[*f*]chromene-2-carbonitrile [79], were found to be effective against HT-29 cells of CRC and -MDA-MB-231 cells of breast cancer, respectively, via a 3-caspase-dependent apoptosis mechanism; therefore, we anticipated that our closely related pyran analogues **4d** and **4k** might be caspase-3 inducers as well. Thus, the real-time

quantitative PCR analyses of caspase-3-gene levels following treatment with compounds **4d** and **4k** at a concentration of 10 mg/mL for 24 h, were performed to investigate their potential as proapoptotic agents.

As shown in Figure 19, the treated HCT-116 cultures showed significant expression of caspase-3 gene as compared to the positive (5-FU-treated) and the negative (pure HCT-116 cells) control cultures. The transcription levels of the caspase-3 gene in HCT-116 in treated cultures were increased 7.31-, 4.62- and 2.55-fold by 5-FU, **4k** and **4d**, respectively, as compared to the negative control. These results indicated a concentration of 10 mg/mL for increasing the expression of caspase-3 gene and subsequent induction of mitochondrial apoptosis of the HCT-116 cells.



**Figure 19.** The expression profiles of caspase-3 gene in lysates of HCT-116 cells treated with 5-FU and pyrans **4d** and **4k** as compared to the untreated HCT-116 cells (negative control).

Overall, pyrans **4d** and **4k** can be considered interesting candidates to be subjected to further studies in order to investigate their usefulness in developing new anti-CRC agents capable of inhibiting the proliferation of HCT-116 cells through inducing cell-cycle arrest at the G1/S boundary by targeting CDK2 and enhancing the apoptosis of cancerous cells via activation of the caspase-3 gene.

### 2.3. Physicochemical and Pharmacokinetic Properties and Lipinski's Rule of Five

Six physicochemical parameters, comprising Lipophilicity (LIPO), Size, Polarity (POLAR), Insolubility (INSOL), Unsaturation (UNSAT) and Flexibility (FLEX) were predicted for the tested compounds using the bioavailability radar chart [80], in which the pink-colored zone (Figure 20) indicates the suitability of physicochemical properties to have good in vivo bioavailability.

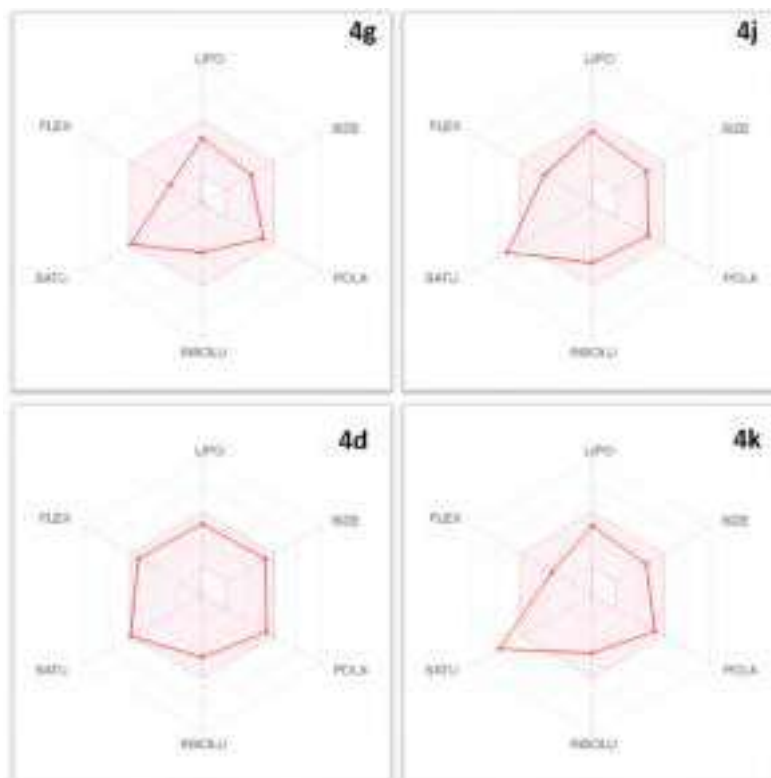
The results indicated that, compounds **4g** and **4d** did not violate any parameters in the radar chart, while **4j** and **4k** derivatives violated only the UNSAT parameter, which is acceptable. The calculated log *p* values were intermediate (2.27 for **4g**, 2.99 for **4j**, 2.98 for **4d** and 2.80 for **4k**). Based on these data, it can be predicted that all the tested derivatives would have good bioavailability profiles, especially the molecules **4g** and **4d**.

The SwissADME server provides a BOILED-EGG chart to indicate human intestinal absorption (white part), blood–brain barrier penetration (yellow part) and the probability of the tested compound acting as a substrate (PGP<sup>+</sup>, blue color) or not a substrate (PGP<sup>−</sup>, red color) for permeability glycoprotein (PGP).

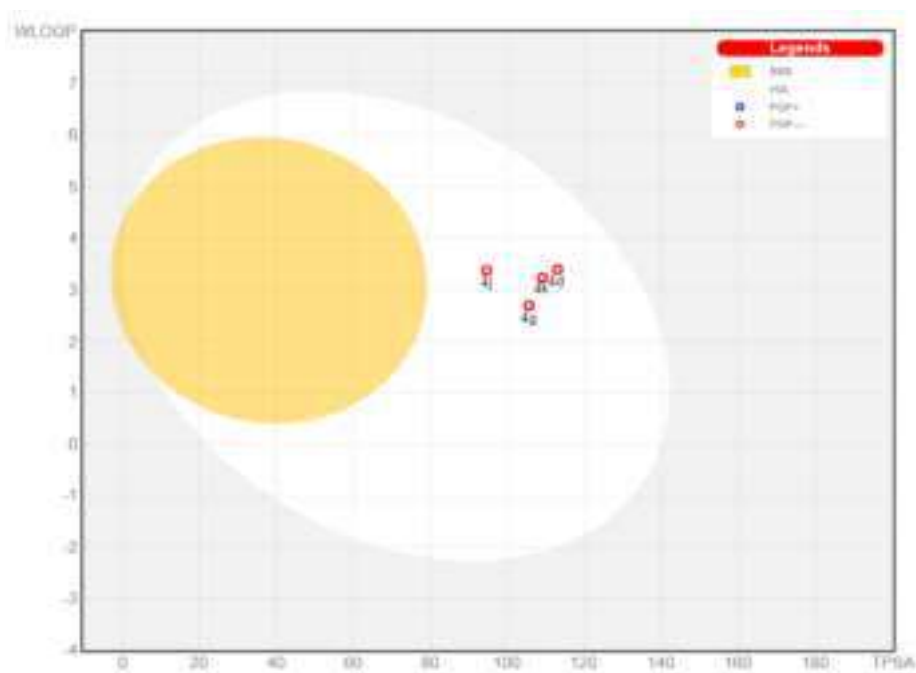
The results (summarized in Figure 21) showed that all the tested derivatives can be expected to be of good oral absorption, which is indicated by their presence in the white



area. Moreover, they would not penetrate the blood–brain barrier (BBB, egg yolk area); thus, they would not cause CNS toxicity. Finally, the four compounds are red-colored, which means that they are not anticipated to be substrates for PGP; therefore, they would not suffer from restricted entry to the target cells through efflux pumps [81].



**Figure 20.** The bioavailability radar plots for the tested compounds (the colored zone is the suitable physicochemical space for oral bioavailability).



**Figure 21.** The BOILED-EGG chart for the studied compounds.

Eventually, the drug-likeness and good oral bioavailability characteristics for the studied compounds were predicted using the Lipinski's rule of five filter [82]. As shown in Table 6 no compound did violate any parameter of the rule, which states that no violation or even one violation indicates expected good oral bioavailability.

**Table 6.** Drug-likeness of the tested compounds.

Comp. No.	Properties	Comment
4g	<ul style="list-style-type: none"> <li>Log P = 2.27 (&lt;5)</li> <li>Molecular weight = 334.75 g/mol (&lt;500)</li> <li>No. of H-bond donor groups (OHs + NHs) = 3 (<math>\leq 5</math>)</li> <li>No. of H-bond acceptor atoms (Os + Ns) = 6 (<math>\leq 10</math>)</li> </ul>	No violation
4j	<ul style="list-style-type: none"> <li>Log P = 2.99 (&lt;5)</li> <li>Molecular weight = 376.41 g/mol (&lt;500)</li> <li>No. of H-bond donor groups (OHs + NHs) = 2 (<math>\leq 5</math>)</li> <li>No. of H-bond acceptor atoms (Os + Ns) = 6 (<math>\leq 10</math>)</li> </ul>	No violation
4d	<ul style="list-style-type: none"> <li>Log P = 2.99 (&lt;5)</li> <li>Molecular weight = 436.46 g/mol (&lt;500)</li> <li>No. of H-bond donor groups (OHs + NHs) = 2 (<math>\leq 5</math>)</li> <li>No. of H-bond acceptor atoms (Os + Ns) = 8 (<math>\leq 10</math>)</li> </ul>	No violation
4k	<ul style="list-style-type: none"> <li>Log P = 2.80 (&lt;5)</li> <li>Molecular weight = 371.39 g/mol (&lt;500)</li> <li>No. of H-bond donor groups (OHs + NHs) = 2 (<math>\leq 5</math>)</li> <li>No. of H-bond acceptor atoms (Os + Ns) = 6 (<math>\leq 10</math>)</li> </ul>	No violation

Although the in-silico predictions are promising, these results are preliminary and should be confirmed experimentally.

### 3. Materials and Methods

#### 3.1. Chemistry

##### 3.1.1. General

All reagents were used as supplied commercially. The IR spectra were obtained using potassium bromide (KBr) discs and recorded on a PerkinElmer FTIR spectrophotometer, Spectrum BX 1000 in wave number ( $\text{cm}^{-1}$ ). Nuclear magnetic resonance spectroscopy was performed on a Bruker Avance 500 spectrometer, operating at 500 MHz for  $^1\text{H}$  and 125 MHz for  $^{13}\text{C}$  at 25 °C (Research Unit, College of Pharmacy, Prince Sattam Bin Abdulaziz University, Al-Kharj, KSA), or on an Eclipse 300 FT NMR spectrometer operating at 300 MHz spectrometer for  $^1\text{H}$  and at 75 MHz for  $^{13}\text{C}$  at 25 °C (College of Science, King Saud University, Riyadh, KSA). The chemical shifts are expressed in ppm and tetramethyl silane (TMS) was used as internal standard; mass spectra were recorded on a Shimadzu Qp-2010 Plus Mass Spectrometer using Ionization Mode: EI (Micro Analytical Center, Cairo University, Egypt). Percentages of C, H and N in the new compounds were evaluated at the regional center for Mycology and Biotechnology (RCMB), Al-Azhar University.

##### 3.1.2. General Procedures for the Synthesis of 6-Amino-5-cyano-4-(aryl)-2-methyl-4H-pyran-3-carboxylic Acid Esters **4a–m**

To an ethanolic mixture (20 mL) of benzaldehyde derivative **1a–k** (0.004 mol), namely, 2-formyl-benzoic acid, 3-methoxy-2-nitro benzaldehyde, 3,4,5-trimethoxy benzaldehyde, biphenyl-3-carbaldehyde, 2-chloro-3-hydroxy-benzaldehyde, 2,4,6-trimethoxy benzaldehyde, 4-fluorobenzaldehyde, 4-methoxybenzaldehyde, 4-formyl-benzonitrile, 2-chloro-benzaldehyde, or 2,4-dichlorobenzaldehyde, and malononitrile **2** (0.004 mol, 0.264 g), piperidine (0.8 mL) and the appropriate  $\beta$ -ketoester derivative **3a–c** (0.004 mol) namely;

methyl acetoacetate, ethyl acetoacetate or benzyl acetoacetate were added. The resulting reaction mixture in each was stirred at room temperature for 24 h, then it was worked up as described below to obtain the desired product.

#### 6-Amino-4-(2-carboxy-phenyl)-5-cyano-2-methyl-4H-pyran-3-carboxylic acid methyl ester **4a**

Filtration of the obtained reaction suspension afforded a yellow solid, which was washed with H<sub>2</sub>O/dil. HCl, air dried and recrystallized from EtOH to give shiny white crystals, yield (63%), m.p. 216–218 °C;  $\nu_{\max}$  (KBr)/cm<sup>-1</sup> 3328 (broad OH and NH<sub>2</sub>), 3193 (CH-Ar), 2895 (CH-aliphatic), 2656, 2544, 2196 (CN), 1716 (C=O-ester), 1675 (C=O-carboxylic), 1605 (C=C), 1445 1405, 1377, 1325, 1264, 1226, 1182, 1124, 1068, 1042, 955, 876, 842, 803, 749, 728, 648, 624, 518, 442;  $\delta_{\text{H}}$  (500 MHz; DMSO-*d*<sub>6</sub>) 7.73 (1H, dd, *J* = 7.7, 1.1 Hz, CH-Ar), 7.50 (1H, t, *J* = 7.3 Hz, CH-Ar), 7.29–7.25 (2H, m, 2 × CH-Ar), 6.85 (2H, br. s, NH<sub>2</sub>), 5.63 (1H, s, C<sup>4</sup>H-pyran), 3.46 (3H, s, O-CH<sub>3</sub>), 2.31 (3H, s, CH<sub>3</sub>);  $\delta_{\text{C}}$  (125 MHz; DMSO-*d*<sub>6</sub>), 168.60 (C=O), 165.83 (C=O), 158.73, 157.04, 146.03, 131.95, 130.48, 129.36, 129.01, 126.39, 119.27, 107.59 (4 × CH-Ar, 2 × C<sub>q</sub>-Ar, 3 × C<sub>q</sub>-pyran, CN), 56.05 and 51.29 (C<sup>5</sup>-pyran and O-CH<sub>3</sub>), 32.72 (C<sup>4</sup>H-pyran), 18.40 (CH<sub>3</sub>); MS (EI) *m/z* (%) [M<sup>+</sup>] 314.85 (0.24) for C<sub>16</sub>H<sub>14</sub>N<sub>2</sub>O<sub>5</sub>, 268.90 (39.95), 252.85 (14.51), 236.90 (100.00), 208.90 (11.83), 192.90 (10.28), 133.00 (31.62), 116.05 (21.80), 105.00 (41.68), 89.00 (27.86), 77.05 (77.39), 66.00 (29.21), 57.05 (15.98). Anal. Calcd. for C<sub>16</sub>H<sub>14</sub>N<sub>2</sub>O<sub>5</sub>: C, 61.14; H, 4.49; N, 8.91. Found; C, 61.36; H, 4.70; N, 9.07.

#### 6-Amino-5-cyano-4-(3-methoxy-2-nitro-phenyl)-2-methyl-4H-pyran-3-carboxylic acid ethyl ester **4b**

The excess solvent was evaporated and the resulting yellow solid was washed with water, air dried and recrystallized from EtOH to afford a pure product as a pale yellow solid, yield (85%), m.p. 220–222 °C;  $\nu_{\max}$  (KBr)/cm<sup>-1</sup> 3475 (asymmetric NH<sub>2</sub>), 3351 (symmetric NH<sub>2</sub>), 3168 and 3098 (CH-Ar), 2989, 2940, 2898 and 2847 (CH-aliphatic), 2192 (CN), 1679 (C=O), 1629 and 1586 (C=C), 1530 (NO<sub>2</sub>), 1478, 1449, 1372, 1332, 1277, 1210, 1122, 1056, 1018, 956, 908, 851, 802, 655, 613, 562, 512, 443;  $\delta_{\text{H}}$  (500 MHz; DMSO-*d*<sub>6</sub>) 7.51 (1H, t, *J* = 8.2 Hz, CH-Ar), 7.18 (1H, d, *J* = 8.4 Hz, CH-Ar), 7.06 (2H, br. s, NH<sub>2</sub>), 6.88 (1H, d, *J* = 7.9 Hz, CH-Ar), 4.35 (1H, s, C<sup>4</sup>H-pyran), 3.96 (2H, q, *J* = 7.1 Hz, O-CH<sub>2</sub>-CH<sub>3</sub>), 3.87 (3H, s, O-CH<sub>3</sub>), 2.32 (3H, s, CH<sub>3</sub>), 0.99 (3H, t, *J* = 7.1 Hz, O-CH<sub>2</sub>-CH<sub>3</sub>);  $\delta_{\text{C}}$  (125 MHz; DMSO-*d*<sub>6</sub>), 164.76 (C=O), 158.89, 158.08, 149.97, 139.63, 137.79, 131.78, 120.83, 118.79, 111.67, 105.54 (3 × CH-Ar, 3 × C<sub>q</sub>-Ar, 3 × C<sub>q</sub>-pyran, CN), 60.21 (O-CH<sub>2</sub>), 56.55 and 55.80 (C<sup>5</sup>-pyran and O-CH<sub>3</sub>), 34.43 (C<sup>4</sup>H-pyran), 18.22 (2 × CH<sub>3</sub>); MS (EI) *m/z* (%) [M<sup>+</sup>] 359.80 (0.40) for C<sub>17</sub>H<sub>17</sub>N<sub>3</sub>O<sub>6</sub>, 341.85 (35.07), 324.85 (5.56), 311.90 (6.19), 296.85 (4.09), 283.85 (8.98), 272.90 (12.99), 297.90 (43.20), 251.90 (11.35), 237.90 (10.52), 226.90 (34.93), 206.90 (11.00), 178.90 (12.93), 160.95 (11.26), 140.05 (6.60), 127.05 (9.20), 115.05 (20.68), 102.00 (23.05), 90.00 (29.84), 76.05 (69.38), 67.00 (100.00), 59.01 (38.59), 51.05 (33.51); Anal. Calcd. for C<sub>17</sub>H<sub>17</sub>N<sub>3</sub>O<sub>6</sub>: C, 56.82; H, 4.77; N, 11.69. Found: C, 57.11; H, 4.83; N, 11.97.

#### 6-Amino-5-cyano-4-(3-methoxy-2-nitro-phenyl)-2-methyl-4H-pyran-3-carboxylic acid benzyl ester **4c**

Addition of ice/H<sub>2</sub>O to the reaction mixture and filtration gave the crude product as a yellow precipitate which was air dried and recrystallized from EtOH/petroleum ether to obtain the pure product as a yellow powder, yield (64%), m.p. 190–192 °C;  $\nu_{\max}$  (KBr)/cm<sup>-1</sup> 3434 (asymmetric NH<sub>2</sub>), 3321 (symmetric NH<sub>2</sub>), 3221; 3190 and 3090, 3031 (CH-Ar), 2942 and 2846 (CH-aliphatic), 2195 (CN), 1716 (C=O), 1673 and 1603 (C=C), 1528 (NO<sub>2</sub>), 1479, 1449, 1406, 1370, 1315, 1285, 1225, 1174, 1181, 1133, 1063, 963, 912, 847, 804, 756, 695, 662, 566, 524, 435;  $\delta_{\text{H}}$  (300 MHz; DMSO-*d*<sub>6</sub>) 7.55–7.46 (2H, m, 2 × CH-Ar), 7.30–7.17 (3H, m, 3 × CH-Ar), 7.08 (2H, br. s, NH<sub>2</sub>), 7.07–7.01 (2H, m, 2 × CH-Ar), 6.87 (1H, d, *J* = 7.5 Hz, CH-Ar), 5.07 and 4.98 (2H, AB q, *J* = 12.6 Hz, O-CH<sub>2</sub>-Ph), 4.39 (1H, s, C<sup>4</sup>H-pyran), 3.88 (3H, s, O-CH<sub>3</sub>), 2.32 (3H, s, CH<sub>3</sub>);  $\delta_{\text{C}}$  (75 MHz; DMSO-*d*<sub>6</sub>), 164.11 (C=O), 158.80, 158.06, 150.11, 139.42, 137.64, 135.98, 131.82, 128.22, 127.79, 127.48, 120.89, 118.67, 111.77, 105.49 (8 × CH-Ar, 4 × C<sub>q</sub>-Ar, 3 × C<sub>q</sub>-pyran, CN), 65.56 (O-CH<sub>2</sub>-Ph), 56.64, 55.89 (C<sup>5</sup>-pyran

and O-CH<sub>3</sub>), 34.65 (C<sup>4</sup>H-pyran), 18.48 (CH<sub>3</sub>); MS (EI) *m/z* (%) [M<sup>+</sup> + 1] 422.10 (0.25) for C<sub>22</sub>H<sub>19</sub>N<sub>3</sub>O<sub>6</sub>, 404.00 (1.48), 360.10 (1.07), 343.05 (0.02), 309.10 (0.76), 291.10 (1.16), 283.05 (1.27), 268.05 (3.94), 252.05 (1.83), 227.00 (4.78), 201.00 (2.05), 153.05 (0.43), 140.05 (0.78), 107.10 (2.60), 92.05 (8.02), 91.05 (100.00), 77.05 (3.46), 65.00 (12.07), 51.00 (3.09); Anal. Calcd. for C<sub>22</sub>H<sub>19</sub>N<sub>3</sub>O<sub>6</sub>: C, 62.70; H, 4.54; N, 9.97; O, 22.78. Found: C, 62.59; H, 4.68; N, 10.19.

#### 6-Amino-5-cyano-2-methyl-4-(3,4,5-trimethoxy-phenyl)-4H-pyran-3-carboxylic acid benzyl ester **4d**

Filtration of the resulting mixture afforded a yellowish-white powder. Recrystallization from MeOH/petroleum ether afforded shiny white crystals, yield (57%), m.p. 158–160 °C;  $\nu_{\max}$  (KBr)/cm<sup>-1</sup> 3430 (asymmetric NH<sub>2</sub>), 3327 (symmetric NH<sub>2</sub>), 3181 (CH-Ar), 2940 and 2887 (CH-aliphatic), 2373, 2192 (CN), 1711 (C=O), 1689, 1641 and 1593 (C=C), 1503, 1463, 1427, 1378, 1322, 1252, 1222, 1120, 1059, 995, 888, 856, 802, 759, 719, 693, 662, 578, 515 cm<sup>-1</sup>;  $\delta_{\text{H}}$  (300 MHz; DMSO-*d*<sub>6</sub>) 7.37–7.25 (3H, m, 3 × CH-Ar of benzyl group), 7.18–7.11 (2H, m, 2 × CH-Ar of benzyl group), 6.92 (2H, br. s, NH<sub>2</sub>), 6.37 (2H, s, 2 × CH-Ar of trimethoxyphenyl group), 5.10 and 5.02 (2H, ABq, *J* = 12.9 Hz, O-CH<sub>2</sub>-Ph), 4.32 (1H, s, C<sup>4</sup>H-pyran), 3.68 (6H, s, 2 × O-CH<sub>3</sub>), 3.64 (3H, s, O-CH<sub>3</sub>), 2.35 (3H, s, CH<sub>3</sub>);  $\delta_{\text{C}}$  (75 MHz; DMSO-*d*<sub>6</sub>), 165.45 (C=O), 158.44, 157.36, 152.89, 140.52, 136.47, 135.89, 140.52, 136.47, 135.89, 128.27, 127.88, 127.56, 119.76, 106.73, 104.351 (7 × CH-Ar, 5 × C<sub>q</sub>-Ar, 3 × C<sub>q</sub>-pyran, CN), 65.77 (O-CH<sub>2</sub>-Ph), 59.99, 57.29 and 55.76 (C<sup>5</sup>-pyran and 3 × O-CH<sub>3</sub>), 39.30 C<sup>4</sup>H-pyran, 18.30 (CH<sub>3</sub>); MS (EI) *m/z* (%) [M<sup>+</sup> + 1] 437.05 (6.98) for C<sub>24</sub>H<sub>24</sub>N<sub>2</sub>O<sub>6</sub>, [M<sup>+</sup>] 436.05 (24.88), 345.00 (36.17), 327.00 (2.08), 301.05 (3.55), 284.00 (5.49), 269.05 (9.70), 244.00 (3.34), 221.00 (2.36), 168.00 (2.28), 134.05 (1.57), 128.05 (0.90), 109.05 (1.08), 91.05 (100.00), 65.00 (9.29), 51.00 (2.45). Anal. Calcd. for C<sub>24</sub>H<sub>24</sub>N<sub>2</sub>O<sub>6</sub>: C, 66.04; H, 5.54; N, 6.42. Found: C, 66.21; H, 5.59; N, 6.64.

#### 6-Amino-4-biphenyl-3-yl-5-cyano-2-methyl-4H-pyran-3-carboxylic acid ethyl ester **4e**

The resulting mixture was poured onto ice/H<sub>2</sub>O and filtered to give a pale-yellow powder, air dried and recrystallized from EtOH/petroleum ether to afford white crystals, yield (73%); m.p. 186–190 °C;  $\nu_{\max}$  (KBr)/cm<sup>-1</sup> 3374 (asymmetric NH<sub>2</sub>), 3213 (asymmetric NH<sub>2</sub>), 3060 and 3032 (CH-Ar), 2976 and 2922 (CH-aliphatic), 2368, 2340, 2188 (CN), 1708 (C=O), 1676 and 1602 (C=C), 1475, 1419, 1373, 1321, 1262, 1211, 1180, 1132, 1069, 951, 902, 868, 774, 746, 698, 647, 545, 513;  $\delta_{\text{H}}$  (500 MHz; DMSO-*d*<sub>6</sub>) 7.62 (2H, d, *J* = 7.5 Hz, 2 × CH-Ar), 7.52 (1H, d, *J* = 7.9 Hz, CH-Ar), 7.48 (2H, t, *J* = 7.55 Hz, 2 × CH-Ar), 7.44–7.41 (2H, m, 2 × CH-Ar), 7.38 (1H, t, *J* = 7.3 Hz, CH-Ar), 7.17 (1H, d, *J* = 7.8 Hz, CH-Ar), 6.98 (2H, br. s, NH<sub>2</sub>), 4.43 (1H, s, C<sup>4</sup>H-pyran), 3.98 (2H, q, *J* = 7.1 Hz, O-CH<sub>2</sub>-CH<sub>3</sub>), 2.35 (3H, s, CH<sub>3</sub>), 1.02 (3H, t, *J* = 7.1 Hz, O-CH<sub>2</sub>-CH<sub>3</sub>);  $\delta_{\text{C}}$  (125 MHz; DMSO-*d*<sub>6</sub>), 165.46 (C=O), 158.54, 156.81, 145.60, 140.21, 140.04, 129.19, 128.97, 127.48, 126.58, 126.21, 125.51, 125.28, 119.76, 107.07 (9 × CH-Ar, 3 × C<sub>q</sub>-Ar, 3 × C<sub>q</sub>-pyran, CN), 60.16 (O-CH<sub>2</sub>-Ph), 57.15 (C<sup>5</sup>-pyran), 38.85 (C<sup>4</sup>H-pyran), 18.22 (CH<sub>3</sub>), 13.67 (CH<sub>3</sub>); MS (EI) *m/z* (%) [M<sup>+</sup> + 1] 360.85 (9.65) and [M<sup>+</sup>] 359.90 (36.27) for C<sub>22</sub>H<sub>20</sub>N<sub>2</sub>O<sub>3</sub>, 330.85 (26.30), 313.90 (24.30), 293.90 (4.77), 286.90 (15.54), 270.90 (8.75), 228.90 (10.19), 206.90 (100.00), 178.90 (24.65), 160.95 (15.76), 133.05 (6.67), 115.00 (10.63), 105.05 (15.92), 88.00 (16.94), 77.05 (22.94), 67.00 (44.11), 51.00 (14.94); Anal. Calcd. for C<sub>22</sub>H<sub>20</sub>N<sub>2</sub>O<sub>3</sub>: C, 73.32; H, 5.59; N, 7.77. Found: C, 73.59; H, 5.71; N, 7.98.

#### 6-Amino-4-(2-chloro-3-hydroxy-phenyl)-5-cyano-2-methyl-4H-pyran-3-carboxylic acid methyl ester **4f**

The resulting mixture was poured on ice–dil. HCl mixture, then filtered and the obtained solid was air dried to obtain an off-white powder. Recrystallization from EtOH/petroleum ether gave a shiny white powder yield (85%), m.p. 238–240 °C;  $\nu_{\max}$  (KBr)/cm<sup>-1</sup> 3478 (OH), 3319 (NH<sub>2</sub>), 3015 (CH-Ar), 2946 and 2843 (CH-aliphatic), 2366, 2200 (CN), 1713 (C=O), 1674, 1634 and 1593 (C=C), 1462, 1403, 1374, 1349, 1261, 1227.7, 1187, 1133, 1074, 976, 853, 801, 759, 726, 667, 547, 500, 443;  $\delta_{\text{H}}$  (500 MHz; DMSO-*d*<sub>6</sub>) 10.09 (1H, s, OH), 7.08 (1H, t, *J* = 7.9 Hz, CH-Ar), 6.85 (2H, br. s, NH<sub>2</sub>), 6.81 (1H, dd, *J* = 8.1, 1.1 Hz, CH-Ar), 6.60 (1H, dd, *J* = 7.6, 1.1 Hz, CH-Ar), 4.93 (1H, s, C<sup>4</sup>H-pyran), 3.49 (3H, s, O-CH<sub>3</sub>), 2.34 (3H, s, CH<sub>3</sub>);  $\delta_{\text{C}}$

(125 MHz; DMSO- $d_6$ ), 165.82 (C=O), 158.60, 157.52, 152.94, 143.39, 127.38, 119.63, 119.50, 119.30, 119.23, 114.55, 106.22 (3 × CH-Ar, 3 × C<sub>q</sub>-Ar, 3 × C<sub>q</sub>-pyran, CN), 56.45 and 51.41 (C<sup>5</sup>-pyran and O-CH<sub>3</sub>), 35.28 (C<sup>4</sup>H-pyran), 18.12 (CH<sub>3</sub>); MS (EI)  $m/z$  (%) [M<sup>+</sup> + 1, <sup>37</sup>Cl] 322.80 (0.92); [M<sup>+</sup>, <sup>37</sup>Cl] 321.80 (4.70); [M<sup>+</sup> + 1, <sup>35</sup>Cl] 320.80 (3.09) and [M<sup>+</sup>, <sup>35</sup>Cl] 319.80 (13.67) for C<sub>15</sub>H<sub>13</sub>ClN<sub>2</sub>O<sub>4</sub>, 306.80 (1.28), 304.80 (3.81), 285.85 (10.38), 284.90 (58.22), 272.85 (1.03), 270.85 (0.36), 252.85 (5.53), 246.85 (1.34), 244.85 (3.08), 224.90 (4.03), 222.90 (1.39), 193.90 (10.96), 192.90 (100.00), 175.90 (9.94), 160.95 (28.16), 127.05 (6.44), 114.00 (10.61), 105.05 (20.05), 99.00 (12.74), 89.00 (23.42), 77.05 (19.61), 67.00 (54.84), 59.05 (37.40), 57.05 (11.01), 51.05 (10.88). Anal. Calcd. for C<sub>15</sub>H<sub>13</sub>ClN<sub>2</sub>O<sub>4</sub>: C, 56.17; H, 4.09; N, 8.73. Found: C, 56.44; H, 4.32; N, 8.99.

#### 6-Amino-4-(2-chloro-3-hydroxy-phenyl)-5-cyano-2-methyl-4H-pyran-3-carboxylic acid ethyl ester **4g**

The resulting reaction mixture was poured onto ice-dil. HCl mixture, then filtered and the obtained solid was air dried to afford an off-white powder. Recrystallization from EtOH/petroleum ether gave a shiny off white powder (65%), m.p. 212–213 °C;  $\nu_{\max}$  (KBr)/cm<sup>-1</sup> 3454 (OH), 3350 (NH<sub>2</sub>), 3197 (CH-Ar), 2974 and 2853 (CH-aliphatic), 2642, 2574, 2372, 2203 (CN), 1713 (C=O), 1669 and 1606 (C=C), 1583, 1465, 1408, 1375, 1322, 1293, 1234, 1185, 1134, 1073, 975, 862, 807, 763, 727, 670, 560, 487;  $\delta_{\text{H}}$  (300 MHz; DMSO- $d_6$ ) 10.10 (1H, s, OH), 7.08 (1H, t,  $J$  = 7.1 Hz, CH-Ar), 6.95 (2H, br. s, NH<sub>2</sub>), 6.83 (1H, d,  $J$  = 7.8 Hz, CH-Ar), 6.60 (1H, d,  $J$  = 7.8 Hz, CH-Ar), 4.90 (1H, s, C<sup>4</sup>H-pyran), 3.94 (2H, q,  $J$  = 7.2 Hz, O-CH<sub>2</sub>-CH<sub>3</sub>), 2.38 (3H, s, CH<sub>3</sub>), 0.98 (3H, t,  $J$  = 7.2 Hz, O-CH<sub>2</sub>-CH<sub>3</sub>);  $\delta_{\text{C}}$  (75 MHz; DMSO- $d_6$ ), 165.28 (C=O), 158.55, 157.39, 152.98, 143.49, 127.42, 119.48, 119.29, 114.48, 106.37 (3 × CH-Ar, 3 × C<sub>q</sub>-Ar, 3 × C<sub>q</sub>-pyran, CN), 60.09 (O-CH<sub>2</sub>), 56.26 (C<sub>q</sub>-pyran), 34.6 (C<sup>4</sup>H-pyran), 18.08 (CH<sub>3</sub>), 13.62 (CH<sub>3</sub>); MS (EI)  $m/z$  (%) [M<sup>+</sup> + 1, <sup>37</sup>Cl] 337.00 (0.63), [M<sup>+</sup>, <sup>37</sup>Cl] 336.00 (3.06), [M<sup>+</sup> + 1, <sup>35</sup>Cl] 335.00 (2.34) and [M<sup>+</sup>, <sup>35</sup>Cl] 334.00 (8.94) for C<sub>16</sub>H<sub>15</sub>ClN<sub>2</sub>O<sub>4</sub>, 307.00 (5.17), 305.00 (14.95), 300.05 (15.37), 299.10 (81.62), 291.00 (92.77), 289.00 (7.87), 271.05 (3.09), 261.00 (9.05), 225.00 (6.39), 208.00 (12.99), 207.00 (100.00), 179.00 (31.94), 161.00 (17.35), 133.05 (6.00), 127.05 (4.38), 115.05 (3.79), 105.05 (5.32), 89.05 (6.04), 77.05 (3.88), 67.00 (15.90), 63.00 (11.37), 57.05 (3.59), 51.00 (4.07); Anal. Calcd. for C<sub>16</sub>H<sub>15</sub>ClN<sub>2</sub>O<sub>4</sub>: C, 57.41; H, 4.52; N, 8.37. Found: C, 57.57; H, 4.41; N, 8.56.

#### 6-Amino-5-cyano-2-methyl-4-(2,4,6-trimethoxy-phenyl)-4H-pyran-3-carboxylic acid ethyl ester **4h**

Filtration of the resulting reaction mixture afforded a yellow solid, which was washed with water and air dried. Recrystallization from EtOH afforded the pure product as a yellow powder, yield (60%), m.p. 196–198 °C;  $\nu_{\max}$  (KBr)/cm<sup>-1</sup> 3465 (asymmetric NH<sub>2</sub>), 3330 (symmetric NH<sub>2</sub>), 3228 and 3192 (CH-Ar), 2940 and 2839 (CH-aliphatic), 2371, 2198 (CN), 1709 (C=O), 1688 and 1602 (C=C), 1460, 1404, 1330, 1226, 1150, 1119, 1062, 948, 922, 816, 785, 717, 649, 606, 500;  $\delta_{\text{H}}$  (300 MHz; DMSO- $d_6$ ) 6.54 (2H, br. s, NH<sub>2</sub>), 6.18 (2H, s, 2 × CH-Ar), 4.88 (1H, s, C<sup>4</sup>H-pyran), 3.90 (2H, q,  $J$  = 6.9 Hz, O-CH<sub>2</sub>-CH<sub>3</sub>), 3.75 (3H, s, O-CH<sub>3</sub>), 3.71 (6H, s, 2 × O-CH<sub>3</sub>), 2.23 (3H, s, CH<sub>3</sub>), 1.02 (3H, t,  $J$  = 6.9 Hz, O-CH<sub>2</sub>-CH<sub>3</sub>);  $\delta_{\text{C}}$  (75 MHz; DMSO- $d_6$ ) 166.31 (C=O), 159.85, 159.700, 159.13, 156.94, 120.54, 112.39, 105.44, 91.41 (2 × CH-Ar, 4 × C<sub>q</sub>-Ar, 3 × C<sub>q</sub>-pyran, CN), 59.78, 56.36, 56.12, 55.96, 55.27 (O-CH<sub>2</sub>, C<sup>5</sup>-Pyran, 3 × O-CH<sub>3</sub>), 27.26 (C<sup>4</sup>H-pyran), 18.08 (CH<sub>3</sub>), 13.91 (CH<sub>3</sub>); MS (EI)  $m/z$  (%) [M<sup>+</sup> + 1] 375.00 (5.63) and [M<sup>+</sup>] 374.05 (24.69) for C<sub>19</sub>H<sub>22</sub>N<sub>2</sub>O<sub>6</sub>, 345.00 (17.76), 343.00 (29.18), 329.05 (6.42), 313.00 (4.86), 297.00 (100.00), 285.05 (18.39), 269.05 (13.20), 257.05 (21.80), 241.05 (4.48), 227.00 (4.35), 207.00 (11.32), 179.00 (12.32), 161.00 (11.25), 134.05 (10.03), 77.00 (8.03), 66.95 (15.11), 57.00 (5.43), 51.00 (3.59). Anal. Calcd. for C<sub>19</sub>H<sub>22</sub>N<sub>2</sub>O<sub>6</sub>: C, 60.95; H, 5.92; N, 7.48. Found: C, 61.17; H, 6.08; N, 7.71.

#### 6-Amino-5-cyano-4-(4-fluoro-phenyl)-2-methyl-4H-pyran-3-carboxylic acid benzyl ester **4i**

The resulting reaction mixture was poured onto iced water and the precipitated solid was filtered off to obtain a yellow powder, which was washed with plenty of water, air dried, recrystallized from EtOH/ petroleum ether to give a pale yellow powder, yield (80%),

m.p. 124–126 °C;  $\nu_{\max}$  (KBr)/ $\text{cm}^{-1}$  3458 (asymmetric  $\text{NH}_2$ ), 3324 (symmetric  $\text{NH}_2$ ), 3238 and 3095 (CH-Ar), 2939 (CH-aliphatic), 2370, 2199 (CN), 1721 (C=O), 1680 and 1602 (C=C), 1504, 1450, 1405, 1376, 1321, 1219, 1177, 1119, 1056, 958, 852, 763, 742, 696, 595, 521, 466;  $\delta_{\text{H}}$  (300 MHz;  $\text{DMSO-}d_6$ ) 7.31–7.27 (3H, m, 3  $\times$  CH-Ar), 7.13–7.09 (6H, m, 6  $\times$  CH-Ar), 6.94 (2H, br. s,  $\text{NH}_2$ ), 5.07 and 4.98 (2H, ABq,  $J = 16.4$  Hz, O- $\text{CH}_2$ -Ph), 4.34 (1H, s,  $\text{C}^4\text{H-pyran}$ ), 2.32 (3H, s,  $\text{CH}_3$ );  $\delta_{\text{C}}$  (75 MHz;  $\text{DMSO-}d_6$ ), 164.65 (C=O), 157.80, 156.91, 140.17, 135.43, 128.80, 128.72, 127.98, 127.63, 127.42, 115.06, 114.78, 106.18 (9  $\times$  CH-Ar, 3  $\times$   $\text{C}_q$ -Ar, 3  $\times$   $\text{C}_q$ -pyran, CN), 65.48 (O- $\text{CH}_2$ -Ph), 56.99 ( $\text{C}^5$ -pyran), 38.74 ( $\text{C}^4\text{H-pyran}$ ), 18.04 ( $\text{CH}_3$ ); MS (EI)  $m/z$  (%) [ $\text{M}^+ + 1$ ] 365.05 (0.42) and [ $\text{M}^+$ ] 364.05 (1.41) for  $\text{C}_{21}\text{H}_{17}\text{FN}_2\text{O}_3$ , 273.05 (44.27), 269.10 (9.28), 251.05 (0.71), 229.00 (3.41), 213.00 (2.77), 200.00 (0.74), 184.00 (1.45), 158.00 (1.24), 145.05 (1.10), 133.05 (1.33), 121.05 (0.83), 91.05 (100.00), 77.00 (2.43), 65.00 (13.54), 51.00 (3.00).

#### 6-Amino-5-cyano-4-(4-methoxy-phenyl)-2-methyl-4H-pyran-3-carboxylic acid benzyl ester **4j**

The resulting reaction mixture was poured onto iced water and the precipitate was filtered off to obtain a yellow solid, which was washed with plenty of water, air dried and recrystallized from EtOH–petroleum ether to give off-white shiny crystals, yield (87%), m.p. 170–172 °C;  $\nu_{\max}$  (KBr)/ $\text{cm}^{-1}$  3407 (asymmetric  $\text{NH}_2$ ), 3328 (symmetric  $\text{NH}_2$ ), 3263, 3219 and 3009 (CH-Ar), 2958 (CH-aliphatic), 2370, 2189 (CN), 1698 (C=O), 1678, 1646 and 1603 (C=C), 1511, 1417, 1379, 1334, 1261, 1208, 1174, 1113, 1059, 1032, 1004, 948, 852, 813, 771, 692, 601, 568, 527;  $\delta_{\text{H}}$  (300 MHz;  $\text{DMSO-}d_6$ ) 7.31–7.29 (3H, m, 3  $\times$  CH-Ar), 7.12–7.09 (2H, m, 2  $\times$  CH-Ar), 7.00 (2H, dd,  $J = 8.4, 2.7$  Hz, 2  $\times$  CH-Ar), 6.94 (2H, br. s,  $\text{NH}_2$ ), 6.84 (2H, dd,  $J = 8.4, 2.72$  Hz, 2  $\times$  CH-Ar), 5.05 and 5.3 (2H, ABq,  $J = 12.6$  Hz, O- $\text{CH}_2$ -Ph), 4.27 (1H, s,  $\text{C}^4\text{H-pyran}$ ), 3.74 (3H, s, O- $\text{CH}_3$ ), 2.31 (3H, s,  $\text{CH}_3$ );  $\delta_{\text{C}}$  (75 MHz;  $\text{DMSO-}d_6$ ), 165.39 (C=O), 158.25, 158.14, 156.76, 136.82, 135.79, 128.24, 127.84, 127.63, 119.74, 113.83, 107.18 (9  $\times$  CH-Ar, 3  $\times$   $\text{C}_q$ -Ar, 4  $\times$   $\text{C}_q$ -pyran, CN), 65.67 (O- $\text{CH}_2$ -Ph), 57.57, 55.04 ( $\text{C}^5$ -pyran and O- $\text{CH}_3$ ), 38.92 ( $\text{C}^4\text{H-pyran}$ ), 18.23 ( $\text{CH}_3$ ); MS (EI)  $m/z$  (%) [ $\text{M}^+ + 1$ ] 377.05 (0.99) and [ $\text{M}^+$ ] 376.05 (3.61) for  $\text{C}_{22}\text{H}_{20}\text{N}_2\text{O}_4$ , 310.05 (0.77), 285.05 (51.33), 269.05 (6.84), 241.05 (6.47), 225.00 (4.71), 212.00 (0.68), 184.00 (3.11), 161.00 (4.63), 135.05 (2.31), 108.05 (1.55), 91.05 (100.00), 77.00 (4.75), 65.00 (13.86), 51.00 (3.36).

#### 6-Amino-5-cyano-4-(4-cyano-phenyl)-2-methyl-4H-pyran-3-carboxylic acid benzyl ester **4k**

Evaporation of the excess solvent afforded a sticky, dark-red residue, which was treated with iced water, to resolve it into a dark-red precipitate. Filtration, air drying and recrystallization from EtOH gave shiny golden crystals, yield (58%), m.p. 156–158 °C;  $\nu_{\max}$  (KBr)/ $\text{cm}^{-1}$  3407 (asymmetric  $\text{NH}_2$ ), 3301 (symmetric  $\text{NH}_2$ ), 3265, 3224, 3196 and 3061 (CH-Ar), 2964 and 2887 (CH-aliphatic), 2373, 2203 (CN), 1720 (C=O), 1685 and 1607 (C=C), 1497, 1449, 1405, 1376, 1319, 1258, 1216, 1182, 1129, 1057, 913, 864, 797, 752, 696, 615, 549, 507, 484, 437;  $\delta_{\text{H}}$  (300 MHz;  $\text{DMSO-}d_6$ ) 7.76 (2H, d,  $J = 8.1$  Hz, 2  $\times$  CH-Ar), 7.33–7.27 (5H, m, 5  $\times$  CH-Ar), 7.08–7.02 (4H, m, 2  $\times$  CH-Ar and  $\text{NH}_2$ ), 5.08 and 4.96 (2H, ABq,  $J = 12.6$  Hz, O- $\text{CH}_2$ -Ph), 4.44 (1H, s,  $\text{C}^4\text{H-pyran}$ ), 2.34 (3H, s,  $\text{CH}_3$ );  $\delta_{\text{C}}$  (75 MHz;  $\text{DMSO-}d_6$ ), 164.98 (C=O), 158.50, 158.38, 150.35, 135.64, 132.57, 128.23, 127.92, 127.74, 119.31, 118.76, 109.61, 105.66 (9  $\times$  CH-Ar, 3  $\times$   $\text{C}_q$ -Ar, 3  $\times$   $\text{C}_q$ -pyran, 2  $\times$  CN), 65.79 (O- $\text{CH}_2$ -Ph), 56.33 ( $\text{C}^5$ -pyran), 34.85 ( $\text{C}^4\text{H-pyran}$ ), 18.43 ( $\text{CH}_3$ ); MS (EI)  $m/z$  (%) [ $\text{M}^+$ ] 371.00 (0.94) for  $\text{C}_{22}\text{H}_{17}\text{N}_3\text{O}_3$ , 280.00 (55.65), 269.05 (16.00), 236.00 (2.30), 178.95 (2.02), 128.05 (1.20), 107.05 (2.71), 91.05 (6.47), 65.00 (12.33), 51.00 (3.64).

#### 6-Amino-4-(2-chloro-phenyl)-5-cyano-2-methyl-4H-pyran-3-carboxylic acid benzyl ester **4l**

Filtration of the resulting reaction suspension afforded a pale-yellow solid that was washed with plenty of water, air dried and recrystallized from MeOH–petroleum ether to give white crystals, yield (70%), m.p. 162–164 °C;  $\nu_{\max}$  (KBr)/ $\text{cm}^{-1}$  3467 (asymmetric  $\text{NH}_2$ ), 3321 (symmetric  $\text{NH}_2$ ), 3217, 3180, 3058 and 3030 (CH-Ar), 2955 (CH-aliphatic), 2368, 2200 (CN), 1724 (C=O), 1678 and 1598 (C=C), 1467, 1440, 1402, 1378, 1321, 1229, 1177, 1127, 1060, 958, 830, 745, 698, 674, 616, 577, 499, 420;  $\delta_{\text{H}}$  (300 MHz;  $\text{DMSO-}d_6$ ) 7.37–7.14 (7H, m, 7  $\times$  CH-Ar), 7.02–6.90 (4H, m, 2  $\times$  CH-Ar and  $\text{NH}_2$ ), 5.07 and 4.98 (2H, ABq,

$J = 12.6$  Hz, O-CH<sub>2</sub>-Ph), 4.91 (1H, s, C<sup>4</sup>H-pyran), 2.36 (3H, s, CH<sub>3</sub>);  $\delta_C$  (75 MHz; DMSO-*d*<sub>6</sub>), 165.34 (C=O), 158.59, 158.56, 140.06, 135.77, 132.06, 129.74, 129.49, 128.42, 128.27, 127.82, 127.57, 119.19, 105.76 (9 × CH-Ar, 3 × C<sub>q</sub>-Ar, 3 × C<sub>q</sub>-pyran, CN), 65.76 (O-CH<sub>2</sub>-Ph), 56.19 (C<sup>5</sup>-Pyran), 35.02 (C<sup>4</sup>H-pyran), 18.39 (CH<sub>3</sub>); MS (EI)  $m/z$  (%) [ $M^+$ , <sup>37</sup>Cl] 382.05 (0.64) and [ $M^+$ , <sup>35</sup>Cl] 380.05 (1.17) for C<sub>21</sub>H<sub>17</sub>ClN<sub>2</sub>O<sub>3</sub>, 291.00 (8.32), 289.00 (24.11), 271.05 (0.47), 269.10 (12.27), 247.00 (0.67), 245.00 (3.25), 209.00 (1.63), 207.00 (0.46), 181.00 (1.10), 179.00 (0.92), 167.00 (0.95), 165.00 (1.23), 136.05 (0.29), 134.10 (0.90), 91.05 (100.00), 77.05 (3.48), 65.00 (16.45), 51.00 (4.41). Anal. Calcd. for C<sub>21</sub>H<sub>17</sub>ClN<sub>2</sub>O<sub>3</sub>: C, 66.23; H, 4.50; N, 7.36. Found: C, 66.48; H, 4.73; N, 7.57.

#### 6-Amino-5-cyano-4-(2,4-dichloro-phenyl)-2-methyl-4H-pyran-3-carboxylic acid benzyl ester **4m**

Filtration of the reaction suspension and recrystallization of the obtained solid from ethanol gave a white powder, yield (57%), m.p. 146–148 °C;  $\nu_{\max}$  (KBr)/cm<sup>-1</sup> 3466 (asymmetric NH<sub>2</sub>), 3322 (symmetric NH<sub>2</sub>), 3223 and 3190 (CH-Ar), 2957 (CH-aliphatic), 2371, 2341, 2202 (CN), 1720 (C=O), 1683, 1642 and 1603 (C=C), 1462, 1402, 1375, 1223, 1176, 1124, 1098, 1060, 1005, 956, 844, 745, 698, 647, 584, 517, 455;  $\delta_H$  (300 MHz; DMSO-*d*<sub>6</sub>) 7.45 (1H, d,  $J = 2.1$  Hz, CH-Ar), 7.35 (1H, dd,  $J = 8.4, 2.1$  Hz, CH-Ar), 7.28–7.18 (4H, m, 4 × CH-Ar), 7.05–6.93 (4H, m, 2 × CH-Ar, NH<sub>2</sub>), 5.09 (1H, d,  $J = 12.6$  Hz, one of O-CH<sub>2</sub>-Ph), 4.92 (1H, d,  $J = 12.6$  Hz, one of O-CH<sub>2</sub>-Ph), 4.87 (1H, s, C<sup>4</sup>H-pyran), 2.36 (3H, s, CH<sub>3</sub>);  $\delta_C$  (75 MHz; DMSO-*d*<sub>6</sub>), 164.50 (C=O), 158.46, 158.09, 140.88, 135.27, 132.54, 131.57, 130.72, 128.37, 127.78, 127.50, 127.37, 118.61, 104.89 (8 × CH-Ar, 4 × C<sub>q</sub>-Ar, 3 × C<sub>q</sub>-pyran, CN), 65.37 (O-CH<sub>2</sub>), 55.30 (C<sup>5</sup>-pyran), 34.64 (C<sup>4</sup>H-pyran), 18.01 (CH<sub>3</sub>); MS (EI)  $m/z$  (%) [ $M^+$ , <sup>37</sup>Cl] 416.00 (0.58), [ $M^+$ , <sup>35</sup>Cl] 414.00 (0.79) for C<sub>21</sub>H<sub>16</sub>Cl<sub>2</sub>N<sub>2</sub>O<sub>3</sub>, 324.90 (19.35), 322.90 (29.45), 307.90 (0.29), 305.90 (0.37), 280.95 (1.65), 279.95 (0.60), 269.05 (13.68), 270.00 (4.80), 243.00 (1.44), 221.90 (0.76), 207.95 (1.20), 186.95 (0.94), 164.00 (1.00), 134.05 (1.62), 92.05 (8.02), 91.05 (100.00), 79.05 (2.57), 65.00 (14.26), 57.05 (5.88), 51.00 (3.42). Anal. Calcd. for C<sub>21</sub>H<sub>16</sub>Cl<sub>2</sub>N<sub>2</sub>O<sub>3</sub>: C, 60.74; H, 3.88; N, 6.75. Found: C, 60.95; H, 4.12; N, 6.93.

#### 3.1.3. General Procedures for Synthesis of 6-Amino-4-(aryl)-3-methyl-2,4-dihydro-pyrano[2,3-*c*]pyrazole-5-carbonitrile **5a,b**

To a mixture of ethyl acetoacetate **3b** (0.003, 0.39 g, 0.38 mL) and hydrazine hydrate (2.1 equiv., 0.0062, 0.31 g, 0.3 mL), the appropriate aromatic aldehyde **1e** or **1f** (0.003 mol) was added, followed by malononitrile **2** (0.003, 0.2 g), EtOH (20 mL) and Et<sub>3</sub>N (0.0007 mol, 0.07 g, 0.1 mL). The resulting reaction mixture was heated under reflux for 12 h.

#### 6-Amino-4-(2-chloro-3-hydroxy-phenyl)-3-methyl-2,4-dihydro-pyrano[2,3-*c*]pyrazole-5-carbonitrile **5a**

Evaporation of the excess solvent and recrystallization of the remaining product from EtOH afforded a beige solid, yield (65%), m.p. 240–242 °C;  $\nu_{\max}$  (KBr)/cm<sup>-1</sup> 3377 and 3309 (OH, NH<sub>2</sub> and NH), 3159 (CH-Ar), 2929 (CH-aliphatic), 2698, 2368, 2171 (CN), 1650 and 1597 (C=C), 1515, 1486, 1458, 1412, 1344, 1291, 1257, 1189, 1161, 1102, 1051, 962, 863, 834, 782, 724, 670, 604, 559, 462;  $\delta_H$  (300 MHz; DMSO-*d*<sub>6</sub>) 12.12 (1H, s, NH), 10.18 (1H, br. s, OH), 7.11 (1H, t,  $J = 7.8$  Hz, Ar-H), 6.90 (2H, br. s, NH<sub>2</sub>), 6.84 (1H, dd,  $J = 8.0, 1.1$  Hz, Ar-H), 6.58 (1H, apparent d,  $J = 7.5$  Hz, Ar-H), 5.06 (1H, s, C<sup>4</sup>H-pyran), 1.82 (3H, s, CH<sub>3</sub>);  $\delta_C$  (75 MHz; DMSO-*d*<sub>6</sub>) 161.19, 154.92, 153.01, 135.28, 127.4, 120.47, 119.26, 114.52, 97.57, (3 × CH-Ar, 3 × C<sub>q</sub>-Ar, 3 × C<sub>q</sub>-pyran, C<sub>q</sub>-pyrazole, CN), 55.99 (C<sup>5</sup>-pyran), 30.67 (C<sup>4</sup>H-pyran), 9.55 (CH<sub>3</sub>); MS (EI)  $m/z$  (%) [ $M^+ + 1$  <sup>37</sup>Cl] 304.95 (1.37), [ $M^+$ , <sup>37</sup>Cl], 304.00 (7.36), [ $M^+ + 1$  <sup>35</sup>Cl] 303.00 (5.84) and [ $M^+$ , <sup>35</sup>Cl] 302.00 (22.49) for C<sub>14</sub>H<sub>11</sub>ClN<sub>4</sub>O<sub>2</sub>, 278.00 (1.13), 276.00 (3.31), 269.05 (0.21), 267.05 (1.22), 237.00 (1.99), 201.00 (18.55), 176.00 (10.65), 175.00 (100.00), 128.05 (1.25), 115.10 (5.92), 105.05 (1.99), 99.00 (2.82), 89.00 (4.58), 77.00 (3.02), 66.00 (7.52), 63.00 (8.23), 57.05 (3.77), 51.00 (4.44). Anal. Calcd. for C<sub>14</sub>H<sub>11</sub>ClN<sub>4</sub>O<sub>2</sub>: C, 55.55; H, 3.66; N, 18.51. Found: C, 55.79; H, 3.78; N, 18.68.

### 6-Amino-3-methyl-4-(2,4,6-trimethoxy-phenyl)-2,4-dihydro-pyrano[2,3-c]pyrazole-5-carbonitrile **5b**

The resulting reaction mixture was cooled down and poured onto ice/water to obtain a pale-yellow precipitate. Recrystallization from EtOH/DMF afforded a yellow/mustard solid (70%), m.p. 182–184 °C;  $\nu_{\max}$  (KBr)/ $\text{cm}^{-1}$  3183 and 3183 (NH<sub>2</sub> and NH), 3002 (CH-Ar), 2940 and 2841 (CH-aliphatic), 2696, 2372, 2184 (CN), 1655 and 1599 (C=C), 1490, 1462, 1409, 1334, 1281, 1226, 1149, 1118, 1040, 951, 922, 828, 759, 733, 650, 581, 526;  $\delta_{\text{H}}$  (300 MHz; DMSO-*d*<sub>6</sub>) 11.75 (1H, s, NH), 6.54 (2H, s, 2 × Ar-H), 6.14 (2H, br. s, NH<sub>2</sub>), 5.02 (1H, s, CH-pyran), 3.72 (3H, s, OCH<sub>3</sub>), 3.64 (6H, s, 2 × OCH<sub>3</sub>), 1.86 (3H, s, CH<sub>3</sub>);  $\delta_{\text{C}}$  (75 MHz; DMSO-*d*<sub>6</sub>) 161.68, 159.29, 155.09, 133.60, 120.28, 111.57, 97.63, (2 × CH-Ar, 4 × C<sub>q</sub>-Ar, 3 × C<sub>q</sub>-pyran, C<sup>3</sup>-pyrazole, CN), 55.80, 55.24, 54.79 (C<sup>5</sup>-pyran and 3 × O-CH<sub>3</sub>), 24.3 (C<sup>4</sup>H-pyran), 8.89 (CH<sub>3</sub>); MS (EI) *m/z* (%) [M<sup>+</sup>] 302.00 (22.49) for C<sub>17</sub>H<sub>18</sub>N<sub>4</sub>O<sub>4</sub>, 342.05 (15.25), 327.05 (29.93), 311.00 (100.00), 295.00 (5.77), 276.05 (14.53), 245.00 (54.35), 230.00 (8.58), 201.00 (4.44), 175.00 (26.46), 139.10 (8.45), 121.05 (6.39), 98.05 (11.78), 77.05 (10.21), 65.05 (7.86), 57.05 (15.75).

## 3.2. Biology

### 3.2.1. Antioxidant Assays

The in vitro antioxidant potential of the synthesized compounds was assessed by two different techniques and compared to butylated hydroxytoluene (BHT), a widely used commercial antioxidant which was taken as the positive control.

#### DPPH Radical Scavenging Assay

The compounds' capacities to scavenge the stable radical 1,1 diphenyl-2-picrylhydrazyl (DPPH) formed in solution by donation of a hydrogen atom or an electron was investigated according to the method described by Bersuder and coworkers [83]. Due to the fact that the initial blue/purple solution of diphenyl picrylhydrazine changes to yellow in the presence of compounds with a capacity to scavenge DPPH free radicals, this reaction is used as a measure of a compound's ability to scavenge any free radical. Briefly, a 0.5 mL volume of DPPH ethanolic solution was mixed with an equal volume of each sample concentration (0.03 to 1 mg/mL), shaken strongly and incubated at room temperature for 1 h in darkness. The absorbance of the residual DPPH radicals was measured at 519 nm and compared to that of the control (without the tested compound). DPPH radical scavenging was calculated using the following formula: Scavenging effect (%) =  $(1 - A_{\text{compound}}/A_{\text{Control}}) \times 100$ , where  $A_{\text{compound}}$  and  $A_{\text{control}}$  are the absorbances of the tested compound and of the control, respectively. A plot of the scavenging effect (%) versus the sample concentration was also performed to determine the compound concentration providing 50% inhibition (IC<sub>50</sub>).

#### Reducing Power Assay

The reducing power of the studied compounds was assessed according to Oyaizu's method [84]. Briefly, different concentrations (ranging from 0 to 1 mg/mL) of each tested compound were first mixed with 1 mL of 0.2 M sodium phosphate buffer (pH 6.6) and 1 mL of 1% potassium ferricyanide (K<sub>3</sub>Fe(CN)<sub>6</sub>) and incubated at 50 °C for 20 min. After the addition of 1.25 mL of 20% trichloroacetic acid (TCA), the mixture was centrifuged for 10 min at 3000 rpm and the upper layer solution was then mixed with 0.5 mL of 0.1% fresh ferric chloride and an equal volume of deionized water. Finally, the absorption of the resulting mixture was measured at 700 nm using a UV spectrophotometer against distilled water as the blank, while butylated hydroxytoluene (BHT) was used as a positive control. The sample ferric reducing power capability was indicated by increased absorbance.

### 3.2.2. Antibacterial Activity

The antibacterial activity of all synthesized compounds was evaluated against the Gram-negative strains *E. coli* (ATCC 25966), *K. pneumonia* (ATCC 700603), *P. aeruginosa* (ATCC 27853) and *S. enteric* (ATCC 43972) and against the Gram-positive strains *B. cereus*



(ATCC 14579), *B. subtilis* (ATCC 6633), *E. faecalis* (ATCC 29122), *S. aureus* (ATCC 25923) and *S. epidermidis* (ATCC 14990), using the agar diffusion method through measuring the appearance of the inhibition zone on the surface of the top agar, as reported by Berghe and Vlietinck [85]. Ampicillin (10 µg/well) was used as the positive reference standard. Bacterial viability was also investigated by determining the colony-forming ability (CFU) of bacteria incubated at different time intervals without or with appropriate amounts of the compound, which were mixed with  $2 \times 10^7$  CFU/mL in sterile BHI and incubated under shaking for 60 min at 37 °C. Samples were serially diluted into sterile BHI, streaked onto media agar plates and incubated for 24 h at 37 °C. The antibacterial potency of the tested compounds was expressed as the residual number of CFUs with reference to the initial inoculums. The results presented as the half-maximal (50 %) inhibitory concentration (IC<sub>50</sub>) values are the means of three different measurements.

### 3.2.3. Cell Culture

Cytotoxic potency was examined for a human colon cancer cell line HCT-116 (American Type Culture Collection; Manassas, VA, USA) using various amounts of each compound (10, 25, 50 and 100 µg). Samples were diluted in Dulbecco's Modified Eagle's Medium, consisting of 10% Fetal Bovine Serum, and added to cells grown and cultured for 24 h in a 5% CO<sub>2</sub>-humidified incubator at 37 °C. Then, the activity of lactate dehydrogenase released from damaged cells was determined in the collected supernatant aliquots using an ELISA endpoint assay (Benchmark Plus, Bio-Rad, Hercules, CA, USA). As positive and negative controls, respectively, 0.1% Triton X-100 in the assay medium and the assay medium only were used. Cell viability, shown as mean values ± SDs (n = 3), was expressed as a relative percentage of the OD values determined at 600 nm in compound-treated cells and the control.

### 3.2.4. CDK2 Inhibitory Assay

CDK-2 inhibition activity of the studied compounds **4d** and **4k** was evaluated using a commercial CDK2 ELISA Kit (cat. no.: 79599; BPS Biosciences, San Diego, CA, USA) following the manufacturer's instructions. Briefly, different concentrations of each compound or the positive control **BMS-265246** (0.01, 0.1, 1 or 10 µM) were incubated with 20 µL of diluted CDK2/CyclinA2 enzyme at 30 °C for 45 min. Following the addition of 50 µL Kinase-Glo<sup>®</sup> Reagent to each well, the plate was incubated at room temperature for 15 min. Then, the luminescence signal was measured using the microplate reader. The CDK2 inhibitory activity was expressed as inhibition percentage, which was determined by comparison with a control experiment for comparative purposes. IC<sub>50</sub> values were deduced from the curves. All measurements were performed in triplicate.

### 3.2.5. In Vitro Quantitative Determination of CDK2 Concentration in HCT-116 Cells

The in vitro quantitative measurement of concentration of CDK2 in lysates of HCT-116 cells was carried out using a commercial Human CDK2 ELISA Kit (cat. no.: LS-F22176; LifeSpan Biosciences Inc., Seattle, WA, USA) in the presence or absence of the studied compounds (**4d** and **4k**), following the manufacturer's instructions. Briefly, standards, blanks or samples were first incubated in the corresponding wells for 90 min at 37 °C. Then, biotinylated detection antibody was added to each well and the plate was incubated for 1 h at 37 °C followed by the addition of an Avidin–Horseradish Peroxidase (HRP) conjugate which binds to the biotin. After incubation of the mixture for 30 min at 37 °C, unbound Avidin–HRP conjugate was washed away and a TMB substrate was then added which reacts with the HRP enzyme, resulting in color development. After that, the reaction was stopped using a sulfuric acid stop solution to terminate the color-development reaction and the optical density of each well was measured using a microplate reader at 450 nm. **BMS-265246** was used as the standard drug for inhibition of CDK2. All measurements were performed in triplicate.

### 3.2.6. Gene Expression Profiles

#### Design of the Primer

Primers specific for the cyclin-dependent kinase-2 (CDK2) and caspase-3 genes were designed using primer blast (<https://www.ncbi.nlm.nih.gov/tools/primer-blast/>, accessed on 31 October 2021) or primer3 (<https://primer3.ut.ee/>, accessed on 31 October 2021) software. The selected genes covered the two main groups of the cyclin-dependent kinase-2 (CDK2) gene and the caspase-3 gene. Primers were used in RT-qPCR analysis to amplify fragments of 100–200 bp in length (Table 7).

**Table 7.** Oligonucleotide primer pairs used for quantitative real-time polymerase chain reaction (RT-qPCR) analysis.

Gene Name	Forward Primer	Reverse Primer
Caspase-3	F 5'-GGAAGCGAATCAATGGACTCTGG-3'	R 5'-GCATCGACATCTGTACCAGACC-3'
Housekeeping gene (GAPDH)	F 5'-GCACCGTCAAGGCTGAGAAC-3'	R 5'-ATGGTGGTGAAGACGCCAGT-3'

#### RNA Isolation and Reverse Transcription

Total RNA was extracted from each cell culture flask using the RNeasy extraction kit (RNeasy micro kit, cat. no. 74004). Up to  $1 \times 10^6$  cells, depending on the cell line, were disrupted in buffer RLT and homogenized and disrupted. Ethanol was then added to the lysate, creating conditions that promote the selective binding of RNA to the RNeasy membrane. The samples were then applied to the RNeasy Mini spin column. Total RNA binds to the membrane, contaminants were efficiently washed away and high-quality RNA was eluted in RNase-free water. All bind, wash and elution steps were performed by centrifugation in a micro-centrifuge, with DNase I treatment. The amount of extracted RNA was quantified by estimating the absorbance at 260 nm. The purity of the RNA was checked by measuring the ratio of the absorbance at 260 and 280 nm, where a ratio ranging from 1.8 to 2.0 was taken to be pure. The absence of degradation of the RNA was verified by RNA electrophoresis on a 1.5% agarose gel containing ethidium bromide. First-strand cDNA was generated from 1  $\mu$ g of each flask using the High-Capacity cDNA Archive Kit, Model for One-Step RT-PCR procedures (RT-PCR kit- BioRad-USA, cat. no. 345-0412), according to the manufacturer's protocol.

#### Quantitative Real-Time PCR (qRT-PCR)

Quantitative real-time PCR was carried out with the Thermal Cycler Rotorgene Real-Time System II (Rotorgene, South Korea) with the SYBR kit. The primer sequences are shown in Table 5. The PCR reaction was carried out in triplicate in 96-well plates. The mixture included 12.5  $\mu$ L SYBR premix ExTag, 1  $\mu$ L of 60 ng cDNA as the template, 5  $\mu$ L of 2  $\mu$ mol/L primer premix and 6.5  $\mu$ L of DNase-free nuclease water at a total volume of 25  $\mu$ L. The thermal profile of the real-time system was one step at 95 °C for 30 s, followed by 30 to 45 cycles at 95 °C for 10 s (denaturation) and at 55 °C for 30 s (annealing and extension), followed by an added dissociation pattern. The actin gene was used as an internal control gene, was abundant and remained constant, and GAPDH was used as an internal standard (housekeeping gene).

#### Data Analysis

The relative expression levels through the average cycle threshold (CT) were successfully detected. Average CT values were calculated from the triplicate experiment conducted for each gene; the CT value was detected by subtracting the average CT value of genes from the CT value of actin and GAPDH genes. The relative expression levels of the target genes were calculated using the  $\Delta\Delta$  Ct method [86] and the reference genes GAPDH for the cancer cell line. Finally, a fold change equation ( $2^{-1}$ ) was used to estimate relative expression levels, while the standard deviation was calculated from the replicated experimental data.

### 3.3. In Silico Studies

The cyclin-dependent kinase 2 (CDK2) enzyme was selected as the molecular target to investigate the underlying molecular mechanism of the antiproliferative effects based on similarity to previously reported antitumoral pyran derivatives, which induced cell-cycle arrest via targeting CDK2 enzyme [35–37]. The structure of the target protein was retrieved from the Protein Data Bank ([www.rcsb.org](http://www.rcsb.org) accessed on 10 January 2022). Thus, the three-dimensional crystal structure (PDB code: 1DI8) of CDK2 in complex with 4-[3-hydroxy anilino]-6,7-dimethoxyquinazoline (**DTQ**) was used.

The protein was prepared with a protein preparation wizard available in the Schrodinger suite, using the standard protocol recommended by Schrodinger, which involved removal of water/solvent molecules, fixing of non-standard residues and adding hydrogens and partial charges.

The structures of the studied compounds (ligands), including **4d**, **4f**, **4k**, **BMS-265246** and **DTQ**, were sketched using the built-in panel of Maestro 11.

Ligand preparation is a capability of the Schrodinger software suite that combines tools for generating 3D structures and 2D (SDF) representations as well as performing ligand geometry minimization. By employing the Ligprep protocol, all the ligands were organized using OPLS3 with default settings, and the output file was saved in maegz format automatically [87].

The Glide module [88] in extra precision (XP) mode [89] was used for flexible molecular docking of all the molecules inside the active site (ATP binding site of the kinase) [90], using default settings, as recommended in the manual for the Glide module from Schrodinger. The residues Lys33, Glu51 and Asp145, constituting the active site, were set as flexible residues. For validation of the docking protocol, the co-crystallized ligand **DTQ** (4-[3-hydroxyanilino]-6,7-dimethoxyquinazoline) was redocked, with an RMSD of 0.34 Å.

Upon completion of each docking calculation, a maximum of 100 poses per ligand were generated, which were passed through a series of filters, and the final best docked structures were ranked using a Glide score function and Glide energy. The Glide score of the predicted poses, which is the scoring energy for the best pose (lowest energy) of each ligand in the binding site, and the Glide energy were used to quantify the binding strength of the different compounds to the target protein. The protein–ligand complexes were analyzed to examine various types of interactions. For the best-scored ligands, the 2D and 3D plots of molecular ligand–receptor interactions were analyzed for hydrogen bonds and halogen bonds.

### ADME Evaluation

SwissADME [91] is a free web tool for evaluating the pharmacokinetics, drug-likeness and medicinal chemistry friendliness of small molecules.

It was accessed on 10 January 2022 to predict the ADME properties of the bioactive synthesized compounds **4g**, **4j**, **4d** and **4k**.

## 4. Conclusions

Eleven new derivatives of 2-amino-4*H*-pyran and one 2,4-dihydropyrano[2,3-*c*]pyrazole were synthesized, fully characterized and examined for antioxidant and antibacterial activities as well as cytotoxicity on a HCT-116 cell line of colorectal cancer. Derivatives **4g** and **4j** showed promising antioxidant potencies as compared to BHT. Moreover, these analogues were more potent than ampicillin, displaying lowered IC<sub>50</sub> values against the Gram-positive strains *B. subtilis* (ATCC 6633), *S. aureus* (ATCC 25923) and *S. epidermidis* (ATCC 14990) and *E. faecalis* (ATCC 29122). The cell viability assays showed that compounds **4d** and **4k** exhibited the strongest antiproliferative activities, whereas **4g** and **4j** were found to be inactive. Thus, the latter analogues would be suitable candidates for further toxicity studies to evaluate their potential as safe antioxidant and anti-Gram-positive bacterial agents that could be used as preventive and adjuvant therapeutic agents against CRC. The antiproliferative mechanism of action of **4d** and **4k** was investigated using molecular

docking simulations within the ATP binding site of CDK-2. The docking results revealed that **4d** and **4k** would inhibit CDK2 activity by competing with ATP to bind on the kinase site through establishing hydrogen bonds with backbone amino acid residues and by establishing hydrophobic interactions with side chains of surrounding residues. In addition, the docking results revealed that a more powerful inhibitor for CDK2 requires a bulkier ring to be attached to the pyran ring through a flexible chain of two to three atoms. Moreover, H-bond donors or acceptors on the central scaffold could substantially enhance binding with the receptor. Further mechanistic studies, including kinase inhibitory assays, quantitative measurement of CDK-2 protein and real-time PCR profiling of CDK-2 gene in HCT-116 treated cells, confirmed that the antiproliferative actions of **4d** and **4k** could be attributed to inhibiting the activity and downregulating the expression level of CDK-2 protein and gene as well. Consequently, these derivatives would be useful leads for the generation of new anti-CRC agents that do not cause chemotherapy-induced alopecia and arrest the cell cycle without sensitization of the epithelium. Finally, investigation of the proapoptotic potential of these analogues using real-time PCR profiling of the caspase-3 gene in HCT-116 treated cells indicated that the concentration of 10 mg/mL of **4d** or **4k** is optimal for inducing mitochondrial apoptosis of the HCT-116 cells via upregulating the expression of caspase-3; therefore, further studies on this topic will be pursued in the future. Despite the in-silico predictions of the ADME profiles and drug-likeness properties of the bioactive candidates **4g**, **4j**, **4d** and **4k** using the bioavailability radar plots, the BOILED-EGG chart and Lipinski's rule of five filter provided a first glance at the potential of these derivatives to be orally bioactive, though more in vivo investigations using animal models are needed to confirm the validity of these predictions.

**Supplementary Materials:** The following supporting information can be downloaded at <https://www.mdpi.com/article/10.3390/ph15070891/s1>: Representative spectra of the synthesized compounds.

**Author Contributions:** Conceptualization, N.N.E.E.-S., Z.M.A. and M.E.A.Z.; methodology and analysis, N.N.E.E.-S., Z.M.A. (chemistry), A.B.B. (biological screening), M.B., V.H.M. (molecular docking and ADME profiling) and H.S.O. (gene expression); writing—original draft preparation, N.N.E.E.-S., A.B.B. and M.B.; funding acquisition, M.E.A.Z. and S.A.A.-H.; writing—review and editing, N.N.E.E.-S., M.E.A.Z. and S.A.A.-H. All authors have read and agreed to the published version of the manuscript.

**Funding:** This research was funded by the Deanship of Scientific Research at Imam Mohammad bin Saud Islamic University, Riyadh, Saudi Arabia, through research group no.: RG.21-09-76.

**Institutional Review Board Statement:** Not applicable.

**Informed Consent Statement:** Not applicable.

**Data Availability Statement:** Data is contained within the article.

**Conflicts of Interest:** The authors declare no conflict of interest.

## References

1. Bray, F.; Ferlay, J.; Soerjomataram, I.; Siegel, R.L.; Torre, L.A.; Jemal, A. Global cancer statistics 2018: GLOBOCAN estimates of incidence and mortality worldwide for 36 cancers in 185 countries. *CA Cancer J. Clin.* **2018**, *68*, 394–424. [[CrossRef](#)] [[PubMed](#)]
2. Xi, Y.; Xu, P. Global colorectal cancer burden in 2020 and projections to 2040. *Transl. Oncol.* **2021**, *14*, 101174–101181. [[CrossRef](#)]
3. Currais, P.; Rosa, I.; Claro, I. Colorectal cancer carcinogenesis: From bench to bedside. *World J. Gastrointest. Oncol.* **2022**, *14*, 654–663. [[CrossRef](#)] [[PubMed](#)]
4. Malumbres, M.; Carnero, A. Cell cycle deregulation: A common motif in cancer. *Prog. Cell Cycle Res.* **2003**, *5*, 5–18.
5. Pizzimenti, S.; Toaldo, C.; Pettazoni, P.; Dianzani, M.U.; Barrera, G. The “two-faced” effects of reactive oxygen species and the lipid peroxidation product 4-hydroxynonenal in the hallmarks of cancer. *Cancers* **2010**, *2*, 338–363. [[CrossRef](#)] [[PubMed](#)]
6. Tian, T.; Wang, Z.; Zhang, J. Pathomechanisms of oxidative stress in inflammatory bowel disease and potential antioxidant therapies. *Oxidative Med. Cell. Longev.* **2017**, *2017*, 4535194. [[CrossRef](#)] [[PubMed](#)]
7. Carini, F.; Mazzola, M.; Rappa, F.; Jurjus, A.; Geagea, A.G.; Al Kattar, S.; Bou-Assi, T.; Jurjus, R.; Damiani, P.; Leone, A.; et al. Colorectal carcinogenesis: Role of oxidative stress and antioxidants. *Anticancer Res.* **2017**, *37*, 4759–4766. [[CrossRef](#)]

8. Aggarwal, V.; Tuli, H.S.; Varol, A.; Thakral, F.; Yerer, M.B.; Sak, K.; Varol, M.; Jain, A.; Khan, M.; Sethi, G. Role of reactive oxygen species in cancer progression: Molecular mechanisms and recent advancements. *Biomolecules* **2019**, *9*, 735. [[CrossRef](#)]
9. Zahra, K.F.; Lefter, R.; Ali, A.; Abdellah, E.C.; Trus, C.; Ciobica, A.; Timofte, D. The involvement of the oxidative stress status in cancer pathology: A double view on the role of the antioxidants. *Oxidative Med. Cell. Longev.* **2021**, *2021*, 9965916. [[CrossRef](#)]
10. Park, C.H.; Eun, C.S.; Han, D.S. Intestinal microbiota, chronic inflammation, and colorectal cancer. *Intest. Res.* **2018**, *16*, 338–345. [[CrossRef](#)]
11. Zou, S.; Fang, L.; Lee, M.H. Dysbiosis of gut microbiota in promoting the development of colorectal cancer. *Gastroenterol. Rep.* **2018**, *6*, 1–12. [[CrossRef](#)] [[PubMed](#)]
12. Leung, A.; Tsoi, H.; Yu, J. Fusobacterium and escherichia: Models of colorectal cancer driven by microbiota and the utility of microbiota in colorectal cancer screening. *Expert Rev. Gastroenterol. Hepatol.* **2015**, *9*, 651–657. [[CrossRef](#)] [[PubMed](#)]
13. Antonic, V.; Stojadinovic, A.; Kester, K.E.; Weina, P.J.; Brücher, B.L.; Protic, M.; Avital, I.; Izadjoo, M. Significance of infectious agents in colorectal cancer development. *J. Cancer* **2013**, *4*, 227–240. [[CrossRef](#)] [[PubMed](#)]
14. Gao, Z.; Guo, B.; Gao, R.; Zhu, Q.; Qin, H. Microbiota dysbiosis is associated with colorectal cancer. *Front. Microbiol.* **2015**, *6*, 20. [[CrossRef](#)]
15. Dai, Z.; Zhang, J.; Wu, Q.; Chen, J.; Liu, J.; Wang, L.; Chen, C.; Xu, J.; Zhang, H.; Shi, C.; et al. The role of microbiota in the development of colorectal cancer. *Int. J. Cancer* **2019**, *145*, 2032–2041. [[CrossRef](#)]
16. Geravand, M.; Fallah, P.; Yaghoobi, M.H.; Soleimanifar, F.; Farid, M.; Zinatizadeh, N.; Yaslianifard, S. Investigation of enterococcus faecalis population in patients with polyp and colorectal cancer in comparison of healthy individuals. *Arq. Gastroenterol.* **2019**, *56*, 141–145. [[CrossRef](#)]
17. Ting, N.L.N.; Lau, H.C.H.; Yu, J. Cancer pharmacomicrobiomics: Targeting microbiota to optimise cancer therapy outcomes. *Gut* **2022**, *71*, 1412–1425. [[CrossRef](#)]
18. Bhat, S.; Muthunatarajan, S.; Mulki, S.S.; Archana Bhat, K.; Kotian, K.H. Bacterial infection among cancer patients: Analysis of isolates and antibiotic sensitivity pattern. *Int. J. Microbiol.* **2021**, *2021*, 8883700. [[CrossRef](#)]
19. Benítez-Chao, D.F.; León-Buitimea, A.; Lerma-Escalera, J.A.; Morones-Ramírez, J.R. Bacteriocins: An overview of antimicrobial, toxicity, and biosafety assessment by in vivo models. *Front. Microbiol.* **2021**, *12*, 677–695. [[CrossRef](#)] [[PubMed](#)]
20. Martelli, G.; Giacomini, D. Antibacterial and antioxidant activities for natural and synthetic dual-active compounds. *Eur. J. Med. Chem.* **2018**, *158*, 91–105. [[CrossRef](#)]
21. Stone, W.L.; Krishnan, K.; Campbell, S.E.; Palau, V.E. The role of antioxidants and pro-oxidants in colon cancer. *World J. Gastrointest. Oncol.* **2014**, *6*, 55–66. [[CrossRef](#)] [[PubMed](#)]
22. Lamb, R.; Ozsvari, B.; Lisanti, C.L.; Tanowitz, H.B.; Howell, A.; Martinez-Outschoorn, U.E.; Sotgia, F.; Michael, P.; Lisanti, M.P. Antibiotics that target mitochondria effectively eradicate cancer stem cells, across multiple tumor types: Treating cancer like an infectious disease. *Oncotarget* **2015**, *6*, 4569–4584. [[CrossRef](#)]
23. Nguyen, H.T.; Duong, H.Q. The molecular characteristics of colorectal cancer: Implications for diagnosis and therapy. *Oncol. Lett.* **2018**, *16*, 9–18. [[CrossRef](#)] [[PubMed](#)]
24. Gordon, E.M.; Ravicz, J.R.; Liu, S.; Chawla, S.P.; Hall, F.L. Cell cycle checkpoint control: The cyclin G1/Mdm2/p53 axis emerges as a strategic target for broad-spectrum cancer gene therapy—A review of molecular mechanisms for oncologists. *Mol. Clin. Oncol.* **2018**, *9*, 115–134. [[CrossRef](#)] [[PubMed](#)]
25. Mani, S.; Wang, C.; Wu, K.; Francis, R.; Pestell, R. Cyclin-dependent kinase inhibitors: Novel anticancer agents. *Expert Opin. Investig. Drugs* **2000**, *9*, 1849–1870. [[CrossRef](#)]
26. Ding, L.; Cao, J.; Lin, W.; Chen, H.; Xiong, X.; Ao, H.; Yu, M.; Lin, J.; Cui, Q. The roles of cyclin-dependent kinases in cell-cycle progression and therapeutic strategies in human breast cancer. *Int. J. Mol. Sci.* **2020**, *21*, 1960. [[CrossRef](#)]
27. Coxon, C.R.; Anscombe, E.; Harnor, S.J.; Martin, M.P.; Carbain, B.; Golding, B.T.; Hardcastle, I.R.; Harlow, L.K.; Korolchuk, S.; Matheson, C.J.; et al. Cyclin-dependent kinase (CDK) inhibitors: Structure-activity relationships and insights into the CDK-2 selectivity of 6-substituted 2-arylamino-purines. *J. Med. Chem.* **2017**, *60*, 1746–1767. [[CrossRef](#)]
28. Cam, W.R.; Masaki, T.; Shiratori, T.Y.; Kato, N.; Okamoto, M.; Yamaji, Y.; Igarashi, K.; Sano, T.; Omata, M. Activation of cyclin e-dependent kinase activity in colorectal cancer. *Dig. Dis. Sci.* **2001**, *46*, 2187–2198. [[CrossRef](#)]
29. Lim, T.G.; Lee, S.Y.; Huang, Z.; Lim, D.Y.; Chen, H.; Jung, S.K.; Bode, A.M.; Lee, K.W.; Dong, Z. Curcumin suppresses proliferation of colon cancer cells by targeting CDK2. *Cancer Prev. Res.* **2014**, *7*, 466–474. [[CrossRef](#)]
30. Shi, X.N.; Li, H.; Yao, H.; Liu, X.; Li, L.; Leung, K.S.; Kung, H.F.; Lin, M.C. Adapalene inhibits the activity of cyclin-dependent kinase 2 in colorectal carcinoma. *Mol. Med. Rep.* **2015**, *12*, 6501–6508. [[CrossRef](#)]
31. Ikwu, F.A.; Isyaku, Y.; Obadawo, B.S.; Lawal, H.A.; Ajibowu, S.A. In silico design and molecular docking study of CDK2 inhibitors with potent cytotoxic activity against HCT116 colorectal cancer cell line. *J. Genet. Eng. Biotechnol.* **2020**, *18*, 51–63. [[CrossRef](#)] [[PubMed](#)]
32. Li, K.; You, J.; Wu, Q.; Meng, W.; He, Q.; Yang, B.; Zhu, C.; Cao, J. Cyclin-dependent kinases-based synthetic lethality: Evidence, concept, and strategy. *Acta Pharm. Sin. B* **2021**, *11*, 2738–2748. [[CrossRef](#)]
33. Afifi, T.H.; Okasha, R.M.; Ahmed, H.E.; Ilaš, J.; Saleh, T.; Abd-El-Aziz, A.S. Structure-activity relationships and molecular docking studies of chromene and chromene based azo chromophores: A novel series of potent antimicrobial and anticancer agents. *EXCLI J.* **2017**, *16*, 868–902. [[CrossRef](#)] [[PubMed](#)]
34. Al Nasr, I.S.; Jentzsch, J.; Shaikh, A.; Singh Shuveksh, P.; Koko, W.S.; Khan, T.A.; Ahmed, K.; Schobert, R.; Ersfeld, K.; Biersack, B. New pyrano-4H-benzo[g]chromene-5, 10-diones with antiparasitic and antioxidant activities. *Chem. Biodivers.* **2021**, *18*, e2000839–e2000851. [[CrossRef](#)] [[PubMed](#)]

35. Mouineer, A.; Zaher, A.; El-Malah, A.; Sobh, E.A. Design, synthesis, antitumor activity, cell cycle analysis and ELISA assay for cyclin dependant kinase-2 of a new (4-aryl-6-fluoro-4H-benzo [4,5] thieno [3,2-b] pyran) derivatives. *Mediterr. J. Chem.* **2017**, *6*, 165–179. [[CrossRef](#)]
36. Zaher, A.F.; Abuel-Maaty, S.M.; El-Nassan, H.B.; Amer, S.A.; Abdelghany, T.M. Synthesis, antitumor screening and cell cycle analysis of novel benzothieno [3,2-b] pyran derivatives. *J. Enzym. Inhib. Med. Chem.* **2016**, *31*, 145–153. [[CrossRef](#)] [[PubMed](#)]
37. Samir, N.; George, R.F.; Elrazaz, E.Z.; Ayoub, I.M.; Shalaby, E.M.; Plaisier, J.R.; Demitri, N.; Wink, M. Synthesis of some tropane-based compounds targeting colon cancer. *Future Med. Chem.* **2020**, *12*, 2123–2140. [[CrossRef](#)] [[PubMed](#)]
38. Yang, Z.J.; Gong, Q.T.; Wang, Y.; Yu, Y.; Liu, Y.H.; Wang, N.; Yu, X.Q. Biocatalytic tandem multicomponent reactions for one-pot synthesis of 2-Amino-4H-Pyran library and in vitro biological evaluation. *Mol. Catal.* **2020**, *491*, 110983–110992. [[CrossRef](#)]
39. de Souza Siqueira, M.; da Silva-Filho, L.C. NbCl<sub>5</sub>-promoted the synthesis of 4H-pyrans through multicomponent reaction. *Tetrahedron Lett.* **2016**, *57*, 5050–5052. [[CrossRef](#)]
40. Rahman, N.; Nongthombam, G.S.; Rani, J.W.; Nongrum, R.; Kharmawlong, G.K.; Nongkhaw, R. An environment-friendly magnetic organo-nanomaterial as a potent catalyst in synthesis of pyranopyrazole derivatives. *Curr. Organocatal.* **2018**, *5*, 150–161. [[CrossRef](#)]
41. Peng, Y.; Song, G. Amino-functionalized ionic liquid as catalytically active solvent for microwave-assisted synthesis of 4H-pyrans. *Catal. Commun.* **2007**, *8*, 111–114. [[CrossRef](#)]
42. Al-Kadasi, M.A.; Osman, H.A.; Nazeruddin, G.M. Silica ammonium acetate as an efficient and recyclable heterogeneous catalyst for synthesis of 4H-pyran derivatives under ultrasound irradiation at ambient conditions. *Am. Chem. Sci. J.* **2014**, *4*, 587–599. [[CrossRef](#)]
43. Shehab, W.S.; Ghoneim, A.A. Synthesis and biological activities of some fused pyran derivatives. *Arab. J. Chem.* **2016**, *9*, S966–S970. [[CrossRef](#)]
44. Shahbazi, S.; Ghasemzadeh, M.A.; Shakib, P.; Zolfaghari, M.R.; Bahmani, M. Synthesis and antimicrobial study of 1, 4-dihydropyrano [2,3-c] pyrazole derivatives in the presence of amino-functionalized silica-coated cobalt oxide nanostructures as catalyst. *Polyhedron* **2019**, *170*, 172–179. [[CrossRef](#)]
45. Kumar, D.; Reddy, V.B.; Sharad, S.; Dube, U.; Kapur, S. A facile one-pot green synthesis and antibacterial activity of 2-amino-4H-pyrans and 2-amino-5-oxo-5,6,7,8-tetrahydro-4H-chromenes. *Eur. J. Med. Chem.* **2009**, *44*, 3805–3809. [[CrossRef](#)]
46. Shukla, P.; Sharma, A.; Fageria, L.; Chowdhury, R. Novel spiro/nonspiro pyranopyrazoles: Eco-friendly synthesis, in-vitro anticancer activity, DNA binding, and in-silico docking studies. *Curr. Bioact. Compd.* **2019**, *15*, 257–267. [[CrossRef](#)]
47. Wang, D.C.; Xie, Y.M.; Fan, C.; Yao, S.; Song, H. Efficient and mild cyclization procedures for the synthesis of novel 2-amino-4H-pyran derivatives with potential antitumor activity. *Chin. Chem. Lett.* **2014**, *25*, 1011–1013. [[CrossRef](#)]
48. Saleh, N.M.; El-Gazzar, M.G.; Aly, H.M.; Othman, R.A. Novel anticancer fused pyrazole derivatives as EGFR and VEGFR-2 dual TK inhibitors. *Front. Chem.* **2020**, *7*, 917–929. [[CrossRef](#)]
49. El-Husseiny, W.M.; El-Sayed, M.A.A.; Abdel-Aziz, N.I.; El-Azab, A.S.; Ahmed, E.R.; Abdel-Aziz, A.A.M. Synthesis, antitumor and antioxidant activities of novel  $\alpha$ ,  $\beta$ -unsaturated ketones and related heterocyclic analogues: EGFR inhibition and molecular modelling study. *J. Enzyme Inhib. Med. Chem.* **2018**, *33*, 507–518. [[CrossRef](#)]
50. El-Sayed, N.N.; Al-Otaibi, T.M.; Alonazi, M.; Masand, V.H.; Barakat, A.; Almarhoon, Z.M.; Ben Bacha, A. Synthesis and characterization of some new quinoxalin-2(1H) one and 2-methyl-3H-quinazolin-4-one derivatives targeting the onset and progression of CRC with SAR, molecular docking, and ADMET analyses. *Molecules* **2021**, *26*, 3121. [[CrossRef](#)]
51. El-Sayed, N.N.; Almanai, N.M.; Ben Bacha, A.; Al-Obeed, O.; Ahmad, R.; Abdulla, M.; Alafeefy, A.M. Synthesis and evaluation of anticancer, antiphospholipases, antiproteases, and antimetabolic syndrome activities of some 3H-quinazolin-4-one derivatives. *J. Enzyme Inhib. Med. Chem.* **2019**, *34*, 672–683. [[CrossRef](#)] [[PubMed](#)]
52. Shahidi, F.; Zhong, Y. Measurement of antioxidant activity. *J. Funct. Foods* **2015**, *18*, 757–781. [[CrossRef](#)]
53. Champlin, F.R.; Ellison, M.L.; Bullard, J.W.; Conrad, R.S. Effect of outer membrane permeabilisation on intrinsic resistance to low triclosan levels in pseudomonas aeruginosa. *Int. J. Antimicrob. Agents* **2005**, *26*, 159–164. [[CrossRef](#)] [[PubMed](#)]
54. Kulkarni, A.P.; Nagvekar, V.C.; Veeraraghavan, B.; Warriar, A.R.; Ts, D.; Ahdal, J.; Jain, R. Current perspectives on treatment of gram-positive infections in India: What is the way forward? *Interdiscip. Perspect. Infect. Dis.* **2019**, *2019*, 7601847. [[CrossRef](#)] [[PubMed](#)]
55. Arnaout, M.K.; Tamburro, R.F.; Bodner, S.M.; Sandlund, J.T.; Rivera, G.K.; Pui, C.H.; Ribeiro, R.C. Bacillus cereus causing fulminant sepsis and hemolysis in two patients with acute leukemia. *J. Pediatr. Hematol. Oncol.* **1999**, *21*, 431–435. [[CrossRef](#)]
56. Olmos, C.; Vilacosta, I.; López, J.; Sáez, C.; Anguita, M.; García-Granja, P.E.; Sarriá, C.; Silva, J.; Álvarez-Álvarez, B.; Martínez-Monzonis, M.A.; et al. Short-course antibiotic regimen compared to conventional antibiotic treatment for gram-positive cocci infective endocarditis: Randomized clinical trial (SATIE). *BMC Infect. Dis.* **2020**, *20*, 417–424. [[CrossRef](#)]
57. Cascioferro, S.; Parrino, B.; Carbone, D.; Pecoraro, C.; Diana, P. Novel strategies in the war against antibiotic resistance. *Future Med. Chem.* **2021**, *13*, 529–531. [[CrossRef](#)]
58. Fathima, A.; Rao, J.R. Selective toxicity of Catechin—A natural flavonoid towards bacteria. *Appl. Microbiol. Biotechnol.* **2016**, *100*, 6395–6402. [[CrossRef](#)]
59. Damo, S.; Chazin, W.J.; Skaar, E.P.; Kehl-Fie, T.E. Inhibition of bacterial superoxide defense: A new front in the struggle between host and pathogen. *Virulence* **2012**, *3*, 325–328. [[CrossRef](#)]
60. Donadio, G.; Mensitieri, F.; Santoro, V.; Parisi, V.; Bellone, M.L.; De Tommasi, N.; Izzo, V.; Dal Piaz, F. Interactions with microbial proteins driving the antibacterial activity of flavonoids. *Pharmaceutics* **2021**, *13*, 660. [[CrossRef](#)]

61. Arakawa, H.; Maeda, M.; Okubo, S.; Shimamura, T. Role of hydrogen peroxide in bactericidal action of catechin. *Biol. Pharm. Bull.* **2004**, *27*, 277–281. [[CrossRef](#)] [[PubMed](#)]
62. Grzesik, M.; Bartosz, G.; Stefaniuk, I.; Pichla, M.; Namieśnik, J.; Sadowska-Bartosz, I. Dietary antioxidants as a source of hydrogen peroxide. *Food Chem.* **2019**, *278*, 692–699. [[CrossRef](#)] [[PubMed](#)]
63. Zubair, M.S.; Anam, S.; Khumaidi, A.; Susanto, Y.; Hidayat, M.; Ridhay, A. Molecular docking approach to identify potential anticancer compounds from Begonia (*Begonia* sp.). In Proceedings of the 1st International Conference on Science and Technology 2015 (ICST-2015), Universitas Gadjah Mada, Indonesia, 21 July 2016; Volume 1755, pp. 080005–080007.
64. Chohan, T.A.; Qian, H.; Pan, Y.; Chen, J.Z. Cyclin-dependent kinase-2 as a target for cancer therapy: Progress in the development of CDK2 inhibitors as anti-cancer agents. *Curr. Med. Chem.* **2015**, *22*, 237–263. [[CrossRef](#)] [[PubMed](#)]
65. Li, Y.; Zhang, J.; Gao, W.; Zhang, L.; Pan, Y.; Zhang, S.; Wang, Y. Insights on structural characteristics and ligand binding mechanisms of CDK2. *Int. J. Mol. Sci.* **2015**, *16*, 9314–9340. [[CrossRef](#)]
66. García-Sosa, A.T.; Mancera, R.L. The effect of a tightly bound water molecule on scaffold diversity in the computer-aided de novo ligand design of CDK2 inhibitors. *J. Mol. Model.* **2006**, *12*, 422–431. [[CrossRef](#)]
67. Bramson, H.N.; Corona, J.; Davis, S.T.; Dickerson, S.H.; Edelstein, M.; Frye, S.V.; Gampe, R.T.; Harris, P.A.; Hassell, A.; Holmes, W.D.; et al. Oxindole-based inhibitors of cyclin-dependent kinase 2 (CDK2): Design, synthesis, enzymatic activities, and X-ray crystallographic analysis. *J. Med. Chem.* **2001**, *44*, 4339–4358. [[CrossRef](#)]
68. Misra, R.N.; Xiao, H.Y.; Rawlins, D.B.; Shan, W.; Kellar, K.A.; Mulheron, J.G.; Sack, J.S.; Tokarski, J.S.; Kimball, S.D.; Webster, K.R. 1H-pyrazolo [3,4-b] pyridine inhibitors of cyclin-dependent kinases: Highly potent 2,6-difluorophenacyl analogues. *Bioorg. Med. Chem. Lett.* **2003**, *13*, 2405–2408. [[CrossRef](#)]
69. Łukasik, P.; Baranowska-Bosiacka, I.; Kulczycka, K.; Gutowska, I. Inhibitors of cyclin-dependent kinases: Types and their mechanism of action. *Int. J. Mol. Sci.* **2021**, *22*, 2806. [[CrossRef](#)]
70. Davis, S.T.; Benson, B.G.; Bramson, H.N.; Chapman, D.E.; Dickerson, S.H.; Dold, K.M.; Eberwein, D.J.; Edelstein, M.; Frye, S.V.; Gampe, R.T.J.; et al. Prevention of chemotherapy-induced alopecia in rats by CDK inhibitors. *Science* **2001**, *291*, 134–137. [[CrossRef](#)]
71. Deshpande, A.; Sicinski, P.; Hinds, P.W. Cyclins and cdks in development and cancer: A perspective. *Oncogene* **2005**, *24*, 2909–2915. [[CrossRef](#)]
72. Li, J.-Q.; Miki, H.; Ohmori, M.; Wu, F.; Funamoto, Y. Expression of cyclin E and cyclin-dependent kinase 2 correlates with metastasis and prognosis in colorectal carcinoma. *Hum. Pathol.* **2001**, *32*, 945–953. [[CrossRef](#)] [[PubMed](#)]
73. Thoma, O.M.; Neurath, M.F.; Waldner, M.J. Cyclin-dependent kinase inhibitors and their therapeutic potential in colorectal cancer treatment. *Front. Pharmacol.* **2021**, *12*, 757120–757129. [[CrossRef](#)] [[PubMed](#)]
74. Zhang, L.; Yu, J. Role of apoptosis in colon cancer biology, therapy, and prevention. *Curr. Colorectal. Cancer Rep.* **2013**, *9*, 331–340. [[CrossRef](#)] [[PubMed](#)]
75. Abdullah, M.; Syam, A.F.; Meilany, S.; Laksono, B.; Prabu, O.G.; Bektı, H.S.; Indrawati, L.; Makmun, D. The value of caspase-3 after the application of annona muricata leaf extract in COLO-205 colorectal cancer cell line. *Gastro. Res. Prac.* **2017**, *2017*, 4357165. [[CrossRef](#)]
76. Hosseini, S.S.; Hajikhani, B.; Faghihloo, E.; Goudarzi, H. Increased expression of caspase genes in colorectal cancer cell line by nisin. *Arch. Clin. Infect. Dis.* **2020**, *15*, e97734. [[CrossRef](#)]
77. Yadav, P.; Yadav, R.; Jain, S.; Vaidya, A. Caspase-3: A primary target for natural and synthetic compounds for cancer therapy. *Chem. Biol. Drug Des.* **2021**, *98*, 144–165. [[CrossRef](#)]
78. Ahagh, M.H.; Dehghan, G.; Mehdipour, M.; Teimuri-Mofrad, R.; Payami, E.; Sheibani, N.; Ghaffari, M.; Asadi, M. Synthesis, characterization, anti-proliferative properties and DNA binding of benzochromene derivatives: Increased Bax/Bcl-2 ratio and caspase-dependent apoptosis in colorectal cancer cell line. *Bioorg. Chem.* **2019**, *93*, 103329–103344. [[CrossRef](#)]
79. Elgaafary, M.; Fouda, A.M.; Mohamed, H.M.; Hamed, A.; El-Mawgoud, H.K.; Jin, L.; Ulrich, J.; Simmet, T.; Syrovets, T.; El-Agrody, A.M. Synthesis of  $\beta$ -enaminonitrile-linked 8-methoxy-1H-benzo [f] chromene moieties and analysis of their antitumor mechanisms. *Front. Chem.* **2021**, *9*, 759148. [[CrossRef](#)]
80. Daina, A.; Michielin, O.; Zoete, V. SwissADME: A free web tool to evaluate pharmacokinetics, drug-likeness and medicinal chemistry friendliness of small molecules. *Sci. Rep.* **2017**, *7*, 42717. [[CrossRef](#)]
81. Sharom, F.J. The P-glycoprotein efflux pump: How does it transport drugs? *J. Memb. Bio.* **1997**, *160*, 161–175. [[CrossRef](#)]
82. Giménez, B.G.; Santos, M.S.; Ferrarini, M.; Fernandes, J.P.S. Evaluation of blockbuster drugs under the rule-of-five. *Die Pharm.* **2010**, *65*, 148–152. [[CrossRef](#)]
83. Bersuder, P.; Hole, M.; Smith, G. Antioxidants from a heated histidine-glucose model system. I: Investigation of the antioxidant role of histidine and isolation of antioxidants by high-performance liquid chromatography. *J. Am. Oil Chem. Soc.* **1998**, *75*, 181–187. [[CrossRef](#)]
84. Oyaizu, M. Studies on products of browning reaction antioxidative activities of products of browning reaction prepared from glucosamine. *Jpn. J. Nutr. Diet.* **1986**, *44*, 307–315. [[CrossRef](#)]
85. Vanden Berghe, D.A.; Vlietinck, A.J. Screening methods for antibacterial agents from higher plants. In *Methods in Plant Biochemistry: Assays for Bioactivity*; Dey, P.M., Harborne, J.B., Hostettman, K., Eds.; Academic Press: London, England, 1991; Volume 6, pp. 47–69.
86. Gomez, K.A.; Gomez, A.A. *Statistical Procedures for Agricultural Research*, 2nd ed.; John Wiley & Sons: Hoboken, NJ, USA, 1984; p. 680.
87. Schrödinger, LLC. *Release 2015-2 (2015) LigPrep*; Version 3.4; Schrödinger, LLC: New York, NY, USA, 2015; p. 26400175.

88. Friesner, R.A.; Banks, J.L.; Murphy, R.B.; Halgren, T.A.; Klicic, J.J.; Mainz, D.T.; Repasky, M.P.; Knoll, E.H.; Shelley, M.; Perry, J.K.; et al. Glide: A new approach for rapid, accurate docking and scoring. 1. Method and assessment of docking accuracy. *J. Med. Chem.* **2004**, *47*, 1739–1749. [[CrossRef](#)]
89. Friesner, R.A.; Murphy, R.B.; Repasky, M.P.; Frye, L.L.; Greenwood, J.R.; Halgren, T.A.; Sanschagrin, P.C.; Mainz, D.T. Extra precision glide: Docking and scoring incorporating a model of hydrophobic enclosure for protein—Ligand complexes. *J. Med. Chem.* **2006**, *49*, 6177–6196. [[CrossRef](#)]
90. Sumirtanurdin, R.; Sungkar, S.; Hisprastin, Y.; Sidharta, K.D.; Nurhikmah, D.D. Molecular docking simulation studies of curcumin and its derivatives as cyclin-dependent kinase 2 inhibitors. *Turk. J. Pharm. Sci.* **2020**, *17*, 417–423. [[CrossRef](#)]
91. Available online: <http://www.swissadme.ch/index.php> (accessed on 10 January 2022).



## Article

# QSAR, Molecular Docking, MD Simulation and MMGBSA Calculations Approaches to Recognize Concealed Pharmacophoric Features Requisite for the Optimization of ALK Tyrosine Kinase Inhibitors as Anticancer Leads

Rahul D. Jawarkar <sup>1,\*</sup>, Praveen Sharma <sup>1</sup>, Neetesh Jain <sup>1</sup>, Ajaykumar Gandhi <sup>2</sup>, Nobendu Mukerjee <sup>3</sup>, Aamal A. Al-Mutairi <sup>4</sup>, Magdi E. A. Zaki <sup>4,\*</sup>, Sami A. Al-Hussain <sup>4</sup>, Abdul Samad <sup>5</sup>, Vijay H. Masand <sup>6</sup>, Arabinda Ghosh <sup>7</sup> and Ravindra L. Bakal <sup>8</sup>



**Citation:** Jawarkar, R.D.; Sharma, P.; Jain, N.; Gandhi, A.; Mukerjee, N.; Al-Mutairi, A.A.; Zaki, M.E.A.; Al-Hussain, S.A.; Samad, A.; Masand, V.H.; et al. QSAR, Molecular Docking, MD Simulation and MMGBSA Calculations Approaches to Recognize Concealed Pharmacophoric Features Requisite for the Optimization of ALK Tyrosine Kinase Inhibitors as Anticancer Leads. *Molecules* **2022**, *27*, 4951.

<https://doi.org/10.3390/molecules27154951>

Academic Editors: Kulandaisamy Arulsamy, Muralikannan Maruthamuthu, Nagendran Tharmalingam and Irini Doytchinova

Received: 30 May 2022

Accepted: 22 July 2022

Published: 3 August 2022

**Publisher's Note:** MDPI stays neutral with regard to jurisdictional claims in published maps and institutional affiliations.



**Copyright:** © 2022 by the authors. Licensee MDPI, Basel, Switzerland. This article is an open access article distributed under the terms and conditions of the Creative Commons Attribution (CC BY) license (<https://creativecommons.org/licenses/by/4.0/>).

- <sup>1</sup> Faculty of Pharmacy, Oriental University, Indore 453555, Madhya Pradesh, India; praveen140581@gmail.com (P.S.); drnkjain9781@gmail.com (N.J.)
  - <sup>2</sup> Department of Chemistry, Government College of Arts and Science, Aurangabad 431004, Maharashtra, India; gascajay18@gmail.com
  - <sup>3</sup> Department of Microbiology, Ramakrishna Mission Vivekananda Centenary College, Kolkata 700118, West Bengal, India; nabendu21@rkmvccrahara.org
  - <sup>4</sup> Department of Chemistry, Faculty of Science, Imam Mohammad Ibn Saud Islamic University, Riyadh 13318, Saudi Arabia; aamutairi@imamu.edu.sa (A.A.A.-M.); sahussain@imamu.edu.sa (S.A.A.-H.)
  - <sup>5</sup> Department of Pharmaceutical Chemistry, Faculty of Pharmacy, Tishk International University, Erbil 44001, Kurdistan Region, Iraq; abdul.samad@tiu.edu.iq
  - <sup>6</sup> Department of Chemistry, Vidyabharati Mahavidyalaya, Camp Road, Amravati 444602, Maharashtra, India; vijaymasand@gmail.com
  - <sup>7</sup> Microbiology Division, Department of Botany, Gauhati University, Guwahati 781014, Assam, India; dra.ghosh@gauhati.ac.in
  - <sup>8</sup> Department of Medicinal Chemistry, Dr. Rajendra Gode Institute of Pharmacy, University-Mardi Road, Amravati 444603, Maharashtra, India; rlbakal@gmail.com
- \* Correspondence: rahuljawarkar@gmail.com (R.D.J.); mezaki@imamu.edu.sa (M.E.A.Z.); Tel.: +91-7385178762 (R.D.J.)

**Abstract:** ALK tyrosine kinase ALK TK is an important target in the development of anticancer drugs. In the present work, we have performed a QSAR analysis on a dataset of 224 molecules in order to quickly predict anticancer activity on query compounds. Double cross validation assigns an upward plunge to the genetic algorithm–multi linear regression (GA-MLR) based on robust univariate and multivariate QSAR models with high statistical performance reflected in various parameters like, fitting parameters;  $R^2 = 0.69\text{--}0.87$ ,  $F = 403.46\text{--}292.11$ , etc., internal validation parameters;  $Q^2_{\text{LOO}} = 0.69\text{--}0.86$ ,  $Q^2_{\text{LMO}} = 0.69\text{--}0.86$ ,  $\text{CCC}_{\text{cv}} = 0.82\text{--}0.93$ , etc., or external validation parameters  $Q^2_{\text{F1}} = 0.64\text{--}0.82$ ,  $Q^2_{\text{F2}} = 0.63\text{--}0.82$ ,  $Q^2_{\text{F3}} = 0.65\text{--}0.81$ ,  $R^2_{\text{ext}} = 0.65\text{--}0.83$  including  $\text{RMSE}_{\text{tr}} < \text{RMSE}_{\text{cv}}$ . The present QSAR evaluation successfully identified certain distinct structural features responsible for ALK TK inhibitory potency, such as planar Nitrogen within four bonds from the Nitrogen atom, Fluorine atom within five bonds beside the non-ring Oxygen atom, lipophilic atoms within two bonds from the ring Carbon atoms. Molecular docking, MD simulation, and MMGBSA computation results are in consensus with and complementary to the QSAR evaluations. As a result, the current study assists medicinal chemists in prioritizing compounds for experimental detection of anticancer activity, as well as their optimization towards more potent ALK tyrosine kinase inhibitor.

**Keywords:** ALK tyrosine kinase inhibitors; QSAR; anticancer; molecular docking; MD simulation; MMGBSA

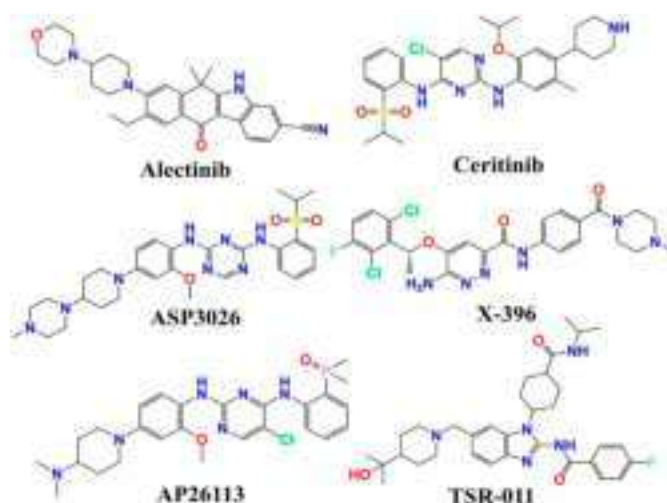
## 1. Introduction

The cancer kinome is currently acknowledged as a powerful target for the treatment of cancer; it comprises over 500 protein kinases, however only a few of them possess

therapeutic activity. The term ALK was coined from a chromosomal rearrangement inside anaplastic large cell lymphoma (ALCL) that was described as a front companion but discovered in 1994 [1]. Anaplastic lymphoma kinase (ALK) is a kind of oncogenic protein that is often expressed in the brain, small intestine, or testis but not in normal lymphoid cells [2]. The main physiologic aspect inhibited by the anaplastic lymphoma kinase (ALK) gene is brain development, which can keep many cancers altered, including non-small-cell lung cancer (NSCLC) or anaplastic large cell lymphomas (ALCL) [3].

Moreover, ALK gene activation appears to contribute to the initiation of carcinogenesis in a variety of human cancers such as anaplastic large cell lymphoma, lung cancer, inflammatory myofibroblastic tumors, and neuroblastoma, with the end result of fusion with additional oncogenes (NPM, EML4, TIM, etc.) and gene amplification, mutation, and protein overexpression [4]. As a basis for the researchers' involvement with the tyrosine kinase as a specific target in cancer treatment, the ALK fusion protein was created. TK plays a major role in signal transduction and is classified as a protein kinase up to the point where it is separated from the phosphate group by a tyrosine residue [5]. ALK is a recognized molecular target in a variety of ALK mutated malignancies, including non-small cell lung cancer. On the other hand, the rise of drug resistance has almost completely restricted the scientific advantage of targeting ALK with tyrosine kinase inhibitors (TKI) [6]. Furthermore, because of the treatment of ALK rearranged cancer, ALK has been suggested as a therapeutic target protein.

Academic institutions and the pharmaceutical sector are working hard to develop potent ALK inhibitors. Currently, the US Food and Drug Administration (US FDA) has approved crizotinib, Entrectinib, ceritinib, or alectinib for the treatment of patients with metastatic "ALK-positive" NSCLC [7–12]. Small-molecular inhibitors of ALK, such as AP26113 [13] and lorlatinib (PF-06463922) [14], are currently being evaluated in clinical studies (See Figure 1). On the other hand, irreversible drug resistance is rapidly spreading over the world, endangering the efficacy of chemotherapy containing these drugs. Alectinib [2], ceritinib [3], ASP3026 [4], PF-0643922, X-396, AP26113, and TSR-011 are examples of small molecules of ALK inhibitors that have been developed and are now being tested in clinical studies) [15–17].



**Figure 1.** Demonstration of some ALK Tyrosine kinase inhibitors presently under clinical trials.

We conducted a quantitative structure activity relationship (QSAR) investigation on a dataset of 224 compounds, including clinically installed ALK tyrosine kinase inhibitory activity ( $K_i$ ), in order to evaluate the critical structural and physicochemical requirements for ALK inhibitors as potent anticancer agents.

Following are the most common QSAR modelling steps: (I) selection of a dataset of molecules that cover a wide chemical space along with verified bio-activity expressed in terms of  $K_i$ ,  $IC_{50}$  or  $EC_{50}$ ; (II) generation of 3D-structures of the molecules followed

by their optimization using appropriate molecular mechanics; (III) molecular descriptor calculation and data pruning using an acceptable statistical method, if required; (IV) QSAR model development using an appropriate technique that recommends promising molecular descriptor selection; and (V) double cross validation of the developed QSAR models. Statistical QSAR evaluates the bioactivity of a chemical based on its *in vitro* modification and *in vivo* testing in a wet lab. Furthermore, illustrative QSAR legitimately vary along with the statistical parameters between QSAR models that provide deep understanding for the pharmacokinetic then optimization of the lead drug [18–26].

Therefore, in the present study, we have attempted to create a QSAR model by utilizing a dataset of 224 structurally diverse compounds whose ALK tyrosine kinase inhibitory activity was previously determined experimentally (Ki). Additionally, the most active compounds in the current dataset have been examined for molecular docking studies, which have been followed by MD simulation and MMGBSA calculations. The primary goal of the current work is to uncover the array of Pharmacophoric characteristics involved in the binding affinity or stability of the drug-ALK complex. Furthermore, the stability on the drug receptor complex was observed and analyzed using MD simulation or MMGBSA techniques. The QSAR model developed in this work should provide useful information to the synthetic chemists in the discovery and development of leads to more powerful ALK Tyrosine kinase inhibitors.

## 2. Results

All the statistical parameters associated with fitting, double validation, or Y-scrambling for the generation of de-novo-QSAR models 1.1–1.2, along with the respective threshold values for half of the parameters are displayed in Table 1 (at the bottom of the table).

**Table 1.** The statistical parameters connected with the fitting, double validation and Y-scrambling for models 1.1 and 1.2.

Statistical Parameters	Model-1.1 (Univariate Dividedset Model)	Model-1.2 (Multivariate DividedSet Model)
Fitting		
$R^2$	0.699	0.86
$R^2_{adj}$	0.692	0.86
$R^2 - R^2_{adj}$	0.001	0.003
LOF	0.57	0.25
$K_{xx}$	0.00	0.29
Delta K	0.83	0.14
$RMSE_{tr}$	0.74	0.48
$MAE_{tr}$	0.57	0.38
$RSS_{tr}$	101.03	42.10
$CCC_{tr}$	0.81	0.93
S	0.75	0.49
F	403.4	292.1
Internal Validation		
$Q^2_{LOO}$	0.68	0.86
$R^2 - Q^2_{LOO}$	0.005	0.007
$RMSE_{cv}$	0.75	0.49
$MAE_{cv}$	0.58	0.39
$PRESS_{cv}$	102.9	44.6
$CCC_{cv}$	0.81	0.92
$Q^2_{LMO}$	0.68	0.86
$R^2_{Yscr}$	0.005	0.02
$RMSE_{AV_{Yscr}}$	1.35	1.3
$Q^2_{Yscr}$	−0.01	0.03
External Validation		
$RMSE_{ext}$	0.79	0.57
$MAE_{ext}$	0.61	0.45
$PRESS_{ext}$	27.8	14.3
$R^2_{ext}$	0.65	0.83

Table 1. Cont.

Statistical Parameters	Model-1.1 (Univariate DividedSet Model)	Model-1.2 (Multivariate DividedSet Model)
$Q^2_{-F1}$	0.64	0.82
$Q^2_{-F2}$	0.63	0.82
$Q^2_{-F3}$	0.65	0.81
$CCC_{ext}$	0.80	0.90
$r^2m_{aver.}$	0.52	0.75
$r^2m_{delta}$	0.10	0.15
$k'$	0.99	0.99
$K$	0.98	0.99
$Clos'$	0.10	0.04
$Clos$	0.01	0.0

Fitting parameters such as  $R^2$ ,  $R^2_{adj}$ , and  $CCC_{tr}$ , among others, have achieved values well above the mentioned threshold limits, indicating the statistical acceptability of comprehensive QSAR models with a wide variety of chemical descriptors in them.  $Q^2_{LOO}$ ,  $Q^2_{LMO}$ , and so on are internal validation parameters whose values indicate the statistical robustness of QSAR models. High values for external validation parameters  $R^2_{ext}$ ,  $Q^2_{-Fn}$ , and so on indicate external predictability for both models which is reflected in a graph of experimental endpoint versus model predicted endpoint (Figure 2A,C). Williams plots that support applicability domain (AD) on the developed QSAR models are shown in Figure 2. To exclude the possibility of occasional improvement in QSAR models, appropriate threshold values based on sufficient parameters and minimal correlation among molecular descriptors must be maintained (See Supplementary Materials File S5 for the detailed formulas for the calculation of various QSAR model performance parameters). Statistical robustness and high external predictability are strong arguments in favor of these models.

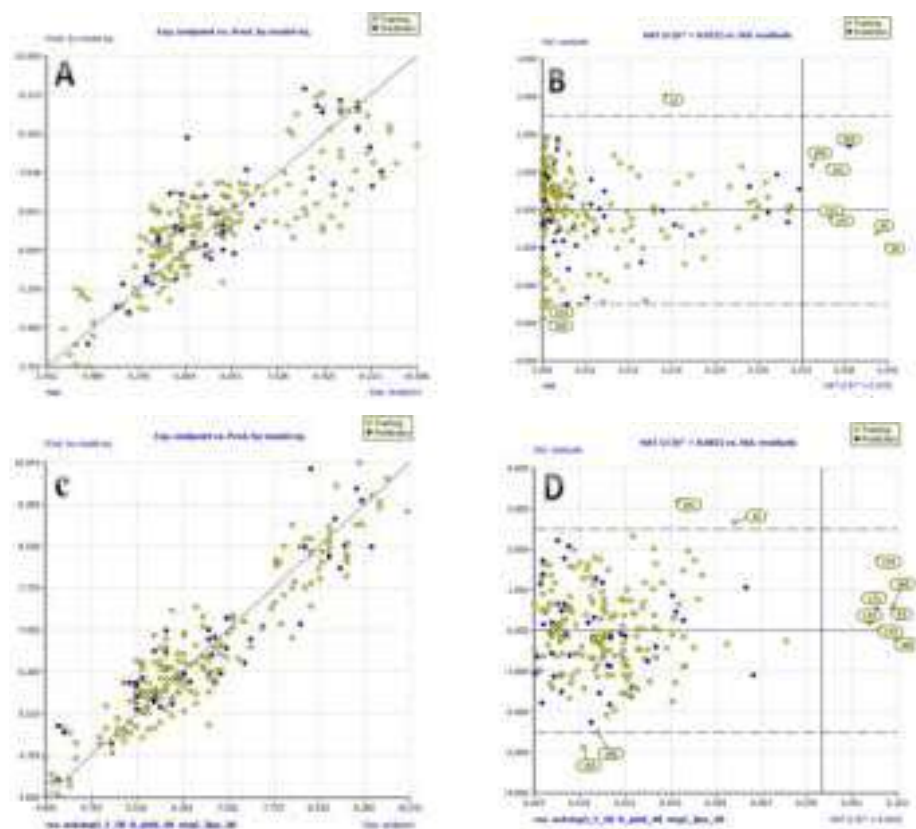


Figure 2. (A) Graph of experimental vs. Predicted pKi values for model 1.1; (B) Williams plot for model 1.1; (C) Graph of experimental vs. Predicted pKi values for model 1.2; (D) Williams plot for model 1.2.

### 2.1. Model. 1.1 (Univariate Analysis)

The univariate statistical analysis of the divided dataset QSAR model revealed that the dataset molecules have a gradual then spectacular outset ( $R^2 = 0.690$ ) with the descriptor *rsa*, which stands for ratio of surface area (ratio of molecular surface area to the solvent accessible surface area). The developed univariate QSAR model is as follow:

$$pKi = -8.9 (\pm 1.5) + 25.0 (\pm 2.4) \times rsa \quad (1)$$

### 2.2. Model. 1.2 (Multivariate Analysis)

The another QSAR model with multiple variable is given below;

$$pKi = -6.7 (\pm 1.09) + 21.6 (\pm 2.1) \times rsa + 1.08 (\pm 0.16) \times \text{notringO\_F\_5B} + 0.06 (\pm 0.03) \times \text{N\_plaN\_4B} + -0.03 (\pm 0.02) \times \text{ringC\_lipo\_2B} \quad (2)$$

(Supplementary Materials Tables S3 and S4.)

## 3. Discussion

A precisely validated correlation between visible features of molecules, as embodied by molecular descriptors and their ALK TK inhibitory potency, amplifies the records about mechanistic features of molecules, as well as specificity and volume (presence and even absence) of various structural characteristics for favorable anticancer activity. In a broad sense, the ALK TK inhibitory efficacy of the compounds in the current dataset is the aggregate of four chemical descriptors that emerged in the developed univariate and multivariate QSAR models. Molecular descriptors may be classified into two groups based on their sign between sophisticated QSAR models.

The molecular descriptors *rsa*, *notringO\_F\_5B*, and *N\_plaN\_4B* performed well in the established QSAR models. Amplification of the values of these chemical descriptors can also contribute to an increase in the compound's ALK TK inhibitory efficacy.

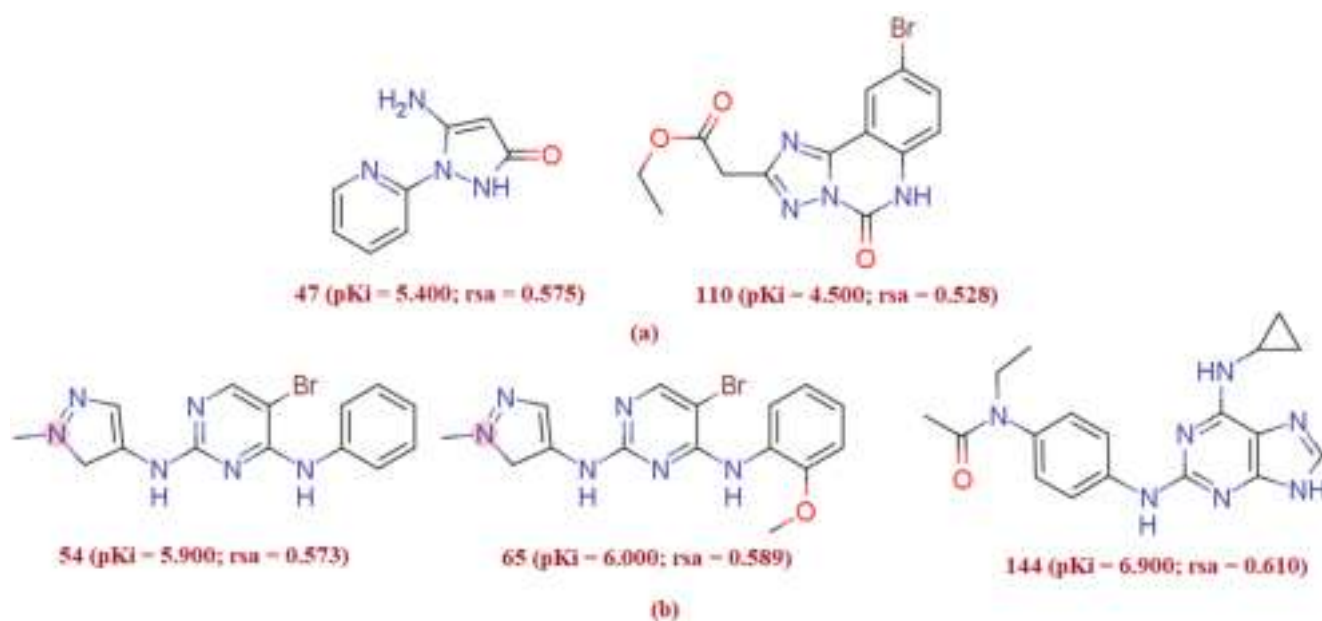
The raised QSAR models include the molecular descriptor *ringC\_lipo\_2B* with a negative coefficient, and by decreasing the value of that molecular descriptor the compound's ALK TK inhibitory efficacy may be increased. The value of these four molecular descriptors is highlighted in the next section by comparing the variation in ALK TK inhibitory potency of the molecules (expressed in terms of *Ki* and *pKi*) with the shift in the values of the molecular descriptors seen in the QSAR models. However, the compound's bioactivity is the result of the combined action of several molecular descriptors that may or may not have been included in QSAR models.

### 3.1. Mechanistic Interpretation

#### 3.1.1. *rsa*

The present QSAR evaluation performed on a given dataset marked the ratio of molecular surface area (*All\_MSA*, molecular surface area) to the solvent accessible surface area (*All\_SASA*) encoded by *rsa* (ratio of surface area) as one of the best performing molecular descriptors with a positive relationship with ALK TK inhibitory potency of the molecule. The chemical descriptor *rsa* (ratio of surface area) encrypts information on the molecular surface area (*All\_MSA*: molecular surface area of the molecule (all atoms)) to the solvent accessible surface area (*All\_SASA*: solvent accessible surface area of the molecule (all atoms)) ratio, and has a positive relationship with the molecule's ALK TK inhibitory potency. A small change in *rsa* results in a big change in the inhibitory activity of ALK TK. Because *rsa* is the ratio of the value of *All\_MSA* to the value of *All\_SASA*, the large possible value of *All\_SASA* to the small value of *All\_SASA* will set the *rsa* to the larger value, thus increasing the molecule's ALK tyrosine kinase inhibitory efficacy. This is demonstrated by comparing molecule 178 (*pKi* = 10, *rsa* = 0.68, *All\_MSA* = 400.5, *All\_SASA* = 587.6) to molecule 181 (*pKi* = 9.252, *rsa* = 0.66, *All\_MSA* = 426.6, *All\_SASA* = 639.9). The significance of *rsa* may be demonstrated by another pair of molecules 110 (*pKi* = 4.5, *rsa* = 0.528) and 47 (*pKi* = 5.4, *rsa* = 0.575) that also corroborate the observation (see Figure 3a). A triad of

compound 54 (pKi = 5.9, rsa = 0.573), compound 65 (pKi = 6.0, rsa = 0.589), and compound 144 (pKi = 6.9, rsa = 0.610) also highlights the importance of high value of ratio of surface area (see Figure 3b).



**Figure 3.** Illustration of the molecular descriptor *rsa* for the molecular pair 47 and 110 (a), and for the molecular pair; 54, 65 and 144 (b) only.

### 3.1.2. N\_plaN\_4B

The molecular descriptor N\_plaN\_4B represents the number of Nitrogen atoms with four bonds from the planar Nitrogen atom and it has a positive coefficient in the developed QSAR model. A significant number of such booster pairs of Nitrogen and planar Nitrogen may provide a more powerful ALK TK inhibitory activity. This observation is reinforced by comparing the molecule 92 (pKi = 6.8, N\_plaN\_4B = 5) with five booster Nitrogen pairs to the molecule 78 (pKi = 5.9, N\_plaN\_4B = 2) with just two booster Nitrogen pairs.

Moreover, in clinical trial agent AP26113 has such booster pairs, i.e. planar Nitrogen within four bonds from the Nitrogen atoms. The present observation confirmed that the QSAR model has successfully identified similar Pharmacophoric traits which are also present in clinical trial agents AP26113. Therefore, the planar Nitrogen within 4 bonds from the Nitrogen atom is mandatory for enhancing the affinity of ALK tyrosine kinase inhibitors (see Figure 4).



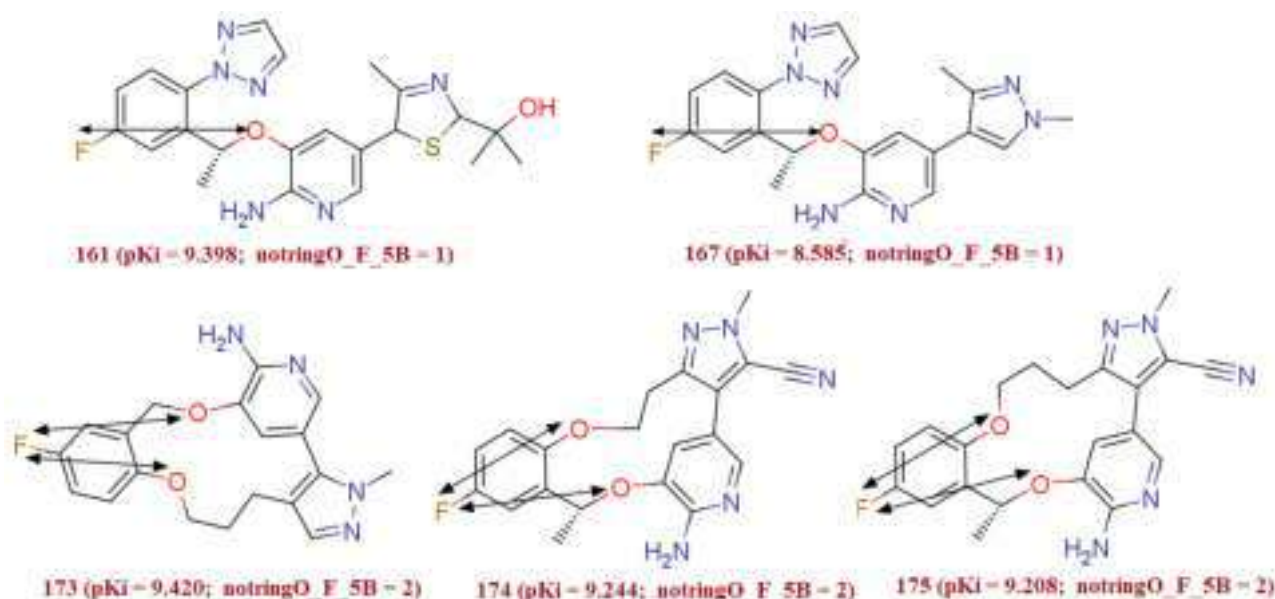
**Figure 4.** Illustration of Molecular descriptor N\_plaN\_4B in clinical trial molecule AP26113 (IC<sub>50</sub> = 0.07 nM).

Additionally, replacement of the molecular descriptor N\_plaN\_4B with *fplaN\_4B* (represent the frequency of occurrence of Nitrogen atom exactly at four bonds from the planer Nitrogen atom) ( $Q^2_{100} = 0.85$ ,  $R^2 = 0.85$ ) and *ringN\_plaN\_6B* (occurrence of planar Nitrogen within six bonds from the ring Nitrogen atom) ( $Q^2_{100} = 0.85$ ,  $R^2 = 0.85$ ) led to the

diminution in the statistical presentation of the model. Thus, it can be concluded that the molecular descriptor  $N\_plaN\_4B$  is the better choice for predicting the ALK TK inhibitory potency. Consequently, the optimal value of distance between planar nitrogen and nitrogen atom is four bonds.

### 3.1.3. notringO\_F\_5B

The molecular descriptor  $notringO\_F\_5B$  represents the number of Fluorine atoms within five bonds from the non-ring Oxygen atom. This molecular descriptor has a positive relationship with the ALK TK inhibitory activity of the compound, and therefore augmenting its value could offer a more potent ALK TK inhibitor. The significance of the presence and large value of a pair of Fluorine within five bonds from non-ring Oxygen can be rationalized from the fact that in the present dataset, the relatively least active compounds with  $pKi \geq 7.400$  (with very few exceptions) either Fluorine atoms itself absent or such booster pair of Fluorine and non-ring Oxygen is absent, i.e.  $notringO\_F\_5B = 0$ . Whereas, in most active compounds with  $pKi \geq 9.155$  at least one such Fluorine is five bonds away from the non-ring Oxygen atom ( $notringO\_F\_5B \geq 1$ ). In addition to this, there are 36 such diverse sets of compounds in the entire dataset which comprises one to two such a pair of oxygen atom and fluorine atom present within five bonds. Moreover, the compounds such as, 174 ( $pKi = 9.24$ ,  $notringO\_F\_5B = 2$ ), 175  $pKi = 9.20$ ,  $notringO\_F\_5B = 2$ ), 165, and 167 were present in prediction set while; the rest of 32 active compounds were exist in training set. Around 16% of the molecule comprises this molecular descriptor. The occurrence of the molecular descriptor  $notringO\_F\_5B$  was not only limited to the series of homologues molecules, but it occurs in the diverse set of molecules like 161 and 167 also. Additional evidence in support is the molecule 161 ( $pKi = 9.398$ ,  $notringO\_F\_5B = 1$ ) with the molecule 173 ( $pKi = 9.420$ ,  $notringO\_F\_5B = 2$ ) (see Figure 5).

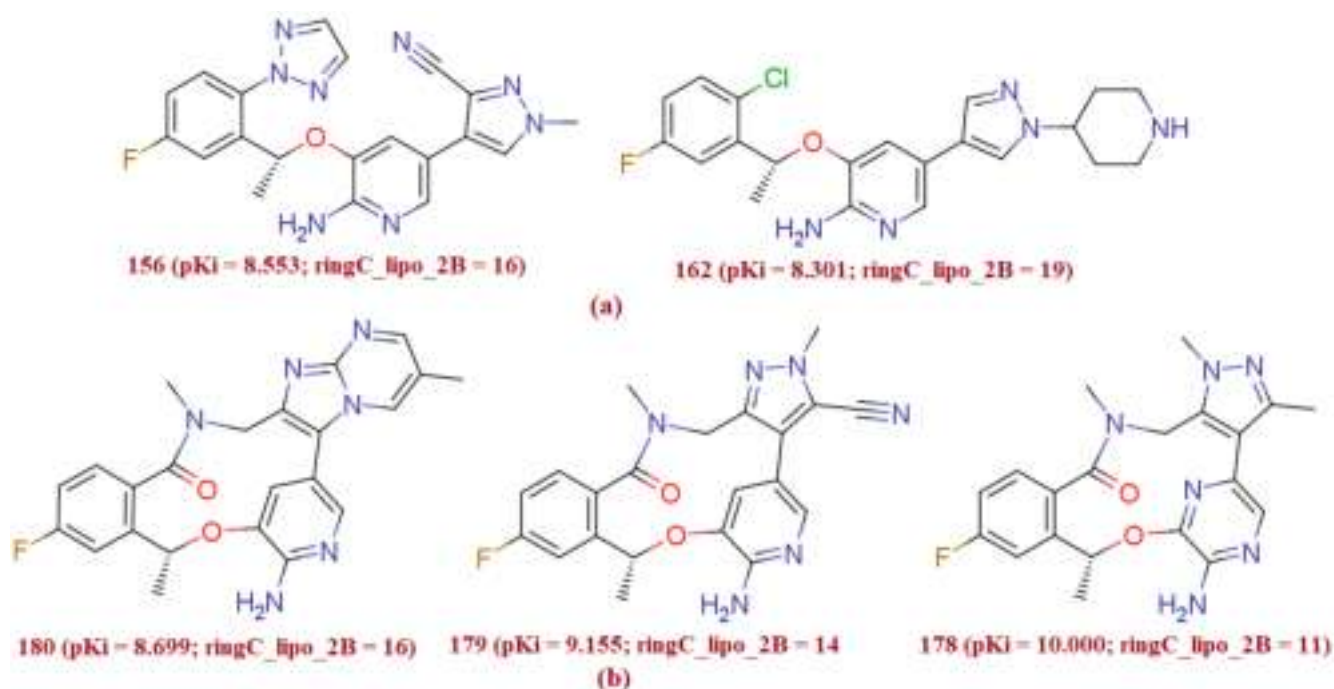


**Figure 5.** Illustration of molecular descriptor  $notringO\_F\_5B$  for the molecules 161 and 173, 174 and 175, and 167.

From this observation it is revealed that the combination of Fluorine atom with non-ring Oxygen atom is independently important for inhibitory potency of ALK TK; but shifting a fluorine atom with any sulfur atom [i.e.,  $notringO\_S\_5B$  ( $Q^2_{LOO} = 0.7219$ ,  $R^2 = 0.7344$ )] that represent the occurrence of Sulfur atom within five bonds from the non-ring Oxygen atom] or any acceptor atom [i.e.,  $notringO\_Acc\_5B$  ( $Q^2_{LOO} = 0.7244$ ,  $R^2 = 0.7350$ )] that represent the occurrence of acceptor atom within five bonds from the non-ring Oxygen atom] significantly diminishes the statistical presentation of the QSAR model. Therefore, the presence of a fluorine atom has good correlation with the  $Ki$  value.

### 3.1.4. ringC\_lipo\_2B

The molecular descriptor ringC\_lipo\_2B encodes information on the occurrence of the ring carbon atoms within two bonds from lipophilic atoms. This observation is supported by comparing the pKi value of the molecule 156 (pKi = 8.55, ringC\_lipo\_2B = 14) with the molecule 162 (pKi = 8.30, ringC\_lipo\_2B = 19), for which decrease in the value of the molecular descriptor ringC\_lipo\_2B for the molecule 162 to 14 resulted into an increase in the pKi value by about 0.25 per unit. The triad of the molecules 180 (pKi = 8.699, ringC\_lipo\_2B = 16), 179 (pKi = 9.155, ringC\_lipo\_2B = 14), 178 (pKi = 10, ringC\_lipo\_2B = 11) also signifies the importance of the molecular with this Pharmacophoric future (see Figure 6a,b). This is obvious as the macrolides and aromatic rings are quite abundant in the present dataset molecules.



**Figure 6.** Presentation of the molecular descriptor ringC\_lipo\_2B for the molecular pair 156 and 162 (a) and for another molecular pair; 180, 179 and 178 (b) only (the ring carbon atoms within 2 bonds from the lipophilic carbon atoms are highlighted by blue ball).

On the other hand, when we have shifted molecular descriptor ringC\_lipo\_2B with the descriptors ringC\_lipo\_1B and fringCnotringC1B in which the statistical performance of the QSAR model was meaningfully improved with the molecular descriptor fringCnotringC1B ( $Q^2_{\text{LOO}} = 0.87$ ,  $R^2 = 0.87$ ); while performance slightly goes down with the descriptor ringC\_lipo\_1B ( $Q^2_{\text{LOO}} = 0.84$ ,  $R^2 = 0.85$ ). Therefore, from the present observation, it is revealed that with an increase in numbers of the non-ring carbon atoms attached directly to the ring carbon atoms, TK inhibitory potency could increase. Based on this observation, the optimal distance between non ring carbon atom/lipophilic atom and ring carbon atom must be one. Moreover, we have highlighted the structure of molecule 156 and 162 to rationalize the impact of the molecular descriptor ringC\_lipo\_2B. Absence of the triazole ring, methyl group on the pyrazole ring and carbonitrile group significantly affects the TK inhibitory potency, and may be the possible reason for the decline in the potency of the molecule 162.

### 3.2. Molecular Docking

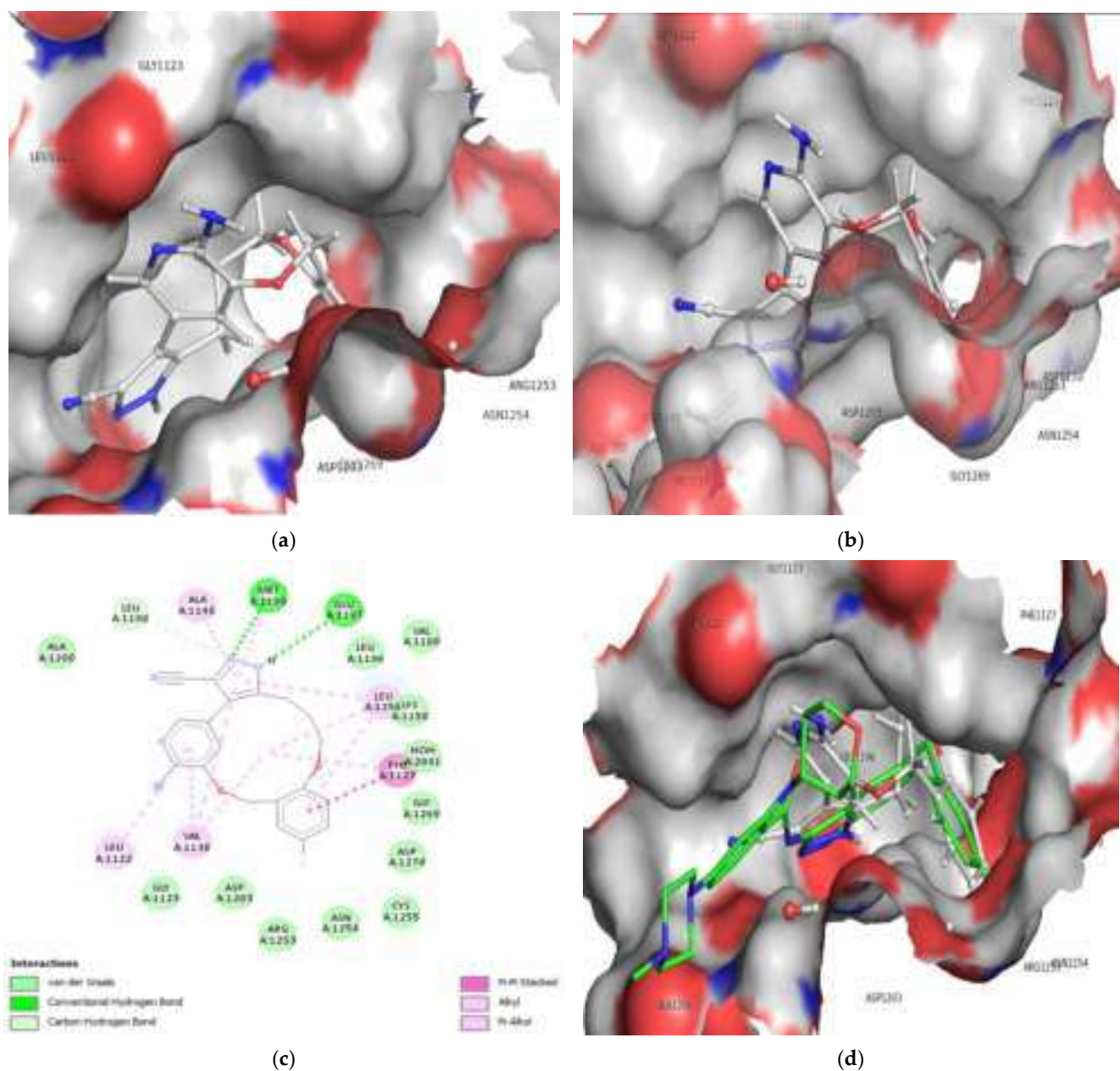
ALK was discovered to be a new receptor tyrosine kinase (RTK) with an external ligand-binding domain (1030 amino acids), a transmembrane domain (28 amino acids), and an intracellular tyrosine kinase domain based on the amino acid sequences (561 amino



acids) [26,27]. While the human ALK tyrosine kinase domain is very comparable to the insulin receptor, its extracellular domain is unique among the RTK family in that it comprises two MAM domains (meprin, A5 protein, as well as receptor protein tyrosine phosphatase mu), an LDLa domain (low-density lipoprotein receptor class A), and a glycine-rich region [27,28].

ALK's ATP binding site has 27 residues, and to boost selectivity against other kinases, residues that differ from ALK were targeted. The ALK Leu1198 residue is preserved in 26 percent of the kinome and is typically Phe or Tyr in other kinases. By expanding into this pocket and bumping against the bigger Phe and Tyr residues, this smaller Leu residue might potentially provide selectivity against the majority of kinases (60 percent) [14].

The protein data bank provided the ALK tyrosine kinase pdb file (pdb id-5fto, Resolution 1.7 Å). The pdb 5fto was chosen for its X-ray resolution or sequel completeness. The protein 5ft was prepared by UCF Chimera chimera-1.16-win64 software (<https://www.cgl.ucsf.edu/Visitors/index.html>, Oakland, California, accessed on 2 March 2022). During protein preparation, we have retained water molecules. High affinity for a protein target must be attained as it is a crucial component of drug design. Although there are statistical mechanics-based formal mathematical equations that can be used to calculate binding free energies, doing so in practice is quite challenging, especially when the effect is caused by a single water molecule rather than the bulk properties of water and it is impossible to capture solvation effects. It is impossible to avoid these granular effects; a review of PDB structures reveals that each ligand-protein combination contains 4–6 ligand-bound water molecules. Furthermore, water not only stabilizes ligand interactions but plays a biological role in dictating specificity. Therefore, the improved protein with water molecules was appropriate for docking analysis. Before the docking investigation, the natural ligand (Entrectinib) was removed; in the present study, the binding site for native ligand, namely the active site, has been studied. As a result, the compounds were docked between the active site, where the native ligand was originally bound orthosterically along ALK tyrosine kinase, and the docking pose for the most active molecules 172 and 178, and an example is shown here for convenience (see Figure 7a,b). Based on the activity profile, we have carried out molecular docking analysis of the compounds 172 and 178 only. The docking analysis of compound 172 into the ALK tyrosine kinase binding pocket revealed conventional hydrogen bonding, carbon hydrogen bonding, pi-pi stacked, and pi-alkyl hydrophobic interactions (See Figure 7c), with a docking score of  $-8.009$  kcal/mol (RMSD = 0.84 Å) and binding energy of  $-77.42$  kcal/mol (see Table 2). In the binding pocket of the ALK tyrosine kinase, compound 172 adopts the same collapsed conformation as the co-crystallized ligand Entrectinib (See Figure 7d). The hydrogen atom on the N1 nitrogen between the pyrazole ring performs conventional hydrogen bonding with the oxygen atom of the residue GLU1197 forming the hinge region with the interatomic association of 2.87 Å, where the oxygen atom of the stated residue acted as hydrogen bond acceptor, and the hydrogen atom on the N1 nitrogen atom acted as hydrogen bond donor. Alongside, another conventional hydrogen bond was discovered in the hydrogen atom on the N2 pyrazole nitrogen with the residue MET1199 of the hinge region (interatomic distance 2.17 Å), within which pyrazole nitrogen appeared as like a hydrogen bond acceptor along MET1199 residue emerged as a hydrogen bond donor in the current composite 172-ALK tyrosine kinase complex. Table 2 displays the full docking results for the composite 172. Furthermore, the gatekeeper residue LEU1198 was attached with N2 nitrogen over the pyrazole ring through carbon hydrogen bonding along an interatomic distance of 2.82 Å. It was reported that the LEU1198 decide the selectivity of the ligand against variety of the kinases. The present observation in the docking analysis supports this fact.



**Figure 7.** Depiction of alignment of compound 172 within the active site of ALK tyrosine kinase (a,b), 2D interaction of compound 172 with ALK tyrosine kinase (c) and Superimposed conformation of compound 172 with the pdb 5fto ligand (green colored); Entrectinib (d).

Moreover, at an interatomic distance of 4.81 Å, the pi-pi stacking hydrophobic contact has been facilitated by the indulgence of the pi orbital of the benzene ring and the pi orbital of the PHE1127. Furthermore, in compound 172, the pyrimidine ring is anchored with VAL1130 (interatomic distance 4.28 Å) and LEU1256 (interatomic distance 4.56 Å) and is coupled to the benzene cyclonaphane ring by alkyl hydrophobic contact. VAL1130 (interatomic distance 4.48 Å) and LEU1256 (interatomic distance 5.07 Å) make pi-alkyl hydrophobic contact with the pyrimidine ring and the cyclonaphane ring at the same time. Furthermore, the presence of an ether linkage in the unsaturated cyclonaphane ring amplifies the hydrophobicity of compound 172 as compared to the saturated benzene ring and, to a lesser extent, pyrimidine ring carbons. These findings validate the significance of the cyclonaphane ring in the molecule 172, which is primarily responsible for the compound's efficacy as mediated by the hydrophobic contact with the ALK tyrosine kinase.

**Table 2.** Presentation of docking interactions of the compound 172.

Residue	Distance in Å	Type of Interaction	Type of Bonding	From	Nature	To	Nature	Angle DHA	Angle HAY
MET1199:H	2.17	Hydrogen Bond	Conventional Hydrogen Bond	MET1199	H-Donor	O:N	H-Acceptor	142.364	93.83
GLU1197	2.87	Hydrogen Bond	Conventional Hydrogen Bond	O:H	H-Donor	GLU1197	H-Acceptor	111.868	157.456
LEU1198	2.82	Hydrogen Bond	Carbon Hydrogen Bond	LEU1198	H-Donor	O:N	H-Acceptor	140.175	119.444
PHE1127	4.81	Hydrophobic	Pi-Pi Stacked	PHE1127	Pi-Orbitals	0	Pi-Orbitals		
VAL1130	4.28	Hydrophobic	Alkyl	VAL1130	Alkyl	0	Alkyl		
LEU1256	4.59	Hydrophobic	Alkyl	LEU1256	Alkyl	0	Alkyl		
PHE1127	4.48	Hydrophobic	Pi-Alkyl	PHE1127	Pi-Orbitals	0	Alkyl		
VAL1130	5.07	Hydrophobic	Pi-Alkyl	0	Pi-Orbitals	VAL1130	Alkyl		
ALA1148	3.54	Hydrophobic	Pi-Alkyl	0	Pi-Orbitals	ALA1148	Alkyl		
MET1199	5.43	Hydrophobic	Pi-Alkyl	0	Pi-Orbitals	MET1199	Alkyl		
LEU1256	4.62	Hydrophobic	Pi-Alkyl	0	Pi-Orbitals	LEU1256	Alkyl		
LEU1122	4.93	Hydrophobic	Pi-Alkyl	0	Pi-Orbitals	LEU1122	Alkyl		
VAL1130	3.94	Hydrophobic	Pi-Alkyl	0	Pi-Orbitals	VAL1130	Alkyl		
LEU1256	4.17	Hydrophobic	Pi-Alkyl	0	Pi-Orbitals	LEU1256	Alkyl		

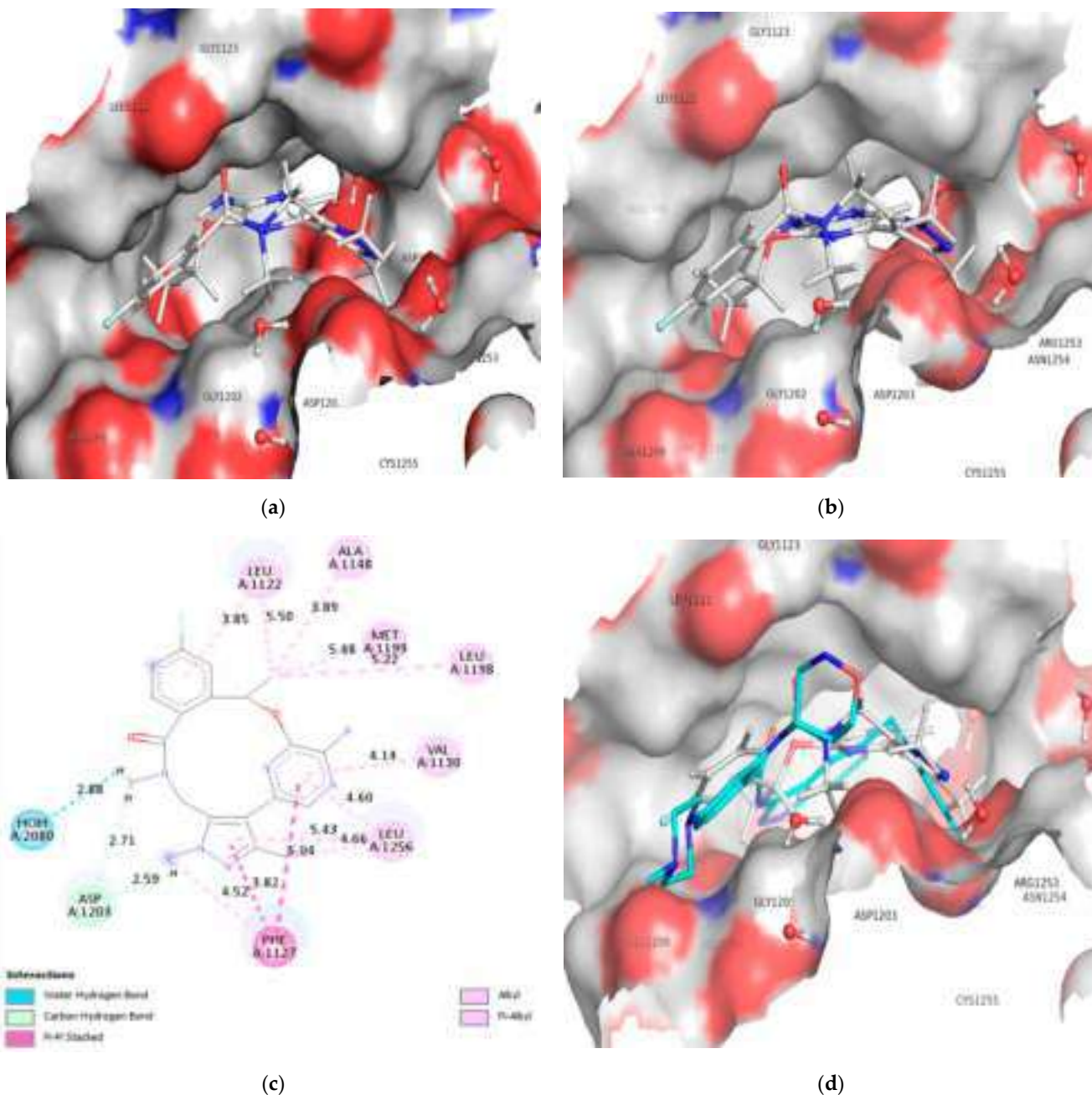
As a result, it can be concluded that the molecule 172 that binds to the ALK tyrosine kinase and drug receptor complex was mostly stabilized via conventional hydrogen, carbon hydrogen, pi-pi cation contact, alkyl hydrophobic and pi-alkyl hydrophobic interactions (See Figure 7).

Moreover, the residues: ALA1148 (interatomic distance 3.54 Å), MET1199 (interatomic distance 5.43 Å), LEU1256 (interatomic distance 4.62 Å), LEU1122 (interatomic distance 4.93 Å), VAL1130 (interatomic distance 3.94 Å) and LEU1256 forming part of a glycine rich loop (interatomic distance 4.17 Å) establishes a pi-alkyl hydrophobic interaction with the pi electrons of the pyrimidine and benzene rings, strengthening the molecule 172-ALK tyrosine receptor complex.

Furthermore, the docking analyses for compound 178 reveal the stability of the drug receptor complex through the formation of water-mediated hydrogen bonds, carbon hydrogen bonds, pi-pi stacking hydrophobic contacts, alkyl and pi-alkyl interactions, and a binding energy of  $-87.50$  kcal/mol (docking score  $-7.84$  kcal/mol, RMSD: 1.06 Å). The HOH2080 water molecules display hydrogen bonding contact with the N7 nitrogen atom of the cyclonaphane ring with an interatomic distance of 2.87 Å (see Figure 8a,b). At the same time, hydrogen of the N7 nitrogen produced by keto-enol tautomerism binds to the ASP1203 residue (interatomic distance 2.58 Å). This interaction is mediated by the presence of N7 nitrogen as a hydrogen bond donor and the oxygen atom of the ASP1203 residue. In addition, ASP1203 and the N1 nitrogen atom of the pyrazine ring in compound 178 formed another carbon hydrogen bond (see Figure 8a,b) (see Table 3). The superimposed conformation of compound 178 with the pdb-5fto ligand Entrectinib into the binding pocket of ALK TK is shown in Figure 8c,d.

Interestingly, the two pi-pi stacking hydrophobic contact into the drug receptor complex has been sustained and facilitated by the involvement of pi electrons from the pyrazine ring, pyrimidine ring, as well as pi electrons from the saturated benzene ring in residue A: PHE1127 (Interatomic distances 5.03 and 3.82 Å resp.). As a result, the residues A: ALA1148 (Interatomic distance 3.88 Å), A: LEU1122 (Interatomic distance 5.49 Å), A: LEU1198 (Interatomic distance 5.22 Å), and A: MET1199 (Interatomic distance 5.47 Å) establish an alkyl hydrophobic contact with the cyclonaphane ring's C4 substituted methyl moiety. Furthermore, the pi electrons of the benzene ring at residue A: PHE1127 (interatomic distance 4.51 Å) establish pi-alkyl hydrophobic contact with the alky moieties of the pyrazine and pyrimidine rings. The pyrazine ring and pyrazine then form a two pi-alkyl contact with the residue A: LEU1256, with interatomic distances of 5.43 and 4.60 Å, respectively.

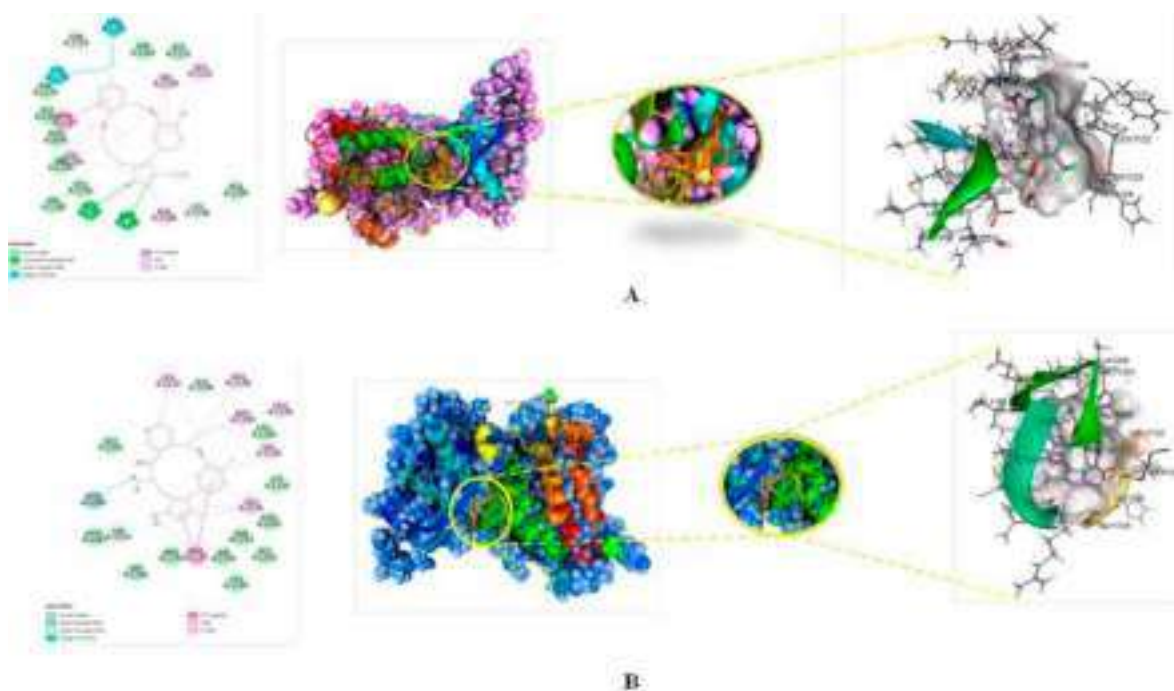
Similarly, the residues A: VAL1130 and A: LEU1122 were linked with the pyrimidine ring and benzene ring via pi-alkyl hydrophobic interactions (Interatomic distances 4.14 Å and 3.84 Å, respectively). The Figure 9A,B displays the 2D interaction and surface view for the compound 172 and 178.



**Figure 8.** Depiction of alignment of compound 178 within the active site of ALK tyrosine kinase (a,b), 2D interaction of compound 178 with ALK tyrosine kinase (c), and Superimposed conformation of compound 178 with the pdb-5fto ligand (cyan colored): Entrectinib (d).

**Table 3.** Presentation of docking interactions of the compound 178.

Residue	Distance in Å	Type of Interaction	Types of Bonding	From	Nature	To	Nature	Angle DHA	Angle HAY
HOH2080	2.87	Hydrogen Bond	Water Hydrogen Bond; Carbon Hydrogen Bond	O:H3	H-Donor	HOH2080	H-Acceptor	114.83	91.8
ASP1203	2.58	Hydrogen Bond	Carbon Hydrogen Bond	O:H1	H-Donor	ASP1203	H-Acceptor	119.9	102.5
ASP1203	2.70	Hydrogen Bond	Carbon Hydrogen Bond	O:H1	H-Donor	ASP1203	H-Acceptor	147.9	110.3
PHE1127	5.03	Hydrophobic	Pi-Pi Stacked	PHE1127	Pi-Orbitals	0	Pi-Orbitals		
PHE1127	3.82	Hydrophobic	Pi-Pi Stacked	0	Pi-Orbitals	PHE1127	Pi-Orbitals		
ALA1148	3.88	Hydrophobic	Alkyl	ALA1148	Alkyl	O:C	Alkyl		
LEU1256	4.66	Hydrophobic	Alkyl	O:C	Alkyl	LEU1256	Alkyl		
LEU1122	5.49	Hydrophobic	Alkyl	O:C	Alkyl	LEU1122	Alkyl		
LEU1198	5.22	Hydrophobic	Alkyl	O:C	Alkyl	LEU1198	Alkyl		
MET1199	5.47	Hydrophobic	Alkyl	O:C	Alkyl	MET1199	Alkyl		
PHE1127	4.51	Hydrophobic	Pi-Alkyl	PHE1127	Pi-Orbitals	O:C	Alkyl		
LEU1256	5.43	Hydrophobic	Pi-Alkyl	0	Pi-Orbitals	LEU1256	Alkyl		
VAL1130	4.14	Hydrophobic	Pi-Alkyl	0	Pi-Orbitals	VAL1130	Alkyl		
LEU1256	4.60	Hydrophobic	Pi-Alkyl	0	Pi-Orbitals	LEU1256	Alkyl		
LEU1122	3.84	Hydrophobic	Pi-Alkyl	0	Pi-Orbitals	LEU1122	Alkyl		



**Figure 9.** (A) Best docked pose of 172 with ALK displaying 2D interaction plot on the left panel. Pink dashed lines indicating the Pi-Alkyl bond and residues embedded in light green sphere indicating to involve in Van der Waals interactions. On the center panel, surface view of ALK displaying binding cavity of 172 and right panel displaying the zoomed out binding pocket having amino acid residues surrounding the 172 molecule; (B) Best docked pose of 178 with ALK displaying 2D interaction plot on the left panel. Pink dashed lines indicating the Pi-Alkyl bond and residues embedded in light green sphere indicate involvement in Van der Waals interactions. On the center panel, surface view of ALK displaying binding cavity of 178 and right panel displaying the zoomed out binding pocket having amino acid residues surrounding the 178 molecules.

In case of the molecule 178, there is a complete reversal of the conformation in comparison with the reported pdb 4CMU for the molecule 178. In the present work, we have used pdb 5fto for performing docking for the most active molecules 172 and the 178. The co-crystallized native ligand was docked along the 172 and the molecule 178. The RMSD values for the molecule 178 was found to be 1.06 Å, while co-crystallized ligand (pdb-5fto) displayed a RMSD of 1.19 Å, which was less than the molecule 178. This observation revealed the good fit of the molecule 178 into the binding pocket of the ALK tyrosine kinase due to the relatively higher flexibility of the ligand. The success rates in binding mode prediction for different docking programs such as, AutoDock 4 version (v4.2.6), FlexX 1.8, FRED (OEDocking 4.1.2.1), Glide 6.7, CCDC GOLD Suite 5.3, and ICM-Pro docking on the numerous known ligands when the RMSD cutoff ranges from 1.0 to 3.0 Å [29]. The same docked complex of the molecule 178 with ALK TK was analysed for the stability by MD simulation and MMGBSA. Although most of the existing docking programs were developed as a general methodology for different systems, they do have their own strengths and limitations and may show different performances on specific applications.

The simulation studies revealed the stability of 178 into the binding pocket of ALK TK, although it displayed reverse conformation. Moreover, the reversal of the conformation could also be attributed to the large size of active site of ALK TK (See Figure 8a,b), which allows adoption of different conformations for molecule 178. Additionally, recent studies point out that current docking software like AutoDock 4 version (v4.2.6), Dock (version 3 and 6), NRG Suite (PyMOL versions 1.2 and above) etc. and respective algorithms for docking scores are inclined toward flexibility of ligands which in turn is associated with loss of ligand conformational entropy on binding. Various factors such as binding site characteristics, one-dimensional properties of the compound library, the type of the binding pocket, ligand and protein flexibility and input differences apparently decide the docking performance [30]. Therefore, the molecule 178 (docking score  $-7.84$  kcal/mol) with lower binding affinity for ALK TK has displayed a high degree of flexibility. Thus, all these combined factors resulted in an artificially more favorable binding score for more flexible decoys than for actives.

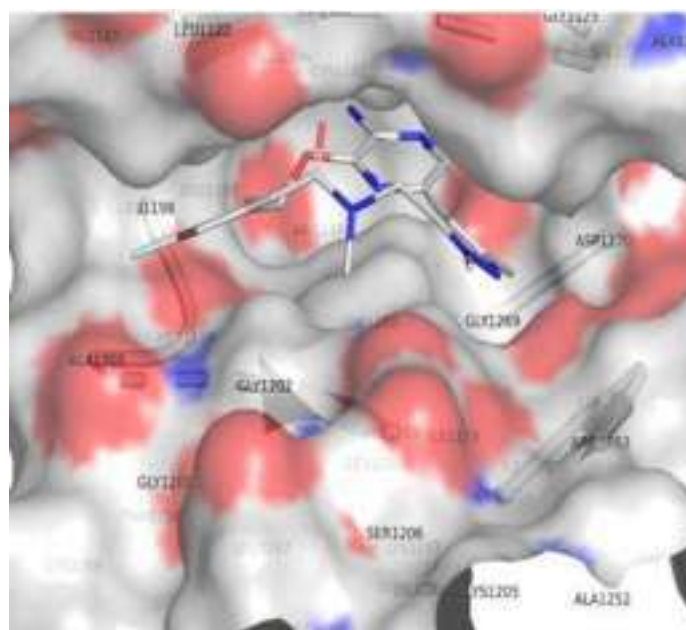
In addition to this, when we have redock the molecule 178 again into the binding pocket of ALK TK for comparing the docking results with the QSAR findings, it has attained similar conformation as that of the co-crystallized ligand (pdb-5fto) and the molecule 172. This observation supports the reported finding related to the loss of bioactive conformation due to the high degree of flexibility.

### 3.3. Comparison of Molecular Docking Results with the Reported X-ray Evidences

For comparing the docking results with the QSAR findings, it has attained similar conformation to that of the co-crystallized ligand (pdb-5fto) and the molecule 172. The docking position of molecule 172 shows that the phenyl with fluorine as a substituent is within the cavity formed by GLY1269 and ASN1254. Maria Menichincheri et al. [31] reported a similar observation. The molecule 171 has a comparable benzene ring with a fluorine substituent; however, the docking position shows that the fluorine carrying ring is unable to occupy the cavity produced by GLY1269 and ASN1254. Furthermore, conformation is completely reversed for molecules 171 and 172. One probable explanation is the existence of an extra carbon atom in molecule 172, which has resulted in increased flexibility and rsa (ratio of surface areas = ALL\_MSA/ALL-SASA). As a result, QSAR and docking led to consistent and complementary results (see Figure 10).

Similarly, comparing molecules 176 and 178 indicates an intriguing impact of the N\_Plan\_4B and ringC\_lipo\_2B on docking position and activity profile. When compared to molecule 176, molecule 178 has a larger number of N\_Plan\_4B and a lower value of ringC\_lipo\_2B. This might be the explanation for the docking conformation reversal and variances in binding affinities. The added planer nitrogen appears to be boosting the polarity of the molecule (see Figure 11a,b).



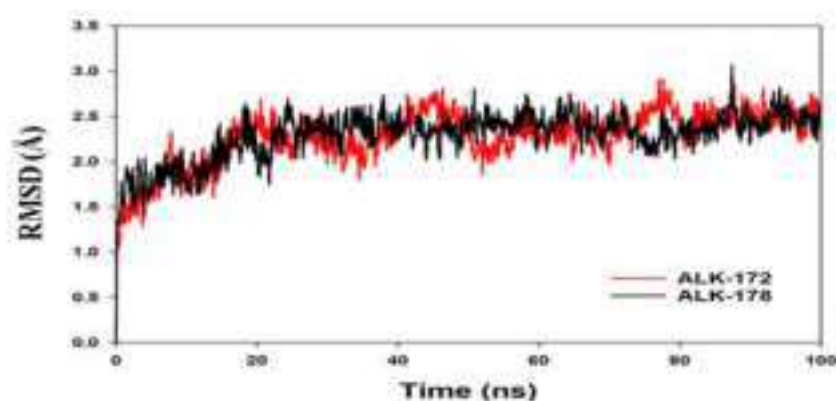


(b)

**Figure 11.** Depiction of the docking pose for the molecule 178 (a) and 176 (b) within the binding pocket of the ALK tyrosine kinase.

### 3.4. Molecular Dynamics Simulation (MD)

Molecular dynamics and simulation (MD) experiments were performed to investigate the stability or convergence of the most active compounds 172 and 178 bound ALK complex. Based on the activity profile and molecular docking results, we have used dock complexes of the compound 172 and 178 for MD simulation analysis. When the root mean square deviation (RMSD) data were compared, each simulation including 100 ns revealed stable conformation. The C-backbone of ALK bound to 172 exhibited a deviation of about 2.2 Å (see Figure 12) while the C-backbone of ALK bound to 178 exhibited a deviation of about 1.8 Å (Figure 12); RMSD plots are within the acceptable range signifying the stability of proteins in the 172 and 178 bound state earlier than or after simulation; however, it can also be suggested that the two ligands, 172 and 178 bound to ALK is quite stable within complex.

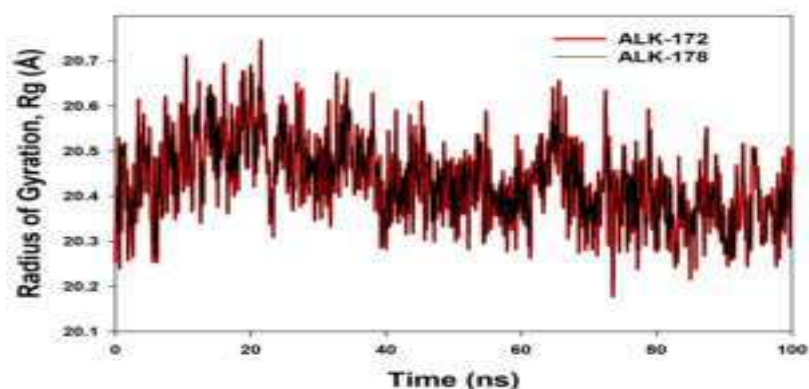


**Figure 12.** MD simulation trajectory analysis of Root Mean Square Deviations (RMSD) of 172 and 178 bound with ALK at 100 ns time frame displayed H-Bond plot of 172 bound ALK (red), 178 bound ALK (black).

The radius of gyration is a measure of the protein's compactness. The Radius of Gyration was reduced in 172 and 178 bound proteins, respectively (see Figure 13). According to

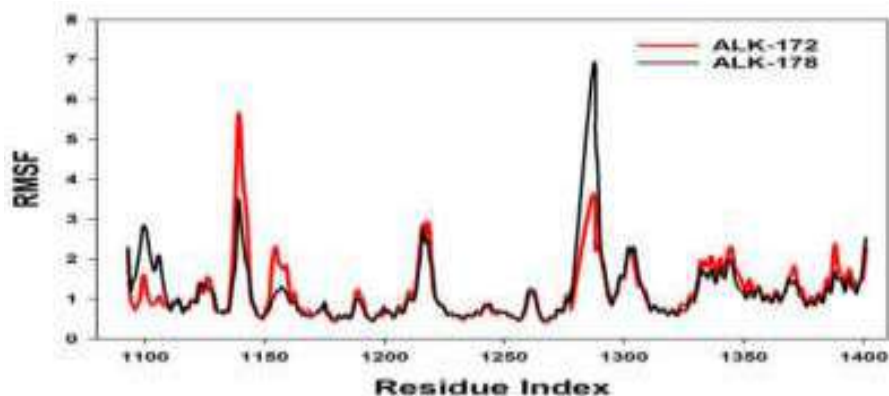


the overall quality analysis based on RMSD and Rg, 172 or 178 bound to the protein targets subsequently in the binding cavities and plays a significant role in the protein stability.



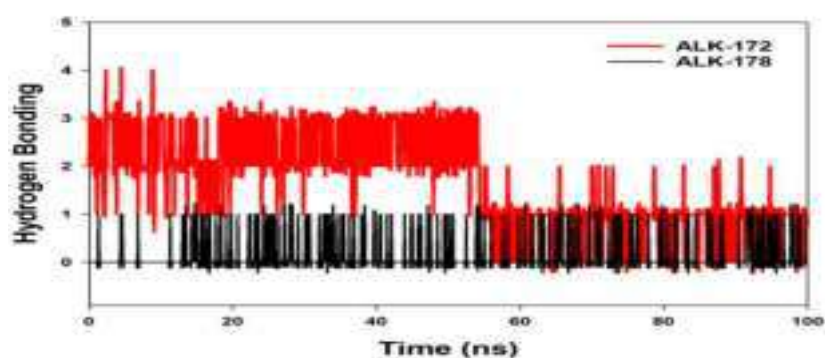
**Figure 13.** MD simulation trajectory analysis of Radius of gyration (Rg) of 172 and 178 bound with ALK at 100 ns time frame displayed H-Bond plot of 172 bound ALK (red), 178 bound ALK (black).

Plots for root mean square fluctuations (RMSF) of amino acid residues are shown at a time function of 100 ns. From the 100 ns simulation runs on ALK shown in Figure 14, ligand 172 has few variations peaks at residue indices 1145, 1220, and 1290, but ligand 178 has fluctuations at residues 1139, 1220, 1275, and 1345, although it was subsequently stabilized. As a result of the RMSF plots, it is reasonable to conclude that the protein structures were stable throughout the simulation within the 172, 178 bound conformation.



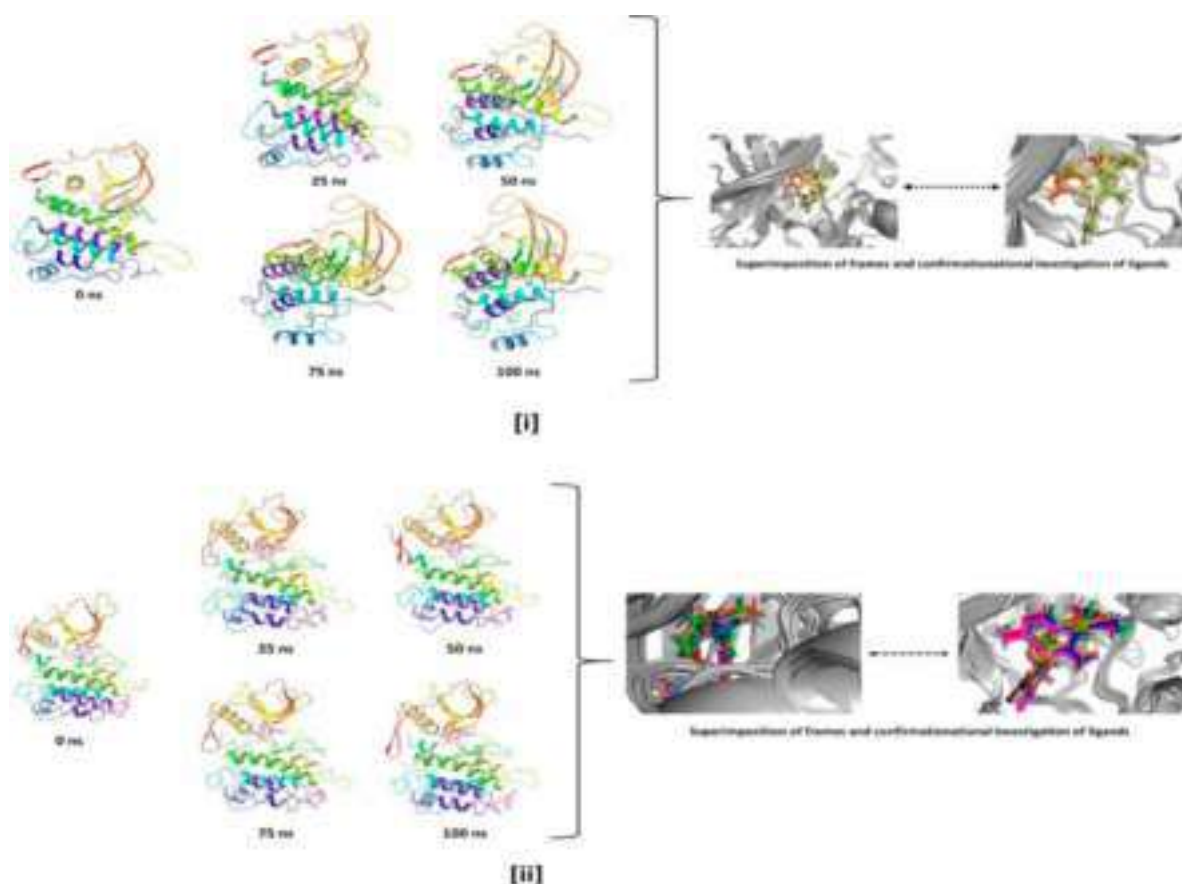
**Figure 14.** MD simulation trajectory analysis of Root Mean Square Fluctuations (RMSF) of 172 and 178 bound with ALK at 100 ns time frame displayed H-Bond plot of 172 bound ALK (red), 178 bound ALK (black).

The average hydrogen bonds established in 172 and 178 or the corresponding proteins throughout the 100 ns simulation were also noticed and recorded in Figure 15. From 0 ns to a 100 ns, an average of one hydrogen bonding is seen throughout the simulation or the same for MD simulations on 172 and 178 including ALK (Figure 15). Overall, three hydrogen bonds were generated during the simulation, as determined by a 2D ligand binding plot of 172 bound ALK protein, whereas in 178 bound along ALK, an average of one hydrogen bonding was produced. The quantity of hydrogen bonding over ALK along 172 and 178 hold strengthened the binding, assisting in making it more stable during the simulation (See Figure 15). In molecular docking studies, we have observed from the 2D interaction diagram where in ALK-172, we can see two hydrogen bonds were formed, on the other hand for ALK-178 we have observed single hydrogen bonding, therefore the same pattern for Molecular Dynamics.



**Figure 15.** MD simulation trajectory analysis of Hydrogen Bonding (H-Bonds) of 172 and 178 bound with ALK at 100 ns time frame displayed H-Bond plot of 172 bound ALK (red), 178 bound ALK (black).

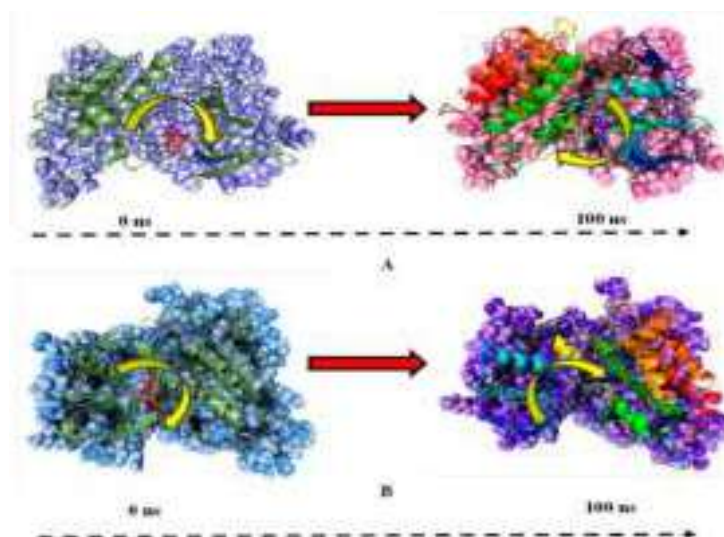
The step wise analysis of the stimulation trajectory of every 25 ns from beginning to end is depicted in Figure 16. The simulation trajectories exhibited the ligand 172 and 178 having no significant conformational changes throughout the 100 ns simulation. This signifies that the simulation complexes of ALK-172 and ALK-178 are stable and the ligand conformations at the active binding pocket of the ALK remains significantly unaltered (See Figure 16).



**Figure 16.** Stepwise trajectory analysis for every 25 ns displaying the protein and ligand conformation during 100 ns of simulation of [i] ALK-172 and [ii] ALK-178.

### 3.5. Molecular Mechanics Generalized Born and Surface Area (MMGBSA) Calculations and Energy Calculations

The MMGBSA technique is widely used to calculate the binding energy of ligands to protein molecules. With ALK, ligand 172 has the lowest binding energy of  $-49.3$  kcal/mol, whereas 178 has a binding energy of  $-52.5$  kcal/mol. The  $G_{\text{bindvdW}}$ ,  $G_{\text{bindLipo}}$ , and  $G_{\text{bindCoulomb}}$  energies contributed the most to the common binding energy of all kinds of interactions.  $G_{\text{bind}}$  is governed by non-bonded interactions such as  $G_{\text{bindCoulomb}}$ ,  $G_{\text{bindCovalent}}$ ,  $G_{\text{bindHbond}}$ ,  $G_{\text{bindLipo}}$ ,  $G_{\text{bindSolvGB}}$ , and  $G_{\text{bindvdW}}$ . Across all interactions, the  $G_{\text{bindvdW}}$ ,  $G_{\text{bindLipo}}$ , and  $G_{\text{bindCoulomb}}$  energies contributed the most to the average binding energy. On the other hand, the  $G_{\text{bindSolvGB}}$  and  $G_{\text{bindCovalent}}$  energies contributed the least to the final average binding energies. Furthermore, the  $G_{\text{bindHbond}}$  interaction values of the 172-ALK and 178-ALK complexes indicated stable hydrogen bonds with amino acid residues.  $G_{\text{bindSolvGB}}$  and  $G_{\text{bindCovalent}}$  had negative energy contributions in all of the compounds, and so opposed binding. When coupled,  $G_{\text{bindSolvGB}}$  and  $G_{\text{bindCovalent}}$  verified adverse energy contributions and hence resisted binding. Figure 17 (left panel) shows that 172 and 178 at the ALK binding pocket experienced an angular shift of the angle (curved to straight) after post simulation at pre-simulation (0 ns) (100 ns) (see Figure 17). These conformational alterations result in improved binding pocket acquisition and engagement with residues, resulting in increased stability and binding energy (see Table 4).



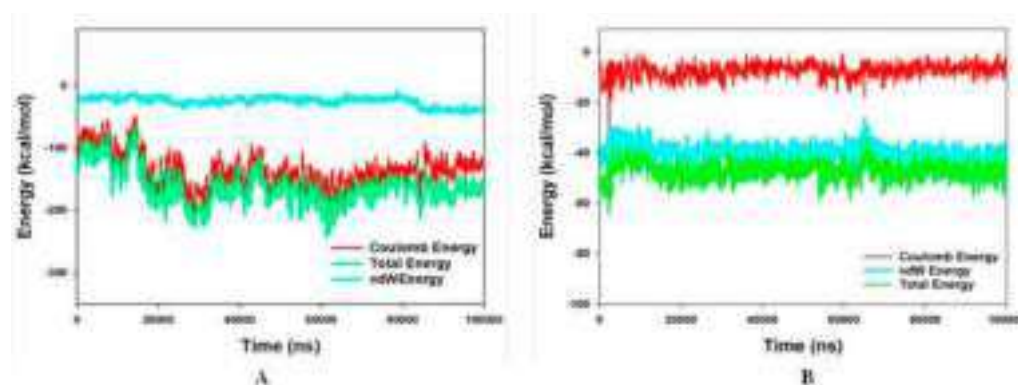
**Figure 17.** MMGBSA trajectory (0 ns, before simulation and 100 ns, after simulation) exhibited conformational changes upon binding the ligands with the protein, (A) ALK-172; (B) ALK-178. The arrows indicating the overall positional variation (movement and pose) of 172 and 178 at the binding site cavity.

**Table 4.** Binding energy calculation of 172 and 178 with ALK and non-bonded interaction energies from MMGBSA trajectories. (\* indicates mean value of energy parameters).

Energies (kcal/mol) *	ALK-172	ALK-178
$\Delta G_{\text{bind}}$	$-49.4 \pm 4.2$	$-52.6 \pm 3.0$
$\Delta G_{\text{bindLipo}}$	$-17.4 \pm 0.6$	$-19.5 \pm 1.5$
$\Delta G_{\text{bindvdW}}$	$-41.1 \pm 3.2$	$-44.8 \pm 3.1$
$\Delta G_{\text{bindCoulomb}}$	$-9.1 \pm 3.5$	$-5.7 \pm 2.2$
$\Delta G_{\text{bindHbond}}$	$-1.4 \pm 0.6$	$-0.3 \pm 0.2$
$\Delta G_{\text{bindSolvGB}}$	$19.7 \pm 3.1$	$18.2 \pm 1.8$
$\Delta G_{\text{bindCovalent}}$	$1.0 \pm 0.9$	$1.3 \pm 1.2$

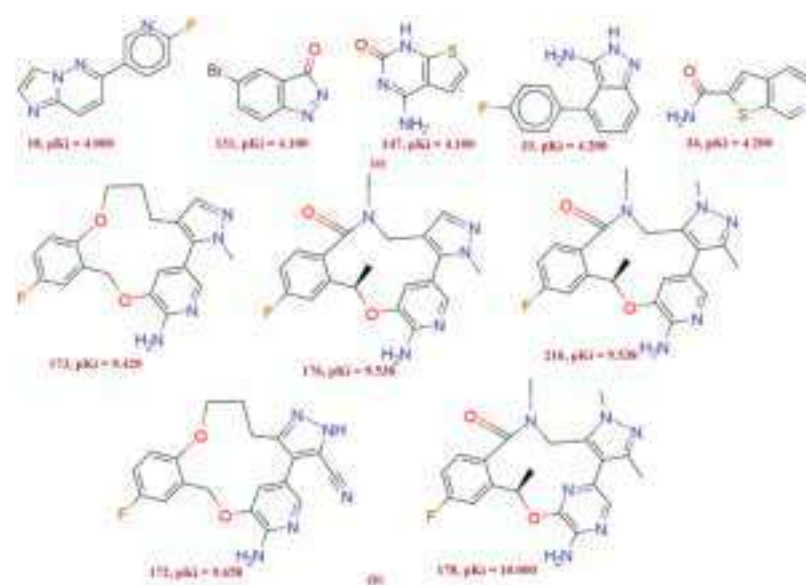
As a result, it is possible that the 172 (See Figure 18A) and 178 (See Figure 18B) molecules have a high affinity for the primary target ALK. In ALK bounded 172 complex systems, the average total energy was  $-130.00$  kcal/mol (green), while van der Waal's

energy (vdW) seemed to be merged over the total energy with an average energy of  $-30.00$  kcal/mol, which was seen as the primary contributor to the stability of the ALK172 complex (cyan). Furthermore, coulombic interactions had a little impact on system stability, contributing an average energy of  $-101.00$  kcal/mol (red) (See Figure 18). The energy profiles of the protein, ALK, and 178 complex systems were chosen to demonstrate the overall system's stability. In this regard, the Total Energy of the ALK-178 system has demonstrated to be completely stable, with an average total energy of  $-55.00$  kcal/mol (dark green). However, van der Waal's energy (vdW) remained merged up-on the total energy with an average energy of  $-40$  kcal/mol, taking into account as the primary contributor to the ALK-178 complex's stability (cyan). Furthermore, coulombic interactions performed a minimal influence in system stability, supplying an average energy of  $-10.00$  kcal/mol (red) as seen in Figure 18.



**Figure 18.** Energy plot of protein ALK with; (A) 172 complex system during the entire simulation event of 100 ns; (B) 178 complex system during the entire simulation event of 100 ns. The total energy (light green), van der Waal's energy (cyan) and coulomb energy (red) of the entire system indicating the stability of the individual systems bound to molecule.

Thus, MM-GBSA calculations resulted from MD simulation trajectories that were well justified with the binding energy obtained from docking results. Furthermore, the last frame (100 ns) of MMGBSA displayed the positional change of the 172 and 178 as compared to the 0 ns trajectory, indicating the better binding pose for best fitting in the protein's binding cavity (See Figure 19).



**Figure 19.** Variations in the  $K_i$  and chemical structure in the present dataset of ALK tyrosine kinase inhibitors: Five most active compounds (b), and five least active compounds (a) from the present series.

## 4. Materials and Methods

### 4.1. Selection of Data-Set

For the current study, 224 molecules with diverse structural features were selected due to the presence of different scaffolds and the substantial variation in the activity profile with an experimentally determined inhibition coefficient ( $K_i$ ) for ALK tyrosine kinase [32–35].  $K_i$  values ranging from 0.1 to 100,000 nM were changed to  $pK_i$  ( $K_i = -\log K_i$ ) before actual QSAR evaluation for the ease of handling the data. The Figure 19 depicts five most active molecules followed by five least active molecules, indicating the heterogeneity of bio-activity and chemical properties. The Table 5 displays SMILES notations alongside ChEMBL id [36] and reported  $K_i$  and  $pK_i$  values for several sample compounds. (See Table S1 in Supplementary Materials displaying Sr no, ChEMBL id, smiles notation,  $K_i$  value, and  $pK_i$  values).

**Table 5.** Presentation of Serial number, ChEMBL ID, Smiles,  $pK_i$  and  $K_i$  value of 10 most active and 10 least active molecules in the dataset as representative examples only.

Sn	CHEMBL ID	Smiles	$pK_i$	$K_i$ in nM
178	CHEMBL3286823	<chem>Cc1nn(C)c2c1-c1cnc(N)c(n1)O[C@H](C)c1cc(F)ccc1C(=O)N(C)C2</chem>	10	0.1
172	CHEMBL3286815	<chem>N#Cc1[nH]nc2c1-c1cnc(N)c(c1)OCc1cc(F)ccc1OCCC2</chem>	9.68	0.22
176	CHEMBL3286820	<chem>Cc1nn(C)c2c1-c1cnc(N)c(c1)O[C@H](C)c1cc(F)ccc1C(=O)N(C)C2</chem>	9.58	0.29
216	CHEMBL4286522	<chem>Cc1[nH][n+](C)c2c1-c1cnc(N)c(c1)O[C@H](C)c1cc(F)ccc1C(=O)N(C)C2</chem>	9.53	0.29
173	CHEMBL3286816	<chem>Cn1ncc2c1-c1cnc(N)c(c1)OCc1cc(F)ccc1OCCC2</chem>	9.42	0.38
161	CHEMBL3128064	<chem>Cc1nc(C(C)(C)O)sc1-c1cnc(N)c(O[C@H](C)c2cc(F)ccc2-n2nccn2)c1</chem>	9.39	0.4
181	CHEMBL3286832	<chem>C[C@H]1Oc2nc(cnc2N)-c2c(nc3ccc(C#N)cn23)CN(C)C(=O)c2ccc(F)cc21</chem>	9.25	0.56
174	CHEMBL3286818	<chem>C[C@H]1Oc2cc(cnc2N)-c2c(nn(C)c2C#N)CCOc2ccc(F)cc21</chem>	9.24	0.57
175	CHEMBL3286819	<chem>C[C@H]1Oc2cc(cnc2N)-c2c(nn(C)c2C#N)CCCOc2ccc(F)cc21</chem>	9.20	0.61
179	CHEMBL3286830	<chem>C[C@H]1Oc2cc(cnc2N)-c2c(nn(C)c2C#N)CN(C)C(=O)c2ccc(F)cc21</chem>	9.1	0.7
110	CHEMBL1995765	<chem>Nc1cc(=O)[nH]n1-c1ccccn1</chem>	4.5	31,622.7
13	CHEMBL1972934	<chem>Nc1ncnc2sccc12</chem>	4.4	39,810.7
39	CHEMBL1975212	<chem>Nc1ncnc2scc(-c3ccccc3)c12</chem>	4.4	39,810.7
48	CHEMBL1949855	<chem>O=c1[nH]cnc2c(Cl)cccc12</chem>	4.4	39,810.7
107	CHEMBL1994159	<chem>CC(=O)c1cccc(-c2ccc3nccn3n2)c1</chem>	4.3	50,118.7
129	CHEMBL2000879	<chem>c1ccc(C2CCc3[nH]nc3C2)cc1</chem>	4.3	50,118.7
33	CHEMBL1971519	<chem>Nc1n[nH]c2cccc(-c3ccc(F)cc3)c12</chem>	4.2	63,095.7
34	CHEMBL1971534	<chem>NC(=O)c1cc2ccncc2s1</chem>	4.2	63,095.7
50	CHEMBL1975921	<chem>O=c1[nH]c2cc(Br)cnc2[nH]1</chem>	4.2	63,095.7
131	CHEMBL2007097	<chem>Nc1nc(=O)[nH]c2sccc12</chem>	4.1	79,432.8

### 4.2. Molecular Structure Drawing and Optimization

The complete 224 molecules' 2D structures were drawn using free and open source software's ChemSketch 12 Freeware (<https://www.acdlabs.com/resources/free-chemistry->

[software-apps/chemsketch-freeware/](#) accessed on 2 March 2022, version 2021), while their 3D structures were generated using Open Babel 2.4, respectively. Furthermore, optimization of the full dataset molecules was achieved using the MMFF94 force field provided in TINKER (default settings), whilst Open3DAlign was used for molecular alignment, respectively [37].

#### 4.3. Molecular Descriptor Calculation and Objective Feature Selection (OFS)

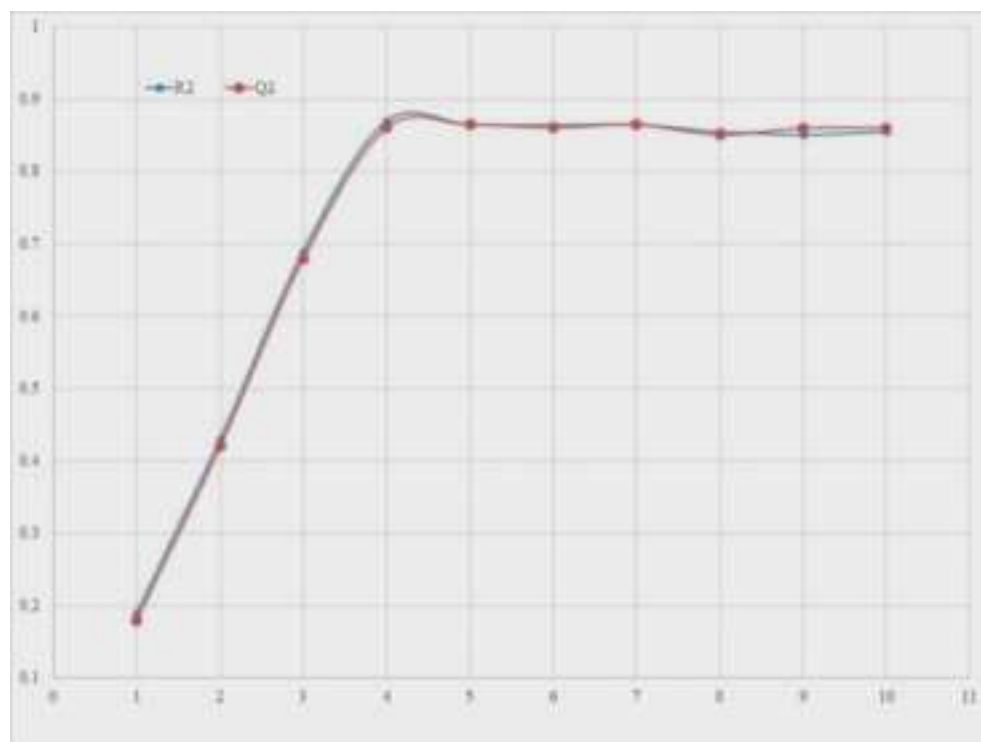
PyDescriptor, which is available as a plugin in the PyMOL 2.5 software application, was used to calculate descriptors for each molecule [38]. Molecular descriptors with almost constant values (>95 percent) and co-linearity ( $|R|$ ) greater than 0.95 were eliminated using objective feature selection (OFS) stability among QSARINS v2.2.4 [39]. This approach removed unnecessary molecular descriptors that impact multi-collinear and mock variables in the GA-MLR model. As a result, following OFS treatment, about 3339 molecular descriptors were separated in order to develop QSAR models.

#### 4.4. Subjective Feature Selection, QSAR Model—Development and Validation

The condensed pool of computed molecular descriptors includes 1D- and 3D-descriptors, as well as molecular properties or value descriptors, and so on. Coinciding with a huge molecule, followed by a vivid gap. After developing robust QSAR models, the Subjective Feature Selection (SFS) function in QSARINS v2.2.4 is used to run Genetic Algorithm (GA) based multi linear regression (MLR). QSAR models were developed in accordance with OECD guidelines and were then subjected to extensive internal or external statistical validation, Y-scrambling, or Applicability domain examination. The following steps are included in the QSAR model development practice. The whole dataset was utilised to create QSAR models, which were mostly based on the undivided (training set) dataset, however in this study, we are presenting one univariate divided set and another divided set multivariate QSAR models

1. The QSAR techniques have been anticipated to use a loosely split operation in QSARINSv2 software v2.2.4 based on a divided dataset. It divided a given dataset into 80% training (180 molecules in the training set) and 20% prediction (44 molecules in prediction set). The 180 molecules from the training set were used to generate the QSAR model, and external validation was completed on 44 compounds from the prediction set.
2. The QSARINS software v2.2.4 program was used to construct GA-MLR mainly based QSAR models, incorporating default parameters.  $Q^2_{LOO}$  is utilised as a fitness parameter to accomplish subjective feature selection. While doing SFS, the  $Q^2_{LOO}$  value was extraordinarily prolonged up to the four variables, but an insignificant uplift was seen after that. Thus, in order to keep the QSAR model from over-fitting, SFS was previously limited to a set of four descriptors. This resulted in the creation of simple and predictive QSAR models. (See Supplementary Materials Table S2 values for the selected four molecular descriptors present in QSAR models).

An important aspect of developing a good QSAR model with minimal over-fitting and appropriate interpretability is to have an enough number of molecular descriptors in QSAR the model. In the present study, a plan (see Figure 20) was projected in the large range of molecular descriptors included among the model yet  $R^2_{tr}$  and  $Q^2_{LOO}$  values to get the so-called breaking point. As a result, the variety of chemical descriptors related to the breakdown point used to be prioritized for model construction. Figure 20 shows that the breakage point correlates with four different factors. As a result, QSAR models with more than four descriptors were rejected.



**Figure 20.** Plot of number of descriptors against Coefficient of Determination  $R^2$  and Leave-One-Out Coefficient of Determination  $Q^2$  to identify the optimum number of descriptors.

To perform acceptable validation, QSARINS v2.2.4 was used to do (a) leave-one-out (LOO) or leave-many-out (LMO) parameter-based internal validation; (b) external validation; (c) Y-scrambling or model applicability domain (AD) analysis in accordance with OECD requirements. The robustness of the GA-MLR-based QSAR model was previously assessed on the basis of how well the various statistical parameters perform on the respective starting value. Two QSAR models (1.1 and 1.2) consisting of univariate divided set and multivariate divided set models with excellent values on these parameters and best predictive capability were chosen for the analysis, but the rest of the QSAR models failed to fulfil some of these factors above-mention values and were omitted [35].

#### 4.5. Molecular Docking

The protein data bank provided the ALK tyrosine kinase pdb file (pdb id-5fto, Resolution 1.7). For its X-ray resolution or sequel completeness, the pdb 5fto was carefully chosen. The optimized protein is appropriate for docking analysis. The protein preparation was carried by UCF chimera-1.16-win64 software (See Supplementary Materials for the detail procedure of protein preparation by chimera-1.16 software). Before the docking investigation, the natural ligand (Entrectinib) was removed. In the present study, the binding site for native ligand, namely the active site, has been studied. As a result, the compounds were docked between the active site, where the native ligand was originally bound along ALK tyrosine kinase, and the docking posture for the most active molecules 172 and 178 is shown below for convenience. The NRGSuite programme (PyMOL versions 1.2 and above) was used to do the molecular docking investigation. Because this is a free and open source software program, it may also be utilised as a PyMOL plugin [35]. It detects surface holes in a protein and uses them as target binding sites for docking simulations with the help of FlexAID [40]. It employs a genetic algorithm for function conformational search, model ligand and side-chain flexibility, and allows for covalent binding simulation. To achieve substantial performance with NRGSuite, the flexible-rigid docking approach was employed in conjunction with the following default settings: Because of the binding sites, the input technique is spherical (diameter: 17); the spacing on the three-dimensional grid is

0.385; facet band flexibility is no; ligand flexibility is yes; ligand posture is no; restrictions are no. Hetero groups-cloud molecules included; van der Waals permeability  $-0.1$ ; solvent types-none; variation on chromosomes—1000; variation on generations—1000; fitness model-share; copy model-population boom; and variation on top complexes—5. After the docking process was validated, the molecule Entrectinib, a discovered tyrosine kinase inhibitor, was employed for validation.

#### 4.6. MD Simulation Analysis

The virtual screening findings are utilised to evaluate the most active Molecule 178 with a docking score of  $-7.8$  kcal/mol and Molecule 172 ( $-8.0$  Kcal/mol) in molecular dynamics and simulation using the Schrodinger Desmond versus 2020.1 (MD simulation). The SPC (Simple factor charge) model was utilised to bind protein ligands using the docking complexes Molecule 178 and Molecule 172. In this system, the OPLS-2005 pressure subject and explicit solvent model with SPC water molecules were applied. To neutralise the charge, Na<sup>+</sup> ions were added [41]. To imitate the physiological environment, 0.15 M NaCl alternatives are provided to the computer [42]. The Nose–Hoover chain coupling approach was employed to build up the NPT ensemble with temperature 300 K, leisure time of 1.0 ps, and pressure 1 bar, which was once as soon as maintained in all simulations. A 2 fs time step will be employed. The barostat approach with the Martyna–Tuckerman–Klein chain coupling scheme [43] was originally utilised for pressure control with a leisure time of 2 ps. The particle mesh Ewald technique [44] was used to calculate long-range electrostatic interactions with a radius of 9 for Coulomb interactions. The non-bonded forces were estimated using the RESPA integrator. The root mean square deviation (RMSD), root mean square fluctuation (RMSF), radius of gyration (Rg), and protein ligand interactions were assessed to have a check at the stability of the complex in MD simulations.

#### 4.7. Molecular Mechanics Generalized Born and Surface Area (MMGBSA) Calculations

The binding free energy ( $G_{\text{bind}}$ ) of docked complexes was determined using the molecular mechanics generalized born surface region (MM-GBSA) module in MD simulations comprising 5fto bonded with the most active molecule 178 and the molecule 172. (Schrodinger suite, LLC, New York, NY, USA, 2017-4). At around the same time, the binding free energy was estimated using the OPLS 2005 force field, the VSGB solvent model and rotamer search techniques [45]. Following the MD run, the MD trajectories frames were chosen at 10 ns intervals. The total free energy binding used to be calculated the usage of Equation (1):

$$\Delta G_{\text{bind}} = G_{\text{complex}} - (G_{\text{protein}} + G_{\text{ligand}}) \quad (3)$$

where,

$\Delta G_{\text{bind}}$  = binding free energy,

$G_{\text{complex}}$  = free energy of the complex,

$G_{\text{protein}}$  = free energy of the target protein, and

$G_{\text{ligand}}$  = free energy of the ligand.

## 5. Conclusions

A cheminformatics technique was used effectively in the current investigation to predict ALK Tyrosine kinase inhibitory activity in order to uncover fundamental structural aspects important for anticancer activity. Two statistically robust univariate and four parametric QSAR models with exceptional external predictive capability were built, and the right number of molecular features were accurately positioned. The QSAR analysis effectively identified a combination based on previously unknown Pharmacophoric properties. The existence of fluorine atoms on the phenyl ring, as well as the presence of planar nitrogen atoms, must be retained in future drug design, coupled with some novel Pharmacophoric qualities such as *rsa*. The molecular descriptors identified in the developed QSAR models, such as the ratio of surface area (*rsa*), planar nitrogen within four bonds from the nitrogen



atom, fluorine atom within five bonds from the non-ring oxygen atom, lipophilic atoms within two bonds from the ring carbon atoms, and so on, can potentially enhance the ALK Tyrosine kinase inhibition potency. QSAR and molecular docking studies have successfully identified certain significant Pharmacophoric traits, such as the presence of an extra carbon atom in molecule 172, which results in increased flexibility and *rsa*; comparison of molecule 176 with 178 reveals an interesting influence of the N\_PlanN\_4B and ringC\_lipo\_2Bon docking pose and activity profile; and reversal in docking conformation and differences in the binding affinities of compounds 176 and 178. Moreover, identification of the additional polar nitrogen in QSAR analysis responsible for increasing the polarity of the molecule. This observation reveals that the QSAR and docking results are completely consistent with one another. The molecular docking studies on the 172 and 178 with the ALK tyrosine kinase receptor revealed that these compounds anchored to the ALK tyrosine kinase along the orientation or position extremely close to co-crystallized ligand; Entrectinib that resulted from crystallographic analysis of the ALK tyrosine kinase protein including its actual ligand. As a result, the created QSAR models meet the threshold values for several statistical parameters required to get the accuracy and applicability of a QSAR model. As a result, the obtained QSAR models include an appropriate mix of quantitative and qualitative characteristics. The pharmacophoric properties found in QSAR models show tremendous potential for optimizing dataset compounds in accordance with more potent ALK tyrosine kinase inhibitors as anticancer leads. Furthermore, MD simulation and binding free energy analyses support the findings of the QSAR and molecular docking studies.

**Supplementary Materials:** The following supporting information can be downloaded at: <https://www.mdpi.com/article/10.3390/molecules27154951/s1>, Table S1: The SMILES notation for two hundred twenty four (224) ALK tyrosine kinase leads, along with their reported  $K_i$  and  $pK_i$  values. Table S2: The values for selected molecular descriptors present in QSAR models. Table S3: Details regarding performance of Univariate Divided set model 1.1. containing Different graphs associated with model, Table S4: Details regarding performance of Multivariate divided set model comprising Different graphs associated with model 1.2. Statistical parameters for used for validation of QSAR models. File S5: Description of the performance parameters in QSARINS.

**Author Contributions:** R.D.J.: Conceptualization, Data Curation and Draft Review and Editing, P.S.: Formal Analysis, Editing, N.J.: Formal Analysis, A.G. (Ajaykumar Gandhi): Review and editing, N.M.: Discussion, Editing, Formal Analysis, A.A.A.-M.: Review, Discussion and Editing, M.E.A.Z.: Review, Discussion and Editing, S.A.A.-H.L.: Formal Analysis, A.S.: Formal Analysis, V.H.M.: Discussion and Formal Analysis, A.G. (Arabinda Gosh): Discussion, Review and Editing, R.L.B.: Formal Analysis, Editing. All authors have read and agreed to the published version of the manuscript.

**Funding:** The authors Magdi E.A. Zaki, Sami A. Al-Hussain, and Aamal A. Al-Mutairi extend their sincere thanks the Deanship of Scientific Research, Imam Mohammad Ibn Saud Islamic University, Saudi Arabia, for its support of this research through the Research Group No RG-21-09-76.

**Institutional Review Board Statement:** Not applicable.

**Informed Consent Statement:** Not applicable.

**Data Availability Statement:** The data is available in the Supplementary Materials section.

**Acknowledgments:** The authors are thankful to Paola Gramatica and her team for providing QSARINS-v2.2.4 and developers of TINKER, ChemSketch 12 Freeware (ACD labs), and PyDescriptor for providing the free versions of their software. Rahul Jawarkar are grateful to the Rajendra Gode Institute of Pharmacy, Amravati, Maharashtra, India. Magdi E.A. Zaki and Sami A. Al-Hussain are thankful to the Deanship of Scientific Research at Imam Mohammad Ibn Saud Islamic University, Riyadh, KSA, for its support of this research through the Research group number 21-09-77.

**Conflicts of Interest:** The authors declare no conflict of interest.

**Sample Availability:** Samples of the compounds are available from the authors.

## References

- Hallberg, B.; Palmer, R.H. The role of the ALK receptor in cancer biology. *Ann. Oncol.* **2016**, *27*, iii4–iii15. [[CrossRef](#)]
- Morris, S.W.; Kirstein, M.N.; Valentine, M.B.; Dittmer, K.G.; Shapiro, D.N.; Saltman, D.L.; Look, A.T. Fusion of a kinase gene, ALK, to a nucleolar protein gene, NPM, in non-Hodgkin's lymphoma. *Science* **1994**, *263*, 1281–1284. [[CrossRef](#)] [[PubMed](#)]
- Holla, V.R.; Elamin, Y.Y.; Bailey, A.M.; Johnson, A.M.; Litztenburger, B.C.; Khotskaya, Y.B.; Sanchez, N.S.; Zeng, J.; Shufean, M.A.; Shaw, K.R.; et al. ALK: A tyrosine kinase target for cancer therapy. *Cold Spring Harb. Mol. Case Stud.* **2017**, *3*, a001115. [[CrossRef](#)]
- Della Corte, C.M.; Viscardi, G.; Di Liello, R.; Fasano, M.; Martinelli, E.; Troiani, T.; Ciardiello, F.; Morgillo, F. Role and targeting of anaplastic lymphoma kinase in cancer. *Mol. Cancer* **2018**, *17*, 30. [[CrossRef](#)]
- Kumar, N.M.; Mathew, M.; Anila, K.N.; Priyanka, S. A review on newer tyrosine kinase inhibitors and their uses. *J. Clin. Diagn. Res.* **2018**, *12*, XE01–XE06. [[CrossRef](#)]
- Lin, J.J.; Riely, G.J.; Shaw, A.T. Targeting ALK: Precision Medicine Takes on Drug Resistance. *Cancer Discov.* **2017**, *7*, 137–155. [[CrossRef](#)] [[PubMed](#)]
- Shaw, A.T.; Kim, D.-W.; Nakagawa, K.; Seto, T.; Crinó, L.; Ahn, M.-J.; De Pas, T.; Besse, B.; Solomon, B.J.; Blackhall, F.; et al. Crizotinib versus Chemotherapy in Advanced ALK-Positive Lung Cancer. *N. Engl. J. Med.* **2013**, *368*, 2385–2394. [[CrossRef](#)] [[PubMed](#)]
- Solomon, B.J.; Mok, T.; Kim, D.-W.; Wu, Y.-L.; Nakagawa, K.; Mekhail, T.; Felip, E.; Cappuzzo, F.; Paolini, J.; Usari, T.; et al. First-line crizotinib versus chemotherapy in ALK-positive lung cancer. *N. Engl. J. Med.* **2014**, *371*, 2167–2177. [[CrossRef](#)]
- Shaw, A.T.; Kim, D.W.; Mehra, R.; Tan, D.S.; Felip, E.; Chow, L.Q.; Camidge, D.R.; Vansteenkiste, J.; Sharma, S.; De Pas, T.; et al. Ceritinib in ALK-rearranged non-small-cell lung cancer. *N. Engl. J. Med.* **2014**, *370*, 1189–1197. [[CrossRef](#)] [[PubMed](#)]
- Kim, D.-W.; Mehra, R.; Tan, D.S.W.; Felip, E.; Chow, L.Q.M.; Camidge, D.R.; Vansteenkiste, J.; Sharma, S.; De Pas, T.; Riely, G.J.; et al. Activity and safety of ceritinib in patients with ALK-rearranged non-small-cell lung cancer (ASCEND-1): Updated results from the multicentre, open-label, phase 1 trial. *Lancet Oncol.* **2016**, *17*, 452–463. [[CrossRef](#)]
- Ou, S.-H.I.; Ahn, J.S.; De Petris, L.; Govindan, R.; Yang, J.C.-H.; Hughes, B.; Lena, H.; Moro-Sibilot, D.; Bearz, A.; Ramirez, S.V.; et al. Alectinib in crizotinib-refractory ALK-rearranged non-small-cell lung cancer: A phase II global study. *J. Clin. Oncol.* **2015**, *34*, 661–668. [[CrossRef](#)] [[PubMed](#)]
- Shaw, A.T.; Gandhi, L.; Gadgeel, S.; Riely, G.J.; Cetnar, J.; West, H.; Camidge, D.R.; Socinski, M.A.; Chiappori, A.; Mekhail, T.; et al. Alectinib in ALK-positive, crizotinib-resistant, non-small-cell lung cancer: A single-group, multicentre, phase 2 trial. *Lancet Oncol.* **2016**, *17*, 234–242. [[CrossRef](#)]
- Katayama, R.; Khan, T.M.; Benes, C.; Lifshits, E.; Ebi, H.; Rivera, V.M.; Shakespeare, W.C.; Iafrate, A.J.; Engelman, J.A.; Shaw, A.T. Therapeutic strategies to overcome crizotinib resistance in non-small cell lung cancers harboring the fusion oncogene EML4-ALK. *Proc. Natl. Acad. Sci. USA* **2011**, *108*, 7535–7540. [[CrossRef](#)] [[PubMed](#)]
- Johnson, T.W.; Richardson, P.F.; Bailey, S.; Brooun, A.; Burke, B.J.; Collins, M.R.; Cui, J.J.; Deal, J.G.; Deng, Y.L.; Dinh, D.; et al. Discovery of (10R)-7-Amino-12-fluoro-2,10,16-trimethyl-15-oxo-10,15,16,17-tetrahydro-2H-8,4-(metheno)pyrazolo[4,3-h][2,5,11]-benzoxadiazacyclotetradecine-3-carbonitrile (PF-06463922), a macrocyclic inhibitor of anaplastic lymphoma kinase (ALK) and c-ros oncogene 1 (ROS1) with preclinical brain exposure and broad-spectrum potency against ALK-resistant mutations. *J. Med. Chem.* **2014**, *57*, 4720–4744. [[PubMed](#)]
- Shaw, A.T.; Yeap, B.Y.; Solomon, B.J.; Riely, G.J.; Gainor, J.; Engelman, J.A. Effect of crizotinib on overall survival in patients with advanced non-small-cell lung cancer harbouring ALK gene rearrangement: A retrospective analysis. *Lancet Oncol.* **2011**, *12*, 4–12. [[CrossRef](#)]
- Bellacasa, R.P.; Karachaliou, N.; Estrada-Tejedor, R.; Teixidó, J.; Costa, C.; Borrell, J.I. ALK and ROS1 as a joint target for the treatment of lung cancer: A review. *Transl. Lung Cancer Res.* **2013**, *2*, 72–86.
- Roskoski, R., Jr. Anaplastic lymphoma kinase (ALK): Structure, oncogenic activation, and pharmacological inhibition. *Pharmacol. Res.* **2013**, *68*, 68–94. [[CrossRef](#)] [[PubMed](#)]
- Cherkasov, A.; Muratov, E.N.; Fourches, D.; Varnek, A.; Baskin, I.I.; Cronin, M.; Dearden, J.; Gramatica, P.; Martin, Y.C.; Todeschini, R.; et al. QSAR modeling: Where have you been? Where are you going to? *J. Med. Chem.* **2014**, *57*, 4977–5010. [[CrossRef](#)] [[PubMed](#)]
- Fujita, T.; Winkler, D.A. Understanding the Roles of the “two QSARs”. *J. Chem. Inf. Model.* **2016**, *56*, 269–274. [[CrossRef](#)] [[PubMed](#)]
- Huang, J.; Fan, X. Why QSAR fails: An empirical evaluation using conventional computational approach. *Mol. Pharm.* **2011**, *8*, 600–608. [[CrossRef](#)] [[PubMed](#)]
- Chirico, N.; Gramatica, P. Real external predictivity of QSAR models. Part 2. New intercomparable thresholds for different validation criteria and the need for scatter plot inspection. *J. Chem. Inf. Model.* **2012**, *52*, 2044–2058. [[CrossRef](#)] [[PubMed](#)]
- Gramatica, P.; Cassani, S.; Roy, P.P.; Kovarich, S.; Yap, C.W.; Papa, E. QSAR modeling is not “Push a button and find a correlation”: A case study of toxicity of (Benzo-)triazoles on Algae. *Mol. Inform.* **2012**, *31*, 817–835. [[CrossRef](#)] [[PubMed](#)]
- Martin, T.M.; Harten, P.; Young, D.M.; Muratov, E.N.; Golbraikh, A.; Zhu, H.; Tropsha, A. Does rational selection of training and test sets improve the outcome of QSAR modeling? *J. Chem. Inf. Model.* **2012**, *52*, 2570–2578. [[CrossRef](#)]
- Masand, V.H.; Mahajan, D.T.; Nazeruddin, G.M.; Hadda, T.B.; Rastija, V.; Alfeefy, A.M. Effect of information leakage and method of splitting (rational and random) on external predictive ability and behavior of different statistical parameters of QSAR model. *Med. Chem. Res.* **2015**, *24*, 1241–1264. [[CrossRef](#)]
- Gramatica, P. On the development and validation of QSAR models. *Methods Mol. Biol.* **2013**, *930*, 499–526.

26. Iwahara, T.; Fujimoto, J.; Wen, D.; Cupples, R.; Bucay, N.; Arakawa, T. Molecular characterization of ALK, a receptor tyrosine kinase expressed specifically in the nervous system. *Oncogene* **1997**, *14*, 439–449. [[CrossRef](#)]
27. Morris, S.W.; Naeve, C.; Mathew, P.; James, P.L.; Kirstein, M.N.; Cui, X.; Witte, D.P. ALK, the chromosome 2 gene locus altered by the t(2;5) in non-Hodgkin's lymphoma, encodes a novel neural receptor tyrosine kinase that is highly related to leukocyte tyrosine kinase (LTK). *Oncogene* **1997**, *14*, 2175–2188. [[CrossRef](#)] [[PubMed](#)]
28. Loren, C.E.; Scully, A.; Grabbe, C.; Edeen, P.T.; Thomas, J.; McKeown, M. Identification and characterization of DAlk: A novel *Drosophila melanogaster* RTK which drives ERK activation in vivo. *Genes Cells* **2001**, *6*, 531–544. [[CrossRef](#)] [[PubMed](#)]
29. Huang, S.Y. Comprehensive assessment of flexible-ligand docking algorithms: Current effectiveness and challenges. *Brief. Bioinform.* **2018**, *19*, 982–994. [[CrossRef](#)]
30. Menichincheri, M.; Ardini, E.; Magnaghi, P.; Avanzi, N.; Banfi, P.; Bossi, R.; Buffa, L.; Canevari, G.; Ceriani, L.; Colombo, M.; et al. Discovery of Entrectinib: A new 3-aminoindazole as a potent anaplastic lymphoma kinase (ALK), c-ros oncogene 1 kinase (ROS1), and pan-tropomyosin receptor kinases (Pan-TRKs) inhibitor. *J. Med. Chem.* **2016**, *59*, 3392–3408. [[CrossRef](#)]
31. Gramatica, P. Principles of QSAR Modeling. *Int. J. Quant. Struct. Prop. Relatsh.* **2020**, *5*, 61–97. [[CrossRef](#)]
32. Zaki, M.E.A.; Al-Hussain, S.A.; Masand, V.H.; Akasapu, S.; Lewaa, I. QSAR and Pharmacophore Modeling of Nitrogen Heterocycles as Potent Human N-Myristoyltransferase (Hs-NMT) Inhibitors. *Molecules* **2021**, *26*, 1834. [[CrossRef](#)]
33. Consonni, V.; Ballabio, D.; Todeschini, R. Comments on the definition of the Q2 parameter for QSAR validation. *J. Chem. Inf. Model.* **2009**, *49*, 1669–1678. [[CrossRef](#)]
34. Consonni, V.; Todeschini, R.; Ballabio, D.; Grisoni, F. On the Misleading Use of QF32 for QSAR Model Comparison. *Mol. Inform.* **2019**, *38*, 1800029. [[CrossRef](#)]
35. Chirico, N.; Gramatica, P. Real external predictivity of QSAR models: How to evaluate It? Comparison of different validation criteria and proposal of using the concordance correlation coefficient. *J. Chem. Inf. Model.* **2011**, *51*, 2320–2335. [[CrossRef](#)] [[PubMed](#)]
36. Gaulton, A.; Hersey, A.; Nowotka, M.; Bento, A.P.; Chambers, J.; Mendez, D.; Motow, P.; Atkinson, F.; Bellis, L.J.; Cibrián-Uhalte, E.; et al. The ChEMBL database in 2017. *Nucleic Acids Res.* **2017**, *45*, D945–D954. [[CrossRef](#)] [[PubMed](#)]
37. Tosco, P.; Balle, T.; Shiri, F. Open3DALIGN: An open-source software aimed at unsupervised ligand alignment. *J. Comput. Aided Mol. Des.* **2011**, *25*, 777–783. [[CrossRef](#)]
38. Masand, V.H.; Rastija, V. PyDescriptor: A new PyMOL plugin for calculating thousands of easily understandable molecular descriptors. *Chemom. Intell. Lab. Syst.* **2017**, *169*, 12–18. [[CrossRef](#)]
39. Gramatica, P.; Chirico, N.; Papa, E.; Cassani, S.; Kovarich, S. QSARINS: A new software for the development, analysis, and validation of QSAR MLR models. *J. Comput. Chem.* **2013**, *34*, 2121–2132. [[CrossRef](#)]
40. Gaudreault, F.; Morency, L.P.; Najmanovich, R.J. NRGsuite: A PyMOL plugin to perform docking simulations in real time using FlexAID. *Bioinformatics* **2015**, *31*, 3856–3858. [[CrossRef](#)]
41. Bowers, K.J.; Chow, D.E.; Xu, H.; Dror, R.O.; Eastwood, M.P.; Gregersen, B.A.; Klepeis, J.L.; Kolossvary, I.; Moraes, M.A.; Sacerdoti, F.D.; et al. Scalable algorithms for molecular dynamics simulations on commodity clusters. In Proceedings of the SC '06: 2006 ACM/IEEE Conference on Supercomputing, Tampa, FL, USA, 11–17 November 2006; IEEE: New York, NY, USA, 2006; p. 43. [[CrossRef](#)]
42. Jorgensen, W.L.; Maxwell, D.S.; Tirado-Rives, J. Development and testing of the OPLS all-atom force field on conformational energetics and properties of organic liquids. *J. Am. Chem. Soc.* **1996**, *118*, 11225–11236. [[CrossRef](#)]
43. Shivakumar, D.; Williams, J.; Wu, Y.; Damm, W.; Shelley, J.; Sherman, W. Prediction of Absolute Solvation Free Energies using Molecular Dynamics Free Energy Perturbation and the OPLS Force Field. *J. Chem. Theory Comput.* **2010**, *6*, 1509–1519. [[CrossRef](#)] [[PubMed](#)]
44. Martyna, G.J.; Klein, M.L.; Tuckerman, M. Nosé–Hoover chains: The canonical ensemble via continuous dynamics. *J. Chem. Phys.* **1992**, *97*, 2635–2643. [[CrossRef](#)]
45. Ylilauri, M.; Pentikäinen, O.T. MMGBSA as a Tool to Understand the Binding Affinities of Filamin–Peptide Interactions. *J. Chem. Inf. Model.* **2013**, *53*, 2626–2633. [[CrossRef](#)] [[PubMed](#)]

Article

# QSAR Evaluations to Unravel the Structural Features in Lysine-Specific Histone Demethylase 1A Inhibitors for Novel Anticancer Lead Development Supported by Molecular Docking, MD Simulation and MMGBSA

Rahul D. Jawarkar <sup>1,\*</sup>, Ravindra L. Bakal <sup>1,†</sup>, Nobendu Mukherjee <sup>2,3,†</sup>, Arabinda Ghosh <sup>4,†</sup>, Magdi E. A. Zaki <sup>5,\*</sup>, Sami A. AL-Hussain <sup>5</sup>, Aamal A. Al-Mutairi <sup>5</sup>, Abdul Samad <sup>6</sup>, Ajaykumar Gandhi <sup>7,†</sup> and Vijay H. Masand <sup>8,†</sup>

- <sup>1</sup> Department of Medicinal Chemistry and Drug Discovery, Dr Rajendra Gode Institute of Pharmacy, University Mardi Road, Amravati 444603, India; rlbakal@gmail.com
- <sup>2</sup> Department of Microbiology, Ramakrishna Mission Vivekananda Centenary College, Kolkata 700118, India; nabendu21@rkmvcrahar.org
- <sup>3</sup> Department of Health Sciences, Novel Global Community Educational Foundation, Hebersham, NSW 2770, Australia
- <sup>4</sup> Microbiology Division, Department of Botany, Gauhati University, Guwahati 781014, India; dra.ghosh@gauhati.ac.in
- <sup>5</sup> Department of Chemistry, Faculty of Science, Imam Mohammad Ibn Saud Islamic University, Riyadh 13318, Saudi Arabia; sahusain@imamu.edu.sa (S.A.A.-H.); aamutairi@imamu.edu.sa (A.A.A.-M.)
- <sup>6</sup> Department of Pharmaceutical Chemistry, Faculty of Pharmacy, Tishk International University, Erbil 44001, Iraq; abdul.samad@tiu.edu.iq
- <sup>7</sup> Department of Chemistry, Government Arts and Science College, Karur 639005, India; gacjay18@gmail.com
- <sup>8</sup> Department of Chemistry, Vidyabharati Mahavidyalaya, Camp, Amravati 444602, India; vijaymasand@gmail.com
- \* Correspondence: rahuljawarkar@gmail.com (R.D.J.); mezaki@imamu.edu.sa (M.E.A.Z.)
- † These authors contributed equally to this work.



**Citation:** Jawarkar, R.D.; Bakal, R.L.; Mukherjee, N.; Ghosh, A.; Zaki, M.E.A.; AL-Hussain, S.A.; Al-Mutairi, A.A.; Samad, A.; Gandhi, A.; Masand, V.H. QSAR Evaluations to Unravel the Structural Features in Lysine-Specific Histone Demethylase 1A Inhibitors for Novel Anticancer Lead Development Supported by Molecular Docking, MD Simulation and MMGBSA. *Molecules* **2022**, *27*, 4758. <https://doi.org/10.3390/molecules27154758>

Academic Editor: Athanassios C. Tsipis

Received: 14 June 2022

Accepted: 19 July 2022

Published: 25 July 2022

**Publisher's Note:** MDPI stays neutral with regard to jurisdictional claims in published maps and institutional affiliations.



**Copyright:** © 2022 by the authors. Licensee MDPI, Basel, Switzerland. This article is an open access article distributed under the terms and conditions of the Creative Commons Attribution (CC BY) license (<https://creativecommons.org/licenses/by/4.0/>).

**Abstract:** Using 84 structurally diverse and experimentally validated LSD1/KDM1A inhibitors, quantitative structure–activity relationship (QSAR) models were built by OECD requirements. In the QSAR analysis, certainly significant and understated pharmacophoric features were identified as critical for LSD1 inhibition, such as a ring Carbon atom with exactly six bonds from a Nitrogen atom, partial charges of lipophilic atoms within eight bonds from a ring Sulphur atom, a non-ring Oxygen atom exactly nine bonds from the amide Nitrogen, etc. The genetic algorithm–multi-linear regression (GA-MLR) and double cross-validation criteria were used to create robust QSAR models with high predictability. In this study, two QSAR models were developed, with fitting parameters like  $R^2 = 0.83–0.81$ ,  $F = 61.22–67.96$ , internal validation parameters such as  $Q^2_{LOO} = 0.79–0.77$ ,  $Q^2_{LMO} = 0.78–0.76$ ,  $CCC_{cv} = 0.89–0.88$ , and external validation parameters such as,  $R2_{ext} = 0.82$  and  $CCC_{ex} = 0.90$ . In terms of mechanistic interpretation and statistical analysis, both QSAR models are well-balanced. Furthermore, utilizing the pharmacophoric features revealed by QSAR modelling, molecular docking experiments corroborated with the most active compound's binding to the LSD1 receptor. The docking results are then refined using Molecular dynamic simulation and MMGBSA analysis. As a consequence, the findings of the study can be used to produce LSD1/KDM1A inhibitors as anticancer leads.

**Keywords:** LSD1; KDM1A; QSAR; anticancer; molecular docking; MD simulation; genetic algorithm–multi linear regression; MMGBSA

## 1. Introduction

Lysine-specific histone demethylase 1A (LSD1), also known as lysine (K)-specific demethylase 1A (KDM1A), is a crucial member of the monoamine oxidases family. LSD1

catalyzes two important and completely opposing enzymatic reactions with flavin adenine dinucleotide (FAD) as a cofactor: transcription repression via de-methylation at histone 3 lysine 4 methyl 1/2 (H3K4me1/2) and transcription activation via de-methylation at histone 3 lysine 9 methyl 1/2 (H3K9me1/2) [1]. LSD1 is also involved in the de-methylation of TP53, E2F1, and DNMT1 [2]. The typical healthy physiological condition is characterized by regimented epigenetic control of cyclic cellular processes, including rejuvenation, differentiation, and proliferation. LSD1 modulates differentiation and proliferation pathways in highly proliferative and widely metastatic small-cell lung cancer (SCLC) [3]. LSD1 overexpression is also found in other cancer types, including prostate cancer, breast cancer, colorectal cancer, and neuroblastoma [1–3].

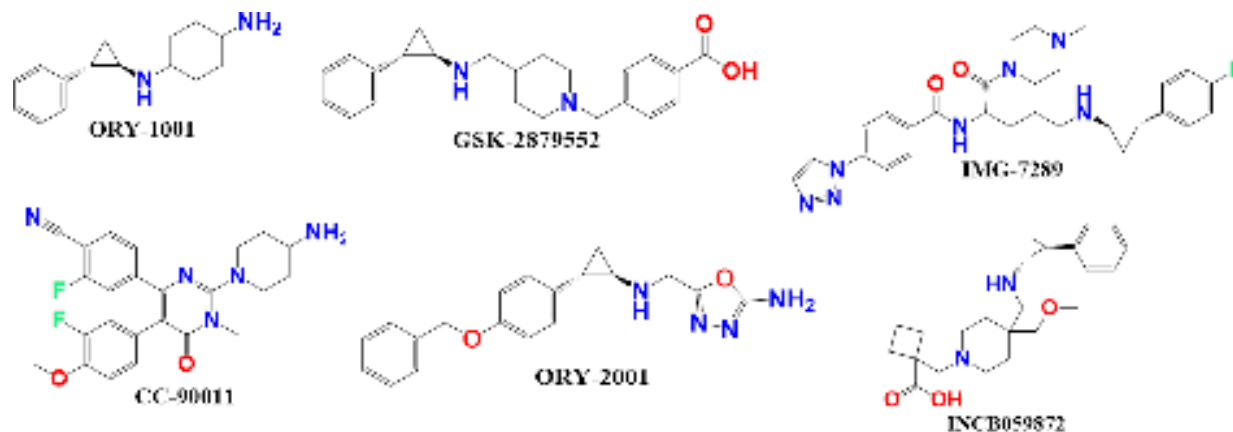
According to reports, if LSD1 overexpression is reduced in several forms of blood malignancies (haematological sarcomas) such as leukaemia, multiple myeloma, and solid tumours, cell differentiation is also reduced. This makes LSD1 an appealing target for anticancer medication development [1].

There have been several reports of reversible LSD1 inhibitors to date [4]. Sorna et al. used high-throughput virtual screening to identify reversible LSD1 inhibitors; however, these drugs appeared to have considerable off-target and nonspecific effects [4,5]. Ma et al. found several pyrimidine–thiourea hybrids that showed a high sensitivity to LSD1 inhibition in vitro and in tumour xenografts. [4]. Furthermore, Li et al. developed a series of [1–3] triazolo [4,5-d] pyrimidine derivatives as selective LSD1 inhibitors, which were reported to block tumour cell migration [5]. The activity of documented reversible inhibitors, on the other hand, did not meet the advances of covalent inhibitors, due in part to the huge size and polarity of the LSD1 substrate binding pocket [6]. Furthermore, the reported compounds' erroneous binding techniques and the lack of theoretical research motivated us to hunt for hidden and buried structural features that are required for developing effective, efficient, and reversible LSD1 inhibitors. This convergence of circumstances encouraged us to do a computational study on the proven reversible LSD1 inhibitors from the appropriate database, as well as examine the underlying structural elements influencing the design and inhibition of potent and effective LSD1 inhibitors.

QSAR is a statistically-based intersectional plan of activities and standardized technique for identifying the mathematical relationship between the structural property of a molecule and its biological activity. General QSAR modelling protocol involves: (I) selecting a sufficiently abundant, admissible molecular dataset with accurate biological activity; (II) 3D-structure creation and optimization; (III) molecular descriptor calculation and constrained trimming using appropriate statistical methods; (IV) QSAR model development using an algorithm that fits favourable molecular descriptors; and (V) sufficient validation of the existing QSAR model (s) [5]. Circumstantial QSAR analysis quantifies the relationship between conspicuous but seemingly confusing molecule structural features and their experimentally studied biological activity. Statistical QSAR analysis predicts the biological activity of a drug prior to wet lab manufacturing and experimental in vivo testing. A QSAR that is conceptually neutral, illustrative, and statistically enhances pharmacokinetics knowledge [6,7]. This emphasizes the value of the QSAR study in promoting lead optimization.

QSAR models for LSD1 inhibitors have been discussed by a number of researchers. Rahman Abdizadeh et al. developed a 3D QSAR model for the set of tranylcypromine derivatives as a data set that performed similarly to the CoMFA ( $q^2 = 0.67$ ;  $r^2_{ncv} = 0.93$ ;  $r^2_{pred} = 0.97$ ), CoMFA-RF ( $q^2 = 0.69$ ;  $r^2_{ncr} = 0.93$ ;  $r^2_{pred} = 0.93$ ), CoMSIA ( $q^2 = 0.83$ ;  $r^2_{ncv} = 0.96$ ;  $r^2_{pred} = 0.96$ ), and HQSAR models ( $q^2 = 0.85$ ;  $r^2_{ncv} = 0.90$ ;  $r^2_{pred} = 0.73$ ) for training as well as the test set of LSD1 inhibition. Moreover, the significant gap between the  $q^2$  and the  $r^2$  values indicate the overfitting in both the CoMFA and CoMSIA models. However, because of the absence of mechanistic interpretation and atom-by-atom pharmacophoric features in CoMFA and CoMSIA investigations, their use has been limited to the optimization of a few pharmacological classes [8]. To date, several LSD1 inhibitors have been approved, and some of them, including ORY-1001, GSK-2879552, IMG-7289,

INCB059872, CC-90011, and ORY-2001 (See Figure 1), are currently being studied in clinical trials for cancer treatment, particularly in small lung cancer cells (SCLC) and acute myeloid leukaemia (AML) [9].



**Figure 1.** Presentation of the Structures of some clinical trial molecules.

A moderate-sized dataset-based QSAR with enough predictive capability and mechanistic understanding is clearly useful for boosting lead potency. In this study, we used molecular docking, MD simulation, and MMGBSA to create robust QSAR models for 84 structurally varied molecules with empirically established LSD1 inhibitory efficacy.

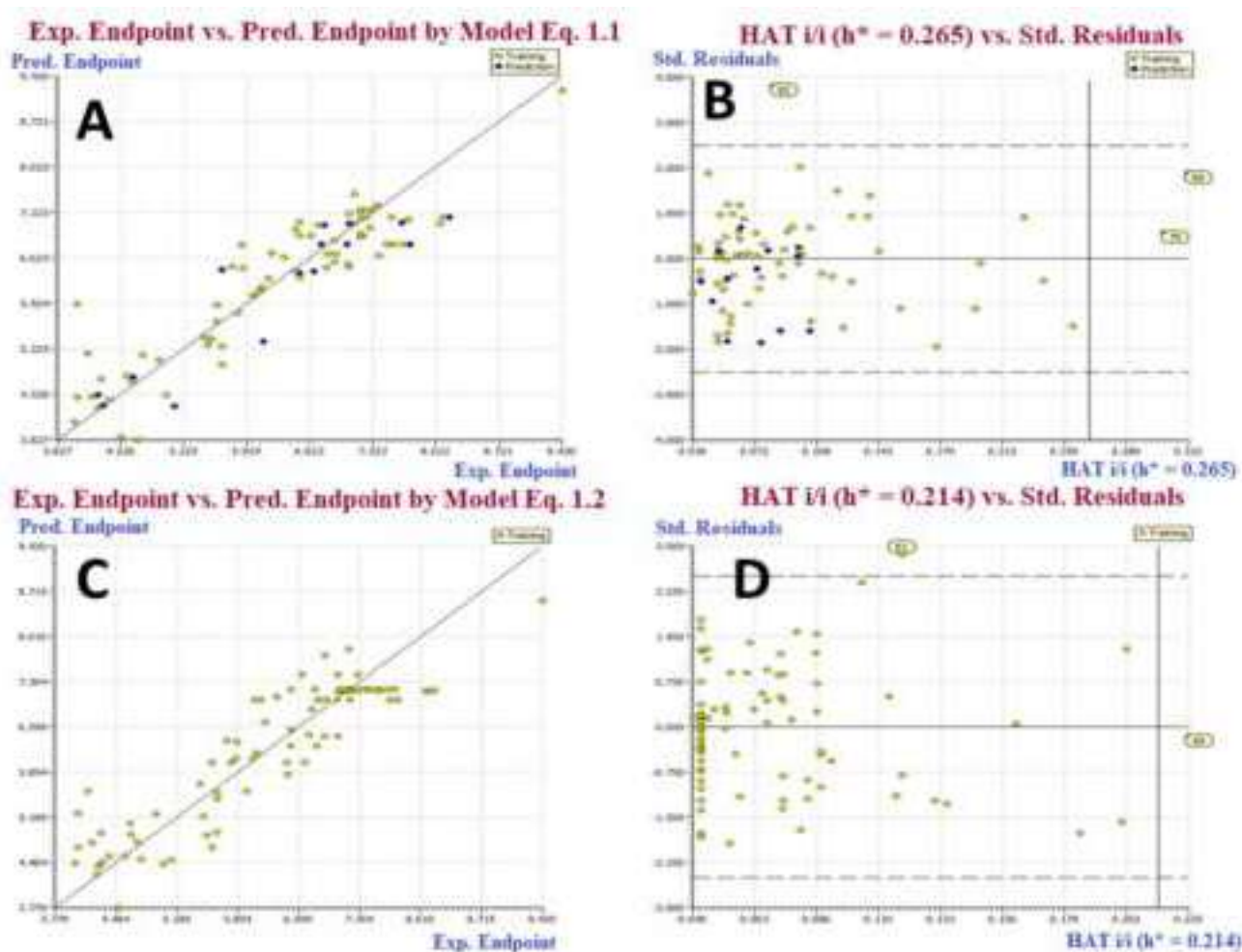
## 2. Results

Despite the fact that the current study is based on a moderate size dataset of 85 molecules, the existence of multiple molecular scaffolds, functional groups, substituents, diverse rings viz. non-aromatic, homoaromatic, heteroaromatic, fused rings; spiro compounds, etc., has significantly covered a vast chemical space. The QSAR models developed are based on a split and entire data set.  $R^2$ ,  $R^2_{adj}$ ,  $CCC_{tr}$ , and other fitting metrics have values far above the allowed threshold values, indicating that the QSAR models are statistically tolerable with the required number of chemical descriptors. Internal validation parameters include  $Q^2_{LOO}$ ,  $Q^2_{LMO}$ , and others with values that condescend to give the statistical robustness of the QSAR models. The external predictability of both models can be seen in the high values of external validation aspects like  $R^2_{ex}$  and  $Q^2_{Fn}$ . Model applicability domain is supported by William's plots (See Figure 2) (Applicability Domain). Fulfillment of allowed threshold values for numerous parameters, as well as poor correlation among molecular descriptors, rule out the possibility of serendipitous QSAR model construction [10–14] (see Table S2, Supplementary Information). These grounds validate these models' statistical robustness and strong external prediction.

### 2.1. Outlier Behavior of the Dataset Molecules

The third type of outlier, outliers toward the model, can only be identified after the regression model has been established. They indicate an X-Y link. Because of the variety of chemical structures explored in the study, model outliers are a specific form of outlier that may be found in high numbers in the QSAR/QSPR data set.

Based on the Williams plot, molecule 60 was identified as the third type of outlier in the divided set model, molecule 79 as an X outlier, and molecule 82 as a Y outlier. Figure 3 illustrates the core plot and loading plot of the Descriptor in a split-set QSAR model. The descriptor ring, CH3B, has a significant impact on molecule 60's outlier characteristics, but the descriptors lipo\_ringS\_8Bc and com\_sp2O\_4A have a substantial impact on molecule 82. The descriptor **fringCH3B**, on the other hand, had a major impact on molecule 79. The aforementioned conclusion explained the impact of particular molecular descriptors on the cluster of molecules in the dataset (See Figure 3).



**Figure 2.** (A) Graph of experimental vs. Predicted  $pEC_{50}$  values for model 1.1. (B) Williams plot for model 1.1. (C) Graph of experimental vs. Predicted  $pEC_{50}$  values for model 1.2. (D) Williams plot for model 1.2.

## 2.2. GA-MLR QSAR Models

Model-1.1 (Divided Set: Training Set-80% (67 molecules) and Prediction Set-20% (17 molecules)):

$$pEC_{50} = 13.856 (\pm 1.734) - 0.832 (\pm 0.226) \text{ avg\_molweight} - 0.211 (\pm 0.087) \text{ fringCH3B} + 0.263 (\pm 0.092) \text{ fNringC6B} + 4.482 (\pm 1.892) \text{ lipo\_ringS\_8Bc} - 0.639 (\pm 0.279) \text{ com\_sp2O\_4A}$$

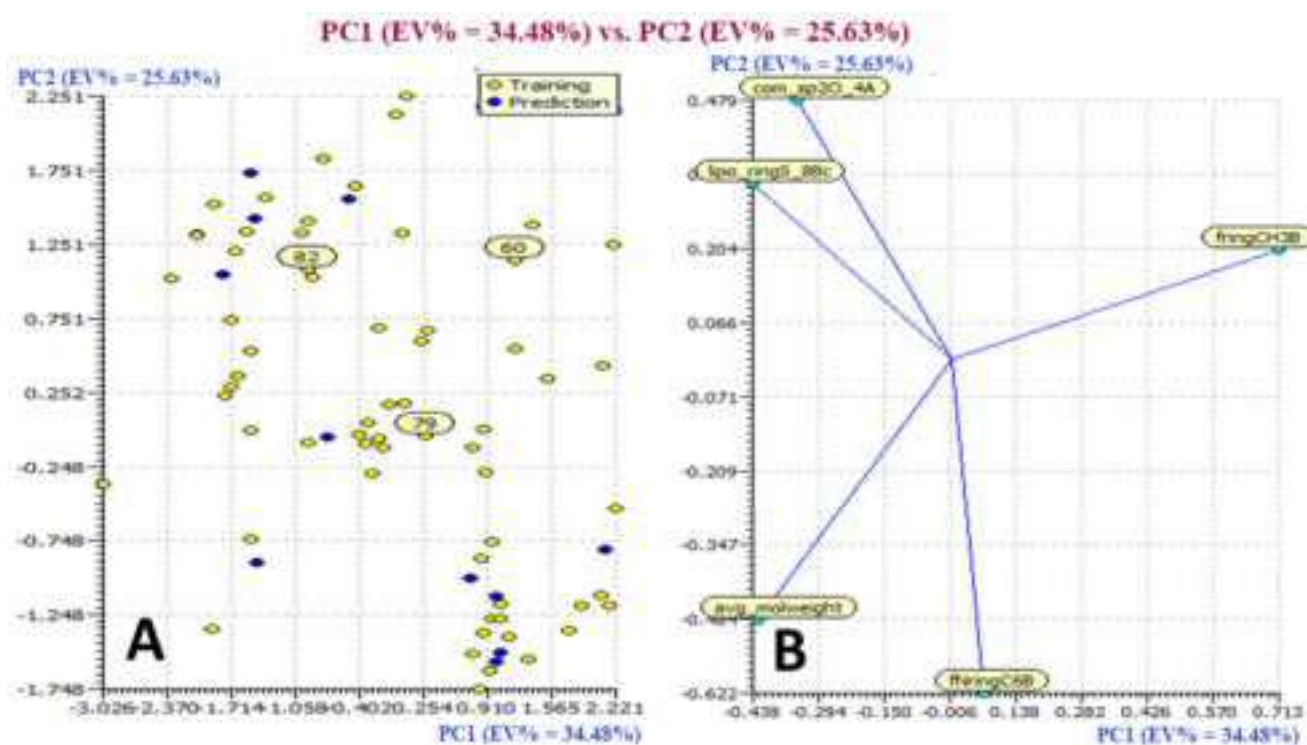
$$[R^2 = 0.83, R^2_{\text{adj}} = 0.82, Q^2_{\text{LOO}} = 0.79, Q^2_{\text{LMO}} = 0.78, \text{RMSE}_{\text{tr}} = 0.49, \text{MAE}_{\text{tr}} = 0.37, \text{RSS}_{\text{tr}} = 16.37, \text{CCC}_{\text{tr}} = 0.91, \text{RMSE}_{\text{cv}} = 0.54, \text{MAE}_{\text{cv}} = 0.40, \text{PRESS}_{\text{cv}} = 20.07, \text{CCC}_{\text{cv}} = 0.89, R^2_{\text{ext}} = 0.82, Q^2_{F1} = 0.81, Q^2_{F2} = 0.81, Q^2_{F3} = 0.81, \text{CCC}_{\text{ex}} = 0.90].$$

Model-1.2 (Full Set: Training Set-100%, (84 molecules)):

$$pEC_{50} = 6.488 (\pm 0.315) - 0.151 (\pm 0.078) \text{ fringCH3B} + 2.921 (\pm 1.496) \text{ lipo\_ringS\_8Bc} + 0.972 (\pm 0.349) \text{ famdNnotringO9B} + 0.347 (\pm 0.104) \text{ fdonsp3C2B} - 0.775 (\pm 0.302) \text{ fsp3CamdN4B}$$

$$[R^2 = 0.81, R^2_{\text{adj}} = 0.80, Q^2_{\text{LOO}} = 0.78, Q^2_{\text{LMO}} = 0.77, \text{RMSE}_{\text{tr}} = 0.51, \text{MAE}_{\text{tr}} = 0.41, \text{RSS}_{\text{tr}} = 22.24, \text{CCC}_{\text{tr}} = 0.90, \text{RMSE}_{\text{cv}} = 0.56, \text{MAE}_{\text{cv}} = 0.45, \text{PRESS}_{\text{cv}} = 26.57, \text{CCC}_{\text{cv}} = 0.88].$$

In this QSAR investigation, model 1.1 was constructed using the extended dataset, whereas model 1.2 was created using the entire dataset. The developed models are distinct in three of the five descriptors out of a total of five. The effects of variation in each molecular descriptor on the biological activity of the associated molecule are demonstrated with examples in the next section, even if the permutation in the bioactivity of each molecule in the dataset is the total of all five molecular descriptors.



**Figure 3.** Presentation of Score Plot (A) and Loading Plot (B) for the Descriptor in divided set QSAR Model.

### 3. Discussion

#### 3.1. Mechanistic Interpretation of Descriptors

**fNringC6B, lipo\_rings\_8Bc, famdNnotringO9B, and fdonsp3C2B:** These four molecular descriptors had positive coefficient values in both the divided and full set models, showing that amplification in the values of these molecular descriptors improves the anticancer potential of LSD1 inhibitors. The importance of some molecular descriptors is demonstrated by comparing variations in the  $pEC_{50}$  or  $EC_{50}$  values with transformations in the values of molecular descriptors.

**fNringC6B** (frequency of occurrence of ring carbon atom exactly at 6 bonds from nitrogen atom). This observation is supported by comparing compound **1** ( $fNringC6B = 1$ ;  $pEC_{50} = 9.42$ ) with compound **6** ( $fNringC6B = 0$ ;  $pEC_{50} = 7.71$ ). Possibly, an increase in the value of  $fNringC6B$  to 1 for compound **6** enhanced its LSD1 inhibitory potency by about two hundred and twenty-two times ( $\Delta pEC_{50} = 2.22$ ) (See Figure 4).

This observation was also seen by comparing the subsequent pair of molecules: **17** ( $pIC_{50} = 7.25$ ,  $fNringC6B = 2$ ) with **18** ( $pIC_{50} = 7.21$ ,  $fNringC6B = 0$ ), **31** ( $pIC_{50} = 7.04$ ,  $fNringC6B = 4$ ) with **32** ( $pIC_{50} = 6.91$ ,  $fNringC6B = 0$ ), **52** ( $pIC_{50} = 6.11$ ,  $fNringC6B = 1$ ) with **56** ( $pIC_{50} = 5.88$ ,  $fNringC6B = 0$ ), etc.

Vianello Paola et al. and colleagues also reported the synthesis of chemical **2** (4-ethyl-N-[3-(methoxymethyl)-2-[(4-[(3R)-pyrrolidin-3-yl] methoxyphenoxy) methyl] phenyl]-4H-thieno [3,2-b] pyrrole-5-carboxamide) from the dataset (see Figure 5). The most efficient basic moiety was compound **2** with pyrrolidin-3-yl-methanol substituent, which had potent inhibitory activity against LSD1 ( $IC_{50} = 0.08570.02$  M) according to structure–activity relationship studies. He went on to say that the polar interaction with two negatively charged regions of the LSD1 catalytic site is responsible for the compound **2**'s increased potency [10] (See Figure 5).



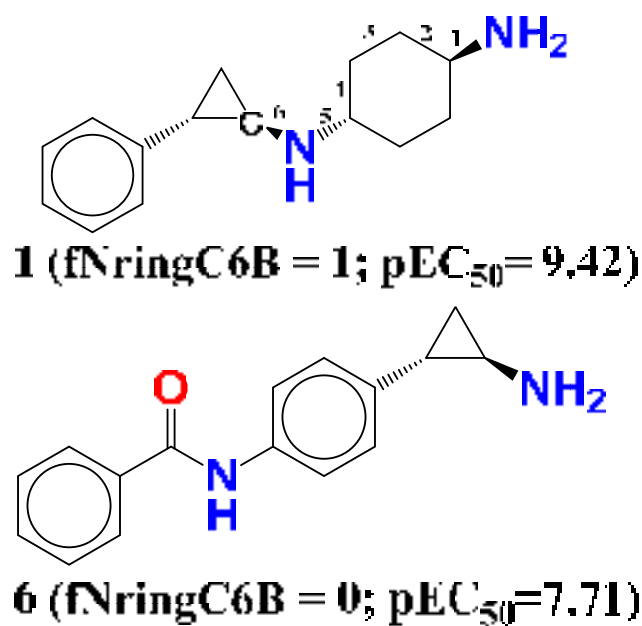


Figure 4. Illustration of molecular descriptor  $fNringC6B$  for the molecules 1 and 6 only.

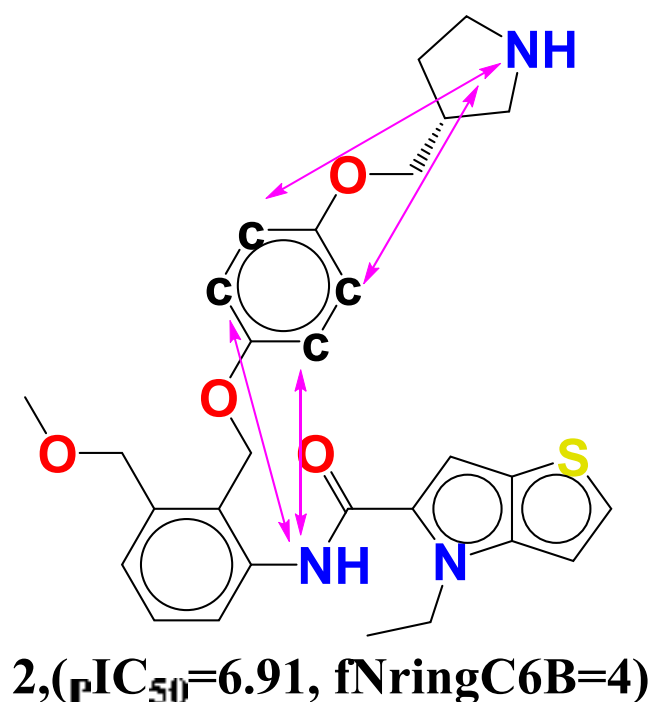


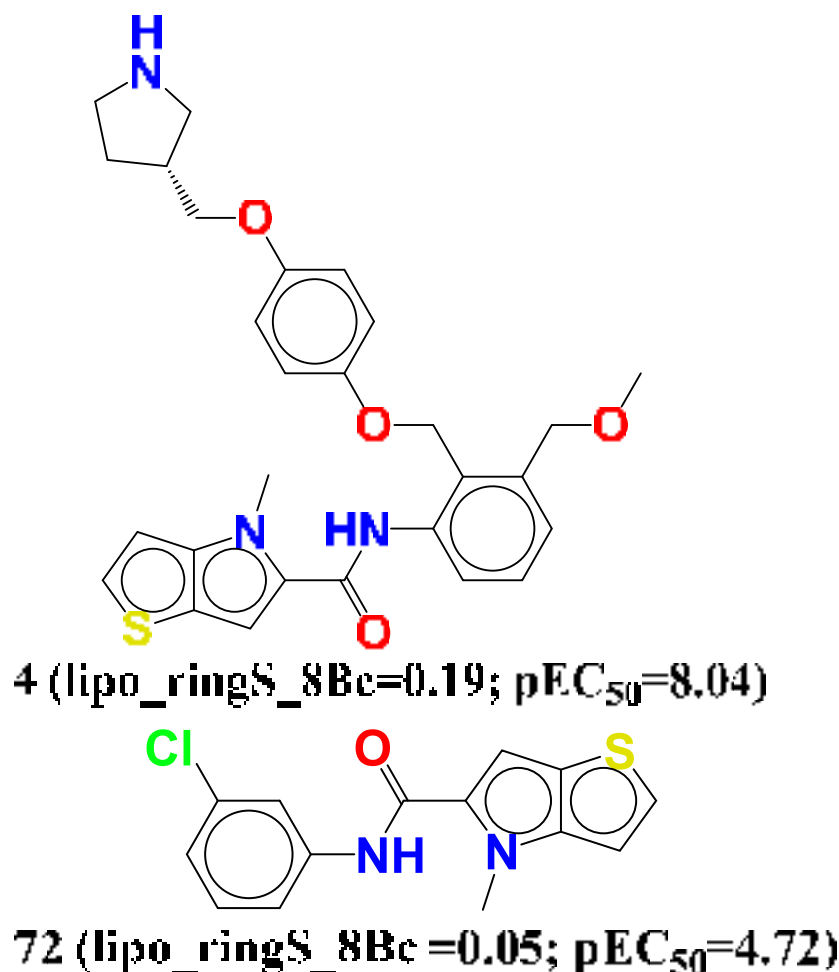
Figure 5. Depiction of the molecular descriptor  $fNringC6B$  in the compound 2.

Thus, the present observation supports that the pyrrolidine ring enhances the polarity of the compound 2 that occurred exactly at 6 bonds. As a whole, the same feature has been captured in the QSAR model through the descriptor  $fNringC6B$ ; therefore, QSAR results are complimentary with the reported findings. At the end, the QSAR model not only identified the polar nitrogen, but it also recognized the lipophilic carbon atom important for LSD1 inhibitory activity.

**lipo\_ringS\_8Bc** (Sum of partial charges of lipophilic atoms within 8 bonds from ring sulfur atom). The molecule with the better LSD1 inhibition might be obtained by enhancing the number of lipophilic atoms that accounted within 8 bonds from the sulfur atom. Just a four-fold amplification in the value of **lipo\_ringS\_8Bc** sufficed about  $2 \times 10^3$

fold more potent ( $\Delta pEC_{50} = 3.32$ ) LSD1 inhibitor compound **4** (**lipo\_ringS\_8Bc** = 0.19;  $pEC_{50} = 8.04$ ) than compound **72** (**lipo\_ringS\_8Bc** = 0.05;  $pEC_{50} = 4.72$ ). Several other pairs of compounds also support this observation: **31** (**lipo\_ringS\_8Bc** =  $-0.23$ ;  $pEC_{50} = 7.046$ ) with **32** (**lipo\_ringS\_8Bc** = 0;  $pEC_{50} = 6.917$ ), **35** (**lipo\_ringS\_8Bc** = 0;  $pEC_{50} = 6.827$ ) with **36** (**lipo\_ringS\_8Bc** =  $-0.28$ ;  $pEC_{50} = 6.81$ ), and **45** (**lipo\_ringS\_8Bc** =  $-0.207$ ;  $pEC_{50} = 6.511$ ) with **46** (**lipo\_ringS\_8Bc** =  $-0.231$ ;  $pEC_{50} = 6.509$ ).

Whence merely adding the number of carbon atoms is restricted (here average\_molweight, i.e., molecular property average molecular weight, is with negative correlation) or inadequate, it is advisable to add electronegative atoms to the carbon atoms within 8 bonds from the ring sulfur to intensify the partial positive charge on the lipophilic atoms that boost up the LSD1 potency of the compound, respectively (see Figure 6).

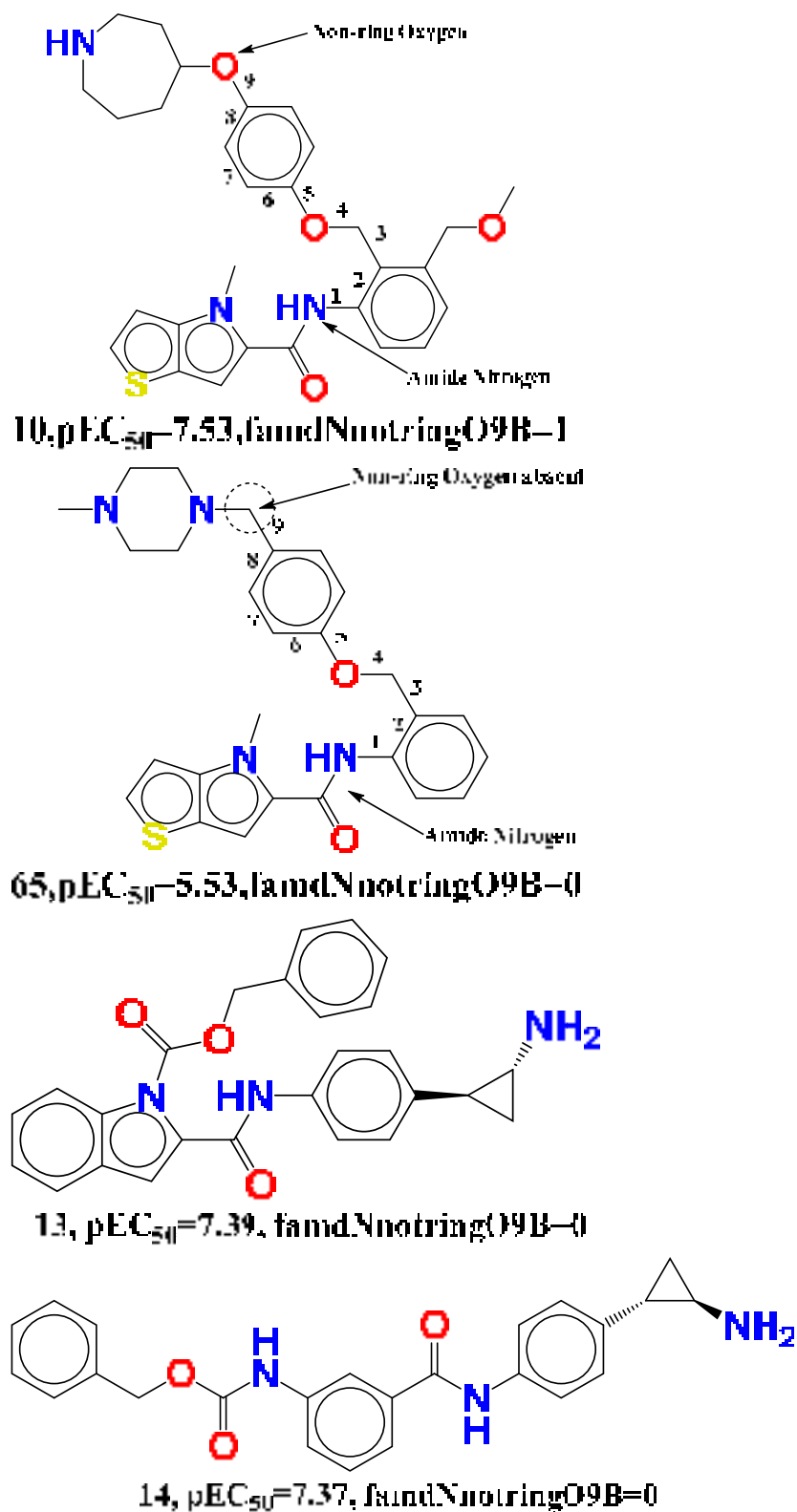


**Figure 6.** Depiction of molecular descriptor **lipo\_ringS\_8Bc** for the molecules **4**, **72**, and reported molecule **28186757** only.

Furthermore, a comparison of compound **4** to the previously reported molecule **28186757** suggests that increasing the amount of carbon atoms at the 8th position, specifically in the ether-containing carbon atom, will enhance the LSD1 inhibitory activity even more [10].

**famdNnotringO9B** (Frequency of occurrence of non-ring oxygen atom exactly at 9 bonds from the amide nitrogen) with a positive coefficient exhibit a direct correlation with LSD1 inhibitory potency. The four displayed compounds, **10**, **65**, **13**, and **14**, in Figure 7 illustrate the influence of the present molecular descriptor on the LSD1 inhibitory potency of the compound. It can be noted that, if the same non-ring carbon atom simultaneously

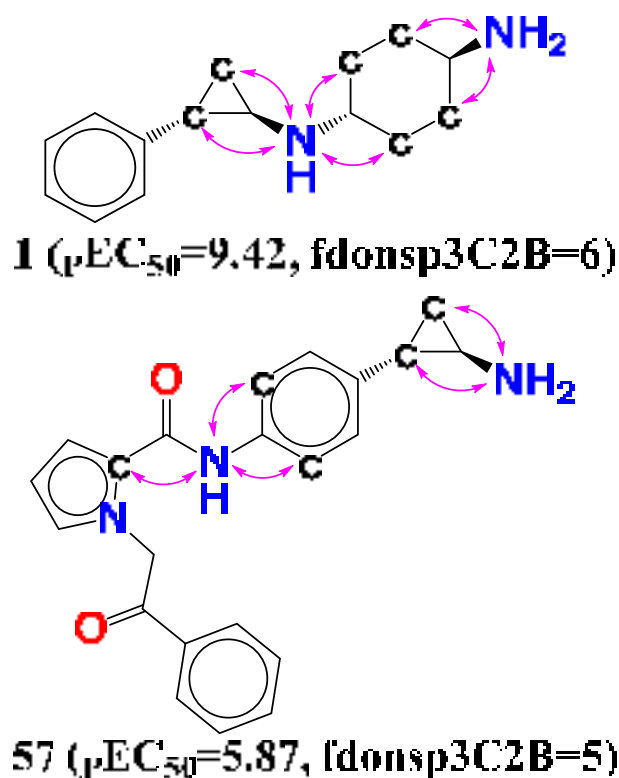
occurred at one to eight bonds or more than 9 bonds from the amide nitrogen, then it is eluded during the calculation of `famdNnotringO9B` (see Figure 7).



**Figure 7.** Pictorial depiction of molecular descriptor `famdNnotringO9B` for the molecules 10, 65, 13, and 14 only.

Non-ring oxygen was detected exactly 9 links from the amide nitrogen in compound **10**, but the same oxygen was missing in compounds **65**, **13**, and **14**. This finding further supports the idea that the appropriate distance between the amide nitrogen and the non-ring oxygen is important for LSD1 inhibition. This helps to explain why molecules **10** and **65**, **13**, and **14** have different LSD1 inhibitory action. Instead, Vianello, Paola, and colleagues found that removing oxygen had only a little effect on the LSD1 inhibitory function. This new discovery backs up the QSAR concept, emphasizing the significance of the oxygen atom in the 9th position from the amide nitrogen. In addition, Vianello Paola emphasized the importance of thieno [3,2-b]pyrrole-5-carboxamides as novel reversible inhibitors of the LSD1 receptor, noting that the same amide nitrogen was successfully detected as `famdNnotringO9B` in QSAR modelling. As a result, the QSAR results are consistent with the stated findings.

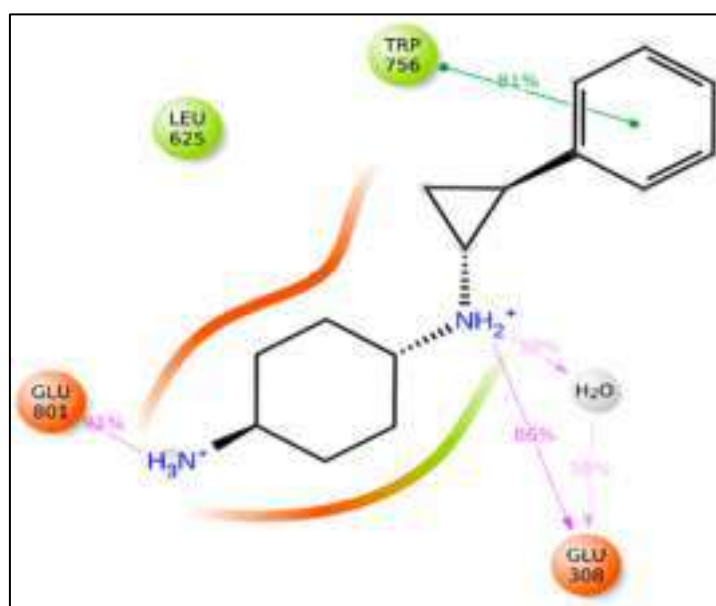
Another key chemical characteristic, `fdonsp3C2B` (frequency of occurrence of sp<sup>3</sup> hybridised carbon atom exactly at 2 bonds from donor atom), is strongly linked with the reported bioactivity of LSD1 inhibitors. When comparing compound **1** to compound **57**, it can be shown that increasing the number of sp<sup>3</sup> hybridised carbon atoms exactly at 2 bonds enhances the LSD1 inhibitory potency (see Figure 8).



**Figure 8.** Pictorial display of molecular descriptor `fdonsp3C2B` for the molecules **1** and **57** only.

Furthermore, the same result holds true for a few other compounds: the most active compound **1** ( $pEC_{50} = 9.42$ ,  $fdonsp3C2B = 6$ ), as well as the compounds **2** ( $pEC_{50} = 8.17$ ,  $fdonsp3C2B = 2$ ), **3** ( $pEC_{50} = 8.10$ ,  $fdonsp3C2B = 2$ ), **4** ( $pEC_{50} = 8.07$ ,  $fdonsp3C2B = 2$ ), and **5** ( $pEC_{50} = 7.49$ ,  $fdonsp3C2B = 2$ ). The LSD1 inhibitory activity will be increased by 3.55 units if the value of the molecular descriptor `fdonsp3C2B` for the molecule **57** is increased from 2 to 6 (about a 35-fold increase in LSD1 inhibitory potency). Furthermore, sp<sup>3</sup> hybridised carbon atoms should be added to boost LSD1 inhibitory activity, according to the current findings. Furthermore, increasing the amount of such sp<sup>3</sup> hybridised carbons along the donor increases the electrical and hydrophobic interaction with the LSD1 receptor, showing lipophilicity.

Following that, it was discovered that during the MD modeling of compound 1 that the NH moiety, which acts as a donor with two bonds from the sp<sup>3</sup> hybridized carbon atom (fdonsp3C2B), demonstrated significant hydrogen bonding with GLU308 (86 percent) and thus plays an important role in the stability of the LSD1–compound 1 complex. Furthermore, by including a water molecule, the same NH moiety created hydrogen bonds with a similar residue (GLU308), increasing the stability of the drug receptor complex. Furthermore, another NH<sub>2</sub> substituent (91 percent) developed hydrogen bonding connections with the Glu801 residue, increasing the stability of the drug receptor complex (see Figure 9). This implies that the QSAR modelling has effectively identified certain important pharmacophores involved in the stability of the drug receptor complex, in addition to finding the many hidden structural elements crucial for LSD1 inhibition. As a consequence, the QSAR findings are entirely consistent with the molecular docking and MD simulation experiments.



**Figure 9.** Depiction of the involvement of the molecular descriptor fdonsp3C2B in the LSD1–Compound 1 interactions during MD simulations.

No one chemical descriptor can explain the variation in inhibitory effectiveness of medicines in a dataset. The performance of the QSAR model is impacted by the synchronous effect of many molecular descriptors, some of which are not included in the QSAR models.

### 3.2. Molecular Docking

The molecular interaction of the five most active molecules with the LSD1 protein at the active site was investigated using molecular docking. The crystal structure of LSD1 was obtained using the RCSB protein data repository (<https://www.rcsb.org/structure/2dw4>, accessed on 24 May 2022) (PDB code: 2DW4). The full length of LSD1 comprises 852 amino acids with three key structure domains [11–14]: N-terminal Swi3-Rsc8-Moira domain (SWIRM domain, residues 172–270); C-terminal amine oxidase-like domain (AOL domain, residues 271–417 and 523–833); and central tower-like domain (Tower domain, residues 418–522). The SWIRM domain of LSD1 consists of six long  $\alpha$ -helices (SW $\alpha$ 1–6) and two stranded  $\beta$ -sheets (SW $\beta$ 1–2), which regulates the chromatin remodeling and histone modification by taking part in protein–protein interactions.

We investigated the probable interactions of inhibitors inside the active site of LSD1 to better understand the SAR and QSAR models of the five most active drugs. With an RMSD of 1.3618 Å, the 2DW4 ligand was redocked into the LSD1 binding pocket. Because the

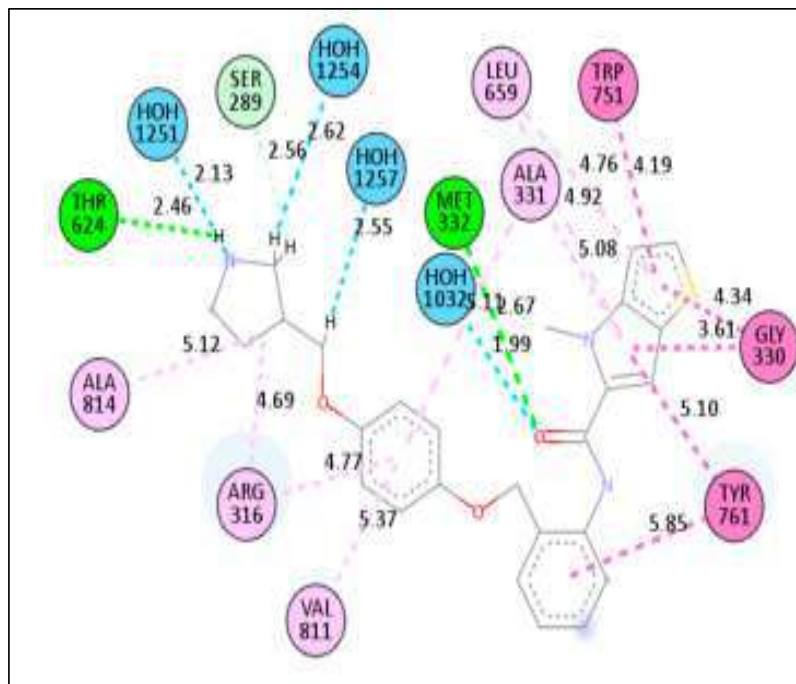
accuracy of the docking results was determined by RMSD, this indicates that NRG Suite docking was able to effectively recognise the correct binding configuration (2.0). The docking scores for the five compounds, **1** ( $EC_{50} = 0.38$  nm), **2** ( $EC_{50} = 6.7$  nm), **3** ( $EC_{50} = 7.8$  nm), **4** ( $EC_{50} = 8.4$ ), **5** ( $EC_{50} = 18$ ), and pdb-2dw4 ligand, were found to be  $-8.33$ (RMSD  $-1.38$  Å),  $-10.47$ (RMSD  $1.82$  Å),  $-11.16$ (RMSD  $1.32$  Å),  $-11.10$ (RMSD  $1.58$  Å),  $-10.96$ (RMSD  $1.13$  Å), and  $-11.31$ (RMSD  $1.36$  Å) Kcal/mol, respectively, demonstrating that docking scores could predict ligand  $EC_{50}$  values. The 2D interactions for the five compounds were displayed in Figures 10–14.

In terms of compound **5**'s low activity, the amide nitrogen forms a conventional hydrogen bond with the neutral non-polar amino acid residue MET332, a water–hydrogen bond with HOH1032, and a neutral polar amino acid residue with the pyrrolidine ring. THR624 forms a second hydrogen bond. With HOH1251, it creates a third water–hydrogen bond. TRP751, GLY330, LEU859, ALA331, TYR761, VAL811, ARG316, and ALA814, on the other hand, have been shown to form hydrophobic bonds with a thiene-pyrrole ring, a benzamide ring, a phenoxy ring, or a pyrrolidine ring (pi-pi T-shaped, amide-pi stacked, alky and pi-alkyl interactions). Despite the wide and flexible structure of compound five, the active conformation and compound-**5**–LSD1 complex were maintained via a variety of hydrophobic interactions and hydrogen bonding.

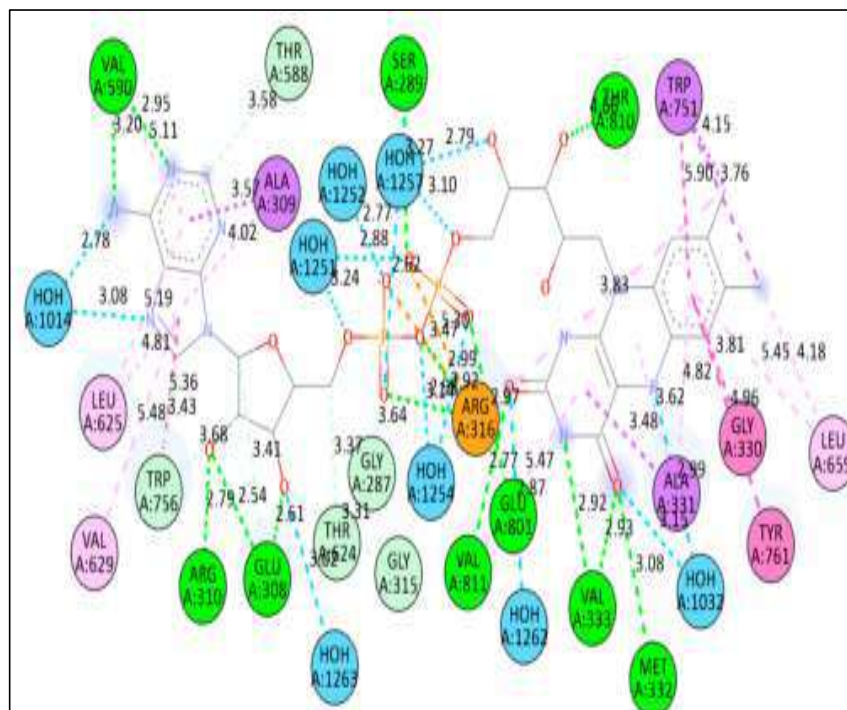
Compound **5** and compound **4** have similar interactions, although compound **4** is three times more powerful than compound **5**. In the structure, compound **5** has a folded shape, whereas compound **4** has an extended conformation akin to the pdb-2dw4 ligand. Within the active area of the LSD1 receptor, chemicals **5** and **4** are diametrically opposed. Except for one hydrophobic interaction with a TYR761 amino acid residue, the thien-pyrrole ring orientation was different. The QSAR models demonstrate the importance of the thiene-pyrrole ring for the reversible inhibition of the LSD1 receptor. The molecular descriptor **lipo\_ringS\_8Bc** indicates the importance of the Sum of partial charges of lipophilic atoms within 8 bonds from ring sulfur atoms. With TRP751, compound **4** (**lipo\_ringS\_8Bc** =  $-0.1869$ ) made more than eight types of hydrophobic connections and one pi-sulphure interaction, whereas compound **5** (**lipo\_ringS\_8Bc** =  $-0.2319$ ) made seven hydrophobic contacts (See Figure 11A,B). The difference in the reactivity of these compounds was linked with the occurrence of positively charged lipophilic atoms. The present observation indicates that the decrease in the negative charge promotes more hydrophobic contacts in the compound **4**. Furthermore, in compound **1** (**lipo\_ringS\_8Bc** = 0), partial positive charges are zero, underlining the observation of declining negative charges and intensifying positive charges within the thiene-pyrrole ring, which promotes better hydrophobic contact with the LSD1 receptor. The compounds **3** (**lipo\_ringS\_8Bc** =  $-0.1869$ ) and **2** (**lipo\_ringS\_8Bc** =  $-0.2339$ ) showed the same behavior. Finally, QSAR analysis was successful in uncovering latent pharmacophoric characteristics that determine not only the LSD1 inhibitory action of these compounds, but also their binding pattern. As a result, the molecular docking analysis results are entirely congruent with the QSAR findings.

Moreover, compound **2** ( $EC_{50} = 6.7$  nm), was marginally more potent than compound **3** ( $EC_{50} = 7.8$  nm). The 2D interactions for compounds **2** and **3** show that compound **2** produced three standard hydrogen bonding contacts with SER760, LYS661, ARG316, and GLU801, but compound **3** did not form any conventional hydrogen bonding interactions with SER760, ALA809, THR810, or HOH1257. Moreover, compound **2** executed more than 11 different hydrophobic contacts with the HIS564, ALA539, VAL333, GLY330, TRP751, VAL811, VAL317, ALA814, etc. Moreover, the thiene-pyrrole ring in the compound didn't contribute in any of the hydrophobic contact, but it aligned over the solvent accessible surface area of the LSD1 receptor (See Figure 12A,B). Furthermore, when the conformations of compounds **2** and **3** are compared to the pdb-2dw4 ligand, it is clear that compound **2** aligns and superimposes entirely along the docked conformation of the pdb ligand. Following that, in compound **3**, the thiene-pyrrole ring aligns vertically in the receptor (LSD1) binding pocket, which is completely different from the bioactive conformation of the pdb ligand and could explain the difference in potency between these compounds

(see Figure 13, green-comp-2, yellow-comp-3, and cyan-pdb-2dw4 ligand). The benzene ring connected to the thiene-pyrrole ring by amide linkage in compound 3 contains a bulky substituent (methoxy ethyl) compared to compound 2 (methoxy methyl), which may have hampered compound 3's ability to achieve the same bioactive conformation as the pdb ligand. This helps to explain the differences in potency and binding affinity for the LSD1 receptor.

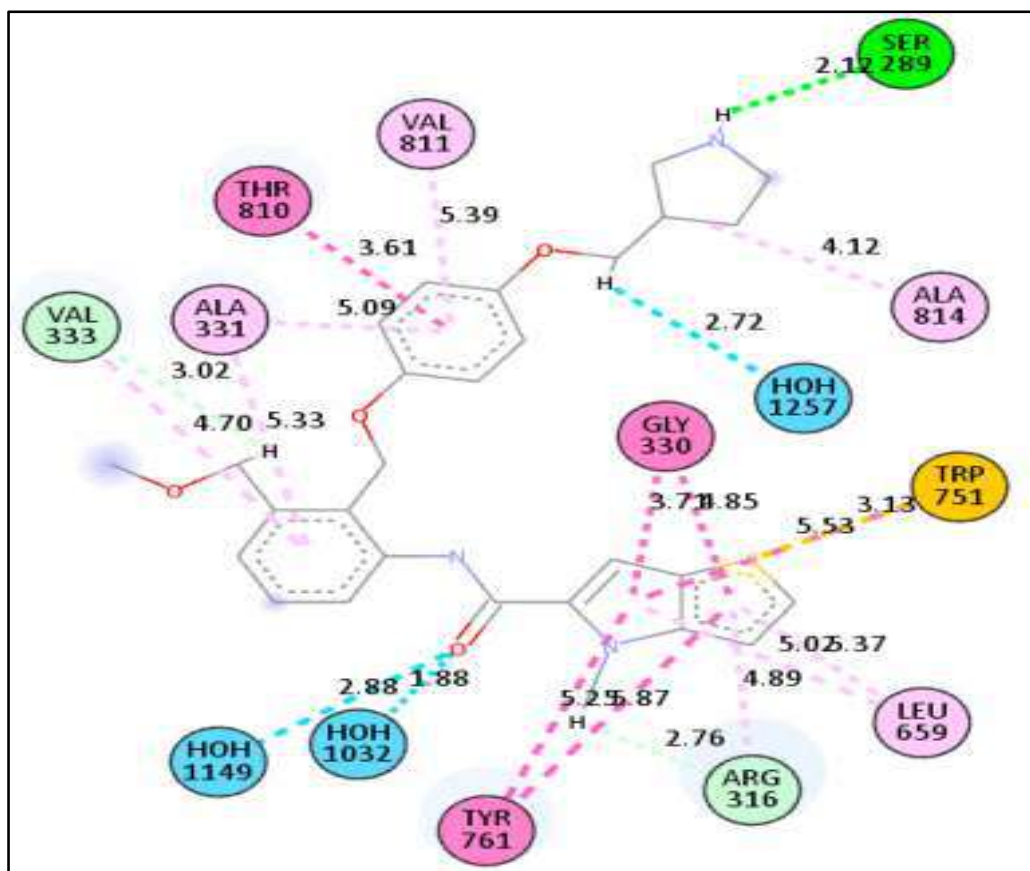


(A)

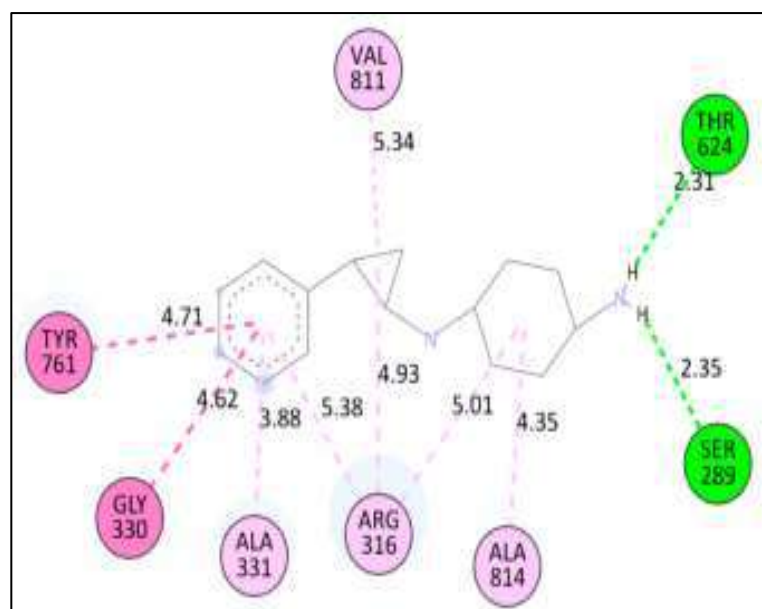


(B)

**Figure 10.** Presentation of the 2D interactions of compound 5 (A) and pdb-2dw4 ligand (B) with LSD1 receptor.



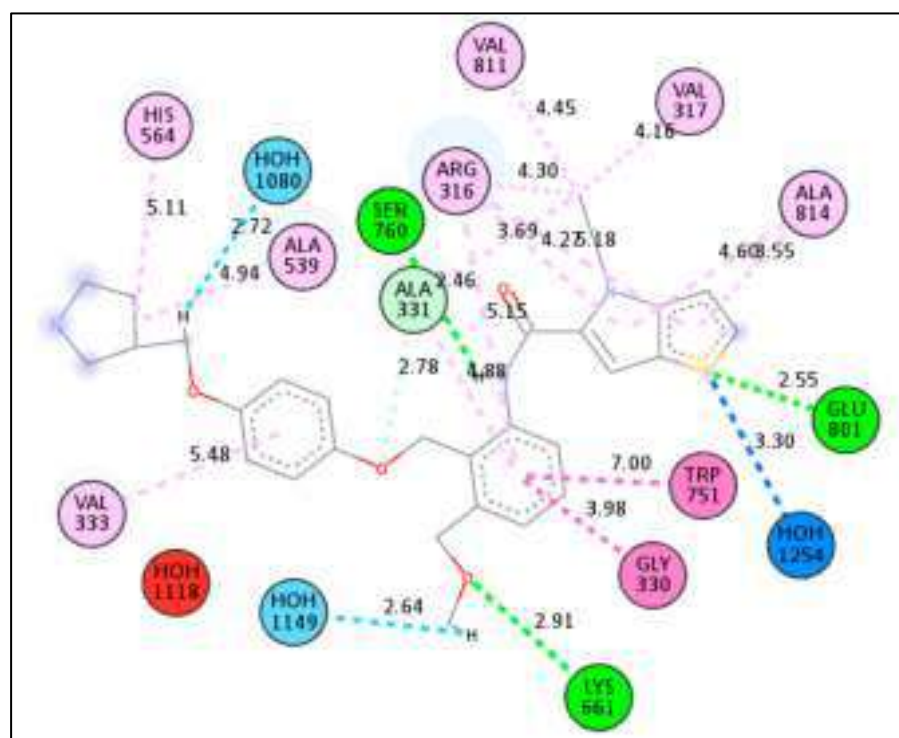
(A)



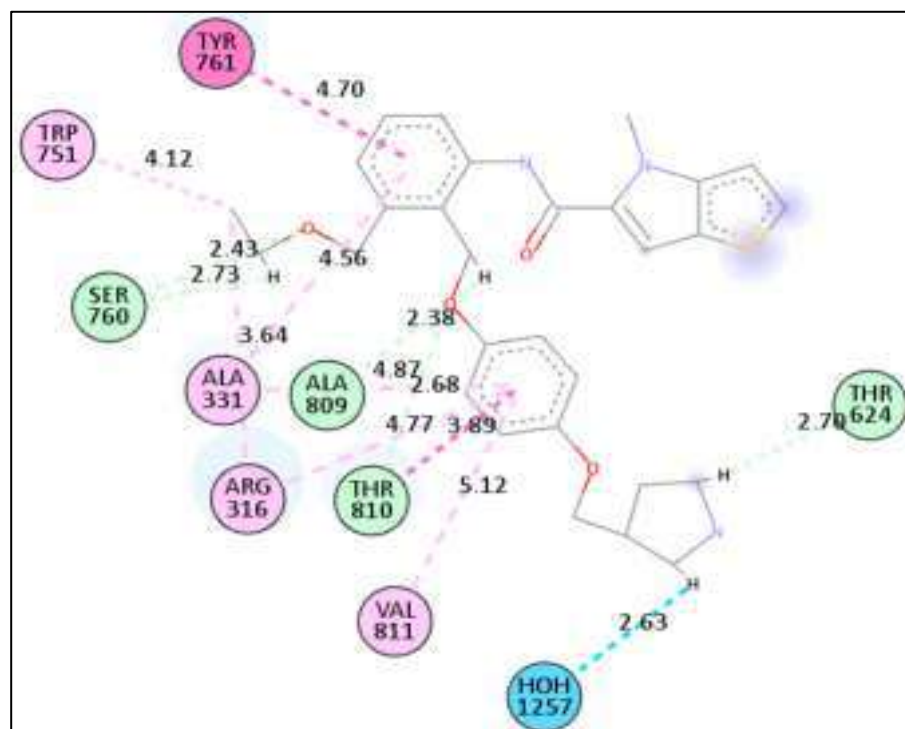
(B)

**Figure 11.** Presentation of the 2D and 3D interactions of compound 4 (A) and compound 1 (B) with LSD1 receptor.



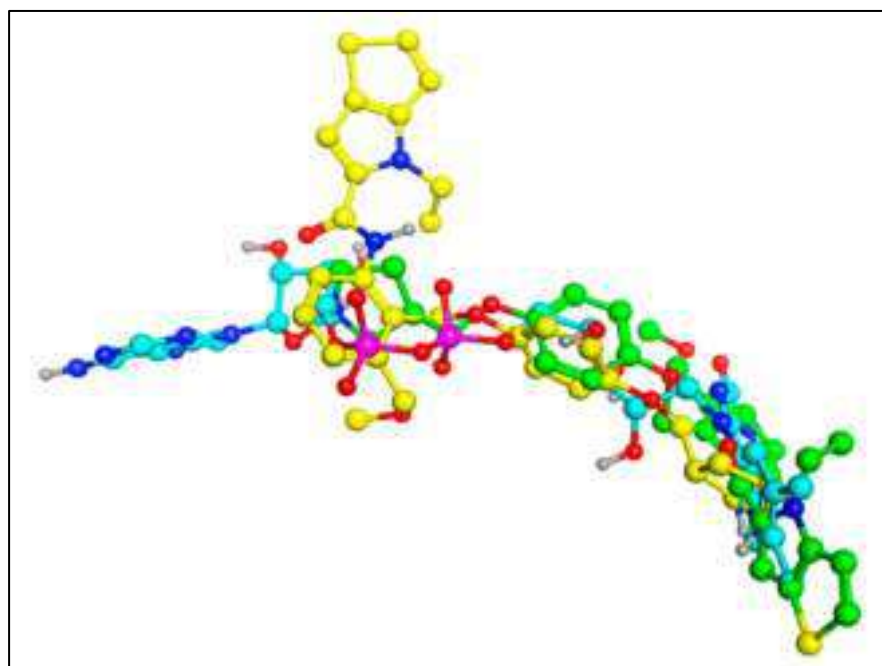


(A)

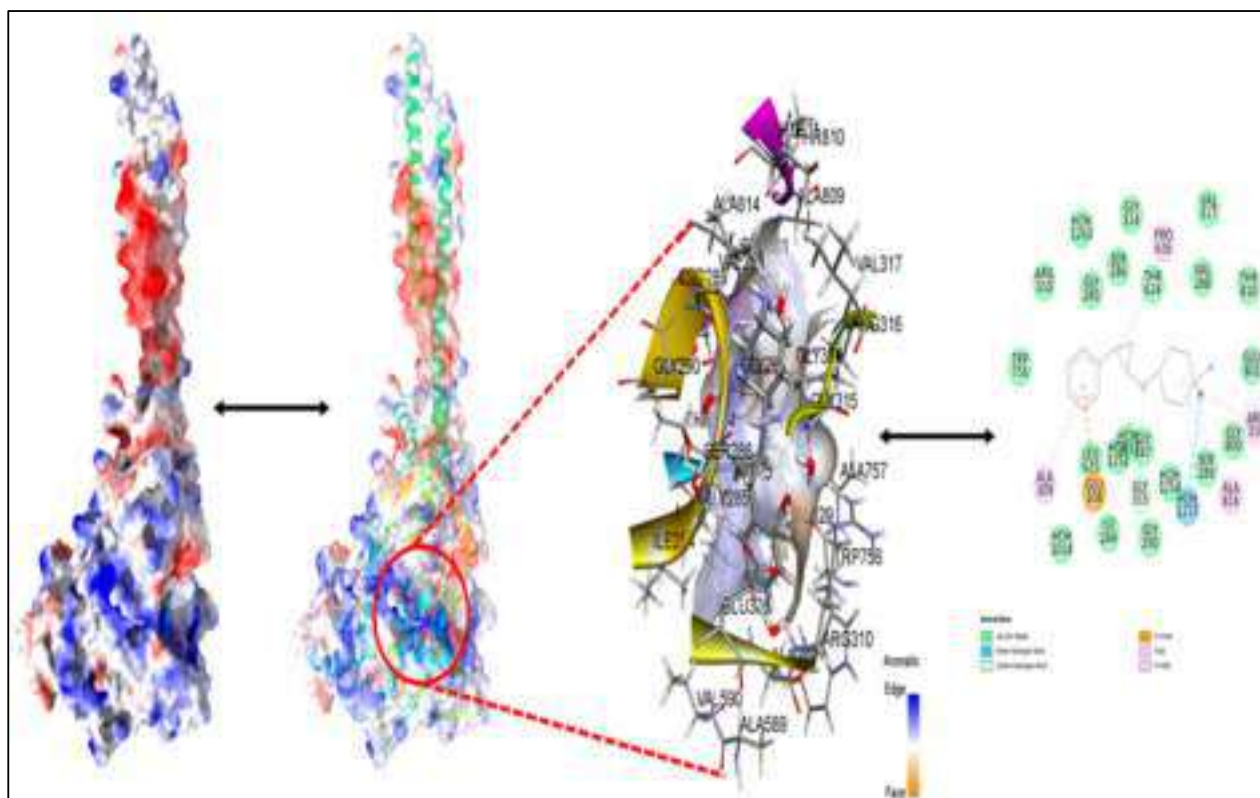


(B)

**Figure 12.** Presentation of the 2D and 3D interactions of compound 4 (A) and compound 1 (B) with LSD1 receptor.



**Figure 13.** Comparison of the docked conformation of the compound 2 and 3 with the pdb-2dw4 ligand. (Green colored—Comp 2; yellow colored—Comp 3; and cyan colored—pdb-2dw4 ligand).



**Figure 14.** Best docked pose of compound 1 with LSD displaying 2D interaction plot on the left panel. Pink dashed lines indicate the Pi-Alkyl bond, and residues embedded in light green sphere indicate the involvement in Van der Waals interactions. On the center panel, surface view of LSD displaying binding cavity of Compound 1 and right panel displaying the zoomed out binding pocket having amino acid residues surrounding the Compound 1.

The compound **2** ( $pIC_{50} = 8.174$ ,  $fdonsp3C2B = 2$ ,  $lipo\_ringS\ 8Bc = -0.2339$ ) and **3** ( $pIC_{50} = 8.174$ ,  $fdonsp3C2B = 2$ ,  $lipo\_ringS\ 8Bc = -0.2339$ ) differed from the compound **1** ( $pIC_{50} = 9.42$ ,  $fdonsp3C2B = 6$ ,  $lipo\_ringS\ 8Bc = 0$ ) in terms of two descriptors: **fdonsp3C2B** and **lipo\_ringS 8Bc**. Compound **3** can't form hydrogen bonds or hydrophobic interactions with the receptor because of its altered orientation. The amide donor produced hydrogen bonds with the SER760 residue in compound **2**, whereas another donor nitrogen of the terminal pyrrolidine ring aligned over the solvent accessible surface region, and the  $sp^3$  hybridised carbon atom made hydrophobic interactions with the receptor. In the QSAR model, the same feature was captured. In addition, the thiene-pyrrole ring sulphure atom formed conventional hydrogen bonds with the ARG316 and GLU 801 residues, as well as a water-hydrogen link with the HOH1254 residue. The relevance of the thiene-pyrrole sulphure atom, which was captured in the QSAR model as **lipo ringS 8Bc** descriptors, is highlighted by this observation. Furthermore, the lipophilic carbon atoms in the benzene ring of compound **2** connected to the thiene-pyrrole ring via amide linkage generate distinct hydrophobic interactions with the receptor. This finding emphasises the significance of positively charged lipophilic carbon atoms in drug receptor interactions. Thus, QSAR modelling was successful in identifying the features required to improve binding affinity, and the results were in perfect agreement with the molecular docking data. In addition, comparison with the most active compound **1** ( $pIC_{50} = 9.42$ ,  $fdonsp3C2B = 6$ ,  $lipo\ ringS\ 8Bc = 0$ ) indicated the importance of the lipophilic, as well as the electronic properties required for binding affinity and, ultimately, LSD1 receptor inhibition.

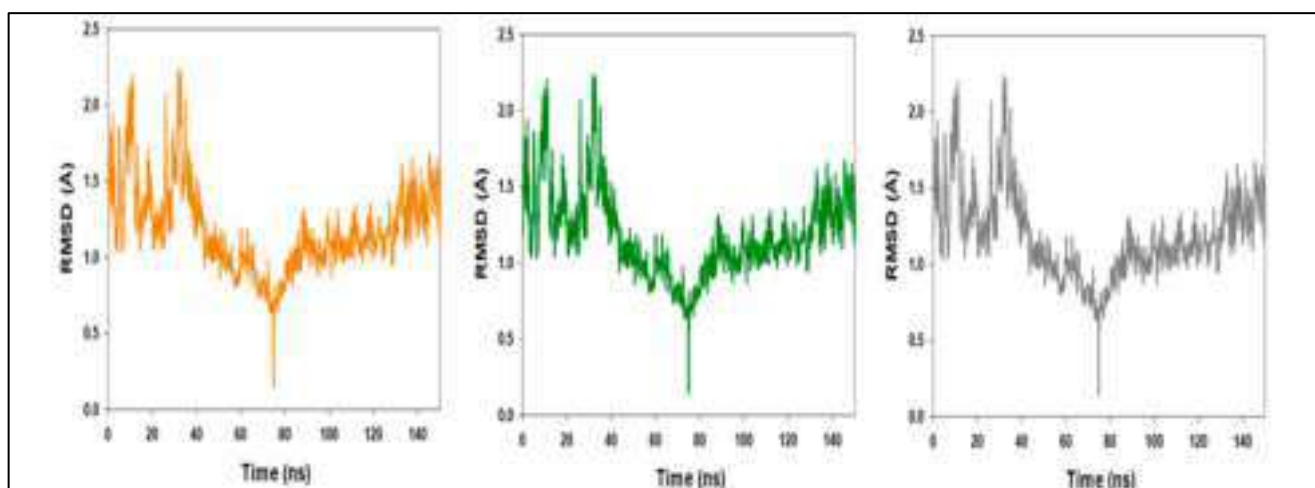
The docking results revealed that the descriptors, **fdonsp3C2B** and **lipo\_ringS\_8Bc**, played important roles in the inhibition of the LSD1 receptor, which was consistent with the QSAR findings.

### 3.3. Molecular Dynamic Simulations

During the simulation, monitoring the protein's RMSD can provide insight into its structural conformation. The RMSD analysis can identify if the fluctuations at the end of the simulation are centred on some thermal average structure if the simulation has equilibrated. For tiny, spherical proteins, changes on the order of 1–3 are perfectly acceptable. Larger changes, on the other hand, imply that the protein is significantly changing form during simulation. It's also crucial that your simulation converges, which means the RMSD values settle around a fixed number. If the average RMSD of the protein is still increasing or dropping at the end of the simulation, your system has not equilibrated, and your simulation may not be lengthy enough to do a thorough analysis. Ligand RMSD (right Y-axis): the ligand RMSD (right Y-axis) shows how stable the ligand is in relation to the protein and its binding pocket.

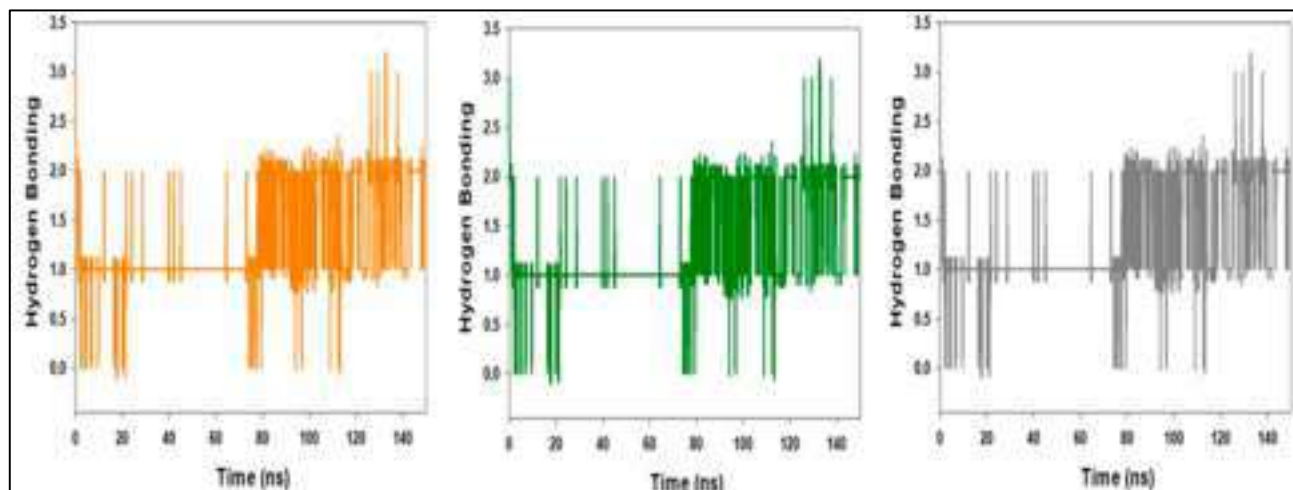
When the protein–ligand complex is aligned on the reference protein backbone first, and then the RMSD of the ligand-heavy atoms is measured, the RMSD of the ligand is plotted. If the observed values are significantly greater than the RMSD of the protein, the ligand has most likely diffused away from its initial binding site.

The above-mentioned diagram is the triple run result of Root Mean Square Deviations (RMSD) MD simulation trajectory analysis. The RMSD plot of the LSD–compound **1** complex (Figure 3) indicates that the complex stabilizes at about 20 ns. After that, for the length of the simulation, swings in RMSD values for target remain within 0.5, which is absolutely acceptable. The ligand fit-to-protein RMSD values fluctuate within 0.7 Angstrom after they have been equilibrated. These findings indicate that the ligands stayed firmly connected to the receptor's binding site throughout the simulation period. The RMSD values for ligand fit to protein do not change much during the simulation duration, showing that the ligands remain securely attached to the receptor's binding site, as shown in Figure 15.



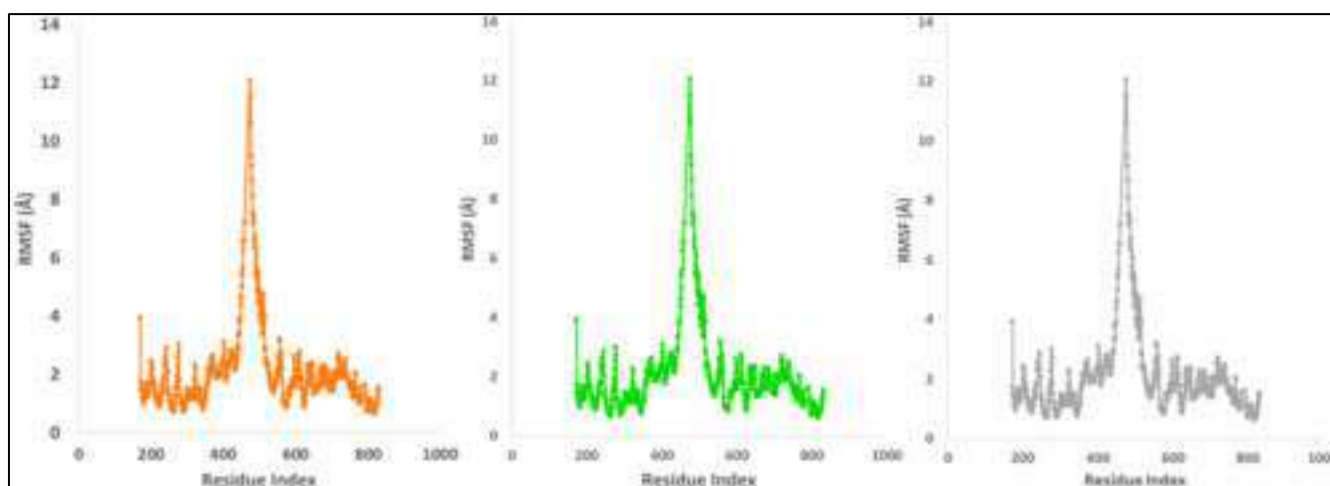
**Figure 15.** MD simulation trajectory analysis of Root Mean Square Divisions (RMSD) of compound 1 bound with LSD; 150 ns time frame in triplicate displayed.

Figure 16 shows the average hydrogen bonds established throughout the 150 ns triple simulation between compound 1 and the various proteins. From 0 to 150 ns, an average of four hydrogen bonds are observed for LSD, and the same is true for triple MD simulations of compound 1 and LSD (Figure 16). Throughout the simulation, two hydrogen bonds were established, as shown by the 2D ligand binding figure. The number of hydrogen bonds between LSD and compound 1 has increased, making the binding stronger and more robust over simulation.



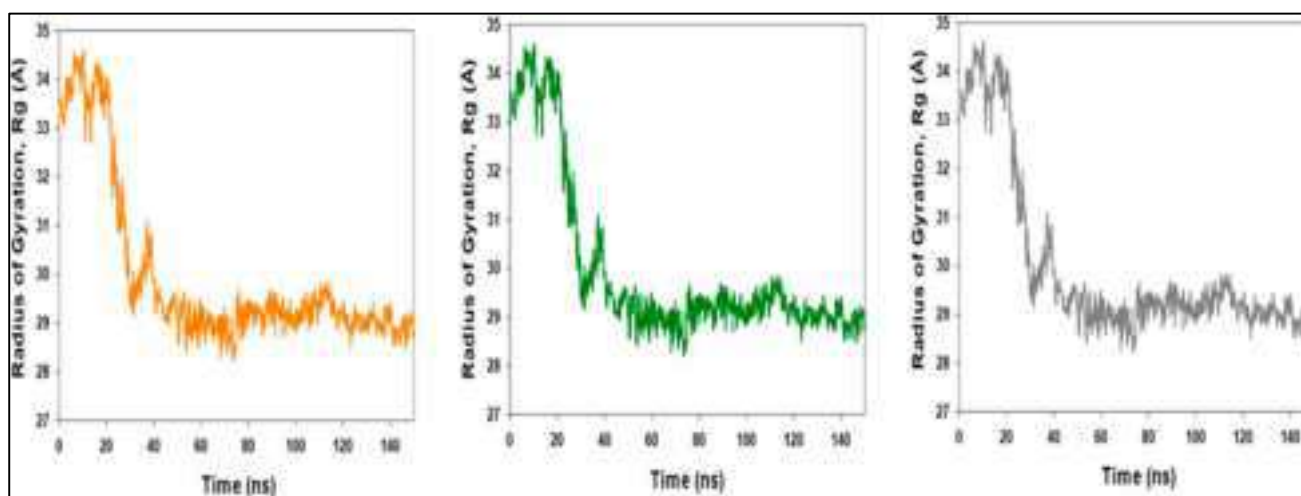
**Figure 16.** MD simulation trajectory analysis of Hydrogen-bonding (H-bonding) of compound 1 bound with LSD 150 ns time frame in triplicate displayed.

On the RMSF plot, peaks represent portions of the protein that fluctuate the most during the simulation. Protein tails (both N- and C-terminal) typically change more than any other part of the protein. Alpha helices and beta strands, for example, are usually stiffer than the unstructured component of the protein and fluctuate less than loop sections. According to MD trajectories, the residues with greater peaks belong to loop areas or N- and C-terminal zones (Figure 17). Although there is some instability between 400 and 600 residues, the stability of ligand binding to the protein is demonstrated by stable RMSF values of binding site residues.



**Figure 17.** MD simulation trajectory analysis of Root Mean Square Fluctuations (RMSF) of compound 1 bound with LSD with their triplicate runs.

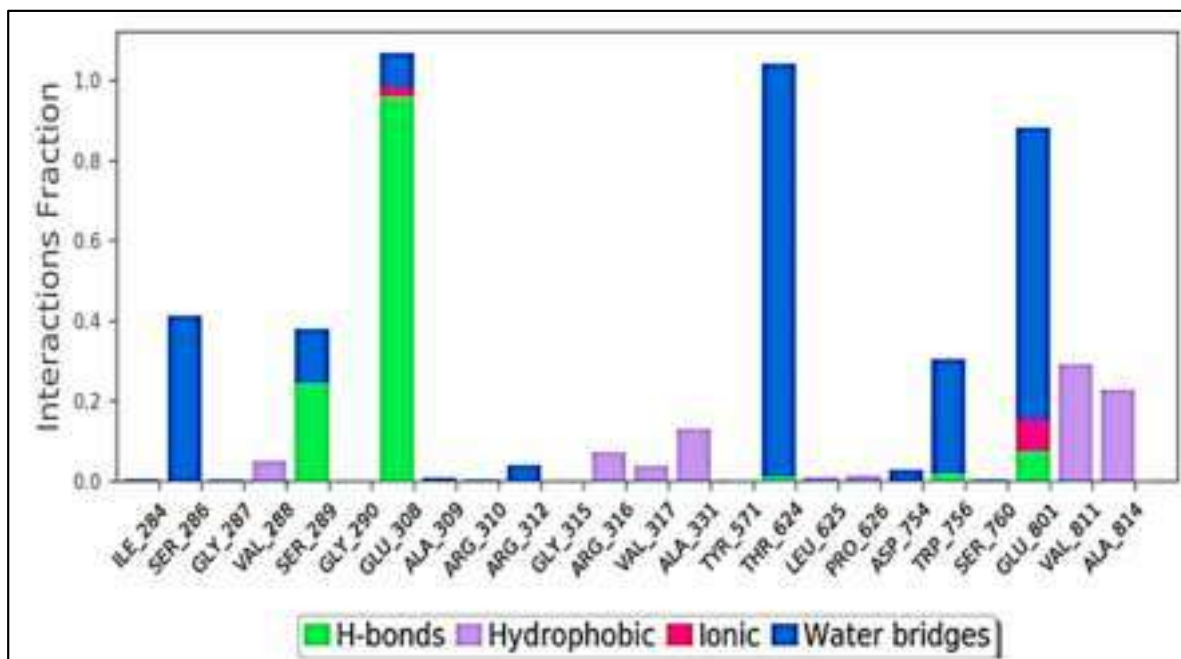
The compactness of proteins is measured by the radius of gyration. The Radius of Gyration of LSD proteins bound to compound 1 was reduced (Figure 18). Compound 1 bonded to the protein targets posthumously in the binding cavities and plays a substantial role in the stability of the proteins, according to the overall quality analysis using RMSD and Rg.



**Figure 18.** MD simulation trajectory analysis of Radius of Gyration (RoG) of compound 1 bound with LSD with their triplicate runs.

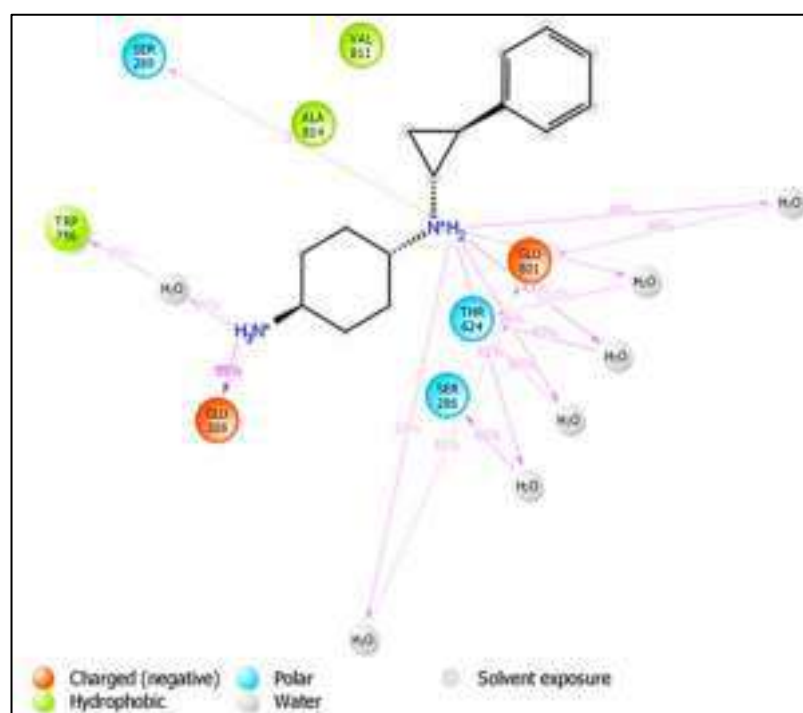
Protein interactions with the ligand can be detected throughout the simulation. These interactions can be categorized and summarized by type, as shown in the graphs below. The four types of protein–ligand interactions (or ‘contacts’) are hydrogen bonds, hydrophobic, ionic, and water bridges. The ‘Simulation Interactions Diagram’ panel in Maestro can be used to analyse the subtypes of each interaction type. Over the course of the trajectory, the stacked bar charts are standardised; for example, a value of 0.7 indicates that the specific interaction is maintained for 70% of the simulation duration. Values exceeding 1.0 are possible because some protein residues may have several interactions with the same subtype of ligand. The majority of the important ligand–protein interactions found by MD are hydrogen bonds and hydrophobic interactions, as shown in Figure 19. In terms of H-bonds, the LSD–compound 14 complex residues VAL 4288, GLY 290, TYR 571, ASP 754, and SER 760 are the most essential. Over the course of the trajectory, the stacked bar charts

were standardised; for example, a value of 1.0 signifies that the specific interaction was maintained for 100% of the simulation duration. Values exceeding 1.0 are possible because some protein residues may have several interactions with the same subtype of ligand.



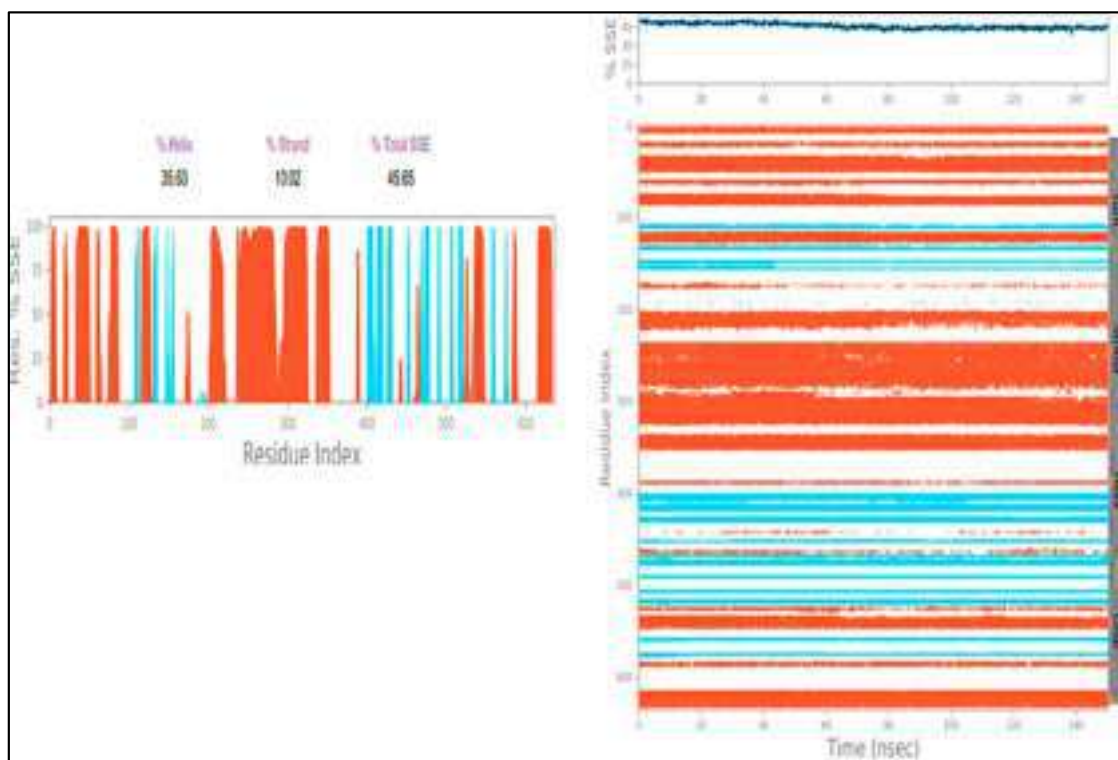
**Figure 19.** Protein-ligand contact histogram (H-bonds, Hydrophobic, Ionic, Water bridges) of LSD and compound 1.

Figure 20 depicts individual ligand atom interactions with protein residues. Interactions that last more than 30.0 percent of the simulation time (0.00 through 150.0 ns) in the chosen trajectory are shown.



**Figure 20.** Ligand atom interactions with the protein residues LSD-compound 1.

The presence of protein secondary structural elements (SSE) such as alpha helices and beta strands is checked throughout the simulation to guarantee that they are not present. The plot above shows the distribution of SSE by residue index over the entire protein structure, and it includes all residues. The graphs at the bottom illustrate the evolution of each residue and its SSE assignment throughout the experiment, in contrast to the charts below, which show a summary of the SSE composition for each trajectory frame during the simulation (as shown in Figure 21).

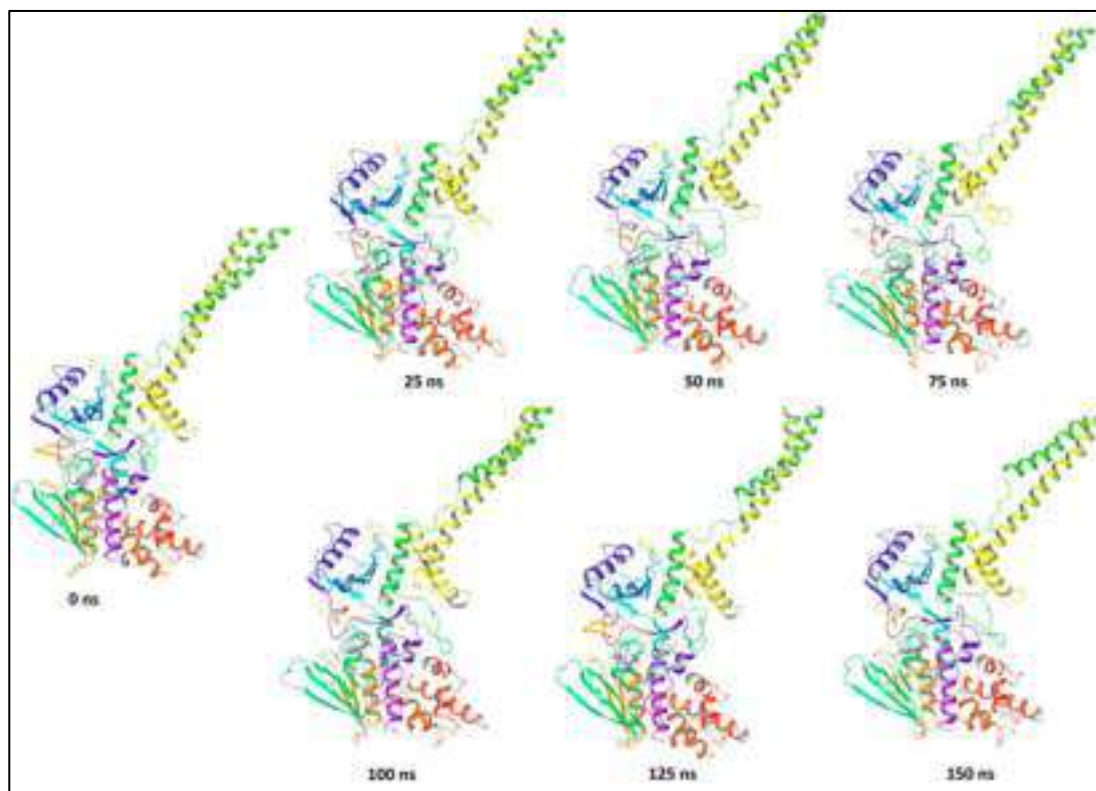


**Figure 21.** Secondary Structure element distribution by residue index throughout the protein structure. Red indicates alpha helices, and blue indicate beta-strands of; LSD-compound 1.

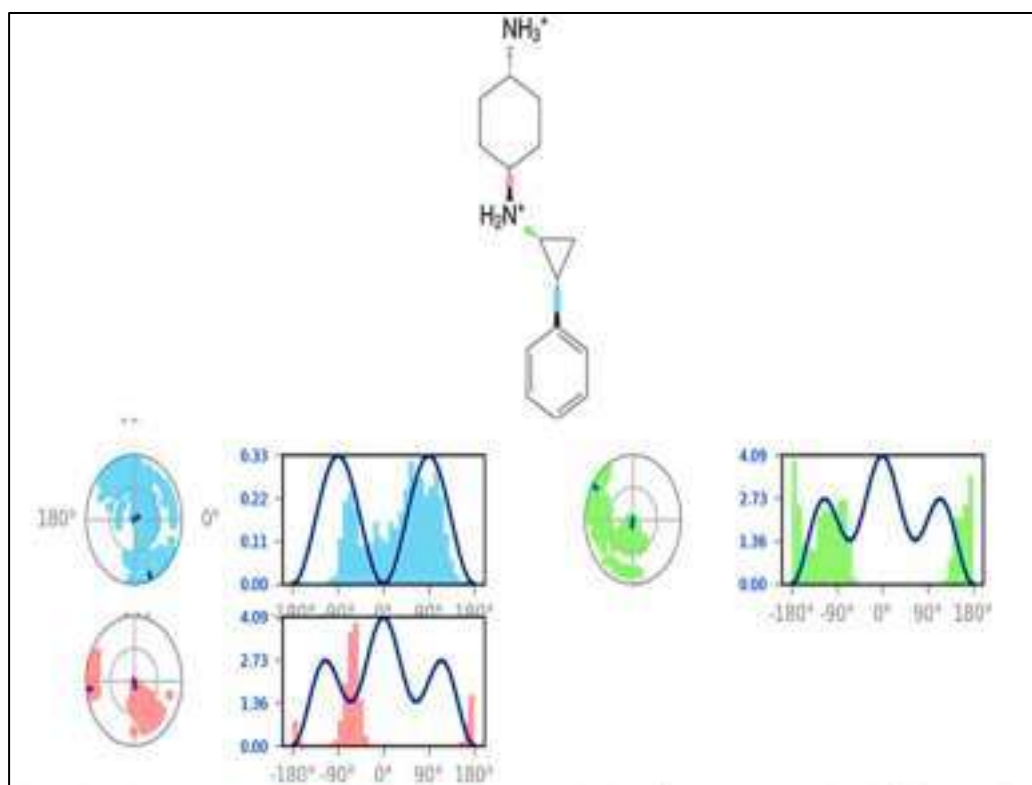
In comparison to the 0 ns structure, the positional change was obvious in the stepwise trajectory analysis of every 25 ns of compound 1 simulation with LSD (Figure 22). In order to achieve conformational stability and convergence, the ligand, compound 1, was discovered to exhibit structural angular mobility at the end frame.

The ligand torsions graphic depicts the conformational evolution of each rotatable bond (RB) in the ligand throughout the simulation trajectory (0.00 through 150.00 ns). The top panel shows a two-dimensional schematic of a ligand with color-coded rotatable bonds. Each rotatable bond torsion is accompanied with a dial plot and a bar plot of the same colour. The structure of the torsion during the simulation is depicted by dial (or radial) charts. The simulation begins in the radial display's centre, and the time evolution is plotted radially outwards.

In the bar charts, which summarize the data from the dial plots, the probability density of the torsion is shown. If torsional potential data is provided, the graphic also displays the potential of the rotatable bond (by summing the potential of the related torsions). The potential values are given in kcal/mol and are displayed on the chart's left Y-axis. The correlations between the histogram and torsion potential can reflect the conformational strain that the ligand undergoes in order to maintain a protein-bound shape (See Figure 23).



**Figure 22.** Stepwise trajectory analysis for every 25 ns displaying the protein and ligand conformation during 150 ns of simulation of LSD-compound 1.



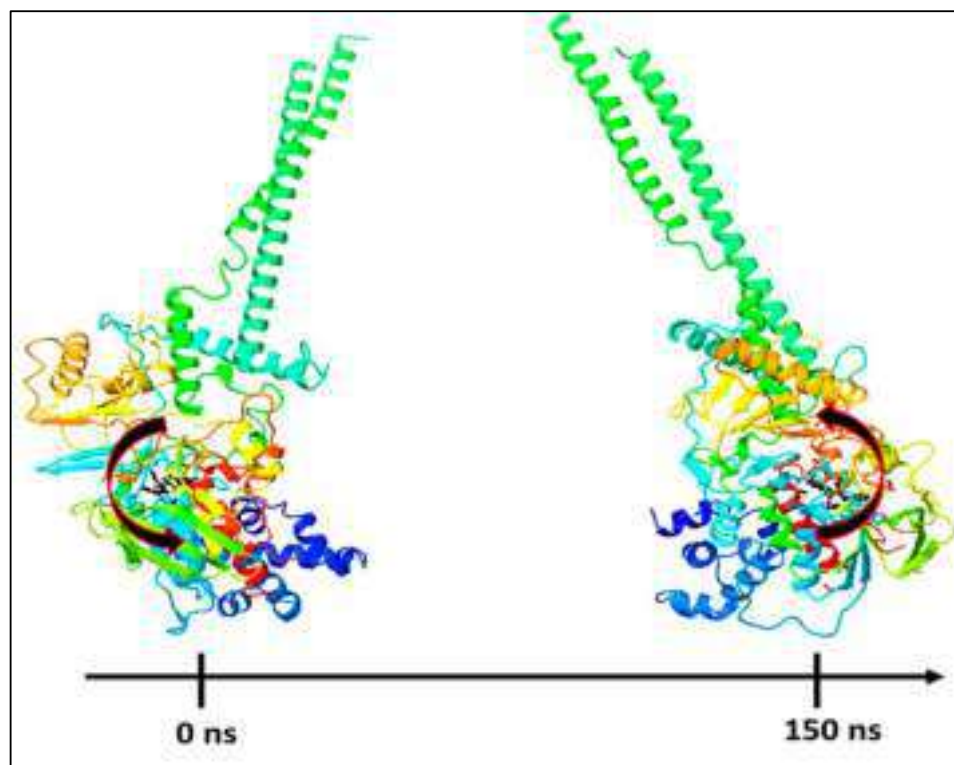
**Figure 23.** Ligand torsion profile of LSD-compound 1 displayed during 150 ns of simulation 1.



Molecular Mechanics Generalized Born and Surface Area (MMGBSA) calculations. The MMGBSA method is often used to determine the binding energy of ligands to protein molecules. The binding free energy of each protein–compound **1** complex was calculated, as well as the influence of the other non-bonded interactions energies (Table 1). The binding energy of ligand compound **1** with LSD is  $-59.78$  kcal/mol.  $G_{\text{bind}}$  is governed by non-bonded interactions such as  $G_{\text{bindCoulomb}}$ ,  $G_{\text{bindCovalent}}$ ,  $G_{\text{bindHbond}}$ ,  $G_{\text{bindLipo}}$ ,  $G_{\text{bindSolvGB}}$ , and  $G_{\text{bindvdW}}$ . The  $G_{\text{bindvdW}}$ ,  $G_{\text{bindLipo}}$ , and  $G_{\text{bindCoulomb}}$  energies contributed the most to the average binding energy across all types of interactions. These conformational alterations result in improved binding pocket acquisition and engagement with residues, resulting in increased binding energy and stability. Thus, the binding energy obtained from docking results was well justified by MM-GBSA calculations. Furthermore, the last frame (150 ns) of MMGBSA displayed the positional change of compound **1** as compared to the 0 ns trajectory, indicating a better binding pose for best fitting in the protein's binding cavity (see Figure 24).

**Table 1.** Binding energy calculation of compound **1** with LSD and non-bonded interaction energies from MMGBSA trajectories. (star indicates mean of all th energy value).

Energies (kcal/mol) Mean *	LSD1 + Comp-1
$\Delta G_{\text{bind}}$	$-42.18 \pm 7.60$
$\Delta G_{\text{bindLipo}}$	$-07.62 \pm 4.78$
$\Delta G_{\text{bindvdW}}$	$-15.63 \pm 7.77$
$\Delta G_{\text{bindCoulomb}}$	$-12.54 \pm 4.07$
$\Delta G_{\text{bindHbond}}$	$-11.68 \pm 2.00$
$\Delta G_{\text{bindSolvGB}}$	$31.53 \pm 9.70$
$\Delta G_{\text{bindCovalent}}$	$10.22 \pm 4.00$

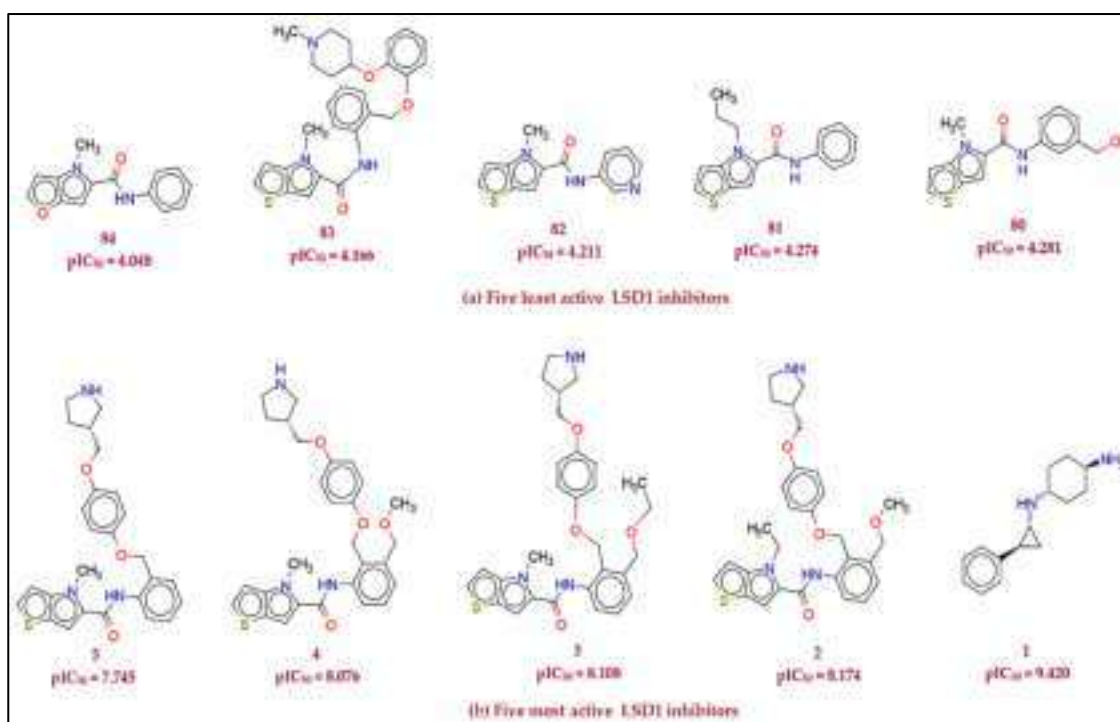


**Figure 24.** MMGBSA trajectory (0 ns, before simulation and 150 ns, after simulation) exhibited conformational changes of compound **1** upon binding with the proteins, LSD, the arrows indicating the overall positional variation (movement and pose) of compound **1** at the binding site cavity.

## 4. Materials and Methods

### 4.1. Preparation of Data Sets/Modeling Set Preparation from ChEMBL Data

Only compounds having experimental LSD1 inhibitory potency tested against a range of LSD1 inhibition assays were used in the ChEMBL [9] database. A limited data set of 84 LSD1 inhibitors with accurate  $EC_{50}$  values (0.38–89500 nM) was created from a crude dataset of 191 compounds with experimental  $EC_{50}$  values after removing structural duplicates, multi-component compounds or salts, and compounds with imprecise  $EC_{50}$  values. The  $EC_{50}$  values in nanomolar (nM) units were converted to molar units first (M). For the sake of data set handling,  $EC_{50}$  (M) values for each molecule were transformed to  $pEC_{50}$  ( $pEC_{50} = -\log EC_{50}$ ). SMILES notations for all 84 substances with experimental  $EC_{50}$  and  $pEC_{50}$  values are listed in Table S1 in Supplementary. Figure 25 shows a representative example of the five least active and five most active LSD1 inhibitors.



**Figure 25.** Representative (a) five least active and (b) five most active LSD1 inhibitors from the selected data set.

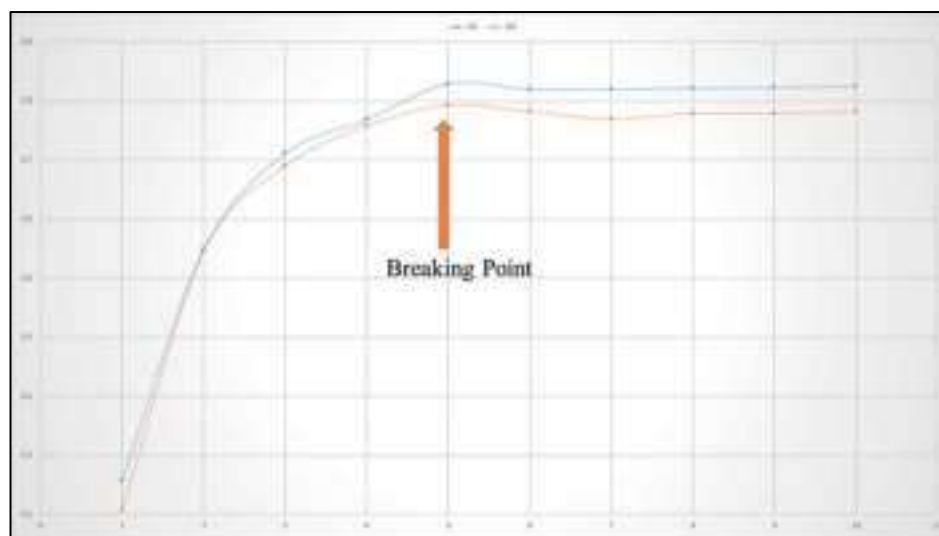
### 4.2. Calculation of Molecular Descriptors and Objective Feature Selection (OFS)

Using Open Babel 3.1, the SMILES notations were translated to 3D structures [15]. The most stable conformation is found in the geometry optimized molecule. As a result, calculating molecular descriptors on a dataset of optimized molecules assures that all physico-chemical attributes for all molecules in the dataset are uniform. Prior to calculating molecular descriptors, all of the compounds in the current dataset were optimized using TINKER (force field MMFF94). An appropriate calculation of many molecular descriptors is required in QSAR analysis to improve mechanistic understanding. A huge collection of more than 30,000 unique 1D- to 3D-molecular descriptors may be found in PyDescriptor, a PyMOL plugin [16]. Data trimming was performed to prevent the risk of overfitting due to noisy duplicated descriptors. Then, using QSARINS-2.2.4 [17], objective feature selection (OFS) was used to exclude near-constant, constant, and significantly inter-correlated ( $|R| > 0.90$ ) molecular descriptors. Despite the fact that only 1733 molecular descriptors were accepted into the contracted molecular descriptor pool, it nevertheless has a wide range of descriptors that cover a wide chemical spectrum.

#### 4.3. Splitting of the Data Set Molecules into Training and External Sets and Subjective Feature Selection

To avoid information leaking, it is critical to divide the entire data set into training and prediction sets with correct configuration and sizes prior to rigorous subjective feature selection [18]. To avoid bias, the entire data set was arbitrarily divided into two sets: training (an 80%, or 67 molecules) and prediction (20%, or 17 molecules). The sole objective of a training set is to select an acceptable number of molecular descriptors for developing QSAR models, whereas the prediction set is used to validate these models externally (Predictive QSAR). The genetic algorithm-reinforced multilinear regression (GA-MLR) method, as implemented in QSARINS-2.2.4, was used to pick acceptable descriptors using  $Q^2_{\text{LOO}}$  as a fitness parameter for subjective feature selection.

To construct a good QSAR model, it is critical to avoid overfitting and to choose an appropriate number of molecular descriptors in order to provide satisfactory interpretability. As a result, a graph of the number of molecular descriptors ( $X$ -axis) involved in the models against  $R^2_{\text{tr}}$  and  $Q^2_{\text{LOO}}$  values ( $Y$ -axis) has been plotted in the current communication to achieve breaking point, with the number of molecular descriptors corresponding to the breaking point being an optimum number of descriptors in QSAR model building. Because the graph in Figure 3 shows a breaking point at five variables, QSAR models with more than five descriptors were eliminated (See Figure 26).



**Figure 26.** Depiction of Plot for the number of descriptors against the Coefficient of Determination  $R^2$  and Leave-One-Out Coefficient of Determination  $Q^2$  to identify the optimum number of descriptors.

#### 4.4. Model Development and Validation

The robustness of the created models was determined using a variety of validation criteria reported in the literature. Internal predictability and statistical quality of the developed model were tested using parameters such as the coefficient of determination ( $r^2$ ), leave-one-out cross-validation ( $Q^2_{\text{LOO}}$ ), and leave-many-out cross-validation to achieve this ( $Q^2_{\text{LMO}}$ ). In addition, for each developed model, the standard error of estimate(s) was defined. For the given QSAR models for the stated dataset, RMSE (Root Mean Squared of Errors) for the training ( $\text{RMSE}_{\text{TR}}$ ) and external prediction sets ( $\text{RMSE}_{\text{ext}}$ ) that denote the complete error of the model that was predicted as an extra portion of the accuracy [5,18] were used.

The QUIK rule (Q Under the Influence of K) was used to examine the inter-correlation between descriptors. To reduce inter-correlation among descriptors, the QUICK rule was set to 0.05. The fit of the randomly reordered  $Y$ -data was checked using  $Y$ -randomization with 2000 iterations to ensure the trustworthiness of the created QSAR model. The dependent variables ( $p\text{EC}_{50}$  value) of the training set were shuffled, and new coefficients of

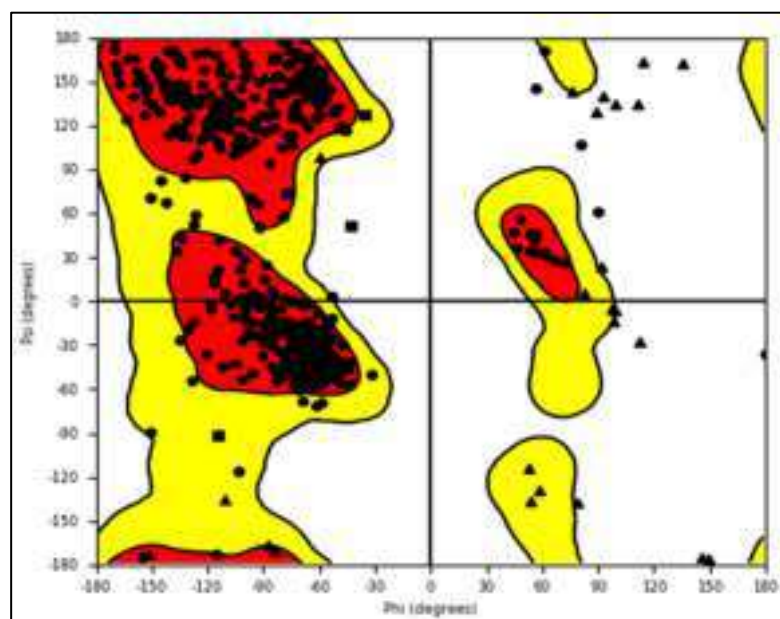
determination were produced for the randomization of the constructed QSAR model. The new models' coefficients of determination are significantly low, indicating that the reported model in this QSAR research was not acquired by chance correlation [19].

All models were externally validated using the following validation criteria:  $r^2_{\text{ext}}$  (external determination coefficient),  $Q^2_{F1}$ ,  $Q^2_{F2}$ ,  $Q^2_{F3}$ , Concordance Correlation Coefficient (CCC),  $CCC_{\text{ex}}$ ,  $r^2_m$ , and  $r^2_o$ . The  $R^2_m$  (overall) parameter penalizes a model when there are big disparities between observed and predicted values of all the compounds in the collection (considering both training and test sets). The difference between the values of the expected and the resultant experimental activity data was assessed using the  $r^2_m$  ( $pEC_{50}$  value). It has been suggested that the observed value for the  $r^2_m$  should be lower than 0.2 if the  $r^2_o$  value is more than 0.5. To validate model reliability and robustness, all QSAR models were examined for validation parameters such as Golbraikh and Tropsha's criterion.

In general, the created QSAR model's predictive ability is determined by how well the anticipated value matches the observed (experimental biological activity) value. Even the presence of a single outlier reduces the generated QSAR model's prediction ability. Following that, we attempted to identify the outliers based on compound with a considerably high residual value in GA-MLR QSAR models. Furthermore, by comparing the predicted value to the standardized residual values, we were able to identify the outlier compounds. Similarly, the leverage effect in Williams' plot revealed structural variation in database compounds. The created QSAR model's applicability domain is determined by combining the leverage and standard residuals [20–23].

#### 4.5. Molecular Docking Analysis

The protein data bank (<https://www.rcsb.org/structure/2DW4>, accessed on 24 May 2022) was used to obtain the pdb file for the LSD1 receptor. The pdb 2dw4 [24] was chosen because of its X-ray resolution and sequence completion. The health of the protein was evaluated before actual docking simulations by plotting Ramchandran's plot [25] (See Figure 27). For docking analysis, the optimized protein is acceptable. Although all of the compounds were docked into the active site, the docking pose for the most active compound 1 as a representative has been shown below for convenience.



**Figure 27.** Ramchandran plot for LSD1 receptor.

The software NRGSuite [26] was utilized for molecular docking analysis. This open-source software is accessible as a PyMOL plugin ([www.pymol.org](http://www.pymol.org), accessed on 7 July 2022). With the help of FlexAID [27], it can detect the surface cavities in a protein and use them as

target-binding sites for docking simulations. It models ligand and side-chain flexibility, as well as covalent docking, and employs a genetic algorithm for conformational search. To gain the best performance using NRGsuite, we used a flexible-rigid docking technique with the following default settings: Side chain flexibility—no; ligand flexibility—yes; ligand pose as reference—no; constraints- no; HET groups- included water molecules; van der Waals permeability—0.1; solvent types—no type; number of chromosomes—1000; number of generations—1000; fitness model—share; reproduction model—population boom; number of TOP complexes—5. The native ligand, a known tranylcypromine inhibitor of LSD1 [24], was used to validate the docking technique for molecular docking.

#### 4.6. Molecular Dynamic Simulation

Desmond, a package from Schrödinger LLC [28], was used to simulate molecular dynamics for 150 nanoseconds. Docking experiments provided the earliest step of protein and ligand complexes for molecular dynamics simulation. In static settings, Molecular Docking Studies can predict the ligand binding state. Because docking provides a static view of a molecule's binding pose in a protein's active site [29], MD simulations tend to compute atom movements over time by integrating Newton's classical equation of motion. The ligand binding status in the physiological milieu was predicted using simulations [30,31].

Protein Preparation Wizard or Maestro was used to preprocess the protein–ligand complex, which included complex optimization and minimization. The System Builder tool was used to prepare all of the systems. TIP3P was chosen as a solvent model with an orthorhombic box (Transferable Intermolecular Interaction Potential 3 Points). In the simulation, the OPLS 2005 force field was used [32]. Counter ions were added to the models to make them neutral. A total of 0.15 M salt (NaCl) was added to replicate physiological circumstances. For the entire simulation, the NPT ensemble with 300 K temperature and 1 atm pressure was chosen. Before the simulation, the models were loosened. After every 100 ps, the trajectories were saved for analysis, and the simulation's stability was determined by measuring the root mean square deviation (RMSD) of the protein and ligand over time.

#### 4.7. Molecular Mechanics Generalized Born and Surface Area (MMGBSA) Calculations

During MD simulations of LSD complexed with complex 1, the binding free energy ( $G_{\text{bind}}$ ) of docked complexes was calculated using the premier molecular mechanics generalized born surface area (MM-GBSA) module (Schrodinger suite, LLC, New York, NY, USA, 2017-4). The binding free energy was calculated using the OPLS 2005 force field, VSGB solvent model, and rotamer search methods [16–18]. After the MD run, 10 ns intervals were used to choose the MD trajectories frames. The total free energy binding was calculated using Equation (1):

$$\Delta G_{\text{bind}} = G_{\text{complex}} - (G_{\text{protein}} + G_{\text{ligand}}) \quad (1)$$

where,  $\Delta G_{\text{bind}}$  = binding free energy,  $G_{\text{complex}}$  = free energy of the complex,  $G_{\text{protein}}$  = free energy of the target protein, and  $G_{\text{ligand}}$  = free energy of the ligand. The MMGBSA outcome trajectories were analyzed further for post-dynamics structural modifications.

## 5. Conclusions

Pharmacophoric traits responsible for improved LSD1 inhibition unraveled by present QSAR evaluation are interconnected and thus easy to incorporate to optimize present LSD1 inhibitors towards more potent analogues; for example, a higher number of Nitrogen atoms precisely at six bonds and a lower number of Hydrogen atoms at three bonds from the ring Carbon atom can be introduced at the same time to optimize the LSD1 inhibitors towards better activity, and a higher number of non-ring Oxygen atoms precisely at nine bonds from the amide Nitrogen and a less frequent occurrence of  $sp^2$  Oxygen within 4Å boosts the LSD1 inhibitory activity. Likewise, the hydrogen bond donor atom at two bonds and amide Nitrogen at four bonds from  $sp^3$  hybridized Carbon atoms enhances the desired

activity. Two of the five descriptors in the split-set model emphasize the relevance of the ring carbon atom, whereas one descriptor represents the importance of the ring Sulphur atom, indicating that there is room for modification of dataset compounds for greater LSD1 inhibition. On the other hand, two out of five descriptors emphasize the relevance of amide nitrogen, suggesting that the current dataset compounds might be optimized for improved LSD1 inhibition. Lipophilic atoms, such as ring carbon atoms, were identified as a possible center for the optimization of LSD1 inhibitors for anticancer efficacy by certain chemical descriptors. As a result, the created QSAR model may be used to improve compounds for better LSD1 inhibition and cancer prevention. The docking results revealed that the descriptors, **fdonsp3C2B** and **lipo\_ringS\_8Bc**, played important roles in the inhibition of the LSD1 receptor, which was consistent with the QSAR findings. The MD simulation results display that the ligands were tightly bound to the binding site of the receptor during the simulation. The ligands are still firmly connected to the receptor's binding site, as evidenced by the fact that the RMSD values for the ligand fit-to-protein does not significantly vary over the course of the simulation. Compound 1's position was altered in the last 150-ns frame of the MMGBSA simulation, compared to the 0-ns trajectory, indicating a more advantageous binding pose for the binding cavity of the protein. Therefore, the MD simulation and MMGBSA analysis strengthens the outcome of the QSAR and Molecular docking studies.

**Supplementary Materials:** The following supporting information can be downloaded at: <https://www.mdpi.com/article/10.3390/molecules27154758/s1>. Table S1: The SMILES notation for 84 leads, along with their reported EC<sub>50</sub> and pEC<sub>50</sub> values. Table S2: The values for selected molecular descriptors present in QSAR models.

**Author Contributions:** Conceptualization, R.D.J., R.L.B. and N.M.—formal analysis; data curation, N.M., A.G. (Arabinda Ghosh), M.E.A.Z. and S.A.A.-H.; formal analysis, N.M., A.A.A.-M.—formal analysis, A.G. (Ajaykumar Gandhi), A.S. and V.H.M.; methodology, N.M., A.G. (Ajaykumar Gandhi) and V.H.M.; writing—original draft, N.M., A.G. (Ajaykumar Gandhi) and S.A.A.-H.; writing—review and editing. All authors have read and agreed to the published version of the manuscript.

**Funding:** The authors extend their sincere appreciation to the Deanship of Scientific Research, Imam Mohammad Ibn Saud Islamic University, Saudi Arabia, for its support of this research through the Research Group No RG-21-09-77.

**Institutional Review Board Statement:** Not applicable.

**Informed Consent Statement:** Not applicable.

**Data Availability Statement:** The data is available in the Supplementary section.

**Acknowledgments:** The authors are thankful to Paola Gramatica and her team for providing QSARINS-v2.2.4, and the developers of TINKER, ChemSketch 12 Freeware (ACD labs), and Py-Descriptor for providing the free versions of their software.

**Conflicts of Interest:** The authors declare no conflict of interest.

**Sample Availability:** Not applicable.

## Abbreviations

CADD	Computer Aided Drug Designing
SMILES	Simplified Molecular-Input Line-Entry System
GA	Genetic Algorithm
MLR	Multiple Linear Regression
QSAR	Quantitative Structure-Activity Relationship
QSARINS	QSAR Insubria
OECD	Organization for Economic Co-operation and Development
OFS	Objective Feature Selection
SFS	Subjective Feature Selection
LSD1	Lysine-specific demethylase 1

## References

1. Maiques-Diaz, A.; Somervaille, T.C.P. LSD1: Biologic roles and therapeutic targeting. *Epigenomics* **2016**, *8*, 1103–1116. [[CrossRef](#)]
2. McGrath, J.P.; Williamson, K.E.; Balasubramanian, S.; Odate, S.; Arora, S.; Hatton, C.; Edwards, T.M.; O'Brien, T.; Magnuson, S.; Stokoe, D.; et al. Pharmacological Inhibition of the Histone Lysine Demethylase KDM1A Suppresses the Growth of Multiple Acute Myeloid Leukemia Subtypes. *Cancer Res.* **2016**, *76*, 1975–1988. [[CrossRef](#)]
3. Mohammad Helai, P.; Smitheman Kimberly, N.; Kamat Chandrashekhar, D.; Soong, D.; Federowicz Kelly, E.; Van Aller Glenn, S.; Schneck Jess, L.; Carson Jeffrey, D.; Liu, Y.; Butticello, M.; et al. A DNA Hypomethylation Signature Predicts Antitumor Activity of LSD1 Inhibitors in SCLC. *Cancer Cell* **2015**, *28*, 57–69. [[CrossRef](#)]
4. Ma, L.-Y.; Zheng, Y.-C.; Wang, S.-Q.; Wang, B.; Wang, Z.-R.; Pang, L.-P.; Zhang, M.; Wang, J.-W.; Ding, L.; Li, J.; et al. Design, Synthesis, and Structure–Activity Relationship of Novel LSD1 Inhibitors Based on Pyrimidine–Thiourea Hybrids As Potent, Orally Active Antitumor Agents. *J. Med. Chem.* **2015**, *58*, 1705–1716. [[CrossRef](#)]
5. Cherkasov, A.; Muratov, E.N.; Fourches, D.; Varnek, A.; Baskin, I.I.; Cronin, M.; Dearden, J.; Gramatica, P.; Martin, Y.C.; Todeschini, R.; et al. QSAR Modeling: Where Have You Been? Where Are You Going To? *J. Med. Chem.* **2014**, *57*, 4977–5010. [[CrossRef](#)]
6. Fujita, T.; Winkler, D.A. Understanding the Roles of the “Two QSARs”. *J. Chem. Inf. Model.* **2016**, *56*, 269–274. [[CrossRef](#)]
7. Abdizadeh, R.; Heidarian, E.; Hadizadeh, F.; Abdizadeh, T. QSAR Modeling, Molecular Docking and Molecular Dynamics Simulations Studies of Lysine-Specific Demethylase 1 (LSD1) Inhibitors as Anticancer Agents. *Anti-Cancer Agents Med. Chem.* **2021**, *21*, 987–1018. [[CrossRef](#)]
8. Fang, Y.; Liao, G.; Yu, B. LSD1/KDM1A inhibitors in clinical trials: Advances and prospects. *J. Hematol. Oncol.* **2019**, *12*, 129. [[CrossRef](#)]
9. Gaulton, A.; Hersey, A.; Nowotka, M.; Bento, A.P.; Chambers, J.; Mendez, D.; Mutowo, P.; Atkinson, F.; Bellis, L.J.; Cibrián-Uhalte, E.; et al. The ChEMBL database in 2017. *Nucleic Acids Res.* **2017**, *45*, D945–D954. [[CrossRef](#)]
10. Vianello, P.; Sartori, L.; Amigoni, F.; Cappa, A.; Fagá, G.; Fattori, R.; Legnaghi, E.; Ciossani, G.; Mattevi, A.; Meroni, G.; et al. Thieno[3,2-b]pyrrole-5-carboxamides as New Reversible Inhibitors of Histone Lysine Demethylase KDM1A/LSD1. Part 2: Structure-Based Drug Design and Structure–Activity Relationship. *J. Med. Chem.* **2017**, *60*, 1693–1715. [[CrossRef](#)]
11. Zheng, Y.-C.; Ma, J.; Wang, Z.; Li, J.; Jiang, B.; Zhou, W.; Shi, X.; Wang, X.; Zhao, W.; Liu, H.-M. A Systematic Review of Histone Lysine-Specific Demethylase 1 and Its Inhibitors. *Med. Res. Rev.* **2015**, *35*, 1032–1071. [[CrossRef](#)]
12. Niwa, H.; Sato, S.; Hashimoto, T.; Matsuno, K.; Umehara, T. Crystal Structure of LSD1 in Complex with 4-[5-(Piperidin-4-ylmethoxy)-2-(p-tolyl)pyridin-3-yl]benzotrile. *Molecules* **2018**, *23*, 1538. [[CrossRef](#)]
13. Stazi, G.; Zwergel, C.; Valente, S.; Mai, A. LSD1 inhibitors: A patent review (2010–2015). *Expert Opin. Ther. Pat.* **2016**, *26*, 565–580. [[CrossRef](#)]
14. Magliulo, D.; Bernardi, R.; Messina, S. Lysine-Specific Demethylase 1A as a Promising Target in Acute Myeloid Leukemia. *Front. Oncol.* **2018**, *8*, 255. [[CrossRef](#)]
15. O’Boyle, N.M.; Banck, M.; James, C.A.; Morley, C.; Vandermeersch, T.; Hutchison, G.R. Open Babel: An open chemical toolbox. *J. Cheminform.* **2011**, *3*, 33. [[CrossRef](#)]
16. Masand, V.H.; Rastija, V. PyDescriptor: A new PyMOL plugin for calculating thousands of easily understandable molecular descriptors. *Chemom. Intell. Lab. Syst.* **2017**, *169*, 12–18. [[CrossRef](#)]
17. Gramatica, P.; Chirico, N.; Papa, E.; Cassani, S.; Kovarich, S. QSARINS: A new software for the development, analysis, and validation of QSAR MLR models. *J. Comput. Chem.* **2013**, *34*, 2121–2132. [[CrossRef](#)]
18. Masand, V.H.; Mahajan, D.T.; Nazeruddin, G.M.; Hadda, T.B.; Rastija, V.; Alfeefy, A.M. Effect of information leakage and method of splitting (rational and random) on external predictive ability and behavior of different statistical parameters of QSAR model. *Med. Chem. Res.* **2014**, *24*, 1241–1264. [[CrossRef](#)]
19. Consonni, V.; Todeschini, R.; Ballabio, D.; Grisoni, F. On the Misleading Use of QF32 for QSAR Model Comparison. *Mol. Inform.* **2019**, *38*, 1800029. [[CrossRef](#)]
20. Krstajic, D.; Buturovic, L.J.; Leahy, D.E.; Thomas, S. Cross-validation pitfalls when selecting and assessing regression and classification models. *J. Cheminform.* **2014**, *6*, 10. [[CrossRef](#)]
21. Martin, T.M.; Harten, P.; Young, D.M.; Muratov, E.N.; Golbraikh, A.; Zhu, H.; Tropsha, A. Does Rational Selection of Training and Test Sets Improve the Outcome of QSAR Modeling? *J. Chem. Inf. Model.* **2012**, *52*, 2570–2578. [[CrossRef](#)]
22. Chirico, N.; Gramatica, P. Real External Predictivity of QSAR Models. Part 2. New Intercomparable Thresholds for Different Validation Criteria and the Need for Scatter Plot Inspection. *J. Chem. Inf. Model.* **2012**, *52*, 2044–2058. [[CrossRef](#)]
23. Roy, P.P.; Kovarich, S.; Gramatica, P. QSAR model reproducibility and applicability: A case study of rate constants of hydroxyl radical reaction models applied to polybrominated diphenyl ethers and (benzo-)triazoles. *J. Comput. Chem.* **2011**, *32*, 2386–2396. [[CrossRef](#)]
24. Mimasu, S.; Sengoku, T.; Fukuzawa, S.; Umehara, T.; Yokoyama, S. Crystal structure of histone demethylase LSD1 and tranylcypromine at 2.25 Å. *Biochem. Biophys. Res. Commun.* **2008**, *366*, 15–22. [[CrossRef](#)]
25. Hollingsworth, S.A.; Karplus, P.A. A fresh look at the Ramachandran plot and the occurrence of standard structures in proteins. *BioMol. Concepts* **2010**, *1*, 271–283. [[CrossRef](#)]
26. Gaudreault, F.; Morency, L.-P.; Najmanovich, R.J. NRGsuite: A PyMOL plugin to perform docking simulations in real time using FlexAID. *Bioinformatics* **2015**, *31*, 3856–3858. [[CrossRef](#)]

27. Gaudreault, F.; Najmanovich, R.J. FlexAID: Revisiting Docking on Non-Native-Complex Structures. *J. Chem. Inf. Model.* **2015**, *55*, 1323–1336. [[CrossRef](#)]
28. Bowers, K.J.A.C.; David, E.; Xu, H.; Dror Ron, O.; Eastwood Michael, P.; Gregersen Brent, A.; Klepeis John, L.; Kolossvary, I.; Moraes, M.A.; Sacerdoti Federico, D.; et al. Scalable Algorithms for Molecular Dynamics Simulations on Commodity Clusters. In Proceedings of the 2006 ACM/IEEE Conference on Supercomputing, Tampa, FL, USA, 11–17 November 2006. [[CrossRef](#)]
29. Ferreira, L.G.; Dos Santos, R.N.; Oliva, G.; Andricopulo, A.D. Molecular docking and structure-based drug design strategies. *Molecules* **2015**, *20*, 13384–13421. [[CrossRef](#)]
30. Hildebrand, P.W.; Rose, A.S.; Tiemann, J.K.S. Bringing Molecular Dynamics Simulation Data into View. *Trends Biochem. Sci.* **2019**, *44*, 902–913. [[CrossRef](#)]
31. Rasheed, M.A.; Iqbal, M.N.; Saddick, S.; Ali, I.; Khan, F.S.; Kanwal, S.; Ahmed, D.; Ibrahim, M.; Afzal, U.; Awais, M. Identification of Lead Compounds against Scm (fms10) in *Enterococcus faecium* Using Computer Aided Drug Designing. *Life* **2021**, *11*, 77. [[CrossRef](#)]
32. Shivakumar, D.; Williams, J.; Wu, Y.; Damm, W.; Shelley, J.; Sherman, W. Prediction of Absolute Solvation Free Energies using Molecular Dynamics Free Energy Perturbation and the OPLS Force Field. *J. Chem. Theory Comput.* **2010**, *6*, 1509–1519. [[CrossRef](#)] [[PubMed](#)]





## OPEN ACCESS

EDITED BY  
Mercè Pallàs,  
University of Barcelona, Spain

REVIEWED BY  
Hoon Kim,  
Sunchon National University,  
South Korea  
Rehan Khan,  
Institute of Nano Science  
and Technology (INST), India  
Anas Shamsi,  
Jamia Millia Islamia, India

\*CORRESPONDENCE  
Nobendu Mukerjee  
nabendu21@arkmvccrahara.org  
Ghulam Md Ashraf  
ashraf.gm@gmail.com  
Arabinda Ghosh  
dra.ghosh@gauhati.ac.in

†These authors have contributed  
equally to this work

SPECIALTY SECTION  
This article was submitted to  
Alzheimer's Disease and Related  
Dementias,  
a section of the journal  
Frontiers in Aging Neuroscience

RECEIVED 17 February 2022  
ACCEPTED 07 July 2022  
PUBLISHED 22 August 2022

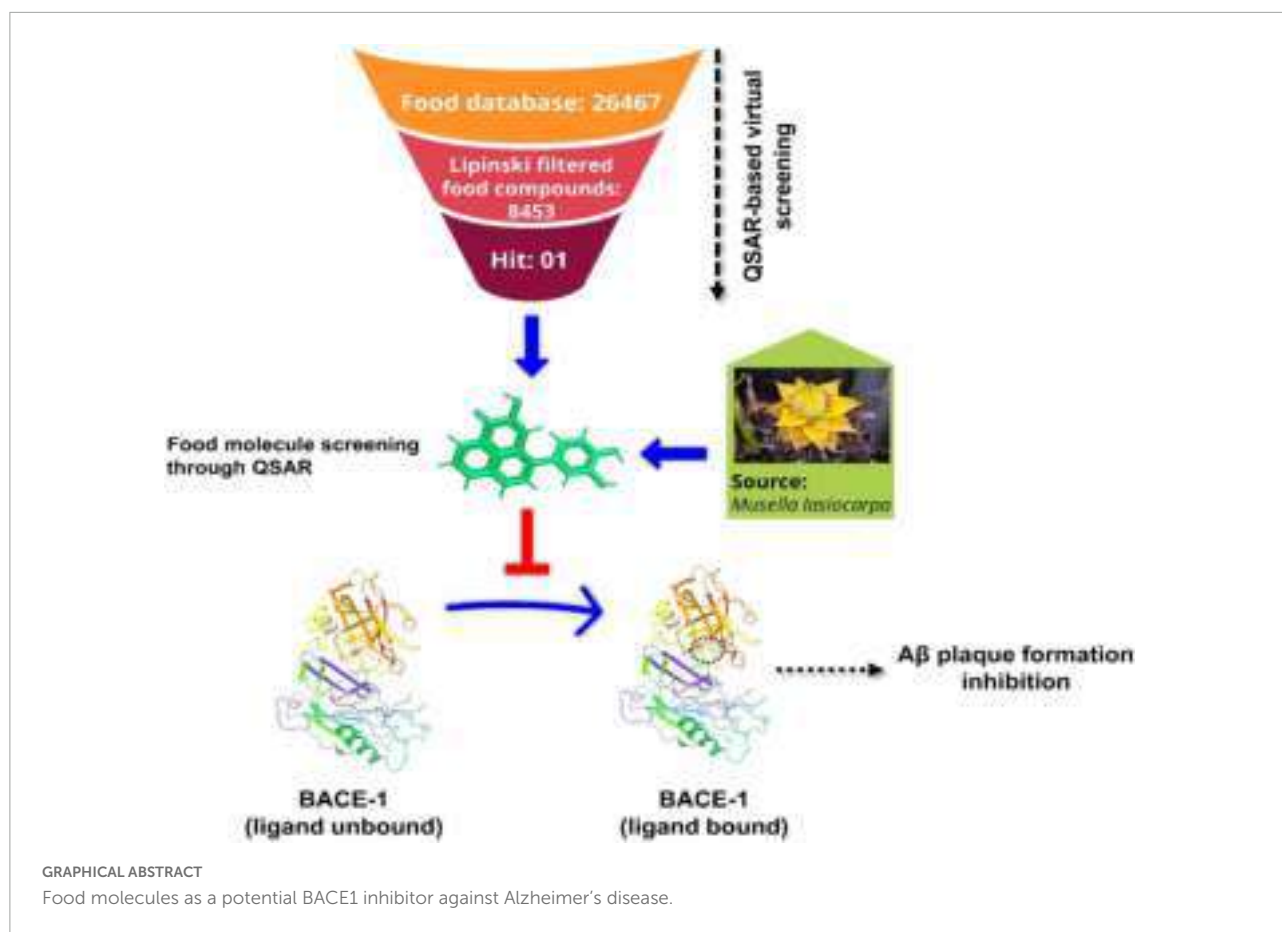
COPYRIGHT  
© 2022 Mukerjee, Das, Jawarkar,  
Maitra, Das, Castrosanto, Paul, Samad,  
Zaki, Al-Hussain, Masand, Hasan,  
Bukhari, Perveen, Alghamdi, Alexiou,  
Kamal, Dey, Malik, Bakal, Abuzenadah,  
Ghosh and Md Ashraf. This is an  
open-access article distributed under  
the terms of the [Creative Commons  
Attribution License \(CC BY\)](https://creativecommons.org/licenses/by/4.0/). The use,  
distribution or reproduction in other  
forums is permitted, provided the  
original author(s) and the copyright  
owner(s) are credited and that the  
original publication in this journal is  
cited, in accordance with accepted  
academic practice. No use, distribution  
or reproduction is permitted which  
does not comply with these terms.

# Repurposing food molecules as a potential BACE1 inhibitor for Alzheimer's disease

Nobendu Mukerjee<sup>1,2\*†</sup>, Anubhab Das<sup>3†</sup>, Rahul D. Jawarkar<sup>4†</sup>, Swastika Maitra<sup>5†</sup>, Padmashree Das<sup>6</sup>, Melvin A. Castrosanto<sup>7</sup>, Soumyadip Paul<sup>1</sup>, Abdul Samad<sup>8</sup>, Magdi E. A. Zaki<sup>9</sup>, Sami A. Al-Hussain<sup>9</sup>, Vijay H. Masand<sup>10</sup>, Mohammad Mehedi Hasan<sup>11</sup>, Syed Nasir Abbas Bukhari<sup>12</sup>, Asma Perveen<sup>13</sup>, Badrah S. Alghamdi<sup>14,15,16</sup>, Athanasios Alexiou<sup>17,18</sup>, Mohammad Amjad Kamal<sup>19,20,21,22</sup>, Abhijit Dey<sup>23</sup>, Sumira Malik<sup>24</sup>, Ravindra L. Bakal<sup>4</sup>, Adel Mohammad Abuzenadah<sup>20,25</sup>, Arabinda Ghosh<sup>26\*</sup> and Ghulam Md Ashraf<sup>15,25\*</sup>

<sup>1</sup>Department of Microbiology, Ramakrishna Mission Vivekananda Centenary College, Khardaha, India, <sup>2</sup>Department of Health Sciences, Novel Global Community Educational Foundation, Hebersham, NSW, Australia, <sup>3</sup>Institute of Health Sciences, Presidency University, Kolkata, India, <sup>4</sup>Department of Medicinal Chemistry, Dr. Rajendra Gode Institute of Pharmacy, Amravati, India, <sup>5</sup>Department of Microbiology, Adamas University, Kolkata, India, <sup>6</sup>Central Silk Board, Guwahati, India, <sup>7</sup>Institute of Chemistry, University of the Philippines Los Baños, Los Baños, Philippines, <sup>8</sup>Department of Pharmaceutical Chemistry, Faculty of Pharmacy, Tishk International University, Erbil, Iraq, <sup>9</sup>Department of Chemistry, Faculty of Science, Imam Mohammad Ibn Saud Islamic University, Riyadh, Saudi Arabia, <sup>10</sup>Department of Chemistry, Vidya Bharati Mahavidyalaya, Amravati, India, <sup>11</sup>Department of Biochemistry and Molecular Biology, Faculty of Life Sciences, Mawlana Bhashani Science and Technology University, Tangail, Bangladesh, <sup>12</sup>Department of Pharmaceutical Chemistry, College of Pharmacy, Jouf University, Sakaka, Saudi Arabia, <sup>13</sup>Glocal School of Life Sciences, Glocal University, Saharanpur, India, <sup>14</sup>Department of Physiology, Faculty of Medicine, King Abdulaziz University, Jeddah, Saudi Arabia, <sup>15</sup>Pre-Clinical Research Unit, King Fahd Medical Research Center, King Abdulaziz University, Jeddah, Saudi Arabia, <sup>16</sup>The Neuroscience Research Unit, Faculty of Medicine, King Abdulaziz University, Jeddah, Saudi Arabia, <sup>17</sup>Department of Science and Engineering, Novel Global Community Educational Foundation, Hebersham, NSW, Australia, <sup>18</sup>AFNP Med, Vienna, Austria, <sup>19</sup>Institutes for Systems Genetics, Frontiers Science Center for Disease-Related Molecular Network, West China Hospital, Sichuan University, Chengdu, China, <sup>20</sup>King Fahd Medical Research Center, King Abdulaziz University, Jeddah, Saudi Arabia, <sup>21</sup>Department of Pharmacy, Faculty of Allied Health Sciences, Daffodil International University, Dhaka, Bangladesh, <sup>22</sup>Enzymoics, Novel Global Community Educational Foundation, Hebersham, NSW, Australia, <sup>23</sup>Department of Life Sciences, Presidency University, Kolkata, India, <sup>24</sup>Amity Institute of Biotechnology, Amity University, Jharkhand, Ranchi, India, <sup>25</sup>Department of Medical Laboratory Sciences, Faculty of Applied Medical Sciences, King Abdulaziz University, Jeddah, Saudi Arabia, <sup>26</sup>Microbiology Division, Department of Botany, Gauhati University, Guwahati, India

Alzheimer's disease (AD) is a severe neurodegenerative disorder of the brain that manifests as dementia, disorientation, difficulty in speech, and progressive cognitive and behavioral impairment. The emerging therapeutic approach to AD management is the inhibition of  $\beta$ -site APP cleaving enzyme-1 (BACE1), known to be one of the two aspartyl proteases that cleave  $\beta$ -amyloid precursor protein (APP). Studies confirmed the association of high BACE1 activity with the proficiency in the formation of  $\beta$ -amyloid-containing neurotoxic plaques, the characteristics of AD. Only a few FDA-approved BACE1 inhibitors



are available in the market, but their adverse off-target effects limit their usage. In this paper, we have used both ligand-based and target-based approaches for drug design. The QSAR study entails creating a multivariate GA-MLR (Genetic Algorithm-Multilinear Regression) model using 552 molecules with acceptable statistical performance ( $R^2 = 0.82$ ,  $Q^2_{loo} = 0.81$ ). According to the QSAR study, the activity has a strong link with various atoms such as aromatic carbons and ring Sulfur, acceptor atoms,  $sp^2$ -hybridized oxygen, etc. Following that, a database of 26,467 food compounds was primarily used for QSAR-based virtual screening accompanied by the application of the Lipinski rule of five; the elimination of duplicates, salts, and metal derivatives resulted in a truncated dataset of 8,453 molecules. The molecular descriptor was calculated and a well-validated 6-parametric version of the QSAR model was used to predict the bioactivity of the 8,453 food compounds. Following this, the food compounds whose predicted activity ( $pKi$ ) was observed above 7.0 M were further docked into the BACE1 receptor which gave rise to the Identification of 4-(3,4-Dihydroxyphenyl)-2-hydroxy-1H-phenalen-1-one (PubChem I.D: 4468; Food I.D: FDB017657) as a hit molecule (Binding Affinity =  $-8.9$  kcal/mol,  $pKi = 7.97$  nM,  $Ki = 10.715$  M). Furthermore, molecular dynamics simulation for 150 ns and molecular mechanics generalized born and surface area (MMGBSA) study aided in identifying structural motifs involved in interactions with the BACE1 enzyme. Molecular docking and QSAR yielded complementary and congruent results. The validated analyses

can be used to improve a drug/lead candidate's inhibitory efficacy against the BACE1. Thus, our approach is expected to widen the field of study of repurposing nutraceuticals into neuroprotective as well as anti-cancer and anti-viral therapeutic interventions.

#### KEYWORDS

beta-site APP cleaving enzyme 1, BACE1, Alzheimer's disease, glioblastoma, QSAR, molecular docking, MD simulations, golden lotus banana

## Introduction

Alzheimer's disease (AD) is a devastating mental illness, which leads to an irreversible, progressive brain disorder that slowly destroys memory skills and learning abilities (De Strooper and Karran, 2016). Though the disease progression and risk factors of AD are not completely understood, a large number of evidence suggest the formation of amyloid-beta ( $A\beta$ ) is central to the pathophysiology of AD (Vassar et al., 1999). AD progression stages vary from mild to severe in middle-aged people to older persons detected with cognitive tests (Hall et al., 2019). During the preclinical stage of AD, patients seem to be symptom-free, but neurodegenerative changes occur in the brain. Abnormal accumulation of  $A\beta$ -containing plaques and hyperphosphorylated tau throughout the brain causes healthy neurons to exhibit loss of synaptic connections, ion-channel dysfunctions, and severe deterioration in neuronal health. This ultimately leads to neuronal cell death and cognitive decline in elderly persons (Musi et al., 2018; Sebastián-Serrano et al., 2018). This progressive accumulation of  $A\beta$  is caused by imbalances in the levels of  $A\beta$  production, aggregation, and clearance (Murphy and LeVine, 2010; Jabir et al., 2021). Moreover, alterations in synaptic plasticity and integral neuronal circuitries severely hamper neurogenesis.

The Special Report examines MCI, including Alzheimer's, from the perspectives of consumers and primary care providers. AD affects 6.5 million Americans who are 65 years old or older. By 2060, this figure may increase to 13.8 million unless medical advances prevent, slow down, or cure AD. A total of 121,499 AD deaths were reported on official death certificates in 2019. According to one COVID-19 report, AD is the sixth most common cause of death in the United States in 2019 and will move up to the seventh most common cause in 2020 and 2021. Among Americans 65 and older, AD is the seventh most common cause of death. Between 2000 and 2019, mortality from HIV, heart disease, and stroke all dropped, whereas AD deaths rose by 145 percent. In 2021, 16 billion hours of care were supplied by over 11 million family members and other unpaid caregivers. These statistics demonstrate a decrease in carers and an increase in the amount of care that each caregiver who is still working gives. \$271.6 billion was

spent on unpaid dementia care in 2021. Family caregivers now have a higher risk of emotional discomfort as well as poorer mental and physical health due to COVID-19. Caregivers of dementia are also impacted by COVID-19. To safeguard their own health and the health of their families, several caregivers have resigned. However, there is a need for more dementia carers. Medicaid payments are more than 22 times greater than Medicare payments, and payments to beneficiaries 65 and older with AD or other dementias are approximately three times more than payments to beneficiaries without these illnesses. Hospice, long-term care, and healthcare for dementia patients will cost \$321 billion in 2022. A poll by the Alzheimer's Association indicates MCI obstacles. The study revealed low MCI knowledge, a lack of desire to seek medical attention for symptoms, and challenges with MCI diagnosis. According to survey findings, clinical trial participation should be increased together with MCI awareness and diagnosis, particularly in impoverished communities (Alzheimer's Association, 2012).

$A\beta$  is a neurotoxic aggregate produced by the consecutive proteolysis of  $\beta$ -amyloid precursor protein (APP) by two aspartyl proteases, beta-site APP cleaving enzyme, Beta-Secretase (BACE1), and finally by  $\gamma$  secretase (Sinha et al., 1999; Vassar et al., 1999; Yan et al., 1999; Cui et al., 2011; Zhang et al., 2011). BACE1 is a novel target, a type 1 transmembrane aspartic protease, related to the pepsin and retroviral aspartic protease families (Moussa-Pacha et al., 2020), having 501 amino acids and is predominantly expressed in the human brain (Zacchetti et al., 2007; Hassan et al., 2018).

As there is a strong association between  $A\beta$  accumulation and AD, the primary therapeutic strategy for the treatment of AD targets lowering the concentration of  $A\beta$ . One such strategy that has come up in recent findings involves inhibiting the enzymes that generate  $A\beta$  in the first place. BACE1 antisense oligonucleotide treatment to APP overexpressing cells is reportedly responsible for a decreased production of  $\beta$ -secretase cleaved APP fragments. Recent studies suggest that the levels of BACE1 protein and their activity were raised to approximately double in patients with AD where BACE1 might initiate or enhance AD pathogenesis. Several studies proved that BACE1 is a vital drug target and active site of the enzyme (Sinha et al., 1999; Vassar et al., 1999; Dingwall, 2001;

Fukumoto et al., 2002; Yang et al., 2003; Li and Südhof, 2004). It is covered by a flexible antiparallel  $\beta$ -hairpin, called a flap (Hussain et al., 2000). It is elucidated that the flap can control substrate access to the receptor site and set the substrate into the perfect orientation for the catalytic process (Lin et al., 2000). Hence, the inhibition of proteases such as BACE1 may represent modifying treatment for AD by controlling the production of A $\beta$  (Tresadern et al., 2011; Arif et al., 2020). Therefore, BACE1 inhibitors may be used to treat AD.

Natural compounds have been investigated for many years for their ability to target a range of *trans*-acetyl peptidases in the search for new medications with fewer side effects due to their high biocompatibility. Apart from their benefits, the majority of natural compounds have a variety of disadvantages, including a high molecular weight, low stability, and in many cases, insufficient solubility. These difficulties can be resolved by using computer-assisted research to generate more effective and selective inhibitors. They are less harmful and more readily absorbed into the body than manufactured drugs. Computational techniques enable the modeling and screening of such compounds in a cost-effective and informative manner from a vast library of choices. The binding sites for various bioactive substances in BACE1 protein were predicted, and their interactions were explored utilizing the Food database and molecular docking. *Musella lasiocarpa*'s bioactive component, 4-(3,4-Dihydroxyphenyl)-2-hydroxy-1H-phenalen-1-one, is found to be the potential inhibitor of BACE1. *M. lasiocarpa*, also known as Chinese Dwarf Banana, is the only species in the genus *Musella*, which belongs to the family of Musaceae. Some novel compounds have also been isolated from this plant, which showed remarkable *in vitro* anticancer activities and some degree of antimicrobial activity (Bo et al., 2000; Dong et al., 2011).

These results demonstrate the potential of the *M. lasiocarpa* as a source of novel drugs, nutraceuticals, and functional foods. The result from this study will inspire the perspective of natural compounds and computer-aided drug discovery and, in the long run, significantly reduce the time required to research and build new lead compounds with specified biological activity and structural variety.

## Methodology

### QSAR modeling

Organization for economic corporation and development guidelines and a standard protocol recommended by different researchers, which involved sequential execution of (1) data collection and its curation, (2) structure generation and calculation of molecular descriptors, (3) objective feature selection (OFS), (4) splitting the dataset into training and external validation sets, and (5) subjective feature selection

involving building a regression model and validation of the developed model, has been followed to build a widely applicable QSAR model for the BACE1 inhibitory activity. This also ensures thorough validation and successful application of the model.

### Selection of data set

The data set of BACE1 inhibitory activity used for building, training, and validating the QSAR model in the present work was downloaded from the ChEMBL database (accessed on 22nd December 2021)<sup>1</sup>, which is a free and publicly accessible database. Initially, the data set comprised of 552 molecules (Davies et al., 2015). Then, as a part of data curation, entries with ambiguous  $K_i$  values, duplicates, salts, metal-based inhibitors, etc., were omitted. The final data set comprises structurally diverse 371 molecules with remarkable variation in structural scaffolds, which were tested experimentally for potency in terms of  $K_i$  (nM). A collection of 371 molecules with various structural configurations with mentioned enzyme inhibitory concentration ( $K_i$ ) was decided on for the existing work (O'Boyle et al., 2011; Tosco et al., 2011; Fujita and Winkler, 2016). The  $K_i$  values ranging from 0.47 to 1,400 nM have been transformed to  $pK_i$  ( $pK_i = -\log K_i$ ) earlier than real QSAR evaluation for ease of dealing with the data. Five least and five most active molecules are depicted in **Figure 1** to illustrate the version in bio-activity with chemical features. The SMILES strings with mentioned  $K_i$  and  $pK_i$  values for all of the molecules are depicted inside **Supplementary Table 1** with the **Supplementary material**.

### Molecular structure drawing and optimization

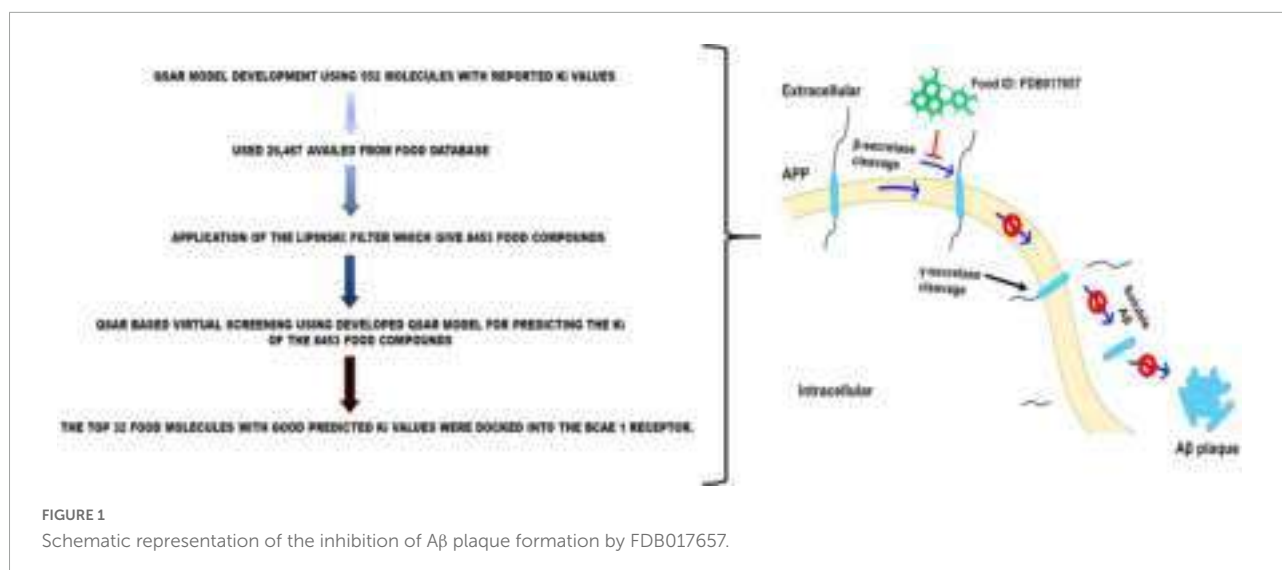
Drawing the 2D structures of all 371 and converting them to their corresponding 3D structures was done using ChemSketch 12 Freeware and Open Babel 2.4, (O'Boyle et al., 2011) both free and open-source software, respectively.<sup>2</sup> After that, the MMFF94 force field available in TINKER (default setting) and Open3DALign is used for optimization and molecular alignment, respectively.

### Molecular descriptor calculation and objective feature selection

PyDescriptor has over 30,000 molecular descriptors for each molecule (Masand and Rastija, 2017). Molecular descriptors with near constant values (>95%) and resonance ( $|R| > 0.95$ ) were eliminated using OFS in QSARINS v2.2.4 (Gramatica et al., 2013, 2014). This work removed duplicate molecular descriptors and prevented collisions of multicollinearity and hypothetical variables in the Genetic Algorithm multiple linear regression (GA-MLR) model. Only 3,281 molecular descriptors

<sup>1</sup> [https://www.ebi.ac.uk/chembl/g/#search\\_results/all/query bace 1](https://www.ebi.ac.uk/chembl/g/#search_results/all/query%20bace%201)

<sup>2</sup> [www.acdlabs.com](http://www.acdlabs.com)



were found in the reduced pool of molecular descriptors generated after OFS processing.

### Subjective feature selection, QSAR model development, and validation

A reduced set of molecular descriptors consisting of 1D to 3D descriptors, molecular properties and charge descriptors, etc., covers a fairly complete descriptor space. A statistically robust genetic algorithm (GA) based on multiple linear regression (MLR) was deployed to run the QSAR model using the subjective feature selection (SFS) task in QSARINS v2.2.4. Models derived according to the organization for economic corporation and development (OECD) principles have been subjected to rigorous internal and external statistical validation, scrambling, and range analysis. The QSAR deployment process goes through the following steps:

To generate a QSAR model from the split data set, a random split operation is performed in QSARINS v2.2.4 to split the given data set into 80% training set (297 molecules) and 20% predictions (74 molecules set). A total of 297 molecules in the training set were used to develop the QSAR model, and external validation was performed on 74 molecules in the prediction set (Gramatica et al., 2013).

The GA-MLR-based QSAR model was built with the default setting QSARINS v2.2.4. Subjective feature selection was performed by setting  $Q^2_{LOO}$  as a fitness feature. The  $Q^2_{LOO}$  score increased significantly to six variables but then increased slightly. Therefore, to avoid overfitting the model, SFS was limited to a set of seven descriptors. This helped to get a simple and informative QSAR model (see **Supplementary Table 2** in **Supplementary information**) for additional information on the six selected molecular descriptors present in the QSAR).

A good QSAR model which has been properly validated using various methods such as cross-validation, external

validation, Y-randomization, and applicability domain (Williams plot) is useful for future utilization in virtual screening, molecular optimization, and decision making, etc. The following statistical parameters and their recommended threshold values are routinely used to validate a model (Bellacasa et al., 2013; Roskoski, 2013; Fujita and Winkler, 2016; Gramatica, 2020):  $R^2_{tr} \geq 0.6$ ,  $Q^2_{loo} \geq 0.5$ ,  $Q^2_{LMO} \geq 0.6$ ,  $R^2 > Q^2$ ,  $R^2_{ex} \geq 0.6$ ,  $RMSE_{tr} < RMSE_{cv}$ ,  $\Delta K \geq 0.05$ ,  $CCC \geq 0.80$ ,  $Q^2_{-Fn} \geq 0.60$ ,  $r^2_m \geq 0.5$ ,  $(1-r^2/r_o^2) < 0.1$ ,  $0.9 \leq k \leq 1.1$  or  $(1-r^2/r_o^2) < 0.1$ ,  $0.9 \leq k' \leq 1.1$ ,  $(r_o^2 - r_o'^2) < 0.3$ ,  $RMSE_{ex}$ ,  $MAE_{ex}$ ,  $R^2_{ex}$ ,  $Q^2_{F1}$ ,  $Q^2_{F2}$ ,  $Q^2_{F3}$ , and low  $R^2_{Yscr}$ ,  $RMSE$  and  $MAE$ . The formulae for calculating these statistical parameters are available in **Supplementary Table 3** in the **Supplementary material**. In addition, the Williams plot was plotted to evaluate the applicability domain of the QSAR model.

### QSAR-based virtual screening

A database of 26,467 food compounds was downloaded from FoodDB (accessed December 28, 2021)<sup>3</sup>, primarily for QSAR-based virtual screening (VS) accompanied through the utility of Lipinski rule of five; the elimination of duplicates, salts, and metal derivatives resulted in a truncated dataset of 8,453 molecules. Therefore, the 8,453-food molecule was mainly used for VS-based QSAR. Prior to the calculation of the molecular descriptor, the 3D molecular system was organized within the same Method as a modeling set. Next, the molecular descriptor was calculated and a well-validated 6-parametric version of the QSAR model was used to predict the bioactivity of the new compound (Gramatica, 2013; Neves et al., 2018; Zaki et al., 2021; Jawarkar et al., 2022; Mukerjee et al., 2022). (The calculated

<sup>3</sup> <http://foodb.ca/>

molecular descriptors along with the predicted pKi and Ki values with smiles strings are given in **Supplementary Table 4** in the **Supplementary material**.

## Virtual screening of natural compounds using molecular docking

The structure-based virtual screening of the compounds was performed using AutoDock vina Version 1.1.2 (Trott and Olson, 2010). Binding sites of BACE1 for screening were predicted using DoGSiteScorer (Volkamer et al., 2012) and information about the binding site of the native ligand. The size of the grid box was set to be  $96 \times 52 \times 56$  Å for BACE1, centered around the identified binding site. The compounds with the best binding affinity (kcal/mol) corroborating ligand-based screening in the QSAR analysis were selected for the studies.

## Preparation of protein and ligand molecule

The target of interest BACE1 (PDB I.D: 2ZHV) crystallographic structure was discovered in the Protein Data Bank's structural database, and a molecular editor with an open-source license was used to import the structure (Discovery studio visualizer 4.0)<sup>4</sup> (Figure 2). To get the structure optimized, the UCSF Chimera utilized the steepest descent to find 1,000 steps, followed by the conjugate gradient of energy minimization approach to optimize the structure of 4-(3,4-dihydroxyphenyl)-2-hydroxy-1H-phenalen-1-one (PubChem I.D: 4468; Food I.D: FDB017657) was acquired from Food Database after screening and QSAR. This dataset was imported into the DS visualizer and saved as PDB files.

The FOOD database was used to obtain the library of ligands by screening the metabolites of *M. lasiocarpa* (Bonvino et al., 2018). The smiles notation and the three-dimensional structures of the selected ligands were downloaded in SDF format from the PubChem database (Kim et al., 2019), and further ligand structure files were converted to PDB format using Open Babel software (O'Boyle et al., 2011). The energy minimization of the ligands was performed in UCSF Chimera software (Pettersen et al., 2004) using the Amber ff 14 sb force field. The receptor used in the study is receptor tyrosine kinase; RCSB Protein Data Bank (PDB) (Berman et al., 2000) was used to download receptors BACE1 with PDB I.D: 2ZHV, Resolution: 1.85 Å. The protein structure was prepared by removing ligand, water molecules, and metal ions. Polar hydrogens were added, and non-polar hydrogens were merged. Finally, Kollman charges were added to the protein molecule before converting to PDBQT format by AutoDock Tools (v.1.5.6) of the MGL software package (Forli et al., 2016).

<sup>4</sup> <https://www.rcsb.org/structure/2ZHV>

## Molecular docking for validation of docking score

The best hits from the QSAR modeling and virtual screening were re-docked against BACE1 (PDB I.D: 2ZHV). Protein and ligand preparations were done using AutoDock Tools (v.1.5.6) (Forli et al., 2016). Gasteiger charges were added to the ligand molecules prior converting to the PDBQT format. Online server DoGSiteScorer and the information about the binding site residues of native ligand were used to construct the grid box. The grid box of dimensions  $96 \times 52 \times 56$  Å for BACE1 with 0.375 Å grid spacing was constructed using auto grid 4.2. Semi-flexible docking was done keeping the receptor molecule rigid and ligands flexible. Molecular docking was done via AutoDock 4.2 (Morris et al., 2009) using the Lamarckian Genetic Algorithm (LGA) scoring function with the number of GA runs = 100, population size = 550, and a maximum number of evaluations = 24,000,000.

## Molecular dynamics simulation (MD-simulation) and free energy landscape (FEL) analysis

The MD simulations studies were carried out in triplicate on dock complexes for BACE1 (PDB I.D: 2ZHV) with FDB017657 using the Desmond 2020.1 from Schrödinger, LLC. The triplicate samplings were made using the same parameters for each MD run to obtain the reproducibility of the results. The OPLS-2005 force field (Bowers et al., 2006; Chow et al., 2008; Shivakumar et al., 2010) and explicit solvent model with the stocktickerSPC water molecules were used in this system (Jorgensen et al., 1983). Na<sup>+</sup> ions were added to neutralize the charge of 0.15 M, and NaCl solutions were added to the system to simulate the physiological environment. Initially, the system was equilibrated using an NVT ensemble for 150 ns to retrain over the protein- FDB017657 complex. Following the previous step, a short run of equilibration and minimization was carried out using an NPT ensemble for 12 ns. The NPT ensemble was set up using the Nose-Hoover chain coupling scheme (Martyna et al., 1994) with the temperature at 27°C, the relaxation time of 1.0 ps, and pressure of 1 bar maintained in all the simulations. A time step of 2fs was used. The Martyna-Tuckerman-Klein chain coupling scheme (Martyna et al., 1992) barostat method was used for pressure control with a relaxation time of 2 ps. The particle mesh Ewald method (Toukmaji and Board, 1996) was used to calculate long-range electrostatic interactions, and the Radius for the Coulomb interactions was fixed at 9Å. RESPA integrator was used for a time step of 2 fs for each trajectory to calculate the bonded forces. The root means square deviation (RMSD), radius of gyration (Rg), root mean square fluctuation (RMSF),

and the number of hydrogen (H-bonds) were calculated to monitor the stability of the MD simulations. The free energy landscape of protein folding on the FDB017657 bound complex was measured using `geo_measures v 0.8` (Kagami et al., 2020). `Geo_measures` include a powerful library of `g_sham` and form the MD trajectory against RMSD and Radius of gyration (Rg) energy profile of folding recorded in a 3D plot using `matplotlib` python package.

## Molecular mechanics generalized born and surface area (MMGBSA) calculations

During MD simulations of BACE1 complexed with FDB017657, the binding free energy ( $G_{\text{bind}}$ ) of docked complexes was calculated using the premier molecular mechanics generalized Born surface area (MM-GBSA) module (Schrodinger suite, LLC, New York, NY, United States, 2017-4). The binding free energy was calculated using the OPLS 2005 force field, VSGB solvent model, and rotamer search methods (Piao et al., 2019). After the MD run, 10 ns intervals were used to choose the MD trajectories frames. The total free energy binding was calculated using equation 1:

$$\Delta G_{\text{bind}} = G_{\text{complex}} - (G_{\text{protein}} + G_{\text{ligand}}) \quad (1)$$

Where,  $\Delta G_{\text{bind}}$  = binding free energy,  $G_{\text{complex}}$  = free energy of the complex,  $G_{\text{protein}}$  = free energy of the target protein, and  $G_{\text{ligand}}$  = free energy of the ligand. The MMGBSA outcome trajectories were analyzed further for post-dynamics structure modifications.

## Dynamic cross-correlation and principal component (PCA) analysis

During a 150 ns MD simulation, a dynamic cross-correlation matrix (DCCM) was constructed across all C-atoms for all complexes to examine domain correlations. During a 150 ns simulation of the BACE1 (PDB I.D- 2ZHV) complexed with FDB017657, PCA analysis was used to recover the global movements of the trajectories. To calculate the PCA, a covariance matrix was created as stated. For conformational analysis of the FDB017657 in bound complex, 20 alternative conformational modes of the main component as movements of trajectories were calculated, and a comparison of the first highest mode (PC2) with PC10 was investigated. `Geo measures v 0.8` was used to calculate the free energy landscape of protein folding on an FDB017657-bound complex (Kagami et al., 2020). The MD trajectory versus PC2 and PC10 energy folding profiles were recorded in a 3D plot using the `matplotlib` python package using `Geo measures`, which includes a comprehensive library of `g_sham`.

## Results

The present QSAR analysis is performed using a moderate-size data set comprising structurally diverse compounds with experimentally measured  $K_i$  in the range from 0.47 to 1,400 nM. Thus, it covers a sufficiently broad chemical and data range. This helped to derive a properly validated (Martin and Muchmore, 2012; Gramatica et al., 2013; Masand et al., 2015; Fujita and Winkler, 2016) genetic algorithm unified with multilinear regression (GA-MLR) model to collect or extend thorough information about the pharmacophoric features that control the desired bio-activity (Descriptive QSAR) and having adequate external predictive capability (Predictive QSAR). The six variable-based GA-MLR QSAR model along with selected internal and external validation parameters (see **Supplementary material** for additional parameters) is as follows:

QSAR Model (Divided Set: Training Set-80% and Prediction Set-20%):

$$pK_i = 4.415 (\pm 0.236) + 0.046 (\pm 0.017) * \text{com\_lipohyd\_5A} + 0.12 (\pm 0.027) * \text{faccC3B} + 0.353 (\pm 0.105) * \text{aroC\_sumpc} + 0.273 (\pm 0.034) * \text{N\_acc\_5B} + 0.109 (\pm 0.02) * \text{aroC\_ringS\_6B} + 0.269 (\pm 0.04) * \text{fsp3OringC8B} +$$

Statistical parameters related to fitting, double cross-validation, and Y-scrambling for the *de novo* QSAR model with thresholds for some parameters (bottom of table) are shown in **Table 1**.

Thresholds for some important statistical parameters:  $R^2 \geq 0.6$ ,  $Q^2_{\text{LOO}} \geq 0.5$ ,  $Q^2_{\text{LMO}} \geq 0.6$ ,  $R^2 > Q^2$ ,  $R^2_{\text{ex}} \geq 0.6$ ,  $\text{RMSE}_{\text{tr}} < \text{RMSE}_{\text{cv}}$ ,  $\Delta K \geq 0.05$ ,  $\text{CCC} \geq 0.80$ ,  $Q^2_{\text{Fn}} \geq 0.60$ ,  $r^2_{\text{m}} \geq 0.6$ ,  $0.9 \leq k \leq 1.1$  and  $0.9 \leq k' \leq 1.1$  at  $\text{RMSE} \approx 2$ ,  $\text{MAE} \approx 0.4 R^2_{\text{adj}}$  of fitting parameter  $R^2$ , etc.) The threshold is significantly exceeded, confirming the adequacy of the number of molecular descriptors in the model and the statistical acceptability of the QSAR model. The values of  $Q^2_{\text{LOO}}$ ,  $Q^2_{\text{LMO}}$ , etc., (internal validation parameters) confirm the statistical robustness of the QSAR model. The high values of the external test parameters  $R^2_{\text{ex}}$ ,  $Q^2_{\text{F1}}$ ,  $Q^2_{\text{F2}}$ ,  $Q^2_{\text{F3}}$ , etc., emphasize the external predictability of the QSAR model. The coverage area of the model (Applicability Domain) is determined from Williams plots for the QSAR model (see **Figure 3**). Almost all statistical parameters reached values well above the accepted threshold, and the minimal correlation between the selected molecular descriptors precluded the possibility of random development of the QSAR model. This data confirms the statistical reliability and high external predictability of the developed QSAR models.

A nicely proven correlation among salient capabilities of the molecules represented through molecular descriptors, and their bioactivity expands statistics approximately mechanistic elements of molecules, specificity, and quantity (presence or even absence) of various structural developments for preferred bioactivity. Although, withinside the QSAR analysis, we've as compared the  $K_i$  values of various molecules in correlation and as an impact of a specific molecular descriptor, a similar

TABLE 1 Statistical parameters for the developed QSAR model.

Statistical parameters	Model
<b>Fitting</b>	
R <sup>2</sup>	0.8120
R <sup>2</sup> <sub>adj</sub>	0.8168
R <sup>2</sup> -R <sup>2</sup> <sub>adj</sub>	0.0037
LOF	0.1807
K <sub>xx</sub>	0.2382
Delta K	0.0928
RMSE <sub>tr</sub>	0.4079
MAE <sub>tr</sub>	0.3276
RSS <sub>tr</sub>	49.5888
CCC <sub>tr</sub>	0.9014
s	0.4128
F	221.7565
<b>Internal validation</b>	
Q <sup>2</sup> <sub>LOO</sub>	0.8120
R <sup>2</sup> -Q <sup>2</sup> <sub>LOO</sub>	0.0085
RMSE <sub>cv</sub>	0.4175
MAE <sub>cv</sub>	0.3352
PRESS <sub>cv</sub>	51.9415
CCC <sub>cv</sub>	0.8968
Q <sup>2</sup> <sub>LMO</sub>	0.8123
R <sup>2</sup> <sub>Yscr</sub>	0.0197
RMSE AV <sub>Yscr</sub>	0.9534
Q <sup>2</sup> <sub>Yscr</sub>	-0.0283
<b>External validation</b>	
RMSE <sub>ext</sub>	0.4604
MAE <sub>ext</sub>	0.3803
PRESS <sub>ext</sub>	15.4724
R <sup>2</sup> <sub>ext</sub>	0.7829
Q <sup>2</sup> <sub>F1</sub>	0.7832
Q <sup>2</sup> <sub>F2</sub>	0.7819
Q <sup>2</sup> <sub>F3</sub>	0.7714
CCC <sub>ext</sub>	0.8742
r <sup>2</sup> <sub>m aver.</sub>	0.6607
r <sup>2</sup> <sub>m delta</sub>	0.1977
K'	0.9967
K	0.9999
Clos'	0.0496
Clos	0.0000

or contrary impact of different molecular descriptors or unknown descriptors has a dominant impact in figuring out the general Ki value of a molecule cannot be neglected. In different words, a single molecular descriptor is incapable of absolutely explaining the experimental Ki value for this sort of numerous set of molecules. That is, the successful usage of the advanced QSAR model is based on the concomitant usage of molecular descriptors.

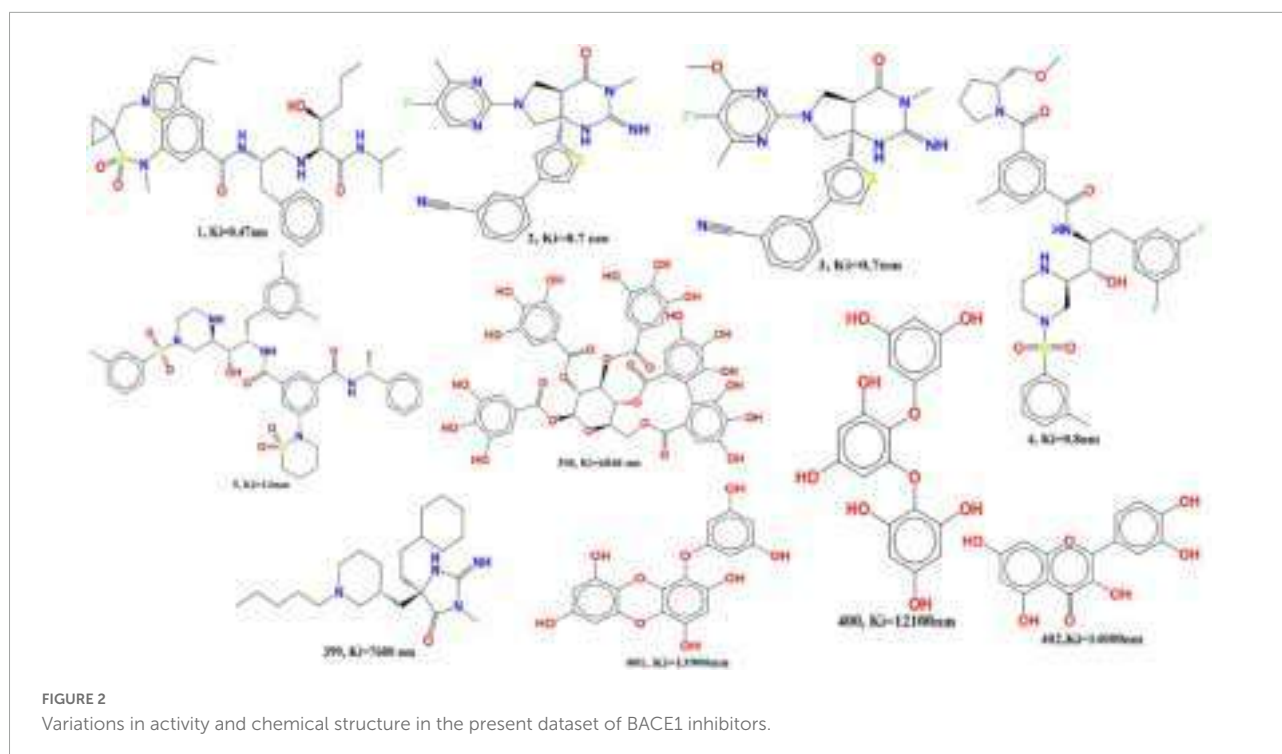
## Mechanistic interpretation

com\_lipohyd\_5A (occurrence of the lipo-hydrophobic atoms within 5A from the center of mass of the molecule) Since this descriptor received a positive coefficient in the developed QSAR model, increasing the value of the molecular descriptor com\_lipohyd\_5A was observed to increase BACE1 inhibitory activity. This can be observed by comparing the compound 368 (pKi = 7.75, com\_lipohyd\_5A = 14) with 48 (pKi = 6.37, com\_lipohyd\_5A = 13) for which an increase in the value of the molecular descriptor com\_lipohyd\_5A from 13 for the molecule 48 to the 14 will give rise to increase in pKi value by about 1 unit (about ten-fold increase in BACE1 inhibitory activity). This observation is further reinforced by the following pair of molecules; 243 (pKi = 7.35, com\_lipohyd\_5A = 8) and 134 (pKi = 6.93, com\_lipohyd\_5A = 7), 211 (pKi = 7.92, com\_lipohyd\_5A = 12) and 207 (pKi = 7.58, com\_lipohyd\_5A = 11), 189 (pKi = 8.4, com\_lipohyd\_5A = 15) and 255 (pKi = 8.19, com\_lipohyd\_5A = 10), 262 (pKi = 5.52, com\_lipohyd\_5A = 15) and 115 (pKi = 4.97, com\_lipohyd\_5A = 13), etc. Shifting the molecular descriptor com\_lipohyd\_5A with com\_lipohyd\_6A statistically improves the performance (R: 0.84) of the developed QSAR model, while replacing com\_lipohyd\_5A with com\_lipohyd\_4A statistically drops the performance of the QSAR model (R: 0.81). This observation underscores the importance of the molecular descriptor com\_lipohyd\_5A. In addition, the optimum distance between lipo-hydrophobic atoms from the center of mass of the molecule should be maintained at 6 Å to show better inhibitory activity against BACE1.

faccC3B (occurrence of the carbon atom exactly at three bonds from the acceptor atom). If the same descriptor exists in two or four bonding at the same time, it will be removed during the calculation of faccC3B. This descriptor received a positive sign in the developed QSAR model. Therefore, further increases in faccC3B value increase the inhibitory efficacy of BACE1 inhibitors. Comparison of the compound 331 (pKi = 7.6, faccC3B = 7) with 142 (pKi = 6.87, faccC3B = 6) illustrate the influence of the molecular descriptor faccC3B. If the value of the molecular descriptor faccC3B is enhanced from 6 for the molecule 142 to 7 will upsurge the pki value by about 1 unit (about 10-fold amplification in the BACE1 inhibitory activity). Following pair from **Figures 3C,D** of molecules support this observation; 295 (pKi = 8.72, faccC3B = 6) and 255 (pKi = 8.19, faccC3B = 4), 262 (pKi = 5.52, faccC3B = 3) and 115 (pKi = 4.97, faccC3B = 2), 258 (pKi = 8.7, faccC3B = 9) and 274 (pKi = 7.58, faccC3B = 8), 128 (pKi = 6.28, faccC3B = 3) and 60 (pKi = 6.1, faccC3B = 2), 169 (pKi = 8.7, faccC3B = 9) and 286 (pKi = 7.55, faccC3B = 7), etc.

This shows that simple carbon atoms along the 3-bond acceptor atom are essential for inhibitory efficacy, but the molecular descriptors faccC3B and fdonC3B (frequency of carbon atoms exactly 3 bonds away from the donor atom). Or





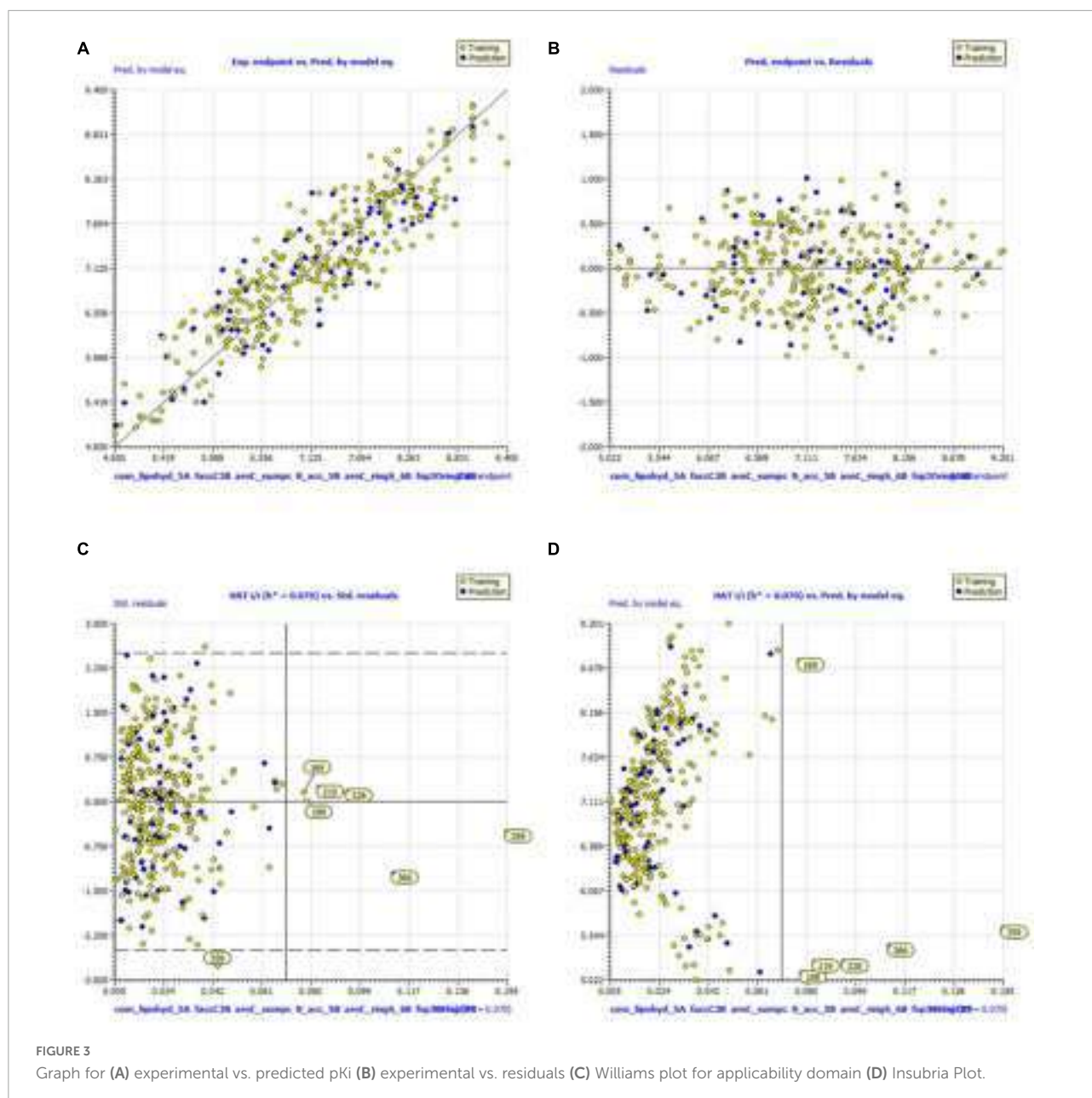
fdonlipo5B (an acceptor atom with exactly 5 bonds from the donor atom) greatly improves the statistical detection power of the developed QSAR model (fdonC3B, R: 0.89) (fdonlipo5B, R: 0.88). This observation shows that the inhibitory effect can be enhanced by replacing the acceptor atom with a donor atom with 3 bonds of the same topology distance, or by moving the carbon atom to any lipophilic atom along the donor by a distance of five bonds. This observation shows that the carbon atom is more important along the donor atom located at the optimum distance of the three bonds. Therefore, since most H-bond donors or acceptors are nitrogen or oxygen, the presence of donor atoms close to the carbon atom may help to enhance the interaction with the polar residues of the receptor (BACE1). In addition, the descriptor also shows the important role that carbon atoms definitely play in lipophilicity.

aroC\_sumpc (sum of partial charges on aromatic carbon atoms in the range of + 0.2 and -0.2). A positive coefficient for aroC\_sumpc indicates that the higher the value of this descriptor, the better the activity profile. The presence of a large number of carbon atoms makes the molecule lipophilic, while the presence of positively or negatively charged carbon atoms causes various types of hydrophobic interactions with the receptor (BACE1), such as pi-alkyl, pi-cation, and pi-pi stacking. This observation underscores the importance of the molecular descriptor aroC\_sumpc. This observation is supported by comparing the following pairs of molecules: 316 (pKi = 8.5, aroC\_sumpc = 0.224000013) and 23 (pKi = 7.4, aroC\_sumpc = -0.088000003),

159 (pKi = 9, aroC\_sumpc = 0.013999997) and 298 (pKi = 8.5, aroC\_sumpc = -0.197999999), 369 (pKi = 9, aroC\_sumpc = 0.356000006) and 109 (pKi = 8.14, aroC\_sumpc = -0.322999999), etc. This observation pointed out that negatively charged carbons are not favorable for BACE1 inhibitory activity, hence, ring carbon atom with neutral or positively charged possesses a better BACE1 inhibitory activity.

Subsequently, shifting the molecular descriptor aroC\_sumpc to the molecular descriptor ringC\_sumpc (sum of partial charges of the ring carbon atom) for future drug optimization increases the statistical power (R: 0.88) of the developed QSAR model. Furthermore, assuming that the molecular descriptor aroC\_sumpc is replaced with the molecular descriptor aroCminus\_sumpc (sum of partial charges of negatively charged aromatic carbon atoms), this reduces the statistical power (R: 0.75) of the QSAR model. Therefore, incorporating the ring carbon atom (ringC\_sumpc) is a better choice for future optimization of hits to the lead molecule for better inhibitory activity of BACE1.

N\_acc\_5B (occurrence of acceptor atom within 5 bonds from the nitrogen atom). The molecular descriptor N\_acc\_5B indicates that the acceptor atom is within the four bonds of the nitrogen atom. This molecular descriptor has a positive coefficient in the developed QSAR model, so increasing the number of such combinations can enhance BACE1 inhibition. The effect of N\_acc\_5B can be explained by comparing the molecule 258 (pKi = 8.7, N\_acc\_5B = 5) and 57 (pKi = 6.4, N\_acc\_5B = 3). For molecule 57, if the value of the molecule descriptor increase from 3 to 5 will further amplify the pKi value



by about 2 units, therefore, enhancing the BACE1 inhibitory activity by about 20 folds. These descriptors pointed out the importance of the nitrogen atom in BACE1 inhibitory activity. Moreover, additional molecular pair also illustrate the effect of N\_acc\_5B on BACE1 inhibitory activity include; 250 (pKi = 7.64, N\_acc\_5B = 5) and 55 (pKi = 6.52, N\_acc\_5B = 3), 189 (pKi = 8.4, N\_acc\_5B = 5) and 252 (pKi = 7.57, N\_acc\_5B = 4), 297 (pKi = 8.0, N\_acc\_5B = 8) and 102 (pKi = 7.17, N\_acc\_5B = 7), 312 (pKi = 8.5, N\_acc\_5B = 4) and 213 (pKi = 6.2, N\_acc\_5B = 3), etc.

The shift of the molecular descriptor N\_acc\_5B by the molecular descriptor N\_acc\_2B (the occurrence of acceptor

atoms within two bonds from the nitrogen atom) strongly affects the statistical performance (R: 0.86) of the developed QSAR model (N\_don\_5B). This observation shows that the subsequent descriptor is N\_acc\_2B, which is useful as a better alternative to future drug optimization and to enhance the BACE1 inhibitor activity. Again, it is suggested that the optimum distance between the acceptor atom and the nitrogen atom may be two bonds.

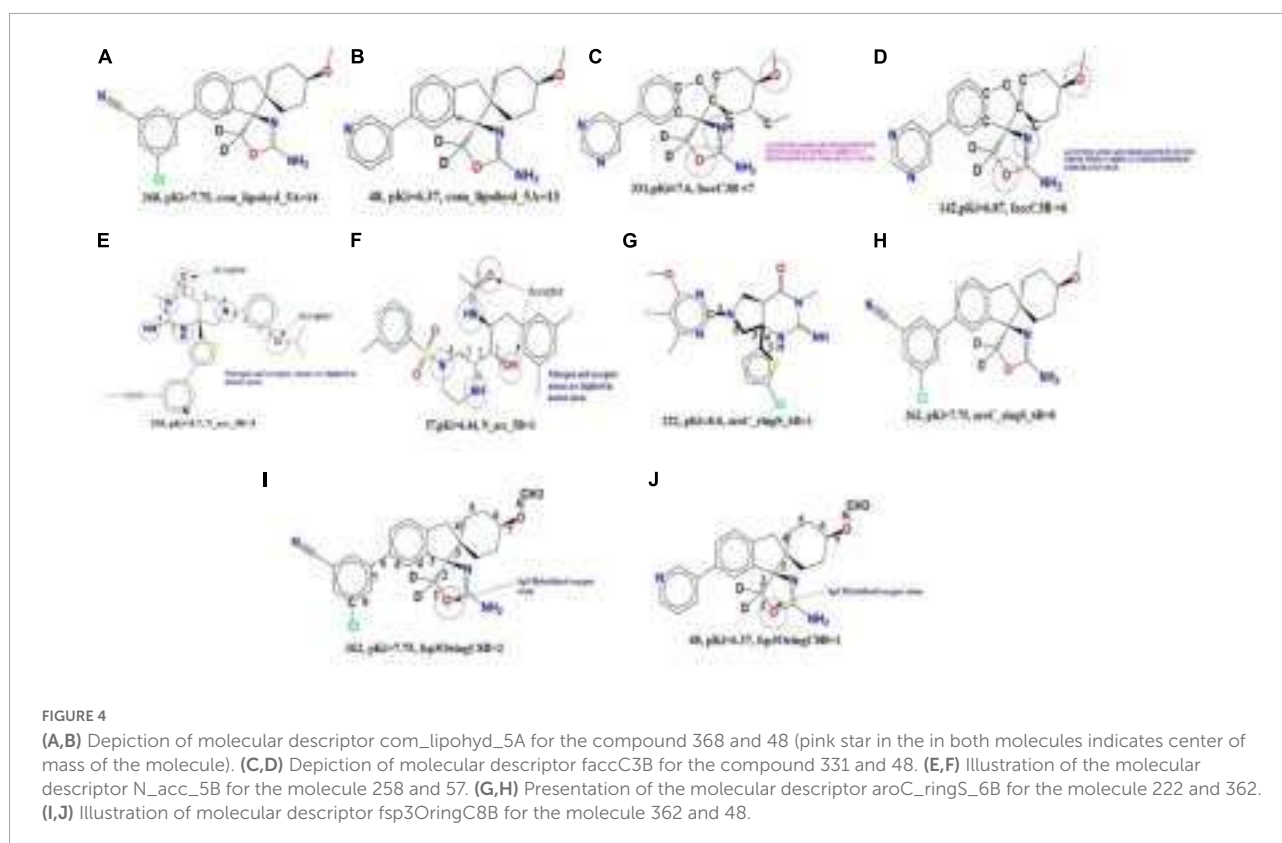
On the other hand, replacing the molecular descriptor N\_acc\_5B with the molecular descriptor N\_don\_5B (the appearance of a donor atom within 5 bonds from the nitrogen atom) significantly increases the statistical power (R: 0.85)

of the developed QSAR model. This remark reveals two strategies for future optimization, consisting of reducing the topological distance from five bonds to two bonds according to the  $N\_acc\_2B$  descriptor, and replacement of acceptors with donors by maintaining the optimal distance of five bonds. This observation underscores the importance of nitrogen atoms and acceptor/donor properties for better inhibitory activity of BACE1.

$aroC\_ringS\_6B$  (occurrence of the ring sulfur atoms within six bonds from the aromatic carbon atoms). The positive coefficient of the developed QSAR model descriptor justifies the increase in the value of the  $aroC\_ringS\_6B$  descriptor and further enhances the BACE1 inhibitory activity. Shifting the molecular descriptor  $aroC\_ringS\_6B$  by  $fringSringC3B$  (frequency of ring carbon atoms in exactly three bonds from the ring sulfur atom) significantly increases the statistical power ( $R:0.91$ ) of the QSAR model. By comparing the molecule 222 ( $pK_i = 8.0$ ,  $aroC\_ringS\_6B = 1$ ) and 362 ( $pK_i = 7.75$ ,  $aroC\_ringS\_6B = 0$ ), the influence of  $aroC\_ringS\_6B$  as illustrated in the **Figures 4A–J**. Moreover, amplification in the value of the molecular descriptor  $aroC\_ringS\_6B$  from 0 to 1 for the molecule will uplift the  $pK_i$  value by about 0.75 units (about 7 fold increase in the BACE1 inhibitory activity). Another pair of molecules also illustrate the effect of  $aroC\_ringS\_6B$  on BACE1 inhibitory activity include; 256 ( $pK_i = 8.5$ ,  $aroC\_ringS\_6B = 2$ ) and 2 ( $pK_i = 7.5$ ,

$aroC\_ringS\_6B = 1$ ), 295 ( $pK_i = 8.7$ ,  $aroC\_ringS\_6B = 2$ ) and 324 ( $pK_i = 7.3$ ,  $aroC\_ringS\_6B = 0$ ), 189 ( $pK_i = 8.4$ ,  $aroC\_ringS\_6B = 2$ ) and 254 ( $pK_i = 8.1$ ,  $aroC\_ringS\_6B = 1$ ), 144 ( $pK_i = 7.8$ ,  $aroC\_ringS\_6B = 2$ ) and 140 ( $pK_i = 7.0$ ,  $aroC\_ringS\_6B = 0$ ), etc.

Furthermore, replacing the molecular descriptor  $aroC\_ringS\_6B$  with  $fringSringC5B$  (frequency of ring carbon atoms in exactly five bonds from the ring sulfur atom) shows an increase in the statistical power ( $r: 0.94$ ) of the developed QSAR model. On the other hand, replacing the molecular descriptor  $aroC\_ringS\_6B$  with  $fringSC6B$  (frequency of carbon atoms appearing in exactly 6 bonds from the ring sulfur atom) significantly reduces the statistical power ( $R: 0.80$ ) of the QSAR model. This observation emphasizes the importance of the ring carbon atom and the ring sulfur atom. Furthermore, it can be concluded that reducing the topology bond distance from six to five bonds strongly affects the inhibitory activity of BACE1. Therefore, in future drug designs, it is recommended to keep the optimal distance between the ring carbon and the ring sprue atom at five bonds in order to increase the inhibitory activity of base 1. Aromatic and heterocyclic rings are very powerful motifs in drug discovery with target proteins such as the classical arene-arene interactions ( $\pi$  stacking),  $\pi$ -sulfur interactions, and arene-cation interaction. It offers many unique and powerful interactions such as bonds (end-face interactions) and recently identified  $\pi$  cations.



fsp3OringC8B (frequency of occurrence of the ring carbon atom exactly at eight bonds from the sp<sup>3</sup> oxygen atom) If the same ring carbon atom occurs simultaneously in seven or nine bonds, it will be bypassed in the fsp3OringC8B calculation. This molecular descriptor has a positive coefficient in the developed QSAR model, so increasing its value can improve the Ki value.

The effect of fsp3OringC8B can be assessed by comparing the molecule 362 9 (pKi = 7.75, fsp3OringC8B = 2) with 48 (pKi = 6.37, fsp3OringC8B = 1). Increasing the value of fsp3OringC8B for molecule 1 to 2 for molecule 48 will upsurge the pKi value by 1.38unit (about 13-fold amplification in the BACE1 inhibitory potential). Following pair of molecules also explain the effect of fsp3OringC8B on BACE1 inhibitory activity; 211 (pKi = 7.9, fsp3OringC8B = 3) and 207 (pKi = 7.5, fsp3OringC8B = 1), 299 (pKi = 8.7, fsp3OringC8B = 2) and 255 (pKi = 8.1, fsp3OringC8B = 1), 352 (pKi = 8.4, fsp3OringC8B = 2) and 30 (pKi = 6.0, fsp3OringC8B = 0), 110 (pKi = 7.5, fsp3OringC8B = 4) and 66 (pKi = 6.5, fsp3OringC8B = 0), etc. Replacing the fsp3OringC8B molecular descriptor with the fsp3OringC9B descriptor significantly reduces the statistical power (R: 0.78) of the developed QSAR model.

This observation underscores the importance of the molecular descriptor fsp3OringC8B. Therefore, future drug designs need to maintain the optimal distance between sp<sup>3</sup> hybridized oxygen and ring carbon atoms at eight bonds in order to achieve better BACE1 inhibitory activity. Most oxygen atoms act as either acceptors or ether linkage, which can confer lipophilicity on the molecule. This may help to enhance both polar and hydrophobic interactions with the BACE1 receptor.

## Molecular docking for validation of docking score

In molecular docking analysis of the BACE1 with FDB017657 in Autodock output, a dock complex displayed the best conformation. Receptors and ligands were saved in the.pdbqt format for subsequent usage using the MGL 1.5.6 suite. Vina was launched from a command prompt using the command line. In the setup, the default grid point spacing was 0.525 and the exhaustiveness was set to 8. The output files were in.pdbqt format, and they were analyzed using PyMol and the Discovery studio visualizer 2021. The ligand-binding was validated and optimized using the co-crystal ligand. Both the receptor and ligands were made by combining 48 polar hydrogen bonds and detecting 1 rotatable bond and adding Kollman and Gasteiger charges. Finally, both receptor and ligand molecules were stored in the.pdbqt format. With the values  $X = -1.655$ ,  $Y = 57.005$ , and  $Z = 133.83$ , a grid box was produced with a spacing of 0.375. Docking experiments of the protein-ligand complex were carried out using Genetic Algorithm (GA) parameters were set with 100, population

TABLE 2 Screening of phytochemicals based on their best binding energy.

Protein-ligand	Binding affinity (kcal/mol)
2zhv_8265	-4.8
2zhv_8263	-4.7
2zhv_8262	-7.3
2zhv_8079	-4.7
2zhv_7888	-5
2zhv_7701	-6.4
2zhv_7594	-6.3
2zhv_7334	-2.9
2zhv_7032	-4.9
2zhv_6574	-5.1
2zhv_5179	-5.6
2zhv_4844	-7.6
2zhv_4817	-5.6
2zhv_4693	-4.9
2zhv_4688	-5.8
2zhv_4605	-5.5
2zhv_4468	-8.9
2zhv_4340	-7.6
2zhv_4009	-5.7
2zhv_3981	-4.6
2zhv_3805	-4.7
2zhv_3207	-5.7
2zhv_2839	-4.8
2zhv_1976	-5.4
2zhv_1749	-5.7
2zhv_734	-7.3
2zhv_686	-6.7
2zhv_673	-8.3
2zhv_603	-6.5
2zhv_442	-4.5
2zhv_41	-3.8
2zhv_4	-5.6

size was made 300 with a maximum number of evaluates was set to low at 2,500,000 and maximum generations of 27,000. Further docking experiments of the protein-ligand complex were carried out using the Lamarckian Genetic Algorithm (LGA) to obtain the lowest free energy of binding (G). The 2ZHV-FDB017657 complex showed free energy of binding ( $\Delta G$ ) -8.9 kcal/mol, inhibitory concentration (Ki) 990.57  $\mu$ M, ligand efficiency -1.26, total internal energy -1.45 kJ/mol, and torsional energy 0.3 kJ/mol. The docking scores are mentioned in **Table 2**.

The principal residues making the binding pocket around 4-(3,4-dihydroxyphenyl)-2-hydroxy-1H-phenalen-1-one (Food I.D: FDB017657) are comprised of THR72, THR231, GLY230, ASP228, GLY34, ILE118, SER35, PHE108, ASP106, LYS107, GLY74, and GLN73 by Van der Waals interaction forces; ASP32

is involved in conventional hydrogen bonding, while TYR71 is involved in forming a conventional Pi-Pi bond (Figure 5, left).

## Molecular dynamics simulation (MD) and free energy landscape analysis

Molecular dynamics and simulation (MD) studies were carried out to determine the stability and convergence of the 4-(3,4-Dihydroxyphenyl)-2-hydroxy-1H-phenalen-1-one (PubChem I.D: 4468; Food I.D: FDB017657) bound BACE1 (PDB I.D: 2ZHV) complex. Each simulation of 150 ns displayed stable conformation while comparing the root mean square deviation (RMSD) values.

The Root Mean Square Deviation (RMSD) is a metric for calculating the average change in the displacement of a group of atoms in relation to a reference frame. It is calculated for each and every frame of the trajectory. The RMSD for frame  $x$  is:

$$RMSD_x = \sqrt{\frac{1}{N} \sum_{i=1}^N (r'_i(t_x) - r_i(t_{ref}))^2}$$

where  $N$  is the number of atoms in the atom selection;  $t_{ref}$  is the reference time (the first frame is usually used as the reference and is treated as time  $t = 0$ ); and where  $r'$  is the position of the selected atoms after superimposing on the reference frame in frame  $x$ , where frame  $x$  is recorded at time  $t_x$ . Every frame in the simulation trajectory is subjected to the same technique (Mayorov and Crippen, 1994).

For characterizing local changes along the protein chain, the Root Mean Square Fluctuation (RMSF) is useful. The RMSF for residue  $i$  is:

$$RMSF_i = \sqrt{\frac{1}{T} \sum_{t=1}^T \langle (r'_i(t) - r_i(t_{ref}))^2 \rangle}$$

The angle brackets indicate that the average of square distance is taken over the selection of atoms in the residue. where  $T$  is the trajectory time over which the RMSF is calculated,  $t_{ref}$  is the reference time,  $r_i$  is the position of residue  $i$   $r'$  is the position of atoms in residue  $i$  after superposition on the reference. Its simulation paths of Desmond were examined. MD trajectory analysis was used to calculate the root mean square deviation (RMSD), root mean square fluctuation (RMSF), and protein–ligand interactions. Protein RMSD: The graphs depict the evolution of a protein's RMSD (left Y-axis). The RMSD is estimated based on the atom selection once all protein frames are aligned on the reference frame backbone.

The  $\alpha$ -backbone of BACE1 bound to 4-(3,4-dihydroxyphenyl)-2-hydroxy-1H-phenalen-1-one (PubChem I.D: 4468; Food I.D: FDB017657) exhibited a deviation of 0.4 Å (Figure 6A). RMSD plots are within the acceptable range signifying the stability of proteins in the FDB017657 bound state before and after simulation and it can also be suggested

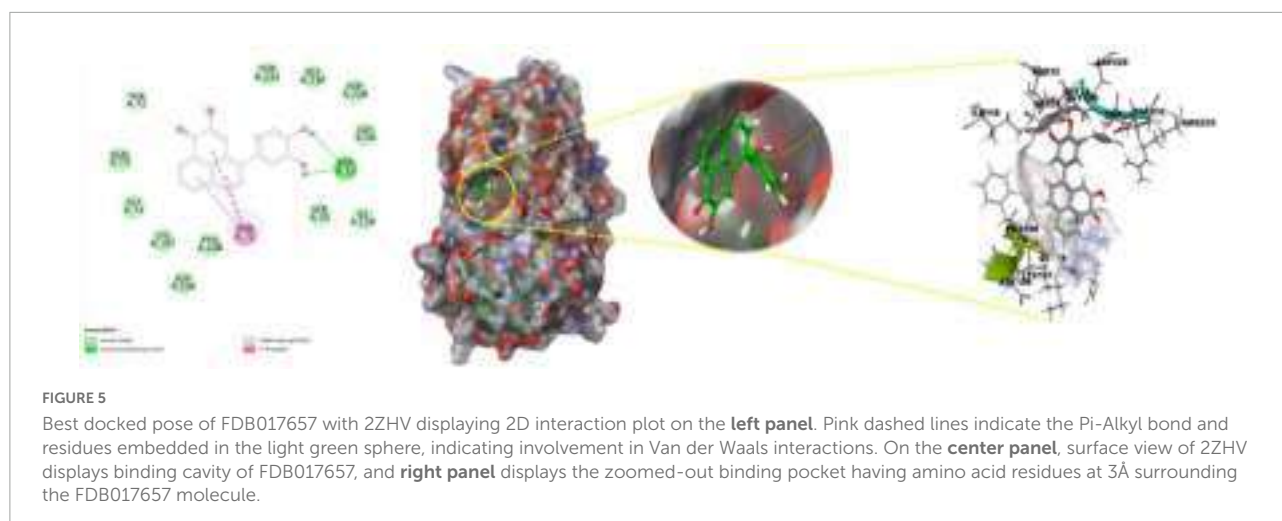
that FDB017657 bound BACE1 (PDB I.D: 2ZHV) is quite stable in the complex might be due to significant binding of the ligand.

The radius of gyration is the measure of the compactness of the protein. FDB017657 bound proteins displayed a lowering of radius of gyration (Rg) (Figure 6B; R1, R2, R3). The lowering of Rg indicates the compactness of the protein–ligand complex. From the overall quality analysis from RMSD and Rg, it can be suggested that FDB017657 bound to the protein targets posthumously in the binding cavities and plays a significant role in the stability of the proteins.

The plots for root mean square fluctuations (RMSF) displayed a significant RMSF in BACE1 protein at a few residues at the specific time function of 150 ns. Peaks show sections of the protein that fluctuate the greatest during the simulation on the RMSF plot. Typically, the tails (N- and C-terminal) of proteins change more than any other portion of the protein. Secondary structural parts such as alpha helices and beta strands are usually more rigid than the unstructured portion of the protein and fluctuate less than loop areas. The residues with higher peaks belong to loop areas or N and C-terminal zones, as determined by MD trajectories (Figure 6C). The stability of ligand binding to the protein is shown by low RMSF values of binding site residues. From the triplicate runs of BACE1, as shown in Figure 6C, a few fluctuating peaks can be seen although mostly the complex is found to be stabilized as shown in Figure 6C. The RMSF values are acceptable for stabilizing the protein–ligand complex. Therefore, in RMSF plots, it can be suggested that the protein structures were stable during simulation in FDB017657 bound conformation.

The average hydrogen bonds formed between FDB017657 and the respective protein, BACE1 (PDB I.D: 2ZHV), during the 150 ns simulation were also recorded (Figure 6D). From 0 ns to 150 ns a formation of hydrogen bonding was found throughout the simulation and the same for triplicate MD simulation of FDB017657 with BACE1 (Figure 6D). Moreover, the pattern of two hydrogen bond formation with BACE1 (PDB I.D: 2ZHV), in docking was corroborated by the number of hydrogen plot analyses after 150 ns molecular dynamics (Figure 6D). The amount of hydrogen bonds between BACE1 with FDB017657 has strengthened the binding and facilitated to conform to a more stable complex during the simulation.

Throughout the simulation, protein interactions with the ligand can be observed. As seen in the graph above, these interactions can be classified and summarized by type. Hydrogen bonds, hydrophobic, ionic, and water bridges are the four forms of protein–ligand interactions (or “contacts”). Each interaction type has a number of subtypes that can be examined using Maestro's “Simulation Interactions Diagram” panel (see Figure 7A). The stacked bar charts are standardized over the course of the trajectory. Some protein residues may make several interactions of the same subtype with the ligand, values above 1.0 are feasible. As shown in Figure 7A, the majority of



the significant ligand–protein interactions discovered by MD are hydrogen bonds and hydrophobic interactions. For 2ZHV-FDB017657, complex residues VAL\_31, ASP\_32, TYR\_71, and THR\_72 are the most important ones in terms of H-bonds.

Individual ligand atom interactions with protein residues are depicted in **Figure 7B**. Interactions that occur for more than 30.0% of the simulation period in the chosen trajectory (0.00 through 150.0 ns) are displayed. From **Figure 7B**, it can be concluded that the amino acid residues: PHE108, TRP76, TYR71, and VAL69 involve a hydrophobic interaction, LYS107, ARG128 possess a positive charge bonding with the ligand, GLN73, SER35, and ASN37 are involved in polar interactions, and ASP32 and ASP228 are involved in negatively charged interaction with the ligand, FDB017657 in 150 ns simulation time scale.

Throughout the simulation, the existence of protein secondary structural elements (SSE) such as alpha helices and beta strands is examined to ensure that they are not present. The plot shown in **Figure 7C** depicts the distribution of SSE by residue index over the complete protein structure, and it encompasses the full protein structure. In contrast to the charts, which show the summary of the SSE composition for each trajectory frame during the course of the simulation, the graphs at the bottom show the evolution of each residue and its SSE assignment throughout the experiment. Throughout the simulation, alpha-helices and beta-strands are monitored as secondary structure elements (SSE). The left graph shows the distribution of SSE across the protein structure by the residue index. The top image highlights the SSE composition for each trajectory frame throughout the simulation, while the bottom plot tracks each residue's SSE assignment through time.

It can be observed from **Figure 7D**, how each rotatable bond (RB) in the ligand alters its conformation throughout the simulation on the ligand torsions map (0.00 through 150.15 ns). The top panel shows a two-dimensional schematic of a ligand with color-coded rotatable bonds. There includes a dial plot

as well as bar plots in the same color for each rotatable bond torsion. The evolution of the torsion's conformation during the simulation is depicted using dial (or radial) graphs. The simulation's time evolution is depicted radially outwards from the simulation's start point at the center of the radial plot. The data from the dial plots are summarized in the bar plots, which show the torsion probability density in the data. Alternatively, if torsional potential data is available, the graphic will also indicate the rotatable bond's potential (by summing the potential of the related torsions) kcal/mol. The potential values are given as kcal/mol and plotted on the graph's left Y-axis. The histogram and torsion potential correlations can reveal the conformational strain that the ligand is under in order to maintain a protein-bound conformational state.

The stepwise trajectory analysis of every 25 ns of simulation of FDB017657 with BACE1 displayed the positional alteration with reference to the 0 ns structure (**Figure 8**). It has been observed that the ligand, FDB017657 has possessed a structural angular movement at the end frame to achieve its conformational stability and convergence.

The free energy landscape (FEL) of achieving global minima of C $\alpha$  backbone atoms of proteins with respect to RMSD and radius of gyration (Rg) is displayed in **Figure 9**, BACE1 bound to the ligand, FDB017657 achieved the global minima (lowest free energy state) at 1.1 Å and Rg 20.9 Å (**Figure 9**). The FEL envisaged a deterministic behavior of BACE1 to the lowest energy state owing to its high stability and best conformation at FDB017657 bound state.

## Molecular mechanics generalized born and surface area calculations

To assess the binding energy of ligands to protein molecules, the MMGBSA technique is commonly employed. The binding free energy of each BACE1– FDB017657 complex, as well

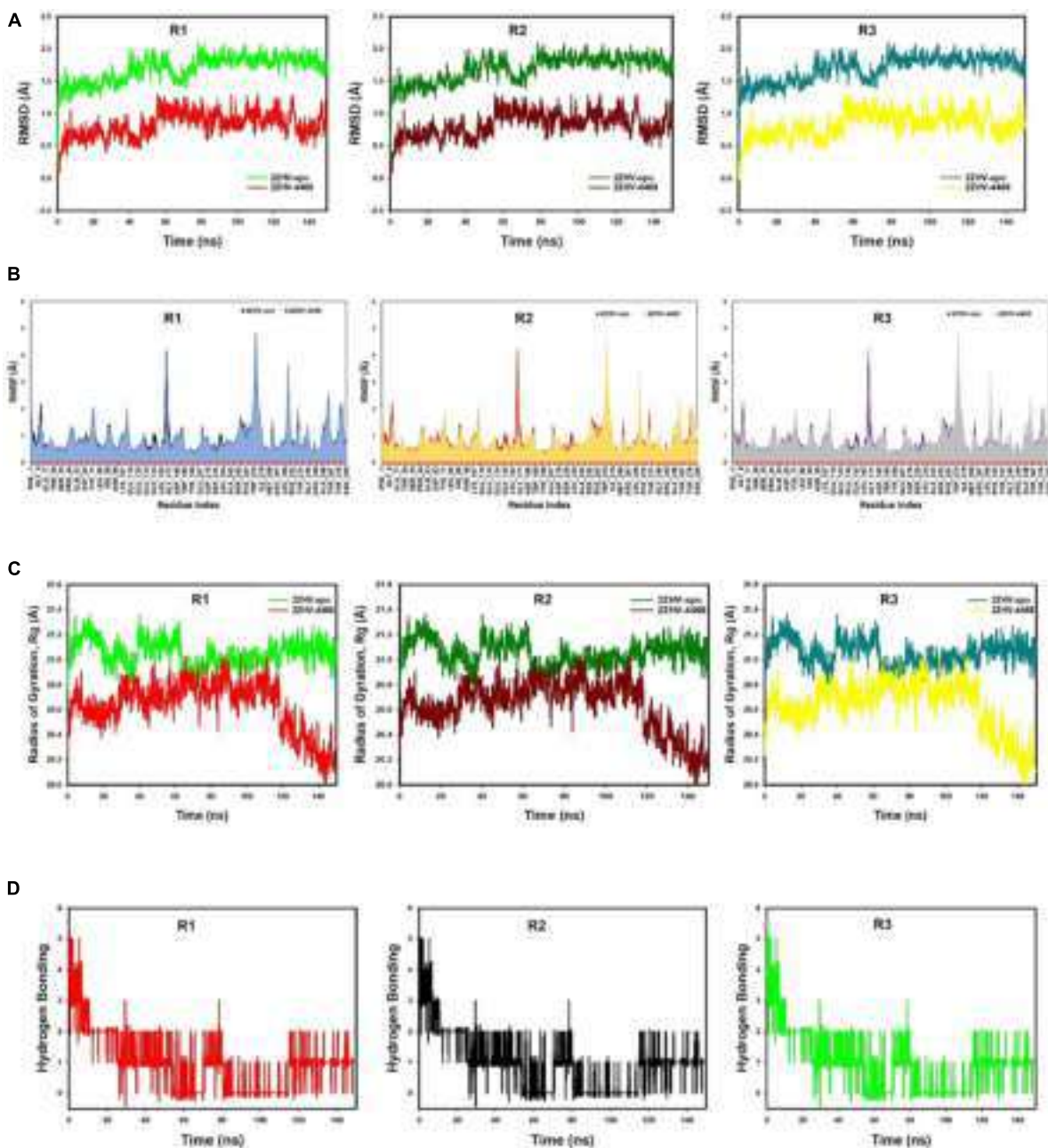


FIGURE 6

(A) MD simulation trajectory analysis of Root Mean Square Deviations (RMSD) of FDB017657 bound with 2ZHV, i.e., BACE1 150 ns time frame in triplicate displayed: R1 (replicate 1) RMSD plot of FDB017657 bound BACE1 (PDB I.D: 2ZHV) (red) with control protein BACE1 (PDB I.D: 2ZHV) (light green); R2 (replicate 2) RMSD plot of FDB017657 bound BACE1 (PDB I.D: 2ZHV) (dark maroon) with control protein BACE1 (PDB I.D: 2ZHV) (juniper green); R3 (replicate 3) RMSD plot of FDB017657 bound BACE1 (PDB I.D: 2ZHV) (lemon yellow) with control protein BACE1 (PDB I.D: 2ZHV) (cyan). (B) MD simulation trajectory analysis of Root Mean Square Fluctuations (RMSF) of FDB017657 bound with BACE1 (PDB I.D: 2ZHV) at 150 ns time frame in triplicate displayed: R1 (replicate 1) RMSF plot of FDB017657 bound BACE1 (PDB I.D: 2ZHV) (navy blue) with control protein BACE1 (PDB I.D: 2ZHV) (black); R2 (replicate 2) RMSF plot of FDB017657 bound BACE1 (PDB I.D: 2ZHV) (canary yellow) with control protein BACE1 (PDB I.D: 2ZHV) (red); R3 (replicate 3) RMSF plot of FDB017657 bound BACE1 (PDB I.D: 2ZHV) (gray) with control protein BACE1 (PDB I.D: 2ZHV) (purple). (C) MD simulation trajectory analysis of Radius of gyration (Rg) of FDB017657 bound with BACE1 (PDB I.D: 2ZHV) at 150 ns time frame in triplicate displayed: R1 (replicate 1) Rg plot of FDB017657 bound BACE1 (PDB I.D: 2ZHV) (red) with control protein BACE1 (PDB I.D: 2ZHV) (light green); R2 (replicate 2) Rg plot of FDB017657 bound BACE1 (PDB I.D: 2ZHV) (dark maroon) with control protein BACE1 (PDB I.D: 2ZHV) (juniper green); R3 (replicate 3) Rg plot of FDB017657 bound BACE1 (PDB I.D: 2ZHV) (cyan) with control protein BACE1 (PDB I.D: 2ZHV) (lemon yellow). (D) MD simulation trajectory analysis of Hydrogen Bonding (H-Bonds) of FDB017657 bound with BACE1 (PDB I.D: 2ZHV) at 150 ns time frame in triplicate displayed: R1 (replicate 1) H-Bond plot of FDB017657 bound BACE1 (PDB I.D: 2ZHV) (red); R2 (replicate 2) H-Bond plot of FDB017657 bound BACE1 (PDB I.D: 2ZHV) (black); R3 (replicate 3) H-Bond plot of FDB017657 bound BACE1 (PDB I.D: 2ZHV) (light green).

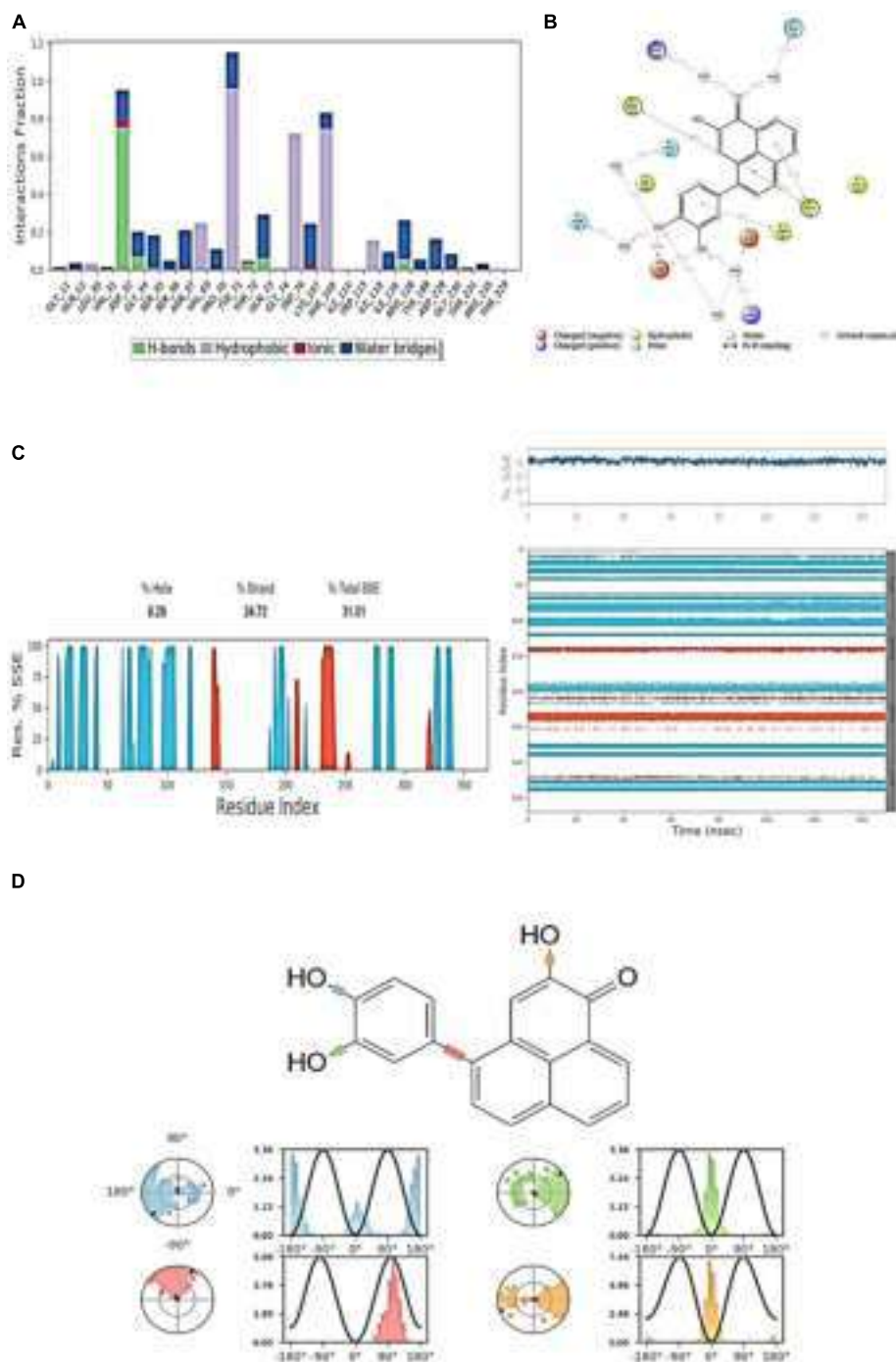


FIGURE 7

(A) Protein-ligand contact histogram (H-bonds, Hydrophobic, Ionic, Water bridges) of the ligand, FDB017657 bound with 2ZHV recorded in a 150 ns simulation interval. (B) Ligand atom interactions with the protein residues of 2ZHV bound with FDB017657. (C) Secondary Structure element distribution by residue throughout the protein structure. Red indicates alpha helices, and blue indicate beta-strands of 2ZHV bound with FDB017657. (D) Ligand torsion profile.

as the impact of other non-bonded interaction energies, were estimated. With BACE1, the ligand FDB017657 has a binding energy of  $-53.4670$  kcal/mol. Non-bonded interactions like  $G_{\text{bindCoulomb}}$ ,  $G_{\text{bindCovalent}}$ ,  $G_{\text{bindHbond}}$ ,  $G_{\text{bindLipo}}$ ,

$G_{\text{bindSolvGB}}$ , and  $G_{\text{bindvdW}}$  govern  $G_{\text{bind}}$ . Across all types of interactions, the  $G_{\text{bindvdW}}$ ,  $G_{\text{bindLipo}}$ , and  $G_{\text{bindCoulomb}}$  energies contributed the most to the average binding energy. On the other side, the  $G_{\text{bindSolvGB}}$  and  $G_{\text{bindCovalent}}$



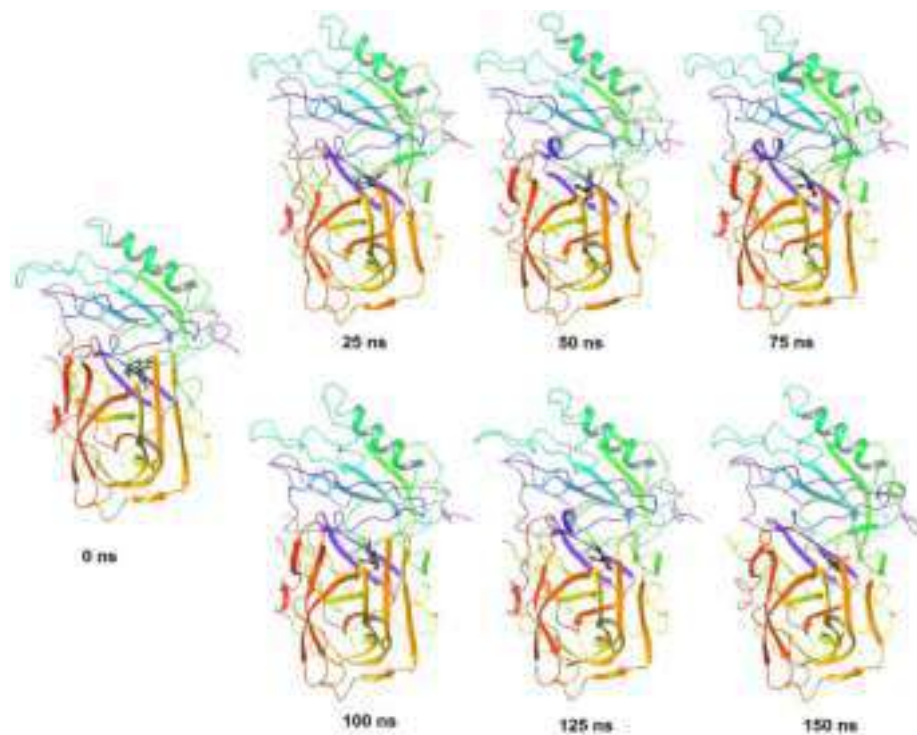


FIGURE 8

Stepwise trajectory analysis for every 25 ns displaying the protein, BACE1 (PDB I.D: 2ZHV) and ligand conformation during 150 ns of simulation of 4-(3,4-Dihydroxyphenyl)-2-hydroxy-1H-phenalen-1-one (PubChem I.D: 4468; Food I.D: FDB017657).

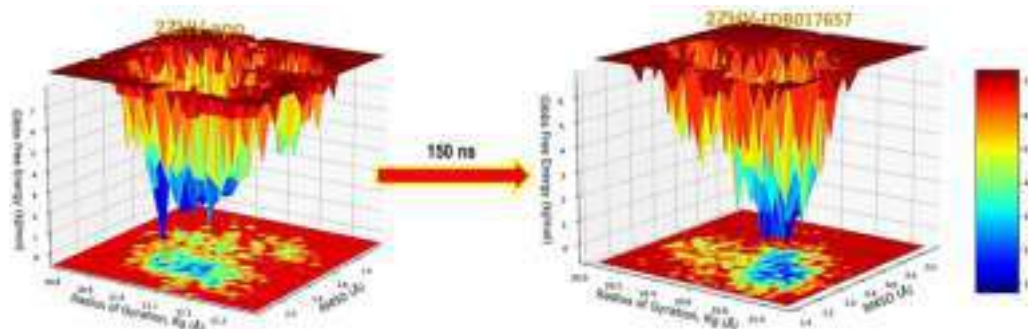


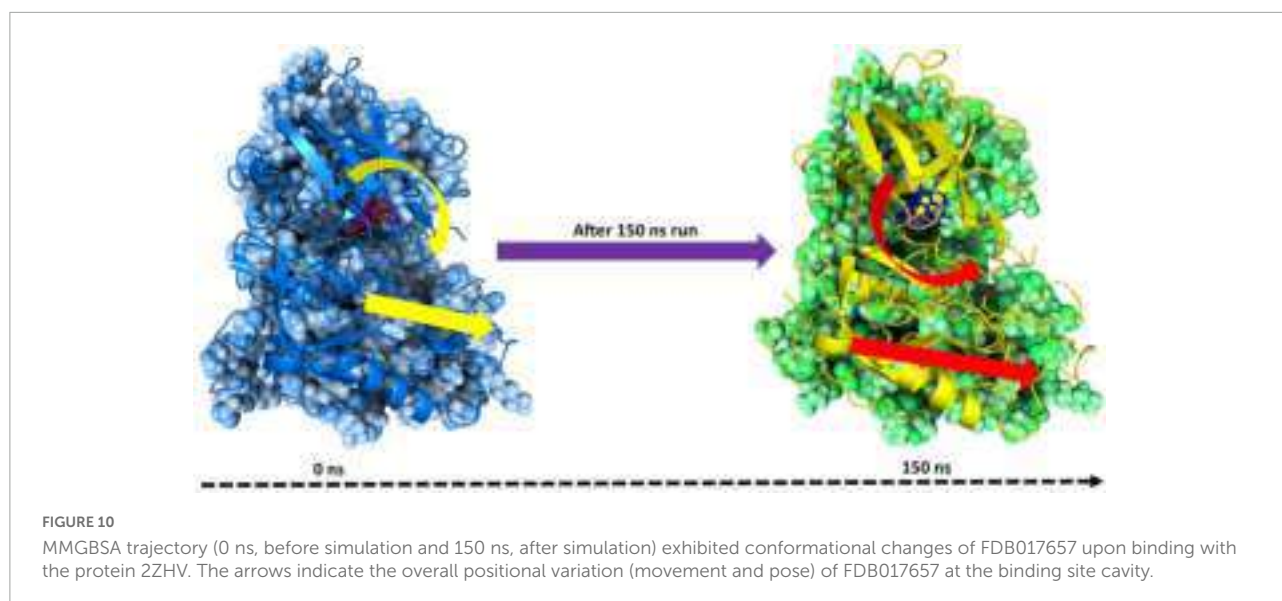
FIGURE 9

Free Energy Landscapes displaying the achievement of global minima ( $\Delta G$ , kJ/mol) of BACE1 in presence of FDB017657 with respect to their RMSD (nm) and Radius of gyration ( $R_g$ , nm).

energies contributed the least to the final average binding energies. Furthermore, the  $G_{\text{bind}}^{\text{Hbond}}$  interaction values of BACE1–FDB017657 complexes demonstrated stable hydrogen bonds with amino acid residues. In all of the compounds,  $G_{\text{bind}}^{\text{SolvGB}}$  and  $G_{\text{bind}}^{\text{Covalent}}$  exhibited unfavorable energy contributions and so opposed binding. **Figure 10** (left panel) reveals that between pre-simulation (0 ns) and post-simulation (150 ns), FDB017657 in the binding pocket of BACE1 has undergone a large angular change in the pose (curved to

straight) (150 ns). These conformational changes lead to better binding pocket acquisition and interaction with residues, which leads to enhanced stability and binding energy (mentioned in **Table 3**).

Thus, MM-GBSA calculations resulted from MD simulation trajectories well justified with the binding energy obtained from docking results; moreover, the last frame (150 ns) of MMGBSA displayed the positional change of FDB017657 as compared to the 0 ns trajectory signifying the better binding



pose for best fitting in the binding cavity of the protein (see [Figure 10](#)).

Therefore, it can be suggested that the FDB017657 molecule has a good affinity for the major target BACE1.

### Dynamic cross-correlation, principal component analysis (PCA), and energy calculations

Molecular dynamics simulation trajectories are analyzed for dynamic cross-correlation among the domains within protein chains bound with the FDB017657 molecule. For correlative dynamic motion, the cross-correlation matrices of BACE1 were generated and displayed in [Figure 11](#). The blue blocks displayed in the figure indicated the residues having high correlated movement and red having the least correlation. The amino acid residues of FDB017657 bound BACE1 showed the concerted movement of residues ([Figure 11](#)).

Principal component analysis (PCA) determines the relationship between statistically meaningful conformations

(major global motions) sampled during the trajectory. PCA of the MD simulation trajectories for BACE1 bound to the FDB017657 molecule was analyzed to interpret the randomized global motion of the atoms of amino acid residues. The internal coordinates mobility into three-dimensional space in the spatial time of 150 ns were recorded in a covariance matrix and the rational motion of each trajectory is interpreted in the form of orthogonal sets or Eigen vectors. In the BACE1 trajectory, PCA indicates statistically significant conformations. It is possible to identify the major motions within the trajectory as well as the critical motions required for conformational changes. In BACE1 bound to FDB017657, two different clusters along the PC1 and PC2 planes are exhibited that indicate a non-periodic conformational shift ([Figure 12A](#)). While these global motions are periodic because the groupings along the PC3 and PC4 planes do not totally cluster separately ([Figure 12B](#)). Moreover, a high periodic global motion was observed along the PC9 and PC10 planes due to the grouping of trajectories in a single cluster at the center of the PCA plot ([Figure 12C](#)). Centering of the trajectories in a single cluster indicates the periodic motion of MD trajectories due to stable conformational global motion.

The energy profiles of the protein, BACE1 and FDB017657 complex systems, were determined to display the stability of the entire system. In this regard, the total energy (ETOT) of the BACE1 bound FDB017657 system was shown to be very stable with an average total energy of  $-69.00$  kcal/mol (green). However, van der Waal's energy (vdW) displayed to be merged over the total energy with an average energy of  $-40.00$  kcal/mol and contemplated as a principal contributor to the stability of the BACE1-FDB017657 complex (cyan). In addition, Coulombic interactions played a minor role in the system stability and contributed to an average energy of  $-32.00$  kcal/mol (red), (see [Figure 12D](#)).

**TABLE 3** Binding energy calculation of FDB017657 with 2ZHV and non-bonded interaction energies from MMGBSA trajectories.

Energies (kcal/mol)	2ZHV
$\Delta G_{\text{bind}}$	$-53.467 \pm 3.001$
$\Delta G_{\text{bindLipo}}$	$-22.124 \pm 2.448$
$\Delta G_{\text{bindvdW}}$	$33.667 \pm 0.0701$
$\Delta G_{\text{bindCoulomb}}$	$-9.827 \pm 5.083$
$\Delta G_{\text{bindHbond}}$	$-1.465 \pm 0.775$
$\Delta G_{\text{bindSolvGB}}$	$-8.989 \pm 1.695$
$\Delta G_{\text{bindCovalent}}$	$-1.079 \pm 1.049$

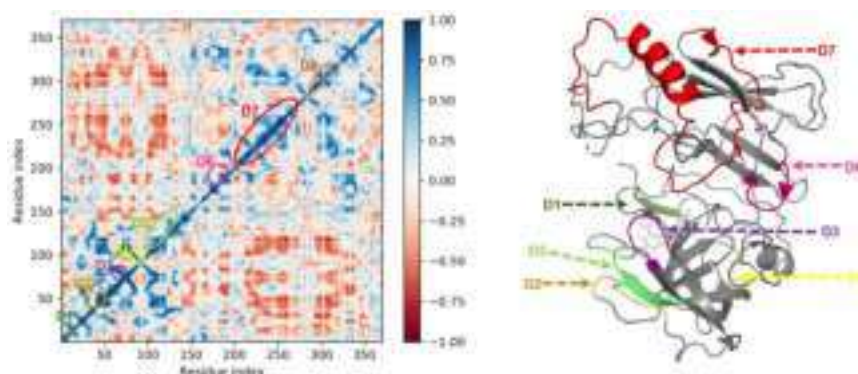


FIGURE 11

Dynamic Cross Correlation matrix (DCCM) of 2ZHV and correlated amino acids conformed into secondary structural domains (colored) and non-correlated domains (gray) of 2ZHV.

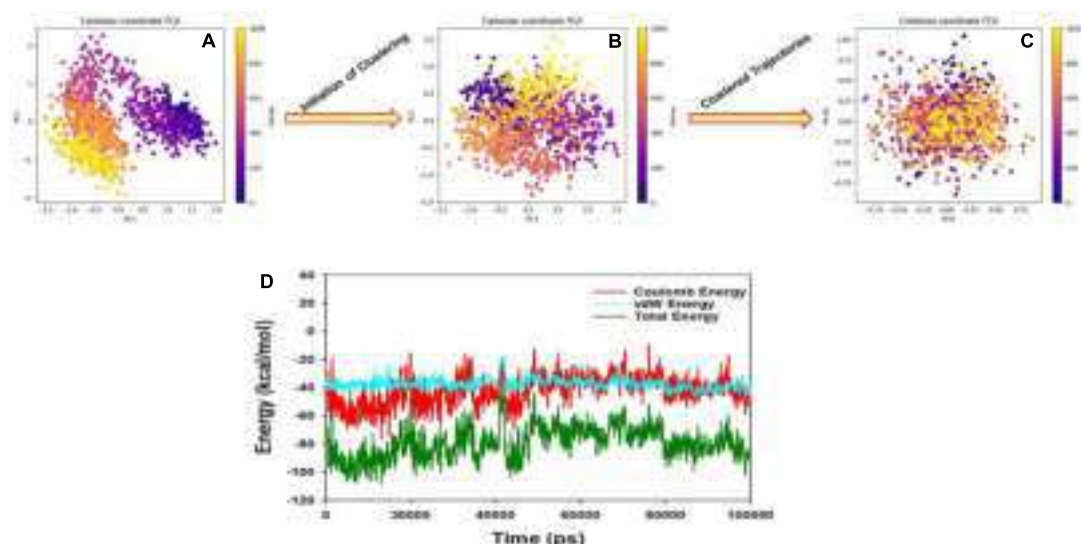


FIGURE 12

(A) PCA of 2ZHV- FDB017657 showing a stable configuration. (B) Energy plot of protein BACE1 and FDB017657 complex system during the entire simulation event of 150 ns. (C,D) The change in PCA movements. The total energy (dark green), van der Waal's energy (cyan) and Coulomb energy (red) of the entire system indicate the stability of the individual systems bound to FDB017657 molecule.

## Discussion

Proteolytic processing of APP by BACE1 is the rate-determining step in A $\beta$  production, hence BACE1 is employed as a therapeutic target for creating innovative lead compounds in AD in this study. According to the earlier reports, it was suggested that the enzyme BACE1 is also associated with different types of cancers and viruses in conjunction with AD. In this study, we have tried to reveal the potential of naturally available food molecules to bind the BACE1's active site in a highly specific binding pattern. The aim of our study is toward the development of a drug from food compounds with the help of computational biology as

it has the additional advantage regarding safety, and lesser chance of side effects. The low toxicity profile of natural products inspired by small-molecule inhibitors may prove to be a great asset during the frenetic development period of drug discovery when time is of the essence. Current state-of-the-art computational approaches can be used to identify structural and pharmacophoric properties of active natural compounds that can be used as drugs. Our results suggest that the selected 8,453 compounds from the Food database are majorly phenols and naphthol metabolites having a high potential of showing inhibitory activity against BACE1. The Food database is a recent database that proved the potential of food metabolites that we use in our daily life and found its

major application in developing different therapeutics treating depressive disorders and others.

A nicely proven correlation among salient capabilities of the molecules represented through molecular descriptors, and their bioactivity expands statistics approximately mechanistic elements of molecules, specificity, and quantity (presence or even absence) of various structural developments for preferred bioactivity. Although, with the QSAR analysis, we've compared the  $K_i$  values of various molecules in correlation and as an impact of a specific molecular descriptor, a similar or contrary impact of different molecular descriptors or unknown descriptors has a dominant impact in figuring out the general  $K_i$  value of a molecule can't be neglected. In other words, a single molecular descriptor is incapable of absolutely explaining the experimental  $K_i$  value for this sort of numerous sets of molecules. That is, the successful usage of the advanced QSAR model is based on the concomitant usage of molecular descriptors.

A QSAR model with multiple chemical descriptors is built using a dataset of 371 compounds. The resulting model was rigorously verified for fitting and internal validation to prove its strong external prediction capacity and resilience. In addition, virtual screening using QSAR yielded a novel food molecule with a better  $K_i$  value of 10.715 nM. Combined QSARs and molecular docking studies offered complimentary information and helped discover prodigious and under-privileged chemical characteristics that might be leveraged to change a molecule to produce better BACE1 inhibitors with higher  $K_i$  values. In the future, structural modifications that result in augmented values for the molecular descriptors with positive coefficients in the developed model for the anti-BACE1 activity will be performed to generate novel hits suitable for construction and *in vitro* evaluation as anti-Alzheimer's (AD) disease therapy. These reports already demonstrated the potential of this plant as a source of novel drugs, nutraceuticals, and functional foods. Our present study perhaps supports a further avenue for *in vivo* and clinical trial of the food molecule, 4-(3,4-dihydroxyphenyl)-2-hydroxy-1H-phenalen-1-one to target BACE1 for any future scope to treat the AD along with viruses and cancer.

## Data availability statement

The original contributions presented in this study are included in the article/**Supplementary material**, further inquiries can be directed to the corresponding authors.

## Author contributions

NM and ADa performed the concept design. NM, AG, SwM, and RJ designed and carried out the experimental procedures. NM, AG, RJ, RB, MC, and VM done the analysis. NM, ADa, PD, AP, GM, SB, BA, and SA-H done the manuscript preparation.

NM, ADe, GM, MK, AAl, ADa, SuM, AMA, and MZ edited the manuscript. All authors contributed to the article and approved the submitted version.

## Funding

This research work was funded by the Institutional Fund Projects under grant no. IFPDP-85-22. This research work was funded by the Institutional Fund Projects under grant no. (IFPDP-85-22). Therefore, authors gratefully acknowledge technical and financial support from Ministry of Education and Deanship of Scientific Research (DSR), King Abdulaziz University, Jeddah, Saudi Arabia.

## Conflict of interest

AA is honorary associated with the scientific board of the company AFNP Med in Austria.

The remaining authors declare that the research was conducted in the absence of any commercial or financial relationships that could be construed as a potential conflict of interest.

## Publisher's note

All claims expressed in this article are solely those of the authors and do not necessarily represent those of their affiliated organizations, or those of the publisher, the editors and the reviewers. Any product that may be evaluated in this article, or claim that may be made by its manufacturer, is not guaranteed or endorsed by the publisher.

## Supplementary material

The Supplementary Material for this article can be found online at: <https://www.frontiersin.org/articles/10.3389/fnagi.2022.878276/full#supplementary-material>

### SUPPLEMENTARY TABLE 1

Smileskipki.

### SUPPLEMENTARY TABLE 2

Descriptor used in QSAR.

### SUPPLEMENTARY TABLE 3

Formulas for calculation of model parameters.

### SUPPLEMENTARY TABLE 4

Food molecules predicted pki and descriptors.

## References

- Alzheimer's Association (2012). 2012 Alzheimer's disease facts and figures. *Alzheimer's Dement.* 8, 131–168.
- Arif, N., Subhani, A., Hussain, W., and Rasool, N. (2020). In silico inhibition of BACE-1 by selective phytochemicals as novel potential inhibitors: Molecular docking and DFT studies. *Curr. Drug Disc. Technol.* 17, 397–411. doi: 10.2174/1570163816666190214161825
- Bellacasa, R. P., Karachaliou, N., Estrada-Tejedor, R., Teixidó, J., Costa, C., and Borrrell, J. I. A. L. K. (2013). and ROS1 as a joint target for the treatment of lung cancer: A review. *Transl. Lung Cancer Res.* 2, 72–86.
- Berman, H. M., Westbrook, J., Feng, Z., Gilliland, G., Bhat, T. N., Weissig, H., et al. (2000). The protein data bank. *Nucleic Acids Res.* 28, 235–242. doi: 10.1093/nar/28.1.235
- Bo, Q., Runhua, L., Hanqing, W., Min, W., Wenpeng, L., and Jinlun, X. (2000). Chemical constituents from *Musella lasiocarpa* (Franch.) CY Wu. *Nat. Product Res. Develop.* 12, 41–44.
- Bonvino, N. P., Liang, J., McCord, E. D., Zafiris, E., Benetti, N., Ray, N. B., et al. (2018). OliveNet<sup>TM</sup>: A comprehensive library of compounds from *Olea europaea*. *Database* 2018:bay016. doi: 10.1093/database/bay016
- Bowers, K. J., Chow, D. E., Xu, H., Dror, R. O., Eastwood, M. P., Gregersen, B. A., et al. (2006). "Scalable algorithms for molecular dynamics simulations on commodity clusters," in *SC'06: Proceedings of the 2006 ACM/IEEE Conference on Supercomputing*, (Tampa, FL: IEEE), 43–43. doi: 10.1109/SC.2006.54
- Chow, E., Rendleman, C. A., Bowers, K. J., Dror, R. O., Hughes, D. H., Gullingsrud, J., et al. (2008). *Desmond performance on a cluster of multicore processors*. New York, NY: DE Shaw Research Technical Report DESRES/TR-2008-01.
- Cui, H., Hung, A. C., Klaver, D. W., Suzuki, T., Freeman, C., Narkowicz, C., et al. (2011). Effects of heparin and enoxaparin on APP processing and  $\text{A}\beta$  production in primary cortical neurons from Tg2576 mice. *PLoS One* 6:e23007. doi: 10.1371/journal.pone.0023007
- Davies, M., Nowotka, M., Papadatos, G., Dedman, N., Gaulton, A., and Atkinson, F. (2015). ChEMBL web services: Streamlining access to drug discovery data and utilities. *Nucleic Acids Res.* 45, D945–D954. doi: 10.1093/nar/gkv352
- De Strooper, B., and Karran, E. (2016). The cellular phase of Alzheimer's disease. *Cell* 164, 603–615. doi: 10.1016/j.cell.2015.12.056
- Dingwall, C. (2001). Spotlight on BACE: The secretases as targets for treatment in Alzheimer disease. *J. Clin. Invest.* 108, 1243–1246. doi: 10.1172/JCI14402
- Dong, L. B., He, J., Li, X. Y., Wu, X. D., Deng, X., Xu, G., et al. (2011). Chemical constituents from the aerial parts of *Musella lasiocarpa*. *Nat. Products Bioprospect.* 1, 41–47. doi: 10.1007/s13659-011-0007-7
- Forli, S., Huey, R., Pique, M. E., Sanner, M. F., Goodsell, D. S., and Olson, A. J. (2016). Computational protein–ligand docking and virtual drug screening with the AutoDock suite. *Nat. Protocols* 11, 905–919. doi: 10.1038/nprot.2016.051
- Fujita, T., and Winkler, D. A. (2016). Understanding the Roles of the "Two QSARs". *J. Chem. Inf. Model* 56, 269–274. doi: 10.1021/acs.jcim.5b00229
- Fukumoto, H., Cheung, B. S., Hyman, B. T., and Irizarry, M. C. (2002).  $\beta$ -Secretase protein and activity are increased in the neocortex in Alzheimer disease. *Arch. Neurol.* 59, 1381–1389. doi: 10.1001/archneur.59.9.1381
- Gramatica, P. (2013). On the development and validation of QSAR models. *Methods Mol. Biol.* 930, 499–526. doi: 10.1007/978-1-62703-059-5\_21
- Gramatica, P. (2020). Principles of QSAR Modeling. *Int. J. Quant. Struct. Property Relation.* 5, 61–97. doi: 10.4018/IJQSPR.2020.0701.oa1
- Gramatica, P., Cassani, S., and Chirico, N. (2014). QSARINS-Chem: Insurbria Datasets and New QSAR/QSPR Models for Environmental Pollutants in QSARINS. *J. Comput. Chem. Softw. News Updates* 35, 1036–1044. doi: 10.1002/jcc.23576
- Gramatica, P., Chirico, N., Papa, E., Kovarich, S., and Cassani, S. (2013). QSARINS: A New Software for the Development, Analysis, and Validation of QSAR MLR Models. *J. Comp. Chem. Softw. News Updates* 34, 2121–2132. doi: 10.1002/jcc.23361
- Hall, A., Pekkala, T., Polvikoski, T., Van Gils, M., Kivipelto, M., Lötjönen, J., et al. (2019). Prediction models for dementia and neuropathology in the oldest old: The Vantaa 85+ cohort study. *Alzheimer's Res. Ther.* 11, 1–2. doi: 10.1186/s13195-018-0450-3
- Hassan, M., Shahzadi, S., Seo, S. Y., Alashwal, H., Zaki, N., and Moustafa, A. A. (2018). Molecular docking and dynamic simulation of AZD3293 and solanezumab effects against BACE1 to treat Alzheimer's disease. *Front. Comput. Neurosci.* 12:34. doi: 10.3389/fncom.2018.00034
- Hussain, I., Powell, D. J., Howlett, D. R., Chapman, G. A., Gilmour, L., Murdock, P. R., et al. (2000). ASP1 (BACE2) cleaves the amyloid precursor protein at the  $\beta$ -secretase site. *Mol. Cell. Neurosci.* 16, 609–619. doi: 10.1006/mcne.2000.0884
- Jabir, N. R., Rehman, M. T., Alsolami, K., Shakil, S., Zughabi, T. A., Alserihi, R. F., et al. (2021). Concatenation of molecular docking and molecular simulation of BACE-1,  $\gamma$ -secretase targeted ligands: In pursuit of Alzheimer's treatment. *Ann. Med.* 53, 2332–2344. doi: 10.1080/07853890.2021.2009124
- Jawarkar, R. D., Bakal, R. L., Zaki, M. E. A., Al-Hussain, S., Ghosh, A., Gandhi, A., et al. (2022). QSAR based virtual screening derived identification of a novel hit as a SARS CoV-229E 3CLpro Inhibitor: GA-MLR QSAR modeling supported by molecular Docking, molecular dynamics simulation and MMGBSA calculation approaches. *Arab. J. Chem.* 15:103499. doi: 10.1016/j.arabj.2021.103499
- Jorgensen, W. L., Chandrasekhar, J., Madura, J. D., Impey, R. W., and Klein, M. L. (1983). Comparison of simple potential functions for simulating liquid water. *J. Chem. Phys.* 79, 926–935. doi: 10.1063/1.445869
- Kagami, L. P., das Neves, G. M., Timmers, L. F. S. M., Caceres, R. A., and Eifler-Lima, V. L. (2020). Geo-Measures: A Pymol plugin for protein structure ensembles analysis. *Comp. Biol. Chem.* 87:107322. doi: 10.1016/j.compbiolchem.2020.107322
- Kim, S., Chen, J., Cheng, T., Gindulyte, A., He, J., He, S., et al. (2019). PubChem 2019 update: Improved access to chemical data. *Nucleic Acids Res.* 47, D1102–D1109. doi: 10.1093/nar/gky1033
- Li, Q., and Südhof, T. C. (2004). Cleavage of amyloid- $\beta$  precursor protein and amyloid- $\beta$  precursor-like protein by BACE 1. *J. Biol. Chem.* 279, 10542–10550. doi: 10.1074/jbc.M310001200
- Lin, X., Koelsch, G., Wu, S., Downs, D., Dashti, A., and Tang, J. (2000). Human aspartic protease memapsin 2 cleaves the  $\beta$ -secretase site of  $\beta$ -amyloid precursor protein. *Proc. Natl. Acad. Sci.* 97, 1456–1460. doi: 10.1073/pnas.97.4.1456
- Maiorov, V. N., and Crippen, G. M. (1994). Significance of root-mean-square deviation in comparing three-dimensional structures of globular proteins. *J. Mol. Biol.* 235, 625–634. doi: 10.1006/jmbi.1994.1017
- Martin, Y. C., and Muchmore, S. W. (2012). Frozen out: Molecular modeling in the age of cryocrystallography. *J. Comput. Aided Mol. Design* 26, 91–92.
- Martyna, G. J., Klein, M. L., and Tuckerman, M. (1992). Nosé–Hoover chains: The canonical ensemble via continuous dynamics. *J. Chem. Phys.* 97, 2635–2643. doi: 10.1063/1.463940
- Martyna, G. J., Tobias, D. J., and Klein, M. L. (1994). Constant pressure molecular dynamics algorithms. *J. Chem. Phys.* 101, 4177–4189. doi: 10.1063/1.467468
- Masand, V. H., Mahajan, D. T., Alafeefy, A. M., Bukhari, S. N., and Elsayed, N. N. (2015). Optimization of antiproliferative activity of substituted phenyl 4-(2-oxoimidazolidin-1-yl) benzenesulfonates: QSAR and CoMFA analyses. *Eur. J. Pharm. Sci.* 77, 230–237.
- Masand, V. H., and Rastija, V. (2017). PyDescriptor: A new PyMOL plugin for calculating thousands of easily understandable molecular descriptors. *Chemom. Intell. Labor. Syst.* 169, 12–18. doi: 10.1016/j.chemolab.2017.08.003
- Morris, G. M., Huey, R., Lindstrom, W., Sanner, M. F., Belew, R. K., Goodsell, D. S., et al. (2009). AutoDock4 and AutoDockTools4: Automated docking with selective receptor flexibility. *J. Comp. Chem.* 30, 2785–2791. doi: 10.1002/jcc.21256
- Moussa-Pacha, N. M., Abdin, S. M., Omar, H. A., Alniss, H., and Al-Tel, T. H. (2020). BACE1 inhibitors: Current status and future directions in treating Alzheimer's disease. *Med. Res. Rev.* 40, 339–384. doi: 10.1002/med.21622
- Mukerjee, N., Das, A., Maitra, S., Ghosh, A., Khan, P., Alexiou, A., et al. (2022). Dynamics of natural product lupenone as a potential fusion inhibitor against the spike complex of novel semliki forest virus. *PLoS One* 17:e0263853. doi: 10.1371/journal.pone.0263853
- Murphy, M. P., and LeVine, III, H. (2010). Alzheimer's disease and the amyloid-beta peptide. *J. Alzheimers Dis.* 19, 311–323. doi: 10.3233/JAD-2010-1221
- Musi, N., Valentine, J. M., Sickora, K. R., Baeuerle, E., Thompson, C. S., Shen, Q., et al. (2018). Tau protein aggregation is associated with cellular senescence in the brain. *Aging cell* 17:e12840. doi: 10.1111/acel.12840
- Neves, B. J., Braga, R. C., Melo-Filho, C. C., Moreira-Filho, J. T., Muratov, E. N., and Andrade, C. H. (2018). QSAR-Based Virtual Screening: Advances and Applications in Drug Discovery. *Front. Pharmacol.* 9:1275. doi: 10.3389/fphar.2018.01275





- O'Boyle, N. M., Banck, M., James, C. A., Morley, C., Vandermeersch, T., and Hutchison, G. R. (2011). Open Babel: An open chemical toolbox. *J. Cheminform.* 3:33. doi: 10.1186/1758-2946-3-33
- Pettersen, E. F., Goddard, T. D., Huang, C. C., Couch, G. S., Greenblatt, D. M., Meng, E. C., et al. (2004). UCSF Chimera—a visualization system for exploratory research and analysis. *J. Comp. Chem.* 25, 1605–1612. doi: 10.1002/jcc.20084
- Piao, L., Chen, Z., Li, Q., Liu, R., Song, W., Kong, R., et al. (2019). Molecular dynamics simulations of wild type and mutants of SAPAP in complexed with Shank3. *Int. J. Mol. Sci.* 20:224. doi: 10.3390/ijms20010224
- Roskoski, R. Jr. (2013). Anaplastic lymphoma kinase (ALK): Structure, oncogenic activation, and pharmacological inhibition. *Pharmacol. Res.* 68, 68–94. doi: 10.1016/j.phrs.2012.11.007
- Sebastián-Serrano, Á., Diego-García, D., and Díaz-Hernández, M. (2018). The neurotoxic role of extracellular tau protein. *Int. J. Mol. Sci.* 19:998. doi: 10.3390/ijms19040998
- Shivakumar, D., Williams, J., Wu, Y., Damm, W., Shelley, J., and Sherman, W. (2010). Prediction of absolute solvation free energies using molecular dynamics free energy perturbation and the OPLS force field. *J. Chem. Theory Comp.* 6, 1509–1519. doi: 10.1021/ct900587b
- Sinha, S., Anderson, J. P., Barbour, R., Basl, G. S., Caccavello, R., Davis, D., et al. (1999). Purification and cloning of amyloid precursor protein  $\beta$ -secretase from human brain. *Nature* 402, 537–540. doi: 10.1038/990114
- Tosco, P., Balle, T., and Shiri, F. (2011). Open3DALIGN: An open-source software aimed at unsupervised ligand alignment. *J. Comp.Aided Mol. Design* 25, 777–783. doi: 10.1007/s10822-011-9462-9
- Toukmaji, A. Y., and Board, J. A. Jr. (1996). Ewald summation techniques in perspective: A survey. *Comp. Phys. Commun.* 95, 73–92. doi: 10.1016/0010-4655(96)00016-1
- Tresadern, G., Delgado, F., Delgado, O., Gijzen, H., Macdonald, G. J., Moechars, D., et al. (2011). Rational design and synthesis of aminopiperazinones as  $\beta$ -secretase (BACE) inhibitors. *Bioorgan. Med. Chem. Lett.* 21, 7255–7260. doi: 10.1016/j.bmcl.2011.10.050
- Trott, O., and Olson, A. J. (2010). AutoDock Vina: Improving the speed and accuracy of docking with a new scoring function, efficient optimization, and multithreading. *J. Comput. Chem.* 31, 455–461. doi: 10.1002/jcc.21334
- Vassar, R., Bennett, B. D., Babu-Khan, S., Kahn, S., Mendiaz, E. A., Denis, P., et al. (1999).  $\beta$ -Secretase cleavage of Alzheimer's amyloid precursor protein by the transmembrane aspartic protease BACE. *Science* 286, 735–741. doi: 10.1126/science.286.5440.735
- Volkamer, A., Kuhn, D., Grombacher, T., Rippmann, F., and Rarey, M. (2012). Combining global and local measures for structure-based druggability predictions. *J. Chem. Inf. Model* 52, 360–372. doi: 10.1021/ci200454v
- Yan, R., Bienkowski, M. J., Shuck, M. E., Miao, H., Tory, M. C., Pauley, A. M., et al. (1999). Membrane-anchored aspartyl protease with Alzheimer's disease  $\beta$ -secretase activity. *Nature* 402, 533–537. doi: 10.1038/990107
- Yang, L. B., Lindholm, K., Yan, R., Citron, M., Xia, W., Yang, X. L., et al. (2003). Elevated  $\beta$ -secretase expression and enzymatic activity detected in sporadic Alzheimer disease. *Nat. Med.* 9, 3–4. doi: 10.1038/nm0103-3
- Zacchetti, D., Chiergatti, E., Bettegazzi, B., Mihailovich, M., Sousa, V. L., Grohovaz, F., et al. (2007). BACE1 expression and activity: Relevance in Alzheimer's disease. *Neurodegener. Dis.* 4, 117–126. doi: 10.1159/000101836
- Zaki, M. E. A., Al-Hussain, S. A., Masand, V. H., Akasapu, S., Bajaj, S. O., El-Sayed, N. N. E., et al. (2021). Identification of Anti-SARS-CoV-2 Compounds from Food Using QSAR-Based Virtual Screening, Molecular Docking, and Molecular Dynamics Simulation Analysis. *Pharmaceuticals* 14:357. doi: 10.3390/ph14040357
- Zhang, Y. W., Thompson, R., Zhang, H., and Xu, H. (2011). APP processing in Alzheimer's disease. *Mol. Brain* 4:3. doi: 10.1186/1756-6606-4-3

## CITATION

Mukerjee N, Das A, Jawarkar RD, Maitra S, Das P, Castrosanto MA, Paul S, Samad A, Zaki MEA, Al-Hussain SA, Masand VH, Hasan MM, Bukhari SNA, Perveen A, Alghamdi BS, Alexiou A, Kamal MA, Dey A, Malik S, Bakal RL, Abuzenadah AM, Ghosh A and Md Ashraf G (2022) Repurposing food molecules as a potential BACE1 inhibitor for Alzheimer's disease. *Front. Aging Neurosci.* 14:878276. doi: 10.3389/fnagi.2022.878276

## Article

# Quinoline Derivatives with Different Functional Groups: Evaluation of Their Catecholase Activity

Mohamed Moutaouakil <sup>1</sup>, Said Tighadouini <sup>1</sup>, Zainab M. Almarhoon <sup>2,\*</sup>, Maha I. Al-Zaben <sup>2</sup>,  
Abir Ben Bacha <sup>3,4</sup>, Vijay H. Masand <sup>5</sup>, Jamal Jamaledine <sup>1</sup> and Rafik Saddik <sup>1,\*</sup>

<sup>1</sup> Laboratory of Organic Synthesis, Extraction, and Valorization, Faculty of Sciences Ain Chock, Hassan II University, Casablanca 20000, Morocco

<sup>2</sup> Department of Chemistry, College of Science, King Saud University, P.O. Box 2455, Riyadh 11451, Saudi Arabia

<sup>3</sup> Biochemistry Department, College of Science, King Saud University, P.O. Box 2245, Riyadh 11495, Saudi Arabia

<sup>4</sup> Laboratory of Plant Biotechnology Applied to Crop Improvement, Faculty of Science of Sfax, University of Sfax, Sfax 3038, Tunisia

<sup>5</sup> Department of Chemistry, Vidya Bharati Mahavidyalaya, Amravati 444 602, India

\* Correspondence: zalmarhoon@ksu.edu.sa (Z.M.A.); rafik.saddik@gmail.com (R.S.)

**Abstract:** In this work, we are interested in finding new catalysts for catecholase, whose principle is based on the oxidation reaction of catechol to *o*-quinone. In this context, we have studied a series of seven quinoline-based compounds. The present work indicates that the complexes formed between seven selected quinoline compounds and the copper salts viz. Cu(OAc)<sub>2</sub>, CuSO<sub>4</sub>, Cu(NO<sub>3</sub>)<sub>2</sub>, and CuCl<sub>2</sub> elicit catalytic activities for the oxidation of catechol to *o*-quinone. The complexes formed with the Cu(OAc)<sub>2</sub> salt show a much higher catalytic activity than the others, whereas the Cu(NO<sub>3</sub>)<sub>2</sub> and CuCl<sub>2</sub> salts formed complexes with low catalytic activity. This study also shows that the oxidation rate depends on two factors, namely the chemical structure of the ligands and the nature of the ions coordinated with the copper.

**Keywords:** catalytic activity; quinoline; catechol oxidase; *o*-quinone



**Citation:** Moutaouakil, M.; Tighadouini, S.; M. Almarhoon, Z.; I. Al-Zaben, M.; Ben Bacha, A.; H. Masand, V.; Jamaledine, J.; Saddik, R. Quinoline Derivatives with Different Functional Groups: Evaluation of Their Catecholase Activity. *Catalysts* **2022**, *12*, 1468. <https://doi.org/10.3390/catal12111468>

Academic Editor: László Poppe

Received: 16 October 2022

Accepted: 15 November 2022

Published: 18 November 2022

**Publisher's Note:** MDPI stays neutral with regard to jurisdictional claims in published maps and institutional affiliations.



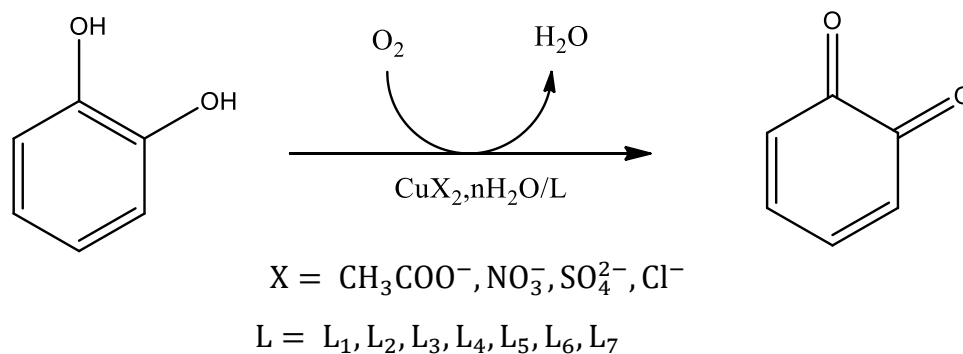
**Copyright:** © 2022 by the authors. Licensee MDPI, Basel, Switzerland. This article is an open access article distributed under the terms and conditions of the Creative Commons Attribution (CC BY) license (<https://creativecommons.org/licenses/by/4.0/>).

## 1. Introduction

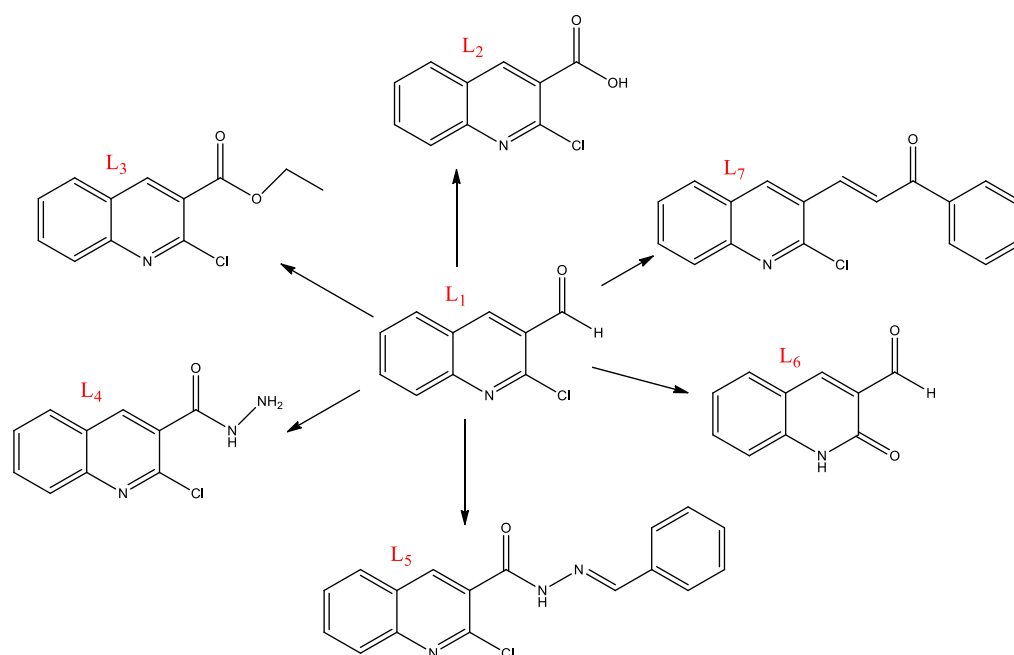
Copper is among the important metals in many catalytic processes and is characterized by its ability to combine with organic ligands to catalyze several diverse biological processes [1]. For example, catechol oxidase is a copper-based moiety that catalyzes the oxidation of phenols to quinones in the presence of oxygen. It is found for example in plants, wherein it plays an essential role in catalyzing the oxidation of catechol to *o*-quinone to produce after polymerization melanin, which gives a dark brown color to damaged fruits [2]. Dopamine is an important neurotransmitter, which after oxidation and polymerization gives polydopamine, an adhesive agent with many industrial applications. The oxidation of phenols to corresponding quinones is a very interesting process that has various applications in many fields [3].

Quinoline derivatives are among the compounds with great pharmacological powers [4], such as antimicrobial [5], anticancer [6–8], antifungal [9,10], antiviral [11], anti-inflammatory [12], antioxidants [13,14], antitumor [15], anti-SARS-CoV-2 [16], corrosion inhibitors [17,18], and antimalarial [19]. On the other hand, copper–quinoline complexes are similar systems that can catalyze many biological processes. For this reason, we are interested in this work to better understand this compelling mechanism and to discover the efficiency of quinoline derivatives in the oxidation of catechol.

This work aims to study the effect of ligands–copper(II) complexes on the oxidation of catechol to *o*-quinone in the presence of O<sub>2</sub> (Scheme 1). In this respect, the reaction was first performed without catalysts, then using the copper salts Cu(OAc)<sub>2</sub>, CuSO<sub>4</sub>, Cu(NO<sub>3</sub>)<sub>2</sub>, and CuCl<sub>2</sub>, then using the synthesized ligands (L<sub>1</sub>, L<sub>2</sub>, L<sub>3</sub>, L<sub>4</sub>, L<sub>5</sub>, L<sub>6</sub>, and L<sub>7</sub>—Scheme 2), and finally, the reaction was catalyzed by the ligands–copper (II) complexes. In order to be able to compare and discuss the obtained results, the oxidation rate for each catechol transformation was calculated.



**Scheme 1.** The oxidation reaction of catechol to *o*-quinone.

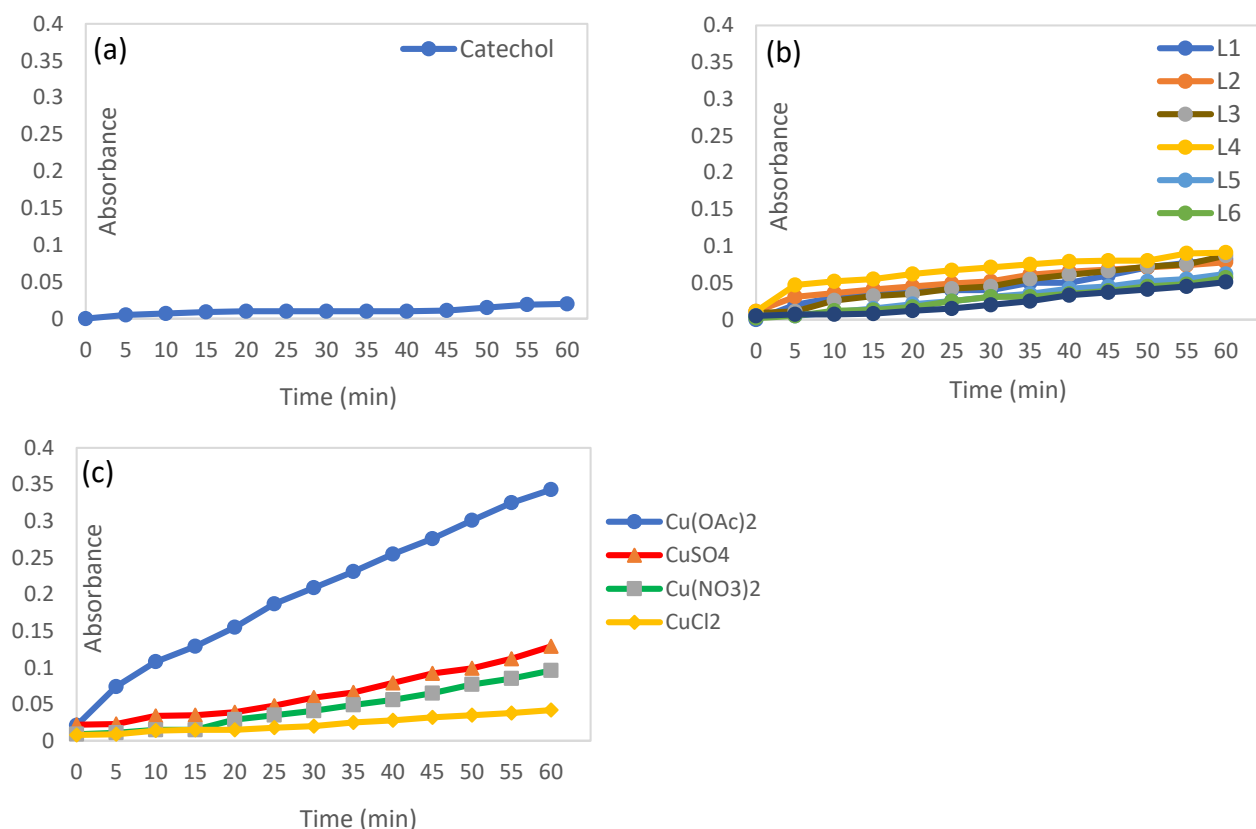


**Scheme 2.** Chemical structure of the studied quinoline ligands.

## 2. Results and Discussions

The results of this study are represented in Figures 1 and 2, which give the absorbance as a function of time for the different cases. Figure 1a presents the oxidation of catechol without any catalyst, while Figure 1b represents the reaction catalyzed by the synthesized ligands. In Figure 1c, the reaction is catalyzed by the metal salts and finally, Figure 2 provides the obtained results using the complexes formed between the synthesized ligands and the metal salts. Table 1 represents the oxidation rate for the different cases.



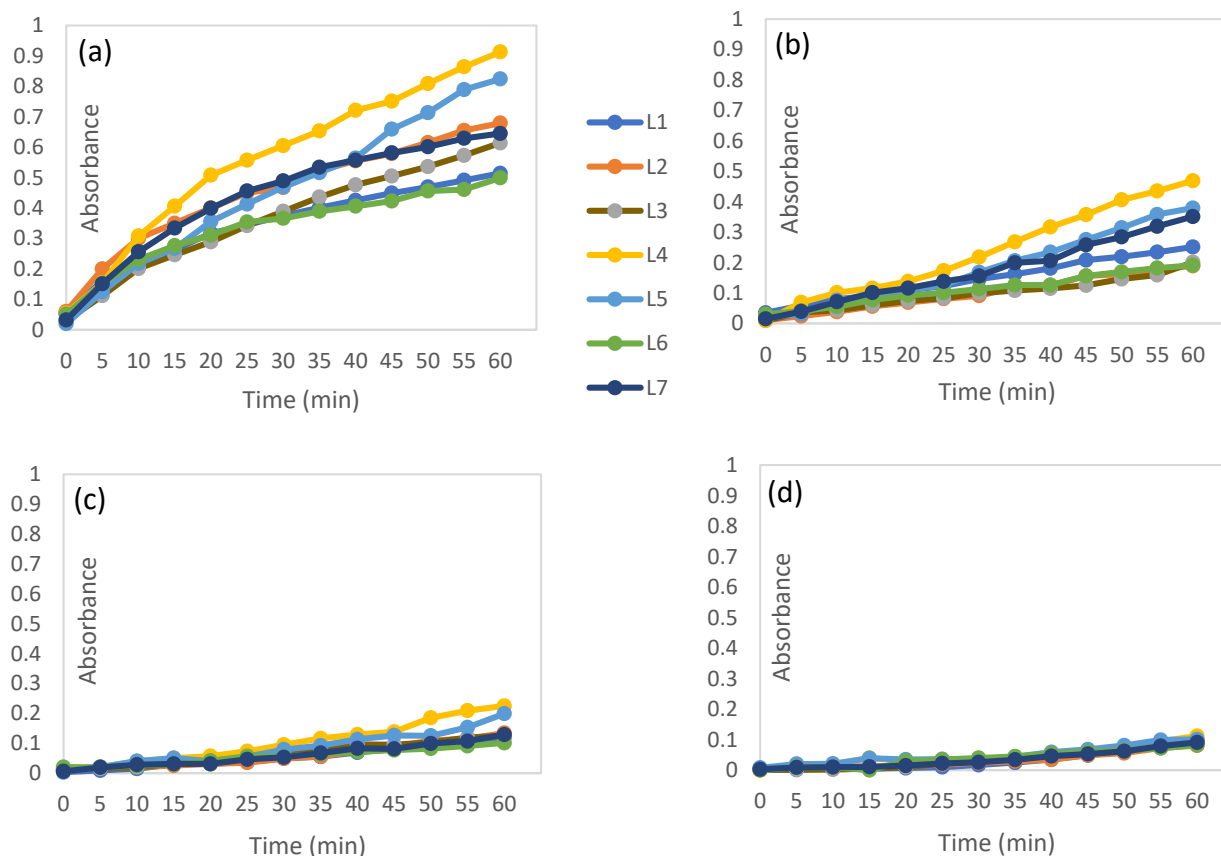


**Figure 1.** Oxidation of catechol to *o*-quinone in the absence of copper complexes: (a) Reaction without any catalyst, (b) reaction catalyzed by the synthesized ligands, and (c) reaction synthesized by the metal salts. Reaction conditions: methanol solutions, 0.15 mL metal salt at  $2 \times 10^{-3}$  mol/L, 0.15 mL ligand at  $2 \times 10^{-3}$  mol/L, 2 mL catechol at  $10^{-1}$  mol/L are mixed,  $T = 25$  °C,  $\lambda = 390$  nm.

**Table 1.** Oxidation rate of catechol to *o*-quinone in ( $\mu\text{mol L}^{-1} \text{s}^{-1}$ ).

	Cu(OAc) <sub>2</sub>	CuSO <sub>4</sub>	Cu(NO <sub>3</sub> ) <sub>2</sub>	CuCl <sub>2</sub>	Ligands Only
L <sub>1</sub>	71.38	34.86	16.53	13.33	11.39
L <sub>2</sub>	94.30	26.25	18.61	11.25	10.83
L <sub>3</sub>	85.27	27.91	17.36	12.22	12.08
L <sub>4</sub>	126.80	65.13	31.25	15.55	12.64
L <sub>5</sub>	114.44	52.63	27.64	14.03	8.61
L <sub>6</sub>	69.30	26.53	14.03	11.39	7.92
L <sub>7</sub>	89.58	48.75	17.91	12.64	7.08
Salt only	47.63	17.91	13.33	5.83	
Without catalysis			2.78		

We notice from Figure 1a that the absorbance remains at almost zero over time and the oxidation rate is very low viz.  $2.78 \mu\text{mol L}^{-1} \text{s}^{-1}$ . Figure 1b also shows a very low absorbance and conversion rate between  $7.08 \mu\text{mol L}^{-1} \text{s}^{-1}$  and  $12.64 \mu\text{mol L}^{-1} \text{s}^{-1}$ . From Figure 1c, we also notice that the absorbance and oxidation rate remain low for the metal salts CuSO<sub>4</sub>, Cu(NO<sub>3</sub>)<sub>2</sub>, and CuCl<sub>2</sub>; however, the salt Cu(OAc)<sub>2</sub> has a better oxidation rate of  $47.22 \mu\text{mol L}^{-1} \text{s}^{-1}$ . Therefore, it can be deduced that the oxidation reaction cannot take place without a catalyst and that neither ligands nor salts alone can catalyze this reaction, except Cu(OAc)<sub>2</sub>, which has a slightly greater catalytic effect compared to the others.



**Figure 2.** Oxidation of catechol to *o*-quinone in the presence of copper complexes: (a) Reaction in the presence of  $\text{Cu}(\text{OAc})_2$  and ligands, (b) reaction in the presence of  $\text{CuSO}_4$  and ligands, (c) reaction in the presence of  $\text{Cu}(\text{NO}_3)_2$  and ligands, and (d) reaction in the presence of  $\text{CuCl}_2$  and ligands. Reaction conditions: methanol solutions, 0.15 mL metal salt at  $2 \times 10^{-3}$  mol/L, 0.15 mL ligand at  $2 \times 10^{-3}$  mol/L, 2 mL catechol at  $10^{-1}$  mol/L are mixed,  $T = 25^\circ\text{C}$ ,  $\lambda = 390$  nm.

The results obtained in Figure 2 show that the complexes formed between the  $\text{Cu}(\text{OAc})_2$  salt and the ligands possess better catalytic activity for the oxidation of catechol, as the obtained oxidation rates are the highest (Figure 2a). The  $\text{L}_4/\text{Cu}(\text{OAc})_2$  complex shows an oxidation rate of  $126.80 \mu\text{mol L}^{-1} \text{s}^{-1}$ , followed by the  $\text{L}_5/\text{Cu}(\text{OAc})_2$  complex ( $114.44 \mu\text{mol L}^{-1} \text{s}^{-1}$ ), then the  $\text{L}_2/\text{Cu}(\text{OAc})_2$ ,  $\text{L}_7/\text{Cu}(\text{OAc})_2$ , and  $\text{L}_3/\text{Cu}(\text{OAc})_2$  complexes with oxidation rates of  $94.30$ ,  $89.58$ , and  $85.27 \mu\text{mol L}^{-1} \text{s}^{-1}$ , respectively, and finally,  $\text{L}_1/\text{Cu}(\text{OAc})_2$  and  $\text{L}_6/\text{Cu}(\text{OAc})_2$ , which give the lowest oxidation rates ( $71.38$  and  $69.30 \mu\text{mol L}^{-1} \text{s}^{-1}$ , respectively).

The complexes formed between the ligands and the  $\text{CuSO}_4$  salt also give high oxidation rates but are generally lower than those obtained in the case of  $\text{Cu}(\text{OAc})_2$ , as the highest oxidation rate is  $65.13 \mu\text{mol L}^{-1} \text{s}^{-1}$  for  $\text{L}_4/\text{CuSO}_4$ , followed by  $\text{L}_5/\text{CuSO}_4$  and  $\text{L}_7/\text{CuSO}_4$ , with oxidation rates of  $52.63$  and  $48.75 \mu\text{mol L}^{-1} \text{s}^{-1}$ , respectively, and then the complexes formed between  $\text{CuSO}_4$  and ligands  $\text{L}_1$ ,  $\text{L}_3$ ,  $\text{L}_6$ , and  $\text{L}_2$  come last with oxidation rates of  $34.86$ ,  $27.91$ ,  $26.53$ , and  $26.25 \mu\text{mol L}^{-1} \text{s}^{-1}$ , respectively (Figure 2b).

The complexes formed between the ligands and  $\text{Cu}(\text{NO}_3)_2$  also catalyze the oxidation reaction, but with slightly lower oxidation rates compared to the previous ones, as the  $\text{L}_3/\text{Cu}(\text{NO}_3)_2$  complex gives the largest oxidation rate of  $31.25 \mu\text{mol L}^{-1} \text{s}^{-1}$ , followed by the  $\text{L}_5/\text{Cu}(\text{NO}_3)_2$  complex ( $27.64 \mu\text{mol L}^{-1} \text{s}^{-1}$ ), and then the complexes formed between  $\text{Cu}(\text{NO}_3)_2$  and the ligands  $\text{L}_2$ ,  $\text{L}_7$ ,  $\text{L}_3$ ,  $\text{L}_1$ , and  $\text{L}_6$ , with oxidation rates of  $18.61$ ,  $17.91$ ,  $17.36$ ,  $16.53$ , and  $14.03 \mu\text{mol L}^{-1} \text{s}^{-1}$ , respectively (Figure 2c).

The complexes formed between the ligands and  $\text{CuCl}_2$  do not show a significant catalytic effect, as there is no significant increase in absorbance in all cases, and the oxidation

rate remains quite low, the largest conversion rate being  $15.55 \mu\text{mol L}^{-1} \text{s}^{-1}$  for  $\text{L}_4/\text{CuCl}_2$  and the smallest being  $11.25 \mu\text{mol L}^{-1} \text{s}^{-1}$  for  $\text{L}_2/\text{CuCl}_2$  (Figure 2d). We deduce from these results that the chemical structure of the ligands and the nature of the copper salts play an important role in the catalytic activity of the studied complexes.

It can be seen from this study that all the complexes formed between the ligands and  $\text{Cu}(\text{OAc})_2$  have very high catalytic activities compared to the complexes formed with the other salts, and this is due to the weak bonding between the  $\text{OAc}^-$  anions and the  $\text{Cu}^{2+}$  cations, which facilitates the coordination between the ligands and copper. On the other hand, the ligands  $\text{L}_4$  and  $\text{L}_5$  form complexes with a very high catalytic activity, because the presence of electron donor groups increases the electron density at the nitrogen atom, which favors the coordination with the metal and the formation of stable complexes. However, in the case of  $\text{L}_1$  and  $\text{L}_6$ , the catalytic activity decreases due to the presence of electron-withdrawing groups (Cl and CO) that weaken the electron density at the oxygen atom and thus disfavor the formation of the copper–metal bond. In the case of complexes formed between the ligands and the metal salt  $\text{CuCl}_2$ , the absorbance remains low, and the catalytic activity decreases because the  $\text{Cl}^-$  anions are strongly bound to copper, and the coordination between the metal and the ligands thus becomes very difficult.

In summary, the catalytic activity of copper salts and quinoline ligands is very low, but their assembly results in complexes that efficiently catalyze the oxidation of catechol to *o*-quinone. The results show that the oxidation rate depends on two factors, namely the ions' nature, and the ligands' chemical structure. The ions strongly bound to copper reduce the coordination of the ligands, resulting in complexes of low catalytic activity, and the reverse is true for the ions weakly bound to copper, which facilitate the coordination of the ligands, giving stable complexes and high catalytic activities. On the other hand, the chemical structure of the ligands plays an essential role, and the presence of electron-donating groups enriches the coordination site in electron density, which increases the stability of the studied complex as well as its catalytic activity. However, the presence of electron-withdrawing groups decreases the electron density at the coordination site, which decreases the stability of the complex and its catalytic activity.

### 3. Materials and Methods

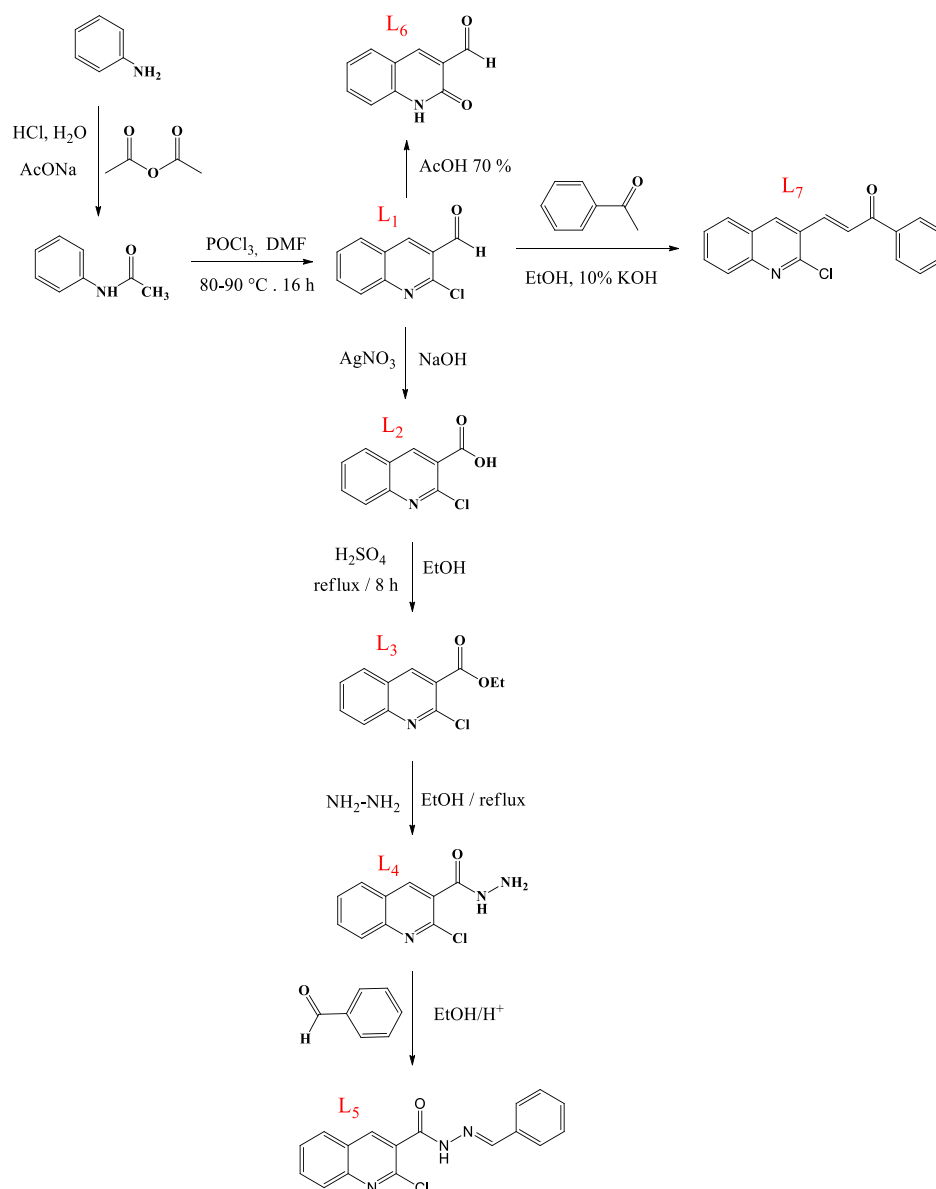
#### 3.1. Reaction and Method

The reaction studied is schematized in Scheme 1, the kinetics of this reaction was followed by measuring the absorbance as a function of time by a UV–Vis spectrophotometer for one hour at 390 nm (absorption maximum of *o*-quinone), under the following conditions:  $T = 25 \text{ }^\circ\text{C}$ ,  $\epsilon = 1.6 \text{ L mol}^{-1} \text{ cm}^{-1}$ . The solutions are prepared by dissolving in methanol, and the complexes are synthesized in situ by mixing 0.15 mL of a solution ( $2 \times 10^{-3} \text{ mol L}^{-1}$ ) of  $\text{CuX}_2$ ,  $n\text{H}_2\text{O}$ , and 0.15 mL of a solution ( $2 \times 10^{-3} \text{ mol L}^{-1}$ ) of the ligand, and then 2 mL of a solution of catechol at a concentration of  $10^{-1} \text{ mol L}^{-1}$  is added [20].

#### 3.2. Synthesis of Ligands

The studied quinoline derivatives were synthesized according to the procedures described in the literature (Scheme 3):

Synthesis of 2-chloroquinoline-3-carbaldehyde (compound  $\text{L}_1$ ): DMF (3 eq) and  $\text{POCl}_3$  (4.5 eq) were stirred for 30 min at  $0 \text{ }^\circ\text{C}$ , then acetanilide (1 eq) in  $\text{CHCl}_3$  (15 mL) was added slowly, and after the addition, the reaction mixture was heated for 16 h ( $80\text{--}90 \text{ }^\circ\text{C}$ ). When the reaction was complete, the mixture was poured into crushed ice and neutralized with saturated  $\text{NaHCO}_3$  solution; the resulting precipitate was filtered, washed with water, and recrystallized in ethyl acetate [21].



**Scheme 3.** Protocol for the synthesis of quinoline derivatives.

Synthesis of 2-chloroquinoline-3-carboxylic acid (compound  $L_2$ ): 89 mg of compound  $L_1$  were dissolved in a minimum of ethanol, then an ethanolic solution of  $\text{AgNO}_3$  (0.7 mmol) and  $\text{NaOH}$  (2.5 mmol) were added. The mixture was left under stirring at room temperature for 4 h; at the end of the reaction, the excess  $\text{AgNO}_3$  was removed by filtration, then a few drops of concentrated sulfuric acid were added to neutralize the solution. The precipitate formed was filtered, washed with water, and dried to give a dark yellow product [22].

Synthesis of ethyl 2-chloroquinoline-3-carboxylate (compound  $L_3$ ): In a minimum of ethanol, 100 mg of compound  $L_2$  and 4 drops of concentrated sulfuric acid were added, and the mixture was refluxed for 8 h. After cooling, the solid formed was recovered by filtration, washed with water, dried, and recrystallized in ethanol [23].

Synthesis of 2-chloroquinoline-3-carbohydrazide (compound  $L_4$ ): 0.5 mmol of compound  $L_3$  and 0.5 mmol of hydrazine were heated at reflux for 4 h in a minimum of ethanol, and at the end of the reaction, 50 g of ice was added to the solution and the obtained precipitate was filtered, washed with water, dried, and recrystallized in ethanol [24].

Synthesis of *N'*-benzylidene-2-chloroquinoline-3-carbohydrazide (compound L<sub>5</sub>): To 15 mL of ethanol, 56 mg of compound L<sub>4</sub> and 40 mg of benzaldehyde and a few drops of acetic acid were added and heated at reflux for 12 h. At the end of the reaction, the reaction mixture was allowed to reach room temperature and the resulting precipitate was filtered, washed with water, dried, and recrystallized in ethanol [25].

Synthesis of 2-oxo-1,2-dihydroquinoline-3-carbaldehyde (compound L<sub>6</sub>): Compound L<sub>1</sub> (1 mmol) was heated to 110 °C for 12 h in acetic acid (70%), and at the end of the reaction, the reaction mixture was allowed to reach room temperature. The precipitate formed was filtered and washed with water, dried, and recrystallized in ethanol [26].

Synthesis of 3-(2-chloroquinolin-3-yl)-1-phenylprop-2-en-1-one (compound L<sub>7</sub>): To 20 mL of ethanol, 1 mmol of acetophenone, 1 mmol of compound L<sub>1</sub>, and 5 mL of 10% NaOH solution were added. After 8 h of stirring at room temperature, the precipitate formed was filtered, washed with water, and recrystallized in ethanol [27].

NMR data of all these ligands are available in the file Supplementary Materials.

#### 4. Conclusions

The results of this study show that the studied quinoline-derived complexes possess catalytic activities, and in particular, the complexes formed between the ligands and the metal salt Cu(OAc)<sub>2</sub> efficiently catalyze the oxidation of catechol to *o*-quinone. The 2-chloroquinoline-3-carbohydrazide ligand (compound L<sub>4</sub>) exhibits the highest catalytic activity, and 2-oxo-1,2-dihydroquinoline-3-carbaldehyde (compound L<sub>6</sub>) exhibits the lowest catalytic activity. In general, the oxidation efficiency of the studied complexes depends on the ions' nature and the ligands' chemical structure. Ions weakly bound to the metal and electron-rich coordination sites yield stable complexes that strongly catalyze catechol oxidation. Further studies are still in progress in our laboratory to synthesize new quinoline derivatives, evaluate their biological and catalytic activities, as well as to obtain more details on this compelling catalytic process.

**Supplementary Materials:** The following supporting information can be downloaded at: <https://www.mdpi.com/article/10.3390/catal12111468/s1>.

**Author Contributions:** R.S. and S.T.: conceptualization, supervision, project administration, methodology, resources, data curation, writing of the original draft, review, and editing; M.M.: conduct of experiment; V.H.M.: review and editing, methodology; J.J.: project administration; Z.M.A., M.I.A.-Z. and A.B.B.: project administration, methodology, writing of original draft and paying publication fees. All authors have read and agreed to the published version of the manuscript.

**Funding:** This research received no external funding.

**Data Availability Statement:** The data presented in this study are available on request from the corresponding author.

**Acknowledgments:** The authors extend their appreciation to the Deanship of Scientific Research at King Saud University for funding this work through research group No (RGP-070).

**Conflicts of Interest:** The authors declare no conflict of interest.

#### References

1. Trammell, R.; Rajabimoghadam, K.; Garcia-Bosch, I. Copper-promoted functionalization of organic molecules: From biologically relevant Cu/O<sub>2</sub> model systems to organometallic transformations. *Chem. Rev.* **2019**, *119*, 2954–3031. [CrossRef] [PubMed]
2. Tripathy, R.; Singha, S.; Sarkar, S. A review on bio-functional models of catechol oxidase probed by less explored first-row transition metals. *J. Coord. Chem.* **2022**, *8*, 1–51. [CrossRef]
3. Hauser, D.; Septiadi, D.; Turner, J.; Petri-Fink, A.; Rothen-Rutishauser, B. From bioinspired glue to medicine: Polydopamine as a biomedical material. *Materials* **2020**, *13*, 1730. [CrossRef] [PubMed]
4. Tabassum, R.; Ashfaq, M.; Oku, H. Current pharmaceutical aspects of synthetic quinoline derivatives. *Mini-Rev. Med. Chem.* **2021**, *21*, 1152–1172. [CrossRef] [PubMed]
5. Insuasty, D.; Vidal, O.; Bernal, A.; Marquez, E.; Guzman, J. Antimicrobial activity of quinoline-based hydroxyimidazolium hybrids. *Antibiotics* **2019**, *8*, 239. [CrossRef]

6. Guan, Y.F.; Liu, X.J.; Yuan, X.Y.; Liu, W.B.; Li, Y.R.; Yu, G.X.; Zhang, S.Y. Design, Synthesis, and Anticancer Activity Studies of Novel Quinoline-Chalcone Derivatives. *Molecules* **2021**, *26*, 4899. [[CrossRef](#)]
7. Diaconu, D.; Antoci, V.; Mangalagiu, V.; Amariuca-Mantu, D.; Mangalagiu, I.I. Quinoline-imidazole/benzimidazole derivatives as dual-/multi-targeting hybrids inhibitors with anticancer and antimicrobial activity. *Sci. Rep.* **2022**, *12*, 1–17. [[CrossRef](#)]
8. Zablotsky, D.; Segal, I.; Zablotskaya, A.; Maiorov, M.; Nguyen, T.A. 19—Antimicrobial Activity of Hybrid Organic-Inorganic Core-Shell Magnetic Nanocomposites. In *Magnetic Nanoparticle-Based Hybrid Materials*; Woodhead Publishing: Cambridge, UK, 2021; pp. 501–507. ISBN 978-0-12-823688-8. [[CrossRef](#)]
9. Ajani, O.O.; Iyaye, K.T.; Ademosun, O.T. Recent advances in chemistry and therapeutic potential of functionalized quinoline motifs—A review. *RSC Adv.* **2022**, *12*, 18594–18614. [[CrossRef](#)]
10. Qin, T.H.; Liu, J.C.; Zhang, J.Y.; Tang, L.X.; Ma, Y.N.; Yang, R. Synthesis and biological evaluation of new 2-substituted-4-amino-quinolines and-quinazoline as potential antifungal agents. *Bioorganic Med. Chem. Lett.* **2022**, *72*, 128877. [[CrossRef](#)]
11. Wyman, K.A.; Girgis, A.S.; Surapaneni, P.S.; Moore, J.M.; Abo Shama, N.M.; Mahmoud, S.H.; Panda, S.S. Synthesis of Potential Antiviral Agents for SARS-CoV-2 Using Molecular Hybridization Approach. *Molecules* **2022**, *27*, 5923. [[CrossRef](#)]
12. Ji, K.L.; Liu, W.; Yin, W.H.; Li, J.Y.; Yue, J.M. Quinoline alkaloids with anti-inflammatory activity from *Zanthoxylum avicennae*. *Org. Biomol. Chem.* **2022**, *20*, 4176–4182. [[CrossRef](#)] [[PubMed](#)]
13. Abdi, B.; Fekadu, M.; Zeleke, D.; Eswaramoorthy, R.; Melaku, Y. Synthesis and Evaluation of the Antibacterial and Antioxidant Activities of Some Novel Chloroquinoline Analogs. *J. Chem.* **2021**, *2021*, 2408006. [[CrossRef](#)]
14. El-Saghier, A.M.; El-Naggar, M.; Hussein, A.H.M.; El-Adasy, A.B.A.; Olish, M.; Abdelmonsef, A.H. Eco-Friendly Synthesis, Biological Evaluation, and In Silico Molecular Docking Approach of Some New Quinoline Derivatives as Potential Antioxidant and Antibacterial Agents. *Front. Chem.* **2021**, *397*, 679967. [[CrossRef](#)] [[PubMed](#)]
15. El Rhabori, S.; El Aissouq, A.; Chtita, S.; Khalil, F. Design of novel quinoline derivatives as anti-breast cancer using 3D-QSAR, molecular docking, and pharmacokinetic investigation. *Anti-Cancer Drugs* **2022**, *33*, 789–802. [[CrossRef](#)] [[PubMed](#)]
16. Gentile, D.; Fuochi, V.; Rescifina, A.; Furneri, P.M. New Anti SARS-CoV-2 Targets for Quinoline Derivatives Chloroquine and Hydroxychloroquine. *Int. J. Mol. Sci.* **2020**, *21*, 5856. [[CrossRef](#)]
17. Verma, C.; Quraishi, M.A.; Ebenso, E.E. Quinoline and its derivatives as corrosion inhibitors: A review. *Surf. Interfaces* **2020**, *21*, 100634. [[CrossRef](#)]
18. Alamiery, A. Investigations on corrosion inhibitory effect of newly quinoline derivative on mild steel in HCl solution complemented with antibacterial studies. *Biointerface Res. Appl. Chem.* **2022**, *2*, 1561–1568.
19. Da Silva Neto, G.J.; Silva, L.R.; Annunziato, Y. Dual quinoline-hybrid compounds with antimalarial activity against *Plasmodium falciparum* parasites. *New J. Chem.* **2022**, *46*, 6502–6518. [[CrossRef](#)]
20. Saddik, R.; Abridach, F.; Benchat, N.; El Kadiri, S.; Hammouti, B.; Touzani, R. Catecholase Activity Investigation for Pyridazinone- and Thiopyridazinone-Based Ligands. *Res. Chem. Intermed.* **2012**, *38*, 1987–1998. [[CrossRef](#)]
21. Belferdi, F.; Merabet, N.; Belkhir, L.; Douara, B. Regioselective demethylation of quinoline derivatives. A DFT rationalization. *J. Mol. Struct.* **2016**, *1118*, 10–17. [[CrossRef](#)]
22. Syniugin, A.R.; Chekanov, M.O.; Volynets, G.P.; Starosyla, S.A.; Bdzhola, V.G.; Yarmoluk, S.M. Design, synthesis, and evaluation of 3-quinoline carboxylic acids as new inhibitors of protein kinase CK2. *J. Enzym. Inhib. Med. Chem.* **2016**, *31*, 160–169. [[CrossRef](#)] [[PubMed](#)]
23. Krishnakumar, V.; Khan, F.-R.N.; Mandal, B.K.; Mitta, S.; Dhasamandha, R.; Govindan, V.N. Quinoline-3-Carboxylates as Potential Antibacterial Agents. *Res. Chem. Intermed.* **2012**, *38*, 1819–1826. [[CrossRef](#)]
24. Abass, M.; Alzandi, A.R.A.; Hassan, M.M.; Mohamed, N. Recent Advances on Diversity Oriented Heterocycle Synthesis of Fused Quinolines and Its Biological Evaluation. *Polycycl. Aromat. Compd.* **2021**, *41*, 2120–2209. [[CrossRef](#)]
25. As, T.; Sal, S. Synthesis and Characterisation of Substituted Quinoline by Vilsmeier-Haack Reagent. *Int. J. Chem. Stud.* **2017**, *5*, 1–4.
26. Hamama, W.S.; Ibrahim, M.E.; Gooda, A.A.; Zoorob, H.H. Recent Advances in the Chemistry of 2-Chloroquinoline-3-Carbaldehyde and Related Analogs. *RSC Adv.* **2018**, *8*, 8484–8515. [[CrossRef](#)] [[PubMed](#)]
27. Li, W.; Xu, F.; Shuai, W.; Sun, H.; Yao, H.; Ma, C.; Xu, S.; Yao, H.; Zhu, Z.; Yang, D.-H.; et al. Discovery of Novel Quinoline-Chalcone Derivatives as Potent Antitumor Agents with Microtubule Polymerization Inhibitory Activity. *J. Med. Chem.* **2019**, *62*, 993–1013. [[CrossRef](#)]



Article

# Pharmacophore Synergism in Diverse Scaffold Clinches in Aurora Kinase B

Vijay H. Masand<sup>1,\*</sup>, Sami A. Al-Hussain<sup>2</sup>, Mithilesh M. Rathore<sup>1</sup>, Sumer D. Thakur<sup>3</sup>, Siddhartha Akasapu<sup>4</sup>, Abdul Samad<sup>5</sup> , Amal A. Al-Mutairi<sup>2</sup> and Magdi E. A. Zaki<sup>2,\*</sup>

<sup>1</sup> Department of Chemistry, Vidya Bharati Mahavidyalaya, Amravati 444602, Maharashtra, India

<sup>2</sup> Department of Chemistry, Faculty of Science, Imam Mohammad Ibn Saud Islamic University, Riyadh 11623, Saudi Arabia

<sup>3</sup> Department of Chemistry, RDIK and NKD College, Badnera, Amravati 444701, Maharashtra, India

<sup>4</sup> Curia Global, Springfield, MO 65807, USA

<sup>5</sup> Department of Pharmaceutical Chemistry, Faculty of Pharmacy, Tishk International University, Erbil 44001, Iraq

\* Correspondence: vijaymasand@gmail.com (V.H.M.); mezaki@imamu.edu.sa (M.E.A.Z.)

**Abstract:** Aurora kinase B (AKB) is a crucial signaling kinase with an important role in cell division. Therefore, inhibition of AKB is an attractive approach to the treatment of cancer. In the present work, extensive quantitative structure–activity relationships (QSAR) analysis has been performed using a set of 561 structurally diverse aurora kinase B inhibitors. The Organization for Economic Cooperation and Development (OECD) guidelines were used to develop a QSAR model that has high statistical performance ( $R^2_{tr} = 0.815$ ,  $Q^2_{LMO} = 0.808$ ,  $R^2_{ex} = 0.814$ ,  $CCC_{ex} = 0.899$ ). The seven-variable-based newly developed QSAR model has an excellent balance of external predictive ability (Predictive QSAR) and mechanistic interpretation (Mechanistic QSAR). The QSAR analysis successfully identifies not only the visible pharmacophoric features but also the hidden features. The analysis indicates that the lipophilic and polar groups—especially the H-bond capable groups—must be present at a specific distance from each other. Moreover, the ring nitrogen and ring carbon atoms play important roles in determining the inhibitory activity for AKB. The analysis effectively captures reported as well as unreported pharmacophoric features. The results of the present analysis are also supported by the reported crystal structures of inhibitors bound to AKB.

**Keywords:** aurora kinase B; QSAR; pharmacophore modeling



**Citation:** Masand, V.H.; Al-Hussain, S.A.; Rathore, M.M.; Thakur, S.D.; Akasapu, S.; Samad, A.; Al-Mutairi, A.A.; Zaki, M.E.A. Pharmacophore Synergism in Diverse Scaffold Clinches in Aurora Kinase B. *Int. J. Mol. Sci.* **2022**, *23*, 14527. <https://doi.org/10.3390/ijms232314527>

Academic Editors: Jesús Vicente de Julián-Ortiz, Gloria Castellano and Francisco Torrens

Received: 19 September 2022

Accepted: 11 November 2022

Published: 22 November 2022

**Publisher's Note:** MDPI stays neutral with regard to jurisdictional claims in published maps and institutional affiliations.



**Copyright:** © 2022 by the authors. Licensee MDPI, Basel, Switzerland. This article is an open access article distributed under the terms and conditions of the Creative Commons Attribution (CC BY) license (<https://creativecommons.org/licenses/by/4.0/>).

## 1. Introduction

The machinery for cell division, also known as mitosis, is completely regulated. Any irregularity or imperfect mitosis results in nondiploid DNA content, which ultimately causes cancer [1]. Researchers have therefore become interested in developing cancer chemotherapeutics that target centrosome maturation and separation, mitotic spindle assembly, chromosomal separation, and cytokinesis involving the participation of numerous important signaling kinases, including aurora, polo-like-kinase (Plk), and cyclin-dependent kinase (Cdk) [2,3]. The successful transition to mitosis depends on the aurora kinase family of serine/threonine kinases [4–7]. Since their discovery in 1995 and the initial detection of their expression in human cancer tissue in 1998 [2,5,7–9], these kinases have received a great deal of attention. This is due to their aberrant and excessive expression in a wide range of solid and liquid tumors, such as pancreatic, lung, liver, and breast tumors, as well as their oncogenic activity [2,4,5,7–11].

The aurora kinase family consists of three isoforms (A, B, and C), each of which differs in the length and amino acid composition of the N-terminal domain, but they share a common and conserved ATP binding site [2,12]. In order for the centrosome to mature, and for spindle assembly, meiosis, and metaphase spindle orientation to occur, aurora-A

is essential [2,12]. In order to achieve precise chromosomal segregation and cytokinesis, aurora kinase B (AKB) is required [2,12]. Massive polyploidization and failure to bio-orientate chromosomes result from AKB inhibition [2,12]. Since aurora kinase C (AKC), which complements the activity of AKB, has received less attention to date, we decided to focus only on AKB in this investigation, due to a lack of data for AKC [12].

Aurora kinases have been suggested as prospective targets for anticancer treatments due to their crucial function in controlling the cell cycle. At this time, none of the ATP-competitive inhibitors targeting AKB that are in clinical development (Figure 1) have been granted approval [4,5,13].



**Figure 1.** Structures of some known aurora inhibitors in different clinical trial stages.

In these conditions, a quick and effective strategy to find AKB inhibitors is still a key goal for medicinal chemists. To fulfill this goal, there is a need to use modern methods such as computer-aided drug design (CADD) to reduce time, costs, trial-and-error procedures, and other required resources [14,15]. The vibrant and developing field of CADD is successful due to the result-oriented performance of molecular docking, QSAR, and its other branches [14–16]. In QSAR, a mathematical model is created to connect chemical descriptors (structural features) to a desired bioactivity profile using a wide range of machine learning techniques [17,18]. In a more pragmatic sense, QSAR allows one to prioritize compounds with desirable attributes for a subsequent (and presumably successful) biological evaluation [17–19]. Traditional QSAR concentrates on producing statistically significant models [17–19]. Previously, different researchers have reported QSAR models for AKB using different techniques. For example, Neaz et al. [20] reported a 3D-QSAR model for a dataset of forty-eight quinazoline derivatives possessing other heterocyclic rings. The developed model had a leave-one-out cross-validated correlation coefficient (Q2LOO) of 0.56. Another 3D-QSAR and molecular docking study of azaindole derivatives as AKB inhibitors was accomplished by Lan and co-workers [21]. The best developed QSAR model based on forty-one molecules had Q2LOO = 0.575. Likewise, Ashraf et al. [22] used a dataset of 57 acylureidoinindolin derivatives to develop a 3D-QSAR model, which had Q2LOO = 0.641, and indicated that electrostatic and hydrophobic fields determine the activity of compounds. Thus, AKB has been the subject of QSAR research; however, the developed QSAR models find little usage due to a lack of generalizability, low predictive power, being based on small datasets comprising limited scaffolds, or a combination of these factors. Therefore, there is a need to develop a robust and balanced QSAR model based on a larger dataset, encompassing diverse structural scaffolds. Consequently, in the present work, a QSAR model has been developed that possesses high external predictive ability and extensive mechanistic interpretations supported by X-ray-resolved structures.

## 2. Results

As stated in Section 1, the focus was on developing a genetic algorithm–multilinear regression (GA–MLR) model with a combination of mechanistic interpretation and high

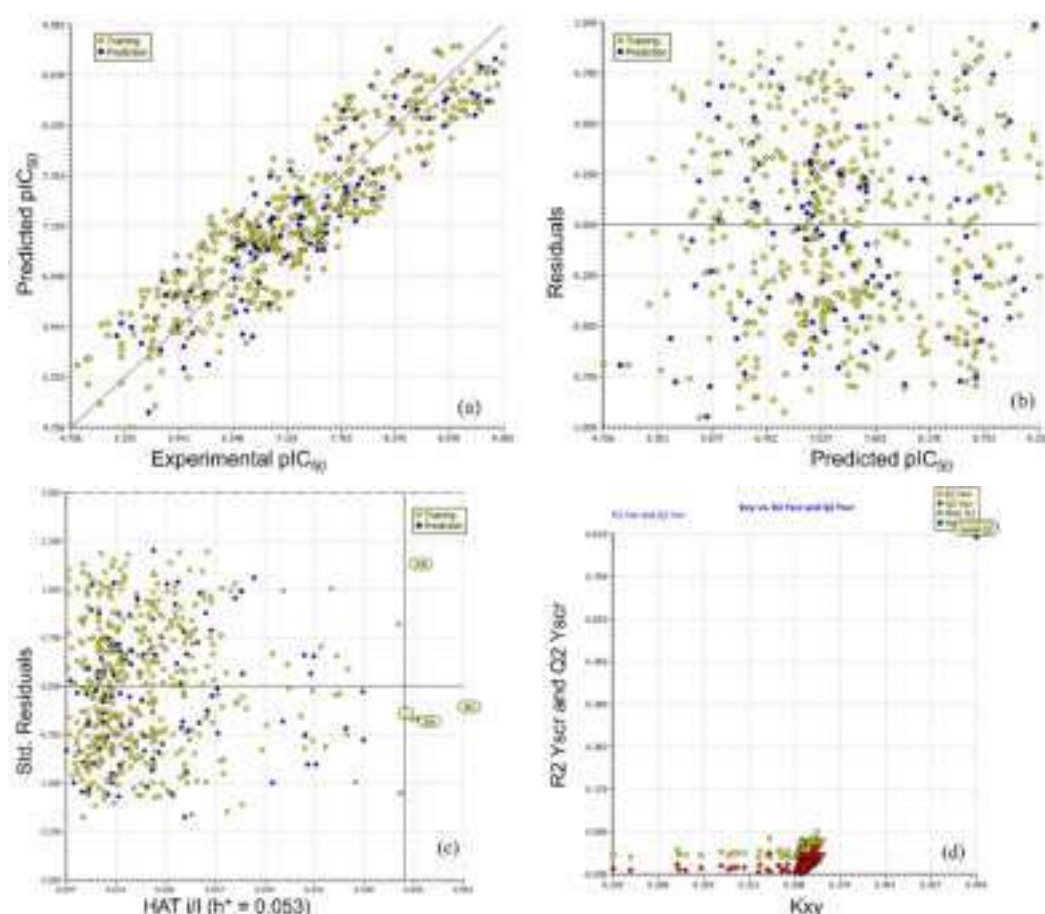


predictive power. We have discovered several structural features in the current investigation. The recently constructed seven-parameter model and its statistical validation parameters are as follows.

Model A:  $\text{pIC}_{50} = 4.611 (\pm 0.224) + 0.559 (\pm 0.105) \times \text{fringNplaN4B} + 0.436 (\pm 0.11) \times \text{fsp3Csp2N5B} + 0.253 (\pm 0.038) \times \text{N\_H\_2B} + 0.164 (\pm 0.035) \times \text{fsp2Osp2C5B} + 0.1 (\pm 0.015) \times \text{da\_lipo\_5B} - 0.317 (\pm 0.056) \times \text{fringNC6B} - 0.262 (\pm 0.048) \times \text{fOringC6B}$ .

Statistical parameters associated with model A:  $R^2_{\text{tr}} = 0.815$ ,  $\text{RMSE}_{\text{tr}} = 0.468$ ,  $\text{MAE}_{\text{tr}} = 0.401$ ,  $\text{CCC}_{\text{tr}} = 0.898$ ,  $s = 0.473$ ,  $F = 277.836$ ,  $R^2_{\text{cv}} (\text{Q2LOO}) = 0.808$ ,  $\text{RMSE}_{\text{cv}} = 0.477$ ,  $\text{MAE}_{\text{cv}} = 0.408$ ,  $\text{CCC}_{\text{cv}} = 0.895$ ,  $\text{Q2LMO} = 0.807$ ,  $R^2_{\text{Yscr}} = 0.016$ ,  $\text{Q2Yscr} = -0.02$ ,  $\text{RMSE}_{\text{ex}} = 0.446$ ,  $\text{MAE}_{\text{ex}} = 0.373$ ,  $R^2_{\text{ex}} = 0.814$ ,  $\text{Q2-F1} = 0.811$ ,  $\text{Q2-F2} = 0.811$ ,  $\text{Q2-F3} = 0.833$ ,  $\text{CCC}_{\text{ex}} = 0.900$ .

Model A is statistically robust, as shown by the high values of various statistical parameters, such as the coefficient of determination ( $R^2_{\text{tr}}$ ) and cross-validated coefficient of determination for leave-one-out ( $R^2_{\text{cv}}$  or  $\text{Q2LOO}$ ), the external coefficient of determination ( $R^2_{\text{ex}}$ ),  $\text{Q2-Fn}$  and the Concordance Correlation Coefficient ( $\text{CCC}_{\text{ex}}$ ), etc., and the low values of lack-of-fit (LOF), root mean square error ( $\text{RMSE}_{\text{tr}}$ ), and mean absolute error (MAE). As a result, model A has high external predictive ability [23–30], is devoid of random correlations [31,32], and meets suggested threshold values for key parameters. The Supplementary Materials contain the formulae to determine these parameters. A Williams plot was used to evaluate the model's applicability domain [33–36]. As a result, it complies with all the OECD-recommended standards and requirements for developing a valuable QSAR model. Different graphs associated with model A are depicted in Figure 2.



**Figure 2.** Different graphs related to model A: (a) experimental vs. predicted  $\text{pIC}_{50}$  (the solid line represents the regression line); (b) experimental vs. residuals; (c) Williams plot for applicability domain (the vertical solid line represents  $h^* = 0.053$  and horizontal dashed lines represent the upper and lower boundaries for applicability domain); (d) Y-randomization plot.

There are seven descriptors in model A, which have been calculated by PyDescriptor [37] and tabulated in Table 1. Of the seven descriptors, five descriptors, viz. fringNplaN4B, fsp3Csp2N5B, N\_H\_2B, fsp2Osp2C5B, and da\_lipo\_5B, have positive coefficients in model A, implying that increasing their value could lead to a better activity profile, whereas the reverse is true for the remaining two descriptors, fOringC6B and fringNC6B, which have negative coefficients in model A. Each molecular descriptor, which is a numeric representation of structural features [37–39], has correlations with different types of pharmacophoric features, which govern the inhibitory profile. However, it is to be noted that a single structural feature can neither explain nor fully determine the final biological activity (IC<sub>50</sub>) of a molecule. The biological activity IC<sub>50</sub>, etc., is an outcome of a combination of different structural features and some unknown factors. Some features enhance the desired pharmacological activity, whereas others are responsible for reversing it. It is believed that two or more pharmacophoric groups concomitantly decide the biological activity (pharmacophore synergism).

**Table 1.** Different molecular descriptors present in model A and their descriptions.

Molecular Descriptor	Description
fringNplaN4B	Frequency of occurrence of planer nitrogen atoms exactly at 4 bonds from ring nitrogen atom
fsp3Csp2N5B	Frequency of occurrence of sp <sup>2</sup> -hybridized nitrogen atoms exactly at 5 bonds from sp <sup>3</sup> -hybridized carbon atoms
N_H_2B	Total number of nitrogen atoms present within 2 bonds from hydrogen atoms
fsp2Osp2C5B	Frequency of occurrence of sp <sup>2</sup> -hybridized carbon atoms exactly at 5 bonds from sp <sup>2</sup> -hybridized oxygen atoms
da_lipo_5B	Total number of lipophilic atoms present within 5 bonds from H-bond donor cum acceptor atoms
fOringC6B	Frequency of occurrence of ring carbon atoms exactly at 6 bonds from oxygen atoms
fringNC6B	Frequency of occurrence of carbon atoms exactly at 6 bonds from ring nitrogen atoms

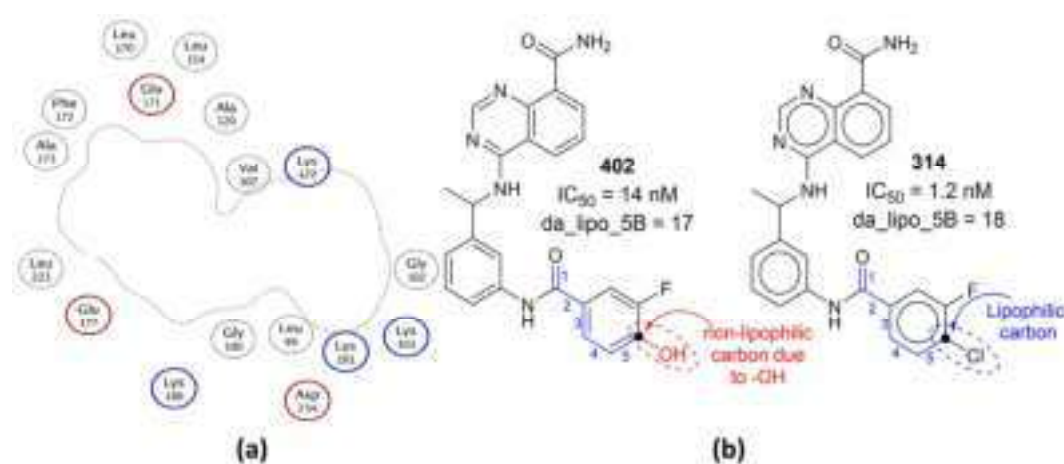
### 3. Discussion

Of the seven descriptors in model A, five descriptors, viz. fringNplaN4B, fsp3Csp2N5B, N\_H\_2B, da\_lipo\_5B, and fringNC6B, indicate the importance of different types of nitrogen atoms in determining the inhibitory activity for aurora kinase B. The same is true for carbon, which is present in four descriptors, viz. fsp3Csp2N5B, da\_lipo\_5B, fringNC6B, and fOringC6B. The relevance of oxygen is due to its presence in three descriptors, viz. fsp2Osp2C5B, da\_lipo\_5B, and fOringC6B. At the same time, it should be noted that the descriptors present in model A are highly interlinked; that is, increasing the value of one descriptor could significantly change the value of another descriptor. This leads to substantial changes in the biological profile of a molecule, pointing toward pharmacophore synergism, as molecular descriptors are mathematical representations of pharmacophores. For example, the values of descriptors fringNplaN4B and fringNC6B vary with the presence/absence of ring nitrogen atoms. Therefore, increasing the value of fringNplaN4B by escalating ring nitrogen atoms could also lead to a higher fringNC6B value. Therefore, in the present work, we have adopted an approach that involves the concomitant consideration of two or more molecular descriptors to explain the variance in the activity profile of matched molecular pairs (MMP). Accordingly, the molecular descriptors whose values have changed for MMP have been discussed concurrently with relevant examples in Section 3.

#### da\_lipo\_5B:

The descriptor da\_lipo\_5B is simultaneously associated with two important aspects of a molecule: lipophilic character and H-bonding-capable (donor and acceptor) atoms. It is to be noted that, in the present work, a carbon atom is non-lipophilic while calculating da\_lipo\_5B, if oxygen or nitrogen is attached to it. The average value of da\_lipo\_5B for the top one hundred active molecules (IC<sub>50</sub> = 0.26 to 4.3 nM) is 15.29, and the value for the

least active one hundred molecules ( $IC_{50} = 611$  to  $16,000$  nM) is 8.51. This reveals that the higher the number of lipophilic atoms within five bonds of a H-bond-capable atom, the higher the activity. This gives an initial impression that lipophilicity (mostly represented by  $\log P$  [40]) is the only governing factor. However, the calculated  $\log P$  ( $clogP$ ), which represents molecular lipophilicity, has a weak correlation of 0.077 with  $pIC_{50}$ , whereas  $da\_lipo\_5B$  has a value of 0.533. Therefore, the conditional occurrence of lipophilic atoms in the vicinity of H-bonding-capable atoms is a better choice. A plausible reason could be the composition of the active site of AKB, which consists of the persistent presence of lipophilic residues such as Gly, Leu, Val, Phe, etc., between the acidic or basic residues such as Glu, Asp, Lys [22]. This is why an aurora kinase B inhibitor also requires the presence of H-bond-capable atoms, preferably with separation by five bonds and the concomitant occurrence of lipophilic atoms in their vicinity. This observation is confirmed by the reported X-ray-resolved structure of aurora kinase B (pdb: 4c2w [41]) (see Figure 3).



**Figure 3.** (a) A 2D depiction of active site of aurora kinase B (pdb: 4c2w). The dotted line represents the contour proximity of active site residues. Acidic and basic residues have been highlighted using red- and blue-colored circles. (b) Comparison of molecule 402 with 314 with respect to  $da\_lipo\_5B$  (blue-colored bonds and numbering).

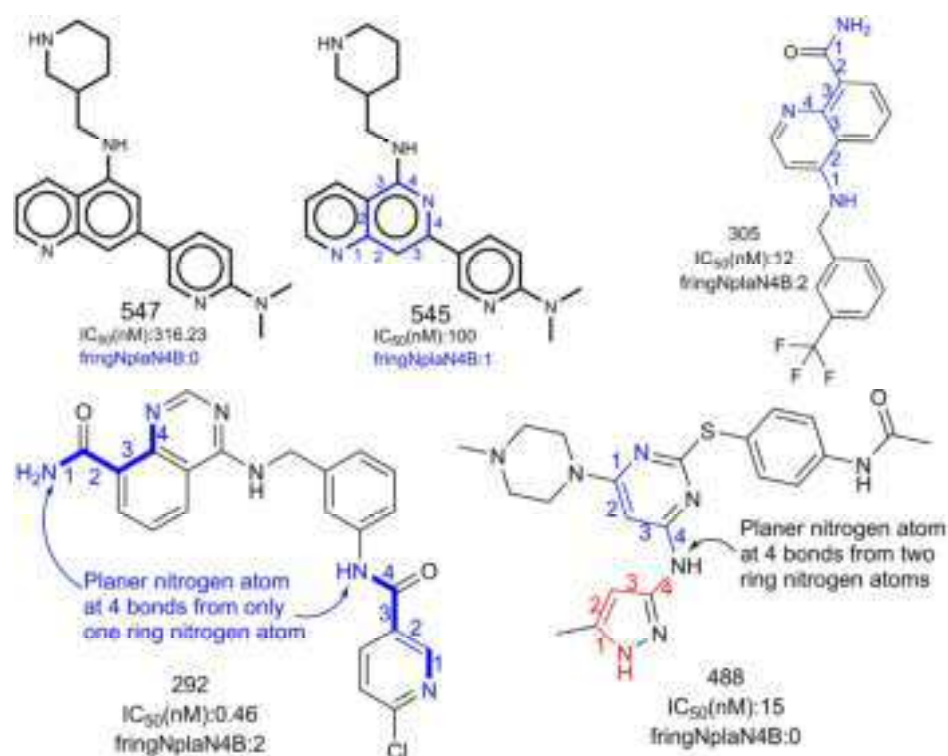
The importance of  $da\_lipo\_5B$  highlights the significance of determining the numbers of donor cum acceptor atoms required to obtain better activity. The average value of donor cum acceptor atoms for the top one hundred active molecules ( $IC_{50} = 0.26$  to  $4.3$  nM) is 3.21, and the value for the least active one hundred molecules ( $IC_{50} = 611$  to  $16,000$  nM) is 2.24. A comparison of the following pairs of molecules as representative examples further highlights the importance of  $da\_lipo\_5B$ : 314 with 402 (see Figure 3), 355 with 347, 206 with 207, 103 with 101, 103 with 99, 61 with 142, 57 with 58, etc.

#### fringNplaN4B:

fringNplaN4B stands for the frequency of occurrence of planer nitrogen atoms exactly at four bonds from a ring nitrogen atom. If the same planer nitrogen atom is also present at  $\leq 4$  bonds from the same or any other ring nitrogen atom through any path, then it is excluded while calculating fringNplaN4B. The importance of fringNplaN4B is reflected by the fact that the most active 110 molecules with  $IC_{50}$  values ranging from 0.26 to 5.9 nM have one or more combinations of planer and ring nitrogen atoms. The reverse is true for less active molecules ( $IC_{50} = 16,000$  to  $611$  nM), with some exceptions, such as molecule numbers 213, 73, 71, 66, 20, etc. Moreover, it was observed that replacing fringNplaN4B with its corresponding equivalents, fringNplaN3B and fringNplaN5B, for three and five bonds led to a reduction in the performance of model A ( $R^2 = 0.770$ , for both). Moreover, fringNplaN3B and fringNplaN5B have a correlation of  $R = 0.084$  and  $0.028$  with  $pIC_{50}$ , respectively, whereas fringNplaN4B is a better choice as a descriptor, with  $R = 0.628$ .

However, at first sight, it appears that, individually, ringN (number of ring nitrogen atoms) or nplanN (number of planer nitrogen atoms) could be an alternative to fringNplaN4B. However, both have a weak correlation of 0.207 and 0.374 with pIC50, respectively. Moreover, a loss in the statistical performance of model A on replacing fringNplaN4B with ringN ( $R^2 = 0.772$ ) or nplanN ( $R^2 = 0.770$ ) again confirmed the importance of fringNplaN4B. Therefore, a combination of ring and planer nitrogen atoms separated exactly by four bonds is an important structural feature to obtain a better pIC50 for AKB.

A literature survey reveals that for pyrrolopyrazole derivatives, a substituted 3-aminopyrazole moiety is important due to its ability to interact with the hinge region of the ATP binding site [2]. The three nitrogen atoms of the N-C-N-N pattern present in 3-aminopyrazole are responsible for binding with the receptor [2]. Unfortunately, it appears that the reported pattern is exclusive to pyrrolopyrazole derivatives bearing a substituted 3-aminopyrazole moiety. Interestingly, the terminal nitrogen atoms of the N-C-N-N pattern are actually ring and planer nitrogen atoms, thereby suggesting the possible presence of fringNplaN4B. However, in many active molecules of the present dataset bearing a substituted 3-aminopyrazole moiety, the value of fringNplaN4B is zero; this is because the planer nitrogen of the N-C-N-N pattern is also present within  $\leq 4$  bonds of the other ring nitrogen atom. However, in several active molecules for AKB, fringNplaN4B is present due to other scaffolds (see Figure 4). In other words, instead of the N-C-N-N pattern or a substituted 3-aminopyrazole moiety, an emphasis on the simultaneous presence of planer and ring nitrogen atoms separated by four bonds in the molecule is a better strategy to enhance the inhibitory profile against AKB. Hence, the present work successfully identified a novel aspect of a reported pattern (N-C-N-N) and extended it for other scaffolds.



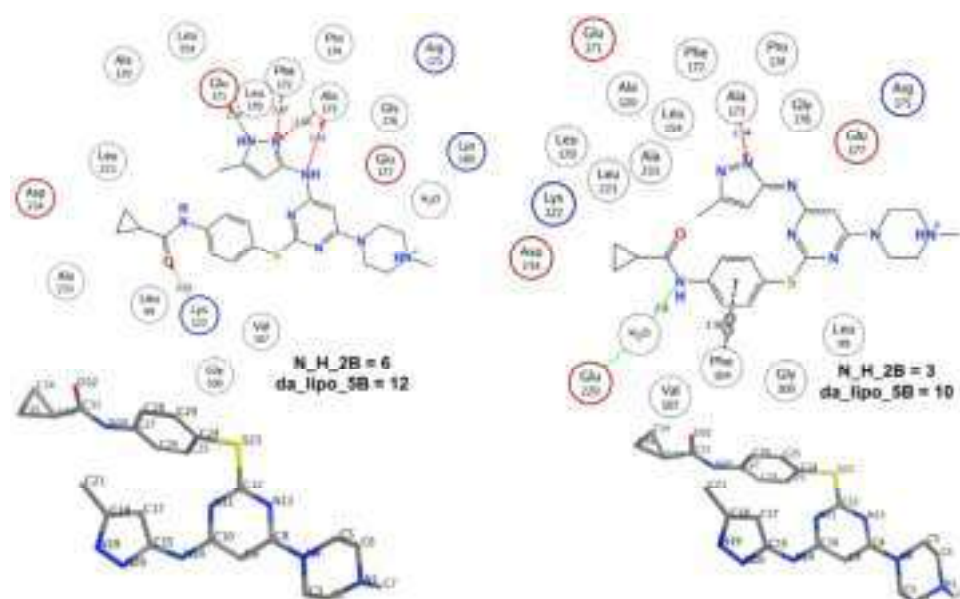
**Figure 4.** Representation of influence of fringNplaN4B on activity profile of AKB inhibitors. The numbers (blue/red) indicate the counting of number of bonds between ring and planer nitrogen.

#### N\_H\_2B:

The positive coefficient for N\_H\_2B indicates that the presence of hydrogen in the vicinity of nitrogen is beneficial to increase the inhibitory activity for aurora kinase B. In many molecules, N\_H\_2B exists due to the direct attachment of a hydrogen atom to a nitrogen atom (N-H) or due to hydrogen atoms bonded to carbon atoms adjacent to

nitrogen (N-CH<sub>n</sub> fragment). N\_H\_2B favors two important structural features that could lead to a better inhibitory profile: (1) the presence of polar hydrogen atoms as N-H or N-CH<sub>n</sub> fragments; (2) steric hindrance or bulkiness in the vicinity of nitrogen atoms, because hydrogen is the smallest among all the elements. The lesser the bulkiness around nitrogen atoms, the better the inhibitory profile. These two structural features in combination allow the polar interactions or H-bond formation between the ligand and the receptor. This observation, and the significance of N\_H\_2B as well as da\_lipo\_5B, is confirmed by the two forms of the ligand VX-680 (molecule number 14) in the pdb 4b8m [42].

The ligand VX-680 exists in two different forms, labeled as TA and TB in the present work, in the two chains of pdb 4b8m. From Figure 5 and Table 2, it is clear that the TA form consists of a higher number of hydrogen atoms than TB, especially in the vicinity of nitrogen atoms. This led to different values for N\_H\_2B for the two forms (see Figure 5). The form TA, having a higher N\_H\_2B value, has a higher number of interactions with the receptor, because the additional hydrogen atoms attached to the nitrogen atoms of the pyrazole (designated as N19 and N20) ring and aminopyrimidine (designated as N14) are responsible for H-bond interactions with Glu171, Phe172, and Ala173 (see Table 2). Meanwhile, these interactions are absent for TB, even though the respective atoms N19 and N14 of TB are more proximate to receptor atoms. The TB form has only one prominent interaction with the receptor due to the nitrogen (designated as N20) of the pyrazole ring in the form of a H-bond with Ala173.



**Figure 5.** Pictorial representation of N\_H\_2B using VX-680 (pdb 4b8m) as an example.

**Table 2.** Distances of different atoms of TA and TB forms of VX-680 (molecule number 14) from the receptor atoms (pdb 4b8m).

TA Form				TB Form			
Residue	Residue Atom	Ligand Atom	Distance	Residue	Residue Atom	Ligand Atom	Distance
GLU171	O	N19	2.97	GLU171	O	N19	2.74
PHE172	CA	N20	3.47	PHE172	CA	N20	3.52
ALA173	N	N20	2.84	ALA173	N	N20	2.74
ALA173	O	N14	2.93	ALA173	O	N14	2.91
HOH2005	O	N13	3.32	HOH2005	O	N30	2.80

The following comparisons of molecules further highlight the importance of N\_H\_2B (see Figure 6): 108 with 75 and 101, 486 with 487 and 484, and 148 with 144, to list a few. A simple analysis of these examples indicates that the presence of a pyrazole ring leads to a better IC<sub>50</sub> for a molecule (see Figure 6). However, it has a negative correlation ( $R = -0.177$ ) with pIC<sub>50</sub>. A plausible reason appears from the present work suggesting that H-bond-capable polar groups are more suitable near the periphery of a molecule, rather than a pyrazole ring, to achieve good interactions with the receptor.



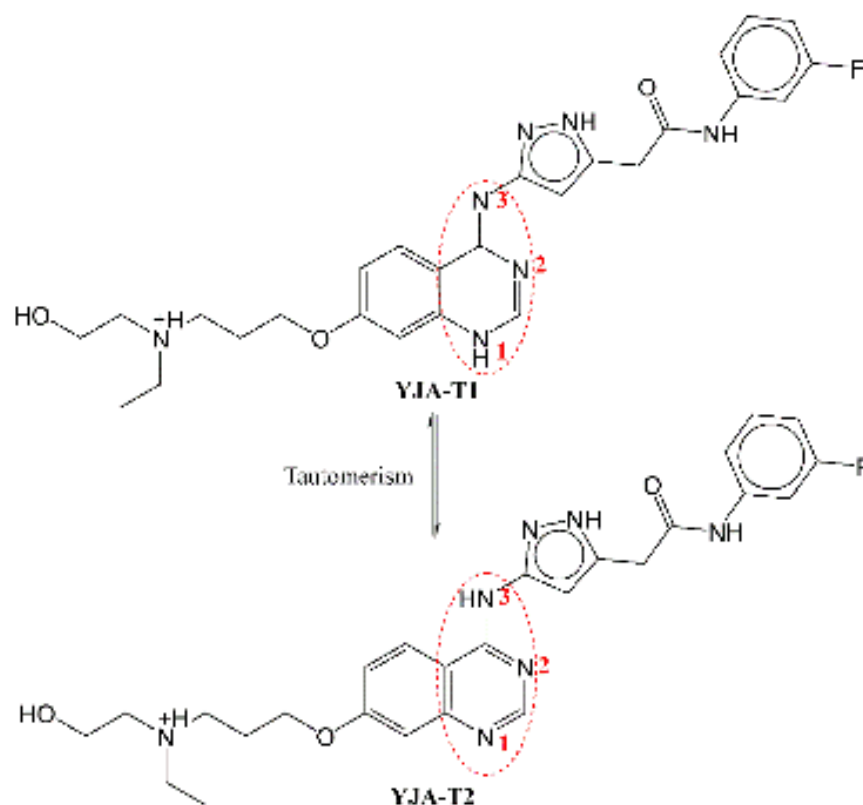
**Figure 6.** Representative examples to understand N\_H\_2B.

### fsp3Csp2N5B:

The descriptor fsp3Csp2N5B is associated with two features, viz. sp<sup>2</sup>-hybridized nitrogen and sp<sup>3</sup>-hybridized carbon atoms. As it has a positive coefficient in model 1, increasing the numbers of such atoms favors the augmentation of pIC<sub>50</sub>. At the same time, increasing fsp3Csp2N5B could influence the values of da\_lipo\_5B and N\_H\_2B, as these descriptors are associated with carbon and nitrogen too. Therefore, it indicates that pharmacophore synergism determines the final inhibitory ability of a molecule for AKB. This is clearly reflected when molecule 435 is compared with molecule 438.

The pdb 4c2v contains two different tautomeric forms of ligand YJA in two different chains, A and B. The influence of fsp3Csp2N5B along with N\_H\_2B is observed for the two tautomeric forms of co-crystallized ligand 'YJA' in the pdb 4c2v [41]. The two tautomeric forms show that YJA-T1 and YJA-T2 (see Figure 7) of ligand YJA have different values for fsp3Csp2N5B and N\_H\_2B (see Table 3). The online tautomer generator from Chemaxon (<https://disco.chemaxon.com/calculators/demo/plugins/tautomers/>, accessed on 28 October 2022) indicates that the ligand YJA can exist in seven different tautomeric forms. However, only two tautomeric forms, YJA-T1 and YJA-T2, predominate, with approximately 16 and 84 percent, respectively. The rest of the tautomeric forms have less than a 0.1% probability of existence.

A comparison of the interactions of YJA-T1 and YJA-T2 with the receptor and the solvent indicates that the two forms have established H-bonds with the similar amino acid residues of the receptor but with different distances (see Figure 8). The YJA-T2 has an additional H-bond with the solvent (HOH2108). Moreover, it has a higher number of interactions with the receptor and the solvent (H<sub>2</sub>O) within 5 Å compared to YJA-T1. Thus, the increased value of fsp3Csp2N5B and N\_H\_2B for these two tautomeric forms correlates with a higher number of receptor atoms in the vicinity, which ultimately leads to an augmented number of interactions. Additional details related to the interactions of YJA-T1 and YJA-T2 with the receptor are available in Table S1 in the Supplementary Materials.



**Figure 7.** Tautomeric forms of ligand YJA (pdb 4c2v). The red colored numbers have been used for indication of nitrogen atoms involved in tautomerism.

**Table 3.** A comparison of two tautomeric forms, YJA-T1 and YJA-T2.

Tautomer with Descriptor Value	H-Bonds Formed with Distance (Å) with Angle (Donor-Hydrogen-Acceptor) (Cut-Off: 5 Å)	List of Receptor Heavy Atoms within 5 Å of N3 atom of Ligand (Residue-Atom-Distance in Å)	List of Receptor Heavy Atoms within 5 Å of N1 Atom of Ligand (Residue-Atom-Distance in Å)
YJA-T1 fsp3Csp2N5B = 0 N_H_2B = 6 fsp2Osp2C5B = 3	LYS122 at 1.668 with 159.8°, GLN145 at 2.251 with 142.4°, ALA173 at 1.952 with 163.9°	VAL107-CB-4.672, VAL107-CG1-4.351, VAL107-CG2-4.419, LU177-OE2-4.842, LEU223-CG-4.608, LEU223-CD1-3.627, LEU223-CD2-4.406	LEU99-CD1-4.259, ALA120-CB-4.501, GLU171-C-4.888, GLU171-O-4.058, PHE172-N-4.808, PHE172-CA-3.818, PHE172-C-3.832, PHE172-CB-4.641, PHE172-CG-4.403, PHE172-CD1-3.550, PHE172-CE1-4.156, ALA173-N-2.936, ALA173-CA-3.743, ALA173-C-4.208, ALA173-O-3.930, ALA173-CB-3.623, LEU223-CD1-4.121

Table 3. Cont.

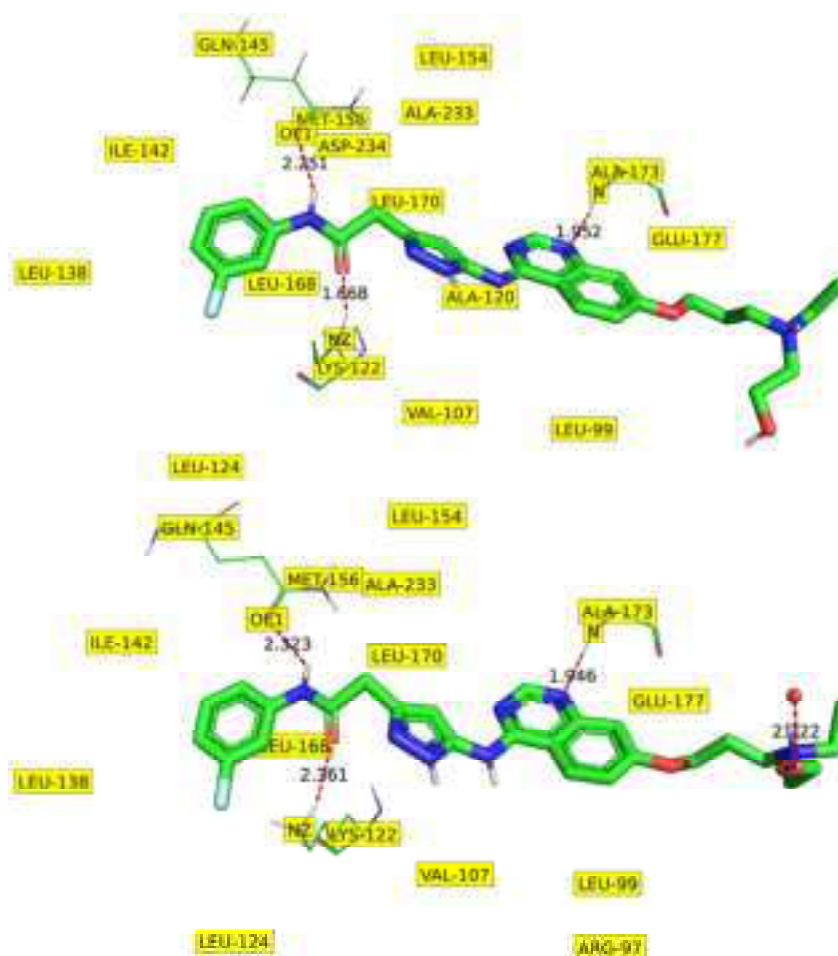
Tautomer with Descriptor Value	H-Bonds Formed with Distance (Å) with Angle (Donor–Hydrogen–Acceptor) (Cut-Off: 5 Å)	List of Receptor Heavy Atoms within 5 Å of N3 atom of Ligand (Residue–Atom–Distance in Å)	List of Receptor Heavy Atoms within 5 Å of N1 Atom of Ligand (Residue–Atom–Distance in Å)
YJA-T2 fsp3Csp2N5B = 1 N_H_2B = 7 fsp2Osp2C5B = 3	LYS122 at 2.361 with 157.8°, GLN145 at 2.323 with 115.7°, ALA173 at 1.946 with 174.4°, HOH2108 2.222 with 106.7°	PHE104-CG-4.358, PHE104-CD2-3.203, PHE104-CE2-3.058, PHE104-CZ-4.124, VAL107-CB-4.591, VAL107-CG1-4.413, VAL107-CG2-4.142, LEU223-CD1-4.047, LEU223-CD2-4.948	LEU99-CD2-3.977, ALA120-CB-4.707, GLU171-C-4.734, GLU171-O-3.872, PHE172-N-4.690, PHE172-CA-3.669, PHE172-C-3.814, PHE172-CB-4.567, PHE172-CG-4.418, PHE172-CD1-3.618, PHE172-CE1-4.265, ALA173-N-2.953, ALA173-CA-3.799, ALA173-C-4.271, ALA173-O-3.915, ALA173-CB-3.635, LEU223-CD1-4.165

**fsp2Osp2C5B:**

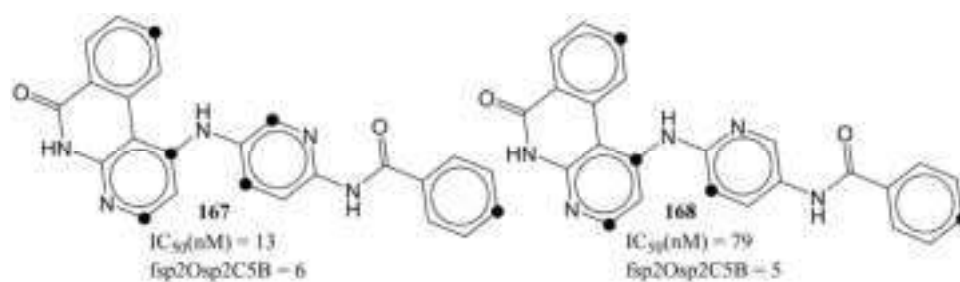
The molecular descriptor fsp2Osp2C5B underlines the influence of a specific combination of sp<sup>2</sup>-hybridized carbon with sp<sup>2</sup>-hybridized oxygen in determining the inhibitory profile for AKB. The positive coefficient for fsp2Osp2C5B indicates that increasing such a combination of oxygen and carbon could lead to a better inhibitory profile. In the present dataset, there are 426 molecules with the presence of at least one such combination of oxygen and carbon. Likewise, the 200 most active molecules with IC<sub>50</sub> values in the range of 0.26 to 24 nM, except molecule numbers 36 and 469, also possess fsp2Osp2C5B >1. A comparison of molecule number 167 with 168 further strengthens this observation (see Figure 9).

A closer analysis revealed that the sp<sup>2</sup>-hybridized carbon with sp<sup>2</sup>-hybridized oxygen, required for the existence of fsp2Osp2C5B are, in general, aromatic carbon atoms and oxygen of the carbonyl group, especially the amide group, respectively. This further highlights the importance of aromatic rings—and in turn lipophilic atoms—as aromatic carbons are mostly lipophilic in nature. The need for an amide group in conjugation points out the necessity of a polar group to enhance the interactions with the receptor. The two tautomeric forms of YJA-T1 and T2 possess such a combination and it results in enhanced interactions with the receptor (see Figure 8). Obviously, a sp<sup>2</sup>-hybridized carbon atom will be at a respective distance of three and five bonds from the nitrogen and oxygen atoms of the same amide group; therefore, we also checked the importance of famdNsp2C3B (frequency of occurrence of sp<sup>2</sup>-hybridized carbon atoms exactly at three bonds from amide nitrogen atoms). It was observed that fsp2Osp2C5B and famdNsp2C3B have a correlation of 0.64 and 0.58, respectively, with pIC<sub>50</sub>. Therefore, fsp2Osp2C5B is a better choice to be considered for future optimizations and activity predictions.





**Figure 8.** Depiction of prominent interactions of YJA-T1 and T2 with the receptor (pdb: 4c2v).

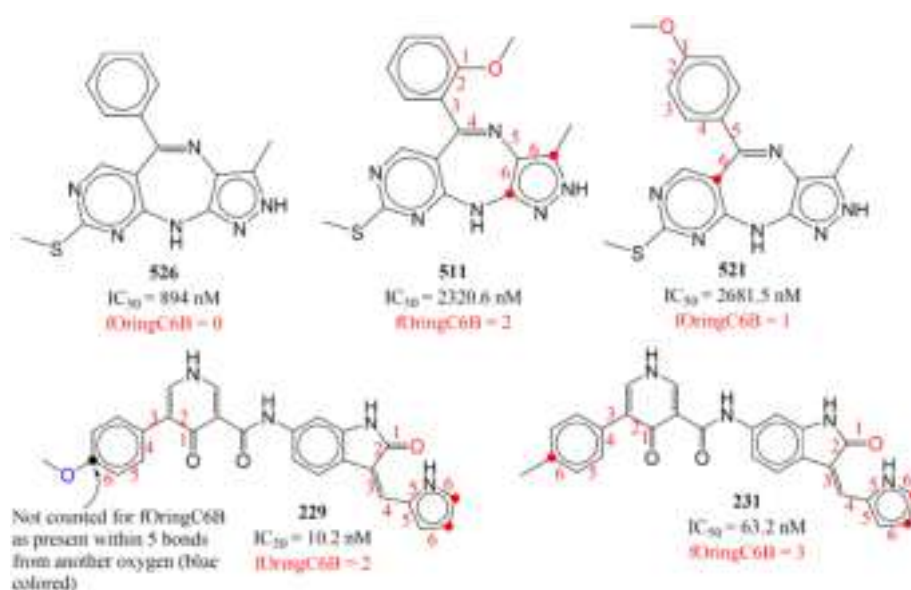


**Figure 9.** Representation of *fsp2Osp2C5B* using molecule numbers 167 and 168 as representative examples. The black circle represents the  $sp^2$ -hybridized carbon at five bonds from  $sp^2$ -hybridized oxygen.

### fOringC6B:

The descriptor *fOringC6B* is associated with the simultaneous and conditional occurrence of polar (oxygen) and lipophilic characters (ring carbons) with an exact separation by six bonds. If a ring carbon is also present within five or less bonds of any other oxygen atom, then it is omitted while calculating *fOringC6B*. The molecular descriptor *fOringC6B* has a negative coefficient in model 1, which means that a higher number of such carbon atoms could reduce the inhibitory profile of a molecule for AKB. This is confirmed when the following pairs of molecules are compared: 526 with 511, 526 with 521, 204 with 205, 229 with 231, 477 with 485, and 256 with 257. The descriptor has been depicted in Figure 10. The red dots indicate the ring carbons, which contribute to *fOringC6B* at exactly six bonds

from the oxygen atom. The six bonds separating such carbon and oxygen atoms have been labeled with numbers.



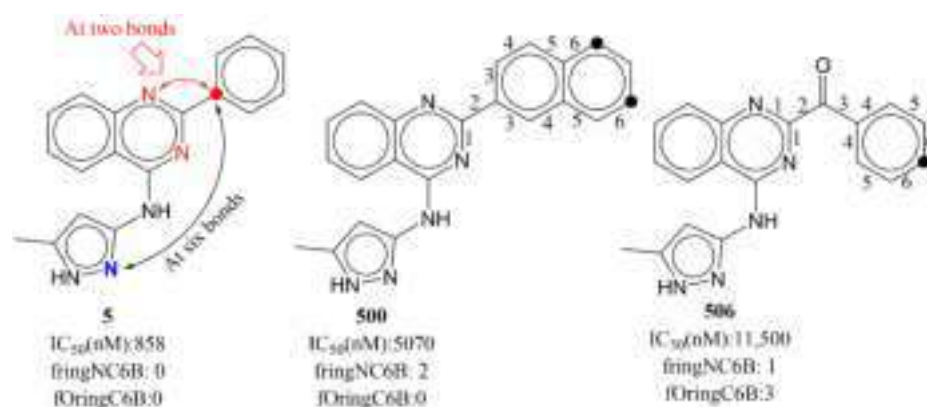
**Figure 10.** Representative examples for fOringC6B. The numbers (red) indicate the counting of number of bonds between ring carbon and oxygen atom.

It appears that reducing the number of ring carbon atoms is a feasible solution to achieve a lower value of fOringC6B, but this will affect negatively other descriptors, viz. da\_lipo\_5B, fsp2Osp2C5B. Instead, a solution is to reduce the number of oxygen atoms or alternatively increase their presence within five or less bonds of ring carbon atoms. The second solution is observed in the case of molecule number 229. The additional -OCH3 led to a decreased value of fOringC6B, because, while calculating fOringC6B, if a ring carbon atom was simultaneously present within six bonds of two or more oxygen atoms, it was excluded.

#### fringNC6B:

The molecular descriptor fringNC6B provides crucial information about the upper limit for separation required between the lipophilic (carbon atoms) and polar (nitrogen atoms) moieties to achieve a better activity profile. While calculating fringNC6B, if a carbon atom is also present within five bonds of any other ring nitrogen, then it is omitted. If a carbon atom is present exactly at a distance of six bonds from a ring nitrogen atom, then it contributes negatively; therefore, such a combination should be avoided. Reducing the bond gap between carbon and ring nitrogen is a feasible and justified solution, as other descriptors, viz. da\_lipo\_5B and fsp3Csp2N5B, also indicate the same. As stated earlier, a plausible reason for this could be the active site of AKB (see Figure 11). The influence of fringNC6B on activity is confirmed when following pairs of molecules are compared: 5 with 500, 5 with 506, 374 with 406, 507 with 514, to list a few.

As stated earlier, the descriptors present in model A are entangled. Therefore, changing one descriptor could result in changes in other descriptors. For example, the descriptors fringNplaN4B and fringNC6B indicate the importance of ring nitrogen atoms. The fringNplaN4B has a positive correlation with pIC50 but fringNC6B has the opposite relation. Therefore, increasing the value of fringNplaN4B by escalating the ring nitrogen atoms could also lead to a higher fringNC6B value. Hence, a balance of the appropriate number and types of nitrogen, carbon, and oxygen could lead to significant inhibitory activity for aurora kinase B.



**Figure 11.** Depiction of fringNC6B using molecule numbers 5, 500, and 506 as representative examples. The carbon present at six bonds from ring nitrogen has been depicted using black dots. The numbers (black) indicate the counting of number of bonds between ring nitrogen and carbon.

#### 4. Materials and Methods

In this work, we adhered to the OECD's and other researchers' suggested standards and recommendations [17–19,32,43,44] for a successful QSAR analysis. The various procedures for creating a model included meticulous dataset selection, data curation, 3D structure production for all molecules, computation and trimming of molecular descriptors, model creation and extensive validation, and mechanistic interpretation [45,46]. To eliminate bias and ensure proper model validation, these stages were carried out one at a time.

##### 4.1. Selection of Dataset

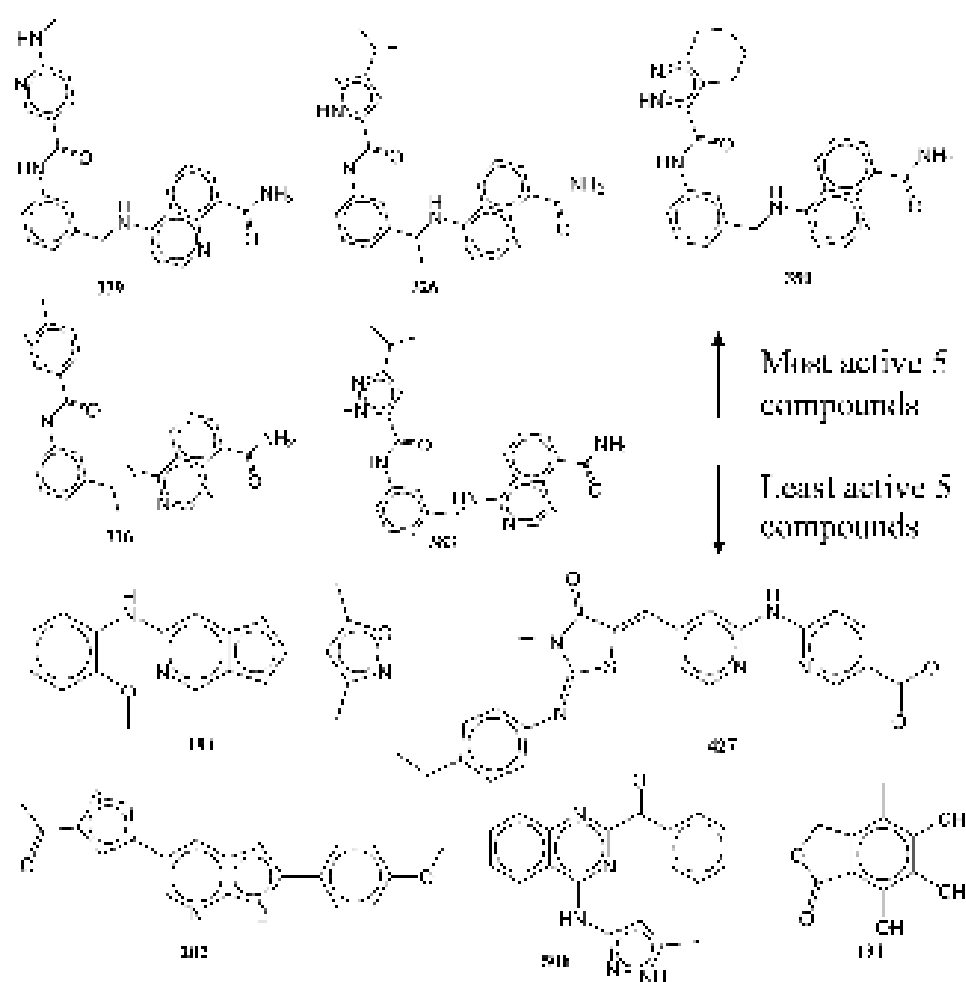
The success and efficacy of a QSAR analysis in the drug discovery pipeline are significantly influenced by the size, composition, and structural diversity of the selected dataset used for the analysis [17–19,32,43,44]. As a result, a sizable dataset of 3398 reported AKB ligands was downloaded from BindingDB (<https://www.bindingdb.org/bind/index.jsp>, accessed on 14 January 2022). The dataset was then reduced to 561 molecules only after duplicates (average value for duplicates), salts, metal derivatives, rule-of-five violators, molecules with undefinable K<sub>i</sub> values, etc., were eliminated during data curation [47]. The condensed dataset still included a variety of molecules, such as stereoisomers, positional and chain isomers, various heterocyclic and aromatic scaffolds, etc. Thus, it covered a broad chemical space. The experimental IC<sub>50</sub> ranged from 0.26 to 16,000 nM. The experimental IC<sub>50</sub> values were converted to pIC<sub>50</sub> for a better QSAR analysis ( $-\log_{10} \text{IC}_{50}$ ). Figure 12 and Table 4 comprise some molecules that are very active and those that are least active, to help the readers to understand the structural variation present in the dataset.

**Table 4.** SMILES notation, IC<sub>50</sub> (nM), and pIC<sub>50</sub> (M) of five most and least active molecules of the selected dataset.

Mol ID	SMILES	IC <sub>50</sub> (nM)	pIC <sub>50</sub> (M)
339	<chem>O=C(Nc1cc(CNc2ncnc3c(C(=O)N)cccc23)ccc1)c1cnc(NC)cc1</chem>	0.26	9.585
326	<chem>O=C(Nc1cc(C(Nc2ncnc3c(C(=O)N)cccc23)C)ccc1)c1[nH]nc(C(C)C)c1</chem>	0.27	9.569
350	<chem>O=C(Nc1cc(CNc2ncnc3c(C(=O)N)cccc23)ccc1)c1[nH]nc2c1CCCC2</chem>	0.3	9.523
316	<chem>O=C(Nc1cc(C(Nc2ncnc3c(C(=O)N)cccc23)C)ccc1)c1cnc(C)cc1</chem>	0.32	9.495
383	<chem>O=C(Nc1cc(CNc2ncnc3c(C(=O)N)cccc23)ccc1)c1[nH]nc(C(C)C)c1</chem>	0.33	9.481
191	<chem>O=C1OCc2c(C)c(O)c(O)c(O)c12</chem>	8690	5.061
506	<chem>O=C(c1nc(Nc2n[nH]c(C)c2)c2c(n1)cccc2)c1cccc1</chem>	11,500	4.939

Table 4. Cont.

Mol ID	SMILES	IC50 (nM)	pIC50 (M)
202	<chem>O=C(C)c1scc(-c2cnc3[nH]c(-c4ccc(OC)cc4)nc3c2)c1</chem>	12,100	4.917
427	<chem>O=C(O)c1cnc(Nc2nccc(/C=C\3/C(=O)N(C)/C(=N/c4ccc(CC)cc4)/S/3)c2)cc1</chem>	12,505.05	4.903
194	<chem>O(C)c1c(Nc2ncc3c([nH]c(-c4c(C)onc4C)c3)c2)cccc1</chem>	16,000	4.796



**Figure 12.** Representative examples from the selected dataset (five most active and five least active molecules).

#### 4.2. Calculation of Molecular Descriptors and Objective Feature Selection (OFS)

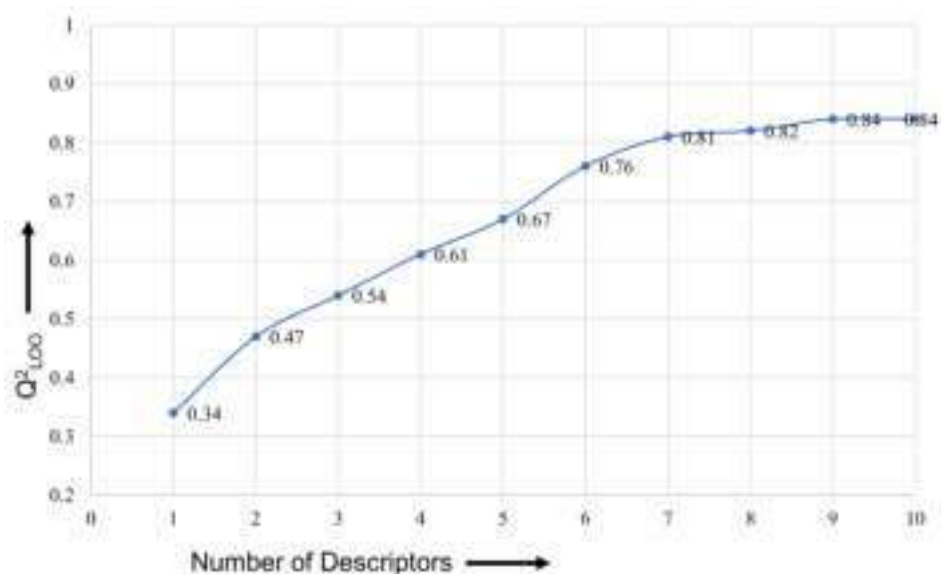
The next step involved applying the proper methodology to convert SMILES notations into 3D-optimized structures. OpenBabel 3.1 [48] was used to translate SMILES to SDF for this. Then, utilizing PM3 as a force field for structure optimization and partial charge assignment, SDF was converted to MOL2 using MOPAC [49] 2016. After this, PyDescriptor [37] and PaDEL [50], which together offered more than 40,000 molecular descriptors for each molecule, were used for molecular descriptor calculation. Although using a large number of molecular descriptors increases the likelihood that a QSAR analysis will be effective, with a balance of predictive and mechanistic interpretation abilities, it also raises the risk of overfitting due to noisy redundancy in the descriptors or chance correlations. As a result, OFS was carried out using QSARINS 2.2.4 [51], which eliminated molecular descriptors that were nearly constant (for 90% of molecules) and highly inter-correlated ( $|R| > 0.90$ ). After extensive OFS, only 1150 descriptors were finally included in the reduced set of molecular descriptors, but they nevertheless covered a wide descriptor space because they included

fingerprints, charged-based, 1D to 3D, and a good number of atom-pair descriptors. The likelihood of a mechanistic interpretation of the model increased because a significant portion of the descriptors could be readily interpreted in terms of structural traits.

#### 4.3. Splitting the Dataset into Training and External Sets and Subjective Feature Selection (SFS)

SFS is one of the most important steps in the QSAR model-building process that involves choosing the right feature selection technique with an adequate number and set of molecular descriptors. Before developing the QSAR model, the dataset was randomly divided into a training set (80%, or 449 molecules) and a prediction set (20%, or 112 molecules), to allow for proper training and validation of the model. In order to eliminate bias, reduce information leakage [32], confirm the model's external predictive ability to predict for molecules other than the training set, and to improve the composition of the training and prediction sets, the dataset was randomly divided at a ratio of 80:20. The selection of molecular descriptors was done using the training set only. The prediction set, also known as the test set or external set, was used exclusively for judging the external predictive ability of the model.

To prevent over- and underfitting, the QSAR model must have an ideal number of molecular descriptors (variables). Consequently, the ideal number of descriptors for the model was identified using a straightforward graphical (or breaking point) method [45,46,52]. The value of  $Q^2_{LOO}$  typically increases considerably when a new variable (molecular descriptor) is added in stages to an MLR model until the desired elevation is reached. After this, the value of  $Q^2_{LOO}$  increases slightly or negligibly. As a result, the number of molecular descriptors that match the elevation point is ideal for creating a QSAR model. A graph of this is shown in Figure 13. The last elevation point in Figure 13 corresponds to seven molecular descriptors. Therefore, the genetic algorithm (GA) in combination with multi-regression (GA-MLR) method, using QSARINS 2.2.4, was used for the exhaustive search to identify seven molecular descriptors to develop the QSAR model. For GA-MLR,  $Q^2_{LOO}$  was used as the fitness parameter.



**Figure 13.** Plot of number of descriptors against leave-one-out coefficient of determination ( $Q^2_{LOO}$ ) to identify the optimum number of descriptors.

#### 4.4. Building Regression Model and Its Validation

Different combinations of various molecular descriptors were eventually found during the search for seven molecular descriptors for the QSAR model using GA-MLR. However, due to the statistical performance and the satisfaction of adhering to strict parameters and criteria, which have been recommended [17–19,23,27,32,33,44–46,52–57] by a significant

number of researchers, only one combination of molecular descriptors was chosen. The following threshold values and conditions were used to select the model:

$R^2_{tr} \geq 0.6$ ,  $Q2LOO \geq 0.5$ ,  $Q2LMO \geq 0.6$ ,  $R^2 > Q2LOO$ ,  $R^2_{ex} \geq 0.6$ ,  $RMSE_{tr} < RMSE_{cv}$ ,  $\Delta K \geq 0.05$ ,  $CCC \geq 0.80$ ,  $Q2-Fn \geq 0.60$ ,  $r2m \geq 0.5$ ,  $(1-r2/ro2) < 0.1$ ,  $0.9 \leq k \leq 1.1$  or  $(1-r2/r'o2) < 0.1$ ,  $0.9 \leq k' \leq 1.1$ ,  $|ro2 - r'o2| < 0.3$ ,  $RMSE_{ex}$ ,  $MAE_{ex}$ ,  $R^2_{ex}$ ,  $Q2F1$ ,  $Q2F2$ ,  $Q2F3$ , and low  $R2Y_{scr}$ ,  $RMSE$  and  $MAE$ .

The model's application domain must be identified for additional validation. In order to assess the application domain of the QSAR model, we employed a Williams plot (standardized residuals vs. hat values).

## 5. Conclusions

In relation to different features influencing the inhibitory activity for AKB, the present analysis successfully highlighted the significance of different types of atoms, groups, patterns, and tautomerism. Additionally, it emphasized the significance of specific patterns of atoms of different hybridization and their inter-relations in determining the final activity. The conditional presence of lipophilic (carbon) atoms or groups with respect to nitrogen atoms was also successfully recognized by model A as being beneficial for obtaining higher inhibitory for AKB. The present work, for the first time, pointed out the role played by tautomerism for AKB inhibitors. Model A performed statistically well, which was indicative of its strong external prediction power. As the current work successfully recognized both previously described and novel pharmacophoric properties associated with AKB inhibition, the results are of immense use throughout the drug discovery pipeline for the development of lead/drug candidates against AKB.

**Supplementary Materials:** The following supporting information can be downloaded at: <https://www.mdpi.com/article/10.3390/ijms232314527/s1>.

**Author Contributions:** V.H.M. and M.E.A.Z.: conceptualization, project design, and experimental studies; V.H.M. and S.A.A.-H.: drafting, resources, and funding management; M.M.R., S.A. and S.D.T.: data collection and curation, drafting, and data compilation; S.A., A.S. and A.A.A.-M.: draft revision and analysis. All authors have read and agreed to the published version of the manuscript.

**Funding:** The authors acknowledge the Deanship of Scientific Research at Imam Mohammad Ibn Saud Islamic University, Riyadh, Saudi Arabia, for its support of this research through research group number RG-21-09-76.

**Institutional Review Board Statement:** Not applicable.

**Informed Consent Statement:** Not applicable.

**Data Availability Statement:** Data are contained within the article and Supplementary Materials.

**Acknowledgments:** V.H.M. is grateful to Paola Gramatica (Italy) and her team for providing the free copy of QSARINS 2.2.4.

**Conflicts of Interest:** The authors declare no conflict of interest.

## Abbreviations

SMILES	Simplified molecular-input line-entry system
GA	Genetic algorithm
MLR	Multiple linear regression
QSAR	Quantitative structure–activity relationship
WHO	World Health Organization
OLS	Ordinary least squares
QSARINS	QSAR Insubria
OECD	Organization for Economic Cooperation and Development

## References

1. Du, R.; Huang, C.; Liu, K.; Li, X.; Dong, Z. Targeting AURKA in Cancer: Molecular mechanisms and opportunities for Cancer therapy. *Mol. Cancer* **2021**, *20*, 15. [[CrossRef](#)] [[PubMed](#)]
2. Garuti, L.; Roberti, M.; Bottegioni, G. Small Molecule Aurora Kinases Inhibitors. *Curr. Med. Chem.* **2009**, *16*, 1949–1963. [[CrossRef](#)] [[PubMed](#)]
3. Pollard, J.R.; Mortimore, M. Discovery and Development of Aurora Kinase Inhibitors as Anticancer Agents. *J. Med. Chem.* **2009**, *52*, 2629–2651. [[CrossRef](#)] [[PubMed](#)]
4. Jing, X.L.; Chen, S.W. Aurora kinase inhibitors: A patent review (2014–2020). *Expert Opin. Ther. Pat.* **2021**, *31*, 625–644. [[CrossRef](#)] [[PubMed](#)]
5. Willems, E.; Dedobbeleer, M.; Digregorio, M.; Lombard, A.; Lumapat, P.N.; Rogister, B. The functional diversity of Aurora kinases: A comprehensive review. *Cell Div.* **2018**, *13*, 7. [[CrossRef](#)]
6. Borisa, A.C.; Bhatt, H.G. A comprehensive review on Aurora kinase: Small molecule inhibitors and clinical trial studies. *Eur. J. Med. Chem.* **2017**, *140*, 1–19. [[CrossRef](#)]
7. Bavetsias, V.; Linardopoulos, S. Aurora Kinase Inhibitors: Current Status and Outlook. *Front. Oncol.* **2015**, *5*, 278. [[CrossRef](#)]
8. Kollareddy, M.; Zheleva, D.; Dzubak, P.; Brahmshatriya, P.S.; Lepsik, M.; Hajduch, M. Aurora kinase inhibitors: Progress towards the clinic. *Investig. New Drugs* **2012**, *30*, 2411–2432. [[CrossRef](#)]
9. Lok, W.; Klein, R.Q.; Saif, M.W. Aurora kinase inhibitors as anti-cancer therapy. *Anticancer Drugs* **2010**, *21*, 339–350. [[CrossRef](#)]
10. He, Y.; Fu, W.; Du, L.; Yao, H.; Hua, Z.; Li, J.; Lin, Z. Discovery of a novel Aurora B inhibitor GSK650394 with potent anticancer and anti-aspergillus fumigatus dual efficacies in vitro. *J. Enzym. Inhib. Med. Chem.* **2022**, *37*, 109–117. [[CrossRef](#)]
11. Keen, N.; Taylor, S. Mitotic drivers—Inhibitors of the Aurora B Kinase. *Cancer Metastasis Rev.* **2009**, *28*, 185–195. [[CrossRef](#)]
12. Kong, Y.; Bender, A.; Yan, A. Identification of Novel Aurora Kinase A (AURKA) Inhibitors via Hierarchical Ligand-Based Virtual Screening. *J. Chem. Inf. Model.* **2018**, *58*, 36–47. [[CrossRef](#)]
13. Durlacher, C.T.; Li, Z.L.; Chen, X.W.; He, Z.X.; Zhou, S.F. An update on the pharmacokinetics and pharmacodynamics of alisertib, a selective Aurora kinase A inhibitor. *Clin. Exp. Pharmacol. Physiol.* **2016**, *43*, 585–601. [[CrossRef](#)]
14. Imam, S.S.; Gilani, S.J. Computer Aided Drug Design: A Novel Loom to Drug Discovery. *Org. Med. Chem.* **2017**, *1*, 1–6. [[CrossRef](#)]
15. Baig, M.H.; Ahmad, K.; Roy, S.; Ashraf, J.M.; Adil, M.; Siddiqui, M.H.; Khan, S.; Kamal, M.A.; Provaznik, I.; Choi, I. Computer Aided Drug Design: Success and Limitations. *Curr. Pharm. Des.* **2016**, *22*, 572–581. [[CrossRef](#)]
16. Macalino, S.J.; Gosu, V.; Hong, S.; Choi, S. Role of computer-aided drug design in modern drug discovery. *Arch. Pharm. Res.* **2015**, *38*, 1686–1701. [[CrossRef](#)]
17. Gramatica, P. Principles of QSAR Modeling. *Int. J. Quant. Struct.-Prop. Relatsh.* **2020**, *5*, 61–97. [[CrossRef](#)]
18. Fujita, T.; Winkler, D.A. Understanding the Roles of the “Two QSARs”. *J. Chem. Inf. Model.* **2016**, *56*, 269–274. [[CrossRef](#)]
19. Cherkasov, A.; Muratov, E.N.; Fourches, D.; Varnek, A.; Baskin, I.I.; Cronin, M.; Dearden, J.; Gramatica, P.; Martin, Y.C.; Todeschini, R.; et al. QSAR modeling: Where have you been? Where are you going to? *J. Med. Chem.* **2014**, *57*, 4977–5010. [[CrossRef](#)]
20. Neaz, M.; Muddassar, M.; Pasha, F.; Cho, S.J. Structural studies of B-type Aurora kinase inhibitors using computational methods. *Acta Pharmacol. Sin.* **2010**, *31*, 244–258. [[CrossRef](#)]
21. Lan, P.; Chen, W.N.; Sun, P.H.; Chen, W.M. 3D-QSAR and molecular docking studies of azaindole derivatives as Aurora B kinase inhibitors. *J. Mol. Model.* **2011**, *17*, 1191–1205. [[CrossRef](#)] [[PubMed](#)]
22. Ashraf, S.; Ranaghan, K.E.; Woods, C.J.; Mulholland, A.J.; Ul-Haq, Z. Exploration of the structural requirements of Aurora Kinase B inhibitors by a combined QSAR, modelling and molecular simulation approach. *Sci. Rep.* **2021**, *11*, 18707. [[CrossRef](#)] [[PubMed](#)]
23. Gramatica, P. External Evaluation of QSAR Models, in Addition to Cross-Validation Verification of Predictive Capability on Totally New Chemicals. *Mol. Inform.* **2014**, *33*, 311–314. [[CrossRef](#)] [[PubMed](#)]
24. Chirico, N.; Gramatica, P. Real external predictivity of QSAR models. Part 2. New intercomparable thresholds for different validation criteria and the need for scatter plot inspection. *J. Chem. Inf. Model.* **2012**, *52*, 2044–2058. [[CrossRef](#)] [[PubMed](#)]
25. Chirico, N.; Gramatica, P. Real external predictivity of QSAR models: How to evaluate it? Comparison of different validation criteria and proposal of using the concordance correlation coefficient. *J. Chem. Inf. Model.* **2011**, *51*, 2320–2335. [[CrossRef](#)]
26. Gramatica, P. Principles of QSAR models validation internal and external. *QSAR Comb. Sci.* **2007**, *26*, 694–701. [[CrossRef](#)]
27. Gramatica, P. On the development and validation of QSAR models. *Methods Mol. Biol.* **2013**, *930*, 499–526. [[CrossRef](#)]
28. Rao, R.B.; Fung, G.; Rosales, R. On the Dangers of Cross-Validation. An Experimental Evaluation. In *Proceedings of the 2008 SIAM International Conference on Data Mining (SDM)*; Society for Industrial and Applied Mathematics: Philadelphia, PA, USA, 2008; pp. 588–596. [[CrossRef](#)]
29. Tropsha, A.; Gramatica, P.; Gombar, V.K. The Importance of Being Earnest Validation is the Absolute Essential for Successful Application and Interpretation of QSPR Models. *QSAR Comb. Sci.* **2003**, *22*, 69–77. [[CrossRef](#)]
30. Hawkins, D.M.; Basak, S.C.; Mills, D. Assessing model fit by cross-validation. *J. Chem. Inf. Comput. Sci.* **2003**, *43*, 579–586. [[CrossRef](#)]
31. Lučić, B.; Batista, J.; Bojović, V.; Lovrić, M.; Sović Kržić, A.; Bešlo, D.; Nadramija, D.; Vikić-Topić, D. Estimation of Random Accuracy and its Use in Validation of Predictive Quality of Classification Models within Predictive Challenges. *Croat. Chem. Acta* **2019**, *92*, 379–391. [[CrossRef](#)]

32. Masand, V.H.; Mahajan, D.T.; Nazeruddin, G.M.; Hadda, T.B.; Rastija, V.; Alfeefy, A.M. Effect of information leakage and method of splitting (rational and random) on external predictive ability and behavior of different statistical parameters of QSAR model. *Med. Chem. Res.* **2014**, *24*, 1241–1264. [[CrossRef](#)]
33. Kar, S.; Roy, K.; Leszczynski, J. Applicability Domain: A Step Toward Confident Predictions and Decidability for QSAR Modeling. In *Computational Toxicology*; Humana Press: New York, NY, USA, 2018; pp. 141–169. [[CrossRef](#)]
34. Roy, P.P.; Kovarich, S.; Gramatica, P. QSAR model reproducibility and applicability A case study of rate constants of hydroxyl radical reaction models applied to polybrominated diphenyl ethers and (benzo-)triazoles. *J. Comput. Chem.* **2011**, *32*, 2386–2396. [[CrossRef](#)]
35. Sushko, I.; Novotarskyi, S.; Korner, R.; Pandey, A.K.; Cherkasov, A.; Li, J.; Gramatica, P.; Hansen, K.; Schroeter, T.; Muller, K.R.; et al. Applicability domains for classification problems: Benchmarking of distance to models for Ames mutagenicity set. *J. Chem. Inf. Model.* **2010**, *50*, 2094–2111. [[CrossRef](#)]
36. Tropsha, A.; Golbraikh, A. Predictive QSAR modeling workflow, model applicability domains, and virtual screening. *Curr. Pharm. Des.* **2007**, *13*, 3494–3504. [[CrossRef](#)]
37. Masand, V.H.; Rastija, V. PyDescriptor: A new PyMOL plugin for calculating thousands of easily understandable molecular descriptors. *Chemom. Intell. Lab. Syst.* **2017**, *169*, 12–18. [[CrossRef](#)]
38. Todeschini, R.; Consonni, V. *Molecular Descriptors for Chemoinformatics*; Wiley-VCH: Weinheim, Germany, 2009.
39. Todeschini, R.; Consonni, V. *Handbook of Molecular Descriptors*; Wiley-VCH: Weinheim, Germany, 2000; Volume 11.
40. Di, L.; Kerns, E.H. *Drug-like Properties: Concepts, Structure Design and Methods: From ADME to Toxicity Optimization*, 2nd ed.; Elsevier/AP: Amsterdam, The Netherlands; Boston, MA, USA, 2016; 560p.
41. Sessa, F.; Villa, F. Structure of Aurora B-INCENP in complex with barasertib reveals a potential transinhibitory mechanism. *Acta Crystallogr. F Struct. Biol. Commun.* **2014**, *70 Pt 3*, 294–298. [[CrossRef](#)]
42. Elkins, J.M.; Santaguida, S.; Musacchio, A.; Knapp, S. Crystal structure of human aurora B in complex with INCENP and VX-680. *J. Med. Chem.* **2012**, *55*, 7841–7848. [[CrossRef](#)]
43. Masand, V.H.; Mahajan, D.T.; Gramatica, P.; Barlow, J. Tautomerism and multiple modelling enhance the efficacy of QSAR: Antimalarial activity of phosphoramidate and phosphorothioamidate analogues of amiprofos methyl. *Med. Chem. Res.* **2014**, *23*, 4825–4835. [[CrossRef](#)]
44. Masand, V.H.; Mahajan, D.T.; Ben Hadda, T.; Jawarkar, R.D.; Alafeefy, A.M.; Rastija, V.; Ali, M.A. Does tautomerism influence the outcome of QSAR modeling? *Med. Chem. Res.* **2014**, *23*, 1742–1757. [[CrossRef](#)]
45. Zaki, M.E.A.; Al-Hussain, S.A.; Bukhari, S.N.A.; Masand, V.H.; Rathore, M.M.; Thakur, S.D.; Patil, V.M. Exploring the Prominent and Concealed Inhibitory Features for Cytoplasmic Isoforms of Hsp90 Using QSAR Analysis. *Pharmaceuticals* **2022**, *15*, 303. [[CrossRef](#)]
46. Zaki, M.E.A.; Al-Hussain, S.A.; Al-Mutairi, A.A.; Masand, V.H.; Samad, A.; Jawarkar, R.D. Mechanistic Analysis of Chemically Diverse Bromodomain-4 Inhibitors Using Balanced QSAR Analysis and Supported by X-ray Resolved Crystal Structures. *Pharmaceuticals* **2022**, *15*, 745. [[CrossRef](#)]
47. Fourches, D.; Muratov, E.; Tropsha, A. Trust, but verify: On the importance of chemical structure curation in cheminformatics and QSAR modeling research. *J. Chem. Inf. Model.* **2010**, *50*, 1189–1204. [[CrossRef](#)]
48. O'Boyle, N.M.; Banck, M.; James, C.A.; Morley, C.; Vandermeersch, T.; Hutchison, G.R. Open Babel: An open chemical toolbox. *J. Cheminform.* **2011**, *3*, 33. [[CrossRef](#)]
49. Stewart, J.J.P. MOPAC: A semiempirical molecular orbital program. *J. Comput.-Aided Mol. Des.* **1990**, *4*, 1–103. [[CrossRef](#)]
50. Yap, C.W. PaDEL-descriptor: An open source software to calculate molecular descriptors and fingerprints. *J. Comput. Chem.* **2011**, *32*, 1466–1474. [[CrossRef](#)]
51. Gramatica, P.; Chirico, N.; Papa, E.; Cassani, S.; Kovarich, S. QSARINS: A new software for the development, analysis, and validation of QSAR MLR models. *J. Comput. Chem.* **2013**, *34*, 2121–2132. [[CrossRef](#)]
52. Bukhari, S.N.A.; Elsherif, M.A.; Junaid, K.; Ejaz, H.; Alam, P.; Samad, A.; Jawarkar, R.D.; Masand, V.H. Perceiving the Concealed and Unreported Pharmacophoric Features of the 5-Hydroxytryptamine Receptor Using Balanced QSAR Analysis. *Pharmaceuticals* **2022**, *15*, 834. [[CrossRef](#)]
53. Consonni, V.; Todeschini, R.; Ballabio, D.; Grisoni, F. On the Misleading Use of Q2F3 for QSAR Model Comparison. *Mol. Inf.* **2019**, *38*, e1800029. [[CrossRef](#)]
54. Golbraikh, A.; Muratov, E.; Fourches, D.; Tropsha, A. Data set modelability by QSAR. *J. Chem. Inf. Model.* **2014**, *54*, 1–4. [[CrossRef](#)]
55. Martin, T.M.; Harten, P.; Young, D.M.; Muratov, E.N.; Golbraikh, A.; Zhu, H.; Tropsha, A. Does rational selection of training and test sets improve the outcome of QSAR modeling? *J. Chem. Inf. Model.* **2012**, *52*, 2570–2578. [[CrossRef](#)]
56. Gramatica, P.; Cassani, S.; Roy, P.P.; Kovarich, S.; Yap, C.W.; Papa, E. QSAR Modeling is not Push a Button and Find a Correlation: A Case Study of Toxicity of (Benzo-)triazoles on Algae. In *Molecular Informatics*; Wiley Online: Hoboken, NJ, USA, 2012; Volume 31, pp. 817–835.
57. Huang, J.; Fan, X. Why QSAR fails: An empirical evaluation using conventional computational approach. *Mol. Pharm.* **2011**, *8*, 600–608. [[CrossRef](#)] [[PubMed](#)]





OPEN

## Magnetic solid phase extraction of Sunitinib malate in urine samples assisted with mixed hemimicelle and spectrophotometric detection

Eslem Pourbasheer<sup>1✉</sup>, Leila Malekpour<sup>2</sup>, Zhila Azari<sup>3</sup>, Vijay H. Masand<sup>4</sup> & Mohammad Reza Ganjali<sup>5,6</sup>

The mixed hemimicelle-based solid phase extraction method using the coated sodium dodecyl sulfate by magnetic iron oxide nanoparticles as adsorbent was developed for extraction and determination of Sunitinib malate in real samples prior to determination by UV–Visible spectrophotometry. For the characterization of synthesized nanoparticles, Fourier transform infrared spectroscopy, and scanning electron microscopy was used. The influences of different factors affecting the extraction efficiency of Sunitinib malate, including the pH, the adsorbent amount, the volume and eluent type, the amount of the surfactant, the ionic strength, extraction, and desorption time, were investigated. At the optimized conditions, a good linearity with correlation coefficients of 0.998 and 0.999 was obtained over the concentration ranges of 1–22 and 1–19  $\mu\text{g}/\text{mL}$  for water and urine samples, in order. The good recoveries of 97% and 99% and also, the limits of detection equal with 0.9, and 0.8  $\mu\text{g}/\text{mL}$  for water and urine samples were enhanced, respectively. These results demonstrate that mixed hemimicelle solid phase extraction is a fast, efficient, economical and selective sample preparation method for the extraction and determination of Sunitinib malate in different water and urine sample solutions.

### Abbreviations

MHSPE	Mixed hemimicelle-based solid phase extraction
SDS	Sodium dodecyl sulfate
SDS-MIONPs	Sodium dodecyl sulfate—magnetic iron oxide nanoparticles
SM	Sunitinib malate
FT-IR	Fourier transform infrared spectroscopy
SEM	Scanning electron microscopy
LOD	Limits of detection
LOQ	Limit of quantification
TKI	Tyrosine kinase inhibitor
VEGFR	Vascular endothelial growth factor receptors
PDGF	Platelet derived-growth factor receptor
GIST	Gastrointestinal stromal tumors
LC–MS/MS	Liquid chromatography-tandem mass spectrometry
HPLC	High-performance liquid chromatography
LLE	Liquid–liquid extraction
SPE	Solid-phase extraction
CPE	Cloud point extraction
MIONPs	Magnetic iron oxide nanoparticles
CTAB	Cetyltrimethyl ammonium bromide

<sup>1</sup>Department of Chemistry, Faculty of Science, University of Mohaghegh Ardabili, P.O. Box 179, Ardabil, Iran. <sup>2</sup>Department of Chemistry, Payame Noor University, P.O. Box 19395-4697, Tehran, Iran. <sup>3</sup>Department of Chemistry, Faculty of Sciences, Azarbaijan Shahid Madani University, 35 Km Tabriz-Marageh Road, P.O. Box 53714-161, Tabriz 5375171379, Iran. <sup>4</sup>Department of Chemistry, Vidyabharati Mahavidyalaya, Camp, Amravati, Maharashtra 444602, India. <sup>5</sup>Center of Excellence in Electrochemistry, Faculty of Chemistry, University of Tehran, Tehran, Iran. <sup>6</sup>National Institute of Genetic Engineering and Biotechnology (NIGEB), Tehran, Iran. ✉email: e.pourbasheer@uma.ac.ir

PZC	Point of zero charge
FeCl <sub>3</sub> ·6H <sub>2</sub> O	Ferric chloride hexahydrate
FeCl <sub>2</sub> ·4H <sub>2</sub> O	Ferrous chloride tetrahydrate
NaOH	Sodium hydroxide
HCl	Hydrochloric acid
NaCl	Sodium chloride

Sunitinib malate is a novel oral multi-targeted tyrosine kinase inhibitor with established efficacy in treating metastatic renal cell carcinoma and imatinib-resistant gastrointestinal stromal tumor<sup>1–4</sup>. Sunitinib malate prevents the growth of cancer cells by obstructing a group of closely linked tyrosine kinase receptors, containing vascular endothelial growth factor receptors platelet-derived growth factor receptor, FMS-related tyrosine-kinase 3 and stem cell factor receptor (FCF c-KIT) at nanomolar concentrations<sup>5–9</sup>. In addition, SM is approved for the therapy of kidney cancer, advanced renal cell carcinoma, and gastrointestinal stromal tumors<sup>10–12</sup>. Therefore, the determination of Sunitinib malate in water and also in biological fluids has found significance. To date, various analytical techniques have been introduced for the determination of Sunitinib malate, such as LC–MS/MS, HPLC, and high-performance liquid chromatography–UV methods<sup>13–15</sup>. The need for the complicated instruments, on the one hand, and being inexpensive and time-consuming, on the other hand, arouse us to utilize spectrophotometry measurements which presents not only quick analysis but also ease of operation and being economic<sup>16–18</sup>.

An accurate and sensitive procedure such as sample purification and preconcentration are essential prior to instrumental analysis<sup>19–27</sup>. Several pre-treatment methods have been employed for the extraction of Sunitinib malate, including LLE, SPE, and CPE<sup>28–31</sup>. Solid phase extraction has gained more research interest due to being simple, and also flexible in terms of selecting the desirable solid phase as adsorbent, which results in the maximum preconcentration factor, short extraction time and low cost according to the low usage of the organic solvents<sup>32,33</sup>.

More recently, MIONPs have been widely applied in analytical research as a flexible adsorbent for the extraction and determination of various chemical analytes<sup>34–39</sup>. The magnetic nanoparticles provide some advantages over the traditional sorbents, for instance, the high surface area, short diffusion route, high number of surface-active sites, and superparamagnetic features, which lead to the maximum extraction recovery, rapid extraction, and simplicity of extraction for samples with large volumes<sup>40–43</sup>. Nanoparticles are inconstant because of the high level of surface energy, which might end in the nanoparticles agglomeration and less yield of operation<sup>44,45</sup>. To inhibit this problem and improve the extraction efficiency, the surface of the nanoparticles is modified with different organic and, or inorganic materials<sup>46,47</sup>. Surfactants are such organic subcategory that is utilized in this research according to some advantages. First and foremost, SPE is based on the adsorption of surfactant on the surface of the adsorbent, which makes mixed (hemimicelles and, or admicelles) (MHSPE), act as a solid–liquid interface and could be utilized for the extraction and preconcentration of any types of samples from various matrices<sup>17,30,31,48</sup>. Secondly, the modification procedure is simple and could be performed during the extraction; accordingly, it is time-consuming<sup>48</sup>. In this called method, as MHSPE, the ionic surfactants such as SDS, CTAB and, etc., were adsorbed on the surface of the mineral oxides such as, silica, titanium dioxide, alumina, and iron oxides<sup>32,45</sup>. The combination of mixed hemimicelles with solid phase extraction and magnetic nanoparticles has plenty of advantages, such as high extraction yield, regeneration of sorbent, high breakthrough volume, easy analytes elution, and no clean-up steps<sup>31</sup>. Facile process, being fast and modifying at the same time of extraction, another motivational reason to select it as the pretreatment method for most drugs and pollutants<sup>10,33,40,47</sup>.

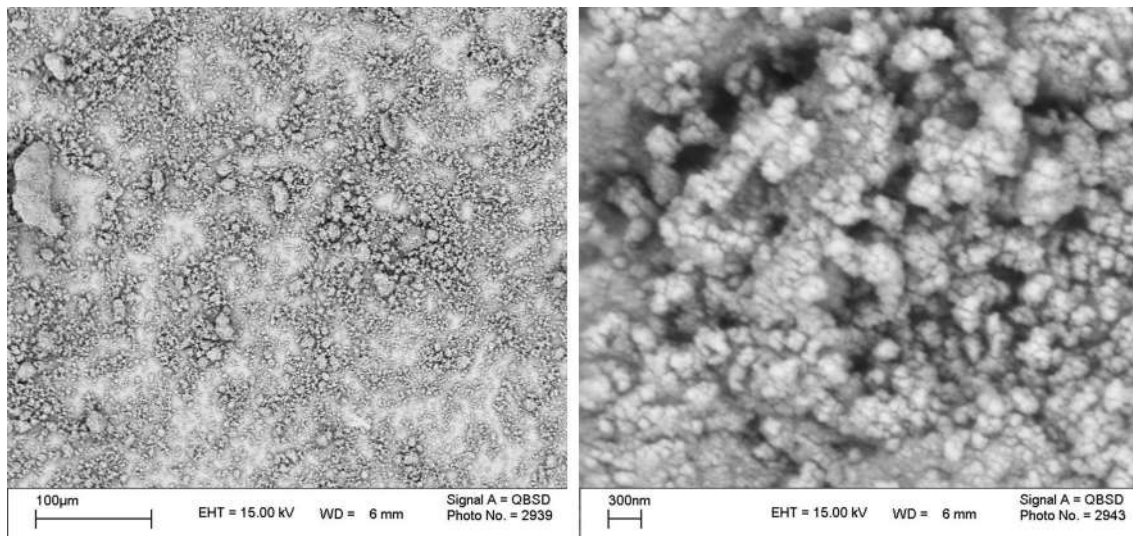
In this study, modified Fe<sub>3</sub>O<sub>4</sub> nanoparticles with sodium dodecyl sulfate was formed mixed based solid-phase extraction method, which was successfully employed for extraction and determination of Sunitinib malate in urine and water samples by UV–Visible spectrophotometry technique. According to our literature survey, it is for the first time that the mixed hemimicelles solid phase extraction has been applied for the extraction and determination of Sunitinib malate in urine and water samples.

## Results and discussion

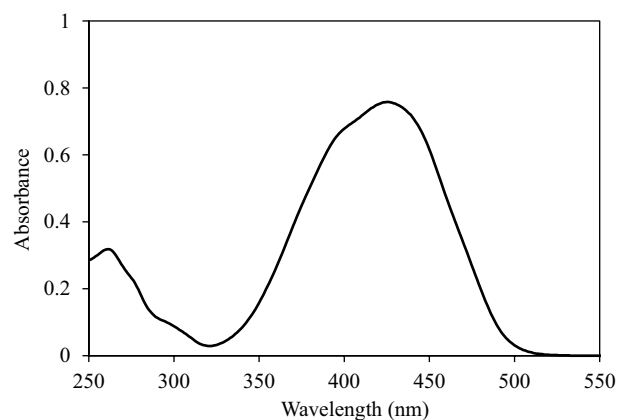
**Characterization of magnetic iron oxide nanoparticles.** The SEM and IR were utilized to characterize the synthesized adsorbent, which modified with SDS. According to our previous work<sup>45</sup>, absorption bands appeared at 529, 477 and 3202 cm<sup>−1</sup> confirm the true synthesis of Fe<sub>3</sub>O<sub>4</sub> since they are related to the FeO, Fe<sub>2</sub>O<sub>3</sub>, and the surface OH group of the magnetic nanoparticles, respectively. After modification, new peaks, which stand for the S=O group and stretching mode of the aliphatic C-H groups of SDS were, emerged at 1252 and both 2928 & 2842 cm<sup>−1</sup>, respectively. These peaks demonstrated that the surface of MIONPs was successfully modified with SDS. Furthermore, SEM images (Fig. 1) show the uniform spherical shape of the modified magnetic nanoparticle with the size of about 39–59 nm.

**Mixed hemimicelles-based solid-phase extraction optimization conditions.** To maximize the extraction efficiency of Sunitinib malate, the influences of different factors such as the pH, the amounts of adsorbent, and surfactant, the ionic strength, eluent type and volume and extraction /desorption time were investigated and optimized. All the experiments were done three times and the averages of the results were applied for optimization. The UV–vis spectra of Sunitinib malate is shown in Fig. 2. All detections were performed at λ<sub>max</sub> = 425 nm.

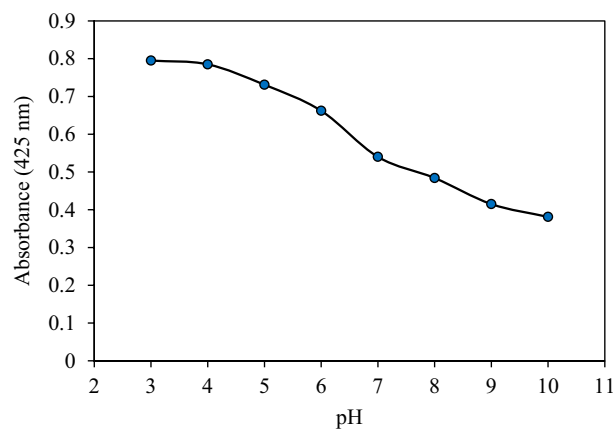
**Effect of pH.** The most significant parameter affecting the formation of mixed-hemimicelles based on the solid adsorbent is the pH of the sample solution<sup>49</sup>. The pH range of 3–10, which was adjusted by applying of 0.1 M HCl or NaOH solution, was investigated. As it is shown in Fig. 3, the highest absorption amount is related



**Figure 1.** SEM images of SDS-MIONPs nanoparticles.



**Figure 2.** Absorbance spectra of Sunitinib Malate (10 µg/mL).



**Figure 3.** Effect of the pH on extraction efficiency (Extraction conditions: sorbent amount, 30 mg; eluent, 5 mL of methanol; Sample volume: 10 mL; Sample concentration: 10 µg/mL; extraction time, 5 min; desorption time, 5 min).

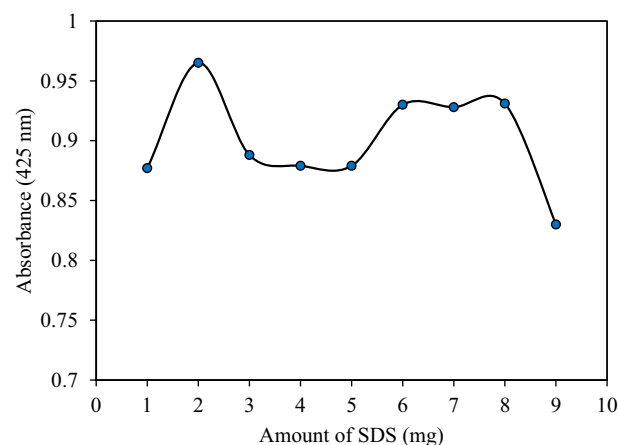
to pH 3, and a more increase in the pH from 3 to 10, leads to a reduction in the adsorption of SM. This can be related to the decrease in positive charge density on the MIONPs surface, on the other hand, the positively charged surface of MIONPs in acidic solutions was desirable for the adsorption of anionic surfactants like SDS. The point of zero charge of MIONPs is about 6.5<sup>50</sup>. When the pH of the solution is above the isoelectric point of the MIONPs, the surface charge density of the MIONPs becomes less positive; hence, adsorption of SDS on nanoparticle surfaces is reduced due to the lack of the formation of mixed. Therefore, electrostatic attraction, between the negative head group of SDS as anionic surfactant and the positive surface of MIONPs is potent enough to produce hemimicelles. Despite the mentioned reason, the acidic solution sustains the positive charge of Sunitinib malate and provides the suitable electrostatic attraction with the negative head group of SDS, which is placed at the second layer of mixed hemimicelle. Accordingly, for the optimum value, pH = 3 was selected.

**Effect of SDS amount.** The SDS concentration effect, on the extraction efficiency of Sunitinib malate, was considered by adding different concentrations of SDS from 1 to 9 mg/mL to the sample solution. As shown in Fig. 4, in the absence of SDS, the Sunitinib malate hardly adsorbed on the surface of the adsorbent; on the other hand, the adsorption of SM on the surface of magnetic iron oxide nanoparticles is in strict need of modification. The notably increased adsorption is enhanced by the addition of 2 mg of surfactant, which is large enough for the formation of admicelles. By the movements toward smaller amounts of SDS the structure of admicelles changes to mixed hemimicelles and hemimicelles which are not proper for the adsorption of SM. Higher amounts of 2 mg are the beginning point of micelle formation which lead to the gradual decrease in adsorption of SM due to the redistribution of Sunitinib malate in the bulk solution. Therefore, 2 mg of SDS was chosen as the optimum value for the next experiments.

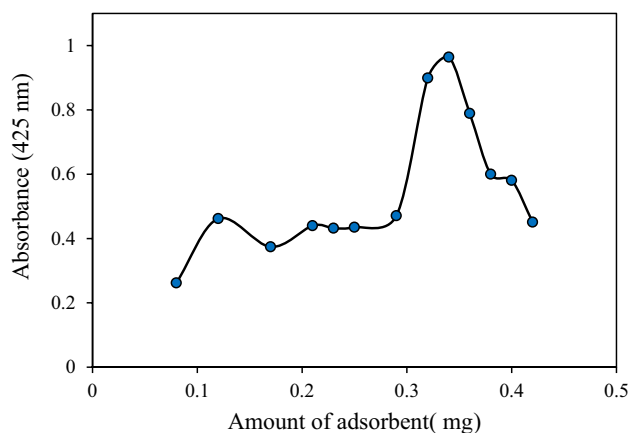
**Effect of ionic strength.** The ionic strength of the studied solution on extraction efficiency was evaluated by the utilization of NaCl with various concentrations of 1–10% (w/v). The results indicate that in the presence of salt, especially in extensive amounts, desorption of Sunitinib malate is diminished based on the competitive behaviour of SM and salt for the adsorption on the surface of adsorbent. Accordingly, no salt addition was utilized for the rest of experiments.

**Effect of the MIONPs amount.** The amount of the adsorbent definitely affects the mechanism of adsorption and extraction efficiency. In order to choose the required quantity of adsorbent (MIONPs) for the extraction of Sunitinib malate, different concentrations of MIONPs suspension were used in the range of 0.08–0.42 mg/mL. Nanoparticles have a higher surface area than ordinary sorbents (micron-size particle sorbents), which result in high extraction capacity and fast extraction dynamics. Therefore, satisfactory results can be obtained with fewer amounts of sorbents. As shown in Fig. 5, the extraction recovery of Sunitinib malate increased with increasing sorbent amounts from 80 up to 320 mg/mL of Fe<sub>3</sub>O<sub>4</sub> nanoparticles, due to the increased accessible adsorption sites. The more addition of the adsorbent diminished the adsorption of SM, due to the dramatic reversal in admicelle formation, which ended in mixed and, or hemimicelles structures. Therefore, 320 mg/mL of the magnetic adsorbent amount was selected as the optimum.

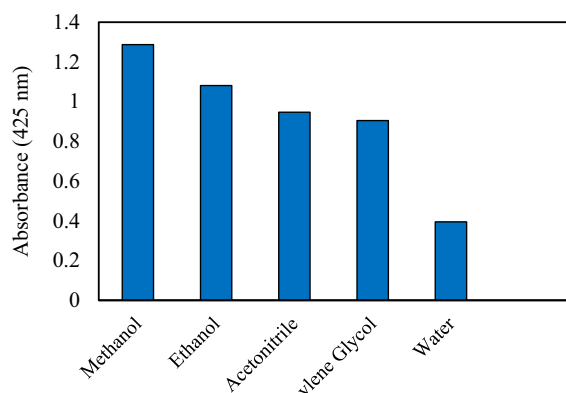
**The influence of kind and the volume of the eluent.** To enhance the maximum release of SM, different organic solvents such as acetonitrile, ethanol, methanol, ethylene glycol and water were studied. As shown in Fig. 6a, the highest extraction recovery of Sunitinib malate was obtained by the use of methanol which conforms to the necessity of the utilization of organic solvent for the disruption of admicelles, structure. Furthermore, the highest solubility of SM in methanol in comparison with others might be the reason for the highest absorbance.



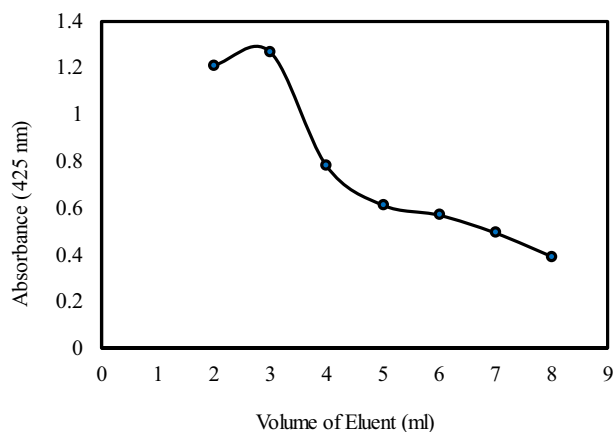
**Figure 4.** Effect of SDS concentration on extraction efficiency (Extraction conditions: sample pH, 3.0; sorbent amount, 30 mg; eluent, 5 mL of methanol; Sample volume: 10 mL; Sample concentration: 10 µg/mL; extraction time, 5 min; desorption time, 5 min).



**Figure 5.** Effect of MIONPs amount on extraction efficiency (Extraction conditions: sample pH, 3.0; SDS concentration: 2 mg/mL; eluent, 5 mL of methanol; Sample volume: 10 mL; Sample concentration: 10 µg/mL; extraction time, 5 min; desorption time, 5 min).



**(a)**



**(b)**

**Figure 6.** Effect of eluent type **(a)** and eluent volume **(b)** on extraction efficiency (Extraction conditions: sample pH, 3.0; sorbent amount, 320 mg; SDS concentration: 2 mg/mL; eluent volume, 5 mL; Sample volume: 10 mL; Sample concentration: 10 µg/mL; extraction time, 1 min; desorption time, 7 min).

Figure 6b exhibits the effect of different volumes of methanol in the range from 2 to 8 mL on the extraction efficiency of Sunitinib malate. By incrementing the volume to 3 mL, the extraction efficiency increased, and the diminution was observed for the higher amounts 3 to 8 mL. It would attribute to the analytes dilution in the high volumes of the eluent. Hence, for the optimum eluent volume, 3 mL of methanol was selected. Moreover, our primary solution, which extracted was acidic, and therefore, 3 mL of the basic solution (methanol: water; 94:6 v/v) demonstrated the best extraction efficiency, and was selected as the desirable extractor.

**The impact of time on both extraction and back extraction.** Extraction/back extraction time is defined as the needed time to bring both solution and adsorbent into contact in order to enhance the complete transfer of analyte to adsorbent/extractor solvent and in solid phase extraction is measured as the time for the shaking by the application of a shaker<sup>45</sup>. This extraction/ back extraction time must be long enough to make solution/adsorbent approximately bare of analyte. In this study, the effect of extraction and back extraction times on the extraction efficiency of Sunitinib malate were investigated in the range of 1–5 and 1–9 min, respectively. The results showed that the highest extraction efficiency was obtained in the shortest tested time as extraction time (1 min). After 1 min, the adsorption remained constant with less reduction. Also, the maximum desorption was observed at 7 min. The desorption's were incomplete in the times shorter than 7 min and then decreased. The rapid dynamic process and high surface area of MIONPs along with homogeneous distribution of the nano-sorbent throughout the sample and could be the possible reasons for gaining a rapid extraction process. In a word, MIONPs-based MHSPE is a method with the capability of a fast separation procedure which leads to a short analysis time. Therefore, 1 and 7 min were selected as the optimized adsorption and desorption time.

**Analytical performance.** In order to validate the proposed method, at the optimized experimental conditions, some figures of merits such as the limit of detection and quantification, the linear range of calibration curve, correlation of determinations ( $R^2$ ), and the accuracy and precision of the method were examined. The analytical performances of the presented method are presented in Table 1. The calibration curve was linear in the range from 1 to 22 and 1 to 19  $\mu\text{g/mL}$  with determination coefficients of 0.998 and 0.999 for water and urine samples, respectively. The LOD and LOQ were defined according to the IUPAC recommendation as follows:  $\text{LOD} = 3.3 (\text{SD}/S)$  and  $\text{LOQ} = 10 (\text{SD}/S)$  where SD is the standard deviation of the blank and S is the slope of calibration curve. The LODs were 0.9 and 0.8  $\mu\text{g/mL}$  and also the LOQs were 2.9 and 2.6  $\mu\text{g/mL}$  for determination of Sunitinib malate in water and urine samples, respectively. Moreover, to determine the relative standard deviation (%) of the analytical method five replicates were done for each concentration. The method accuracy was investigated by the measurement of relative error which is 100 multiplied by the resulting subtraction of founded and added concentration of SM in spiked samples divided to added concentrations. As the results reveal in Table 1, the proposed method exhibited good linearity, appropriate precision and low LOD and LOQ for the determination of the analyte.

**Real sample analysis.** Under the optimized conditions, the mixed hemimicelles SPE method was applied for the extraction and determination of Sunitinib malate in spiked tap water and urine samples. Since Sunitinib malate was not detected in the real samples, 10  $\mu\text{g/mL}$  of Sunitinib malate was added into the water and urine samples, and extraction was done based on the procedure. The analytical results are summarized in Table 2. It can be seen, that the enhanced recoveries are about 97% and 99% for water samples and urine samples, respectively, which indicate the suitability of MIONPs sorbents for selective extraction and determination of Sunitinib malate in real samples. Also, the relative standard deviations (RSDs %) for five replicate extractions were 0.67 and 0.41% and the gained relative errors were 3.1 and 0.04 for water and urine, respectively; indicating the proper precision and accuracy of the method. Also, the performance of the proposed method was compared to that of other reported methods for determination of Sunitinib Malate and the results are presented in Table 3.

Sample	LOD ( $\mu\text{g/mL}$ )	LOQ ( $\mu\text{g/mL}$ )	Regression equation	$R^2$	EP (%) <sup>a</sup>	LDR (mg/L) <sup>b</sup>
Water	0.9	2.9	$y = 0.0362x + 0.1134$	0.998	97	1–22
Urine	0.8	2.6	$y = 0.0415x + 0.0031$	0.999	99	1–19

**Table 1.** Figures of merit for the applied MHSPE in real samples. <sup>a</sup>Extraction percentage. <sup>b</sup>Linear dynamic range.

Sample	$C_{\text{added}}$ ( $\mu\text{g/mL}$ )	$C_{\text{found}}$ ( $\mu\text{g/mL}$ )	RSD (%) (n = 5)	$R^2$	Relative recovery (%)	Relative error (%)
Water	10	10.31	0.67	0.998	97	+ 3.1
Urine	10	10.60	0.41	0.999	99	+ 6.04

**Table 2.** Determination of Sunitinib Malate (SM) in real samples.

Sample	Detection system	LOD (ng/mL)	LOQ (ng/mL)	LDR (ng/mL) <sup>b</sup>	R <sup>2</sup>	References
Plasma	LC-MS/MS	– <sup>a</sup>	1.37	1.37–1000	0.99	4
Plasma	LC-MS/MS	–	2	2–250	0.9919	10
Plasma	LC-MS/MS	–	0.10	0.10–150	0.998	12
Plasma	HPLC-UV-Vis	–	10	20–200	–	13
Plasma	LC-MS/MS	–	0.2	0.2–500	0.9950	15
Urine	UV-Visible	0.8 (mg/L)	2.6 (mg/L)	1–19 (mg/L)	0.999	This work
Water	UV-Visible	0.9 (mg/L)	2.9 (mg/L)	1–22 (mg/L)	0.998	This work

**Table 3.** Comparison of the proposed MHSPE method with some of the methods reported in the literature for determination of Sunitinib Malate. <sup>a</sup>Data not reported. <sup>b</sup>Linear dynamic range.

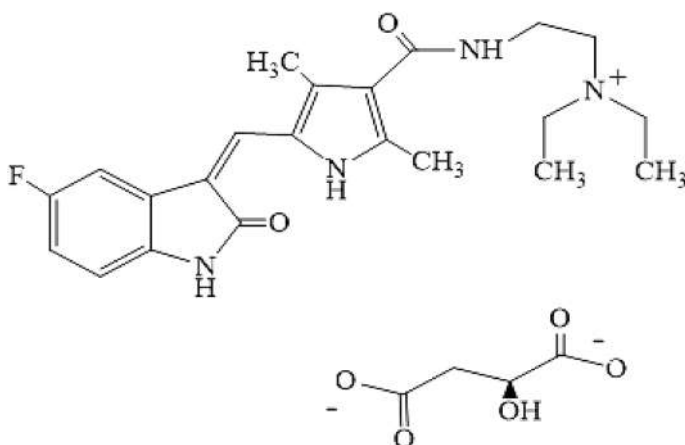
## Conclusion

The proposed mixed hemimicelles solid phase extraction was developed for extraction and determination of Sunitinib malate in tap water and urine samples prior to spectrophotometric determination. Sodium dodecyl sulfate was utilized for the modification of magnetic iron oxide nanoparticles and the construction of mixed hemimicelles. The proposed method provides various advantages like short analysis time, simplicity, low cost, high extraction efficiency, low detection limits and proper recoveries. This method presents satisfactory repeatability and accuracy for the extended dynamic linear ranges of 1–22 and 1–19 µg/ml for water and urine samples, respectively. Also, the satisfactory recoveries and precision of the proposed MHSPE method indicate that MIONPs sorbents have considerable potential for the extraction and determination of Sunitinib malate from biological fluids. Finally, this method was handled for designation of SM in water and urine samples with low detection limits and proper recoveries of 97 and 99, respectively. Hence, the proposed analysis method could be successfully applied for extraction and determination of drugs in real samples.

## Experimental

**Materials and instruments.** All used reagents were of analytical grade and distilled water was used for making of all the aqueous solutions. The FeCl<sub>3</sub>·6H<sub>2</sub>O, FeCl<sub>2</sub>·4H<sub>2</sub>O, SDS, NaOH (99%), HCl (37%), aqueous ammonia (25 wt%), NaCl, methanol, ethanol, ethylene glycol, acetonitrile, dimethyl sulfoxide and Sunitinib malate were purchased from Merck (Darmstadt, Germany). The molecular structure of Sunitinib malate is presented in Fig. 7. A stock solution of the Sunitinib malate (100 mg/L) was prepared by dissolving proper amount of Sunitinib malate in dimethyl sulfoxide and methanol and stored at 4 °C. All the solutions were prepared by suitable diluting of the stock solution with distilled water. The Climo-Shaker ISF1-X (Kuhner AG, Switzerland) was used for shaking of the mixtures. A Jenway model 4510 (Stone, UK), pH meter with a glass electrode was applied for the pH measurements. All of spectrophotometric measurements of the solutions were done by a Analytic Jena SPECORD 250 UV-vis spectrophotometer (Germany). The UV detection of Sunitinib malate was performed at 425 nm. The FT-IR spectra of the prepared nanoparticles was carried out by a Shimadzu prestige-21 (Japan) FT-IR spectrophotometer in the range of 400–4000 cm<sup>-1</sup>. The structure of the synthesized nanoparticles was characterized by a scanning electron microscopy (SEM, LEO 1430VP).

**Magnetic iron oxide nanoparticles preparation.** The nanoparticles of Fe<sub>3</sub>O<sub>4</sub> were synthesized with the help of a conventional co-precipitation method similar to our previous works<sup>45</sup>. The 4.3 g of FeCl<sub>2</sub>·4H<sub>2</sub>O and



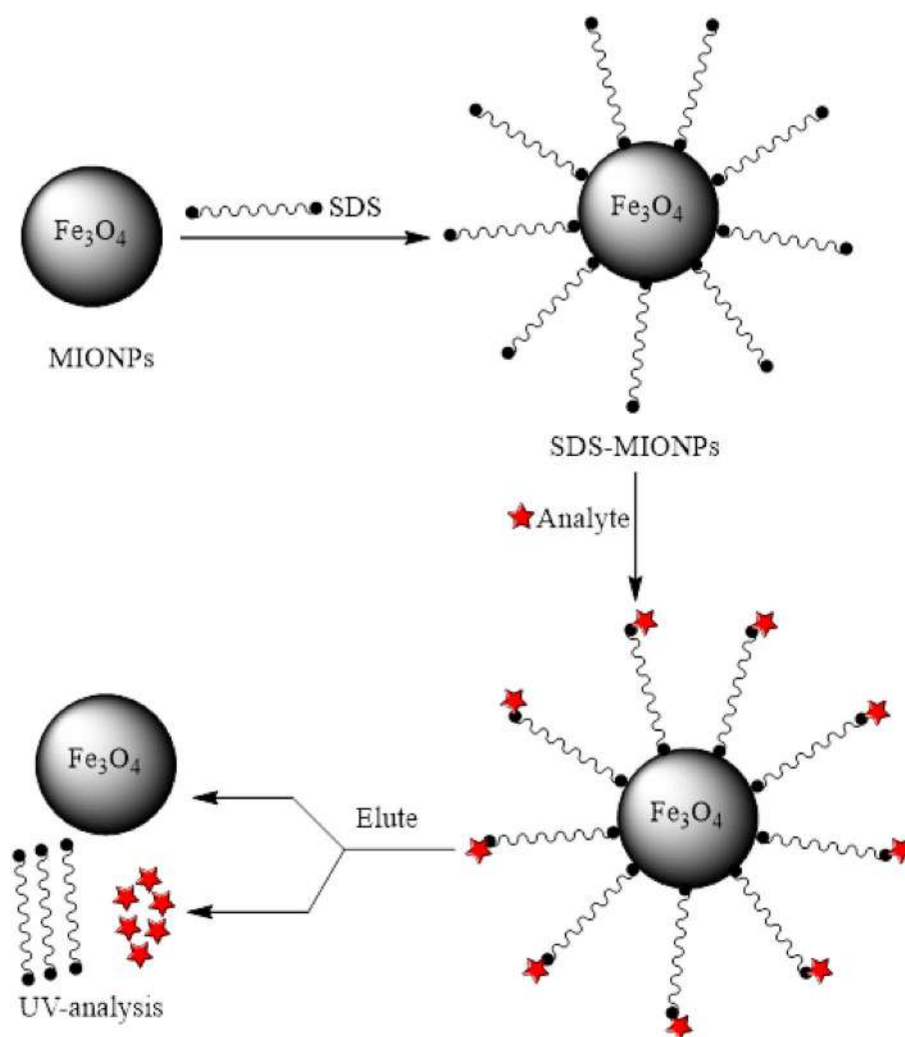
**Figure 7.** Structure of Sunitinib Malate (SM).

11.68 g of  $\text{FeCl}_3 \cdot 6\text{H}_2\text{O}$  were dissolved in 200 mL of deionized water under a nitrogen atmosphere at 85 °C. An ammonia solution (20 mL, 30% w/w) was added dropwise into the mixture with vigorous stirring (400 rpm) for 30 min. The orange color of the solution changed to black quickly. After cooling down to room temperature, the obtained MNPs precipitate was separated from the reaction mixture under the magnetic field. The magnetite precipitates were eluted twice with deionized water, and once with 0.02 mol/L sodium chloride.

**Preparation of real samples.** The efficiency of this method was evaluated by the application of water and urine as real samples. Tap water samples were freshly prepared from our analytical laboratory (Ardabil, Iran). Water samples were just filtered with a Millipore filter before extraction. The urine samples were taken from a voluntary female. The collected urine samples were centrifuged at 2500 rpm for 20 min at room temperature to sediment white lipidic solid, then filtered with a 0.2  $\mu\text{m}$  syringe filter. The spiked urine samples were diluted 1:10 using distilled water, in order to decrease the matrix effect.

**Ethics declaration.** The urine sample preparation method was carried out in accordance with relevant guidelines and regulations. The urine sample was taken from a voluntary female and informed consent of participating subject, was obtained. The researchers institute did not require approval for the use of urine in experiments in this instance.

**Magnetic MHSPE procedure.** The step-by-step procedure to accomplish MHSPE of Sunitinib malate, was as follows (Fig. 8): a 10 mL of the aqueous solution containing Sunitinib malate (10  $\mu\text{g}/\text{mL}$ ) was transferred into a 25 mL beaker. Next, an amount of 0.5 mL (30 mg/mL) of  $\text{Fe}_3\text{O}_4$  NPs suspension and 0.2 mL of the SDS solution (2 mg/mL) were sequentially added. In order to complete the extraction process, the mixtures were shaken and permitted for 5 min. After that, the SDS-coated MIONPs were isolated from the solutions using an external magnet. After 2 min, the solutions became clear and supernatant solutions were decanted. The 5 mL of



**Figure 8.** A schematic diagram of magnetic MHSPE procedure.



methanol was used for the elution of pre-concentrated analyte from the isolated adsorbent. The concentration of Sunitinib malate was determined at a wavelength of 425 nm using a UV–Vis spectrophotometer.

## Data availability

All data supporting the conclusions of this research article are included within the manuscript.

Received: 9 January 2023; Accepted: 22 February 2023

Published online: 27 February 2023

## References

- Speed, B. et al. Pharmacokinetics, distribution, and metabolism of [14C] sunitinib in rats, monkeys, and humans. *Drug Metab. Dispos.* **111**, 042853 (2011).
- He, L. et al. LC-ESI-MS/MS determination of simotininib, a novel epidermal growth factor receptor tyrosine kinase inhibitor: application to a pharmacokinetic study. *J. Chromatogr. B* **947**, 168–172 (2014).
- Qiu, F., Bian, W., Li, J. & Ge, Z. Simultaneous determination of sunitinib and its two metabolites in plasma of Chinese patients with metastatic renal cell carcinoma by liquid chromatography–tandem mass spectrometry. *Biomed. Chromatogr.* **27**, 615–621 (2013).
- Zhou, Q. & Gallo, J. M. Quantification of sunitinib in mouse plasma, brain tumor and normal brain using liquid chromatography–electrospray ionization–tandem mass spectrometry and pharmacokinetic application. *J. Pharm. Biomed. Anal.* **51**, 958–964 (2010).
- Rodamer, M., Elsinghorst, P. W., Kinzig, M., Gütschow, M. & Sörgel, F. Development and validation of a liquid chromatography/tandem mass spectrometry procedure for the quantification of sunitinib (SU11248) and its active metabolite, N-desethyl sunitinib (SU12662), in human plasma: application to an explorative study. *J. Chromatogr. B* **879**, 695–706 (2011).
- Oberoi, R. K., Mittapalli, R. K., Fisher, J. & Elmquist, W. F. Sunitinib LC–MS/MS assay in mouse plasma and brain tissue: application in CNS distribution studies. *Chromatographia* **76**, 1657–1665 (2013).
- Rizwana, I., Prakash, K. V. & Mohan, G. K. Analytical method development and validation for the estimation of sunitinib malate in bulk and its pharmaceutical dosage form using RP-HPLC. *Indo. Am. J. Pharm. Res.* **4**, 561–565 (2014).
- van Erp, N. P. et al. Pharmacogenetic pathway analysis for determination of sunitinib-induced toxicity. *J. Clin. Oncol.* **27**, 4406–4412 (2009).
- de Bruijn, P. et al. Bioanalytical method for the quantification of sunitinib and its n-desethyl metabolite SU12662 in human plasma by ultra performance liquid chromatography/tandem triple-quadrupole mass spectrometry. *J. Pharm. Biomed. Anal.* **51**, 934–941 (2010).
- Andriamanana, I., Gana, I., Duret, B. & Hulin, A. Simultaneous analysis of anticancer agents bortezomib, imatinib, nilotinib, dasatinib, erlotinib, lapatinib, sorafenib, sunitinib and vandetanib in human plasma using LC/MS/MS. *J. Chromatogr. B* **926**, 83–91 (2013).
- Ghazaghi, M., Mousavi, H. Z., Shirkanloo, H. & Rashidi, A. Ultrasound assisted dispersive micro solid-phase extraction of four tyrosine kinase inhibitors from serum and cerebrospinal fluid by using magnetic nanoparticles coated with nickel-doped silica as an adsorbent. *Microchim. Acta.* **183**, 2779–2789 (2016).
- Musijowski, J., Piórkowska, E. & Rudzki, P. J. Determination of sunitinib in human plasma using liquid chromatography coupled with mass spectrometry. *J. Sep. Sci.* **37**, 2652–2658 (2014).
- Blanchet, B. et al. Development and validation of an HPLC–UV–visible method for sunitinib quantification in human plasma. *Clin. Chim. Acta.* **404**, 134–139 (2009).
- Lankheet, N. A. et al. Method development and validation for the quantification of dasatinib, erlotinib, gefitinib, imatinib, lapatinib, nilotinib, sorafenib and sunitinib in human plasma by liquid chromatography coupled with tandem mass spectrometry. *Biomed. Chromatogr.* **27**, 466–476 (2013).
- Minkin, P. et al. Quantification of sunitinib in human plasma by high-performance liquid chromatography–tandem mass spectrometry. *J. Chromatogr. B* **874**, 84–88 (2008).
- Bagheri, H., Zandi, O. & Aghakhani, A. Extraction of fluoxetine from aquatic and urine samples using sodium dodecyl sulfate-coated iron oxide magnetic nanoparticles followed by spectrofluorimetric determination. *Anal. Chim. Acta.* **692**, 80–84 (2011).
- Ershad, S. & Razmara, A. Extraction and pre-concentration of indomethacin with magnetic nanoparticles adsorbent prior to its spectrophotometric determination. *Int. J. PharmTech Res.* **9**, 55–61 (2016).
- Kolaei, M., Dashtian, K., Rafiee, Z. & Ghaedi, M. Ultrasonic-assisted magnetic solid phase extraction of morphine in urine samples by new imprinted polymer-supported on MWCNT-Fe<sub>3</sub>O<sub>4</sub>-NPs: CENTRAL composite design optimization. *Ultrason. sonochem.* **33**, 240–248 (2016).
- Zhao, J., Liao, W. & Yang, Y. Magnetic solid-phase extraction for determination of sulphiride in human urine and blood using high-performance liquid chromatography. *Biomed. Chromatogr.* **29**, 1871–1877 (2015).
- Mirabi, A. & Aliakbari, N. Preparation of modified magnetic nanocomposites dithiooxamide/Fe<sub>3</sub>O<sub>4</sub> for pre-concentration and determination of trace amounts of cobalt ions in food and natural water samples. *J. Chem. Health Risks.* **6**, 291–303 (2016).
- Pourbasheer, E., Qasemi, F., Rouhi, M., Azari, Z. & Ganjali, M. R. Pre-concentration and determination of 2-mercaptobenzimidazole by dispersive liquid–liquid microextraction and experimental design. *J. Sep. Sci.* **40**, 2467–2473 (2017).
- Razmi, R. et al. Pre-concentration and determination of ceftazidime in real samples using dispersive liquid–liquid microextraction and high-performance liquid chromatography with the aid of experimental design. *J. Sep. Sci.* **39**, 4116–4123 (2016).
- Banaei, A., Vojoudi, H., Karimi, S., Bahar, S. & Pourbasheer, E. Synthesis and characterization of new modified silica coated magnetite nanoparticles with bisaldehyde as selective adsorbents of Ag(I) from aqueous samples. *RSC Adv.* **5**, 83304–83313 (2015).
- Rouhi, M., Pourbasheer, E. & Ganjali, M. R. Optimization of dispersive liquid–liquid microextraction combined with high performance liquid chromatography for the analysis of dipyrindamole in water and urine samples. *Monatsh Chem.* **146**, 1593–1601 (2015).
- Pourbasheer, E., Sadafi, S., Ganjali, M. R. & Abbasghorbani, M. Dispersive liquid–liquid microextraction for pre-concentration and determination of phenytoin in real samples using response surface methodology–high performance liquid chromatography. *RSC Adv.* **4**, 62190–62196 (2014).
- Borgul, P. et al. Oxidized thin aluminum films used as the polarized liquid–liquid interface support for norcocaine detection. *Sens. Actuators B. Chem.* **373**, 132651 (2022).
- Roosendaal, J. et al. Development and validation of LC–MS/MS methods for the quantification of the novel anticancer agent guadecitabine and its active metabolite β-decitabine in human plasma, whole blood and urine. *J. Chromatogr. B Anal. Technol. Biomed. Life Sci.* **1109**, 132–141 (2019).
- Parham, H. & Rahbar, N. Solid phase extraction–spectrophotometric determination of salicylic acid using magnetic iron oxide nanoparticles as extractor. *J. Pharm. Biomed. Anal.* **50**, 58–63 (2009).
- Gholivand, M. B. & Torkashvand, M. Electrooxidation behavior of warfarin in Fe<sub>3</sub>O<sub>4</sub> nanoparticles modified carbon paste electrode and its determination in real samples. *Mater. Sci. Eng. C.* **48**, 235–242 (2015).

30. Du, J. et al. Mixed hemi/ad-micelle SDS-coated magnetic Fe<sub>2-x</sub>Al<sub>x</sub>O<sub>3</sub> (x= 0.4) nanoparticles for the capture of gatifloxacin and prulifloxacin coupled with fluorimetric determination. *Anal. Methods*. **8**, 2778–2785 (2016).
31. Bavili Tabrizi, A. & Dehghani Teymurlouie, N. Application of sodium dodecyl sulfate coated iron oxide magnetic nanoparticles for the extraction and spectrofluorimetric determination of propranolol in different biological samples. *J. Mex. Chem. Soc.* **60**, 108–116 (2016).
32. Esmaeili-Shahri, E. & Es'haghi, Z. Superparamagnetic Fe<sub>3</sub>O<sub>4</sub>@SiO<sub>2</sub> core-shell composite nanoparticles for the mixed hemimicelle solid-phase extraction of benzodiazepines from hair and wastewater samples before high-performance liquid chromatography analysis. *J. Sep. Sci.* **38**, 4095–4104 (2015).
33. Amoli-Diva, M., Pourghazi, K. & Poursadollah-Karani, H. Surfactant coated magnetic nanoparticle-based solid-phase extraction coupled with spectrophotometric detection for determination of ultra-trace amounts of indomethacin in biological fluids. *Micro Nano Lett.* **10**, 135–139 (2015).
34. Tabrizi, A. B., Rashidi, M. R. & Ostadi, H. A nanoparticle-based solid-phase extraction procedure followed by spectrofluorimetry to determine carbaryl in different water samples. *J. Braz. Chem. Soc.* **25**, 709–715 (2014).
35. Zandipak, R. & Taghavi, L. Synthesis of 2, 4-dinitrophenylhydrazine loaded sodium dodecyl sulfate-coated magnetite nanoparticles for adsorption of Hg (II) ions from an aqueous solution. *Environ. Health Eng. Manage. J.* **3**, 183–189 (2016).
36. Ganjali, M. R., Pourbasheer, E. & Rezapour, M. Dextran capped Gd<sup>3+</sup>-doped Fe<sub>3</sub>O<sub>4</sub> nanoparticles: electrochemical synthesis and characterization. *Anal. Bioanal. Electrochem.* **10**, 394–403 (2018).
37. Asfaram, A., Ghaedi, M., Goudarzi, A., Soylak, M. & Mehdizadeh Langroodi, S. Magnetic nanoparticle based dispersive micro-solid-phase extraction for the determination of malachite green in water samples: optimized experimental design. *New J. Chem.* **39**, 9813–9823 (2015).
38. Habila, M. A. et al. Mercaptobenzothiazole-functionalized magnetic carbon nanospheres of type Fe<sub>3</sub>O<sub>4</sub>@SiO<sub>2</sub>@C for the preconcentration of nickel, copper and lead prior to their determination by ICP-MS. *Microchim. Acta* **183**, 2377–2384 (2016).
39. Habila, M. A., Allothman, Z. A., El-Toni, A. M., Labis, J. P. & Soylak, M. Synthesis and application of Fe<sub>3</sub>O<sub>4</sub>@SiO<sub>2</sub>@TiO<sub>2</sub> for photocatalytic decomposition of organic matrix simultaneously with magnetic solid phase extraction of heavy metals prior to ICP-MS analysis. *Talanta* **154**, 539–547 (2016).
40. Faraji, M., Yamini, Y. & Rezaee, M. Extraction of trace amounts of mercury with sodium dodecyl sulphate-coated magnetite nanoparticles and its determination by flow injection inductively coupled plasma-optical emission spectrometry. *Talanta* **81**, 831–836 (2010).
41. Ranjbari, E., Hadjmohammadi, M. R., Kiekens, F. & De Wael, K. Mixed hemi/Ad-micelle sodium dodecyl sulfate-coated magnetic iron oxide nanoparticles for the efficient removal and trace determination of rhodamine-B and rhodamine-6G. *Anal. Chem.* **87**, 7894–7901 (2015).
42. Sharifabadi, M. K., Tehrani, M. S., Mehdinia, A., Azar, P. A. & Husain, S. W. Fast removal of citalopram drug from waste water using magnetic nanoparticles modified with sodium dodecyl sulfate followed by UV-spectrometry. *J. Chem. Health Risks*. **3** (2013).
43. Sobhanardakani, S., Zandipak, R. & Cheraghi, M. Synthesis of DNPH/SDS/Fe<sub>3</sub>O<sub>4</sub> nanoparticles for removal of Cr (VI) ions from aqueous solution. *Avicenna J. Environ. Health Eng.* **3**, e7789–e7798 (2016).
44. Mashhadizadeh, M. H. & Amoli-Diva, M. Atomic absorption spectrometric determination of Al<sup>3+</sup> and Cr<sup>3+</sup> after preconcentration and separation on 3-mercaptopropionic acid modified silica coated-Fe<sub>3</sub>O<sub>4</sub> nanoparticles. *J. Anal. At. Spectrom.* **28**, 251–258 (2013).
45. Azari, Z., Pourbasheer, E. & Beheshti, A. Mixed hemimicelles solid-phase extraction based on sodium dodecyl sulfate (SDS)-coated nano-magnets for the spectrophotometric determination of Fingolomid in biological fluids. *Spectrochim. Acta, Part A* **153**, 599–604 (2016).
46. Banaei, A. et al. Synthesis of silica gel modified with 2, 2'-(hexane-1, 6-diylbis (oxy)) dibenzaldehyde as a new adsorbent for the removal of Reactive Yellow 84 and Reactive Blue 19 dyes from aqueous solutions: equilibrium and thermodynamic studies. *Powder Technol.* **319**, 60–70 (2017).
47. Banaei, A. et al. Adsorption equilibrium and thermodynamics of anionic reactive dyes from aqueous solutions by using a new modified silica gel with 2, 2'-(pentane-1, 5-diylbis (oxy)) dibenzaldehyde. *Chem. Eng. Res. Des.* **123**, 50–62 (2017).
48. Muthukumar, C., Sivakumar, V. M. & Thirumarimurugan, M. Adsorption isotherms and kinetic studies of crystal violet dye removal from aqueous solution using surfactant modified magnetic nanoadsorbent. *J. Taiwan Inst. Chem. Eng.* **63**, 354–362 (2016).
49. Beiraghi, A., Pourghazi, K. & Amoli-Diva, M. Mixed supramolecular hemimicelles aggregates and magnetic carrier technology for solid phase extraction of ibuprofen in environmental samples prior to its HPLC-UV determination. *Chem. Eng. Sci.* **108**, 103–110 (2014).
50. Rajabi, A. A., Yamini, Y., Faraji, M. & Nourmohammadian, F. Modified magnetite nanoparticles with cetyltrimethylammonium bromide as superior adsorbent for rapid removal of the disperse dyes from wastewater of textile companies. *Nanochem. Res.* **1**, 49–56 (2016).

## Author contributions

E.P. acted as the corresponding author, supervising the overall research and the manuscript preparation. L.M. and Zh.A. performed the experiments. V.H.M., and M.R.G. supported the experiments and preparation of the manuscript. All authors reviewed the manuscript.

## Competing interests

The authors declare no competing interests.

## Additional information

**Correspondence** and requests for materials should be addressed to E.P.

**Reprints and permissions information** is available at [www.nature.com/reprints](http://www.nature.com/reprints).

**Publisher's note** Springer Nature remains neutral with regard to jurisdictional claims in published maps and institutional affiliations.



**Open Access** This article is licensed under a Creative Commons Attribution 4.0 International License, which permits use, sharing, adaptation, distribution and reproduction in any medium or format, as long as you give appropriate credit to the original author(s) and the source, provide a link to the Creative Commons licence, and indicate if changes were made. The images or other third party material in this article are included in the article's Creative Commons licence, unless indicated otherwise in a credit line to the material. If material is not included in the article's Creative Commons licence and your intended use is not permitted by statutory regulation or exceeds the permitted use, you will need to obtain permission directly from the copyright holder. To view a copy of this licence, visit <http://creativecommons.org/licenses/by/4.0/>.

© The Author(s) 2023

## Terms and Conditions

Springer Nature journal content, brought to you courtesy of Springer Nature Customer Service Center GmbH (“Springer Nature”).

Springer Nature supports a reasonable amount of sharing of research papers by authors, subscribers and authorised users (“Users”), for small-scale personal, non-commercial use provided that all copyright, trade and service marks and other proprietary notices are maintained. By accessing, sharing, receiving or otherwise using the Springer Nature journal content you agree to these terms of use (“Terms”). For these purposes, Springer Nature considers academic use (by researchers and students) to be non-commercial.

These Terms are supplementary and will apply in addition to any applicable website terms and conditions, a relevant site licence or a personal subscription. These Terms will prevail over any conflict or ambiguity with regards to the relevant terms, a site licence or a personal subscription (to the extent of the conflict or ambiguity only). For Creative Commons-licensed articles, the terms of the Creative Commons license used will apply.

We collect and use personal data to provide access to the Springer Nature journal content. We may also use these personal data internally within ResearchGate and Springer Nature and as agreed share it, in an anonymised way, for purposes of tracking, analysis and reporting. We will not otherwise disclose your personal data outside the ResearchGate or the Springer Nature group of companies unless we have your permission as detailed in the Privacy Policy.

While Users may use the Springer Nature journal content for small scale, personal non-commercial use, it is important to note that Users may not:

1. use such content for the purpose of providing other users with access on a regular or large scale basis or as a means to circumvent access control;
2. use such content where to do so would be considered a criminal or statutory offence in any jurisdiction, or gives rise to civil liability, or is otherwise unlawful;
3. falsely or misleadingly imply or suggest endorsement, approval, sponsorship, or association unless explicitly agreed to by Springer Nature in writing;
4. use bots or other automated methods to access the content or redirect messages
5. override any security feature or exclusionary protocol; or
6. share the content in order to create substitute for Springer Nature products or services or a systematic database of Springer Nature journal content.

In line with the restriction against commercial use, Springer Nature does not permit the creation of a product or service that creates revenue, royalties, rent or income from our content or its inclusion as part of a paid for service or for other commercial gain. Springer Nature journal content cannot be used for inter-library loans and librarians may not upload Springer Nature journal content on a large scale into their, or any other, institutional repository.

These terms of use are reviewed regularly and may be amended at any time. Springer Nature is not obligated to publish any information or content on this website and may remove it or features or functionality at our sole discretion, at any time with or without notice. Springer Nature may revoke this licence to you at any time and remove access to any copies of the Springer Nature journal content which have been saved.

To the fullest extent permitted by law, Springer Nature makes no warranties, representations or guarantees to Users, either express or implied with respect to the Springer nature journal content and all parties disclaim and waive any implied warranties or warranties imposed by law, including merchantability or fitness for any particular purpose.

Please note that these rights do not automatically extend to content, data or other material published by Springer Nature that may be licensed from third parties.

If you would like to use or distribute our Springer Nature journal content to a wider audience or on a regular basis or in any other manner not expressly permitted by these Terms, please contact Springer Nature at

[onlineservice@springernature.com](mailto:onlineservice@springernature.com)

See discussions, stats, and author profiles for this publication at: <https://www.researchgate.net/publication/370559563>

# QSAR modeling approaches to identify a novel ACE2 inhibitor that selectively bind with the C and N terminals of the ectodomain

Article in *Journal of biomolecular Structure & Dynamics* · May 2023

DOI: 10.1080/07391102.2023.2205948

CITATIONS

0

READS

87

10 authors, including:



**Rahul Jawarkar**

Dr Rajendra Gode Institute of Pharmacy Amravati Maharashtra

71 PUBLICATIONS 534 CITATIONS

[SEE PROFILE](#)



**Magdi E. A. Zaki**

University of Minho

213 PUBLICATIONS 1,735 CITATIONS

[SEE PROFILE](#)



**Abdul Samad**

Tishk International University

42 PUBLICATIONS 557 CITATIONS

[SEE PROFILE](#)




## QSAR modeling approaches to identify a novel ACE2 inhibitor that selectively bind with the C and N terminals of the ectodomain

Rahul D. Jawarkar, Magdi E. A. Zaki, Sami A. Al-Hussain, Aamal A. Al-Mutairi, Abdul Samad, Nobendu Mukerjee, Arabinda Ghosh, Vijay H. Masand, Long Chiau Ming & Summya Rashid



To cite this article: Rahul D. Jawarkar, Magdi E. A. Zaki, Sami A. Al-Hussain, Aamal A. Al-Mutairi, Abdul Samad, Nobendu Mukerjee, Arabinda Ghosh, Vijay H. Masand, Long Chiau Ming & Summya Rashid (2023): QSAR modeling approaches to identify a novel ACE2 inhibitor that selectively bind with the C and N terminals of the ectodomain, Journal of Biomolecular Structure and Dynamics, DOI: [10.1080/07391102.2023.2205948](https://doi.org/10.1080/07391102.2023.2205948)

To link to this article: <https://doi.org/10.1080/07391102.2023.2205948>

 [View supplementary material](#) 

 Published online: 05 May 2023.

 [Submit your article to this journal](#) 

 [View related articles](#) 

 [View Crossmark data](#) 



## QSAR modeling approaches to identify a novel ACE2 inhibitor that selectively bind with the C and N terminals of the ectodomain

Rahul D. Jawarkar<sup>a</sup>, Magdi E. A. Zaki<sup>b</sup>, Sami A. Al-Hussain<sup>b</sup>, Aamal A. Al-Mutairi<sup>b</sup>, Abdul Samad<sup>c</sup>, Nobendu Mukerjee<sup>d</sup>, Arabinda Ghosh<sup>e</sup>, Vijay H. Masand<sup>f</sup>, Long Chiau Ming<sup>g</sup> and Summya Rashid<sup>h</sup>

<sup>a</sup>Department of Medicinal Chemistry and Drug Discovery, Dr Rajendra Gode Institute of Pharmacy, Amravati, Maharashtra, India; <sup>b</sup>Department of Chemistry, Faculty of Science, Imam Mohammad Ibn Saud Islamic University, Riyadh, Saudi Arabia; <sup>c</sup>Department of Pharmaceutical Chemistry, Faculty of Pharmacy, Tishk International University, Erbil, Kurdistan Region, Iraq; <sup>d</sup>Department of Microbiology, Ramakrishna Mission Vivekananda Centenary College, Kolkata, India; <sup>e</sup>Microbiology Division, Department of Botany, Gauhati University, Guwahati, India; <sup>f</sup>Department of Chemistry, Vidyabharati Mahavidyalaya, Amravati, Maharashtra, India; <sup>g</sup>School of Medical and Life Sciences, Sunway University, Sunway City, Malaysia; <sup>h</sup>Department of Pharmacology & Toxicology, College of Pharmacy, Prince Sattam Bin Abdulaziz University, Al-Kharj, Saudi Arabia

### ABSTRACT

Due to the high rates of drug development failure and the massive expenses associated with drug discovery, repurposing existing drugs has become more popular. As a result, we have used QSAR modeling on a large and varied dataset of 657 compounds in an effort to discover both explicit and subtle structural features requisite for ACE2 inhibitory activity, with the goal of identifying novel hit molecules. The QSAR modelling yielded a statistically robust QSAR model with high predictivity ( $R^2_{tr}=0.84$ ,  $R^2_{ex}=0.79$ ), previously undisclosed features, and novel mechanistic interpretations. The developed QSAR model predicted the ACE2 inhibitory activity ( $pIC_{50}$ ) of 1615 ZINC FDA compounds. This led to the detection of a  $pIC_{50}$  of 8.604 M for the hit molecule (ZINC000027990463). The hit molecule's docking score is  $-9.67$  kcal/mol (RMSD 1.4). The hit molecule revealed 25 interactions with the residue ASP40, which defines the N and C termini of the ectodomain of ACE2. The HIT molecule conducted more than thirty contacts with water molecules and exhibited polar interaction with the ARG522 residue coupled with the second chloride ion, which is 10.4 nm away from the zinc ion. Both molecular docking and QSAR produced comparable findings. Moreover, MD simulation and MMGBSA studies verified docking analysis. The MD simulation showed that the hit molecule-ACE2 receptor complex is stable for 400 ns, suggesting that repurposed hit molecule 3 is a viable ACE2 inhibitor.

### ARTICLE HISTORY

Received 25 January 2023  
Accepted 17 April 2023

### KEYWORDS



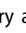
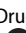
Angiotensin converting enzyme-2; QSAR; molecular docking; MD simulation; MMGBSA


## 1. Introduction

The signalling mechanism known as the renin-angiotensin system (RAS) controls vascular function in a homeostatic manner (Crowley et al., 2005). Modulation of blood volume, natriuresis, and blood pressure are some of its systemic effects. RAS controls local blood flow and controls trophic responses to various stimuli, but it also serves an important local purpose. The majority of tissues express and work with the type 1 integral membrane glycoprotein; ACE2 (Tipnis et al., 2000). The highest levels of ACE2 expression are seen in the kidney, endothelium, lungs, and heart (Donoghue et al., 2000). The major RAS effector, angiotensin II (Ang II), increases vasoconstriction, salt retention, oxidative stress, inflammation, and fibrosis while decreasing baroreceptor sensitivity to sustain heart rate. Various studies support ACE2's critical function of effectively degrading Ang II to Ang-(1-7), which antagonizes Ang II's effects (Figure 1). Ang-(1-7) works on the MAS receptor, which decreases blood

pressure through vasodilation, promotes salt and water excretion by the kidney, and reduces inflammation by increasing nitric oxide production (Figure 1). ACE, on the other hand, transforms Ang I into Ang II, which works at the type 1 angiotensin receptor (AT1R) to raise blood pressure by promoting vasoconstriction, increasing salt and water reabsorption by the kidney, and causing oxidative stress to promote inflammation and fibrosis (Figure 1) (Crowley et al., 2005).

The RAS regulates body fluid, electrolyte homostasis, and vascular tone (Yim & Yoo, 2008). These RAS actions are mediated by angiotensin effector peptides such as Ang II, III, and 1-7 (Sparks et al., 2014). The main effector peptide, Ang II, is produced in the blood and affects the kidneys, adrenal glands, sympathetic nervous system, and baroreceptor reflexes (Atlas, 2007; Reid, 1992). Local RAS has been discovered in a variety of different tissues, including the brain (Ganten et al., 2009; Reid, 1992). Angiotensinogen is produced by astrocytes in the central nervous system, and is

**CONTACT** Rahul D. Jawarkar  rahuljawarkar@gmail.com  Department of Medicinal Chemistry and Drug Discovery, Dr Rajendra Gode Institute of Pharmacy, University mardi road, Amravati 444603, Maharashtra, India; Magdi E. A. Zaki  Mezaki@imamu.edu.sa  Department of Chemistry, Faculty of Science, Imam Mohammad Ibn Saud Islamic University, Riyadh 13318, Saudi Arabia

 Supplemental data for this article can be accessed online at <https://doi.org/10.1080/07391102.2023.2205948>.

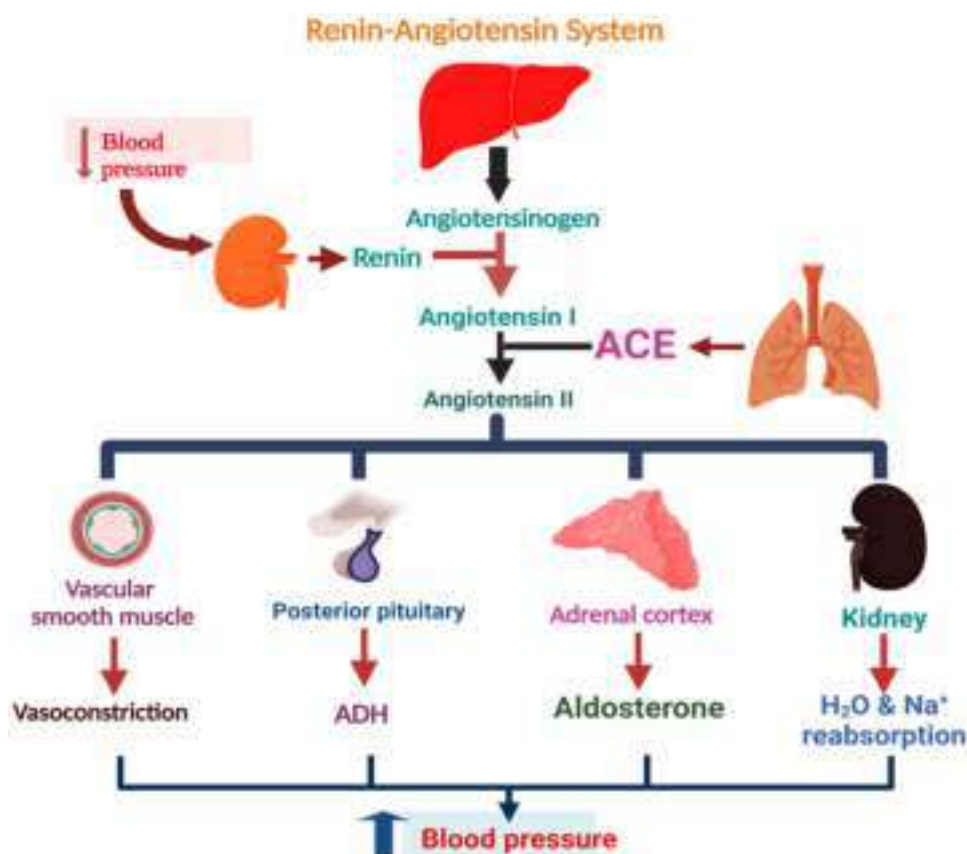


Figure 1. Functional scheme of the renin-angiotensin system.

then degraded by renin, angiotensin converting enzyme (ACE), amino peptidases or ACE2 and Nephilysin (Lin et al., 1996). Despite some speculation, it is unknown the locality of brain these RAS enzymes are produced (Bodiga & Bodiga, 2013). The RAS in the brain regulates learning, memory, anxiety, sorrow, cognition, and emotional stress (McKinley et al., 2003), but it also supports the actions of the peripheral RAS (Bodiga & Bodiga, 2013). Importantly, there is growing evidence that RAS in the brain has a role in the development of neurodegenerative diseases such as Alzheimer's disease (Paul et al., 2006; Zhu et al., 2011).

Although some studies have shown a link between RAS and toxic peptide accumulation (Tian et al., 2012), tau phosphorylation (Murphy et al., 2010), oxidative stress (Tian et al., 2012), mitochondrial dysfunction, neuroinflammation, and cholinergic dysfunction (Chrissobolis et al., 2012), it is still unclear how medications that act on the RAS system affect Alzheimer's disease.

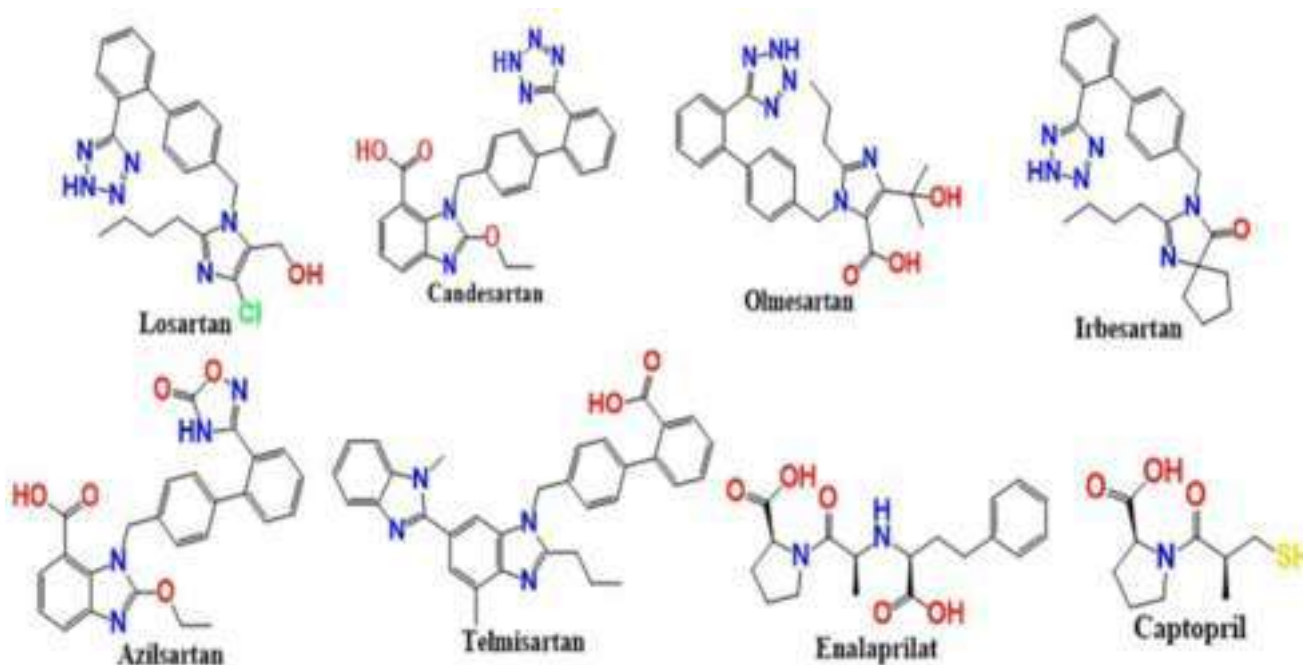
Literature survey reveals that, there are Angiotensin-Receptor Blockers (ARBs) and ACE inhibitors which have varied effects on ACE2 levels (Burchill et al., 2012; Burrell et al., 2005; Ferrario et al., 2005; 2020; Furuhashi et al., 2015; Hamming et al., 2008; Igase et al., 2005; Ishiyama et al., 2004; Lakshmanan et al., 2012; Ocaranza et al., 2006; Soler et al., 2009; Sukumaran et al., 2011; 2012; 2017; Vuille-dit-Bille et al., 2015; Zhong et al., 2011). ACE inhibitors and angiotensin-receptor blockers (ARBs) are notable in that their effects on angiotensin II are unique from one another

(Vaduganathan et al., 2020). Some of the important ACE 2 blockers and inhibitors are shown in Figure 2.

Subsequently, recombinant human ACE2 is known as therapeutic RAS modulator. Supplementation with recombinant human ACE2 results in lowering of Ang II and increase of Ang-(1-7)/Ang II ratio (Basu et al., 2017). GSK2586881, a recombinant human ACE2 was found to decrease the level of Ang II with increase of Ang (1-7) in acute respiratory distress syndrome patients (Khan et al., 2017).

In order to retain its high binding affinity for ACE2, a novel therapeutic drug must be designed that has a better ADMET (Absorption, Distribution, Metabolism, Excretion, and Toxicity) profile. For this, it is crucial to understand the pharmacophoric characteristics connected to ACE2 binding affinities using a large, structurally varied dataset with sufficient fluctuations in activity space. Due to its effectiveness in terms of time and cost, computer-aided drug design (CADD) is a modern and practical approach to achieving these goals (Baig et al., 2016; Imam & Gilani, 2017). A flourishing and well acknowledged subfield of CADD called ligand-based drug designing (LBDD) has a greater percentage of success in identifying important pharmacophoric characteristics. If the target protein's 3D structure is unavailable, this approach should be used (Baig et al., 2016). Quantitative Structure-Activity Relationship (QSAR) is an effective, interdisciplinary method for identifying prominent and subtle pharmacophoric characteristics in the context of LBDD (Gramatica, 2013; 2020; Huang & Fan, 2011).





**Figure 2.** Chemical structures of the angiotensin-receptor blockers (ARBs; azilsartan, candesartan, irbesartan, losartan, olmesartan, telmisartan) (A) and angiotensin converting enzyme (enalaprilat, captopril) inhibitors (B).

Several researchers have utilised various scaffold patterns in QSAR analyses for the ACE2 receptor. QSARs of nine peptide datasets of angiotensin-converting enzyme inhibitor (ACE-inhibitor) oligopeptides were investigated by Xiaoyu Wang and colleagues. According to Xiaoyu, the hydrophobic and stereospecific amino acid residues for the ACE-inhibitor dipeptides are essential for the ACE2 inhibitory activities (Wang et al., 2011). Additionally, Fangfang Wang and colleagues proposed that the steric field has a beneficial impact on the ACE2 inhibitory bioactivity, supporting the finding made by Wang and colleagues (Wang & Zhou, 2020). Additionally, Regulska and colleagues provided evidence corroborating Wang and colleagues' finding that the hydrophobic feature plays a critical role in determining ACE2 inhibitory activity (Regulska et al., 2014). As a result, Prabhakar and colleagues investigated the structure-activity relationship study, and they came to the conclusion that ACE's hydrophobicity and polar interaction play a significant role in its inhibitory effect. Despite the fact that these investigations helped to identify certain significant structural characteristics, the created QSAR models lacked wide application because they were either based on limited datasets or just particular scaffolds. Additionally, its use for lead optimization pipeline is constrained by limited external predictive ability. An extensive knowledge of the relationship between structural characteristics and desired bioactivity is provided by a QSAR study that uses a wide variety of compounds and balances predictive and mechanistic interpretation (Fujita & Winkler, 2016; Gramatica, 2020; Masand et al., 2021). In order to determine the structural characteristics that are very important for ACE2 ligands, QSAR analysis has been carried out in the current work employing a large and diverse dataset that covers a broad chemical and activity space. In addition, we have found a new (ZINC000027990463) inhibitor

against ACE2 employing a wide range of computational approaches, including drug repurposing, QSAR-based virtual screening, molecular docking supplemented by molecular dynamic simulation, and molecular mechanics generalised borne surface area (MMGBSA). Therefore, it would be a good idea to do drug repurposing on these drugs that have received clinical approval once again. Repurposing clinically approved medications has the advantage that their side effects are known, making them great candidates for ACE2 inhibition. As a result, the hit compound can be suggested for a number of disorders linked to ACE2 receptor activation.

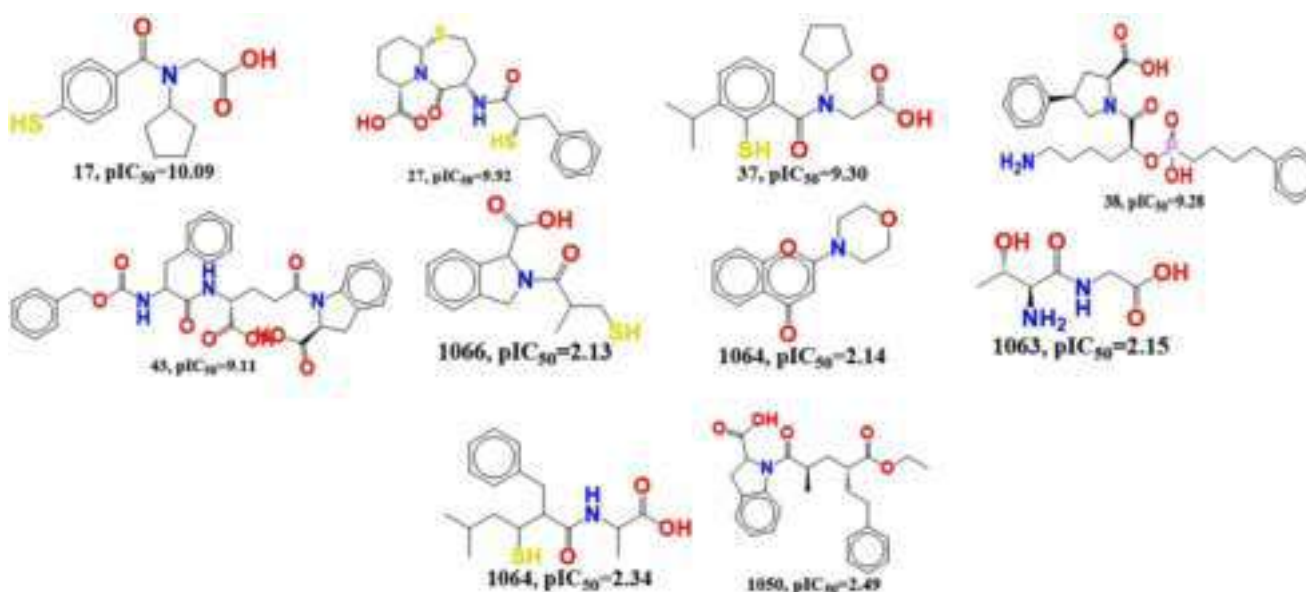
## 2. Materials and methods

### 2.1. Preparation of datasets

There are 1075 compounds in the ChEMBL database whose ACE 2 potency has been measured experimentally using the  $IC_{50}$  (Gaulton et al., 2017). An updated dataset including 657 ACE inhibitors with precise  $IC_{50}$  values is constructed after deleting duplicates, multi-component compounds or salts, and compounds with incorrect  $IC_{50}$  values. The  $pIC_{50}$  values  $M$  were calculated by first converting  $IC_{50}$  nM values to  $M$  molar concentrations ( $pIC_{50} = -\log IC_{50} M$ ). The structures of the five most active and five least active molecules of the dataset are shown in Figure 3. (See Supplemental Information Table for SMILES notations for all 657 compounds with  $IC_{50}$ , molecular descriptor, and  $pIC_{50} M$  values).

### 2.2. QSAR model development and validation

For virtual screening, molecular optimization, and decision-making, a robust QSAR model validated by cross-validation, external validation, Y-randomization, and applicability



**Figure 3.** Showing the representative examples of five most active and five least active compounds along with their  $pIC_{50}$  values.

domain (William's plot), among others, is helpful. For this study, we used ChemSketch to sketch 2D structures for all 657 compounds, Open Babel 3.1.1 (O'Boyle et al., 2011) to convert these to 3D structures, and hyperchem (Ivanciuc, 1996) to optimise these 3D structures using a semi-empirical PM6 approach (Bikadi & Hazai, 2009).

A PyMOL plugin called PyDescriptor calculated molecular descriptors using the resulting conformers. Topological, geometrical, and constitutional chemical space of molecules are all included in PyDescriptor (Masand & Rastija, 2017). Prefiltering the descriptors (removing the semi-constant and highly inter-correlated ones) yields 2081 descriptors. In order to build and test a QSAR model, a total of 657 molecules were split into training (80%, or 527) and test (20%, or 130) sets. Multiple linear regression was employed in QSAR Model development. Descriptors for the training set were selected with the help of the full subset and the QSARINS 2.2.4 used for Analyzing Genetic function algorithm Method (Dearden et al., 2009; Fujita & Winkler, 2016; Gramatica, 2014; 2020; Gramatica et al., 2013; 2014).

There are a variety of validation criteria available in the literature that may be used to determine how well the model actually works. QSAR model internal predictability and statistical quality were tested using  $r^2$ , leave-one-out, and leave-many-out cross-validation ( $Q^2_{LMO}$ ). The estimate standard error for each model is also provided. To further improve the QSAR models' accuracy, we additionally provided the Root Mean Squared Error (RMSE) for both the training (RMSE<sub>tr</sub>) and external prediction (RMSE<sub>ext</sub>) sets. To reduce the amount of overlap between the various descriptors, QUICK was set to 0.05. The QSAR model's reliability was tested using a Y-randomization test with 2000 repetitions to eliminate spurious correlations.

External validation was performed using  $r^2_{ext}$ ,  $Q^2_{F1}$ ,  $Q^2_{F2}$ ,  $Q^2_{F3}$ , CCC<sub>ext</sub>,  $r^2_m$ , and  $r^2_m$ .  $R^2_m$  penalises a model for large disparities between actual and anticipated chemical values (considering both training and test sets). The metric  $Q^2_{F3}$  is particularly well-suited for comparing the external

predictivity of different models developed on the same training dataset. The  $r^2_m$  measures discordance between predicted and actually observed levels of activity ( $pIC_{50}$  M value). The proposed threshold for external validation's correlation coefficient,  $r^2_m$ , is more than 0.5. All QSAR models were evaluated using the criteria established by Golbraikh and Tropsha to guarantee reliability and stability. The degree to which a QSAR model's projected value agrees with the measured biological activity determines the model's predictive accuracy. The predictive power of a QSAR model declines as soon as an outlier is included. To continue, we scoured GAMLIR-based QSAR models for substances with very high residual values. Comparison of the predicted value to the residual data helped find the outlier compounds. As William demonstrated, leverage effects brought attention to inherent diversity in database structure. The range of validity for a QSAR model is determined by the residuals and leverage (Consonni et al., 2019; Harit et al., 2017).

### 2.3. Drug repositioning and QSAR based virtual screening

We utilised a 1650-compound Zinc FDA database for QSAR-based virtual screening. Previously, 3D-molecular structures were structured as a modelling set for descriptor calculations. The six-parameter QSAR model was used to predict ACE2 inhibitory activity of 1650 FDA molecules (Bakal et al., 2022; Ghosh et al., 2022; Jawarkar et al., 2022).

### 2.4. Molecular docking study

Protein Data Bank (<https://www.rcsb.org/structure/1O86>) has the human ACE PDB file. PDB ID:1O86 was determined based on X-ray resolution and sequence completion. The docking-ready protein is tuned. The active site in the pdb was determined on the basis of bound ligand; lisinopril. For clarity, the docking stance for the most active molecule 3 is shown as a

symbol. NRGSuite was used to study molecular docking. This is a PyMOL plugin (<https://www.pymol.org>). It can determine protein surface cavities for docking simulations using FlexAID (Gaudreault et al., 2015). It models ligand and side-chain flexibility and simulates covalent docking. In this study, a flexible-rigid docking technique with default settings was utilised to optimise NRGSuite performance: Biovia Discovery studio software was used to visualise with the setting of 1000 chromosomes, 1000 generations, fitness model share, reproduction model population boom, and 5 TOP complexes were retained.

### 2.5. Molecular dynamics simulation (MD-simulation)

The MD simulations were carried out in triplicate using the Desmond 2020.1 from Schrödinger, LLC on dock complexes for Mpro (PDB I.D: 1o86) and molecule 3 (ZINC I.D: ZINC000027990463). To ensure that the results were repeatable, duplicate samplings were performed with the same parameters for each MD run. This system utilizes the OPLS-2005 force field (Shivakumar et al., 2010) and an explicit solvent model with SPC water molecules. To neutralize the charge, Na<sup>+</sup> ions were added. To imitate the physiological environment, 0.15 M NaCl solutions were introduced to the system. To retrain over the protein-compound 4 complex, the system was first equilibrated using an NVT ensemble for 400 ns. Following the preceding phase, an NPT ensemble was used to execute a short equilibration and minimization run for 12 ns. In all simulations, the NPT ensemble was set up using the Nose-Hoover chain coupling scheme (Jorgensen et al., 1983), with a temperature of 27 °C, a relaxation duration of 1.0 ps, and a pressure of 1 bar. A 2 fs time step was chosen. With a relaxation duration of 2 ps, the Martyna-Tuckerman-Klein chain coupling scheme (Martyna et al., 1992) barostat method was employed for pressure control. Long-range electrostatic interactions were calculated using the particle mesh Ewald method (Toukmaji & Board, 1996), with the Coulomb interaction Radius set at 9. The bonded forces were calculated using the RESPA integrator with a time step of 2 fs for each trajectory. To check the stability of the MD simulations, the root mean square deviation (RMSD), radius of gyration (Rg), root mean square fluctuation (RMSF), and quantity of hydrogen (H-bonds) were computed. Geo measures v 0.872 was used to calculate the free energy landscape of protein folding on a chemical 4 bound complex (Kagami et al., 2020). The MD trajectory versus RMSD and Radius of gyration (Rg) energy profile of folding was recorded in a 3D plot using the matplotlib python package utilizing Geo measures, which includes a sophisticated library of g\_sham (Ghosh et al., 2022).

### 2.6. Molecular mechanics generalized born and surface area (MMGBSA) calculations

During MD simulations of ACE2 complexed with hit molecule 3, binding free energy (Gbind) was calculated using MMGBSA module. (Schrodinger Suite, 2017-4, NY). OPLS 2005, VSGB, and rotamer search methods were used to compute

binding free energy. After MD, 10 ns intervals of trajectory frames were picked. Total free energy binding was calculated using equation 1:

$$\Delta G_{\text{bind}} = G_{\text{complex}} - (G_{\text{protein}} + G_{\text{ligand}})$$

Where,  $\Delta G_{\text{bind}}$  = binding free energy,  $G_{\text{complex}}$  = free energy of the complex,  $G_{\text{protein}}$  = free energy of the target protein, and  $G_{\text{ligand}}$  = free energy of the ligand.

## 3. Results and discussion

The current study relies on a sizable dataset (657 molecules), but it has already significantly spanned a large area of chemistry due to the presence of numerous molecular scaffolds, functional groups, substituents, diverse rings (including non-aromatic, homoaromatic, heteroaromatic, fused rings; spiro compounds; etc.). The QSAR model was constructed using a divided data set. Values of  $R^2$ ,  $R^2_{\text{adj}}$ , CCC<sub>tr</sub>, and other fitting parameters that are much above the allowable threshold values demonstrate that the QSAR models are statistically acceptable with the required number of chemical descriptors.

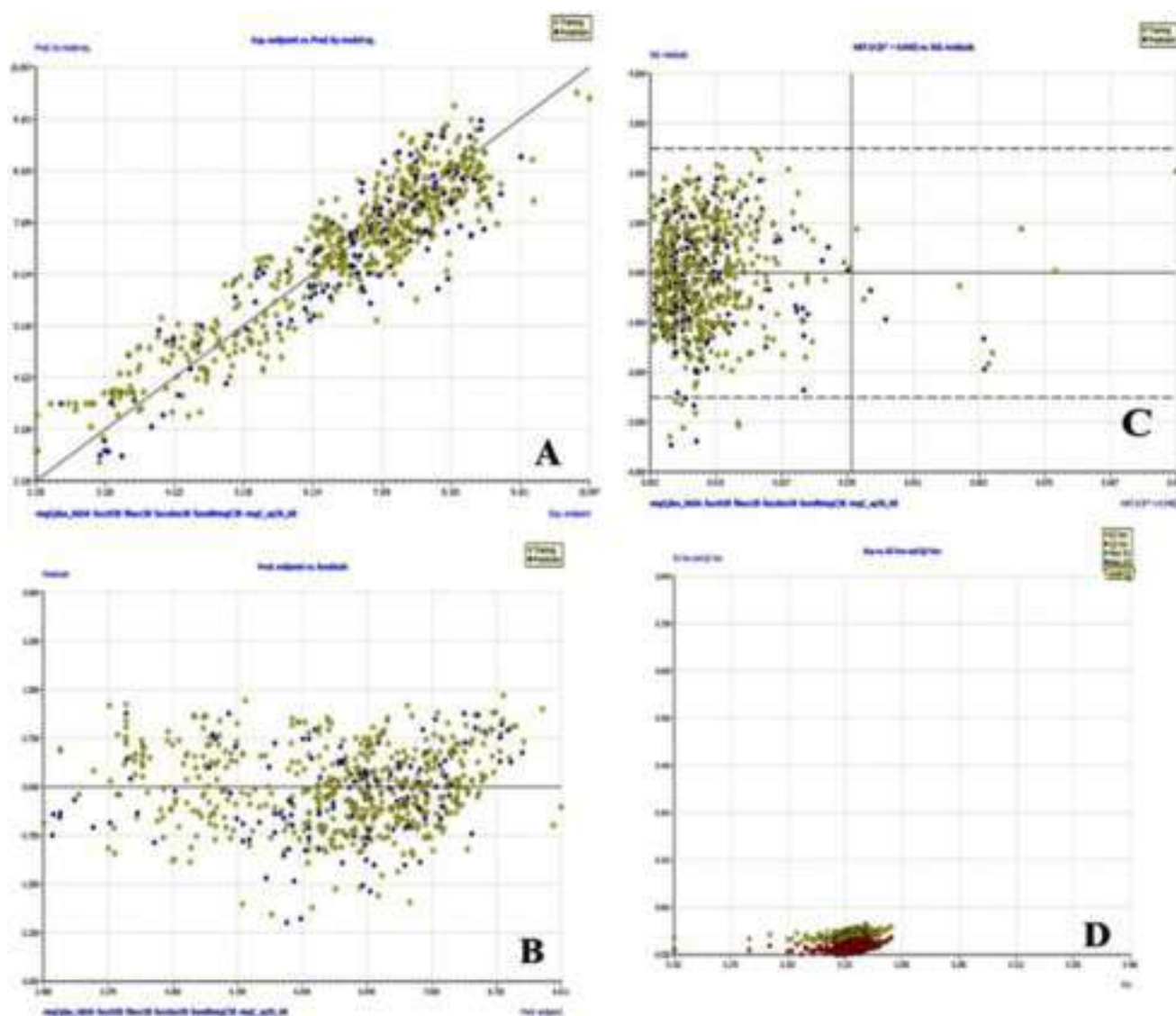
### 3.1. QSAR model

$Q^2_{\text{LOO}}$ ,  $Q^2_{\text{LMO}}$ , and other internal validation parameters have values that suggest the statistical robustness of the QSAR models and define the superiority of the QSAR model.

### 3.2. Model

$\text{PIC}_{50} = 4.541 (\pm 0.184) + 0.021 (\pm 0.002) * \text{ringCplus\_AbSA} + -0.228 (\pm 0.028) * \text{facch3B} + 0.8 (\pm 0.057) * \text{fNacc3B} + -1.606 (\pm 0.129) * \text{faccdon3B} + 0.441 (\pm 0.044) * \text{famDnringC3B} + 0.136 (\pm 0.015) * \text{sp3S\_ringC\_6B}$   
 $R^2: 0.8485, R^2_{\text{adj}}: 0.8468, R^2_{-R^2_{\text{adj}}}: 0.0018, \text{LOF}: 0.3794, \text{Kxx}: 0.2694, \text{Delta K}: 0.0963, \text{RMSE}_{\text{tr}}: 0.6019, \text{MAE}_{\text{tr}}: 0.4925, \text{RSS}_{\text{tr}}: 190.5623, \text{CCC}_{\text{tr}}: 0.9181, \text{s}: 0.6059, \text{F}: 484.5475, Q^2_{\text{LOO}}: 0.8441, R^2-Q^2_{\text{LOO}}: 0.0044, \text{RMSE}_{\text{cv}}: 0.6107, \text{MAE}_{\text{cv}}: 0.4994, \text{PRESS}_{\text{cv}}: 196.1450, \text{CCC}_{\text{cv}}: 0.9156, Q^2_{\text{LMO}}: 0.8428, R^2_{\text{Yscr}}: 0.0111, Q^2_{\text{Yscr}}: -0.0158, \text{RMSE}_{\text{AV}_{\text{Yscr}}}: 1.5379, \text{RMSE}_{\text{ext}}: 0.6982, \text{MAE}_{\text{ext}}: 0.5729, \text{PRESS}_{\text{ext}}: 63.8534, R^2_{\text{ext}}: 0.7997, Q^2_{-F1}: 0.7834, Q^2_{-F2}: 0.7828, Q^2_{-F3}: 0.7962, \text{CCC}_{\text{ext}}: 0.8900, r^2_{\text{m aver.}}: 0.7172, r^2_{\text{m delta}}: 0.0067, \text{Exp}(x) \text{ vs. } \text{Pred}(y): R^2: 0.8441, R^2_{\text{o}}: 0.8177, k': 0.9919, \text{Clos}': 0.0313, r^2_{\text{m}}: 0.7069, \text{Pred}(x) \text{ vs. } \text{Exp}(y): R^2: 0.8441, R^2_{\text{o}}: 0.8441, k: 0.9998, \text{Clos}: 0.0000, r^2_{\text{m}}: 0.8422, \text{Exp}(x) \text{ vs. } \text{Pred}(y): R^2: 0.7997, R^2_{\text{o}}: 0.7899, k': 0.9737, \text{Clos}': 0.0123, R^2_{\text{m}}: 0.7205, \text{Pred}(x) \text{ vs. } \text{Exp}(y): R^2: 0.7997, R^2_{\text{o}}: 0.7882, k: 1.0165, \text{Clos}: 0.0144, r^2_{\text{m}}: 0.7139.$

William's plot illustrated the applicability of the model. Figure 4c displays William's plot, which shows that all of the molecules fall within the model's application domain (the solid line at the top of the plot represents  $h^* = 0.021$ , and the dotted lines at the bottom of the plot reflect the upper and lower limits of standard residuals). The dataset of compound Kxy (Inter-correlation among descriptors) vs  $Q^2_{\text{LMO}}$  (Leave-many-out cross-validated square of the (multiple) correlation coefficient) is shown in Figure 4a. The scatter plot of



**Figure 4.** Different graphs associated with the model (a) experimental vs. predicted  $pK_i$  (the solid line represents the regression line); (b) experimental vs. residuals; (c) William's plot for applicability domain (the vertical solid line represents  $h^* = 0.021$  and horizontal dashed lines represent the upper and lower boundaries for applicability domain; (d) Y-randomization plot.

Kxy against  $R^2_{Yscr}$  ( $R^2$  of the training set with Y-scrambling) and  $Q^2_{Yscr}$  ( $Q^2_{LOO}$  of the training set with Y-scrambling) is shown in Figure 4d. The score plot for the Descriptor in the QSAR model's split set is shown in Figure 4d. As such, it complies with all the OECD-approved recommendations and requirements for developing a practical QSAR model (Cherkasov et al., 2014; Chirico & Gramatica, 2011; 2012; Consonni et al., 2009; Gramatica, 2013; Gramatica et al., 2007; Krstajic et al., 2014; Rao et al., 2008; Tropsha et al., 2003).

## 4. Discussion

### 4.1. QSAR mechanistic interpretation

Understanding the mechanism of action of molecules, the basis for their specificity, and the pharmacophoric attributes/groups responsible for the desired bioactivity can be improved by validating the relationship between influential

structural properties or molecular descriptors of molecules and bioactivity. A synergistic or reverse effect of other molecular descriptors or unknown factors having a remarkable influence in determining a molecule's overall  $IC_{50}$  value cannot be ignored, despite the fact that we have compared the  $IC_{50}$  values of numerous molecules in relation to and as a result of a specific molecular descriptor (or feature) in the present analysis. That is, the experimental  $IC_{50}$  value cannot be determined or fully explained by a single chemical descriptor or attribute for such a vast and structurally diverse range of compounds. That is to say, taking into account the synergistic effects of component molecular descriptors are crucial for making use of a validated QSAR model effectively. The updated QSAR model has a total of six characterizations (Fujita & Winkler, 2016; Gramatica, 2020) (See Table 1).

**ringCplus\_AbSA:** This description denotes the presence of absolute surface area for the positively charged ring carbon atom. Because the descriptor has a positive coefficient in the proposed QSAR model, increasing the value of this

**Table 1.** Shows details of molecular descriptors used to develop QSAR model.

Molecular descriptors	Description	Correlation
ringCplus_AbSA	Occurrence of absolute surface area of the positively charged ring carbon atom.	Positive
facch3B	Frequency of the occurrence of hydrogen atom exactly at the three bonds of the acceptor atom.	Negative
Nacc3B	Frequency of occurrence of the acceptor atom exactly three bonds from the nitrogen atoms.	Positive
faccdon3B	Frequency of occurrence of donor atom exactly at three od from the acceptor atom.	Negative
famdNringC3B	Frequency of occurrence of ring carbon atom exactly at three bonds from the amide nitrogen.	Positive
sp3S_ringC_6B	Occurrence of the ring carbon atom within 6 bonds from Sp3 hybridized sulphur atom.	Positive

descriptor further boosts the ACE2 inhibitory action. This may be shown by comparing molecule 80 (ringCplus\_AbSA = 86.14,  $pIC_{50}$ : 8.58) with molecule 274 (ringCplu\_AbSA = 34.02,  $pIC_{50}$ : 7.82). For molecule 358, increasing the value of this molecular descriptor from 34 to 86 results in a 0.76 unit improvement in ACE inhibitory activity. (About 5.75-fold increase in the inhibitory potency for ACE2). In one of the active compounds 80, no substitution at the 5th position of the pyrrolidine ring is observed, but inclusion of carbonyl group at the 5th position in molecule 274 greatly decreases the absolute surface area for the positively charged ring carbon atom, thus lowering lipophilicity. This finding indicates that inclusion of a carbonyl group decreases the lipophilicity and increases the polarity of compound 274. As a result, lipophilicity (expressed as LogP) is critical for ACE 2 inhibitory activity. This might be the cause of the discrepancy in ACE2 inhibitory activity of compound 80 and 274. Following that, R G Almquist and coworkers reported the same result and commented on the impact of substitution at positions 2 and 5 of the hexanoic acid unit on ACE2 inhibitory activity (Almquist et al., 1982) (See Figure 5). Therefore, QSAR results are in complete agreement with the reported findings. The same observation was found to be true in case of following pair of molecules, 157 (ringCplus\_AbSA = 33.91,  $pIC_{50}$ : 8.237) and 530 (ringCplus\_AbSA = 26.887,  $pIC_{50}$ : 6.854), 575 (ringCplus\_AbSA = 0,  $pIC_{50}$ : 6.62) and 378 (ringCplus\_AbSA = 38.50,  $pIC_{50}$ : 7.456), 205 (ringCplus\_AbSA = 68.539,  $pIC_{50}$ : 8.076) and 597 (ringCplus\_AbSA = 20.724,  $pIC_{50}$  = 6.523), 447 (ringCplus\_AbSA = 72.708,  $pIC_{50}$ : 7.215) and 892 (ringCplus\_AbSA = 41.886,  $pIC_{50}$  = 4.444), 489 (ringCplus\_AbSA = 97.094,  $pIC_{50}$ : 7.046) and 900 (ringCplus\_AbSA = 40.443,  $pIC_{50}$ : 4.41), etc.

Statistical performance ( $R^2 = 0.88$ ) can significantly enhance for established QSAR model by replacing the molecular descriptor ringCplus\_AbSA with the molecular descriptor Cplus\_AbSA (absolute surface area for the positively charged carbon atom). As a result, simple carbon atoms that are aliphatic in nature are indeed a better choice for increasing ACE2 inhibitory effectiveness. Again, replacing the molecular descriptor ringCplus AbSA with lipo\_AbSA

(occurrence of absolute surface area for the positively charged lipophilic atom) results in a slight increase in the statistical performance of the generated QSAR model ( $R^2 = 0.80$ ). This observation demonstrated that positively charged carbon atoms alone are sufficient to increase the ACE2 inhibitory efficacy when compared to positively charged ring carbon atoms. Based on this result, it is imperative that positively charged ring carbon atoms must be retained in future drug design in order to developed more potent ACE2 inhibitors.

**facch3B:** This descriptor describes the frequency of the hydrogen atoms occurring precisely three bonds away from the acceptor atom. As a result of this descriptor's negative association with ACE2 inhibitory activity, its value increases while the  $pIC_{50}$  decreases. The pair of molecules 1047 (facch3B = 4,  $pIC_{50}$ : 2.6), and 983 (facch3B = 2,  $pIC_{50}$ : 3.45) might be used to examine this (see Figure 6). This finding shows that as the hydrogen atom count rises, the inhibitory activity of ACE2 decreases.

Less bulkiness close to the acceptor atom is very helpful for raising the  $pIC_{50}$  values because hydrogen is smaller than other elements and substituting it with any other element will increase the steric bulk. As a result, having fewer hydrogen atoms increases the action of an ACE2 inhibitor. The variance in the ACE2 inhibitory activity may therefore result from this. Shufen Wu and coworker has performed COMFA and COMSIA QSAR modeling of bitter peptides and highlight the importance of steric field in ACE2 inhibition (Wu et al., 2014). Additionally, Xiaoyu Wang and colleagues studied oligopeptide QSAR modelling and deduced that the steric and electrical characteristics are the most crucial ones for determining the inhibition of ACE2 (Wang et al., 2011). The electrical parameter was explained by the presence of acceptor atoms, but the steric parameter was emphasized by the absence of as many hydrogen atoms. Both instances occurring at three bonds highlights the molecule's ACE2 inhibitory activity. Therefore, the results of the QSAR are in perfect accord with the conclusions of the literature based on this observation.

**Figure 5.** Depiction of the molecular descriptor ringCplus\_AbSA for the molecules 80 and 274 only.

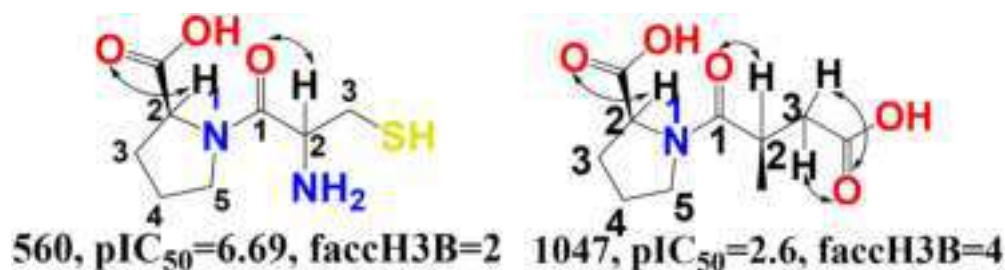


Figure 6. Presentation of the molecular descriptor  $faccH3B$  for the molecules 983 and, 1047 only.

Subsequently, if we have decreased the value of the molecular descriptor from 4 to 2 for the molecule 1047 will result into increase in the ACE inhibitory activity by 4.09 Unit (about 12,302.68-fold amplification in the inhibitory potency for ACE receptor). Same observation has been highlighted by the following pairs of molecules; 470 ( $faccH3B=3$ ,  $pIC_{50}:7.11$ ) and 736 ( $faccH3B=4$ ,  $pIC_{50}:5.66$ ), 79 ( $faccH3B=5$ ,  $pIC_{50}:8.58$ ) and 553 ( $faccH3B=9$ ,  $pIC_{50}:6.75$ ), 226 ( $faccH3B=4$ ,  $pIC_{50}:8$ ) and 321 ( $faccH3B=6$ ,  $pIC_{50}:7.36$ ), 78 ( $faccH3B=2$ ,  $pIC_{50}:8.58$ ) and 514 ( $faccH3B=7$ ,  $pIC_{50}:6.95$ ), 150 ( $faccH3B=2$ ,  $pIC_{50}:8.27$ ) and 779 ( $faccH3B=7$ ,  $pIC_{50}:5.39$ ), 545 ( $faccH3B=3$ ,  $pIC_{50}:6.77$ ) and 983 ( $faccH3B=5$ ,  $pIC_{50}:3.45$ ), 1047 ( $faccH3B=4$ ,  $pIC_{50}:2.6$ ) and 794 ( $faccH3B=3$ ,  $pIC_{50}:5.31$ ), etc.

In addition, the statistical performance ( $R^2 = 0.78$ ) of the proposed QSAR model will be significantly reduced when the molecular descriptor  $faccH3B$  is substituted with the molecular descriptor plus  $acc\ 4B$  (presence of acceptor atom within 4 bonds from the positively charged atom). In particular, to have better ACE2 inhibitory activity, the minimum bonding distance between the acceptor atom and the hydrogen atom must be maintained at three bonds. Likewise, when we exchange the molecular descriptor  $faccH3B$  with the molecular descriptor  $H\_acc\_3B$  (presence of the acceptor atom within three bonds from the hydrogen atom), the created QSAR model will statistically maintain its performance ( $R^2=0.84$ ). In order to increase the ACE2 inhibitory effectiveness, the acceptor atom must be kept in the future drug design at a precise distance of three bonds or less from the hydrogen atom.

**fNacc3B:** This descriptor identified the acceptor atom's frequency of occurrence precisely at three bonds from the nitrogen atom. The acceptor atoms which occur at 2 or 4 bonds will be excluded while calculation of molecular descriptor  $fNacc3B$ . In the developed QSAR model, this descriptor  $a$  has acquired a positive coefficient, so an increase in its value further increases the ACE2 inhibitory

activity. The effect of molecular descriptor can be seen by comparing the molecules 98 ( $fNacc3B=4$ ,  $pIC_{50}:8.50$ ) and 924 ( $fNacc3B=2$ ,  $pIC_{50}:4.11$ ), where increasing the value of the descriptor for the molecule 924 from 2 to 4 will result in an increase in the ACE2 inhibitory activity by 4.39 Unit (about 24,547.08-fold increase in ACE2 inhibitory potency) (see Figure 7). The Acyl tripeptide analogues of enalapril were synthesized by William J. Greenlee and a colleague claimed that the proline portion's carboxy group substitution improved the AC2 inhibitory activity. The identical carboxy OH and CO are the acceptor atoms and are spaced three bonds apart from the nitrogen atom in the proline. Furthermore, according to William J. Greenlee, the carboxy part engaged in interaction with the zinc atom at the active site (Greenlee et al., 1985). Therefore, the QSAR results are analogous with the reported findings.

The following molecule pairings demonstrate this observation; 98 ( $fNacc3B=4$ ,  $pIC_{50}:8.509$ ) and 427 ( $fNacc3B=2$ ,  $pIC_{50}:7.292$ ), 157 ( $fNacc3B=4$ ,  $pIC_{50}:8.237$ ) and 301 ( $fNacc3B=3$ ,  $pIC_{50}:7.721$ ), 111 ( $fNacc3B=4$ ,  $pIC_{50}:8.432$ ) 378 ( $fNacc3B=2$ ,  $pIC_{50}:7.456$ ), 162 ( $fNacc3B=4$ ,  $pIC_{50}:8.222$ ) and 552 ( $fNacc3B=3$ ,  $pIC_{50}:6.745$ ), 140 ( $fNacc3B=2$ ,  $pIC_{50}:8.301$ ) and 531 ( $fNacc3B=2$ ,  $pIC_{50}:6.854$ ), 175 ( $fNacc3B=3$ ,  $pIC_{50}:8.155$ ) and 597 ( $fNacc3B=2$ ,  $pIC_{50}:6.523$ ), 355 ( $fNacc3B=5$ ,  $pIC_{50}:7.538$ ) and 396 ( $fNacc3B=4$ ,  $pIC_{50}:7.398$ ), 88 ( $fNacc3B=4$ ,  $pIC_{50}:8.538$ ) and 475 ( $fNacc3B=3$ ,  $pIC_{50}:7.092$ ), etc.

To verify the influence of molecular descriptor  $fNacc3B$  on ACE2 inhibitory activity, we have replaced the molecular descriptor  $fNacc3B$  with another equivalent molecular descriptor  $fNsp2O3B$  (frequency of occurrence of  $Sp^2$  hybridised oxygen atom exactly at three bonds from the nitrogen atom) will significantly improve the statistical performance ( $R^2=0.90$ ) of the developed QSAR model. This observation revealed that the  $sp^2$  hybridized oxygen atom as an acceptor is the most preferred substituent placed precisely at 3 bonds

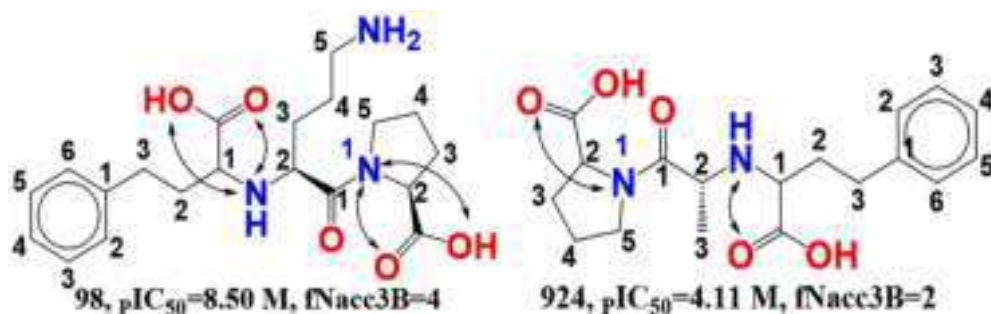


Figure 7. Presentation of molecular descriptor  $fNacc3B$  for the molecule 98 and 924.

from the element nitrogen required to enhance the ACE2 inhibitory activity. This observation also points out that the optimum bonding distance between acceptor atom and element nitrogen must be 3 bonds to have better ACE2 inhibitory activity. In addition to this, we have shifted the molecule descriptor fNacc3B again with the molecular descriptor fnsP3O3B (frequency of occurrence of Sp<sup>3</sup> hybridised oxygen atom precisely at three bonds from the nitrogen atom). This alteration significantly increases the statistical performance ( $R^2=0.92$ ) of the developed QSAR model. This observation revealed that the sp<sup>3</sup> hybridised oxygen is the better option as an acceptor to improve ACE2 inhibitory potency. Moreover, it also observed that the sp<sup>3</sup> hybridised oxygen atom as an acceptor pharmacophore is the better choice over sp<sup>2</sup> hybridised oxygen atom to uplift ACE2 inhibitory potency. As a result, to enhance ACE2 inhibitory activity, the Sp<sup>3</sup> hybridised oxygen atom must be kept in the future drug design.

**faccdon3B:** This descriptor signifies the frequency of occurrence of a donor atoms exactly at 3 bonds from the acceptor atoms. This descriptor highlight the significance of hydrogen bond forming capable moieties at specific distance. However, this descriptor has acquired negative coefficient in the developed QSAR model, therefore decrease in the bonding distance between donor and acceptor atom could increases the ACE2 inhibitory potency. ( $IC_{50}$ ). This can be observed by comparing the molecular pair; 274 and 464. If the value of the molecular descriptor for 464 is altered from 38.61 to 34.02, the ACE2 inhibitory potency of compound 464 will increase by 0.6 Unit (about a 3.98-fold increase in inhibitory potency) (see [Figure 8](#)).

Following pairs of molecules revealed the same observation: 464 (faccdon3B=0,  $pIC_{50}$ : 7.149) and 919 (faccdon3B=1,  $pIC_{50}$ : 4.18), 447 (faccdon3B=0,  $pIC_{50}$ : 7.215) and 892 (faccdon3B=1,  $pIC_{50}$ : 4.444), 754 (faccdon3B=0,  $pIC_{50}$ : 5.572) and 981 (faccdon3B=1,  $pIC_{50}$ : 3.471), 645 (faccdon3B=0,  $pIC_{50}$ : 6.31) and 931 (faccdon3B=1,  $pIC_{50}$ : 4.05), 794 (faccdon3B=0,  $pIC_{50}$ : 5.319) and 104 (faccdon3B=0,  $pIC_{50}$ : 8.481), etc.

To observed the effect of molecular descriptor on ACE2 inhibitory potency, we have replaced the molecular descriptor faccdon3B with another molecular descriptor; fdonCON3B (frequency of occurrence of nitrogen atom precisely at three bonds form the carbonyl oxygen atom). This will significantly enhances the statistical performance ( $R^2 = 0.91$ ) of the developed QSAR model. From these observations, it can be inferred that the oxygen atom is a better candidate as an acceptor and that pure nitrogen is a good donor to replace

three bonds apart from each other. Moreover, to observed the effect of bonding distance between donor and acceptor atoms, we have replaced the molecular descriptor faccdon3B was replaced with fsp2O\_3B (frequency of occurrence of non-ring nitrogen atom exactly at three bonds from the Sp<sup>2</sup> hybridised oxygen atom). This changes significantly alter the statistical performance ( $R^2 = 0.92$ ) of the proposed QSAR model. Based on this finding, the non-ring nitrogen atom (donor atom) and the Sp<sup>2</sup> hybridised oxygen (acceptor atom) atom are the superior options as a donor and acceptor for enhancing the ACE2 inhibitory activity must be place within 3 bonding distance, and not exactly at 3 bonds in future drug design.

**famdNringC3B:** This represents the frequency of occurrence of ring carbon atoms precisely at three bonds from the amide nitrogen atom. This means that if same combination of ring carbon and amide nitrogen occurs at 2 or 4 bonds will not be calculated during calculation of the molecular descriptor **famdNringC3B**. This descriptor has a positive coefficient in the established QSAR model, therefore an increase in the value of this descriptor boosts the ACE2 inhibitory activity even more. This may be seen by comparing the molecules 180 and 470, where an increase in this descriptor's value from 0 to 1 for the molecule 470 will result in a 1.04 Unit improvement in ACE2 inhibitory activity (about 10.96-fold increase in ACE2 inhibitory potency) (see [Figure 9](#)). Molecule 180 has one ring carbon atom, exactly at three bonds from the amide nitrogen atom, while molecule 470 has none. This result lends credence to the theory that the disparity between molecules 180 and 470 in their inhibitory activity on ACE 2 is due to their distinct chemical structures.

The same observation has been found in the subsequent pair of molecules, Molecule 145 (famdNringC3B= 3,  $pIC_{50}$ : 8.301) 180 (famdNringC3B= 1,  $pIC_{50}$ : 8.155), 366 (famdNringC3B= 2,  $pIC_{50}$ : 7.509) and 503 (famdNringC3B= 0,  $pIC_{50}$ : 7), 201 (famdNringC3B= 4,  $pIC_{50}$ : 8.097) and 227 (famdNringC3B= 8, and  $pIC_{50}$ : 0), 91 (famdNringC3B= 3,  $pIC_{50}$ : 8.538) and 188 (famdNringC3B= 2,  $pIC_{50}$ : 8.149), 92 (famdNringC3B= 2,  $pIC_{50}$ : 8.538) and 128 (famdNringC3B= 0,  $pIC_{50}$ : 8.387), 56 (famdNringC3B= 2,  $pIC_{50}$ : 8.824) and 720 (famdNringC3B= 0,  $pIC_{50}$ : 5.772), 279 (famdNringC3B= 2,  $pIC_{50}$ : 7.796) and 567 (famdNringC3B= 6.668,  $pIC_{50}$ : 0), 222 (famdNringC3B= 3,  $pIC_{50}$ : 8) and 546 (famdNringC3B= 1,  $pIC_{50}$ : 6.77), 27 (famdNringC3B= 4,  $pIC_{50}$ : 9.921) and 246 (famdNringC3B= 1,  $pIC_{50}$ : 7.921), 162 (famdNringC3B= 4,  $pIC_{50}$ : 8.222) and 445 (famdNringC3B= 2,  $pIC_{50}$ : 7.222), 378 (famdNringC3B= 3,  $pIC_{50}$ : 7.456) and 850 (famdNringC3B= 0,  $pIC_{50}$ : 4.907), etc.



**Figure 8.** Presentation of molecular descriptor faccdon3B for the molecules; 274 and 464 only.



Figure 9. Presentation of molecular descriptor famdNringC3B for the molecule 180 and 470.

To examine the influence of molecular descriptor famdNringC3B, we have replaced this descriptor with fNringC3B (frequency of occurrence of ring carbon atom exactly at three bonds from the ring nitrogen atom). The shifting of molecular descriptor subsequently improved the developed QSAR model's statistical performance ( $R^2=0.88$ ). Thus, the aforementioned observation shows that mere nitrogen instead of ring nitrogen is sufficient to increase the ACE2 inhibitory potency when it is situated precisely three bonds from the ring carbon atom. Additionally, the statistical performance of the QSAR model will be significantly decreased ( $R^2=0.80$ ) when the molecule famdNringC3B is shifted with the chemical descriptor ringC\_N\_3B (occurrence of element nitrogen within 3 bonds from the ring carbon atom). The factual meaning of this descriptor is the placing of nitrogen atom at 1 or 2 or 3 bonds from the ring carbon atom and not precisely at 3 bonds from the ring carbon atoms. Based on these findings, it is clear that decreasing the bonding distance between nitrogen atoms in rings and amides has a profound effect on statistical performance and, by extension, biological activity. It follows that the ideal distance for optimum inhibitory activity is precisely three bonds between the amide oxygen and nitrogen atoms.

**sp3S\_ringC\_6B:** The presence of a ring carbon atoms within six bonds from the sp<sup>3</sup> hybridized sulphur atom is indicated by this descriptor. Since the developed QSAR model has given this descriptor a positive coefficient. Therefore, raising its value will increase its ACE 2 inhibitory activity. By comparing the molecules 174 and 736, it can be seen how increasing the descriptor value from 0 to 3 for the latter increases the ACE2 inhibitory activity by 2.49 units (about 309.02-fold increase in ACE2 inhibitory potency) (see Figure 10). The sp<sup>3</sup> hybridised sulphur atom was absent in molecule 736, while it was present in molecule 174 within six bonds from three of the ring-like carbon atoms. The observation explains how the molecules 174 and 736 differ

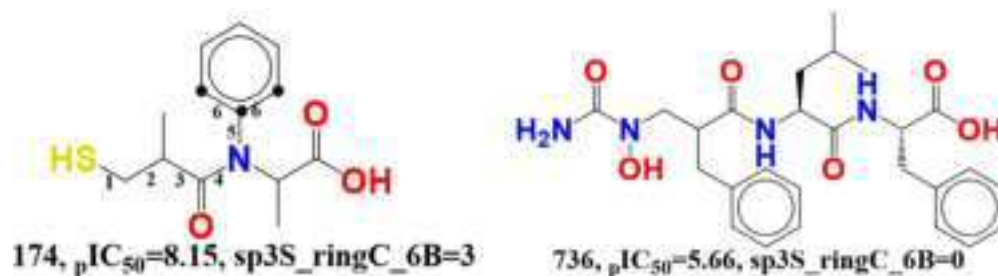


Figure 10. Presentation of the molecular descriptor ringC\_sp3S\_6B for the molecule 174 and 736.

in their bioactivity. The same observation was found to be true in the following molecular pairs; 252 (sp3S\_ringC\_6B=10,  $pIC_{50}$ : 7.921) and 602 (sp3S\_ringC\_6B=0,  $pIC_{50}$ :6.523), 603 (sp3S\_ringC\_6B=6,  $pIC_{50}$ : 6.523) and 722 (sp3S\_ringC\_6B=3,  $pIC_{50}$ :5.77), 317 (sp3S\_ringC\_6B=10,  $pIC_{50}$ :7.658) and 283 (sp3S\_ringC\_6B=0,  $pIC_{50}$ :7.77), 273(sp3S\_ringC\_6B=9,  $pIC_{50}$ :7.824) and 343 (sp3S\_ringC\_6B=5,  $pIC_{50}$ : 7.585), 340 (sp3S\_ringC\_6B=0,  $pIC_{50}$ :7.6) and 415 (sp3S\_ringC\_6B=0,  $pIC_{50}$ : 7.347).

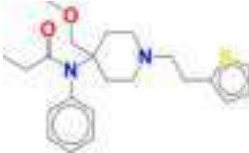



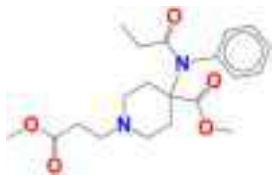


The statistical performance ( $R^2=0.88$ ) of the constructed QSAR model will be significantly improved when the molecular descriptor sp3S\_ringC\_6B is switched out for the molecular descriptor S\_ringC\_5B (presence of ring carbon atom within 5 bonds from the sulphur atom). As a result, adding a single carbon atom is enough to increase the ACE2 inhibitory efficacy. Additionally, the sulphur atom must be precisely positioned at the optimal topological distance of five bonds. This finding also showed that reducing the topological distance from 6 to 5 links will massively improve the ACE2 inhibitory activity. However, the statistical result ( $R^2=0.80$ ) of the developed QSAR model is reduced when the molecular descriptor sp3S\_ringC\_6B is substituted with the molecular descriptor sp3S\_ARO\_4B (presence of aromatic carbon atom within 4 bonds from the Sp<sup>3</sup> hybridised sulphur atom). Based on this discovery, shifting descriptors suggest that the ideal bonding distance between the ring carbon atom and the sulphur atom must be five bonds in order to have higher ACE2 inhibitory activity.

#### 4.2. QSAR based virtual screening

Following the development of QSAR model, we have carried out QSAR based virtual screening using 1650 FDA molecules for prediction ACE2 inhibitory activity. The 11 hit molecules were obtained as repurposed drug candidate against ACE2 receptor. Amongst the top hit molecules, molecule 3 was




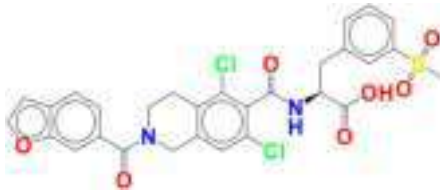


**Table 2.** Presentation of 11 hit molecules identified in QSAR based virtual screening along with their structures and zinc i.d.

SN	ZINC_ID	Structures	pIC <sub>50</sub> in M
1	ZINC00000538386		8.71
2	ZINC000003927822		8.696
3	ZINC000027990463		8.604
4	ZINC000169621231		8.418
5	ZINC000000538283		8.358
6	ZINC000169677008		8.343
7	ZINC000169289388		8.329

(continued)

Table 2. Continued.

SN	ZINC_ID	Structures	pIC <sub>50</sub> in M
8	ZINC000000538658		8.184
9	ZINC000000621893		8.109
10	ZINC000003932831		8.043
11	ZINC000084668739		8.029

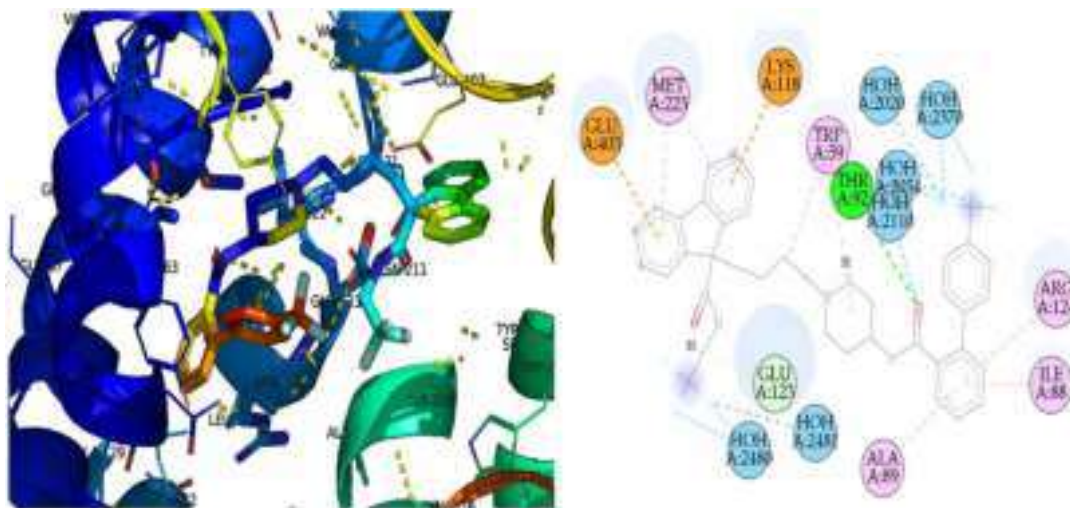
selected as prominent hit depending upon its docking score and RMSD value. The [Supplementary Materials](#) file comprises the SMILES notations, calculated molecular descriptor values, and pIC<sub>50</sub> for the 1615 FDA molecules availed from the zinc database. The top 11 hit molecules are depicted in the [Table 2](#).

### 4.3 Molecular docking analysis

The carboxy terminal His-Leu dipeptide of angiotensin I is cleaved by the angiotensin-converting enzyme (ACE), releasing the strong vasopressor octapeptide angiotensin II. ACE inhibitors are first-line medications for hypertension, heart failure, myocardial infarction, and diabetic nephropathy. The same gene produces two distinct isoforms of ACE that are expressed in different tissues. It appears in sperm cells as a lower-molecular-mass glycoform with 701 amino acids, but in somatic tissues it is a glycoprotein made up of a single, long polypeptide chain with 1,277 amino acids. The somatic form consists of two homologous domains (N and C domain), each of which has an active site with a conserved HEXXH zinc binding motif. The two histidine residues in

these active sites function as zinc ligands, and a glutamate 24 residues downstream serves as the third ligand. The peptide N-acetyl-seryl-aspartyl-lysyl-proline, which controls haematopoietic stem cell differentiation and proliferation, and the bradykinin-potentiating peptide angiotensin II are both N-domain-specific substrates (Soubrier et al., 1988). The C domain seems to be necessary and sufficient for controlling blood pressure and cardiovascular function, suggesting that the C domain is the dominant angiotensin-converting site. An N-terminal 'lid' formed by helices  $\alpha 1$ ,  $\alpha 2$  and  $\alpha 3$  sits on top of the molecule (all three containing several charged residues). The N and C termini of the ectodomain are defined by residues Asp 40 ( $\alpha 1$ ) and Gly 615 (five residues downstream of  $\alpha 20$ ), which is consistent with earlier tACE mutagenesis and cleavage-secretion investigations. The natural structure had a total of 504 water molecules. Several ordered water molecules occupy the active-site pocket (Chubb et al., 2002).

Zinc is an essential component of ACE. At the active site, one highly organized zinc ion (B-factor 16.3 Å in tACE-native) is bound. The HEXXH zinc-binding motif, with its two zinc-coordinating histidines, is found on helix  $\alpha 13$  (His 383 and His 387) (Ehlers & Riordan, 1991). Moreover, the substrate



**Figure 11.** Best docked pose of hit molecule 3 with ACE2 displaying 3D (a), and 2D (B) interactions (green: H-bond interaction, cyan: Water hydrogen bond, orange: pi-cation and pi-anion interactions, pink: Pi-alkyl interaction, and lime green: carbon hydrogen bond).

hydrolysis by ACE is substrate-dependently induced by chloride ion. The first chloride ion (Cl1, 20.7 distant from the zinc ion) is surrounded by a hydrophobic shell of four tryptophans and is bound to four ligands: Arg 489 (NH1), Arg 186 (NE), Trp 485 (NE1), and water. The second (Cl2, 10.4 away from the zinc ion) ligand is bound to Arg 522 (NE, 3.1), which is consistent with a previous report indicating that Arg 1098 (the analogous Arg residue in the C domain of somatic ACE) is required for chloride dependence of ACE activity. Tyr 224 and a water molecule are the other two Cl 2 ligands (Bünning & Riordan, 1983; Shapiro et al., 1983).

QSAR-based virtual screening was used in the current study to find and repurpose 1650 clinically established FDA compounds as new inhibitors of angiotensin converting enzyme 2. We have put into practise the blend of mix methodology, which combines molecular docking and QSAR based virtual screening. In this study, we used the 2.0Å resolution X-ray structure of human testicular ACE2 in association with one of the most popular inhibitors, lisinopril (N2 -[(S)-1-carboxy - 3 - phenylpropyl] - L - lysyl - L-proline; commonly known as Prinivil or Zestril). The structure of ace2 in complex with lisinopril was selected on the basis of resolution and the completion of sequence, and the active site was determined on the basis of native ligand bound to ace2. The hit molecule which has identified with good predicted activity has been subjected to the molecular docking analysis.

In the present work, we have got around 11 hit molecules by QSAR based virtual screening with good  $PI_{C50}$  value ranging from 8.0-8.71. These molecules have been subjected to the docking analysis using crystal structure of human angiotensin converting enzyme 2 in complex with Lisinopril (PDB ID- 1o86) (Natesh et al., 2003). The crystal structure was verified for the sequence completion and good resolution (2 Å). The molecular docking analysis reveals that the hit molecule 3 emerge with good docking score of  $-9.67$  with the RMSD of 1.40 Å, although all the hit molecules showed good docking score but hit molecule 3 showed less RMSD value than 1.50Å with the comparable docking score. Moreover, it

shows predictive  $pIC_{50}$  of 8.60 M. The active site of the molecule was found using the structure of the tACE-lisinopril combination. The active site of ACE 2 enzyme consists of non-polar lipophilic residues like; alanine, glycine, leucine, phenylalanine, proline, and tyrosine, while polar or acidic/basic residues are arginine, asparagine, aspartic acid (or aspartate), lysine, serine, and threonine (see Figure 11). Chemically the hit molecule 3 is 1 - (4-(9-((2,2,2, trifluoromethyl) carbonyl)-9H-fluoren-9-yl) butyl)-4-(4'-(trifluoromethyl)-[1,1'biphenyl]-2- carboxamido) piperidin-1-ium.

The hit molecule 3's extended conformation, in which the substituted phenyl executed three alkyl hydrophobic contacts with ARG105, ARL88, and ALA89 residues, and it was pointing toward the lid of the active site, can be seen in the docked complex of the hit molecule 3 bound with tACE. The hit molecule 3 was deeply buried inside the binding pocket of ACE2 enzyme about 10 to 12 Å into the active site.

The analysis reveals that the molecule 3 gave rise to polar and nonpolar contacts comprising conventional hydrogen bonding, water hydrogen bonding, C-H bond,  $\pi$ -cation,  $\pi$ -anion interaction and  $\pi$ -alkyl hydrogen contacts (see Table 3). Significant interactions between the molecules 3 and ASP40 residue, which define the N and C termini of the ectodomain of ACE2, have been described. 25 contacts were made by molecule 3 using ASP30.

The N and C termini of the ectodomain of the ACE2 enzyme's molecule 3 showed substantial contact with them, according to this finding. The molecule 3 depicted the formation of more than 30 water hydrogen bonds with the water molecules present in binding pocket; like trifluoroethyl moiety form water hydrogen bond with H-O-H2110, H-O-H2054, H-O- H2370 and H-O-H2020. Additionally, there were about 10 water hydrogen bonds executed with trifluoro group. Most of the water molecules were occurred within 5 Å from the molecule 3. The hit molecule displayed a coordination with the nearby residue GLU403 with no contact reported with the acetate ion. The GLU403 executed  $\pi$ -cation and  $\pi$ -anion type of interaction with the terminal benzene

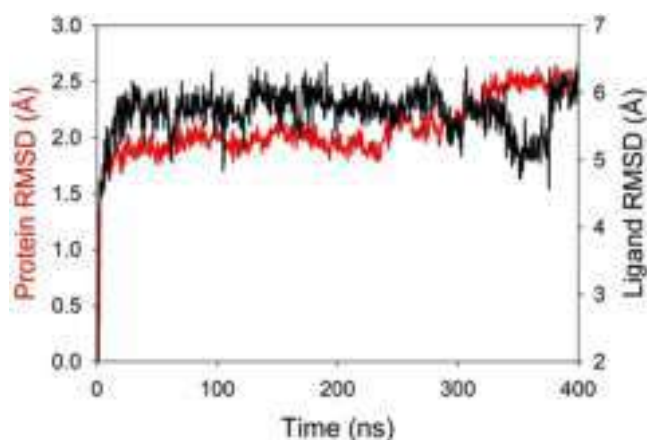
**Table 3.** Presentation of hydrogen bonding, polar and nonpolar interaction of ACE2-Molecule 3 complex.

Name of the molecule	H-bonds formed with distance (Å)	List of receptor atoms exhibited polar contacts with the molecule 3	List of receptor atoms exhibited non-polar contacts with the molecule 3 with distance (Å)
Molecule 3	THR92-CB-0H2-3.986, THR92-CG2-0H1-4.950, THR92-CG2-0H2-3.635, THR92-OG1-0H1-4.713, THR92-OG1-0H2-3.191, HOH2005-O-0H2-4.232, HOH2020-O-0C-4.116, HOH2020-O-0F-4.268, HOH2020-O-0H-4.570, HOH2054-O-0F-3.019, HOH2055-O-0H2-4.257, HOH2108-O-0O-4.178, HOH2110-O-0H1-2.409, HOH2110-O-0H2-3.063, HOH2111-O-0H1-3.950, HOH2152-O-0C-4.211, HOH2152-O-0H-4.136, HOH2300-O-618N-4.772, HOH2300-O-618CH3-4.030, HOH2300-O-618H-4.506, HOH2300-O-618HH31-2.946, HOH2300-O-618HH32-4.431, HOH2300-O-618HH33-4.544, HOH2370-O-0C-4.807, HOH2370-O-0F-4.698, HOH2370-O-0H-4.949, HOH2371-O-0F-4.958, HOH2478-O-0F-4.495, HOH2480-O-0O-4.510, HOH2480-O-0N-4.362, HOH2566-O-618N-2.550, HOH2566-O-618CH3-2.198, HOH2566-O-618H-2.378, HOH2566-O-618HH31-1.437, HOH2566-O-618HH32-2.544, and HOH2566-O-618HH33-3.139.	ASP40, ALA42, GLU43, TYR51, TRP59, TYR62, ASN66, ASN85, MET86, ILE88, ALA89, THR92, LYS118, ASP121, GLU123, ARG124, ALA125, LEU132, ASN136, TYR213, SER222, MET223, ASN265, GLU267, GLY268, PRO269, TYR360, ALA400, GLU403, ASN406, PRO407, PRO519, ARG522, PHE570, LYS613, TRP616, and PRO617.	ASP40-N-39C-1.313, ASP40-N-39O-2.233, ASP40-N-39CH3-2.423, ASP40-N-39HH31-3.333, ASP40-N-39HH32-2.704, ASP40-N-39HH33-2.703, ASP40-CA-39C-2.449, ASP40-CA-39O-2.769, ASP40-CA-39CH3-3.833, ASP40-CA-39HH31-4.620, ASP40-CA-39HH32-4.127, ASP40-CA-39HH33-4.127, ASP40-C-39C-3.725, ASP40-C-39O-4.259, ASP40-C-39CH3-4.883, ASP40-C-39HH32-4.994, ASP40-C-39HH33-4.994, ASP40-O-39C-4.705, ASP40-CB-39C-3.027, ASP40-CB-39O-2.921, ASP40-CB-39CH3-4.442, ASP40-CB-39HH33-4.583, ASP40-CG-39C-4.534, ASP40-CG-39O-4.387, ASP40-OD1-39O-4.981, GLU41-N-39C-4.085, GLU41-N-39O-4.846, GLU41-N-39CH3-4.960, GLU41-N-39HH33-4.788, ALA42-CB-39HH32-4.872, GLU43-OE2-39O-4.981, TYR62-CB-0H-4.492, TYR62-CG-0C-4.340, TYR62-CG-0H-3.389, TYR62-CD1-0C-4.547, TYR62-CD1-0H-3.559, TYR62-CD2-0C-3.732, TYR62-CD2-0H-3.012, TYR62-CE1-0C-4.224, TYR62-CE1-0H-3.410, TYR62-CE2-0C-3.313, TYR62-CE2-0H-2.820, TYR62-CZ-0C-3.592, TYR62-CZ-0H-3.035, TYR62-OH-0C-3.964, TYR62-OH-0H-3.714, ASN85-ND2-0C-4.965, ASN85-ND2-0H-4.615, ILE88-CB-0H-4.616, ILE88-CG1-0H-4.451, ILE88-CG2-0C-4.470, ILE88-CG2-0H-3.651, ILE88-CD1-0C-4.346, ILE88-CD1-0H-3.667, LEU122-O-0H1-4.416, LEU122-O-0H2-4.401, GLU123-CB-0H1-4.116, GLU123-CB-0H2-4.995, GLU123-CG-0O-4.393, GLU123-CG-0H1-4.749, GLU123-CD-0O-3.259, GLU123-CD-0N-4.388, GLU123-CD-0H1-4.055, GLU123-CD-0H2-4.865, GLU123-OE1-0O-3.268, GLU123-OE1-0N-3.882, GLU123-OE1-0H1-3.449, GLU123-OE1-0H2-4.645, GLU123-OE2-0O-3.022, GLU123-OE2-0N-4.193, GLU123-OE2-0H1-4.586, and MET223-SD-0O-4.674.

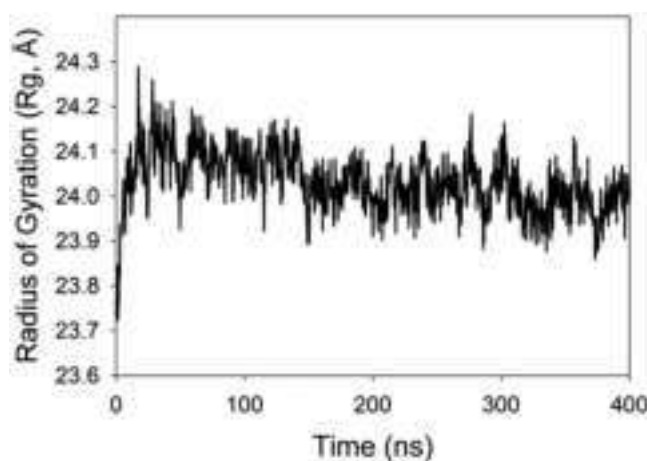
ring of the fluorine nucleus of molecule 3. Subsequently, the molecule 3 gave rise to the polar contact with the ARG522 residue which was bound with the second chloride ion just 10.4 Å away from the zinc ion. In the current docking experiment, we have emphasized the hit molecule 3's specific pattern of ACE2 enzyme binding. The recently discovered hit molecule 3 is a highly selective ACE inhibitor targeted to the C domain of the ACE2 enzyme by structure-based, rational drug design, according to overall docking study.

Additionally, the 2-carboximido segment's carbonyl oxygen created one hydrogen bond with THR-92. The carbonyl group served as the hydrogen bond acceptor in the current interaction. The descriptor acH3B, in which the first biphenyl ring containing hydrogen and another hydrogen in a 2-carboximido group were located precisely at 3 bonds from the

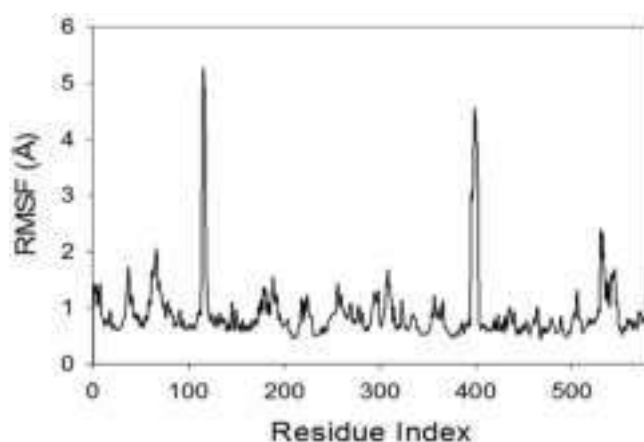
acceptor carbonyl oxygen, underlined the same characteristic. The significance of steric and electronic features is emphasized by this descriptor. The trifluoroethyl group on the 9-carboximido group then made three hydrogen bonding connections with the water molecules HOH2480 and HOH2481. The fluorine atom, which was precisely three bonds from the nitrogen atom in the drug-water molecule interactions at hand, served as the hydrogen bond acceptor. This finding emphasises the significance of the molecular descriptor Nacc3B. In addition, three of the four such ring carbon atoms are located precisely three bonds apart from the amide nitrogen atoms. Two carbon atoms from the fluorene ring were discovered, but they didn't appear to be in touch. In contrast, two other carbon atoms from the biphenyl segment's phenyl ring engaged with ARG105,



**Figure 12.** A 400 ns time frame for ACE2-Molecule 3 complex display root mean square deviation (RMSD) plot confirm the stable complex.

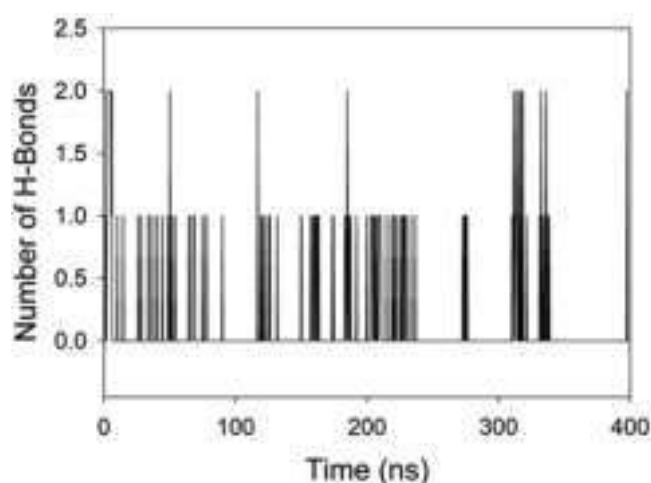


**Figure 13.** MD simulation trajectory analysis of radius of gyration (Rg) of molecule 3 bound with ACE2 at 400 ns time frame.



**Figure 14.** MD simulation trajectory analysis of root mean square fluctuations (RMSF) of the molecule 3 bound with ACE2 at 400 ns time frame.

ARL88, and ALA89 residues through alkyl hydrophobic interactions. This finding demonstrates the role of the molecular descriptor *famdNringC3B* in interactions between drug receptors. The current description emphasises the significance of the ring carbon atom required to preserve the molecule's lipophilicity. These findings show that the QSAR results and the docking results are entirely consistent with one another.



**Figure 15.** MD simulation trajectory analysis of hydrogen bonding (H-Bonds) formation of molecule 3 bound with ACE2 at 400 ns time frame.

#### 4.4. Molecular dynamic simulation analysis

MD studies were performed to determine whether the hit molecule 3 bound ACE2 complex is stable or convergent. We employed the dock complex of hit molecule 3 for MD simulation based on its activity profile and molecular docking data. RMSD data showed steady conformation in every simulation, including 400 ns ones. The C-backbone of arginase-1 protein attached to the ligand, molecule 3, revealed a 2.4 divergence (see Figure 12). RMSD graphs indicate ACE2 protein stability in the molecule 3 bound state before or after simulation.

Radius of gyration determines protein compactness (Rg). The radius of gyration of molecule 3-bound ACE2 protein was reduced from 24.1 to 24.0 Å. Lowering of Rg of 0.1 Å deviation means more compactness from initial to final MD simulation over 400 ns time scale (see Figure 13). Yet, the shift in gyrational radius is insufficient. Moreover, it can be deduced that the drug receptor complex showed a consistent value of radius of gyration during the whole 400 ns of simulation time, with only minor fluctuations. However, Low Rg value point toward long-lasting interactions between proteins and their ligands. Thus, binding of ligand during MD simulations marginally altered the global conformation or size of the ACE2 protein (Liddle et al., 2012; Lobanov et al., 2008). Literature survey revealed that the highest radius of gyration value depicting poor compactness (Parida et al., 2020; Priya et al., 2017). Thus, molecule 3 has a higher affinity and binds to the ACE2 protein target in the binding cavities, impacting protein stability based on RMSD and Rg.

C-atom amino acid residue RMSF plots are presented using a 400 ns time function (Figure 14). Molecule 3 shows bound protein C-atoms displayed small alterations except at peaks at residue indices 120 and 400, which may conform into loops, but the fluctuations diminished afterwards. RMSF plots suggest that ACE2 protein structure was stable and stiff throughout simulation in the molecule 3 bound state.

Figure 15 illustrates the average hydrogen bonds generated between molecule 3 and proteins during 400 ns. An

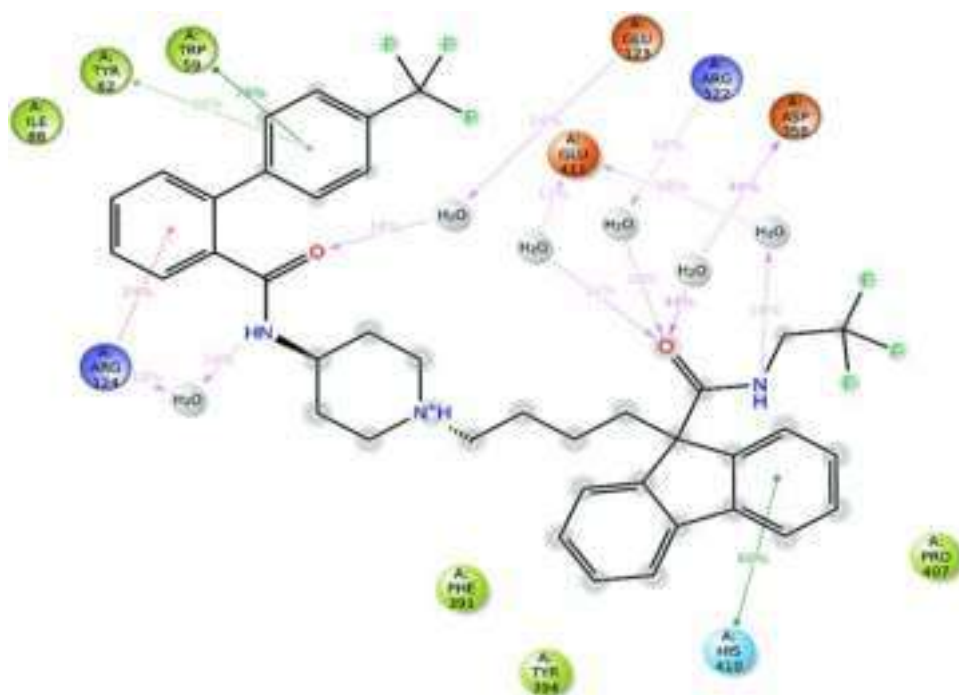


Figure 16. Presentation of the 2D interactions of a molecule 3 with the ACE2 receptor.

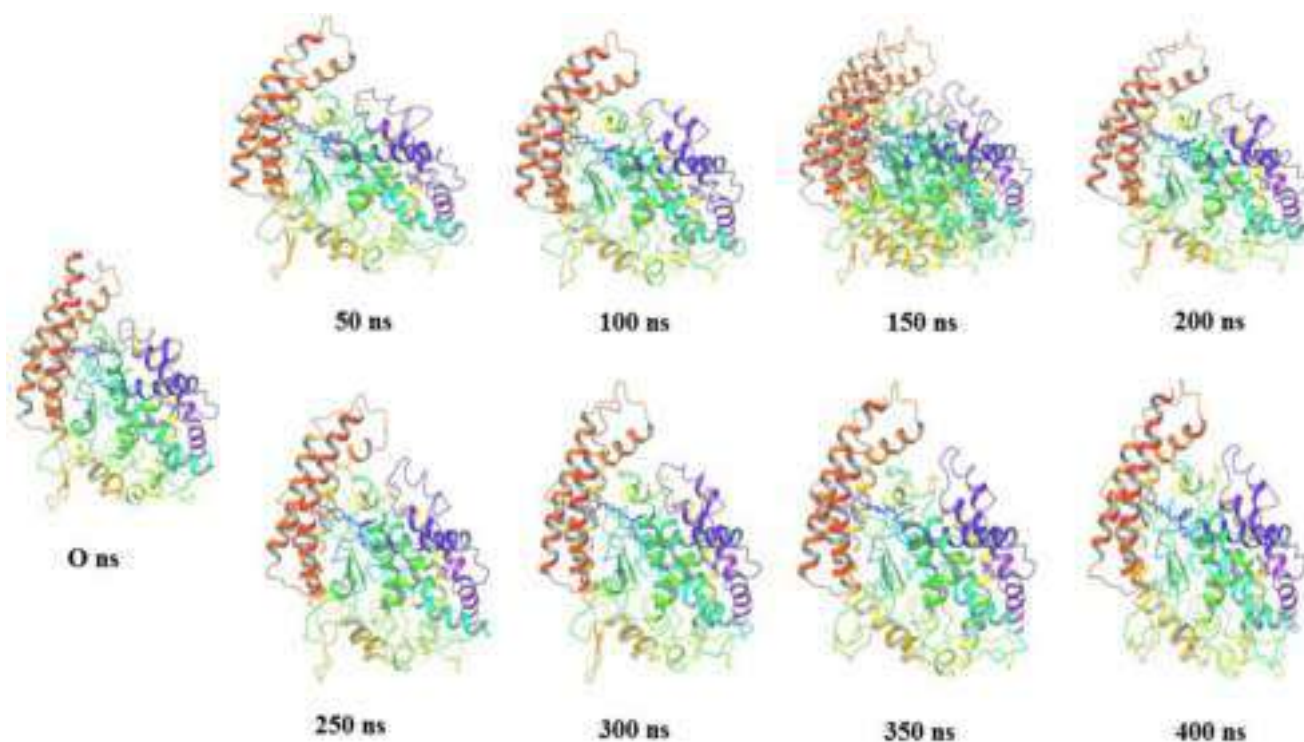


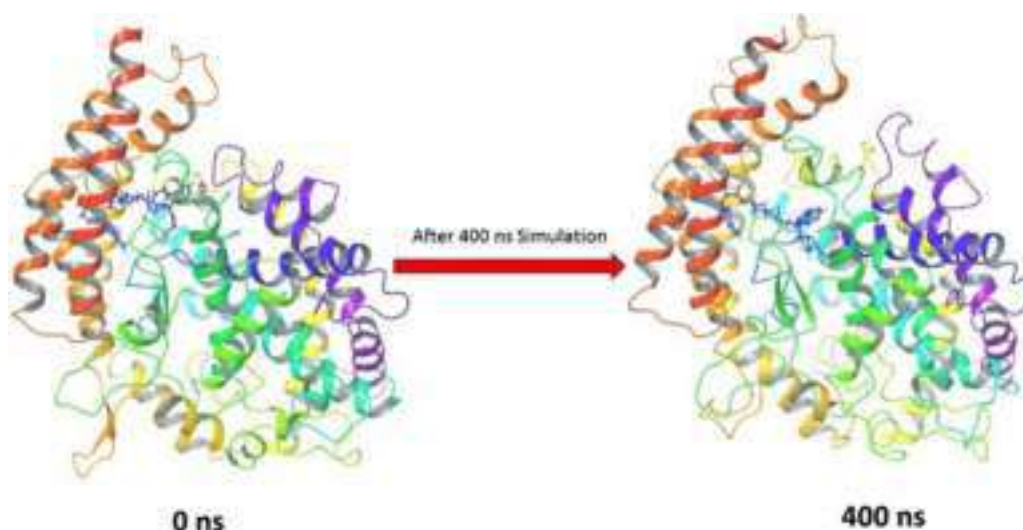
Figure 17. Stepwise trajectory analysis for every 50 ns displaying the protein and ligand conformation during 400 ns of simulation of ACE2 bound molecule 3.

average of Three hydrogen bonding with ARG522, ASP358, and HIS410 during the simulation from 0 to 400 ns, or the same for MD simulations of molecule 3 with ACE2. A 2D ligand binding diagram of the bound ACE2 protein to molecule 3 showed three hydrogen bonds (Figure 16).

Hydrogen bonding between ACE2 and molecule 3 enhanced binding strength, making simulations more stable. The 2D interaction diagram from molecular docking tests

indicates one hydrogen bond and more than 30 water hydrogen bonding contacts in the ACE2-molecule 3-complex.

Figure 17 depicts a 50-ns stimulation trajectory from start to completion. Simulation trajectories indicated that ligand molecule 3's conformation did not change substantially over the 400 ns simulation. This reveals that ACE2-molecule 3 simulation complexes are stable and the ALK ligand conformations are mainly impacted (See Figure 17).



**Figure 18.** MMGBSA trajectory (0 ns, before simulation and 400 ns, after simulation) exhibited conformational changes upon binding of the molecule 3 with the ACE2 receptor.

**Table 4.** Binding energy calculation of 172 and 178 with ALK and non-bonded interaction energies from MMGBSA trajectories. (\* indicates mean value of energy parameters).

Energies (kcal/mol) *	ACE2-Molecule 3
$\Delta G_{\text{bind}}$	$-76.93 \pm 5.15$
$\Delta G_{\text{bindLipo}}$	$-27.65 \pm 3.68$
$\Delta G_{\text{bindvdW}}$	$-72.26 \pm 5.40$
$\Delta G_{\text{bindCoulomb}}$	$-27.18 \pm 9.11$
$\Delta G_{\text{bindHbond}}$	$-1.21 \pm 0.28$
$\Delta G_{\text{bindSolvGB}}$	$61.91 \pm 9.46$
$\Delta G_{\text{bindCovalent}}$	$4.02 \pm 3.02$

#### 4.5. Molecular mechanics generalized born and surface area (MMGBSA) calculations and energy calculations

The ligand-protein binding energy is measured using MMGBSA. The binding energy of molecule 3- ACE2 complex is  $-76.93 \pm 5.15$ . All of the binding energies were influenced by the  $G_{\text{bindvdW}}$ ,  $G_{\text{bindLipo}}$ , and  $G_{\text{bindCoulomb}}$  energies. Beside this, non-bonded interactions include  $G_{\text{bindCoulomb}}$ ,  $G_{\text{bindCovalent}}$ ,  $G_{\text{bindHbond}}$ ,  $G_{\text{bindLipo}}$ ,  $G_{\text{bindSolvGB}}$ , and  $G_{\text{bindvdW}}$ . Among these, the  $G_{\text{bindvdW}}$ ,  $G_{\text{bindLipo}}$ , and  $G_{\text{bindCoulomb}}$  energies had a profound effect on all interactions. The final average binding energies were influenced the least by the  $G_{\text{bindSolvGB}}$  and  $G_{\text{bindCovalent}}$  energies. The stable hydrogen bonds between amino acid residues in Molecule 3-ACE2 were shown by high  $G_{\text{bindHbond}}$  inter-action values. When tested with a range of compounds, both  $G_{\text{bindSolvGB}}$  and  $G_{\text{bindCovalent}}$  failed to bind. Due to their negative energy contributions,  $G_{\text{bindSolvGB}}$  and  $G_{\text{bindCovalent}}$  were unable to form a bond. It can be seen in the left panel of Figure 17 that the pre-simulation (0 ns) (400 ns) caused molecule 3 in the ACE2 binding pocket to extend (become straight) (see Figure 18). Through enhancing binding pocket acquisition and residue engagement, conformational changes boosted stability and binding energy (see Table 4).

## 5. Conclusions

According to the analysis, pharmacophoric characteristics such as the positively charged ring carbon atom's absolute surface area, the hydrogen atom's exact location at the acceptor

atom's three bonds, the acceptor atom's exact location at the nitrogen atom's three bonds, the donor atom's exact location at the acceptor atom's three bonds, the ring carbon atom's exact location at the amide nitrogen's three bonds, and the ring carbon atom's High levels of external predictability, fitting robustness, and internal validation characterised the QSAR model. With an  $IC_{50}$  of 2.48 nM, Lomitapide was successfully identified as a novel FDA chemical using QSAR-based virtual screening and drug repositioning. According to molecular docking, identified hit binds to ASP40 of the C and N terminal ectodomain. The interaction between identified hit and ace2 was studied using molecular docking, and more than 30 water hydrogen bonds were found. The pharmacophoric properties of drug receptor interactions revealed by QSAR are reflected in the molecular docking results. Additionally, identified hit interacted with the ARG522 residue connected to the second chloride ion of the ACE2 receptor. Thus, the identified hit's strong affinity for ACE2 and ability to bind to it energetically expands the market for ACE2 inhibitors. Drug receptor complex stability after 400 ns of simulation with considerable binding energy was shown by MD simulation and MMGBSA analysis. The findings may help in the development of a novel ACE2 therapy.

## Acknowledgments

The author Rahul D. Jawarkar indebted to honorable President; Shri Yogendraji Gode Sir, President, Indira Bahuddeshiya Shikshan sanstha, Buldhana, for his extended support during entire course of Research work. The author R.D. Jawarkar is thankful to Paola Gramatica and her team for providing the free copy of QSARINS 2.2.4.

## Disclosure statement

No potential conflict of interest was reported by the authors.

## Funding

The authors acknowledge the Deanship of Scientific Research at Imam Mohammad ibn Saud Islamic University, Riyadh, KSA, for its support of this research.

## Author contributions

Rahul D. Jawarkar, Nobendu Mukerjee: conceptualization, editing and formal analysis. Magdi E.A. Zaki: Conceptualization, editing and review, Sami-AL-Hussain: Formal Analysis and Review. Aamal A. Al-Mutairi: formal analysis. Arabinda Ghosh: Review, editing and formal analysis.; Long chiau Ming; Review and editing. Abdul Samad; Formal Analysis and Review. Vijay H. Masand; Review and editing.

## References

- Almquist, R. G., Crase, J., Jennings-White, C., Meyer, R. F., Hoefle, M. L., Smith, R. D., Essenburg, A. D., & Kaplan, H. R. (1982). Derivatives of the potent angiotensin converting enzyme inhibitor 5(S)-benzamido-4-oxo-6-phenylhexanoyl-L-proline: Effect of changes at positions 2 and 5 of the hexanoic acid portion. *Journal of Medicinal Chemistry*, 25(11), 1292–1299. <https://doi.org/10.1021/jm00353a005>
- Atlas, S. A. (2007). The renin-angiotensin aldosterone system: Pathophysiological role and pharmacologic inhibition. *Journal of Managed Care Pharmacy: JMCP*, 13(8 Suppl B), 9–20. <https://doi.org/10.18553/jmcp.2007.13.s8-b.9>
- Baig, M. H., Ahmad, K., Roy, S., Ashraf, J. M., Adil, M., Siddiqui, M. H., Khan, S., Kamal, M. A., Provazník, I., & Choi, I. (2016). Computer aided drug design: Success and limitations. *Current Pharmaceutical Design*, 22(5), 572–581. <https://doi.org/10.2174/1381612822666151125000550>
- Bakal, R. L., Jawarkar, R. D., Manwar, J. V., Jaiswal, M. S., Ghosh, A., GaNDhi, A., Zaki, M. E. A., Al-Hussain, S., Samad, A., Masand, V. H., Mukerjee, N., Nasir Abbas Bukhari, S., Sharma, P., & Lewaa, I. (2022). Identification of potent aldose reductase inhibitors as antidiabetic (Anti-hyperglycemic) agents using QSAR based virtual Screening, molecular Docking, MD simulation and MMGBSA approaches. *Saudi Pharmaceutical Journal: SPJ: The Official Publication of the Saudi Pharmaceutical Society*, 30(6), 693–710. <https://doi.org/10.1016/j.jpsp.2022.04.003>
- Basu, R., Poglitsch, M., Yogasundaram, H., Thomas, J., Rowe, B. H., & Oudit, G. Y. (2017). Roles of angiotensin peptides and recombinant human ACE2 in heart failure. *Journal of the American College of Cardiology*, 69(7), 805–819. <https://doi.org/10.1016/j.jacc.2016.11.064>
- Bikadi, Z., & Hazai, E. (2009). Application of the PM6 semi-empirical method to modeling proteins enhances docking accuracy of AutoDock. *Journal of Cheminformatics*, 1(1). <https://doi.org/10.1186/1758-2946-1-15>
- Bodiga, V. L., & Bodiga, S. (2013). Renin angiotensin system in cognitive function and dementia. *Asian Journal of Neuroscience*, 2013, 1–18. <https://doi.org/10.1155/2013/102602>
- Bünning, P., & Riordan, J. F. (1983). Activation of angiotensin converting enzyme by monovalent anions. *Biochemistry*, 22(1), 110–116. <https://doi.org/10.1021/bi00270a016>
- Burchill, L. J., Velkoska, E., Dean, R. G., Griggs, K., Patel, S. K., & Burrell, L. M. (2012). Combination renin-angiotensin system blockade and angiotensin-converting enzyme 2 in experimental myocardial infarction: Implications for future therapeutic directions. *Clinical Science (London, England: 1979)*, 123(11), 649–658. <https://doi.org/10.1042/CS20120162>
- Burrell, L. M., Risvanis, J., Kubota, E., Dean, R. G., MacDonald, P. S., Lu, S., Tikellis, C., Grant, S. L., Lew, R. A., Smith, A. I., Cooper, M. E., & Johnston, C. I. (2005). Myocardial infarction increases ACE2 expression in rat and humans. *European Heart Journal*, 26(4), 369–375. <https://doi.org/10.1093/eurheartj/ehi114>
- Cherkasov, A., Muratov, E. N., Fourches, D., Varnek, A., Baskin, I. I., Cronin, M., Dearden, J., Gramatica, P., Martin, Y. C., Todeschini, R., Consonni, V., Kuz'min, V. E., Cramer, R., Benigni, R., Yang, C., Rathman, J., Terfloth, L., Gasteiger, J., Richard, A., & Tropsha, A. (2014). QSAR modeling: Where have you been? where are you going to? *Journal of Medicinal Chemistry*, 57(12), 4977–5010. <https://doi.org/10.1021/jm4004285>
- Chirico, N., & Gramatica, P. (2011). Real external predictivity of QSAR models: How to evaluate it? Comparison of different validation criteria and proposal of using the concordance correlation coefficient. *Journal of Chemical Information and Modeling*, 51(9), 2320–2335. <https://doi.org/10.1021/ci200211n>
- Chirico, N., & Gramatica, P. (2012). Real external predictivity of QSAR models. Part 2. New intercomparable thresholds for different validation criteria and the need for scatter plot inspection. *Journal of Chemical Information and Modeling*, 52(8), 2044–2058. <https://doi.org/10.1021/ci300084j>
- Chrissobolis, S., Banfi, B., Sobey, C. G., & Faraci, F. M. (2012). Role of Nox isoforms in angiotensin II-induced oxidative stress and endothelial dysfunction in brain. *Journal of Applied Physiology (Bethesda, MD: 1985)*, 113(2), 184–191. <https://doi.org/10.1152/jappphysiol.00455.2012>
- Chubb, A. J., Schwager, S. L. U., Woodman, Z. L., Ehlers, M. R. W., & Sturrock, E. D. (2002). Defining the boundaries of the testis angiotensin I-converting enzyme ectodomain. *Biochemical and Biophysical Research Communications*, 297(5), 1225–1230. [https://doi.org/10.1016/s0006-291x\(02\)02324-0](https://doi.org/10.1016/s0006-291x(02)02324-0)
- Consonni, V., Ballabio, D., & Todeschini, R. (2009). Comments on the definition of the Q2 parameter for QSAR validation. *Journal of Chemical Information and Modeling*, 49(7), 1669–1678. <https://doi.org/10.1021/ci900115y>
- Consonni, V., Todeschini, R., Ballabio, D., & Grisoni, F. (2019). On the misleading use of QF32 for QSAR model comparison. *Molecular Informatics*, 38(1–2), 1800029. <https://doi.org/10.1002/minf.201800029>
- Crowley, S. D., Gurley, S. B., Oliverio, M. I., Pazmino, A. K., Griffiths, R., Flannery, P. J., Spurney, R. F., Kim, H.-S., Smithies, O., Le, T. H., & Coffman, T. M. (2005). Distinct roles for the kidney and systemic tissues in blood pressure regulation by the renin-angiotensin system. *The Journal of Clinical Investigation*, 115(4), 1092–1099. <https://doi.org/10.1172/JCI23378>
- Dearden, J. C., Cronin, M. T. D., & Kaiser, K. L. E. (2009). How not to develop a quantitative structure-activity or structure-property relationship (QSAR/QSPR). *SAR and QSAR in Environmental Research*, 20(3–4), 241–266. <https://doi.org/10.1080/10629360902949567>
- Donoghue, M., Hsieh, F., Baronas, E., Godbout, K., Gosselin, M., Stagliano, N., Donovan, M., Woolf, B., Robison, K., Jeyaseelan, R., Breitbart, R. E., & Acton, S. (2000). A novel angiotensin-converting enzyme-related carboxypeptidase (ACE2) converts angiotensin I to angiotensin 1-9. *Circulation Research*, 87(5), E1–E9. <https://doi.org/10.1161/01.RES.87.5.e1>
- Ehlers, M. R. W., & Riordan, J. F. (1991). Angiotensin-converting enzyme: Zinc- and inhibitor-binding stoichiometries of the somatic and testis isozymes. *Biochemistry*, 30(29), 7118–7126. <https://doi.org/10.1021/bi00243a012>
- Ferrario, C. M., Ahmad, S., & Groban, L. (2020). Mechanisms by which angiotensin-receptor blockers increase ACE2 levels. *Nature Reviews. Cardiology*, 17(6), 378–378. <https://doi.org/10.1038/s41569-020-0387-7>
- Ferrario, C. M., Jessup, J., Chappell, M. C., Averill, D. B., Brosnihan, K. B., Tallant, E. A., Diz, D. I., & Gallagher, P. E. (2005). Effect of angiotensin-converting enzyme inhibition and angiotensin II receptor blockers on cardiac angiotensin-converting enzyme 2. *Circulation*, 111(20), 2605–2610. <https://doi.org/10.1161/CIRCULATIONAHA.104.510461>
- Fujita, T., & Winkler, D. A. (2016). Understanding the roles of the “two QSARs. *Journal of Chemical Information and Modeling*, 56(2), 269–274. <https://doi.org/10.1021/acs.jcim.5b00229>
- Furuhashi, M., Moniwa, N., Mita, T., Fuseya, T., Ishimura, S., Ohno, K., Shibata, S., Tanaka, M., Watanabe, Y., Akasaka, H., Ohnishi, H., Yoshida, H., Takizawa, H., Saitoh, S., Ura, N., Shimamoto, K., & Miura, T. (2015). Urinary angiotensin-converting enzyme 2 in hypertensive patients may be increased by olmesartan, an angiotensin II receptor blocker. *American Journal of Hypertension*, 28(1), 15–21. <https://doi.org/10.1093/ajh/hpu086>
- Ganten, D., Hermann, K., Unger, T., et al. (2009). The tissue Renin-Angiotensin Systems: Focus on brain angiotensin, adrenal gland and arterial wall. *Clinical and Experimental Hypertension Part A: Theory and Practice*, 5(7–8), 1099–1118.
- Gaudreault, F., Morency, L.-P., & Najmanovich, R. J. (2015). NRGsuite: A PyMOL plugin to perform docking simulations in real time using FlexAID. *Bioinformatics*, 31(23), 3856–3858. <https://doi.org/10.1093/bioinformatics/btv458>



- Gaulton, A., Hersey, A., Nowotka, M., Bento, A. P., Chambers, J., Mendez, D., Mutowo, P., Atkinson, F., Bellis, L. J., Cibrián-Uhalte, E., Davies, M., Dedman, N., Karlsson, A., Magariños, M. P., Overington, J. P., Papadatos, G., Smit, I., & Leach, A. R. (2017). The ChEMBL database in 2017. *Nucleic Acids Research*, 45(D1), D945–D954. <https://doi.org/10.1093/nar/gkw1074>
- Ghosh, A., Mukerjee, N., Sharma, B., Pant, A., Kishore Mohanta, Y., Jawarkar, R. D., Bakal, R. L., Terefe, E. M., Batiha, G. E.-S., Mostafa-Hedeab, G., Aref Albezrah, N. K., Dey, A., & Baishya, D. (2022). Target specific inhibition of protein tyrosine kinase in conjunction with cancer and SARS-COV-2 by olive nutraceuticals. *Frontiers in Pharmacology*, 12. <https://doi.org/10.3389/fphar.2021.812565>
- Gramatica, P. (2013). On the development and validation of QSAR models. *Computational Toxicology. Methods in Molecular Biology*, 499–526.
- Gramatica, P. (2014). External evaluation of QSAR models, in addition to cross-validation: verification of predictive capability on totally new chemicals. *Molecular Informatics*, 33(4), 311–314. <https://doi.org/10.1002/minf.201400030>
- Gramatica, P. (2020). Principles of QSAR modeling. *International Journal of Quantitative Structure-Property Relationships*, 5(3), 61–97. <https://doi.org/10.4018/IJQSPR.20200701.0a1>
- Gramatica, P., Cassani, S., & Chirico, N. (2014). QSARINS-chem: Insubria datasets and new QSAR/QSPR models for environmental pollutants in QSARINS. *Journal of Computational Chemistry*, 35(13), 1036–1044. <https://doi.org/10.1002/jcc.23576>
- Gramatica, P., Chirico, N., Papa, E., Cassani, S., & Kovarich, S. (2013). QSARINS: A new software for the development, analysis, and validation of QSAR MLR models. *Journal of Computational Chemistry*, 34(24), 2121–2132. <https://doi.org/10.1002/jcc.23361>
- Gramatica, P., Giani, E., & Papa, E. (2007). Statistical external validation and consensus modeling: A QSPR case study for Koc prediction. *Journal of Molecular Graphics & Modelling*, 25(6), 755–766. <https://doi.org/10.1016/j.jmglm.2006.06.005>
- Greenlee, W. J., Allibone, P. L., Perlow, D. S., Patchett, A. A., Ulm, E. H., & Vassil, T. C. (1985). Angiotensin-converting enzyme inhibitors: Synthesis and biological activity of acyltripeptide analogs of enalapril. *Journal of Medicinal Chemistry*, 28(4), 434–442. <https://doi.org/10.1021/jm00382a008>
- Hamming, I., van Goor, H., Turner, A. J., Rushworth, C. A., Michaud, A. A., Corvol, P., & Navis, G. (2008). Differential regulation of renal angiotensin-converting enzyme (ACE) and ACE2 during ACE inhibition and dietary sodium restriction in healthy rats. *Experimental Physiology*, 93(5), 631–638. <https://doi.org/10.1113/expphysiol.2007.041855>
- Harit, T., Bellaouchi, R., Rokni, Y., Riahi, A., Malek, F., & Asehrou, A. (2017). Synthesis, characterization, antimicrobial activity, and docking studies of new triazolic tripod ligands. *Chemistry & Biodiversity*, 14(12), e1700351. <https://doi.org/10.1002/cbdv.201700351>
- Huang, J., & Fan, X. (2011). Why QSAR fails: An empirical evaluation using conventional computational approach. *Molecular Pharmaceutics*, 8(2), 600–608. <https://doi.org/10.1021/mp100423u>
- Igase, M., Strawn, W. B., Gallagher, P. E., Geary, R. L., & Ferrario, C. M. (2005). Angiotensin II AT1 receptors regulate ACE2 and angiotensin-(1–7) expression in the aorta of spontaneously hypertensive rats. *American Journal of Physiology. Heart and Circulatory Physiology*, 289(3), H1013–H1019. <https://doi.org/10.1152/ajpheart.00068.2005>
- Imam, S. S., & Gilani, S. J., editors. (2017). *Computer aided drug design: A novel loom to drug discovery*.
- Ishiyama, Y., Gallagher, P. E., Averill, D. B., Tallant, E. A., Brosnihan, K. B., & Ferrario, C. M. (2004). Upregulation of angiotensin-converting enzyme 2 after myocardial infarction by blockade of angiotensin II receptors. *Hypertension (Dallas, TX: 1979)*, 43(5), 970–976. <https://doi.org/10.1161/01.HYP.0000124667.34652.1a>
- Ivanciuc, O. (1996). HyperChem release 4.5 for windows. *Journal of Chemical Information and Computer Sciences*, 36(3), 612–614. <https://doi.org/10.1021/ci950190a>
- Jawarkar, R. D., Bakal, R. L., Zaki, M. E., Al-Hussain, S., Ghosh, A., Gandhi, A., Mukerjee, N., Samad, A., Masand, V. H., & Lewaa, I. (2022). QSAR based virtual screening derived identification of a novel hit as a SARS CoV-229E 3CLpro Inhibitor: GA-MLR QSAR modeling supported by molecular Docking, molecular dynamics simulation and MMGBSA calculation approaches. *Arabian Journal of Chemistry*, 15(1), 103499. <https://doi.org/10.1016/j.arabjc.2021.103499>
- Jorgensen, W. L., Chandrasekhar, J., Madura, J. D., Impey, R. W., & Klein, M. L. (1983). Comparison of simple potential functions for simulating liquid water. *The Journal of Chemical Physics*, 79(2), 926–935. <https://doi.org/10.1063/1.445869>
- Kagami, L. P., das Neves, G. M., Timmers, L F S M. e. d., Caceres, R. A., & Eifler-Lima, V. L. (2020). Geo-Measures: A PyMOL plugin for protein structure ensembles analysis. *Computational Biology and Chemistry*, 87, 107322. <https://doi.org/10.1016/j.compbiolchem.2020.107322>
- Khan, A., Benthin, C., Zeno, B., Albertson, T. E., Boyd, J., Christie, J. D., Hall, R., Poirier, G., Ronco, J. J., Tidswell, M., Harges, K., Powley, W. M., Wright, T. J., Siederer, S. K., Fairman, D. A., Lipson, D. A., Bayliffe, A. I., & Lazaar, A. L. (2017). A pilot clinical trial of recombinant human angiotensin-converting enzyme 2 in acute respiratory distress syndrome. *Critical Care*, 21(1). <https://doi.org/10.1186/s13054-017-1823-x>
- Krstajic, D., Buturovic, L. J., Leahy, D. E., & Thomas, S. (2014). Cross-validation pitfalls when selecting and assessing regression and classification models. *Journal of Cheminformatics*, 6(1). <https://doi.org/10.1186/1758-2946-6-10>
- Lakshmanan, A. P., Thandavarayan, R. A., Watanabe, K., Sari, F. R., Meilei, H., Giridharan, V. V., Sukumaran, V., Soetikno, V., Arumugam, S., Suzuki, K., & Kodama, M. (2012). Modulation of AT-1R/MAPK cascade by an olmesartan treatment attenuates diabetic nephropathy in streptozotocin-induced diabetic mice. *Molecular and Cellular Endocrinology*, 348(1), 104–111. <https://doi.org/10.1016/j.mce.2011.07.041>
- Liddle, J., Bamborough, P., Barker, M. D., Campos, S., Chung, C.-W., Cousins, R. P. C., Faulder, P., Heathcote, M. L., Hobbs, H., Holmes, D. S., Ioannou, C., Ramirez-Molina, C., Morse, M. A., Osborn, R., Payne, J. J., Pritchard, J. M., Rumsey, W. L., Tape, D. T., Vicentini, G., Whitworth, C., & Williamson, R. A. (2012). 4-Phenyl-7-azaindoles as potent, selective and bioavailable IKK2 inhibitors demonstrating good in vivo efficacy. *Bioorganic & Medicinal Chemistry Letters*, 22(16), 5222–5226. <https://doi.org/10.1016/j.bmcl.2012.06.065>
- Lin, C.-G., Pan, C.-Y., & Kao, L.-S. (1996). Rab3A delayed catecholamine secretion from bovine adrenal chromaffin cells. *Biochemical and Biophysical Research Communications*, 221(3), 675–681. <https://doi.org/10.1006/bbrc.1996.0655>
- Lobanov, M. Y., Bogatyreva, N. S., & Galzitskaya, O. V. (2008). Radius of gyration as an indicator of protein structure compactness. *Molecular Biology*, 42(4), 623–628. <https://doi.org/10.1134/S0026893308040195>
- Martyna, G. J., Klein, M. L., & Tuckerman, M. (1992). Nosé–Hoover chains: The canonical ensemble via continuous dynamics. *The Journal of Chemical Physics*, 97(4), 2635–2643. <https://doi.org/10.1063/1.463940>
- Masand, V. H., & Rastija, V. (2017). PyDescriptor: A new PyMOL plugin for calculating thousands of easily understandable molecular descriptors. *Chemometrics and Intelligent Laboratory Systems*, 169, 12–18. <https://doi.org/10.1016/j.chemolab.2017.08.003>
- Masand, V. H., Patil, M. K., El-Sayed, N. N. E., Zaki, M. E., Almarhoon, Z., & Al-Hussain, S. A. (2021). Balanced QSAR analysis to identify the structural requirements of ABBV-075 (Mivebresib) analogues as bromodomain and extraterminal domain (BET) family bromodomain inhibitor. *Journal of Molecular Structure*, 1229, 129597. <https://doi.org/10.1016/j.molstruc.2020.129597>
- McKinley, M. J., Albiston, A. L., Allen, A. M., Mathai, M. L., May, C. N., McAllen, R. M., Oldfield, B. J., Mendelsohn, F. A. O., & Chai, S. Y. (2003). The brain renin–angiotensin system: Location and physiological roles. *The International Journal of Biochemistry & Cell Biology*, 35(6), 901–918. [https://doi.org/10.1016/s1357-2725\(02\)00306-0](https://doi.org/10.1016/s1357-2725(02)00306-0)
- Murphy, M. P., LeVine, H., & Lovell, M. A. (2010). Alzheimer’s disease and the amyloid- $\beta$  peptide. *Journal of Alzheimer’s Disease: JAD*, 19(1), 311–323. <https://doi.org/10.3233/JAD-2010-1221>
- Natesh, R., Schwager, S. L. U., Sturrock, E. D., & Acharya, K. R. (2003). Crystal structure of the human angiotensin-converting enzyme–lisinopril complex. *Nature*, 421(6922), 551–554. <https://doi.org/10.1038/nature01370>
- O’Boyle, N. M., Banck, M., James, C. A., Morley, C., Vandermeersch, T., & Hutchison, G. R. (2011). Open Babel: An open chemical toolbox. *Journal of Cheminformatics*, 3(1). <https://doi.org/10.1186/1758-2946-3-33>

- Ocaranza, M. P., Godoy, I., Jalil, J. E., Varas, M., Collantes, P., Pinto, M., Roman, M., Ramirez, C., Copaja, M., Diaz-Araya, G., Castro, P., & Lavandero, S. (2006). Enalapril attenuates downregulation of angiotensin-converting enzyme 2 in the late phase of ventricular dysfunction in myocardial infarcted rat. *Hypertension (Dallas, TX: 1979)*, 48(4), 572–578. <https://doi.org/10.1161/01.HYP.0000237862.94083.45>
- Parida, P. K., Paul, D., & Chakravorty, D. (2020). The natural way forward: Molecular dynamics simulation analysis of phytochemicals from Indian medicinal plants as potential inhibitors of SARS-CoV-2 targets. *Phytotherapy Research*, 34(12), 3420–3433. <https://doi.org/10.1002/ptr.6868>
- Paul, M., Poyan Mehr, A., & Kreutz, R. (2006). Physiology of local renin-angiotensin systems. *Physiological Reviews*, 86(3), 747–803. <https://doi.org/10.1152/physrev.00036.2005>
- Priya, R., Sneha, P., Rivera Madrid, R., Doss, C. P., Singh, P., & Siva, R. (2017). Molecular modeling and dynamic simulation of arabidopsis thaliana carotenoid cleavage dioxygenase gene: A comparison with *bixa orellana* and *crocus sativus*. *Journal of Cellular Biochemistry*, 118(9), 2712–2721. <https://doi.org/10.1002/jcb.25919>
- Rao, R. B., Fung, G., & Rosales, R. (2008). *On the dangers of cross-validation. An experimental evaluation* [Paper presentation]. Proceedings of the 2008 SIAM International Conference on Data Mining, p. 588–596. <https://doi.org/10.1137/1.9781611972788.54>
- Regulska, K., Stanisz, B., Regulski, M., & Murias, M. (2014). How to design a potent, specific, and stable angiotensin-converting enzyme inhibitor. *Drug Discovery Today*, 19(11), 1731–1743. <https://doi.org/10.1016/j.drudis.2014.06.026>
- Reid, I. A. (1992). Interactions between ANG II, sympathetic nervous system, and baroreceptor reflexes in regulation of blood pressure. *The American Journal of Physiology*, 262(6 Pt 1), E763–E778. <https://doi.org/10.1152/ajpendo.1992.262.6.E763>
- Shapiro, R., Holmquist, B., & Riordan, J. F. (1983). Anion activation of angiotensin converting enzyme: Dependence on nature of substrate. *Biochemistry*, 22(16), 3850–3857. <https://doi.org/10.1021/bi00285a021>
- Shivakumar, D., Williams, J., Wu, Y., Damm, W., Shelley, J., & SheRMan, W. (2010). Prediction of absolute solvation free energies using molecular dynamics free energy perturbation and the OPLS force field. *Journal of Chemical Theory and Computation*, 6(5), 1509–1519. <https://doi.org/10.1021/ct900587b>
- Soler, M. J., Ye, M., Wysocki, J., William, J., Lloveras, J., & Batlle, D. (2009). Localization of ACE2 in the renal vasculature: Amplification by angiotensin II type 1 receptor blockade using telmisartan. *American Journal of Physiology. Renal Physiology*, 296(2), F398–F405. <https://doi.org/10.1152/ajprenal.90488.2008>
- Soubrier, F., Alhenc-Gelas, F., Hubert, C., Allegrini, J., John, M., Tregear, G., & Corvol, P. (1988). Two putative active centers in human angiotensin I-converting enzyme revealed by molecular cloning. *Proceedings of the National Academy of Sciences of the United States of America*, 85(24), 9386–9390. <https://doi.org/10.1073/pnas.85.24.9386>
- Sparks, M. A., Crowley, S. D., Gurley, S. B., et al. (2014). Classical renin-angiotensin system in kidney physiology. *Comprehensive Physiology*, 1201–1228.
- Sukumaran, V., Tsuchimochi, H., Tatsumi, E., Shirai, M., & Pearson, J. T. (2017). Azilsartan ameliorates diabetic cardiomyopathy in young db/db mice through the modulation of ACE-2/ANG 1–7/Mas receptor cascade. *Biochemical Pharmacology*, 144, 90–99. <https://doi.org/10.1016/j.bcp.2017.07.022>
- Sukumaran, V., Veeraveedu, P. T., Gurusamy, N., Lakshmanan, A. P., Yamaguchi, K., Ma, M., Suzuki, K., Nagata, M., Takagi, R., Kodama, M., & Watanabe, K. (2012). Olmesartan attenuates the development of heart failure after experimental autoimmune myocarditis in rats through the modulation of ANG 1–7 mas receptor. *Molecular and Cellular Endocrinology*, 351(2), 208–219. <https://doi.org/10.1016/j.mce.2011.12.010>
- Sukumaran, V., Veeraveedu, P. T., Gurusamy, N., Yamaguchi, K., Lakshmanan, A. P., Ma, M., Suzuki, K., Kodama, M., & Watanabe, K. (2011). Cardioprotective effects of telmisartan against heart failure in rats induced by experimental autoimmune myocarditis through the modulation of angiotensin-converting enzyme-2/angiotensin 1-7/mas receptor axis. *International Journal of Biological Sciences*, 7(8), 1077–1092. <https://doi.org/10.7150/ijbs.7.1077>
- Tian, M., Zhu, D., Xie, W., & Shi, J. (2012). Central angiotensin II-induced Alzheimer-like tau phosphorylation in normal rat brains. *FEBS Letters*, 586(20), 3737–3745. <https://doi.org/10.1016/j.febslet.2012.09.004>
- Tipnis, S. R., Hooper, N. M., Hyde, R., Karran, E., Christie, G., & Turner, A. J. (2000). A human homolog of angiotensin-converting enzyme. *The Journal of Biological Chemistry*, 275(43), 33238–33243. <https://doi.org/10.1074/jbc.M002615200>
- Toukmaji, A. Y., & Board, J. A. (1996). Ewald summation techniques in perspective: A survey. *Computer Physics Communications*, 95(2–3), 73–92. [https://doi.org/10.1016/0010-4655\(96\)00016-1](https://doi.org/10.1016/0010-4655(96)00016-1)
- Tropsha, A., Gramatica, P., & Gombar, V. K. (2003). The importance of being earnest: Validation is the absolute essential for successful application and interpretation of QSPR models. *QSAR & Combinatorial Science*, 22(1), 69–77. <https://doi.org/10.1002/qsar.200390007>
- Vaduganathan, M., Vardeny, O., Michel, T., McMurray, J. J. V., Pfeffer, M. A., & Solomon, S. D. (2020). Renin-angiotensin-aldosterone system inhibitors in patients with covid-19. *The New England Journal of Medicine*, 382(17), 1653–1659. <https://doi.org/10.1056/NEJMr2005760>
- Vuille-dit-Bille, R. N., Camargo, S. M., Emmenegger, L., Sasse, T., Kummer, E., Jando, J., Hamie, Q. M., Meier, C. F., Hunziker, S., Forras-Kaufmann, Zs. o. fia., Kuyumcu, S., Fox, M., Schwizer, W., Fried, M., Lindenmeyer, M., Götz, O., & Verrey, F. (2015). Human intestine luminal ACE2 and amino acid transporter expression increased by ACE-inhibitors. *Amino Acids*, 47(4), 693–705. <https://doi.org/10.1007/s00726-014-1889-6>
- Wang, F., & Zhou, B. (2020). Investigation of angiotensin-I-converting enzyme (ACE) inhibitory tri-peptides: A combination of 3D-QSAR and molecular docking simulations. *RSC Advances*, 10(59), 35811–35819. <https://doi.org/10.1039/d0ra05119e>
- Wang, X., Wang, J., Lin, Y., Ding, Y., Wang, Y., Cheng, X., & Lin, Z. (2011). QSAR study on angiotensin-converting enzyme inhibitor oligopeptides based on a novel set of sequence information descriptors. *Journal of Molecular Modeling*, 17(7), 1599–1606. <https://doi.org/10.1007/s00894-010-0862-x>
- Wu, S., Qi, W., Su, R., Li, T., Lu, D., & He, Z. (2014). CoMFA and CoMSIA analysis of ACE-inhibitory, antimicrobial and bitter-tasting peptides. *European Journal of Medicinal Chemistry*, 84, 100–106. <https://doi.org/10.1016/j.ejmech.2014.07.015>
- Yim, H. E., & Yoo, K. H. (2008). Renin-angiotensin system - considerations for hypertension and kidney. *Electrolyte & Blood Pressure*, 6(1), 42. <https://doi.org/10.5049/EBP.2008.6.1.42>
- Zhong, J.-C., Ye, J.-Y., Jin, H.-Y., Yu, X., Yu, H.-M., Zhu, D.-L., Gao, P.-J., Huang, D.-Y., Shuster, M., Loibner, H., Guo, J.-M., Yu, X.-Y., Xiao, B.-X., Gong, Z.-H., Penninger, J. M., & Oudit, G. Y. (2011). Telmisartan attenuates aortic hypertrophy in hypertensive rats by the modulation of ACE2 and profilin-1 expression. *Regulatory Peptides*, 166(1–3), 90–97. <https://doi.org/10.1016/j.regpep.2010.09.005>
- Zhu, D., Shi, J., Zhang, Y., Wang, B., Liu, W., Chen, Z., & Tong, Q. (2011). Central angiotensin II stimulation promotes  $\beta$  amyloid production in sprague dawley rats. *PLoS One*, 6(1), e16037. <https://doi.org/10.1371/journal.pone.0016037>

## Article

# Synthesis and Biological Evaluation of Some New 3-Aryl-2-thioxo-2,3-dihydroquinazolin-4(1H)-ones and 3-Aryl-2-(benzylthio)quinazolin-4(3H)-ones as Antioxidants; COX-2, LDHA, $\alpha$ -Glucosidase and $\alpha$ -Amylase Inhibitors; and Anti-Colon Carcinoma and Apoptosis-Inducing Agents

Nahed Nasser Eid El-Sayed <sup>1,\*</sup>, Taghreed M. Al-Otaibi <sup>2</sup>, Assem Barakat <sup>2</sup>, Zainab M. Almarhoon <sup>2,\*</sup>, Mohd. Zaheen Hassan <sup>3</sup>, Maha I. Al-Zaben <sup>2</sup>, Najeh Krayem <sup>4</sup>, Vijay H. Masand <sup>5</sup> and Abir Ben Bacha <sup>6</sup>

<sup>1</sup> National Organization for Drug Control and Research, Egyptian Drug Authority (EDA), 51 Wezaret El-Zeraa St., Giza 35521, Egypt

<sup>2</sup> Department of Chemistry, College of Sciences, King Saud University, P.O. Box 2455, Riyadh 11451, Saudi Arabia; chemst222@gmail.com (T.M.A.-O.); ambarakat@ksu.edu.sa (A.B.); mzaben@ksu.edu.sa (M.I.A.-Z.)

<sup>3</sup> Department of Pharmaceutical Chemistry, College of Pharmacy, King Khalid University, Abha 62529, Saudi Arabia; zaheen@kku.edu.sa

<sup>4</sup> Laboratoire de Biochimie et de Génie Enzymatique des Lipases, ENIS, Université de Sfax, Route de Soukra 3038, Sfax BP 1173, Tunisia; krayemnajeh@yahoo.fr

<sup>5</sup> Department of Chemistry, Vidya Bharati College, Camp, Amravati, Maharashtra 444602, India; vijamasand@gmail.com

<sup>6</sup> Biochemistry Department, College of Sciences, King Saud University, P.O. Box 22452, Riyadh 11495, Saudi Arabia; aalghanouchi@ksu.edu.sa

\* Correspondence: nahed.elsayed@edaegypt.gov.eg (N.N.E.E.-S.); zalmarhoon@ksu.edu.sa (Z.M.A.)



**Citation:** El-Sayed, N.N.E.; Al-Otaibi, T.M.; Barakat, A.; Almarhoon, Z.M.; Hassan, M.Z.; Al-Zaben, M.I.;

Krayem, N.; Masand, V.H.; Ben Bacha, A. Synthesis and Biological Evaluation of Some New

3-Aryl-2-thioxo-2,3-dihydroquinazolin-4(1H)-ones and 3-Aryl-2-(benzylthio)quinazolin-4(3H)-ones as Antioxidants; COX-2, LDHA,  $\alpha$ -Glucosidase and  $\alpha$ -Amylase Inhibitors; and Anti-Colon Carcinoma and Apoptosis-Inducing Agents. *Pharmaceuticals* **2023**, *16*, 1392. <https://doi.org/10.3390/ph16101392>

Received: 16 July 2023

Revised: 17 September 2023

Accepted: 20 September 2023

Published: 1 October 2023



**Copyright:** © 2023 by the authors. Licensee MDPI, Basel, Switzerland. This article is an open access article distributed under the terms and conditions of the Creative Commons Attribution (CC BY) license (<https://creativecommons.org/licenses/by/4.0/>).

**Abstract:** Oxidative stress, COX-2, LDHA and hyperglycemia are interlinked contributing pathways in the etiology, progression and metastasis of colon cancer. Additionally, dysregulated apoptosis in cells with genetic alternations leads to their progression in malignant transformation. Therefore, quinazolinones **3a–3h** and **5a–5h** were synthesized and evaluated as antioxidants, enzymes inhibitors and cytotoxic agents against LoVo and HCT-116 cells. Moreover, the most active cytotoxic derivatives were evaluated as apoptosis inducers. The results indicated that **3a**, **3g** and **5a** were efficiently scavenged DPPH radicals with lowered IC<sub>50</sub> values (mM) ranging from 0.165 ± 0.0057 to 0.191 ± 0.0099, as compared to 0.245 ± 0.0257 by BHT. Derivatives **3h**, **5a** and **5h** were recognized as more potent dual inhibitors than quercetin against  $\alpha$ -amylase and  $\alpha$ -glucosidase, in addition to **3a**, **3c**, **3f** and **5b–5f** against  $\alpha$ -amylase. Although none of the compounds demonstrated a higher efficiency than the reference inhibitors against COX-2 and LDHA, **3a** and **3g** were identified as the most active derivatives. Molecular docking studies were used to elucidate the binding affinities and binding interactions between the inhibitors and their target proteins. Compounds **3a** and **3f** showed cytotoxic activities, with IC<sub>50</sub> values ( $\mu$ M) of 294.32 ± 8.41 and 383.5 ± 8.99 (LoVo), as well as 298.05 ± 13.26 and 323.59 ± 3.00 (HCT-116). The cytotoxicity mechanism of **3a** and **3f** could be attributed to the modulation of apoptosis regulators (Bax and Bcl-2), the activation of intrinsic and extrinsic apoptosis pathways via the upregulation of initiator caspases-8 and -9 as well as executioner caspase-3, and the arrest of LoVo and HCT-116 cell cycles in the G2/M and G1 phases, respectively. Lastly, the physicochemical, medicinal chemistry and ADMET properties of all compounds were predicted.

**Keywords:** colorectal cancer; oxidative stress; inflammation; COX-2; Warburg effect; LDHA; post prandial hyperglycemia; apoptosis; quinazolinone; ADMET

## 1. Introduction

Colorectal cancer (CRC) was ranked third and second in terms of incidence and mortality, respectively, accounting for 1.9 million of all new cancer cases and 900,000 deaths in 2020 worldwide. Notably, the incidence of CRC has shown a rising trend among individuals aged less than 50 years [1].

CRC neo-tumorigenesis is a complex and multistep process, linked to factors of oncogenesis such as oxidative stress (OS), chronic inflammation, reprogrammed glucose metabolism and diabetes mellitus (DM). In addition, defective signaling or changes in the expression of proteins regulating programmed cell death “apoptosis” play crucial roles in the evolution of normal mucosa cells towards neoplastic transformations and the acquisition of new characteristics, among which evading cell death [2].

OS is a pathological state featuring the over-generation of cellular reactive oxygen and/or nitrogen species (RO/NS) as a result of a dysregulated intracellular metabolism, tissue inflammation or exposure to exogenous stimuli at an extent that exceeds the cellular antioxidant defenses [3]. In fact, OS is considered as a hallmark of carcinogenesis [3].

Regarding CRC, OS on intestinal mucosal cells is proven to damage phospholipid biological membranes via lipid peroxidation by free radicals [4]. Therefore, it causes rupture of the phospholipid bilayer of the cytoplasmic cellular membrane, with the loss of cellular homeostasis. It promotes the destruction of the two lipid bilayers of the endoplasmic reticulum (ER), the dynamic reservoir of  $\text{Ca}^{2+}$ , leading to disruption of ER- $\text{Ca}^{2+}$  homeostasis, which is implicated in the initiation and propagation of cancer [5]. Also, it causes oxidative damage to the mitochondrial membranes, which disrupts the cell energy metabolism [6].

Another aspect of involvement of OS in CRC pathogenesis is through production of malondialdehyde (MDA, one of the end products of lipid peroxidation), which promotes oxidative DNA damage via formation of adducts with DNA bases; deoxyguanosine and deoxyadenosine, thus initiating mutations in tumor suppressor genes and proto-oncogenes [6,7].

Furthermore, free radicals may modify proteins, thus diminishing or enhancing their catalytic activity. Also, free radicals may stimulate cell and tissue lesions by oxidizing carbohydrates [8], and they may exert pro-inflammatory and pro-proliferative roles via oxidizing cholesterol to oxysterols [9]. Interestingly, cancerous cells can maintain certain levels of ROS to promote their proliferation and invasion [4]. Moreover, ROS are key constituents of cancer cells' survival via the generation of resistance to chemo- and radiotherapies [10]. Accordingly, several studies have indicated that antioxidant compounds were supplemented or tested as adjuvants in cancer therapy to reverse resistance mechanisms, to reduce systemic toxicity during chemo- or radiotherapy [11] and to prevent cancer cell invasion [12].

Chronic inflammation is another principal effector in colorectal carcinogenesis. Inflammation can be induced by different stimuli, including pathogens, toxic compounds and OS-damaged cells. This inflammation enhances the affected tissues to overexpress the inducible cyclooxygenase isoform-2 (COX-2), which is typically absent or rarely expressed in healthy tissues. COX-2 catalyzes the conversion of arachidonic acid (AA) to prostaglandins (PGs)  $\text{H}_2$ , which are further metabolized by prostaglandin synthases to  $\text{PGD}_2$ ,  $\text{E}_2$ ,  $\text{I}_2$ ,  $\text{F}_{2\alpha}$  and thromboxane  $\text{A}_2$ . Extensive clinical and experimental studies conducted over the last few decades have provided convincing data indicating that high levels of COX-2 and  $\text{PGE}_2$  are implicated in the pathogenesis of colorectal carcinoma [13–15], and that they are associated with poorer survival outcomes [16]. The key roles of the COX-2/ $\text{PGE}_2$  pathway in CRC pathogenesis include generating an immunosuppressive tumor microenvironment [17], participating in tumor initiation, promoting sustained angiogenesis and thus favoring tumor growth, inducing tumor cell invasion, encouraging migration, reducing apoptotic rate and enhancing chemotherapeutic resistance [18,19]. Therefore, inhibition of COX-2 to reduce  $\text{PGE}_2$  synthesis is considered an important therapeutic approach in prevention and modulation of CRC progression [20]. Consistent with these findings, a number of meta-analyses and in vitro studies have reported that classical non-steroidal

anti-inflammatory drugs (NSAIDs) [21] and selective COX-2 inhibitors [22] provided protection against CRC incidence, reduced mortality and improved chemosensitivity and the efficacy of anticancer drugs when co-administrated [23].

Furthermore, the reprogrammed energy metabolism or Warburg effect [24] is a prominent metabolic characteristic of malignant cells [25]. The common features of this abnormal, less-energy-efficient metabolic pathway include increased glucose uptake, production of two moles of pyruvate and less ATP (2 moles/ glucose molecule) and rapid cytoplasmic fermentation of pyruvate to lactate under catalysis of lactate dehydrogenase A (LDHA). Lactate is then exported to the extracellular environment, which, in the presence of hydrogen ion, generate an acidic tumor microenvironment (TME). Lactic acidosis has been observed in different cancer types and it is linked to tumor aggressiveness [26]. In this regard, several clinical studies have revealed that hyperlactatemia is involved not only in tumor growth but also in the evasion of immune surveillance [27], local invasion, metastasis, chemoresistance and patient survival [28]. Consequently, targeting glycolysis via inhibiting LDHA would suppress hyperlactatemia and prevent its protumorigenic effects, in addition to depriving cancerous cells of nutrients, thereby killing them [29]. Indeed, several studies have shown that inhibition of LDHA activity impedes tumor progression, induces significant oxidative stress and necrosis [30], induces G2/M cell cycle arrest, increases sensitivity to ionizing radiation and 5-Fluorouracil (5-FU) [31,32] and attenuates cell invasion and migration [33].

DM is a multifactorial chronic metabolic disorder affecting millions of people worldwide. DM is categorized into Type 1 (T1DM, caused by the autoimmune destruction of the pancreatic  $\beta$ -cells leading to little, or the absolute lack of, insulin production), Type 2 (T2DM, arises due to complex interactions between genes and some risk factors, mainly obesity, smoking and hypertension, leading to insulin resistance) and gestational (GDM, occurs in pregnant women). T2DM is the most prevalent type, accounting for about 90% of all diabetic cases [34]. Besides its deadly cardiovascular complications, T2DM has also been associated with an increased risk for the development of certain types of cancers [35]. In particular, the positive correlation between CRC and T2DM is attributed to sharing some common risk factors including obesity, alcohol consumption, cigarette smoking and a Western-pattern diet. In addition, genome-wide association studies have identified transcription factor 7-like 2 (TCF7L2), gremlin 1 (GREM1) and tumor protein p53 inducible nuclear protein 1 (TP53INP1), among other genes, as being pleiotropically related to T2DM as well as CRC prognosis and tumorigenesis [36]. Moreover, T2DM-related metabolic changes, such as hyperinsulinemia, hyperglycemia, OS, inflammation induced by adipose tissue dysfunction, impaired immunological surveillance and gastrointestinal motility disorder have been implicated in carcinogenesis [37].

With regard to hyperglycemia, it influences the neoplastic transformations by providing glucose that is essential for the growth and proliferation of cancerous cells under the Warburg state [38]. It leads to the irreversible formation of advanced glycosylated end-products (AGEs) with proteins, lipids and nucleic acids, as well as their buildup, resulting in the development of OS and chronic inflammations, which are intrinsically linked to induction and development of cancer. Furthermore, elevated expressions of AGEs and their receptors contribute to the invasion and metastasis of CRC [39]. Also, the activations of the polyol, hexosamine and protein kinase C metabolic pathways [40] are other putative mechanisms by which hyperglycemia contributes to the cell proliferation, invasion and tumor progression of colon cancer. In addition, hyperglycemia may negatively affect CRC patients' quality of life by reducing the chemotherapeutic efficacy and inducing adverse effects [36].

Thus, over the years, researchers have worked on various targets to moderate the onset or worsening of diabetes, from which some antihyperglycemic therapies have been approved by the US FDA and other regulatory agencies, which exhibit different mechanisms of action via targeting single or multiple established molecular pathways involved in the pathogenesis of the disease [41]. Amongst these validated pathways is the breakdown of complex carbohydrates into absorbable monosaccharides, which takes place under

the catalysis of alpha-glucosidase (AG) and alpha-amylase (AA). Thus, inhibitors (Is) of these enzymes would manage T2DM by delaying the carbohydrate metabolism and turning down the rate of glucose absorption to reduce the post prandial blood glucose level (PPBGL). Indeed, carbohydrate mimics [34], including voglibose (natural sugar), miglitol (semisynthetic iminosugar) and 1-deoxynojirimycin (DNJ), all of which inhibit AG, in addition to acarbose (an oligosaccharide), which can also inhibit AA [42], are marketed as antidiabetic drugs. Despite the helpful impacts of these glucose-lowering drugs, morbidity and mortality remain significant in T2DM patients. In addition, these medications have many drawbacks, such as poor compliance with treatment, expense and adverse effects [43,44]. Therefore, there are a lot of synthetic efforts towards the development of new inhibitors, particularly annulated sugars [45], iminosugars [46,47] and novel classes of drugs derived from the structural hybrids of different key molecules and heterocycles [48], with the aim to develop new effective inhibitors that are escorted by better compliance, socioeconomic benefits and safety [49].

Additionally, apoptosis is a well-characterized form of programmed cell death (PCD), which occurs normally for regulating tissue homeostasis and regeneration during development. However, it is also activated as an immune defense mechanism against damaged or stressed cells in response to stimuli such as reactive oxygen species (produced by some chemotherapeutic agents) or DNA damage (from irradiation or anticancer drugs) to remove these potentially harmful cells [50]. If apoptosis is not controlled properly (insufficient apoptosis/extreme cell proliferation), mutations will potentially accumulate in the unwanted cells, which eventually could lead to the induction of cancer. Indeed, resisting apoptosis is considered as one of the hallmarks of cancer [51].

Apoptosis can be triggered by two different pathways: the extrinsic (death receptor) and the intrinsic (mitochondrial) pathways. The extrinsic pathway is initiated via the binding of certain extracellular ligands (members of the tumor necrosis factor super family, TNF) to their cognate cell surface death receptors, resulting in caspase 8 activation. This activation can directly induce apoptosis, or activate effector caspase 3 or Bid, which lead to apoptosis. While the intrinsic apoptotic pathway is initiated via mitochondrial outer membrane permeabilization (MOMP), a process controlled by the members of the B-cell lymphoma (BCL-2) family and p53 proteins [52]. MOMP is considered as the point of no return in this apoptotic cascade, since it leads to the release of the apoptogenic proteins cytochrome c and Smac from the mitochondria into the cell cytoplasm, which activate caspases directly or indirectly, respectively [53,54]. According to the direct mode, cytochrome c interacts with apoptotic protease activating factor-1 (APAF1), thus transforming it into an apoptosome complex, which activates pro-caspase-9 to initiator caspase 9, which in turn activates caspase-3, leading to the activation of the final cascade and, consequently, the fragmentation of the nucleus after its membrane rupture [55]. After the activation of all signaling cascade mediators, the two pathways meet up at the final caspases' activation (caspases 3, 7), resulting in the cleavage of different integrated cell proteins and the execution of the apoptotic steps [55].

Furthermore, the BCL-2 family of proteins [56], which tightly regulate the intrinsic pathway, is subclassified into three subgroups; the first comprises the pro-apoptotic proteins or apoptosis effectors that positively regulate apoptosis, and they include Bcl-2 antagonist killer 1 (Bak) and Bcl-2-associated X protein (Bax), which can directly execute MOMP when activated.

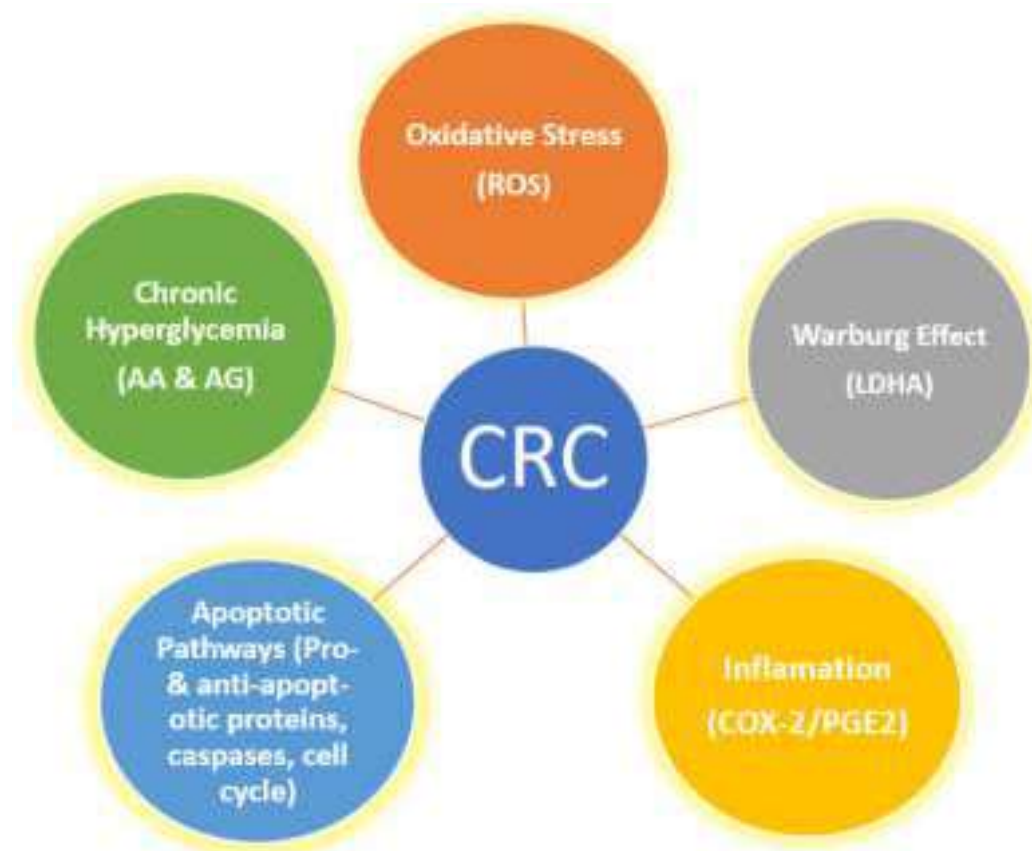
The second comprises the pro-survival members that negatively regulate apoptosis, and they include B cell lymphoma-2 (Bcl-2) itself, B cell lymphoma extra-large (Bcl-xL), B cell lymphoma-w (Bcl-W), B cell lymphoma-like protein 2 (Bcl-B), myeloid leukemia cell 1 (MCL-1) and Bcl-2-related protein A1/Bcl-2-related isolated from fetal liver-11 (A1/BFL-1).

The third group is the pro-apoptotic BH3-only proteins, which include p53-upregulated modulator of apoptosis (Puma), Bcl-2-interacting mediator of cell death (Bim) and the Bcl-2 Homology 3 interacting death agonist (Bid), which act as activators to Bax and Bak. This group comprises also other proteins, called sensitizers, which do not associate with Bax

and Bak, but antagonize the pro-survival members, including the Bcl-2 associated agonist of cell death (Bad), Bcl-2 interacting t killer 1 (Bik), Noxa, BMF and HRK.

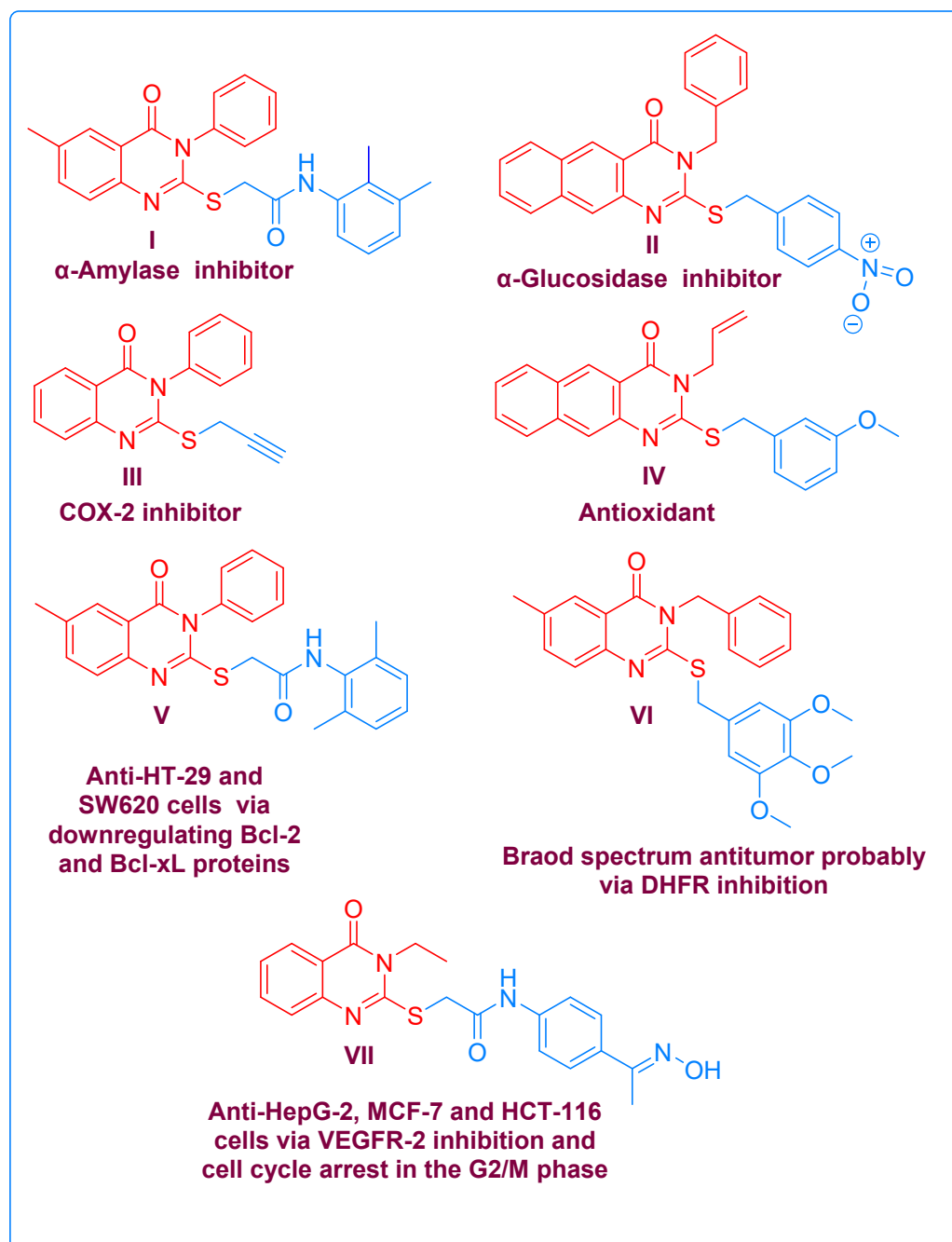
In healthy cells, the pro- and anti-apoptotic proteins are held in a fine, delicate balance. Conversely, during cancer development, the malignant cells alter this balance, by overexpressing various anti-apoptotic proteins and/or abnormally reduce the expression levels of pro-apoptotic members, and thus they become unresponsive to stimuli that otherwise trigger apoptosis in sensitive cells, which leads to cellular proliferation and cancer progression, in addition to therapeutic resistance [57]. Therefore, inhibiting the anti-apoptotic [58,59] and activating pro-apoptotic members [60] of the Bcl-2 family have been suggested as plausible selective strategies for cancer therapy and to overcome drug resistance.

Taken together, the complexity of CRC and the manifold and heterogeneous association of this malignancy with OS, inflammation, Warburg effect and hyperglycemia highlight the need for the development of new pharmaceuticals capable of the simultaneous targeting of these risk factors as well as the apoptotic pathways (Figure 1).



**Figure 1.** Various risk factors and pathways implicated in cancer, which serve as targets for multi-potent agents.

The innovation of multi-targeted therapies represents a promising and prevailing anticancer drug discovery paradigm among medicinal chemists [61]. In line with this principle, quinazolinone scaffolds have proven to be easily accessible pharmacophores, possessing multipotent pharmacological activities both *in vitro* and *in vivo* [62]. They have been presented as core structures in inhibitors for; AA [63] I, AG [64] II, and COX-2 [65] III, as well as antioxidant agent [66] IV, and anti-cancer candidates (V, VI and VII), which produce their cytotoxic effects through different molecular mechanisms [63,67,68], as portrayed in Figure 2.



**Figure 2.** Selected examples of biologically active compounds containing quinazolinone cores.

In light of the above, in this study, we designed a number of new quinazolinone derivatives bearing 4-nitro-phenyl, in addition to fluorine containing 4- or 3-(trifluoromethyl)phenyl moiety at position 3, due to the significant impact of fluorine atoms in enhancing the binding affinity to the targeted protein, as well as improving pharmacokinetic and physicochemical properties including metabolic stability and membrane permeation [69]. Also, various substituents such as Br, Cl and OCH<sub>3</sub> were located at the 6 and/or 6,7 positions on the quinazolinone core, to span different electronic, steric and lipophilic characters that would produce different pharmacological responses, which would increase the probability of the discovery of active agents. Subsequently, these compounds were evaluated in vitro as antioxidants as well as AA, AG, COX-2 and LDHA inhibitors. Structure–activity relationships regarding the antioxidant activity were discussed. Additionally, molecular docking simulations were performed to confirm the results of the in vitro enzymatic inhibitory



assays and to predict the conformations of the potential inhibitors upon binding to the target proteins, as well as to calculate the binding affinities between them.

Moreover, all compounds were screened for their cytotoxic effects on LoVo and HCT-116 human colon carcinoma cells at 200 µg/mL, and then the IC<sub>50</sub> values of the most active cytotoxic candidates were calculated from the concentration–response curves and compared with that of 5-FU. Afterwards, they were evaluated against non-tumoral human umbilical vein endothelial cells (HUVEC) to explore their safety profiles. Furthermore, the capability of the cytotoxic candidates to modulate apoptosis regulators (Bax and Bcl2), to activate caspases-8, 9 and 3 and to disturb the cell cycles of LoVo and HCT-116 cells were investigated. Finally, the physicochemical, medicinal chemistry and ADMET properties of all compounds were predicted and discussed in detail for some active compounds as model examples.

## 2. Results and Discussion

### 2.1. Chemistry

The target compounds were synthesized as depicted in Scheme 1.

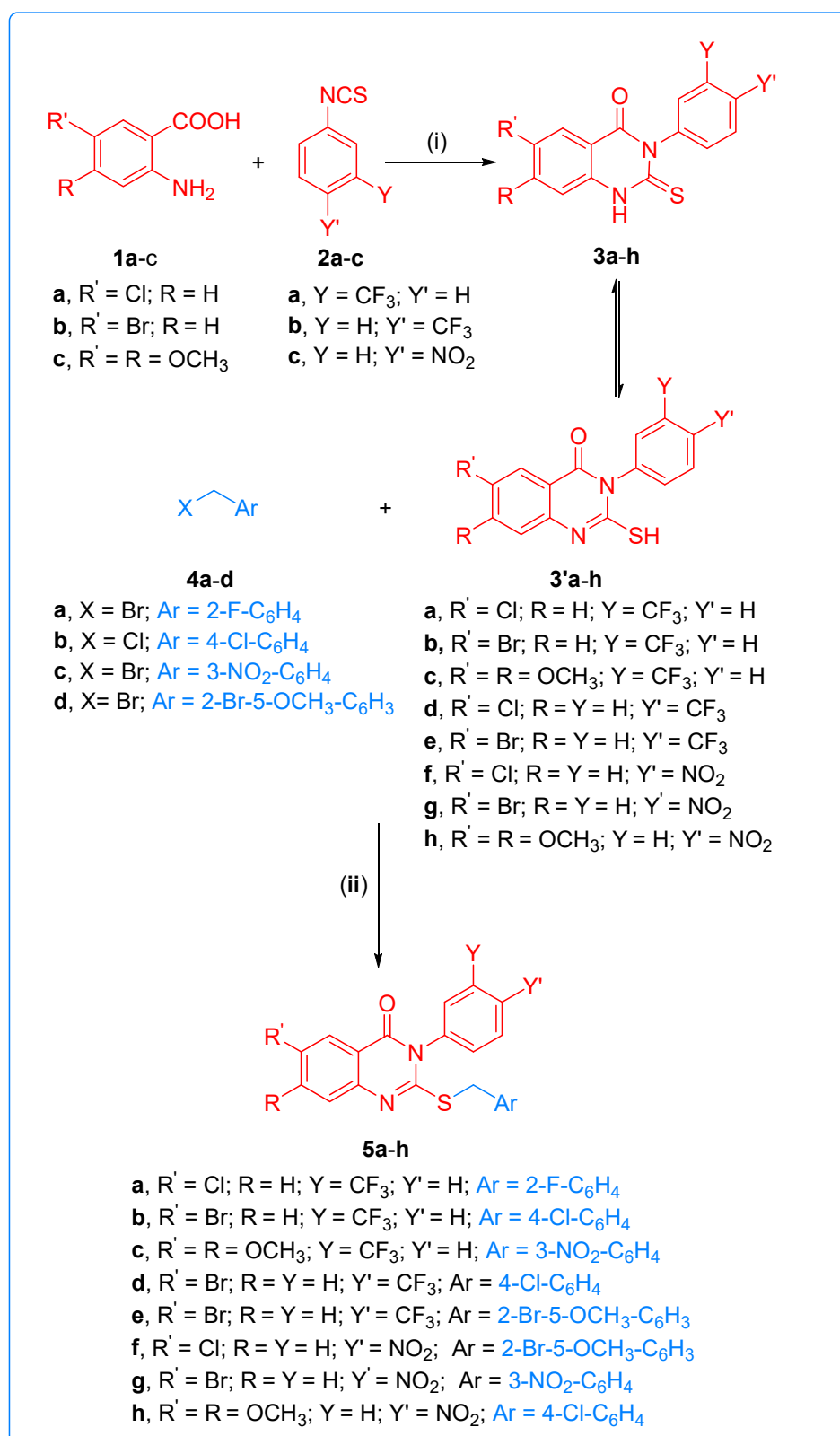
Initially, refluxing mixtures of 5-substituted or 4,5-disubstituted anthranilic acid derivatives **1a–c** and 3-substituted or /4-substituted phenyl isothiocyanate derivatives **2a–c** in glacial acetic for 10 h [70] yielded the new 6-substituted or 6,7-disubstituted-3-aryl-2-thioxo-2,3-dihydro-1*H*-quinazolin-4-one derivatives **3a–h**, which can potentially also exist in their tautomeric forms **3'a–h** due to thiocarbonyl–thiol tautomerization. Subsequently, the arylation of the acidic thiol groups using various aryl halides **4a–d** under basic catalysis with potassium carbonate in refluxing dry acetone for 6 h [50] produced eight new 2-(benzylsulfanyl)-3-aryl-3*H*-quinazolin-4-one derivatives, **5a–h**. The structures of the synthesized derivatives were elucidated based on IR, <sup>1</sup>H-NMR, <sup>13</sup>C-NMR and mass spectrometric analyses.

All the spectroscopic data indicated the predominance of the thiocarbonyl tautomeric form for compounds **3a–h** in the solid state (IR) and in the DMSO solution (NMR), which is in agreement with the reported data [71]. Thus, their IR spectra showed stretching absorption bands for the NH groups at a  $\nu_{\max}$  ranging from 3155 to 3245 cm<sup>-1</sup>. In addition, the <sup>1</sup>HNMR spectra demonstrated the NH protons as singlet peaks at  $\delta_{\text{H}} = 12.91\text{--}13.24$  ppm, while the <sup>13</sup>CNMR spectra exhibited characteristic signals for C=S at a  $\delta_{\text{C}}/\text{ppm}$  ranging from 174.38 to 176.28.

Contrarily, the IR and <sup>1</sup>HNMR spectra of derivatives **5a–h** indicated the disappearance of the NH protons, and their <sup>13</sup>CNMR spectra confirmed the absence of the peaks corresponding to the C=S groups and the presence of the benzylic methylene groups.

As representative examples, the IR spectrum of compound **3c** showed the stretching absorption bands at  $\nu_{\max} = 3178$  and  $1698$  cm<sup>-1</sup>, corresponding to the NH and C=O groups, respectively. The <sup>1</sup>H-NMR spectrum of this compound (500 MHz; DMSO-d<sub>6</sub>) showed a characteristic one-proton singlet peak at  $\delta_{\text{H}} = 12.91$  ppm for the NH proton. Additionally, the four aromatic protons of the 3-trifluoromethylphenyl ring exhibited a one-proton doublet peak (coupling constant *J* value = 7.5 Hz), a one-proton singlet peak, an apparent triplet peak (*J* value = 8.05 Hz) and a doublet peak (*J* value = 8.5 Hz) at chemical shift values of  $\delta_{\text{H}} = 7.73, 7.69, 7.66, 7.24$  and  $7.56$  ppm, respectively. The two aromatic protons of the dimethoxyphenyl ring were detected as two singlet peaks at  $\delta = 7.24$  and  $6.95$  ppm.

Lastly, the two methoxy groups exhibited two singlet peaks, each integrating to three protons at  $\delta_{\text{H}} = 3.83$  and  $3.77$  ppm. With regard to its <sup>13</sup>C-NMR spectrum (125 MHz; DMSO-d<sub>6</sub>), it was characterized by a distinctive peak at  $\delta_{\text{C}}/\text{ppm} = 174.66$  attributed to C=S group, in addition to seventeen peaks, as expected, at  $\delta_{\text{C}}/\text{ppm} = 159.34$  (C=O), 155.41, 146.58, 140.23, 135.63, 133.62, 130.03, 129.80, 126.38, 125.03, 124.89, 122.87, 108.66, 106.94, 97.98 (6 × CH-aromatic, 6 × C<sub>q</sub>-aromatic and C<sub>q</sub>F<sub>3</sub>), 56.01 and 55.84 (2 × OCH<sub>3</sub>). Finally, the MS spectrum of this compound showed a molecular ion peak [M<sup>+</sup> + 1] at  $m/z = 383.17$  (27.26%) for C<sub>17</sub>H<sub>13</sub>F<sub>3</sub>N<sub>2</sub>O<sub>3</sub>S, and the base peak was detected at  $m/z = 382.16$ , which corresponds to [M<sup>+</sup>].



**Scheme 1.** Reagents and conditions: (i) Glacial AcOH, reflux 10 h. (ii) Dry acetone, K<sub>2</sub>CO<sub>3</sub>, reflux 6 h.

On the other hand, the IR spectrum (KBr) of compound **5c** indicated the disappearance of the stretching absorption band due to NH group of its precursor **3c**. The <sup>1</sup>H-NMR spectrum (300 MHz, DMSO-d<sub>6</sub>) endorsed the absence of NH proton and the presence of the characteristic benzylic protons as an AB quartet signal at δ<sub>H</sub> = 4.53 ppm, with a coupling

constant of  $J = 13.5$  Hz. In addition, it displayed eight peaks corresponding to ten aromatic protons as follows: a one-proton apparent doublet of the doublet peak ( $J$  values = 6.3, 2.1 Hz); an apparent one-proton doublet of the doublet peak ( $J$  values = 8.4, 2.4 Hz); a one-proton singlet; a two-proton doublet peak ( $J = 7.8$  Hz); a two-proton multiplet peak; a one-proton triplet peak ( $J = 7.8$  Hz); a one-proton singlet peak and a one-proton singlet peak, which were resonating at  $\delta_{\text{H}} = 8.52, 8.09, 7.98, 7.93, 7.83\text{--}7.77, 7.60, 7.37$  and  $7.24$  ppm, respectively, confirming the installation of the 3-nitrophenyl moiety on the sulfur atoms. The  $^{13}\text{C}$ -NMR spectrum (150 MHz; DMSO- $d_6$ ) revealed the absence of the peak due to the C=S group and the presence a new characteristic  $\text{CH}_2$ -benzylic peak at  $\delta_{\text{C}} = 35.12$  ppm. The mass spectrum of this compound indicated the presence of the molecular ion peaks  $[\text{M}^+ + 2]$  and  $[\text{M}^+ + 1]$  at  $m/z$  (%) = 519.10 (6.53) and 518.19 (29.95), respectively, for  $\text{C}_{24}\text{H}_{18}\text{F}_3\text{N}_3\text{O}_5\text{S}$ . The base peak, which represents  $[\text{M}^+]$  ion was recorded at  $m/z = 517.18$ .

## 2.2. Biological Evaluation

The synthesized compounds were subjected to multiple in vitro biological evaluations as described in the following sections.

### 2.2.1. Antioxidant Evaluation via 2,2-Diphenyl-1-picryl-hydrazyl-hydrate (DPPH) Assay

The DPPH free radical scavenging method is used for the determination of the antioxidant potency of compounds **3a-h** and **5a-h**, expressed as mean  $\text{IC}_{50}$  values; half maximal inhibitory concentrations. The results are summarized in Table 1.

**Table 1.** Mean  $\text{IC}_{50}$  values in mg/mL (mM) for scavenging initial DPPH radicals using the synthesized compounds  $\pm$  SD of three independent replicates. BHT was used as the reference drug.

Comp. # (MW)	Mean Values of Half Maximal Inhibitory Potency in mg/mL $\pm$ SD (mM)
<b>3a</b> (356.75)	<b>0.068 <math>\pm</math> 0.004 (0.191 <math>\pm</math> 0.011)</b>
<b>3b</b> (401.20)	0.161 $\pm$ 0.016 (1.520 $\pm$ 0.039)
<b>3c</b> (382.36)	0.100 $\pm$ 0.014 (0.262 $\pm$ 0.037)
<b>3d</b> (356.75)	0.179 $\pm$ 0.016 (0.502 $\pm$ 0.045)
<b>3e</b> (401.20)	0.290 $\pm$ 0.028 (0.723 $\pm$ 0.070)
<b>3f</b> (333.75)	0.227 $\pm$ 0.010 (0.680 $\pm$ 0.030)
<b>3g</b> (378.20)	<b>0.0625 <math>\pm</math> 0.002 (0.165 <math>\pm</math> 0.005)</b>
<b>3h</b> (359.36)	0.325 $\pm$ 0.007 (0.904 $\pm$ 0.0195)
<b>5a</b> (464.86)	<b>0.080 <math>\pm</math> 0.002 (0.172 <math>\pm</math> 0.004)</b>
<b>5b</b> (525.77)	0.167 $\pm$ 0.010 (0.318 $\pm$ 0.019)
<b>5c</b> (517.48)	0.186 $\pm$ 0.006 (0.359 $\pm$ 0.012)
<b>5d</b> (481.31)	0.200 $\pm$ 0.028 (0.416 $\pm$ 0.058)
<b>5e</b> (600.25)	0.225 $\pm$ 0.021 (0.375 $\pm$ 0.035)
<b>5f</b> (532.79)	0.241 $\pm$ 0.013 (0.452 $\pm$ 0.024)
<b>5g</b> (513.32)	0.200 $\pm$ 0.014 (0.390 $\pm$ 0.027)
<b>5h</b> (483.92)	0.364 $\pm$ 0.020 (0.752 $\pm$ 0.041)
BHT (220.35)	<b>0.054 <math>\pm</math> 0.006 (0.245 <math>\pm</math> 0.027)</b>

In principle, the antioxidant power of a compound in this assay is correlated to its tendency to reduce the stable, purple-colored DPPH radical through a hydrogen atom transfer (HAT) mechanism and/or a single electron transfer mechanism [72], thereby converting it to the yellow-colored 2,2-diphenyl-1-picrylhydrazine, whereby this reduction is accompanied by a depletion in the amount of the initial DPPH radicals and a change in the absorbance of the test solution accordingly, which can be detected relative to the blank solution at  $\lambda = 517$  nm.

The antioxidant potency of a compound depends on its structural characteristics due to the electronegativity, position and number of substituents. Therefore, among the tested compounds (Table 1), the quinazolinone derivatives **3a**, **3g** and **5a** demonstrated the lowest mean half maximal concentrations for scavenging DPPH radicals with  $\text{IC}_{50}$  values (mM)

of  $0.191 \pm 0.011$ ,  $0.165 \pm 0.005$  and  $0.172 \pm 0.004$ , respectively, which were lower than  $0.245 \pm 0.027$ , the value of the reference antioxidant drug, butylated hydroxy toluene (BHT), indicating that these quinazolinones are more potent antioxidants than BHT. The rest of the compounds exhibited  $IC_{50}$  (mM) values ranging from  $0.262 \pm 0.037$  to  $1.520 \pm 0.039$ .

For quinazolinones **3a–3h** and **5a–5h**, the  $IC_{50}$  (mM) values spanned from  $0.191 \pm 0.011$  to  $1.520 \pm 0.039$ , and from  $0.172 \pm 0.004$  to  $0.752 \pm 0.041$ , respectively. Generally, it was observed that all *S*-arylated derivatives were more efficient than their thioxo precursors, except for derivatives **5c** and **5g**, which were less active than their counter substrates **3a** and **3g**, respectively; this may be attributed to the arylation of the *S*-atom by the 3-nitrobenzyl group.

Interestingly, among the derivatives of the **3a–h** series, the highest and the poorest scavenging efficiencies were associated with derivatives **3g** and **3b**, which share the 6-bromo-2-thioxo-2,3-dihydroquinazolin-4(1*H*)-one core, but differ in the type and location of the substituents on the 3-phenyl groups, where the former possessed 3-(4-nitrophenyl), whereas the latter possessed 3-(3-(trifluoromethyl)phenyl) moiety. Along this line, comparing the efficiencies of compounds **3a**, **3c** and **3b** having the 3-(3-(trifluoromethyl)phenyl) group and different substituents on the 2-thioxo-2,3-dihydroquinazolin-4(1*H*)-one core including 6-Cl, 6,7-di-MeO and 6-Br, respectively, revealed the superiority of compounds **3a** (8.0-fold) and **3c** (5.8-fold) to derivative **3b**. Furthermore, comparing the antiradical potencies of analogs **3b** and **3e** having exactly the same structure, but with the trifluoromethyl(CF<sub>3</sub>) substituent located at positions 3 and 4 on the 3-phenyl group, respectively, indicated that introducing CF<sub>3</sub> at position 4 enhanced the activity by 2.1-fold.

Additionally, comparing derivatives **3a**, **3d** and **3f**, which possessed the 6-chloro-2-thioxo-2,3-dihydroquinazolin-4(1*H*)-one nucleus, revealed that the 3-(3-CF<sub>3</sub>)phenyl group and the 3-(4-CF<sub>3</sub>)phenyl group enhanced the antioxidant potency by 3.6- and 1.4-fold, respectively, as compared to the 3-(4-NO<sub>2</sub>)phenyl substituent.

All of these observations indicated that in series **3a–h**, the combination of the 3-(3-(trifluoromethyl)phenyl) group with a 6-chloro-2-thioxo-2,3-dihydroquinazolin-4(1*H*)-one core improved the antiradical efficiency (as in case of **3a**). Contrarily, its combination with 6-bromo-2-thioxo-2,3-dihydroquinazolin-4(1*H*)-one core (as in case of **3b**) greatly reduced the activity, which was improved upon tethering the 4-chlorobenzyl moiety to the *S*-atom by 4.8-fold (as in case of **5b**). The weakest antioxidant in the **5a–h** series was **5h**, which possessed the 6,7-dimethoxy-3-(4-nitrophenyl)quinazolin-4(3*H*)-one core and lacked substituents at the *o* or *m*-positions on the 3-phenyl and the *S*-benzyl groups.

## 2.2.2. In Vitro Enzyme Inhibition Assays

### Cyclooxygenase-2 (COX-2) Assay

The inhibitory potential of compounds **3a–h** and **5a–h** towards the inducible pro-inflammatory COX-2 enzyme was examined at 0.100 and 0.200 mg/mL concentrations and the results are presented in Table 2.

Although the obtained data indicated that the inhibitory efficiency increased by duplicating the concentration of the tested compounds by 1.41- (**5c**) up to 2.58 (**5h**)-fold, only **3a** and **3g** exhibited potent inhibitory efficiencies of  $97.050 \pm 1.344$  and  $98.900 \pm 1.556\%$ , respectively, at 0.200 mg/mL (i.e., at 0.561 mM and 0.529 mM, respectively) as compared with the  $100.00 \pm 0.00\%$  inhibitory effectiveness of celecoxib at 0.10 mg/mL (0.262 mM). Moreover, at 0.200 mg/mL concentration, compound **5a** produced an inhibitory efficiency equal to  $63.150 \pm 5.869\%$  and the rest of the compounds exhibited poor inhibitory capabilities ranging from  $10.750 \pm 2.475$  to  $52.000 \pm 2.828\%$ .

**Table 2.** COX-2 inhibitory potency of the synthesized compounds expressed as mean % inhibition  $\pm$  SD of three independent replicates. The increase in inhibitory efficiency by duplicating the concentration was obtained by dividing the % inhibition at 0.200 mg/mL by the % inhibition at 0.100 mg/mL and was expressed in fold. Celecoxib was used as the reference COX-2 inhibitor at 0.1 mg/mL concentration.

Comp. #	Mean Values of % Inhibition $\pm$ SD	
	At 0.100 mg/mL	At 0.200 mg/mL (Fold)
<b>3a</b>	<b>57.000 <math>\pm</math> 2.828</b>	<b>97.050 <math>\pm</math> 1.344 (1.70)</b>
<b>3b</b>	6.250 $\pm$ 1.768	10.750 $\pm$ 2.475 (1.72)
<b>3c</b>	9.850 $\pm$ 1.626	20.200 $\pm$ 1.131(2.05)
<b>3d</b>	20.200 $\pm$ 1.131	32.750 $\pm$ 2.475 (1.62)
<b>3e</b>	10.400 $\pm$ 1.697	15.650 $\pm$ 0.494975 (1.50)
<b>3f</b>	11.450 $\pm$ 0.778	26.750 $\pm$ 3.889 (2.34)
<b>3g</b>	<b>60.000 <math>\pm</math> 2.828</b>	<b>98.900 <math>\pm</math> 1.556 (1.65)</b>
<b>3h</b>	14.550 $\pm$ 0.636	27.650 $\pm$ 2.192 (1.900)
<b>5a</b>	<b>34.200 <math>\pm</math> 1.697</b>	<b>63.150 <math>\pm</math> 5.869 (1.85)</b>
<b>5b</b>	9.250 $\pm$ 1.768	19.500 $\pm$ 2.121 (2.11)
<b>5c</b>	18.650 $\pm$ 3.465	26.250 $\pm$ 4.031 (1.41)
<b>5d</b>	26.300 $\pm$ 1.839	44.050 $\pm$ 1.344 (1.68)
<b>5e</b>	31.000 $\pm$ 2.828	51.650 $\pm$ 4.879 (1.67)
<b>5f</b>	28.900 $\pm$ 2.687	52.000 $\pm$ 2.828 (1.80)
<b>5g</b>	14.250 $\pm$ 1.768	26.000 $\pm$ 2.828 (1.83)
<b>5h</b>	11.200 $\pm$ 0.990	28.900 $\pm$ 0.283 (2.58)
Celecoxib at 0.1 mg/mL	<b>100.000 <math>\pm</math> 0.000</b>	<b>ND<sup>1</sup></b>

<sup>1</sup> ND: not determined.

#### Lactate Dehydrogenase A (LDHA) Assay

Furthermore, the studied compounds were assessed for their LDHA inhibitory potency (Table 3) at 0.100 and 0.200 mg/mL concentrations using sodium oxamate as the reference inhibitor. Again, the inhibitory efficiencies of the tested compounds at 0.200 mg/mL were increased by 0.20- (3c) up to 1.84 (3a)-fold than at the 0.100 mg/mL concentration. Also, each compound in the 3a–h series was found to be more active than its counterpart in the 5a–h series at both concentrations, except for derivative 3f (34.250  $\pm$  1.768%) and its S-alkylated product 5f (51.050  $\pm$  3.606%), which may indicate the importance of the NH group for LDHA inhibition.

Overall, derivatives 3g and 3a were recognized as the most active derivatives, with inhibitory efficiencies of 100.000  $\pm$  0.000 and 98.450  $\pm$  1.344 at 0.200 mg/mL (0.561 mM and 0.529 mM), respectively, as compared with the 100.000  $\pm$  0.000% inhibitory efficiency of sodium oxamate at 0.111 mg/mL (1 mM). Moreover, derivatives 3d and 5f demonstrated inhibitory effectiveness of 53.500  $\pm$  2.121% and 51.050  $\pm$  3.606% at 0.200 mg/mL (0.561 and 0.375 mM, respectively), whereas the rest of the compounds exerted inhibitory efficiencies ranging from 14.300  $\pm$  1.556 to 43.900  $\pm$  1.556%.

Although analogs 3a and 3d as well as 3b and 3e have exactly the same structure, except for locating the CF<sub>3</sub> group on the 3-phenyl moiety in each pair at positions 3 and 4, respectively, it was observed that the structures with 3-CF<sub>3</sub> were more potent than those with 4-CF<sub>3</sub>, implying the importance of this substituent at the position 3 for LDHA inhibition.

**Table 3.** LDHA inhibitory potency of the synthesized compounds at 0.1 mg/mL and 0.2 mg/mL concentrations expressed as mean % inhibition  $\pm$  SD of three independent replicates. The increase in inhibitory efficiency by duplicating the concentration was obtained by dividing the % inhibition at 0.200 mg/mL by % the inhibition at 0.100 mg/mL and was expressed in fold. Sodium oxamate was used as the reference drug at 0.111 mg/mL (1 mM) concentration.

Comp. #	Mean Values of % Inhibition $\pm$ SD	
	At 0.1 mg/mL	At 0.2 mg/mL (Fold Change as Compared to 0.1 mg/mL)
3a	53.500 $\pm$ 1.131	98.450 $\pm$ 1.344 (1.84)
3b	29.150 $\pm$ 2.192	42.350 $\pm$ 1.909 (1.45)
3c	17.800 $\pm$ 1.556	30.750 $\pm$ 1.7678 (0.2)
3d	33.500 $\pm$ 2.121	53.500 $\pm$ 2.121 (1.59)
3e	22.150 $\pm$ 1.202	35.950 $\pm$ 1.344 (1.62)
3f	21.500 $\pm$ 1.556	34.250 $\pm$ 1.768 (1.59)
3g	68.250 $\pm$ 4.596	100.000 $\pm$ 0.000 (1.7)
3h	29.850 $\pm$ 1.768	43.900 $\pm$ 1.556 (1.47)
5a	24.000 $\pm$ 1.697	38.900 $\pm$ 1.131 (1.62)
5b	14.500 $\pm$ 1.131	22.500 $\pm$ 1.697 (1.55)
5c	8.550 $\pm$ 1.061	14.300 $\pm$ 1.556 (1.67)
5d	13.850 $\pm$ 2.051	20.400 $\pm$ 1.980 (1.47)
5e	15.150 $\pm$ 1.768	19.650 $\pm$ 2.334 (1.29)
5f	31.950 $\pm$ 2.475	51.050 $\pm$ 3.606 (1.60)
5g	15.750 $\pm$ 2.050	27.700 $\pm$ 2.546 (1.75)
5h	15.350 $\pm$ 1.202	21.750 $\pm$ 1.344 (1.42)
Sodium Oxamate at 0.111 mg/mL (1 mM)	100.000 $\pm$ 0.000	ND <sup>1</sup>

<sup>1</sup> ND: not determined.

In the view of the COX-2 and LDHA inhibitory assays, the IC<sub>50</sub> values in  $\mu$ g/mL and ( $\mu$ M) for the most active compounds, **3a** and **3g**, were determined to be 281.374  $\pm$  10.545 and 251.780  $\pm$  22.023 against COX-2, respectively, as compared with 0.136  $\times$  10<sup>-3</sup>  $\pm$  0.006  $\times$  10<sup>-3</sup> for celecoxib. Likewise, the IC<sub>50</sub> values against LDHA were calculated to be 273.345  $\pm$  16.087 and 242.279  $\pm$  31.298, respectively, compared to 140.503  $\pm$  7.647 by sodium oxamate, as presented in Table 4.

**Table 4.** Mean IC<sub>50</sub> values of the potential COX-2 and LDHA inhibitors and their reference inhibitors, celecoxib and sodium oxamate, respectively, in  $\mu$ g/mL ( $\mu$ M)  $\pm$  SD of three independent replicates.

Comp. # (MW)	Mean IC <sub>50</sub> Values in $\mu$ g/mL $\pm$ SD/( $\mu$ M $\pm$ SD)	
	COX-2	LDHA
3a (356.75)	100.380 $\pm$ 3.762/ (281.374 $\pm$ 10.545)	97.516 $\pm$ 5.739/ (273.345 $\pm$ 16.087)
3g (378.20)	95.223 $\pm$ 8.329/ (251.780 $\pm$ 22.023)	91.630 $\pm$ 11.837/ (242.279 $\pm$ 31.298)
Celecoxib (381.373)	0.0517 $\times$ 10 <sup>-3</sup> $\pm$ 0.0021 $\times$ 10 <sup>-3</sup> / (0.136 $\times$ 10 <sup>-3</sup> $\pm$ 0.006 $\times$ 10 <sup>-3</sup> )	ND <sup>1</sup>
Sodium oxamate (111.03)	ND <sup>1</sup>	15.600 $\pm$ 0.849/ (140.503 $\pm$ 7.647)

<sup>1</sup> ND: not determined.

#### Alpha-Glucosidase (AG) and Alpha-Amylase (AA) Assays

The studied compounds were evaluated in vitro for their AG and AA inhibitory activities via the determination of their IC<sub>50</sub> values in  $\mu$ g/mL and  $\mu$ M, which were compared with quercetin as the reference drug (Table 5).

**Table 5.**  $\alpha$ -Glucosidase and  $\alpha$ -amylase inhibitory potencies of the synthesized compounds expressed as mean  $IC_{50}$  values  $\pm$  SD of three independent replicates. Quercetin was used as the reference inhibitor.

Comp. # (MW)	Mean $IC_{50}$ Values in $\mu\text{g/mL} \pm \text{SD}$ ( $\mu\text{M} \pm \text{SD}$ )	
	$\alpha$ -Glucosidase (AG)	$\alpha$ -Amylase (AA)
<b>3a</b> (356.75)	11.200 $\pm$ 0.300 (31.395 $\pm$ 0.841)	<b>124.333 <math>\pm</math> 4.042 (348.516 <math>\pm</math> 11.330)</b>
<b>3b</b> (401.20)	26.033 $\pm$ 0.503 (64.888 $\pm$ 1.254)	17171.333 $\pm$ 4.163 (427.051 $\pm$ 10.376)
<b>3c</b> (382.36)	7.867 $\pm$ 0.306 (20.5 $\pm$ 0.800)	<b>92.000 <math>\pm</math> 3.000 (240.611 <math>\pm</math> 7.846)</b>
<b>3d</b> (356.75)	37.200 $\pm$ 0.361 (104.275 $\pm$ 1.012)	335.667 $\pm$ 3.055 (940.903 $\pm$ 8.563)
<b>3e</b> (401.20)	30.500 $\pm$ 0.819 (76.022 $\pm$ 2.041)	252.00 $\pm$ 4.583 (628.116 $\pm$ 11.423)
<b>3f</b> (333.75)	5.233 $\pm$ 0.153 (15.679 $\pm$ 0.458)	<b>111.667 <math>\pm</math> 3.512 (334.583 <math>\pm</math> 10.523)</b>
<b>3g</b> (378.20)	12.500 $\pm$ 0.889 (33.051 $\pm$ 2.351)	179.333 $\pm$ 7.768 (474.175 $\pm$ 20.539)
<b>3h</b> (359.36)	<b>4.633 <math>\pm</math> 0.153 (12.882 <math>\pm</math> 0.426)</b>	<b>122.000 <math>\pm</math> 4.583 (339.492 <math>\pm</math> 12.753)</b>
<b>5a</b> (464.86)	<b>5.833 <math>\pm</math> 0.252 (12.548 <math>\pm</math> 0.542)</b>	<b>86.667 <math>\pm</math> 4.509 (186.437 <math>\pm</math> 9.700)</b>
<b>5b</b> (525.77)	37.033 $\pm$ 0.252 (70.436 $\pm$ 4.793)	<b>162.000 <math>\pm</math> 5.568 (308.120 <math>\pm</math> 10.590)</b>
<b>5c</b> (517.48)	41.367 $\pm$ 1.002 (79.939 $\pm$ 1.936)	<b>197.333 <math>\pm</math> 4.509 (381.335 <math>\pm</math> 8.713)</b>
<b>5d</b> (481.31)	38.100 $\pm$ 0.656 (79.159 $\pm$ 1.363)	<b>181.667 <math>\pm</math> 5.508 (377.443 <math>\pm</math> 11.444)</b>
<b>5e</b> (600.25)	43.133 $\pm$ 2.055 (71.858 $\pm$ 3.424)	<b>150.333 <math>\pm</math> 3.512 (250.451 <math>\pm</math> 5.851)</b>
<b>5f</b> (532.79)	23.600 $\pm$ 0.400 (44.295 $\pm$ 0.751)	<b>106.667 <math>\pm</math> 5.033 (200.205 <math>\pm</math> 9.446)</b>
<b>5g</b> (513.32)	20.633 $\pm$ 0.737 (40.195 $\pm$ 1.436)	339.000 $\pm$ 4.000 (660.407 $\pm$ 7.792)
<b>5h</b> (483.92)	<b>6.100 <math>\pm</math> 0.458 (12.605 <math>\pm</math> 0.946)</b>	<b>117.667 <math>\pm</math> 3.055 (243.154 <math>\pm</math> 6.313)</b>
Quercetin (302.236)	<b>3.967 <math>\pm</math> 0.208 (13.126 <math>\pm</math> 0.688)</b>	<b>121.667 <math>\pm</math> 3.055 (402.566 <math>\pm</math> 10.108)</b>

The results showed that the tested compounds exhibited  $IC_{50}$  values ( $\mu\text{M}$ ) ranging from 12.548  $\pm$  0.542 to 104.275  $\pm$  1.012 against AG, and ranging from 186.437  $\pm$  9.700 to 940.903  $\pm$  8.978.563 against AA, compared with 13.126  $\pm$  0.688 and 402.566  $\pm$  10.108 for quercetin, respectively. Accordingly, derivatives **3h**, **5a** and **5h** were proven to be more potent AG inhibitors than quercetin. Congruently, eleven derivatives, **3a**, **3c**, **3f**, **3h** and **5a–5f**, as well as **5h**, exhibited superior inhibitory efficiencies (lowered  $IC_{50}$  in  $\mu\text{M} \pm \text{SD}$ , ranging from 186.437  $\pm$  9.700 by **5a** to 381.335  $\pm$  8.713 by **5c**) to that of quercetin against AA. In addition, compound **3b** exhibited a modest potency against AA, with an  $IC_{50}$  value of 427.051  $\pm$  10.376  $\mu\text{M}$ .

Overall, compounds **3h**, **5a** and **5h** were recognized as dual inhibitors for AG and AA; thus, they would have the potential as hypoglycemic and anti-DM-type 2 agents.

It is noticeable that the dual inhibitors **3h** and **5h** possessed the same 6,7-dimethoxy-3-(4-nitrophenyl)quinazolin-4(3H)-one core, implying the importance of this moiety for the inhibition of both enzymes.

With regard to derivatives **3a** and **5a**, which possessed the 6-chloro-3-(3-(trifluoromethyl)phenyl)quinazolin-4(3H)-one core, only **5a** was found to be efficient against AG, which implies the importance of the 2-fluorobenzyl group for the inhibition of the AG enzyme.

Moreover, the dual inhibitor **5a** is also a potent radical scavenger; therefore, it may contribute to antidiabetic activities both directly, through inhibiting AA and AG, and indirectly, via its antioxidant properties.

### 2.2.3. Cytotoxic Activity

The anticancer activities of all the synthesized compounds were assessed against two human colon carcinoma cell lines, namely LoVo and HCT-116 (Table 6), via the determination of the mean percents of the viable cancerous cells remaining after being incubated with 200  $\mu\text{g/mL}$  of each test compound for 48 h using LDH assay [73].

**Table 6.** Cytotoxic effects of the synthesized compounds on LoVo and HCT-116 human colon carcinoma cell lines expressed as mean % of viable cells after being treated with 200 µg/mL of the test compounds for 48 h ± SD of three independent assays. Assay medium and 0.1% Triton X-100 were used as negative and positive control experiments, respectively. The cytotoxic effects of the potential antiproliferative candidates were further assessed on non-tumoral human umbilical vein endothelial cells (HUVEC) at the same concentration.

Comp. #	Mean % of Viable Cells ± SD		
	LoVo	HCT-116	HUVEC
<b>3a</b>	<b>23.500 ± 1.500</b>	<b>26.833 ± 1.258</b>	<b>97.000 ± 2.646</b>
<b>3b</b>	62.000 ± 3.606	70.667 ± 2.517	ND <sup>1</sup>
<b>3c</b>	<b>47.333 ± 2.517</b>	65.000 ± 3.606	<b>99.667 ± 0.577</b>
<b>3d</b>	87.000 ± 1.732	96.000 ± 1.732	ND <sup>1</sup>
<b>3e</b>	90.667 ± 3.512	92.333 ± 2.517	ND <sup>1</sup>
<b>3f</b>	<b>22.667 ± 2.082</b>	<b>4.667 ± 0.577</b>	<b>99.667 ± 0.577</b>
<b>3g</b>	55.667 ± 3.055	<b>42.333 ± 2.517</b>	<b>98.667 ± 1.155</b>
<b>3h</b>	64.000 ± 3.000	70.333 ± 3.786	ND <sup>1</sup>
<b>5a</b>	90.333 ± 1.528	89.667 ± 3.055	ND <sup>1</sup>
<b>5b</b>	<b>37.667 ± 2.517</b>	60.333 ± 2.517	<b>96.333 ± 0.577</b>
<b>5c</b>	78.333 ± 3.512	82.333 ± 2.517	ND <sup>1</sup>
<b>5d</b>	76.000 ± 1.732	86.667 ± 1.528	ND <sup>1</sup>
<b>5e</b>	64.333 ± 2.082	79.667 ± 2.517	ND <sup>1</sup>
<b>5f</b>	84.333 ± 3.512	76.000 ± 1.732	ND <sup>1</sup>
<b>5g</b>	74.667 ± 2.517	66.333 ± 3.055	ND <sup>1</sup>
<b>5h</b>	81.667 ± 3.055	91.000 ± 2.646	ND <sup>1</sup>
Positive Control (Triton X-100, 0.1%)	0.000	0.000	ND <sup>1</sup>
Negative Control (Assay medium) 5-FU	99.500 ± 0.707	100.000 ± 0.000	57.333 ± 2.517

<sup>1</sup> ND: not determined.

The results shown in Table 6 indicated that **3a** and **3f** were the most active derivatives against both cell lines by reducing their viability percents to 23.500 ± 1.500 and 22.667 ± 2.082% (LoVo) and 26.833 ± 1.258 and 4.667 ± 0.577% (HCT-116), respectively. Three other compounds, namely **3g** (against HCT-116) and **3c** and **5b** (against LoVo) showed moderate antiproliferative effects with viability % of 42.333 ± 2.517, 47.333 ± 2.517 and 37.667 ± 2.517, respectively. The rest of the compounds demonstrated poor cytotoxic profiles, with viability percentages ranging from 55.667 ± 3.055 to 90.667 ± 3.512 (LoVo cells) and from 60.333 ± 2.517 to 96.000 ± 1.732 (HCT-116 cells).

Accordingly, the cytotoxic effects of the compounds **3a**, **3c**, **3f**, **3g** and **5b**, which showed growth inhibitory efficiencies of less than 50% on one or both tumoral cells, were determined at the same test concentration against non-tumoral human umbilical vein endothelial cells (HUVEC) and were found to be 97.000 ± 2.646, 99.667 ± 0.577, 99.667 ± 0.577, 98.667 ± 1.155 and 96.333 ± 0.577, respectively, as compared to 57.333 ± 2.517% exerted by 5-fluorouracil (**5-FU**), the reference anticancer drug (Table 6).

Based on the results of the viability assays, the IC<sub>50</sub> values for the most active cytotoxic candidates, **3a**, **3c**, **3f**, **3g** and **5b**, in µg/mL (µM) were calculated from the concentration–response curves and compared with that of **5-FU**, as shown in Table 7.

It is noteworthy to indicate that the viability of the normal HUVEC upon being treated with 200 µg/mL (1537.515 µM) of **5-FU** was reduced to 57.333 ± 2.517% and its IC<sub>50</sub> was determined to be 298.500 ± 19.092 µg/mL (2294 ± 146.77 µM). On the other hand, the IC<sub>50</sub> values (µg/mL) of **5-FU** were calculated to be 2.910 ± 0.028 (LoVo) and 11.850 ± 0.354 (HCT-116), implying its higher selectivity towards the examined cancerous cells, as indicated by the calculated selectivity indices (SIs, represent the ratio of IC<sub>50 normal cell</sub> to IC<sub>50 cell line</sub>) [74], which were equal to 102.577 (LoVo) and 25.190 (HCT-116), respectively.



**Table 7.** Mean IC<sub>50</sub> values of the compounds, which exhibited cell viabilities of less than 50%, expressed in µg/mL (µM) ± SD of three independent replicates. 5-Flurouracil was used as the reference drug.

Comp. # (MW)	Mean IC <sub>50</sub> Values in µg/mL/(µM) ± SD		
	LoVo cells	HCT-116 cells	HUVEC
<b>3a</b> (356.75)	105.000 ± 3.000/ (294.324 ± 8.409)	106.333 ± 4.726/ (298.060 ± 13.247)	
<b>3c</b> (382.36)	275.333 ± 4.509/ (720.088 ± 11.792)	281.000 ± 3.606/ (734.910 ± 9.431)	
<b>3f</b> (333.75)	128.000 ± 3.000/ (383.521 ± 8.989)	108.000 ± 1.000 (323.596 ± 2.996)	
<b>3g</b> (378.20)	221.667 ± 3.512/ (586.111 ± 9.286)	168.333 ± 3.512/ (444.090 ± 9.286)	
<b>5b</b> (525.77)	161.000 ± 3.606/ (306.218 ± 6.859)	246.000 ± 1.732/ (467.885 ± 3.294)	
5-FU (130.08)	2.910 ± 0.028/ (22.371 ± 0.215)	11.850 ± 0.354/ (91.098 ± 2.721)	298.500 ± 19.092 (2294 ± 146.77)

#### 2.2.4. Investigation of the Apoptosis-Inducing Properties as a Potential Molecular Basis for the Observed Cytotoxicity for Derivatives **3a** and **3f**

##### Effects of **3a** and **3f** on the Expressional Levels of Bcl-2 and Bax, Regulators of the Intrinsic Pathway

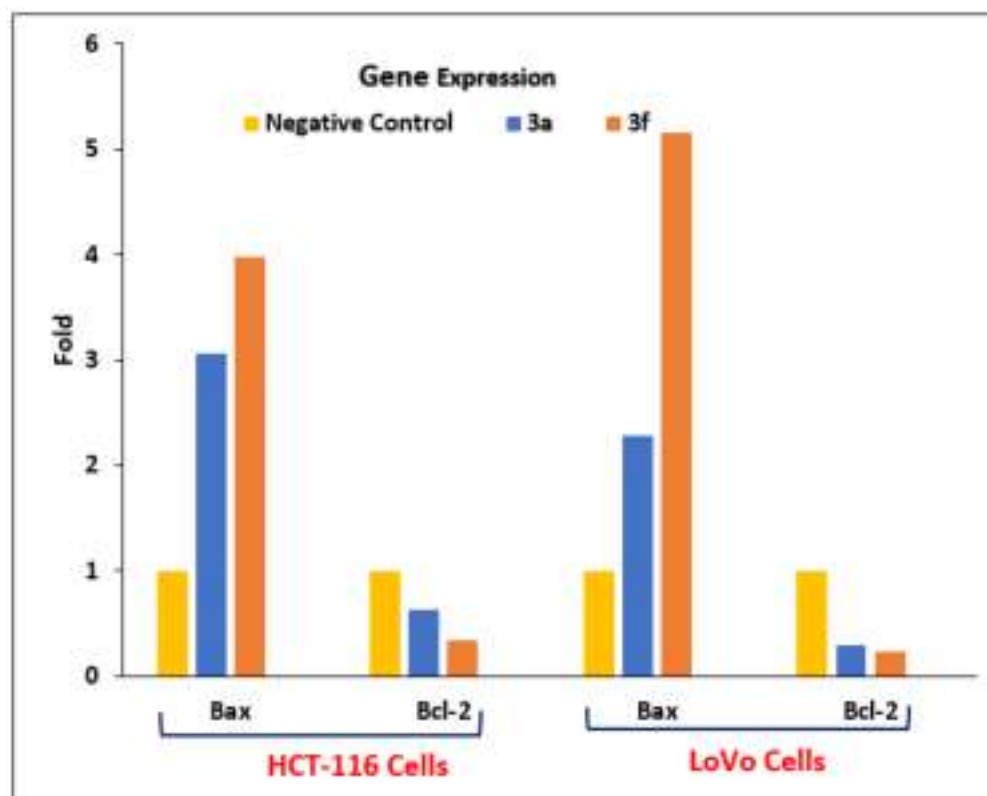
Collectively, the viability assays showed that derivatives **3a** and **3f** were the most active cytotoxic derivatives against both tested colon cell lines. However, the enzymatic inhibitory assays showed that only **3a** was active against COX-2 and LDHA; in addition, it is documented that HCT-116 cells are COX-2 negative [75]. Consequently, these observations imply that molecular targets other than COX-2 and LDHA could be responsible for the observed cytotoxicity on the tested cancerous cells.

Impaired apoptosis plays a main role in cancer cell survival, tumor progression and resistance to chemotherapy. In particular, the inhibition of the intrinsic apoptotic pathway depends partly on disturbing the balance between the expression of the Bcl-2 and Bax genes. Bcl-2 protein is a member of the anti-apoptotic (pro-survival) subgroup, and its expressional level in tumor cells is much higher than in normal cells; therefore, molecules targeting this protein would have little effect on normal cells [56]. On the other hand, Bax is a proapoptotic protein, whose overexpression induced by several agents enhances apoptosis, but its loss contributes to drug resistance in human cancers [76].

Bcl-2 inhibits apoptosis by forming a heterodimer with Bax or by inhibiting the activities of caspase-9, 3, 6, and 7, resulting in a prolonged survival time of tumor cells, thus causing their malignant transformation [56]. On the other hand, the activated Bax levels promote cell apoptosis by binding to the mitochondrial membranes, and increasing their permeability and cytochrome c releasing [77].

Considering these facts, enhancing apoptosis has been extensively studied as a potential drug target in cancer therapy [78], therefore, in this study, we investigated the effects of the most cytotoxic compounds, **3a** and **3f**, (at 10 µg/mL, 24 h incubation) on the expressional levels of these apoptotic regulator genes (Bax and Bcl-2) using quantitative reverse transcription–polymerase chain reactions (qRT-PCR).

The results were compared with the negative control (untreated cells) cultures. The recorded results (Figure 3) in the expressional level of anti-apoptotic gene Bcl-2 (by 0.635- and 0.345-fold) in the **3a**- and **3f**-treated HCT-116 cell cultures, respectively, as compared to negative control culture.



**Figure 3.** qRT-PCR analysis of the expressional levels of Bax and Bcl2 genes in cultures of LoVo and HCT-116 treated with 10 µg/mL of the cytotoxic candidates 3a and 3f for 24 h, as compared to negative control (untreated cells).

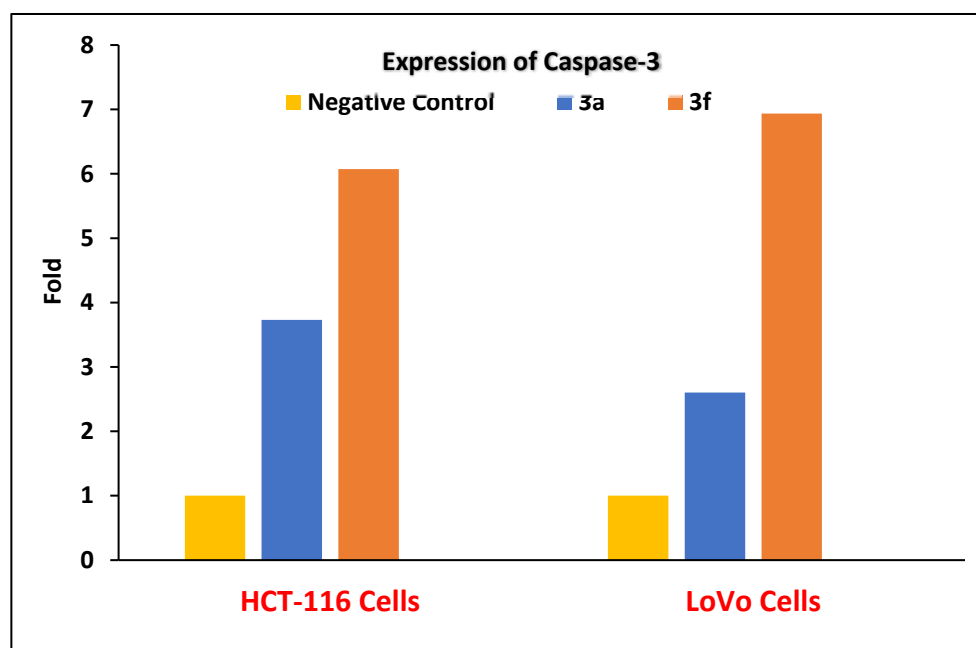
#### Caspases Activation Induced by Derivatives 3a and 3f

The two distinctive apoptotic pathways converge on caspases activation. The extrinsic apoptosis pathway is mediated by the death receptor, while the intrinsic mitochondrial pathway is triggered via the interaction of cytochrome c with apoptotic protease activating factor-1 (APAF1) resulting activation of caspases [79]. In general, caspase -9 is activated by cytochrome c, released by the mitochondria in the intrinsic pathway, while the extrinsic pathway activates caspase-8. After the activation of these initiator caspases (-8 and -9), the effector step of apoptosis is then triggered by the activation of caspases -3, -6 and -7. The activities of these effectors induce observed morphological changes in the apoptotic cells, especially DNA fragmentation, after chromatin condensation and the apoptotic bodies' formation [80].

Therefore, in this study the expressional levels of caspase-3 as a major apoptosis effector were evaluated in 3a- and 3f-treated HCT-116 and LoVo cell cultures (10 µg/mL, for 24 h incubation), using qRT-PCR analysis. As shown in Figure 4, the expression levels of this gene were upregulated by 3.731- and 6.071-fold (in HCT-116), and by 2.6026- and 6.9340-fold (in LoVo) after treatment by 3a and 3f, respectively, as compared to the negative control culture.

Furthermore, in order to confirm the implication of these compounds in the apoptotic pathways triggered by caspases, the proteins levels of caspases 8 and 9 were evaluated using Western blot analysis for the HCT-116 and LoVo carcinoma cells lysates after treatment with compounds 3a and 3f (50 µg/mL for 48 h); the untreated cells were used as a negative control.

HCT-116 and LoVo carcinoma cells lysates were prepared for the Western blot analysis of caspase-8 and caspase-9.

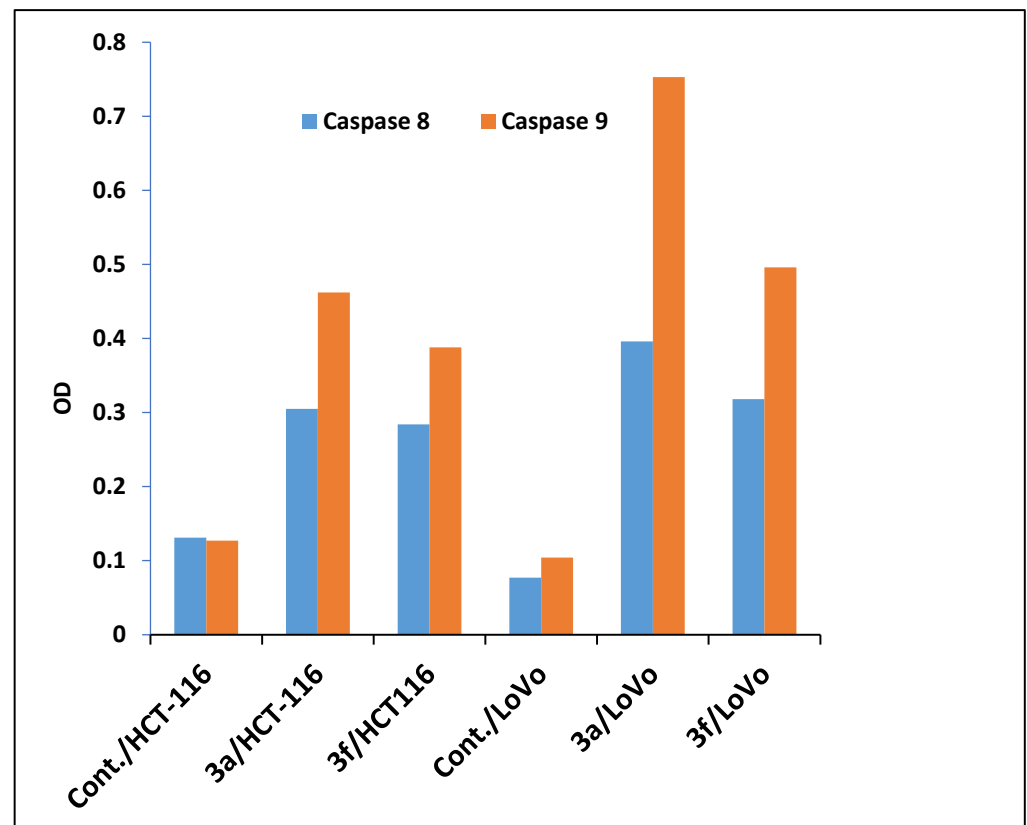


**Figure 4.** qRT-PCR analysis of the expressional levels of caspase-3 gene in cultures of LoVo and HCT-116 treated with 10  $\mu\text{g}/\text{mL}$  of the cytotoxic candidates **3a** and **3f** for 24 h, as compared to negative control (untreated cells).

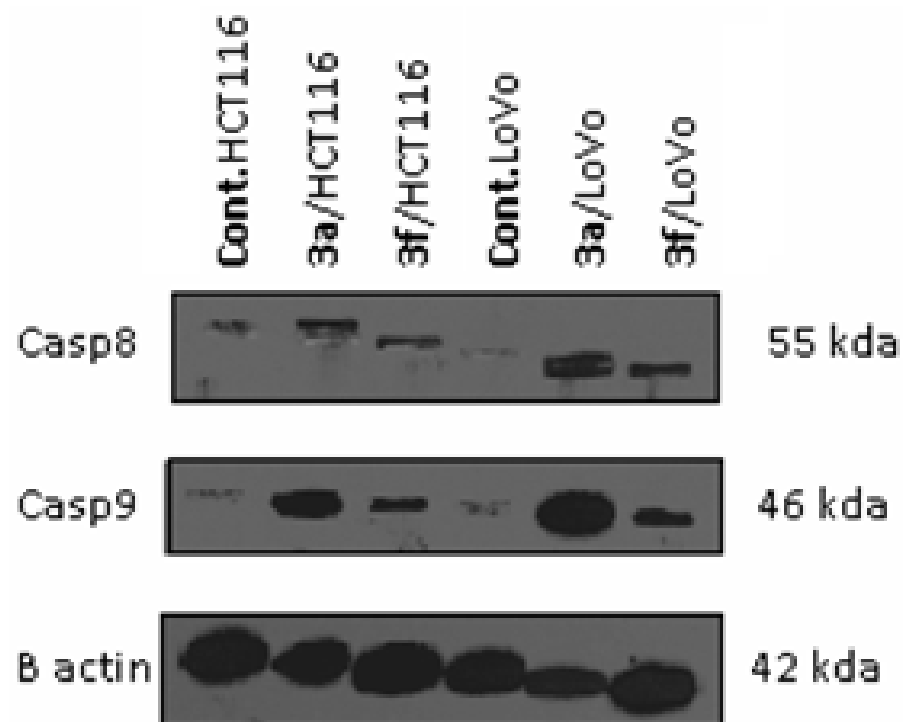
Compared to the negative control (untreated cells), compounds **3a** and **3f** induced higher expressional levels of caspase-9 with the HCT-116 and LoVo cells than that of caspase-8 in both cultures. The increase in the expressional level of caspase 8 ranged between 2.3 and 2.2 times in the lysates of HCT-116, and between 5.1 and 4.1 times in the lysates of the LoVo cells following a 48 h treatment with **3a** and **3f**, respectively, whereas the expression levels of caspase-9 increased by 3.6 and 3.1 times in the lysates of HCT-116, and between 7.2 and 4.8 times in the lysates of the LoVo cells (Figures 5 and 6). Thus, both proteins were more activated in the cultures of LoVo cells than those of the HCT-116 cells. These results clearly demonstrate that compounds **3a** and **3f** are apoptogenic molecules that are able to induce apoptosis in HCT-116 and LoVo colon cancer cells, predominantly through the intrinsic pathway. Indeed, the caspase-8 levels confirmed that apoptotic cell death caused by **3a** and **3f** was triggered through the extrinsic-mediated pathway, whereby the ligand–receptor binding activated caspase-8. The mitochondrial intrinsic-mediated pathway of apoptosis is also activated in HCT-116 and LoVo-treated cells through the release of high levels of caspase-9 [81]. Both pathways eventually meet up and lead to the hierarchical activation of caspases -3, 6 and 7, which are responsible for the morphological changes in apoptotic cells.

#### Annexin-V Externalization Induced by Compounds **3a** and **3f**

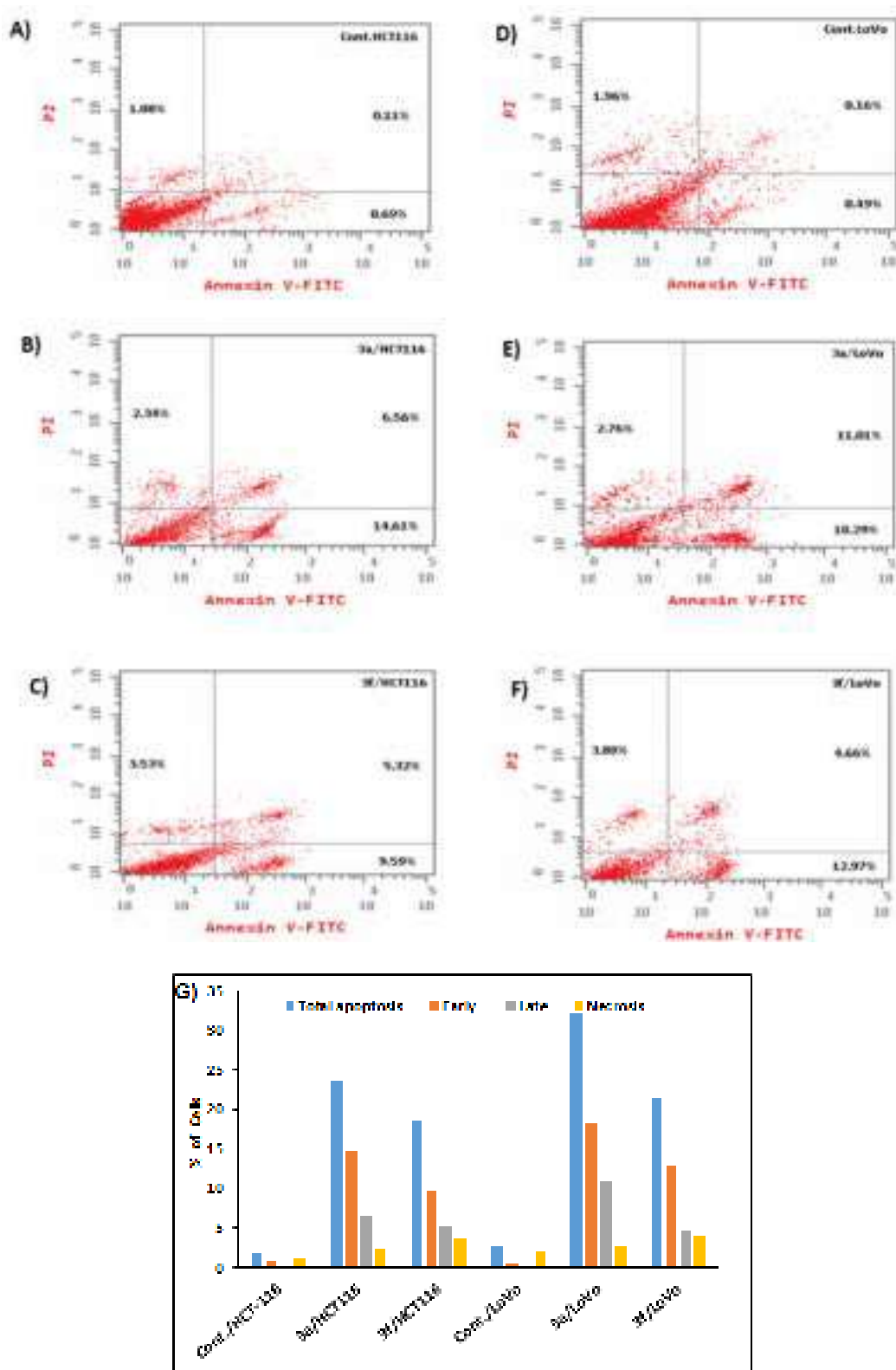
In order to examine the effect of compounds **3a** and **3f** on the apoptosis of HCT-116 and LoVo carcinoma cells, the Annexin-V-FITC probe was used and flow cytometry analyses were performed (Figure 7).



**Figure 5.** Expressional levels of caspase-8 and caspase-9 in lysates of HCT-116 and LoVo carcinoma cells following treatment with 50  $\mu\text{g}/\text{mL}$  of the compounds 3a and 3f for 48 h.



**Figure 6.** Effects of 3a and 3f compounds on protein expressional levels of caspases-8 and 9 after a 48 h treatment of the cells with 50  $\mu\text{g}/\text{mL}$  of each compound via immunoblotting, using polyclonal antibodies against caspases -8 and -9.  $\beta$ -Actin was used as the protein loading control.



**Figure 7.** Apoptosis rates of HCT-116 and LoVo cells treated with 50  $\mu\text{g}/\text{mL}$  of compounds **3a** and **3f**, detected via flow cytometry, after 48 h treatment (A) Untreated HCT-116 cells; (B,C) treated HCT-116 cells with 50  $\mu\text{g}/\text{mL}$  of compounds **3a** and **3f**, respectively. (D) Non treated LoVo cells; (E,F) LoVo cells treated with 50  $\mu\text{g}/\text{mL}$  of compounds **3a** and **3f**, respectively. (G) Quantification of the apoptosis rate in HCT-116 and LoVo cells undergoing early and late apoptosis detected via Annexin V-FITC/PI dual-staining flow cytometry.

The percentages of the early apoptotic cells (Annexin-V positive and propidium iodide, PI negative) and late apoptotic cells (both Annexin-V and PI positive) were then calculated. Annexin V-PI staining was also performed to distinguish apoptotic and necrotic cell deaths. The data showed that compounds **3a** and **3f** in each cell line caused more apoptotic cell death rather than necrosis (Figure 7G), since necrotic cells represent less than 5% of the total cells' population. The late apoptotic percentages of the HCT-116 cells was increased to 6.56% (Figure 7B) and 5.32% (Figure 7C) after treatment with **3a** and **3f**, respectively, for 48 h, compared with the untreated cells (Figure 7A).

Similarly, the late apoptotic percentages of the LoVo cells treated with **3a** and **3f** were increased to 11.01% (Figure 7E) and 4.66% (Figure 7F), respectively, while the percentage of the untreated LoVo cells was only 0.16% (Figure 7D). The early apoptotic populations were augmented to 14.6% (Figure 7B) and 18.29% (Figure 7E) for the HCT-116 and LoVo cells treated with compound **3a**, respectively. After the 48 h treatment with **3f**, the percentages of the early apoptotic population of the HCT-116 and LoVo cells reached 9.59% (Figure 7C) and 12.97% (Figure 7F), respectively. These observations clearly imply that compounds **3a** and **3f** effectively induced apoptosis in both tested colon carcinoma cell lines.

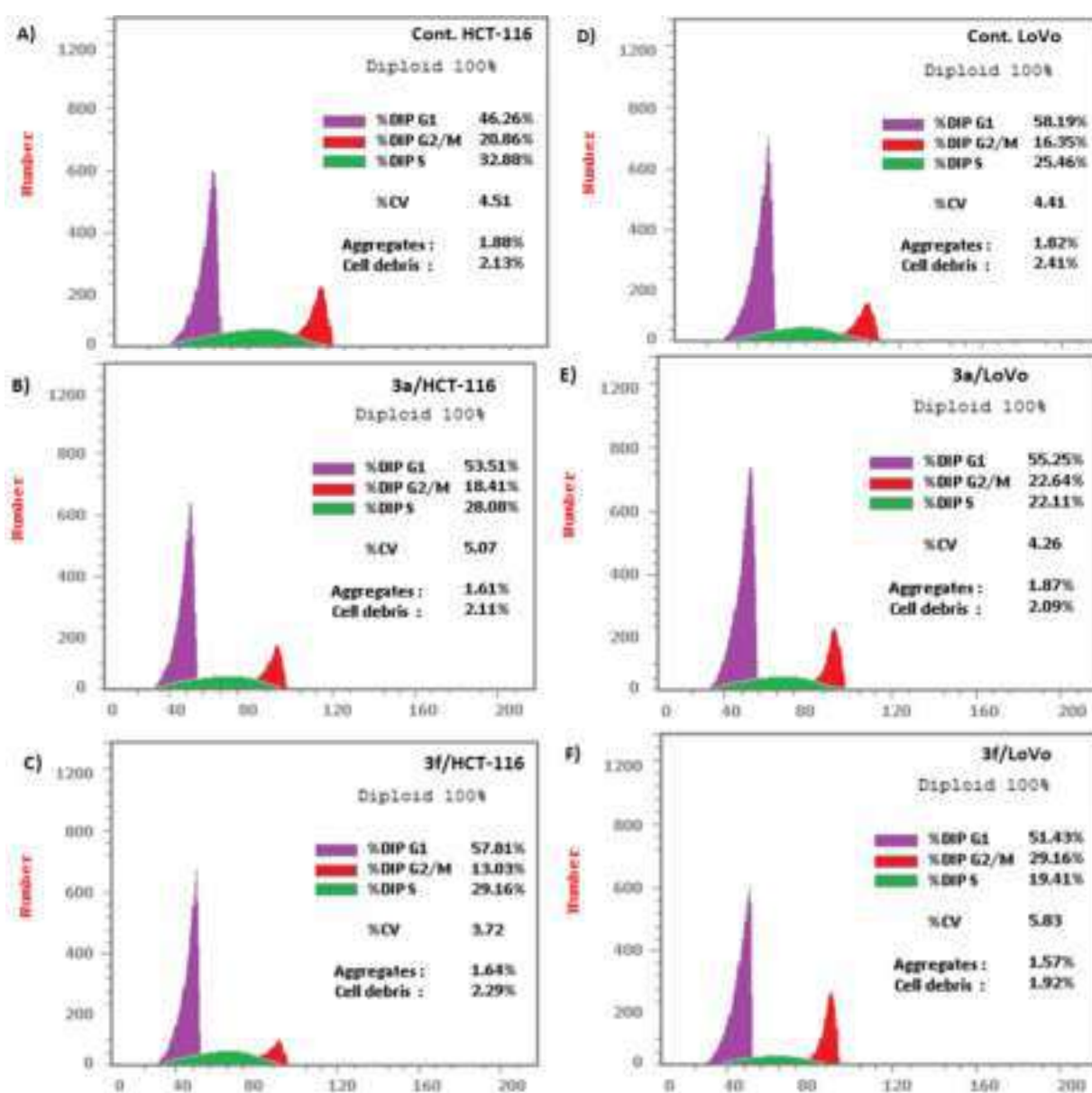
#### Compounds **3a** and **3f** Induced Apoptosis in HCT-116 and LoVo Carcinoma Cells Associated with Cell Cycle Arrest

The viability of the cells is maintained by a complete cell cycle life, which is generally developed in the order of the G1-S-G2-M phases. When DNA integrity is impaired by certain factors, cells cannot pass through the G1/S phase and/or the G2/M detection points, and cell proliferation is eventually blocked [82].

In the current study, the cell cycle distribution of the treated HCT-116 and LoVo carcinoma cells with compounds **3a** and **3f** was assessed by labeling the cell's DNA with PI stain in order to determine if the induction of apoptosis in carcinoma cells could be related to the cell cycle arrest (Figure 8A–F). The intensity of the PI stain is proportional to the cell's DNA content (Figure 9). As shown in Figure 8, there was a significant G1 phase arrest in the HCT-116 cells after the 48 h treatment with **3a** and **3f**, where the percentage of the cells at this phase significantly increased from 46.26% (untreated negative control, Figure 8A) to 53.51% and 57.81%, respectively, as shown in Figure 8B,C. Likewise, for the LoVo cell derivatives, **3a** and **3f** induced cell cycle arrest in the G2/M phase, wherein the percentage of the cells' population in the G2/M phase increased to 22.64% (Figure 8E) and 29.16% (Figure 8F), respectively, compared to the untreated cells (16.35%). The ability of the tested compounds (**3a** and **3f**) to block the cell cycle progression in LoVo and HCT-116 cells confirmed their anticancer potential against these colon carcinoma cell lines and could explain the mechanism of the observed cytotoxicity.

#### 2.3. Molecular Docking Simulations

In order to confirm the results concluded from the in vitro enzymatic inhibitory assays, molecular docking studies were performed. Thus, the relative binding affinities, binding interactions and conformations of the most active candidates within the active sites of their target proteins were identified.



**Figure 8.** Flow cytometry analysis of cell cycle distribution changes of HCT-116 and LoVo cells treated with 50 µg/mL of compounds **3a** and **3f** over 48 h. (A) Control HCT-116; (B) treated HCT-116 with **3a**; (C) treated HCT-116 with **3f**; (D) control LoVo; (E) treated LoVo with **3a**; (F) treated LoVo with **3f**.

### 2.3.1. Docking against Human Pancreatic Alpha-Amylase (HPA; PDB ID: 3BAJ)

Representative examples for the most active AA inhibitors from the **3a–h** and **5a–h** series, namely **3c**, **3f**, **3h**, **5a**, **5f** and **5h**, as well as the reference inhibitor quercetin and the co-crystal ligand acarbose, were docked against human pancreatic alpha-amylase (PDB ID: 3BAJ) [83] using AutoDock 4.2.2 with a Lamarckian genetic algorithm-implemented program suite.

Initially, the docking protocol was validated by redocking the co-crystal ligand, **acarbose**, within the active site, with a cutoff of root mean square positional deviation (RMSD) < 2 Å (Figure 10) [84].

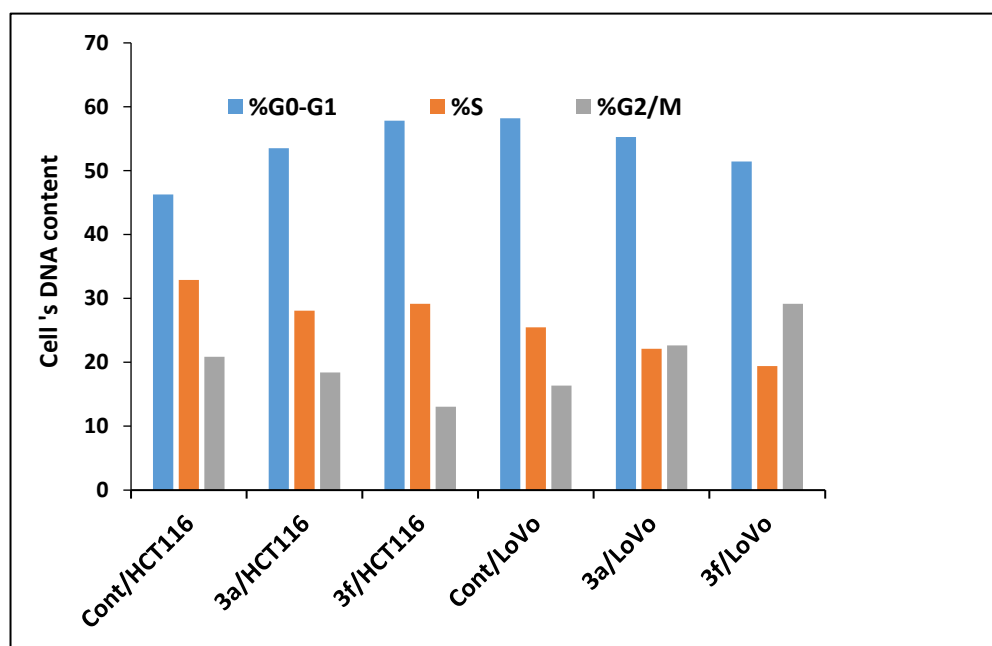


Figure 9. Quantification of the cell cycle distribution of HCT-116 and LoVo cells.

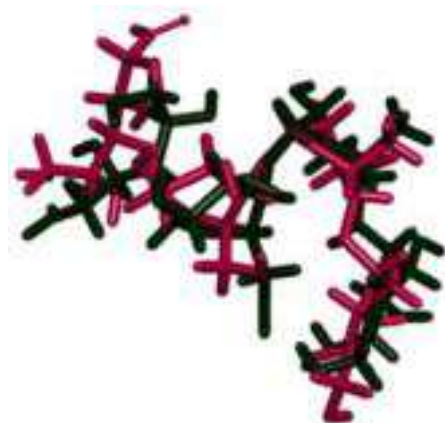


Figure 10. The validation of the accuracy and performance of the docking protocol by redocking acarbose ligands in pink and green within the active site of HPA.

The analysis of the results of the docking simulations clearly showed that the studied compounds fitted nicely within the active site and formed hydrogen bonds, Van der Waals,  $\pi$ - $\pi$  stacking and alkyl and  $\pi$ -alkyl interactions with the active site amino acid residues (Figure 11). Their binding free energies (Table 8) were ranged from  $-8.4$  to  $-9.1$  kcal/mol as compared to  $-9.3$  and  $-5.4$  kcal/mol for quercetin and acarbose, respectively, indicating a considerable affinity between the docked quinazolinones and the enzyme alpha-amylase.

Table 8. Binding free energies of the docked conformations of the studied compounds in the active sites of  $\alpha$ -Amylase (AA) and  $\alpha$ -Glucosidase (AG).

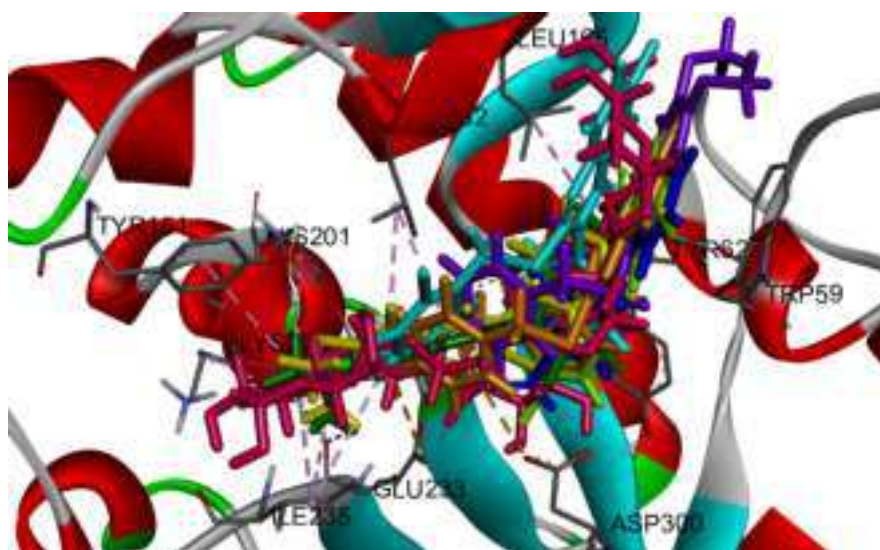
Comp.#	Binding Energies (kcal/mol)	
	$\alpha$ -Amylase	$\alpha$ -Glucosidase
3c	$-8.7$	$-5.6$
3f	$-8.4$	$-5.2$
3h	$-9.1$	$-4.8$



Table 8. Cont.

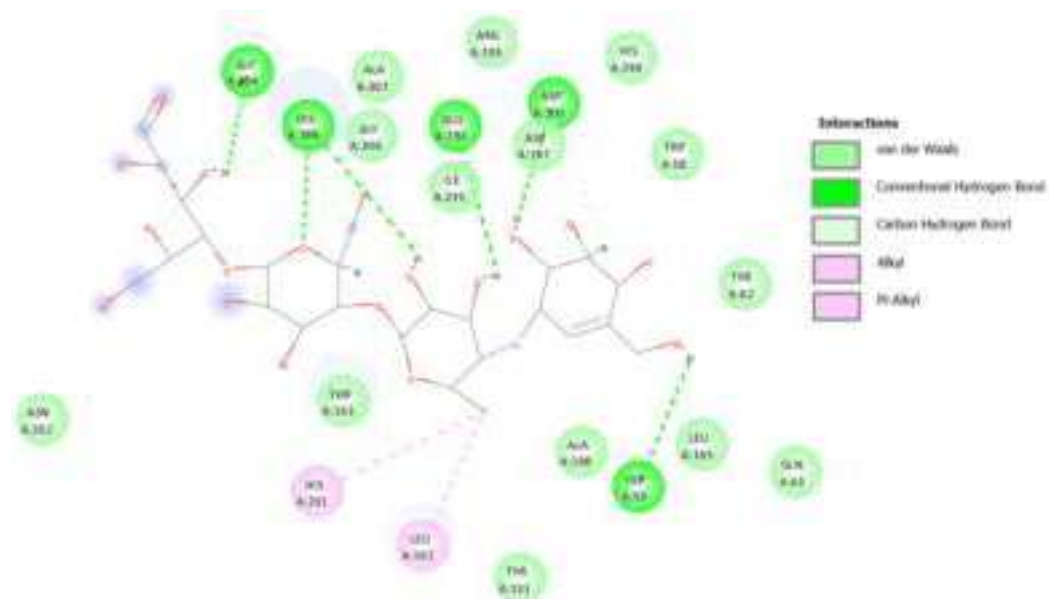
Comp.#	Binding Energies (kcal/mol)	
	$\alpha$ -Amylase	$\alpha$ -Glucosidase
5a	−8.9	−9.0
5f	−8.7	ND <sup>1</sup>
5h	−8.4	−5.7
Quercetin	−9.3	−7.0
Acarbose	−5.4	<sup>1</sup> ND
1-Deoxyojirimycin	<sup>1</sup> ND	−5.7

<sup>1</sup> ND: not determined.



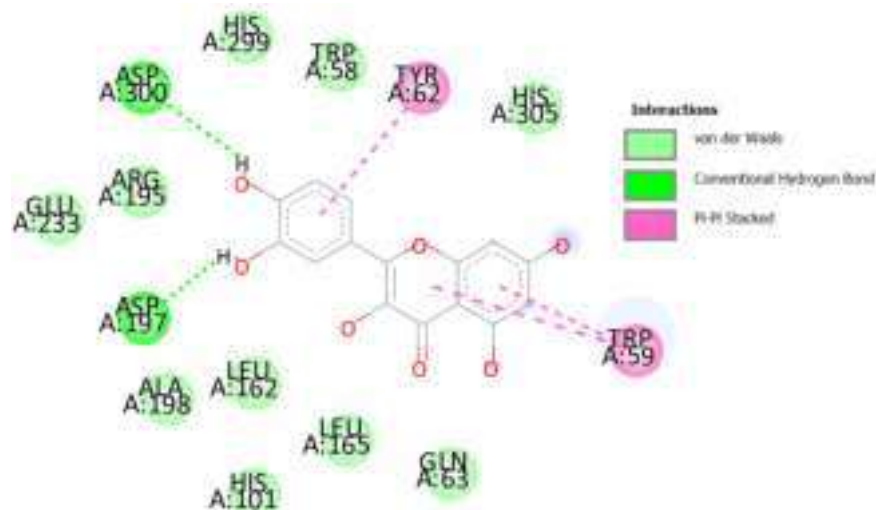
**Figure 11.** Three-dimensional docked poses of **3c** (green), **3f** (blue), **3h** (yellow), **5a** (orange), **5f** (cyan), **5h** (purple), quercetin (lime) and acarbose (pink) within the active site of HPA (PDB ID: 3BAJ).

As shown in Figure 12, acarbose is stabilized in the active catalytic site by six H-bonds, which were formed with the amino acid residues Trp59, Glu233, Asp300, Gly304 and His305 (two interactions). Additionally, acarbose exhibited alkyl interactions with Leu162 and His201.



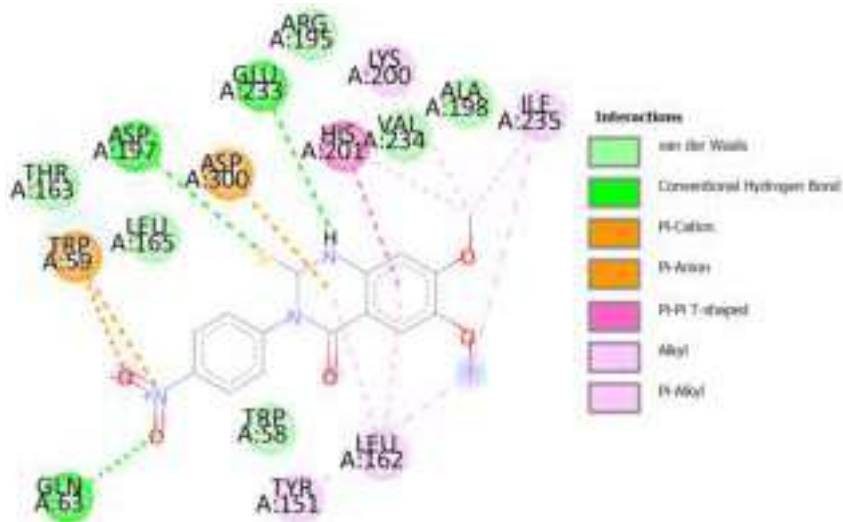
**Figure 12.** Two-dimensional docked conformation of acarbose at the active site of HPA (PDB ID: 3BAJ).

With regard to quercetin, its 3,4-dihydroxyl groups at the terminal phenyl ring formed two hydrogen bonds with the active site residues Asp197 and Asp 300; additionally, the aromatic rings formed  $\pi$ - $\pi$  stacking with the Trp59 and Tyr62 residues (Figure 13).



**Figure 13.** Two-dimensional docked conformation of **quercetin** and the main interactions stabilizing it at the active site of HPA (PDB ID: 3BAJ).

Among the docked ligands, **3h** manifested the strongest binding affinity to the target enzyme, with the highest binding free energy value. Compound **3h** established  $\pi$ - $\pi$  stacking interactions with the His201 residue,  $\pi$ -anion and  $\pi$ -cation interactions with Trp59, as well as three hydrogen bonds with amino acid residues Gln63, Asp197 and Glu233. Further stabilizing interactions include the alkyl interactions with amino acid residues Lys200, His 201 and Ile235, as well as the  $\pi$ -alkyl interactions with Leu162 (Figure 14).



**Figure 14.** Two-dimensional docked conformation of the best compound, **3h**, and the main interactions stabilizing it at the active site of HPA (PDB ID: 3BAJ).

Altogether, it can be concluded that these docking simulations affirmed the results of the *in vitro* AA inhibitory assay, and thereby both studies showed the promising nature of the studied quinazolinone derivatives for alpha-amylase inhibitory activity.

### 2.3.2. Docking against Recombinant Human Lysosomal Acid-Alpha-Glucosidase (rhGAA, PDB ID: 5NN5)

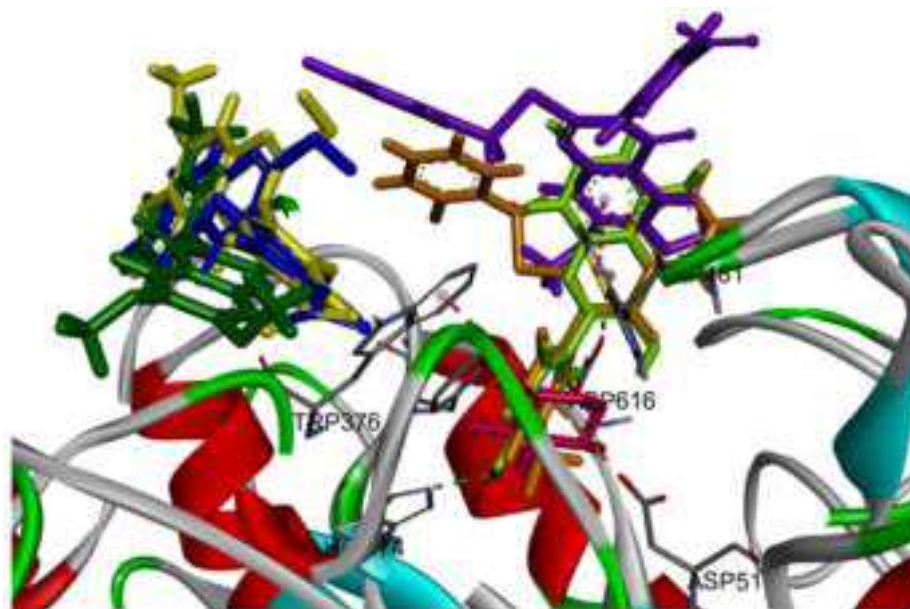
Molecular docking simulations were performed against the recombinant human lysosomal acid-alpha-glucosidase (rhGAA, PDB ID: 5NN5) [85] using derivatives **5a**, **3h** and **5h**, which exerted lower IC<sub>50</sub> values, as well as compounds **3c** and **3f**, which showed slightly higher IC<sub>50</sub> values as compared to quercetin.

First, the docking protocol was validated by redocking the native ligand 1-deoxynojirimycin (DNJ) at the active pocket with the RMSD deviation < 2 Å, implying the accuracy of the docking procedures (Figure 15).



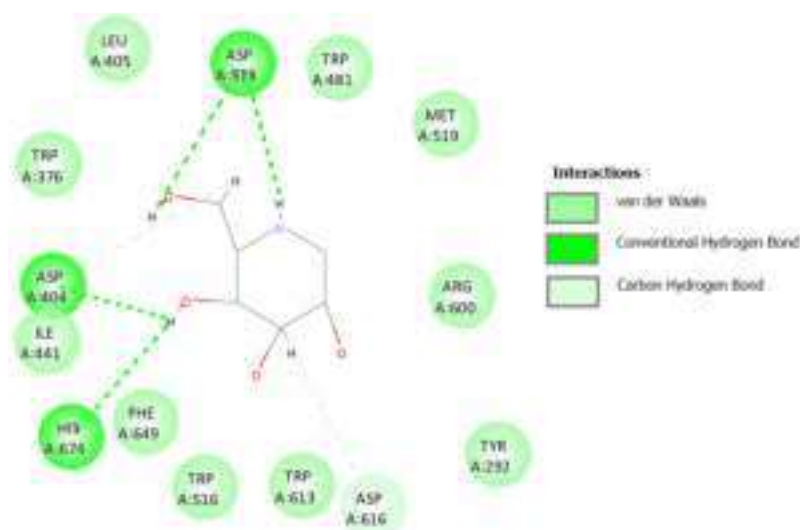
**Figure 15.** The validation of the accuracy and performance of the docking protocol by redocking 1-deoxynojirimycin (pink) in the active pocket of rhGAA, and the calculation of the RMSD value as compared to the native conformation (green).

The docking results showed that ligands **3c**, **3f** and **3h** bound differently from **5a**, **5h**, quercetin and DNJ (Figure 16).



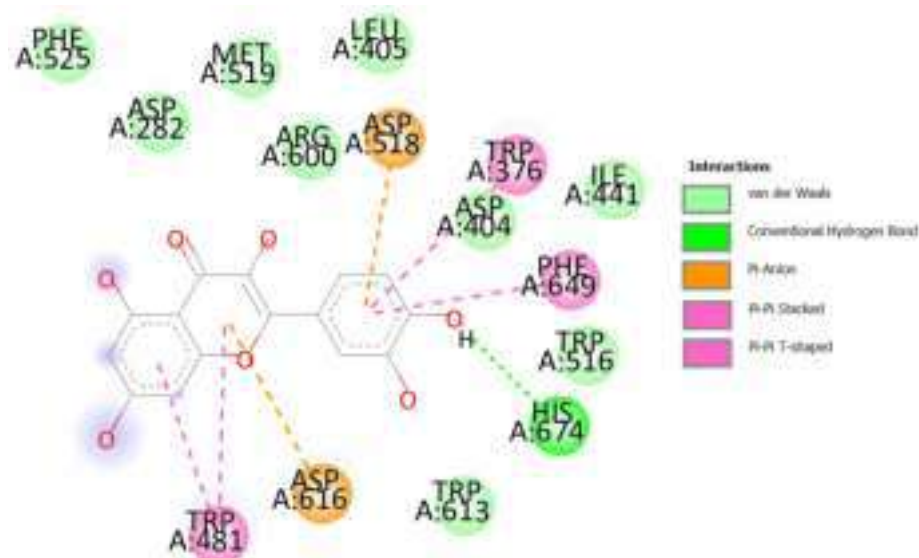
**Figure 16.** Three-dimensional docked poses of ligands **3c** (green), **3f** (blue), **3h** (yellow), **5a** (orange), **5h** (purple), quercetin (lime) and 1-deoxynojirimycin (pink) within the active site of rhGAA (PDB ID: 5NN5).

Thus, the analysis of the 2D docked conformation of the native ligand DNJ within the active pocket of rhGAA (binding free energy =  $-5.7$  Kcal/mol) revealed the establishment of four H-bonds with amino acid residues Asp404, Asp518 (two interactions) and His674. Further stabilizing interactions were provided via Van der Waals forces with Asp404 and Asp616 (Figure 17).



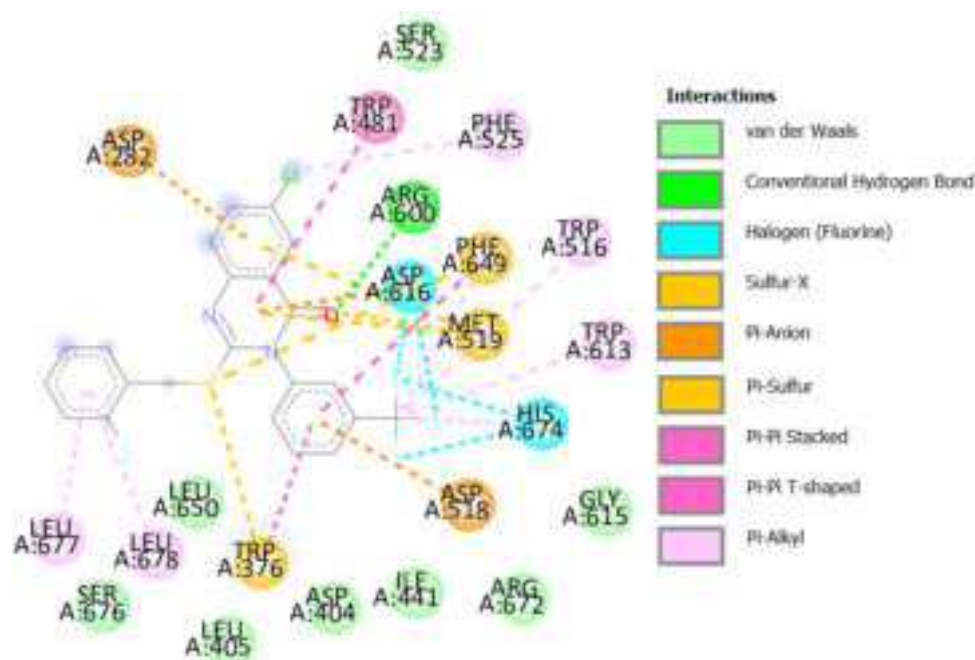
**Figure 17.** Two-dimensional docked conformation of 1-deoxynojirimycin (DNJ) at the active site of rhGAA (PDB ID: 5NN5).

Quercetin showed strong interactions and fitted inside the active pocket, with a binding energy of  $-7.0$  kcal/mol (Table 8). The para-hydroxyl group at the 2-phenyl substituent formed one hydrogen bond with His674. Moreover, the aromatic rings of quercetin showed  $\pi$ - $\pi$  stacking with the Trp376, Trp481 and Phe649 amino acid residues (Figure 18).



**Figure 18.** Two-dimensional docked conformation of quercetin and the main interactions stabilizing it at the active site of rhGAA (PDB ID: 5NN5).

Among the studied quinazolinones, derivative **5a** showed a strong affinity to the active site of the enzyme and fitted properly, with the highest binding energy value of  $-9.0$  kcal/mol (Table 8). Its oxo group formed a hydrogen bonding interaction with amino acid residue Arg600. Other stabilizing interactions were provided via the  $\pi$ - $\pi$  stacking with Trp376, Trp481 and Phe649 residues, in addition to several  $\pi$ -S, halogen and  $\pi$ -alkyl interactions (Figure 19).



**Figure 19.** Two-dimensional docked conformation of compound **5a** and the main interactions stabilizing it at the active site of rhGAA (PDB ID: 5NN5).

Collectively, the findings from the docking simulations correlated well to the results of the in vitro AA and AG inhibition experiments.

### 2.3.3. Docking against Lactate Dehydrogenase A (LDHA, PDB code: 1I10)

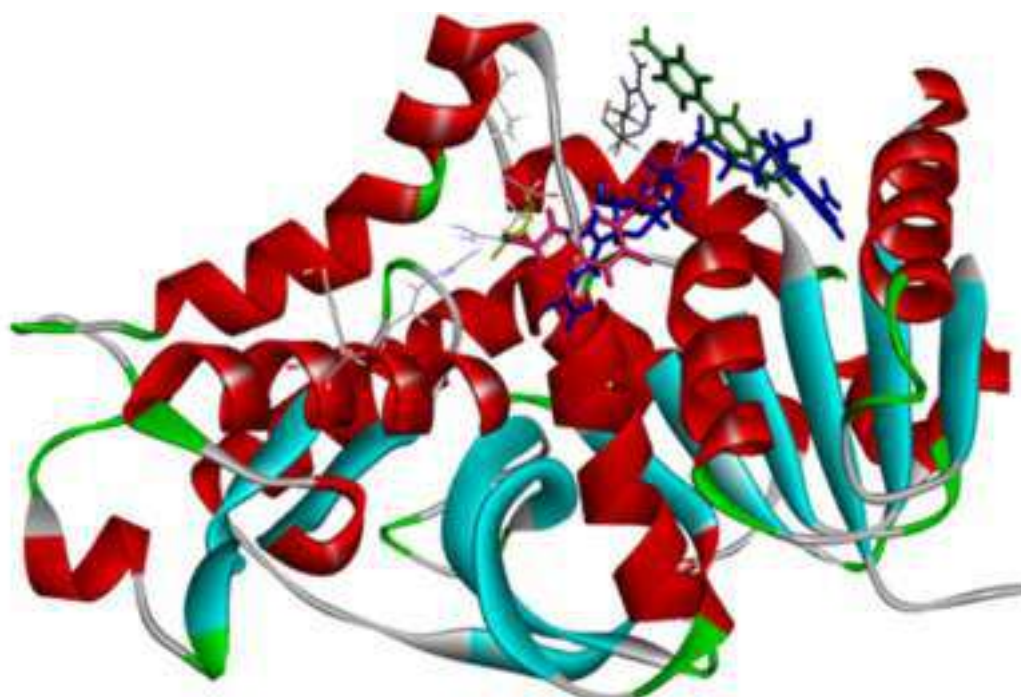
The 3D structure of LDHA was modelled using the known structure of human muscle LDHA (PDB code: 1I10), which comprises four subunits [86].

The docking method was validated by removing and redocking the co-crystallized ligand (oxamate) in order to determine the ability of the AutoDock v. 4.2.2 program to reproduce the orientation and position of the native ligand observed in the experimentally crystallized protein structure. As shown in Figure 20, the redocked conformation of the ligand oxamate is superimposed on the co-crystallized one and the RMSD deviation is  $<2 \text{ \AA}$ , which ensures the accuracy and reliability of the docking results.



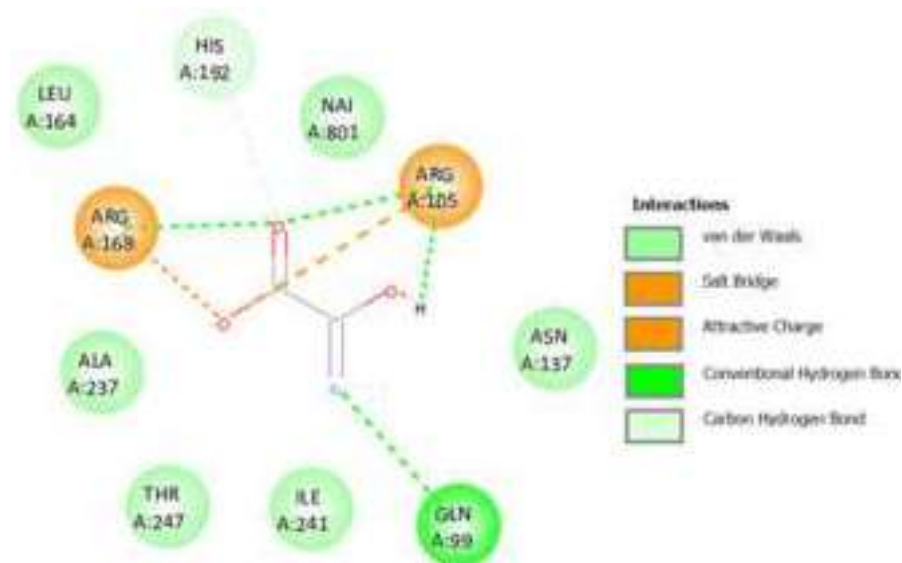
**Figure 20.** The validation of the accuracy and performance of the docking protocol by redocking oxamate (pink), and the calculation of the RMSD value as compared to native conformation (green).

Thereafter, the most promising LDHA inhibitors, **3a** and **3g**, as well as the reference inhibitor, oxamate, were docked inside the active site of lactate dehydrogenase A (PDB code: 1I10) [86] using the Autodock v. 4.2.2 program (Figure 21).



**Figure 21.** Three-dimensional docked conformation of compounds **3a** (pink), **3g** (green), oxamate (yellow) and NADH (blue) at the active site of LDHA (PDB code: 1I10).

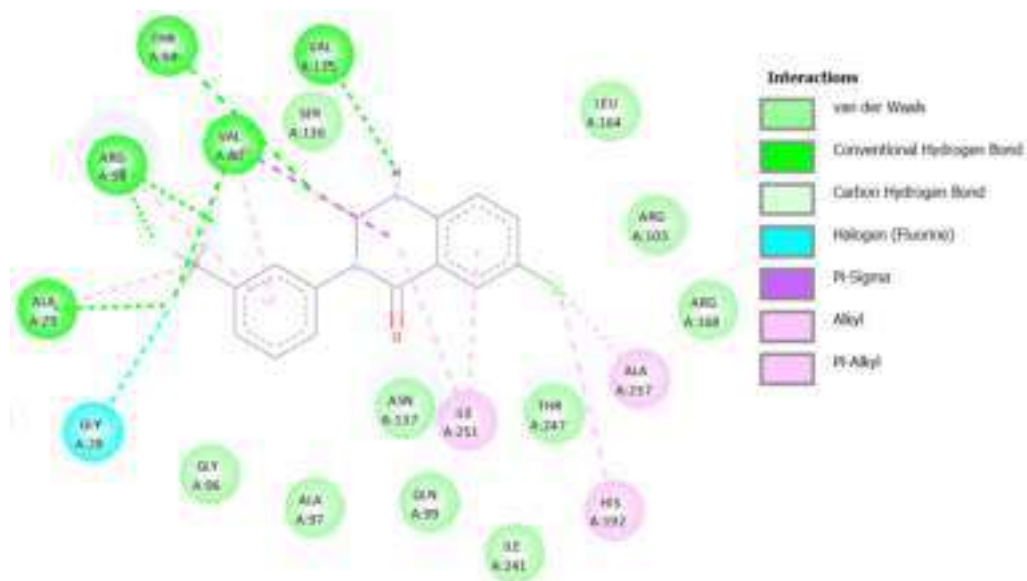
Previous studies have shown that oxamate, a competitive analogue of pyruvate, formed hydrogen bonds with the Arg105 guanidinium group, the 3'-OH-group of the NADH nicotinamide and the backbone oxygen of Ala97 [87]; thus, this region was identified as the active site of the LDHA (Figure 21). Among these, the interaction with Arg105 in the loop plays an essential role in stabilizing the transition state during the substrate conversion. Our results also showed three hydrogen bonding interactions of oxamate with Gln99, Arg105 and Arg168 (Figure 22).



**Figure 22.** Two-dimensional docked conformation of **oxamate** at the active site of LDHA (PDB code: 1I10).

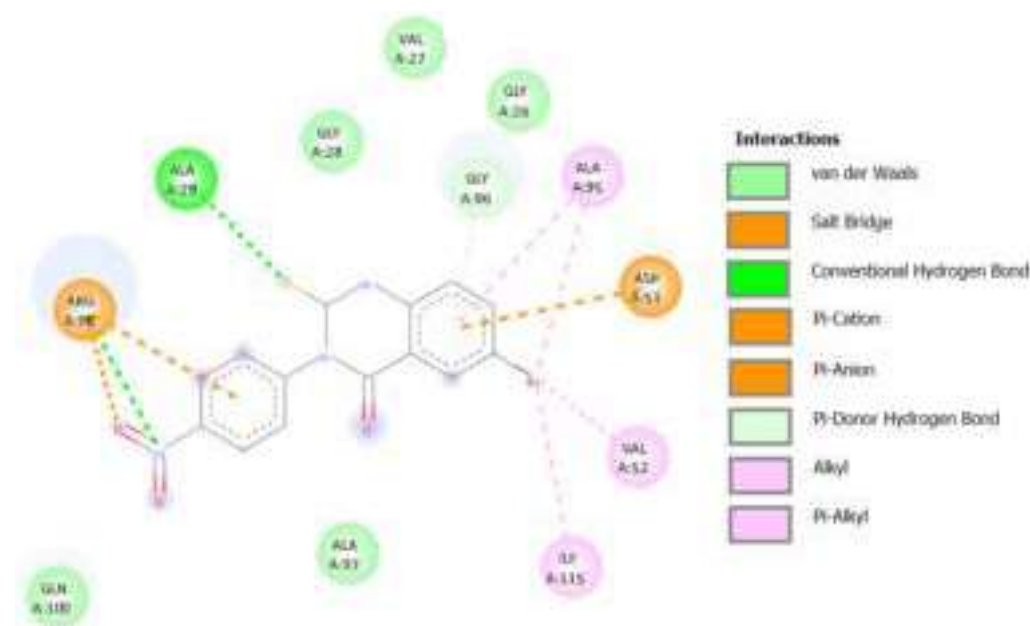
When docked into the same active site, compounds **3a** and **3g** occupied the same pocket in proximity with the NADH, with different interactions.

Regarding compound **3a**, it was stabilized in the active site by establishing six hydrogen bonding interactions; two of them were between the thioxo and NH groups with Thr94 and Val135, respectively. Additionally, the trifluoromethyl group formed four hydrogen bonds with the Ala29, Val30 and Arg98 (two interactions) amino acid residues. The distal phenyl ring fitted onto the lipophilic pocket, forming a  $\pi$ -alkyl stacking interaction (Figure 23). These interactions are different from those observed in previous studies [87], which may account for its reduced inhibitory efficiency as compared to oxamate. However, the binding free energy of compound **3a** was  $-9.2$  kcal/mol, indicating its significant affinity to the enzyme.



**Figure 23.** Two-dimensional docked conformation of compound **3a** at the active site of LDHA (PDB code: 1110).

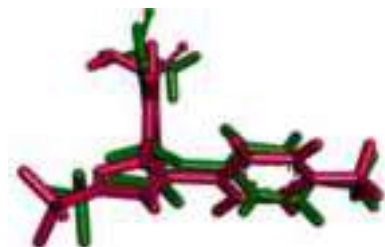
On the other hand, compound **3g** fitted within the catalytic active site, with a binding free energy of  $-5.9$  kcal/mol, by forming only two hydrogen bonds with the Ala29 and Arg98 residues (Figure 24).



**Figure 24.** Two-dimensional docked conformation of compound **3g** at the active site of LDHA (PDB code: 1110).

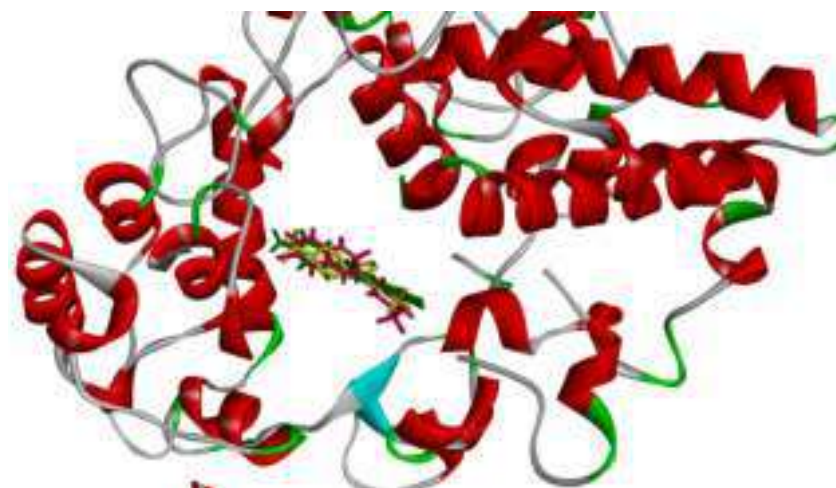
#### 2.3.4. Docking against COX-2 (PDB ID: 3LN1)

Moreover, molecular docking studies of compounds **3a** and **3g** were carried out in order to identify their selectivity and interactions with the target enzyme COX-2 (PDB ID: 3LN1) [88] after reproducing the conformation of celecoxib (shown in pink) with the RMSD deviation  $< 2 \text{ \AA}$ , as compared to the native conformation (shown in green) (Figure 25).



**Figure 25.** The validation of the accuracy and performance of the docking protocol by redocking celecoxib (pink), and the calculation of the RMSD value as compared to the native conformation (green).

The molecular docking studies revealed that both the quinazolinone derivatives, **3a** and **3g**, showed good interactions with the amino acid residues in the enzyme active site, with binding energies of  $-9.4$  and  $-9.0$  kcal/mol, respectively, as compared with the standard drug celecoxib ( $-7.1$  kcal/mol) (Figure 26).

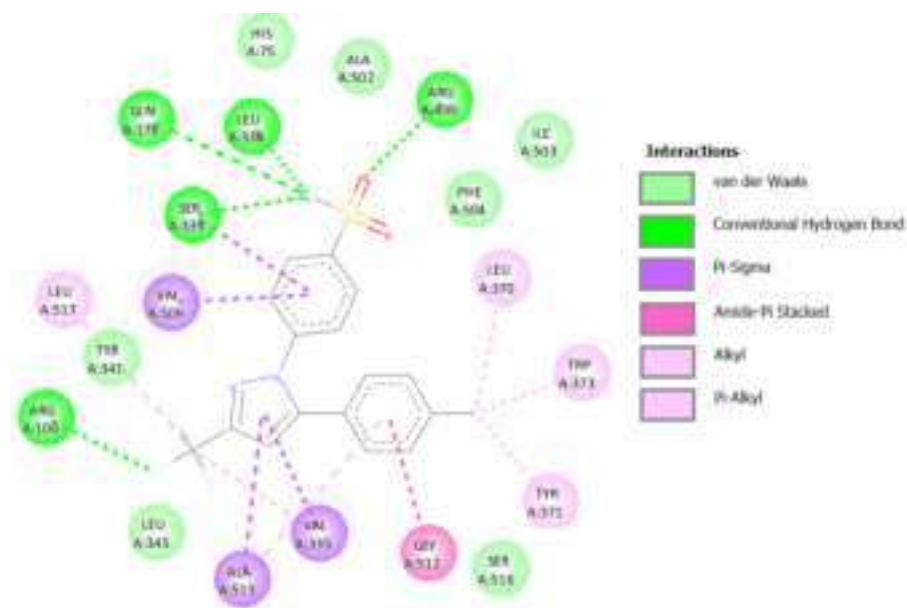


**Figure 26.** Three-dimensional docked conformation of compounds **3a** (pink), **3g** (green) and celecoxib (yellow) at the active site of COX-2 (PDB code: 3LN1).

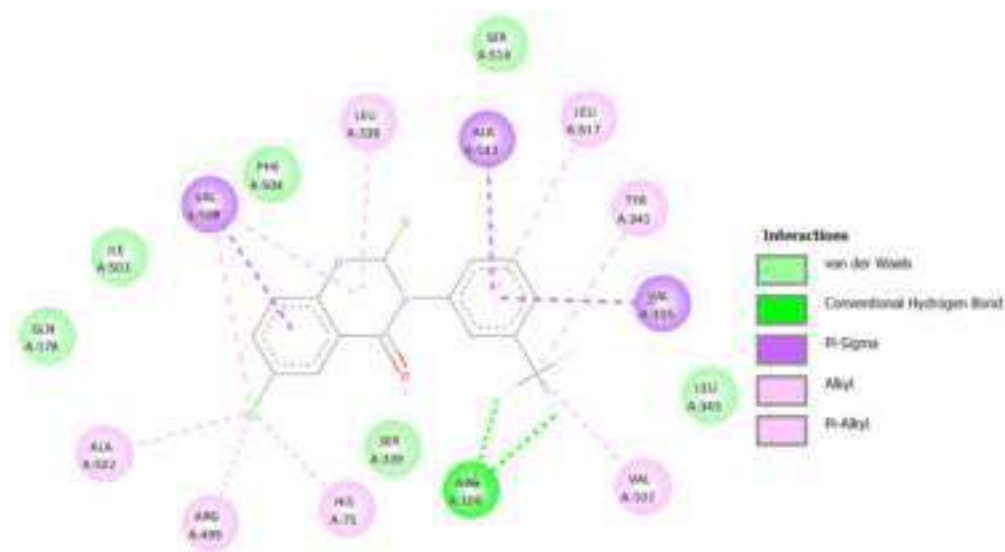
The sulfonamide group of celecoxib showed hydrogen bonding with Gln 178, Leu 338, Ser 339 and Arg 499. The pyrazole ring and phenyl ring showed  $\pi$ -sigma interactions with Ala513, Val335 and Val509 Arg 106 (Figure 27).

Compounds **3a** and **3g** occupied the same pocket, but with different interactions. Derivative **3a** showed two hydrogen bonds with Arg106 (Figure 28), whereas **3g** showed three hydrogen bonds with Arg499, Ile503 and Phe504 (Figure 29). Thus, it can be concluded that these interactions contributed to the measured inhibitory activity of these quinazolinone analogues.





**Figure 27.** Two-dimensional docked conformation of celecoxib at the active site of COX-2 (PDB ID: 3LN1).



**Figure 28.** Two-dimensional docked conformation of compound **3a** at the active site of COX-2 (PDB ID: 3LN1).

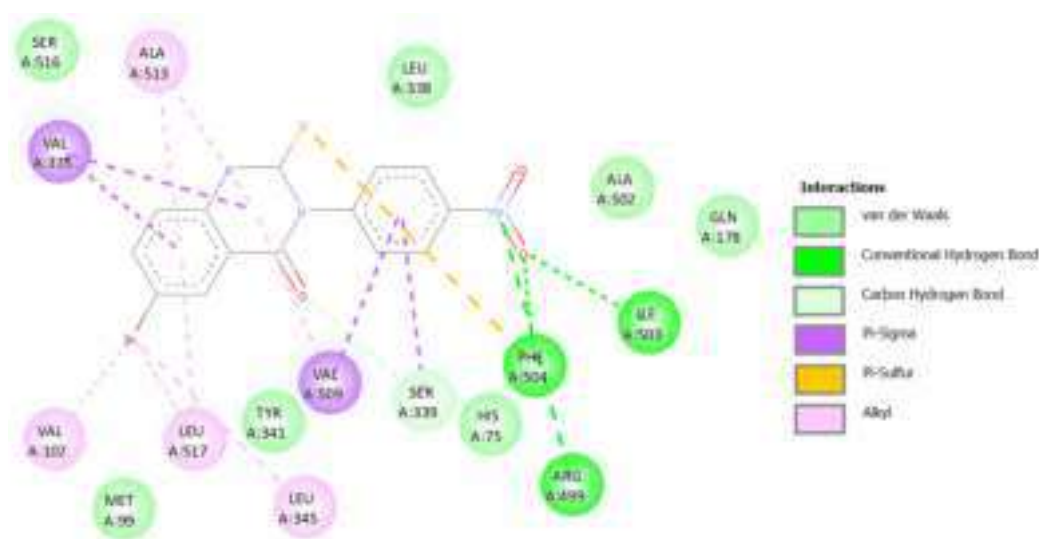
#### 2.4. *In Silico* Physicochemical, Medicinal and ADMET Predictions

The data for all the synthesized compounds are available in the Supplementary Materials.

##### 2.4.1. Physicochemical Properties of the Most Biologically Active Candidates

The physicochemical, medicinal chemistry and ADMET properties of all synthesized compounds were predicted (Supplementary Materials) using ADMETLab2.0 [89].

Considering derivatives **3a** (antioxidant, COX-2 inhibitor, LDHA inhibitor, AA inhibitor, cytotoxic agent), **3c** (AA inhibitor), **3f** (AA inhibitor, cytotoxic agent), **3g** (antioxidant, COX-2 inhibitor, LDHA inhibitor), **3h** (AA inhibitor, AG inhibitor), **5a** (antioxidant, AA inhibitor, AG inhibitor), **5b** (AA inhibitor), **5c** (AA inhibitor), **5d** (AA inhibitor), **5e** (AA inhibitor), **5f** (AA inhibitor) and **5h** (AA inhibitor, AG inhibitor), which exhibited promising biological activities, their molecular descriptors were predicted as presented in Table 9.



**Figure 29.** Two-dimensional docked conformation of compound **3g** at the active site of COX-2 (PDB ID: 3LN1).

**Table 9.** In silico predictions for molecular descriptors for derivatives **3a**, **3c**, **3f**, **3g**, **3h**, **5a**, **5b**, **5c**, **5d**, **5e**, **5f** and **5h**.

Comp.#	MW <sup>1</sup>	nHA <sup>1</sup>	nHD <sup>1</sup>	nRot <sup>1</sup>	TPSA <sup>1</sup>	LogS <sup>1</sup>	LogP <sup>1</sup>	LogD <sup>1</sup>	Fsp3	nRig
<b>3a</b>	356.00	3	1	2	37.79	−4.594	3.762	3.732	0.067	19
<b>3c</b>	382.06	5	1	4	56.25	−4.421	2.886	3.295	0.176	19
<b>3f</b>	333.00	6	1	2	80.83	−4.032	2.871	2.633	0	20
<b>3g</b>	376.95	6	1	2	80.93	−4.102	3.076	2.493	0	20
<b>3h</b>	359.06	8	1	4	99.39	−3.934	2.011	2.284	0.125	20
<b>5a</b>	464.04	3	0	5	34.89	−7.104	5.561	4.422	0.091	24
<b>5b</b>	523.96	3	0	5	34.89	−7.588	6.153	4.22	0.091	24
<b>5c</b>	517.09	8	0	8	96.49	−6.868	4.228	3.921	0.167	25
<b>5d</b>	480.01	3	0	5	34.89	−7.543	6.039	4.385	0.091	24
<b>5e</b>	597.92	4	0	6	44.12	−7.779	6.228	4.13	0.13	24
<b>5f</b>	530.97	7	0	6	87.26	−7.54	5.344	4.046	0.091	25
<b>5h</b>	483.07	3	0	7	96.49	−6.87	4.192	3.788	0.13	25

MW<sup>1</sup>: Molecular weight; nHA<sup>1</sup>: number of H-bond acceptors; nHD<sup>1</sup>: number of H-bond donors; TPSA<sup>1</sup>: topological polar surface area in Å<sup>2</sup>; LogS<sup>1</sup>: the logarithm of aqueous solubility value; LogP: the logarithm of *n*-octanol/water partition coefficient; LogD<sup>1</sup>: the logarithm of octanol/buffer (at pH 7.4) distribution coefficient; Fsp3: the number of sp<sup>3</sup> hybridized carbons/total carbon count; nRig: number of rigid bonds.

#### 2.4.2. Medicinal Chemistry of the Most Biologically Active Candidates

The same set of compounds were further evaluated for their suitability in medicinal chemistry using a number of well-known measures, rules and filters.

##### The Quantitative Estimate of Drug-likeness (QED) Score

This is a measure of drug-likeness based on the concept of desirability, estimated from eight properties, including MW, LogP, nHA, nHD, TPSA, nRot, the number of aromatic rings (NAr) and the number of alerts for undesirability. This descriptor ranks compounds having a mean QED score of  $\geq 0.67$  as attractive; on the other hand, unattractive compounds would have a QED score of  $0.67 > \text{QED} \geq 0.34$ . Moreover, unattractive and too complex compounds would have a mean QED score of  $< 0.34$  [90]. The predicted data indicated that **3a** (0.641), **3c** (0.64), **3f** (0.441), **3g** (0.419) and **3h** (0.437) would be ranked as unattractive, whereas **5a** (0.197), **5b** (0.21), **5c** (0.136), **5d** (0.233), **5e** (0.179), **5f** (0.131), and **5h** (0.153) could be categorized as unattractive and too complex compounds.

### Lipinski's Rule of Five Filter

Lipinski's rule of five [91] is a widely used filter to evaluate a compound's drug-likeness physicochemical characteristics and its suitability for oral administration. The four parameters of this rule, which are associated with absorption and/or permeability, include the molecular weight, the number of H-bond acceptors (HBAs, expressed as sum of Os and Ns), the number of hydrogen bond donors (HBDs expressed as the sum of HOs and HNs) and the LogP value, which is a measure of a compound's hydrophilicity and it represents the logarithm of its partition coefficient between *n*-octanol and water ( $\log(c_{\text{octanol}}/c_{\text{water}})$ ) were predicted using ADMTLab 2.0.

As presented in Table 9, all the studied compounds were found to have molecular weights with a range of 333.00 ~ 483.07 Da, which are within the permissible limit ( $\leq 500$ ), except for compounds **5b** (523.96), **5c** (517.09), **5e** (597.92) and **5f** (530.97).

The number of HBAs ranged from three to eight; thus, they do not exceed the limit ( $\leq 10$ ). Similarly, the number of HBDs ranged from zero to one, which complies with the acceptance value ( $\leq 5$ ). The LogP values were predicted to span from 2.011 to 6.228 (limit  $\leq 5$ ); thus, all studied compounds would possess desirable lipophilic characteristics, except for derivatives **5a** (5.561), **5b** (6.153), **5d** (6.039), **5e** (6.228) and **5f** (5.3438).

Overall, derivatives **3a**, **3c**, **3f**, **3g**, **3h** and **5h**, which fulfilled the thresholds of the Lipinski Ro5, as well as quinazolinones **5a**, **5c** and **5d**, which exhibited one violation, would be expected to be absorbed by the intestinal walls, whereas derivatives **5b**, **5e** and **5f**, which showed two violations (Table 10), would be poorly absorbed by the intestinal walls, as indicated by the rule [91].

**Table 10.** In silico predictions for medicinal chemistry characteristics.

Comp. #	QED <sup>1</sup>	Lipinski	Pfizer	Golden Triangle
<b>3a</b>	0.641	Accepted	Rejected	Accepted
<b>3c</b>	0.64	Accepted	Accepted	Accepted
<b>3f</b>	0.441	Accepted	Accepted	Accepted
<b>3g</b>	0.419	Accepted	Accepted	Accepted
<b>3h</b>	0.437	Accepted	Accepted	Accepted
<b>5a</b>	0.197	Accepted	Rejected	Accepted
<b>5b</b>	0.21	Rejected	Rejected	Rejected
<b>5c</b>	0.136	Accepted	Accepted	Rejected
<b>5d</b>	0.233	Accepted	Rejected	Accepted
<b>5e</b>	0.179	Rejected	Rejected	Rejected
<b>5f</b>	0.131	Rejected	Accepted	Rejected
<b>5h</b>	0.153	Accepted	Accepted	Accepted

QED<sup>1</sup>: the quantitative estimate of drug-likeness.

### Pfizer Rule

According to this rule, the combination of a high LogP with a low TPSA increases the likelihood of adverse outcomes; this is due to a low polar surface area (TPSA < 75), and a higher LogP (LogP > 3) increases the ability of a compound to cross biological membranes and distribute widely into off-target tissue compartments [92]. Therefore, the high/low thresholds for LogP and TPSA have cutoffs of 3.0 and 75, and when both risk factors are present, the compound is likely to be toxic. Thus, according to data presented in Table 9, only compounds **3c**, **3f**, **3g**, **3h**, **5c**, **5f** and **5h** complied with the Pfizer rule (Table 10).

### GlaxoSmithKline (GSK) Rule

This rule highlights the importance of a lower molecular weight and LogP physicochemical properties to obtain improved ADMET parameters. The cutoff limits are MW  $\leq 400$  and LogP  $\leq 4$  [93]. Thus, **3a**, **3c**, **3f**, **3g** and **3h**, satisfied this rule.

### Golden Triangle

This visualization tool [94] was developed to aid in identifying metabolically stable, permeable and potent drug candidates, which would have values of  $200 \leq MW \leq 500$ , and  $-2 \leq \text{LogD} \leq 5$ . As per the data in Table 9, compounds **5b**, **5c**, **5e** and **5f** violate this rule (Table 10); thus, they are expected to have unfavorable ADMET profiles.

The ADMET profiles of the dual AA and AAG inhibitors, **3h**, **5a** and **5h**, are discussed in detail in Section 2.4.3.

### Pan-Assay Interference Compounds (PAINS) Filter

This filter aids in detecting substructural features that may interfere with bioactivity detection technology that are frequently found in problematic compounds, making them give false positive results in bioactivity assays for a number of reasons [95–97]. Also, compounds bearing interference moieties tend to have therapeutic limitations due to these moieties often being associated with reactivity, toxicity or metabolic liability [97]. Consequently, the screening results showed that none of studied compounds were flagged to contain PAINS alters.

### 2.4.3. Drug Metabolism and Pharmacokinetic (DMPK) Analysis for the AA and AG Dual Inhibitors: **3h**, **5a** and **5h**

Because undesirable ADMET profiles, Absorption, Distribution, Metabolism, Excretion and Toxicity, are the main reasons for high attrition rates in drug development, computer-aided models are being relied on for the prediction of these properties for drug candidates in the early stages of drug discovery programs, thus saving extensive efforts and reducing cost and duration as compared to in vivo models [98]. Therefore, the ADMET parameters were predicted for the AA and AG dual inhibitors, **3h**, **5a** and **5h**, using the ADMETlab 2.0 server [89], which was freely accessed on 22<sup>nd</sup> August 2023 at <https://admetmesh.scbdd.com/>.

For simplification, the computed values for all descriptors will be listed in the order of **3h**, **5a** and **5h**, respectively.

#### Absorption Prediction

The absorption profile of a drug is influenced by specific biochemical characteristics, including the water/lipid solubility, bioavailability and permeability across barriers—including the gastrointestinal tract lining, which can be predicted as human intestinal absorption (HIA)—as well as the interaction with transporters and metabolizing enzymes in the gut wall.

#### Solubility (LogS)

The computed descriptor used to assess the aqueous solubility is LogS; the logarithm of molar solubility is expressed as Log mol/L, and the empirical decision indicated that compounds with values falling within the range from  $-6$  to  $0.5$  log mol/L would be considered proper; thus, derivative **3h** is expected to show a good water solubility, with a LogS value of  $-3.934$  (Table 9), whereas derivatives **5a** and **5h** would be insoluble, with LogS values of  $-7.104$ , and  $-6.875$ , respectively; accordingly, they might not be orally bioactive.

Solubility is essentially influenced by the presence of molecular entities ( $\text{NH}_2$ ,  $\text{OH}$ ,  $\text{NO}_2$  and  $\text{OCH}_3$ ) that are capable of H-bond formation with water molecules or those conferring lipid solubility (aromatic groups (Cl, Br and I; the effect of F can vary). Thus, the order of solubility based on the computed LogS values is as follows: **3h** > **5h** > **5a**, which is consistent with the type of substituents and functional groups incorporated in each of them, as **3h** possessed  $\text{NO}_2$ ,  $\text{OCH}_3$  and  $\text{NH}$  groups, **5h** possessed  $\text{NO}_2$ ,  $\text{OCH}_3$  and Cl, and **5a** possessed Cl,  $\text{CF}_3$  and F.

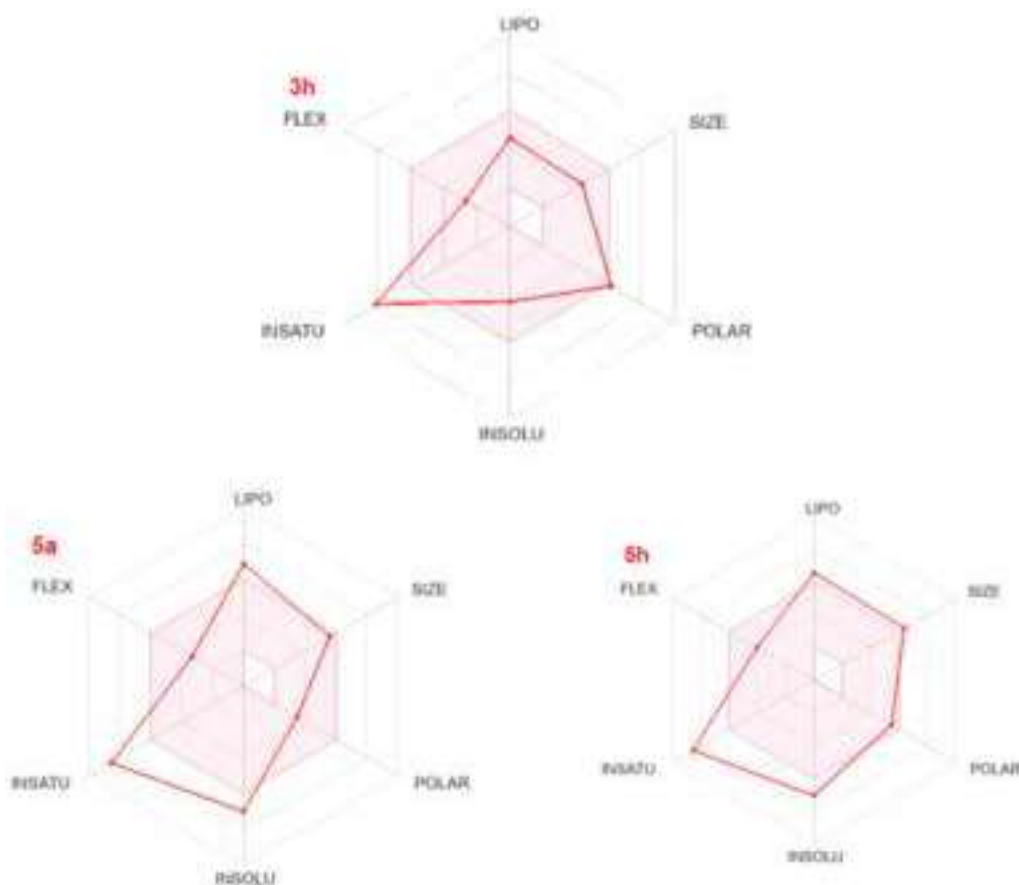
#### Human Intestinal Absorption (HIA)

The HIA of an oral drug is an essential prerequisite for its apparent efficacy; in addition, it can be used as an alternative indicator for oral bioavailability. The molecules are classified as category 0 (HIA−) with a HIA of > 30%, or as category 1 (HIA+) with a HIA of < 30%, with the output value indicating the probability of being of HIA+ within the range of 0 to 1. The estimated scores were 0.008, 0.003 and 0.004, respectively, implying that they are not expected to belong to HIA+ category.

#### The Human Oral Bioavailability (HOB)

Human oral bioavailability (HOB) is an important parameter used to measure the amount of a drug that actually enters circulation after ingestion. The high oral bioavailability of a drug would reduce the amount of administration needed to achieve the expected pharmacological action, which can reduce the side effects and toxicity risks brought by the drug.

The oral bioavailability radar plots shown in Figure 30 were predicted with the SwissADMET web tool [95]. This graph is based on six physicochemical descriptors arranged on the corners of a hexagon, including insolubility (LogS), polarity (TPSA), size (MW), flexibility (FLEX, based on number of nRot/nRig), lipophilicity (Lipo, based on LogPoc-tanol/water) and unsaturation. The colored zone is the suitable physicochemical space for oral bioavailability.



**Figure 30.** The bioavailability radar hexagons for derivatives **3h**, **5a** and **5h**, predicted using the SwissADME web tool. The pink area represents the optimal range for each property and the red lines define the oral bioavailability properties of the studied compounds.

As shown in the bioavailability radar hexagons (Figure 30), the three compounds possessed suitable sizes, flexibilities and polarities. However, all of them demonstrated high unsaturation fractions, indicated by the off-shoot of the INSATU vertex, which may affect their solubility since it was hypothesized that increasing the  $sp^3$  fraction might

increase the complexity of the molecules, improving their solubility and providing a three-dimensionality that could contribute to greater selectivity and fewer off-target effects [99].

Additionally, compounds **5a** and **5h** possessed unsuitable lipophilicity and solubility characteristics. The link between solubility and lipophilicity is well established; as the LogP increases, solubility decreases on average [93]. Therefore, the order of LogP among the three compounds is as follows: **5a** > **5h** > **3h**, which is the reverse order of solubility.

The Human Oral Bioavailability Factors 20% ( $F_{20\%}$ ) and 30% ( $F_{30\%}$ )

Moreover, two cutoffs can be used to assess the HOB; the first is,  $F_{20\%}$ , wherein the molecules with a bioavailability of  $\geq 20\%$  are classified as category 0 ( $F_{20\%-}$ ), whereas molecules with a bioavailability of  $< 20\%$  are classified as category 1 ( $F_{20\%+}$ ). The output value is the probability of being  $F_{20\%+}$  within the range of 0 to 1. The estimated scores for the studied compounds were 0.002, 0.002 and 0.001, implying that the compounds have negligible probabilities for being  $F_{20\%+}$ .

The second is  $F_{30\%}$ , whereby the molecules with a bioavailability of  $\geq 30\%$  are classified as category 0 ( $F_{30\%-}$ ), whereas molecules with a bioavailability of  $< 30\%$  are classified as category 1 ( $F_{30\%+}$ ). The output value is the probability of being  $F_{30\%+}$  within the range of 0 to 1. The calculated scores were 0.002, 0.003 and 0.004, respectively, implying that the three compounds have negligible probabilities of being  $F_{30\%+}$ .

#### Permeability

After an orally administered drug is dissolved in the gastro-intestinal tract, it must then be sufficiently permeable through the biological membranes present to enter the systemic circulation. Permeation is often mimicked in laboratories using artificial membrane assays such as the Caucasian colon adenocarcinoma cell line (Caco-2) and the Madin Darby Canine Kidney cell line (MDCK).

With regard to Caco-2 permeability descriptor, the computed values expressed in log cm/s of the studied compounds were  $-4.737$ ,  $-5.065$ , and  $-4.771$ , respectively; thus, all of them comply with the respected range for this property (value  $> -5.15$  log cm/s).

Respecting the MDCK permeability as another tool, which is assessed using the apparent permeability coefficient  $P_{app}$  in cm/s, the predicted values were  $5.25 \times 10^{-5}$ ,  $1.13 \times 10^{-5}$  and  $2.43 \times 10^{-5}$ , respectively, whereby the standard limits for  $P_{app}$  in cm/s and their significance are a high permeability of  $> 20 \times 10^{-6}$ , medium permeability of  $20-2 \times 10^{-6}$ , and low permeability of  $< 2 \times 10^{-6}$ . Thus, all derivatives have a high passive MDCK permeability.

#### P-glycoprotein (P-gp) Efflux

The P-glycoprotein (P-gp) efflux is considered one of the determinants of oral bioavailability as well as the rate and amount of a drug that diffuses across the basolateral membrane to enter the general circulation. Therefore, P-gp efflux screening is a key step in the early drug discovery stage. Compounds are classified as non-inhibitors (category 0) and inhibitors (category 1), with the output value representing the probability of being an inhibitor within the range of 0 to 1. With regard to **3h**, **5a** and **5h**, they are anticipated to be P-gp inhibitors as per their scores of 0.978, 0.991 and 0.994, respectively. So, these derivatives are expected to show drug–drug interactions (DDIs) with co-administrated P-gp substrates.

With respect to P-gp substrate properties, the compounds may belong to category 0 if they are non-substrates, or to category 1 if they are substrates, with the output value indicating the probability of being a substrate within the range of 0 to 1. The predicted value for the three compounds was 0.001, implying that they have a low probability for being substrates, which is beneficial, since it is known that therapeutic agents which are substrates of P-gp usually exhibit a poor bioavailability due to P-gp blocking their absorption [100]. In addition, they can be considered as safe from having significant DDIs when co-administrated with other Pgp inhibitors.

## Distribution

After the drug is absorbed, it enters the systematic circulation to be distributed throughout the body, where it is reversibly transferred between various tissues, organs and cells. Thus, this property is essential for the prediction of pharmacodynamic and toxicodynamic properties [101].

Four descriptors were predicted to assess the efficiency of the drug distribution throughout the body: plasma protein binding (PPB), the volume of distribution (VD), the fraction unbound in plasma ( $f_u$ ), and uptake by the blood–brain barrier (BBB).

### The Degree of Plasma Protein Binding (PPB)

This refers to the binding of the drug to plasma proteins such as albumin, which significantly influences the distribution of the drug between the plasma and the tissue of interest; hence, it determines the efficacy of a given drug as well as its clearance (Cl).

Generally, only the free or unbound fraction of a drug is active; therefore, if there is little inclination that a drug molecule will bind with plasma proteins (predicted PPB value  $\leq 90\%$ ), as a consequence, this compound is considered to have a high therapeutic index, meaning that it can circulate more efficiently and freely within the blood stream and hence has access to the target site. In contrast, a compound with a PPB value of  $> 90$  is expected to be poorly distributed. For the studied compounds, the PPB values were calculated to be 84.49, 100.92 and 100.40, respectively; as a consequence, only **3h** is expected to demonstrate a high therapeutic efficiency. It is noteworthy to indicate that many marketed drugs have PPB values of  $> 90\%$  [102]; thus, for **5a** and **5h**, their high values can be tolerated if they have a high rate of dissociation. Also, this high tendency for PPB can be advantageous, as the plasma–drug complex is considered as a reservoir for free drug concentration whenever it is eliminated from the body, thus prolonging the duration of the drug's action [102].

### The Fraction Unbound in Plasma ( $f_u$ )

The  $f_u$  is an indicator of the free amount of a drug in the plasma, and it determines a compound's capability to traverse biological barriers and gain access to target tissues and organs. As a consequence, the more plasma-bound a compound is, the less efficiently it can traverse biological barriers. The standard scores for high, medium and low fractions unbound in plasma are as follows:  $> 20\%$ ;  $5\text{--}20\%$ ; and  $< 5\%$ , respectively. With regard to the predicated values of the investigated compounds, they are equal to 13.85, 0.66 and 0.55, respectively; thus, again, only derivative **3h** is expected to have a moderate therapeutic efficiency.

### Volume of Distribution (VD)

As a drug is absorbed, its distribution throughout the body must be considered, since it determines if the compound will produce a pharmacological response or not. The VD value (L/Kg) can be used to predict the distribution characters for an unknown drug, including its conditions of binding to plasma proteins, its distribution amount in the body's fluid and its uptake amount in tissues. The optimal range of the VD for proper distribution is between 0.04 and 20 L/Kg, otherwise it is poor. For the studied compounds, the computed VD values were 0.497, 0.686 and 0.132, respectively, implying that they are likely to be well distributed throughout the body's tissues and will not be confined to the plasma.

### Penetration of Blood–Brain Barrier (BBB)

This is an important descriptor to anticipate the capability of a compound to distribute into the brain. It is measured as  $\text{LogBB}$  in  $\text{cm}^2/\text{s}$ , and if a compound has a  $\text{LogBB} > -1$ , it will penetrate the BBB and thus, it is classified as category 1 (BBB+); however, it will be poorly distributed to the brain if it has a  $\text{LogBB}$  of  $\leq -1$ , and will be classified as category 0 (BBB–). The output value is the probability of being BBB+, within the range of 0–1. The calculated values for the specified inhibitors were 0.18, 0.298 and 0.212, respectively; thus, all of them are not expected to penetrate the BBB, implying that they are not associated with CNS toxicity.

## Metabolism

Drug metabolism is a very complex process, which begins once a compound penetrates the gastrointestinal tract and passes through the portal vein to the liver. Two phases may be involved in metabolizing drugs: phase I, in which reactions such as oxidations, reductions, hydrolysis and dealkylations take place; and phase II, in which conjugation reactions with endogenous substances occur.

Cytochrome P-450 (CYP450) is a superfamily of isoenzymes that catalyze the phase I metabolism. For an orally delivered drug to be distributed beyond the liver to exert its pharmacological action on the target organ, some fraction of this drug must survive the hepatic metabolism. Therefore, the property of being a substrate or an inhibitor to these hepatic enzymes is crucial. Also, it may induce DDIs, whereby one drug may enhance the toxicity or reduce the therapeutic effect of another drug. The major CYP450 isoforms, which are responsible for most of the metabolic reactions, include CYP1A2, CYP2C19, CYP2C9, CYP2D6 and CYP3A4.

According to the results presented in the Supplementary Materials, the compounds showed varied probabilities of being substrates or inhibitors for these cytochromes. The utilized database classified the compounds in two categories: category 0 for non-substrates/non-inhibitors; and category 1 for substrates/inhibitors. The output values indicate the probability of being a substrate/inhibitor, within the range of 0 to 1.

With respect to CYP1A2, the computed probabilities for **3h** of being an inhibitor and a substrate were 0.124 and 0.97, respectively, indicating that it is a possible substrate for this enzyme. The probabilities for **5a** were anticipated to be 0.885 and 0.238, respectively, indicating that it is a possible inhibitor. Lastly, the computed probabilities for **5h** were 0.245 and 0.826, respectively; thus, it appeared to be a substrate for CYP1A2.

The predicted probabilities of being an inhibitor and a substrate for CYP2C19 were 0.325 and 0.553 (**3h**), 0.062 and 0.929 (**5a**), and 0.894 and 0.177 (**5h**), respectively. Thus, **5a** and **5h** are highly expected to be a substrate and an inhibitor for the CYP2C19 isoform, respectively.

As regards CYP2C9, the measured inhibitor/substrate probabilities were 0.163/0.832 (**3h**), 0.929/0.858 (**5a**), and 0.901/0.904 (**5h**), respectively. Accordingly, all of them have a high probability of being substrates; in addition, **5a** and **5h** appeared to be possible inhibitors for this cytochrome.

Concerning CYP2D6, the measured inhibitor/substrate probabilities were 0.01/0.468 (**3h**), 0.347/0.396 (**5a**), and 0.046/0.69 (**5h**), respectively. Therefore, there is no expected incidence of 2D6 isoenzyme inhibition by **3h** and **5h**, but medium probability for inhibition by **5a**. In addition, there are moderate probabilities for all of them for being 2D6 substrates.

Lastly, regarding the inhibitor/substrate probabilities for CYP3A4, they were predicted as follows: 0.277/0.826 (**3h**), 0.567/0.641 (**5a**) and 0.727/0.929 (**5h**), respectively, implying that very high probabilities exist for **3h** and **5h** as substrates and moderate probabilities for **5a** and **5h** as inhibitors.

## Excretion

Total clearance parameters (CLs), which are expressed as  $\text{mL}/\text{min}/\text{kg}$ , are used to predict the removal rate of a compound from the systemic circulation by all methods: "renal clearance; hepatic clearance via metabolic loss; and loss into milk, sweat and saliva".

The CLs are inversely proportional to a compound's in vivo half-life time; thus, a higher CL value implies that a compound is more rapidly removed from the body by any method, which may impact its potency. Consequently, CLs define, together with the volume of distribution, the dosing frequency of a drug [103]. The standard scores in  $\text{mL}/\text{min}/\text{kg}$  for high, moderate and low clearance are  $>15$ , 5–15 and  $< 5$ , respectively.

The calculated CL ( $\text{mL}/\text{min}/\text{kg}$ ) results were 6.455, 3.838 and 4.054, implying that the clearance for **3h** is moderate, whereas it is expected to be low for **5a** and **5h**.

For the half-life of a drug ( $T_{1/2}$  in hour), the database subdivided molecules as category 0 ( $T_{1/2-}$ ) with a  $T_{1/2}$  of  $> 3$ , and category 1 ( $T_{1/2+}$ ) for molecules with a  $T_{1/2}$  of  $\leq 3$  h. The output value is the probability of being  $T_{1/2+}$  with score ranges of 0–0.3, 0.3–0.7 and



0.7–1.0 for excellent, medium and poor, respectively. The calculated values for the studied compounds were 0.692, 0.025 and 0.145, respectively, indicating that the probability for having a  $T_{1/2}$  of  $\leq 3$  h is low for **5a** and **5h**, whereas it is moderate for **3h**.

### Toxicity

ADMETLab2.0 provides several descriptors to identify potential toxicities which could associate drugs and drug candidates. The most important properties will be discussed in the following section.

- The human ether-a-go-go-related gene (hERG) blockers

The hERG encodes a voltage-gated potassium channel, which is involved in the regulation of the exchange of cardiac action potential and resting potential. A blockade of hERG may result in long QT syndrome (LQTS), arrhythmia, and Torsade de Pointes (TdP), which may lead to palpitations, fainting, or even sudden death. Therefore, the molecules are classified for their inhibitory potential against hERG as category 0 (hERG-), which represents molecules exerting an  $IC_{50}$  of more than 10  $\mu$ M or demonstrate less than 50% inhibition at 10  $\mu$ M, and category 1 (hERG+), referring to molecules with an  $IC_{50}$  of less than 10  $\mu$ M or more than 50% inhibition at 10  $\mu$ M. The output value reflects the probability of being hERG+ blockers, within the range of 0–1. The compounds' scores for being hERG+ blockers were predicted to be 0.01, 0.279 and 0.549, respectively, implying that **3h** and **5a** are weak hERG+ blockers, and can accordingly be regarded as non-cardiotoxic, whereas **5h** is expected to be a medium hERG+ blocker, indicating its hazard as a cardiotoxic agent.

- The human hepatotoxicity (H-HT)

The compounds were further screened for their hepatotoxicity. The ADMETLab 2.0 categorizes the molecules as category 0 if they are H-HT negative (–) or category 1 if they are H-HT positive (+), with the output value being the probability of being toxic, within the range of 0 to 1. The reported scores for the studied derivatives were 0.882, 0.851 and 0.228, respectively. Thus, only **5h** is not expected to cause hepatic injuries, whereas **3h** and **5a** might induce adverse hepatic effects.

- Drug-induced liver injury (DILI)

Over the past 50 years, DILI has become the most common safety issue causing drug withdrawal from the market. Therefore, the molecules are classified as category 0 if they are DILI negative (–), or category 1 if they are DILI positive (+) and the output value is the probability of being toxic, within the range of 0 to 1. As the predicted scores of the investigated compounds were 0.963, 0.923 and 0.971, thus all of them are expected to cause DILI.

- AMES Toxicity for mutagenicity

This assay is a widely used method to test chemicals for mutagenicity, which is positively correlated to carcinogenicity. According to the used platform, the compounds are identified as category 0 (AMES negative (–, nontoxic)) or category 1 (AMES positive (+, toxic)), with the output value reflecting the probability of being toxic, within the range of 0 to 1. The recorded AMES scores were 0.984, 0.504 and 0.986, respectively, indicating that **3h** and **5h** are strong mutagenic agents, while **5a** is a medium agent. The predicted scores were 0.606, 0.025 and 0.038, respectively; thus, **5a** and **5h** are considered nontoxic, whereas **3h** is likely to cause toxicity.

- Rat oral acute toxicity (ROA)

The used web interface categorizes compounds according to the risk of causing acute toxicity in mammals upon administration into category 0 (low-toxicity, >500 mg/kg) and category 1 (high-toxicity, <500 mg/kg). The output value is the probability of being toxic, within the range of 0 to 1. The predicted scores were 0.606, 0.025 and 0.038, respectively, which indicates that **5a** and **5h** are expected to be nontoxic, whereas **3h** has a medium probability of being a toxic molecule.

- FDA Maximum Recommended Daily Dose (FDAMDD)

This descriptor estimates the toxic dose threshold of chemicals in humans. The compounds are categorized as category 1 (FDAMDD positive (+, toxic),  $\leq 0.011$  mmol/kg of body weight (bw)/day); or category 0 (FDAMDD negative (−, nontoxic),  $> 0.011$  mmol/kg of bw/day). The output value is the probability of being toxic, within the range of 0 to 1. The computed scores were 0.881, 0.909 and 0.891, respectively, indicating that all of the compounds would be toxic substances.

- Carcinogenicity

This endpoint is assessed via the perdition of the  $TD_{50}$ : the dose required to produce a toxic effect in 50% of the population. Molecules are designated as inactive (category 0; non-carcinogens) or active (category 1; carcinogens) according to their  $TD_{50}$  values. The output value is the probability of being toxic, within the range of 0 to 1. According to the computed values of 0.937, 0.425 and 0.866, respectively, only **5a** would be a moderately carcinogenic compound, whereas **3h** and **5h** are expected to be highly carcinogenic.

- Respiratory Toxicity

Herin, the compounds are labeled as category 1 (respiratory toxicants) or category 0 (non-respiratory toxicants), with the output value is the probability of being toxic, within the range of 0 to 1. As per the computed scores of 0.944, 0.647 and 0.864, respectively, only **5a** is accompanied by a medium risk of being a respiratory toxicant, whereas **3h** and **5h** would be strong respiratory toxicants.

- Eye irritation/eye corrosion (EI/EC)

The chemical may be classified as category 1 (irritant or corrosive) or category 0 (non-irritant/non-corrosive) with the output value is the probability of being toxic, within the range of 0 to 1. The computed values for the toxic probabilities were 0.03, 0.157 and 0.148 for eye irritation, and 0.003 for all of them as corrosives; thus, none of the compounds is likely to cause eye irritation or corrosion.

- Predicting the toxicology in the 21st century (Tox21) program

Furthermore, the toxicity of the compounds was evaluated according to the Tox21 dataset, which consists of two major panels: a nuclear receptor (NR) signaling panel and a stress response (SR) panel, which together comprise 12 in vitro assays.

#### *Nuclear receptor pathway toxicity*

Seven assays were used to evaluate the compounds for their capabilities of interacting with nuclear receptors (either as inhibitors or activators) that may cause the disruption of normal endocrine function, as well as interfere with metabolic homeostasis, reproduction, and developmental and behavioral functions.

1. Nuclear receptor–Androgen receptor (NR-AR)

The androgen receptor (AR) is a nuclear hormone receptor that plays a critical role in androgen-related diseases such as AR-dependent prostate cancer. Therefore, the used web tool categorizes the compounds either as category 1 (activator or agonist) or category 0 (inactivator). The output value is the probability of being AR agonists, within the range of 0 to 1. The predicted probability values were 0.134, 0.338 and 0.607, respectively. Accordingly, **3h** is not a possible agonist, whereas **5a** and **5h** have medium probabilities of being AR agonists.

2. Nuclear receptor–Androgen receptor ligand binding domain (NR-AR-LBD)

This receptor is also implicated in androgen-related diseases; thus, in this bioassay, chemicals which are capable of binding to the AR-LBD belong to category 1 (active) and the output value is the probability of being active, within the range of 0 to 1. The predicted probability values were 0.554, 0.025 and 0.225, respectively, indicating that **3h** and **5h** may bind with this receptor, whereas **5a** may not bind with it.

### 3. Nuclear receptor–Aryl hydrocarbon Receptor (NR-AhR)

The AhR is pivotal for adaptive responses against environmental pollutants such as aromatic hydrocarbons and environmental changes through the induction of phase I and II enzymes; in addition, it interacts with other nuclear receptor signaling pathways. The molecules may belong to category 0, or category 1, wherein molecules labeled as category 1 act to activate the aryl hydrocarbon receptor signaling pathway, with the output value is the probability of being an activator, within the range of 0 to 1. The computed values were 0.885, 0.511 and 0.846, respectively; thus, **3h** and **5h** have a high probability of being AhR activators, whereas **5a** can be considered as a moderate activator.

### 4. NR-Aromatase

Aromatase catalyzes the conversion of androgen to estrogen and plays a crucial role in maintaining the balance between the two hormones in many of the endocrine disrupting chemical (EDC)-sensitive organs. The compounds may be labelled as category 1 (active) or category 0 (inactive). The label of category 1 designates aromatase inhibitors, with the output probability value being within the range of 0 to 1. The predicted values were 0.885, 0.902 and 0.924, respectively. Thus, all the compounds have a high probability of being aromatase inhibitors and could cause an imbalance between androgen and estrogen.

### 5. Nuclear receptor–Estrogen receptor (NR-ER)

Certain chemicals may interact with steroid hormone receptors like the ER, thus causing the disruption of normal endocrine function; these chemicals are called endocrine disrupting chemicals (EDCs). Therefore, chemicals and drugs are assessed for their effect on the ER signaling pathway as being either category 1 (active) or category 0 (inactive), with the output value indicating the probability of being active within the range of 0 to 1. The computed values were 0.552, 0.474 and 0.519, implying that the three compounds have medium probabilities for interfering with the ER signaling pathway.

### 6. Nuclear receptor–Estrogen receptor $\alpha$ ligand binding domain (NR-ER-LBD)

Likewise, compounds may be labeled as active or inactive towards the NR-ER-LBD. The output value is the probability of being active, within the range of 0 to 1. The predicted values were 0.491, 0.102 and 0.362; as a consequence, the probability that **5a** interferes with the ER-LBD pathway is negligible, whereas **3h** and **5h** have medium probabilities for interference with this pathway.

### 7. Nuclear receptor–peroxisome proliferator-activated receptors gamma (NR-PPAR $\gamma$ )

Furthermore, the compounds may be categorized as active (category 1) or inactive (category 0) for their interference with the PPAR $\gamma$  receptor (also known as the glitazone reverse insulin resistance receptor), which is involved in the regulation of the glucose and lipid metabolism. The output value is the probability of being active within the range of 0 to 1. The estimated values were 0.446, 0.933 and 0.807, respectively; thus, **5a** and **5h** have medium probabilities, whereas **3h** has a moderate probability for interference with PPAR $\gamma$ .

#### *Stress response (SR) panel*

Toxicity may also lead to cellular oxidative stress, which in turn leads to apoptosis. Thus, the compounds were also screened with regard to five stress response assays, as follows:

#### 1. The antioxidant response element signaling pathway (SR-ARE)

The ARE directly reacts to cellular stress; therefore, the chemicals are labelled as category 1 (active) or category 0 (inactive), with the output value indicating the probability of being active within the range of 0 to 1. According to the computed values of 0.816, 0.912 and 0.912, all compounds have a high probability for being active in ARE signaling.

#### 2. ATPase family AAA domain-containing protein 5 (SR-ATAD5)

According to this assay, compounds which are expected to cause DNA damage, thus enhancing the levels of genome instability gene 1 (ELG1; human ATAD5) protein, are labeled as category 1 (active), while those would not cause DNA damage are labeled as category 0 (inactive), with the output value is the probability of being active within the range of 0 to 1. The predicted values were 0.749, 0.012 and 0.542, respectively, indicating the safety of **5a** with regard to this indicator, whereas **3h** and **5h** have medium probabilities for being inducers to genomic instability.

### 3. Heat shock factor response element (SR-HSE)

This pathway is activated in response to stresses (such as elevated temperature, oxidant accumulation and abrupt alterations in osmolarity) that damage cellular proteins. Therefore, the compounds were evaluated as being activators (category 1) or non-activators (category 0) for the HSE, with the output value indicating the probability of being active within the range of 0 to 1. The computed values were 0.593, 0.314 and 0.091, respectively, implying that **3h** has a medium probability of being a stressor, whereas **5a** and **5h** have negligible probabilities as stressors; accordingly, they are safer.

### 4. Mitochondrial membrane potential (SR-MMP, $\Delta\Psi_m$ )

Compounds may cause mitochondrial toxicity via different mechanisms of action, one of them being influencing the MMP. Compounds that disrupt mitochondrial function may induce adverse effects such as liver injury. Therefore, the compounds were evaluated as being active (category 1) or inactive (category 0) with regard to disrupting the MMP, with the output value indicating the probability of being active within the range of 0 to 1. The predicted values were 0.875, 0.898 and 0.926; thus, all of the compounds are expected to cause MMP.

### 5. p53, a tumor suppressor protein (SR- p53)

This pathway is a well-known cancer pathway, which is activated following DNA damage or other cellular stressors. Thus, compounds which do not activate p53 are labelled (category 0), while those activate it are labeled category 1 and they are considered as toxic molecules. The output value is the probability of being an activator within the range of 0 to 1. The estimated values were 0.893, 0.909 and 0.916, respectively; accordingly, all of them are potential toxic molecules via activating the p53 pathway.

- The prediction of the existence or absence of toxicophores and compliance with toxicity rules:
  1. The number of toxic substructures (toxicophores) present in the studied compounds were 5, 1 and 3, respectively;
  2. Based on the genotoxic carcinogenicity rule, the molecules possessed 5, 0 and 5 substructures, respectively, which would cause carcinogenicity or mutagenicity through genotoxic mechanisms;
  3. Based on the non-genotoxic carcinogenicity rule, the molecules possessed 0, 1 and 1 substructures, respectively, which would cause carcinogenicity through nongenotoxic mechanisms;
  4. Based on the skin sensitization rule, the molecules possessed 1, 1 and 2 substructures, respectively, which would cause skin irritation;
  5. Based on the non-biodegradable rule, the molecules possessed 2, 2 and 3 substructures, respectively, which would make them non-biodegradable;
  6. Based on the SureChEMBL rule, the molecules did not have any structural alerts to have a MedChem unfriendly status.
- Predictions of environmental toxicity
  1. Bioconcentration Factor (BCF)

The BCF is used to reflect on secondary poisoning potential and evaluate risks to human health via the food chain. The unit of BCF is  $\log_{10}(L/kg)$  and it is calculated based on the ratio of a chemical concentration in the organism as a

result of absorption via the respiratory and dermal surfaces to that in water at a steady state. Substances are considered highly bioaccumulative (should be severely restricted) with a BCF value of  $\geq 3.7$ , accumulative with BCF ranging between 3 and 3.3, and non-accumulative having BCF values of  $< 3$ , according to the US Environmental Protection Agency under the Toxic Substances Control Act [104]. For the studied compounds the computed values were 0.741, 1.7 and 2.212; thus, all of them would be non-bioaccumulative, and so they are considered to be non-ecotoxic.

2. The 50% growth inhibitory concentration ( $IGC_{50}$ ) for *Tetrahymena pyriformis*  
This value indicates aquatic toxicity by estimating the concentration of a chemical in water in mg/L that causes 50% growth inhibition to *Tetrahymena pyriformis* after 48 h. The predicted values in units of  $[-\log_{10}[(\text{mg/L})/(1000 \times \text{MW})]]$  were 4.771, 5.339 and 5.222, respectively.
3. The median lethal concentration values against fathead minnow ( $LC_{50FM}$ )  
This value refers to the concentration of a molecule in water in mg/L that causes 50% of fathead minnow to die after 96 h, expressed in  $[-\log_{10}[(\text{mg/L})/(1000 \times \text{MW})]]$ . The computed values were 5.083, 6.709 and 6.738 unit.
4. The median lethal concentration values against *Daphnia magna* ( $LC_{50DM}$ )  
This value is defined as the concentration of a compound in water in mg/L which causes death to 50% of a population of *Daphnia magna* after 48 h. The recorded values for the compounds were 5.959, 6.99 and 6.865  $[-\log_{10}[(\text{mg/L})/(1000 \times \text{MW})]]$ , respectively.

### 3. Materials and Methods

#### 3.1. Chemistry

##### 3.1.1. General

All reagents were supplied commercially and they were used without further purification. The melting points ( $^{\circ}\text{C}$ ) were determined using an electronic melting point apparatus (Electrothermal, Essex, UK) and they were uncorrected. IR spectra were recorded on the Perkin Elmer FT-IR system, spectrum BX, as wave numbers ( $\text{cm}^{-1}$ ) using KBr discs. The NMR analyses were performed in deuterated dimethyl sulfoxide ( $\text{DMSO-}d_6$ ) and they were recorded on different Spectrometers (Tokyo, Japan) including, an Eclipse 300 FT NMR Spectrometer at 300 MHz and on a JNM-Ecx500II FT NMR system spectrometer at 500 MHz for the  $^1\text{H}$ NMR analysis, whereas the  $^{13}\text{C}$ NMR on the Agilent NMR-600, was working at 150 MHz. Chemical shifts ( $\delta$ ) were expressed in ppm relative to tetramethylsilane (TMS) as the internal standard; the coupling constant values ( $J$ ) were expressed in Hz and the splitting patterns of  $^1\text{H}$ NMR were designated as s (singlet), d (doublet), t (triplet), dd (double-doublet), app. (apparent), m (multiplet) and q (quartet). Mass spectra were carried out on a direct probe controller inlet part of a single quadrupole mass analyzer in the Thermo Scientific GCMS model (ISO Lt) using Thermo X-Calibur Software 3.0.

##### 3.1.2. General Procedures for the Synthesis of 6-substituted or 6,7-disubstituted-3-aryl-2-thioxo-2,3-dihydro-1*H*-quinazolin-4-one **3a-h**

To a suspension of anthranilic acid derivative **1a-c** (0.054 mol) namely; 5-chloro anthranilic acid, 5-bromo anthranilic or 4,5-dimethoxy anthranilic acid in glacial acetic acid (50 mL), the appropriate phenyl isothiocyanate derivative **2a-c** (0.054 mol) namely; 3-(trifluoromethyl)phenyl isothiocyanate, 4-(trifluoromethyl)phenyl isothiocyanate or 4-nitrophenyl isothiocyanate was added. After refluxing the resulting reaction mixture for 10 h [70], the formed solid in each case was collected via filtration, washed with an excess of water, air-dried and recrystallized from ethanol to give the pure compound. The obtained products would exist in two tautomeric forms, **3a-h** and **3'a-h** (6,7-disubstituted-2-mercapto-3-aryl-3*H*-quinazolin-4-one derivatives). The IR as well as the  $^1\text{H}$  and  $^{13}\text{C}$ NMR data proved the predominance of the **3a-h** tautomeric forms.

*6-Chloro-2-thioxo-3-(3-trifluoromethyl-phenyl)-2,3-dihydro-1H-quinazolin-4-one (3a)*, off-white, yield (80%), m.p. 275–276 °C;  $\nu_{\max}$  (KBr)/ $\text{cm}^{-1}$  3245 (NH), 3108 and 3038 (CH-aromatic), 1888, 1838, 1664 (C=O), 1619; 1523 and 1484 (C=C), 1450, 1389, 1332, 1269, 1212, 1174, 1129, 1069, 1003, 919, 864, 833, 800, 761, 724, 694, 663, 615, 563, 540, 474;  $^1\text{H-NMR}$  (500 MHz; DMSO- $d_6$ )  $\delta_{\text{H}}$ : 13.19 (1H, s, NH), 7.84 (1H, d,  $J = 1.5$  Hz, CH-aromatic), 7.81 (1H, app. dd,  $J = 8.5, 1.5$  Hz, CH-aromatic), 7.78–7.75 (2H, m,  $2 \times$  CH-aromatic), 7.70 (1H, t,  $J = 7.5$  Hz, CH-aromatic), 7.58 (1H, d,  $J = 7.5$  Hz, CH-aromatic), 7.42 (1H, d,  $J = 8.5$  Hz, CH-aromatic);  $^{13}\text{C-NMR}$  (150 MHz; DMSO- $d_6$ )  $\delta_{\text{C}}$ : 176.24 (C=S), 159.39 (C=O), 140.31, 138.86, 136.00, 133.93, 130.61, 130.31, 130.09, 128.70, 126.67, 125.57, 125.27, 123.44, 118.45, 118.24 ( $7 \times$  CH-aromatic,  $5 \times$  C<sub>q</sub>-aromatic, and CF<sub>3</sub>); MS (EI)  $m/z$  (%) [ $\text{M}^+ + 2, ^{37}\text{Cl}$ ] 360.11 (2.11), [ $\text{M}^+ + 1, ^{37}\text{Cl}$ ] 359.05 (5.22), [ $\text{M}^+, ^{37}\text{Cl}$ ] 358.08 (16.11), [ $\text{M}^+ + 1, ^{35}\text{Cl}$ ] 357.07 (43.94), [ $\text{M}^+, ^{35}\text{Cl}$ ] 356.10 (60.87) for C<sub>15</sub>H<sub>8</sub>ClF<sub>3</sub>N<sub>2</sub>OS, 355.04 (100.00), 337.42 (3.36), 322.97 (8.39), 287.11 (6.40), 287.03 (7.52), 259.98 (4.42), 195.89 (1.34), 180.93 (2.94), 168.23 (2.13), 153.01 (4.97), 145.28 (4.29), 132.31 (4.01), 125.20 (14.72), 107.94 (5.36), 90.19 (11.34), 75.04 (16.95), 74.10 (17.68), 69.03 (59.01), 50.24 (5.78), 43.14 (5.14).

*6-Bromo-2-thioxo-3-(3-trifluoromethyl-phenyl)-2,3-dihydro-1H-quinazolin-4-one (3b)*, off-white powder, yield (72%), m.p. 282–283 °C;  $\nu_{\max}$  (KBr)/ $\text{cm}^{-1}$  3164 (NH), 3094 (CH-aromatic), 2996, 2935, 1726 (C=O), 1616; 1532 and 1475 (C=C), 1452, 1432, 1389, 1334, 1264, 1211, 1170, 1115, 1071, 998, 910, 855, 810, 757, 693, 612, 549, 436;  $^1\text{H-NMR}$  (500 MHz; DMSO- $d_6$ )  $\delta_{\text{H}}$ : 13.18 (1H, s, NH), 7.97 (1H, d,  $J = 2.0$  Hz, CH-aromatic), 7.92 (1H, app. dd,  $J = 8.5, 2.0$  Hz, CH-aromatic), 7.75–7.73 (2H, m,  $2 \times$  CH-aromatic), 7.68 (1H, t,  $J = 7.5$  Hz, CH-aromatic), 7.58 (1H, d,  $J = 7.5$  Hz, CH-aromatic), 7.35 (1H, d,  $J = 8.5$  Hz, CH-aromatic);  $^{13}\text{C-NMR}$  (150 MHz; DMSO- $d_6$ )  $\delta_{\text{C}}$ : 176.28 (C=S), 159.27 (C=O), 140.30, 139.17, 138.69, 133.93, 130.63, 130.30, 130.09, 129.68, 126.66, 125.58, 125.26, 123.46, 118.59, 116.41 ( $7 \times$  CH-aromatic,  $5 \times$  C<sub>q</sub>-aromatic, and CF<sub>3</sub>); MS (EI)  $m/z$  (%) [ $\text{M}^+ + 1, ^{81}\text{Br}$ ] 403.06 (4.16), [ $\text{M}^+, ^{81}\text{Br}$ ] 402.04 (11.42), [ $\text{M}^+ + 1, ^{79}\text{Br}$ ] 401.06 (15.01), [ $\text{M}^+, ^{79}\text{Br}$ ] 400.05 (16.06) for C<sub>15</sub>H<sub>8</sub>BrF<sub>3</sub>N<sub>2</sub>OS, 197.12 (1.48), 333.14 (1.50), 169.05 (2.24), 145.10 (4.86), 133.13 (2.55), 125.19 (4.29), 106.23 (1.66), 90.15 (13.78), 75.04 (28.55), 74.11 (14.98), 69.08 (100.00), 63.12 (43.07), 50.07 (6.06), 43.17 (2.07).

*6,7-Dimethoxy-2-thioxo-3-(3-trifluoromethyl-phenyl)-2,3-dihydro-1H-quinazolin-4-one (3c)*, off-white solid, yield (68%), m.p. 304–305 °C;  $\nu_{\max}$  (KBr)/ $\text{cm}^{-1}$  3178 (NH), 3115 and 3035 (CH-aromatic), 2973 (CH-aliphatic), 2279, 1698 (C=O), 1626; 1548 and 1512 (C=C), 1459, 1429, 1399, 1332, 1290, 1248, 1203, 1174, 1113, 1032, 992, 977, 819, 761, 698, 654, 597, 556, 456;  $^1\text{H-NMR}$  (500 MHz; DMSO- $d_6$ )  $\delta_{\text{H}}$ : 12.91 (1H, s, NH), 7.73 (1H, d,  $J = 7.5$  Hz, CH-aromatic), 7.69 (1H, s, CH-aromatic), 7.66 (1H, app t,  $J = 8.0$  Hz, CH-aromatic), 7.56 (1H, d,  $J = 8.5$  Hz, CH-aromatic), 7.24 (1H, s, CH-aromatic), 6.95 (1H, s, CH-aromatic), 3.83 (3H, s, OCH<sub>3</sub>), 3.77 (3H, s, OCH<sub>3</sub>);  $^{13}\text{C-NMR}$  (125 MHz; DMSO- $d_6$ )  $\delta_{\text{C}}$ : 174.66 (C=S), 159.34 (C=O), 155.41, 146.58, 140.23, 135.63, 133.62, 130.03, 129.80, 126.38, 125.03, 124.89, 122.87, 108.66, 106.94, 97.98 ( $6 \times$  CH-aromatic,  $6 \times$  C<sub>q</sub>-aromatic, and CF<sub>3</sub>), 56.01 (OCH<sub>3</sub>), 55.84 (OCH<sub>3</sub>); MS (EI)  $m/z$  (%) [ $\text{M}^+ + 2$ ] 384.11 (4.47), [ $\text{M}^+ + 1$ ] 383.17 (27.26), [ $\text{M}^+$ ] 382.16 (100.00) for C<sub>17</sub>H<sub>13</sub>F<sub>3</sub>N<sub>2</sub>O<sub>3</sub>S, 381.18 (49.46), 367.08 (21.32), 349.00 (8.35), 336.13 (17.89), 321.03 (1.88%), 308.23 (5.29), 280.19 (1.52), 267.24 (1.27), 145.23 (1.91), 69.15 (19.97).

*6-Chloro-2-thioxo-3-(4-trifluoromethyl-phenyl)-2,3-dihydro-1H-quinazolin-4-one (3d)*, white powder, yield (84%), m.p. 375–377 °C;  $\nu_{\max}$  (KBr)/ $\text{cm}^{-1}$  3164 (NH), 3095 and 3001 (CH-aromatic), 2341, 1925, 1840, 1800, 1702 (C=O), 1618; 1534 and 1482 (C=C), 1435, 1395, 1330, 1262, 1214, 1162, 1111, 1066, 1021, 990, 956, 913, 822, 760, 715, 680, 650, 596, 536, 475, 420;  $^1\text{H-NMR}$  (500 MHz; DMSO- $d_6$ )  $\delta_{\text{H}}$ : 13.20 (1H, s, NH), 7.85–7.79 (4H, m,  $4 \times$  CH-aromatic), 7.52 (2H, d,  $J = 8.5$  Hz,  $2 \times$  CH-aromatic), 7.42 (1H, d,  $J = 9.0$  Hz, CH-aromatic);  $^{13}\text{C-NMR}$  (150 MHz; DMSO- $d_6$ )  $\delta_{\text{C}}$ : 176.00 (C=S), 159.25 (C=O), 143.20, 138.88, 136.00, 130.64, 129.26, 128.70, 126.56, 125.41, 123.59, 118.45, 118.14 ( $7 \times$  CH-aromatic,  $5 \times$  C<sub>q</sub>-aromatic, and CF<sub>3</sub>); MS (EI)  $m/z$  (%) [ $\text{M}^+ + 1, ^{37}\text{Cl}$ ] 358.91 (1.63), [ $\text{M}^+, ^{37}\text{Cl}$ ] 358.03 (28.37), [ $\text{M}^+ + 1, ^{35}\text{Cl}$ ] 357.01 (18.30), [ $\text{M}^+, ^{35}\text{Cl}$ ] 356.09 (64.18) for C<sub>15</sub>H<sub>8</sub>ClF<sub>3</sub>N<sub>2</sub>OS, 355.09 (100.00), 337.03 (6.02), 322.95 (10.78), 297.27 (7.64), 285.99 (9.01), 277.45 (4.42), 261.29 (6.04), 236.61 (2.79), 228.19 (3.05),

195.87 (5.98), 179.29 (3.94), 153.18 (11.88), 133.17 (5.08), 126.15 (25.96), 114.32 (4.67), 90.21 (15.36), 75.09 (41.28), 69.16 (56.28%), 50.16 (14.81), 43.28 (6.46).

**6-Bromo-2-thioxo-3-(4-trifluoromethyl-phenyl)-2,3-dihydro-1H-quinazolin-4-one (3e)**, white powder, yield (67%), m.p. 359–360 °C;  $\nu_{\max}$  (KBr)/ $\text{cm}^{-1}$  3161 (NH), 3089 (CH-aromatic), 2996, 2938, 2373, 2342, 1921, 1850, 1798, 1705 (C=O), 1616; 1533 and 1478 (C=C), 1432, 1393, 1329, 1261, 1213, 1163, 1067, 1022, 989, 957, 927, 901, 821, 761, 710, 651, 595, 531, 440;  $^1\text{H-NMR}$  (500 MHz; DMSO- $d_6$ )  $\delta_{\text{H}}$ : 13.19 (1H, s, NH), 7.97 (1H, d,  $J = 1.5$  Hz, CH-aromatic), 7.92 (1H, app. dd,  $J = 8.5, 2.0$  Hz, CH-aromatic), 7.82 (2H, d,  $J = 9.0$  Hz, CH-aromatic), 7.51 (2H, app. d,  $J = 8.5$  Hz,  $2 \times$  CH-aromatic), 7.35 (1H, app. d,  $J = 8.5$  Hz, CH-aromatic);  $^{13}\text{C-NMR}$  (150 MHz; DMSO- $d_6$ )  $\delta_{\text{C}}$ : 176.04 (C=S), 159.16 (C=O), 143.24, 139.25, 138.69, 130.63, 129.64, 126.56, 118.65, 118.54, 116.38 ( $7 \times$  CH-aromatic,  $5 \times$  C<sub>q</sub>-aromatic, and CF<sub>3</sub>); MS (EI)  $m/z$  (%) [ $\text{M}^+ + 1$ ,  $^{81}\text{Br}$ ] 402.94 (10.26), [ $\text{M}^+$ ,  $^{81}\text{Br}$ ] 401.98 (29.26), [ $\text{M}^+ + 1$ ,  $^{79}\text{Br}$ ] 401.09 (39.11), [ $\text{M}^+$ ,  $^{79}\text{Br}$ ] 400.04 (39.62) for C<sub>15</sub>H<sub>8</sub>BrF<sub>3</sub>N<sub>2</sub>OS, 399.06 (22.17), 381.07 (3.47), 369.02 (3.38), 330.94 (36.62), 320.92 (3.04), 292.29 (2.57), 239.87 (1.76), 182.97 (1.57), 145.09 (2.87), 89.23 (2.30), 75.01 (5.70), 69.10 (100.00%), 50.2 (1.54).

**6-Chloro-3-(4-nitro-phenyl)-2-thioxo-2,3-dihydro-1H-quinazolin-4-one (3f)**, yellow powder, yield (68%), m.p. 343–344 °C;  $\nu_{\max}$  (KBr)/ $\text{cm}^{-1}$  3157 (NH), 3088, (CH-aromatic), 2995, 1698 (C=O), 1616; 1519 and 1475 (C=C), 1432, 1392, 1348, 1256, 1211, 1085, 1017, 990, 912, 823, 760, 694, 647, 587, 535, 475, 426;  $^1\text{H-NMR}$  (500 MHz; DMSO- $d_6$ )  $\delta_{\text{H}}$ : 13.24 (1H, s, NH), 8.34–8.27 (2H, m,  $2 \times$  CH-aromatic), 7.85 (1H, d,  $J = 3.0$  Hz, CH-aromatic), 7.81 (1H, app. dd,  $J = 8.5, 3.0$  Hz, CH-aromatic), 7.62–7.57 (2H, m,  $2 \times$  CH of 4-NO<sub>2</sub>-C<sub>6</sub>H<sub>4</sub>), 7.42 (1H, d,  $J = 9.0$  Hz, CH-aromatic);  $^{13}\text{C-NMR}$  (75 MHz; DMSO- $d_6$ )  $\delta_{\text{C}}$ : 175.63 (C=S), 159.04 (C=O), 147.38, 145.24, 138.69, 135.86, 131.07, 128.64, 126.46, 124.56, 118.28, 117.94 ( $7 \times$  CH-aromatic and  $5 \times$  C<sub>q</sub>-aromatic); MS (EI)  $m/z$  (%) [ $\text{M}^+$ ,  $^{37}\text{Cl}$ ] 335.05 (26.91), [ $\text{M}^+ + 1$ ,  $^{35}\text{Cl}$ ] 334.10 (33.29), [ $\text{M}^+$ ,  $^{35}\text{Cl}$ ] 333.06 (57.07) for C<sub>14</sub>H<sub>8</sub>ClN<sub>3</sub>O<sub>3</sub>S, 332.07 (44.01), 302.82 (3.742), 285.97 (24.99), 257.94 (1.91), 231.34 (2.62), 215.77 (2.31), 183.85 (5.07), 153.03 (3.33), 133.00 (5.69), 124.26 (20.51), 110.11 (5.45), 90.08 (18.18), 75.22 (55.60), 63.18 (100.00), (50.19 (22.63), 46.12 (15.38).

**6-Bromo-3-(4-nitro-phenyl)-2-thioxo-2,3-dihydro-1H-quinazolin-4-one (3g)**, yellow powder, yield (65%), m.p. 340–341 °C;  $\nu_{\max}$  (KBr)/ $\text{cm}^{-1}$  3155 (NH), 3084 (CH-aromatic), 2992, 1698 (C=O), 1614; 1517 and 1471 (C=C), 1429, 1390, 1346, 1256, 1210, 1071, 989, 906, 852, 821, 760, 690, 646, 587, 526, 444, 421;  $^1\text{H-NMR}$  (500 MHz; DMSO- $d_6$ )  $\delta_{\text{H}}$ : 13.23 (1H, s, NH), 8.33–8.28 (2H, m,  $2 \times$  CH of 4-NO<sub>2</sub>-C<sub>6</sub>H<sub>4</sub>), 7.97 (1H, d,  $J = 2.0$  Hz, CH<sup>5</sup>-quinazolin-4(3H)-one), 7.93 (1H, dd,  $J = 8.5, 2.0$  Hz, CH<sup>7</sup>-quinazolin-4(3H)-one), 7.62–7.56 (2H, m,  $2 \times$  CH of 4-NO<sub>2</sub>-C<sub>6</sub>H<sub>4</sub>), 7.35 (1H, d,  $J = 8.5$  Hz, CH<sup>8</sup>-quinazolin-4(3H)-one);  $^{13}\text{C-NMR}$  (75 MHz; DMSO- $d_6$ )  $\delta_{\text{C}}$ : 175.62 (C=S), 158.86 (C=O), 147.38, 145.17, 139.01, 138.54, 131.07, 129.46, 124.56, 118.43, 118.28, 116.30 ( $7 \times$  CH-aromatic and  $5 \times$  C<sub>q</sub>-aromatic); MS (EI)  $m/z$  (%) [ $\text{M}^+ + 2$ ,  $^{81}\text{Br}$ ] 381.07 (2.28), [ $\text{M}^+ + 1$ ,  $^{81}\text{Br}$ ] 380.11 (8.00), [ $\text{M}^+$ ,  $^{81}\text{Br}$ ] 379.05 (35.08), [ $\text{M}^+ + 1$ ,  $^{79}\text{Br}$ ] 378.01 (47.20), [ $\text{M}^+$ ,  $^{79}\text{Br}$ ] 377.02 (39.84) for C<sub>14</sub>H<sub>8</sub>BrN<sub>3</sub>O<sub>3</sub>S, 376.01 (39.79), 361.40 (1.64), 344.03 (2.49), 332.03 (16.15), 298.12 (4.51), 271.96 (2.41), 239.99 (2.86), 224.17 (3.44), 197.08 (10.80), 168.09 (5.36), 133.10 (11.22), 116.23 (6.34), 108.09 (5.97), 90.12 (43.77), 75.18 (48.59), 50.08 (13.32), 46.07 (6.82).

**6,7-Dimethoxy-3-(4-nitro-phenyl)-2-thioxo-2,3-dihydro-1H-quinazolin-4-one (3h)**, yellow powder, yield (54%), m.p. 328–329 °C;  $\nu_{\max}$  (KBr)/ $\text{cm}^{-1}$  3177 (NH), 3113 and 3033 (CH-aromatic), 2972 (CH-aliphatic), 1696 (C=O), 1625; 1550 and 1514 (C=C), 1428, 1400, 1348, 1292, 1247, 1200, 1156, 1064, 1024, 988, 855, 818, 756, 708, 684, 647, 607, 581, 498, 426;  $^1\text{H-NMR}$  (500 MHz; DMSO- $d_6$ )  $\delta_{\text{H}}$ : 12.96 (1H, s, NH), 8.32–8.24 (2H, m,  $2 \times$  CH-aromatic), 7.62–7.54 (2H, m,  $2 \times$  CH-aromatic), 7.24 (1H, s, CH-aromatic), 6.95 (1H, s, CH-aromatic), 3.83 (3H, s, OCH<sub>3</sub>), 3.77 (3H, s, OCH<sub>3</sub>);  $^{13}\text{C-NMR}$  (75 MHz; DMSO- $d_6$ )  $\delta_{\text{C}}$ : 174.38 (C=S), 159.33 (C=O), 155.69, 147.24, 146.82, 145.59, 135.86, 131.17, 124.40, 108.77, 107.08, 98.23 ( $6 \times$  CH-aromatic and  $6 \times$  C<sub>q</sub>-aromatic), 56.23 (OCH<sub>3</sub>), 56.06 (OCH<sub>3</sub>); MS (EI)  $m/z$  (%) [ $\text{M}^+ + 2$ ] 361.20 (4.32), [ $\text{M}^+ + 1$ ] 360.21 (17.90), [ $\text{M}^+$ ] 359.19 (100.00) for C<sub>16</sub>H<sub>13</sub>N<sub>3</sub>O<sub>5</sub>S, 358.20 (55.20), 343.20 (2.79), 326.17 (4.69), 312.18 (4.66), 297.15 (3.91), 269.11 (5.30), 255.12 (6.26), 222.13 (3.54), 205.15 (3.67), 179.20 (22.25), 164.14 (50.57), 150.15 (21.00), 136.12 (55.73), 120.11 (12.10), 108.13 (29.19), 90.13 (21.26), 76.11 (20.09), 63.15 (35.96), 50.15 (23.96), 44.12 (8.94).

### 3.1.3. Synthesis of 2-(benzylsulfanyl)-3-aryl-3H-quinazolin-4-one Derivatives 5a–h General Procedures

Potassium carbonate (3 equiv., 0.0054 mol, 0.74 g) was added [63] to an equimolar mixture (0.0018 mol) of 6-substituted or 6,7-disubstituted-3-aryl-2-thioxo-2,3-dihydro-1H-quinazolin-4-one **3a–h** and aryl halide derivative Ar-CH<sub>2</sub>-X **4a–d**, namely (in order) 2-fluoro benzyl bromide, 4-chlorobenzyl chloride, 3-nitro benzyl bromide or 2-bromo-5-methoxy benzyl bromide in dry acetone (20 mL). After refluxing the reaction mixture for 6 h, it was filtered while hot to isolate potassium carbonate and the filtrate was concentrated under reduced pressure to give the crude solid product. The obtained solid in each case was washed with water, air-dried and recrystallized from the appropriate solvent to give compounds **5a–h** in pure forms.

*2-(2-Fluoro-benzylsulfanyl)-6-chloro-3-(3-trifluoromethyl-phenyl)-3H-quinazolin-4-one (5a)*, white powder (EtOH/CHCl<sub>3</sub>), yield (80%), m.p. 148–149 °C;  $\nu_{\max}$  (KBr)/cm<sup>-1</sup> 3084 (CH-aromatic), 2989 and 2929 (CH-aliphatic), 1923, 1797, 1699 (C=O), 1547 (C=N), 1466 and 1402 (C=C), 1333, 1304, 1282, 1248, 1199, 1170, 1120, 1095, 1071, 976, 895, 873, 833, 807, 763, 696, 612, 540, 562, 420; <sup>1</sup>H-NMR (300 MHz; DMSO-*d*<sub>6</sub>)  $\delta_{\text{H}}$ : 8.12–7.50 (8H, m, 8 × CH-aromatic), 7.38–7.04 (3H, m, 3 × CH-aromatic), 4.46 (2H, s, S-CH<sub>2</sub>); <sup>13</sup>C-NMR (75 MHz; DMSO-*d*<sub>6</sub>)  $\delta_{\text{C}}$ : 162.27 (C=O), 159.97 (C=N), 159.02 (C<sub>q</sub>-F), 156.83 145.99, 136.50, 135.17, 133.97, 131.94, 1130.98, 130.30, 129.90, 129.80, 128.43, 127.08, 126.79, 125.59, 124.56, 121.13, 115.56, 115.28 (11 × CH-aromatic, 6 × C<sub>q</sub>-aromatic, and CF<sub>3</sub>), 29.79 (CH<sub>2</sub>); MS (EI) *m/z* (%) [M<sup>+</sup>, <sup>37</sup>Cl] 467.21 (2.86), [M<sup>+</sup> + 1, <sup>35</sup>Cl] 466.06 (3.45), [M<sup>+</sup>, <sup>35</sup>Cl] 465.32 (1.41) for C<sub>22</sub>H<sub>13</sub>ClF<sub>4</sub>N<sub>2</sub>OS, 464.10 (19.39), 430.49 (3.42), 411.50 (6.55), 377.95 (3.80), 355.03 (9.71), 339.47 (11.09), 320.17 (52.77), 308.94 (13.30), 296.96 (16.64), 287.14 (47.96), 269.09 (10.39), 253.19 (41.03), 244.25 (6.72), 233.28 (5.24), 225.90 (1.93), 191.88 (3.35), 168.39 (6.01), 145.14 (3.60), 132.93 (7.28), 124.01 (8.68), 109.12 (100.00), 83.14 (16.33), 76.04 (7.36), 69.36 (1.67), 63.56 (14.33), 57.31 (4.36), 44.95 (7.26).

*2-(4-Chloro-benzylsulfanyl)-6-bromo-3-(3-trifluoromethyl-phenyl)-3H-quinazolin-4-one (5b)*, off-white solid (EtOH/CHCl<sub>3</sub>), yield (80%), m.p. 193–194 °C;  $\nu_{\max}$  (KBr)/cm<sup>-1</sup> 3056 (CH-aromatic), 2935 (CH-aliphatic), 2298, 1907, 1690 (C=O), 1541 (C=N), 1490 and 1463 (C=C), 1331, 1289, 1249, 1176, 1125, 1092, 1067, 1013, 977, 910, 836, 809, 784, 744, 696, 610, 538, 507, 440; <sup>1</sup>H-NMR (300 MHz; DMSO-*d*<sub>6</sub>)  $\delta_{\text{H}}$ : 8.14 (1H, d, *J* = 2.4 Hz, CH-aromatic), 8.08–7.807.68 (5H, m, 5 × CH-aromatic), 7.68 (1H, d, *J* = 8.7 Hz, CH-aromatic), 7.59 (2H, d, *J* = 8.4, 2 × CH-aromatic), 7.35 (2H, d, *J* = 8.4 Hz, 2 × CH-aromatic), 4.43 (2H, AB q, *J* = 13.5 Hz, S-CH<sub>2</sub>); <sup>13</sup>C-NMR (150 MHz; CDCl<sub>3</sub>)  $\delta_{\text{C}}$ : 160.35 (C=O), 156.60 (C=N), 146.35, 138.11, 135.87, 134.55, 133.57, 132.68, 130.64, 130.42, 129.73, 128.75, 128.05, 127.08, 126.37, 121.08, 119.44 (11 × CH-aromatic, 7 × C<sub>q</sub>-aromatic, and CF<sub>3</sub>), 36.37 (CH<sub>2</sub>); MS (EI) *m/z* (%) [M<sup>+</sup> + 2, <sup>81</sup>Br and <sup>37</sup>Cl] 528.05 (24.98), [M<sup>+</sup> + 1, <sup>81</sup>Br and <sup>37</sup>Cl] 527.05 (31.94), [M<sup>+</sup>, <sup>81</sup>Br and <sup>37</sup>Cl] 526.03 (100.00), [M<sup>+</sup> + 1, <sup>79</sup>Br and <sup>35</sup>Cl] 525.07 (24.52), [M<sup>+</sup>, <sup>79</sup>Br and <sup>35</sup>Cl] 524.05 (82.52) for C<sub>22</sub>H<sub>13</sub>BrClF<sub>3</sub>N<sub>2</sub>OS, 509.04 (2.46), 507.07 (5.47), 493.07 (44.88), 491.09 (35.03), 458.12 (3.28), 456.09 (3.77), 320.12 (4.10), 268.91 (1.50).

*2-(3-Nitrobenzylsulfanyl)-6,7-dimethoxy-3-(3-trifluoromethyl-phenyl)-3H-quinazolin-4-one (5c)*, off-white powder (EtOH/CHCl<sub>3</sub>), yield (51%), m.p. 245–246 °C;  $\nu_{\max}$  (KBr)/cm<sup>-1</sup> 3067 (CH-aromatic), 2971 and 2938 (CH-aliphatic), 2831, 1918, 1849, 1681 (C=O), 1613 (C=N), 1580; 1535 and 1499 (C=C), 1454, 1388, 1352, 1330, 1273, 1240, 1171, 1129, 1072, 1027, 1002, 981, 922, 868, 846, 808, 758, 695, 675, 588, 528; <sup>1</sup>H-NMR (300 MHz; DMSO-*d*<sub>6</sub>)  $\delta_{\text{H}}$ : 8.52 (1H, app. dd, *J* = 6.3, 2.1 Hz, CH-aromatic), 8.09 (1H, app. dd, *J* = 8.4, 2.4 Hz, CH-aromatic), 7.98 (1H, s, CH-aromatic), 7.93 (2H, d, *J* = 7.8 Hz, 2 × CH-aromatic), 7.83–7.77 (2H, m, 2 × CH-aromatic), 7.60 (1H, t, *J* = 7.8 Hz, CH-aromatic), 7.37 (1H, s, CH-aromatic), 7.24 (1H, s, CH-aromatic), 4.53 (2H, AB q, *J* = 13.5 Hz, S-CH<sub>2</sub>); 3.99 (3H, s, OCH<sub>3</sub>), 3.85 (3H, s, OCH<sub>3</sub>); <sup>13</sup>C-NMR (150 MHz; DMSO-*d*<sub>6</sub>)  $\delta_{\text{C}}$ : 160.55 (C=O), 155.47 (C=N), 154.15 (2 × C<sub>q</sub>-O), 148.48, 147.74, 143.81, 140.41, 137.27, 136.68, 134.42, 131.20, 130.26, 127.15, 125.21, 122.55, 112.68, 107.45, 106.06 (10 × CH-aromatic, 6 × C<sub>q</sub>-aromatic, and CF<sub>3</sub>), 56.43 (OCH<sub>3</sub>), 56.19 (OCH<sub>3</sub>), 35.12 (CH<sub>2</sub>); MS (EI) *m/z* (%) [M<sup>+</sup> + 2] 519.10 (6.53), [M<sup>+</sup> + 1] 518.19 (29.95), [M<sup>+</sup>] 517.18 (100.00) for C<sub>24</sub>H<sub>18</sub>F<sub>3</sub>N<sub>3</sub>O<sub>5</sub>S 501.23 (3.23), 500.21 (9.57), 484.26 (3.90), 381.12 (4.91),



395.07 (1.59), 372.13 (1.22), 350.20 (2.09), 339.51 (1.92), 323.13 (2.02), 294.26 (2.49), 179.09 (2.06), 164.08 (1.62), 150.16 (1.78), 145.06 (1.30), 136.22 (8.05), 121.29 (1.38), 90.21 (15.71), 89.20 (15.26), 77.05 (2.71), 63.25 (4.11).

2-(4-Chloro-benzylsulfanyl)-6-chloro-3-(4-trifluoromethyl-phenyl)-3H-quinazolin-4-one (**5d**), off-white solid (EtOH), yield (80%), m.p. 259–260 °C;  $\nu_{\max}$  (KBr)/ $\text{cm}^{-1}$  3091 and 3063 (CH-aromatic), 2926 and 2856 (CH-aliphatic), 2369, 2340, 1898, 1850, 1776, 1695 (C=O), 1571 (C=N), 1549; 1464 and 1413 (C=C), 1328, 1269, 1203, 1162, 1114, 1066, 1019, 968, 930, 826, 784, 734, 712, 678, 642, 598, 543, 499, 466, 424;  $^1\text{H-NMR}$  (300 MHz;  $\text{CDCl}_3$ )  $\delta_{\text{H}}$ : 7.73 (1H, app. s, CH-aromatic), 7.34 (2H, d,  $J = 8.1$  Hz,  $2 \times$  CH-aromatic), 7.25 (1H, dd,  $J = 8.7, 2.4$  Hz, CH-aromatic), 7.15 (1H, d,  $J = 8.7$  Hz, CH-aromatic), 6.97 (2H, d,  $J = 8.1$  Hz,  $2 \times$  CH-aromatic), 6.88–6.77 (4H, m,  $4 \times$  CH-aromatic), 3.91 (2H, s, S- $\text{CH}_2$ );  $^{13}\text{C-NMR}$  (150 MHz;  $\text{DMSO-}d_6$ )  $\delta_{\text{C}}$ : 160.17 (C=O), 157.11 (C=N), 146.25, 139.78, 136.46, 135.51, 132.34, 131.69, 131.07, 130.59, 128.72, 127.15, 125.89, 121.35 ( $11 \times$  CH-aromatic,  $7 \times$  C<sub>q</sub>-aromatic, and  $\text{CF}_3$ ), 35.43 ( $\text{CH}_2$ ); MS (EI)  $m/z$  (%) [ $\text{M}^+ + 1, ^{37}\text{Cl}$ ] 485.19 (4.80), [ $\text{M}^+, ^{37}\text{Cl}$ ] 484.08 (16.22), [ $\text{M}^+ + 3, ^{35}\text{Cl}$ ] 483.08 (23.67), [ $\text{M}^+ + 2, ^{35}\text{Cl}$ ] 482.07 (79.35), [ $\text{M}^+ + 1, ^{35}\text{Cl}$ ] 481.21 (60.81), [ $\text{M}^+, ^{35}\text{Cl}$ ] 480.14 (100.00) for  $\text{C}_{22}\text{H}_{13}\text{Cl}_2\text{F}_3\text{N}_2\text{OS}$ , 479.59 (35.24), 478.93 (10.15), 449.00 (52.76), 447.10 (72.05), 412.25 (7.68), 355.00 (34.48), 337.13 (4.68), 335.03 (3.09), 322.23 (1.40), 320.10 (2.93), 304.29 (1.46), 268.93 (3.28).

2-(2-Bromo-5-methoxybenzylsulfanyl)-6-bromo-3-(4-trifluoromethyl-phenyl)-3H-quinazolin-4-one (**5e**), off-white solid (EtOH/ $\text{CHCl}_3$ ), yield (93%), m.p. 206–207 °C;  $\nu_{\max}$  (KBr)/ $\text{cm}^{-1}$  3067 (CH-aromatic), 2929 and 2862 (CH-aliphatic), 1691 (C=O), 1544 (C=N), 1462 (C=C), 1326, 1241, 1203, 1161, 1120, 1063, 1018, 967, 832, 660;  $^1\text{H-NMR}$  (500 MHz;  $\text{CDCl}_3$ )  $\delta_{\text{H}}$ : 8.33 (1H, d,  $J = 2.5$  Hz, CH-aromatic), 7.84 (1H, dd,  $J = 8.5, 2.5$  Hz, CH-aromatic), 7.78 (2H, d,  $J = 8.0$  Hz,  $2 \times$  CH of 4- $\text{CF}_3$ - $\text{C}_6\text{H}_4$ ), 7.57 (1H, d,  $J = 8.5$  Hz, CH-aromatic), 7.43–7.40 (3H, m,  $3 \times$  CH-aromatic), 7.13 (1H, d,  $J = 3.0$  Hz, CH-aromatic), 6.68 (1H, dd,  $J = 9.0, 3.0$  Hz, CH-aromatic), 4.50 (2H, s, S- $\text{CH}_2$ ), 3.74 (3H, s,  $\text{OCH}_3$ );  $^{13}\text{C-NMR}$  (125 MHz;  $\text{CDCl}_3$ )  $\delta_{\text{C}}$ : 160.39 (C=O), 158.83 (C=N), 156.73, 146.43, 138.48, 138.13, 136.47, 133.49, 129.79, 128.03, 127.01, 126.98, 124.63, 122.46, 121.10, 119.39, 117.31, 115.24, 114.92 ( $10 \times$  CH-aromatic,  $8 \times$  C<sub>q</sub>-aromatic, and  $\text{CF}_3$ ), 55.45 ( $\text{OCH}_3$ ), 37.52 ( $\text{CH}_2$ ); MS (EI)  $m/z$  (%) [ $\text{M}^+, ^{81}\text{Br}$ ] 600.15 (40.51), [ $\text{M}^+ + 1, ^{79}\text{Br}$ ] 599.29 (19.34), for  $\text{C}_{23}\text{H}_{15}\text{Br}_2\text{F}_3\text{N}_2\text{O}_2\text{S}$ , 566.81 (89.90), 552.96 (73.88), 520.49 (26.10), 467.86 (43.53), 440.74 (47.66), 437.83 (20.21), 422.12 (28.05), 337.38 (78.36), 290.43 (21.89), 222.37 (26.16), 202.73 (58.44), 201.11 (32.20), 191.45 (81.52), 186.76 (23.12), 156.47 (27.10), 144.50 (58.73), 116.18 (64.60), 106.18 (28.17), 87.12 (64.64), 74.20 (60.82), 69.66 (16.26), 57.86 (33.61).

2-(2-Bromo-5-methoxybenzylsulfanyl)-6-chloro-3-(4-nitro-phenyl)-3H-quinazolin-4-one (**5f**), white powder (MeOH/ $\text{CHCl}_3$ ), yield (67%), m.p. 215–216 °C;  $\nu_{\max}$  (KBr)/ $\text{cm}^{-1}$  3082 (CH-aromatic), 2962 and 2862 (CH-aliphatic), 1682 (C=O), 1548 (C=N), 1520 and 1469 (C=C), 1399, 1347, 1304, 1246, 1199, 1164, 1111, 1018, 968, 919, 840, 810, 730, 698, 644, 597, 542, 496, 465, 424;  $^1\text{H-NMR}$  (300 MHz;  $\text{DMSO-}d_6$ )  $\delta_{\text{H}}$ : 8.40 (2H, d,  $J = 9.0$  Hz,  $2 \times$  CH-aromatic), 8.00 (1H, d,  $J = 2.4$  Hz, CH-aromatic), 7.96–7.74 (4H, m,  $4 \times$  CH-aromatic), 7.48 (1H, d,  $J = 9.0$  Hz, CH-aromatic), 7.30 (1H, d,  $J = 3.3$  Hz, CH-aromatic), 6.80 (1H, dd,  $J = 8.7, 3.3$  Hz, CH-aromatic), 4.51 (2H, s, S- $\text{CH}_2$ ), 3.72 (3H, s,  $\text{OCH}_3$ );  $^{13}\text{C-NMR}$  (150 MHz;  $\text{CDCl}_3$ )  $\delta_{\text{C}}$ : 160.38 (C=O), 158.82 (C=N), 155.87, 148.63, 146.01, 140.88, 136.29, 135.56, 133.51, 132.00, 130.58, 127.92, 126.61, 125.07, 120.60, 117.36, 115.21, 114.95 ( $10 \times$  CH-aromatic,  $8 \times$  C<sub>q</sub>-aromatic), 55.45 ( $\text{OCH}_3$ ), 37.54 ( $\text{CH}_2$ ); MS (EI)  $m/z$  (%) [ $\text{M}^+ + 1, ^{81}\text{Br}$  and  $^{37}\text{Cl}$ ] 536.07 (5.84), [ $\text{M}^+, ^{81}\text{Br}$  and  $^{37}\text{Cl}$ ] 535.04 (32.01), [ $\text{M}^+ + 1, ^{81}\text{Br}$  and  $^{35}\text{Cl}$ ] 534.07 (34.13), [ $\text{M}^+, ^{81}\text{Br}$  and  $^{35}\text{Cl}$ ] 533.05 (100.00), [ $\text{M}^+ + 1, ^{79}\text{Br}$  and  $^{35}\text{Cl}$ ] 532.09 (30.17), [ $\text{M}^+, ^{79}\text{Br}$  and  $^{35}\text{Cl}$ ] 531.07 (90.35), for  $\text{C}_{22}\text{H}_{15}^{81}\text{BrClN}_3\text{O}_4\text{S}$ , 502.04 (8.58), 500.03 (13.17), 499.10 (5.81), 453.69 (4.52), 378.36 (1.34), 345.05 (2.04), 286.12 (1.85), 254.15 (1.48), 201.06 (2.19), 120.84 (1.31), 77.21 (3.92), 76.17 (1.32), 63.14 (1.28).

2-(3-Nitro-benzylsulfanyl)-6-bromo-3-(4-nitro-phenyl)-3H-quinazolin-4-one (**5g**), white powder (MeOH/ $\text{CHCl}_3$ ), yield (67%), m.p. 251–252 °C,  $\nu_{\max}$  (KBr)/ $\text{cm}^{-1}$  3118 and 3065 (CH-aromatic), 2929 and 2856 (CH-aliphatic), 1690 (C=O), 1548 (C=N), 1518 and 1464 (C=C), 1349, 1264, 1199, 1098, 1013, 967, 899, 856, 826, 750, 719, 695, 656, 528, 415;  $^1\text{H-NMR}$

(300 MHz; DMSO- $d_6$ )  $\delta_H$ : 8.47–8.35 (3H, m, 3  $\times$  CH-aromatic), 8.15–8.00 (3H, m, 3  $\times$  CH-aromatic), 7.95 (1H, d,  $J$  = 7.2 Hz, CH-aromatic), 7.83 (2H, d,  $J$  = 8.7 Hz, 2  $\times$  CH-aromatic), 7.69 (1H, d,  $J$  = 8.7 Hz, CH-aromatic), 7.59 (1H, t,  $J$  = 7.8 Hz, CH-aromatic), 4.56 (2H, s, S-CH<sub>2</sub>); <sup>13</sup>C-NMR (75 MHz; DMSO- $d_6$ )  $\delta_C$ : 159.65 (C=O), 156.40 (C=N), 148.46, 147.66, 146.18, 141.43, 139.87, 138.03, 136.40, 131.40, 129.94, 128.72, 128.52, 124.95, 124.45, 122.35, 121.50, 118.46 (11  $\times$  CH-aromatic and 7  $\times$  C<sub>q</sub>-aromatic), 34.96 (CH<sub>2</sub>); MS (EI)  $m/z$  (%) [ $M^+$  + 2, <sup>81</sup>Br] 517.03 (1.36), [ $M^+$ , <sup>81</sup>Br] 515.08 (18.24), [ $M^+$  + 1, <sup>79</sup>Br] 514.56 (12.55), [ $M^+$ , <sup>79</sup>Br] 513.11 (19.77) for C<sub>21</sub>H<sub>13</sub>BrN<sub>4</sub>O<sub>5</sub>S, 511.51 (41.12), 497.04 (73.71), 495.04 (63.14), 467.95 (33.54), 434.27 (2.01), 387.96 (5.03), 376.89 (6.86), 346.06 (16.36), 331.06 (9.28), 311.17 (4.59), 304.07 (31.73), 300.12 (20.05), 266.70 (4.79), 223.20 (7.92), 207.82 (10.64), 196.83 (1.84), 136.18 (46.62), 122.16 (9.11), 116.19 (1.37), 105.16 (17.00), 90.17 (100.00), 89.16 (77.70), 77.16 (35.65). 2-(4-Chloro-benzylsulfanyl)-6,7-dimethoxy-3-(4-nitro-phenyl)-3H-quinazolin-4-one (**5h**), yellow powder (EtOH/CHCl<sub>3</sub>), yield (77%), m.p. 250–251 °C;  $\nu_{max}$  (KBr)/cm<sup>-1</sup> 3072 (CH-aromatic), 2960 and 2833 (CH-aliphatic), 1684 (C=O), 1610 (C=N), 1554; 1518 and 1495 (C=C), 1461, 1437, 1388, 1356, 1308, 1277, 1240, 1210, 1175, 1149, 1075, 1009, 971, 868, 840, 774, 749, 711, 602, 502, 430; <sup>1</sup>H-NMR (300 MHz; DMSO- $d_6$ )  $\delta_H$ : 8.40 (2H, d,  $J$  = 5.4 Hz, 2  $\times$  CH-aromatic), 7.81 (2H, d,  $J$  = 5.4 Hz, 2  $\times$  CH-aromatic), 7.56–7.12 (6H, m, 6  $\times$  CH-aromatic), 4.44 (2H, s, S-CH<sub>2</sub>), 3.98 (3H, s, OCH<sub>3</sub>), 3.86 (3H, s, OCH<sub>3</sub>); <sup>13</sup>C-NMR (150 MHz; DMSO- $d_6$ )  $\delta_C$ : 160.15 (C=O), 155.65 (C=N), 153.73, 148.60, 143.93, 142.25, 136.29, 132.42, 131.77, 131.67, 128.82, 125.12, 112.61, 107.70, 106.14 (10  $\times$  CH-aromatic and 8  $\times$  C<sub>q</sub>-aromatic), 56.65 (OCH<sub>3</sub>), 56.28 (OCH<sub>3</sub>), 35.41 (CH<sub>2</sub>); MS (EI)  $m/z$  (%) [ $M^+$  + 1, <sup>37</sup>Cl] 486.20 (18.25), [ $M^+$ , <sup>37</sup>Cl] 485.02 (33.61), [ $M^+$  + 1, <sup>35</sup>Cl] 484.03 (46.89), [ $M^+$ , <sup>35</sup>Cl] 483.03 (100.00) for C<sub>23</sub>H<sub>18</sub>ClN<sub>3</sub>O<sub>5</sub>S, 481.05 (15.67), 467.98 (2.89), 452.25 (13.58), 450.37 (28.43), 437.86 (2.75), 421.58 (1.59), 407.04 (7.06), 373.34 (4.96), 361.05 (12.05), 348.66 (8.75), 331.55 (12.43), 329.19 (53.67), 295.92 (2.68), 282.07 (3.70), 258.41 (2.80), 158.09 (1.56), 143.15 (2.27), 125.08 (2.33), 76.29 (2.21), 63.01 (2.86).

### 3.2. Biology

#### 3.2.1. DPPH Radical Scavenging Assay

The antioxidant potencies of all synthesized compounds were investigated using a 1,1 diphenyl-2-picrylhydrazyl (DPPH) radical scavenging assay according to the protocol described by Bersuder et al. [105]. In brief, a 0.5 mL volume of DPPH ethanolic solution was mixed with an equal volume of each sample concentration (i.e., the test compound or butylated hydroxytoluene, BHT, which was used as the reference antioxidant in the positive control experiment), shaken strongly, and incubated at room temperature for 1 h in darkness. The absorbance of the residual DPPH radicals was measured at  $\lambda$  = 519 nm and compared to the negative control (without the test compound or reference antioxidant). The DPPH radical scavenging power was calculated using the following formula: scavenging efficiency (%) =  $(1 - A_{\text{compound}}/A_{\text{Control}}) \times 100$ , where  $A_{\text{compound}}$  and  $A_{\text{Control}}$  are the absorbance of the tested compound and the negative control, respectively. The standard curve was obtained by plotting the scavenging effect (%) versus the compound concentration and it was used to determine the compound's concentration providing 50% inhibition (IC<sub>50</sub>) in mg/mL, which was converted into mM units. Additionally, the  $\pm$  SD values were calculated from three independent triplicate measurements.

#### 3.2.2. COX-2 Inhibition Assay

Each compound of the two series, **3a–h** and **5a–h**, was resuspended in 100% DMSO at a final concentration of 10 mg/mL. Each compound was investigated in triplicates at different concentrations (50, 100, 200 and 300  $\mu$ g/mL) using a commercial COX-2 inhibitory screening assay kit (Catalog Number: 701080; Cayman Chemical Company) following the manufacturer's instructions. Briefly, 10  $\mu$ L of the tested compound was added to a mixture of the reaction buffer solution (160  $\mu$ L of 0.1 M Tris-HCl, pH 8.0, in the presence of 2 mM phenol and 5 mM EDTA), COX-2 (10  $\mu$ L) and heme (10  $\mu$ L). After a 10 min incubation at 37 °C, the reaction was started by adding arachidonic acid (10  $\mu$ L), rapidly mixed and kept at 37 °C for 2 min. PGF<sub>2</sub> $\alpha$  generated via PGH<sub>2</sub> reduction with stannous

chloride (30  $\mu$ L) was incubated at room temperature for 5 min. The  $\text{PGF}_{2\alpha}$  amount was then determined via an enzyme immunoassay. Prior to incubation with the COX-2 reaction (at room temperature 18 h), the 96-well plate was previously coated with a mouse anti-rabbit monoclonal antibody. Unbound reagents were removed by washing the plate followed by adding Ellman's reagent to the well. The reaction product displaying a distinct yellow color was measured at 410 nm using a UV microplate reader. The % inhibition was calculated by comparing the  $\text{PGF}_{2\alpha}$  produced in the compound-treated samples with a control sample, using the following equation: % inhibition is equal to  $[(\text{PGF}_{2\alpha}]_{\text{control}} - [\text{PGF}_{2\alpha}]_{\text{sample}}] / [\text{PGF}_{2\alpha}]_{\text{control}} \times 100$ . Celecoxib was used as the standard inhibitor for COX-2. The COX-2 inhibitory efficiency was expressed as an inhibition percentage, which was determined via a comparison with the negative control experiments. The  $\text{IC}_{50}$  values were deduced for the most active candidates from their calibration curves.

### 3.2.3. Lactate Dehydrogenase A (LDHA) Inhibitory Assay

The LDHA inhibitory effectiveness was investigated by measuring the amounts of consumed NADH [73]. Briefly, different concentrations of each compound (50, 100, 200 and 300  $\mu\text{g}/\text{mL}$ ) were incubated in a buffer containing 20 mM of HEPES-K+ (pH 7.2), 20  $\mu\text{M}$  of NADH, 2 mM of pyruvate and 10 ng of purified recombinant human LDHA protein for 10 min. The fluorescence of NADH, which has an excitation wavelength of 340 nm and an emission wavelength of 460 nm, was detected using a spectrofluorometer. Sodium oxamate at 1 mM was used as a standard inhibitor of LDHA. The LDHA inhibitory efficiency was expressed as an inhibition percentage, which was determined via a comparison with the negative control experiments. The  $\text{IC}_{50}$  values were calculated for the most active candidates from their calibration curves.

### 3.2.4. In Vitro $\alpha$ -Glucosidase (AG) Inhibitory Activity

The AG inhibitory activities of the synthesized quinazolinone derivatives were assessed based on the detection of the release of 4-nitrophenol (NP) from 4-nitrophenyl  $\alpha$ -D-glucopyranoside (4-NPGP) using the method reported by Andrade-Cetto and collaborators [106]. Concisely, 20  $\mu\text{L}$  of each compound at different concentrations ranging from 0 to 50  $\mu\text{g}/\text{mL}$ , DMSO or quercetin (used as the positive control) at the same concentration of the tested compounds was mixed with 180  $\mu\text{L}$  of the  $\alpha$ -glucosidase enzyme from *Saccharomyces Cerevisiae*, and the resulting mixture was incubated at 37  $^{\circ}\text{C}$  for 2 min. Then, the reaction was allowed to start by adding 150  $\mu\text{L}$  of the color reagent 4-NPGP and the resulting mixture was incubated for additional 15 min at 37  $^{\circ}\text{C}$ . Collectively, the colorimetric assay medium contained 2U of  $\alpha$ -glucosidase, 5 mM of 4-NPGP and 10 mM of the potassium phosphate buffer with a pH of 6.9. Reading the assay was carried out using a microplate reader (Bio-Tek ELX-800, Thermo Fischer Scientific, Agilent Technologies, New York, USA) at 405 nm. The  $\alpha$ -glucosidase inhibition was calculated as follows: % inhibition =  $100 - (X2_{\text{sample}} - X1_{\text{sample}} / X2_{\text{control}} - X1_{\text{control}}) \times 100$ , where X1 is the absorbance of the initial reading and X2 is the absorbance of the final reading, and control is the absorbance of the assay without the compound and with DMSO instead. The inhibitory efficiency of each compound was expressed as  $\text{IC}_{50}$   $\mu\text{g}/\text{mL}$  (as well as  $\mu\text{M}$ ), which was calculated from the corresponding calibration curve.

### 3.2.5. In Vitro $\alpha$ -Amylase (AA) Inhibition Assay

In this experiment, the  $\alpha$ -amylase inhibitory activities of the compounds **3a-h** and **5a-h** were evaluated according to the reported methodology [107]. Precisely, 10  $\mu\text{L}$  of  $\alpha$ -amylase enzyme (3,3 U, EC 3.2.1.1, Sigma Chemical Co., St. Louis, MO, USA) was mixed with 10  $\mu\text{L}$  of each compound at different concentrations ranging from 20 to 200  $\mu\text{g}/\text{mL}$ , DMSO or quercetin (used as the positive control at the same compound concentrations) at 37  $^{\circ}\text{C}$  for 5 min. Then, 180  $\mu\text{L}$  of Labtest (the amylase substrate) was added and the samples were incubated for 8 min, followed by measuring the first reaction at 620 nm to obtain (X1). Afterwards, the reaction mixture was incubated for an additional 5 min at 37  $^{\circ}\text{C}$ ; then,

the second reaction was measured to obtain the final reading (X2). Notably, the amylase substrate, Labtest, was diluted in distilled water (1:1) before being added to the microplate (Bio Tek ELX-800, USA). The  $\alpha$ -amylase inhibitory efficiency was calculated as follows: % inhibition =  $100 - (X2 \text{ sample} - X1 \text{ sample} / X2 \text{ control} - X1 \text{ control}) \times 100$ , where control is the absorbance of the assay with DMSO instead the test compound. The results were expressed as IC<sub>50</sub>  $\mu\text{g}/\text{mL}$  (as well as  $\mu\text{M}$ ) and were determined from the standard curves.

### 3.2.6. Viability Assay

The cytotoxic potencies of the studied quinazolinone derivatives were examined on two human colon cancer cell line types: HCT-116 and Lovo (American Type Culture Collection; Manassas, VA, USA), using various amounts of tested compounds (50, 100, 200 and 400  $\mu\text{g}$ ). The samples were diluted in Dulbecco's Modified Eagle's Medium, consisting of 10% fetal bovine serum (FBS), added to cells grown and cultured for 24 h in a 5% CO<sub>2</sub>-humidified incubator at 37 °C. Thereafter, the activity of lactate dehydrogenase released from damaged cells was determined [73] in the collected supernatant aliquots using an ELISA end-point assay (Benchmark Plus, Bio-Rad, CA, USA); 0.1% Triton X-100 in the assay medium and the assay medium only were used as the positive and negative controls, respectively. Cell viability was expressed as a relative percentage of the OD values (at 550 nm) for compound-treated cells (final concentration of 200  $\mu\text{g}/\text{mL}$ ) and the negative control, which was shown as the mean %  $\pm$  SD (n = 3). The results of the viability assays for the potential cytotoxic candidates were compared with the % of viable human umbilical vein endothelial cells (HUVEC) at the same concentration. These cells were grown in Dulbecco's Modified Eagle's Medium (PAN-Biotech; Barcelona, Spain) containing 10% FBS (Sigma Aldrich; St. Quentin-Fallavier, France), 2 mM Glutamine (Sigma Aldrich), 100 units/mL penicillin and 100 mg/mL streptomycin (Life Technologies; Paisley, UK).

A plot of the cell viability (%) versus the compound concentration ( $\mu\text{g}/\text{mL}$ ) was also performed to determine the compound concentration providing 50% inhibition (IC<sub>50</sub>) in  $\mu\text{g}/\text{mL}$ , which was converted to  $\mu\text{M}$ .

### 3.2.7. Statistical Analysis

The obtained results were presented as the mean  $\pm$  standard deviation (SD) from three experiments. The statistical significance between pairs of means was evaluated using Student's t test. A value of  $p < 0.05$  or  $p < 0.01$  was the criteria for a statistical significance.

The IC<sub>50</sub> value for each tested compound was obtained using the Quest Graph™ IC<sub>50</sub> Calculator, AAT Bioquest, Inc. (<https://www.aatbio.com/tools/ic50-calculator>) online resource accessed on 2 February 2023.

### 3.2.8. Determination of the Expressional Levels of Bax, caspase-3 and Bcl-2 Genes Cell Culture

Briefly, in a 25 mL flask ( $1 \times 10^6$  cells/flask), the human colon cancer cell lines (HCT-116 and LoVo) were grown for 24 h. After replacing the culture media with a medium containing 1% FBS for 24 h, the cells were treated with 10  $\mu\text{g}/\text{mL}$  of each tested compound in 2 mL of fresh medium containing 1% FBS, or 0.25% DMSO, which was used as the negative control. The cells were adherent cells and they were detached using trypsin after being washed with ice-cold phosphate-buffered saline (PBS).

### Design of the Primer

Primers specific for the Bax, Bcl-2 and Caspase-3 genes were designed using the primer blast (<https://www.ncbi.nlm.nih.gov/tools/primer-blast/> accessed on 9 January 2023) software. The primers were used in the RT-qPCR analysis to amplify fragments of 100–200 bp in length (Table 11).

**Table 11.** Description of primers used for qPCR.

Gene	Primer Sequence (5' to 3')
Bax	F 5'-TCAGGATGCGTCCACCAAGAAG-3',R 5'-TGTGTCCACGGCGCAATCATC-3'.
Bcl-2	F 5'-ATCGCCCTGTGGATGACTGAGT -3',R 5'-GCCAGGAGAAATCAAACAGAGGC-3'.
Caspase 3	F 5'-GGAAGCGAATCAATGGACTCTGG-3',R 5'-GCATCGACATCTGTACCAGACC -3'.
GAPDH	F 5'-GTCTCCTCTGACTTCAACAGCG-3' R 5'-ACCACCCTGTTGCTGTAGCCAA-3'

### Reverse-Transcription PCR (RT-PCR)

The RNeasy Mini Kit (Qiagen, Hilden, Germany) was used to extract the total RNA. The RNA purity, quality and quantity were checked using a Nanodrop 8000 spectrophotometer (Thermo Fisher Scientific, USA). The Hyperscript Kit (GeneAll, Seoul, Korea) and random hexamers (GeneAll, Seoul, Korea) were used to reverse-transcript 1 µg of RNA from each sample into cDNA as described in the manufacturer's protocol.

### Quantitative Real-Time PCR

A QuantStudio 7Flex Detection System (Applied Biosystems, Thermo Fischer Scientific, Inc., USA) was used to measure the mRNA expression of Bax, Caspase-3 and Bcl-2. The reactions for the synthesis of cDNA were carried out using an iScript One-Step RT-PCR Kit with SYBR Green (cat no: 170–8892; Bio-Rad, Inc., Hercules, CA, USA). Briefly, primers (Table 10) were added to the reaction mixture at a final concentration of 10 pM. Thus, 5 µL of each cDNA sample were added to a 20 µL PCR mixture consisting of 12.5 µL of 2 × iScript One-Step RT-PCR Kit with SYBR Green, 0.5 µL of primers for Bax, Caspase-3 and Bcl-2 as well as GAPDH (Macrogen, Seoul, Korea), and 7 µL RNase/DNase-free water (Qiagen, DE). The thermal cycling conditions for Bax, Caspase-3 and Bcl-2 were established as 5 min at 95 °C, followed by 40 cycles of 30 s at 95 °C and 30 s at 60 °C, and finally 10 s at 95 °C. The presence of a single melting temperature peak verified the specificity of each primer. The expression of a house-keeping gene, GAPDH, was used as an endogenous control for the current work.

#### 3.2.9. Annexin-V-FITC Assay

The distribution of early and late apoptotic cells after treatment with compounds **3a** and **3f** was carried out using an Annexin V-FITC Apoptosis Detection Kit (BioVisionResearch Products—USA). HCT-116 and LoVo carcinoma cells were seeded in 60 mm<sup>2</sup> culture dishes and treated with the vehicles DMSO, and compounds **3a** and **3f** (50 µg/mL) for 48 h. Cells were then harvested, washed twice with PBS and resuspended in an Annexin-V binding buffer (BioVisionResearch Products—USA). Finally, the cells were stained with Annexin V-FITC and propidium iodide (PI). The fluorescent intensity of the stained cancer cells was determined using an FITC signal detector (usually FL1) and PI staining with the phycoerythrin emission signal detector (through quadrant statistics for necrotic and apoptotic cell populations).

#### 3.2.10. Cell Cycle Assay

Changes in cell cycle distribution induced by compounds **3a** and **3f** were analyzed using a flow cytometric analysis according to Nicoletti et al. 1991 [108] using a Propidium Iodide Flow Cytometry Kit for Cell Cycle Analysis (Abcam-UK). HCT-116 and LoVo carcinoma cells (5 × 10<sup>4</sup> cells/mL) were treated with DMSO as a negative control, and compounds **3a** and **3f** (50 µg/mL), for 48 h. After the centrifugation of the treated cells at 1800 rpm for 5 min, the pellet was washed twice with PBS. Then, the cells were fixed by mixing 700 mL of 90% cold ethanol, and stained with propidium iodide (PI) for 1 h at 37 °C. RNase A at 10 mg/mL was added in order to limit the ability of the PI to bind only

to the DNA molecules. The stained cells were analyzed for their DNA content using a BD FACSC flow cytometer.

### 3.2.11. Immunoblot Experiments

In order to determine the levels of production of caspases 8 and 9 by the treated carcinoma cells, Western blot analysis was carried out using a FLAG<sup>®</sup> Western Detection Kit (Agilent Technologies, USA). Exponentially growing HCT-116 and LoVo cells were treated with 50 µg/mL of derivatives **3a** and **3f** for 48 h. After incubation, the cells were harvested and lysed using a Lysis buffer consisting of 10 mM of Tris, 100 mM of NaCl, 25 mM of ethylenediaminetetra acetic acid (EDTA), 25 mM of Ethylene glycol bis(2-aminoethyl)tetraacetic acid (EGTA), 0.1% Sodium dodecyl sulfate (SDS), 1% (*v/v*) Triton X-100 and 2% (*v/v*) NP-40 (pH 7.4), with a 1:200 protease inhibitor cocktail (Sigma-Adrich) and a 1:300 phosphatase inhibitor cocktail tablet (Roche Applied Science, Mannheim, Germany). The protein concentrations of each sample were determined calorimetrically using the Bradford method before proceeding to carry out the Western blotting [109]. Equal amounts (20 µg) of the protein samples were mixed and boiled with SDS Loading buffer for 10 min, allowed to cool on ice and then loaded into SDS-polyacrylamide gel and separated using a Cleaver electrophoresis unit (Cleaver, Warwickshire, UK), before being transferred onto polyvinylidene fluoride (PVDF) membranes (Bio-Rad, USA) for 30 min using a Semi-dry Electroblotter (Biorad, USA) at 2.5 A and 25 V for 30 min. The membrane was blocked with 5% nonfat dry milk in TBS-T for two hours at room temperature, in order to reduce non-specific protein interactions between the membrane and the antibody. The blocked membrane was incubated overnight at 4 °C with primary antibodies (Cell Signaling Technology, Massachusetts, USA) and β-actin (Sigma). The blots were then washed three times (10 min each) with TBS-T. The membrane was then incubated with the corresponding horse radish peroxidase (HRP)-linked secondary antibodies (Dako, Hamburg, Germany) for another hour at room temperature, followed by washing three times (10 min each) with TBS-T. The chemiluminescent Western ECL substrate (Perkin Elmer, Waltham, MA, USA) was applied to the blot according to the manufacturer's recommendation. Briefly, the membranes were incubated for 1 min with a mixture of equal volumes of ECL solution A and ECL solution B. The chemiluminescent signals were captured using a CCD camera-based imager (Chemi Doc imager, Biorad, USA), and the bands' intensities were then measured using ImageLab v3.0 (Bio-Rad). Protein-sized markers were used in all gels to localize the gel transfer regions for specific proteins and determine the transfer efficiency. Following an overnight incubation with the primary antibodies, HRP conjugated secondary antibodies were added and incubated for 1 h. The proteins were detected using an enhanced chemiluminescence (ECL) detection system (Thermo Fischer Scientific, USA). The intensities of the bands were quantified using the NIH ImageJ software v3.0.1 (<http://rsb.info.nih.gov/ij/>).

### 3.3. In Silico Studies

#### 3.3.1. Molecular Docking Studies

- Preparation of the protein

The crystal structures of the protein–ligand complexes for alpha-amylase (PDB ID: 3BAJ) (<https://doi.org/10.1021/bi701652t>) accessed on 5 March 2023, human lysosomal acid-alpha-glucosidase (PDB ID: 5NN5) (<https://doi.org/10.1038/s41467-017-01263-3>) on 5 March 2023, lactate dehydrogenase A (PDB ID: 1I10) ([https://doi.org/10.1002/1097-0134\(20010501\)43:2<T1>textless{}175:aid-prot1029\T1>textgreater{}3.0.co;2-#](https://doi.org/10.1002/1097-0134(20010501)43:2<T1>textless{}175:aid-prot1029\T1>textgreater{}3.0.co;2-#)) on 24 May 2023 and cyclooxygenase-2 (PDB ID: 3LN1) (<https://doi.org/10.1016/j.bmcl.2010.07.054>) 25 May 2023 were used for the docking calculations. They were retrieved from the Research Collaboratory for Structural Bioinformatics (RCSB) Protein Data Bank. For each crystal structure, the crystallographic water molecules were removed, the missing hydrogen atoms were added and the inhibitor from the crystal structure was used to define the active site.

- Preparation of ligands

The structures of all the quinazolinone compounds were sketched using Chemdraw ultra 13.0 and converted into 3D structures using the Hyperchem pro 8.0 software ([www.hyper.com](http://www.hyper.com)). Geometry optimization was carried out using the PM3 method via the MOPAC program (<http://OpenMOPAC.net>). Finally, all the compounds were saved in a .pdb format for further docking studies.

- Docking studies

Autodock tools (ADT) version 1.5.6 ([www.autodock.scrips.edu](http://www.autodock.scrips.edu)) was used to prepare the molecular docking. The Lamarckian genetic algorithm methodology was employed for the docking simulations. The best binding conformation was selected from the docking log (.dlg) file for each ligand and further interaction analysis was performed using PyMol and Discovery Studio Visualizer 4.0.

### 3.3.2. ADMET Analysis

The ADMET analysis was performed using the standard protocol recommended in ADMETLab 2.0 (<https://admetmesh.scbdd.com>) [89]. For this, the canonical SMILES (simplified molecular-input line-entry system) of all molecules were submitted serially to the 'ADMET Evaluation' option of the 'services' section of the ADMETLab 2.0 server. After submitting, the server led to the calculation and display of a good number of the ADMET properties of a molecule. The results were then saved in a '.csv' file. The same file is available as a Supplementary Material.

### 3.3.3. The Bioavailability Radar Charts

These were studied using the SwissADME free web tool [95] (<http://www.swissadme.ch/idex.php>), accessed on 26 May 2023.

## 4. Conclusions

Quinazolinone derivatives **3a–h** and their *S*-arylated analogues **5a–h** were synthesized and characterized by various spectroscopic techniques. Multi-target biological screening revealed the significance of **3a**, **3g** and **5a** as potent DPPH radical scavengers with lowered IC<sub>50</sub> values (mM) of  $0.191 \pm 0.011$ ,  $0.165 \pm 0.005$  and  $0.172 \pm 0.004$ , respectively, as compared with  $0.245 \pm 0.027$  by BHT. Despite this, none of the screened compounds showed an improved inhibitory efficiency to celecoxib (IC<sub>50</sub> =  $0.136 \times 10^{-3} \pm 0.006 \times 10^{-3}$  μM) and sodium oxamate (IC<sub>50</sub> =  $140.503 \pm 7.647$  μM) against COX-2 and LDHA, respectively; quinazolinones **3a** (IC<sub>50</sub> values =  $281.374 \pm 10.545$  and  $273.345 \pm 16.087$  μM) and **3g** (IC<sub>50</sub> values =  $251.780 \pm 22.023$  and  $242.279 \pm 31.298$ ) were recognized as the most active derivatives against these enzymes, respectively. Notably, quinazolinones **3h**, **5a** and **5h** with IC<sub>50</sub> values ranging from  $12.548 \pm 0.542$  to  $12.882 \pm 0.426$  μM against AG, and derivatives **3a**, **3c**, **3f**, **3h** and **5a–5f** as well as **5h**, with IC<sub>50</sub> values spanning from  $186.437 \pm 9.700$  to  $381.335 \pm 8.713$  μM against AA, exerted superior activity to quercetin (IC<sub>50</sub> =  $13.126 \pm 0.688$  and  $402.566 \pm 10.108$ , respectively). Therefore, **3h**, **5a** and **5h** can be considered as dual inhibitors for AG and AA.

In addition, the viability assays identified **3a** and **3f** as the most active antiproliferative agents with IC<sub>50</sub> (μM) values of  $294.324 \pm 8.409$  and  $383.521 \pm 8.989$  (LoVo cells), and  $298.060 \pm 13.247$  and  $323.596 \pm 2.996$  (HCT-116 cells) as compared with  $22.371 \pm 0.215$  (LoVo) and  $91.098 \pm 2.721$  (HCT-116) by 5-FU. Interestingly, these compounds did not inhibit the growth of non-tumoral HUVEC at 560.617 and 599.251 μM, with viability percents of  $97.000 \pm 2.646$  and  $99.667 \pm 0.577$ , respectively. Quantitative real-time PCR measurements confirmed the capability of **3a** and **3f** at 10 μg/mL to upregulate the expression levels of Bax and Caspase-3 genes, along with the downregulation of the expression level of the Bcl-2 gene in the cultures of the treated HCT-116 and LoVo cells as compared to the negative control cultures. Moreover, the Western blotting analyses indicated that **3a** and **3f** were able to induced apoptosis in HCT-116 and LoVo colon cancer cells via pathways triggered by caspases, and predominantly through the intrinsic pathway mediated by caspase-9. Furthermore, the two compounds induced more death for the HCT-116 and LoVo cells via

apoptosis than via necrosis; in addition, they induced cell cycle arrest for the LoVo cells in the G2/M phase and for the HCT-116 cells in the G1 phase. Therefore, the observed cytotoxicity of these derivatives could be attributed to the induction of apoptosis and the blocking of cell cycle progression in both cell lines. Molecular docking analyses of the active or potential candidates corroborated the observed inhibitory efficiencies in the in vitro assays against AA, AG, LDAH and COX-2. Lastly, the physicochemical properties, the suitability in medicinal chemistry and the ADMET characteristics were predicted for all the synthesized compounds and explained in detail for some representative active compounds. Collectively, these quinazolinone derivatives may be considered to be suitable candidates for further optimization and exploration against CRC and its risk factors, particularly oxidative stress and DM-type 2.

**Supplementary Materials:** The following supporting information can be downloaded at <https://www.mdpi.com/article/10.3390/ph16101392/s1>; The Excel file is for all physicochemical and ADMET predictions and the PDF file is for the spectroscopic analyses of the synthesized compounds.

**Author Contributions:** Conceptualization, N.N.E.E.-S. and A.B.B.; validation, M.Z.H.; formal analysis, N.N.E.E.-S., A.B.B., N.K., V.H.M. and M.Z.H.; investigation, N.N.E.E.-S.; resources, N.N.E.E.-S., T.M.A.-O., Z.M.A. and A.B.B.; data curation, N.N.E.E.-S., A.B.B., Z.M.A., N.K. and M.Z.H.; writing—original draft preparation, N.N.E.E.-S., N.K., A.B.B. and T.M.A.-O.; writing—review and editing, N.N.E.E.-S., M.Z.H., A.B., Z.M.A., N.K., A.B.B. and M.I.A.-Z.; supervision, N.N.E.E.-S. and A.B.; project administration, N.N.E.E.-S. and Z.M.A.; funding acquisition, Z.M.A. and M.I.A.-Z. All authors have read and agreed to the published version of the manuscript.

**Funding:** Research Center of the Female Scientific and Medical Colleges, Deanship of Scientific Research, King Saud University.

**Institutional Review Board Statement:** Not applicable.

**Informed Consent Statement:** Not applicable.

**Data Availability Statement:** Data is contained within the article and supplementary material.

**Acknowledgments:** We extend our appreciation to “Research Center of the Female Scientific and Medical Colleges”, Deanship of Scientific Research, King Saud University.

**Conflicts of Interest:** The authors declare no conflict of interest.

## References

1. Xi, Y.; Xu, P. Global colorectal cancer burden in 2020 and projections to 2040. *Trans. Oncol.* **2021**, *14*, 101174. [[CrossRef](#)] [[PubMed](#)]
2. Orlandi, G.; Roncucci, L.; Carnevale, G.; Sena, P. Different Roles of Apoptosis and Autophagy in the Development of Human Colorectal Cancer. *Int. J. Mol. Sci.* **2023**, *24*, 10201. [[CrossRef](#)] [[PubMed](#)]
3. Zhou, L.; Zhang, Z.; Huang, Z.; Nice, E.; Zou, B.; Huang, C. Revisiting cancer hallmarks: Insights from the interplay between oxidative stress and non-coding RNAs. *Mol. Biomed.* **2020**, *1*, 4. [[CrossRef](#)] [[PubMed](#)]
4. Bardelčíková, A.; Šoltys, J.; Mojžiš, J. Oxidative Stress, Inflammation and Colorectal Cancer: An Overview. *Antioxidants* **2023**, *12*, 901. [[CrossRef](#)]
5. Zheng, S.; Wang, X.; Zhao, D.; Liu, H.; Hu, Y. Calcium homeostasis and cancer: Insights from endoplasmic reticulum-centered organelle communications. *Trends Cell Biol.* **2023**, *33*, 312–323. [[CrossRef](#)]
6. Xiao, M.; Zhong, H.; Xia, L.; Tao, Y.; Yin, H. Pathophysiology of mitochondrial lipid oxidation: Role of 4-hydroxynonenal (4-HNE) and other bioactive lipids in mitochondria. *Free Radic. Biol. Med.* **2017**, *111*, 316–327. [[CrossRef](#)]
7. Gentile, F.; Arcaro, A.; Pizzimenti, S.; Daga, M.; Cetrangolo, G.P.; Dianzani, C.; Lepore, A.; Graf, M.; Ames, P.R.J.; Barrera, G. DNA damage by lipid peroxidation products: Implications in cancer, inflammation and autoimmunity. *AIMS Genet.* **2017**, *4*(2), 103–137. [[CrossRef](#)]
8. Martemucci, G.; Costagliola, C.; Mariano, M.; D’andrea, L.; Napolitano, P.; D’Alessandro, A.G. Free Radical Properties, Source and Targets, Antioxidant Consumption and Health. *Oxygen* **2022**, *2*, 48–78. [[CrossRef](#)]
9. Kloudova, A.; Guengerich, F.P.; Soucek, P. The Role of Oxysterols in Human Cancer. *Trends Endocrinol. Metab.* **2017**, *28*, 485–496. [[CrossRef](#)]
10. Kumari, S.; Badana, A.K.; Murali Mohan, G.; Shailender, G.; Malla, R. Reactive Oxygen Species: A Key Constituent in Cancer Survival. *Biomark. Insights* **2018**, *13*, 1177271918755391. [[CrossRef](#)]



11. Krejbich, P.; Birringer, M. The Self-Administered Use of Complementary and Alternative Medicine (CAM) Supplements and Antioxidants in Cancer Therapy and the Critical Role of Nrf-2-A Systematic Review. *Antioxidants* **2022**, *11*, 2149. [[CrossRef](#)] [[PubMed](#)]
12. Ho, B.Y.; Wu, Y.M.; Chang, K.J.; Pan, T.M. Dimeric acid inhibits SW620 cell invasion by attenuating H<sub>2</sub>O<sub>2</sub>-mediated MMP-7 expression via JNK/C-Jun and ERK/C-Fos activation in an AP-1-dependent manner. *Int. J. Biol. Sci.* **2011**, *7*, 869–880. [[CrossRef](#)]
13. Sheng, J.; Sun, H.; Yu, F.B.; Li, B.; Zhang, Y.; Zhu, Y.T. The Role of Cyclooxygenase-2 in Colorectal Cancer. *Int. J. Med. Sci.* **2020**, *17*, 1095–1101. [[CrossRef](#)]
14. Roelofs, H.M.; Te Morsche, R.H.; van Heumen, B.W.; Nagengast, F.M.; Peters, W.H. Over-expression of COX-2 mRNA in colorectal cancer. *BMC Gastroenterol.* **2014**, *14*, 9005–9010. [[CrossRef](#)]
15. Wilson, D.J.; DuBois, R.N. Role of Prostaglandin E2 in the Progression of Gastrointestinal Cancer. *Cancer Prev. Res.* **2022**, *15*, 355–363. [[CrossRef](#)]
16. Rahman, M.; Selvarajan, K.; Hasan, M.R.; Chan, A.P.; Jin, C.; Kim, J.; Chan, S.K.; Le, N.D.; Kim, Y.B.; Tai, I.T. Inhibition of COX-2 in colon cancer modulates tumor growth and MDR-1 expression to enhance tumor regression in therapy-refractory cancers in vivo. *Neoplasia* **2012**, *14*, 624–633. [[CrossRef](#)] [[PubMed](#)]
17. Thumkeo, D.; Punyawatthanakool, S.; Prasongtanakij, S.; Matsuura, R.; Arima, K.; Nie, H.; Yamamoto, R.; Aoyama, N.; Hamaguchi, H.; Sugahara, S.; et al. PGE2-EP2/EP4 signaling elicits immunosuppression by driving the mregDC-Treg axis in inflammatory tumor microenvironment. *Cell Rep.* **2022**, *39*, 110914–110928. [[CrossRef](#)] [[PubMed](#)]
18. Wang, D.; Fu, L.; Sun, H.; Guo, L.; DuBois, R.N. Prostaglandin E2 Promotes Colorectal Cancer Stem Cell Expansion and Metastasis in Mice. *Gastroenterology* **2015**, *149*, 1884–1895.e4. [[CrossRef](#)]
19. Sun, Y.; Tang, X.M.; Half, E.; Kuo, M.T.; Sinicrope, F.A. Cyclooxygenase-2 overexpression reduces apoptotic susceptibility by inhibiting the cytochrome c-dependent apoptotic pathway in human colon cancer cells. *Cancer Res.* **2002**, *62*, 6323–6328.
20. Karpishev, V.; Nikkhoo, A.; Hojjat-Farsangi, M.; Namdar, A.; Azizi, G.; Ghalamfarsa, G.; Sabz, G.; Yousefi, M.; Yousefi, B.; Jadidi-Niaragh, F. Prostaglandin E2 as a potent therapeutic target for treatment of colon cancer. *Prostaglandins Other Lipid Mediat.* **2019**, *144*, 106338. [[CrossRef](#)]
21. Wang, L.; Zhang, R.; Yu, L.; Xiao, J.; Zhou, X.; Li, X.; Song, P.; Li, X. Aspirin Use and Common Cancer Risk: A Meta-Analysis of Cohort Studies and Randomized Controlled Trials. *Front. Oncol.* **2021**, *11*, 690219. [[CrossRef](#)] [[PubMed](#)]
22. Arber, N.; Eagle, C.J.; Spicak, J.; Rácz, I.; Dite, P.; Hajer, J.; Zavoral, M.; Lechuga, M.J.; Gerletti, P.; Tang, J.; et al. Celecoxib for the prevention of colorectal adenomatous polyps. *N. Engl. J. Med.* **2006**, *355*, 885–895. [[CrossRef](#)] [[PubMed](#)]
23. Chen, W.S.; Liu, J.H.; Liu, J.M.; Lin, J.K. Sequence-dependent effect of a cyclooxygenase-2 inhibitor on topoisomerase I inhibitor and 5-fluorouracil-induced cytotoxicity of colon cancer cells. *Anti Cancer Drugs* **2004**, *15*, 287–294. [[CrossRef](#)] [[PubMed](#)]
24. Warburg, O. On the origin of cancer cells. *Science* **1956**, *123*, 309–314. [[CrossRef](#)]
25. El Sayed, S.M. Biochemical Origin of the Warburg Effect in Light of 15 Years of Research Experience: A Novel Evidence-Based View (An Expert Opinion Article). *Onco Targets Ther.* **2023**, *16*, 143–155. [[CrossRef](#)]
26. Kliebhan, J.; Besse, A.; Kampa-Schittenhelm, K.; Schittenhelm, M.; Driessen, C. Mutant TP53 driving the Warburg Effect in Mantle Cell lymphoma. *Clin. Case Rep.* **2022**, *10*, e6296–e6300. [[CrossRef](#)] [[PubMed](#)]
27. Brand, A.; Singer, K.; Koehl, G.E.; Kolitzus, M.; Schoenhammer, G.; Thiel, A.; Matos, C.; Bruss, C.; Klobuch, S.; Peter, K.; et al. LDHA-Associated Lactic Acid Production Blunts Tumor Immunosurveillance by T and NK Cells. *Cell Metab.* **2016**, *24*, 657–671. [[CrossRef](#)] [[PubMed](#)]
28. de la Cruz-López, K.G.; Castro-Muñoz, L.J.; Reyes-Hernández, D.O.; García-Carrancá, A.; Manzo-Merino, J. Lactate in the Regulation of Tumor Microenvironment and Therapeutic Approaches. *Front. Oncol.* **2019**, *9*, 1143. [[CrossRef](#)] [[PubMed](#)]
29. Daverio, Z.; Balcerzyk, A.; Rautureau, G.J.P.; Panthu, B. How Warburg-Associated Lactic Acidosis Rewires Cancer Cell Energy Metabolism to Resist Glucose Deprivation. *Cancers* **2023**, *15*, 1417. [[CrossRef](#)]
30. Le, A.; Cooper, C.R.; Gouw, A.M.; Dinavahi, R.; Maitra, A.; Deck, L.M.; Royer, R.E.; Vander Jagt, D.L.; Semenza, G.L.; Dang, C.V. Inhibition of lactate dehydrogenase A induces oxidative stress and inhibits tumor progression. *Proc. Natl. Acad. Sci. USA* **2010**, *107*, 2037–2042. [[CrossRef](#)]
31. Zhai, X.; Yang, Y.; Wan, J.; Zhu, R.; Wu, Y. Inhibition of LDH-A by oxamate induces G2/M arrest, apoptosis and increases radiosensitivity in nasopharyngeal carcinoma cells. *Oncol. Rep.* **2013**, *30*, 2983–2991. [[CrossRef](#)] [[PubMed](#)]
32. Han, J.H.; Kim, M.; Kim, H.J.; Jang, S.B.; Bae, S.J.; Lee, I.K.; Ryu, D.; Ha, K.T. Targeting Lactate Dehydrogenase A with Catechin Resensitizes SNU620/5FU Gastric Cancer Cells to 5-Fluorouracil. *Int. J. Mol. Sci.* **2021**, *22*, 5406. [[CrossRef](#)]
33. Maftouh, M.; Avan, A.; Sciarrillo, R.; Granchi, C.; Leon, L.G.; Rani, R.; Funel, N.; Smid, K.; Honeywell, R.; Boggi, U.; et al. Synergistic interaction of novel lactate dehydrogenase inhibitors with gemcitabine against pancreatic cancer cells in hypoxia. *Br. J. Cancer* **2014**, *110*, 172–182. [[CrossRef](#)] [[PubMed](#)]
34. Liu, Z.; Ma, S. Recent Advances in Synthetic  $\alpha$ -Glucosidase Inhibitors. *Chem. Med. Chem.* **2017**, *12*, 819–829. [[CrossRef](#)]
35. Tomic, D.; Shaw, J.E.; Magliano, D.J. The burden and risks of emerging complications of diabetes mellitus. *Nat. Rev. Endocrinol.* **2022**, *18*, 525–539. [[CrossRef](#)] [[PubMed](#)]
36. Cheng, H.C.; Chang, T.K.; Su, W.C.; Tsai, H.L.; Wang, J.Y. Narrative review of the influence of diabetes mellitus and hyperglycemia on colorectal cancer risk and oncological outcomes. *Transl. Oncol.* **2021**, *14*, 101089. [[CrossRef](#)] [[PubMed](#)]
37. Yu, G.H.; Li, S.F.; Wei, R.; Jiang, Z. Diabetes and colorectal cancer risk: Clinical and therapeutic implications. *J. Diabetes Res.* **2022**, *2022*, 1747326. [[CrossRef](#)]

38. Yeh, C.S.; Wang, J.Y.; Chung, F.Y.; Lee, S.C.; Huang, M.Y.; Kuo, C.W.; Yang, M.J.; Lin, S.R. Significance of the glycolytic pathway and glycolysis related-genes in tumorigenesis of human colorectal cancers. *Oncol. Rep.* **2008**, *19*, 81–91. [CrossRef]
39. Schröter, D.; Höhn, A. Role of Advanced Glycation End Products in Carcinogenesis and their Therapeutic Implications. *Curr. Pharm. Des.* **2018**, *24*, 5245–5251. [CrossRef]
40. Vekic, J.; Zeljkovic, A.; Stefanovic, A.; Giglio, R.V.; Ciaccio, M.; Rizzo, M. Diabetes and Colorectal Cancer Risk: A New Look at Molecular Mechanisms and Potential Role of Novel Antidiabetic Agents. *Int. J. Mol. Sci.* **2021**, *22*, 12409. [CrossRef]
41. Dahlén, A.D.; Dashi, G.; Maslov, I.; Attwood, M.M.; Jonsson, J.; Trukhan, V.; Schiöth, H.B. Trends in Antidiabetic Drug Discovery: FDA Approved Drugs, New Drugs in Clinical Trials and Global Sales. *Front. Pharmacol.* **2022**, *12*, 807548. [CrossRef]
42. Ferey-Roux, G.; Perrier, J.; Forest, E.; Marchis-Mouren, G.; Puigserver, A.; Santimone, M. The human pancreatic alpha-amylase isoforms: Isolation, structural studies and kinetics of inhibition by acarbose. *Biochim. Biophys. Acta* **1998**, *1388*, 10–20. [CrossRef]
43. Hedrington, M.S.; Davis, S.N. Considerations when using alpha-glucosidase inhibitors in the treatment of type 2 diabetes. *Expert Opin. Pharmacother.* **2019**, *20*, 2229–2235. [CrossRef] [PubMed]
44. Hossain, A.; Pervin, R. Current Antidiabetic Drugs: Review of Their Efficacy and Safety. In *Nutritional and Therapeutic Interventions for Diabetes and Metabolic Syndrome*, 2nd ed.; Bagchi, D., Nair, S., Eds.; Elsevier Academic Press: Oxford, UK, 2018; Chapter 34, pp. 445–473. [CrossRef]
45. Rajasekaran, P.; Ande, C.; Vankar, Y.D. Synthesis of (5,6 & 6,6)-oxa-oxa annulated sugars as glycosidase inhibitors from 2-formyl galactal using iodocyclization as a key step. *Arkivoc* **2022**, *2022*, 5–23. [CrossRef]
46. Tseng, P.S.; Ande, C.; Moremen, K.W.; Crich, D. Influence of side chain conformation on the activity of glycosidase inhibitors. *Angew. Chem. Int. Ed. Engl.* **2023**, *62*, e202217809. [CrossRef] [PubMed]
47. Compain, P.; Martin, O.R. (Eds.) *Iminosugars: From Synthesis to Therapeutic Applications*; John Wiley & Sons Ltd.: Chichester, UK, 2007; pp. 7–123. Available online: [http://library.navoiy-uni.uz/files/martin%20o.%20r.%20-%20iminosugars-%20from%20synthesis%20to%20therapeutic%20applications%20\(2007\)\(456s\).pdf](http://library.navoiy-uni.uz/files/martin%20o.%20r.%20-%20iminosugars-%20from%20synthesis%20to%20therapeutic%20applications%20(2007)(456s).pdf) (accessed on 11 August 2023).
48. Singh, A.; Singh, K.; Sharma, A.; Kaur, K.; Kaur, K.; Chadha, R.; Bedi, P.M.S. Recent developments in synthetic  $\alpha$ -glucosidase inhibitors: A comprehensive review with structural and molecular insight. *J. Mol. Struct.* **2023**, *1281*, 135115. [CrossRef]
49. Chaudhury, A.; Duvoor, C.; Reddy Dendi, V.S.; Kraleti, S.; Chada, A.; Ravilla, R.; Marco, A.; Shekhawat, N.S.; Montales, M.T.; Kuriakose, K.; et al. Clinical Review of Antidiabetic Drugs: Implications for Type 2 Diabetes Mellitus Management. *Front. Endocrinol.* **2017**, *8*, 6. [CrossRef]
50. Elmore, S. Apoptosis: A review of programmed cell death. *Toxicol. Pathol.* **2007**, *35*, 495–516. [CrossRef]
51. Hanahan, D.; Weinberg, R.A. Hallmarks of cancer: The next generation. *Cell* **2011**, *144*, 646–674. [CrossRef]
52. Kiraz, Y.; Adan, A.; Kartal Yandim, M.; Baran, Y. Major apoptotic mechanisms and genes involved in apoptosis. *Tumor Biol.* **2016**, *37*, 8471–8486. [CrossRef]
53. Du, C.; Fang, M.; Li, Y.; Li, L.; Wang, X. Smac, a mitochondrial protein that promotes cytochrome c-dependent caspase activation by eliminating IAP inhibition. *Cell* **2000**, *102*, 33–42. [CrossRef]
54. Chinnaiyan, A.M. The apoptosome: Heart and soul of the cell death machine. *Neoplasia* **1999**, *1*, 5–15. [CrossRef]
55. Hill, M.M.; Adrain, C.; Duriez, P.J.; Creagh, E.M.; Martin, S.J. Analysis of the composition, assembly kinetics and activity of native Apaf-1 apoptosomes. *EMBO J.* **2004**, *23*, 2134–2145. [CrossRef]
56. Qian, S.; Wei, Z.; Yang, W.; Huang, J.; Yang, Y.; Wang, J. The role of BCL-2 family proteins in regulating apoptosis and cancer therapy. *Front. Oncol.* **2022**, *12*, 985363. [CrossRef]
57. Kaloni, D.; Diepstraten, S.T.; Strasser, A.; Kelly, G.L. BCL-2 protein family: Attractive targets for cancer therapy. *Apoptosis* **2023**, *28*, 20–38. [CrossRef]
58. Zhang, X.; Liu, X.; Zhou, D.; Zheng, G. Targeting anti-apoptotic BCL-2 family proteins for cancer treatment. *Future Med. Chem.* **2020**, *12*, 563–565. [CrossRef] [PubMed]
59. Yangnok, K.; Innajak, S.; Sawasjirakij, R.; Mahabusarakam, W.; Watanapokasin, R. Effects of Artonin E on Cell Growth Inhibition and Apoptosis Induction in Colon Cancer LoVo and HCT116 Cells. *Molecules* **2022**, *27*, 2095. [CrossRef] [PubMed]
60. Liu, Z.; Ding, Y.; Ye, N.; Wild, C.; Chen, H.; Zhou, J. Direct Activation of Bax Protein for Cancer Therapy. *Med. Res. Rev.* **2016**, *36*, 313–341. [CrossRef] [PubMed]
61. Fu, R.G.; Sun, Y.; Sheng, W.B.; Liao, D.F. Designing multi-targeted agents: An emerging anticancer drug discovery paradigm. *Eur. J. Med. Chem.* **2017**, *136*, 195–211. [CrossRef]
62. Radwan, A.A.; Alanazi, F.K. Biological activity of quinazolinones. In *Quinazolinone and Quinazoline Derivatives*; Al-kaf, A.G., Ed.; IntechOpen: London, UK, 2020; Chapter 2; pp. 11–38. Available online: <https://www.intechopen.com/chapters/70910> (accessed on 24 February 2023).
63. El-Sayed, N.N.E.; Almaneai, N.M.; Ben Bacha, A.; Al-Obeed, O.; Ahmad, R.; Abdulla, M.; Alafeefy, A.M. Synthesis and evaluation of anticancer, antiphospholipases, antiproteases, and antimetabolic syndrome activities of some 3H-quinazolin-4-one derivatives. *J. Enzyme Inhib. Med. Chem.* **2019**, *34*, 672–683. [CrossRef]
64. Al-Salahi, R.; Ahmad, R.; Anouar, E.; Nor Azman, N.I.I.; Marzouk, M.; Abuelizz, H.A. 3-Benzyl(phenethyl)-2-thioxobenzo[g]quinazolines as a new class of potent  $\alpha$ -glucosidase inhibitors: Synthesis and molecular docking study. *Future Med. Chem.* **2018**, *10*, 1889–1905. [CrossRef]

65. Moussa, G.; Alaeddine, R.; Alaeddine, L.M.; Nassra, R.; Belal, A.S.F.; Ismail, A.; El-Yazbi, A.F.; Abdel-Ghany, Y.S.; Hazzaa, A. Novel click modifiable thioquinazolinones as anti-inflammatory agents: Design, synthesis, biological evaluation and docking study. *Eur. J. Med. Chem.* **2018**, *144*, 635–650. [[CrossRef](#)]
66. Al-Salahi, R.; Taie, H.A.A.; Bakheit, A.H.; Marzouk, M.; Almehezia, A.A.; Herqash, R.; Abuelizz, H.A. Antioxidant activities and molecular docking of 2-thioxobenzof[*g*]quinazoline derivatives. *Pharmacol. Rep.* **2019**, *71*, 695–700. [[CrossRef](#)]
67. El-Messery, S.M.; Hassan, G.S.; Nagi, M.N.; Habib, E.E.; Al-Rashood, S.T.; El-Subbagh, H.I. Synthesis, biological evaluation and molecular modeling study of some new methoxylated 2-benzylthio-quinazoline-4(3H)-ones as nonclassical antifolates. *Bioorg. Med. Chem. Lett.* **2016**, *26*, 4815–4823. [[CrossRef](#)] [[PubMed](#)]
68. Mahdy, H.A.; Ibrahim, M.K.; Metwaly, A.M.; Belal, A.; Mehany, A.B.M.; El-Gamal, K.M.A.; El-Sharkawy, A.; Elhendawy, M.A.; Radwan, M.M.; Elsohly, M.A.; et al. Design, synthesis, molecular modeling, in vivo studies and anticancer evaluation of quinazolin-4(3H)-one derivatives as potential VEGFR-2 inhibitors and apoptosis inducers. *Bioorg. Chem.* **2020**, *94*, 103422. [[CrossRef](#)] [[PubMed](#)]
69. Gillis, E.P.; Eastman, K.J.; Hill, M.D.; Donnelly, D.J.; Meanwell, N.A. Applications of Fluorine in Medicinal Chemistry. *J. Med. Chem.* **2015**, *58*, 8315–8359. [[CrossRef](#)] [[PubMed](#)]
70. Hamidian, H.; Tikdari, A.M.; Khabazzadeh, H. Synthesis of New 4(3H)-Quinazolinone Derivatives Using 5(4H)-Oxazolones. *Molecules* **2006**, *11*, 377–382. [[CrossRef](#)]
71. Mohamed, M.A.; Ayyad, R.R.; Shaver, T.Z.; Abdel-Aziz, A.A.; El-Azab, A.S. Synthesis and antitumor evaluation of trimethoxyanilides based on 4(3H)-quinazolinone scaffolds. *Eur. J. Med. Chem.* **2016**, *112*, 106–113. [[CrossRef](#)] [[PubMed](#)]
72. Ichikawa, K.; Sasada, R.; Chiba, K.; Gotoh, H. Effect of Side Chain Functional Groups on the DPPH Radical Scavenging Activity of Bisabolane-Type Phenols. *Antioxidants* **2019**, *8*, 65. [[CrossRef](#)]
73. Kim, E.Y.; Choi, H.J.; Park, M.J.; Jung, Y.S.; Lee, S.O.; Kim, K.J.; Choi, J.H.; Chung, T.W.; Ha, K.T. Myristica fragrans Suppresses Tumor Growth and Metabolism by Inhibiting Lactate Dehydrogenase A. *Am. J. Chin. Med.* **2016**, *44*, 1063–1079. [[CrossRef](#)]
74. Lica, J.J.; Wieczór, M.; Grabe, G.J.; Heldt, M.; Jancz, M.; Misiak, M.; Gucwa, K.; Brankiewicz, W.; Maciejewska, N.; Stupak, A.; et al. Effective Drug Concentration and Selectivity Depends on Fraction of Primitive Cells. *Int. J. Mol. Sci.* **2021**, *22*, 4931. [[CrossRef](#)] [[PubMed](#)]
75. Tsai, F.M.; Wu, C.C.; Shyu, R.Y.; Wang, C.H.; Jiang, S.Y. Tazarotene-induced gene 1 inhibits prostaglandin E2-stimulated HCT116 colon cancer cell growth. *J. Biomed. Sci.* **2011**, *18*, 88. [[CrossRef](#)]
76. Paul-Samojedny, M.; Kokocińska, D.; Samojedny, A.; Mazurek, U.; Partyka, R.; Lorenz, Z.; Wilczok, T. Expression of cell survival/death genes: Bcl-2 and Bax at the rate of colon cancer prognosis. *Biochim. Biophys. Acta* **2005**, *1741*, 25–29. [[CrossRef](#)]
77. Hauseman, Z.J.; Harvey, E.P.; Newman, C.E.; Wales, T.E.; Bucci, J.C.; Mintseris, J.; Schweppe, D.K.; David, L.; Fan, L.; Cohen, D.T.; et al. Homogeneous Oligomers of Pro-apoptotic BAX Reveal Structural Determinants of Mitochondrial Membrane Permeabilization. *Mol. Cell* **2020**, *79*, 68–83.e7. [[CrossRef](#)]
78. Wani, A.K.; Akhtar, N.; Mir, T.U.G.; Singh, R.; Jha, P.K.; Mallik, S.K.; Sinha, S.; Tripathi, S.K.; Jain, A.; Jha, A.; et al. Targeting Apoptotic Pathway of Cancer Cells with Phytochemicals and Plant-Based Nanomaterials. *Biomolecules* **2023**, *13*, 194. [[CrossRef](#)]
79. Ocker, M.; Höpfner, M. Apoptosis-modulating drugs for improved cancer therapy. *Eur. Surg. Res.* **2012**, *48*, 111–120. [[CrossRef](#)] [[PubMed](#)]
80. Zorofchian Moghadamtousi, S.; Karimian, H.; Rouhollahi, E.; Paydar, M.; Fadaeinasab, M.; Abdul Kadir, H. Annona muricata leaves induce G<sub>1</sub> cell cycle arrest and apoptosis through mitochondria-mediated pathway in human HCT-116 and HT-29 colon cancer cells. *J. Ethnopharmacol.* **2014**, *156*, 277–289. [[CrossRef](#)]
81. Lee, S.T.; Wong, P.F.; Cheah, S.C.; Mustafa, M.R. Alpha-tomatine induces apoptosis and inhibits nuclear factor-kappa B activation on human prostatic adenocarcinoma PC-3 cells. *PLoS ONE* **2011**, *6*, e18915. [[CrossRef](#)]
82. Xiang, L.; He, B.; Liu, Q.; Hu, D.; Liao, W.; Li, R.; Peng, X.; Wang, Q.; Zhao, G. Antitumor effects of curcumin on the proliferation, migration and apoptosis of human colorectal carcinoma HCT-116 cells. *Oncol. Rep.* **2020**, *44*, 1997–2008. [[CrossRef](#)] [[PubMed](#)]
83. Maurus, R.; Begum, A.; Williams, L.K.; Fredriksen, J.R.; Zhang, R.; Withers, S.G.; Brayer, G.D. Alternative catalytic anions differentially modulate human alpha-amylase activity and specificity. *Biochemistry* **2008**, *47*, 3332–3344. [[CrossRef](#)]
84. Hassan, M.Z.; Alsayari, A.; Asiri, Y.I.; Bin Muhsinah, A. 1, 2, 4-Triazole-3-Thiones: Greener, One-Pot, Ionic Liquid Mediated Synthesis and Antifungal Activity. *Polycycl. Aromat. Compd.* **2023**, *43*, 167–175. [[CrossRef](#)]
85. Roig-Zamboni, V.; Cobucci-Ponzano, B.; Iacono, R.; Ferrara, M.C.; Germany, S.; Bourne, Y.; Parenti, G.; Moracci, M.; Sulzenbacher, G. Structure of human lysosomal acid  $\alpha$ -glucosidase—a guide for the treatment of Pompe disease. *Nat. Commun.* **2017**, *8*, 1111. [[CrossRef](#)]
86. Read, J.A.; Winter, V.J.; Eszes, C.M.; Sessions, R.B.; Brady, R.L. Structural basis for altered activity of M- and H-isozyme forms of human lactate dehydrogenase. *Proteins* **2001**, *43*, 175–185. [[CrossRef](#)] [[PubMed](#)]
87. Kim, E.Y.; Chung, T.W.; Han, C.W.; Park, S.Y.; Park, K.H.; Jang, S.B.; Ha, K.T. A Novel Lactate Dehydrogenase Inhibitor, 1-(Phenylseleno)-4-(Trifluoromethyl) Benzene, Suppresses Tumor Growth through Apoptotic Cell Death. *Sci. Rep.* **2019**, *9*, 3969. [[CrossRef](#)] [[PubMed](#)]
88. Wang, J.L.; Limburg, D.; Graneto, M.J.; Springer, J.; Hamper, J.R.; Liao, S.; Pawlitz, J.L.; Kurumbail, R.G.; Maziasz, T.; Talley, J.J.; et al. The novel benzopyran class of selective cyclooxygenase-2 inhibitors. Part 2: The second clinical candidate having a shorter and favorable human half-life. *Bioorg. Med. Chem. Lett.* **2010**, *20*, 7159–7163. [[CrossRef](#)]

89. Xiong, G.; Wu, Z.; Yi, J.; Fu, L.; Yang, Z.; Hsieh, C.; Yin, M.; Zeng, X.; Wu, C.; Lu, A.; et al. ADMETlab 2.0: An integrated online platform for accurate and comprehensive predictions of ADMET properties. *Nucleic Acids Res.* **2021**, *49*, W5–W14. [[CrossRef](#)]
90. Bickerton, G.R.; Paolini, G.V.; Besnard, J.; Muresan, S.; Hopkins, A.L. Quantifying the chemical beauty of drugs. *Nat. Chem.* **2012**, *4*, 90–98. [[CrossRef](#)]
91. Lipinski, C.A.; Lombardo, F.; Dominy, B.W.; Feeney, P.J. Experimental and computational approaches to estimate solubility and permeability in drug discovery and development settings. *Adv. Drug Deliv. Rev.* **1997**, *23*, 3–25. [[CrossRef](#)]
92. Hughes, J.D.; Blagg, J.; Price, D.A.; Bailey, S.; Decrescenzo, G.A.; Devraj, R.V.; Ellsworth, E.; Fobian, Y.M.; Gibbs, M.E.; Gilles, R.W.; et al. Physicochemical drug properties associated with in vivo toxicological outcomes. *Bioorg. Med. Chem. Lett.* **2008**, *18*, 4872–4875. [[CrossRef](#)]
93. Gleeson, M.P. Generation of a set of simple, interpretable ADMET rules of thumb. *J. Med. Chem.* **2008**, *51*, 817–834. [[CrossRef](#)]
94. Johnson, T.W.; Dress, K.R.; Edwards, M. Using the Golden Triangle to optimize clearance and oral absorption. *Bioorg. Med. Chem. Lett.* **2009**, *19*, 5560–5564. [[CrossRef](#)] [[PubMed](#)]
95. Daina, A.; Michielin, O.; Zoete, V. SwissADME: A free web tool to evaluate pharmacokinetics, drug-likeness and medicinal chemistry friendliness of small molecules. *Sci. Rep.* **2017**, *7*, 42717. [[CrossRef](#)] [[PubMed](#)]
96. Capuzzi, S.J.; Muratov, E.N.; Tropsha, A. Phantom PAINS: Problems with the Utility of Alerts for Pan-Assay Interference Compounds. *J. Chem. Inf. Model.* **2017**, *57*, 417–427. [[CrossRef](#)]
97. Baell, J.B.; Holloway, G.A. New substructure filters for removal of pan assay interference compounds (PAINS) from screening libraries and for their exclusion in bioassays. *J. Med. Chem.* **2010**, *53*, 2719–2740. [[CrossRef](#)]
98. Waring, M.J.; Arrowsmith, J.; Leach, A.R.; Leeson, P.D.; Mandrell, S.; Owen, R.M.; Pairaudeau, G.; Pennie, W.D.; Pickett, S.D.; Wang, J.; et al. An analysis of the attrition of drug candidates from four major pharmaceutical companies. *Nat. Rev. Drug Discov.* **2015**, *14*, 475–486. [[CrossRef](#)]
99. Lovering, F.; Bikker, J.; Humblet, C. Escape from flatland: Increasing saturation as an approach to improving clinical success. *J. Med. Chem.* **2009**, *52*, 6752–6756. [[CrossRef](#)]
100. Nguyen, T.T.; Duong, V.A.; Maeng, H.J. Pharmaceutical Formulations with P-Glycoprotein Inhibitory Effect as Promising Approaches for Enhancing Oral Drug Absorption and Bioavailability. *Pharmaceutics* **2021**, *13*, 1103. [[CrossRef](#)] [[PubMed](#)]
101. Boobis, A.; Gundert-Remy, U.; Kremers, P.; Macheras, P.; Pelkonen, O. In silico prediction of ADME and pharmacokinetics. Report of an expert meeting organised by COST B15. *Eur. J. Pharm. Sci.* **2002**, *17*, 183–193. [[CrossRef](#)]
102. Kratochwil, N.A.; Huber, W.; Müller, F.; Kansy, M.; Gerber, P.R. Predicting Plasma Protein Binding of Drugs: A New Approach. *Biochem. Pharmacol.* **2002**, *64*, 1355–1374. [[CrossRef](#)]
103. Van De Waterbeemd, H.; Gifford, E. ADMET in silico modelling: Towards prediction paradise? *Nat. Rev. Drug Discov.* **2003**, *2*, 192–204. [[CrossRef](#)]
104. Babalola, S.; Igie, N.; Odeyemi, I. Molecular Docking, Drug-Likeness Analysis, In Silico Pharmacokinetics, and Toxicity Studies of p-Nitrophenyl Hydrazones as Anti-inflammatory Compounds against COX-2, 5-LOX, and H<sup>+</sup>/K<sup>+</sup> ATPase. *Pharm. Fronts* **2022**, *4*, e250–e266. [[CrossRef](#)]
105. Bersuder, P.; Hole, M.; Smith, G. Antioxidants from a heated histidine-glucose model system. I: Investigation of the antioxidant role of histidine and isolation of antioxidants by high-performance liquid chromatography. *J. Am. Oil Chem. Soc.* **1998**, *75*, 181–187. [[CrossRef](#)]
106. Andrade-Cetto, A.; Becerra-Jiménez, J.; Cárdenas-Vázquez, R. Alfa-glucosidase-inhibiting activity of some Mexican plants used in the treatment of type 2 diabetes. *J. Ethnopharmacol.* **2008**, *116*, 27–32. [[CrossRef](#)]
107. Subramanian, R.; Asmawi, M.Z.; Sadikun, A. In vitro alpha-glucosidase and alpha-amylase enzyme inhibitory effects of *Andrographis paniculata* extract and andrographolide. *Acta Biochim. Polym.* **2008**, *55*, 391–398. [[CrossRef](#)]
108. Nicoletti, I.; Migliorati, G.; Pagliacci, M.; Grignani, F.; Riccardi, C. A rapid and simple method for measuring thymocyte apoptosis by propidium iodide staining and flow cytometry. *J. Immunol. Methods* **1991**, *139*, 271–279. [[CrossRef](#)]
109. Bradford, M.M. A rapid and sensitive method for the quantitation of microgram quantities of protein utilizing the principle of protein-dye binding. *Anal. Biochem.* **1976**, *72*, 248–254. [[CrossRef](#)]

**Disclaimer/Publisher's Note:** The statements, opinions and data contained in all publications are solely those of the individual author(s) and contributor(s) and not of MDPI and/or the editor(s). MDPI and/or the editor(s) disclaim responsibility for any injury to people or property resulting from any ideas, methods, instructions or products referred to in the content.

See discussions, stats, and author profiles for this publication at: <https://www.researchgate.net/publication/370322209>

# In silico study to recognize novel angiotensin-converting-enzyme-I inhibitors by 2D-QSAR and constraint-based molecular simulations

Article in *Journal of biomolecular Structure & Dynamics* · April 2023

DOI: 10.1080/07391102.2023.2203261

CITATIONS

0

READS

159

9 authors, including:



**Sapan Shah**

Priyadarshini J L College of Pharmacy

28 PUBLICATIONS 126 CITATIONS

SEE PROFILE



**Vijay H. Masand**

Vidya Bharati Mahavidyalaya, Amravati, Maharashtra, India.

130 PUBLICATIONS 1,708 CITATIONS

SEE PROFILE



**Magdi E. A. Zaki**

University of Minho

213 PUBLICATIONS 1,735 CITATIONS

SEE PROFILE



**Ashish Shah**

Sumandeep Vidyapeeth University

58 PUBLICATIONS 160 CITATIONS

SEE PROFILE



## *In silico* study to recognize novel angiotensin-converting-enzyme-I inhibitors by 2D-QSAR and constraint-based molecular simulations

Sapan Shah<sup>a</sup> , Dinesh Chaple<sup>a</sup>, Vijay H. Masand<sup>b</sup> , Magdi E.A Zaki<sup>c</sup> , Sami A. Al-Hussain<sup>c</sup>, Ashish Shah<sup>d</sup> , Sumit Arora<sup>e</sup> , Rahul Jawarkar<sup>f</sup>  and Mohammad Tauqeer<sup>g</sup>

<sup>a</sup>Department of Pharmaceutical Chemistry, Priyadarshini J. L. College of Pharmacy, Nagpur, Maharashtra, India; <sup>b</sup>Department of Chemistry, Vidya Bharati Mahavidyalaya, Amravati, Maharashtra, India; <sup>c</sup>Department of Chemistry, Faculty of Science, Imam Mohammad Ibn Saud Islamic University, Riyadh, Saudi Arabia; <sup>d</sup>Department of Pharmacy, Sumandeep Vidyapeeth, Vadodara, Gujarat, India; <sup>e</sup>Department of Pharmacognosy, Gurunanak College of Pharmacy, Nagpur, Maharashtra, India; <sup>f</sup>Department of Medicinal Chemistry and Drug Discovery, Dr. Rajendra Gode Institute of Pharmacy, Amravati, India; <sup>g</sup>Department of Pharmacognosy, Dr. Arun Motghare College of Pharmacy, Kosra-Kondha, Maharashtra, India

Communicated by Ramaswamy H. Sarma

### ABSTRACT

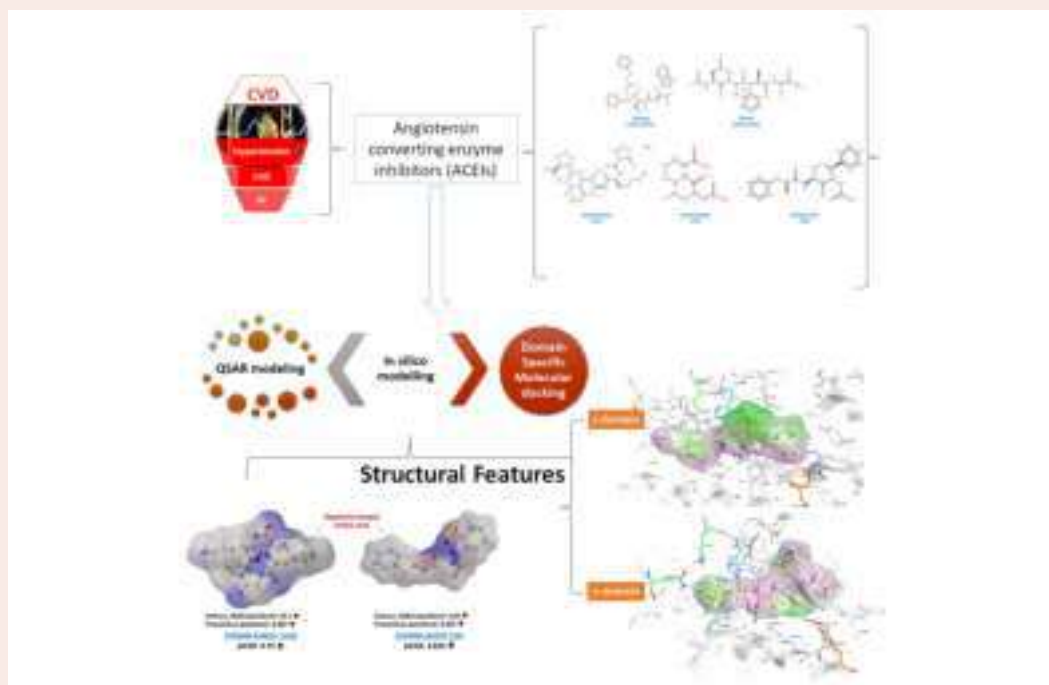
Cardiovascular diseases (CVD) such as heart failure, stroke, and hypertension affect 64.3 million people worldwide and are responsible for 30% of all deaths. Primary inhibition of the angiotensin-converting enzyme (ACE) is significant in the management of CVD. In the present study, the genetic algorithm-multiple linear regressions (GA-MLR) method is used to generate highly predictive and statistically significant ( $R^2 = 0.70-0.75$ ,  $Q^2_{LOO} = 0.67-0.73$ ,  $Q^2_{LMO} = 0.66-0.72$ ,  $CCC_{ex} = 0.70-0.78$ ) quantitative structure-activity relationships (QSAR) models conforming to OECD requirements using a dataset of 255 structurally diverse and experimentally validated ACE inhibitors. The models contain simply illustratable Padel, Estate, and PyDescriptors that correlate structural scaffold requisite for ACE inhibition. Also, constraint-based molecular docking reveals an interaction profile between ligands and enzymes which is then correlated with the essential structural features associated with the QSAR models. The QSAR-based virtual screening was utilized to find novel lead molecules from a designed database of 102 thiadiazole derivatives. The Applicability domain (AD), Molecular Docking, Molecular dynamics, and ADMET analysis suggest two compound D24 and D40 are inflexibly linked to the protein binding site and follows drug-likeness properties.

### ARTICLE HISTORY

Received 8 November 2022  
Accepted 10 April 2023

### KEYWORDS

Cardiovascular diseases; angiotensin-converting enzyme inhibitors; QSAR; validation; molecular docking; structural features



## 1. Introduction

The complications like hypertension, dysrhythmia, heart failure (HF), myocardial infarction, etc. are the main factors associated with cardiovascular diseases (CVD) accounting for 32% of the overall mortality in developed and many developing countries (Dariush et al., 2016). The experimental evidence suggests that control of the renin-angiotensin-aldosterone system (RAAS) is very important in the pathophysiology of CVD through Angiotensin-Converting-Enzyme-I (ACE-I) inhibition (McMurray, 2011).

ACE-I which catalyzes the conversion of angiotensin-I to angiotensin-II is a membrane-bound dipeptidyl carboxyl peptidase that has two important active sites viz. zinc-binding site and cationic binding site and occupies an important niche in the regulation of extracellular volume by the rennin angiotensin system (Gonzalez Amaya et al., 2020; Khan & Imig, 2018). There are many trends in which ACE-related exploration requisite like deficiencies attributed to the current generation of these drugs, overcoming side effects such as dry cough or angioedema, development of irreversible ACE-I inhibitors (ACEIs), and improving the selectivity of drugs towards c-domain for antihypertensive activity (Regulska et al., 2014; Zheng et al., 2022).

*In silico* techniques have proven crucial in drug discovery efforts because of their multifaceted use for data collection, pre-processing, analysis, and inference. Wet-lab chemical experimentation has been minimized in the last few years by molecular modelling and virtual experimentation, which use the foundational concepts of basic sciences including mathematics, chemistry, physics, and algorithms (Jawarkar, Bakal, et al., 2022; Schaduangrat et al., 2020).

Quantitative structure-activity relationship (QSAR) and molecular simulations are recognized *In silico* approaches in ligand-based drug design and structure-based drug design, which when applied in harmony give critical and superlative evidence essential for lead/drug optimization (Masand et al., 2017). QSAR is a mathematical expression to correlate biological activities with chemical structures of different classes of compounds which will be helpful to design and predict the activity of novel drug candidates without sacrificing animals (Khan et al., 2019; Olasupo et al., 2019).

The current challenge in the QSAR is to fill data gaps by predicting biological activity from known structural features of novel designed ACEIs comprising scaffolds that might not have been tested experimentally (Roy et al., 2017). A combination of esoteric e-Dragon or PaDEL descriptors along with PyDescriptor descriptors is useful for deriving statistically robust QSAR models further valuable for qualitative, quantitative, and mechanistic interpretations (Masand & Rastija, 2017). Molecular simulation techniques identify the most favorable conformation (position and relative orientation) of bioactive at a catalytic site to study interaction with a target that was knotty with conventional biological assay (Hadaji et al., 2022; Karadžić et al., 2017).

There have been a large number of computational studies performed (Carli et al., 2014; Gonzalez Amaya et al., 2020; Politi et al., 2009; Sagardia et al., 2013; Shah et al., 2023; Stoičkov et al., 2018; Yan et al., 2020) so far for designing new

ACE-I inhibitors, but still, we are far from finding a potentially small non-peptide moiety as ACEIs. ACE inhibitors are mostly composed of a group such as a carboxyl (lisinopril), phosphonate (fosinopril), and sulfhydryl (captopril) that chelates with the divalent zinc ion through various interactions lead to different domain specificity (Zheng et al., 2022). Theazole group's nucleus, the thiadiazole moiety, is a flexible pharmacophore with a wide range of biological functions (Almutairi et al., 2022; Hu et al., 2014; Jain et al., 2013; Palakkeezhillam et al., 2023). In addition to these, thiadiazole shows the potential to act as a cardiovascular drug in the treatment of hypertension (El-Enany et al., 2020; Turner et al., 1988). The main aim of this research work is to develop good, rational, and statistically robust *in silico* models that can correctly interpret the structural features, with high external predictability to screen novel ACEIs with more favorable clinical profiles than current generation drugs. New thiadiazole derivatives were designed according to the classical synthetic scheme also considering structural requirements suggested by *in silico* studies. The QSAR-based virtual screening was utilized to find novel lead molecules from a designed thiadiazole derivative. Moreover, selected compounds with favorable docking scores were subjected to molecular dynamics and ADMET analysis. Additionally, such *in silico* models could be useful to explore the binding mode of inhibitors with ACE-I to gain further insight into the structure-activity relationship.

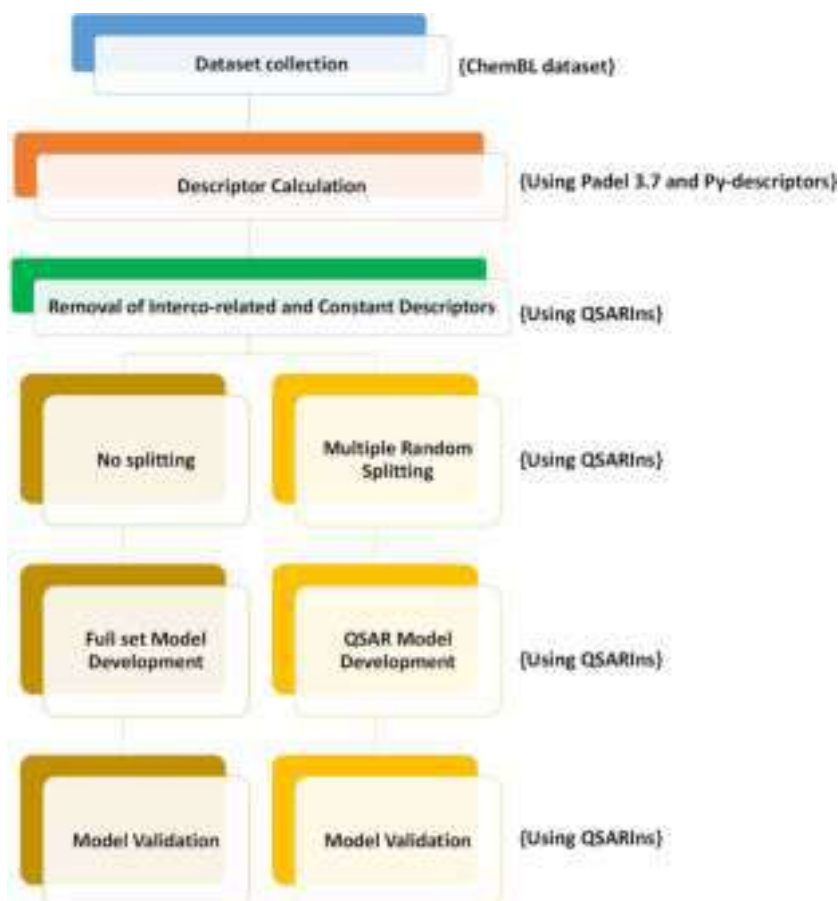
## 2. Experimental methodology

### 2.1. Datasets selection

Molecular structural datasets of 255 compounds with inhibitory activity against the angiotensin-converting enzyme of *Rattus norvegicus* were collected from the ChEMBL database (<https://www.ebi.ac.uk/chembl>). The dataset was prepared to contain diverse classes of heterocyclic compounds selected in which inhibitory activity was expressed in  $IC_{50}$  (nM). The reported  $IC_{50}$  (nM) values for enzyme inhibitory activity were converted to molar units and then calculated  $pIC_{50}$  ( $-\log_{10}IC_{50}$ ) were used before QSAR analysis. SMILES notations of all chemical compounds are retrieved from ChEMBL database which was then converted to SDF format using OpenBabel considering 3D geometry optimization. Molecular structures are energy-optimized using the MMFF94 force field in Marvin from ChemAxon ([www.chemaxon.com](http://www.chemaxon.com)). Before calculating descriptors, we curated all chemical compounds to develop significant QSAR models (see [supplementary information S1](#), Sheet1).

### 2.2. Descriptor calculation and pre-treatment

In this section, we have calculated only 2D descriptors using three approaches, namely Py-Descriptor(16251) (Masand & Rastija, 2017) (Constitutional, geometric, circular fingerprint, quantum chemical and topological), Estate Descriptors (calculates n-octanol/water partition coefficient; Tetko et al., 2001) and PaDEL-Descriptor 2.20 (1444) (Yap, 2011) (for extended topochemical atom indices) (see [supplementary information S2](#)). Since all the calculated descriptors (>17730) do not



**Figure 1.** Steps Involved in QSAR Model Development.

contain significant information; we have performed data curation manually, to eliminate the descriptors with missing or near-constant values. Descriptors are filtered which are constant (>95%) and highly correlated ( $|R| > 95\%$ ) before particular feature selection using QSARINS 2.2.4 (Gramatica et al., 2013). This led to a set of only 620 interpretable descriptors for ACE-I inhibitory activity. The reduced set of descriptors still comprises a wide array of speculative molecular descriptors that takes into account different structural features, viz. constitutional, geometric, autocorrelation, topological, quantum chemical, and circular fingerprints capturing the diverse aspects of the chemical structures.

## 2.3. QSAR model development

### 2.3.1. QSAR model

The principle and application of QSAR analysis define key characteristics of structural features to envisage the anticipated activity of compounds before their actual synthesis and biological evaluation. The dataset was divided into training (70%) and prediction (or test) (30%) sets randomly before descriptor selection. We utilized the training set to generate the QSAR models and then validated our results using the test set. The superlative set of descriptors was selected using the GA-MLR module of QSARINS 2.2.4. Multiple Diversified QSAR models ensure the retention of complete information on structural features governing the biological inhibitory

activity of molecules. The steps applied in the development of the QSAR model have been briefed in Figure 1.

### 2.3.2. Statistical validation of the generated 2D-QSAR models

In the present work, we have applied various statistical methodologies like internal (regression coefficient:  $R^2$ , leave-one-out/many-out cross-validated correlation coefficient:  $Q^2_{LOO}$ , Avg  $R_m^2_{LOO}$ , and  $\Delta R_m^2$ ) and external ( $Q^2-F^1$ ,  $Q^2-F^2$ ,  $R_m^2$  parameters, and concordance correlation coefficient: CCC) validation methods to assure the significant level of the generated models (Tropsha, 2010). Additionally, the Y-randomization test (Kumar et al., 2020), checked applicability domain criteria was checked, using the Williams plot—the plot of HAT  $i/i(h^*)$  versus standardized cross-validated residuals was used (Roy et al., 2015). Consideration of all these criteria together advances the predictive efficiency of the QSAR model (Shah & Chaple, 2021). The details of various statistical validation parameters are discussed in Table 2.

## 2.4. Molecular docking

In this analysis, we have applied the molecular docking studies to investigate the binding pattern of molecules (most active, least active, and intermediately active compounds from the dataset) with the C-domain (PDB ID: 1O86) and N-domain (PDB ID:3NXQ) of ACE-I, obtained from the protein data bank



(<https://www.rcsb.org>). The orally active ACEIs have so far been the preeminent drugs in lowering blood vessel pressure both in renovascular and fundamental hypertension. The molecular docking study was performed by using MOE 2015 software (Chemical Computing Group, Montreal, Canada). Before the docking analysis, we prepared the target protein and selected ligands from the dataset using a standard protocol (See [supplementary information S4](#)). Pharmacophore constraints were generated using the Pharmacophore query editor containing metal chelation constraint and one positional constrain amide/amine Nitrogen with 1 Å constraint sphere. This pharmacophore was used in the docking using the pharmacophore placement method at a site centered on co-crystallized ligand atoms and the top 1000 poses ranked by the London dG scoring function. From these poses, the best 30 poses were ranked and then minimized using MMFF94x forcefield within a rigid receptor. The resulting poses were then refined and scored using the Generalized-Born Volume Integral/Weighted Surface area (GBVI/WSA) dG scoring function which estimates the binding free energy for an obtained pose of the ligand. The final results were analyzed, and visualized based on docking scores and pose using Discovery Studio 2020 Client (Biovia, 2016), Ligplot v.4.5.3 (Wallace et al., 1995), and PyMol software (L DeLano, 2002) considering bound ligand as standard. Visualization of protein-ligand interaction reflects, the number of interactions and active residues responsible for the significant binding at the active site target enzyme.

### 2.5. Modeling of new compounds

About 102 novel thiaziazole derivatives were designed using DataWarrior software according to the synthetic route considering structural requirements indicated by the developed QSAR model (Sander et al., 2015). The chemical similarity analysis with the compounds database in ChEMBL reveals that designed analogues are novel and have not been experimented with before for ACEIs. All compounds generated were 3D optimized using MMFF94 force-field by OpenBabel and descriptors are calculated as discussed above. The best acceptable and predictable QSAR model was used to predict the applicability domain of the optimized designed compounds using QSARINs and the activity ( $pIC_{50}$ ) was predicted for the generated compounds exhibited HAT  $i/i$  ( $h^*=0.1676$ ) or less.

### 2.6. ADMET study of designed compounds

The selected 102 designed thiaziazole analogues were subjected to drug-likeness properties according to Lipinski, Ghose, Veber, Egan, and Muegge filters. The pharmacokinetic profile (ADME) and Toxicity predictions of ligands were conducted using SwissADME (<http://www.swissadme.ch>) and pkCSM (<http://biosig.unimelb.edu.au/pkcsm/prediction>). To analyze the toxicological properties of ligands SMILES notations or SDF files uploaded followed by selecting required models for generating numerous information about structure-related effects (Arora et al., 2020; Shah et al., 2021).

### 2.7. Molecular dynamics

Desmond version 2020.1 with OPLS3e force field from Schrodinger was used to study the dynamic behaviour of most active Molecules D24 with a docking score of  $-6.257$  kcal/mol, Molecule D40 ( $-6.697$  kcal/mol) and standard RXPA380 ( $-8.753$  kcal/mol) complexes in presence of explicit water molecules (Harder et al., 2016). The System Builder module was used for system preparation using SPC module for solvation and volume occupancy in an orthorhombic box with periodic boundary conditions. The solvated system was neutralised by the addition of appropriate anion ( $Cl^-$ ) and cation ( $Na^+$ ) with a salt concentration of 0.15 mol/L. The Nose-Hoover chain coupling approach was employed to build up the NPT ensemble with temperature 300 K, leisure time of 1.0 ps, and pressure 1 bar, which was once as soon as maintained in all simulations. A 2 fs time step will be employed. The barostat approach with the Martyna-Tuckerman-Klein chain coupling scheme was originally utilized for pressure control with a leisure time of 2 ps. The particle mesh Ewald technique was used to calculate long-range electrostatic interactions with a radius of 9 for Coulomb interactions. The non-bonded forces were estimated using the RESPA integrator. The root mean square deviation (RMSD), root mean square fluctuation (RMSF), a radius of gyration (Rg), and protein-ligand interactions were assessed to check the stability of the complex in MD simulations (Jawarkar, Sharma, et al., 2022).

## 3. Results

### 3.1. QSAR models

A total of four QSAR models based on GA analysis were generated where all models are statistically analogous and relate

Box 1. Reaction scheme for the design of thiaziazole derivatives.



**Table 1.** QSAR model developed against ACE-I enzyme.

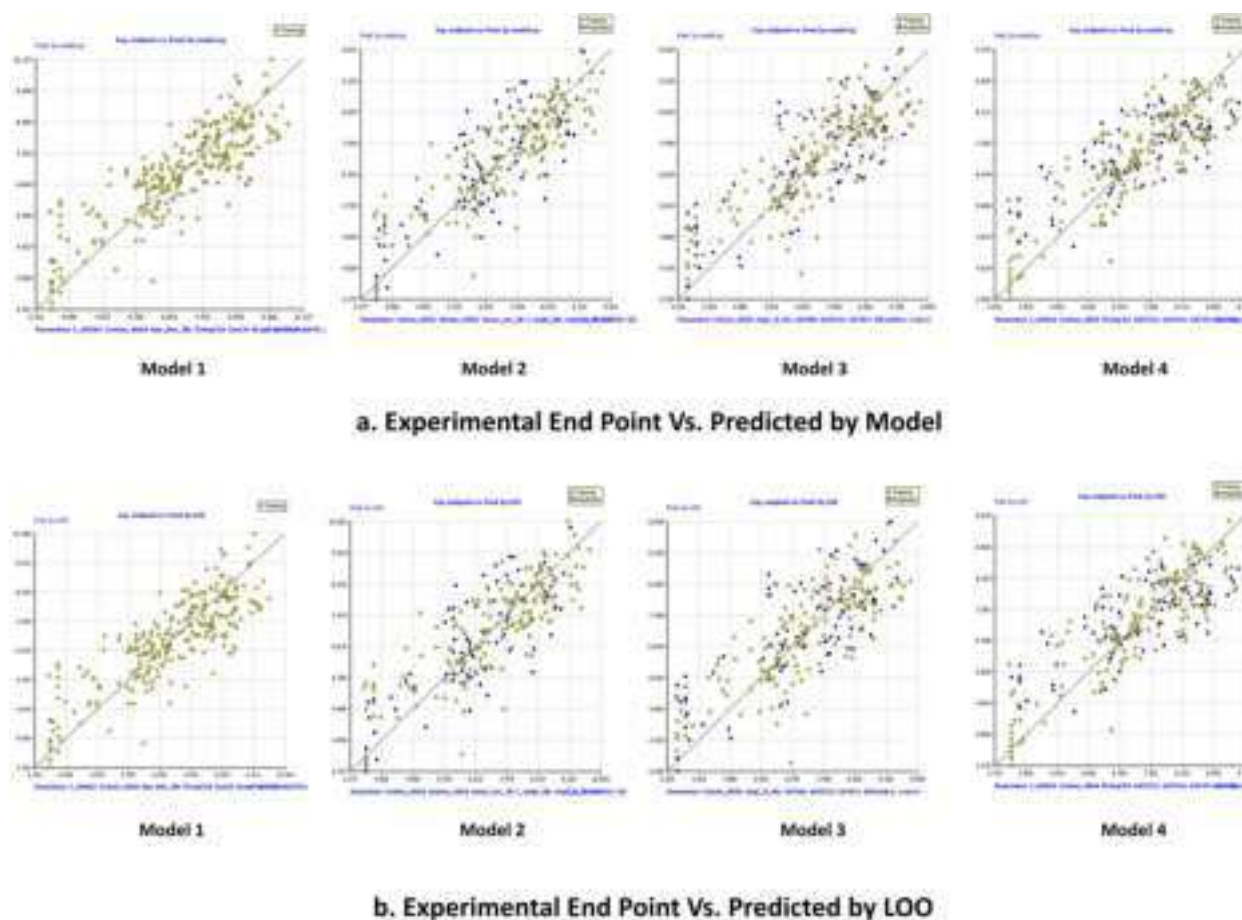
Model 1 (Undivided)	$\text{pIC}_{50} = 2.17088 + 8.3221(\pm 1.3209) \text{fmsaminus} - 0.1781(\pm 0.0252) \text{C\_HASA2} + 0.0403 (\pm 0.0089) \text{Cminus\_AbSA} - 5.8539(\pm 0.7665) \text{lipo\_don\_3Bc} - 0.1182(\pm 0.0232) \text{fCringC5A} + 0.0442(\pm 0.0163) \text{SaaCH} - 0.2705(\pm 0.0517) \text{ALogP} + 2.2208 (\pm 0.4424) \text{AATSC7i} + 1.7636(\pm 0.2408) \text{GATS7e}$
Model 2 (Divided)	$\text{pIC}_{50} = -2.0928 + 8.0956 (\pm 1.656) \text{fmsaminus} + 0.0693(\pm 0.011) \text{Cminus\_AbSA} + 0.0207 (\pm 0.0042) \text{Sminus\_SASA} + 0.0878(\pm 0.021) \text{minus\_acc\_3B} + 1.2740 (\pm 0.4115) \text{C\_ringN\_2Bc} - 0.1000 (\pm 0.0193) \text{ringC\_S\_5B} + 11.5138 (\pm 1.2883) \text{MATS3c} + 1.3922 (\pm 0.4451) \text{GATS7m} + 0.8866(\pm 0.1904) \text{GATS7s}$
Model 3 (Divided)	$\text{pIC}_{50} = -1.7419 + 13.2854(\pm 1.528) \text{fmsaminus} + 0.0854(\pm 0.0104) \text{Cminus\_AbSA} + 2.7259 (\pm 0.6713) \text{ringC\_N\_4Ac} - 0.3158 (\pm 0.066) \text{AATS8s} + 687.2595(\pm 71.96) \text{AATSC3c} + 1.7160(\pm 0.1856) \text{GATS7s} + 1.860 (\pm 0.059) \text{SHCsats}$
Model 4 (Divided)	$\text{pIC}_{50} = -2.5203 + 12.5040(\pm 1.3908) \text{fmsaminus} - 0.1644(\pm 0.0272) \text{C\_HASA2} + 0.0804(\pm 0.0096) \text{Cminus\_AbSA} - 0.0420(\pm 0.0164) \text{fCringC5A} + 537.3100 (\pm 70.27) \text{AATSC3c} + 0.9097(\pm 0.417) \text{GATS7m} + 1.4798(\pm 0.2397) \text{GATS7e} + 0.9601(\pm 0.2848) \text{GATS8p}$

**Table 2.** Statistical performance of developed QSAR models.

Sr. No.	Statistical parameter	Model 1	Model 2	Model 3	Model 4
		Undivided	Divided	Divided	Divided
1.	$N_{tr}$	255	179	180	180
2.	$N_{test}$	0	76	75	75
3.	No. of descriptors	9	9	7	8
Fitting criteria					
4.	$R^2_{tr}$	0.7161	0.7405	0.7096	0.7480
5.	$R^2_{adj}$	0.7057	0.7267	0.6977	0.7361
6.	$R^2 - R^2_{adj}$	0.0104	0.0138	0.0118	0.0119
7.	LOF	0.8319	0.8237	0.8173	0.7659
8.	Kxx	0.3314	0.3204	0.281	0.2852
9.	DeltaK	0.0429	0.0505	0.0579	0.0558
10.	$RMSE_{tr}$	0.8477	0.8163	0.8342	0.7969
11.	$MAE_{tr}$	0.663	0.6301	0.6574	0.6195
12.	$RSS_{tr}$	183.2378	119.2823	125.2716	113.6803
13.	$CCC_{tr}$	0.8346	0.8509	0.8301	0.8558
14.	S	0.8648	0.8401	0.8534	0.8177
15.	F	68.6637	53.5776	60.0267	63.0619
Internal validation criteria					
16.	$R^2_{cv} (Q^2_{LOO})$	0.6932	0.7083	0.6732	0.7225
17.	$R^2 - Q^2_{LOO}$	0.0229	0.0322	0.0363	0.0254
18.	$RMSE_{cv}$	0.8812	0.8655	0.8849	0.8362
19.	$MAE_{cv}$	0.6898	0.6678	0.6924	0.6512
20.	$PRESS_{cv}$	198.0217	134.0909	140.9372	125.1548
21.	$CCC_{cv}$	0.8214	0.8327	0.8095	0.8414
22.	$Q^2_{LMO}$	0.6866	0.6996	0.6629	0.7168
23.	$R^2_{Y_{scr}}$	0.0355	0.05	0.0389	0.0459
24.	$Q^2_{Y_{scr}}$	-0.045	-0.0665	-0.0535	-0.0587
25.	$RMSE_{AV_{Y_{scr}}}$	1.5623	1.5617	1.5174	1.5504
External validation criteria					
26.	$\theta^*$		-7.4174	-9.9624	-17.8467
27.	$RMSE_{ex}$		0.9879	1.0493	1.0449
28.	$MAE_{ex}$		0.8109	0.8525	0.8792
29.	$PRESS_{ext}$		74.1668	82.5792	82.9744
30.	$R^2_{ex}$		0.6229	0.624	0.5816
31.	$Q^2 - F^1$		0.6074	0.6173	0.5732
32.	$Q^2 - F^2$		0.5844	0.6071	0.5731
33.	$Q^2 - F^3$		0.6199	0.5405	0.5667
34.	$CCC_{ex}$		0.7874	0.7812	0.7091
35.	$r^2_{m \text{ aver.}}$		0.4943	0.4906	0.3478
36.	$r^2_{m \text{ delta}}$		0.0475	0.17	0.3607
Predictions by LOO					
37.	$R^2$		0.7087	0.6739	0.7228
38.	$R^2_{o'}$		0.6128	0.5489	0.6341
39.	$k'$		0.9866	0.9863	0.9874
40.	$1 - (R^2/R^2_{o'})$		0.1353	0.1855	0.1227
41.	$r^2_{m}$		0.4892	0.4356	0.5076
42.	$R^2_{o}$		0.7083	0.6733	0.7225
43.	K		0.9991	0.9986	0.9988
44.	$1 - (R^2 - ExPy/R_o^2)$		0.0006	0.0009	0.0003
45.	$r^2_{m}$		0.6943	0.6576	0.7120

the biological activity (response dependable) to a set of molecular descriptors (independent variable) resulting in a mathematical equation correlating them (see [supplementary information S3, Sheet1](#)). Model 1 is generated using an undivided dataset whereas the other three using divided can

be useful to locate importantly and obscured structural topographies that have a significant correlation with the activity. Therefore, we have developed GA-MLR-based multiple QSAR models for ACE-I inhibitory activity following OECD guidelines ([Table 1](#)).



**Figure 2.** Plot of the predicted training set and test set versus experimental pIC50 values (a) by developed QSAR models (b) by LOO method.

### 3.2 Validation of QSAR models

The developed GA-based models are examined in terms of the statistical quality of their results to evaluate their predictive power (Table 2). The results suggest that developed QSAR models are statistically robust and possess acceptable external predictive power.

The QSAR model is said to be valid as it meets the predicted  $R^2$  criteria  $>0.6$  (Golbraikh et al., 2003). The displayed linear relationship (Figure 2) was observed in the plot of the predicted value of the training set versus experimental pIC50 values ( $R^2 = 0.70\text{--}0.75$ ). For all the developed models, the value of  $R^2_{\text{adj}}$  is quite close to  $R^2_{\text{tr}}$ , low value of LOF (Lack of fit) and  $k$  (computes inter-correlation between descriptors) suggesting that the number of descriptors in the models is not too high, thereby, indicating that the models are free from over-fitting (Gramatica, 2014).

All the developed QSAR models are statistically robust based on high values of cross-validation parameters  $Q^2$ ,  $Q^2_{\text{LMO}}$ ,  $\text{CCC}_{\text{CV}}$ , and condition  $\text{RMSE}_{\text{tr}} < \text{RMSE}_{\text{cv}}$  is fulfilled by all the developed models (Figure 3). The low value of  $R^2_{\text{Yscr}}$  and  $Q^2_{\text{Yscr}}$  for all the models indicates that the models have not been developed by chance. A high value of various statistical parameters like  $R^2_{\text{exv}}$ ,  $Q^2\text{-F}^1$ ,  $Q^2\text{-F}^2$ ,  $Q^2\text{-F}^3$ ,  $\text{CCC}_{\text{exv}}$  etc. indicates the models possess high external predictivity. This is additionally upheld by the low value of  $\text{RMSE}_{\text{exv}}$ ,  $\text{MAE}_{\text{exv}}$  and  $\text{PRESS}_{\text{ext}}$ .

Figure 4 depicts the Williams plot of the ACEIs dataset, in which the Hat diagonal values are plotted against

standardized residuals by the developed model and the LOO method gives information about outliers and outstanding chemicals in the models.

The applicability domain is fixed up inside a defined domain where all the datasets were inside the limit  $\pm 3$  for residuals and a leverage threshold  $h^*(h^* = 3p^0/n)$  where  $p^0$  is the number of descriptors and  $n$  is the number of compounds; Roy et al., 2015).

Applicability domain analysis examination reveals that most of the compounds of the training and test set were within the domain. Also, none of the statistical values was the distant outlier with standardized residuals  $>3d$  for the selected dataset. The Y-randomization graph evaluates the reliability and robustness of the model which confirms that the developed model is not by chance correlation (Figure 5).

### 3.3. Molecular docking

#### 3.3.1. Validation of docking protocol

Before proceeding toward the docking analysis of selected compounds from the dataset, the docking protocol was validated by re-docking the native ligands (Lisinopril and RXP407 compounds) from crystal structures (PDB ID: 1O86 and 3NXQ) into its binding pocket. The shape and large dimension of the binding site are always a challenge for docking of ACEIs. Therefore, in both cACE and nACE molecular docking calculations, constraints are needed to obtain

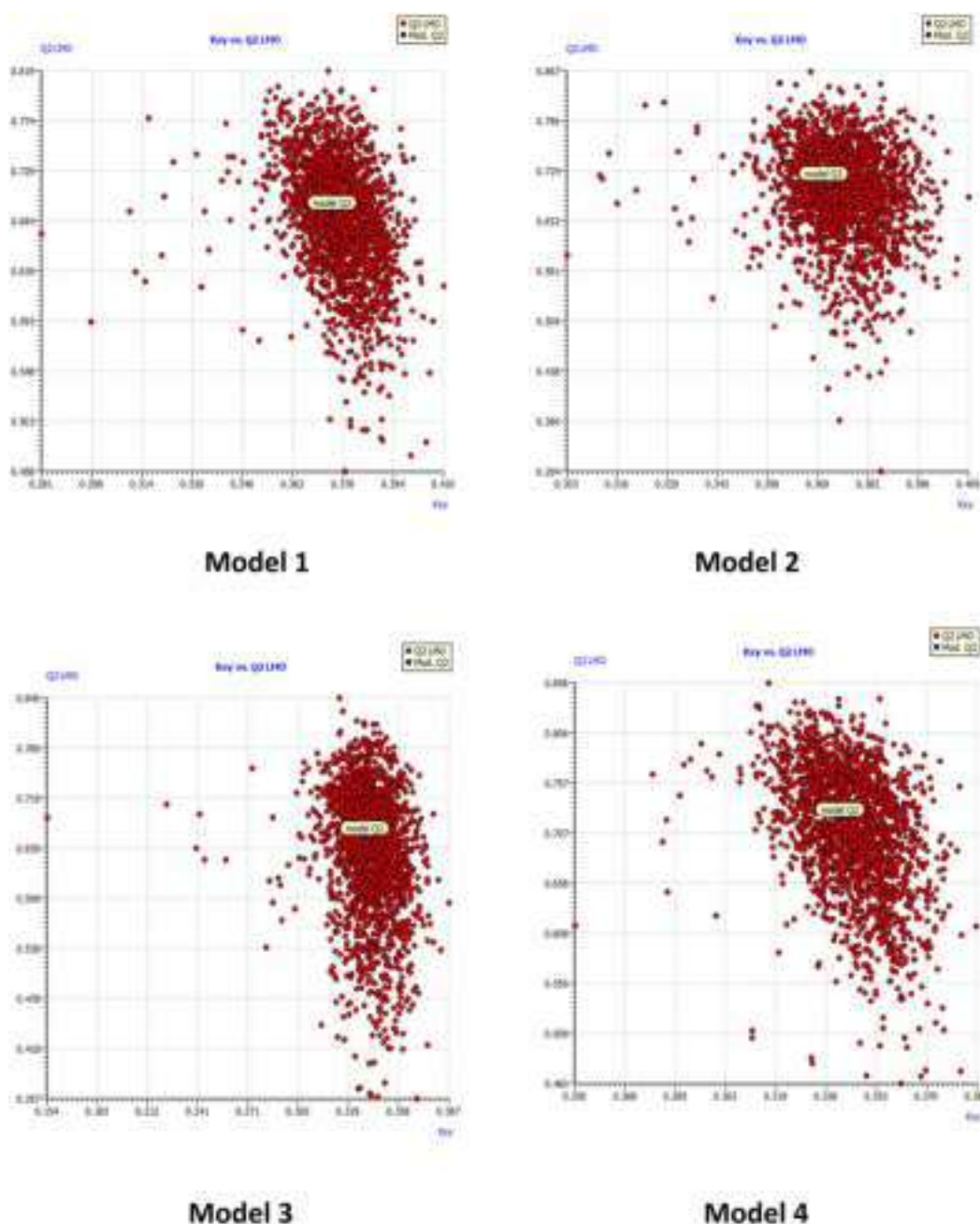


Figure 3. Plot of LMO validations compared with the original model.

reliable orientations of ligands such that pose that contains hydrogen bonds with His331 and/or His491 (nACE) or His353 and/or His513 (cACE) along with metal-chelator interactions are reliable (Caballero, 2020). The results showed that docked poses of native ligands are maximally superimposed with co-crystallized ligands in protein structure (Figure 6). This implies that the docking protocol is well enough for the virtual screening of dataset compounds.

### 3.3.2. Molecular docking results

The developed QSAR model is statistically robust in predicting the binding affinity of ligands against the target protein ACE-I. However, the ACE-I binding site is composed of the subsites S2', S1', S1, and S2 (Figure 10). Conventional ACE

inhibitors bind to the catalytic region of the active sites of nACE and cACE *via* chelation with the central  $Zn^{2+}$ , while the groups P2', P1', P1, and P2, mimicking substrate peptides, are placed inside these subsites (Caballero, 2020). To unfold correlations between structural features of developed QSAR models and site-specific ligand binding interactions, we have dock cACE specific inhibitor (RXP380), nACE specific inhibitor (RXP407), and the dataset molecules 120 (most active), 104 (moderately active), 225 (least active) into the active binding pocket of both the domains of ACE-I (cACE, PDB ID: 1O86 and nACE, PDB ID: 3NXQ) in this study (Figure 10 and Table 3). The resulting docking pose that has metal-acceptor interaction and H-bonding with His353 and/or His513 (cACE) or H-bonding with H331 and/or H491 (nACE) are selected for assessments.

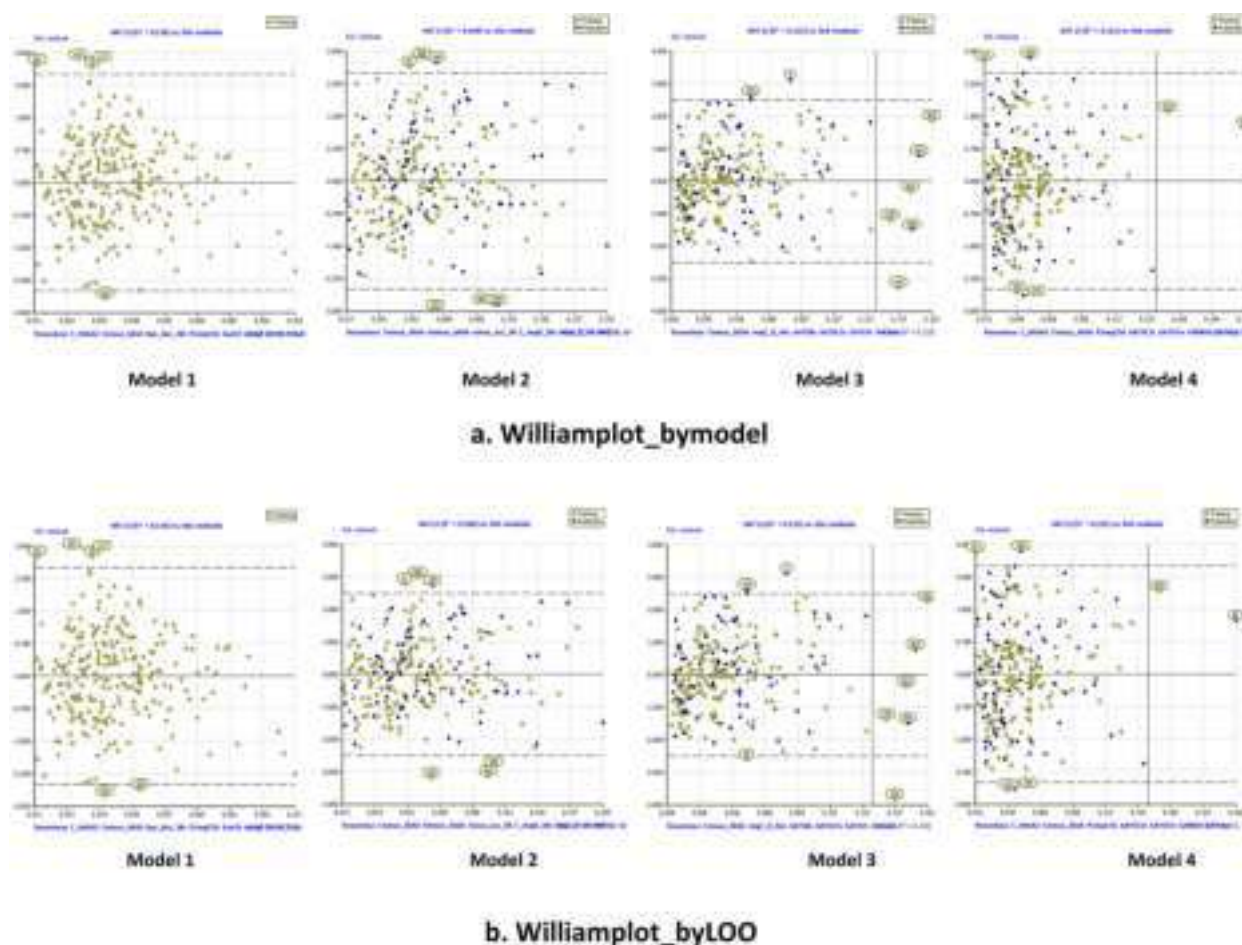


Figure 4. Williams plot. Hat diagonal values versus standardized residuals (a) by developed QSAR models (b) by LOO method.

## 4. Discussions

### 4.1. QSAR results evaluation

It can be observed that model 4 is statistically better than all other models based on fitting criterion ( $R^2_{tr}$ ,  $RMSE_{tr}$ ,  $CCC_{tr}$ , and  $F$  values) and internal validation criterion ( $Q^2_{LOO}$ ,  $RMSE_{cv}$ ,  $CCC_{cv}$ ,  $Q^2_{LMO}$ ). However, model 2 is more predictive of the external validation criterion ( $RMSE_{ex}$ ,  $Q^2-F^1$ ,  $Q^2-F^2$ ,  $Q^2-F^3$ ,  $r^2_m$  average).

The contribution of each descriptor for inhibitory activity is expressed by the values of standardized coefficients. For instance, in Model 2, the descriptor 'MATS3c' has the maximum positive coefficient value of 11.514 for ACE-I inhibition. The meaning of each descriptor that is selected in the developed QSAR model is summarized in Table 4.

#### 4.1.1 Elucidation of descriptors

The challenges that come across during QSAR analysis are the interpretation and relationship of structural features with selected descriptors. Hence, in the current work, effectively interpretable descriptors that are straightforwardly connected with the presence or absence of structural attributes were considered. Further, molecular docking studies predict the predominant binding modes of structural scaffolds with target enzymes. This could be highly beneficial to the design

and synthesis of a new chemical moiety having the potential to inhibit the ACE-I enzyme.

Among the selected descriptors, many typical QSAR parameters, such as PyDescriptors (Cminus\_AbSA, fCringC5A, lipo\_don\_3Bc, minus\_acc\_3B, ringC\_N\_4Ac, ringC\_S\_5B, Sminus\_SASA, ringC\_S\_5B, Sminus\_SASA) and Padel descriptors which include ALogP, autocorrelation (AATS8s, AATSC3c, AATSC7i, GATS7e, GATS7m, GATS7s, GATS8p, MATS3c) and atom-type electrotopological state (SaaCH, SHCsats) contribute significantly in angiotensin-converting enzyme inhibition activity.

The properties of atoms including relative positions and their properties calculated in terms of the number of bonds or Euclidean distance through PyDescriptors. The quantum chemical descriptors C\_ringN\_2Bc and ringC\_N\_4Ac show a positive contribution to angiotensin-converting enzyme inhibition. These descriptors point out that an increase in partial charges of carbon atoms present within 2 bonds from ring Nitrogen atoms or partial charges on ring carbon atoms within a distance of 4 Å to nitrogen favor the ACE-I inhibitory activity as found in compounds 120 (pIC50: 9.75) and 147 (pIC50: 9.45) with a higher numerical value of these descriptors (Figure 7). In contrast, compounds like 33 (pIC50: 3.823) and 96 (pIC50: 3.823) have no such charges and show lower inhibitory activity (Figure 7a). The 3rd quantum chemical descriptor lipo\_don\_3BC represents the sum of partial charges of lipophilic atoms presents within 3 bonds from donor atoms like -NH or -OH. It shows a negative correlation

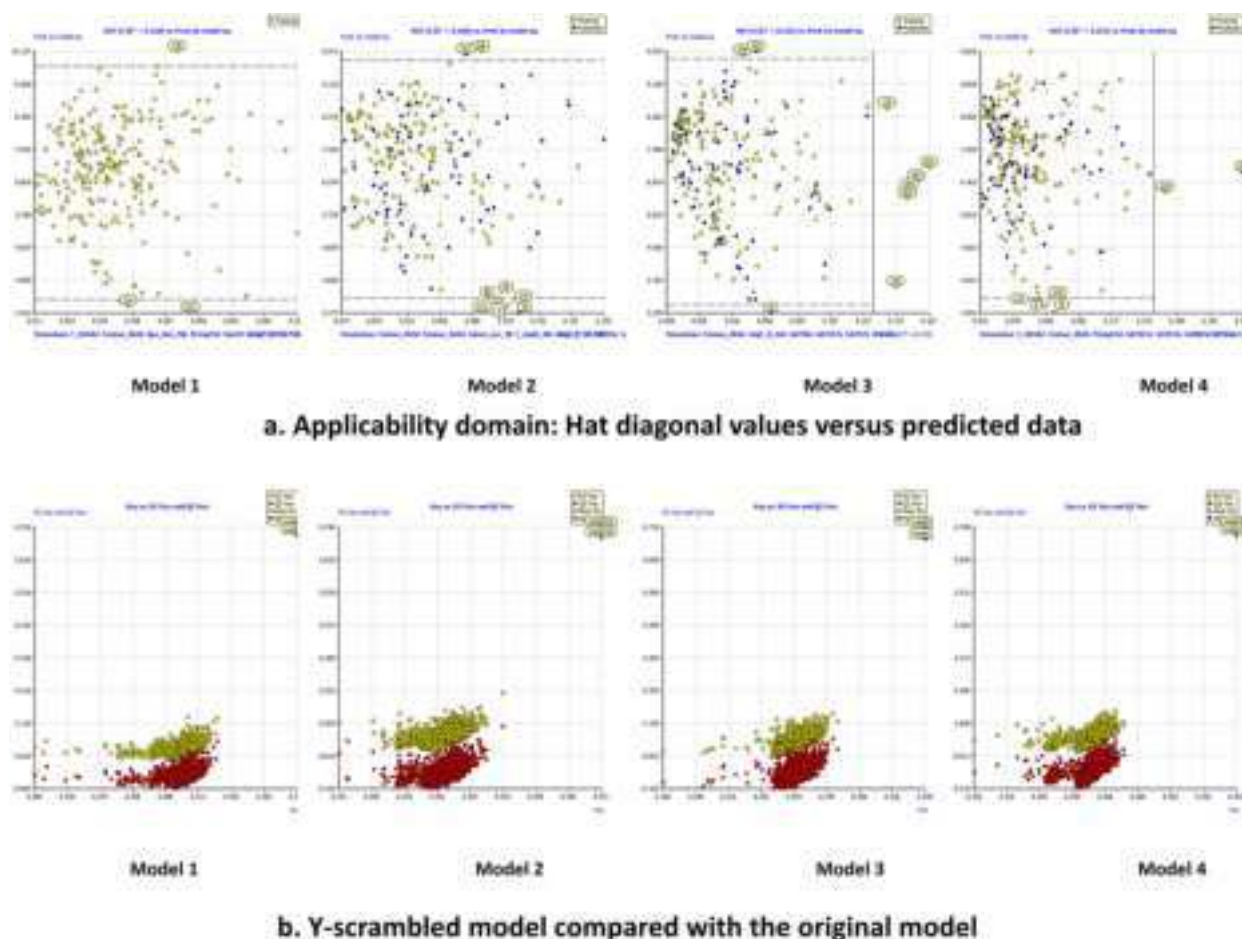


Figure 5. Statistical criterion of the model (a) Applicability domain: Hat diagonal values versus predicted data (b) Y-scrambled evaluation.

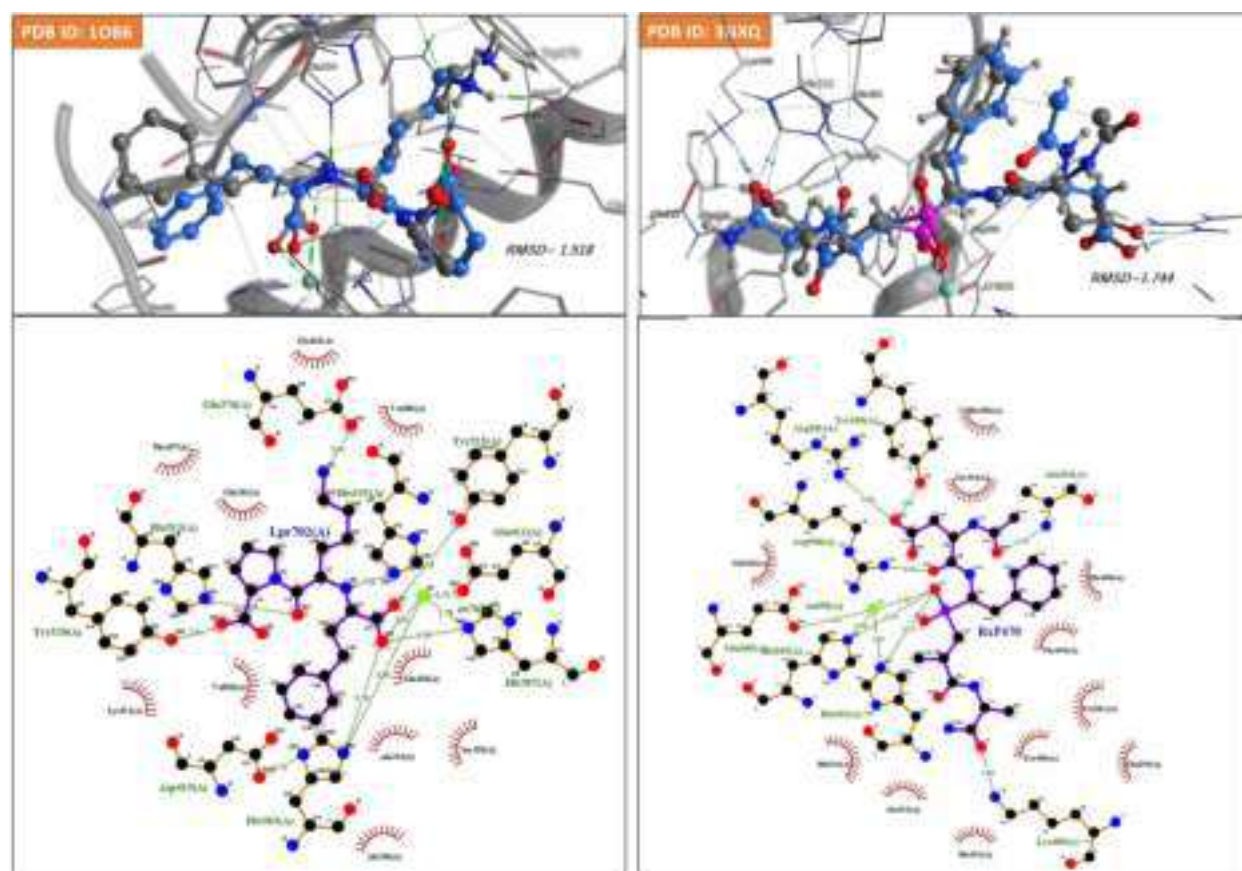


Figure 6. Validation of docking protocol by re-docking the native ligands (Lisinopril and RXPA407) at active binding site and interacting amino acid residues.

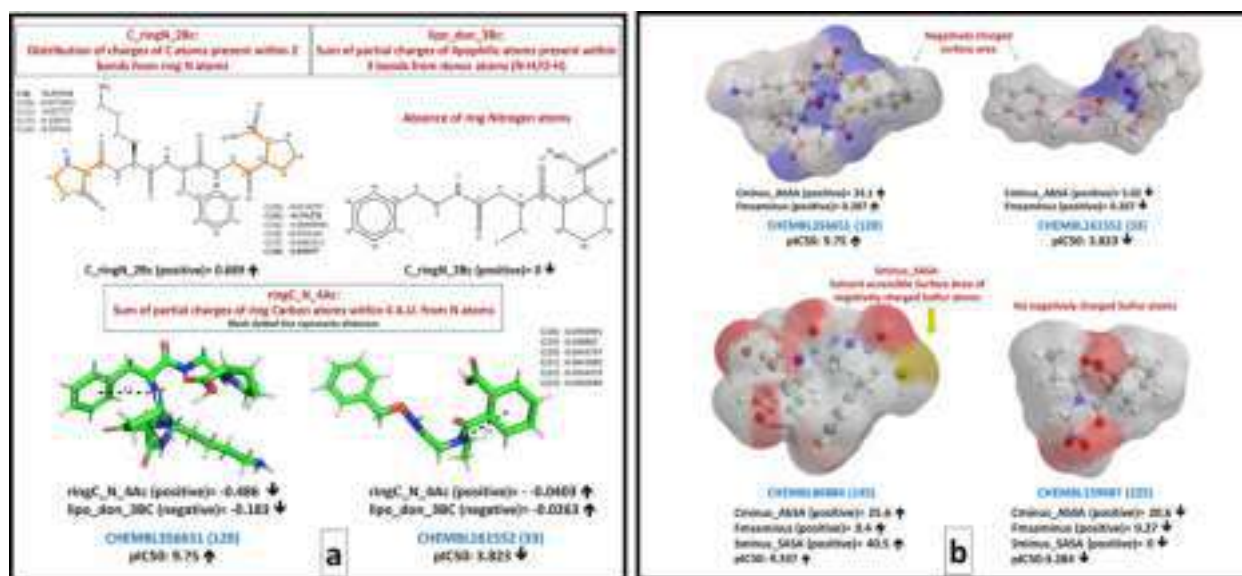
**Table 3.** Molecular docking results of selected dataset against cACE (PDB ID:1O86) and nACE (PDB ID:3NXQ).

Co. No.	pIC50	nACE (PDB ID: 3NXQ)				cACE (PDB ID: 1O86)			
		Arg 381	Tyr369	Binding energy	RMSD	Glu 403	Phe 391	Binding energy	RMSD
RXPA380	Ki = 3.0 nM	5.83 (C-38)	5.64 (C-38)	-6.549	1.77	3.43 (O-6, H-bond)	3.27 (C-43)	-8.753	1.42
RXP407	Ki = 7.0 nM	2.09 (O-10, H-bond)	2.81 (O-10, H-bond)	-9.887	1.83	5.16 (C-34)	3.87 (C-34)	-6.754	1.93
120	9.75	3.88(C-40)	3.25(C-39)	-7.313	2.53	2.44 (O-40, H-bond)	3.33 (O-39)	-9.155	1.56
104	7.137	9.25 (O-3)	7.34 (O-1)	-4.768	1.36	4.15 (C-17)	4.38 (C-18)	-7.036	1.2
225	3.284	7.09 (C-1)	5.96 (O-8)	-3.536	1.3	8.66 (O-8)	8.53 (O-8)	-5.914	1.87

\*Each bounding pose is evaluated by measuring the distance between the ligand atoms indicated in brackets and N atom from Arg381, O atom from Tyr369 in the nACE with the distance between the nearest C atom from Phe391 and O atom of Glu403 in the cACE.

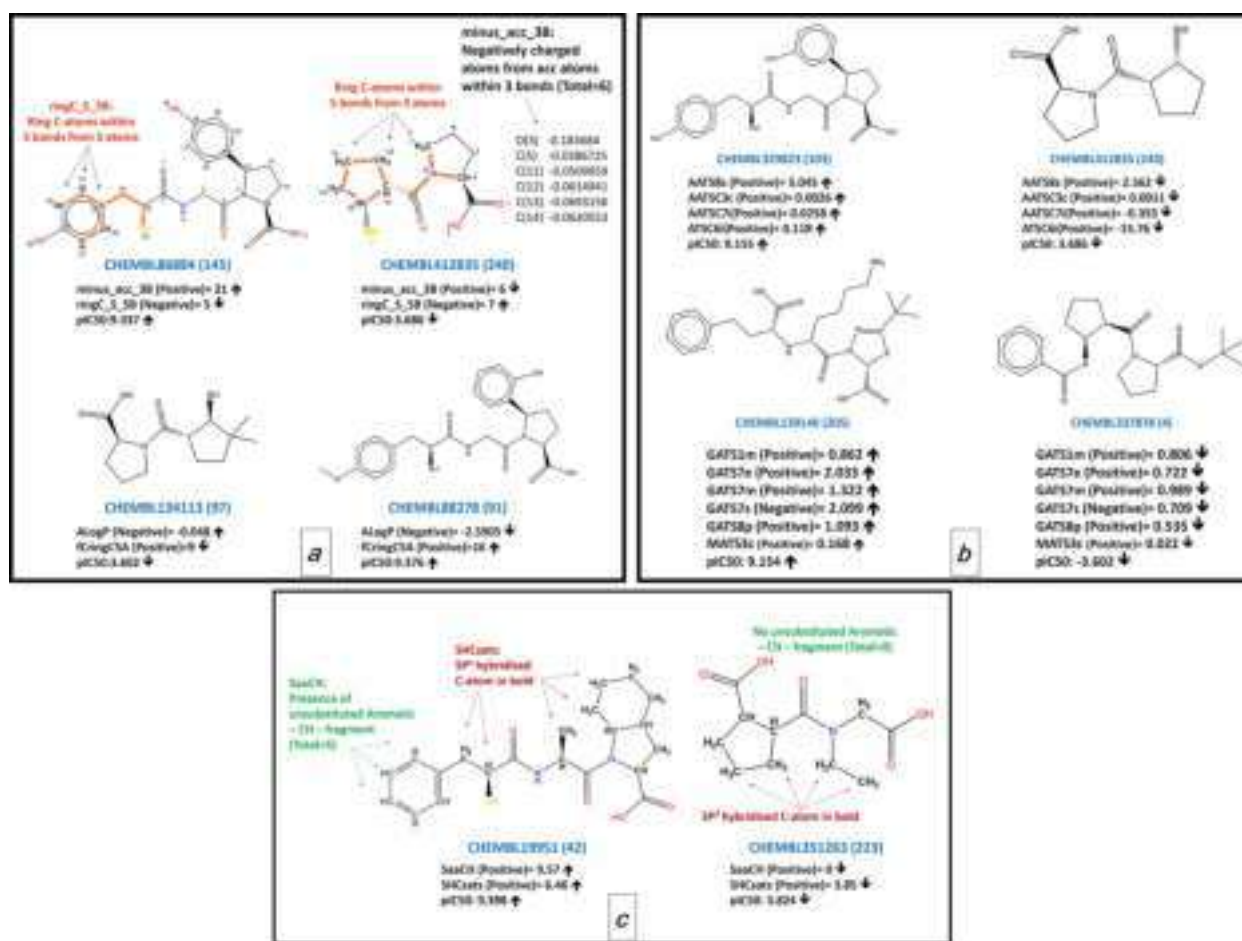
**Table 4.** Symbols and definitions for the descriptors selected in QSAR models.

Name	Brief description	Descriptor type
Cminus_AbSA	Absolute Surface Area of negatively charged carbon atoms	Geometric
fmsaminus	Frequency of occurrence of negatively charged molecular surface area	Geometric
fCringC5A	Frequency of occurrence of ring Carbon atoms exactly at 5 Angstrom from Carbon atoms	Circular fingerprint
minus_acc_3B	Number of negatively charged atoms from acc atoms within 3 bonds	Topological
ringC_5_5B	Number of ring Carbon atoms within 5 bonds from 5 atoms	Topological
C_HASA2	Solvent Accessible Surface Area of Carbon atoms having partial charge in the range 0.10 to 0.20	Geometric
Sminus_SASA	Solvent accessible Surface Area of negatively charged Sulfur atoms	Geometric
C_ringN_2Bc	Sum of partial charges of Carbon atoms present within 2 bonds from ring Nitrogen atoms	Quantum chemical
lipo_don_3Bc	Sum of partial charges of lipophilic atoms present within 3 bonds from donor atoms	Quantum chemical
ringC_N_4Ac	Sum of partial charges of ring Carbon atoms within 4 A.U. from N atoms	Quantum chemical
ALOGP	Ghose-Crippen LogKow	ALOGP (Lipophilicity)
AATS8s	Average Broto-Moreau autocorrelation - lag 8 / weighted by I-state	Topological Autocorrelation
AATSC3c	Average centered Broto-Moreau autocorrelation - lag 3 / weighted by charges	Topological Autocorrelation
AATSC7i	Average centered Broto-Moreau autocorrelation - lag 7 / weighted by first ionization potential	Topological Autocorrelation
GATS7e	Geary autocorrelation - lag 7 / weighted by Sanderson electronegativities	Topological Autocorrelation
GATS7m	Geary autocorrelation - lag 7 / weighted by mass	Topological Autocorrelation
GATS7s	Geary autocorrelation - lag 7 / weighted by I-state	Topological Autocorrelation
GATS8p	Geary autocorrelation - lag 8 / weighted by polarizabilities	Topological Autocorrelation
MATS3c	Moran autocorrelation - lag 3 / weighted by charges	Topological Autocorrelation
SaaCH	Sum of atom-type E-State: :CH:	Atom type electrotopological state
SHCsats	Sum of atom-type H E-State: H on C sp3 bonded to saturated C	Atom type electrotopological state

**Figure 7.** Impact of (a) quantum chemical descriptors (C<sub>ringN\_2Bc</sub> and ringC<sub>N\_4Ac</sub> and lipo<sub>don\_3Bc</sub>) on ACE-I enzyme (b) geometric descriptors (Cminus<sub>AbSA</sub>, fmsaminus, and Sminus<sub>SASA</sub>) on ACE-I enzyme inhibitory activity.

with activity as shown in model-1 and reflects from descriptor values  $-0.0263$  (for compound 33) and  $-0.183$  (for compound 120) that the higher the score lower the potency of a compound.

The descriptors Cminus<sub>AbSA</sub> (Absolute SA of negatively charged C-atoms), fmsaminus (Frequency of occurrence of negatively charged SA), and Sminus<sub>SASA</sub> (Solvent accessible SA of negatively charged S-atoms) are geometric



**Figure 8.** Impact of (a) Topological (minus\_acc\_3B, ringC\_S\_5B), Circular fingerprint (fCringC5A), and ALogP (b) 2D Autocorrelation descriptors (ATS, GATS, and MATS) (c) 2D atom type electro-topological state descriptors (SaaCH and SHCsats) on ACE-I enzyme inhibitory activity.

PyDescriptors contributing positively to the response (Figure 7b). So, the greater occurrence of these features correlates to higher ACE-I enzyme inhibitory activity as observed in compounds numbers 145 (pIC50: 9.337), and 103 (pIC50: 9.155), while the absence of this feature correlates to lower potency of ACE-I enzyme inhibitory activity as observed in compounds 33 (pIC50: 3.824) and 225 (pIC50: 3.284).

Topological descriptors, minus\_acc\_3B defining the number of negatively charged atoms from acceptors atoms within 3 bonds, positively influences ACE-I inhibitory activity in model-2. Whereas, another descriptor ringC\_S\_5B defines the number of ring carbon atoms within 5 bonds from S atoms that negatively influence activity. This is witnessed by compounds 145 (pIC50: 9.337) and 240 (pIC50: 3.686) where the positive contribution of minus\_acc\_3B descriptor and the opposite is seen in compounds 4 (pIC50: 3.602) and 41 (pIC50: 9.585) (negative contribution of ringC\_S\_5B descriptor) as depicted in Figure 8a.

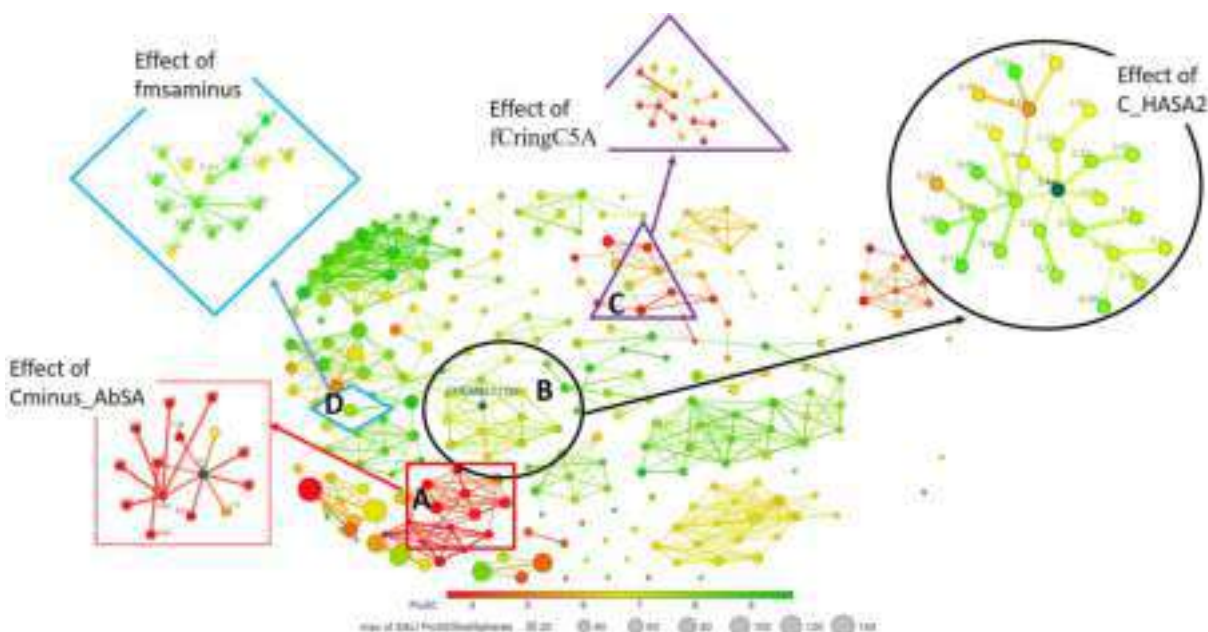
The descriptors fCringC5A is a circular fingerprint that represents the frequency occurrence of ring Carbon atoms exactly at 5 Å from Carbon atoms. The 2D descriptors ALogP shows a negative coefficient in developed QSAR model 1 based on an undivided dataset. It indicates that the hydrophobic carbon chain plays an important role in the control of angiotensin-converting enzyme inhibition. AlogP is defined as Ghose-Crippen LogKo/w, which interprets that the

number of heteroatoms present is indirectly proportional to the hydrophobicity of the molecules (Ghose et al., 1998). As the descriptors contribute negatively to the inhibitory activity against the ACE-I enzyme. So, the compounds 97 (pIC50: 3.602) and 251 (pIC50: 3.668) with high lipophilicity or showing higher descriptors values showed ACE-I enzyme inhibitory activity in a lower range. Conversely, compound 91 (pIC50: 9.376) showed higher range ACE-I enzyme inhibitory activity due to the absence of lipophilicity (Low descriptor value).

All the developed QSAR models contained 2D Autocorrelation descriptors of Broto-Moreau (ATS), Geary (GATS), and Moran (MATS; Hollas, 2003), which defines the distribution of physicochemical properties along the topological surfaces of the molecules as a positive coefficient (except GATS7s in model-5), hence, its value must be kept as high as possible. All 2D autocorrelation descriptor contributes positively to the ACE-I inhibitory activity as specified by the positive regression coefficient. Thus, the molecules bearing such fragments may have enhanced ACE-I inhibitory activity as presented in compounds 103 (pIC50: 9.155) and 205 (pIC50: 9.154). Although the compounds containing no such features have lower inhibitory activity as shown in compounds 240 (pIC50: 3.686) and 4 (pIC50: -3.602) (Figure 8b).

The models also contained positively correlated 2D atom type electro-topological state descriptors SaaCH (indicates





**Figure 9.** Activity cliff and SAR study. Molecules are clustered by chemical similarity considering SkelSpheres. The colors of the markers signify the pIC<sub>50</sub> value, where red color indicates the lowest and Green color indicates the highest pIC<sub>50</sub>.

the presence of un-substituted aromatic—CH—fragment; Edraki et al., 2016) and SHCsats (the hydrogen E-states sum on the sp<sup>3</sup> hybridized carbon atom of the saturated bond). SHCsats reflect weak interactions with non-polar sites in the biomolecular targets (Przybyłek, 2020). The positive contribution of these descriptors suggests that the numerical value of descriptors is directly related to the ACE-I inhibitory activity. The impact of these electro-topological state descriptors is depicted in compound 42 (pIC<sub>50</sub>: 9.398) (Enzyme inhibitory activity increases with the corresponding rise in numerical descriptor values), whereas the inverse phenomena have been observed in compound 223 (pIC<sub>50</sub>: 3.824) (Enzyme inhibitory activity decreases on lowering corresponding numerical descriptor value) in Figure 8c.

#### 4.1.2. Activity cliff analysis

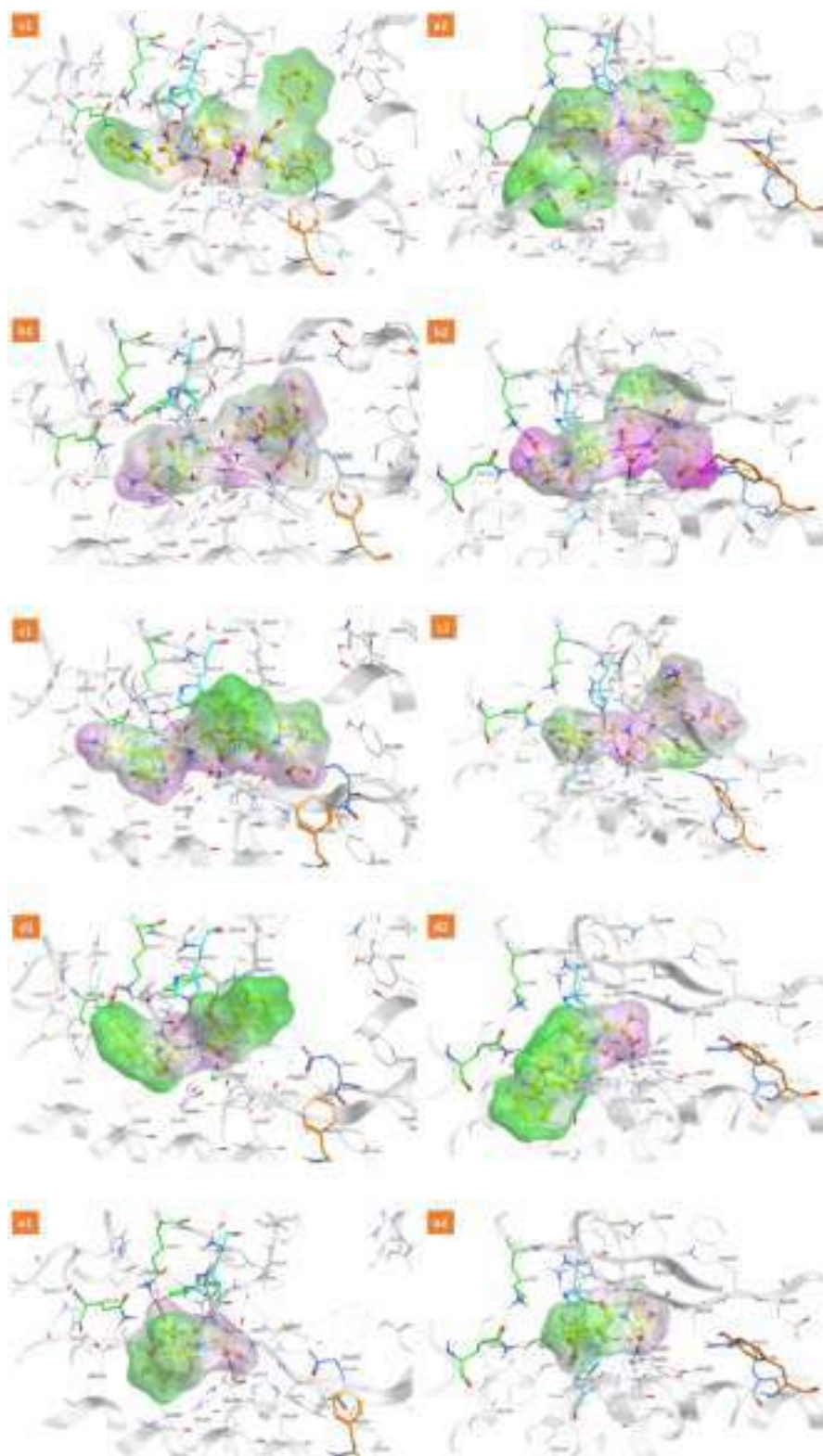
In descriptive SAR study, activity cliff analysis helps in the determination of specific and minor structural changes that influence biological activity. This relationship between structural features and biological activity can be visualized by calculating the structure-activity landscape index (SALI) using DataWarrior (Blay et al., 2021; Kumar et al., 2021). The SALI plot of selected dataset compounds represents the relative position in 2D space comparing biological activity with structural features (Figure 9). Similar compounds are connected with a line and the markers are colored by ACE-I inhibitory activity (pIC<sub>50</sub>) of the compounds from green (active, ≥ 7) to red (inactive, ≤ 5). In the landscape, connected with lines building green colored clusters represents similar compounds with analogous ACE-I inhibitory activity. It helps rationalize structural modification for the betterment of pharmacokinetic parameters with strengthened biological activity (Egieyeh et al., 2016). In Figure 9 encircled cluster 'B', contains green markers (active) connected to yellow

(intermediately active) and red (inactive). These compounds are structurally similar but have varied biological activity signifies characteristic activity cliffs (Stumpfe et al., 2019). Similar observations are also indicated by clusters A, C, and D. Such clusters are helpful in the identification of structural differences between a pair of compounds with varied bio-activity (Victoria-Muñoz et al., 2022).

#### 4.2. Molecular docking analysis

RXPA380 is a c-domain-specific inhibitor with 3000 folds lower K<sub>i</sub> (3.0 nM) compared to the n-domain of ACE-I. c-domain specificity of RXPA380 (binding energy, −8.753) is attributed because of the hydrophobic interaction with residue Phe391 (subsite S1) and H-bonding of residue Glu403 (subsite S2) with group P2 (benzyl ring). Further, the P1' and P2' groups of RXPA380 enhanced stability by forming π-alkyl and π-ionic interactions with residue His513 (subsite S1') and Lys511 (subsite S2') respectively. In disparity, equivalent residues Arg381 (subsite S2) and Tyr369 (subsite S1) in nACE fail to form these important interactions (binding energy, −6.549). RXP407 is an n-domain specific inhibitor with 2500 folds lower K<sub>i</sub> (7.0 nM) compared to the c-domain of ACE-I. Formation of salt bridge interaction with residue Arg381 (subsite S2) and conventional H-bonding with residue Tyr369 (subsite S1) contributes to n-domain selectivity (binding energy, −9.887). These polar interactions lose their specificity in cACE due to the replacement of Tyr369 by Phe391. The resulting interactions of RXPA380 and RXP407 are in agreement with previously reported work, which means that the docking protocol is agreeable (Cozier et al., 2018; Fienberg et al., 2018).

In the cACE domain, the most active compound (120) from the dataset (pIC<sub>50</sub> = 9.747) is accompanied by a



**Figure 10.** Schematic representation of 3D docked pose of compounds (a1) RXP380-cACE (a2) RXP380-nACE (b1) RXP407-cACE (b2) RXP407-nACE (c1) 120-cACE (c2) 120-nACE (d1) 104-cACE (d2) 104-nACE (e1) 225-cACE and (e2) 225-nACE bind to the catalytic region of the active sites via a chelation interaction with the zinc atom. The poses are overlaid with molecular surfaces according to lipophilicity (green-lipophilic, white-neutral, and magenta-hydrophilic regions).

docking score of  $-9.155$  with RMSD 1.56 by forming eight hydrogen bonds (conventional and carbon-hydrogen bonds) with Glu403, His513, Glu162, Gln369, Glu411, His387, Glu376, and Asp377 similarly to that of RXP380. In the nACE domain, with a docking score of  $-7.313$  and RMSD 2.53, compound (120) forms nine hydrogen bonds (conventional

and carbon-hydrogen bonds) with Trp335, Ser333, His361, Asp43, Thr496, Gln259, Ala332, Glu362, and His491 analogous to RXP407 (Figure 10). Chemically, compound 120 (ChEMBL356651) is ((R)-3-oxopyrrolidine-2-carbonyl)-L-lysyl-L-phenylalanyl-glycyl-D-proline. The terminal carboxyl group of proline is anchored with conventional H-bonding interaction

with residue Glu403 (cACE) and Gln259 (nACE). Equally, the carboxyl group of lysyl structure hydrogen bonds with the positively charged residues His353/His513 (cACE) and Ala332(nACE), while the carboxyl group of phenylalanyl forms ionic interactions with Zn metal (both domains) necessary for reliable conformation of ligand pose. The identical observation is indicated by using the descriptors Cminus\_AbSA and fmsaminus, highlighting the significance of the negatively charged surface area. Further, descriptor minus\_acc\_3B signifies the presence of the total number of negatively charged atoms (O-17 and O-28) from acceptor atoms (–NH) within 3 bonds in the ligand molecule accompanying the above interactions. This rationalizes that, the QSAR model showed a factual correlation with the docking results. Subsequently, the descriptor SaaCH indicates the presence of an unsubstituted aromatic—CH—fragment which facilitates the appropriate binding and alignment of a molecule into the active pockets. The aromatic ring of the phenylalanyl group forms alkyl and pi-alkyl interaction with hydrophobic residue Val518 and Ser355 at the S2 subsite (cACE). However, docking poses of RXP407 and compound 120 in the nACE domain do not show these interactions. Moreover, autocorrelation descriptors MATS3c (Secondary amine) and GATS7s (phenyl/alkyl attached carbamate derivative) are responsible for binding to target proteins. So, the high value of descriptors MATS3c, GATS7s, and SaaCH and docking analysis show the importance of hydrophobicity in ligands for c-domain specificity compared to the n-domain. This exhibits that, QSAR analysis correctly identified imperative structural characteristics decisive for ACE-I inhibition. Compounds 104 (ChEMBL71746) and 225 (ChEMBL159987) are small molecular sizes that don't have such kind of combination in large active pockets which may additionally drop the binding affinity against both domain cACE and nACE.

The resemblance in features obtained from QSAR modeling and molecular docking are in agreement and important for predicting ACE-I inhibitory activity. Consequently, the developed QSAR models can be considered to be able to predict the angiotensin-converting enzyme inhibitory activity of diverse structures with supremacy in comparison to the previously reported models (Gonzalez Amaya et al., 2020).

#### 4.3. AD, molecular docking, and ADMET analysis of designed compounds

The applicability domain screening of 102 novel thiadiazole derivatives simplified the identification of 65 probable leads with the potential to inhibit ACE-I (Figure 11). The predicted  $pIC_{50}$  values are based on rigorous validation with exhibited HAT  $i/i$  ( $h^* = 0.1676$ ) or less. The structure molecular docking score and predictive activity of the recognized compounds have been shown in Table 5.

Further ADMET analysis shows that a total of 21 designed compounds with better-predicted activity follow drug-likeness parameters with no violations for Lipinski, Ghose, Veber, Egan, and Muegge filters. Moreover, all 21 designed compounds pass the pan assay interference compound (PAINS) test. Additionally, it is predicted that designed compounds D1 to

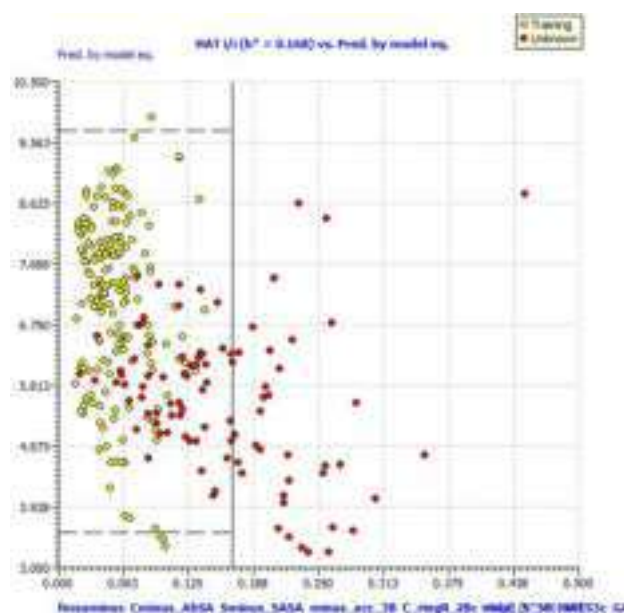


Figure 11. Applicability domain analysis of novel designed compounds using winner model-2.

D5, D9 to D11, and D16 do not show AMES toxicity, hepatotoxicity, or skin sensitivity, and does not inhibit hERG-I and II (low risk of cardiac toxicity). Designed compound D24 (cACE,  $-6.257$  kcal/mol) and D40 (cACE,  $-6.697$  kcal/mol) shows comparatively better docking score and selectivity for cACE over the nACE domain than other designed derivatives. However, both of these molecules predicted that they do not show potential to inhibit hERG-I only but may have a certain affinity for hERG-II protein (Supplementary information S5).

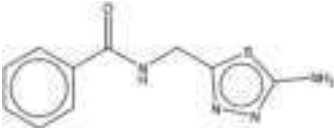
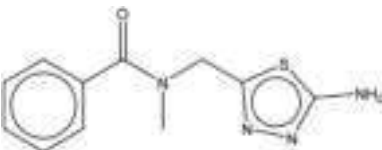
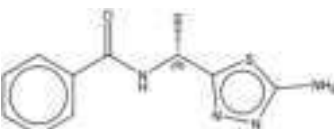
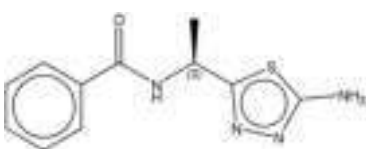
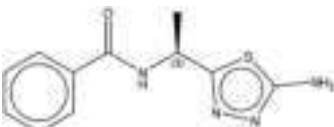
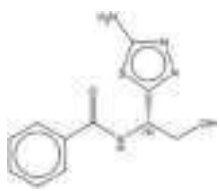
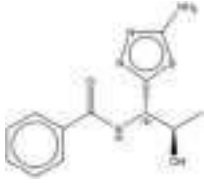
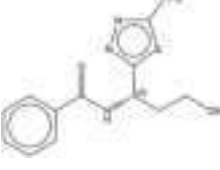
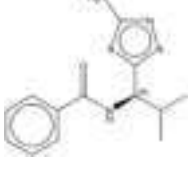
#### 4.4. Molecular dynamic simulation studies

Molecular Dynamics simulation studies were carried out to understand the stability of protein–ligand interaction. As discussed earlier, the two best ligands having the highest docking score were selected for MD simulation studies.

RXPA380 was considered the standard inhibitor with the c-domain-specificity inhibitor. Backbone root mean square deviation (RMSD) analysis was carried out to evaluate the stability of RXPA380 into the binding pocket of cACE (PDB ID: 1O80) protein. When the root mean square deviation (RMSD) data were compared, each simulation including 100 ns revealed stable conformation. It was observed that RXPA380 formed H-bond with various amino acid residues such as Tyr62, Asn66, Glu143, His353, Ser355, Tyr360, His513, Ser516 and Ser517 whereas hydrophobic bond interaction with Trp59, Arg124, Ala354, Trp357, Val380, His383, His387, Phe391, His410, Phe457, Lys511, Val518, Arg522, and Tyr523. The RMSD and RMSF plot of protein–ligand and the ligand–protein contacts for RXPA380 are shown in Figure 12 and Figure 13 respectively.

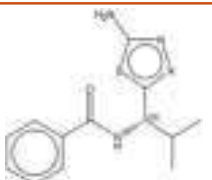
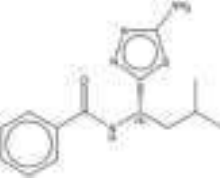
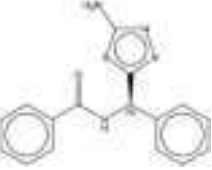
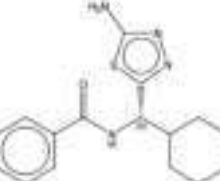
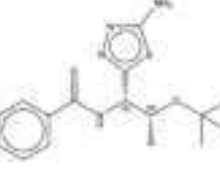
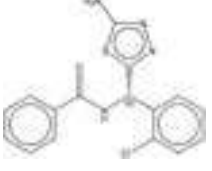
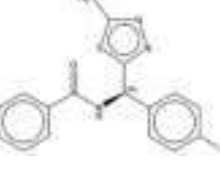
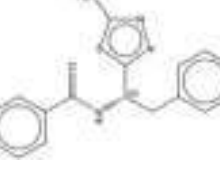
Similarly, the interactions of D24 at different time intervals were analyzed and checked for stability which showed that the proteins got stabilized and the ligand was forming interaction with the protein (RMSD difference  $\leq 2.5$  Å). D24 was

**Table 5.** Molecular docking score and predictive activity.

Designed Compounds ID	Structures	Constraint Docking (MOE)		
		cACE Score	nACE Score	pIC50 value (Pred. by model eq.)
D1		-5.04076	-4.12513	7.2996
D2		-4.98171	-4.24858	7.2996
D3		-5.05719	-4.12859	6.1324
D4		-5.73965	-5.75091	5.975
D5		-5.63515	-5.73591	6.0084
D6		-5.2706	-5.51041	7.5089
D8		-5.1148	-5.21678	6.6008
D9		-4.83491	-3.48704	5.9597
D10		-5.78887	NA	6.0491

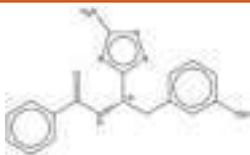
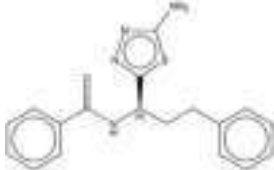
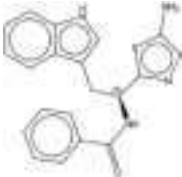
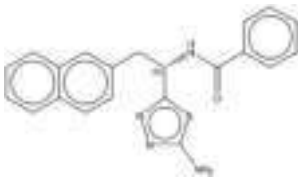
(continued)

Table 5. Continued.

Designed Compounds ID	Structures	Constraint Docking (MOE)		
		cACE Score	nACE Score	pIC50 value (Pred. by model eq.)
D11		-5.51545	-1.43169	5.9849
D16		-5.5154	-1.44846	5.8639
D23		-5.85387	-2.28013	7.3894
D24		-6.25657	-1.09322	6.0035
D32		-6.25957	-4.18712	4.967
D40		-6.69737	-3.14666	6.1763
D41		-6.55797	NA	6.4006
D42		-6.50319	-2.43959	4.6983

(continued)

Table 5. Continued.

Designed Compounds ID	Structures	Constraint Docking (MOE)		
		cACE Score	nACE Score	pIC50 value (Pred. by model eq.)
D43		-5.83596	-2.60598	5.4627
D44		-6.0223	-0.08135	5.3869
D56		-6.26933	-1.09785	5.1441
D65		-6.58994	-4.53265	5.3906

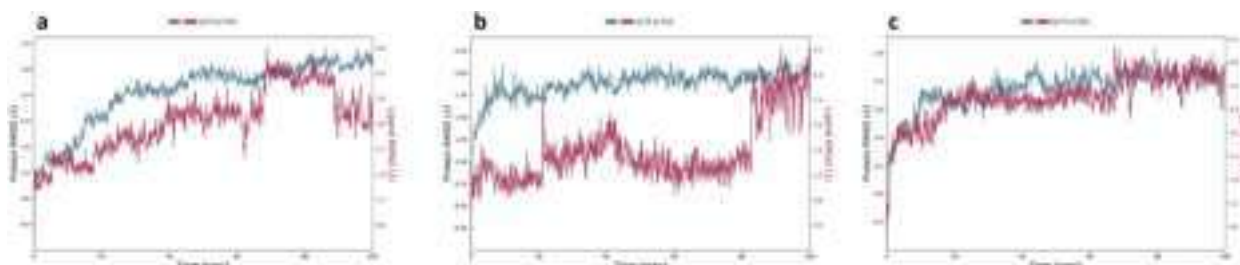


Figure 12. RMSD of the protein backbone along the simulation trajectory for the protein and ligand docked complexes. The overall structure of cACE did not change much after the binding of (a) RXPA380 (b) D24 and (c) D40.

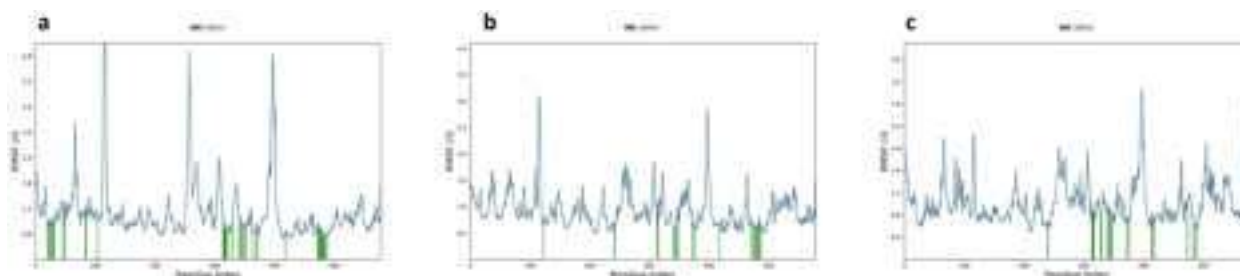
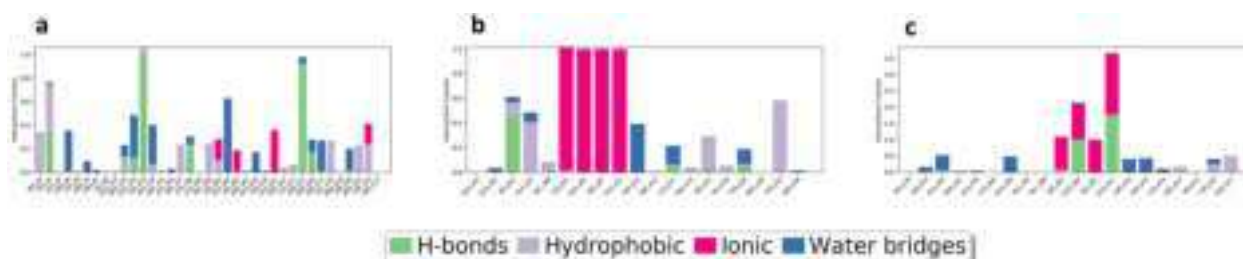


Figure 13. RMSF of the amino acids comprising the cACE. No abrupt fluctuations were observed in any region of the protein with the three ligands (a) RXPA380 (b) D24 and (c) D40.

forming H-bond interactions with Gln281, His353, Lys511, His513, Tyr520 and Tyr523 while hydrophobic interactions with His353, Ala354, Val380, His383, Phe457, Lys511, Phe512, His513, Val518 and Tyr523. The RMSD of D24 is shown in Figure 12.

On the other hand, D40 was showing stable interactions throughout the simulation period (100 ns) which indicates the stability of the ligand in the binding site pocket of the protein (RMSD Difference = 2.8 Å). D40 was interacted with amino acid such as His353, Ala354, Ser355, Ala356, Gln369, His383,



**Figure 14.** Hydrogen bond occupancy of various important residues of the cACE during the simulation run in case of binding with (a) RXPA380 (b) D24 and (c) D40.

Glu384, His387, Glu411, Phe457, Tyr523 and Phe527 residues by forming Ionic, H-bond and hydrophobic interactions. The RMSF plot for D40 is shown in Figure 13.

All three molecule complexes generated various interactions such as hydrogen bonds, hydrophobic contacts, ionic interactions, and water bridges with distinct substrates in the binding sites. Although hydrophobic and hydrogen bonds, are weaker compared to ionic bonds, they are too exploited most for the design of new drug candidates (Bhardwaj et al., 2021; Yunta, 2017). Therefore, interactions pattern generated with the surrounding amino acids in the cACE domain by RXPA380 were found to be used to predict the binding features of the novel compounds over the entire 100 ns simulation trajectory.

MD simulations trajectories revealed that D24 (Figure 14b) was making more ionic bonds in comparison to D40 (Figure 14c) and RXPA380 (Figure 14a) over the entire simulation trajectory. Tyr62, Glu143, His353, Tyr360, His513, Ser516, and Ser517 are all conserved amino acid residues that play key roles in docked chemical identification *via* H-bonding interaction. Correspondingly, compound RXPA380 shows the formation of weak hydrophobic interaction with Phe391 and water bridge interaction with Glu403 suggesting its cACE domain-specific inhibitor. Furthermore, stability is provided by ionic interaction made by His383, His387, Glu411, and Tyr523 amino acid residues. Design compounds D24 and D40 were found to form significant key interactions similar to RXPA380 towards the substrate binding pocket of cACE and could probably be the novel lead molecules for the inhibition of the cACE enzyme.

Thus, MD simulation trajectories are well supported with the binding potential scores calculated from the constraint-based docking results. Therefore, it can be suggested that the compound D24 and D40 has good affinity for the cACE domain of the enzyme. Also, both the compounds, D24 and D40 show drug-likeness properties as they follow Lipinski, Ghose, Veber, Egan, and Muegge's rule. Furthermore, both compounds do not have AMES toxicity, skin sensitivity, or minnow toxicity and are not a good substrate for hERG I which suggests compounds are safe to use. Thus, they could be considered for further synthesis and subsequent screening as novel therapeutics for cACE inhibition and in the management of hypertension.

## 5. Conclusion

The GA-MLR-based approach was utilized to establish validated QSAR models obeying OECD principles to envisage the

inhibitory activities of 255 compounds against the angiotensin-converting-enzyme-I of *Rattus norvegicus*. The development of multiple QSAR models helped in identifying less dominant, but very useful descriptors, which have a significant correlation with the activity. The obtained results demonstrated PyDescriptors (Geometric, circular fingerprint, topological and quantum chemical) and Padel descriptors (2D Autocorrelation and atom type electrotopological state) are the most significant descriptors with an inverse correlation between ALogP value and ringC\_S\_5B descriptors compared to all other calculated descriptors against the inhibitory activity. Molecular docking reveals a binding pattern between the c-domain of the ACE-I enzyme and ligands. Amongst all designed thiadiazole derivatives, 21 compounds show anticipated inhibitory activity and follow drug-likeness parameters. Further results from Molecular dynamics studies demonstrated that ligands D24 and D40 were tightly bound to the binding site of the receptor with low RMSD values observed during the 100 ns simulation does not significantly vary during the progression of the simulation. Consequently, Molecular dynamics analysis strengthens the outcome of the QSAR and docking studies. In conclusion, the validated QSAR models and *in silico* analysis could be used to design new molecules against ACE-I inhibitory activity.

## Acknowledgment

The authors are thankful to Mr. M. I. Bashir, University Sains, Malaysia for providing facilities to conduct molecular docking studies.

## Disclosure Statement

The authors have no relevant financial or non-financial interests to disclose.

## Ethics Approval

All authors certify that they have no affiliations with or involvement in any organization or entity with any financial interest or non-financial interest in the subject matter or materials discussed in this manuscript.

## Consent for Publication

All authors agree to publish the article.

## Funding

The authors acknowledge the Deanship of Scientific Research at Imam Mohammad Ibn Saud Islamic University, Riyadh, Saudi Arabia, for its support of this research work.

## ORCID

Sapan Shah  <http://orcid.org/0000-0002-8155-9361>  
 Vijay H. Masand  <http://orcid.org/0000-0001-9300-4147>  
 Magdi E.A Zaki  <http://orcid.org/0000-0002-4305-934X>  
 Ashish Shah  <http://orcid.org/0000-0003-0817-5940>  
 Sumit Arora  <http://orcid.org/0000-0001-9453-6057>  
 Rahul Jawarkar  <http://orcid.org/0000-0003-3563-6642>

## Authors' Contributions

In the present research all authors have contributed and have given cooperation throughout to approve the manuscript. S. K. Shah and D. R. Chaple: Conceptualization, Writing - Original Draft, Formal analysis, Final Drafting, Implementation of methodology and result analysis. V. H. Masand: Review & Editing, Descriptor Calculation, and Data Curation. Magdi E.A. Zaki and Sami A Al-Hussain: Writing, Figures and Tables and Molecular docking. Rahul Jawarkar: Molecular dynamics simulation and Interpretation of results. Ashish Shah, Sumit Arora, and Mohammad Tauqeer: Original Draft, Review of style and content.

## References

- Almutairi, T. M., Rezki, N., Aouad, M. R., Hagar, M., Bakr, B. A., Hamed, M. T., Hassen, M. K., Elwakil, B. H., & Moneer, E. A. (2022). Exploring the antiparasitic activity of tris-1,3,4-thiadiazoles against *Toxoplasma gondii*-infected mice. In *Molecules*, 27(7), 2246. <https://doi.org/10.3390/molecules27072246>
- Arora, S., Lohiya, G., Moharir, K., Shah, S., & Yende, S. (2020). Identification of potential flavonoid inhibitors of the SARS-CoV-2 main protease 6YNQ: A molecular docking study. *Digital Chinese Medicine*, 3(4), 239–248. <https://doi.org/10.1016/j.dcm.2020.12.003>
- Bhardwaj, V. K., Singh, R., Sharma, J., Rajendran, V., Purohit, R., & Kumar, S. (2021). Identification of bioactive molecules from tea plant as SARS-CoV-2 main protease inhibitors. *Journal of Biomolecular Structure and Dynamics*, 39(10), 3449–3458. <https://doi.org/10.1080/07391102.2020.1766572>
- Biovia, D. S. (2016). *Discovery studio modeling environment, release 2017*, San Diego. Dassault Systèmes.
- Blay, V., Dong, J., & Moya, A. (2021). Machine learning study of the molecular drivers of natural product prices. *Biofuels, Bioproducts and Biorefining*, 15(6), 1820–1834. <https://doi.org/10.1002/bbb.2281>
- Caballero, J. (2020). Considerations for docking of selective angiotensin-converting enzyme inhibitors. *Molecules*, 25(2), 295. <https://doi.org/10.3390/molecules25020295>
- Carli, N., Massarelli, I., & Bianucci, A. M. (2014). A new neural network (tiling-contextual neural network for structures, TC-NNfs) enabling the treatment of relatively small datasets of therapeutic interest: An application to a small dataset of ACE inhibitors. *Chemometrics and Intelligent Laboratory Systems*, 137, 1–9. <https://doi.org/10.1016/j.chemolab.2014.06.001>
- Cozier, G. E., Schwager, S. L., Sharma, R. K., Chibale, K., Sturrock, E. D., & Acharya, K. R. (2018). Crystal structures of sampatrilat and sampatrilat-Asp in complex with human ACE – a molecular basis for domain selectivity. *The FEBS Journal*, 285(8), 1477–1490. <https://doi.org/10.1111/febs.14421>
- Edraki, N., Das, U., Hemateenejad, B., Dimmock, J. R., & Miri, R. (2016). Comparative QSAR analysis of 3,5-bis (Arylidene)-4-piperidone derivatives: The development of predictive cytotoxicity models. *Iranian Journal of Pharmaceutical Research : IJPR*, 15(2), 425–437. <https://pubmed.ncbi.nlm.nih.gov/27642313>
- Egijeh, S. A., Syce, J., Malan, S. F., & Christoffels, A. (2016). Prioritization of anti-malarial hits from nature: Chemo-informatic profiling of natural products with in vitro antiparasitic activities and currently registered anti-malarial drugs. *Malaria Journal*, 15(1), 50. <https://doi.org/10.1186/s12936-016-1087-y>
- El-Enany, W. A. M. A., Gomha, S. M., El-Ziaty, A. K., Hussein, W., Abdulla, M. M., Hassan, S. A., Sallam, H. A., & Ali, R. S. (2020). Synthesis and molecular docking of some new bis-thiadiazoles as anti-hypertensive  $\alpha$ -blocking agents. *Synthetic Communications*, 50(1), 85–96. <https://doi.org/10.1080/00397911.2019.1683207>
- Fienberg, S., Cozier, G. E., Acharya, K. R., Chibale, K., & Sturrock, E. D. (2018). The design and development of a potent and selective novel dipropyl derivative that binds to the N-domain of angiotensin-I converting enzyme. *Journal of Medicinal Chemistry*, 61(1), 344–359. <https://doi.org/10.1021/acs.jmedchem.7b01478>
- Ghose, A. K., Viswanadhan, V. N., & Wendoloski, J. J. (1998). Prediction of hydrophobic (lipophilic) properties of small organic molecules using fragmental methods: An analysis of ALOGP and CLOGP methods. *The Journal of Physical Chemistry A*, 102(21), 3762–3772. <https://doi.org/10.1021/jp980230o>
- Golbraikh, A., Shen, M., Xiao, Z., Xiao, Y.-D., Lee, K.-H., & Tropsha, A. (2003). Rational selection of training and test sets for the development of validated QSAR models. *Journal of Computer-Aided Molecular Design*, 17(2-4), 241–253. <https://doi.org/10.1023/A:1025386326946>
- Gonzalez Amaya, J. A., Cabrera, D. Z., Matallana, A. M., Arevalo, K. G., & Guevara-Pulido, J. (2020). In-silico design of new enalapril analogs (ACE inhibitors) using QSAR and molecular docking models. *Informatics in Medicine Unlocked*, 19, 100336. <https://doi.org/10.1016/j.imu.2020.100336>
- Gramatica, P. (2014). External evaluation of QSAR models, in addition to cross-validation: Verification of predictive capability on totally new chemicals. *Molecular Informatics*, 33(4), 311–314. <https://doi.org/10.1002/minf.201400030>
- Gramatica, P., Chirico, N., Papa, E., Cassani, S., & Kovarich, S. (2013). QSARINS: A new software for the development, analysis, and validation of QSAR MLR models. *Journal of Computational Chemistry*, 34(24), 2121–2132. <https://doi.org/10.1002/jcc.23361>
- Hadaji, E., Bouachrine, M., El Hamdani, H., & Ouammou, A. (2022). QSAR and molecular docking study of quinolin derivatives with topoisomerase I inhibitory properties as potential anticancer agents using statistical methods. *Materials Today: Proceedings*, 51, 1838–1850. <https://doi.org/10.1016/j.matpr.2020.08.032>
- Harder, E., Damm, W., Maple, J., Wu, C., Reboul, M., Xiang, J. Y., Wang, L., Lupyran, D., Dahlgren, M. K., Knight, J. L., Kaus, J. W., Cerutti, D. S., Krilov, G., Jorgensen, W. L., Abel, R., & Friesner, R. A. (2016). OPLS3: A force field providing broad coverage of drug-like small molecules and proteins. *Journal of Chemical Theory and Computation*, 12(1), 281–296. <https://doi.org/10.1021/acs.jctc.5b00864>
- Hollas, B. (2003). An analysis of the autocorrelation descriptor for molecules. *Journal of Mathematical Chemistry*, 33(2), 91–101. <https://doi.org/10.1023/A:1023247831238>
- Hu, Y., Li, C.-Y., Wang, X.-M., Yang, Y.-H., & Zhu, H.-L. (2014). 1,3,4-thiadiazole: Synthesis, reactions, and applications in medicinal, agricultural, and materials chemistry. *Chemical Reviews*, 114(10), 5572–5610. <https://doi.org/10.1021/cr400131u>
- Jain, A. K., Sharma, S., Vaidya, A., Ravichandran, V., & Agrawal, R. K. (2013). 1,3,4-Thiadiazole and its derivatives: A review on recent progress in biological activities. *Chemical Biology & Drug Design*, 81(5), 557–576. <https://doi.org/10.1111/cbdd.12125>
- Jawarkar, R. D., Bakal, R. L., Zaki, M. E. A., Al-Hussain, S., Ghosh, A., Gandhi, A., Mukerjee, N., Samad, A., Masand, V. H., & Lewaa, I. (2022). QSAR based virtual screening derived identification of a novel hit as a SARS CoV-229E 3CLpro Inhibitor: GA-MLR QSAR modeling supported by molecular Docking, molecular dynamics simulation and MMGBSA calculation approaches. *Arabian Journal of Chemistry*, 15(1), 103499. <https://doi.org/10.1016/j.arabj.2021.103499>
- Jawarkar, R. D., Sharma, P., Jain, N., Gandhi, A., Mukerjee, N., Al-Mutairi, A. A., Zaki, M. E. A., Al-Hussain, S. A., Samad, A., Masand, V. H., Ghosh, A., & Bakal, R. L. (2022). QSAR, molecular docking, MD simulation and MMGBSA calculations approaches to recognize concealed pharmacophoric features requisite for the optimization of ALK tyrosine kinase inhibitors as anticancer leads. *Molecules*, 27(15), 4951. <https://doi.org/10.3390/molecules27154951>
- Karadžić, M. Ž., Jevrić, L. R., Mandić, A. I., Markov, S. L., Podunavac-Kuzmanović, S. O., Kovačević, S. Z., Nikolić, A. R., Oklješa, A. M., Sakač, M. N., & Penov-Gaši, K. M. (2017). Chemometrics approach based on chromatographic behavior, in silico characterization and molecular



- docking study of steroid analogs with biomedical importance. *European Journal of Pharmaceutical Sciences : Official Journal of the European Federation for Pharmaceutical Sciences*, 105, 71–81. <https://doi.org/10.1016/j.ejps.2017.05.004>
- Khan, M. A. H., & Imig, J. D. B. T.-R. M. (2018). *Antihypertensive drugs*. Elsevier. <https://doi.org/10.1016/B978-0-12-801238-3.96704-7>
- Khan, K., Roy, K., & Benfenati, E. (2019). Ecotoxicological QSAR modeling of endocrine disruptor chemicals. *Journal of Hazardous Materials*, 369, 707–718. <https://doi.org/10.1016/j.jhazmat.2019.02.019>
- Kumar, V., De, P., Ojha, P. K., Saha, A., & Roy, K. (2020). A multi-layered variable selection strategy for QSAR modeling of butyrylcholinesterase inhibitors. *Current Topics in Medicinal Chemistry*, 20(18), 1601–1627. <https://doi.org/10.2174/1568026620666200616142753>
- Kumar, S., Nair, A. S., Bhashkar, V., Sudevan, S. T., Koyiparambath, V. P., Khames, A., Abdelgawad, M. A., & Mathew, B. (2021). Navigating into the chemical space of monoamine oxidase inhibitors by artificial intelligence and cheminformatics approach. *ACS Omega*, 6(36), 23399–23411. <https://doi.org/10.1021/acsomega.1c03250>
- L DeLano, W. (2002). Pymol: An open-source molecular graphics tool. {CCP4} Newsletter on Protein Crystallography.
- Masand, V. H., El-Sayed, N. N. E., Mahajan, D. T., Mercader, A. G., Alafeefy, A. M., & Shibi, I. G. (2017). QSAR modeling for anti-human African trypanosomiasis activity of substituted 2-Phenylimidazopyridines. *Journal of Molecular Structure*, 1130, 711–718. <https://doi.org/10.1016/j.molstruc.2016.11.012>
- Masand, V. H., & Rastija, V. (2017). PyDescriptor: A new PyMOL plugin for calculating thousands of easily understandable molecular descriptors. *Chemometrics and Intelligent Laboratory Systems*, 169, 12–18. <https://doi.org/10.1016/j.chemolab.2017.08.003>
- McMurray, J. J. V. (2011). CONSENSUS to EMPHASIS: The overwhelming evidence which makes blockade of the renin–angiotensin–aldosterone system the cornerstone of therapy for systolic heart failure. *European Journal of Heart Failure*, 13(9), 929–936. <https://doi.org/10.1093/eurjhf/hfr093>
- Mozaffarian, D., Benjamin, E. J., Go, A. S., Arnett, D. K., Blaha, M. J., Cushman, M., Das, S. R., De Ferranti, S., Després, J. P., Fullerton, H. J., Howard, V. J., Huffman, M. D., Isasi, C. R., Jiménez, M. C., Judd, S. E., Kissela, B. M., Lichtman, J. H., Lisabeth, L. D., Liu, S., ... Turner, M. B. (2016). Heart Disease and Stroke Statistics—2016 Update. *Circulation*, 133(4), e38–e360. <https://doi.org/10.1161/CIR.0000000000000350>
- Olasupo, S. B., Uzairu, A., Shallangwa, G., & Uba, S. (2019). QSAR analysis and molecular docking simulation of norepinephrine transporter (NET) inhibitors as anti-psychotic therapeutic agents. *Heliyon*, 5(10), e02640. <https://doi.org/10.1016/j.heliyon.2019.e02640>
- Palakkeezhillam, V. N. V., Haribabu, J., Manakkadan, V., Rasin, P., Varughese, R. E., Gayathri, D., Bhuvanesh, N., Echeverria, C., & Sreekanth, A. (2023). Synthesis, spectroscopic characterizations, single crystal X-ray analysis, DFT calculations, in vitro biological evaluation and in silico evaluation studies of thiosemicarbazones based 1,3,4-thiadiazoles. *Journal of Molecular Structure*, 1273, 134309. <https://doi.org/10.1016/j.molstruc.2022.134309>
- Politi, A., Durdagi, S., Moutevelis-Minakakis, P., Kokotos, G., Papadopoulos, M. G., & Mavroustakos, T. (2009). Application of 3D QSAR CoMFA/CoMSIA and in silico docking studies on novel renin inhibitors against cardiovascular diseases. *European Journal of Medicinal Chemistry*, 44(9), 3703–3711. <https://doi.org/10.1016/j.ejmech.2009.03.040>
- Przybyłek, M. (2020). Application 2D descriptors and artificial neural networks for beta-glucosidase inhibitors screening. *Molecules*, 25(24), 5942. <https://doi.org/10.3390/molecules25245942>
- Regulska, K., Stanis, B., Regulski, M., & Murias, M. (2014). How to design a potent, specific, and stable angiotensin-converting enzyme inhibitor. *Drug Discovery Today*, 19(11), 1731–1743. <https://doi.org/10.1016/j.drudis.2014.06.026>
- Roy, K., Ambure, P., & Aher, R. B. (2017). How important is to detect systematic error in predictions and understand statistical applicability domain of QSAR models? *Chemometrics and Intelligent Laboratory Systems*, 162, 44–54. <https://doi.org/10.1016/j.chemolab.2017.01.010>
- Roy, K., Kar, S., & Ambure, P. (2015). On a simple approach for determining applicability domain of QSAR models. *Chemometrics and Intelligent Laboratory Systems*, 145, 22–29. <https://doi.org/10.1016/j.chemolab.2015.04.013>
- Sagardia, I., Roa-Ureta, R. H., & Bald, C. (2013). A new QSAR model, for angiotensin I-converting enzyme inhibitory oligopeptides. *Food Chemistry*, 136(3–4), 1370–1376. <https://doi.org/10.1016/j.foodchem.2012.09.092>
- Sander, T., Freyss, J., von Korff, M., & Rufener, C. (2015). DataWarrior: An open-source program for chemistry aware data visualization and analysis. *Journal of Chemical Information and Modeling*, 55(2), 460–473. <https://doi.org/10.1021/ci500588j>
- Schaduangrat, N., Lampa, S., Simeon, S., Gleeson, M. P., Spjuth, O., & Nantasenamat, C. (2020). Towards reproducible computational drug discovery. *Journal of Cheminformatics*, 12(1), 9. <https://doi.org/10.1186/s13321-020-0408-x>
- Shah, S., Arora, S., Chaple, D., Badne, P., Yende, S., Khonde, S., & Deshmukh, S. (2023). 2D-QSAR modeling of chalcone analogues as angiotensin converting enzyme inhibitor. *Biointerface Research in Applied Chemistry*, 13(4), 1–23.
- Shah, S. K., & Chaple, D. R. (2021). 2D-QSAR modeling of quinazolinone derivatives as angiotensin II Type 1a receptor blockers. *International Journal of Quantitative Structure-Property Relationships*, 7(2), 1–20. <https://doi.org/10.4018/IJQSPR.290012>
- Shah, S., Chaple, D., Arora, S., Yende, S., Moharir, K., & Lohiya, G. (2021). Exploring the active constituents of *Oroxylum indicum* in intervention of novel coronavirus (COVID-19) based on molecular docking method. *Network Modeling Analysis in Health Informatics and Bioinformatics*, 10(1), 8. <https://doi.org/10.1007/s13721-020-00279-y>
- Stoicikov, V., Šarić, S., Golubović, M., Zlatanović, D., Krtinić, D., Dinić, L., Mladenović, B., Sokolović, D., & Veselinović, A. M. (2018). Development of non-peptide ACE inhibitors as novel and potent cardiovascular therapeutics: An in silico modelling approach. *SAR and QSAR in Environmental Research*, 29(7), 503–515. <https://doi.org/10.1080/1062936X.2018.1485737>
- Stumpfe, D., Hu, H., & Bajorath, J. (2019). Evolving concept of activity cliffs. *ACS Omega*, 4(11), 14360–14368. <https://doi.org/10.1021/acsomega.9b02221>
- Tetko, I. V., Tanchuk, V. Y., & Villa, A. E. P. (2001). Prediction of n-octanol/water partition coefficients from PHYSPROP database using artificial neural networks and e-state indices. *Journal of Chemical Information and Computer Sciences*, 41(5), 1407–1421. <https://doi.org/10.1021/ci010368v>
- Tropsha, A. (2010). Best practices for QSAR model development, validation, and exploitation. *Molecular Informatics*, 29(6–7), 476–488. <https://doi.org/10.1002/minf.201000061>
- Turner, S., Myers, M., Gadie, B., Nelson, A. J., Pape, R., Saville, J. F., Doxey, J. C., & Berridge, T. L. (1988). Antihypertensive thiadiazoles. 1. Synthesis of some 2-aryl-5-hydrazino-1,3,4-thiadiazoles with vasodilator activity. *Journal of Medicinal Chemistry*, 31(5), 902–906. <https://doi.org/10.1021/jm00400a003>
- Victoria-Muñoz, F., Sánchez-Cruz, N., Medina-Franco, J. L., & Lopez-Vallejo, F. (2022). Cheminformatics analysis of molecular datasets of transcription factors associated with quorum sensing in *Pseudomonas aeruginosa*. *RSC Advances*, 12(11), 6783–6790. <https://doi.org/10.1039/D1RA08352J>
- Wallace, A. C., Laskowski, R. A., & Thornton, J. M. (1995). LIGPLOT: A program to generate schematic diagrams of protein-ligand interactions. *Protein Engineering*, 8(2), 127–134. <https://doi.org/10.1093/protein/8.2.127>
- Yan, W., Lin, G., Zhang, R., Liang, Z., Wu, L., & Wu, W. (2020). Studies on molecular mechanism between ACE and inhibitory peptides in different bioactivities by 3D-QSAR and MD simulations. *Journal of Molecular Liquids*, 304, 112702. <https://doi.org/10.1016/j.molliq.2020.112702>
- Yap, C. W. (2011). PaDEL-descriptor: An open source software to calculate molecular descriptors and fingerprints. *Journal of Computational Chemistry*, 32(7), 1466–1474. <https://doi.org/10.1002/jcc.21707>
- Yunta, M. (2017). It is important to compute intramolecular hydrogen bonding in drug design? *American Journal of Modelling and Optimization*, 5, 24–57. <https://doi.org/10.12691/ajmo-5-1-3>
- Zheng, W., Tian, E., Liu, Z., Zhou, C., Yang, P., Tian, K., Liao, W., Li, J., & Ren, C. (2022). Small molecule angiotensin converting enzyme inhibitors: A medicinal chemistry perspective. *Frontiers in Pharmacology*, 13, 968104. <https://www.frontiersin.org/articles/10.3389/fphar.2022.968104> <https://doi.org/10.3389/fphar.2022.968104>

## Leveraging nitrogen occurrence in approved drugs to identify structural patterns

Vijay H. Masand<sup>a</sup>, Sami Al-Hussain<sup>b</sup>, Abdullah Y. Alzahrani<sup>c</sup>, Nahed N. E. El-Sayed<sup>d</sup>, Chien Ing Yeo<sup>e</sup>, Yee Seng Tan<sup>e</sup> and Magdi E.A. Zaki<sup>b</sup>

<sup>a</sup>Department of Chemistry, Vidya Bharati Mahavidyalaya, Amravati, India; <sup>b</sup>Department of Chemistry, Faculty of Science, Imam Mohammad Ibn Saud Islamic University, Riyadh, Saudi Arabia; <sup>c</sup>Department of Chemistry, Faculty of Science and Arts, King Khalid University, Mohail Assir, Saudi Arabia; <sup>d</sup>National Organization for Drug Control and Research, Egyptian Drug Authority (EDA), Giza, Egypt; <sup>e</sup>Sunway Biofunctional Molecules Discovery Centre, School of Medical and Life Sciences, Sunway University, Sunway City, Malaysia

### ABSTRACT

**Background:** The process of drug development and discovery is costly and slow. Although an understanding of molecular design principles and biochemical processes has progressed, it is essential to minimize synthesis-testing cycles. An effective approach is to analyze key heteroatoms, including oxygen and nitrogen. Herein, we present an analysis focusing on the utilization of nitrogen atoms in approved drugs.

**Research design and methods:** The present work examines the frequency, distribution, prevalence, and diversity of nitrogen atoms in a dataset comprising 2,049 small molecules approved by different regulatory agencies (FDA and others). Various types of nitrogen atoms, such as  $sp^3$ -,  $sp^2$ -,  $sp$ -hybridized, planar, ring, and non-ring are included in this investigation.

**Results:** The results unveil both previously reported and newly discovered patterns of nitrogen atom distribution around the center of mass in the majority of drug molecules.

**Conclusions:** This study has highlighted intriguing trends in the role of nitrogen atoms in drug design and development. The majority of drugs contain 1–3 nitrogen atoms within 5Å from the center of mass (COM) of a molecule, with a higher preference for the ring and planar nitrogen atoms. The results offer invaluable guidance for the multiparameter optimization process, thus significantly contributing toward the conversion of lead compounds into potential drug candidates.

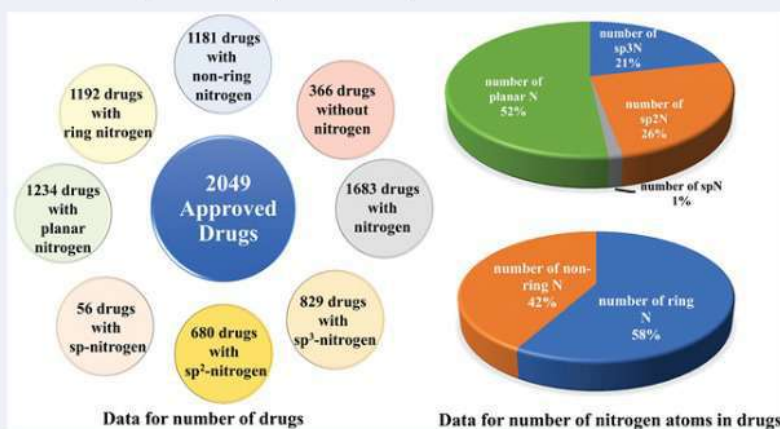
### ARTICLE HISTORY

Received 27 July 2023

Accepted 2 October 2023

### KEYWORDS

Drug design; drug discovery; heteroatoms; molecule distribution; multiparameter optimization; nitrogen atoms



## 1. Introduction

Advancements in the fields of drug design and biomedical research have enhanced the understanding of biomolecules, molecular interactions, pharmacophoric patterns, and biochemical processes, driving dynamic and progressive developments in these domains [1]. The conversion of compounds to drugs requires a collaboration of diverse disciplines and involves a series of sequential steps [2]. In general, the process

of successful drug development involves five major steps, which have been depicted in Figure 1.

Early drug discovery requires multiple efforts, which involve disease and target identification, assay development along with wet lab synthesis of a library of molecules. A lot of researchers nowadays use contemporary methods like pharmacophore modeling, LBDD (Ligand-based Drug Designing), and SBDD (Structure-based Drug Designing) in combination to identify

Impact Factor-8.575 (SJIF)

ISSN-2278-9308

# *B.Aadhar*

**Single Blind Peer-Reviewed & Refreed Indexed**  
**Multidisciplinary International Research Journal**

FEBRUARY 2023

**New Directions in Humanities**



Chief Editor

**Prof. Virag S. Gawande**

Director

Aadhar Social

Research & Development

Training Institute Amravati

Editor

**Dr. Pradnya S. Yenkar**

Principal,

Vidya Bharati Mahavidyalaya,

Camp, Amravati



This Journal is indexed in :

- Scientific Journal Impact Factor (SJIF)
- Cosmos Impact Factor (CIF)
- International Impact Factor Services (IIFS)

For Details Visit To : [www.aadharsocial.com](http://www.aadharsocial.com)

**Aadhar P**UBLICATIONS



Impact Factor – (SJIF) –8.575

ISSN – 2278-9308

# B.Aadhar

**Single Blind Peer-Reviewed & Refereed Indexed**

**Multidisciplinary International Research Journal**

**FEBRUARY 2023**

ISSUE No - 390

**Sciences, Social Sciences, Commerce,  
Education, Language & Law**

**Prof. Virag.S.Gawande**

Chief Editor

Director

Aadhar Social Research &, Development Training Institute, Amravati.

**Dr. Pradnya S. Yenkar**

Editor

Principal,

Vidya Bharati Mahavidyalaya,

Camp, Amravati

**Aadhar International Publication**

For Details Visit To : [www.aadharsocial.com](http://www.aadharsocial.com)

© All rights reserved with the authors & publisher



## Editorial Board

### **Chief Editor -**

**Prof.Virag S.Gawande,**

**Director,**

Aadhar Social Research &

Development Training Institute, Amravati. [M.S.] INDIA

### Executive-Editors -

❖ **Dr.Dinesh W.Nichit** - Principal, Sant Gadge Maharaj Art's Comm,Sci Collage,  
Walgaon.Dist. Amravati.

❖ **Dr.Sanjay J. Kothari** - Head, Deptt. of Economics, G.S.Tompe Arts Comm,Sci Collage  
Chandur Bazar Dist. Amravati

### Advisory Board -

❖ **Dr. Dhnyaneshwar Yawale** - Principal, Sarswati Kala Mahavidyalaya , Dahihanda, Tq-Akola.

❖ **Prof.Dr. Shabab Rizvi** ,Pillai's College of Arts, Comm. & Sci., New Panvel, Navi Mumbai

❖ **Dr. Udaysinh R. Manepatil** ,Smt. A. R. Patil Kanya Mahavidyalaya, Ichalkaranji,

❖ **Dr. Sou. Parvati Bhagwan Patil** , Principal, C.S. Shindure College Hupri, Dist Kolhapur

❖ **Dr.Usha Sinha** , Principal ,G.D.M. Mahavidyalay,Patna Magadh University.Bodhgay Bihar

### Review Committee -

❖ **Dr. D. R. Panzade**, Assistant Pro. Yeshwantrao Chavan College, Sillod. Dist. Aurangabad (MS)

❖ **Dr.Suhas R.Patil** ,Principal ,Government College Of Education, Bhandara, Maharashtra

❖ **Dr. Kundan Ajabrao Alone** ,Ramkrushna Mahavidyalaya, Darapur Tal-Daryapur, Dist-Amravati.

❖ **DR. Gajanan P. Wader** Principal , Pillai College of Arts, Commerce & Science, Panvel

❖ **Dr. Bhagyashree A. Deshpande**, Professor Dr. P. D. College of Law, Amravati]

❖ **Dr. Sandip B. Kale**, Head, Dept. of Pol. Sci., Yeshwant Mahavidyalaya, Seloo, Dist. Wardha.

❖ **Dr. Hrushikesh Dalai** , Asstt. Professor K.K. Sanskrit University, Ramtek

*Our Editors have reviewed paper with experts' committee, and they have checked the papers on their level best to stop furtive literature. Except it, the respective authors of the papers are responicible for originality of the papers and intensive thoughts in the papers.*

- **Executive Editor**

### Published by -

**Prof.Virag Gawande**

**Aadhar Publication** ,Aadhar Social Research & Development Training Institute, New Hanuman Nagar,

In Front Of Pathyapustak Mandal, Behind V.M.V. College,Amravati

( M.S ) India \_Pin- 444604 **Email :** [aadharpublication@gmail.com](mailto:aadharpublication@gmail.com)

**Website :** [www.aadharsocial.com](http://www.aadharsocial.com) **Mobile :** [9595560278 /](tel:9595560278)

**INDEX**

No.	Title of the Paper	Authors' Name	Page No.
1	Impact Of Covid-19 And Lockdown On Mental Health Of Various Sections	<b>Prof.Dr .Devdas S.Ramteke</b>	1
2	An Overview of the Development of Education System in India	<b>Dr. Rajesh M. Deshmukh</b>	6
3	COVID-19:Challenges and Opportunities in Indian Economy	<b>Dr. Devendra S. Rangachary , Prof.Dr. Mithilesh Rathore</b>	12
4	Echo of Ecocriticism in Maneka Gandhi's 'Love Story'	<b>Dr. Shitalbabu Ambadas Tayade</b>	16
5	Importance Of English Language In The Present Scenario	<b>Dr. Nishigandh Satav</b>	20
6	Socio-Cultural challenges in Indian Education System: with Special Reference to Indian Women	<b>Dr. Rizawana B. Gadakari</b>	23
7	Importance of Good Communication Skills	<b>Mrs. Anjali Deshmukh</b>	26
8	The Modern Trends In Literary Forms Of Media: Photography And Internet	<b>Prof. Purushottam V.Bathe</b>	29
9	Experiment-Based Subjects: A Challenge To Learn In An Online Mode	<b>C. N. Jadhav</b>	33
10	Nostalgic Sense for Past in Tennessee Williams' 'The Glass Menagerie A Strategy of Survival in Oddity	<b>N. G. Jadhao</b>	37
11	Effect Of COVID-19 Pandemic in Learning and Teaching Science Subjects: A Challenge to Both Teachers And Student	<b>P. P. Nalawade , J. R. Bansod , N.N. Kakpure</b>	40
12	Unaccustomed Earth:Generational Shift in tackling the Emotional Conflicts by Indian Immigrants	<b>Dr. Nakul D. Gawande</b>	44
13	Synthesis And Characterization Of Cu-Nanoparticles By Using O.Sanctum And M.Panniculata	<b>L.P.Khalid , P.V.Pulate , N.G.Kokateand , J.B.Patil</b>	47
14	Stress among the positive patients during the Covid-19 pandemic	<b>Manjusha Jagannath Barbudhe</b>	52
15	Recent Trends in Humanities, Commerce, Science and Technology	<b>Mr. Shrirang Deshmukh</b>	57
16	The Impact of Financial Constraints on Student Enrolment in Higher Education: A Major Challenge in Higher Education	<b>Dr. Sanjay B. Kadu</b>	59
17	Human Predicament in the select stories of Guy de Maupassant and Thomas Mann	<b>Dr. R. M. Patil</b>	67
18	COVID 19 impacts on woman with Poly Cystic Ovary Syndrome on their pre-existing mental health issues in Vidarbha:Thematic Study	<b>Apeksha Bandebuche , Dr. D. S. Ramteke</b>	72
19	Innovations in EdTech: Improving Access and Outcomes for Learners	<b>Dr. Pratik B. Upase</b>	



20	The Effect of Job Vulnerability on Pandemic Prevalent Concern: Loneliness Dr. S. D. Wakode , Ujjwala Godbole Kulkarni	
21	A study of Coping Strategies of Frontline and Non-Frontline workers. Dr. S.D. Wakode ,Vanita SachinRaut	
22	मध्ययुगीन मराठी गद्य साहित्यातील संवाद शैलीचे स्वरूप डॉ. अण्णा वैद्य	
23	जनसाहित्य संशोधन पद्धती डॉ. दिनेश की. राऊत	
24	मराठी समकालिन साहित्य विचारातील नवे प्रवाह प्रा विक्रान्त कृष्णराव मेश्राम	
25	कोरोनोत्तर शैक्षणिक स्थिती प्रा.डॉ.गजानन रामचंद्र लोहवे	
26	पारधी समाजाची संस्कृती आणि पारधी स्त्रियांची स्थितिगती कु.सारिका विष्णुपंत वनवे	
27	भारतीय संविधानातील कलम 21 अंतर्गत आरोग्याचा अधिकार : एक विश्लेषण डॉ. विजय रा. ढेंगळे	
28	'भारतीय स्त्रीयांचे दृष्टीने मानवतावादी स्थान एक अभ्यास' प्रा. डॉ. टि. डी. राजगुरे	
29	मानव्य विज्ञानातील नवी दिशा संदीप महादेवराव हाडोळे	
30	आंबेडकरी गेय कवितेतील मूल्यदर्शन प्रा.डॉ. संजय शेजव	
31	दलित आत्मकथनातील स्त्री-पुरुष संबंध डॉ. गजानन बनसोड	
32	समकालीन लेखिकेच्या कादंबरीतील स्त्री नायिका आणि जीवनचित्रण (मेघना पेठे, कविता महाजन,अरुणा सबाने) तोष्णा बी.बोंदाडे (मोकडे) , प्रा.डॉ. गजानन बनसोड	
33	संसर्गजन्य रोगामुळे मानसिकतेवर परिणाम होऊन जीवनशैली विस्कळीत – एक विश्लेषण प्रा. ए. एम. वानखडे	
34	राष्ट्रसंतांनी मांडलेला मानवतावादी विचार एक चिकित्सक अभ्यास प्रा. अनुप अरुण नांदगावकर	
35	श्री गोविंदप्रभु विषयक साहित्यातील जननिष्ठा प्रा. डॉ. कल्पना त्र्यं. मेहरे	
36	कोविड-१९ आणि सद्याचे बदलते जागतिक राजकारण अमित पुरुषोत्तम इंगोले	
37	तुकडोजी महाराजांचे साहित्यातून स्वातंत्र्याला योगदान प्रा. अमृता दीपक तायडे	
38	थेरीगाथा आणि आधुनिक स्त्रीवादी कादंबरीतून व्यक्त झालेला स्त्रीवाद : चिकित्सक अध्ययन प्रा. डॉ. विश्वजीत कांबळे,	
39	डॉ. सुखदेव ढाणके यांच्या 'पिंडपातविषयी – आशयअभिव्यक्ती कु. ज्योती भिकुसा शेंदुरजणे प्रा. गजानन बनसोड,	
40	कोविड-१९ नंतर वाढलेली अर्थव्यवस्थेतील डिजिटल पेमेंट पध्दती प्रा. राजेश माथुरकर	



41	कोरोना विषाणूचा प्रादुर्भाव झालेल्या स्त्री पुरुषांचा बाध्यता ग्रस्तता या समायोजन नसविकृती घटकावर झालेल्या परिणामाचा तुलनात्मक अभ्यास प्रा. अरुणा तसरे प्रो.डॉ. एस.डी. वाकोडे	
----	---	--





## The Impact of Financial Constraints on Student Enrolment in Higher Education: A Major Challenge in Higher Education

**Dr. Sanjay B. Kadu**

Head & Professor, Commerce Department, Vidya Bharti Mahavidyalay, Amravati. (MS)  
Mobile- 9420189295 , Email- drkadu2122@gmail.com

**Abstract:** This study aims to examine the impact of financial constraints on student enrolment in higher education through a desktop research approach. The objective of the study is to understand the extent of the problem of financial constraints on student enrolment in higher education and to identify the socio-economic factors that contribute to these constraints. The study will review existing literature and data on the topic, including government reports, academic studies, and other relevant sources.

The study will analyze data on the cost of higher education, access to financial assistance and scholarships, and the financial literacy and planning of students and families. The study will also explore the prevalence of financial constraints as a barrier to student enrolment in higher education in India.

The results of the study will provide valuable insights into the impact of financial constraints on student enrolment in higher education in India. The study will contribute to the broader understanding of the challenges faced by students in accessing higher education and the role of financial constraints in limiting enrolment.

### **Introduction:**

Higher education is widely considered as a critical factor in economic and social development. Access to higher education is not only a pathway for individuals to acquire the skills and knowledge necessary for success in the modern economy, but also to increase their social mobility and improve their quality of life. However, despite the recognized importance of higher education, many students around the world face significant financial barriers that limit their ability to pursue further education.

In India, financial constraints are a major challenge for students seeking to enroll in higher education. Despite recent efforts to expand access to higher education, including the creation of new institutions and the expansion of financial aid programs, many students still face significant financial hurdles that limit their ability to pursue further education. The high cost of tuition and related expenses, combined with limited access to scholarships and other forms of financial assistance, creates substantial barriers to student.

In order to better understand the impact of financial constraints on student in higher education in India, it is necessary to examine the various socio-economic factors that contribute to these constraints. These factors may include poverty, limited access to financial resources, inadequate support from families, and lack of access to financial services. Additionally, structural factors, such as the limited capacity of higher education institutions and the high cost of tuition and related expenses, may also play a role in creating financial barriers for students.

### **Literature review:**

The literature review for the study "The impact of financial constraints on student in higher education" will focus on identifying the socio-economic factors that contribute to financial constraints and their impact on student. The literature review will also aim to understand the extent of the problem of financial constraints on student in higher education.

In this regard, various studies have been conducted on financial constraints and their impact on higher education in different countries including India. A study by B.S. Yadav and A. Kumar (2015) investigated the financial constraints faced by students in higher education in India and found that more than 60% of students face financial difficulties in pursuing their education. The study also found that the majority of students come from low-income families, which limits their ability to pay for higher education.

Another study by S.A. Adebayo (2017) found that financial constraints were the main barrier to access to higher education in Nigeria. The study also found that students from low-income families were more likely to face financial constraints and were less likely to enroll in higher education.



Additionally, a study by M.A. Park (2017) explored the impact of financial constraints on student in South Korean higher education institutions. The study found that students from low-income families were more likely to face financial constraints and were less likely to enroll in higher education.

**Objectives:**

The objectives of the study are:

- (1) Understand the extent of the problem of financial constraints on student in higher education;
- (2) Identify the socio-economic factors that contribute to financial constraints and their impact on student.

**Methodology:**

This study is entirely qualitative in approach. Researchers primarily used secondary data for this investigation. Secondary data was gathered from publicly available sources such as articles, research papers, census data, general reports, websites, etc.

The impact of financial constraints on student in higher education is a significant issue in many countries, including India. Financial constraints refer to the lack of financial resources or the inability to access funds that are necessary to pursue higher education. This can include difficulties in paying for tuition fees, transportation costs, books, and other educational expenses. As a result, many students are unable to enroll or continue their studies in higher education institutions, thereby limiting their opportunities for personal and professional growth.

There are several socio-economic factors that contribute to financial constraints in higher education. For example, students from low-income families and rural areas often face the highest barriers to higher education due to their limited financial resources. In addition, the rising cost of higher education has made it increasingly difficult for students from economically weaker sections of society to pursue higher education.

Studies have shown that financial constraints have a significant impact on student in higher education. The All India Survey on Higher Education (AISHE) reported that the Gross Ratio (GER) in higher education in India was 26.3% in 2018-19, which is lower than the GER of many developed countries. A study conducted by the Ministry of Human Resource Development (MHRD) found that financial constraints are the most significant barrier to higher education in India, with more than 50% of students dropping out of college due to financial difficulties.

The National Sample Survey Office (NSSO) reported that only 14% of students from economically weaker sections of society were enrolled in higher education in India, compared to 35% of students from the general population. A study by the University Grants Commission (UGC) revealed that students from rural areas and low-income families face the highest financial barriers to higher education in India.

To address the problem of financial constraints on student in higher education, various government and non-government organizations have implemented programs and initiatives aimed at providing financial assistance and support to students in need. These can include scholarships, student loans, and other forms of financial aid. Additionally, many institutions have implemented cost-saving measures, such as online learning and open-source materials, to make higher education more accessible and affordable.

In conclusion, the impact of financial constraints on student in higher education is a critical issue that requires attention and action. Addressing this issue is crucial in ensuring that students from all socio-economic backgrounds have equal access to higher education and the opportunities that it offers.

Some important statistical insights

1. According to the All India Survey on Higher Education (AISHE) report (2018-19), the Gross Ratio (GER) in higher education in India was 26.3%, which is lower than the GER of many developed countries.
2. A study conducted by the Ministry of Human Resource Development (MHRD) found that financial constraints are the most significant barrier to higher education in India, with more than 50% of students dropping out of college due to financial difficulties.
3. The National Sample Survey Office (NSSO) reported that only 14% of students from economically weaker sections of society were enrolled in higher education in India, compared to 35% of students from the general population.
4. A study by the University Grants Commission (UGC) revealed that students from rural areas and low-income families face the highest financial barriers to higher education in India.



5. A report by the Centre for the Study of Developing Societies (CSDS) found that the cost of higher education has risen by more than 50% in India in the past decade, making it increasingly difficult for students from low-income families to pursue higher education.

**Findings:**

The impact of financial constraints on student in higher education is a widely studied and documented issue. Financial constraints are a major barrier for students to pursue higher education, particularly for those from low-income families, rural areas, and economically weaker sections of society. Several studies have found that financial difficulties are the primary reason for students dropping out of college, with the cost of higher education continuing to rise in many countries. Additionally, socio-economic factors such as family income, geographic location, and economic background are significant contributors to financial constraints. Addressing the issue of financial constraints and providing financial assistance and support to students is crucial to improving student in higher education and increasing access to education for all.

**Conclusion:**

In conclusion, the impact of financial constraints on student in higher education is a significant issue that requires attention. The lack of financial resources can prevent students from pursuing higher education and can lead to a reduction in the number of students enrolled in colleges and universities. This can have a negative impact on the socio-economic development of a country as it can reduce the number of highly educated individuals who can contribute to the growth of the economy. Therefore, it is important to address the issue of financial constraints in higher education by providing financial assistance and scholarships to students who are unable to afford the cost of higher education. This will help to increase the of students in higher education and support the development of the country.

**References:**

- Yadav, B.S., Kumar, A. (2015). Financial Constraints Faced by Students in Higher Education in India. *International Journal of Humanities and Social Science Research*, 5(10), 170-176.
- Chaudhary, R. (2017). Financial Constraints and Access to Higher Education: Evidence from India. *Journal of International and Comparative Education*, 6(1), 41-52.
- Kaur, G., & Kaur, H. (2017). Financial Constraints and Access to Higher Education: Evidence from Punjab. *Education and Development*, 5(3), 44-52.
- Dutta, R. (2017). Financial Constraints and Access to Higher Education: Evidence from West Bengal. *International Journal of Economics, Commerce and Management*, 5(9), 1-7.
- "Financial Constraints to Education: Empirical Evidence and Policy Implications" by J. Ethan Pandithurai, *International Journal of Educational Development*, 2008. (<https://www.sciencedirect.com/science/article/pii/S073805930800059X>)
- "Financial Constraints and Access to Higher Education: A Study of Household Behaviour in India" by Santosh Mehrotra, *Economic and Political Weekly*, 2011. (<https://www.epw.in/journal/2011/35/special-articles/financial-constraints-and-access-higher-education.html>)
- "The Financial Constraints to Higher Education: A Study of Rural and Urban Households in India" by S. Mukhopadhyay and A. Kumar, *Education Economics*, 2006. (<https://www.tandfonline.com/doi/abs/10.1080/09645290600728381>)
- "Financial Constraints and Higher Education: An Analysis of Student Loan Schemes in India" by N. Kapur, *Journal of Educational Planning and Administration*, 2008. (<https://www.jstor.org/stable/40939077?seq=1>)

Impact Factor-8.575 (SJIF)

ISSN-2278-9308

# *B.Aadhar*

**Single Blind Peer-Reviewed & Refreed Indexed**  
**Multidisciplinary International Research Journal**

FEBRUARY 2023

**New Directions in Humanities**



Chief Editor

**Prof. Virag S. Gawande**

Director

Aadhar Social

Research & Development

Training Institute Amravati

Editor

**Dr. Pradnya S. Yenkar**

Principal,

Vidya Bharati Mahavidyalaya,

Camp, Amravati



This Journal is indexed in :

- Scientific Journal Impact Factor (SJIF)
- Cosmos Impact Factor (CIF)
- International Impact Factor Services (IIFS)

For Details Visit To : [www.aadharsocial.com](http://www.aadharsocial.com)

**Aadhar P**UBLICATIONS



Impact Factor – (SJIF) –8.575

ISSN – 2278-9308

# B.Aadhar

**Single Blind Peer-Reviewed & Refereed Indexed**

**Multidisciplinary International Research Journal**

**FEBRUARY 2023**

ISSUE No - 390

**Sciences, Social Sciences, Commerce,  
Education, Language & Law**

**Prof. Virag.S.Gawande**

Chief Editor

Director

Aadhar Social Research &, Development Training Institute, Amravati.

**Dr. Pradnya S. Yenkar**

Editor

Principal,

Vidya Bharati Mahavidyalaya,

Camp, Amravati

**Aadhar International Publication**

For Details Visit To : [www.aadharsocial.com](http://www.aadharsocial.com)

© All rights reserved with the authors & publisher



## Editorial Board

### **Chief Editor -**

**Prof.Virag S.Gawande,**

**Director,**

Aadhar Social Research &

Development Training Institute, Amravati. [M.S.] INDIA

### Executive-Editors -

❖ **Dr.Dinesh W.Nichit** - Principal, Sant Gadge Maharaj Art's Comm,Sci Collage,  
Walgaon.Dist. Amravati.

❖ **Dr.Sanjay J. Kothari** - Head, Deptt. of Economics, G.S.Tompe Arts Comm,Sci Collage  
Chandur Bazar Dist. Amravati

### Advisory Board -

❖ **Dr. Dhnyaneshwar Yawale** - Principal, Sarswati Kala Mahavidyalaya , Dahihanda, Tq-Akola.

❖ **Prof.Dr. Shabab Rizvi** ,Pillai's College of Arts, Comm. & Sci., New Panvel, Navi Mumbai

❖ **Dr. Udaysinh R. Manepatil** ,Smt. A. R. Patil Kanya Mahavidyalaya, Ichalkaranji,

❖ **Dr. Sou. Parvati Bhagwan Patil** , Principal, C.S. Shindure College Hupri, Dist Kolhapur

❖ **Dr.Usha Sinha** , Principal ,G.D.M. Mahavidyalay,Patna Magadh University.Bodhgay Bihar

### Review Committee -

❖ **Dr. D. R. Panzade**, Assistant Pro. Yeshwantrao Chavan College, Sillod. Dist. Aurangabad (MS)

❖ **Dr.Suhas R.Patil** ,Principal ,Government College Of Education, Bhandara, Maharashtra

❖ **Dr. Kundan Ajabrao Alone** ,Ramkrushna Mahavidyalaya, Darapur Tal-Daryapur, Dist-Amravati.

❖ **DR. Gajanan P. Wader** Principal , Pillai College of Arts, Commerce & Science, Panvel

❖ **Dr. Bhagyashree A. Deshpande**, Professor Dr. P. D. College of Law, Amravati]

❖ **Dr. Sandip B. Kale**, Head, Dept. of Pol. Sci., Yeshwant Mahavidyalaya, Seloo, Dist. Wardha.

❖ **Dr. Hrushikesh Dalai** , Asstt. Professor K.K. Sanskrit University, Ramtek

*Our Editors have reviewed paper with experts' committee, and they have checked the papers on their level best to stop furtive literature. Except it, the respective authors of the papers are responicible for originality of the papers and intensive thoughts in the papers.*

- **Executive Editor**

### Published by -

**Prof.Virag Gawande**

**Aadhar Publication** ,Aadhar Social Research & Development Training Institute, New Hanuman Nagar,

In Front Of Pathyapustak Mandal, Behind V.M.V. College,Amravati

( M.S ) India \_Pin- 444604 **Email :** [aadharpublication@gmail.com](mailto:aadharpublication@gmail.com)

**Website :** [www.aadharsocial.com](http://www.aadharsocial.com) **Mobile :** [9595560278 /](tel:9595560278)

**INDEX**

No.	Title of the Paper	Authors' Name	Page No.
1	Impact Of Covid-19 And Lockdown On Mental Health Of Various Sections	<b>Prof.Dr .Devdas S.Ramteke</b>	1
2	An Overview of the Development of Education System in India	<b>Dr. Rajesh M. Deshmukh</b>	6
3	COVID-19:Challenges and Opportunities in Indian Economy	<b>Dr. Devendra S. Rangachary , Prof.Dr. Mithilesh Rathore</b>	12
4	Echo of Ecocriticism in Maneka Gandhi's 'Love Story'	<b>Dr. Shitalbabu Ambadas Tayade</b>	16
5	Importance Of English Language In The Present Scenario	<b>Dr. Nishigandh Satav</b>	20
6	Socio-Cultural challenges in Indian Education System: with Special Reference to Indian Women	<b>Dr. Rizawana B. Gadakari</b>	23
7	Importance of Good Communication Skills	<b>Mrs. Anjali Deshmukh</b>	26
8	The Modern Trends In Literary Forms Of Media: Photography And Internet	<b>Prof. Purushottam V.Bathe</b>	29
9	Experiment-Based Subjects: A Challenge To Learn In An Online Mode	<b>C. N. Jadhav</b>	33
10	Nostalgic Sense for Past in Tennessee Williams' 'The Glass Menagerie A Strategy of Survival in Oddity	<b>N. G. Jadhao</b>	37
11	Effect Of COVID-19 Pandemic in Learning and Teaching Science Subjects: A Challenge to Both Teachers And Student	<b>P. P. Nalawade , J. R. Bansod , N.N. Kakpure</b>	40
12	Unaccustomed Earth:Generational Shift in tackling the Emotional Conflicts by Indian Immigrants	<b>Dr. Nakul D. Gawande</b>	44
13	Synthesis And Characterization Of Cu-Nanoparticles By Using O.Sanctum And M.Panniculata	<b>L.P.Khalid , P.V.Pulate , N.G.Kokateand , J.B.Patil</b>	47
14	Stress among the positive patients during the Covid-19 pandemic	<b>Manjusha Jagannath Barbudhe</b>	52
15	Recent Trends in Humanities, Commerce, Science and Technology	<b>Mr. Shrirang Deshmukh</b>	57
16	The Impact of Financial Constraints on Student Enrolment in Higher Education: A Major Challenge in Higher Education	<b>Dr. Sanjay B. Kadu</b>	59
17	Human Predicament in the select stories of Guy de Maupassant and Thomas Mann	<b>Dr. R. M. Patil</b>	67
18	COVID 19 impacts on woman with Poly Cystic Ovary Syndrome on their pre-existing mental health issues in Vidarbha:Thematic Study	<b>Apeksha Bandebuche , Dr. D. S. Ramteke</b>	72
19	Innovations in EdTech: Improving Access and Outcomes for Learners	<b>Dr. Pratik B. Upase</b>	



20	The Effect of Job Vulnerability on Pandemic Prevalent Concern: Loneliness Dr. S. D. Wakode , Ujjwala Godbole Kulkarni	
21	A study of Coping Strategies of Frontline and Non-Frontline workers. Dr. S.D. Wakode ,Vanita SachinRaut	
22	मध्ययुगीन मराठी गद्य साहित्यातील संवाद शैलीचे स्वरूप डॉ. अण्णा वैद्य	
23	जनसाहित्य संशोधन पद्धती डॉ. दिनेश की. राऊत	
24	मराठी समकालिन साहित्य विचारातील नवे प्रवाह प्रा विक्रान्त कृष्णराव मेश्राम	
25	कोरोनोत्तर शैक्षणिक स्थिती प्रा.डॉ.गजानन रामचंद्र लोहवे	
26	पारधी समाजाची संस्कृती आणि पारधी स्त्रियांची स्थितिगती कु.सारिका विष्णुपंत वनवे	
27	भारतीय संविधानातील कलम 21 अंतर्गत आरोग्याचा अधिकार : एक विश्लेषण डॉ. विजय रा. ढेंगळे	
28	'भारतीय स्त्रीयांचे दृष्टीने मानवतावादी स्थान एक अभ्यास' प्रा. डॉ. टि. डी. राजगुरे	
29	मानव्य विज्ञानातील नवी दिशा संदीप महादेवराव हाडोळे	
30	आंबेडकरी गेय कवितेतील मूल्यदर्शन प्रा.डॉ. संजय शेजव	
31	दलित आत्मकथनातील स्त्री-पुरुष संबंध डॉ. गजानन बनसोड	
32	समकालीन लेखिकेच्या कादंबरीतील स्त्री नायिका आणि जीवनचित्रण (मेघना पेठे, कविता महाजन,अरुणा सबाने) तोष्णा बी.बोंदाडे (मोकडे) , प्रा.डॉ. गजानन बनसोड	
33	संसर्गजन्य रोगामुळे मानसिकतेवर परिणाम होऊन जीवनशैली विस्कळीत – एक विश्लेषण प्रा. ए. एम. वानखडे	
34	राष्ट्रसंतांनी मांडलेला मानवतावादी विचार एक चिकित्सक अभ्यास प्रा. अनुप अरुण नांदगावकर	
35	श्री गोविंदप्रभु विषयक साहित्यातील जननिष्ठा प्रा. डॉ. कल्पना त्र्यं. मेहरे	
36	कोविड-१९ आणि सद्याचे बदलते जागतिक राजकारण अमित पुरुषोत्तम इंगोले	
37	तुकडोजी महाराजांचे साहित्यातून स्वातंत्र्याला योगदान प्रा. अमृता दीपक तायडे	
38	थेरीगाथा आणि आधुनिक स्त्रीवादी कादंबरीतून व्यक्त झालेला स्त्रीवाद : चिकित्सक अध्ययन प्रा. डॉ. विश्वजीत कांबळे,	
39	डॉ. सुखदेव ढाणके यांच्या 'पिंडपातविषयी – आशयअभिव्यक्ती कु. ज्योती भिकुसा शेंदुरजणे प्रा. गजानन बनसोड,	
40	कोविड-१९ नंतर वाढलेली अर्थव्यवस्थेतील डिजिटल पेमेंट पध्दती प्रा. राजेश माथुरकर	





41	कोरोना विषाणूचा प्रादुर्भाव झालेल्या स्त्री पुरुषांचा बाध्यता ग्रस्तता या समायोजन नसविकृती घटकावर झालेल्या परिणामाचा तुलनात्मक अभ्यास प्रा. अरुणा तसरे प्रो.डॉ. एस.डी. वाकोडे	
----	---	--



## Innovations in EdTech: Improving Access and Outcomes for Learners

**Dr. Pratik B. Upase**

Assistant Professor Department of Commerce Vidya Bharati Mahavidyalaya  
Amravati ,pratik.upase@gmail.com,8390091615

**Abstract:** The integration of technology in education has been increasing in recent years, leading to the development of innovative EdTech solutions aimed at improving access and outcomes for learners. However, despite the numerous benefits that EdTech offers, many challenges remain, including accessibility, equity, and privacy concerns. The purpose of this research study is to investigate the impact of EdTech on access and outcomes for learners through a qualitative approach, including exploring the perceptions and experiences of teachers, students, and educational administrators.

**Keywords:** EdTech, Technology in Education, Access, Learning Outcomes, Digital Divide, Quality Education, Marginalized Communities, Educational Equity

**Introduction:** The integration of technology in education has been a topic of growing interest in recent years, as the development of innovative EdTech solutions has shown the potential to improve access and outcomes for learners. EdTech offers numerous benefits, including increased engagement and motivation, personalized learning experiences, and improved educational equity. For instance, digital platforms and tools can provide learners with access to a wider range of educational resources and support individualized learning, while virtual and augmented reality technologies can enhance the immersive and interactive learning experiences.

However, despite these advantages, the use of EdTech in education also faces several challenges, including accessibility, privacy, and equity concerns. In some cases, the cost of technology and lack of infrastructure can limit access for some learners, particularly those from underprivileged communities. Additionally, concerns about privacy and the safety of personal data have been raised, as the use of technology in education often involves the collection and storage of sensitive information. Given these challenges, it is critical to understand the impact of EdTech on access and outcomes for learners. This is particularly important as the use of technology in education continues to grow and evolve. The purpose of this research study is to examine the impact of EdTech on access and outcomes for learners through a qualitative approach. The research will explore the perceptions and experiences of teachers, students, and educational administrators regarding the impact of EdTech on access and outcomes for learners. The qualitative approach will provide a rich and nuanced understanding of the key themes and patterns related to the impact of EdTech on access and outcomes for learners.

**Literature review:** In recent years, EdTech has become increasingly popular in India, as both the public and private sectors have invested heavily in the development of EdTech solutions to improve access to quality education and learning outcomes. This literature review examines research into the impact of EdTech on access and learning outcomes in India.

The primary focus of research in this area has been on the use of EdTech to bridge the digital divide and to provide access to education in remote and rural areas. A study by the United Nations Educational, Scientific and Cultural Organization (UNESCO) found that EdTech can help to improve student engagement, motivation and learning outcomes (2020). In addition, the Indian government has launched initiatives such as the 'Digital India' program to promote the use of EdTech in schools (The Economic Times, 2020).

Research has also examined the impact of EdTech on the quality of education in India. A number of studies have found that EdTech can be used to improve the learning outcomes of students (Kaur et al., 2019; Raval et al., 2018; Thakur et al., 2016). Furthermore, EdTech has been used to provide access to quality education for marginalized and vulnerable communities (The Economic Times, 2020).

In conclusion, EdTech has become increasingly popular in India in recent years and is being used to improve access to education and learning outcomes. Research into the impact of EdTech has found that it can be used to bridge the digital divide, improve student engagement and motivation, and to provide access to quality education for vulnerable communities.

**Methodology:** The qualitative methodology outlined in this paper will provide a comprehensive understanding of the current state of EdTech and its potential to improve access and outcomes for



learners. The collection and analysis of verbal, visual, and written data will provide an understanding of the challenges and benefits associated with EdTech, as well as potential solutions for making EdTech more effective. By utilizing this methodology, the researcher will be able to effectively answer the research question and provide meaningful insight into the future of EdTech.

Research question frame by the researcher here is - What are the innovations in EdTech that are improving access and outcomes for learners, and what challenges and potential solutions exist for making EdTech more effective?

**Discussion:**In recent years, the education technology (EdTech) industry has seen rapid expansion and growth. EdTech has become an integral part of the educational experience, providing students with access to a wide range of learning resources, increased opportunities for collaboration, and improved outcomes. With the rise of technology and its capabilities, EdTech has become an indispensable tool for educators across the world. This paper will explore the various innovations in EdTech that are improving access and outcomes for learners. It will discuss the benefits and challenges of using EdTech tools in the classroom, as well as potential solutions to those challenges. It will also discuss the importance of EdTech in providing equitable access to learning opportunities, and the potential of EdTech to create a more inclusive learning environment.

**Benefits of EdTech:** EdTech provides a range of benefits to learners and educators alike. EdTech tools can be used to facilitate collaboration and communication between students, teachers, and parents. The use of EdTech tools also allows students to access content and resources that may otherwise be inaccessible due to geographic or financial barriers. Additionally, EdTech can provide students with personalized learning experiences that can be tailored to their individual needs and interests. EdTech can also be used to track student progress and provide feedback, allowing educators to better understand their students' strengths and weaknesses.

**Challenges of EdTech:** Despite the numerous benefits that EdTech can provide, there are also challenges associated with its use. Many EdTech tools require significant upfront investments in terms of both time and resources. Additionally, there is a lack of standardization among EdTech tools, making it difficult for educators to evaluate the efficacy of different tools. Additionally, there is a lack of understanding among educators regarding how to most effectively use EdTech tools in the classroom. **Potential Solutions** In order to address the challenges associated with the use of EdTech, it is essential that educators receive adequate training and support. Professional development programs should be provided to ensure that educators are equipped with the necessary knowledge and skills to effectively use EdTech tools. Additionally, EdTech providers should strive to create tools that are simple to use and easily accessible to all students. Furthermore, education systems should invest in EdTech tools that are tailored to the specific needs of their students and educators.

1. **Adaptive Learning:** Adaptive learning technology uses algorithms to tailor instruction to the individual student's pace and needs. By adapting the curriculum to each student, this technology enables them to achieve mastery at their own pace, while also providing customized feedback and guidance.

2. **Gamification:** Gamification is the use of game elements and game design techniques to facilitate learning. It incentivizes students to complete tasks and encourages them to work harder and stay engaged.

3. **Virtual Reality:** Virtual reality is a computer-generated environment that simulates real life. This technology brings the classroom to life and enables teachers to take students on virtual field trips, explore new concepts, and gain hands-on experience.

4. **Artificial Intelligence:** Artificial intelligence is a branch of computer science that enables computers to learn from data, identify patterns, and make decisions. AI can be used to personalize instruction for every student, identify academic issues, and provide feedback.

Challenges, few more:

1. **Accessibility:** EdTech can be expensive and inaccessible for many students, particularly those from low-income backgrounds.

2. **Quality:** The quality of EdTech can vary greatly, and it's important to ensure that the technology is actually improving student outcomes.

3. **User-Friendliness:** EdTech can be intimidating and confusing for students and teachers alike. If the technology isn't easy to use, students won't be able to take advantage of its benefits.

Potential Solutions:



1. Increase Accessibility: Governments should provide financial support to schools to help them purchase EdTech and make it more accessible to all students.
2. Enhance Quality: Governments and schools should ensure that EdTech is high-quality and effective before purchasing and implementing it.
3. Improve User-Friendliness: Schools should provide training and support to help teachers and students learn how to use EdTech effectively. Additionally, EdTech vendors should focus on designing user-friendly interfaces.

Some statistical fact to show relation between EdTech Access and Outcomes:

1. India is a hub of EdTech startups and investments, with over 600 EdTech startups, more than any other country in the world. (TechCrunch, 2020)
2. In 2020, EdTech investments in India amounted to over \$2.2 billion, an increase of over 70% from the previous year. (KPMG, 2021)
3. EdTech is being used to bridge the digital divide by providing access to education for learners in rural and remote areas. (The Economic Times, 2020)
4. Over 80% of schools in India are now using EdTech to deliver remote learning. (The Economic Times, 2020)
5. The Indian government has launched several initiatives to promote the use of EdTech in schools, including the 'Digital India' program. (The Economic Times, 2020)

**Findings:** This research study examined the impact of EdTech on access and learning outcomes in India. The findings of the study revealed the following:

1. EdTech is being used to bridge the digital divide and to provide access to education in remote and rural areas.
2. EdTech can help to improve student engagement, motivation and learning outcomes.
3. EdTech is also being used to improve access to quality education for marginalized and vulnerable communities.

Overall, this research study demonstrates that EdTech can be used to improve access to education and learning outcomes.

**Conclusion:** In conclusion, this research study has demonstrated that EdTech can be used to improve access to education and learning outcomes. EdTech is being used to bridge the digital divide and to provide access to education in remote and rural areas, as well as to improve student engagement and motivation. Furthermore, EdTech is being used to improve access to quality education for marginalized and vulnerable communities. However, it is important to note that EdTech also has its limitations, such as the potential for digital divides to persist in certain areas and the need to ensure that EdTech is used in a way that is most beneficial to students and educators. Ultimately, EdTech can be a powerful tool for improving access to education and learning outcomes, but it is important to be aware of its potential drawbacks.

**References:**

1. Ertmer, P. A., & Ottenbreit-Leftwich, A. T. (2010). Teacher beliefs and technology integration practices: A study of change. *Journal of Research on Technology in Education*, 42(4), 255-284.
2. Mishra, P., & Koehler, M. J. (2006). Technological pedagogical content knowledge: A framework for teacher knowledge. *Teachers College Record*, 108(6), 1017-1054.
3. Manca, S., & Ranieri, M. (2016). The "level of use" of ICT in education: A critical review of the literature (2003-2014). *Journal of Educational Technology Development and Exchange*, 9(1), 1-27.
4. Suhr, D., & Thomas, K. (2015). An exploratory study of teachers' beliefs and practices regarding technology integration. *Journal of Research on Technology in Education*, 47(4), 363-384.
5. TechCrunch. (2020). India has the most Edtech startups in the world, with over 600. Retrieved from <https://techcrunch.com/2020/03/19/india-has-the-most-edtech-startups-in-the-world-with-over-600/>
6. Kaur, P., Gill, S. K., & Grewal, J. (2019). Impact of EdTech on quality education in India. *International Journal of Research in Education and Science*, 5(3), 566-574.
7. Thakur, P., & Kaur, G. (2016). Technology in Education: Impact on Student Learning Outcomes in India. *International Journal of Education and Research*, 4(7), 63-72.
8. The Economic Times. (2020). EdTech in India: Improving access and outcomes for learners. Retrieved from <https://economictimes.indiatimes.com/industry/services/education/edtech-in-india-improving-access-and-outcomes-for-learners/articleshow/77603513.cms>



- 
9. UNESCO. (2020). Harnessing the Power of EdTech to Create Quality Learning Opportunities for All. Retrieved from [https://en.unesco.org/sites/default/files/harnessing\\_the\\_power\\_of\\_edtech\\_to\\_create\\_quality\\_learning\\_opportunities\\_for\\_all.pdf](https://en.unesco.org/sites/default/files/harnessing_the_power_of_edtech_to_create_quality_learning_opportunities_for_all.pdf)
10. KPMG. (2021). India EdTech Report 2020. Retrieved from <https://assets.kpmg/content/dam/kpmg/in/pdf/2020/india-edtech-report-2020.pdf>
11. UNESCO. (2020). Harnessing the Power of EdTech to Create Quality Learning Opportunities for All. Retrieved from [https://en.unesco.org/sites/default/files/harnessing\\_the\\_power\\_of\\_edtech\\_to\\_create\\_quality\\_learning\\_opportunities\\_for\\_all.pdf](https://en.unesco.org/sites/default/files/harnessing_the_power_of_edtech_to_create_quality_learning_opportunities_for_all.pdf)

Impact Factor-8.575 (SJIF)

ISSN-2278-9308

# B.Aadhar

Single Blind Peer-Reviewed & Refreed Indexed  
Multidisciplinary International Research Journal

FEBRUARY 2023

(CCCLXXXVIII) 390

New Directions in Humanities



**SOCIAL SCIENCES  
AND HUMANITIES**

**Sociology**

Anthropology, Infant, Research, Injustice, Parent, Design, Fashion, Mental Health, Regulations, Communicate, Food preparation, Food security, Cognitive, Behaviour, Garments, Inquiry, Secondary source, Culture, Primary source, Record, Recipe, Nutrients, Identity, Group behaviour, Trends, Nutrition, Investigate, Psychology, Bias, Human origins, Metabolism, Fabrics, Equality, Family, Human mind, Thesis, Children, Assess, Analyz, Human mind

Chief Editor  
**Prof. Virag S. Gawande**  
Director  
Aadhar Social  
Research & Development  
Training Institute Amravati

Editor  
**Dr. Pradnya S. Yenkar**  
Principal,  
Vidya Bharati Mahavidyalaya,  
Camp, Amravati



This Journal is indexed in :

- Scientific Journal Impact Factor (SJIF)
- Cosmos Impact Factor (CIF)
- International Impact Factor Services (IIFS)

For Details Visit To : [www.aadharsocial.com](http://www.aadharsocial.com)

Aadhar PUBLICATIONS



Scanned with OKEN Scanner

**INDEX**

No.	Title of the Paper	Authors' Name	Page No.
1	Pandemic stress and challenges in education Dr. Vikas T. Adlok , Dr. Govind M. Tirmanwar		1
2	Challenges for Academic Libraries in Pandemic COVID 19 Dr. Vishalsingh Rameshsingh Shekhawat		4
3	Pandemic and Psychophysical Health Challenges	Dr. Sheetal Shinde	9
4	Impact of pandemic Covid-19 on Fisheries Dr. Anju P. Khedkar (Vikhar)		11
5	New Challenges in psycho-physical health in post-covid-19 Dr. P. B. Ingle		14
6	Historical Perspective of Pandemic in India	Prof. P. D. Shrungare	17
7	A Study on Use of Technology in Education: An Opportunity or A Challenge Dr. Pallavi Mandaogade (Jain)		21
8	The Relationship of Humanities to other Knowledge Domains Prof. Dr. Ananda B. Kale , Prof. Manisha Kirtane		26
9	R.K. Narayan's Malgudi days: The mirror of Society	Savita.M. Lonare	28
10	Student's Perspectives On Learning Physics During Pandemic R. B. Butley		30
11	Use of Surprise and Twist in the Short Stories of O. Henry Prof.V.P. Shekokar		35
12	A study of the Mental Stress and Mental health of Police Employee during Corona period Vidhya T. Ambhore		37
13	Relationship Between Narcissism, Social Media Use And Self Esteem Sonali Ramesh Khandekar , Dr. Shafiq Yusufkhan Pathan		42
14	Use of Technology in Education during the Pandemic Dr.Suraj K. Rodde		47
15	कोवीड-19 कालावधीनंतर महाविद्यालयीन विद्यार्थ्यांच्या मानसिक स्वास्थ्याचा अभ्यास वैशाली ढोले , रमेश पठारे		50
16	कोविड-१९ साथीच्यारोगाचा भारतीय अर्थव्यवस्थेवर होणारा आर्थिक व सामाजिक परिणाम प्रा. दिपाली अतुल पडोळे		58
17	कोव्हीड नंतरचे मानसिकस्वास्थ्य, आव्हाने व उपाय डॉ. गजानन र. रत्नपारखी		60
18	शिक्षण आणि आव्हाने डॉ. दामोदर दुधे		63
19	नंदा खरे यांच्या साहित्यातील नवजाणिवा अभिजित अशोक इंगळे		67
20	शैक्षणिक समस्यांचे विश्लेषणात्मक अध्ययन प्रा. अमरिश एस. गावंडे		70
21	डॉ. सुखदेव ढाणके यांच्या पिंडपातविषयी - आशयअभिव्यक्ती कु. ज्योती भिकुसा शेंदुरजणे , प्रा. गजानन बनसोड		74



## Use of Technology in Education during the Pandemic

**Dr.Suraj K. Rodde**

Associate Professor Vidya Bharati Mahavidyalaya, Amravati

### Abstract:

The terrible 2020 year filled the peaceful atmosphere with a very small but new effective organism known as novel coronavirus which had given a halt to the economy, trade and commerce, technology and education of the world.

Most of the educational institutes in India were unprepared for digital learning. Despite the challenges in education during the lockdown period, paradigm shift from offline learning to online learning took place. The rapid transition from offline learning to online learning could be achieved by means of science and technology. The traditional classroom confined to four walls with desks and benches, blackboards, whiteboards and textbooks are drastically replaced by technology. This paper aims to investigate use of technology in education during the pandemic focusing on teaching and learning imparted online.

**Keywords:** Technology, Education, Digital Learning, Pandemic

### Introduction

The educational system in India mostly follows conventional methods of teaching. When the nationwide lockdown was declared, it gave a sudden spasm to the flow of education creating tremendous impact on the students as well as teachers. Initially, the people of the world were unable to adjust to the corona pandemic but gradually people got themselves accustomed to the situation and started to adapt to new life situations. Though people have undergone many crises, problems and difficulties in all the perspectives yet the most affected one is Education. Literally speaking, education is the modification of human behavior. Education shapes and moulds the behavior of the students. Before the lockdown in the country, students could avail their education according to the conveniences of the society, community or region. The mode of teaching was also simple. But in the year 2020, education for the students especially in the remote rural regions was a very challenging task as the poorest students are affected the most by the closing of institutions during the pandemic. Thus it has become more complex. Hence the learning experiences and the behavior of the students continued to be moulded via technology.

The pandemic has compelled the nature of teaching and learning to embrace online learning employing various methods of technology but access to electronic devices became the main hurdle.

### Objective

The main objective of this paper is to obtain the experience of students studying in various classes by employing technology during the pandemic.

### Methodology

In this study the researcher used secondary data for this investigation which was gathered from research articles, journals, published reports and sources and information available on websites. This paper considers some factors such as faculty teaching tools, and student satisfaction in learning and assessment, and how pandemic affects the teaching and learning process. It is also noted that the psychology of the students in welcoming the online mode of learning or the acceptance of the students towards technology centered learning are addressed.

### Education during Pandemic

#### Readiness to learn online during pandemic

Students though vulnerable to stress and the burdens of pandemic, yet their desire, their readiness and the willingness to keep learning never ceased. Many students lack adequate ICT literacy skills but indicate that most of the students showed their readiness to learn during the pandemic. Once they are completely equipped with the required mobile devices, the excitement and the joy of learning through the usage of technology could not stop them from exploring many things and discovering many innovative ideas.

#### Emotional and mental condition of students during pandemic

Though the students showed their readiness to learn online yet some of students were mentally and emotionally disturbed and some was mentally stressed. This indicates that they were psychologically unstable and unprepared for their online learning. Anxiety among students occurs





during the lockdown because everyone was required to stay at home and all teaching and learning platforms took part virtually. Students' lost connection with human presence therefore it affects them mentally and emotionally. The education scenario during the lockdown was not impressive. There were many hurdles in facilitating the students' learning via online platform.

#### **Socio-economic status of students**

For online learning, electronic devices and gadgets such as android mobile phones, laptops, tablets are minimum requirements. There are few colleges which could really provide online learning to students. Thanks to Technology which introduced especially to deliver lectures and content presentations through Google Classroom, Google Meet, WhatsApp, Graphic Tablets etc. These apps and platforms helped to interact with students successfully. Introducing simple animations during their virtual classes to seek their attention and interest of the students really attentive and curious and enjoy learning and hence the attention span of the students was achieved.

#### **Google Classroom experience**

Assignments on various topics for various semesters are assigned in the Google Classroom. Tests are conducted using the Google Forms and Google Classroom as the students found it user friendly. Study materials are also provided in the Google Classroom. Semester examinations are conducted in blended mode i.e, online and offline. Technology and the internet has immensely contributed to the future career of our students as it has made learning more accessible. Despite many challenges everything became possible and was successfully achieved.

#### **Purchasing of new mobile phones**

The use of technology in education was undoubtedly a dream within a dream. To continue with the teaching and learning during the lockdown period, it was indeed very tough for the students to attend their classes online for few specific reasons such as poor internet connection, lack of availability of android phones, establishment of suitable place, lack of support from economic circumstances parents etc. Most of the students could equip themselves with necessary devices, yet another issue with some students could not obtain the gadgets thereby creating imbalance in imparting online classes. There was another serious problem posed before the parents and the guardians as they are not in a position to render technical guidance and assistance to prepare their children or their wards for online lessons adequately.

#### **Internet connectivity**

When the attendance of students was checked through Google Classroom it was found that some of the students missed their classes. When the investigator inquired their reason it was due to lack of proper internet connectivity they could not attend their classes. It is seen that some of the students had poor internet connectivity. It is suggested that the state government should take immediate steps in assisting the students with poor internet connectivity so that students do not miss their classes and can achieve better interaction with the teachers as well as with their peer friends.

#### **Google Classroom and Google Meet after Pandemic**

Students encountering trouble in accessing the online learning are dissatisfied with the ongoing teaching learning process as they could not avail the education being provided through online mode. As most of the students are not in favour of the online mode of learning through Google Classroom and Google Meet as the abrupt transition from direct learning to virtual learning has generated intense pressure in the students as well as parents.

#### **Suggestion and recommendation**

Online learning with different online learning tools and applications is undoubtedly not going to ensure learning of students effectively but it can be instruments for teachers to keep their students continue their learning even after pandemic to interact and communicate via online platforms. Though pandemic has created many difficulties and challenges in the lives of students, teachers and parents yet there are many ways in which technology has added a value to the student's academic achievement. It has also created in the students the desire and the passion and also the curiosity to learn. Students from higher Semesters i.e, recently passed out students are not only self-motivated to learn but taking the benefits of such platforms they attended webinars, online meetings and discussions and discover their innate skills and dispositions. They keep accessing plenty of resources on the internet and continue to study during lockdowns as they were on the verge of completing their graduation program to obtain a positive learning outcome. Thus the achievement motivation is attained.





The need of hour for the students is to have proper and adequate facilities in the educational system to experience and learn in real and virtual classrooms so that when unexpected times like pandemic and other consequences, students will not panic instead prepare themselves to overcome any problems.

#### **Conclusion**

From the overall analysis, it is understood that pandemic attacked the globe when most of the educational institutes were unprepared for online learning physically, mentally, emotionally and digitally. Despite the challenges in education during the lockdown period, paradigm shift from offline learning to online learning took place which has been clearly experience. The rapid transition from offline learning to online learning could be achieved by means of science and technology. At the first stage of using means of technology, the teachers and the students were less familiar with various modes of online learning platforms and virtual classrooms. Teachers had to adapt to new pedagogical skills and knowledge which requires self-training. Eventually, the teachers did not lose hope and they struggled to keep in touch with students. Teachers are to be applauded and appreciated for keeping the students involved and engaged even during the hard times of pandemic.

#### **References**

1. Nasir M.Khalid M. "The Influence of Social Presence on Students' Satisfaction toward Online Course" *Open Praxis*, 12, pp. 485-493, 2020
2. <https://www.frontiersin.org/articles/10.3389/fpsyg.2021.656776/ful>
3. <https://coed.dypvp.edu.in/educational-resurgence-journal>
4. <https://timesofindia.indiatimes.com/>
5. <http://sersc.org/journals/index.php/IJAST/article/view/25414>
6. <https://www.ericsson.com/en/blog/2020/5/impact-of-technology-on-education>
7. <https://www.brookings.edu/blog/education-plus-development/2021/08/23/>
8. <https://www.tandfonline.com/doi/full/10.1080/2331186X.2021.1964690>
9. <https://www.bgca.org/news-stories/2020/July/Teacher-Shares-Eye-Opening-Effect-of-School-Changes-and-COVID-19-on-Americas-Youth?>
10. <https://www.online-journals.org/index.phpand-infuse-it-into-a-current-educational-framework-1724540-2020-09-25>

## THE ROLE OF OPEN EDUCATIONAL RESOURCES (OERS) IN PROMOTING AFFORDABLE AND ACCESSIBLE HIGHER EDUCATION

Dr. Pratik. B. Upase Assistant Professor  
Department of Commerce, Vidya Bharati Mahavidyalaya, Amravati  
Maharashtra, India  
pratik.upase@gmail.com

### ABSTRACT

The study used a comprehensive review of existing literature on the use of OERs in higher education, including a systematic search of relevant databases and specific inclusion and exclusion criteria. The key findings indicate that OERs have the potential to significantly reduce the cost of higher education and increase accessibility for students, particularly those from disadvantaged backgrounds. The study also identifies several challenges and gaps in the literature, including issues related to OER quality and sustainability, faculty adoption, and institutional support. The review concludes with recommendations for policymakers, administrators, and educators on how to effectively implement and promote the use of OERs in higher education to improve affordability and accessibility. Overall, the study highlights the importance of OERs as a means of promoting affordable and accessible higher education, and calls for continued research and development in this area.

**Keywords:** Open Educational Resources (OERs), Higher Education, Affordability, Accessibility, Student Success, Institutional Support

### Introduction

The cost of higher education has been a major concern for students, parents, and policymakers for several decades. This has led to a significant increase in student debt and has made higher education increasingly unaffordable for many students.

In response to these challenges, there has been growing interest in the role of Open Educational Resources (OERs) in promoting affordable and accessible higher education. OERs are educational resources. They include materials such as textbooks, course materials, videos, and other educational resources that can be accessed online for free.

The use of OERs has the potential to significantly reduce the cost of higher education for students. By providing free access to educational materials, OERs can eliminate the need for students to purchase expensive textbooks and other course materials, which can save them hundreds or thousands of dollars per year. OERs also provide greater flexibility and customization options for course materials, which can lead to more effective teaching and learning.

In addition to promoting affordability, OERs can also enhance accessibility to higher education. By providing free access to educational resources, OERs can help to level the playing field and provide greater opportunities for students from diverse backgrounds to access higher education.

### Research Question and Objectives

**Research Question:** What does existing research suggest about the role of Open Educational Resources (OERs) in promoting affordable and accessible higher education, and what are the implications for higher education institutions, policymakers, and educators?

**Objectives:**

1. To conduct a comprehensive review of existing literature on the use of OERs in higher education and their impact on affordability and accessibility.
2. To identify trends, gaps, and challenges in the existing literature on the use of OERs in higher education.
3. To provide recommendations for policymakers, administrators, and educators on how to effectively implement and promote the use of OERs in higher education to improve affordability and accessibility based on the findings of the literature review.

### Methodology

The methodology used was a comprehensive review of existing literature on OERs in higher education. This methodology involved conducting a systematic search of relevant databases. Data were extracted and synthesized from the selected studies to identify trends, gaps, challenges, and effectiveness of OERs in promoting affordability and accessibility in higher education. The findings were then critically evaluated and

used to provide recommendations for policymakers, administrators, and educators on how to effectively implement and promote the use of OERs in higher education to improve affordability and accessibility.

### Literature Review

The existing literature (OERs) in promoting affordable and accessible higher education is vast and diverse, with a range of studies examining different aspects of the topic. The literature can be broadly categorized into three areas: (1) the impact of OERs on affordability and accessibility, (2) the challenges and opportunities of implementing OERs in higher education institutions, and (3) best practices .

Despite the potential benefits of OERs, several challenges and gaps exist in the literature. One of the major challenges is the lack of awareness and adoption of OERs by faculty and administrators (Atenas, 2015). A study by Jhangiani et al. (2018) found that while 88% of faculty members were aware of OERs, only 20% had adopted them in their courses.

Another challenge is the lack of quality control and curation of OERs (Weller, 2014). Since OERs are often created by individuals or small teams without rigorous peer review, there is a risk of inaccuracies, biases, and outdated information in these resources. Additionally, the lack of standardization and interoperability of OERs makes it difficult for educators to find, use, and adapt them for their specific needs (Hilton, 2016).

The use of Open Educational Resources (OERs) in higher education has gained significant attention over the past decade due to its potential to enhance affordability and accessibility. According to Stagg (2020), OERs are openly licensed resources that can be used for teaching, learning, and research purposes. These resources include textbooks, videos, podcasts and other learning materials.

Numerous studies have examined the impact of OERs on affordability and accessibility in higher education. For instance, Hilton (2016) conducted a meta-analysis of 16 studies and found that students who used OERs performed as well or better than those who used traditional textbooks, and also saved a significant amount of money on textbook costs. Similarly, a study by Kimmons and Veletsianos (2016) found that students who used OERs reported higher levels of satisfaction with their course materials and increased engagement with the course content.

In higher education, as a means of improving affordability and accessibility for students. OERs are defined as "teaching, learning and research resources that are free of cost and may be reused, revised, remixed and redistributed" (UNESCO, 2012). They can include a wide range of digital content, such as textbooks, videos, simulations, and interactive learning objects.

Many studies have examined the impact of OERs on various aspects of higher education, including student learning outcomes, student engagement, faculty adoption, and institutional sustainability. Some studies have found that OERs can improve student learning outcomes and engagement, by providing more flexible and personalized learning experiences (Cronin, 2017; Wiley et al., 2014). Other studies have focused on the barriers and challenges to OER adoption, such as the lack of incentives for faculty, the need for technical support, and concerns about quality (Petrides et al., 2011; Bliss et al., 2013).

Despite these challenges, many universities and colleges around the world have embraced OERs as a means of improving access to education. For example, the Open University in the UK has developed a comprehensive OER policy that promotes the use and creation of OERs across all disciplines (Ferguson et al., 2011). In the US, the Open Textbook Network has developed a network of over 800 institutions that have adopted open textbooks as a means of reducing textbook costs (Hilton et al., 2016).

In terms of recommendations for policymakers, administrators, and educators, several studies have highlighted the importance of creating supportive institutional policies and providing faculty with training and resources to effectively use OERs (Hilton et al., 2013; Stacey et al., 2015). Others have suggested the need for collaborative approaches to OER development and dissemination, such as the creation of OER consortia and partnerships between universities and publishers (Atkins et al., 2007; Neumann et al., 2017).

Studies on the impact of OERs on affordability and accessibility have found that the use of OERs can significantly reduce the cost of higher education for students. OERs can eliminate the need for students to purchase expensive textbooks and other course materials, which can save them hundreds or thousands of dollars per year. OERs also provide greater flexibility and customization options for course materials, which can lead to

more effective teaching and learning. In addition, OERs can enhance the accessibility of higher education by providing free access to educational resources for students from disadvantaged backgrounds.

However, studies have also identified several challenges and opportunities of implementing OERs in higher education institutions. These include issues related to copyright and licensing, technical infrastructure, faculty awareness and support, and the need for effective policies and guidelines to promote the use of OERs. Despite these challenges, studies have also identified several best practices and strategies for effectively implementing OERs in higher education institutions, including the use of faculty incentives and training, collaboration between institutions and stakeholders, and the development of effective policies and guidelines.

To effectively implement and promote the use of OERs in higher education, several recommendations have been proposed in the literature. First, there is a need for increased awareness and education about OERs among faculty, administrators, and students (Atenas et al., 2015). This can be achieved through professional development opportunities, workshops, and training programs that focus on the benefits and effective use of OERs in teaching and learning.

Second, there is a need for increased collaboration and networking among OER practitioners and advocates to promote the sharing and dissemination of high-quality OERs (Weller, 2014). This can be achieved through the establishment of OER repositories, open licensing policies, and peer-review mechanisms for OERs.

According to Hilton III (2019), students who use OERs are more likely to complete their courses successfully and have better grades compared to those who use traditional resources. Additionally, the cost savings associated with the use of OERs can be substantial, with studies showing savings of up to \$128 per student per course (Hilton III et al., 2019).

However, despite the potential benefits of OERs, their adoption and implementation in higher education institutions remain limited. Factors that have been identified as barriers to the adoption and implementation of OERs include a lack of awareness and understanding of OERs, the absence of incentives for faculty to adopt OERs, and the lack of institutional support (Hilton 2019). Furthermore, the quality and relevance of OERs have also been questioned, with some scholars arguing that OERs may not always be of high quality and may not meet the needs of all students (Allen & Seaman, 2017).

Despite these challenges, there have been efforts to promote the use of OERs in higher education. For example, the U.S. Department of Education has launched the Open Textbook Pilot program, which provides grants to colleges and universities to promote the use of OERs (Lindshield & Adhikari, 2019). Additionally, some institutions have implemented policies that require faculty to consider OERs when selecting course materials (Hilton III et al., 2019).

Overall, the existing literature suggests that the use of OERs has the potential to promote affordable and accessible higher education, but effective implementation requires careful consideration of the challenges and opportunities involved. Further research is needed to explore the long-term impact of OERs on affordability and accessibility in higher education and to identify additional best practices and strategies for promoting their use.

The existing literature suggests that the use of OERs has the potential to promote affordability and accessibility in higher education. However, there are several challenges that must be addressed to ensure the effective adoption and implementation of OERs. Higher education institutions should provide faculty with the necessary support and incentives to adopt OERs, while policymakers should consider implementing policies that encourage the use of OERs. Educators should also be aware of the potential benefits and limitations of OERs and be able to effectively integrate them into their teaching.

### **Discussion of the Key Theories, Concepts, and Debates in the Literature**

OERs in promoting affordable and accessible higher education is underpinned by several key theories, concepts, and debates. These include:

1. **Open education:** The concept of open education is central to the use of OERs in higher education. Open education is an approach to teaching and learning that emphasizes the free and open sharing of knowledge and resources. OERs are a key component of open education, as they enable educators to share course materials, textbooks, and other resources freely with students.
2. **Cost and affordability:** OERs can significantly reduce the cost of higher education for students. Studies have found that the cost of textbooks and other course materials can be a major barrier to

higher education for students from disadvantaged backgrounds. OERs provide a way to eliminate this cost barrier and make higher education more accessible.

3. **Access and equity:** The use of OERs can also enhance the accessibility of higher education by providing free access to educational resources for students from disadvantaged backgrounds. This is particularly important in countries and regions where access to higher education is limited by economic, social, or geographical factors.
4. **Copyright and licensing:** One of the key challenges of using OERs is navigating the complex landscape of copyright and licensing laws. The reuse and remixing of OERs can be limited by copyright restrictions, and educators need to be aware of these limitations when using OERs in their teaching.
5. **Faculty awareness and support:** Another challenge of using OERs is the need for faculty awareness and support. Many educators may be unfamiliar with OERs or may be resistant to using them in their teaching. Institutions need to provide training and support to faculty to ensure that they are aware of the benefits of OERs and how to use them effectively.
6. **Policy and governance:** The use of OERs also requires effective policy and governance structures to promote their adoption and implementation. Institutions and policymakers need to develop guidelines and policies that promote the use of OERs, support faculty in using them effectively, and ensure that they are sustainable and scalable over time.

Overall, the literature on the role of OERs in promoting affordable and accessible higher education highlights the importance of open education, cost and affordability, access and equity, copyright and licensing, faculty awareness and support, and policy and governance. These concepts and debates are central to understanding how OERs can be effectively used in higher education to promote affordability and accessibility.

The increasing cost of textbooks and other educational materials has led to the emergence of OERs as an alternative to traditional, costly resources. OERs have the potential to promote affordable and accessible higher education, but their effectiveness in achieving this goal has been the subject of much research and debate. This study provides existing research on the role of OERs in promoting affordability and accessibility in higher education and its implications for higher education institutions, policymakers, and educators.

## **Findings and Conclusion**

### **Summary of the key findings:**

The analysis of the existing literature on the role of Open Educational Resources (OERs) in promoting affordable and accessible higher education has yielded several key findings. First, the use of OERs has the potential to significantly reduce the cost of higher education for students, particularly in developing countries where access to affordable educational resources is limited. Second, OERs have been shown to improve student engagement and learning outcomes, as well as increase access to higher education for underrepresented groups such as low-income and minority students.

Third, the implementation and adoption of OERs in higher education institutions are influenced by a variety of factors, including institutional policies, faculty attitudes and beliefs, technical infrastructure, and funding. Fourth, while there is a growing body of research on the use of OERs in higher education, there are still significant gaps in the literature, particularly regarding the long-term sustainability and impact of OER initiatives.

Finally, the implications of these findings for higher education institutions, policymakers, and educators are clear. Institutions should prioritize the adoption and implementation of OERs as a means of promoting affordability and accessibility, and policymakers should provide support and funding for OER initiatives. Educators should be trained and supported in the use of OERs to enhance student learning, and efforts should be made to address the digital divide and ensure that all students have access to the necessary technology to use OERs effectively. Overall, the findings suggest that OERs have the potential to play a significant role in promoting affordable and accessible higher education, but continued research and investment are needed to fully realize this potential.

### **Conclusion**

Overall, the existing literature suggests that the use of OERs can promote affordability and accessibility in higher education. However, there are challenges that need to be addressed to ensure the effective adoption and implementation of OERs. Higher education institutions, policymakers, and educators should work together to address these challenges and promote the use of OERs to improve the quality and accessibility of higher education.

### Scope of Further Research

Despite the growing body of research on the role of Open Educational Resources (OERs) in promoting affordable and accessible higher education, there are still some areas that require further exploration. One possible avenue for future research is to investigate the potential impact of OERs on students' long-term academic and professional outcomes. Additionally, more research is needed to understand the factors that influence the adoption and implementation of OERs in different educational contexts, as well as the challenges that educators face when designing and delivering OER-enabled courses.

Another area of future research is to explore the effectiveness of different strategies for promoting the adoption and use of OERs among students and educators, such as incentives, training, and support. It may also be useful to investigate the potential of OERs to enhance the quality and relevance of higher education, and to provide learners with more flexible and personalized learning experiences. Finally, future research could explore the role of OERs in promoting equity and social justice in higher education, and the extent to which OERs can help to address disparities in access to education and opportunities for learning.

### References

- Atenas, J., Havemann, L., & Priego, E. (2015) "Open data as open educational resources: Towards transversal skills and global citizenship". *Open Praxis*, 7(4), 377-389. <https://doi.org/10.5944/openpraxis.7.4.233>
- Atkins, D., Brown, J., & Hammond, A. (2007). "A review of the open educational resources (OER) movement: Achievements, challenges, and new opportunities" Report to The William and Flora Hewlett Foundation.
- Bliss, T., Hilton, J., Wiley, D., & Thanos, K. (2013). "The cost and quality of online open textbooks: Perceptions of community college faculty and students". *First Monday*, 18(1). <https://doi.org/10.5210/fm.v18i1.3972>
- Bliss, T. J., Robinson, T. J., Hilton, J., & Wiley, D. A. (2013). "An OER framework, heuristic, and lens: Tools for understanding lecturers' adoption of OER". *Journal of Interactive Media in Education*, 1(18), 1-16. <https://doi.org/10.5334/2013-18>
- Colvard, N., Watson, C., & Park, H. (2018). "The impact of open educational resources on various student success metrics." *International Journal of Teaching and Learning in Higher Education*, 30(2), 262-276.
- Cronin, C. (2017). "Open education, open questions." *Learning, Media and Technology*, 42(2), 117-120. <https://doi.org/10.1080/17439884.2017.1416323>
- DeRosa, R., & Robinson, T. (2017). From OER to open pedagogy: Harnessing the power of open. *Journal of Interactive Media in Education*, 1(5), 1-10. <https://doi.org/10.5334/jime.440>
- Ferguson, R., Scanlon, E., & Harris, L. (2011). "Institutional policies supporting effective OER practices: A synthesis of findings from the Open University UK" In *Proceedings of the 4th OER Workshop*.
- Hilton III, J. (2016). "Open educational resources and college textbook choices: A review of research on efficacy and perceptions". *Educational Technology Research and Development*, 64(4), 573-590. <https://doi.org/10.1007/s11423-016-9434-9>
- Hilton III, J., Fischer, L., Wiley, D., & Williams, L. (2016). "Maintaining momentum toward graduation: OER and the course throughput rate" *International Review of Research in Open and Distributed Learning*, 17(6), 18-27.
- Hilton III, J., & Wiley, D. (2010). "A sustainable future for open educational resources?" *The Journal of Distance Education*, 24(2), 1-13. <https://doi.org/10.1080/01587919.2010.503062>
- Jhangiani, R., & Jhangiani, S. (2017). "Investigating the perceptions, use, and impact of open textbooks: A survey of post-secondary students in British Columbia." *The International Review of Research in Open and Distributed Learning*, 18(4). <https://doi.org/10.1007/s11423-016-9434-9>
- Li, Y., & Zhang, Y. (2019). "The influence of open educational resources on students' learning outcomes: A meta-analysis". *Educational Technology & Society*, 22(1), 1-13.
- Mulder, F. (2013). "Open educational resources: A catalyst for innovation, educational research and innovation". OECD Publishing. doi: 10.1787/9789264185363-en
- National Institute of Open Schooling. (2016). "Open educational resources. Retrieved from <https://www.nios.ac.in/media/documents/OER.pdf>"
- Rolfe, V. (2016). "Open educational resources: Staff attitudes and awareness", *Research in Learning Technology*, 24.
- Smith, M., & Casserly, C. (2006). "The promise of open educational resources. *Change: The Magazine of Higher Learning*" 38(5), 8-17. doi: 10.3200/CHNG.38.5.8-17
- Stagg, A. (2014) "A guide to developing digital literacies in new teachers: Models, frameworks and exemplars" *Australian Journal of Teacher Education*, 39(6), 146-163.
- Weller, M. (2014). "Battle for open: How openness won and why it doesn't feel like victory. London:" Ubiquity Press. doi: 10.5334/bam

Wiley, D., & Hilton III, J. (2018) "Defining OER-enabled pedagogy" *The International Review of Research in Open and Distributed Learning*, 19(4), 133-147.



## Transition from IPv4 to IPv6 Network in IoT Security Based Upon Transition Methods

Ms. Shilpa B. Sarvaiya<sup>1</sup>, Dr. D. N. Satange<sup>2</sup>

<sup>1</sup>Department of Computer Science, Vidyabharati Mahavidyalaya, Amravati, Maharashtra, India

<sup>2</sup>Director, Student Development, S. G. B. A. University, Amravati, Maharashtra, India

-----\*\*\*-----  
**Abstract:** While deployments of IPv6 networks have increased over recent years, especially in IoT Paradigm. Today there are two types of internet protocol versions that are currently working in the global internet to transfer data from one electronic device to another. IPv4 which consists of 32 bits long addresses and IPv6 which consists of 128 bits long addresses which is more effective as it can handle billions of devices and can assign each device different IP address. This paper will present an overview of the main migration technologies that can be used to transition from an IPv4 network to an IPv6 network, this paper will also research on finding and comparing the effects of IPv6 transition methods such as Dual Stack, Tunneling and Network Address Translation-Protocol Translation will be compared on variant parameters to find the best performing transition method in IoT Network in terms of security.

**Keywords:** IoT (Internet of Things), IPv4 (Internet Protocol Version 4), IPv6 (Internet Protocol Version 6), Transition Methods, Dual Stack, Tunneling, NAT-PT.

### 1. Introduction:

In the modern area there are two types of internet protocol versions that are currently working in the global internet to transfer data from one electronic device to another. IP address are assigned to every device and every device has its unique address generated through binary values consists of 0 and 1. Today these two versions of Internet protocol are widely used to connect different networks to each other. IPv4 is the earlier version of IPv6. IPv4 consists of 32 bits long addresses and each unique address is assigned to each device so data can be transmitted to that specific address [1].

The new version of Internet Protocol was published in 1996 called IPv6 which consists of 128 long bits addresses. Due to large number of growths in electronic

devices, an IPv4 address was not enough to cover all the devices. To resolve the issue IPv6 introduced which can handle billions of devices and more than that and assign each device different unique address that is IP address. IPv6 found out much better and efficient in addressing of devices, routing of networks, security of information and data, translation of network address also in support of configuration of protocol. Assign a unique IP address IoT devices establish a secure communication channel, their connection should be bootstrapped through the so-called device binding process and visualize sensor data, users can easily understand the physical environment and operate the devices [2].

A variety of transition methods are available to facilitate the migration to IPv6. These methods have been observed and compared with each other and the effects of these transition methods on IPv6 in IoT security. These transition strategies are observed and compared that are Dual-Stack, Tunneling and NAT-PT. Each method or technique has its own pros and cons and each method performs its own strategy [3].

### 1.1. Importance of IPV6 Network in IoT Security:

The internet communications have evolved rapidly after the creation of IPv6 Internet Protocol version 6. The major difference of IPv6 is that it allows more unique addresses to create. There are five major reasons why IPv6 is more important and better option for the IoT network paradigm than IPv4 Internet Protocol version 4.

#### First and most important one is the security:

Security is the most important feature used to secure the communication between the IoT devices from threats, virus, attacks, etc. IPv6 uses end-to-end encryption technology which can encrypt the data so it can be secured and cannot be hacked. IPv6 also supports more secure and safe name resolution than IPv4.

**Second is the scalability:** Ipv6 protocol provides the connections of devices in more scalable form. It provides large area of devices so they can connect together on a large scale communicating over a long distance as well [4].

**Third is the connect ability:** which means connecting billions of devices to each other and allow a networking protocol so they can transfer data to each other. IPv6 allows much more addresses than IPv4 so billions of devices can connect to each other.

**Fourth is Internet Protocol version 6 uses multicasting:** To transmit data packets from one

destination to another means IPv6 supports multicasting of packets at one time in different destinations.

**Fifth is IP Protocol version 6 providing Authentication:** IP version 4 does not provide authentication whereas IP version 6 provides Authentication as well as Confidentiality, Integration, and Access control of each data packet [5].

The overall graph of the adoption of IPv6 by Internet users since late 2015 to 2025 is shown in figure 1.

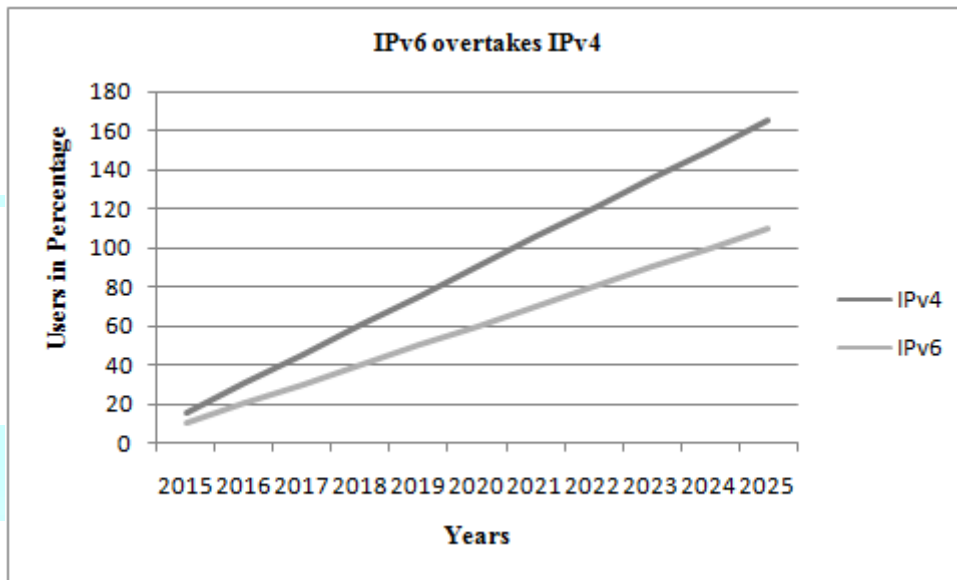


Figure 1: Growth from IPv6 to IPv4 Network

**2. History:**

In late 1960's there was a great need and demand of research centres and universities to develop a protocol or networking system to exchange data. To overcome this need ARPA (Advanced Research Project Agency) developed a net called ARPANET from 1972 it renamed DARPA from ARPANET [6].

In 1981 the ARPANET developed a transfer control protocol called IPv4 which was a huge success [7].

After 1990's IPv4 address space was getting full and at that time there was not enough addresses left to assign the new devices [8].

The new version of Internet Protocol was published in 1996 called IPv6 which consists of 128 long bits addresses. IPv6 found out much valuable and impressive as compared to IPv4 and it found out much better and efficient in addressing of devices, routing of networks, security of information and data, translation of network address and in support of configuration of protocol [9].

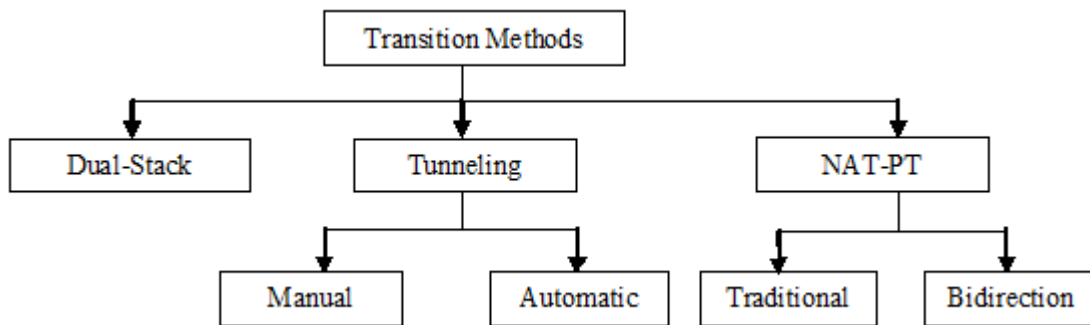
Still now these two versions are using. Both internet protocols have different configurations and are used in different environment. A census of the Internet's connected devices would readily number in the tens of billions of devices. If they all needed a globally unique permanent IP address, IPv6 would have been an imperative over a decade ago [10].

**3. Transition from IPV4 to IPV6 Network in IoT Security:**

There is not complete transition from IPv4 to IPv6 because IPv6 is not backward compatible. However; there are three methods, which can convert IPv4 to IPv6. The methods that can convert IPv4 to IPv6 are described as below.

**3.1. Transition Methods:**

One of the most important parts of implementing IPv6 is being able to gracefully transition from IPv4. The methods discussed in this paper can each be used as option when beginning an IPv6 deployment and should each be looked over for applicability depending on the specific requirements of an organization. There are three main methods that can be used when transitioning a network from IPv4 to IPv6 in IoT environment. These methods are 1) Dual-Stack, 2) Tunneling and 3) NAT-PT is explained in this section.

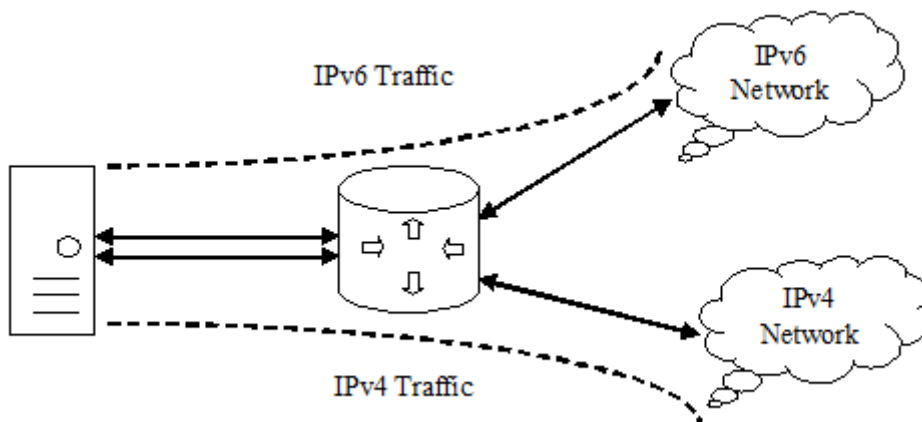


**Figure 2: Types of Transition Methods**

**3.1.1. Dual-Stack Method**

Dual Stack can process both IPv4 and IPv6 traffic simultaneously. The increase of devices day by day, it seems we are running out of IP address in IPv4 for each format which seems a big issue. IPv6 is the solution which is a new IP address format. The ISPs (Internet Service Provider) task is to provide net connections to their customers which are IPv4-to-IPv4 or IPv6-to-IPv6 but because of Dual Stack, every network is configured on both IPv4 and IPv6 and data can follow or both protocols simultaneously. Dual Stack equipped with both of the stacks, it can disable any of the stack when required either IPv4 or IPv6 and also can run both at same time [11].

Dual Stack is a simple transition method or solution that supports both internet protocols. Dual Stack devices like PC, a router or a server and other IoT (internet of things) can support both IPv4 and IPv6. This transition method is effective because IPv4 is not compatible sometimes on IPv6 devices and vice versa. Dual Stack includes both protocols working parallel which can be applied on both end system to establish connection and flow [12].



**Figure 3: Dual Stack Router Connectivity**

In the above figure 3, a server having IPv4 as well as IPv6 address configured for it can now speak with all the hosts on both the IPv4 as well as the IPv6 networks with the help of a Dual Stack Router. The dual Stack Router can communicate with both the networks. It provides a medium for the hosts to access a server without changing their respective IP versions.

### 3.1.2. Tunneling Method

For minimizing the transitions, all the routers on the way between the two IPv6 nodes do need to support IPv6. This method of transition is called Tunneling. Primarily IPv6 packets are placed inside IPv4 packets then the packets are routed through the IPv4 routers.

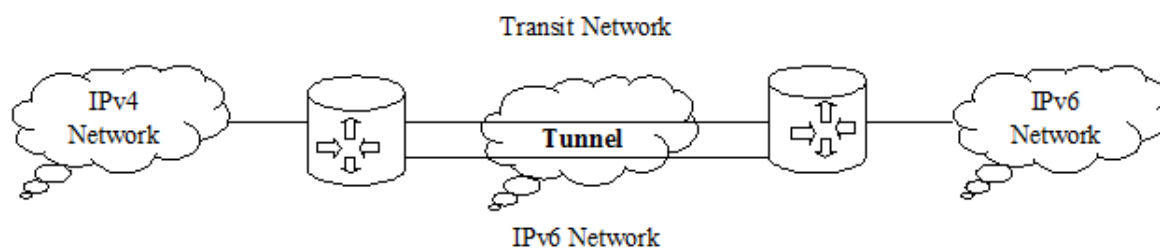
Tunneling is another transition method that provides a way or a tunnel to use IPv4 infrastructure to carry traffic of IPv6. This method uses routing infrastructure of one internet protocol to carry internet protocol traffic via channel also called tunnelling. Tunneling can be used as Router-to-Router or Host-to-Router or Host-Host or Router-to-Host. Most of the internet traffic is carried from one router or host to another via tunnels to migrate from IPv4 to IPv6 as the different devices uses different versions. IPv4 which is a 32-bit address can support around 4.3 billion devices where as IPv6 uses 128-bit address and support much more devices i.e. 2 times to 128 power [12].

The Tunneling method is also divided into two types of methods one is Manual Tunneling and another one is Automatic Tunneling are listed below.

**Manual Tunneling:** Tunnels which uses peer to peer topology and need manual configuration called manual IPv6 tunnel.

**Automatic Tunneling:** Tunneling uses the embedded address information of IPv4 in IPv6 packet then this type of tunnelling known as Automatic Tunneling.

In a scenario where different IP versions exist on intermediate path or transit networks, tunneling provides a better solution where user's data can pass through a non-supported IP version.



**Figure 4: Tunneling Between Ipv6 over IPv4 Network**

The above figure 4 depicts how remote IPv4 networks can communicate via a Tunnel, where the transit network was on IPv6. Vice versa is also possible where the transit network is on IPv6 and the remote sites that intend to communicate are on IPv4.

### 3.1.3. Network Address Translation-Protocol Translation (NAT-PT)

This is another important method of transition to IPv6 by means of a Network Address Translation-Protocol Translation (NAT-PT) enabled device. With the help of a NAT-PT device, actual can take happens between IPv4 and IPv6 packets and vice versa.

Network Address Translation ( NAT) method facilitates communication between IPv4-only and IPv6-only network by translating two different IP address families. This method translates IPv6 from IPv4 and gives consistent Internet experience to the users by accessing contents over the Internet, which have Ipv4 services. NAT-PT is similar to the NAT system utilized in IPv4 that is frequently used for converting private (RFC 1918) IPv4 address to public IPv4 address and vice versa. It is used to convert IPv4 address to IPv6 address and vice versa. This method should be used only when there are no other techniques to allow IPv6-only devices to communicate with IPv4-only devices [13].

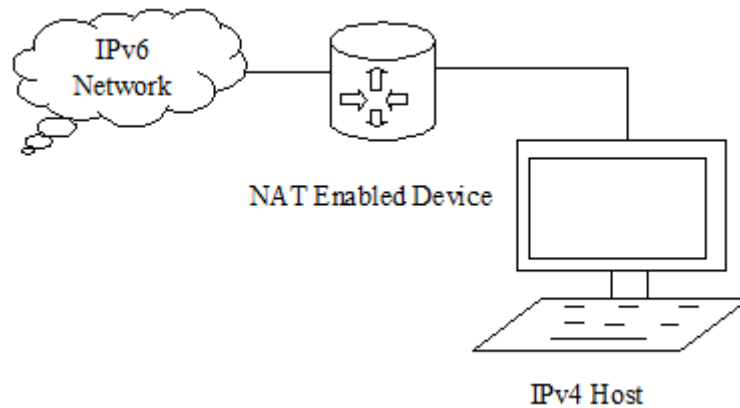


Figure 5: NAT-Protocol Translation Basic Operation

In the above figure 5, a host with IPv4 address sends a request to an IPv6 enabled server on Internet that does not understand IPv4 address. In this scenario, the NAT-PT device can help them communicate. When the IPv4 host sends a request packet to the IPv6 server, the NAT-PT device/router strips down the IPv4 packet, removes IPv4 header, and adds IPv6 header and passes it through the Internet. When a response from the IPv6 server comes for the IPv4 host, the router does vice versa.

In IPv6, there are two types of NAT-PT

**Traditional:** Traditional NAT-PT where sessions from IPv6 network are unidirectional. In this type, it allows hosts that are in IPv6 network to access the hosts that are in IPv4 network.

**Bidirectional:** In Bidirectional NAT-PT, sessions from both networks can be initiated i.e. from hosts in the IPv6 network as well as in the IPv4 network.

NAT-PT transition method main task is to migrate from IPv4 to IPv6 and also to provide connection bidirectional between IPv6 and IPv4.

#### 4. Comparison between Transition Methods of IPv6 over IPv4:

All three transition methods are observed, compared and the effect of transition methods in IoT security. All transition methods are useful in some way and all of them has pros and cons according to the system. Comparison has been observed and studied that is presented below [14, 15].

Table1: Comparative Analysis of Three Transition Methods

Parameters/Transition Methods	Dual-Stack	Tunneling	NAT-PT
Latency	Medium	Low	High
Throughput	Moderate	Highest	Lowest
Packet Loss	High	Low	High
Traffic	High	Low	Medium
Packet Delivery	Fast	Fast	Slow
Delay	Minimum	Minimum	Maximum
Security	Higher	Lowest	Average
Connectivity	Bidirectional	Bidirectional	Bidirectional
Transition Approach	Simplest	Complex	More Complex
Flexibility	Greatest	Moderate	Lowest
Cost	Low	High	Medium
Advantages	Easy to implement. Already supported in all Operating System and Devices.	Simple Deployment. No Additional Management.	Solve Network Issues. The Router is used as a Translation Communicator.

<b>Drawbacks</b>	Required additional Memory and CPU Power. Two Routing Tables.	Harder to troubleshooting and Network Management Vulnerable to security attacks	Complexity increases in IP addresses. Reduction in the overall value and utility of the network.
<b>Limitations</b>	Two firewalls sets of policies.	Have single points of failure.	Harder to control on a larger scale
<b>Performance Analysis</b>	Dual-Stack transition method shows better performance in the network compared to Tunneling in terms of Latency and Delay.	Better deliverables are produced in terms of Packet Delivery and Delay.	Rapid Deployment mechanism is convenient and easy to manage. However it has low flexibility.

**5. Problems and Discussion:**

It is most important that the transition from IPv4 to IPv6 is stable and Non-Interruptive to exiting services. The effect of IPv6 over IPv4 transition methods in IoT security includes the problems in the following majors' areas: Address Architecture, Connectivity, 3) High Availability, 4) Applications and 5) Network Management [16, 17].

- 1. Address Architecture Problems:** IPv6 has much larger address space in comparison with IPv4. Due to the large IPv6 address space, special attention is needed when designing the IPv6 network since it differs from the fragmented and smaller IPv4 address design.
- 2. Connectivity Problems:** While shifting the transition from IPv6 to IPv4 network to provide continuity of services to the users. The Dual-Stack is the natural approach but due to the depletion of IPv4 address, cost and up-gradation of the network to IPv6-only.
- 3. High Availability:** High Availability is the major requirement for every service and network service. An application running on IPv6 may need to failover to IPv4 network due to network failure during transitioning.
- 4. Applications Problems:** During the transition process, IPv4 and IPv6 applications will co-exist in the network. Regardless of what technology providers choose to use, services should be provided to the customers. Users should find out the best for the transition without affecting the services they provide.
- 5. Network Management:** New technologies and methods may be introduced during the transition process. These new technologies and techniques require new operation models.

**6. Conclusion:**

In this paper, the three transition methods of the IPv4 to IPv6 transition have been discussed, deployed and compare. It has been found that these three methods have distinct advantages, drawback and features. The appropriate transition mechanism will be chosen for the network based on various parameters like the size of the network, the availability of the latest devices, the cost, and the security concern. If Latency, Throughput and Packet Loss are considered then Tunneling method is the best choice as compare to the Dual-Stack and NAT-PT. But the Tunneling method has vulnerable to security attacks, solved these security issues by IPSec (IP Security). So, our recommendation is to use Tunneling mode with IPSec for the transition purpose. The Dual-Stack remains more popular and practical with low cost in implementation and supported by wide range of devices. Transition Methods, like Tunneling and NAT-PT, are not optimally supported for the networks during a transition from IPv4 to IPv6. Thus; Dual-Stack seems the preferable method to begin adopting IPv6 with upgradable devices in order to securely manage the exiting IPv4 infrastructure. The deployment of IPv6 over IPv4 network is the best way for the growth of IoT's devices as well as also improvement in terms of their security.

**7. References:**

1. Farhan Anwar Ghumman, "Effects of IPv4/IPv6 Transition Methods in IoT (Internet of Things): A survey" SSRN-ID: 3402664, PP. 01-06, 19 June 2019.
2. Abubakar Isa and Idris Abdulmumine, "Design and Comparison Migration between IPv4 and IPv6 Transition Techniques", Proceedings of the

- 3<sup>rd</sup> Yusuf Maitama Sule University, Kano, PP. 179-189, November 2017.
3. Steffen Hermann and Benjamin Fabian, "A Comparison of Internet Protocol (IPv6) Security Guidelines", Future Internet 2015, ISSN: 1999-5903, PP. 01-61, 24 May 2015.
4. C. V. Ravi Kumar et al, "Performance Analysis of IPv4 to IPv6 Transition Methods", Indian Journal of Science and Technology, ISSN: 0974-6846, Vol. 9, PP. 01-08, May 2016.
5. Aparna Sivaprakash and S. Kayalvizhi, "A Survey on Optimal IPv4 to IPv6 Transition Techniques" International Journal of Research Granthaalayah, ISSN: 2350-0530, Vol. 4, Issue 4; PP. 90-96 April 2016.
6. Iman Akour, "Between Transition from IPv4 and IPv6 Adaption: The Case of Jordanian Government", International Journal of Advanced Computer Science and Applications (IJACSA), Vol. 7, No. 9, PP. 248-252, 2016.
7. Md. Asif Hossain et al, "Performance Analysis of Three Transition Mechanisms between IPv6 Network and IPv4 Network: Dual Stack, Tunneling and Translation", International Journal of Computer (IJC), ISSN: 2307-4523, Vol. 20, No. 1, PP. 217-228, 2015.
8. Daniel Enache et al, " A Study of the Technology Transition From IPv4 to IPv6 For An ISP", Review of the Air Force Academy, Vol. 1, PP. 117-121, 2016.
9. I Kullayamma et al, "Scenarios in Migration of Networks from IPv4 to IPv6", International Journal of Lates Trends in Engineering and Technology-ISSN: 2278-621XVol. 8, Issue 1, PP. 097-105, 2015.
10. Edwin S. Cordeiro, "Comparison between IPv4 to IPv6 Transition Techniques", arXiv, PP. 01-11, 1 Dec 2016.
11. Peng Wu et al, "Transition from IPv4 to IPv6 a State-of-the-Art Survey", In IEEE Communications Surveys and Tutorials, Accepted for Publication, 2015.
12. Pyung Soo Kim, "Analysis and Comparison of Tunneling based IPv6 Transition Mechanisms", International Journal of Applied Engineering Research, ISSN: 0973-4562, Vol. 12, No. 6, PP. 894-897, 2017.
13. Nellore Karthikeyan and K. Chandra Mouli, "Corporate Migration from IPv4 to IPv6 using Different Transition Mechanisms", International Journal of Engineering Science and Research Technology, ISSN: 2277-9655, Vol. 5, PP. 802-808 October 2016.
14. B. I. D. Kumar et al, "A Hybrid Transition for IPv4-IPv6 Co-existence in Small Size Organization" International Journal of Engineering and Advanced Technology(IJEAT), ISSN: 2249-8958, Vol. 9 Issue 2, PP. 3416-3421, December 2019.
15. Fuiang Li et al, "A Case Study of IPv6 Network Performance: Packet Delay, Loss, and Reordering", Hindawi Mathematical Problems in Engineering, Article ID: 3056475, Vol. 2017 PP. 01-11, 2017.
16. Dr. Jitendranath Mungara et al, "Survey on IPv4 and IPv6 Using Dual Stack, Tunneling and Translation", International Journal of Advanced Research in Computer and Communication Engineering, ISSN: 2278-1021, vol. 7, Issue 2PP. 187-189, February 2018.
17. Julianne S. et al, "IPv4 to IPv6 Transition Strategies for Enterprise Networks in Developing Countries", Institute for Computer Sciences, Social Informatics and Telecommunications Engineering, PP. 94-104, 2015



# IJRASET

International Journal For Research in  
Applied Science and Engineering Technology



---

# INTERNATIONAL JOURNAL FOR RESEARCH

IN APPLIED SCIENCE & ENGINEERING TECHNOLOGY

---

**Volume: 10    Issue: VII    Month of publication: July 2022**

**DOI: <https://doi.org/10.22214/ijraset.2022.45604>**

**[www.ijraset.com](http://www.ijraset.com)**

**Call:  08813907089**

**E-mail ID: [ijraset@gmail.com](mailto:ijraset@gmail.com)**



# Analysis of IoT Data Transfer Messaging Protocols on Application Layer

Ms. Shilpa B.Sarvaiya<sup>1</sup>, Dr. D.N. Satange<sup>2</sup>, Prof. Ather Iqbal<sup>3</sup>

<sup>1</sup>Department of Computer Science Vidyabharati Mahavidyalaya, Amravati,

<sup>2</sup>Department of Computer Science Narsamma Hirayya Arts Commerce & Science, Amravati,

<sup>3</sup>HOD Department of Computer Science Vidyabharati Mahavidyalaya, Amravati

**Abstract:** Now on a daily basis during a smarter embedded world, have Internet of Things. IoT have lot of things for the embedded systems, and it's the potential to remodel our world with the assistance of it. Internet of Things (IoT) or Web of Things (WoT) is emerging technology and it wireless network between two or more objects or smart things connect via Internet. IoT classified in two types first is within IoT and second side is outside of IoT.

In inside IoT consider as protocols in IoT. In outside of IoT consider as sensor, actuators, etc., those are physically possible. In within IoT consider as protocol and IoT have own Protocol Stack. Protocol Stack has different layer like Application Layer, Transport Layer, Internet Layer and Physical/Link Layer. The judgmental role goal of IoT is to confirm effectual communication between two objects and build a sustained bond among them using different application. The application Layer liable for providing services and determining a group of protocol for message passing at the application Layer. This paper understands Application Layer Data Transfer Messaging Protocol like MQTT, AMQT, COAP, XMPP, DDS, HTTP, RESTFULL, and WEB-SOCKET. Also describe which sort of architecture (like Request/Response, Client/Server and Publish/Subscribe) and security (like DTLS, TCL/SSL and HTTPS) support in those protocols that decide upon appropriate protocol supported application needs.

**Keywords:** IoT, WoT, M2H, M2M, MQTT, AMQT, COAP, XMPP, DDS, HTTP, RESTFULL, WEB-SOCKET.

## I. INTRODUCTION

IoT has significantly changed ones perspective of living style. It has enabled many non-living objects to behave smartly and intellectually according to the circumstance and environment. A growing number of physical objects are being connected to the Internet at an unprecedented rate realizing the idea of the Internet of Things (IoT).

The IoT envisions hundreds or thousands of end-devices with sensing, actuating, processing, and communication capabilities able to be connected to the Internet [1]. The captured data needs a direction to be Transferred, Modified, Controlled, Acknowledged, Stored or Exported to other devices. These tasks can be performed through suitable protocols. Typically, IoT is expected to offer advanced connectivity of devices, systems, and services that goes beyond, Human-to-Machine (H2M), Machine-to-Machine (M2M) communications. In section 2 studies the literature review, in section 3 explain the working of the data transfer protocols between the transmitter and the receiver is given. Section 4 Analyse the result and discuss, section 5 gives the conclusion of the work, the comparisons of the messaging protocols is important to choose a suitable design platform.

1) *Human To Machine Communications In IoT ( H2M):* Human to Machine communication originally emerged from Telemetry technology, and its main aim was to measure data and automatically transmit it from remote sources typically by cable or a radio. Nowadays, plethora of sensors are being developed, which have better perceptual abilities than humans and can detect information that humans cannot.

Affordable electronic devices halved to an increasing number of them being connected to the Internet. The smart IoT devices open up the possibility to reduce the burden on the user end by equipping everyday objects. Human-to-Machine communication is a very important development in Internet of Things. Figure 1 shows the human to machine interaction and its relation to the IoT. Figure 1 shows the elaborate human to machine interaction which demonstrates the use of sensors, actuators, cognition unit and processing unit.

The data transfer in HMI model is based on the cognitive ability of the human. The machine sends the control data to the actuator unit to perform the required action.

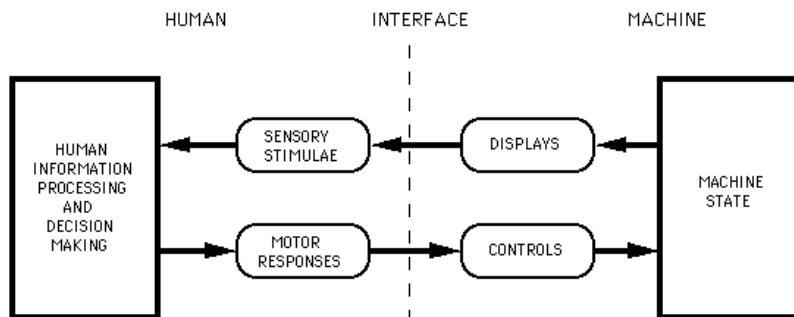


Figure 1: Human to Machine Interaction

2) *Machine To Machine Communications In Iot ( M2m)*: Machine to Machine (M2M) is a broad term that can be used to describe any technology that enables networked devices to exchange information and perform actions without the manual assistance of humans. It forms the basis for a concept known as the Internet of Things (IoT). Key components of an M2M system include sensors, RFID, a Wi-Fi or cellular communications link and autonomic computing software programmed to help a networked device interpret data and make decisions. M2M communications expands telemetry's role beyond its common use in science and engineering and places it in an everyday setting. People already are using M2M, but there are many more potential applications as wireless sensors networks and computers improve, benefitting the concept to be amalgamated with other technology. The main goal of M2MC is to enable the sharing of information between electronic systems autonomously; Figure 2 shows the amalgamation of Machine to Machine and IoT in real time. In other words Machine to Machine refers to technologies that allow both wireless and wired systems to communicate with other devices. M2M application protocols take a fundamental role in communication efficiency: Protocol overheads, necessary number of management or control and information messages, reliability and security. All these impact the number and size of transmissions consequently, the energy and bandwidth consumptions in a mobile device. It finds its major application in protocols namely MQTT, AMQP, COAP, XMPP, DDS, HTTP, RESTFULL, and WEB-SOCKET.

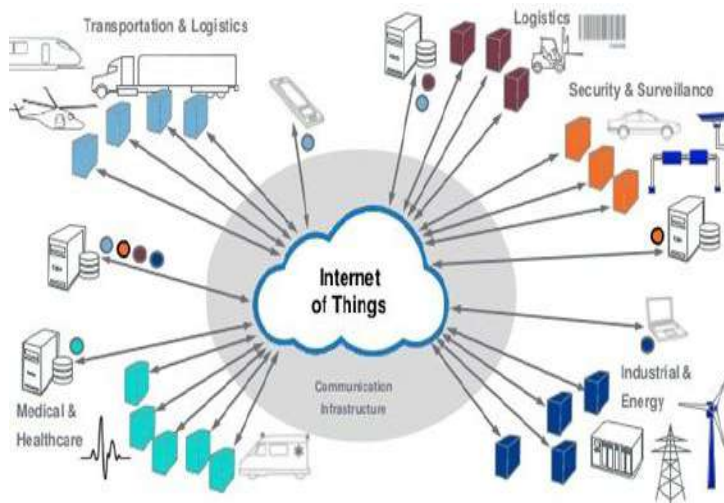


Figure 2: Amalgamation of M2M and IoT

## II. RELATED WORK

Internet of Things (IoT) is emerging technology. Show in previous section inside of IoT describe as protocols. By studying paper regarding IoT and IoT protocol related IETF standards paper show Application Layer protocols focus basically on message exchange between applications and the Internet [2]. A Data Transfer Protocol is a standardised format for transmitting data between two devices. The type of protocol used can determine the variables. Application Layer work with other layer like Transport Layer, Internet Layer and Physical Layer. In this paper our aim to provide comprehensive survey to describe all main eight Application Layer Protocols.

A. IoT Ecosystem

Figure 3 shows a 7-Layer model of IoT Ecosystem. At the bottom Layer is the market or application domain. The second layer consists of sensors that enable the application. The third layer consists of interconnection layer that allows the data generated sensors to be communicated, usually to a computing facility, data centre, or a cloud. Finally the top layer consists of services that enable the market and may include energy management, health management, education, transportation etc. [3].



Figure 3: IoT Ecosystem

In this paper, we concentrate on the Session Layer. This layer itself can be shown in a Multi-Layer stack as shown in figure 4. We have shown only the Data link, Network, and Transport or Session Layers. The data link layer connects two IoT elements which generally could be two sensors or the sensor and the gateway device that connects a set of sensors to the Internet. Often there is a need for multiple sensors to communicate and aggregate information before to the Internet. Specialized protocols have been designed for routing among sensors and part of the routing layer. The Session Layer protocols enable messaging among various elements of the IoT communication subsystem. A number of security and management protocol have also been developed for IoT as shown in the figure.

<b>Session</b>		MQTT, SMQTT, CoRE, DDS, AMQP, XMPP, CoAP, ...	<b>Security</b>	<b>Management</b>
<b>Network</b>	<b>Encapsulation</b>	6LowPAN, 6TISCH, 6Lo, Thread, ...	TCG, Oath 2.0, SMACK, SASL, ISASecure, ace, DTLS, Dice, ...	IEEE 1905, IEEE 1451, ...
	<b>Routing</b>	RPL, CORPL, CARP, ...		
<b>Datalink</b>		WiFi, Bluetooth Low Energy, Z-Wave, ZigBee Smart, DECT/ULE, 3G/LTE, NFC, Weightless, HomePlug GP, 802.11ah, 802.15.4e, G.9959, WirelessHART, DASH7, ANT+, LTE-A, LoRaWAN, ...		

Figure 4: Protocols for IoT

III. IOT APPLICATION LAYER MESSAGING PROTOCOLS

A communication protocol is nothing but a language that is used by objects to interact among them. In simple words, a protocol is a set of rules that must be obeyed by the communicating objects. Communication Protocols are extremely essential in heterogeneous systems; where the objects interacting may be heterogeneous in nature, needing a common framework for them to interact. This section reviews standards and protocols for message passing in IoT Application Layer proposed by different standardization [2]. All most Web-based application and IoT application are IP based and they use TCP and UDP for transport. However, there are several message distribution functions that are common among many IoT applications; it is desirable that these functions be implemented in an interoperable standard ways by different applications. Those protocols are:

- 1) *MQTT (Message Queuing Telemetry Transport Protocol)*: MQTT (Message Queue Telemetry Transport) was develop by or introduce by IBM in 1999 and standardized by OASIS in 2013 to target come up with lightweight M2M communication [3]. It is Publish/Subscribe Protocol architecture similar to Client/Server Protocol show in figure 5 below. The importance of MQTT Protocol is due to its simplicity and the no need of high CPU and memory usage (reason is the lightweight protocol) [4].MQTT

supports a wide range of different devices and mobile platforms. At Transport Layer TLS/SSL security provides to MQTT. Show above figure 5 there three components are there Publishers, a Broker and Subscribers. Publishers are generally lightweight sensors that connect with a broker and send data to a broker and go back to sleep. Subscribers are IoT applications that interested in data send by sensors and also connect with a broker, so broker send interested data to subscribers. The brokers classify sensor data in Topics and send them to subscribers interested in the Topics. This all thing is on IoT point of View [5].

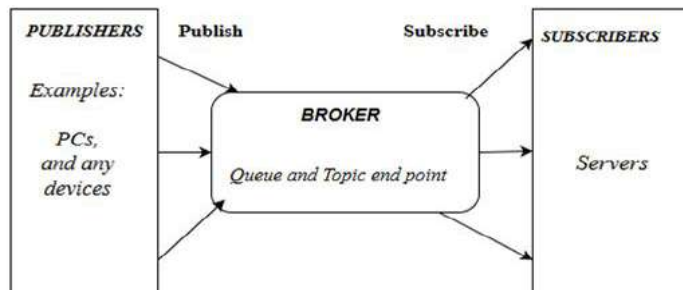


Figure 5: Working of MQTT Protocol

- 2) *CoAP (Constrained Application Protocol)*: CoAP (Constrained Application Protocol) is used for low power and low memory embedded devices where it can be used for communication instead of HTTP. Currently there is HTTP Protocol available with Request/Response paradigm but HTTP has many features and more footprint [5]. HTTP runs over TCP where TCP will need more resources due to three way handshake and many more complex mechanism. Now for low power embedded devices, there is no need of this heavy protocols and we can optimize it to run over TCP. As CoAP is a Restful web Transfer Protocol for use with constrained networks. CoAP uses Client/Server model of approach same as HTTP. It is designed for constrained networks with low overhead and lower footprint [6].

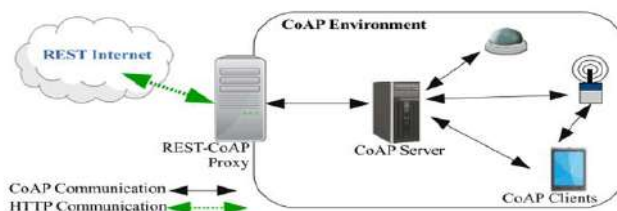


Figure 6: Constrained Application Protocol

- 3) *AMQP (Advanced Message Queuing Protocol)*: The Advanced Message Queuing Protocol (AMQP) is a protocol that across from the financial industry. Security is managed with the use of the TLS/SSL Protocols. Its run over TCP. AMQP is follow Publish/Subscribe communication Protocol for messaging [6,7]. AMQP is same like MQTT but AMQP have advantage its store data then forward it, and this features used at when network disruptions that time ensures reliability. Show in figure 7 below a broker divide into two part Exchange and Queue. Exchange responsibility to receive Publishers messages and distribute to Queue. A queue is based on Pre-define Roles and Condition and it's basically send message to subscribers who subscribe those data.

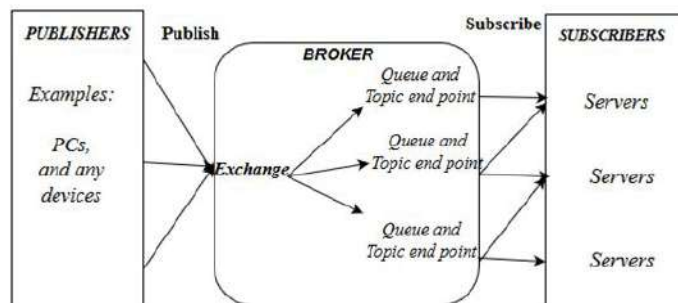


Figure 7: Advanced Message Queuing Protocol

- 4) *XMPP (Extensible Messaging and Presence Protocol)*: Extensible Messaging and Presence Protocol (XMPP) is a Messaging Protocol that was designed originally for chatting and message exchange applications. It was standardized by IETF in 1999 named as jabber. In all Application Layer Protocols only XMPP Protocol support Publish /Subscribe and Request/Response model and it's depend on application developers to develop application which model they use [8]. It does not provide any quality of service guarantees and, hence, is not practical for M2M communications. XMPP is IP based communication protocol with Extensible Mark-up Language (XML) support [9].

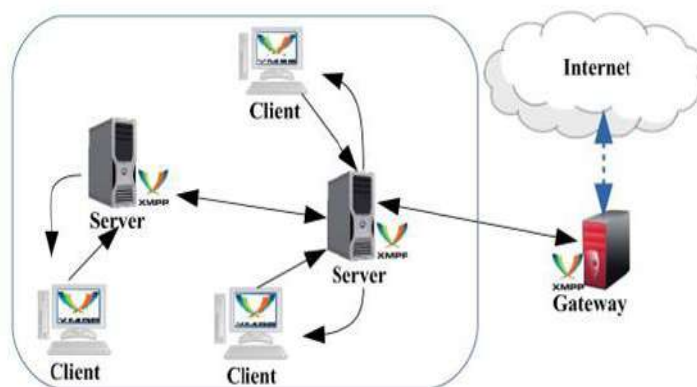


Figure 8: Extensible Messaging and Presence Protocol

- 5) *DDS (Data Distribution Service)*: Data Distribution Service (DDS) is another Publish/Subscribe Protocol that is designed by the Object Management Group (OMG) for M2M communications. It defines two sub layers: Data-Centric Publish-Subscribe (DCPS) which disseminates information to subscribers and Data-Local Reconstruction Layer (DLRL) which is an optional and is an interface to the DCPS functionalities. It shares data among distributed objects [9].

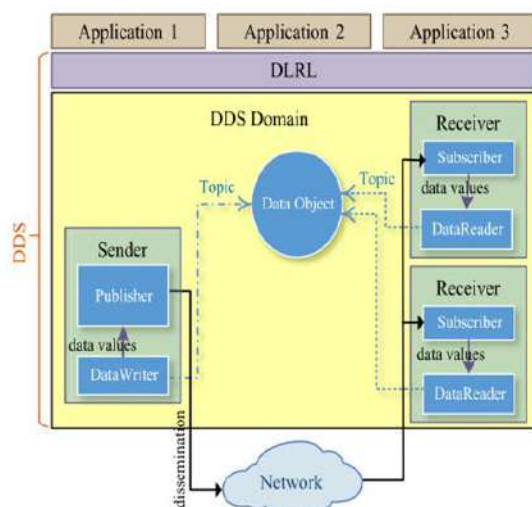


Figure 9: Data Distribution Service

- 6) *HTTP (Hyper Text Transfer Protocol)*: HTTP is specially designed for Internet. It was developed by Tim Berners Lee and later standardized by IETF in 1997. Though HTTP uses Request/Response architecture, it doesn't use topics. HTTP is based on Representational State Transfer (REST), an architectural style that makes information available as resources identified by URIs [8]. HTTP is simple text based protocol where no fixed header size is defined. It has features on Persistent and Non-Persistent connections. By default TCP is used as HTTP's Transport Protocol, but HTTP doesn't have any QoS support [9]. HTTP is very powerful protocol, but it's relatively expensive in implementation and network resource usage. This makes it difficult to adopt HTTP as it is for IoT networks. HTTP transfers a large number of small packets over web but overhead of HTTP causes many problems, such as consumption of network resources and large delays [10].

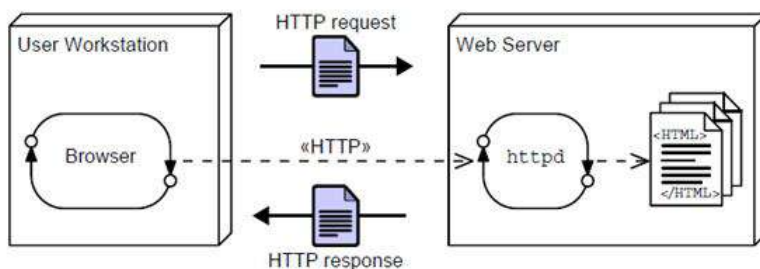


Figure 10: Working of Hyper Text Transfer Protocol

7) **RESTFULL (REpresentational State Transfer):** Representational State Transfer ( RESTFUL Services) is an engineering that gives web administrations which permit correspondence and information trade between various gadgets utilizing HTTP in IoT condition [5]. REST utilizes the HTTP strategies GET, POST, PUT, and DELETE to give an asset arranged informing framework where all activities can be performed essentially by utilizing the synchronous request/response HTTP commands. RESTFUL services use the secure and reliable HTTP which is the proven worldwide Internet language. It can make use of TLS/SSL for security [9].

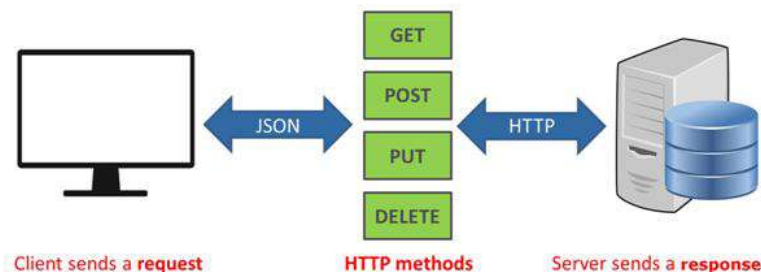


Figure 11: Working of RESTFULL Protocol

8) **WEB-SOCKET:** The WEB-SOCKET Protocol provides two ways for communication between clients and a remote server. Web-Socket provides security similar to the security model used HTTPS Protocol. For browsing Application Layer used and web-Socket work on TCP Transport Layer Protocol, so they need to interact and communicate with host those who connect with remote. Web-Socket is a Web-based Protocol that works on the single TCP channel and provides full duplex communications. Web-Socket starts session without Publish/Subscribe and Request/Response models like previous protocols [9, 10].

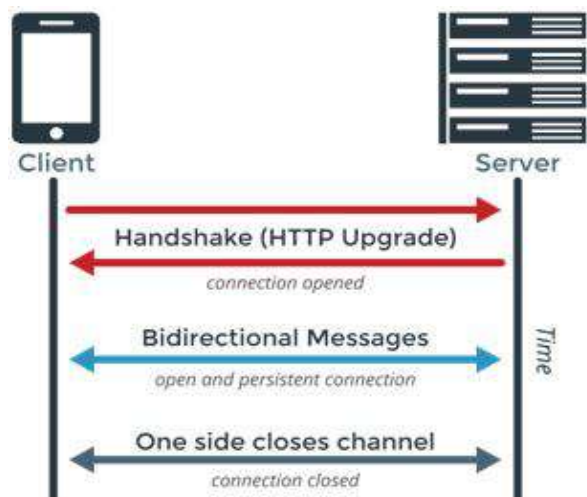


Figure 12: Working of WEB-SOCKET Protocol

#### IV. RESULT AND DISCUSSION

To interconnect objects to transfer data and to publish information over a network without requiring Human-to Human or Human-to-Computer interaction is now possible. That is why the IoT application programmers are faced with the challenges of choosing an appropriate communication protocols for their resource-constrained applications.

Performance Evaluation: In The process of Subscription-Publication, the challenge is to accomplish the message delivery with a high efficiency, a low latency and a low packet loss rate using one of reliability and QoS level. Otherwise, it is up to the application to select the appropriate QoS level for its publications and subscriptions, thus the decision to use one of these levels impacts on the application performance as well as on the use of bandwidth and battery life of devices. However, although the traditional protocol's effectiveness, the need for a suitable protocol for IoT applications involving constrained devices is necessary because the biggest obstacle in the functioning of these devices is energy consumption. Both MQTT and CoAP protocols are being implemented for Mesh-Networking applications in networks in order to allow inter-standard communication between lightweight end nodes. Data transfer Protocols are rapidly emerging and integrating the IoT market as leading lightweight messaging protocols for constrained devices.

Each protocol offers unique benefits and each poses challenges and tradeoffs. The strengths and issues of these eight protocols are summarized in Table 1 [9, 10]. The purpose of this evaluation is to choose the use of either MQTT or CoAP according to the best throughput and lowest latency resulted in the presence of different criteria. AMQP can be integrated with TLS in order to ensure secure communication. DDS, RESTFUL, and WEB-SOCKET is an excellent quality of service levels and reliability guarantees. XMPP is very secure protocol which supports encryption, authentication, and access control. MQTT and CoAP use different transmission protocols of TCP and UDP. CoAP present the best performances in terms of both throughput and latency.

Table 1: Comparative Analysis of IoT Data Transfer Messaging Protocols

Sr.No	Criteria	MQTT	CoAP	AMQP	XMPP	DDS	HTTP	RESTFUL	WEBSOCKET
1	Year	1999	2010	2003	1999	2004	1997	2000	2011
2	RESTFUL	No	Yes	No	No	No	Yes	Yes	yes
3	Transport Protocol	TCP	UDP	TCP	TCP	TCP/UDP	TCP	TCP/UDP	TCP
4	Publish/Subscribe Model	Yes	Yes	Yes	Yes	Yes	No	No	No
5	Request/Response	No	Yes	No	Yes	No	Yes	Yes	YES
6	Security	SSL	DTLS	SSL	SSL	SSL/DTLS	SSL	SSL/TLS	TLS
7	QoS	yes	Yes	Yes	No	Yes	No	NO	NO
8	Header Size	2	4	8	-----	-----	-----	-----	-----
9	XML Support	No	No	No	Yes	No	Yes	Yes	Yes
10	Encoding Format	Binary	Binary	Binary	Character	Binary	Text	Text	Text
11	Default Port	1883/8883	5683/5684	5671/5672	5222/5223	7400/7401	80/443	23450/tcp	RFC 6455
12	Proxy Support	Partial	Yes	Yes	Yes	Yes	Yes	Yes	Yes

#### V. CONCLUSION

In this paper, we made a shot to supply survey on the embedded world and/or Machine to Human (M2H), Machine to Machine (M2M) communication around Data transfer Messaging Protocols. During this paper we have analyzed and compared messaging protocols for IoT systems. Started our discussion with MQTT then discussed, MQTT, AMQT, COAP, XMPP, DDS, HTTP, RESTFULL, and WEB-SOCKET. Each of these protocols has their different pros, cons and is meant for particular scenarios. Also we performed comparative analysis of this protocol which is in a position to assist us to choose appropriate messaging protocol depending upon application requirements.

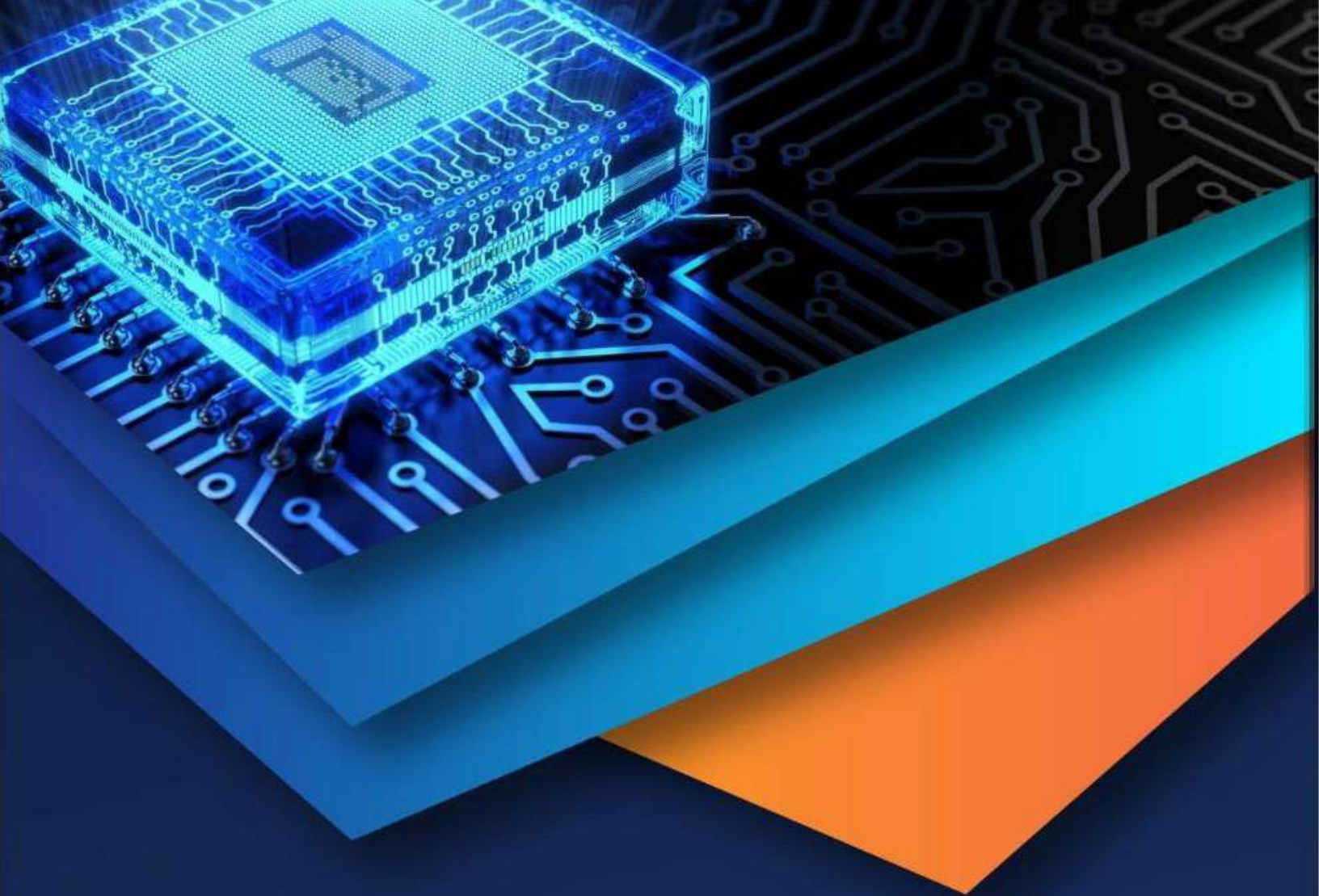
There are three major components for implementing IoT on different applications: Security, Privacy and Trust. While increasing the expansion of IoT, Security is more important for reliable data transferred among the billions of smart objects. This paper concentrates on Application Layer Data Transfer Messaging Protocols on IoT devices. CoAP having light weight and consume low energy; CoAP is utilized on many applications of IoT. To secure data transferred, CoAP combined with DTLS Protocols named as Datagram Transport Layer Security Protocols because the safety agent. So, in future we concentrate on Security in Application Layer Protocols.



## REFERENCES

- [1] Ms .B.Sarvaiya, Dr.S.S. Sherekar, Dr.V.M.Thakare, "Study of Security Challenges in Multi-layered Structure and Various Attacks on IOT", AIC 2K18 Annual IETE Convention International Journal of Electronics, Communication And Soft Computing Science & Engineering ( IJECSCSE),Impact Factor- 4.526, ISSN :2277-9477, 29 and 30 September-2018.
- [2] Jayavardhana Gubbi et al. "Internet of Things (IoT): A Vision, Architecture Elements, and Future Directions", In Future Generation Computer Systems, PP.1645-1660, and ISSN: 0167-739X, 2013 IEEE.
- [3] Kushal Reshamdalal, "A Comprehensive Study of Application Layer Protocols (ALP)", International Journal of Innovations & Advancement in Computer Science (IJACS), ISSN 2347-8616, Volume 6, Issue 10 October 2017 IEEE.
- [4] Tanya Mohan Tukade, R.M.Banakar, "Data Transfer Protocols in IoT-An Overview", International Journal of Pune and Applied Mathematics, ISSN: 1311-8080, Volume 118, No.16 2018 IEEE.
- [5] Fathia Ouakasse, Said Rakrak, "A Comparative Study of MQTT and CoAP Application Layer Protocols via. Performances Evaluation", Journal of Engineering and Applied Sciences. ISSN: 6053-6061, Volume 13, No 15.2018 IEEE.
- [6] Yuang Chen,Thomas Kunz, "Performance Evaluation of IoT Protocols under a Constrained Wireless Access Network",2016 International Conference on Selected Topics in Mobile & Wireless Networking(MoWNeT).ISSN:5090-1743,2016 IEEE.
- [7] Danish Bilal Ansari, Atteeq-Ur-Rehman, Rizwan Ali Mughal, "Internet of Things (IoT) Protocols: A Brief Exploration of MQTT and CoAP", International Journal of Computer Applications.ISSN: 0975-8887, Volume 179, No.27, March 2018 IEEE.
- [8] Suvam Monanty, Sagar Sharma, Vaibhav Vishal, "MQTT-Messaging Queue Telemetry Transport IoT based Messaging Protocol", International Research Journal of Engineering and Technology (IRJET).ISSN:2395-0056, Volume 03, Issue 09, SEP 2016 IEEE.
- [9] Makkad Asim, "A Survey on Application Layer Protocols for Internet of Things (IoT)", International Journal of Advanced Research in Computer Science, ISSN: 0976-5697, Volume 8, No.3, March-April 2017 IEEE.
- [10] Sagar P Jaikar, Dr.Kamatchi R.Iyer, "A Survey of Messaging Protocols for IoT Systems", International Journal of Advanced in Management Technology and Engineering Sciences, ISSN: 2249-7455, Volume 8, Issue II, FEB 2018 IEEE.





10.22214/IJRASET



45.98



IMPACT FACTOR:  
7.129



IMPACT FACTOR:  
7.429



# INTERNATIONAL JOURNAL FOR RESEARCH

IN APPLIED SCIENCE & ENGINEERING TECHNOLOGY

Call : 08813907089  (24\*7 Support on Whatsapp)

# Trustworthy IoT Traditional Network Security to Authentication and Access Control Model for Heterogeneous Devices

Ms.Shilpa B.Sarvaiya<sup>1</sup>, Dr.D.N.Satange<sup>2</sup>

<sup>1</sup>*Department of Computer Science, Vidyabharati Mahavidyalaya, Amravati*

<sup>2</sup>*Director, Students' Development, S.G.B.A. University, Amravati*

**Abstract-**Security is the basic requirement of any user for Internet of Things (IoT) traditional network. An internet user will not share his confidential and important data on the network unless the traditional network is trusted. IoT is considered as a collection of heterogeneous devices, such as, radio frequency identification, sensors and actuators, which form a huge traditional network, enabling not connected to computer in the network to produce a trustworthy world of services. Security and privacy are the two most important aspects of the IoT network, which includes authentication, authorization, data protection, network security, and access control. Additionally, traditional network security cannot be directly used in IoT traditional networks due to its limitations on computational capabilities and heterogeneous devices storage capacities. Authentication and Access control is the mainstay of the IoT traditional network, as all components undergo an authentication process before establishing communications between heterogeneous devices therefore, securing authentication and access control is essential to ensure that resources are only granted to the authorized users. With authentication and access control information, it sets the access rights of the subject to the object and protects heterogeneous devices from unauthorized access to ensure confidentiality and integrity of the system resources in the send and receive data signal is one of the basic security services. Current access control technology can be divided into Role-based Access Control (RBAC) and Resource Role Hierarchy Based Access Control (RRBAC). The first kind of access control model is RBAC, which is widely used in traditional networks and second is suitable for multiple security domains with different applications. In this paper focused on IoT security particularly on their authentication and access control model. Also, studies on existing evaluation schemes of IoT authentication and access control.

**Keywords-** Access Control, Authentication, Attribute-Based Access Control (ABAC), Role-Based Control (RBAC), Resource Role Hierarchy Based Access Control (RRBAC).

## 1. INTRODUCTION

The fundamental question that needs to be answered is how we can trust the validity of the data being generated in the first place. IoT therefore needs to improve its trustworthiness before it can be used to solve challenging economic and environmental problems tied to our social lives.

Due to huge number of IoT devices and machine to machine communication feature of IoT, legacy authentication and authorization techniques are not viable for it. Devices must authenticate each other before exchanging any information between them (M2M communication) which is a challenge for researcher due to massive number of heterogeneous devices. IoT is focusing on Machine to Machine (M2M) mode of communication. For such communication nodes authentication is very important for insuring security and privacy. When two or more nodes are communicating with each other for a common objective they should authenticate each other first in order to block fake node attack. However, there is no efficient authentication mechanism for massive number of IoT devices. Authentication and access control mechanisms are capable of preventing unauthorized users from accessing the data of sensor nodes on the IoT perception layer and guaranteeing the data security effectively. User authentication is to allow legitimate user to access resources as well as to decline malicious person or attacker [1]. After authentication, access control is to restrict authenticated user to access the only data that have the privileges. However, due to the characteristics of

wireless sensor network, secure access is faced with more severe challenges. The trustworthiness to heterogeneous device authentication and access control model in IoT traditional network are discussed here. In this paper, authors focus various evaluation techniques with their parameters and supporting equations. This paper presents an overview of the existing work on trust authentication, access control models in IoT. The first access control model is role-based access control (RBAC), which is widely used in traditional networks. Adopt ABAC-based authorization method in order to access various resources and data in this type of model, users require certain certificate information that falls into ABAC. If a user has some special attributes in ABAC, it is possible to access a particular resource or piece of data. ABAC is a more flexible and scalable that abstract identity, role, and resources information of the traditional access control into entity attributes. Additionally, ABAC can support either fine-grained access control in the complex system or dynamic extension of large-scale users. The second access control model RRBAC is suitable for multiple security domains with different applications [2, 3].

The paper focuses on building an access control model and system based on trust computing, which is a new field of access control techniques that includes Access Control, Trust Computing, Internet of Things, network attacks, and cheating detection technologies. Because target access control systems can be very complex to manage, there has been substantial research in this domain, most of which has been related to attacks like self-promotion and ballot stuffing where a node falsely promotes its importance and boosts the reputation of a malicious node (by providing good recommendations) to engage in a collusion-style attack. The traditional trust computation model is inefficient in differentiating a participant object in IoT, which is designed to win trust by cheating. There is an urgent need to put forward more suitable and effective methods to ensure the security of IoT

This paper is organized as follows. Section II describes the authentication model for IoT security. Section III presents Access control model for IoT security. In section IV Authentication Evaluation Techniques for IoT security, Section V presents Access Control Evaluation Techniques for IoT security finally, section VI concludes the paper and future research.

## 2. AUTHENTICATION MODEL FOR IOT SECURITY

Authentication allows communicating entities to convince the identity of each other and exchange session keys. In wireless sensor network, user and terminal nodes in the communication process require mutual authentication to ensure network security, while terminal nodes require authentication mutually to prevent malicious nodes attacks. Encryption mechanism ensures confidentiality to prevent data from being stolen during communication process via encoding the data. Usually, the authentication is divided into two parts [4, 5].

(1) Authentication: authentication between user and terminal nodes ensures only the legitimate User can access the network.

(2) Key establishment: session keys should be created between the user and nodes for secure Communication.

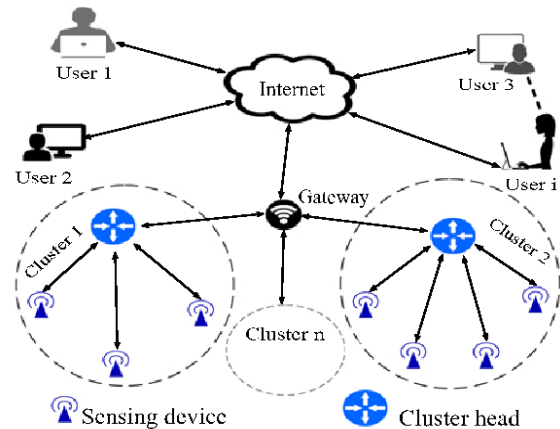


Figure 1: Authentication Model for IoT security

## 3. ACCESS CONTROL MODEL FOR IOT SECURITY

As discussed in Section 3, access control is the most fundamental component in trustworthy security. Many access control models have been developed in the past three decades and among all these models, Role-Based Access Control (RBAC) models [6] are most widely used in enterprises and other organizations. Role-based models can greatly cut down the cost for policy specification. Also, Role hierarchy in RBAC provides a natural representation (role hierarchy) of the structure of the users in an organization. Role faithfully describes the responsibility and authority of

the user in the position represented by the role. The RBAC model focuses on building a hierarchy of the subjects to reduce the overhead in access right specification and management but does not consider the same for the objects (i.e., the resources to be accessed). In IoT security, there are an enormous number of resources. If permissions have to be assigned for individual IoT resources to roles, permission assignment and management can have a very high complexity, likely to be infeasible [7]. RBAC model also has limitations in highly open environment where no role hierarchy can be formulated [8] In RBAC, the only alignment required for interoperability is to map the roles from one domain to another and role mapping techniques has been well explored [9]. For interoperability in ABAC, need to align the attributes as well as the values for the attributes. If two systems do not have equivalent attributes, it is impossible to align them. Extended the RBAC model and created the RRBAC (Resource and Role hierarchy Based Access Control) model [10] to circumvent the problems in RBAC and ABAC discussed above. Similar to role hierarchy, IoT resources can be organized in a hierarchy and permissions can be assigned based on the resource hierarchy. By providing resource hierarchy as a part of the access control model, we can greatly simplify access rights assignments using the resource groups and privilege inheritance concept on the resource hierarchy. The high level RRBAC model is formally specified in Section 3.1. For the dynamic and open IoT systems develop a “resource role hierarchy” based access control model to support easy policy specification. An entity in the system can build a resource role hierarchy to specify its view of the other entities in the system without knowing the specific entities. Integrate the RBAC model with RRBAC so that access control policies can be specified based on the relative role hierarchy and resource hierarchy [11]. When a dynamic IoT network is formed, the other entities are mapped to the relative role hierarchy of entity based on their attributes. The attribute values are obtained by mining the societal databases and social networks. The resource role hierarchy concept is presented in Section 3.2.

3.1 Role-Based Access Control Model (RBAC)

Role-Based Access Control approach (RBAC), a policy mechanism defined roles and privileges. This approach scales better than other models. However,

when talking about a huge amount of devices, managing roles for individual entities the possibility of grouping sensors and assigning roles to those that have the same rights is a good solution for this problem. For providing access rights to user, it is important to know the user’s responsibilities assigned by the organization. RBAC try to reduce the gap by combining the forced organizational constraints with flexibility of explicit authorizations [12]. RBAC mostly used for controlling the access to computer resources. RBAC is very useful method for controlling what type of information users can utilize on the computer, the programs that the users execute, and the changes that the users can make. In RBAC roles for users are assigned statically, which is not used in dynamic environment. It is more difficult to change the access rights of the user without changing the specified roles of the user. RBAC is mostly preferable access control model for the local domain. Due to the static role assignment, it does not have complexity. Therefore, it needs the low attention for maintenance [13, 14]. Role is nothing but the abstractions of the user behaviour and their assigned duties [15].

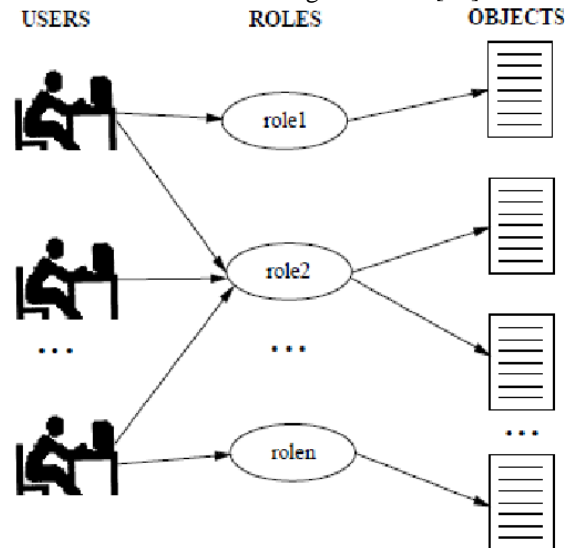


Figure 2: Role-Based Access Control Model

Essentially, in role-based access control policies need to identify the roles in the system, a role can be defined as a set of responsibilities and actions associated with a particular working activity. In an Access control security model, a role is considered as a job-related access right which can be given to the authorized users within an organization. It allows authorized user to achieve its associated responsibilities [14, 15].

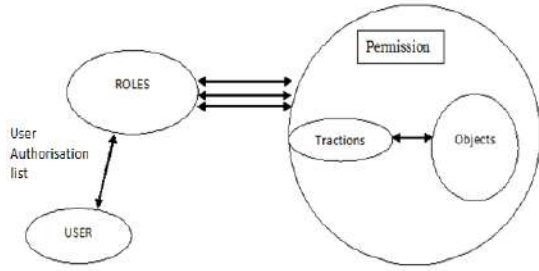


Figure 3: User-Role-Permission Mapping

A permission  $p$  is a pair  $\langle \text{trans}, \text{objset} \rangle$ , where  $\text{trans}$  represents the transaction that executes on the set of objects that is  $\text{objset}$ . Consider  $P$  indicate the universal set of permissions,  $\text{Trans}$  indicate the universal set of transactions, and  $\text{Obj}$  indicates the set of objects.

### 3.2 Resource and Role Hierarchy Based Access Control (RRBAC)

The big difference between RRBAC and (ABAC). RRBAC is suitable for multiple security domains with different applications. Figure 4 is the structure graph of RRBAC model. From Figure 4, the users are distributed anywhere, in a school, in a company etc. In every security domain, the administrator is charge of managing the sessions and roles. Usually, the session IDs are randomly generated as a procedure for a user to perform actions. The roles are man-made according to the registration of the resources. The resources are also distributed. After a resource registers and passes the examination, it can become a legitimate resource. Surely, a valid resource is treated as a part of the domain [16].

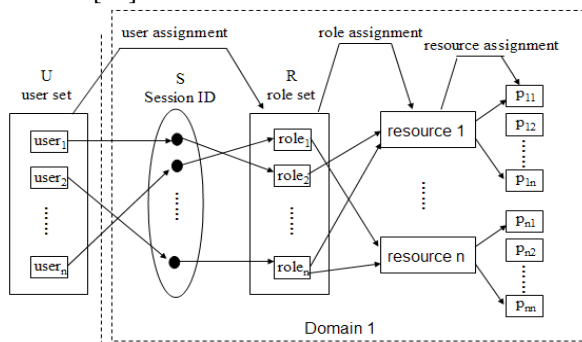


Figure 4: The structure graph of RRBAC Model [16]

## 4. IOT AUTHENTICATION EVALUATION TECHNIQUES

As the new and challenging authentication techniques are necessary to protect the IoT environment from

various emerging attacks, evaluation of those proposed schemes are equally important to check their potency. In this section, discuss several evaluation techniques with their parameters and supporting equations [17].

### A. Average Response Time

Response time is assumed to be the time taken by the server to result in the response of a request to the client. This can be affected by few factors, such as, number of users, number of request, type of requests, think time, network bandwidth, and server configuration. First response time can be executed by the time of client request and the time of first response, which is defined in equation 1.

$$T_{res} = t_{res} - t_{req} \quad (1)$$

Here  $T_{res}$ ,  $t_{res}$ ,  $t_{req}$  are response time, time of client request and time of first response respectively. Average response time is calculated by the mean of all response time, which is determined in equation 2.

$$T_{avg\_res} = (n/r) - T_{think} \quad (2)$$

Where  $T_{avg\_res}$  is the average response time,  $n$  is the number of concurrent users.  $r$  is the number of requests per second the server receives.  $T_{think}$  is the average think time (in seconds). However, to obtain an accurate response time result, a user should always include think time in the equation.

### B. Impact on Throughput

Throughput (TP) can be described as the amount of data passes through a system in a unit of time. In the traditional network of IoT, find out the total number of transmitted data preserved in a second. The TP can be defined in equation 3.

$$TP = \sum (Q_i^f * l_i) / T_w \quad (3)$$

Here, TP denotes throughput, while  $Q_i^f$  is the Quantity and  $l_i$  is the length of the  $i^{th}$  kind, and  $T_w$  denotes as the whole time of the simulation.

### C. Packet Delivery Ratio

Packet Delivery Ratio is calculated based on the number of packets sent by the sender and the number of packets successfully received at the receiver end. However, it depends on several factors like network configuration, device capabilities, and bandwidth; therefore, it is difficult to test the network performance. Equation 4 can be used to calculate the packet delivery ratio.

$$PDR = N_{rp} / N_{sp} \quad (4)$$

Where  $PDR$  is Packet Delivery Ratio;  $N_{sp}$  is the total

number of sent packets, and  $N_{rp}$  is the total number of received packets. It has been identified that throughput falls when the number of nodes increases in a network. In the wireless sensor network, packet-sending circumstances are defined in the energy model, like that; energy is consumed when a packet is sent over the network. Therefore, more packet transfer cost core energy consumption. Ultimately, the packet can be discarded due to less energy or long-distance travel [17].

D. Handshake Duration

Handshaking is the process of negotiation between two network parties in the IoT network. These parties can be user, sensor, actuator, server or other nodes. As shown in Figure 5, handshaking takes place by completing the two-roundtrip message, whereas, client's discovery offers by the server and again the client's request acknowledges by the server. Duration to a handshake  $T_{hs}$  is computed at the client-end using equation 5.

$$T_{hs} = T_s + T_{res} + T_p \quad (5)$$

Where  $T_s$  is the time taken by whole session request,  $T_{res}$  is client response time and  $T_p$  denotes as processing time at the server. However, to calculate the handshake duration, a user must perform several random numbers of handshakes between the client and the server.

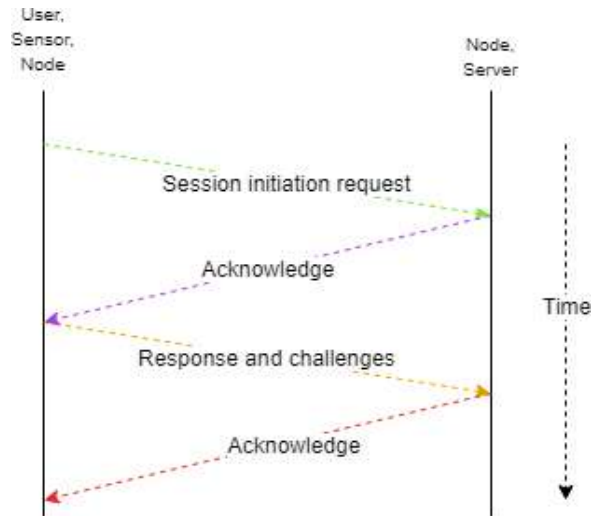


Figure 5: Four Way Authentication Handshaking.

E. End-To-End Delay

End-to-End Delay or E2ED denotes the average time to deliver packets from sender to receiver. E2ED can be calculated by using equation 6.

$$E2ED = \sum (T^r_i - T^s_i) / n \quad (6)$$

Here,  $i$  is the number of packets and  $n$  is the number of received packets, while  $T^r_i$  is the received and  $T^s_i$  denotes the sent timestamp for  $i^{th}$  packet. E2ED is proportional to the number of sensors in the IoT network. Therefore, an increased number of nodes put up the congestion in the network.

5. IOT ACCESS CONTROL EVALUATION TECHNIQUES

Access Control technologies are known as the main elements to address the security and privacy issues in the Internet of Things. Any effective access control system should satisfy the main security properties of confidentiality (preventing unauthorized divulgence of resources), integrity (preventing resource to be modified without authorization resources), and availability (assuring access to resource by legitimate users when needed). In addition, the classification of IoT heterogeneous devices by assigning them a particular class according to their evaluation techniques. These evaluation techniques will help in building an adequate access control framework to achieve the required security level for each domain application.

A. Quantitative and Qualitative Evaluation techniques  
In this section, we evaluate in both quantitative and qualitative way towards access control in IoT and their versatility for preserving security and privacy by referring to the above Role-Based Access Control Model (RBAC) and Resource Role Hierarchy Based Access Control (RRBAC) Model based on the described legend below this evaluation is highlighted as follow [18].

Legend: VH= Very High=> 5, H= High =>4, M=Medium =>3, L= Low => 2, VL= Very Low =>1, No= Null => 0

Each quality criteria is assigned a value ranging from 0 to 5, where 0 signifies not defined, 1 signifies a very low quality sufficiency, 2 signifies a low quality sufficiency, 3 signifies a medium quality sufficiency, 4 signifies a high quality sufficiency while 5 signifies a very high quality sufficiency. These values are then used to indicate the sufficiency of each access control model's interoperability between heterogeneous devices for each security and privacy preserving analysis for IoT.

## B. Evaluation of Access Control based on RBAC and RRBAC Model

The web service technology is known to provide great interoperability between heterogeneous devices. For this reason, we classify all the devices that adopt the web of think approach (based on web service) as high-quality sufficiencies in term of interoperability based on RBAC model have the following issues [18].

(1) Interoperability: the difficulty to approve a real consensus regarding the meaning of role to be shared with different applications, platforms, domains and enterprises.

(2) Role explosion: The role explosion issue justifies the critical dynamicity aspect of RBAC. Actually, RBAC defines access permissions in a static and fixed manner without taking the context of the access into consideration. As a result, a pure RBAC solution may be inappropriate for defining fine-grained access permissions based on context, and dynamics of IoT environment.

(3) Critical scalability: policies cannot evolve easily. In fact, the creation of new roles can lead to rebuilding the entire model.

(4) Nonsupport of delegation: a subject cannot grant access rights to another subject, as well as grant the right to further delegate all or part of the granted rights.

## 6. ANALYSIS AND DISCUSSION

The current concept of network and connectivity is going to be changed in the next few years. As it is predicted that the number of connected heterogeneous devices in the world will take over the headcount of human beings soon, this can be possible because of the expansion of the authentication and access control evaluation techniques in Internet of Things. However, security on IoT is still searching for its way to improve so that it can provide reliability and protection against threats. Again, suitable selection of authentication and access control model is one of the main important parts in security, because it is the gateway of a user or device to introduce in a network. In addition, a proper selection of authenticate devices to protect the network from attacks. Due those issues, basic RBAC model is not really a suitable solution to perform authorization functions in IoT domain applications requiring high level of interoperability/scalability, such as smart grids and smart cities. Authentication and access control is the process for giving the authority to access the

specific resources, applications and system. Access control defines a set of criteria to access the heterogeneous devices of the IoT system and its resources. In Role Based model creates different authorities permissions by assigning access rights to specific roles or jobs within the IoT system then role based access control assigns these roles to users, It is effectively implemented in an environment because command and resources are assigned according to the roles.

## 7. CONCLUSION

The data can be perceived from any device at any moment. The powerful IoT heterogeneous devices authentication and Access Control is needed to make sure connected devices on the IoT can be trusted and access to the device resources to be what they intend to be. Accordingly, each IoT device needs a distinctive identity that can be authenticated when the device connected to the traditional network, it can track every device communicate securely with it, and inhibit it from executing detrimental processes. If a device shows unforeseen behaviour can simply revoke its privileges and compulsory to verify that the data do not change during transit. Then the network checks if this information is correct or not and ensures that the device is connected to the right network or not. It can be done using authentication and access control mechanism.

This paper is to propose a flexible Resource and Role Hierarchy Based Access Control (RRBAC) model for the dynamic IoT environment. Working from the RBAC access control model, the RRBAC access control model is more extendable, flexible and trustworthy. The main contribution of this paper is to understand the trust models enable the owners and roles to determine the trustworthiness of individual roles and users in the RBAC system respectively. RRBAC allow the data owners to use the trust evaluation techniques to decide to save their data in the IoT environment. RRBAC model provides a flexible approach for many security domains. Authentication and Access Control models supports different types of resources sharing to reduce the impact of any wrong data signal on the IoT traditional network. As a consequence, the RRBAC model provides a self-adaptive framework which is reliable enough too attached to any heterogeneous devices in the IoT environments.

REFERENCE

- [1] Ms.S.B.Sarvaiya, Dr.S.S.Sherekar, Dr.V.M .Thakare,” Taxonomy of Authentication Techniques in Security Attacks of Internet of Things”, NCETS “Research Journey” International E- Research journal, Impact Factor 6.261 ISSN: 2348-7143,February-2019.
- [2] Inayant Ali, Sonia, Sabir, Zahid Ullah," Internet of Things Security, Device Authentication and Access Control: A Review”, International Journal of Computer Science and Information Security (IJCSIS), vol. 14, no. 8, August 2016.
- [3] Sowmya Ravidas, et al. " Access Control in Internet-of-Things: A Survey”, ResearchGate March 29, 2019.
- [4] Antonio L.Maia Neto et al., " AoT: Authentication and Access Control for the Entire IoT Device Life-Cycle” November 2016.
- [5] Yungpeng Zhang,Xuqing Wu, " Access Control in Internet of Things: A Survey”, Asia-Pacific Engineering and Technology Conference, ISBN: 978-1-60595-443-1, 02 October 2018.
- [6] R. Sandhu, E. Coyne, H. Feinstein and C. Youman, "Role- based access control models," IEEE Computer, vol. 29, no. 2, pp. 38-47, 1996.
- [7] E. Yuan and J. Tong, "Attribute based access control (ABAC) for web services," in IEEE International Conference on Web Services, 2005.
- [8] C. Hu, D. Ferraiolo, D. Kuhn, A. Schnitzer, K. Sandlin, R. Miller and K. Scarfone, "Guide to attribute-based access control (abac) definition and considerations," in NIST Special Publication 800-162, 2014.
- [9] B. Shafiq, J. Joshi, E. Bertino and A. Ghafour, "Secure interoperation in a multidomain environment employing RBAC policies," IEEE TKDE, vol. 17, no. 11, pp. 1557- 1577.
- [10]N. Solanki, Y. Huang, I.-L. Yen, F. Bastani and Y. Zhang, "Resource and role hierarchy-based access control for resourceful systems," in CompSAC, 2018.
- [11]Xingdong Li, Zhengping Jin “Resource and Role Based Access Control Model”, 3<sup>rd</sup> International Conference on Mechatronics and Industrial Informatics (ICMII 2015).
- [12]Bokefode Jayant.D., Ubale Swapnaja A,Apte Sulbha S,Modani Dattatray G,” Analysis of DAC MAC RBAC Access Control based Model for Security”, International Journal of Computer Applications (0975-8887) Volume 104-No.5,October 2014.
- [13]Zhuo Tang, Juan Wei, Ahmed Sallam, Kenli Li, and Ruixuan Li,” A New RBAC Based Access Control Model for Cloud Computing Springer-Verlag Berlin Heidelberg 2012.
- [14]Yizhu Zhao, Yanhua Zhao, Hongwei Lu,” A flexible role-and resource-based access control model”, International Colloquium on Computing, Communication, Control, and Management 2018 ISECS
- [15]H.L.F.Ravi Sandhu, Edward J.Coyne, C.E. Youman. Role-based Access Control Models. IEEE Computer, 29 February 1996.
- [16]Nidhiben Solanki,Yongtao Huang,I-Ling Yen,Farokh Bastani,Yuqun Zhang,”Resource and Role Hierarchy Based Access Control for Resourceful Systems, International Conference on Computer Software and Applications 2018 42<sup>nd</sup> IEEE.
- [17]Tarak Nandy,Rafidah MD Noor,et al. " Review on Security of Internet of Things Authentication Mechanism ",IEEE,vol.7, August 26,2019.
- [18]Aafaf Ouaddah, et al.," Access control in The Internet of Things: Big challenges and new opportunities”, ScienceDirect, ISSN:1389-1286 17 January 2018.



look healthier and freour.

### Conclusion

Recognizing women's and men's distinct roles in family nutrition is a key to improving food security at the household level. To tackle this issue, FAO bases its approach to nutrition on the economic and cultural context of the area, FAO bases its approach to nutrition on the economic and cultural context of the area concerned, and considers that food security depends not only on the availability of food, but also on access to food, as well as on food adequacy and acceptability to consumers. Other underlying causes of malnutrition must also be addressed. These include dietary intake and diversity, health and disease, and maternal and child care – areas in which women play decisive roles.

### Recommendations

1. Olive oil can help reduce risk of certain cancers, blood pressure problems and heart disease, but there are 100 calories in each tablespoon so it is crucial to use it sparingly. One can either add a little in salad or use it in cooking.

2. Water-soluble vitamins include the vitamin B-complex and vitamin C, and are essential nutrients needed daily by the body in very small quantities.

### References

- Hotz Christine, González-Cossío (2016). The American Society for Nutritional Sciences, The Effect of Micronutrient Deficiencies on Child Growth: A Review of Results from Community-Based Supplementation Trials. <http://jn.nutrition.org/content/133/11/4010S.full>.
- Hector, Cori; Kumar (2014), "Fortification of cereals, rice, oil and sugar" Proceeding of the International Conference on Micronutrient Fortification of Food Science, application and management held at Delhi", pg 35-36.
- Orphan Nutrition (2016). An International Organization. Report: An Initiative of a child's best start to improve nutrition and feeding orphaned children Micronutrient Malnutrition. What is micronutrient deficiency? What is Vitamin- D Deficiency? [http://www.orphan nutrition.org/understanding-malnutrition/micronutrient-malnutrition/Vitamin\\_D](http://www.orphan nutrition.org/understanding-malnutrition/micronutrient-malnutrition/Vitamin_D).

10

## Misconceptions of Covid-19 Vaccine among College Students

S. D. Wakode

Head, Department of Psychology,  
Vidya Bharati Mahavidyalaya, Amravati

Ms. Vidhya Ambhore

Department of Psychology,  
Mahatma Fule Mahavidyalaya, Amravati

**Abstract:** The study aimed to reveal vaccine related misconceptions among college students. A questionnaire based on seven misconceptions identified by UNICEF was used. Online survey was conducted. Nine hundred eighty nine respondents replied the questionnaire. The study revealed that majority of respondents (80.50%) believed in natural immunity. Study stream was a partial factor in vaccine related misconceptions. Lower income group (0-1 Lakhs) exhibited significantly higher vaccine related misconceptions. It is also evident that gender is not a crucial factor in vaccine related misconceptions.

### Introduction

The emergence of a novel Corona virus indicates that our understanding of its mutations and risk factors for infection is still limited. Therefore, the tragedy that we are facing today makes us search for answers and corrective actions urgently for the survival of humans. But due to the information boom caused by internet and social media there are enormous misconceptions about this disease. Misconceptions related to corona virus disease-2019 (COVID-19) has been spread out broadly and the World Health Organization declared these as a major challenge to fight against the pandemic. Therefore,

**The Effect of Job Vulnerability on Pandemic Prevalent Concern: Loneliness.****Dr. S. D. Wakode**

HOD, Department of Psychology, Vidyabharati Mahavidyalaya, Amravati

**Ujjwala Godbole Kulkarni**

Research Scholar, Vidyabharati Mahavidyalaya, Amravati.

**Abstract:**

Imposition of lockdown and subsequent isolation during Covid19 pandemic made Loneliness (is a subjective experience, painful, unwanted and difficult to tolerate) worse and job profile and working pattern of and every professional has changed drastically during and post pandemic period. This research aims to study the effect of job profile on pandemic prevalent concern-Loneliness. The profiles under consideration are (a) most vulnerable people – Medical Professionals and (b) less vulnerable than medical professionals i.e. – Non-Medical Professionals. Survey method was used to obtain the information. Study includes sample of 80 professionals (40 Medical, 40 Non-Medical) selected randomly from Amravati District. Standardized UCLA Loneliness Scale (Version3) by Daniel w. Russell was used. Mean, Standard Deviation and T-values were computed. Statistical analysis reveals that there is no significant difference between loneliness experienced by medical and non-medical professionals.

**Key Words:** Job Vulnerability, Medical Professionals, Non-Medical Professionals, Loneliness, COVID 19 Pandemic.

1. Introduction The mankind has been experiencing manmade or natural disasters since centuries. Societies have also tried to come out of or get rid of such situations. But, the world has witnessed many drastic changes in the way we live and lead our daily life from last 3 to 4 decades more prominently. Rapid technological revolution in automation, digital revolution, loss of geographical barriers due to modernized way of transport and communication, global environmental changes, global witness of new diseases and epidemics and growing number of natural disasters are the main contributing factors for these drastic changes. These changes have also brought in changes in values and beliefs of masses. It is observed that along with the advent of these changes, daily living of general population is not only modernised, advanced and innovative but also complex, competitive and stressful at the same time.

Till recently, type of disaster, type of devastation thereon and subsequent mental problems were different at different geographies or families. Present day Covid-19 pandemic is unique disaster in a sense that whole world or world population have experienced same disaster and same mental problems at the same time. Due to imposed pandemic countering measures like heavy medication, getting quarantined, lockdowns etc. and inadequate resources like medicines, oxygen etc.; almost every individual have experienced helplessness, fear of death and loneliness. We have not experienced such disaster across the globe in recent century.

Consequently, job profiles have changed drastically with particular reference to current pandemic. Professionals working in medical field were in great demand. Even students pursuing their last semester of doctorate degree had to work in Covid wards. Medical professionals have undergone the most stressful situation due to responsibility of others' life and concern of self-life at the same time. Professionals, other than medical field have to change their working pattern to a greater extent. During this period of pandemic, medical professionals were mostly insecure and level of risk faced by them was highest among all other professionals

Thus, the situation has brought forth challenge for every individual to be fittest so as to come out of and sustain in this situation and situation here forth.

As such situations may recur in future, this is the best and unique opportunity provided by time to us to study the effect of job profile on pandemic prevalent prominent mental concern: Loneliness.

For the present study the job profiles under consideration are (a) most vulnerable people – Medical Professionals and (b) less vulnerable than medical professionals i.e. – Non-Medical Professionals.

Amravati District experienced a unique situation from February 2021 i.e. emergence of a new mutant and drastic rise in infection thereon. Hence, all class of people in the district have undergone



more stressful situation than any other districts. So for collection of the sample Amravati district is considered as a population for the present study.

### 1.1 Loneliness

Loneliness is a subjective feeling. Being alone is different from loneliness. One may perceive himself/herself as lonely even when surrounded by friends and loved ones. Loneliness is something everyone feels at some point of life. Human beings have a fundamental need of belongingness. If this need is not satisfied they may experience problems like anxiety, frustration, emotional disturbances, depression and various other psychosomatic difficulties.

The deficit in social participation and relationships can lead individuals to report higher level of loneliness.

Loneliness is a subjective experience, which is painful, unwanted, aversive and difficult to tolerate.

Loneliness can be defined as the discrepancy between desired and actual quantity and quality of social relationships. (Peplau and Perlman, 1982)

Loneliness is an emotional state, not necessarily, the objective state of being alone – it is dissatisfaction with social relationships, regardless of how few or numerous, infrequent or active (Hawkley and Cacioppo, 2010).

The American Psychological Association defines loneliness as an affective and cognitive discomfort or uneasiness from being or perceiving oneself to be alone or otherwise solitary.

### 1.2 Objective

To assess the effect of Job Vulnerability on loneliness and find out whether medical and non-medical professionals differ significantly from each other or not.

### 1.3 Hypothesis

There will be significant difference in the level of loneliness experienced by medical and non-medical professionals; Medical professionals will experience lower level of loneliness than non-medical professionals.

## 2. Review of literature

The review of literature is a text of earlier researches which include correct knowledge including valuable findings and aid to situate the current study within the body of literature. Many researchers have tried to explore how job profile is related to and affects important trait like loneliness.

2.1) María Cabello, Ana Izquierdo, Itziar et al (2021) conducted study on Loneliness and not living alone is what impacted on the healthcare professional's mental health during the COVID-19 outbreak in Spain. This study was aimed at exploring the role of loneliness in the healthcare professionals' mental health during the COVID-19 outbreak in Spain.

This study has showed that, after controlling for other covariates, the presence of feelings of loneliness was related to lower mental health in healthcare professionals. The prevalence of health professionals with feelings of loneliness was 53% in this study. This number is very high if we consider that the prevalence of people who have feelings of loneliness is around 30% in the Spanish adult population (Martín-María et al., 2020).

Study concluded that presence of loneliness was positively related to higher mental health problems after controlling for other covariates. Other factors related to higher mental health problems were a higher COVID-19 risk perception, being in quarantine, checking COVID-19-related news several times a day and having a lower training on managing infectious diseases.

2.2) Sonam Joshi in her article in Times Of India (Oct 8, 2020) wrote that among 3 in 5 (60%) Indian professionals have felt lonely at some point while working remotely in the last few months, while 73% still feel lonely now. These are the findings of the LinkedIn Workforce Confidence Index, an online survey of 16,199 Indian professionals conducted between April and September to understand the impact of the pandemic and remote work on their mental health.

2.3) Lauren Vogel (2018) in his article published in Harvard Business Review Stated that Doctors and lawyers are among America's loneliest workers, followed by people who work in engineering and science. Researchers surveyed 1624 full-time employees on the degrees of loneliness and social support they experienced daily, both in and out of the workplace. Respondents with graduate degrees reported higher levels of loneliness than those who had completed only undergraduate studies or high school. Lawyers and doctors were the loneliest by far, reporting levels of loneliness 25% higher than respondents with bachelor's degrees and 20% higher than those with PhDs.



2.4) Joanne M. Stubbs, Helen M. Achat(2022) conducted a survey of Health Care Workers and stated that Loneliness in HCWs is a legitimate concern, negatively impacting their well-being during a health crisis. Contact with family and friends, the support provided by living with one's partner and a sense of camaraderie with colleagues were associated with mental well-being and indicate potential avenues to ameliorate the adverse consequences of loneliness.

### 3. Research Methodology

**3.1 Research Method** - Survey descriptive method was used for this study.

**3.2 Population** – For the present study population includes professionals from Amravati District of the age ranging from 25 years to 55 years which are categorized into two groups' medical and non- medical professionals.

Medical Professionals of Amravati District - general and specialized physicians and surgeons, dentists, nurses, dieticians, physiotherapists, speech therapists, pathologists, lab Technicians, ward boys, Pharmacists, Psychologist.

Non-Medical professionals of Amravati district – All professionals other than Medical Professionals. (Administrative staff, educationist, bankers, police, self-employed, businessmen etc.)

**3.3 Sample-** The sample of the present study consisted of 80 professionals with equal number of medical and non- medical Professionals i.e. 40 each. The samples were selected randomly from different hospitals, school, shops, banks and offices. This Sample is free from distinguishing factors like Gender, Area (rural and Urban) and Education.

### 3.4 Research Tool

Standardized Psychological test: UCLA loneliness scale (version 3)- by Daniel W. Russell was used for the present study. It contains 20 items. The test is highly reliable, both in terms of internal consistency (coefficient alpha ranging from 0.89 to 0.94) and test-retest reliability over a 1 year period ( $r = 0.73$ )

**3.5 Procedure-** The researcher briefed the participants regarding purpose of the study and assisted them while solving the UCLA Loneliness scale (version 3) as per the need of the participants. Participants were given sufficient time to complete the UCLA Loneliness scale (version 3).

**3.6 Statistical Techniques-** In order to draw out the results the researcher used statistical techniques like Mean, Standard deviation, and T-test

### 3.7 Statistical Results and Findings

Professionals	N	Mean	S.D.	t-value	Significance
Medical	40	38.45	9.462341	0.146436	Not Significant at 0.05 level ( $p > 0.05$ )
Non-Medical	40	38.75	8.851336		

Table 1

**4. Discussion-** A perusal of table 1 reveals that mean loneliness scale scores of medical and non-medical professional were 38.45 and 38.75, with S.D. 9.462341 and 8.851336 respectively. The t- value between the means of two groups was found to be 0.146436 which is not significant at 0.05 level of significance. It shows that there is no significant difference between loneliness experienced by medical and non-medical professionals. This finding is in the line with the findings of Lauren Vogel (2018) and Sonam Joshi (2020). Thus the hypothesis is rejected.

### 5. Conclusion

Conclusion of the study is Medical and non-medical professionals do not differ significantly from each other on the level of Loneliness. Medical Professionals and non-medical professionals have experienced a same level of loneliness.

### 6. Scope and Limitations of the study

#### 6.1 Scope

1. Medical and non-medical professionals are included in this study. People, who are not medical professionals, were treated as non-medical professionals.
2. The sample data was collected form people of Amravati district.
3. An important pandemic prevalent concern: loneliness was considered in this study.

#### 6.2 Limitations

1. The sample data was collected form people of Amravati district only.
2. The sample size was small.
3. The sample was not distinguished between gender, area (rural and urban) and education.



4. Sample was collected from literate people only.
5. Though Pandemic situation may have brought many prevalent concerns on the surface only loneliness was taken into account for study.
6. Consistently the nature of covid variant is changing that's why there is a possibility in severity and changes in system.
7. The research was done using self-report questionnaires, so there is a possibility that the responses given by the respondents to be false.

**REFERENCES**

- 1) Cabello,M.,Itzier,A.I. et al (2021). Loneliness and not living alone is what impacted on the healthcare professional's mental health during the COVID-19 outbreak in Spain. *In health and social care in community* retrived from <https://doi.org/10.1111/hsc.13260>
- 2) Eng, A (2016). Understanding Loneliness. Retrieved from <https://sites.northwestern.edu/nphr/files/2019/01/nphr-2016-eng-loneliness-z94prz.pdf>
- 3) <https://dictionary.apa.org/loneliness>
- 4) Joanne M. Stubbs, Helen M. Achat (2022) Are healthcare workers particularly vulnerable to loneliness? The role of social relationships and mental well-being during the COVID-19 pandemic In *Psychiatry Research Communications*, 2(2),retrieved from <https://doi.org/10.1016/j.psycom.2022.100050>
- 5) Joshi, S., (Oct 8,2020) Around 3 in 5 (60%) Indian professionals have felt lonely at .. *In Times of India*[http://timesofindia.indiatimes.com/articleshow/78550390.cms?utm\\_source=contentofinterest&utm\\_medium=text&utm\\_campaign=cppst](http://timesofindia.indiatimes.com/articleshow/78550390.cms?utm_source=contentofinterest&utm_medium=text&utm_campaign=cppst)
- 6) Lauren Vogel(2018)Medicine is one of the loneliest professions In *CMAJ* August 07, 2018 **190 (31) E946; Retrieved from DOI: <https://doi.org/10.1503/cmaj.109-5640>**
- 7) Pagan, R. (2020). Gender and Age Differences in Loneliness: Evidence for People without and with Disabilities. In *International Journal of Environmental Research and Public Health*. Retrieved from <https://www.mdpi.com/journal/ijerph>
- 8) Sunny, A.M., Jacob, J.G., Jimmy N., Shaji, D.T., & Dominic, C (2018). Emotional maturity variation among college students with perceived loneliness. In *International Journal of Scientific and Research Publications*. Retrieved from <http://dx.doi.org/10.29322/IJSRP.8.5.2018.p7736>

**A study of Coping Strategies of Frontline and Non-Frontline workers.****Dr. S.D. Wakode**

HOD, Department of Psychology Vidyabharati Mahavidyalaya, Amravati.

**Vanita Sachin Raut**

Research Scholar Vidyabharati Mahavidyalaya, Amravati.

**Abstract:**

Frontline and Non-Frontline workers were critically working hard for normal functioning of the society during Covid19 pandemic.

Aim of this research is to understand the difference between Coping Strategies of frontline and Non-Frontline workers. Survey method was used to collect the sample size of 80 workers (frontline-40 and Non-frontline-40) using random sampling method. Standardized psychological test named Coping Techniques Scale by Dr.Vijaya Lakshmi and Dr. ShrutiNarain was used. Mean standard deviation and T-values were computed. Statistical analysis revealed that Frontline Worker's Coping Strategies are significantly different from Non-Frontline workers.

Key Words: Frontline Workers, Non-Frontline Workers, Coping Strategies, COVID 19 Pandemic.

**1. Introduction**

Man has witnessed many challenges posed by diseases across centuries that caused havoc across the world. Diseases like plague, cholera, flue, etc. affected people across the globe in varying magnitude and caused innumerable deaths of human beings. The latest pandemic that the world witnessed of late was COVID-19. It had its origin in China and later spread to every part of the world. It killed thousands and is still causing damage to human health and lives.

Governments in different parts of the world took various measures to tackle the pandemic, from containing it to making people immune to the disease. One common measure was locking down all the economic activities and confining people to their homes. Even though the measures were aimed at protecting human lives, it caused immense financial distress especially to those who earned their living on daily wages. The collateral damage was even severe if one were to consider the mental issues that plagued many because of the restricted movements.

Government machinery & certain other institutions needed to function even during the onslaught of the pandemic. Institutions like state and central police organizations, armed forces, home guards and civil defense including disaster managements and municipalities, health care, banks, prisons, revenue departments functioned as usual for surveillance and containment activities. Within these institutions there were two categories of workers, viz.; Frontline workers and Non-frontline workers. Frontline workers were the officials engaged in containment and surveillance activities etc and non-frontline workers were officials engaged in the field of education, agriculture and food production, critical retail (i.e. grocery stores, hardware stores, mechanics), critical trades (construction workers, electricians, plumbers, etc.), workers involved in transportation, officials of nonprofit and social service organizations and self-employed people.

Both frontline workers and non-frontline workers were critical for normal functioning of the society and the containment of the pandemic. They not only ensured that those who were confined to homes received regular supply of essential commodities and medicines but also took care of those who were affected by the disease. But since these were the ones who constantly came in contact with people and were exposed to disease at every step, they had to take extra precaution in order to discharge their duties efficiently and at the same time remain healthy themselves. Extended working hours, work overload, and constant exposure to spreading disease lead to problems like stress and deterioration of both mental and physical health among frontline and non-frontline workers.

Work related stress is not new. It leads to various mental issues like depression and anxiety. Heightened performance expectations, demanding work schedules, fear of losing job, being in wrong profession, etc are some of the reasons for work related stress. In case of frontline and non-frontline workers during pandemic the fear of getting infected and passing on the infection to family, alienation from society and even the fear of death were other dominant factors for deterioration of mental health.



This problem became acute due to the prolonged period of pandemic and lockdowns. Therefore, maintaining positive mental health became a priority for workers in pandemic situations.

Different coping strategies have also been designed to address the issues of mental health. General awareness about such coping strategies is essential especially among officials working in pandemic like situations. If followed proactively, these strategies will help maintain good mental health to all who are subject to mental stress.

This research is aimed at understanding different coping strategies and their effectiveness in maintaining sound mental health. The outcomes of this study may be useful in providing inputs to various institutions in framing policies in future for frontline and non-frontline workers.

**Definition:****Coping strategies:**

1- Coping Strategies refer to the specific efforts, both Behavioral and Psychological that people employ to master tolerate, reduce, or minimize stressful events. (Holahan & Moos, 1987).

2- Coping resources are predictive of psychological wellbeing and act as buffers emotional disorder. (McCarthy et al, 2006)

**1.2 Objective**

To Study the Coping Strategies of Frontline and Non-Frontline Workers, to find out whether they differ significantly from each other or not.

**1.3 Hypothesis**

There will be significant difference in coping strategies of Frontline and Non-Frontline Workers; frontline workers will exhibit adaptive coping strategies than non-frontline workers.

**2. Review of literature**

The review of literature is a text of earlier researches which include correct knowledge including valuable findings and aid to situate the current study within the body of literature.

2.1. "Emotional responses and coping strategies in nurses and nursing students during Covid-19 outbreak: A comparative study". by Long Huang, Wansheng Lei, Fuming Xu, Hairong Liu, Liang Yu (2020). In this study they investigate nurses' emotional responses and coping styles, and conduct a comparative study with nursing college students. This study was conducted through the online survey questionnaire. The results found that women showed more severe anxiety and fear than men. Participants from cities exhibited these symptoms more than participants from rural areas, however rural participants experienced more sadness than urban participants.

2.2. "Exploring stress coping strategies of frontline emergency health workers dealing Covid-19 in Pakistan: A qualitative inquiry." This study examines the psychological impact of COVID-19 on emergency HCWs and to understand how they are dealing with COVID-19 pandemic, their stress coping strategies or protective factors, and challenges while dealing with COVID-19 patients. In the result they found that participants practiced and recommended various coping strategies to deal with stress and anxiety emerging from COVID-19 pandemic. Media was reported to be a principal source of raising stress and anxiety among the public. Religious coping as well as their passion to serve humanity and country were the commonly employed coping strategies.

2.3. "Challenges, experience, and coping of health professionals in delivering healthcare in an urban slum in India during the first 40 days of COVID-19 crisis: a mixed method study" By Carolin Elizabeth George, Shon Rajukutty, Luc P de Witte Correspondence to Dr Carolin Elizabeth George; (2020). This study describes the initial dilemmas, mental stress, adaptive measures implemented and how the healthcare team collectively coped while providing healthcare services in a large slum in India, during the COVID-19 pandemic.

**3. Research Methodology**

**3.1 Research Method** - Survey descriptive method was used for this study.

**3.2 Population** – For this study population includes workers from Amravati District of the age ranging from 22 years to 60 years which are categorized into two groups Frontline and Non-Frontline workers.

(Frontline workers of Amravati District – Medical Professional, Bankers, and police

Non-Frontline workers of Amravati district – Administrative staff, educationist, self-employed.)

**3.3 Sample**- The sample of the present study consisted of 80 workers with equal number of Frontline and Non-Frontline workers i.e. 40 each. The samples were selected randomly from different hospitals, school, shops, banks and offices. This Sample is free from distinguishing factors like Gender, Area (rural and Urban) and Education.



### 3.4 Research Tool

**Standardized Psychological test: Coping Techniques Scale:( Dr.Vijaya Lakshmi and Dr. ShrutiNarain)**In this test two types of coping strategies are measure. First is adaptive coping and second is maladaptive coping. This scale meant for individuals from 15 years and above of age. There is fix time limit as such. However, it generally takes about 20 to 25 minutes in its completion. The scoring of all the items of this scale can be done by giving a score 5, 4,3,2,1, for always, almost always, sometime, almost never, never respectively. Reliability check by Test re test Methods and Split half Methods. All reliability coefficients were significant at .01 level. This test was validated against the COPE inventory (Carver,Scheier and Weintraub ,1989 ) The concurrent validity 0.80 was significant. The qualitative interpretation of the obtained score is as under; high, moderate, low, high, moderate low.

**3.5 Procedure-** The researcher briefed the participants regarding purpose of the study and assisted them while solving the Coping Techniques Scale as per the need of the participants. Participants were given sufficient time to complete the test

**3.6 Statistical Techniques-** In order to draw out the results the researcher used statistical techniques like Mean, Standard deviation, and T-test.

### 3.7 Statistical Results and Findings

**Table 1**

Workers type	N	Mean	S.D.	t-value	Significance
Frontline	40	135.125	12.85857	2.08	Significant at 0.05 level (p<0.05)
Non- Frontline	40	129.775	9.92		

### 4. Discussion

A perusal of table 1 reveals that mean adaptive coping strategies scale scores of Frontline and non-Frontline workers are 135.125 and 129.775 with S.D.12.86 and 9.92 respectively. The t- value between the means of two groups is 2.08 which is significant at 0.05 level of significance. It shows that there is a significant difference between adaptive coping strategies of frontline and non-frontline workers. It indicates that Frontline workers exhibit better adaptive coping strategies as compare to non-frontline workers. Thus the hypothesis is accepted.

### 5. Conclusion

Conclusion of the study is that there is a significant difference in coping strategies of Frontline and Non-Frontline Workers; frontline workers exhibits better adaptive coping strategies than non-frontline workers.

### 6. Scope and Limitations of the study

#### 6.1 Scope

- This study is useful for the pandemic warriors in understanding their mental and taking steps for their wellbeing.
- This study will be useful for understanding coping strategies of pandemic workers.
- The study is useful in providing inputs for framing welfare policies for the pandemic warriors.

#### 6.2 Limitations

1. The sample data was collected form people of Amravati district only.
2. The sample size was small.
3. The sample was not distinguished between gender, area (rural and urban) and education.
4. Sample was collected from literate people only.
5. The research was done using self-report questionnaires, so there is a possibility that the responses given by the respondents to be false.

### REFERENCES:

- 1.) Carver, C. S., & Connor-Smith, J. (2010). Personality and coping. *Annual review of psychology*, 61, 679–704. <https://doi.org/10.1146/annurev.psych.093008.100352>
- 2.) George CE, Inbaraj LR, Rajukutty S, et al. 2020. Challenges, experience and coping of health professionals in delivering healthcare in an urban slum in India during the first 40 days of COVID-19 crisis: a mixed method study. *BMJ Open*2020;10:e042171. <https://doi:10.1136/bmjopen-2020-042171>
- 3.) Heffer T, Willoughby T (2017) A count of coping strategies: A longitudinal study investigating an alternative method to understanding coping and adjustment. *PLoS ONE* 12(10): e0186057. <https://doi.org/10.1371/journal.pone.0186057>
- 4.) <https://dictionary.apa.org/coping-strategy>





- 
- 5.) Huang L, Lei W, Xu F, Liu H, Yu L (2020) Emotional responses and coping strategies in nurses and nursing students during Covid-19 outbreak: A comparative study. *PLoS ONE* 15(8): e0237303. <https://doi.org/10.1371/journal.pone.0237303>
- 6.) Munawar, Khadeeja&Choudhry, Fahad. (2020). Exploring Stress Coping Strategies of Frontline Emergency Health Workers dealing Covid-19 in Pakistan: A Qualitative Inquiry. *American Journal of Infection Control*. 49. <https://doi.org/10.1016/j.ajic.2020.06.214>

75  
Azadi Ka  
Amrit Mahotsav



ऋते ज्ञानान्न मुक्तिः

# Srujan Prabhat

A Biannual Research Journal

ISSN : 2249-1171 | Volume - II | October 2022 | Issue - II

**SPECIAL EDITION**



**Government Vidarbha Institute of Science  
And Humanities (Autonomous), Amravati**

NAAC Re-accredited 'A' Grade with CGPA 3.32



43	स्थानिक स्वराज्य आणि महिला नेतृत्व	डॉ. अर्चना ज्ञा. पाटील	191-195
44	स्थानिक स्वराज्य आणि महिला नेतृत्व	प्रा. देवेंद्र उत्तमराव ठाकरे	196-199
45	७३ वी घटना दुरुस्ती व पंचायत राज व्यवस्था	डॉ. सुनंदा तिडके	200-202
46	स्थानिक स्वराज्य संस्थेसमोरील आव्हाने	डॉ. प्रशांत विघे	203-207
47	स्थानिक स्वराज्य संस्था आणि महिला नेतृत्व	अमित पुरुषोत्तम इंगोले प्रा.डॉ. विनायक कोडापे	208-211
48	महात्मा गांधी आणि ग्रामीण विकास	डॉ. डी.के. खोकले	212-214
49	स्थानिक स्वराज्य संस्थेतील महिला नेतृत्वाचा विकास : एक अवलोकन	प्रा.डॉ.शुद्धोधन एस. गायकवाड	215-219
50	स्थानिक स्वराज्य संस्था आणि महिला सबलीकरण	डॉ. स्वप्ना त्र्यं. लेंडे	220-224
51	स्थानिक स्वराज्य संस्था आणि गांधी विचारांची प्रासंगिकता	डॉ. विष्णु पुंजाजी पवार	225-229
52	स्थानिक स्वराज्य संस्था आणि ग्रामीण विकास विशेष-संदर्भ:- गोंदिया जिल्हा	डॉ. एच. पी. पारधी	230-235
53	स्थानिक स्वराज्य संस्थांचे महत्त्व	प्रा. मेघराज आर. शिंदे	236-237
54	ग्रामव्यवस्थेचा व्हास व नागरीकरण	डॉ. दिनेश स. धाकडे	239-242
55	स्थानिक स्वराज्य संस्था आणि स्थानिक लोकांचा लोकसहभाग	प्रा. डॉ. आशिष दि. काळे	243-245
56	स्थानिक स्वराज्य संस्था आणि गांधीवादी विचारांची प्रासंगिकता	डॉ. प्रविण जयकृष्ण गुल्हाने	246-250
57	स्थानिक स्वराज्य संस्था आणि ग्रामीण विकास	डॉ. एल. जी. सोनुले	251-253
58	सत्तेचे विकेंद्रीकरण व ग्रामस्वराज्याची संकल्पना	डॉ. पंकज परसराम नंदेश्वर डॉ. प्रिया अनिरुद्ध सांगोले	254-256
59	महात्मा गांधी यांची स्थानिक स्वशासन संकल्पना	डॉ. प्रमोद एम. तालन डॉ. निना चवरे	257-259
60	स्थानिक स्वराज्य संस्था आणि ग्रामीण विकास	प्रा. डॉ. कल्पना एस. गोडघाटे	260-263
61	ग्रामीण विकासात स्थानिक शासनाची भूमिका	प्रा. डॉ. चावरे एम. व्ही.	264-267
62	महात्मा गांधीचे सर्वोदयी विचार आणि ग्रामीण विकास	प्रा. डॉ. रविंद्र भणगे	268-276
63	ग्रामीण विकास आणि महिला नेतृत्व (विशेष संदर्भ चंद्रपूर जिल्हा)	प्रा. डॉ. राजेंद्र सदाशिव मुद्दमवार	277-282

## स्थानिक स्वराज्य संस्था आणि महिला नेतृत्व

अमित पुरोषोत्तम इंगोले

राज्यशास्त्र विभाग प्रमुख

विद्याभारती महाविद्यालय, अमरावती

### प्रस्तावना

'स्थानिक स्वराज्य संस्था' हा राज्य व्यवस्थेचा प्रमुख आधारस्तंभ मानला जातो. प्रामुख्याने भारतातील पंचायत राज व्यवस्था ग्रामीण विकासाच्या दृष्टीने महत्त्वाची प्रशासकीय यंत्रणा आहे. पंचायत राज व्यवस्थेचे जिल्हा पातळीवर जिल्हा परिषद, विकास गट पातळीवर पंचायत समिती आणि पायाभूत समजल्या जाणाऱ्या ग्राम किंवा खेडे पातळीवर ग्रामपंचायत अशी प्रशासकीय रचना आढळून येते. यातील ग्रामपंचायत म्हणजे प्राचीन पंचायतीचे आधुनिक स्वरूप होय. ग्रामीण भागात राहणाऱ्या जवळपास ७० टक्के लोकसंख्येची निगडित ग्रामपंचायतीची भूमिका असते. प्राचीन कालखंडापासून पंचायतीतील महिलांचा सहभाग अपवादात्मक राहिला आहे. मात्र १९९२ च्या ७३ व्या घटनादुरुस्तीने महिलांना ग्रामपंचायतीतील ३३ टक्के आरक्षण देऊन निर्णय निर्धारण प्रक्रियेतील त्यांच्या राजकीय प्रवेशाचा मार्ग सुकर केला. अर्थात ग्रामपंचायतला दीर्घ इतिहास लाभला असला तरी त्यातील महिला सहभाग ही नवीन संकल्पना आहे.

सत्याचे विकेंद्रीकरण हा केंद्रबिंदू म्हणून महाराष्ट्राचे शिल्पकार कै. यशवंतराव चव्हाण यांनी पंचायत राज व्यवस्थेची मुहूर्तमेढ रोवली. महाराष्ट्रातील पंचायत राज व्यवस्था ही आदर्श व्यवस्था म्हणून संपूर्ण देशात मान्य झाली आहे. ७३ व्या घटना दुरुस्तीमुळे पंचायत राज संस्थांना विशेष करून ग्रामपंचायत व ग्रामसभा या शेवटच्या स्तरावरील संस्थांना घटनात्मक अधिकार प्राप्त झालेले आहेत. त्यामुळे राज्यातील पंचायत राज व्यवस्थेला बळकटी प्राप्त झालेली आहे. देशातील महिलांना सत्तेत प्रत्यक्ष सहभाग देण्यात महाराष्ट्र अग्रेसर राहिला आहे. महिलांना सबळ करण्याच्या पथावरील ग्रह करावे घटना दुरुस्ती हे महत्त्वाचे पाऊल आहे. याची जाणीव असल्यामुळे प्रथम जिल्हा परिषदेच्या पातळीवर महिला व बालविकास समितीची स्थापना करण्यात आली आणि पंचायतराज व्यवस्थेत ३३ टक्के जागा मुलांसाठी राखून ठेवण्यात आल्या.

### संशोधनाची उद्दिष्ट्ये-

महिलांचा राजकीय सहभागाचा अर्थ अभ्यासणे

स्थानिक स्वराज्य संस्थेतील महिलांची भूमिका अभ्यास

### संशोधन पध्दती

प्रस्तुत शोधनिबंधासाठी संकलित तथ्यांचे संकलन हे प्रामुख्याने दुय्यम स्रोतांच्या माध्यमातून केले आहे. यासाठी प्रामुख्याने स्थानिक स्वराज्य संस्थेच्या संदर्भात पुस्तके, महिलांचे नेतृत्व या संबंधीत साहित्याचा आढावा घेतला आहे.

### महिलांचा राजकीय सहभागाचा अर्थ

राजकारणातील सहभाग ही लोकशाही राजकीय व्यवस्थेच्या यशस्वी तेथील अत्यावश्यक व महत्त्वाची बाब

होय. लोकशाही समाज हा सहभागीतापूर्ण समाज असून जातसत्ता लोकप्रतिनिधीच्या अंतर्गत असते. यात सामान्य नागरिकांचा शासकीय प्रक्रियेतील सहभाग अपेक्षित असतो. यामध्ये लिंग, जात, वर्ग, धर्म या बाबी गुण असतात. पालमर म्हणतात, 'लोकशाही व्यवस्थेत नागरिकांचा राजकीय बाबतीतील क्रियाशील सहभाग महत्त्वाचा असतो कारण त्यामुळे व्यवस्थेला आधी मान्यता प्राप्त होऊन ती बलशाली बनते.' म्हणून राजकीय सहभागाची व्याख्या करताना ते म्हणतात, 'राजकीय सहभाग म्हणजे नागरिकांचा राजकीय क्रिया मधील सहभाग असून, तो प्रत्यक्ष-अप्रत्यक्षरीत्या निर्धारण कर्त्यांच्या वर्तणुकीवर प्रभाव कार्य ठरतो.

राजकीय सहभागा विविध मार्गातून होत असतो. हे राजकीय सहभागाचे शान फिल्म १० मार्ग सांगितले आहेत, व्हर्बानी मतदानात सहभाग, राजकीय मोहिमेत सहभाग, सहकार्य पूर्ण व लोक संपर्क जनसंपर्क इत्यादी मार्ग सांगितलेले आहेत.

महिलांच्या राजकीय सहभागाबाबतचा विचार हा १९७५ पासून म्हणजे आंतरराष्ट्रीय महिला वर्ष नंतर सुरू झाला. महिलांच्या राजकीय सहभागावर अनेक बाबींचा प्रभाव पडत असतो. त्या संदर्भात अनेक विद्वानांमध्ये एक मत नाही. महिलांच्या राजकीय सहभागाबाबत मिल ब्रेथ व गोयल म्हणतात, 'सामान्यतः परंपरेने राजकारण हे पुरुषांचे क्षेत्र राहिले व महिला त्यात अत्यल्प मिसळलेल्या आहेत. आजच्या आधुनिकीकरणात व कारखानदारीमुळे लिंगभेद कमी झाला असला तरी परंपरेमुळे तो बहुतांशी दिसून येतो. तरीही पुरुष मानसशास्त्रीय दृष्ट्या स्त्रियांपेक्षा राजकारणात अधिक प्रमाणात सहभागी होतात.

महिलांच्या राजकीय सहभागाबाबत युनेस्को (UNESCO) मी केलेल्या सात दक्षिण पूर्व आशियाई राष्ट्रांच्या सर्वेक्षणात असे आढळले की, (ऑस्ट्रेलिया भारत बांगलादेश नेपाळ थायलंड मलेशिया व फिलिपाईंस ) पक्ष सदस्यत्वात निवडणुकीत मतदानात व राजकीय महिलांच्या बाबतीत महिलांचा राजकीय सहभाग एवढासा प्रभावी दिसत नाही. त्यातील बहुतांशी महिलांचे पती किंवा अन्य नातेवाईक राजकारणात सक्रिय असलेले दिसतात. म्हणून सर्वसाधारणपणे महिलांचा राजकीय सहभाग खालील प्रमाणे स्पष्ट दिसते.

१. परंपरेमुळे व मानसशास्त्रीय दृष्ट्या महिला राजकारणातून उदासीन असतात.
२. शिक्षणाचा अभाव.
३. कुटुंबाच्या राजकीय पार्श्वभूमीचा प्रभाव महिलांच्या राजकीय सहभागावर पडतो.
४. महिलांच्या राजकारणाबद्दल नकारात्मक दृष्टिकोन देखील राजकीय सहभागावर करतो.
५. महिलांचे कुटुंब प्रति असलेल्या जबाबदारी अशा अनेक महिलांच्या राजकीय सहभागावर काही प्रमाणात प्रभाव पडतात.

भारताने स्वातंत्र्यानंतर लोकशाही समाजवाद कल्याणकारी राज्य व धर्मनिरपेक्षता इत्यादी बाबी उद्देश पत्रिकेच्या माध्यमातून नागरिकांना लेखी हमी देऊन समाजाचा सर्वांगीण विकास होण्यास मदत होईल, असे चित्र स्पष्ट झाले असले तरीही लोकशाही शासन प्रणाली आपणास नवीन असल्यामुळे भारतीयांना लोकशाहीचे राजकीय शिक्षण देण्याची आवश्यकता होती व असे प्रशिक्षण देण्यासाठी नागरिकांचा जास्तीत जास्त राजकीय सहभाग आवश्यक असतो. लोकशाहीत निवडणुकीच्या माध्यमातून राजकीय सहभाग वाढतो व लोकशाही मजबूत बनते. राजकीय सहभागामुळे

राष्ट्रीय समस्यांची अधिक चांगल्या प्रकारे सोडवणूक होते. एवढेच नव्हे, तर देशातील निकोप राजकीय प्रक्रियेसाठी जास्तीत जास्त नागरिकांनी सहभाग घेतला पाहिजे. पुरुषांप्रमाणे स्त्रियांचा सहभाग वाढला पाहिजे.

### स्थानिक स्वराज्य संस्थेतील महिलांची भूमिका

ग्रामपंचायत पंचायत समिती व जिल्हा परिषद या तिन्ही स्तरावरील स्थानिक स्वराज्य संस्थेमध्ये महिलांचा सहभाग उल्लेखनीय आहे. महिलांसाठी केवळ जागा राखून ठेवून आमचे काम भागत नाही, तर त्यांना सक्षम करणे, त्यांच्या प्रशिक्षणातून कौशल्य विकास करून एक कार्यक्षम लोकप्रतिनिधी बनविणे, ही काळाची गरज आहे. त्यासाठी महाराष्ट्रातील पंचायत राज प्रशिक्षण केंद्रीय व यशवंतराव चव्हाण विकास प्रशासन प्रबोधिनी, पुणे यांच्या माध्यमातून अनुक्रमे ग्रामपंचायत, पंचायत समिती व जिल्हा परिषद पातळीवरील नवनिर्वाचित सदस्यांना घटक कार्यक्रमांतर्गत प्रशिक्षणाचे काम सुरू केले असून, या प्रशिक्षण कार्यक्रमास प्रतिसादही चांगला मिळत आहे. महिला आरक्षण स्थानिक स्वराज्य संस्थांना लागू करण्यात आले. त्यामुळे महिलांना दिलेल्या संधीमुळे महिलांचे प्रश्न पुढे आले. त्यांचा आत्मविश्वास वाढला. सार्वजनिक जीवनात त्यांच्या सहभागाला महत्त्व आहे. नेतृत्वाच्या दिशेने वाटचाल सुरू झाली असली तरी स्त्रियांची राजकारणातील सहभागाची बेरीज अजून बरोबर झाली नाही.

महिलांचे राजकारणातील प्रवेशाबद्दल कौतुक केले जाते. तिचा गौरव केला जातो. मात्र, नंतर राजकीय मंडळींच्या ओळखी झाल्या किंवा एखाद्या महत्त्वाचे पद मिळाले की, बाहेरून वावड्या उठतात. तिच्यावर टीका सुरू होते. ती पुढे जाईल म्हणून तिचा पान उतारा केला जातो व त्यातूनच आरक्षणाची ससे होलपट सुरू होते आणि मग कुटुंब की राजकारण हे उत्तर देणे तिला अशक्य होते. त्यामुळेच आज पर्यंतचा स्त्रियांचा राजकारणाचा प्रवास आरक्षण आहे म्हणून येणे व पाच वर्षेप्रामाणिकपणे काम करणे व पुढे आरक्षण नाही म्हणून बाजूला जाणे आपले कुटुंब मुला बाळांचे संगोपन करणे हेच राहिले आहे. त्यासाठी महिलांनी कोणत्याही मार्गाने स्थानिक स्वराज्य संस्थांमध्ये प्रवेश मिळाल्यानंतर आपल्या स्वतःच्या कर्तृत्वाने व अक्कल हुशारीने आपण त्या पदासाठी पात्र आहोत, हे दाखविले व त्यांना या राजकारणातील प्रवास अधिक सुलभ होईल यात शंका नाही.

महिलांचे अनेक प्रश्न व समस्या आहेत. त्या सोडविण्याकरता सातत्याने प्रयत्न सुरू आहेत. महिलांना सामाजिक दृष्ट्या आर्थिक सबलीकरण तसेच नियोजन व निर्णय प्रक्रियेतील सहभाग या प्रक्रियेत सामावून घेणे अगत्याचे आहे. विकास प्रक्रियेत महिलांवर विश्वासाने जबाबदारी सोपविली तर त्या दृष्टीने पार पाडतात, हा अनुभव आहे. या प्रक्रियेतून सक्षम गट तयार झाला तर भविष्यात महिला आरक्षणाची गरज भासणार नाही. महिलांना सामाजिक सुरक्षा मिळावी, त्यांचे शोषण, लैंगिक छळ याबाबत शासकीय पातळीवर खास प्रयत्न होत आहेत. शिक्षण व आर्थिक बळामुळे बऱ्याच महिला स्वावलंबी व आत्मनिर्भर होऊ लागल्या आहेत. त्यातूनच आज आधुनिक काळात स्त्रिया राजकारण समाजकारण आणि प्रशासन यामध्ये आपले नेतृत्व प्रभावीपणे निर्माण करताना दिसून येत आहेत.

### महिलांचे नेतृत्व आणि घटनात्मक तरतूदी

भारतीय स्वातंत्र्यानंतर महिलांचा राजकीय विकास घडवून आणण्यासाठी पंचायती राज संस्थांना घटनात्मक दर्जा प्राप्त करून देण्यासाठी ७३ वी घटना दुरुस्ती करण्यात आली. ही घटना दुरुस्ती करून महिलांचे आरक्षणाला कायदेशीर अधिष्ठान दिले आणि पंचायती राज संस्थातील महिलांचा सहभाग वाढविण्याचा जाणीवपूर्वक प्रयत्न करण्यात

आला आहे. या घटना दुरुस्ती नंतर गेल्या दशकापासून महिला आरक्षणाची अंमलबजावणी सुरू झाली आहे. पंचायत राज संस्थातील ३३ टक्के आरक्षण म्हणजे भारतातील अध्याय लोकांचे स्वतंत्र आहे. भारतीय समाजातील एक नवे पर्व व नवे परिवर्तन आहे. या सामाजिक व राजकीय परिवर्तनामुळे पंचायती राज संस्थातील राजकारणाला अनन्यसाधारण महत्त्व प्राप्त झालेली आहे. आज देशातील लोकसभा व विधानसभेच्या निवडणुकीपेक्षा ही पंचायती राज संस्थांच्या निवडणुका या जनतेच्या व राजकीय पक्षांच्या आरक्षण केंद्र बनले आहेत.

महिलांचे नेतृत्व वाढविण्यासाठी उपाय

१. महिलांचा राजकीय क्षेत्रातील सहभाग वाढवायचा असेल तर त्यांना राजकारणात जास्तीत जास्त संधी देणे गरजेचे आहे व अशी संधी देण्याचे कार्य राजकीय पक्ष अधिक प्रभावीपणे करू शकतात.
२. महिलांना अधिकाधिक उमेदवारी देऊन महिलांना राजकीय दृष्ट्या सक्रिय बनविण्याचे कार्य राजकीय पक्ष करू शकतात.
३. आज प्रत्येक राजकीय पक्ष महिलांना अधिक अधिक उमेदवारी दिली पाहिजे, असे म्हणतात. मात्र, प्रत्यक्षात कृती केली जात नाही असे दिसते. याबाबतीत सर्वच राजकीय पक्ष उदासीन दिसून येतात.

निष्कर्ष

७३ व्या घटना दुरुस्तीमुळे पंचायत राज संस्थांना विशेष करून ग्रामपंचायत व ग्रामसभा या शेवटच्या स्तरावरील संस्थांना घटनात्मक अधिकार प्राप्त झालेले आहेत. महिलांना सबळ करण्याच्या पथावरील ७३ वी घटनादुरुस्ती हे महत्त्वाचे पाऊल आहे. ग्रामपंचायत, पंचायत समिती व जिल्हा परिषद या तिन्ही स्तरावरील स्थानिक स्वराज्य संस्थांमध्ये महिलांचा सहभाग उल्लेखनीय आहे. कोणत्याही प्रकारचे बौद्धिक क्षमता अभिसमता चिकाटी व धडाडी याबाबतीत पुरुषाहून कमी नसलेली स्त्री सामाजीकरणातून समाज मान्य स्त्री सुलभ गुण शकते. स्त्रियांचे जीवन आदर्शवत होण्यासाठी स्त्रियांचे त्यांच्या भविष्य वर अंशतः तरी नियंत्रण पाहिजे. त्यासाठी स्त्री शिक्षणाचा देशव्यापी व अखंड अशा शिक्षणाचा घडक कार्यक्रम स्वीकारण्याची अत्यंत आवश्यक आहे. २१ व्या शतकात भविष्यकाळातील आव्हानांना सामोरे जाण्यासाठी आता स्त्रिने कंबर कसली आहे. प्रेम मातृत्व दयाशीलता या भारतीय संस्कृतीमधील मूलभूत नियमाचे पालन तर ती करतेच आहे पण बाका प्रसंग समोर उभा टाकल्यावर खंबीरपणे आलेल्या प्रसंगाला सामोरे जाण्याची ही तयारी करण्यास सिद्ध झाल्याचे दिसते.

संदर्भ-

- तिवडी व चौधरी- भारत पंचायती राज, ऋचा प्रकाशन, जयपूर, १९९५.  
शर्मा प्रज्ञा, महिला आरक्षण और राजनीतिक सहभागिता महिला विकास, और सशक्तीकरण .  
सरदार अण्णासाहेब, पंचायत राज पध्दती आणि विकास योजना, ऑगस्ट २००४.

\*\*\*\*\*

75  
Azadi Ka  
Amrit Mahotsav



ऋते ज्ञानात् मुक्तिः

# Srujan Prabhat

A Biannual Research Journal

ISSN : 2249-1171 | Volume - II | October 2022 | Issue - II

**SPECIAL EDITION**



- PUBLISHED BY -  
Government Vidarbha Institute of Science  
And Humanities (Autonomous), Amravati  
NAAC Re-accredited 'A' Grade with CGPA 3.32



Scanned with OKEN Scanner



# B.Aadhar

Single Blind Peer-Reviewed & Refreed Indexed  
Multidisciplinary International Research Journal

FEBRUARY 2023

(CCCLXXXVIII) 390

New Directions in Humanities



Chief Editor

**Prof. Virag S. Gawande**

Director

Aadhar Social

Research & Development

Training Institute Amravati

Editor

**Dr. Pradnya S. Yenkar**

Principal,

Vidya Bharati Mahavidyalaya,

Camp, Amravati

This Journal is indexed in :

- Scientific Journal Impact Factor (SJIF)
- Cosmos Impact Factor (CIF)
- International Impact Factor Services (IIFS)



Impact Factor-8.575 (SJIF)

ISSN-2278-9308

# *B.Aadhar*

Single Blind Peer-Reviewed & Refreed Indexed  
Multidisciplinary International Research Journal

FEBRUARY 2023

New Directions in Humanities



VOLUME -B



Chief Editor  
Prof. Virag S. Gawande  
Director  
Aadhar Social  
Research & Development  
Training Institute Amravati

Editor  
Dr. Pradnya S. Yenkar  
Principal,  
Vidya Bharati Mahavidyalaya,  
Camp, Amravati



This Journal is indexed in :

- Scientific Journal Impact Factor (SJIF)
- Cosmos Impact Factor (CIF)
- International Impact Factor Services (IIFS)

For Details Visit To : [www.aadharsocial.com](http://www.aadharsocial.com)

Aadhar PUBLICATIONS



**INDEX**

No.	Title of the Paper	Authors' Name	Page No.
1	Pandemic stress and challenges in education	Dr. Vikas T. Adlok , Dr. Govind M. Tirmanwar	1
2	Challenges for Academic Libraries in Pandemic COVID 19	Dr. Vishalsingh Rameshsingh Shekhawat	4
3	Pandemic and Psychophysical Health Challenges	Dr. Sheetal Shinde	9
4	Impact of pandemic Covid-19 on Fisheries	Dr. Anju P. Khedkar (Vikhar)	11
5	New Challenges in psycho-physical health in post-covid-19	Dr. P. B. Ingle	14
6	Historical Perspective of Pandemic in India	Prof. P. D. Shringare	17
7	A Study on Use of Technology in Education: An Opportunity or A Challenge	Dr. Pallavi Mandaogade (Jain)	21
8	The Relationship of Humanities to other Knowledge Domains	Prof. Dr. Ananda B. Kale , Prof. Manisha Kirtane	26
9	R.K. Narayan's Malgudi days: The mirror of Society	Savita.M. Lonare	28
10	Student's Perspectives On Learning Physics During Pandemic	R. B. Butley	30
11	Use of Surprise and Twist in the Short Stories of O. Henry	Prof.V.P. Shekokar	35
12	A study of the Mental Stress and Mental health of Police Employee during Corona period	Vidhya T. Ambhore	37
13	Relationship Between Narcissism, Social Media Use And Self Esteem	Sonali Ramesh Khandekar , Dr. Shafiq Yusufkhan Pathan	42
14	Use of Technology in Education during the Pandemic	Dr.Suraj K. Rodde	47
15	कोवीड-19 कालावधीनंतर महाविद्यालयीन विद्यार्थ्यांच्या मानसिक स्वास्थ्याचा अभ्यास	वैशाली ढोले , रमेश पठारे	50
16	कोविड-१९ साथीच्यारोगाचा भारतीय अर्थव्यवस्थेवर होणारा आर्थिक व सामाजिक परिणाम	प्रा. दिपाली अतुल पडोळे	58
17	कोव्हीड नंतरचे मानसिकस्वास्थ्य, आव्हाने व उपाय	डॉ. गजानन र. रत्नपारखी	60
18	शिक्षण आणि आव्हाने	डॉ. दामोदर दुधे	63
19	नंदा खरे यांच्या साहित्यातील नवजाणिवा	अभिजित अशोक इंगळे	67
20	शैक्षणिक समस्यांचे विश्लेषणात्मक अध्ययन	प्रा. अमरिश एस. गावंडे	70
21	डॉ. सुखदेव ढाणके यांच्या पिंडपातविषयी – आशयअभिव्यक्ती	कु. ज्योती भिकुसा शेंदुरजणे , प्रा. गजानन बनसोड	74



22	कोविड-१९ नंतर वाढलेली अर्थव्यवस्थेतील डिजिटल पेमेंट पध्दती प्रा. राजेश माथुरकर	77
23	कोरोना विषाणूचा प्रादुर्भाव झालेल्या स्त्री पुरुषांचा बाध्यता ग्रस्तता या समायोजन नसविकृती घटकावर झालेल्या परिणामाचा तुलनात्मक अभ्यास प्रा. अरुणा तसरे , प्रो.डॉ. एस.डी. वाकोडे	81
24	डॉ. पंजाबराव देशमुख यांचे सामाजिक कार्य प्रा. डॉ. मंजुषा धापुडकर	85
25	समाजातील स्त्रिया, दर्जा व अधिकार प्रा डॉ दीपक आनंदराव चौरपगार	88
26	श्री गोविंदप्रभु विषयक साहित्यातील जननिष्ठा प्रा. डॉ. कल्पना त्र्यं. मेहरे	91
27	कोविड-१९ आणि सद्याचे बदलते जागतिक राजकारण अमित पुरुषोत्तम इंगोले	94
28	तुकडोजी महाराजांचे साहित्यातून स्वातंत्र्याला योगदान प्रा. अमृता दीपक तायडे	101
29	शेरीगाथा आणि आधुनिक स्त्रीवादी कादंबरीतून व्यक्त झालेला स्त्रीवाद : चिकित्सक अध्ययन प्रा. डॉ. विश्वजीत कांबळे	108
30	स्वातंत्र्योत्तर महाराष्ट्रातील सार्वजनिक आरोग्य सुविधा : एक ऐतिहासिक अध्ययन इ.स. १९५१ ते १९७२ डॉ. विशाल अ. दौलतकार	131
31	Teaching and Learning After Post Covid – 19 : A Systematic Literature Review Mr. Sandeep Bodade, Dr. P. S. Yenkar	125
32	Is English a Global Language? Kishor P.Chapke, Dr.Pradnya S.Yenkar ,	129
33	Future of Humanities in India R. M. Patil,	135
34	The Role of Communication in Human Interaction Prof. Shubhangi A. Joshi	138
35	Brainstorming: A Magical Technique for Speaking at Length in English Dr.Shivraj N. Kombe	142
36	New challenges in psycho-physical health pandemic Stress Dr. Dnyaneshwari S. Wankhade	146
37	The Role of Electronic Technology in Pandemic Dr. R. J. Gajbe, Mr. B. D. Bundele, Mr. C. R. Chaudhari	153



22	कोविड-१९ नंतर वाढलेली अर्थव्यवस्थेतील डिजिटल पेमेंट पध्दती प्रा. राजेश माथुरकर	77
23	कोरोना विषाणूचा प्रादुर्भाव झालेल्या स्त्री पुरुषांचा बाध्यता ग्रस्तता या समायोजन नसविकृती घटकावर झालेल्या परिणामाचा तुलनात्मक अभ्यास प्रा. अरुणा तसरे , प्रो.डॉ. एस.डी. वाकोडे	81
24	डॉ. पंजाबराव देशमुख यांचे सामाजिक कार्य प्रा. डॉ. मंजुषा धापुडकर	85
25	समाजातील स्त्रिया, दर्जा व अधिकार प्रा डॉ दीपक आनंदराव चौरपगार	88
26	श्री गोविंदप्रभु विषयक साहित्यातील जननिष्ठा प्रा. डॉ. कल्पना त्र्यं. मेहरे	91
27	कोविड-१९ आणि सद्याचे बदलते जागतिक राजकारण अमित पुरूषोत्तम इंगोले	94
28	तुकडोजी महाराजांचे साहित्यातून स्वातंत्र्याला योगदान प्रा. अमृता दीपक तायडे	101
29	धेरीगाथा आणि आधुनिक स्त्रीवादी कादंबरीतून व्यक्त झालेला स्त्रीवाद : चिकित्सक अध्ययन प्रा. डॉ. विश्वजीत कांबळे	108
30	स्वातंत्र्योत्तर महाराष्ट्रातील सार्वजनिक आरोग्य सुविधा : एक ऐतिहासिक अध्ययन इ.स. १९५१ ते १९७२ डॉ. विशाल अ. दौलतकार	131
31	Teaching and Learning After Post Covid – 19 : A Systematic Literature Review Mr. Sandeep Bodade, Dr. P. S. Yenkar	125
32	Is English a Global Language? Kishor P.Chapke, Dr.Pradnya S.Yenkar ,	129
33	Future of Humanities in India R. M. Patil,	135
34	The Role of Communication in Human Interaction Prof. Shubhangi A. Joshi	138
35	Brainstorming: A Magical Technique for Speaking at Length in English Dr.Shivraj N. Kombe	142
36	New challenges in psycho-physical health pandemic Stress Dr. Dnyaneshwari S. Wankhade	146
37	The Role of Electronic Technology in Pandemic Dr. R. J. Gajbe, Mr. B. D. Bundele, Mr. C. R. Chaudhari	153



## कोविड-१९ आणि सद्याचे बदलते जागतिक राजकारण अमित पुरुषोत्तम इंगोले

राज्यशास्त्र विभाग विद्याभारती महाविद्यालय, अमरावती

जगात आतापर्यंत माथीचे व विंगर साथीचे रोग बरेच आलेले आहेत. कॉलरा, प्लेग, मनेरिया, डेंग्यू, फ्ल्यु हे माथीचे आजार आहेत. तर देवी, टॉयफॉईड, एडस, कॅन्सर या सारखे आजार हे विंगर साथीचे आहेत.

जगात ४०० वर्षांचा काळ असा आहे की, दर १०० वर्षांना साथीचा रोग आलेला दिसतो. इ. स. १७२० मध्ये प्लेगची फार मोठी साथ जगात आली. भारतात प्लेगने त्यावेळेस जवळपास १ कोटी १५ हजारलोक मरण पावलेत. चीनमध्येही जवळपास ५० लाख लोक मरण पावलेत. जपानमध्ये जवळपास १७ लाख लोक मरण पावलेत. मात्र इंग्लंड, फ्रान्स, इटाली, अमेरिका, पोलंड, हॉलंड, स्विझर्लंड या पाश्चात्य देशांमध्ये केवळ हजारांच्या संख्येनेच लोक मरण पावलेत. कारण त्यांनी लस व गोळ्या शोधून काढल्यात. व प्लेग आटोक्यात आणला.

इ. स. १८२० मध्ये कॉलराची साथ जगात आली. यात भारतात २० लाख लोक मरण पावलेत. चीनमध्ये ५५ लाख लोक मरण पावलेत. आफ्रिकेमध्ये तर १ कोटीच्या वर लोक मरण पावलेत. मात्र फ्रान्स, इटाली, इंग्लंड, अमेरिकेत व इतर पाश्चात्य राष्ट्रांमध्ये केवळ हजारांच्या संख्येनेच लोक मेलेत. कारण या सुधारीत राष्ट्रांनी कॉलराची लस, गोळ्या, औषधे शोधून काढून कॉलरा आटोक्यात आणला.

१९२० मध्ये फ्ल्यु ची साथ जगात आली. फ्ल्युमुळे भारतात ३० लाख लोक मरण पावलेत. चीन मध्ये १६ लाख लोक मरण पावलेत. आफ्रिकेत १ कोटी २ लाख लोक मरण पावलेत. फ्रान्स, इटाली, इंग्लंड, अमेरिका या पाश्चात्य राष्ट्रांमध्ये हजारांच्या संख्येनेच लोक मेलेत. कारण त्यांनी लस शोधून काढली. गोळ्या, इंजेक्शने शोधली व आपापल्या देशात साथ आटोक्यात आणली.

२०२० मध्ये कोवीड - १९ किंवा कोरोनाची साथ आली. हा एक अनाकलनीय असा साथीचा रोग आहे. चीनमधील वुहान शहरात आणि वुहान प्रांतात याचा फैलाव पहील्यांदा झाला. या साथीच्या रोगाचे विषाणू वटवाघूळापासून तयार झालेले आहेत. हे चीनच्या शास्त्रज्ञांनी सांगितले. त्याचप्रमाणे अमेरिका, इंग्लंड, फ्रान्स, ईझराईल, जापान, रशिया येथील शास्त्रज्ञांनी सुद्धा वटवाघूळापासून हा विषाणू तयार झाला हे सांगितले. प्रामुख्याने चीनने या साथीच्या रोगाची माहिती दोन अडीच महीनेपर्यंत जागतिक आरोग्य संघटनेला सांगितली नाही. त्यामुळे पुढे हा साथीचा रोग चीन व्यतिरिक्त फ्रान्स, इटाली, अमेरिका, स्पेन, ब्राझील, पोलंड, हॉलंड, फिलीपाईन्स, जापान, इराण, सीदी अरेबिया, आफ्रिका, पाकिस्तान, भारत व जगातील सर्वच राष्ट्रांमध्ये फैलावला.

या रोगाविषयी पाश्चात्य देशातील अमेरिका, फ्रान्स, इटाली, आस्ट्रेलिया यांचे मत असे कि, हा मानव निर्मीत विषाणू चीनने मुद्दाम तयार केला. जगात मिसाईलच्या माध्यमातून हे विषाणू सोडून सर्व मानवजात धोक्यात आणून आपली सत्ता जगात स्थापन करण्यासाठी चीनने हे दृष्ट कृत्य केले असा अमेरिकेचा सरळ आरोप आहे. त्यांनी चीनच्या अनेक पुराव्यानिशी टि. व्ही मिडीयावर हे सिद्ध केलेले आहे. त्यामुळे कोरोनाच्या संदर्भातील विषाणूविषयी अजूनही जगात त्याची खरी परिक्षा व संशोधन झालेले नाही. व त्याची लसही तयार झालेली नाही, हे सत्य आहे. मात्र या विषाणूने सर्व जगत कधी नव्हे एवढा धुमाकूळ घातला. औषधे, गोळ्या, इंजेक्शने यांचा उपयोग फ्ल्यु, बर्डफ्ल्यु, स्वाईनफ्ल्यु या रोगांसारखा करण्यात येत आहे. अमेरिका, ईझराईल, जापान, ऑस्ट्रेलिया, या राष्ट्रांनी याची लस तयार करण्याचा दावा केला. पण तो दावा अजूनही फारसा सिद्ध झालेला नाही. हा विषाणू वेळोवेळी आपले वैशिष्ट्ये बदलतो. तो जमिनीच्या पृष्ठभागावर राहतो. तर कधी हवेतही तरंगतो. हा विषाणू निर्जीव आहे असेही मानल्या जाते. हा विषाणू प्रामुख्याने नाक आणि तोंड यातून शरीरात प्रवेश करतो. घसा, श्वासनलिका, दोन्ही फुफुसे यामध्ये प्रवेश करून त्यांना मोठ्या प्रमाणात बाधित करतो. या जंतूचा फैलाव वाऱ्यासारखा होतो. ऑक्सिजनवर रूग्णाला ठेवावे लागते. कोवीड - १९, अगोदर चीनमध्येच फ्ल्यु, बर्डफ्ल्यु आणि पुढे स्वाईनफ्ल्यु ची साथ फैलावली. त्यामुळे चीनच्या शास्त्रज्ञांनी फ्ल्युला १७, स्वाईनफ्ल्युला १८ आणि आताच्या कोरोना ला किंवा कोविड १९ असे क्रमांक दिलेले आहेत. त्यामुळे कोवीड १९, किंवा कोरोना चा उपचार हा फ्ल्यु, स्वाईनफ्ल्यु सारखाच करावा लागतो. तिच औषधे यावर



कोरोनाचा आशय घेऊनच पाकिस्तानने चीनच्या सांगण्यावरून हे सर्व हल्ले केलेले आहेत. पाकव्याप्त काश्मिर हा भारताचा अविभाज्य भाग आहे. व आज ना उद्या भारत ताब्यात घेईल या भीतीने पाकिस्तानने हा भाग चीनच्या ताब्यात दिलेला असून या ठिकाणी चीनने अनेक प्रकल्प टाकलेले आहेत. ते प्रकल्प भारताने जर पाकव्याप्त काश्मिर ताब्यात घेतला तर चीनला सोडावे लागतील. व चीनचे फार मोठे आर्थिक नुकसान होऊन चीनची पाकिस्तानवरची हुकूमत नष्ट होईल या भीतीने चीनने कोरोना काळातच पाकिस्तानला मोठ्या प्रमाणात अतिरेकी हल्ले करावयास सांगितले. व पाकिस्तान चीनच्या सांगण्यावरून असे अतिरेकी हल्ले करित आहे. कोरोना काळातच चीनने लडाख भागात फार मोठे सैन्य जमवून भारताचा भूभाग बळकावण्याचा प्रयत्न केलेला आहे. परंतु भारताने मोठ्या सैन्याचा समुदाय जमवून चीनला मोठ्या प्रमाणात प्रतिबंध केलेला आहे. कोरोना काळातच हे युद्धाचे व अतिरेकी कारवायांचे राजकारण पाकिस्तान व चीनने आखले आहे. कोरोनाच्या व्यवस्थापनात भारत गुंतेल व सहज भारताचा भाग जिंकता येईल या ईर्ष्येने पाकिस्तान व चीनने हे हल्ले केलेले आहेत यात वाद नाही.

५) वर्णव्देषाचे जागतिक राजकारण :-

कोरोना काळातच वर्णव्देषाची ठिणगी जी अमेरिकेत पडली तिने उग्र रूप धारण केले. व ट्रम्फ सरकारलाही मोठा धक्का बसला आहे. अमेरिकेतील रिपब्लिकन पक्ष हा वर्णव्देष बाळगणारा पक्ष आहे. ट्रम्फ हे रिपब्लिकन पक्षाचे असून त्यांनी बहुमताने अमेरिकेचे अध्यक्षपद मिळविलेले आहे. व त्यांच्या विरोधी हिलरी क्लिंटनचा परामव केला. कोरोनाच्या अमेरिकेतील लॉकडाऊनच्या काळात पोलीसांनी एका ह्युस्टन शहरातील जॉर्ज फ्लॉईडस या काळ्या वर्णाच्या व्यक्तीस खूप मारले. हा व्यक्ती निग्रो वंशाचा असल्यामुळे अमेरिकेतील पूर्ण निग्रो लोकांनी तसेच गोऱ्या लोकांनी सुद्धा पोलीसांविरुद्ध उग्र आंदोलने केलीत. एका पोलीस इन्स्पेक्टरने आपला पाय त्याच्या मानेवर एक दिड तास दाबून ठेवला. बाकीच्या पोलीसांनी त्याला लाठीने मारले. त्याचा दम घोटून तो मेला. आणि त्याच्या पोस्टमार्टममध्ये दम घोटल्यामुळे तो मेला हे सिद्ध झाले. ही घटना अमेरिकेच्या मोठमोठ्या शहरात वाऱ्यासारखी पसरली. आणि अमेरिकेतील निग्रो लोकांनी आठ दहा दिवसापासून उग्र आंदोलने कोरोना काळातच केली. वर्णव्देष असा ऊफाळून आला याला कोरोनाचा लॉकडाऊन काळ कारणीभूत ठरला. सरकारला त्याची फार मोठी आर्थिक मदत करावी लागली. शेवटी ह्युस्टनशहरात त्याचा अंत्यविधी झाला. ज्या अमेरिकेत अब्राहम लिंकन सारखा निग्रो वंशाच्या विचारवंताने फार मोठी वैचारिक क्रांती करून अमेरिकेचे अध्यक्षपद भुषविले त्याच अमेरिकेत जॉर्ज फ्लॉईडसचा वर्णव्देषातून वध व्हावा हे अमेरिकेला शोभणारे नाही. कोरोनामुळेच वर्णव्देषातून गोऱ्या पोलीसांनी काळ्या वर्णीय निग्रोंवर खूप अत्याचार केलेत हे कटुसत्य आहे. या संदर्भात वेस्ट इंडिजचा अग्रगण्य क्रिकेटपटू ख्रिस गिलने आपले वक्तव्य जागतिक पातळीवर केले आणि आपल्याला सुद्धा इतर देशात तिरस्कारपूर्वक वागणूक दिल्या जाते हे सांगितले. तेव्हा हे उदाहरण बोलके आहे. सर्व विचारवंतानी अमेरिकेतील या वर्णव्देषाचा धिक्कार केलेला आहे. वर्णव्देष नष्ट करण्यासाठी महात्मा गांधींनी १९३२ मध्ये आफ्रिकेत जाऊन गोऱ्यांविरुद्ध आंदोलन केले. व वर्णभेद नाहीसा करण्याचा प्रयत्न केला. गांधीजींना सुद्धा खूप छळ सहन करावा लागला होता. पण गोऱ्यांच्या मनातून काळ्यांचा व्देष अजूनही गेलेला नाही. हे कोरोना काळातच सिद्ध झाले आहे. आणि वर्णव्देषाचे राजकारण नव्याने पाहायला मिळाले ते कोरोनाच्या लॉकडाऊन काळामुळेच !

६) जागतिक शस्त्रस्पर्धेला नव्याने उधाण आले :-

चीनने हा विषाणू तयार केला. त्यामुळे चीन हा व्हायरस मिसाईलच्या माध्यमातून भावी काळात वेगवेगळ्या देशांमध्ये सोडेल. याबदल पाश्चात्य राष्ट्रे खवळून उठली आहेत. चीनमधील प्रसिद्ध प्राणीशास्त्रज्ञ डॉ. लिली गियांग या स्त्रीला अमेरिकेत केंब्रीज विद्यापीठात तज्ञ म्हणून फेलोशिप देऊन तिने केंब्रीज विद्यापीठात खूप संशोधन केले. पुढे ती चीनमध्ये गेली. तिने चीनच्या बुहान शहराच्या प्रयोगशाळेत वटवाघूळावर प्रयोग करून हा विषाणू तयार केला. हा विषाणू तयार करतांना तिने इंग्रजीतून एक वाक्य म्हटले ते पाहण्यासारखे आहे This is only Trailor, but remaining picture is very dangerous. यासारख्या वक्तव्याने युरोप खंडातील सर्व राष्ट्रे चिडली. प्रामुख्याने अमेरिकेचे अध्यक्ष डोनाल्ड ट्रम्फ व रिपब्लिकन पक्षाचे अनेक सिनेटर्स यांनी डॉ. लिली गियांगच्या या वक्तव्याचा पूर्ण फायदा करून कोरोना हा मानवनिर्मित आहे हे सर्व जगाला ठणकावून सांगितले. चीनने हा विषाणू जगाच्या नाशासाठी केलेला आहे. यात सर्व जगावर हुकूमत गाजविणे व सर्वांना दहशत देणे हा हेतू स्पष्ट होतो. या ईर्ष्यतून अमेरिकेच्या अध्यक्षांनी जास्तीच्या अणुचाचण्या करावयाचे ठरविले. अत्यंत आधुनिक मिसाईल्सच्या याच काळात घेतल्या. त्याचप्रमाणे अणुबॉम्ब व हायड्रोजन बॉम्ब यांच्या चाचण्या घेतल्या. क्षेपणास्त्राच्या चाचण्याही घेतल्या. ही शस्त्रस्पर्धा कोरोनाच्या भीतीतून निर्माण झाली. युरोप खंडातील फ्रान्स, इंग्लंड यांनी सुद्धा आधुनिक शस्त्रांच्या चाचण्या घेतल्या. अमेरिकेच्या मार्गदर्शनाखाली २० राष्ट्रांची एक संघटना अध्यक्ष ट्रम्फ यांनी तयार केली. कोरोनाचे संकट आटोपल्यावर बुहान सारख्या शहरावर बॉम्ब टाकून ते शहर व तेथील प्रयोगशाळा नष्ट करण्याचे मनसुबे व योजनाही त्यांनी आखल्या



आहेत. कोरोना काळातच चीनने भारताच्या लडाख भागात सैन्य मोठ्या प्रमाणात जमा केले. त्यामुळे भारतानेही मोठ्या प्रमाणात सैन्य जमा केले. फ्रान्सकडून अधिक तीन जेट विमाने लडाख साठी भारताने खरेदी केलेत. चीनच्या या विषाणूतून शस्त्रसंधाना खुप चालना मिळाली. दुसऱ्या महायुद्धात जपानवर अमेरिकेने शक्तीशाली बॉम्ब टाकून हिरोशिमा व नागासाकी ही दोन शहरे उध्वस्त केली. भा काळात चीनमधील बुहान शहर पूर्णपणे उध्वस्त करण्याची योजना युरोप खंडातील या समुदायाने आखली आहे. एक दिड वर्षातच हे युध्द होऊ शकते.

७) चीनचा साम्राज्यवाद विस्तार :-

कोरोना काळातच चीनने साम्राज्यवादाचा स्विकार केलेला दिसते. जर चीनने हा विषाणू जगावर दहशत निर्माण करण्याच्या दृष्टिने निर्माण केलेला असेल व युध्दामधून मिसाईल्स मधून त्याचा उपयोग जर चीन भविष्यात करित असेल तर जगावर चीनचे वर्चस्व फार मोठ्या प्रमाणात निर्माण होऊ शकते. इंग्लंड, फ्रान्स, जपान, अमेरिका, आस्ट्रेलिया, भारत, इटाली, ईसाईल या देशातील संशोधकांनी सांगितले की हा मानवनिर्मित विषाणू आहे. नैसर्गिक कॉलन्सासारखा, प्लेगसारखा किंवा डेंग्यूसारखा विषाणू नाही. त्याचे स्वरूपच विचित्र आहे. क्षणोक्षणी त्याचे वैशिष्ट्ये बदलत असतात. हा विषाणू निर्जीव जरी असला तरी मानवाच्या शरीरात जाण्यासाठी तो धडपडत असतो. हा विषाणू संशोधकांना चक्रावून टाकणारा आहे. त्यामुळेच त्याची लसही पूर्णपणे निघाली नाही. सगळेच संशोधक गोंधळून गेलेले आहेत. याचा फायदा घेऊन चीनने या कोरोना काळातच भारताच्या पूर्व लडाख भागात भारताच्या सरहद्ददीत प्रवेश करून आपले सैन्य फार मोठ्या प्रमाणात जमविले आहे. हॉंगकॉंग या प्रदेशावरही आपले वर्चस्व स्थापन केले. हॉंगकॉंगची स्वायत्तता नाकारून तो आपलाच प्रदेश आहे हे चीनच्या संसदेमध्ये चीनने बहुमताने पास करून घेतले. हॉंगकॉंगमध्ये पोलीस व मिलीटरीचा धुमाकूळ चीनने घातलेला आहे. तसेच तायवान या भागालाही त्रास देणेसुरू केले आहे. आणि तायवान हा आपलाच भूभाग आहे म्हणून तोही बळकावण्याचा प्रयत्न चीन करित आहे. तिबेट हा प्रांत जेथे दलाई लामा राहत होते, तो त्यांनी बळजबरीने आपल्या ताब्यात घेतला. आणि तिबेटची स्वायत्तता नष्ट केली. पाकव्याप्त काश्मिरचा भाग पाकिस्तानकडून चीनने वेगवेगळ्या प्रकल्पासाठी घेऊन तेथे अनेक प्रकल्प चीनने सुरू केलेत. हा पाकव्याप्त काश्मिर सुध्दा जिंकून घेण्याचे स्वप्न चीन पाहत आहे. हिंदी महासागरात व अरबी महासागरात चीनने अत्याधुनिक मोठमोठ्या नौका सज्ज करून आपली हुकुमशाही समुद्रावर निर्माण केलेली आहे. अधिक वर्चस्व दाखविण्यासाठी अंतराळ यानाची भाडोत्री पध्दतीने चीनने जाहीरात केलेली असून अंतराळ प्रवास सुध्दा सुरू केलेला आहे. हा खटाटोप करून आपले वर्चस्व जगावर राहावे हा चीनचा कारस्थानाचा भाग आहे. चीनचा हा साम्राज्यवाद कोणालाही खटकल्याशिवाय राहत नाही. नेपाळला हाताशी धरून भारताची तिन शहरे नेपाळच्या नकाशात तेथील पंतप्रधानाने दाखविले आणि तसा प्रस्ताव नेपाळने आपल्या लोकसभेत पास करून घेतला. हे कारस्थान चीनचेच आहे. चीन याबाबत जगात लबाड, कपट कारस्थानी, व धूर्त देश म्हणून ओळखल्या जात आहे. कोरोनाचा विषाणू त्यांच्याच प्रयोगशाळेत जो तयार करण्यात आला तो अनावधानाने निसटून पूर्ण बुहान शहरात व चीनच्या वेगवेगळ्या प्रांतात पसरला व यात चीनचे वरेच लोक मेलेत. भस्मासुरासारखी चीनची स्थिती झाली. कोरोनाचे संकट आम्ही नष्ट केले असून त्यांनी आनंदोत्सव साजरा केला. रोपणाई केली आणि याच काळामध्ये आपल्या साम्राज्यावादाचा विस्तार या कोरोना काळातच मोठ्या प्रमाणात केलेला दिसतो. त्यामुळे जागतिक स्तरावर चीनला सर्व राष्ट्रांनी एकाकी पाडलेले दिसते.

८) कोरोनातूनच वर्गबलह निर्माण होणे :-

कोरोना काळातच भारतासारखे विकसनशिल सारख्या देशात मजुरांची स्थिती फार भयानक झाली. या कोरोना काळातच लॉकडाऊन केल्यानंतर मुंबईच्या कारखान्यातील सर्व भारतातील प्रांतांचा मजूरवर्ग, गुजरात मधील अहमदाबाद, मुरत, बडोदा, राजकोट या औद्योगिक शहरातील कारखान्यातील इतर प्रांतातील मजूरवर्ग, चेन्नई व कलकत्ता या टिकाणच्या कारखान्यातील विविध प्रांतातील मजूरवर्ग, पंजाबातील कारखान्यातील इतर प्रांतातील मजूरवर्ग यांचे जे हाल झाले ते भारतातील वेगवेगळ्या दुरदर्शन वाहीण्यांनी फार बारकाईने दाखविले. हे चित्र पाहून भारतीय विचारवंत व सर्व जगातील विचारवंतांचे डोके चक्रावून गेले । हजार-हजार किलोमिटर पायी जाणे, मायकळीने जाणे, ट्रकमधून जाणे, ट्रॅक्टरमधून अवैध जाणे, कासेही करून कोरोनाच्या भीतीने जे मिळेल त्या वाहनाने आपल्या गावी जाणे, पायांना चालण्यामुळे मोठमोठ्या जखमा होणे यासारखे दुःखी प्रसंग इतर देशात दिसणार नाहीत. भारतासारख्या गरीब देशातच हे दिसू शकते. या मजुरांचे लाखांचे तांडेच्या तांडे पाहून प्रत्येक राज्यसरकारची पाचावर धारण बसली. त्यासाठी गेळे आणि बसेस मोड्याच्या लागल्यात. त्या त्या प्रांताच्या गावी ते बिचारे गेलेत. पण त्यांच्या दारिद्र्याची करुण कहाणी पाहिल्यावर हा वेध किती मांडवतथाही वृत्तीचा आहे हे स्पष्ट झाले. मूठभर भांडवलदार व





वापरावी लागतात. तो साध्य रोग आहे. असाध्य रोग नाही हे ही सिध्द झालेले आहे. त्यामुळे कोरोनाच्या संदर्भात सद्याची उपचार पध्दती फ्ल्यु, स्वाईनफ्ल्यु सारखीच सुरु आहे. जेव्हा लस तयार होईल तेव्हा होईल, तोपर्यंत पारंपारिक फ्ल्यु आणि स्वाईनफ्ल्यु यावरची इंजेक्शने तसेच गोळ्या व औषधे सर्व जगात वापरण्यात येत आहेत. आणि तिच उपचार पध्दती सद्या सुरु आहे. अँलोपॅथी, आयुर्वेद, होमियोपॅथी या शाखेचे तज्ञ याबाबत विचार करून सांगतात कि, कोविड १९ मध्ये प्रतिकारशक्ती वाढविण्यासाठी वेगवेगळ्या औषधांचा उपयोग करावा लागतो.

कोविड - १९ मुळे खऱ्या अर्थाने पाश्चात्य राष्ट्रांमध्ये फार मोठ्या प्रमाणात लोक मरण पावलेले आहेत. अमेरिका, फ्रान्स, इटाली, स्विट्झर्लंड, ब्राझिल, स्पेन, हॉलंड यामध्ये फार मोठ्या प्रमाणात लोक मरण पावलेत. अमेरिका हा पहिल्या क्रमांकावर असून फ्रान्स आणि इटाली हे दुसऱ्या, तिसऱ्या क्रमांकावर आहेत. वास्तविक पाहता पाश्चात्य राष्ट्रे कोणत्याही रोगाचे विषाणू शोधून त्यांची लस तसेच औषधे आणि गोळ्या तयार करण्यात आघाडीवर असतात. पण कोविड - १९ च्या संदर्भात मात्र अमेरिकेसारख्या राष्ट्राची सुध्दा मती गुंग झालेली आहे. आणि एवढ्या मोठ्या सुधारलेल्या राष्ट्रांने या साथीच्या रोगामुळे नांगी टाकलेली आहे. इंग्लंडमध्ये तर तेथील राजे घराण्यात राणी एलिझाबेथला कोरोना संसर्ग झालेला आहे. त्याप्रमाणे इंग्लंडचे पंतप्रधान बोरीस जॉन्सन यांना सुध्दा कोरोना झालेला आहे. वेगवेगळ्या देशातील मोठमोठे राजकारणी, कला क्षेत्रातील लोक हे कोरोना मुळे मरण पावलेले दिसतात.

सर्व राष्ट्रांपेक्षा भारताने यावर बरीच मात केलेली दिसते. परंतू तरीही आजच्या घडीला भारत हा चौथ्या क्रमांकावर आलेला आहे. पुढे भारतात मोठ्या प्रमाणात याचा संसर्ग निश्चीत होऊ शकतो. हे भारतातील तज्ञ डॉक्टरांनी स्पष्ट केलेले आहे. भारताची लोकसंख्या चीनच्या बरोबरीने आहे. त्यामुळे भारताला सर्व जगात फार महत्त्व प्राप्त होऊन भारत कोरोनावर ज्या पध्दतीने ईलाज करीत आहे, त्यांचे अनुकरण पाश्चात्य राष्ट्रे आणि आशिया खंडातील राष्ट्रे तसेच आफ्रिका खंडातील राष्ट्र भारताचे अनुकरण करीत आहेत. या कोरोनाच्या साथीच्या संदर्भात सद्याचे जागतिक राजकारण फार झपाटयाने बदलत आहे. या बदललेल्या राजकारणाचे वेगवेगळे वैशिष्ट्ये पुढीलप्रमाणे स्पष्ट करता येतील.

१) पाश्चात्य देशांनी चीनला वेगळे पाडले :-

बुहान प्रांतातील बुहान शहराच्या प्रयोगशाळेतील कोरोनाचे विषाणू नकळत प्रयोगशाळेतून बातावरणात पसरले. त्यामुळे बुहान शहर आणि बुहान प्रांतात फार मोठ्या प्रमाणात ही साथ फैलावली. बुहान शहरातील चीनचे फार मोठे मटन मार्केट आहे. दुरदर्शन च्या माध्यमातून सर्व जगासमोर हे मटन मार्केट आलेले आहे. या मटन मार्केटमध्ये वेगवेगळे प्राणी, पक्षी, जलचर प्राणी यांचा समावेश आहे. ही साथ चीनने जगापासून अडीच ते तिन महीण्यापासून लपवून ठेवली असा अमेरिकेचा स्पष्ट आरोप आहे. तसेच इंग्लंड, फ्रान्स, इटाली, ब्राझिल, ऑस्ट्रेलिया यांचेही हेच म्हणणे आहे. सर्वात जास्त अमेरिकेतील १ लाखापेक्षा जास्त लोक मरण पावलेले आहेत. त्याखालोखाल इटाली, फ्रान्स व इतर पाश्चात्य राष्ट्रांमध्ये मृत्युंची संख्या आहे. हा विषाणू कसा आहे. त्याचे विक्षेपण या पाश्चात्य राष्ट्रातील वैज्ञानिकांनी वेगवेगळ्या प्रकारे केलेले आहे. आणि चीनला वेगळे पाडले. अमेरिकेचे अध्यक्ष डोनाल्ड ट्रम्प यांनी तर चीनला युध्दाची धमकी दिलेली आहे. अमेरिकेमधील रिपब्लिकन पक्षांच्या सिनेटरांनी चीनवर सरळ आरोप केला कि, चीनने हा विषाणू पाश्चात्य राष्ट्रांत मिसाईलद्वारे सोडण्यासाठी तयार केलेला आहे. त्यामुळे अमेरिकेच्या अर्थशास्त्रांनी चीनशी असलेले राजनैतिक संबंध व आर्थिक संबंध तोडलेले आहेत. अमेरिकेने आपल्या १०२ कंपन्यांमधील शेअर्स काढून घेतलेत. या कंपन्या भारतात नेण्याचा अमेरिकेचा विचार आहे. इतर सर्व पाश्चात्य राष्ट्रांनी या बाबतीत भारताचे सहकार्य आपल्या कंपन्यांमध्ये घेण्याचे ठरविले आहे. सद्याच्या घडीला चीनने भारताचा लडाख मधील भाग सैन्य पाठवून बळकावला. त्यामुळे भारताचे व चीनचे संबंध हे शत्रुत्वाचे निर्माण झालेले आहेत. भारताने चीनशी आर्थिक संबंध पूर्णपणे तोडलेले आहेत. संपूर्ण पाश्चात्य राष्ट्रांनी आणि अमेरिकेने भारताला सहकार्य केलेले आणि चीनला एकाकी पाडले. हा फार महत्वाचा जागतिक राजकारणाचा भाग आहे.

२) आर्थिक महासत्ता होण्याचा विचार कोरोना मुळे चीनने केला :-

कोरोना हा जर चीनने निर्माण केलेला आहे आणि त्यापाठीमागे चीनचा स्पष्ट हेतू हा दिसतो कि सर्व जगावर आपली आर्थिक सत्ता कशी स्थापन करता येईल हा चीनचा धूर्त विचार आहे. इंजेक्शने, गोळ्या, औषधे, मॉस्क, क्वाँटस, लस व इतर आरोग्याची साधने जगाला पुरविणे व अवाढव्य पैसा कमावणे हा चीनचा स्वार्थी हेतू आहेच. तो सर्व जगासमोर उघडा झालेला आहे. फक्त रशिया आणि उत्तर कोरीया यांनीच चीनचे समर्थन केलेले आहे. चीनने अगोदरच वेगवेगळ्या वस्तूंची निर्यात फार मोठ्या प्रमाणात पाश्चात्य देशात आणि आशिया खंडामधील देशांमध्ये केलेली आहे.



यामध्ये मोबाईल, कॉम्प्युटर, लॅपटॉप, टि. व्ही. यंत्रांचे सुटे भाग, रेल्वेचे सुटे भाग, यांचा समावेश आहे. अगदी लहान मुलांच्या खेळण्यांची निर्यात चीनने फार मोठ्या प्रमाणात केलेली आहे. भारतासारख्या देशात दिवाळीच्या पणत्या आणि महालक्ष्मीच्या मुर्त्या याही चीनकडून भारतात निर्यात होत असतात. या सर्व वस्तूंच्या माध्यमातून चीनने फार मोठा आर्थिक लाभ करून घेतलेला आहे. कोरोना विषाणूचा प्रयोगशाळेत संशोधन करून सर्व जगात हा विषाणू कसा फैलावेल याचा विचार चीनने निश्चीतच केलेला आहे. चीनने या संदर्भात लसही निर्माण केलेली आहे. औषधे, गोळ्या आणि इंजेक्शन सुध्दा तयार केलेली आहेत. त्यामुळे त्या देशात त्यांनी कोरोनाच्या साथीला प्रतिबंध घातला. आणि स्वतःला सावरले. साहजिकच पाश्चात्य देश आणि इतर देश यांच्याकडून कोरोनाच्या साथीची इंजेक्शन, गोळ्या, औषधे, किट्स, मास्क आणि इतर उपकरणांची आयात सर्व राष्ट्रांनी चीनकडून केली. यामध्ये अनेक किट्स आणि मास्क व औषधे बोगस निघालीत. व अमेरिका, भारत, ब्राझिल, स्पेन, इटाली या देशांनी ती चीनकडे परत पाठवून दिलीत. या माध्यमातून फार मोठा पैसा जगातील अनेक राष्ट्रांकडून कमाविता येईल या हेतूनेच चीनने हा विषाणू निर्माण केलेला दिसतो. अमेरिका आणि रशिया यांच्यापेक्षा महासत्ता जागतिक पातळीवर बनण्याचा विचार चीनचा निश्चीतच आहे. म्हणजेच आर्थिक महासत्ता अमेरिका रशियापेक्षा आपण व्हावे हा चीनचा हेतू जगासमोर स्पष्ट झालेला आहे.

३) जागतिक धर्मगट कोरोनामुळे निर्माण झालेत :-

कोरोना या साथीच्या रोगामुळे कधी नव्हे एवढे जागतिक पातळीवर धर्मगट प्रभावी झालेत. ख्रिश्चन धर्म सर्व युरोप खंडातील देशांमध्ये आहे. हे युरोप खंडातील ख्रिश्चनधर्मीय देश एकत्र आलेत. आणि चीनवर आक्रमण करण्याचा वेत ते आखीत आहेत. अमेरिकेसारखा ख्रिश्चनधर्मीय देश युरोप खंडाचे नेतृत्व करीत आहे. अध्यक्ष डोनाल्ड ट्रम्फ च्या नेतृत्वाखाली इंग्लंडचे पंतप्रधान बोरीस जॉनसन हे त्यामध्ये सहभागी आहेत. इटाली, फ्रान्स, ब्राझील हे सर्व ख्रिश्चन राष्ट्रे एकत्र आली आहेत. ख्रिश्चन धर्माचा कधी नव्हेत एवढा त्यांना आता अभिमान वाटत आहे. व आशिया खंडातील चीनला त्यांनी नेस्तनाबूत करून टाकण्याचे ठरविले आहे. अमेरिकेने विमान सेवा बंद केली. व्यापार व आर्थिक संबंध तोडून टाकलेत. बाकीच्या युरोप खंडातील राष्ट्रांनी सुध्दा चीनशी संबंध तोडलेत. बहुसंख्य ख्रिश्चन धर्मीय लोकांनी चीनविरुद्ध वहीष्कार पुकारून त्यांच्याशी असलेले राजनैतिक व आर्थिक संबंध तोडून टाकलेले आहेत. त्यांचे असे म्हणणे आहे कि, चीनने मुददाम खोडसाळपणे हा विषाणू तयार केलेला असून युरोप खंडातील देशांमध्ये सोडलेला असून त्यामुळे युरोप खंडातील बहुसंख्य लोक मोठ्या प्रमाणात मरण पावलेले आहेत. अमेरिकेत जवळपास १ लाख १५ हजार लोक मरण पावलेत. इटलीत जवळपास ५५ हजार लोक मरण पावलेत. फ्रान्समध्ये जवळपास ४७ हजार लोक मरण पावलेत. ब्राझिलमध्ये जवळपास ३६ हजार लोक मरण पावलेत. हॉलंडमध्ये जवळपास २४ हजार लोक मरण पावलेत. स्वित्झर्लंडमध्ये जवळपास २२ हजार लोक मरण पावलेत. ऑस्ट्रेलियामध्ये जवळपास २७ हजार लोक मरण पावलेत. एकंदरीत युरोप खंडातील लोक मारण्यासाठी चीनने हा विषाणू व्हायरस वुहानच्या प्रयोगशाळेत तयार केलेला असून त्यामध्ये वटवाघूळाच्या तोंडाची लाळ तसेच पंखावरील किटाणू आणि वटवाघूळाचे रक्त या तिन्हींपासून कोरोना विषाणू तयार केलेला असून तो मानवनिर्मित आहे. नैसर्गिक नाही. प्रामुख्याने मिसाईल्स व्दारे त्यांनी हा विषाणू युरोप खंडामध्ये सोडलेला आहे. आणि मोठ्या प्रमाणात युरोप खंडातील लोक मरत आहेत. व्देषभावनेतून चीनने युरोपखंडावर वर्चस्व गाजविण्यासाठी हा विषाणू तयार केलेला आहे. म्हणून ख्रिश्चन धर्मीय राष्ट्रांनी एकजूट करून चीनशी असलेले सर्व प्रकारचे संबंध तोडून टाकलेले आहेत. सर्व प्रकारच्या वस्तूंची आयात बंद केलेली आहे. कोरोनामुळेच हे धर्माचे राजकारण जागतिक स्तरावर निर्माण झालेले आहे. कोरोनाचे संकट संपल्यानंतर सर्व युरोपखंडातील देश मिळून चीनशी युध्द करून चीनला नेस्तनाबूत करण्याची योजना त्यांनी आखलेली आहे.

४) कोरोना काळात पाकिस्तानचे भारतावरील दहशतवादी आक्रमणे :-

कधी नव्हे एवढे दहशतवादी हल्ले काश्मिर सिमेवर पाकव्याप्त सिमारेषेवरून पाकिस्तान भारतावर करीत आहे. आपल्या देशातील कोरोनाग्रस्त लोकांची काळजी बाजूला ठेऊन त्यांना मरणाच्या दारात लोटून भारत कोरोना रोगाच्या व्यवस्थापनात गुंतला आहे व भारताने कडेकोट लॉकडाऊन केलेले आहे याचा गैर फायदा घेऊन जैश-ए-मुहम्मद, लष्कर-ए-तोयबा, आयसीसी, यासारख्या दहशतवादी संघटना प्रखर हल्ले करीत आहे. भारताचे सैनिक तेवढ्याच जिददीने या अतिरेक्यांचा खिमा करीत आहेत. कोरोनाच्या निमीत्ताने पाकिस्तानने भयानक अतिरेकी हल्ले सुरू केलेले आहेत. कोरोनाच्या काळात चीनने पाकिस्तानला चिथावणी देऊन अतिरेक हल्ले जास्त प्रमाणात करावयास लावलेले आहे. कोरोना काळातच मे महीण्यात १ चीफ कमांडर, २ डिव्हीजनल ऑफीसर्स, २ इन्स्पेक्टर त्यांनी भारताच्या सैन्यातील मारलेले आहेत. फार मोठा हल्ला करण्यासाठी एक स्फोटकांची कहर भारतीय हद्दीत त्यांनी आणली. परंतु भारताच्या गुप्तचर संघटनेने ती कार पकडली. आणि त्यातील स्फोटके जंगलात नेऊन नष्ट केलीत.



१० टक्के राजकारणी भांडवलदार यांच्या हाती गरीबांच्या नाड्या दिसून आल्यात. कार्ल मार्क्स च्या वर्गकलहाचे लॉकडाऊनच्या कोरोना काळात हे विदारक चित्र दिसले. आणि विचारवंतांच्या अंगावर काटे आले. हा गरीब व श्रीमंताचा वर्गकलह जगाच्या राजकारणात भारतात विदारक दिसला. तसेच पाकिस्तानतही दिसला. पाकच्यात काश्मिरातील गरीब मुसलमान तसेच गिलगिट प्रांतातील गरीब मुसलमानांचे हाल पाहण्यासारखे होते. ही माणसे आहेत कि कुत्रे - मांजरे आहेत ? असा भास होतो. हा वर्गकलह जगाच्या राजकारणात भारतात व पाकिस्तानात दिसला तो अंतर्मुख करणारा आहे. कारण कोरोना काळातच तो निर्माण झाला.

९) साम्यवादी राष्ट्रांची एकी :-

या कोरोना काळातच चीनच्या विरोधात जसा युरोप खंड दंड थोपटून उभा राहिला तसेच चीनच्या बाजूने उत्तर कोरीया, रशिया हे साम्यवादी देश चीनच्या बाजूने उभे राहिलेले. पाकिस्तान आणि नेपाळ हे चीनच्या बाजूने उभे राहिलेले. जागतिक आरोग्य संघटनेच्या वतीने त्यांनी चीनला दिलासा दिला. व अमेरिकेचे आरोप फेटाळले. त्यामुळे अमेरिका व युरोप खंड विधरला. रशिया व ओरीया यांनी चीनला दिलासा दिला. जी ७ या जागतिक संघटनेचा विचार कोरोना काळातच अध्यक्ष ट्रॅम्प यांनी केला. चीनची - बाजू रशियाने व दक्षिण कोरीयाने घेतली. या कोरोना काळातच ही साम्यवादी राष्ट्रे चीनच्या बाजूने उभी राहिलीत. त्यामुळे चीनला या मित्र राष्ट्रांचा आधार सध्यातरी मिळालेला आहे.

१०) जागतिक आरोग्य संघटनेशी अमेरिकेने संबंध तोडणे :-

कोरोना काळातच अमेरिका आणि युरोप खंडाच्या आरोपांना जागतिक आरोग्य संघटनेने नाकारले आणि चिन्हे समर्थन केले. त्यामुळे अमेरिकेसारखा श्रीमंत देश हा चिडला. आणि जागतिक आरोग्य संघटनेशी असलेले आपले संबंध तोडून टाकलेले. या जागतिक आरोग्य संघटनेला सर्वात जास्त फंड अमेरिकेकडून मिळत असतो. परंतु ट्रॅम्प यांनी हा फंड देण्यास पूर्णपणे नकार दिला. त्याचे कारण असे की, जागतिक आरोग्य संघटनेने (WHO) चीनला दिलासा देऊन त्याची बाजू घेतली. यामुळे अमेरिका दुखावल्या गेला. म्हणून अमेरिकेने तसेच फ्रान्सने या जागतिक आरोग्य संघटनेशी संबंध तोडला. कोरोना काळातच हे संबंध तोडल्या गेलेले. या अगोदरच्या साथीच्या रोगामध्ये असे काहीही झालेले नव्हते. बाबही अत्यंत महत्वाची आहे. म्हणून

११) जी - ७ संघटनेत भारताला व आणखी तिन राष्ट्रांना स्थान मिळणे :-

अमेरिकेचे अध्यक्ष ट्रॅम्प यांनी जी - ७ या संघटनेत अगोदरच्या सात राष्ट्रांबरोबर भारताला घेण्याची शिफारस अमेरिकेने केली. तसेच भारत व रशिया, ऑस्ट्रेलिया, जापान यांचाही समावेश केला. आणि जी - ७ ऐवजी जी - ११ असे या जागतिक आर्थिक संघटनेचे स्वरूप याच कोरोना काळात निर्माण झाले. त्याचे कारण असे की, ज्यांची आर्थिक उन्नती चांगली झालेली आहे अशा नविन चार राष्ट्रांना या आर्थिक संघटनेत समाविष्ट केलेले आहे. कोरोना काळात हा महत्वाचा बदल झालेला दिसतो.

१२) जागतिक सुरक्षा समितीत भारताला स्थान मिळणे :-

या कोरोना काळातच भारतासारख्या शांतताप्रिय देशाला जगाच्या सुरक्षा समितीत सभासदत्व मिळालेले आहे. ही भारताच्या दृष्टिने गौरवाची बाब आहे. भारताबरोबरच स्वित्झर्लंड यालाही सभासदत्व मिळालेले आहे. हे सभासदत्व तिन तिन वर्षांसाठी मिळालेले आहे. पुढे ते कायमस्वरूपी मिळेल. चीनला शह देण्यासाठी हा विचार या कोरोना काळातच आला. आणि जागतिक सुरक्षा समितीची नव्याने स्थापना झाली.

१३) जागतिक आरोग्य संघटनेच्या अध्यक्षपदी भारताचे डॉ. हर्षवर्धन यांची नियुक्ती होणे :-

ही महत्वाची बाबही कोरोना काळातच झाली. युरोप खंडातील देशांनी भारताला अत्यंत महत्त्व दिले. विशेषतः अमेरिकेने नरेंद्र मोदींना अत्यंत महत्त्व दिले. भारतातील कोरोना नष्ट होण्याच्या दृष्टिने नरेंद्र मोदींनी जी पाऊले उचलली आणि जी शिस्त भारतात निर्माण केली ती सर्व जगाने मान्य केली. त्याचा परिणाम असा झाला कि जगाच्या दृष्टिने भारत मार्गदर्शक ठरला. त्यामुळे या जागतिक आरोग्य संघटनेच्या अध्यक्षपदी डॉ. हर्षवर्धन यांची नेमणुक झाली. ही सुध्दा कोरोना काळातील महत्वाची बाब आहे.

१४) औषधांची जागतिक स्पर्धा निर्माण होणे :-

कधी नव्हे एवढी औषधांच्या बाबतीत जागतिक स्पर्धा निर्माण झालेली आहे. या स्पर्धेत चीन, अमेरिका, फ्रान्स, ईसाईल, जापान, रशिया आणि भारत हे देश उतरलेले आहेत. कोरोनाच्या उपचारासाठी इंजेक्शन, गोळ्या, किटस, मास्क आणि लस निर्माण करण्याची स्पर्धा या देशांमध्ये निर्माण झालेली दिसते. आणि याचा आर्थिक फायदा आपल्याला कसा मिळेल याचेही आयोजन या देशांनी केलेले दिसते.



१५) कधी नव्हे एवढे भारताला महत्व प्राप्त झाले :-

पाश्चात्य राष्ट्रांनी व मुस्लिम राष्ट्रांनी तसेच आशिया खंडातील देशांनी आणि आफ्रिकेमधील देशांनी भारताला फार महत्व दिलेले दिसते. नरेंद्र मोदींनी या सर्व देशांचा वेळोवेळी प्रवास करून त्यांच्याशी फार चांगले नाते निर्माण केलेले असल्यामुळे साहजिकच भारताला जागतिक राजकारणात फार महत्व प्राप्त झालेले दिसते. याचाच परिणाम असा कि, सुरक्षा परिषदेत स्थान मिळणे, जी - ७ आर्थिक संघटनेत स्थान मिळणे आणि भारतासारख्या देशाला जागतिक आरोग्य संघटनेचे अध्यक्षपद मिळणे या गौरवशाली बाबी आहेत हे नाकारून चालणार नाही.

एकंदरीत कोवीड - १९ च्या काळातील सध्याच्या जगाच्या राजकारणाचे अनेक मुद्दे जे मी स्पष्ट केलेले आहेत ते अंतर्मुख करणारे आहेत. कधी नव्हे एवढ्या जलद गतीने कोरोना काळात हे राजकारणाचे सध्याच्या काळातील महत्त्वाचे मुद्दे निर्माण झालेत की याचा परिणाम भविष्यकाळातील अनेक राजकिय तसेच आर्थिक घटनांवर फार मोठ्या प्रमाणावर होणार आहेत हे नाकारून चालता येणार नाही. त्याचबरोबर हेही नमुद करावेसे वाटते की, चीनच्या साम्राज्यवादी वृत्तीला आळा घालण्याच्या दृष्टिने तिसरे महायुद्ध होऊ शकेल अशी संभाव्य भिती निर्माण झालेली आहे. संदर्भ ग्रंथ व संदर्भ लेख सुची :-

- १) सार्थीच्या रोगांचा इतिहास, ले. डॉ. ह. नर. सरदेसाई, पॉप्युलर प्रकाशन मुंबई, प्रथमावृत्ती १९७०,
- २) सार्थीच्या रोगांचे जंतूविज्ञान व सार्थीचे रोग, ले. डॉ. श्यामप्रसाद शुक्ला, नागविदर्भ प्रकाशन नागपूर, प्रथमावृत्ती १९६२
- ३) सार्थीचे रोग व आयुर्वेद चिकित्सा, ले. डॉ. नारायण वामन व्याघ्रळकर, विजय प्रकाशन नागपूर, प्रथमावृत्ती १९७४
- ४) सार्थीचे आणि विंगर सार्थीच्या रोगाची चिकित्सा, ले. डॉ. संजय आनंदराव जोशी, उद्यम प्रकाशन पुणे, प्रथमावृत्ती १९७४.
- ५) पहील्या व दुसऱ्या जागतिक महायुद्धाचा इतिहास, ले. डॉ. स. ना. गुप्ते, कॉन्टीनेण्टल प्रकाशन पुणे, तृतीय आवृत्ती १९८०.
- ६) इतिहासाचे तत्वज्ञान, ले. सदाशिव नारायण आठवले, सुविचार प्रकाशन पुणे, प्रथमावृत्ती १९७८.
- ७) राजकिय तत्वज्ञान, ले. भा. ल. भोळे, पिंपळापुरे प्रकाशन नागपूर, प्रथमावृत्ती १९८१
- ८) हिस्टरी अॅण्ड पॉलिटिक्स, ले. बोरीस मालकम, मॅकमिलन पब्लिकेशन लंडन, प्रथमावृत्ती १९१८.
- ९) पॉलिटीकल हिस्टरी ऑफ वर्ल्ड, ले. डॉ. एडमंड बेकन, मॅकमिलन पब्लिकेशन लंडन प्रथमावृत्ती १४९२.
- १०) फ्रान्सच्या राज्यक्रांतीचा इतिहास, ले. रा. आ. ओक, कॉन्टीनेण्टल प्रकाशन पुणे, प्रथमावृत्ती १९५८
- ११) युरोपचा इतिहास भाग १ आणि २, ले. डॉ. स. ना. गुप्ते, कॉन्टीनेण्टल प्रकाशन पुणे, प्रथमावृत्ती १९८३
- १२) वॉर अॅण्ड पीस, ले. विल्यम टॉलस्टॉय, मॅकमिलन पब्लिकेशन लंडन, प्रथमावृत्ती १९५२.
- १३) अब्राहम लिंकन, ले. वा. ह. शिर्सिकर, मेहता प्रकाशन पुणे, प्रथमावृत्ती १९५४.
- १४) कोरोना-१९ आंतरराष्ट्रीय बातम्या, दै. सकाळ पुणे १५) कोरोनाचा इतिहास, ले. अ. ग. बागाईतकर, १५ एप्रिल २०२०, दैनिक सकाळ, पुणे
- १६) कोरोना एक विश्लेषण, ले. माधव वामन गाडगिळ २७ एप्रिल २०२०, दैनिक सकाळ, पुणे
- १७) अमेरिका व चिन कोरोना वाग्युद्ध, ले. अ. ग. बागाईतकर, ७ मे २०२०, दैनिक सकाळ, पुणे
- १८) कोरोना आणि जागतिक अर्थचक्र, ले. स. ना. बोरीकर, २१ मे २०२०, दै. लोकमत, नागपूर. १९) कोरोनाच्या निमीत्ताने जागतिक धर्मयुद्ध, ले. माधव गाडगिळ २२ मे २०२०, दै. तरुण भारत नागपूर.

Impact Factor-8.575 (SJIF)

ISSN-2278-9308

# B.Aadhar

Single Blind Peer-Reviewed & Refreed Indexed  
Multidisciplinary International Research Journal

FEBRUARY 2023

(CCCLXXXVIII) 390

New Directions in Humanities



Chief Editor

**Prof. Virag S. Gawande**

Director

Aadhar Social

Research & Development

Training Institute Amravati

Editor

**Dr. Pradnya S. Yenkar**

Principal,

Vidya Bharati Mahavidyalaya,

Camp, Amravati



This Journal is indexed in :

- Scientific Journal Impact Factor (SJIF)
- Cosmos Impact Factor (CIF)
- International Impact Factor Services (IIFS)

For Details Visit To : [www.aadharsocial.com](http://www.aadharsocial.com)

Aadhar PUBLICATIONS

**INDEX**

No.	Title of the Paper	Authors' Name	Page No.
1	Impact Of Covid-19 And Lockdown On Mental Health Of Various Sections	Prof.Dr .Devdas S.Ramteke	1
2	An Overview of the Development of Education System in India	Dr. Rajesh M. Deshmukh	6
3	COVID-19:Challenges and Opportunities in Indian Economy	Dr. Devendra S. Rangachary , Prof.Dr. Mithilesh Rathore	12
4	Echo of Ecocriticism in Maneka Gandhi's 'Love Story'	Dr. Shitalbabu Ambadas Tayade	16
5	Importance Of English Language In The Present Scenario	Dr. Nishigandh Satav	20
6	Socio-Cultural challenges in Indian Education System: with Special Reference to Indian Women	Dr. Rizawana B. Gadakari	23
7	Importance of Good Communication Skills	Mrs. Anjali Deshmukh	26
8	The Modern Trends In Literary Forms Of Media: Photography And Internet	Prof. Purushottam V.Bathe	29
9	Experiment-Based Subjects: A Challenge To Learn In An Online Mode	C. N. Jadhav	33
10	Nostalgic Sense for Past in Tennessee Williams' 'The Glass Menagerie A Strategy of Survival in Oddity	N. G. Jadhao	37
11	Effect Of COVID-19 Pandemic Learning and Teaching Science Subjects: A Challenge to Both Teachers And Student	P. P. Nalawade , J. R. Bansod , N.N. Kakpure	40
12	Unaccustomed Earth:Generational Shift in tackling the Emotional Conflicts by Indian Immigrants	Dr. Nakul D. Gawande	44
13	Synthesis And Characterization Of Cu-Nanoparticles By Using O.Sanctum And M.Panniculata	L.P.Khalid , P.V.Pulate , N.G.Kokateand , J.B.Patil	47
14	Stress among the positive patients during the Covid-19 pandemic	Manjusha Jagannath Barbudhe	52
15	Recent Trends in Humanities, Commerce, Science and Technology	Mr. Shrirang Deshmukh	57
16	The Impact of Financial Constraints on Student Enrolment in Higher Education: A Major Challenge in Higher Education	Dr. Sanjay B. Kadu	59
17	Human Predicament in the select stories of Guy de Maupassant and Thomas Mann	Dr. R. M. Patil , Ms. Yogita S. Bhuyar	62
18	COVID 19 impacts on woman with Poly Cystic Ovary Syndrome on their pre-existing mental health issues in Vidarbha:Thematic Study	Apeksha Bandebuche , Dr. D. S. Ramteke	64
19	Innovations in EdTech: Improving Access and Outcomes for Learners	Dr. Pratik B. Upase	68
20	The Effect of Job Vulnerability on Pandemic Prevalent Concern: Loneliness	Dr. S. D. Wakode , Ujjwala Godbole Kulkarni	72



## COVID-19: Challenges and Opportunities in Indian Economy

**Dr. Devendra S. Rangacharya**

Department of Economics

Vidya Bharati Mahavidyalaya, Amravati.

**Prof. Dr. Mithilesh Rathore**

Department of Chemistry

Vidya Bharati Mahavidyalaya, Amravati.

### Abstract

In this paper I have discussed the impacts of COVID-19 on Indian economy and challenges to be faced in future. It presents the so far impact made by the Covid-19 pandemic on the economy and how markets and the economy have reacted sharply to the pandemic and its implications for businesses. The relevant data have been collected from a variety of reports of agencies, journals, newspapers and websites. The paper conclude and gives clear depiction of the impacts of Covid-19 pandemic on Indian economy.

**Key words:** Economy, Market, Pandemic, jeopardizing.

### I. Introduction:

Recently, there has been a sharp decline in the Indian economy. The economy expanded at a six-year low of 4.7 percent during the third quarter of this fiscal year. The last quarter of the current fiscal year has a good chance of recovering. However, the recent coronavirus outbreak has made recovery incredibly challenging in the short to medium term. The outbreak has posed new obstacles for the Indian economy, seriously disrupting both the supply and demand sides and jeopardizing the direction of the nation's economic growth. On January 30, India made the first confirmed case public. However, because there are few instances and most of them are tied to travel, there aren't many indications of community transmission. On the other hand, the domestic situation is still unstable and needs to be closely watched. The virus might have a significant and long-lasting economic impact on India if it were to spread over the entire nation. The impact on trade, investments, and service lines would be unfavourable in nations like China, South Korea, Japan, Italy, and others, but a shutdown in India may be much more detrimental. The purpose of the study is to learn how the business community feels about the possibility that the virus's development and spread could harm the Indian economy.

### II. Literature review:

1. *Maya M A 2021:* Late in 2019, a brand-new coronavirus appeared in Wuhan, China, and started to spread globally. The World Health Organization has given the illness brought on by this virus the official name Coronavirus Disease 2019 (2019). (COVID-19). 2 The spread of COVID-19 is still a concern on a global scale.
2. *VinayAnany 2021:* Unexpected changes brought on by the COVID-19 outbreak have undoubtedly disrupted daily life and led to severe psychological reactions and mental health crises. Finding psychological traits that foreshadowed distress among Indians throughout the spread of a novel Coronavirus was the aim of the study.

### III. India's Growth Projections Revised Down

As a result, the majority of multilateral organisations and credit rating agencies have revised their growth projections for India for 2020 and 2021 to take into account the detrimental effects of travel bans brought on by the coronavirus, supply chain hiccups, and low levels of consumption and investment on both the global and Indian economies.

**FitchRatings-** In addition, Fitch has revised its estimate of India's economic growth in 2019–20 downward from 5.1 percent to 4.9 percent.

**Moodys-Moody's Investors Service** has lowered its India growth prediction for 2020 from 5.4 percent to 5.3 percent, down from 5.4 percent in February.

**S&P Global Ratings-S&P** has decreased India's GDP growth prediction for 2020 to 5.2 percent, down from 5.7 percent previously expected.

**Barclays-India's GDP growth estimate for 2020** has been cut by Barclays from 6.5 percent to 5.6 percent. 2020, Sunil and associates A UN study estimates that India's trade impact from the coronavirus pandemic will exceed \$348 million dollars, and the nation is one of the top 15 economies most impacted by the impact of China's industrial crisis on international commerce. According to the Asian Development Bank (ADB), the loss of consumer expenditure from the Covid-19 outbreak may cost the Indian economy anything from \$387 million to \$29.9 billion (<https://www.livemint.com/>). According to



a survey conducted by FICCI (2020), the majority of respondents from the industry do not anticipate a positive demand account for the entire fiscal year. The present financial crisis has had a severe impact on several businesses, with tourism, hospitality, and aviation being among the worst-affected. Reduced activity in a number of areas, including retail, construction, and entertainment, is also having an impact on consumption. These factors include job losses and a fall in people's income levels, particularly among daily wage workers. Lack of raw materials and parts is a problem for the automotive, pharmaceutical, electronics, chemical, and other sectors.

CII identifies certain policy and regulatory reforms that would make conducting business easier in the aftermath of the COVID-19 pandemic and reduce negative impact on industry and economy.

1. Enhance Validity of licenses / approvals /NoCs
2. Easy & quick disbursal of pending dues
3. Provide speedy clearances
4. Relaxation / dispensation of labour law compliances
5. Contribution to PF& ESIFunds
6. Facilitate ease of doing business for MSMEs
7. Facilitate trading across borders
8. Ease licensing requirement for production of Sanitizer

Ratings for CARE for 2020 The purpose of the study is to learn how the business community feels about the possibility that the virus's development and spread could harm the Indian economy. By June 2020, retail inflation will have increased. Dev and Sengupta & Sengupta Dev (Dev and Sengupta, 2020) A worldwide epidemic is currently wreaking havoc on the economics and healthcare systems of several nations. The health-care crisis is currently receiving the majority of governmental attention, but it will soon become evident that the economy is also experiencing serious problems. India is not alone in this regard. The economic catastrophe caused by the health shock will have an impact on every nation on earth. On the other hand, the calamity in India might be especially bad because the economy was already in ruins when the shock occurred. The economic catastrophe that follows the health shock will have a much more enduring effect on us than the health shock itself.

#### IV. Objectives:

The major objectives of this study are:

1. To comprehend the influence of Covid-19 on the Indian economy as a whole.
2. To comprehend the influence of Covid-19 on various industries.

#### V. Research Methodology:

I chose media that were primarily published in March and April to understand the impact of COVID-19 on the Indian economy and various businesses. I've also read a couple of research papers and news articles over the last two months.

#### Impact of Covid-19 on Indian Economy:

India's economy has been impacted by the coronavirus epidemic, which has claimed lives. With a few notable exceptions, almost all industries have suffered as domestic demand and exports have fallen precipitously. Impacts of several significant industries are evaluated, as are any potential remedies.

##### • Food & Agriculture

Because agriculture is the country's backbone and is included in the government's important category, the impact on both primary agricultural production and agro-input usage is expected to be minimal. Several state governments have previously permitted the unrestricted movement of fruits, vegetables, milk, and other foodstuffs. Uncertain limitations on movement and the halting of logistics vehicles have a significant influence on online food grocery platforms. In the short term, the actions outlined by the RBI and the Finance Minister will benefit the industry and employees. In the next weeks, insulating rural food producing areas will be a fantastic answer to the macro impact of COVID-19 on the Indian food sector as well as the wider economy.

##### • Aviation & Tourism

The Aviation Sector and Tourism both contribute roughly 2.4 percent and 9.2 percent of our GDP, respectively. In fiscal year 2018-19, the tourism industry serviced around 43 million people. The first businesses to be severely impacted by the pandemic were aviation and tourism. COVID, it appears, will have a greater impact on these industries than 9/11 and the 2008 financial crisis. Since the beginning of the epidemic, these two industries have been experiencing serious cash flow problems and





are facing a probable layoff of 38 million people, or 70% of the total workforce. Both white-collar and blue-collar occupations will be affected. According to IATO estimates, travel restrictions might cost these industries almost 85 billion rupees. In the fields of contactless boarding and transport technologies, the Pandemic has sparked a wave of innovation.

- **Telecom**

Even before the Covid-19, there were substantial changes in India's telecom business as a result of brief pricing wars between service providers. Due to restrictions, most important services and sectors were able to continue operating during the epidemic thanks to the establishment of the "work from home" policy. As of 2019, the telecom sector provides roughly 6.5 percent of GDP and employs almost 4 million people, with over 1 billion connections. Increased broadband consumption had a direct influence on the network, putting strain on it. There has been a 10% increase in demand. Telcos, on the other hand, are bracing for a dramatic reduction in new subscriber additions. As a policy recommendation, the government may help the sector by reducing regulatory requirements and providing a moratorium on spectrum dues, which could be utilised by enterprises to expand their networks.

- **Pharmaceuticals**

Since the onset of the Covid-19 pandemic, the pharmaceutical sector has been on the increase, particularly in India, the world's largest producer of generic pharmaceuticals. It has been booming in India, exporting Hydroxychloroquine around the world, especially to the US, UK, Canada, and the Middle East, with a market size of \$55 billion by the start of 2020. The epidemic has caused a recent increase in the price of raw materials imported from China. Generic pharmaceuticals have been hit the most because of the industry's significant reliance on imports, interrupted supply chains, and labour shortages caused by social alienation. Simultaneously, the pharmaceutical business is suffering as a result of government-imposed export bans on vital pharmaceuticals, equipment, and PPE kits in order to secure adequate supplies for the country. The rising demand for these drugs, along with their limited availability, is making things more difficult. In such a critical moment, easing financial stress on pharmaceutical businesses, tax relief, and addressing the labour shortage could be the key elements.

- **Oil and Gas**

The Indian oil and gas business is important in the global perspective; it is the world's third-largest energy user, trailing only the United States and China, and accounts for 5.2 percent of global oil demand. The nationwide lockdown slowed demand for transportation fuels (which represent for two-thirds of total demand in the oil and gas sector), as auto and industrial manufacture plummeted and goods and passenger mobility (both bulk and personal) fell. Despite the fact that crude prices fell during this time, the government increased excise and special excise tax to compensate for the revenue loss, as well as the road cess. To increase demand, the government may consider passing on the benefits of lower crude prices to end consumers via retail outlets as a policy recommendation.

#### **VI. Results and Findings:**

- It has been established that when the global economy is slowing, no emerging economy can grow at its normal rate. COVID-19 aggravated the Indian economy's already-existing challenges. India's GDP has been progressively shrinking since peaking at 7.9 in Q4 of FY 2018, falling to 4.5 in Q2 of FY 2020. Businesses were cautious to invest in capital expenditures due to a lack of demand in the industry. Unemployment was at an all-time high, and exports had been stagnant for several months. The situation in India could deteriorate more and last longer; the country's economy was already in chaos before Covid-19 struck.

- As a result of the efforts taken to prevent the spread of the Coronavirus Disease 2019 (Covid-19), such as social separation and lockdown, non-essential expenditures are being postponed. India's aggregate demand is plummeting as a result of this. In addition to lower demand, there will be major supply chain disruptions as some people stay at home, others return to their villages, imports are hampered, and international travel is halted. In almost every industry, this will have a detrimental influence on production. Manufacturing, mining, agriculture, public administration, and construction will all experience a gradual increase in the shock. Investment, employment, income, and consumption will all suffer as a result, decreasing the economy's total growth rate.

- Several economies around the world, including India, are recognising the pitfalls of being overly reliant on a single market. Making the most of the current circumstance, India may now attempt to gain up to 40%





of their competitor's market share by focusing on domestic manufacturing and increasing the country's Make in India project.

#### VII. Recommendations:

Here are some ideas for policymakers to think about as they prepare to deal with the economic crisis.

1. The first measure must be to safeguard workers in the informal sector, who will be disproportionately affected and lack the necessary savings to weather the storm. This would not be easy, but there are two options: MNREGA (Mahatma Gandhi National Rural Employment Guarantee Act) and Jan Dhan accounts.
2. As previously said, the goal in the organised sector should be to make banks less risk averse in their overall lending while maintaining their ability to distinguish between viable and non-viable enterprises.
3. In order to boost liquidity and consumer confidence in these difficult times, the Indian government should grant a pay roll tax holiday for a quarter.
4. MSMEs should be offered a working capital loan equivalent to one to three months' average annual turnover (depending on the magnitude of the disruption). MSMEs should be provided with three-month concessional loans at a rate of 5% through SIDBI to assist them when global supply networks are disrupted. Over the next three years, the interest payment for such financing can be adjusted as part of GST.
5. Funding from corporate social responsibility should go toward a pandemic response fund.
6. A disaster management framework focusing on disease outbreak management will become critical in the large and highly populated country.

#### VIII. Conclusion:

This has not yet been done in a systematic way in India, and it must be prioritised alongside efforts to alleviate the health crisis. After the measures are implemented, the impact of COVID-19 on the Indian economy could be reduced by lowering tax rates or providing tax relief. Government policymakers would need to implement a significant targeted fiscal stimulus, broader monetary stimulus, and policy rate reductions to help stabilise the economy and combat the economic impact of the rapidly spreading coronavirus. If the COVID-19 problem grows, manufacturers will definitely face challenges on numerous fronts. Other aspects will have to be considered by manufacturers in addition to their own financial viability. They'll have to collaborate closely with the public sector to design plans that are vital to public safety and the financial viability of their workforce, all while keeping the lights on in their operations. a challenging setting Some austerity measures will be required, but they must be mitigated in order to meet long-term objectives.

#### References:

1. [https://bfsi.eletsonline.com/covid-19-and-its-impact-on-indian-economy/\(04/05/2020\)](https://bfsi.eletsonline.com/covid-19-and-its-impact-on-indian-economy/(04/05/2020))
2. <https://www.moneycontrol.com/news/business/markets/covid-19-impact-bumpy-road-ahead-for-indian-economy-global-financial-markets-5165951.html> (04/05/2020)
3. ICRA, Reports on Impact of Covid-19 on India Inc. – What lies ahead?, April-2020 2. CRISIL Ratings Report, "Pandemic to weigh on India Inc credit quality",
4. April-2020 3. KPMG in India analysis, 2020, Potential impact of COVID-19 on the Indian economy, April-2020
5. "Stock markets post worst losses in history; Sensex crashes 3,935 points amid coronavirus lockdown". The Indian Express. 23 March 2020. Retrieved 23 March 2020.
6. "Lockdown hurts economy but saving life is more important: PM Modi". India Today. 14 April 2020. Retrieved 14 April 2020.
7. "Covid-19: Govt allows transportation of all essential, non-essential goods". Business Standard India. PTI. 30 March 2020. Retrieved 30 March 2020.
8. <https://economictimes.indiatimes.com/news/politics-and-nation/coronavirus-faced-with-anunprecedented-challenge-how-is-india->
9. [https://en.wikipedia.org/wiki/Economic\\_impact\\_of\\_the\\_2019%E2%80%932020\\_coronavirus\\_pandemic\\_in\\_India](https://en.wikipedia.org/wiki/Economic_impact_of_the_2019%E2%80%932020_coronavirus_pandemic_in_India)



**दलित आत्मकथनातील स्त्री-पुरुष संबंध****डॉ. गजानन बनसोड**

प्राध्यापक, मराठी विभाग, विद्याभारती महाविद्यालय, अमरावती

दलित आत्मकथनात अंतरीच्या जिद्दाळ्याचे दलित स्त्रियांच्या जीवनाचे दर्शन आत्मकथनकारांनी घडविले आहे. भारत देशात स्त्रियांची लोकसंख्या एकूण लोकसंख्येच्या पन्नास टक्के एवढी आहे. यातील बहुतांश दलित स्त्रिया निरक्षर, दारिद्र्यरेषेखालील, आर्थिकदृष्ट्या मागासलेल्या, सामाजिकदृष्ट्या नाकारलेल्या, झिडकारलेल्या आहेत. मानसन्मान, प्रतिष्ठा, स्वातंत्र्यापासून वंचित ठेवलेल्या आहेत. दलित स्त्रीचे स्वसमाजात व सवर्णीय समाजातही शोषण होते. कबाडकष्ट करणारी, पुरुषांच्या खांद्याला खांद्या लावून मेहनत करीत असली तरी, ती परावलंबी जीवन जगतांना दिसून येते. दुःख, व्यथा, यातना या साखळीत सगळ्याच दलित स्त्रिया बांधल्या गेल्या आहेत. दलित आत्मकथनातून व्यक्त होणाऱ्या दलित स्त्री जीवनाच्या संदर्भात सरिता पदकी म्हणतात, "दलित जीवनातील वेदनेबद्दल बोलता बोलताच ही आत्मचरित्रे त्यांच्या आयुष्यात आलेल्या स्त्रियांबद्दलही खूप काही सांगून गेली. तसे पाहता दलित स्त्रीचे चित्रण मराठी वाङ्मयात अगदीच आले नव्हते असे नव्हे. पण किती झाले तरी दुरून पाहून कल्पनेचे रंग भरून केलेले ते चित्रण होते आणि तेही फार थोडे होते. दलित आत्मचरित्रांनी मात्र दलित स्त्रीचे अगदी जवळून अंतरीच्या जिद्दाळ्याचे दर्शन घडवले, अंगावर चिंध्या पांघरून, फाटक्या पिशाचीत रस्त्यावरचे कागद वेचणारी बाई ही एखाद्याच्या कथेतील पात्र असणे आणि ती बाई त्याची स्वतःची आई असणे यात दोन जगाचा फरक आहे. लग्नाच्या जेवणानंतर उकिरड्यावर टाकलेल्या पत्रावळीतील अन्न खाणाऱ्या व्यक्ती दुरून पाहिलेल्या असणे आणि स्वतःच तसे अन्न चवीने खाणे आणि पुन्हा पुन्हा ते खायला मिळावे म्हणून आईने ते उकळून, वाळवून ठेवणे या दोन अनुभवांतल्या दाहाचा फरक कोणत्या तापमापकाने मोजणार ? दलित स्त्रीच्या आयुष्याचे असे अस्सल आणि निकटचे दर्शन या आत्मचरित्रांनी आपल्यावर घडविले म्हणून त्यांच्या लेखकांचे आभार मानावेत तेवढे थोडेच. कल्पना ताणूनही जे दिसणार नाही

असे स्त्री जीवनाचे भयानक वास्तव या आत्मचरित्रांनी आपल्याला दिले आहे."<sup>१</sup> दलित स्त्रियांच्या जीवनाची अनुभूती अधिक यातनांनी वेदनांनी भरलेली आहे हे सरिता पदकी यांच्या वरील विवेचनातून दिसून येते. दलित स्त्रियांच्या वाट्याला येणारी भूमिका ही बहुरूपी असून सर्वाधिक कष्टाची मागणी करणारी आहे. गो. म. कुलकर्णी दलित स्त्रीच्या मनाबद्दल बोलतात, "दलित स्त्री मुक्तीची उद्याची दिशा काय असेल ती असो, पण आज तरी या दलित स्त्रिया शरीराने विसाव्या शतकाच्या उत्तरार्धात जगत असल्यातरी मनाने मध्ययुगीन तमोयुगातच वावरत आहेत. मग ते जग शहरातील असो किंवा खेड्यातील त्यात तसा काही फरक पडत नाही. या स्त्री जगातील अभावग्रस्तता, अज्ञान, दारिद्र्य, वैफल्य, कोंडमारा, अगतिकता इत्यादी विचारात घेता परंपरेने दलितांवर लादलेल्या साऱ्या दुःखाचे मूर्तीकरण स्त्री जगाच्या रूपाने झाल्याचे दिसते."<sup>२</sup> दलित जीवन जगणाऱ्या स्त्रियांचे जग बाह्य उपाधींनी पछाडलेले आहे. पारंपारिक एकत्र कुटुंबपद्धती, त्यातील हेवेदावे, ताणतणाव, अज्ञातजग, रूढी, परंपरा संकेत समजूती यांचा दलित जीवनात सुकाळ आहे. पुरुष कसाही वागला तरी ते सहन करणे हे या जगातील स्त्रियांचे भाग्येय आहे.

डॉ. शरद व्यवहारे यांच्या मते, "दलित आत्मकथनातील स्त्रीच्या व्यथेला दुःखाला तसेच भावनांना अनेक संदर्भ आहेत. आत्मकथनातील स्त्री जे जीवन जगतांना दिसते ते पाहता त्यातील जीव हरवलेला दिसतो. या स्त्रीचे कारुण्य व्यापक स्वरूपाचे आहे. कारण ही स्त्री अपार दुःख सहन करते. कबाडकष्ट करूनही सुखासमाधानाने तिला दोन घास पोटात घालता येत नाही. विविध तातळ्यांवरून संघर्षाला समोर जाणारी, नवऱ्याचा जाच सहन करूनही त्याच्याशी एकनिष्ठ राहणारी, प्रस्थापित वर्णव्यवस्था आणि गरिबी व अस्पृश्यता अशा दुहेरी स्वरूपाच्या यातना सहन करणारी आणि प्रतिकूल परिस्थितीशी सामना देत सुखाचा भविष्यकाळ पाहू इच्छिणारी स्त्री दलित आत्मकथनात आहे."<sup>३</sup> दलित आत्मकथनातून स्त्रियांची नानाविध रूप आपणास दिसतात. समाजातील भीषण रूढी परंपरेत दलित स्त्री कशी पिळवटून गेली आहे हे वरील विवेचनावरून लक्षात येते.

जनाबाई गिन्हे यांचे 'मरणकळा' हे भटक्या स्त्रीचे पहिले स्त्री आत्मकथन आहे. भटक्या विमुक्त जमातीमधील स्त्री जीवनाचे विदारक सत्य दाहक वास्तव घेऊन अवतरले आहे. चार पाच वर्षांच्या असतांना त्यांनी सांगितलेला अनुभव या समाजाचा दृष्टिकोन स्पष्ट करणारा आहे. त्या लिहितात, "म्या आता चार पाच सालाची झाली हुते तरी माझ्या पाठीवर मायला पोर सोर कायबी झालं न्हाय. तवा आजी, चुलते, काके, बाचं गणगावत, बा ला मनायचे, 'बापू तुही पोर मोठी झालीया, गुजरीला (मायला) कायबी होत नाय. तिला कवर पाणी घालतु या, आम्ही तुला दुसरी बाई करून देतु या, आस म्हनायची ! मायला कोणीच घरात बरं बघत नव्हतं आन मलायी मनायचे 'सपाट पाठीची', हिच्या पाठीवर लेकरू बाळ काय हुत न्हाय. आन आमच्या दोघोनलाबी कोणी बरं बघत नव्हतं."<sup>४</sup> मुलगा नाही, मुलीच्या पाठीवर काही होत नाही. ह्यासाठी दुसऱ्या लग्नाचा आग्रह धरणारे आणि मुलीला 'सपाट पाठीची' म्हणून हिणवणारे हे जग परंपरागत दृष्टिकोनाचे आहे. गोपाळ जातीमध्ये मुलींनी शिकणे फार मोठे अपराध समजला जातो. पहिल्या दिवशी शाळेत घालतांना लेखिकेची आई विरोध करते. भटक्याची पोरगी शाळेत जाते, अशी गोपाळाच्या वस्तीवर चर्चा होते. शाळेत जाणारी मुलगी चांगल्या चालचलनाची नसते, असे त्यांचे मत असते. लेखिकेचे लग्न जुळल्यानंतर गोपाळ समाजातील एक स्त्री तिच्या सासूला वाईट सांगते. तेव्हाचा प्रसंग जनाबाई गिन्हे नोंदवतात, "आगं बायनू, तुम्ही येड्या का शान्या, ही पोर कशाला केली ? ती

मायपोटी एकटी हाय, शिकल्याली हाय आन् ती नांदायची न्हाय. मला माहीत असतं ना, तर म्या तवाच सांगितलं असतं, माय, ही पोर करू नका मून. तिला लेकरू बाळबी व्हायचं न्हाय. तिच्या मायलांबी एकटी झाली अन् तिच्या पाठीवर कायची न्हाय. वया तसंच पोरीचंबी व्हाईल." <sup>4</sup> भटक्या समाजात एक स्त्री दुसऱ्या स्त्रीकडे कोणत्या दृष्टिकोनातून पाहतो, 'स्त्री' हीच स्त्रीची वेरी कशी आहे ? त्याचबरोबर शिक्षित मुलींबद्दल असणारा गैरसमज वरील प्रसंगातून व्यक्त होतो.

अजित मिणेकर आपल्या 'फिरस्तू' या आत्मकथनात सांगतात, "आई चुली पुढे चिमणीच्या उजेडात स्वैपाक करत होती. बाघाच्या आडोश्याला दबा धरून उभा राहिला होता. आई स्वैपाकाची आवरा आवर करून बाहेर पडते न पडते तोंच वानं आईच्या डोक्यात कुन्हाड घातली. डोक्यावरचा नेम चुकला आणि ती कपाळावर आदळली. आई जोरात किंचाळली, आम्ही जवळपास मुलांबरोबर खेळत होतो. आईची किंकाळी ऐकून पळत घराकडं सुटलो तर आई दारातच दोन्ही हातानं कपाळ धरून बसली होती. रक्त भळाभला वाहत होतं. आई रक्ताच्या थारोळ्यांत बसली होती." <sup>5</sup> दारिद्र्याच्या अवस्थेत मुलाबाळांना सांभाळणाऱ्या स्त्रींवर घरातील कर्ताधर्ता व्यसनी पुरुष कुठलीही दयामया न दाखविता कुन्हाडीचा वार करतो. त्यामध्ये ती रक्तवंबाळ होते. दलित पुरुषांमधला अहंपणा, पुरुषी वर्चस्वाची जाणीव वरील प्रसंगात दिसून येते.

अशोक पवार यांच्या 'बिराड' या आत्मकथनात त्यांची आई आपली मनोवेदना व्यक्त करते. "मडं गेल त्या आयी वाचं पिदाड्या नवरा करून देला. मडं समंद वाटोळं केलं. लेक मेली का जिती हाय त्ये बी पाह्यालं आले न्हाय.. आता ह्यांच्या संग मळा जल्म कटत न्हाय. म्या हिरच भरते. मेल्यावर तरी ह्यो सुधरलं. दारू सोडलं, सारा दिवस गांडीत माती जावसतर काम करावं अन् रोज सांच्याला गद्दी सारखा मार खावावं. आता म्हाच्यानं सोसनं व्हत न्हाय...?" <sup>6</sup> नवऱ्याचा अनन्वित अत्याचार सोसून व्यथित झालेलं दुःखीकष्टो मन बोलतांना दिसते. दारू पिऊन मारझोड करणाऱ्या नवऱ्या बद्दल बोलतांना ती आपल्या आईवडिलांनाही दोष देते.

आर्थिकदृष्ट्या दुबळी, सामाजिक दृष्ट्या अगतिक, घरातही दुय्यम स्थान, उरफुटेस्तोवर कष्ट करून मारहाण सहन करणारी अशा दलित स्त्रीला घटनेने दिलेले मानवी हक्क कसे माहीत असणार ? स्त्री शक्ती, स्त्री पुरुष समानता हा दृष्टिकोन तर त्यांना माहितीच नाही. इतकेच नव्हे तर होणाऱ्या अत्याचाराला वाचा फोडण्याचेही स्वातंत्र्य नाही.

स्त्री गुलामापेक्षाही गुलाम पूर्वापार चालत आलेल्या परंपरेच्या साखळ्यांनी त्यांचे जीवन जखडले गेले. दलित स्त्रीच्या वाट्याला आलेली अगतिकता, असहायतेने केवढी मोठी परिसीमा गाठली आहे. याचे दृकप्रत्ययकारी चित्रण आत्मकथनातून दिसते.

दलित स्त्री जीवनाची ससेहोलपट देश स्वातंत्र्यानंतरही कमी झालेली नाही. आत्मकथनात दलित स्त्री शोषणावर डोळसपणे, चिकित्सक वृत्तीने मांडलेले प्रसंगापहून वाचकांचे मन हेलावून जाते. प्रल्हाद चेंदवणकर आपल्या तात्याविषयी सांगतात, "बापू ! ह्या

बायला माझ्यापरासभी लई ताकद हाय... मला ही बायकूच नग s नाकापरास मोती जड." <sup>7</sup> स्त्री समर्थ असली तरीही तिच्यावर अर्नेतिकतेचा शिवका लावून पुरुष मोकळा होतो. तिला पशूप्रमाणे वागवतो. आवाजाच्या, माराच्या जबरेने गप्प बसवतो. स्त्रीवादी चळवळीच्या कार्यकर्त्या सीमा साखरे म्हणतात की, "प्रत्येक स्त्री एक कथा आहे. स्त्रियांची भाषा वेगवेगळी असेल परंतु व्यवस्थेने निर्माण केलेले दुःख एक आहे. कारण ते शोषणातून निर्माण होते." <sup>8</sup> दलित स्त्री ही परावलंबी असून त्या स्त्रीच्या वेदना ह्या जास्त ठसठसणाऱ्या आहेत.

गोपीचंद पवार 'कोल्हाटी' समाजातील स्त्री जीवन मांडतांना सांगतात, "खिग्येमे कुती लभावता का (घरात पळवून आणलेली वाई लपवितो काय) कोंड्याच्या त्वांडानं भळबळ पाणी सालडं, त्यो तिला सोताच्या घरात लपवायला तयार झाला. म्या दोन दिसात येतो. काई तजवीज करतो. असं फुसफुस सांगून भदगुण्या निसाटला. कोंड्यानं कोयली पेटवून रातभर मजा मारली. दोन दिसात भदगुण्या आला. तूच इला घे, म्हणू लागला. कोड्यानं न्हाई, व्हय करून पाचसं रूपयं मोजलं. सरीला घरात घातलं, आन सा मयन्याला आंघ्रातल्या बांडीवर असणाऱ्या बोंडगावच्या भातूला घेतली तेवढ्यातच इकली. सरू सांगत व्हती, 'करमाचा भोग हाय' बाईला गाईची दसा हाय. वापानं गाय इकली आन मी त्येला मुकली ?" <sup>9</sup> दलित स्त्रीच्या जीवनाचा सौदा पुरुषाने करावा यासारखी क्रूर घटना नाही. माणुसकीला काळीमा फासणाऱ्या गोष्टीला जबाबदार घटक म्हणजे अशिक्षितपणा, दारिद्र्य जातीयता वर्णव्यवस्था हीच होय.

डा. किशोर शांताबाई काळे 'कोल्हाट्याचं पोर' मधून जिजीला कृष्णा कोल्हाट्याने कसे गाठले तो अनुभव मांडतात. "कुठं जायच वाई ? लक्ष्मीनं भोळेपणानं सर्व काही सांगितलं. कृष्णा कोल्हाट्यानं लक्ष्मीला आणि तिच्या दोन्ही मुलांना हॉटेलमध्ये नेलं. त्यांना पाटभर खाऊ घातलं. लक्ष्मीच्या भोळ्या स्वभावाच्या कृष्णा कोल्हाट्यानं फायदा उचलला आणि तिला आपल्यासारखं करून घेतलं. कृष्णा कोल्हाट्याला लग्नाची पहिली बायको होती आणि एक मुलगा देखील. त्याचं नाव कोंडिबा. लक्ष्मी कृष्णा कोल्हाट्याची बायको म्हणून राहू लागली. नंतर ती सोलापूरला गेलीच नाही आणि तिला आयुष्यात तिचा महादेव काही भेटला नाही.... याच कोल्हाट्यांमध्ये गंगाराम व्होल वाजवण्यास शिकला. जिजी नाच, कोल्हाट्यां उड्या मारणं आणि इतर कला शिकली. कोंडिबा आयता खात होता. कारण तो लग्नाच्या बायकोचा मुलगा होता ! लक्ष्मीची इच्छा होती की जिजीचं लग्न करून द्यावं. पण कृष्णा कोल्हाट्याला सोन्याची अंडो देणारी कोंवडी हातची जाऊ द्यायची नव्हती." <sup>10</sup> दलित स्त्रीला भावभावना नसतात, तिला इच्छा, आकांक्षा नसतातच तसे गुहित धरून वापाने मुलीच्या जीवनाचा केलेला सत्यानाश दिसतो. धनहीन, विद्याहीन, सत्ताहीन तिची मास्त्रीण होण्याची इच्छाशक्ती थिजवली गेली, गोठवून टाकली.



भगवान इंगळे 'ढोर' या आत्मकथनात आपल्या आईची व्यथा व्यक्त करतांना सांगतात, "आरं या गंगीला पुरीचं लेंढार लागलय. तिला पोर्गा नाय व्हनार. कवर दम धरतोस ? दुसरी कर मनून मागं लागायचा. म्या मुळमुळु रडत रुसून रानात काळं करी न् जिवाचा सनीताप करी"<sup>१२</sup> जननप्रक्रिया स्त्रीला बहाल केलेली निसर्गदत्त देणगी होय. त्यातही स्त्रीला मुलगीच झाली तर तिच्या नावाने बॉव करून तिला नवऱ्याने सोडून द्यावे व दुसरी बायको करावी म्हणजे मुलगा होईल असे एक स्त्री-स्त्रीबद्दल म्हणते. हे आत्मकथनातून दिसून येते.

'वावदान' मध्ये आपल्याला आजीच्या दुःखी, कष्टी जीवनाची माहिती सांगतांना वैशाली सुरवसे यांनी सांगितलेला पुढील प्रसंग पहा- "सटवा म्हणाला, 'झाली की नाही भाकर कालवन अजून ? का डुलत बसलीस चुली म्होरं ? त्यावर तिरवणा घाबरून म्हणाली, 'इ ालं व झालं, जरा दाळ शिजूलाल्याय ? त्यावर सटवाचं डोकसं फिरलं आन तो रागान म्हणालां, 'ती दाळ शिजायला घातलंय का दगडं- बिगडं घातलंय. अजून खी शिजना ती दाळ ? वाड... वाड जसलं आसलं तसलं. जावाव लागतं हामाला कामाला. तुझ्यावानी बसायचाय व्हय ?"<sup>१३</sup>

दलित स्त्री जीवनाची कहानी हीनदीन आणि चिंतनीय असलेली दिसते. त्यात वैविध्यता आहे कुणी वांझ स्त्री म्हणून, तर कुणी मुलीच होतात म्हणून, कुणी अनैतिकतेचा आरोप सहन करीत जगतात. काबाडकष्ट, संसारासाठी खस्ता खाणे हे तर तिच्या पाचवीला पुजलेले दिसते. स्त्री दुःखाच्या नानापरी दलित आत्मकथनातून पहावयास मिळतात.

#### संदर्भ टीपा :

- १) दलित पुरुषांच्या आत्मचरित्रातील स्त्री प्रतिमा / संपा. शोभा भागवत, स्त्रीवाणी प्रकाशन, पुणे, प्र.आ. सप्टेंबर १९९७, पृ. १०२.
- २) तत्रैव, पृ. १४८.
- ३) दलित स्त्री विशेषांक, अस्मितादर्श, औरंगाबाद १९८१/शरद व्यवहारे याचा लेख, पृ. १६८.
- ४) मरणकळा / जनाबाई कचरू गिन्हे, प्रचार प्रकाशन, कोल्हापूर, जुलै १९९२, पृ. २२.
- ५) फिरस्तू / अजित मिणेकर, सलोनी प्रकाशन, इचलकरंजी, ऑगस्ट १९९७.
- ६) विराड / अशोक पवार, दिलीपराज प्रकाशन, पुणे, २००१.
- ७) टाच / प्रल्हाद चेंदवणकर, समता सहकारी ग्रंथ प्रकाशन, मुंबई, ऑगस्ट १९९४.
- ८) कोल्हाटउडी / गोपीचंद पवार, शब्ददान प्रकाशन, नांदेड, जाने. १९९८.
- ९) कोल्हाट्याचं पोर/ किशोर शांताबाई काळे, ग्रंथाली प्रकाशन मुंबई, नोव्हें. १९९४.
- १०) ठोर / भगवान इंगळे, ग्रंथाली प्रकाशन, मुंबई, २८ नोव्हें. १९९९.
- ११) वावदान / वैशाली सुरवसे, शब्ददान प्रकाशन, नांदेड, ऑक्टो. २००१.

समकालीन लेखिकेच्या कादंबरीतील स्त्री नायिका आणि जीवनचित्रण  
(मेघना पेठे, कविता महाजन, अरुणा सबाने)

तोष्णा बी.बोंदाडे (मोकडे)  
मार्गदर्शकसंशोधक विद्यार्थी, मराठी विभाग  
विद्याभारती महाविद्यालय अमरावती.

प्रा.डॉ. गजानन बनसोड  
संशोधक  
मराठी विभाग प्रमुख,  
विद्याभारती महाविद्यालय, अमरावती.

१९६० नंतर मराठी साहित्य विश्वात जे अनेक प्रवाह निर्माण झाले, त्यापैकी एक जोमदार साहित्य प्रवाह म्हणजे, स्त्रीवादी साहित्य प्रवाह होय. आतापर्यंत स्त्रिया लिहित होत्या मात्र, कुठेतरी ते लिखाण पुरुषसत्ताक साहित्याचा पगडा असणारं होतं. प्रथम स्त्री संवेदनांचा बंडखोर हुंकार विभावरी शिरूरकर यांच्या लिखाणातून उमटला. स्त्रिया लिहू लागल्या कधी ठळक तर, कधी संदिग्ध स्वरूपात आत्मशोधाची, आत्माविष्काराची, बंडखोरीची भूमिका येऊ लागली. पुढे-पुढे स्त्रियांच्या लेखनाकडे स्वतंत्रपणे पाहण्याचा दृष्टिकोन विकसित होऊ लागला. पुष्पा भावे, अंजली सोमण, रूपाताई कुळकर्णी, सीमा साखरे, मलिका अमर शेख, प्रज्ञा पवार, ज्योती लांजेवार, उर्मिला पवार वगैरे सह मराठीत सर्व बाजूंनी स्त्रीवादी साहित्याचा प्रवाह स्त्रीवादी चळवळीतून स्वतंत्रपणे आकाराला येऊ लागला. स्त्रीयांना बदलत्या जीवनाचं वास्तव मांडल्याची प्रेरणा मिळाली. यातून स्त्रीवादी साहित्याचं वास्तववादी स्वतंत्र जाणीव प्रतिभाविश्व स्वयंभाषा आणि शैलीसह मराठीच्या साहित्य आणि संस्कृतीच्या प्रांतात येऊ लागलं. मेघना पेठे, कविता महाजन आणि अरुणा सबाने या समकालीन स्त्रीवादी साहित्यिकांनी आपल्या स्वतंत्र दृष्टीचा आणि स्वयंभू शैलीचा प्रत्यय त्यांच्या लिखाणातून घडवून आणला.

मेघना पेठे, कविता महाजन, अरुणा सबाने या तिन्ही लेखिका वयाच्या आणि लेखनाच्या दृष्टीने समवयस्क आणि समकालीन आहेत. त्यांनी कादंबरीतून चितारलेला काळ आणि अनुभव विश्व समकालीन आहे. आयुष्य जगतांना कामानिमित्ताने अवतीभवतीचं जग त्यांनी अनुभवलं तोच अनुभव पण कल्पकतेने तिन्ही लेखिकांनी कादंबरीतून कथात्म पद्धतीने वर्णन केला आहे. यापूर्वी इतक्या उघड्या नागड्या स्वरूपात विषयविश्व साहित्यातून आलेलं नसल्याने या तिन्हीही लेखिकेच्या कादंबऱ्या या मराठी साहित्य विषयाची छाप सोडून जातात .

समकालीन मेघना पेठे कविता महाजन, अरुणा सबाने या लेखिकेच्या कादंबरीतील नायिका आणि त्यांनी जगलेलं वेदनादायी जीवन लेखिकेने अतिशय विदारकपणे चित्रित केलेलं आहे. या कादंबऱ्या वाचताना बोल्ट वाटत असल्या तरी नकोशा वाटत नाही. वास्तवतेच्या परिप्रेक्ष्यातून चितारलेल्या त्या साहित्यकृती व्यवस्थेने दाबून टाकलेले हुंकार उद्गाराच्या स्वरूपात कादंबरीतून प्रगट होताना दिसतात.

मेघना पेठे यांच्या 'नातिचरामि' या कादंबरीतील स्त्री नायिका आणि जीवन चित्रण—

मेघना पेठे मराठीतील निर्भय अभिव्यक्तीच्या आणि स्त्री स्वातंत्र्याचे वेगळे परिमाण मांडणाऱ्या लेखिका आहे. मेघनांनी आतापर्यंत स्त्रियांनी मांडलेल्या शालीन, सोज्वळ, सोशिक संस्कृती प्रधान, परंपरा जपणाऱ्या नायिकांना खो देऊन, स्त्रिया स्वतंत्र व्यक्ती म्हणून जगणाऱ्या नायिका मांडल्या आहे. स्त्री-अस्तित्वाची दखल घ्यायला लावणारी ही नायिका सहजासहजी वाचकांच्या पचनी पडणाऱ्या नसली तरी तिचे अस्तित्व नाकारण्यासारखे नाही.

'नातिचरामि' या कादंबरीत मीरा हे केंद्रवर्ती पात्र आहे. मीरा ही महानगरात शिकलेली आणि मध्यमवर्गीय कुटुंबात वाढलेली मुलगी आहे. उपजीविकेसाठी कारकुनी करणारी सुंदर स्त्री म्हणजे मीरा. मीरा पहिला नवऱ्याच्या पुरुषपणाच्या अहंकाराला कवटाळून वेगळी होते. त्यानंतर ती दुसरं लग्न करते पण, तिला त्यातही यश येत नाही. तिचा दुसरा नवरा डिवोर्स नंतरही मोगशी शरीर संबंध ठेवतो. तिच्यावर अधिकार गाजवतो. मात्र शरीराची गरज ओळखून मीरा हे कॅव्हॉल प्रखर विरोध न करता सहन करते. भरत हा मीराच्या आयुष्यातला सुखाचा विश्वस्तपणाचा एकमेव 'नातिचरामि' स्पर्श करणारा आहे.



मीराच्या आयुष्यातलं एकाकीपण समजून घेणारा वयस्कर गझल गायक मित्र लोभी आहे. मीराच्या दुसऱ्या नवऱ्याची मैत्रीन चंदाबाई ही व्याभिचारी असूनही समाजात सन्मानाने जगताना दिसते. मीराचे शरीरसंबंधाविषयीचे विचार जरी मुक्त असले तरी तिने केवळ तिच्या दोन्ही पतीसोबतच संग केला आहे. तिच्यावर भाळणाऱ्या डॉक्टर किंवा इतर मित्रांशी तिने कधीही जवळिक केली नाही. यातून एक बाब निदर्शनास येते की मीराचे विचार कितीही बोल्ड असले तरी तिची सामाजिक संकेत, लग्न व्यवस्था, वैध सेक्स या चौकटीतच ती राहणारी आहे. मेघनाची भाषा आणि शैली चिंतनशील आणि तात्विक पाखरण करणारी आहे.

कविता महाजन यांच्या कादंबरीतील नायिका आणि जीवनचित्रण —

कविता महाजन यांच्या 'ब्र' आणि 'भिन्न' या दोन्ही कादंबऱ्या मराठी कादंबरी विश्वात नवकोरं विश्व उभं करणारं आहे. कादंबरीतून व्यक्त होणारे समाजचिंतन आणि संशोधनातून येणारे वास्तव अनोख्या स्वरूपात आले आहे.

सुशिक्षित नागरी स्त्रियांना 'ब्र' उच्चारण्याचा अधिकार नसतो. मात्र आदिवासी स्त्रिया हालअपेष्टा सहन करूनही अधिक जागरूक आणि धीटपणे लढतांना दिसते.

कादंबरीतील प्रफुल्ला संसाराचा कोष भेदून प्रगत स्वयंसेवी संस्थेत काम करते. आदिवासी स्त्रियांच्या समस्येवर काम करतांना ती स्वतःला झोकून देऊन काम करते. ती ज्या संस्थेत काम करते त्या संस्थेचा प्रमुख सुमेध हा देखील पाशवी पौरुषाने बरबटलेला पुरुष आहे. त्याची सुमित्रा सारखी सुशील सुसंस्कृत मुलगी ध्येयवादाच्या नादात सुमित सारख्या माणसाचा बळी ठरते. प्रफुल्लाच्या कामाचा आदर्श डॉक्टर दयाळ आणि त्यांची अमेरिकन पत्नी डॉक्टर एंजेला आहे आणि नतदृष्ट लोक त्या दोघांना हूसकाविण्याचा प्रयत्न करून बघतात मात्र ते कधीच त्यांच्या सेवा व्रता पासून परावृत्त होत नाही. मीरा संसाराच्या जाचाला कंटाळून सेवा संस्थेत येते, मात्र तिथेही तिला पूर्ण समाधान मिळत नाही. तरीही मीरा सेवेचा ध्यास सोडतांना दिसत नाही. ती एकनिष्ठपणे सेवेच्या मार्गाने चालत राहते. 'ब्र' या कादंबरीचा शेवट लेखिकेने प्रफुल्ला श्रीप्रिया या मैत्रीणीला मदत आणि नवीन निर्णयासाठी आत्मबल गोळा करण्याच्या हेतूने लिहिलेल्या काव्यात्मक पत्राने केलेला आहे.

'भिन्न' ही कादंबरी महिलांच्या लैंगिक आणि सामाजिक उपेक्षेचा प्रश्न मांडणारी आहे. कादंबरी रचिता —प्रतिभा —लेनिना यातील नायिकांभोवती फिरतांना दिसते.

रचिता शिर्के ही नवऱ्याकडून एचआयव्ही पॉझिटिव्ह आणि एड्सग्रस्त स्त्री आहे. सोबत या स्वयंसेवी संस्थेत प्रतीक्षा कमल आणि लेनिना ह्या दोघी कार्यकर्त्या आहेत. रचिता शिर्के ही मुंबई महानगरमध्ये शेफाली मॅडमच्या लेडीज क्लब मध्ये जिमची इन्स्ट्रक्टर म्हणून नोकरी करणारी बाई. रचिताचा नवरा विठ्ठल अतिशय लफंगा माणूस. रचिताच्या वडिलांचं आणि नवऱ्याचं विद्रूप चित्र किळसवाणे आहे. रचिता एड्स बाधित असल्याचे कळल्यावर रचिताचा संघर्ष सुरू होतो. विठ्ठलला जेव्हा एड्सबाधा झाल्याचे कळते तेव्हा तो आत्महत्या करतो. कुटुंबाची जबाबदारी रचितावर येऊन पडते. ती न डगमगता खंबीरपणे संकटांचा सामना करते. 'सोबत' च्या माध्यमातून एड्सग्रस्तांना जीवन जगण्यासाठी मदतही करते.

प्रतीक्षा कमल ही समाजकार्यात उच्च शिक्षण घेतल्यानंतर मुंबईच्या कामाठीपुऱ्यात वेशावस्तीत एड्स पासून महिलांना जागृत करण्याचं काम करते. पुरुषप्रधान संस्कृतीचा निषेध करित ती स्वतःच्या नावापुढे आईचे नाव लावते. 'सोबत' या स्वयंसेवी संस्थेचे विश्वस्त जे.डी. वाडेकर वर एकतर्फी प्रेम करणारी ती...शेवटी भावनिक संघर्ष असह्य होऊन लोकल ट्रॅकवर आत्महत्या करते.

लेनिना ही 'सोबत'मध्ये पगारी कार्यकर्ता कर्मचारी म्हणून कार्य करणारी आहे. पुरुषव्यवस्थेवर बोलण्यातून — वागण्यातून सतत ताशेरे ओढणारी लेनिना मात्र मुक्त आणि बिनधास्त आहे. 'पुरुष जसा स्त्रियांना वापरतो तसा स्त्रियांनाही पुरुषांना वापरता आलं पाहिजे' या बिनधास्त विचारसरणीची लेनिना मोहक उर्फ प्रसादच्या नकळत प्रेमात पडते. तिच्या आयुष्याची सांगता त्यांनी एकमेकांना स्वीकारण्यात होते.

'ब्र' आणि 'भिन्न' या केवळ साहित्यकृती नाही तर सामाजिक दस्तावेज आहे. कविताने भाषेच्या जिवंत प्रवाहीपणाला स्त्रीत्वाचा खास टच आहे. या साहित्यकृतीची मौलिकता तिच्या सामाजिक वाधिलकी आणि उत्तरदायित्व जपणारी संवेदनशीलता यात दडलेली आहे. या दोन्ही

कादंबऱ्या डॉक्युमेंटेशन स्वरूपाला प्राधान्य देत असून लेखिकेची स्वतंत्र भाषा आहे. लेखिकेने या दोन्हीही कादंबऱ्या लिहून नैतिक आणि सामाजिक संदर्भ संवर्धनाची जबाबदारी निभावलेली आहे. अरुणा सबाने यांच्या कादंबऱ्यातील नायिका आणि जीवनचित्रण :

अरुण सबाने या विदर्भातील स्त्रीवादी चळवळीत सक्रिय कार्य करणाऱ्या सामाजिक कार्यकर्त्या आहेत. विदर्भातील 'आकांक्षा प्रकाशन' चालविणाऱ्या एकमेव स्त्री प्रकाशिका म्हणून त्यांचा गौरव केला जातो. त्यांनी लिहिलेल्या कादंबऱ्या केवळ वाङ्मयीन कलाकृती नाही तर सामाजिक आत्माविष्कार आहे. 'विमुक्ता' आणि 'मुन्नी' या कादंबऱ्यांमध्ये वसुधा आणि वैदेही या दोन्ही नायिकेच्या वाट्याला नवऱ्याला कंटाळून आलेलं एकाकीपण आहे. तरी त्या खंबीरपणे आपलं अस्तित्व सिद्ध करताना दिसतात.

'विमुक्ता' या कादंबऱ्यातील वसुधाचा नवरा शशांक हा वकील आहे. वरवर पाहू जाता सुशांत सुखभावी वाटत असला तरी वसुधेच्या वाट्याला मात्र, अमानुष्य पौरुषत्व, पशुत्व, विकृतीचं भेमुर् रूप आलेलं आहे. नितीन आणि आनंदचे अनैतिक संबंध आहे या संशयावरून तो दररोज मारझोड करणे, मुलांसमोर गलिच्छ बोलणे, दारू पिऊन तिच्यावर जबरदस्ती करणे या जाचाला वसु कंटाळलेली होती. तरीही सर्व अडचणींवर मात करून वार्म या टॉईज कंपनीला जगाच्या बाजारपेठेपर्यंत पोहचवून स्वतःचं वेगळं विश्व साकार करताना दिसते.

आयुष्याकडे पाहण्याचा सकारात्मक दृष्टिकोन आणि जगण्यासाठी करावा लागणारा संघर्ष हा प्रेरक आणि उद्बोधक आहे.

'मुन्नी' या कादंबऱ्यातील नायिका वैदेही तिच्या वाट्याला येणारा मास्तर नवरा हा स्त्रीलंपट आणि अनैतिक पौरुषत्वाचा नमूना आहे. चवचाल मास्तर वैदेही समोर विद्यार्थिनीशी लगट करतो. एक दिवस वैदेहीला आणि तीन मुलांना सोडून विद्यार्थिनी बरोबर पळून जातो. त्यानंतर वैदेही महिलांसाठी काम करण्यासाठी समाज कार्यकर्ती होते. ती मुन्नी आणि सायना सारख्या मुलींना वेश्याव्यवसायातून सोडवण्याचा प्रयत्न करते. कादंबरीत वर्णन केलेला परिसर हा गंगा-जमुना वस्तीचा आहे. मुन्नीची या व्यवसायातून सुटका करून तिला शिकवते आणि पुढे ती आय.ए.एस. अधिकारी होते. सोहम महाजन सारखा हुशार प्राध्यापक तिच्या आयुष्यात येऊन तिच्या आयुष्याचं मोनं करतो.

सायना ही त्याबाबतीत अभागी ठरते. वैदेहीच्या मदतीने ती गंगा-जमुनाच्या जगातून सुटण्याचा मार्ग शोधते, पण तिच्या वाट्याला वस्तीतलेच अनुभव परत-परत येताना दिसतात.

नागपुरी वऱ्हाडी, वेश्या व्यवसायातील भाषिक रूप, लिंगप्रचुर भाषा आणि उघडं-नागडं भयावह आणि विकृत विश्व लेखिकेने चांगलं रंगविलं आहे.

कथानकांचा आणि पात्रांचा विस्तार दोन्ही कादंबऱ्यांनी साधला आहे. कादंबरीतील निवेदन पद्धती पारंपरिक आणि साधी सरळ आहे.

मेघना पेठे, कविता महाजन, अरुणा सबाने यांनी लिहिलेल्या या कादंबऱ्या मराठी कादंबरी विश्वात लक्षणीय भर घालणाऱ्या तर आहेतच सोबत स्त्रियांचे नवे विषय, त्यातील वेगळेपणा, शैली, लेखनातील वैविध्यता आणि स्त्रियांची कादंबरीवरील हुकूमत सांगणाऱ्या आहेत. स्त्रियांनी लेखनाला उर्गीत जरी सुरुवात केली असली, तर दखल घ्यायला लावणारं कादंबरी लेखन त्यांनी सिद्ध केले आहे आहे.

संदर्भ ग्रंथ सूची

- १) पेठे, मेघना (२००५). *नातिचरामि*, राजहंस प्रकाशन, पुणे.
- २) महाजन, कविता (२००५). *ब्र*, राजहंस प्रकाशन, पुणे.
- ३) महाजन, कविता (२००७). *भिन्न*, राजहंस प्रकाशन, पुणे.
- ४) सवाणे, अरुणा (२००६). *विमुक्ता*, आकांक्षा प्रकाशन, नागपूर.
- ५) सवाणे, अरुणा (२०१०). *मुन्नी*, आकांक्षा प्रकाशन, नागपूर.
- ६) कादंबरीचे द्रष्टेपण (२०००), एस. एन. डी. टी. मुंबई चर्चासत्र.
- ७) यानप, किशोर (२०१२). *समकालीन स्त्रियांच्या कादंबऱ्या*, आकांक्षा प्रकाशन, नागपूर



# अक्षरवैदर्भी

ISSN -0976-0296



प्र. मणिष चौण्डे

वर्ष-४०

अंक-२

मे २०२३

प्रकाशन १ मे २०२३

## अंतरंग

लेख-

- सांविधानिक मूल्ये आणि ग्रामगीता-डॉ. योगिता पिंजरकर ९

शोधनिबंध-

- अर्जुन डांगळे यांच्या 'निळे अधोरेखित' मधील निखळ  
आणि प्रखर नोंदी-डॉ. गजानन बनसोड ३१

दोन कथा -

- बलिदान-प्रा. कृष्णकांत पराते १७  
■ जित्याची खोड...-सौ.अपर्णा विचोरे-आठल्ये ६२

अनुभवकथन-

- आम्हाला बेवारस सोडू नका नं मालक-डॉ. माधव जाधव ५१

प्रस्तावना-

- 'कोरोना संग्राम'-डॉ. सुभाष सावरकर ४५

दोन परीक्षणे -

- 'अभिनय चिंतन': तौलनिक अभ्यास भरतमुनी ते बर्टोल्ट ब्रेख्ट  
- प्रो.डॉ.शशिकान्त लोखंडे २७

- 'पद्मकोश': अपार वेदनेतून जगण्याचा सूर शोधण्याची धडपड  
- प्रा. मीनल येवले ४ ०

- 'धोंडी धोंडी पाणी दे' वऱ्हाडी कावयसंग्रह- विशाल मोहोड ५ ७

- 'डबल गेम' झाडीपट्टीतील जीवनाच्या लक्षवेधी कथा  
- रमेश नागेश सावंत ६७

अक्षरगंगेच्या काठी-

- 'अक्षरवैदर्भी': अंतर्यामी वसलेलं नाव- उमेश मोहिते ५

- चाळीशीची स्मृद्ध वाटचाल!-प्रा.व्यंकटेश वळसंगकर ८

अकरा कविता-

ओझं-सुरेश पाचकवडे (७) काही संदर्भ-नीळकंठ गोपाळ मेंढे (२५) भवसागर-  
प्रकाश आमले (२६) कोरी पाटी-नीलकृष्ण देशपांडे (१९) धाक-विनय मिरासे 'अशांत'  
(५५) जोतीबा/वज्रमूठ-निरंजन माधव/गारपीट-अय्युब पठाण लोहगावकर (५६)  
मही माय-धोंडीराम ध.राजपूत (६६) कसे भेटले लोक-नंदकुमार शेंडगे (६९) दिशा-  
संदीप निवृत्ती गवई/रवंथ श्रमाची-माला पारिसे (७०)



## अर्जुन डांगळे यांच्या 'निळे अधोरेखित' मधील निखळ आणि प्रखर नोंदी

डॉ. गजानन बनसोड

प्राध्यापक व मराठी विभागप्रमुख, विद्याभारती महाविद्यालय, अमरावती

आंबेडकरी परिवर्तनवादी विचारवंत लेखक म्हणून एकूणच मराठी साहित्याला अर्जुन डांगळे यांची ओळख आहे. त्यांचे व्यक्तित्व बहुआयामी असून कविता, कथा आणि अभ्यासपूर्ण वैचारिक लेखनातून स्वतःचा ठसा उमटविला आहे. साठोत्तरी पिढीतील मराठी साहित्याची कोंडी फोडण्याचे कार्य ज्या लेखकांनी केले त्यांमधील अर्जुन डांगळे हे महत्त्वपूर्ण नाव आहे. दलित साहित्याच्या पहिल्या फळीतील लेखक म्हणून त्यांची सर्वदूर ओळख आहे. 'छावणी हलते आहे' या कविता संग्रहात त्यांनी आंबेडकरी क्रांतीचे तत्त्वज्ञान मांडले आहे. डॉ. बाबासाहेब आंबेडकरांची चळवळ पुढे नेणारे ते कार्यकर्ते आहेत. पंथर या लढावू संघटनेच्या स्थापनेतही त्यांचा सहभाग होता. त्यांचे वडील उमाजी डांगळे हे त्यावेळच्या रिपब्लिकन चळवळीत असल्यामुळे समाजकार्याचे बाळकडू त्यांचा घरातच मिळाले. माटुंग्याच्या लेबर कॅम्पमध्ये त्यांचे बालपण गेले. हा परिसर रिपब्लिकन कार्यकर्त्यांच्या चळवळीचे प्रमुख केंद्र होते.

वडील उमाजी डांगळे रिपब्लिकन चळवळीत सक्रिय असल्यामुळे अण्णाभाऊ साठे, दादासाहेब गायकवाड, आचार्य अत्रे, बाबुराव बागूल अशा नेते आणि साहित्यिक-कलावंत मंडळीची त्यांच्या घरातच उठबस असे. तेव्हापासून आंबेडकरी चळवळीचे त्यांचे संबंध जुळत गेले. नंतरच्या काळात दलित पंथरचा लढा व दलित साहित्याची चळवळ यांत ते अग्रभागी होते. अखिल दलित साहित्याचे संपादन करण्याचे मोठे काम त्यांनी केले. त्यांनी संपादित केलेल्या 'पॉयझन्ड ब्रेड' या भारतीय दलित साहित्याच्या ग्रंथाची कीर्ती तर नेल्सन मंडेला यांच्यामार्फत पोहोचली आणि १९९८ साली जेव्हा अर्जुन डांगळे दक्षिण आफ्रिकेच्या दौऱ्यावर गेले तेव्हा मंडेला यांनी आत्मचरित्राची प्रत स्वाक्षरी करून डांगळे यांना भेट दिली. आंबेडकरी दलित साहित्य

चळवळीतही त्यांचे स्थान महत्त्वपूर्ण आहे.

अर्जुन डांगळे यांना उत्तम राजकीय भान आहे. त्यामुळे राज्यपातळीवर तिसऱ्या आघाडीचा समर्थ पर्याय उभा करण्यासाठी भारतीय बहुजन महासंघाच्या स्थापनेत त्यांनी प्रकाश आंबेडकरांच्या बरोबरीने वाटा उचलला. रामदास आठवले यांच्यासोबतही त्यांनी काम केले. समाजवादी, आंबेडकरवादी आणि कम्युनिस्ट तिन्ही विचारधारांतील कार्यकर्त्यांशी त्यांचे उत्तम जुळते मिळते होते.

अर्जुन डांगळे यांनी महाराष्ट्राच्या सामाजिक, साहित्यिक, सांस्कृतिक, राजकीय चळवळीत तीस वर्षांहून अधिक काळ सक्रिय सहभाग घेऊन कार्य केले आहे. त्यांचा 'छावणी हलते आहे' हा कवितासंग्रह, 'ही बांधावरची माणसं' हा कथासंग्रह, 'दलित विद्रोह', 'आंबेडकरी चळवळीचे अंतरंग' व 'मैदानातील माणसे', 'निळे अधोरेखित' इ. लेखसंग्रह प्रसिद्ध आहेत. त्यांनी काही ग्रंथांचे संपादन केले आहेत. त्यांमध्ये 'लोकशाहीर अण्णाभाऊ साठे : निवडक वाङ्मय', 'कर्मवीर दादासाहेब गायकवाड : काल आणि कर्तृत्व', 'डॉ. बाबसाहेब आंबेडकर : गौरव ग्रंथ', 'पायझन्ड ब्रेड' इ. ग्रंथ आहेत.

त्यांच्या, 'छावणी हलते आहे' कविता संग्रहास राज्य पुरस्कार मिळाला आहे. दिव्ही येथील प्रजासत्ताक दिनानिमित्ते आकाशवाणीवर होणाऱ्या राष्ट्रीय कवी संमेलनात १९७८ साली त्यांनी मराठीचे प्रतिनिधित्व केले आहे. संदर्भ ग्रंथ म्हणून अनेक विद्यापीठांतील अभ्यासक्रमांत त्यांच्या पुस्तकाचा वापर केला जातो. मुंबई मराठी साहित्य संघाच्या वतीने दिवंगत लालजी पेंडसे यांच्या नावाने दिला जाणारा 'समाजवादी विचारवंत' हा पुरस्कार त्यांना मिळाला आहे.

त्यांनी साने गुरुजी राष्ट्रीय स्मारक ट्रस्टचे अध्यक्ष म्हणून कार्य केले आहे, तसे महाराष्ट्र राज्य साहित्य संस्कृती मंडळामध्ये सदस्य म्हणून कार्य केले आहे.

अर्जुन डांगळे यांच्या 'निळे अधोरेखित' पुस्तकातील सर्व लेख प्रासंगिक असून विचारप्रवृत्त करणारे आहेत. समाज जीवनाची जाणीव ठेवून चिंतनशील मांडणी या लेखांत त्यांनी केली आहे. यातील लेख 'आपलं महानगर' मध्ये प्रकाशित झाले आहेत. समाजातील प्रश्नाला भिडण्याची वृत्ती त्यांची आहे. एका सच्च्या कार्यकर्त्यांच्या मनातील अस्वस्थता त्यांच्या लेखांत जाणवते. त्यासोबतच जागतिक पातळीवर अमणारे त्यांचे आकलन, सूक्ष्म पातळीवर असणारे समाज निरीक्षण या लेखांत पानोपानी जाणवते. समाजाला सजग करण्याची भूमिका त्यांच्या या लेखनामामे आहे.

'खाजगीकरण आणि राखीव जागा' या संदर्भात भाष्य करताना खाजगीकरण ही जागतिक अटळ आणि अपरिहार्य बाब आहे असे सांगितले. परंतु त्यासोबतच जागतिकीकरण आणि खाजगीकरणामुळे सर्वसामान्य मागासवर्गीय व दलितामध्ये काय परिणाम घडणार आहे? एकूणच समाज त्यामध्ये कसा भरडला जाणार आहे? पुन्हा एकदा उद्योग, कार्य आणि नोकरीच्या सर्व संधी कशा सवर्णीयांच्या हातात जाणार आहेत याबाबतचे निरीक्षण या लेखात अर्जुन डांगळे यांनी नोंदवले आहे. भविष्यात खाजगीकरणानंतर होणाऱ्या बदलावर सूचक भाष्य त्यांनी या लेखात केले आहे. 'सामाजिक विषमतेचा बळी ठरलेल्या दलिताना विशेषाधिकार म्हणून, सामाजिक न्यायाच्या नावाखाली ज्या राखीव जागेमुळे उपजिविकेचे साधन उपलब्ध झालेले आहे. त्या राखीव जागांच्या प्रश्नाची सोडवणूक जर समाधानकारक पद्धतीने झाली नाही तर या देशात चादवी शिवाय पर्याय नाही. याचे कारण असे की दलित, मध्यमवर्गीय समाजात शिक्षणाचे प्रमाण वाढत चाललेले आहे. त्याला आपल्या न्याय्य हक्काची जाणीव झालेली आहे. खाजगीकरणाच्या नावाने जर एक वेगळी सामाजिक विषमता उभी राहणार असेल तर ती कदापिही सहन केली जाणार नाही' (पृ. १३-१४) असे प्रखर भाष्य ते या लेखात करतात. दलितांनी राखीव जागांच्या कुबड्या फेकून घ्याव्यात असे बोलले जाते पण आज बौटावर मोजण्याइतक्या सुस्थितीतील दलितांचा अपवाद वगळता अजूनही फार मोठा वर्ग उपेक्षित आहे. शिवाय जागतिकीकरण होत असता हे धोरण राबविणारी मानसिकता उच्चवर्णीय भारतीयांचीच असेल तर? -हा प्रश्नही ते उपस्थित करतात. चिंतनशील वृत्तीने त्यांनी या लेखात खाजगीकरणाचा वेध घेतला आहे.

'निळे अधोरेखित' मधील दुसऱ्या लेखात 'आंबेडकरी चळवळीच्या अस्तित्वाला लागलेलं प्रश्नचिन्ह कोण मिटवणार?' असा सवाल त्यांनी केला आहे. गटागटाच्या तटबंदीमुळे आंबेडकरी ताकदीचे होत असलेले विभाजन पाहून ते अस्वस्थ होतात. आंबेडकरी चळवळीला पुढे न्यायचे असेल तर पुन्हा एकदा ही ताकद एकवटली पाहिजे. बुद्धीजीवी वर्गाने यासाठी एकदिलाने पुढाकार घेतला पाहिजे. आंबेडकरी चळवळीच्या अस्तित्वाला लागलेल्या प्रश्नचिन्हावर मात करण्याची जबाबदारी बुद्धिजीवी मध्यमवर्गाने स्वीकारावी असे मत अर्जुन डांगळे यांनी व्यक्त केले आहे.

ते म्हणतात, 'ज्या चळवळीला क्रांतिकारक नेता आहे आणि तत्त्वज्ञान



डॉ. बाबासाहेब आंबेडकरांच्या चळवळीमध्ये स्त्रियांनी कशाप्रकारे योगदान दिले; स्वतःच्या जीवाची तमा व बाळगता काळाराम मंदिर प्रवेशाच्या वेळी स्त्रियांनी कसा पुढाकार घेतला याची नोंद अर्जुन डांगळे यांनी, 'ज्यांनी इतिहास घडवला त्या भविष्यही घडवू शकतात' या लेखात घेतली आहे. १९३० साली नाशिकला कर्मवीर दादासाहेब गायकवाड यांच्या नेतृत्वाखाली जो प्रदीर्घ असा काळाराम मंदिराचा सत्याग्रह बाबासाहेबांच्या प्रेरणेने झाला, त्यातील स्त्रियांची कामगिरी फारच मोलाची आहे. काळाराम मंदिर सत्याग्रहातील पहिली तीस सत्याग्रहींची तुकडी ही स्त्रियांची होती. इतकेच काय, त्या परिसरात लावलेला प्रतिबंधक कायदा मोडल्यावरून दादासाहेब गायकवाड, अमृतराव रणखांबे, सावळाराम दाणी, हरिभाऊ जाधव, यांच्या बरोबर चौदा स्त्रियांच्या तुकडीलाही शिक्षा ठोठावली गेली. त्यात पा वली संभू काळे नावाची पंच्याहत्तर वर्षाची स्त्री होती. तिलाही पंधरा दिवसाची साधी कैद झाली होती. जवळजवळ चार वर्षे चाललेल्या या सत्याग्रहात सहभागी होणं, सत्याग्रहींची जेवणाखाण्याची व्यवस्था करणं, सत्याग्रहींना धीर देण अशी महत्त्वाची कामे महिलांनी केलेली आहेत.' (पृ.३४) आंबेडकरी चळवळीतील स्त्रियांचा गौरवशाली इतिहास मांडतांना ज्यांनी महाराष्ट्राभर चळवळीचे नेतृत्व केले त्या शांताबाई दाणी आणि मीराताई आंबेडकर यांचा गौरवपूर्ण उल्लेख त्यांनी केला आहे.

तथागत सिद्धार्थ बुद्धांनी, 'बहुजन हिताय बहुजन सुखाय' असा संदेश दिला. पण आज सत्तेच्या राजकारणात 'बहुजन' या शब्दाला नवनव्यां भूलभुल्लय घेले आहे. त्याची पोलखोल 'बहुजनवादः किती वास्तव, किती भ्रामक' या लेख अर्जुन डांगळे यांनी केली आहे. बहुजनवादाविषयी वास्तववादी कोणातून लेखात त्यांनी प्रदीर्घ विवेचन केले आहे.

डॉ. बाबासाहेब आंबेडकर यांच्या सार्वजनिक जीवनात असलेले स्थान त्यांनी एका लेखात मांडले आहे. त्यांच्या सामाजिक सेवांकांची सुरवात, स्वतंत्र मजूर पक्षाची स्थापना, पीपल्स एज्युकेशन सोसायटीची स्थापना, मुंबईच्या मणिभवनातील डॉ. बाबासाहेब आंबेडकर व गांधीजी यांच्या इतिहासातील सर्वात मोठी अंत्ययात्रा, डॉ. बाबासाहेब आंबेडकरांचा आठवणीना या लेखात त्यांनी उजाळा दिला आहे.

साहित्यिक आणि विचारवंताची सामाजिक बांधिलकी तसेच समाजाला दिशा देण्यासाठी त्यांनी पुढाकार घ्यायला

डॉ. बाबासाहेब आंबेडकरांच्या चळवळीमध्ये स्त्रियांनी कशाप्रकारे योगदान दिले; स्वतःच्या जीवाची तमा व बाळगता काळाराम मंदिर प्रवेशाच्या वेळी स्त्रियांनी कसा पुढाकार घेतला याची नोंद अर्जुन डांगळे यांनी, 'ज्यांनी इतिहास घडवला त्या भविष्यही घडवू शकतात' या लेखात घेतली आहे. १९३० साली नाशिकला कर्मवीर दादासाहेब गायकवाड यांच्या नेतृत्वाखाली जो प्रदीर्घ असा काळाराम मंदिराचा सत्याग्रह बाबासाहेबांच्या प्रेरणेने झाला, त्यातील स्त्रियांची कामगिरी फारच मोलाची आहे. काळाराम मंदिर सत्याग्रहातील पहिली तीस सत्याग्रहींची तुकडी ही स्त्रियांची होती. इतकेच काय, त्या परिसरात लावलेला प्रतिबंधक कायदा मोडल्यावरून दादासाहेब गायकवाड, अमृतराव रणखांबे, सावळाराम दाणी, हरिभाऊ जाधव, यांच्या बरोबर चौदा स्त्रियांच्या तुकडीलाही शिक्षा ठोठावली गेली. त्यात पा वली संभू काळे नावाची पंच्याहत्तर वर्षांची स्त्री होती. तिलाही पंधरा दिवसाची साधी कैद झाली होती. जवळजवळ चार वर्षे चाललेल्या या सत्याग्रहात सहभागी होणं, सत्याग्रहींची जेवणाखाण्याची व्यवस्था करणं, सत्याग्रहींना धीर देण अशी महत्त्वाची कामे महिलांनी केलेली आहेत.' (पृ. ३४) आंबेडकरी चळवळीतील स्त्रियांचा गौरवशाली इतिहास मांडतांना ज्यांनी महाराष्ट्राभर चळवळीचे नेतृत्व केले त्या शांताबाई दाणी आणि मोरताई आंबेडकर यांचा गौरवपूर्ण उल्लेख त्यांनी केला आहे.

तथागत सिद्धार्थ बुद्धांनी, 'बहुजन हिताय बहुजन सुखाय' असा संदेश दिला. पण आज सत्तेच्या राजकारणात 'बहुजन' या शब्दाला नवनव्यां भूलभुल्लुप्याने घेरले आहे. त्याची पोलखोल 'बहुजनवादः किती वास्तव, किती भ्रामक' या लेखात अर्जुन डांगळे यांनी केली आहे. बहुजनवादाविषयी वास्तववादी दृष्टिकोणातून या लेखात त्यांनी प्रदीर्घ विवेचन केले आहे.

डॉ. बाबासाहेब आंबेडकर यांच्या सार्वजनिक जीवनात मुंबईचे असलेले स्थान त्यांनी एका लेखात मांडले आहे. त्यांच्या सामाजिक संस्था, साप्ताहिकांची सुरवात, स्वतंत्र मजूर पक्षाची स्थापना, पीपल्स एज्युकेशन सोसायटीची स्थापना, मुंबईच्या मणिभवनातील डॉ. बाबासाहेब आंबेडकर व गांधीजी यांची भेट, मुंबईच्या इतिहासातील सर्वात मोठी अंत्ययात्रा, डॉ. बाबासाहेब आंबेडकरांच्या संदर्भातील सर्व आठवणींना या लेखात त्यांनी उजाळा दिला आहे.

साहित्यिक आणि विचारवंताची सामाजिक बांधिलकी असायला हवी; तसेच समाजाला दिशा देण्यासाठी त्यांनी पुढाकार घ्यायला हवा. समाज ज्यांच्याकडे

आस्थेने पाहतो त्यांनी आपली जबाबदारी स्वीकारायला हवी- असे मत अर्जुन डांगळे यांनी आपल्या लेखात व्यक्त केले आहे. 'विचारवंताची सामाजिक बांधिलकी प्रतिपादन करत असताना त्यांनी मी दलित, विद्रोही, पुरोगामी कवीच्या पातळीवर नेऊन बसवू इच्छित नाही; काहीतर काल्पनिक, भव्य दिव्य लढावू लिखाण करावं अस मला मुळीच वाटत नाही. पण चळवळीला दिशा देणारं, चळवळीचे आदर्श जपणारं लिखाण व्हावं, ही अपेक्षा बाळगल्यास त्यात वावणं ठरू नये' (पृ. ६५) असे मांडले आहे. तसेच साहित्यिकांनी वास्तववादी लिखाण करावं; विचारवंतांनी विज्ञानवादी दृष्टिकोनातून आपला विचार समाजापुढे ठेवावा ही सार्थ अपेक्षा व्यक्त केली आहे.

'निळी पहाट' ही समस्त आंबेडकरी चळवळीतील साहित्यिक कवी, कलावंत आणि कार्यकर्त्यांना आवडणारी प्रतिमा आहे. त्या विषयीचे विवेचन अर्जुन डांगळे यांनी एका लेखात केले आहे. दलित साहित्याने मराठी साहित्याला संपन्न आणि समृद्ध केले आहे. नवे अनुभवविश्व, नवीन अभिव्यक्ती, नवी भाषा घेऊन हे साहित्य वाड्मयाच्या प्रांतात दाखल झाले. यासोबतच नव्या सौंदर्य/समीक्षा शास्त्रासोबत, नव्या शब्दकोषाची आणि परिवर्तनवादी मानसिकतेची गरज दलित साहित्य चळवळीने समोर आणली नवीन प्रतिमाविश्व दलित, आंबेडकरी चळवळीतील लेखकांनी मराठी साहित्यामध्ये आणलं. त्याविषयी सखोल चिंतनपर मांडणी डांगळे यांनी केली आहे.

संपूर्ण समाजाला गतिमान आणि कार्यशील करण्यासाठी, 'निळे अधोरेखित' मधील वेगवेगळ्या लेखातून डांगळे यांनी चिंतनगर्भ लिखाण केले आहे. बदलत्या काळात, केवळ राजकीय नाही तर वैचारिक आघाडीची आवश्यकता ते व्यक्त करतात. त्या संदर्भात आपल्या हळव्या कवीमनाने ते साद घालतात.

'एकाच गावाला निघालेले हे वाटसरू

वेगवेगळ्या वाटांनीच गेले आहेत दूरदूर

खूप दूर खूप दूर, त्यांना मी आता कसा पकारू

कुठचा बर्मनदा, करील का संगीतबद्ध माझी हुरहूर' (पृ. ७४)

बदलत्या काळात राजकीय भान देणाऱ्या या ओळी आहेत. प्रतिगाम्यांना पराभूत करण्यासाठी फक्त राजकीय नाही तर वैचारिक एकवाक्यता असणाऱ्या आघाडीची गरज ते व्यक्त करतात.

'राखीव जागा: उमाळे उसासे नकोत; नवी रणनिती हवी'- या लेखात अर्जुन डांगळे म्हणतात की, 'राखीव जागांचं धोरण म्हणजे समाजातील दडपल्या



अभ्यासक यांना आत्मचिंतन करावना लावणाने आहे. त्या मज्जेचा बाबंकातपणे  
 नसूनच या लेखन प्रसंगाने जाणवते. मनाचाकडे गहन्याचा मनाच्याकडे निमित्त,  
 निकोप, व्यापक व सर्वसमावेश दृष्टिकोन आहे. हेही लक्षात घेते. 'निळे अधोरेखित'  
 मधील लेखांत कुणाविषयी कटुता नसून वास्तववादी नोंदी वेळवेळा स्थानी येऊन  
 आहेत. मूल्यमान असणाऱ्या विचारवंत लेखकांचे हे मनागुही चिंतन आहे.

संदर्भ -

- (१) निळे अधोरेखित - अरुण डंगरे, सहित प्रकाशन, कोल्हापूर, पुणे ३, आ. अंकित. २००५.  
 (२) कुळकर्णी गो.म./ पुंडलिक विद्यालय : दलित साहित्य : एक साम्प्रदायिक अभ्यास, पुणे  
 प्रकाशन पुणे, प्र. आ. १९९४. (३) कुळकर्णी व. वि. मराठी साहित्य : विमर्श आणि विमर्शक,  
 नंदगंधा प्रकाशन पुणे, प्र. आ. २००१. (४) अंतर्गत नानाव : साहित्याचा अन्वयार्थ, मेरु  
 पब्लिशिंग हाऊस, पुणे, प्र. आ. १९९६. (५) खरत संकाय : दलित साहित्य : ज्ञान आणि  
 प्रवृत्ती, इनामदार बंधू प्रकाशन, पुणे, प्र. आ. १९७८. (६) बाबू ए. ए. निळी मराठी प्रकाशन  
 नाट्याच्या मंडळ, वाई, प्र. आ. १९७८.



## कोरी पाटी

होय बुद्धीचाच जेव्हा, कोर करकरीत पाटी  
 घडू होती वा मनाच्या, आठल्या त्या जोगी पाटी॥-  
 वाटते घडते इथे, काही जगाहून वेगळे।  
 चांगलेही टोचते, का हीच आहे जगहाट?॥-  
 तुषारतां द्वारे जरी गंगाहि आली आपसुका।  
 नृगजळाचा भास म्हणुनो कां उगा करता हाकाटो?॥-  
 दानवंताचीहि निंदा गरजवंताच्याच ओठी  
 धमिक धंडाचेहि दिसते पोट गेलेले खपाटी॥-  
 चालवांती वारसा जे अंध गांधारी-कृपेचा।  
 त्यांस वाटे डोळेसांचे विश्व जन्म अनुल्याच पाटी॥-  
 स्वार्थ पुला पोसताना रीत-नीती टांगणीला।  
 साळसूदाच्या सभेला संधिसाधूंचाच दाटी॥-  
 -नीलकृष्ण देशपांडे  
 पोहंडुळ (पुस्तक), वि. बबठनाळ-४३५२०४

नेलेल्या विषयतेचे-मग ती आर्थिक किंवा सामाजिक असो, बळी ठरलेल्या जनसमूहांना विशेष संधी होय' फुले-शाहूंनी मांडलेली ही भूमिका सार्वत्रिक पातळीवर बाबासाहेब आंबेडकरांनी अधिक प्रखर केली (पृ.७८) असे सांगतात. त्यासोबतच सत्ताधान्यांना उखाडून घेण्यासाठी राखीव जागा भरताना सर्वांना समान संधी मिळाली पाहिजे. उखाडून घेण्यासाठी राखीव जागा म्हणजे उपेक्षित, वंचितांना त्यांच्या शैक्षणिक, अर्थी भूमिका ते घेतात. राखीव जागा म्हणजे उपेक्षित, वंचितांना त्यांच्या शैक्षणिक, अर्थी भूमिका ते घेतात. राखीव जागा म्हणजे उपेक्षित, वंचितांना त्यांच्या शैक्षणिक, सामाजिक उत्कर्षासाठी दिली गेलेली संधी आहे असे त्यांना वाटते. यासाठी दलितांनी आपल्यामधील अंतर्विरोध मिटवून एकजुटीने राहण्याची आवश्यकता त्यांनी प्रतिपादन केली आहे.

धर्माच्या नावावर राजकीय फायदा उठवणाऱ्यांना भारतीय जनतेने राजकारणातून उठवलं पाहिजे, तर देशाला भवितव्य आहे. राजकारण्यांनी आतंकवादाला आश्रय दिला असं निरीक्षण 'आतंकवाद: राष्ट्रीय प्रश्न' या लेखात ते नोंदवितात.

'गांधी-आंबेडकर: वैचारिक समन्वय अधोरेखित झाला पाहिजे' या लेखात विवेचन करताना गांधी-आंबेडकर यांमध्ये वैचारिक संघर्ष होता ही बाब आपण कायम मानली तरी दोघांमध्ये नैतिकता होती ती जशी व्यक्तिगत जीवनात दोघांनीही जोपासली तशी सार्वजनिक आयुष्यात देखील जोपासली. माणसाला माणूस म्हणून प्रतिष्ठा मिळाली पाहिजे : जाती, धर्म, लिंग, पंथांच्या आधारे ती उद्ध्वस्त केली जाता कामा नये- या मूल्यांवर ह्या दोघांचाही ठाम विश्वास होता. हेच मूल्य आता उद्ध्वस्त केलं जात असताना गांधी-आंबेडकर संघर्षाचा बाऊ करण्यात काय हंशील आहे? उलट या दोघांतील वैचारिक समन्वय अधोरेखित झाला पाहिजे असे डांगळे यांना वाटते आणि ती आजच्या काळाची गरज आहे.

'निळे अधोरेखित' मधील 'शिवधर्माची स्थापना वैदिक ब्राह्मणी वर्चस्वाला हारदा', 'सहा डिसेंबर', 'खूप झालं आता कामाला लागू या!', 'आंबेडकरी विचारांचं पावर हाउस उभारलं पाहिजे', 'डॉ. आंबेडकरांची भाषणे: वैचारिक प्रबोधनाची दिशा' या काही लेखांतून समाजप्रबोधनाचे कार्य त्यांनी केले आहे. आंबेडकरी चळवळीचा चिंतनशील सखोल अभ्यास अर्जुन डांगळे यांनी केला आहे. इतकेच नव्हे तर ते स्वतः चळवळ जगले, परिवर्तनवादी चळवळीला (पंथरला) मार्गदर्शन केले. रिपब्लिकन चळवळीला सर्वसमावेशक करण्यासाठी ते आयुष्यभर प्रयत्नशील राहिले. म्हणूनच 'निळे अधोरेखित' मधील अर्जुन डांगळे यांचे सर्वच लेख विचारप्रवृत्त करणारे आहेत. आंबेडकरी चळवळीला गतिमान करण्यासाठी ऊर्जा देणारे आहेत. नेते, कार्यकर्ते,

अभ्यासक यांना आत्मचिंतन करायला लावणारे आहेत. एका सच्च्या कार्यकर्त्याची तळमळ या लेखन प्रपंचात जाणवते. समाजाकडे पाहण्याचा त्यांच्याकडे निर्मळ, निकोप, व्यापक व सर्वसमावेश दृष्टिकोन आहे, हेही लक्षात येते. 'निळे अधोरेखित' मधील लेखांत कुणाविषयी कटुता नसून वास्तववादी नोंदी तेवढ्या त्यांनी घेतल्या आहेत. मूल्यमान असणाऱ्या विचारवंत लेखकाचे हे मर्मग्राही चिंतन आहे.

संदर्भ -

- (१) निळे अधोरेखित - अर्जुन डांगळे, सहित प्रकाशन, गोरगाव, मुंबई प्र.आ.ऑक्टो. २००५.
- (२) कुळकर्णी गो.म./ पुंडलिक विद्याधर : दलित साहित्य : एक सांस्कृतिक अभ्यास, सुगावा प्रकाशन पुणे, प्र. आ. १९९४. (३) कुळकर्णी व. दि. मराठी साहित्य : विमर्श आणि विमर्शक, पद्मगंधा प्रकाशन पुणे, प्र. आ. २००१. (४) कोत्तापळे नागनाथ : साहित्याचा अन्वयार्थ, मेहता पब्लिशिंग हाउस, पुणे, प्र. आ. १९९६. (५) खरात शंकरराव : दलित वाङ्मय : प्रेरणा आणि प्रवृत्ती, इनमदार बंधू प्रकाशन, पुणे, प्र. आ. १९७८. (६) जाधव रा. ग. निळी पहाट, प्रज्ञा पाठशाळा मंडळ, वार्ड, प्र. आ. १९७८.



## कोरी पाटी

होय बुद्धीचीच जेव्हा, कोर करकरीत पाटी।  
घट्ट होती या मनाच्या, आतल्या त्या जीर्ण गाठी॥-

वाटते घडते इथे, काही जगाहून वेगळे।  
चांगलेही टोचते, का हीच आहे जगरहाटी?॥-

तुषार्ता द्वारी जरी गंगाहि आली आपसुक।  
मृगजळाचा भास म्हणुनी कां उगा करता हाकाटी?॥-

दानवंताचीहि निंदा गरजवंताच्याच ओठी  
धनिक धेंडाचेहि दिसते पोट गेलेले खपाटी॥-

चालवीती वारसा जे अंध गांधारी-कृपेचा।  
त्यांस वाटे डोळेसांचे विश्व जणु अपुल्याच पाठी॥-

स्वार्थ पुला पोसताना रीत-नीती टांगणीला।  
साळसूदाच्या सभेला संधिसाधूंचीच दाटी॥-

-नीलकृष्ण देशपांडे  
पोहंडुळ (पुसद), जि.यवतमाळ-४४५२०४

गेलेल्या विषयतेचे-मग ती आर्थिक किंवा सामाजिक असो, बळी ठरलेल्या जनसमूहांना विशेष संधी होय' फुले-शाहूंनी मांडलेली ही भूमिका सार्वत्रिक पातळीवर बाबासाहेब आंबेडकरांनी अधिक प्रखर केली (पृ.७८) असे सांगतात. त्यासोबतच सत्ताध्याऱ्यांना खडा सवाल करताना राखीव जागा भरताना सर्वांना समान संधी मिळाली पाहिजे. अशी भूमिका ते घेतात. राखीव जागा म्हणजे उपेक्षित, वंचितांना त्यांच्या शैक्षणिक, सामाजिक उत्कर्षासाठी दिली गेलेली संधी आहे असे त्यांना वाटते. यासाठी दलितांनी आपल्यामधील अंतर्विरोध मिटवून एकजुटीने राहण्याची आवश्यकता त्यांनी प्रतिपादन केली आहे.

घर्मांच्या नावावर राजकीय फायदा उठवणाऱ्यांना भारतीय जनतेने राजकारणातून उठवून पाहिजे, तर देशाला भवितव्य आहे. राजकारण्यांनी आतंकवादाला आश्रय दिला असं निरीक्षण 'आतंकवाद: राष्ट्रीय प्रश्न' या लेखात ते नोंदवितात.

'गांधी-आंबेडकर: वैचारिक समन्वय अधोरेखित झाला पाहिजे' या लेखात विवेचन करताना गांधी-आंबेडकर यांमध्ये वैचारिक संघर्ष होता ही बाब आपण कायम मानली तरी दोघांमध्ये नैतिकता होती ती जशी व्यक्तिगत जीवनात दोघांनीही जोपासली तशी सार्वजनिक आयुष्यात देखील जोपासली. माणसाला माणूस म्हणून प्रतिष्ठा मिळाली पाहिजे : जाती, धर्म, लिंग, पंथांच्या आधारे ती उद्ध्वस्त केली जाता कामा नये- या मूल्यांवर ह्या दोघांचाही ठाम विश्वास होता. हेच मूल्य आता उद्ध्वस्त केलं जात असताना गांधी-आंबेडकर संघर्षाचा बाऊ करण्यात काय हंशील आहे? उलट या दोघांतील वैचारिक समन्वय अधोरेखित झाला पाहिजे असे डांगळे यांना वाटते आणि ती आजच्या काळाची गरज आहे.

'निळे अधोरेखित' मधील 'शिवधर्माची स्थापना वैदिक ब्राह्मणी वर्चस्वाला हार्दरा', 'सहा डिसेंबर', 'खूप झालं आता कामाला लागू या!', 'आंबेडकरी विचारांचं पावर हाउस उभारलं पाहिजे', 'डॉ. आंबेडकरांची भाषणे: वैचारिक प्रबोधनाची दिशा' या काही लेखांतून समाजप्रबोधनाचे कार्य त्यांनी केले आहे. आंबेडकरी चळवळीचा चिंतनशील सखोल अभ्यास अर्जुन डांगळे यांनी केला आहे. इतकेच नव्हे तर ते स्वतः चळवळ जगले, परिवर्तनवादी चळवळीला (पंथरला) मार्गदर्शन केले. रिपब्लिकन चळवळीला सर्वसमावेशक करण्यासाठी ते आयुष्यभर प्रयत्नशील राहिले. म्हणूनच 'निळे अधोरेखित' मधील अर्जुन डांगळे यांचे सर्वच लेख विचारप्रवृत्त करणारे आहेत. आंबेडकरी चळवळीला गतिमान करण्यासाठी ऊर्जा देणारे आहेत. नेते, कार्यकर्ते,

अभ्यासक यांना आत्मचिंतन करायला लावणारे आहेत. एका सच्च्या कार्यकर्त्याची तळमळ या लेखन प्रपंचात जाणवते. समाजाकडे पाहण्याचा त्यांच्याकडे निर्मळ, निकोप, व्यापक व सर्वसमावेश दृष्टिकोन आहे, हेही लक्षात येते. 'निळे अधोरेखित' मधील लेखांत कुणाविषयी कटुता नसून वास्तववादी नोंदी तेवढ्या त्यांनी घेतल्या आहेत. मूल्यभान असणाऱ्या विचारवंत लेखकाचे हे मर्मग्राही चिंतन आहे.

संदर्भ -

- (१) निळे अधोरेखित - अर्जुन डांगळे, सहित प्रकाशन, गोरगाव, मुंबई प्र.आ.ऑक्टो. २००५.
- (२) कुळकर्णी गो.म./ पुंडलिक विद्याधर : दलित साहित्य : एक सांस्कृतिक अभ्यास, सुगावा प्रकाशन पुणे, प्र. आ. १९९४. (३) कुळकर्णी व. दि. मराठी साहित्य : विमर्श आणि विमर्शक, पद्मगंधा प्रकाशन पुणे, प्र. आ. २००१. (४) कोत्तापल्ले नागनाथ : साहित्याचा अन्वयार्थ, मेहता पब्लिशिंग हाउस, पुणे, प्र. आ. १९९६. (५) खरात शंकरराव : दलित वाङ्मय : प्रेरणा आणि प्रवृत्ती, इनामदार बंधू प्रकाशन, पुणे, प्र. आ. १९७८. (६) जाधव रा. ग. निळी पहाट, प्रज्ञा पाठशाळा मंडळ, वाई, प्र. आ. १९७८.

■ ■ ■

## कोरी पाटी

होय बुद्धीचीच जेव्हा, कोर करकरीत पाटी।  
घट्ट होती या मनाच्या, आतल्या त्या जीर्ण गाठी।।-

वाटते घडते इथे, काही जगाहून वेगळे।  
चांगलेही टोचते, का हीच आहे जगरहाटी?।।-

तुषार्ता द्वारी जरी गंगाहि आली आपसुक।  
मृगजळाचा भास म्हणुनी कां उगा करता हाकाटी?।।-

दानवंताचीहि निंदा गरजवंताच्याच ओठी  
धनिक घेंडाचेहि दिसते पोट गेलेले खपाटी।।-

चालवीती वारसा जे अंध गांधारी-कृपेचा।  
त्यांस वाटे डोळेसांचे विश्व जणु अपुल्याच पाटी।।-

स्वार्थ पुला पोसताना रीत-नीती टांगणीला।  
साळसूदाच्या सभेला संधिसाधूंचीच दाटी।।-

-नीलकृष्ण देशपांडे  
पोहंडळ (पुसद), जि.यवतमाळ-४४५२०४

# अजोध्या

ISSN-2249-3034  
UGC CARE Listed Journal

वर्ष १७ वे / अंक २ रा / एप्रिल/मे/जून - २०२३





UGC CARE Listed Journal

ISSN-2249-3034

सर्व साहित्य व कला प्रवाहांना वाहिलेले नियतकालिक  
वर्ष १७ वे । अंक दुसरा। एप्रिल-मे-जून -२०२३

संपादकिय -

लेख -

व्हिंसेंट व्हॅन गॉग आणि सुनील यावलीकर :

दुःखानुभूतीचे सृजनशील अनुबंध - डॉ. अजय देशपांडे/०१

एक मनस्वी चित्रकार : व्हर्मीर - विनया मगरे सहस्त्रबुद्धे/०५

देवानंद गोरडे यांची कविता - सुरेश आकोटकर /०८

अज्ञातवास : सर्जनशील चित्रलिपी/डॉ. मोना चिमोटे/२०

कथा -

डोळ्यात उतरलेला येशू - महावीर जोंधळे/३१

ग्रंथचर्चा -

वर्तमान वास्तवाला भिडणारी कादंबरी- डॉ. वासुदेव मुलाटे/३५

विन चेहऱ्याचे कभिन्न तुकडे - सारिका उबाळे/३८

सूर्याकळानंतरच्या कविता - डॉ. गजानन बनसोड/४१

मुखपृष्ठ - Girl with Pearl earring चित्र जगप्रसिध्द डच चित्रकार योहानेस  
व्हर्मीर (इंटरनेटवरून साभार)

साहित्य पाठविण्याचा पत्ता :

डॉ. अजय देशपांडे, मराठी भाषा व साहित्य विभाग

लोकमान्य टिळक महाविद्यालय, वणी, जि. यवतमाळ ४४५ ३०४

ध्रमणध्वनी- 9850593030 E-mail : deshpandeajay15@gmail.com

अक्षरजुळवणी व मुद्रण :

पूजा कॉम्प्युटर्स , मोतीनगर, अमरावती. मो. 9370616276

E-mail Id : rajeshdeulkar111@gmail.com

\* या अंकात व्यक्त झालेल्या मतांशी संपादक मंडळ सहमत असेलच असे नाही.

# स्मृतीशेष गणेश टाले यांच्या सूर्यकळानंतरच्या कविता

डॉ. गजानन बनसोड

सूर्यकळानंतरच्या कवितासंग्रहात एकूण ५९ कविता आहेत. या कवितेचे आकलन आणि अवलोकन करताना यातील बऱ्याचशा कविता सामाजिक जाणिवंच्याच आहेत. राजकारण, धर्मकारण, समाजकारण व समाजातील दांभिकतेवर त्यांनी आपल्या कवितेतून परखड समाचार घेतला आहे. या कवितेला अत्यंत अभ्यासपूर्ण अशी प्राचार्य डॉ. अशोक पळवेकर यांची प्रस्तावना आहे. या पुस्तकाला अत्यंत देखणा आकार देणाऱ्या मुक्ता प्रकाशनाच्या प्रकाशक सारिका उबाळे यांनी या पुस्तकाचा दर्जा वाढविला आहे.

सूर्यकळानंतरच्या कवितांमध्ये महात्मा ज्योतिबा फुले, क्रांतीमा सावित्रीबाई, डॉ. बाबासाहेब आंबेडकर यांच्या विषयी अपार कृतज्ञता व्यक्त केली आहे. १९५६ च्या धम्मदीक्षेच्या मूल्यांतरानंतर नवशिक्षित आणि नव दीक्षित झालेल्या बौद्ध तरुणांनी डॉ. बाबासाहेब आंबेडकर यांचे विचारकार्य आणि चळवळीच्या प्रेरणा घेऊन आपल्या हातातील लेखणीला तलवारीची धार देऊन आपले जीवनानुभव मांडायला सुरूवात केली. पहिल्यांदा आपल्या मनातील उद्वेग आंबेडकरी विचाराने झपाटलेल्या कवींनी काव्यातून मांडला. समाजातील जातवास्तवाचे, जन्मावरून लादलेल्या दुःखाचे अनेक संदर्भ कवी नामदेव ढसाळ आणि त्यांच्या समकालीन आंबेडकरी कवींच्या काव्यात सापडतात.

सूर्यकळानंतरच्या कविता अभ्यासताना गणेश टाले यांनी सामाजिक दृष्टिकोन आणि वैश्विक भान जपलेले जाणवते. आंबेडकरी कवितेतील सामाजिक जाण त्यांनी जपलेली आहे. एक पत्र बाबासाहेबांना या कवितेत ते म्हणतात,

बाबासाहेब

आपली चळवळ आता वळवळ झालीय

कुणाचं खेटर नाही कुणाच्या पायात

नेतेही सारे लेचेपेचे झालेत बाबासाहेब

दुसऱ्या एका बाबासाहेब या शीर्षकाच्याच कवितेमध्ये ते म्हणतात,

बाबासाहेब

मी नवीन घर बांधले  
 पण माझा मुलगा उत्कर्ष  
 घराच्या सर्व भिंतीवर  
 अक्षर गिरवायला लागला  
 काल तर त्याने कमांलच केली  
 चक्क भिंतीवर  
 जा आणि आपापल्या घराच्या भिंतीवर  
 लिहून ठेवा की आपल्याला शासनकर्ती  
 जमात बनायचे आहे.

या दोन्ही कवितेमध्ये त्यांची चिंतनशीलता जाणवते. नेत्यांचा बेगडीपणा, त्यांचे दुष्टप्रीधीरण, यामुळे भरकटलेला समाज वावर ते मुक्तपणे भाष्य करतात. मोर्चा आंदोलन संघर्ष करणारा नेताच प्रस्थापित लोकांच्या मांडीवर जाऊन बसला आणि त्यांची भाटगिरी करायला लागला तर चळवळीची कशी दुर्दशा होते हे ते बाबासाहेबांना अत्यंतिक भावनाशील होऊन सांगतात. कवी गणेश टाले यांनी मानवाच्या कल्याणासाठी झटणाऱ्या महामानवाविषयी आपल्या कवितेतून आदरभाव व्यक्त केला आहे. तथागत सिद्धार्थ गौतम बुद्ध, महामानव डॉ. बाबासाहेब आंबेडकर, महात्मा ज्योतिबा फुले, क्रांतीज्योती सावित्रीबाई फुले यांच्या विषयी आपल्या कवितेतून अंतःकरणपूर्वक आदरभाव व्यक्त करतात. या कवितासंग्रहामध्ये एकूण सहा कविता बाबासाहेबांच्या चळवळीची, कार्याची, संघर्षाची आंदोलनाची महिमा सांगणाऱ्या आहेत. त्यांच्याचमुळे आज आपण सन्मानाचे जीवन जगतो याची जाणीव या कवीला पदोपदी होते.

गणेश टाले यांचे मन गाव शिवारात, शेतीमातीत रमणारे आहे. कष्टकरी माणसाबद्दल त्यांची अपार आस्था आहे. आपल्या गावची नोंद ते कवितेतून घेतात.

गावात माणसे साधी  
 नात्यात शोधती नाती  
 घरात पडला पेव  
 नाही बुजविण्या माती

बदलत्या गाव खेड्यांचं वर्णन करताना, विकासाच्या नावावर गाव भकास होताना ते पाहतात. आज गावाची संपूर्ण रया गेलेली त्यांना जाणवते म्हणूनच ते कशी वाजेल गा

धूनमध्ये म्हणतात.

खाचर गेलं  
 दमनी गेली  
 गेली पायटांगी

विकासाच्या पाठीवर, खेकड्यांची नांगी

गाव शिवाराशी असलेलं त्याचं सलोख्याचं नातं आहे. गाव, गोटाण अशा कितीतरी कवितेतून ते नाते अधोरेखित होते.

कवी गणेश टाले यांनी आपल्या कवितेमध्ये सरळ साधी व व्यवहारातील लोकभाषा वापरली आहे. वऱ्हाडीचाही ते सुंदर वापर करतात. प्रतिमा, प्रतीके, अलंकार याचा फारसा सोस त्यांच्या कवितेला नाही. कविता म्हणजे त्यांचा एकेक विचार आहे. तो सामान्यातील सामान्य माणसाला समजावा इतकेच या कवीला वाटते. शब्दांची नक्षीदार मांडणी ते आपल्या कवितेत करतात. आदरणीय कविवर्य डॉ. सुखदेव ढाणके यांच्या सहवास त्यांना लाभल्यामुळे कवितेमधील शब्द कसे जपून, तोलून, मोजून वापरवे त्या शब्दांची जातकुळी कोणती हे कवीला ज्ञात आहे. आशयाच्या अंगाने गणेश टाले यांचा कवितेमध्ये गहनता आहे. मुक्तछंद, अभंगवृत्त, गीत इत्यादी प्रकारात त्यांची रचना आहे. ते स्वतःला आंबेडकरी अनुयायी म्हणून घेतात आणि एका कार्यकर्त्यांच्या भूमिकेतून आपल्या समाजातील वैगुण्य ते मांडतात. आपल्या जीवनातील दुःखाचे अभंग गाताना ते म्हणतात,

गर्द काळोखाच्या राती

प्राण भाकरीचा गेला

भूक पोटाला मुकली

पूर आसवांचा आला

तर भाकर या शीर्षकाच्या वेगळ्या एका कवितेत कवी म्हणतो,

भूकच भाकर

भाकरीत भूक

कळो आली चूक

माणसाला

गणेश टाले यांनी अत्यंत सुंदर पद्धतीने भाकरी ही प्रतिमा मानवी जाणिवेशी कशी

संबंधित आहे ते वेगवेगळ्या कवितांतून उलगडून दाखविले आहे. जो माणूस अभावग्रस्त आहे, ज्याने उपास तापास सोसून स्वतःला घडवले आहे, अशा माणसाच्या जीवनात भाकरीचं काय महात्म्य आहे ते त्यांनी भाकर एक, भाकर दोन, भाकरी आणि गोवरी या कवितेतून उलगडून दाखविले आहे. गद्यात्मक शैलीत भाकरीचा प्रवास कुठून कधी केव्हा सुरू झाला हे सांगता येत नाही परंतु विकासाच्या एका टप्प्यावर केव्हातरी माणसाला भाकर गवसली असावी तेव्हापासून वीतभर पोटासाठी, चतकोर भाकरीसाठी संघर्ष सुरू आहे असे कवीला वाटते.

सर्येकळानंतरच्या कवितेमधील कळस म्हणजे बापाच्या कविता. या संपूर्ण कविता संग्रहात दहा कवितेतून कवींनी बापाच्या जीवनाचे त्याच्या कष्टाचे त्याच्या सुखदुःखाचे वर्णन केले आहे.

माझा बाप आज

मातीला गहाण

पायाची वहान

पायातच

बापाच्या कष्टाची जाणीव कवीला आहेच म्हणून पुढे कवितेत तो म्हणतो,

रक्त आटवून

छातीवर गोटा

यासाठीच भेटा

वावरात

किंवा,

बाप मरायाचा रोज

वावरांत कणकण

स्वप्न पेरायचा तरी

आयुष्याची वणवण

यात या कवितेच्या माध्यमातून आपल्या बापाच्या कष्टाची जाणीव अनेक कवितेतून कवीने अधोरेखित केली आहे. या कवितासंग्रहातील बापाची कविता हा स्वतंत्रपणे अभ्यासाचा विषय आहे. अत्यंत ताकदीने बापासंबंधी आपल्या मनातील भावभावना उत्कटपणे कवीने या कवितेतून नोंदवल्या आहेत. बाप म्हणजे काय याची संपूर्ण उकल

कवीने एका कवितेतूनच केली आहे, तो म्हणतो,

बाप म्हणजे वाप्यातील पाणी

बाप म्हणजे बैलाच्या घुंगरातील गाणी

बाप म्हणजे पन्हाटीच्या बोंडातील कापूस

बाप म्हणजे ज्वारीचं भरलेलं कणीस

बाप म्हणजे खाचराला ओढणारे चाक

या अत्यंत सुंदर शब्दातून बापाची महती कवी गातो. बैल, माय, कष्ट, शेत, रावण अशा कितीतरी जीवनविषयक जाणिवा मायबाप एक हिरवं सपन या कवितेतून कवी अधोरेखित करतो. काही व्यक्ती विषयक कविता कवीने या संग्रहात लिहिल्या आहेत. त्यामध्ये राष्ट्रसंत तुकडोजी महाराज तसेच अंधार वाटेवरील सूर्य या कवितेत कविवर्य गझलकार ललित सोनोने यांचे विषयीचा आदरभाव व्यक्त होतो. क्रांतीज्योती सावित्रीबाई फुले यांना ती बहुजन समाजातील ज्ञानाई म्हणतात,

विद्येची आई झालीस

क्रांती सूर्याची सावली

अज्ञानाला गाडले तू

झालीस आमची माऊली

सावित्रीबाई बदल आपल्या अंतःकरणात काय स्थान आहे ते वरील कवितेतून उद्धृत करतात. मराठी भाषेचा महिमाही त्यांनी शाश्वत मराठी या कवितेत साकारला आहे. अभिजात सौंदर्याला/झाली मराठी पारखी/कशी करावी प्रशंसा/माय मावशी सारखी/ अशाप्रकारे मराठी भाषेची महती त्यांनी आपल्या कवितेतून गायली आहे. गणेश टाले यांचे कोरोना काळात दुःखद निधन झाले आहे. परंतु तत्पूर्वी त्यांनी कोरोना आजारावर दोन कविता लिहिल्या आहेत. त्यामध्ये बुद्धा ही कविता अभ्यासनीय आहे. बुद्धा/एखाद्या कोरोना सारखा अतिसूक्ष्म विषाणूही/जगाला कसे सळो की पळो करून सोडतो/आणि वेशीवर टांगतो अख्या मानवजातीची लक्तेरे/तर अशा महाभयानक महामारीच्या काळातही सरकार कशा पद्धतीने आपले इव्हेंट करतो व त्या आधारे कोण आपला व कोण परका हे त्याहाळण्याचे काम करतो त्यावर कवी गणेश टाले वाजवा तुम्ही टाळ्या या कवितेत म्हणतो, वाजवा तुम्ही टाळ्या आणि लावा तुम्ही दिवे/आम्हाला आता ओळखू आले तुमचे धूर्त कावे/कोरोना या अतिभयानक मानव जातीला घातक असणाऱ्या



विषाणूच्या आक्रमणात धर्मांध लोक कशा पद्धतीने आपल्या माणसाची अंध भक्तांची चाचपणी करतात यावर त्यांनी भाष्य केले आहे.

कवी गणेश टाले यांच्या सूर्यकळानंतरच्या कविता संग्रहाद्वारे मराठी वाङ्मयाचे क्षेत्र चौफेर विस्तारित झाले आहे. आंबेडकरी आणि ग्रामीण कवितेचा मेळ या एकूणच कविता संग्रहात जाणवतो. या कवितासंग्रहातील कविता सामाजिक, परिवर्तनवादी आणि डॉ. बाबासाहेब आंबेडकरांच्या चळवळीला गतिमान करणाऱ्या, उपेक्षित, वंचित, कष्टकरी आणि कृषीनिष्ठ जाणिवेच्या आहेत. नामदेव ढसाळ, बाप, अंधार वाटेवरील प्रकाशयात्री कविता जरी व्यक्तीप्रधान असल्या तरी त्यांच्याविषयीचा आदरभाव वरील कवितेतून व्यक्त झालेला आहे. येणाऱ्या पिढीसाठी स्मृतीशेष प्राचार्य डॉ. गणेश टाले यांचा कवितासंग्रह यातील विचार दिशादर्शक ठरणारे आहेत.



सूर्यकळानंतरच्या कविता - प्रथमावृत्ती २०२३

पृष्ठे - ७८

किंमत रु. १३०/-

मुक्ता प्रकाशन, अमरावती

भ्रमणभाषा - ९७३०४१९१५९



**Impact Of Covid-19 And Lockdown On Mental Health Of Various Sections****Prof.Dr .Devdas S.Ramteke**

Professor, Dept. of Psychology, Vidya Bharati Mahavidyalaya, Camp, Amravati (444 602)- M .S.

**Abstract:**

Global panic and worry have been sparked by the COVID-19 epidemic and lockdown. Children may experience short- and long-term psychosocial and mental health effects from this. Developmental age, educational level, pre-existing mental health issues, economic adversity, and quarantine due to infection or fear of infection all have an impact on how minors are affected.

Keyword: Pandemic, Covid-19, Lockdown

**1. Introduction**

28 percent of people on the planet are children, who number over 2.2 billion. The world's population is made up of 16% people aged 10 to 19 years (UNICEF, 2019). The global influence of COVID-19 on kids and teenagers is unmatched. The prevention of COVID-19 infection worldwide requires social isolation and withdrawal (Shen et al., 2020). Some nations have put in place regional and national lockdowns from January 2020. During the lockdown, all schools, educational institutions, and activity centres have been closed. Tension, worry, and helplessness are brought on by inescapable conditions. Children and teenagers may be more negatively impacted by this epidemic than adults in the long run (Shen et al., 2020). The type and extent of influence on this age group depends on a number of sensitive variables, including developmental age, current educational status, special needs, a history of mental illness, and the presence of a child or parent who has been quarantined because of an infection or a fear of an infection. The studies on the mental health of kids and teens affected by the COVID-19 pandemic are discussed in the parts that follow, along with the lockdown procedures used to stop further infection.

**2. Impact on young children**

A child is impacted by stress before birth. Parents, especially expectant mothers, are more susceptible to anxiety and depression under stress, which is medically linked to the wellbeing of the foetus (Biaggi et al., 2016; Kinsella and Monk, 2009). Pandemic and shutdown effects are greater on young children and teenagers than on adults. Youngsters (ages 3-6) were more prone than older children to exhibit clinginess and fear about family members contracting the illness (6-18 years old). Older kids were less focused and kept bringing up COVID-19. No matter their age, all children displayed increased irritability, inattention, and clinging behaviour (Viner et al., 2020a). Parents' surveys reveal that children report feeling unsure, afraid, and alone. Children displayed symptoms of separation anxiety, poor eating, nightmares, and disrupted sleep (Jiao et al., 2020).

**3. Impact on school and college going students**

Prior to the lockdown, kids and teenagers learned most things from peers and mentors around the world. 91% of all pupils worldwide have been impacted by national school closures (Lee, 2020). Children and teens who are kept at home experience uncertainty and worry as a result of the disruptions to their socialisation, physical activity, and education (Jiao et al., 2020). Routine disruption, boredom, and a lack of new ideas for academic and extracurricular activities result from long-term educational unstructuredness. Because they are unable to play outside, interact with peers, or take part in school activities in person, some children experience bad affect (Lee, 2020; Liu et al., 2020; Zhai and Du, 2020). These children are more clingy, attention-seeking, and dependent on their parents as a result of a long-term change in routine. Children may refuse to go to school and may find it difficult to interact with their mentors when the lockdown is lifted. Consequently, restricting their movement could worsen their mental health (Lee, 2020). According to a poll, older youth and teenagers are concerned about academic activities, exchange programmes, and cancelled exams (Lee, 2020). School closures save 2-4 percent more deaths, according to the most recent COVID-19 data, which is less than other social isolation techniques. If long-term social isolation is advised, they advise schools to employ less disruptive strategies (Lee, 2020; Sahu, 2020; Viner et al., 2020a). A protracted closure of institutions like schools looks questionable in the current political atmosphere. Apparently, panic buying is a form of survival (Arafat et al., 2020). The pandemic era has seen an increase in teen hoarding (Oosterhoff et al., 2020a). Youth view social withdrawal as a social responsibility and are more sincere about it if they



are driven to stop others from getting sick (Oosterhoff et al., 2020a). Additionally, spending a lot of time alone at home puts kids at risk for being harassed or mistreated, excessive internet use, and access to harmful content (Cooper, 2020; UNICEF, 2020b). Children in abusive households rarely have the ability to report violence, abuse, and harm during lockdown, when schools, legal, and preventative programmes are not fully operational.

#### **4. Impact on children and adolescents having special needs**

Neurodevelopmental, behavioural, or emotional issues affect 1 in 6 children ages 2 to 8 years (CDC, 2019). Children with behavioural and emotional disorders such as autism, ADHD, cerebral palsy, learning disabilities, developmental delays, and others face difficulties during pandemics and lockdowns (CDC, 2019). They struggle with uncertainty, which is made worse by the imposed restrictions and the unfavourable environment. They struggle to work independently, understand the pandemic, and follow directions. These kids no longer have access to resources, peer relationships, or opportunities to learn and develop crucial social and behavioural skills due to the closing of special schools and daycare facilities. Their symptoms might return when they lose their footing in life (Lee, 2020). Temper tantrums and parent-teen conflict are brought on by these elements. These children experienced difficulties even when attending special schools before the outbreak, but they learned to create a daily schedule (APA, 2020; Cortese et al., 2020; UNICEF, 2020a). Parents who are unable to handle these problems on their own must turn to therapists and schools for help (Dalton et al., 2020). The needs of each child's illness are unique. Children with autism have a hard time adjusting to change. They become agitated if something is changed or tweaked. Self-harm and behavioural problems can get worse. Parenting is challenging when there is autism lockdown. Since online sessions are difficult for children to learn, the termination of speech and occupational therapy sessions may have an impact on their skill development and next milestone (UNICEF, 2020a). Children with ADHD are unable to understand their caregivers' cues. Being confined increases their impulsivity and hyperactivity, making it difficult for caregivers to involve kids in worthwhile activities because it's difficult for them to keep contained and avoid touching infected objects (Cortese et al., 2020). OCD affects 0.25–4 percent of kids and teenagers (CDC, 2019). This pandemic may have a particularly negative impact on children with OCD. People may feel distressed as a result of contamination, hoarding, and somatic fixation obsessions. Cleanliness stops the spread of COVID-19. Six times per day and after handling anything, the United Nations advises washing hands (APA, 2020; United Nations, 2020). Hoarding behaviour has gotten worse because of the lockdown, which has left healthier people worried about food and supplies for prevention like masks and sanitizers (APA, 2020; Mukherjee et al., 2020).

#### **5. Impact of lockdown on underprivileged children**

Inequality and mental health problems are related. Socioeconomic inequality has gotten worse as a result of the epidemic and lockdown's effects on the global economy. Lockdowns deprive disadvantaged children of food and protection in developing nations. Long-term stress could hinder their development. The lockdown impacted 40 million disadvantaged children in India, which has 472 million children. Include street, farm, rural, and migrant children (Dalton et al., 2020; Rosenthal et al., 2020). Due to increased economic, social, and environmental exposure, a rising number of poor and street children are without a stable income, making them more susceptible to abuse and mental health issues (Birla, 2019). Home is where most families find security. People who are poor and in poverty have it backwards. Because of the movement restrictions imposed by lockdown, children are more likely to be exploited, violent, or abused (Cooper, 2020; United Nations, 2020). Director's Assistant at Childline 1098 Since the shutdown started, India recorded a 50% increase in calls (PTI, 2020). This alarming rise has resulted in more youngsters being victims at home. Many low-income families are unable to make a living during lockdown, which causes frustration and helplessness. Violence against children and family strife can result from displacement. Despair, anxiety, and suicide may result from this (Jiao et al., 2020; Petito et al., 2020; Solantaus et al., 2020) Kids may be forced to work if schools are closed or there is economic hardship. Children who are orphaned are more likely to be exploited (United Nations, 2020). During lockdown, many colleges provide students with online or distance learning courses. Because they don't have this option, underprivileged children lack internet learning resources and stimulation. Girls in low-income families are less likely than males to have access to technology, which may lower their engagement in digital education (McQuillan and Neill, 2009). Once the lockdown is lifted, more girls leave school because of the gender gap (Cooper, 2020; PTI, 2020).



## 6. Impact due to quarantine and separation from parents

COVID-19 is expressed variably in children and adolescents. However, child infections have spread globally, forcing quarantines. There are lots of sick parents who are isolated. Children are split from their parents in both situations. To combat COVID-19, many countries have strict quarantine regulations. To stop the spread of the sickness, China has segregated adults, teenagers, and children. Despite being for the community's good, quarantine has psychological effects (Liu et al., 2020). Children who are isolated may develop mental health problems as a result of parental separation melancholy. Parents' absence might have an impact on a child's relationship because they are so important during a child's formative years. A child's mental health could be harmed if they are taken away from their primary caretakers (Cooper, 2020; Jiao et al., 2020; Liu et al., 2020). Children's psychological development can be harmed by sadness, anxiety, fear of death, worry of parent mortality, and fear of hospital isolation (APA, 2020; CDC, 2019; Dalton et al., 2020). Children that have unreleased emotions may become afraid or act out (Liu et al., 2020). Because adolescents lack the knowledge and maturity to understand how the pandemic is affecting their world, they could feel isolated.

## 7. Advisories of international organizations

During COVID-19, international organisations and advisory bodies released guidelines to support mental and preventive health for all. They advise parents to talk to their kids about the epidemic based on their age and capacity to comprehend the issue. Children should be given tasks one at a time, included in family activities, taught social graces and hygiene, and encouraged to play inside and express their creativity. Teenagers should also fulfil obligations and understand their civic responsibility (WHO, 2020b). Adult-supervised initiatives aid them in understanding their concerns. Homeschooling for kids and teenagers has to be more organised. Children should be encouraged to interact online with adults watching them (WHO, 2020a). The advisory groups have also made recommendations for children with neurodevelopmental disorders and special needs (UNICEF, 2020a, 2020b; WHO, 2020a). nervous and traumatised children. Children require early identification and prompt management involving parents and experts to prevent long-term mental health morbidity.

## 9. Young children

- ❖ Teens require less supervision than younger children. They require more time spent playing indoors and their parents' physical presence. Parents should reassure and pay their youngster good attention.
- ❖ Parents must speak in terms that are acceptable for their children's age and in plain language when discussing COVID-19. Children need factual information from government websites made specifically for kids, WHO, UNICEF, or other organisations.
- ❖ Children should only watch fact-based, impartial news channels in order to lessen their anxiety about the uncertain future (Wang et al., 2020). Skip the tabloids.
- ❖ Parents should set an example for their children by using coping mechanisms and preventative actions. Reminders through phone are another option.
- ❖ The child should have a regular schedule that includes time for play, reading, resting, and exercising. Families should play board games and indoor sports with kids instead of playing video games. Parents should establish a regular bedtime. Children might require more time and care before going to bed.
- ❖ The good behaviour of the child should be emphasised above the bad. Parents should place more emphasis on what to do than on what not to do. esteem and social reinforcing over tangible benefits.
- ❖ Children's behaviour could change as a result of pandemics. Parents might think about disregarding behaviour issues if they are minor and do not harm kids or others. This could help both parties give each other space and reduce recurrence.

## 10. Role of school teachers/school counsellors

- ❖ Online academic activities are typically organised by schools and universities, putting teachers in constant contact with students and allowing them to support mental health. Position during the COVID-19 outbreak and lockdown:
- ❖ Teachers can devote time to teaching students about COVID-19 and using international standards to promote preventative health behaviour. During the epidemic, they might impart responsibility to the students. They can demonstrate and engage in prevention.
- ❖ By making courses more interactive, involving students in quizzes, puzzles, and little competitions, and giving more imaginative homework assignments, they can conduct creative online academic and



non-academic sessions. Use textbooks and other academic resources. UNESCO offers online learning materials (UNESCO, 2020)

- ❖ Teachers encourage students' mental well-being. They can talk about a student's wellbeing. Deep breathing, muscle relaxation, diversion, and positive self-talk can be taught. Using actual examples, virtual classes can focus on 'life skills' for managing with stress.
- ❖ Teachers can educate youngsters prosocial conduct and attributes like empathy and patience. This can aid them realise their role in society and how social detachment isn't emotional remoteness.
- ❖ Teachers are required to call or text parents with updates on their children's mental health. They may call their parents, give them their contact information, and schedule time to talk because of the digital divide.
- ❖ They are able to suggest mental health professionals to patients. They serve as a catalyst for communication between parents based on interactions with students and the results of screening tools. If they see a problem, they can speak with the parents and suggest that the kids seek help from mental health specialists.
- ❖ Teachers must ensure that less fortunate students without internet access have access to academic and life skills reading materials with the support of the school administration. If they have internet access.

### **Paediatricians' role**

- Parents who have concerns about their child's health or behaviour during the formative years when their personalities are developing frequently seek doctors. Parents have faith in them and ask questions. Promoting mental health, fostering resilience, identifying mental health disorders, and collaborating with mental health care providers for children all require the engagement of a paediatrician. The functions of paediatricians in COVID 19 include:
  - They must have access to and regularly use teleconsultation. They must provide phone or online consultations for parents.
  - They should provide basic reading materials for mental health promotion online or in handouts and educate parents on the developmental requirements of kids at various ages.
  - Children who exhibit physical symptoms of stress or emotional health issues, such as aches, pains, or self-harm, can be identified by paediatricians.
  - The child's temperament, functioning, school adjustment, peer group, routine, and general activities must be discussed.
  - Analysis can be done on psychosocial, medical, and environmental stressors that affect mental health, such as family history, financial strains, home environment, and neighbourhood.
  - In order to identify ADHD, autism, anxiety disorders, and depression in children, mental health examinations should use quick, standardised screening approaches.
  - Their relationships with clinical psychologists, child psychologists, and psychiatrists need to be established. When specific mental health care is required, they should work with them and refer kids.

### **12. Health system and policy makers**

- Prior to COVID 19, outdated theories and practises for the mental health of kids and teens still apply. To take into consideration the duration of the lockdown and the times that follow, policies must be modified. The following suggestions may aid in directing how the health system operates and how policies are developed for the treatment of mental illness in children:
  - To fulfil the needs of the population's mental health, the healthcare system should prioritise prevention, promotion, and treatment.
  - There is no one approach that can account for children's and adolescents' mental health in many contexts. The contextual elements that differ by country and stage of sickness should serve as the foundation for the health system and regulations.
  - Most developing nations are lacking in mental health professionals. GPs, schools, non-profits, and paediatricians must be involved in inclusive strategies. Short-term training in mental health treatment should be given to these arms.
  - In developing nations, different regulations for rural, suburban, and concrete homes reflect the distinctions between urban, suburban, and rural college regions.



- Regular collaboration with state and/or local public health organisations is required to create adaptable strategies that can be tailored to schools and communities.
- Policies should take into account a child's developmental stage, such as whether they are a toddler, a school-age child, or a teen.
- Unambiguous standards are needed, but full translation of prevailing therapeutic modalities to telehealth compatibility is also necessary.
- People who are prone to illness, underprivileged, disabled, or have developmental disabilities shouldn't be ignored.
- Plans for returning to school should emphasise hygiene and social distance. This should be carried out with young learners' in-person education in mind.
- Assure appropriate funding, oversight, and application for policy implementation.

### 13. Conclusion

Although stress makes them more susceptible, young children and adolescents have a low COVID-19 infection rate. Numerous cross-sectional studies have examined COVID-19 and focused on children and young people. This influence can take several forms and have different effects depending on risk variables such developmental age, educational level, pre-existing mental health issue, economic disadvantage, or quarantine due to infection or infection fear. More clinginess, disturbed sleep, nightmares, poor eating, inattentiveness, and separation issues are seen in young children. Children's academic, psychological, and developmental progress is negatively impacted by prolonged school and activity centre closures, which also cause them to feel alone, anxious, and insecure. Addiction to social media and online gaming makes them more dangerous. Children and teenagers with mental illnesses aren't used to change. Issues with behaviour and symptoms could get worse. Children who receive counselling, training, and other therapies run the danger of losing their access to special education and therapy. Children in poverty are more likely to be used and abused. Children under quarantine run the risk of developing mental health problems. In-person and online interactions are required to increase children's access to mental health services. For this parent network, psychiatric, psychological, paediatric, community volunteer, and non-governmental organisations are required. Telemental health compatibility is required for the general population. This would lessen mental health problems during and after a pandemic in impoverished and vulnerable communities. The primary goals of the health care system and policymakers should be prevention, promotion, and interventions while taking the regional context into account in order to meet the needs of the general population in terms of mental health.

### References:

1. United Nations Policy Brief: The impact of COVID-19 on children. United Nations. 2020:1–17. Policy Brief] [Google Scholar]
2. WHO. (2020a). Healthy parenting. <https://www.who.int/emergencies/diseases/novel-coronavirus-2019/advice-for-public/healthy-parenting>.
3. WHO. (2020b). WHO | COVID-19: resources for adolescents and youth. WHO; World Health Organ. [http://www.who.int/maternal\\_child\\_adolescent/links/covid-19-mncah-resources-adolescents-and-youth/en/](http://www.who.int/maternal_child_adolescent/links/covid-19-mncah-resources-adolescents-and-youth/en/).
4. United Nations Policy Brief: The impact of COVID-19 on children. United Nations. 2020:1–17. Policy Brief] [Google Scholar]
5. UNICEF. (2020b, April 14). UNICEF. UN News. <https://news.un.org/en/tags/unicef>.
6. UNICEF Global population of children 2100. Statista. 2019 <https://www.statista.com/statistics/678737/total-number-of-children-worldwide/> [Google Scholar]
7. McQuillan H., Neill B.O. Gender differences in children's internet use: key findings from Europe. J. Child. Media. 2009;3(4):366–378. doi: 10.1080/17482790903233408. [CrossRef] [Google Scholar]

Impact Factor-8.632 (SJIF)

ISSN-2278-9308  
(CDIX ) 409  
April -2023  
Volumes-B



# *B.Aadhar*

Peer-Reviewed & Refreed Indexed

Multidisciplinary International Research Journal

SPECIAL ISSUE ON  
Konkan Gyanpeeth Uran College  
of Commerce and Arts, Uran organised an

**ICSSR SPONSORED**

NATIONAL CONFERENCE

In association with

Department of History and

Indian Sculpture and Architecture Research Council  
On

Exploring New Research Trends in Ancient Indian Iconography,  
Temples, Caves, Stupas, Chaityagraha and Rock Paintings.

Date : 20<sup>th</sup> & 21<sup>st</sup> March 2023



Chief Editor

Prof. Virag S. Gawande

Executive Editor

Dr Arvind Sontakke

Prof. Dr. Baliram Gaikwad



This Journal is indexed in :

Scientific Journal Impact Factor (SJIF)

Cosmos Impact Factor (CIF)

International Impact Factor Services (IIFS)

For Details Visit To : [www.aadharsocial.com](http://www.aadharsocial.com) Aadhar PUBLICATIONS Amravati (M,S)

**वाकाटककालीन विष्णूशिल्प****डॉ. मिनल खेरडे**

विद्याभारती महाविद्यालय अमरावती, E-mail ID : minalkherde@rediff.com

**प्रस्तावना :-**

विष्णू मूर्ती शिल्प :- भगवान विष्णू ही वैदिक देवता असून इंद्राचा मित्र म्हणून त्याचे वर्णन वेदप्रघात आहे. विष्णूने आपल्या तीन पावलांनी त्रैलोक्य व्यापले म्हणून त्यास 'त्रिविक्रम' म्हणतात याशिवाय खिलसुक्तांत (ऋग्वेदाचे परिशिष्ट) विष्णूची अच्युत, गोविंद, माधव, चक्री, हृषिकेश, अमृतेश, वासुदेव, केशव आणि कृष्ण ही नावे आली आहेत. पुढे महाभारतकाली पांचरात्र आणि गीता ग्रंथात वासुदेव आणि कृष्ण यांना ईश्वरस्वरूप प्राप्त झाले. अर्थात कृष्ण, वासुदेव आणि विष्णू ही एकाच देवतेची नावे आहेत. या ग्रंथांत विष्णूच्या मत्स्य, कच्छ, व वामन अवताराच्या कथाही समाविष्ट आहेत. ब्राह्मण ग्रंथ व उपनिषदात विष्णू हा विश्वाचा भरण पोषण करणारा, जीवात्म्याला मोक्ष प्रदान करणारा म्हटले आहे. अर्थात विष्णू हा परमेश्वर म्हणून वैदिक काळात स्विकृत होता.<sup>१</sup>(केतकर, खंड ४) विष्णूची अनेक नावे आहेत. तसेच वेदातील वर्णन केलेल्या अन्य देवता एकाच परमेश्वराची (विष्णूची) रूपे होत असे विधान वेदग्रंथातच आहे. अर्थात विष्णू या वैदिक देवतेचे नारायण आणि वासुदेव या नावांनी महाभारतकाळी भक्तीसंप्रदाय सुरु झाले होते असे दिसते.

वाकाटक व धर्मसंक्रमण :- महाराष्ट्रातील नाणेघाट येथील पहिल्या शिलालेखांत वासुदेव व संकर्षण या देवांना आरंभीच नमन केले आहे. त्यावरून इसवीसनपूर्व पहिल्या शतकांत, सातवाहनांच्या उदयकाळी महाराष्ट्रात भागवतधर्माचा प्रसार झाला होता हे स्पष्ट होते. सातवाहन राजे हिंदुधर्मिय होते. त्यांनी यज्ञयाग केलेत व पुण्य प्राप्तीस्तव दानधर्मही केला. परंतु त्या काळात श्रौतधर्म मागे पडून पौराणिक भागवतधर्म लोकप्रिय होत होता आणि भक्तीच्या नव्या संदर्भाने लोक याकडे अधिकाधिक आकृष्ट होत होते असे दिसते. सातवाहनांचे उत्तराधिकारी वाकाटक शासकांचे काळांत वैष्णव पंथाने चांगलेच बाळसे धरले होते आणि राजा व प्रजा वैष्णव पंथाचे अनुशिलन करीत होते असे दिसते.

स्वाभाविकरित्या यज्ञांची जटिलता व पुराहितांचे शोषण यापासून मुक्ती मिळाल्यामुळे व पुण्यसंचयाची हमी असल्यामुळे गुप्त वाकाटक काळात भागवत धर्माचा मोठ्या प्रमाणावर प्रसार झाला. अर्थातच भक्तीसाठी सगुणोपासना म्हणजे मंदिरे व मूर्तीची निर्मिती झाली. वाकाटक काळात आरंभिक राजांनी वैदिक यज्ञांचा अवलंब केला असला तरी प्रजाजनांत भागवत धर्माचा परिपोष होणे स्वाभाविकच होते. त्यामुळे शैवपंथाच्या बरोबरीने वैष्णव पंथाचा विकास व विस्तार झालेला दिसून येतो.

भगवान श्री विष्णू पूजा :- शैवधर्माप्रमाणेच वैष्णव धर्मालाही वाकाटक काळात महत्त्व होते. रुद्रसेन द्वितीयचा मांडळ ताम्रपट हा वैष्णवांचा ताम्रपट असल्याचे दिसते. तसेच मांडळ येथील उत्खननात विष्णूची मूर्तीही मिळाली आहे. (देगलुरकर, 1987) ईशा, ईश्वर व शिव ह्या सर्वमान्य ईश्वर विषयक संकल्पना होत्या. वैष्णवपंथीय लोकांमध्ये 'स्वामीन' हे विरुद्ध विष्णूला लावण्यात येत असे. मांडळ येथील उत्खननांत वाकाटक कालीन वैष्णव पंथीय मूर्ती मिळाल्या आहेत. (Shatri, 1992) यावरून असा अंदाज काढणे शक्य आहे की, मांडळच्या आसपासच्या भागात वाकाटकांच्या काळात वैष्णव धर्मीयांचे प्राबल्य होते आणि भागवत धर्माचा प्रसार करण्यात सुद्धा वाकाटकांनी महत्त्वाची कामगिरी बजावली आहे. रामटेक येथील जी मंदिरे आहेत ती विष्णूची असावीत व ती प्रभावती गुप्ताने





बांधली असावीत (Bajpei, 1992) असे मानले जाते. वेरुळ येथील विष्णूचे शिल्प हे वाकाटक काळातील वैष्णव भक्तीचे उदाहरण आहे. (जोशी, 1979) अर्जिठा येथील शैलगृह क्र. १७ मध्ये वराहदेवाचा शिलालेख आहे. त्यात हरिषेणाची तुलना राम, शिव व चंद्र यांच्या सौंदर्याशी केली आहे व त्याला विष्णुसमान प्रतापी म्हटले आहे. (देशपांडे, 1996) वरील सर्व विशेषणे वैष्णव धर्माचे द्योतक आहेत. वाकाटकांची महाराणी म्हणून आल्यानंतर वैष्णव धर्मालाही तेवढेच महत्त्वाचे स्थान प्राप्त झाले होते असे दिसते.

वाकाटक हे मुलतः शैव धर्मीय होते. परंतु गुप्त सम्राट चंद्रगुप्त द्वितीय याची कन्या ही प्रभावती गुप्ता वाकाटकांची महाराणी म्हणून आल्यानंतर वैष्णव धर्मालाही तेवढेच महत्त्वाचे स्थान प्राप्त झाले होते असे दिसते. विष्णूचे आणखी एक देवालय बैतुल जिल्ह्यातील (सध्याचे पट्टन) अश्वत्थखेटक येथे होते. त्यातही महापुरुषाच्या म्हणजे विष्णूच्या पादूकांचीच पूजा केली जात असे. त्या देवळाला जोडून असलेल्या अन्नसत्राला द्वितीय प्रवरसेनाने नारायणराजाचे विनंतीवरून ४०० निवर्तने भूमीदान दिली होती. (मिराशी, 1957) पट्टन ताम्रपटात खालील उल्लेख आहे. (मिराशी, 1957)

अत्र ग्रामे राजक्यमानेन भूमेन्निर्वर्तनशतानि चत्वारि महापुरुषपा दमूलसत्रोपयोज्यं नारायणराजविज्ञाप्येन दत्तम् (1)\*

प्रवरसेनाने लिहिलेले 'सेतुबंध' हे काव्य रामचरित्रावर आधारित आहे. या काव्याचे चार श्लोक विष्णु स्तुतीपर लिहिलेले आहेत." (मिराशी, 1975) कालिदासाच्या 'मेघदूत' काव्यात भगवान विष्णु आषाढ शुद्ध एकादशी किंवा शयनी एकादशीपासून कार्तिक शुक्ल एकादशी किंवा प्रबोधिनी एकादशीपर्यंत शय्येवर निद्रिस्त असतात ही कल्पना मांडली आहे." (मिराशी, 1972) या काव्यांत शापित यक्ष मेघाना आपला दूत बनवून आपल्या पत्नीला त्यांच्यामार्फत संदेश पाठवितो. त्यात आपल्या घराची खूण तो मेघाला सांगतो. त्यात तो म्हणतो,

“शापान्तो मे भूजगशयनादु त्थिते शाङ्-र्गपाणी।

शेषान्मासान्गमय चतुरो लोचने मीलयित्वा ।

पश्चादावां विरहगुणितं तं तमात्माभिलाषं

निर्वेक्ष्यावः परिणतशरच्चन्द्रिकासु क्षपासु ॥“

(भगवान विष्णु आपल्या सर्पशय्येवरून उठतील तेव्हा अर्थात कार्तिक शुक्ल एकादशीला माझ्या शापाची समाप्ती होणार आहे. तेव्हा तू राहिलेले चार महिने डोळे मिटून दुःख सहन करीत घालव, नंतर आपण शरद ऋतूतील शुभ्र चांदण्यात पूर्वीच्या विरहाने ज्यांची गोडी वाढली आहे, अशा अनेक उपभोगांचे सेवन करू. (मिराशी, 1972) यातील भगवान विष्णूचा उल्लेख कालिदास काली वैष्णवधर्म प्रसाराची खूण मानता येईल.

गुप्तकाळात वैष्णवधर्माचा प्रसार झालेला होता. (बाजपेयी, 1992) चंद्रगुप्त द्वितीयची मुलगी व वाकाटक सम्राज्ञी प्रभावती गुप्ताच्या ऋद्धपूर ताम्रपटाची सुरुवात 'जितं भगवता' या विष्णुनामाने होते. या लेखातच रामगिरी स्वामीचाही (रामगिरिस्वामिन) उल्लेख आहे. रामगिरिस्वामी म्हणजे भगवान रामचंद्र होय. (मिराशी, 1957) अर्थात विष्णू व रामचंद्र याची अभिन्नता यावरून स्पष्ट होते. तसेच रामाचे पादूकाजवळ (पादमुलात) हा ताम्रपट दिला होता. त्यातून अतीव निष्ठा प्रगट होते. प्रभावती गुप्ताच्या पुणे ताम्रपटातील ग्रामदान भगवंताच्या नैवद्यासाठी (भगवत्पादमूले निवेद) (मिराशी, 1957) भगवत भक्त आचार्य चनालस्वामीस दिले होते. यातील भगवान म्हणजे श्री विष्णु असावे. कारण याच ताम्रपटात गुप्त सम्राट चंद्रगुप्त द्वितीयचे वर्णन भगवान विष्णूचा एकनिष्ठ उपासक (परमभागवतो महाराजा धिराज श्री चंद्र गुप्तस्य) (मिराशी, 1957) असे करण्यात आले आहे. प्रभावती गुप्ता आपल्या पित्याप्रमाणे वैष्णव



धर्मानुयायी होती हे स्पष्ट दिसते. प्रभावती गुप्ताच्या मोठ्या मुलाचे नाव दामोदरसेन म्हणजे विष्णुद्योतक होते. (मिराशी, 1979) अर्थात विष्णुचा कृपाप्रसाद.

भगवान विष्णुची प्रार्थना :- कालिदासाने 'रघुवंश' या काव्याच्या दहाव्या सर्गात रघूला, भगवान विष्णूने देवांची प्रार्थना ऐकून आपण पृथ्वीवर अवतार घेऊ असे आश्वासन दिल्याचे वर्णन केले आहे. (मिराशी, 1979)

पवनार :- पवनार प्रवरसेन द्वितीयने आपल्या 'सेतूबंध' काव्यात रामाचे वर्णन केले. त्यात तो रामाचे रूपात विष्णु व राम यांचे द्वैत मानीत नसे. प्रवरसेनाने आपल्या मातेकरिता प्रवरपूर (पवनार) येथे बांधलेल्या देवालयाला लावलेल्या शिल्पपट्टापैकी काही रामावतारातील तर काही कृष्णावतारातील प्रसंगाचे होते हे आता पवनारच्या उत्खननामुळे ज्ञान झाले आहे. अर्थात विष्णु, राम व कृष्ण यांचे द्वैत मानले जात नव्हते असे स्पष्ट दिसते. यावरून भगवान विष्णुच्या अवतारांची संकल्पना वाकाटक काळी जनमान्य झाली होती हे स्पष्टपणे दिसून येते.

भगवत :- 'भगवत' या शब्दाने केवळ विष्णू निर्दिष्ट केला जात नाही. ते विशेषण शिव, जिन, बुद्ध यांचेही असू शकते (आपटे, 1838) असे आपट्यांच्या संस्कृत कोषात नमूद आहे. पंतजलीच्या महाभाष्यात 'शिवभागवताः' याचा अर्थ 'भगवान शिव' असा सांगितला आहे. तेव्हा 'भागवत पाद' या शब्दाने रामाप्रमाणेच विष्णु व त्याचे अवतार यांचीही उपासना दर्शविली जाते. (मिराशी, 1979)

शंकराप्रमाणे विष्णुची देवालयेही त्याकाळात बांधली गेली होती. परंतु ती आता अस्तित्वात नाहीत.. वाकाटक नृपती द्वितीय रुद्रसेन हा बहुधा आपली अग्रमहिषी प्रभावती गुप्ता हिच्या प्रभावामुळे विष्णुपासक बनला असावा. (मिराशी, 1979) तसेच भागवत पुराणातील उल्लेखावरून पृथिवीषेण द्वितीय हा सुध्दा 'परमभागवत' किंवा विष्णुचा भक्त होता असे दिसते. (Majumdar 1917) बालाघाट ताम्रपटात असे वर्णन आहे. (मिराशी, 1957) अन्य वाकाटक राजे शिवोपासक होते परंतु वैष्णव धर्माबद्दल अनादर नव्हता असे दिसते.

नारायण :- नागरा, जि. भंडारा येथे १९८१ मध्ये भैरव टेकडी या नावाने प्रसिध्द असलेल्या ठिकाणी उत्खनन करण्यात आले. तेथील मंदिराजवळ पेटिकाशीर्षक ब्राह्मी लिपीत 'नारायण' असे नाव कोरलेली मुद्रा मिळाली आहे. (बोरकर, 2000) यावरून विष्णुचे नारायण हे संबोधन काही ठिकाणी प्रचलित झाले असावे असे दिसते.

मनसर :- मनसर येथील उत्खननात विविध शिल्पाप्रमाणेच अर्धोन्मीलित नेत्र मुद्रा असलेली एक आध्यात्मिक भावसंपन्न वैष्णवी प्रतिमा मिळाली आहे. हिच्या हातात गदा असून तर्जनी वर आहे. (चितळे, 1998) अर्थात वैष्णव सुध्दा स्त्री प्रतिमांची पूजा करित असावेत असे दिसते. परंतु स्त्री प्रतिमांचे उल्लेख अगदी त्रोटक आहेत.

श्रीरामचंद्राची पूजा : वाकाटक काळात रामगिरी (रामटेक) गडावर श्रीरामचंद्राच्या पादूकांची पूजा केली जात होती. याबाबतचा उल्लेख राजमहिषी प्रभावती गुप्ता हिच्या ऋध्दपूर ताम्रपटात 'रामगिरी स्वामिनः पादमुलात' असा आला आहे. (मिराशी, 1957) अर्थात सदर ताम्रपट रामगिरीवरील भगवान रामचंद्राच्या पायाजवळ दिला आहे. प्रभावती गुप्ताच्या पुणे ताम्रपटातही 'भगवत्पादमूले' हा शब्द प्रयोग आहे. (मिराशी, 1957) तसेच प्रवरसेन द्वितीयच्या इंदूर ताम्रपटातही 'भगवत्पाद' हा प्रयोग आहे. (मिराशी, 1957) त्यात दान दिलेल्या गावाचा अर्धा भाग चंद्र नामक वाण्याने विकत घेवून दान दिला. प्रभावती गुप्ता अत्यंत 'भगवदभक्ता' म्हणजे रामभक्त होती. हे तिचेवर माहेरचे संस्कार असावेत. ती रामगिरीवर नियमित रामचंद्र दर्शनास जात असावी व तेथे रामचंद्राचे भव्य देवालय बांधले असावे. तेथे रामचंद्राच्या पादूकांची पूजा होत असावी. (मिराशी, 1957) अगस्ती मूर्तींनी, श्रीराम रामटेकवरून परततांना स्वतः रामाच्या पादूकांची तेथे प्रतिस्थापना केली असे वर्णन मिळते. रामगिरी वाकाटकांच्या नंदिवर्धन राजधानीपासून केवळ तीन मैलावर आहे ही बाब नजरेआड करता येणार नाही.

कालिदासाने लिहिलेल्या 'मेघदूत' काव्यातील रामगिरी येथे आश्रमात राहणाऱ्या शापीत यक्षाने मेघाला अलका नगरीचा रस्ता सांगण्यापूर्वी रामगिरीचे वर्णन व "बन्धे पुंसां रघुपति परदैरदि-तं मेखलासु (मिराशी, 1958) (जेथे श्रीरामचंद्राची वंदनीय पावले उमटली आहेत.) अशा शब्दांत केले आहे. अर्थात रामगिरीला रामचंद्राचे देवालयांत पादूका पूजन होत होते हे स्पष्ट दिसते. मेघदूतातील रामगिरी व रामटेक एकच आहेत. याबाबतचे उल्लेख तेथिल लक्ष्मणाचे देवालयातील यादवकालीन शिलालेखात तसेच ऋध्वपूर व मांडळच्या ताम्रपटात आहेत. (मिराशी, 1958) रामटेकला रामाबरोबरच लक्ष्मणाचेही देवालय आहे. (चतुर्वेदी, 2001)

श्रीराम :- कालिदासाच्या 'रघुवंश' या ग्रंथात रामाच्या पूर्वजांचा इतिहास आहे. तसेच रामाच्या लंका विजयाचे कलात्मक वर्णन आहे. (मिराशी, 1975) द्वितीय प्रवरसेनाच्या 'सेतुबंध' या काव्यात श्रीरामाने सागरावर सेतु बांधण्याचे व लंका विजयाचे चित्रण आहे. (भुसारी, 1979) 'गाथासप्तशती' मध्ये पस्तीसाव्या गाथेत रामाचा उल्लेख आदराधीन आला आहे. (मिराशी, 1975) कालिदासाला मेघदूत काव्याची कल्पना रामायणावरून सुचली असावी असे काही विद्वान मानतात. हनुमान रामदुत होता. रामायणातील रामाच्या विरह व्यथेचे वर्णन आणि हनुमानाने वानर सैन्यास लंकेच्या वाटेचे सांगितलेले वर्णन वरील मताचे समर्थनार्थ देण्यात येते. या सर्व उल्लेखांवरून असे दिसते की, कालिदास काळी म्हणजेच वाकाटक काळी रामकथा जनमानसात लोकप्रिय होती. आणि खंडकाव्य निर्मिती होण्याइतके रामचरिताला महत्त्व प्राप्त झाले होते. एवढेच नव्हे तर राम व कृष्ण भगवान विष्णुचे अवतार होत ही सार्वत्रिक धारणा असल्यामुळे रामाला देवत्व प्राप्त झाले होते आणि रामाच्या मूर्तीची अथवा पादूकांची पूजा केली जात असावी.

वर्धा जिल्ह्यात पवनार (प्रवरपूर) येथे जे उत्खनन झाले आहे, त्यावरून असे दिसते की, धाम नदी तीरावील टेकडीवर (श्री विनोबाजींचा आश्रम) श्री रामचंद्राचे उत्तुंग देवालय असावे. आणि या देवालयाला रामायणातील विविध प्रसंगांच्या शिल्पकृतींनी अलंकृत केले असावे. कारण पवनार येथे उत्खननात भरत भेट- राम, सीता, भरत, लक्ष्मण यांचे शिल्पपट्ट मिळाले आहेत. (मिराशी, 1957)

पवनार म्हणजे द्वितीय प्रवरसेन याने आपल्या कारकिर्दीच्या अकराव्या वर्षानंतर आपल्या नावे बसविलेले प्रवरपूर होय. प्रवरपूर वाकाटकांची राजधानी झाल्यानंतर श्रीरामदर्शनापासून आपली माता प्रभावती गुप्ता वंचीत राहू नये म्हणून मातृभक्त प्रवरसेनने मातेच्या सांगण्यांवरून राममंदिराची निर्मिती केली असावी. कारण प्रभावती गुप्ता ही रामभक्त होती. आज तेथे मंदिर उपलब्ध नाही परंतु अवशेष रूपात शिल्पपट्ट मिळाले आहेत.

द्वादशीला वैष्णव पूजा :- वाकाटक काळात कार्तिक शुक्ल एकादशी शुभ मानली जात असावी. कारण वाकाटकांच्या उपलब्ध ताम्रपटांपैकी चार ताम्रपट कार्तिक शुद्ध द्वादशीला म्हणजे एकादशीच्या पारण्याच्या दिवशी दिलेले आहेत. (मिराशी, 1957) त्यापैकी एक प्रभावती गुप्ताने रामचंद्राच्या पादूका जवळ दिला होता. वैष्णव संप्रदायात एकादशीला मन शुद्धीकरीता उपवास करून दुसऱ्या दिवशी पारण्याला दान धर्म करणे पुण्यप्रद मानले जाते. एकंदरित वाकाटक काळात वैष्णव धर्माचे व राम पूजेचे प्रचलन होते असे दिसते.

श्रीकृष्ण पुजा :- वाकाटक काळात कृष्णभक्तीही प्रचलीत असावी. पांचरात्र या वैदिक संप्रदायात व्युहवाद अंतर्भूत असून वासुदेव, संकर्षण, प्रह्लाद व अनिरुद्ध असा चतुर्व्यूह क्रम दिला आहे. यात सांबाचा नंतर अंतर्भाव केल्या गेला. यातील वासुदेव म्हणजे विष्णु, नारायण किंवा कृष्ण होय. संकर्षण म्हणजे बलराम हा बंधु होय आणि अन्य श्रीकृष्ण पुत्र व प्रपौत्र होत. या पांचांची पुजाअर्चा व उपासनेला व्युहवादात प्राधान्य आहे. यातील मुख्य व प्रधान देवता म्हणजे विष्णु, नारायण, वासुदेव किंवा कृष्ण ही व्युहसृष्टीचे सृजन करणारी एकात्मिक देवता होय. त्यामुळे वैष्णव पंथात वासुदेव भक्तीला विशेष महत्त्व आहे. (पांडे, 1955)



वासुदेव :- सातवाहनांच्या नाणेघाट शिलालेखात संकर्षण, वासुदेव असा उल्लेख आहे. परंतु हा क्रम व्यूहवादाचे क्रमाने नसल्यामुळे सातवाहन काळात व्यूहवाद संलग्न नसावा असे विद्वान प्रतिपादन करतात. (भुसारी, 1979) परंतु वासुदेव म्हणजे कृष्ण भक्तीचा प्रसार सातवाहन काळात बराच झाला असावा. कारण दुसऱ्या सातवाहन राजाचे नाव कण्ह (कृष्ण) असे होते. तसेच गाथासप्तशती या ग्रंथात (भुसारी, 1979) कृष्णाची कण्ह, दामोदर (दोमादर) माधव (माधव) म्हमहण (मधुमथन) अशी अनेक नावे आली आहेत. त्याखेरीज (यशोदा) सहिआ (राधिका) गोवी (गोपी) व अवहू (व्रजवधू) आणि वल्लवी (बल्लभी) ही कृष्णाच्या गोतावळ्याची नावे आली आहेत. सातवाहन काळात विष्णु व कृष्ण यांचे ऐक्य प्रस्थापित झाले होते असे स्पष्ट दिसते. (भुसारी, 1979) वाकाटक काळांत ते दृढ झाले असावे.

सर्वसेनकृत हरिवंश या काव्यात भगवान कृष्णाची वंशावळ दिली आहे (मिराशी, 1979) व महात्म्य वर्णन केले आहे. कालिदासाने आपल्या 'मेघदूत' काव्यात चंबळ नदीचे वर्णन करताना यक्ष मेघास, कृष्णाच्या वर्णाची चोरी करणारा म्हणजे 'तत्सदृशकृष्णवर्ण' असे संबोधितो. (चतुर्वेदी, 2001) अर्थात वाकाटक काळात विष्णु, राम व कृष्ण यांची पूजा व आराधना करणारा मोठा समाज होता असे दिसते. परंतु कृष्ण मंदिरांचा मात्र कुठेच उल्लेख मिळत नाही. किंवा ठावठिकाणा लागत नाही.

बलराम : शक्ती देवता:- बलराम ही वैष्णव पंथातील चातुर्व्यूहापैकी एक देवता होय. बलराम हा शेषाचा अवतार मानल्या जातो. पुराणात पृथ्वी धारण करणारा व विष्णूची शैव्या असलेल्या शेषनागाचे वर्णन आहे. बलरामाने शेवटी शरीर त्याग करून सर्प रूप धारण करून समुद्रात प्रवेश केला असे वर्णन आहे. गीतेत कृष्ण स्वतःला शेषनाग म्हणवितो. अर्थात बलराम पूजेचा संबंध नागपूजेशी आहे असे दिसते. यावरून नागपूजेवर वासुदेव पूजेचा प्रभाव स्पष्ट दिसतो. (पांडे, 1955)

लोकदेवतांचे एकत्रीकरण-महाविलयन होऊन बलराम हे प्रतिक तयार झाले. नाग, भूमिपूजक आणि मद्यप्राशन महत्त्वाचे मानणाऱ्या जमातीच्या समजूती बलरामात एकवटल्या आहेत. मथुरा, उत्तर प्रदेश इत्यादी भागातील काही ठिकाणी बलरामाच्या हातात मद्याचा पेला दिसतो. वैष्णवांनी त्याला शेषनागाचा अवतार म्हणून स्थान दिल्यामुळे तो नागपूजकांचा पूजनीय दैवत बनला. भूमातेची नांगराच्या रूपाने पूजा करणाऱ्या शेतकरी वर्गाला हलधारी बलरामाने दिलासा दिला. विष्णूचा अवतार असणाऱ्या श्रीकृष्णाच्या मोठ्या भावाचा मान त्याला दिला गेला. हरिवंशात श्रीकृष्णासह त्याचेही पराक्रम वर्णिले आहेत.

त्यापैकी एक धेनुकासुरवध कथा होय, गाढवाच्या रूपात आलेल्या असुराला त्याचे मागचे पाय धरून गरगरा फिरविले व ताडाच्या झाडावर उंच भिरकावून दिले. भल्याभल्यांना नमवणारा धेनुकासुर बलरामाने असा लीलया ठार केला. ही कथा विदर्भात अनेक पिढ्या लोकप्रिय असावी. मांडळ आणि पवनारला धेनुकासुरवध करणाऱ्या बलरामाची प्रत्येकी एक प्रतिमा आहे. (कोलते, 1996) मांडळच्या प्रतिमेच मथुरेला सापडलेल्या मूर्तीशी साम्य लक्षणीय आहे. बलरामामागच्या शेषाच्या वेटोळ्याची पध्दत याबाबत अधिक बोलकी आहे. (देगलुकर, 1987) पवनारला धेनुकासुरवधाचे मोठे शिल्प आहे. इथे मध्यप्रदेशातील मंदसोरच्या अशाच धेनुकासुरवधाच्या शिल्पाचा प्रभाव स्पष्ट दिसतो. मांडळ प्रमाणेच या दोन्ही शिल्पात बलरामाचे मागे शेषनाग दिसत नाही. पवनारसारखीच अधिक उठावातली धेनुकासुरवध मूर्ती तळेगाव (दशसहस्र) दशासर इथे आहे. (काळे, 2001)

वराह शिल्प- विष्णूचा तिसरा अवतार वराह रूपात झालेला आहे. वराहावतारात भगवान विष्णुने हिरण्याक्षाला मारून सर्वप्रथम समुद्रतलासी बुडविलेल्या पृथ्वीचा उद्धार केला होता. रामटेक येथे मुख्य मंदिराचे अगोदर प्रचंड अशी वराह मूर्ती आहे. इथे असणारा वराह हा प्राणीसादृश्य असून यालाच 'यज्ञ वराह' अशी संज्ञा आहे. ही मूर्ती प्रभावती गुप्ताने स्थापित केली. यामागे प्रभावतीच्या माहेरचा सार्थ अभिमानच उभा असल्याचे जाणवते. गुप्त घराण वैष्णव



होत. गुप्तानी लोकप्रियता मिळवून ती टिकवण्यासाठी खूप प्रयत्न केले. त्यातलाच एक प्रयत्न म्हणजे वराहाने जशी रसातळाला नेलेली पृथ्वी सामर्थ्याने बाहेर काढली तसाच पराक्रम करून गुप्तानीही धरतीला वाचविले असा संदेश देणाऱ्या वराह अवताराच्या त्यांनी अनेक मूर्ती अनेक ठिकाणी प्रस्थापित केल्या. माहेरचा अभिमान आणि सक्रिय पाठिंबा आपल्याला असल्याचे प्रभावतीला सूचित करायचे असावे. त्यासाठी तिने ही वराहमूर्ती प्रस्थापित केली. या वराह मूर्तीच्या पोटाखालून गेल्यास पापक्षालन होते अशी भावडी समजूत आहे. त्यामुळे भक्तगण या मूर्तीच्या पोटाखालून जाण्याचे कष्ट आजही घेतात. पापपुण्याच्या कल्पनेचा पगडा आजही दिसतो.

नृसिंह :- नृसिंह हा विष्णूचा चवथा अवतार मानलेला आहे. रामटेक येथे नृसिंहाची दोन देऊळे आहे व त्यांत मूर्ती आहेत. नृसिंह पूजा त्याकाळांत प्रचलित झाली होती. रामटेक येथील केवळ नृसिंहाच्या देवळातील मंडपामध्ये प्रभावती गुप्ताच्या मुलीने व मुलाने आईच्या स्मृत्यर्थे केवळ नृसिंहाचे देऊळ बांधले असा खंडीत असलेल्या लेखाचा संदर्भ निघतो. (गोखले, 1958) या मंदिरातील मूर्तीचे नांव त्यांनी 'प्रभावती स्वामिन' असे ठेवले होते. रामटेकला नृसिंहाची दोन देऊळे आहेत. त्यातील नृसिंहाच्या मूर्ती भव्य असून त्यांचे हातात चक्र आहे. दोन्ही मूर्ती सारख्याच आहेत. लक्ष्मणाच्या देवळातील शिलालेखात यासंबंधी पुढीलप्रमाणे उल्लेख आहे.

अतीव तेजः प्रसरप्रतप्तं जगत्समग्रं कृपया ररक्षा।

योऽयं चतुर्थोऽवतरो ऽच्युतस्य श्रीमाननृसिंहोऽपि वसत्यमुष्मिन् ॥

प्रागत्र देवो नृहरिः सुरारेर्बिभेद वक्षः करजैः शिताग्रैः।

तद्रक्तपूरारुणितस्तोऽयं -----U-- UU - U - - - - करजै (मिराशी, 1958)

भगवान विष्णूचा चौथा अवतार नृसिंह हा या गिरीवर राहतो. त्याने कृपावंत होवून आपल्या अत्यंत प्रखर तेजाने पृथ्वीचे रक्षण केले आहे. नृसिंहावतारात भगवान विष्णूने हिरण्यकश्यपूचे वक्षःस्थल आपल्या नखांनी याच पर्वतावर फाडले. त्याच्या रक्ताने हा सर्व पर्वत भरून जाऊन तांबडा लाल झाला असे प्रस्तुत शिलालेखात म्हटले आहे.

रुद्रसेन द्वितीय हा प्रभावतीमुळे विष्णुभक्त झाला होता. त्याचा एकमेव ताम्रपट मांडळ येथे सापडला. त्याच्या मृत्यूनंतर प्रभावती गुप्ताने किंवा तिच्या मुला-मुलीने नृसिंह प्रतिमा उभारलेल्या दिसतात. नृसिंहाप्रमाणे आपला पती पराक्रमी होता हे तिला सुचवायचे होते. तसेच मृत्यूनंतरही तो प्रजारक्षणासाठी सज्ज असल्याचा निर्वाळाच जणू तिला मूर्तीच्या भव्यतेद्वारे द्यायचा होता. ही मंदिरे प्रभावतीच्या त्यागाचे, जिद्दीचे व कुपलत्तेचे प्रतीक होत. नृसिंह मूर्तीचे केवळ, स्थौण गिरीज, लक्ष्मीनृसिंह, विदारण असे विविध प्रकार आहेत. एका मंदिरातील मूर्ती 'केवळ' रूपात दाखविली आहे. दुसरे मंदिर रुद्रनृसिंह म्हणून ओळखले जाते. (मिराशी, 1958)

सिंडरिया, पहावी (जि. जबलपूर) येथील गिरीजा नृसिंह मूर्तीच्या कोरिव कामाचे साम्य रामटेक येथील मूर्तीच्या कोरिव कामाशी आहे. यावरून असे स्पष्ट होते की, कलात्मक मूर्तीकारांचे विदर्भ हे केंद्र होते. वेरूळ येथील नृसिंहाचे शिल्प वाकाटक काळाचेच उदाहरण होय. (त्रिपाठी)

हयग्रीव मूर्ती :- विष्णु अवतार हयग्रीव मूर्ती भंडारा येथील खांबा तलावाकाठी आढळली आहे. ही मूर्ती नागमैपाची वाटते. हयग्रीव हा श्रीकृष्णाचा अवतार असून त्यास हयशीर्ष असेही म्हणतात.

वैदिक साहित्यात हया शीर्षास यज्ञाचा अवतार म्हटले आहे. देवीभागवतात असा उल्लेख आहे. की हयग्रीव असुरास देवीचा वर होता. प्रत्यक्ष भगवतांनी त्याचेच रूप धारण करून त्याला यमसदनी पाठविले, महाभारतातील शांतिपर्वात मधु व कैटभ असुरांचा वध करण्यासाठी श्री विष्णूंनी हयग्रीवाचा अवतार घेतला. असे म्हटले आहे. भंडारा येथील मूर्तीच्या उजव्या हातात असलेले अश्वचे मस्तक हे या मूर्तीचे व्यवच्छेदक लक्षण असून ही मूर्ती हयग्रीवाची



असावी असे मानतात. मूर्तीशास्त्रात ह्यग्रीवाचे अंकन कुषाण काळापासून सुरू झाले. मूर्ती इसवीसन चौथ्या शतकातील असावी. (चितळे, 1989) परंतु ही पूजनिय देवता मानली जात नाही.

त्रिविक्रम (वामन) :- वामन हा विष्णूचा पाचवा अवतार मानल्या जातो. गाथासप्तशतीतील ४०६ व्या गाथेत वामनाचा उल्लेख आहे. वामनाने आपल्या वचनात बळी राजाला बांधून घेतले होते. तिन्ही लोकांचा विजय संपादन करणाऱ्या बळीला तीन पावलांची जागा मागून पाताळात बंदिस्त करण्याच्या वामनाबद्दल देवांना आदर होता. त्यामुळे देव आनंदित होवून त्यांनी वामनरूपी हरीचा जयजयकार केला असे वर्णन आहे. तसेच ४११ व्या गाथेत वामनाच्या त्रिविक्रमरूपाचा उल्लेखही केला आहे. (भुसारी, 1979) रामटेकला उत्तरेकडच्या-टेकडीवर त्रिविक्रमाचे देवालय आहे. ते अतिशय वैशिष्ट्यपूर्ण आहे. हे देवालय वाकाटककालीन आहे. (मिराशी, 1957) त्रिविक्रमाची मूर्ती वामन अवताराची मूर्ती होय.

भोगराम : रामटेक येथे भोगरामाचे मंदिर आहे. (मिराशी, 1958) वराह मंदिरापुढे गेले असता डावीकडे भोगरामाचे पूर्वाभिमुख मंदिर लागते. या भोगरामाचे वर्णन तेथीलच शिलालेखात केले आहे.

श्रीभोगरामभिरामतुनं निरीक्ष्य

क्षीणाखिलावसरणिः शरणे मुरारे ।

भोगानभंगुरसोन्सुचिरं विचित्रान-

प्राप्नोति कल्पशतमल्पितदेवराजः ॥

(श्री भोगरामाचे सुंदर रूप पाहिल्यावर मनुष्याची सर्व पातके नष्ट होऊन तो साक्षात इंद्रापेक्षाही अधिक अशा विविध प्रकारच्या चिरकालीन भोगांचा अनुभव शेकडो कल्पापर्यंत विष्णू लोकांत घेत असतो. (मिराशी, 1958) रामावतारांचीच ही थोडी वेगळी अभिव्यक्ती होय. रामावतार हा जनमान्य झाला होता.

कपटराम : गुप्त राम : रामटेक महात्म्यात रामटेक सोबतच नंदीवर्धन गावातील तीर्थाचा उल्लेख आढळतो रामटेक येथे रुद्रनृसिंह, केवलनृसिंह, वराह, त्रिविक्रम, कपट राम, भोगराम यांची मंदिरे आहेत. कपटम मंदिर हे गुप्त वाकाटक काळातील मंदिर आहे. (बोरकर, 1997)

रामटेक येथे गुप्तरामाचे देवालय आहे. याचे वर्णन रामटेकच्या शिलालेखात येते.

दृष्ट्वा दृष्ट्वा प्रकृष्टमहिमानमनन्तभक्त्या

तं गुप्तराममतिगुप्तपदं च किंचित् A

प्राप्नोति यत्तदिह किं ननु देवराजो

-- u - uuu - uu - u -- AA

जोडमूर्ती :- याशिवाय याच काळात महाराष्ट्रात अन्यत्र आढळणाऱ्या आणखी काही प्रकाराच्या मूर्तींचा उल्लेख येथे करता येईल. त्यांना जोडमूर्ती म्हणता येईल किंवा मिश्रमूर्ती म्हणता येईल. उदाहरणार्थ हरिहर, अर्धनारीनटेश्वर, ब्रह्मेशानजनार्दनार्क इत्यादी मूर्ती याप्रकारात मोडतात. या मूर्ती म्हणजे समन्वयी विचारसरणीचे उत्तम उदाहरण म्हणता येईल, शिव, विष्णु त्याचप्रमाणे पुरुष प्रकृती आणि ब्रह्मा, शिव, विष्णु व सूर्य यांच्या मिश्रमूर्ती त्यांच्यात द्वैत नाही असे दाखविण्यासाठी निर्माण केल्या गेल्या असाव्यात. (देगलुकर, 1987)

शैवपंथ, वैष्णवपंथ, शाक्तपंथ हे प्रमुख पंथ उदयाला आलेत व त्यांचेही अनेक उपपंथ तयार झाले. वाकाटक काळात शैवपंथाचे प्राबल्य असल्याचे दिसून येते. यावरून सातवाहन कालीन समाजात शैव धर्म व शिव पूजा रूढ असावी असे दिसते. वाकाटक काळातही लिंगपूजा सर्वमान्य झाली होती असे उत्खननात प्राप्त पुराव्यावरून स्पष्ट



दिसून येते. लिंगोदभूव शिवमूर्तीचे अंकन मेरु येथील दशावतार लेणे (क्र. १५), कैलास लेणे (क्र. १६), यात आलेले आहे.  
" मांडळ येथील उत्खननात ब्रह्माची मूर्ती मिळाली आहे.

सारांश :-विष्णूच्या अवतारांची प्रतिष्ठा :- वाकाटक काळापर्यंत भगवान विष्णूच्या अवतारांची कल्पना लोकमनात रूढ झाली होती व अवतार प्रतिष्ठीत झाले होते. वाकाटक काळात विष्णूवतारांची पुजाविधी सुरु झाली असावी. तसेच विष्णूवतारांची देवालये निर्मितीमुद्दहा सुरु झाली होती. वाकाटक कालीन अनेक मूर्ती उत्खननांत प्राप्त झाल्यावरून असे मत मांडता येईल.

संदर्भ ग्रंथ :-

- 1.केतकर, व्य. गो. : महाराष्ट्र ज्ञानकोश प्रस्तावना खंड-४, भुसारी आर. एम : प्रचीन महाराष्ट्राचा धार्मिक इतिहास, (इ.स. पूर्व 208 ते इ.स. 1550) प्रथम आवृत्ती, 1965 साहित्य परिषद : हैद्राबाद 1992, पृ. ८४.
- 2.देगलुकर, गो.व. : विदर्भ संशोधन मंडळ, प्रभा १९८७.
- 3.Shastri, A. M. (Ed.): New Vakataka Inscriptions (The Age of the Vakataka), Harman Publishig House; 1992 New Delhi, p. 288, 229.
- 4.Bajpei, K. D. : Location of Ramgiri of Kalidas (Ed. Shastri, A.M. : The Age of the Vakataka) p. 90.
- 5.जोशी, नि. पु. : भारतीय मूर्तीशास्त्र, प्रथम आवृत्ती 1979, कुळकर्णी ज.आ प्रकाशन, पुणे, पृ. ७७.
- 6.देशपांडे, ब्राम्हानंद : शोधामुद्रा खंड-२, द्वितीय आवृत्ती, 1996, कैलास पब्लिकेशन; औरंगबाद, पृ. ३०.
- 7.मिराशी, वा.शि. : वाकाटक नृपती आणि त्यांचा काल, 1957, नागपूर विश्वविद्यालय नागपूर, पृ. २७७.
- 8.पट्टन ताम्रपट, (पूर्वोक्त) पृ. २८२
- 9.मिराशी, वा. वि. कालिदास, तिसरी आवृत्ती, 1975, महाराष्ट्र राज्य साहित्य संस्कृती मंडळ; मुंबई, पृ. ४६
10. मिराशी, वा.वि. संशोधन मुक्तावली, सर ६, प्रथम आवृत्ती, 1972 विदर्भ संशोधन मंडळ; नागपूर, पृ.४६.
11. मिराशी, वा.वि. संशोधन मुक्तावली, सर ६, प्रथम आवृत्ती, 1972 विदर्भ संशोधन मंडळ, नागपूर, पृ. ४७.
12. बाजपेयी, कृष्णदत्त डि. : ऐतिहासिक भारतीय अभिलेख, अभिलेख खंड-१ पब्लिकेशन स्क्रीन प्रथम संस्करण, 1992 जयपूर, पृ. ४७.
13. ऋध्दपूर ताम्रपट ओळ-१ (मिराशी, वा.वि. : वाकाटक नृपती आणि त्यांचा काल), पृ. २३९.
14. पुणे ताम्रपट ओळ-१४ (पूर्वोक्त), पृ. १९२.
15. पूर्वोक्त, ओळ, ६-७.
16. मिराशी, वा.वि. संशोधन मुक्तावली, सर-९, पृ. १६९.
17. मिराशी, वा.वि. संशोधन मुक्तावली, सर-९, पृ. १६६.
18. आपटे, शि.वा. : संस्कृत हिंदी कोश, पृ. ७२७.
19. मिराशी, वा.वि. संशोधन मुक्तावली, सर-९, 1979. विदर्भ संशोधन मंडळ: नागपूर. पृ. १६६.
20. मिराशी, वा.शि. : वाकाटक नृपती आणि त्यांचा काल, पृ. १३४, १३५.
21. Mujudar, R.C. : The Classical Age] 1970 Bharatiya Bhavan; Bombay, Vol. III] p. 184.
22. मिराशी, वा.वि. संशोधन मुक्तावली, सर-९, पृ. १०४.
23. बोरकर, र.रा. : विदर्भातील पुरतत्वीय उत्खनन संशोधन पर लेख
24. चितळे, श्रीपाद : दैनिक लोकसत्ता २७/५/९८ मनसर जागतिक पुरातत्वीय नकाशावर
25. मिराशी, वा.शि. : वाकाटक नृपती आणि त्यांचा काल, पृ. २३५.
26. पुणे ताम्रपट ओळ-१४ (पूर्वोक्त), पृ. १९२.



27. इंदुर ताम्रपट ओळ-२० (पूर्वोक्त), पृ. २४९.
28. मिराशी, वा.शि. : वाकाटक नृपती आणि त्यांचा काल, पृ. १०४.
29. मेघदू श्लोक १२.
30. मिराशी, वा.शि. : मेघदुतातील रामगिरी अर्थात रामटेके, प्रथम आवृत्ती 1958 विदर्भ संशोधन मंडळ ; नागपूर, पृ. ९४, ९६.
31. चतुर्वेदी, सिताराम : कालिदास ग्रंथावली, प्रथम संस्करण सवंत, 2001, अखिल भारतीय विक्रम परिषद ; काशी, पृ. २८९.
32. मिराशी, वा.वि. : कालिदास, पृ. १२७, १२९.
33. पूर्वोक्त पृ. १२८.
34. भूसारी, आर.एम.: आद्य महाराष्ट्र आणि सातवाहन काल, प्रथम आवृत्ती 1979, सहित्य परिषद; हैद्राबाद, पृ. १३२.
35. मिराशी, वा.शि. : वाकाटक नृपती आणि त्यांचा काल, पृ. १३१, १३५.
36. पूर्वोक्त, पृ. १०९.
37. पांडे, चंद्रभान : आद्य सातवाहन साम्राज्य का इतिहास, पृ. १३१, १३५.
38. भूसारी, आर.एम.: आद्य महाराष्ट्र आणि सातवाहन काल, पृ. १११.
39. भूसारी, आर.एम.: आद्य महाराष्ट्र आणि सातवाहन काल पृ. ११३.
40. पूर्वोक्त, पृ. ११४.
41. मिराशी, वा.वि. : संशोधन मुक्तावली, सर-६, पृ. ३०.
42. चतुर्वेदी सिताराम : कालिदास ग्रंथावली, पृ. २९०.
43. पांडे, चंद्रभान : आद्य सातवाहन साम्राज्य का इतिहास, पृ. १३६.
44. कोलते, वि.भी. : प्राचीन विदर्भ व आजचे नागपूर, प्रथम आवृत्ती, 1996, अमरावती विद्यापीठ; अमरावती, पृ. १३०.
45. देगुलकर, गो. व. : विद्वध प्रज्ञा १९८७, पृ. ५०.
46. काळे, भाग्यश्री पाटसकर, दैनिक लोकसत्ता १६/२/२००१.
47. गोखले, शोभना : महाराष्ट्र इतिहास आणि संस्कृती पर्यालोचन.
48. मिराशी, वा.वि. मेघदुतातील रामगिरी अर्थात रामटेक, प्रथम आवृत्ती, 1958 विदर्भ संशोधन मंडळ ; नागपूर, पृ. ६.
49. मिराशी, वा.वि. मेघदुतातील रामगिरी अर्थात रामटेक, पृ. ६.
50. त्रिपाठी, रमाकांत : उत्तरमचरीत चतुर्थ संस्करण १९९९, पृ. १२४.
51. चितळे, भी.के. : विदर्भ संशोधन मंडळ ; वार्षिकांक १९८९, पृ. १५४, १५५.
52. भूसारी, आर.एम.: आद्य महाराष्ट्र आणि सातवाहन काल, पृ. ११५.
53. मिराशी, वा.शि. : वाकाटक नृपती आणि त्यांचा काल, पृ. १३१, १३२.
54. मिराशी, वा.वि. मेघदुतातील रामगिरी अर्थात रामटेक, पृ. १०.
55. पूर्वोक्त
56. बोरकर, र.रा. रामटेक, प्रथम आवृत्ती, 1997 उन्मेष प्रकाशन, नागपूर, पृ. २८, २९.
57. देगुलकर, गो. व. : महाराष्ट्र संस्कृती एक पर्यालोचन, पृ. २१५.





## **COVID 19 impacts on woman with Poly Cystic Ovary Syndrome on their pre-existing mental health issues in Vidarbha:Thematic Study**

**Apeksha Bandebuche**  
Research Scholar(Psychology)  
VidyaBharati Mahavidyalaya,  
Amravati.

**Dr. D. S. Ramteke**  
(M.A., Ph.D.)  
Professor,Department of Psychology  
Vidya Bharati Mahavidyalaya,  
Amravati.

### **Abstract-**

Background COVID-19 Pandemic has far reaching psychosocial implications for chronic health conditions. This is a qualitative study which captured the live experiences of women with PCOS during COVID 19 related lockdown. Woman with PCOS are predisposed to severe cardio-metabolic risk factors which increase the susceptibility to severe COVID-19 and also exhibit increased likelihood of impaired mental health wellbeing.

### **Purpose-**

This study is a review related to exploring the experience of mental Health.in1st national Lockdown on woman with PCOS.

### **Method-**

Cross section study of 15 women with PCOS living in Maharashtra in COVID 19 lockdown recruited to qualitative study. Telephone interview conducted and data subjected to thematic study.Resulting this 5 themes are focused which normal PCOS woman faces through experience.

- 1) My PCOS Journey
- 2) Living through Lockdown with PCOS
- 3) Self care and managing system with PCOS during lockdown.
- 4) Health care on hold: releases uncertainty and anxiety associated withit.
- 5) Exacerbating pre-Existing Issues,  
- worsening of pre-existing mental health issues increases anxiety and isolation.

### **Conclusion-**

This Thematic study for the woman with PCOS in pandemic and first National lockdown was mostly experienced as adding to pre-existing challenges of living with their conditions.

**Keywords.**COVID-19, PCOS, lockdown

### **1. Introduction.**

In March 2020, the World Health organization called on all countries to take action against the COVID-19 pandemic and social isolation implied all over... (1) Based on clinical evidence, it is clear that, in addition to older age and male sex, susceptibility to severe COVID-19 is directly associated with a number of chronic cardio-metabolic diseases- such as obesity, diabetes, hypertension and metabolic syndrome. [2,3] of note, with exception of advance age and male sex; The same cardio metabolic risk factor which are predisposing factor to COVID-19 prevalent among women with PCOS[5,6]Due to which this woman were highly risk factor during COVID-19 pandemic (7)

Prominent features of PCOS include ovarian dysfunction with chronic oligo anovulation and hyperandrogenism. (5, 6, 8) with rottenburg phenomene of PCOS. (18.)To date, despite high prevalence of PCOS and potentially high risk of these patients for severe COVID-19 (7, 14, 15). There is paucity of research on potential effect of COVID- 19 pandemic and related lockdown quarantine measures on this female population. As such, the objective of present study was to capture unique patient experiences of woman with PCOS during pandemic lockdown.By obtaining novel qualitative data addressing research question of what PCOS females experience during pandemic, lockdown condition with her physio-psycho changes.

In overall these all changes collectively described in five themes living throughCOVID 19 pandemic and lockdown as woman with PCOS.

### **2. Review of Literature**

The qualitative study of keegan et al (2003) conducted semi structural interviews with women with PCOS in which women were asked about self image and women used word themselves as disgusting. They shows self-esteem value about themselves much below. Average one third women



reported conspicuous hair growth on their faces always in their mind and they check themselves frequently in mirror.

This includes frustration with primary care services including late diagnosis this includes frustration with primary care services including late diagnosis [19], difficulties accessing treatment and lack of support from healthcare professional's post-diagnosis [18]. As other research has also found, the study participants described significant and enduring difficulties in losing/managing body weight [18], as well as a wide range of mental health issues and detrimental impacts on relationships, work and social lives [16]. Most notably, in line with prior research findings, the participants in this study also described feeling isolated and different from other women [16,17] before being physically isolated by restrictions on social contact.

In literature review of Keegan et al (2003) psychological analysis and according Jahonfar et al (1995) psychological distress reduce motivation and life satisfaction and increases anxiety.

### **3. Material and Methods**

#### **3.1. Study Design**

This is qualitative interview online cross sectional study which done to see a range of physical and psychological effects of COVID-19 pandemic on woman with PCOS (13). Its done to provide further insight into experience of living with PCOS during pandemic and its association restrictions.[14]

#### **3.2. Study Participants**

For present study, 15 woman taken who was previously diagnosed with PCOS. Age of participants were 24 to 42 years, ranged BMI between 22.6 to 53.6 kg/m<sup>2</sup>.

#### **3.3. Procedure**

It taken by online study survey consent of participant taken details of participants who are part of the interviews. It is done alone using survey software Qualtrics XM.

#### **3.4. Data collection**

Telephone interviews are suited to qualitative studies where primary aim to gather more detailed data pertaining to topic exploration quantitatively (20).

#### **3.5. Data Analysis**

Data imported into Nvivo and analyzed being process of inductive thematic analysis, following principal outlined by Braun and Clarke (14).

### **4. Results.**

As it is a thematic analysis research methodology, five main themes are derived.

#### **1) My PCOS Journey**

Here mentioned broad spectrum symptoms of PCOS include absent irregular / heavy / painful periods. Increase body weight, acne, excess hair growth, uncontrolled emotions, low mood depression. Women frequently identified their weight, acne and hair growth as causes of the far-reaching psychological and social aspects of having PCOS, including low self-esteem, low sex drive and challenges with socializing or relationships. This was in addition to experiencing low mood and heightened emotions. As a result, many participants described how the accumulation of symptoms of PCOS had a significant detrimental and enduring effect on their mental health.

#### **2) Living through Lockdown 1**

As all things stuck down, PCOS women feel more restricted in the family and their symptoms increase make them more helpless. That increase stress level, poorer sleep and more about conditions.

#### **3) Self-care and managing symptoms**

This includes PCOS women's restrictions to manage their PCOS symptoms and self care. As hair growth not controlled due lack of saloons, weight control diminished as lack of Gym, which makes them more anxious about their illness.

#### **4) Healthcare on Hold.**

Participants described experiencing reduced access to healthcare professionals and services during the COVID-19-related lockdown. This included access to their usual clinicians, as well as delays to services they were waiting to receive pre-pandemic. Both of these experiences were sources of significant anxiety and distress for these women, delaying them from further understanding and overcoming/managing their symptoms.



- MC. Trottier A, Baillargeon JP. Insulin and hyperandrogenism in women with polycystic ovary syndrome. *J Steroid Biochem Mol Biol*2010;122:42–52.
4. Benson S, Hahn S, Tan S, et al. Prevalence and implications of anxiety in polycysticovary syndrome: results of an internet-based survey in Germany. *Hum Reprod*2009;24:1446–51.
5. Kyritsi, E.M.; Dimitriadis, G.K.; Kyrou, I.; Kaltsas, G.; Randeve, H.S.PCOS remains a diagnosis of exclusion: A concise review of keyendocrinopathies to exclude 5-Conaglen HM, Conaglen JV. *Sexual desire in women presenting for antiandrogenotherapy. J Sex Marital Ther* 2003;29:255–67.
6. Kyrou, I.; Weickert, M.O.; Randeve, H.S. Diagnosis and Management of Polycystic Ovary Syndrome (PCOS). In *Endocrinology and Diabetes: Case Studies, Questions and Commentaries*; Ajjan, R., Orme, S.M., Eds.; Springer:London, UK, 2015; pp. 99–113..
7. Elsenbruch S, Hahn S, Kowalsky D, et al. Quality of life, psychosocial well-being, and sexual satisfaction in women with polycystic ovary syndrome. *J Clin Endocrinol Metab* 2003;88: 5801–7.
8. The Rotterdam ESHRE; ASRM-Sponsored PCOS Consensus Workshop Group. Revised 2003 consensus on diagnostic criteria and long-term health risks related to polycystic ovary syndrome. *Fertil. Steril.*2004, 81,
9. Hahn S, Janssen OE, Tan S, et al. Clinical and psychological correlates of quality-of-life in polycystic ovary syndrome. *Eur J Endocrinol* 2005;153:853–60.
10. Keegan A, Liao L-M, Boyle M. 'Hirsutism': A Psychological Analysis. *J Health Psychol* 2003;8(3):327–45.
11. Kitzinger C, Willmott J. The thief of womanhood: women's experience of polycystic ovarian syndrome. *Soc Sci Med* 2002;54: 349–61
12. Lechner L, Bolman C, van Dalen A. Definite involuntary childlessness: associations between coping, social support and psychological distress. *Hum Reprod*2007;22:288–94.
13. Library, Vidya Bharti Mahavidyalay.
14. Library, Government Vidarbha Institute Science and Humanity (GVISH).
15. Lipton MG, Sherr L, Elford J, et al. Women living with facial hair: the psychological and behavioral burden. *J Psychosom Res* 2006;61: 161–8
16. Oddens BJ, den Tonkelaar I, Nieuwenhuys H. Psychosocial experiences in women facing fertility problems—a comparative survey. *Hum Reprod* 1999;14:255–61.
17. Braun, V.; Clarke, V. Using thematic analysis in psychology. *Qual. Res. Psychol.* 2006, 3, 77–101. [CrossRef].
18. Pfaff, K.A.; Baxter, P.E.; Jack, S.M.; Ploeg, J. Exploring new graduate nurse confidence in interprofessional collaboration: A mixed methods study. *Int. J. Nurs. Stud.* 2014, 51, 1142–1152. [CrossRef]
19. Musselwhite, K.; Cuff, L.; McGregor, L.; King, K.M. The telephone interview is an effective method of data collection in clinical nursing research: A discussion paper. *Int. J. Nurs. Stud.* 2007, 44, 1064–1070. [CrossRef][PubMed]
20. Braun, V.; Clarke, V. Using thematic analysis in psychology. *Qual. Res. Psychol.* 2006, 3, 77–101.
21. Polivy J, Herman CP. Causes of eating disorders. *Annu Rev Psychol*2002;53:187–213.
22. hael FJ, Rodin DA, Peattie A. Ovarian morphology and insulin sensitivity in women with bulimia nervosa. *Clin Endocrinol* 1995; 43:451–5.
21. Rassi A, Veras AB, Peis M, et al. Prevalence of psychiatric disorders in patients with polycystic ovary syndrome. *Compr Psychiat* 2010; 51:599–602
22. Yazici K, Baz K, Yazici AE, et al. Disease-specific quality of life is associated with anxiety and depression in patients with acne. *J Eur Acad Dermatol* 2004;18:435–9.
23. Weiner CL, Primeau M, Ehrmann DA. Androgens and mood dysfunction in women: comparison of women with polycystic ovarian syndrome to healthy controls. *Psychosom Med* 2004;66: 356–62.

# Biometric Authentication & It's Security Purposes

<sup>1</sup>Prof. S.B.Bele, <sup>2</sup>Sakshi R. Bherde, <sup>3</sup>Atharva U. Wadalkar, <sup>4</sup>Sakshi R. Deshmukh

<sup>1</sup>Assistant Professor, Department of MCA, Vidya Bharati Mahavidyalaya, Amaravati, India

<sup>2,3,4</sup>Student, Department of MCA, Vidya Bharati Mahavidyalaya, Amaravati, India

**Abstract - Trusted user authentication is becoming an increasingly important function in a web-enabled world. The effect of an unsecure authentication system in a corporate or enterprise environment can be prosperous and can include dropping of confidential information, rejection of service, and compromise of data integrity. The value of trusted user authentication is not limited to computer or network access. Many other applications in daily life also require user authentication, such as banking, e-commerce, and can benefit from physical access control and enhanced security to computer resources.**

**Keywords:** Biometric, Pattern, Iris, Authentication, Security, Sensors.

## 1. Introduction

Password less authentication plays an important role in improving this situation. By leveraging the unique physical characteristics of individuals to establish their identity, it provides unparalleled security. It locks sensitive, critical information behind the scenes of your fingerprints, iris patterns, facial features, voice patterns, and behavioral patterns like keystroke dynamics. Biometric systems can be deployed in applications ranging from physical authorization and time attendance systems to mobile devices and online transactions. This compatibility enables organizations to apply tighter security measures across multiple touch points, protecting sensitive data and assets.

## 2. Applications of Biometric Authentication

### A) Lawful Applications

**Justice and Law Enforcement:** Biometric technology and law enforcement have a long history, and many important variations in identity management have arrived from this beneficial relationship. Biometrics implemented by the police force today is truly multimodal. Fingerprint, face and voice recognition play a unique role in improving public safety and tracking the people we are looking for.

### B) Government Applications

**Border Control and Airports:** A major area of application for biometric technology is at the boundary. Biometric technology helps automate the boundary crossing process.

Reliable and automated passenger screening initiatives and automated SAS help simplify the international passenger travel experience while improving the efficiency of government agencies and keeping borders more secure than ever.

### C) Health Care Applications

In the healthcare sector, biometrics presents an enhanced model. Medical records are one of the most valuable personal documents; Doctors need to access them quickly and accurately. Lack of privacy and good computing can make the difference between timely and error free detection and health fraud.

### D) Commercial Applications

*Privacy:*

As connectivity spreads across the globe, it's clear that old security methods aren't strong enough to protect what matters most. Fortunately, biometric technology is more accessible than ever, poised to provide added security and convenience for everything from car doors to phone PINs that need to be protected.

*Finance:*

Biometric technology is widely used in finance to enhance security and convenience. By using unique biometric characteristics like fingerprints, iris, voice, and face, customers can securely access their financial data. These biometric modalities, used alone or in combination, help protect against fraud and ensure that the person accessing the account is the authorized user.

*Eyes Movement Applications:*

Eye movement tracking applications have various uses in different industries. In the automotive industry, tracking a driver's eye movements can help measure sleepiness or drowsiness. Screen navigation applications use eye tracking to assist people with disabilities in scrolling web pages or performing actions on computers or mobile devices. In aviation, eye and head movement tracking in flight simulators can analyze pilot behavior and serve as a training tool for new pilots.

#### E) Screen Navigation

Screen navigation applications that track eye movements are indeed crucial for people with disabilities. By using cameras, these applications enable individuals to scroll web pages, write text, and perform actions on computers or mobile devices simply by clicking on buttons. This technology has been gaining significant attention due to the rapid development and the increasing demand for new methods of screen navigation, particularly on mobile devices platforms. It's exciting to see how this innovation is improving accessibility for individuals with disabilities.

#### F) Aviation

Flight simulators track the pilot's eye and head movement to analyze their behavior in realistic scenarios. This helps evaluate their performance based on eye movements and other information. It's also a valuable training tool for new pilots, encouraging them to regularly monitor airplane indicators on the primary flight display (PFD). It's fascinating how technology aids in pilot training and enhances aviation safety.

### 3. Security Needs for Biometric Authentication

According to research papers, security is crucial for biometric authentication due to the following reasons: Non-repudiation: Biometric authentication provides a unique and personal identifier for individuals, making it difficult to deny their actions or presence. Difficult to replicate: Biometric traits, such as fingerprints or iris patterns, are difficult to replicate, making it challenging for unauthorized individuals to gain access. Enhanced protection: Biometric data is stored in encrypted form, adding an extra layer of protection against unauthorized access. Reduced reliance on passwords: Biometric authentication reduces the reliance on traditional passwords, which can be easily forgotten, guessed, or stole.

Continuous authentication: Biometric authentication can provide continuous authentication, ensuring that the authorized user remains present throughout the session. Overall, research emphasizes the importance of security in biometric authentication to protect sensitive data and ensure the integrity of the authentication process.

### 4. Simple Biometric System Architecture

#### A) Sensor

The sensor is the first block of the biometric system which gathered all the crucial data for biometrics. It is the interface between the system and the natural world. Basically, it is an image acquisition system, but it also depends on the peculiarity or characteristics required that it has to be restore or not.

#### B) Pre-Processing

The second block in a biometric system performs pre-processing tasks. Its function is to increase the input and cancel artifacts from the sensor, background noise, etc. It also performs some kind of normalization to prepare the data for further analysis. It is the second block that executes all the pre-rectifying. Its function is to increase the input and to cancel artifacts from the sensor, background noise, etc. It performs some kind of normalization.

#### C) Feature Extractor

The third step in a biometric system is indeed the most important one. It involves extracting features to identify them later on. The goal of a characteristic extractor is to characterize an object using calculation for recognition.

#### D) Template Generation

The template generator plays a crucial role in the biometric system. It generates templates using the extracted features for authentication. These templates can be in the form of a vector of numbers or an image with distinct characteristics. They are stored in the database for differentiates and serve as input for similar.

#### E) Matcher

The matching phase involves using a matcher to compare the acquired template with the stored templates. Various algorithms like Hamming distance are used for this comparison. Once the inputs are matched, the results are generated.

#### F) Application Device

An application device is a device that utilizes the results of a biometric system. Examples of such devices include the Iris recognition system and facial recognition system. They make use of biometric data for identification and authentication purposes.

### 5. Research

In biometric authentication, research methodology involves conducting studies to understand and improve the accuracy and reliability of biometric systems. Researchers start by selecting a specific biometric modality, such as fingerprint, iris, or face recognition. They collect a large dataset of biometric samples from individuals to create a training set. Next, researchers develop algorithms and models to extract unique features from the biometric samples. These features are then used to create templates or reference points

for each individual. The templates are stored securely in a database.

### A) Data overload & accuracy

Data overload and accuracy are important considerations in biometric authentication. When it comes to data overload, it refers to the situation where a large amount of biometric data is collected and processed. This can pose challenges in terms of storage, processing power, and efficiency. It's crucial to strike a balance between collecting enough data for accurate identification and authentication, while also considering the limitations of the system.

In terms of accuracy, biometric authentication systems strive to achieve high levels of precision and reliability. However, it's important to note that no system is perfect and there can be instances of false positives or false negatives. Factors such as environmental conditions, variations in biometric traits, and quality of sensors can impact accuracy. Continuous research and advancements in algorithms and technologies aim to improve the accuracy of biometric authentication systems.

### B) How Biometric authentication help in Security purposes

- Biometric authentication enhances security by using unique physical or behavioral traits for identification.
- These traits, such as fingerprints, iris patterns, or facial features, are difficult to replicate, making it harder for unauthorized individuals to gain access.
- Biometric data is more secure than traditional methods like passwords, as it is inherently tied to the individual and cannot be easily forgotten or stolen.

### C) Biometric System Architecture

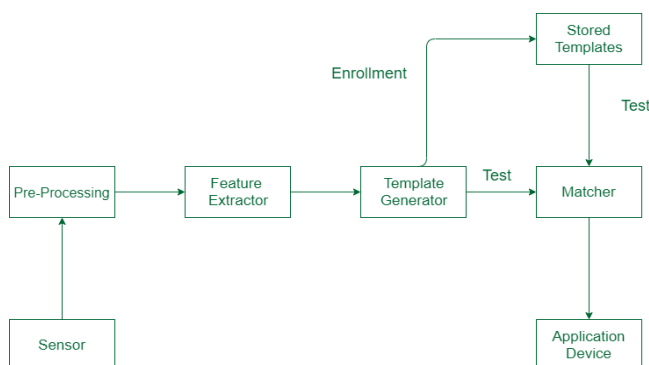


Figure 1: Biometric System Architecture

### D) Research Methodology

In biometric authentication, researchers follow a systematic research methodology. They start by selecting a specific biometric modality, like fingerprint or face

recognition. Then, they collect a dataset of biometric samples and develop algorithms to extract unique features. These features are used to create templates for each individual. Researchers evaluate the system's performance using testing protocols and metrics like False Acceptance Rate and False Rejection Rate. Statistical analysis is done to analyze the results and improve the system.

### E) Discussion

Biometric authentication is a fascinating field that offers secure and convenient ways to verify one's identity. It utilizes unique physical or behavioral characteristics, such as fingerprints, iris patterns, or facial features, to authenticate individuals. This technology has numerous applications, from unlocking smartphones to accessing secure facilities. It provides a higher level of security compared to traditional methods like passwords or PINs, as biometric traits are difficult to forge or replicate. However, it's important to address privacy concerns and ensure that biometric data is securely stored and used ethically. Overall, biometric authentication is an exciting field with promising advancements in enhancing security and user experience.

### F) Future Scope

The future scope of biometric authentication looks promising. Advancements in technology will likely lead to more accurate and reliable biometric systems. We can expect improvements in areas such as multi-modal biometrics, where multiple biometric traits are combined for enhanced security. Additionally, research and development will focus on addressing challenges like spoofing attacks and ensuring the privacy and security of biometric data. Biometric authentication will continue to find applications in various industries, such as banking, healthcare, and travel, providing convenient and secure ways to verify identity it's an exciting field with ongoing innovation and potential for widespread adoption.

## 6. Result

Biometric authentication provides secure and convenient identity verification using unique physical or behavioral characteristics. It offers a higher level of security differentiated to traditional methods like passwords. Advancements in technology continue to improve biometric systems, making them more accurate and reliable. It has various applications in industries such as banking, healthcare, and travel. Overall, biometric authentication has proven to be a successful and effective method of ensuring secure access.

## 7. Conclusion

Biometric authentication is a secure and convenient method of verifying one's identity using unique physical or behavioral characteristics. It offers a higher level of security differentiated to traditional methods like passwords. Advancements in technology continue to improve biometric systems, making them more accurate and reliable. Biometric authentication has found applications in various industries, providing secure access to sensitive information and facilities. It is a promising field with ongoing innovation and potential for widespread adoption.

## REFERENCES

[1] <https://www.seminaronly.com/computer%20science/Bio-metrics%20Based%20Authentication%20Problem.php>

- [2] <https://www.intechopen.com/chapters/65920>
- [3] <https://www.geeksforgeeks.org/what-is-biometrics/>
- [4] [https://www.researchgate.net/publication/46189709\\_Biometric\\_Authentication\\_A\\_Review](https://www.researchgate.net/publication/46189709_Biometric_Authentication_A_Review)
- [5] [https://link.springer.com/chapter/10.1007/1-84628-064-8\\_1](https://link.springer.com/chapter/10.1007/1-84628-064-8_1)
- [6] <https://www.mastercard.com/news/perspectives/2022/brazil-biometric-verification/?cmp=202>
- [7] <https://www.ijert.org/review-paper-on-biometric-authentication>
- [8] <https://www.javatpoint.com/iot-healthcare>

### Citation of this Article:

Prof. S.B.Bele, Sakshi R. Bherde, Atharva U. Wadalkar, Sakshi R. Deshmukh, "Biometric Authentication & It's Security Purposes" Published in *International Research Journal of Innovations in Engineering and Technology - IRJIET*, Volume 7, Issue 10, pp 290-293, October 2023. Article DOI <https://doi.org/10.47001/IRJIET/2023.710037>

\*\*\*\*\*



ISSN(online): 2581-3048

Impact Factor : 5.95

## CERTIFICATE OF PUBLICATION

# INTERNATIONAL RESEARCH JOURNAL OF INNOVATIONS IN ENGINEERING AND TECHNOLOGY

*Is Hereby Awarding this Certificate to*

**Prof. S.B.Bele**

Assistant Professor, Department of MCA, Vidya Bharati Mahavidyalaya,  
Amaravati, India

*In Recognition of the Publication of Manuscript Entitled*

## **Biometric Authentication & It's Security Purposes**

*Published in International Research Journal of Innovations in  
Engineering and Technology (IRJIET)*

**Volume 7, Issue 10, pp 290-293, October-2023**

<https://doi.org/10.47001/IRJIET/2023.710037>

**Manuscript ID :** IRJIET710037

**Date of Issue :** October 30, 2023



Editor-In-Chief  
IRJIET

Managing Editor  
IRJIET

Mail us at: [editor@irjiet.com](mailto:editor@irjiet.com) / [irjietjournal@gmail.com](mailto:irjietjournal@gmail.com)

Journal Website : [www.irjiet.com](http://www.irjiet.com)



# Comparative Analysis of Robotic Operating Systems

<sup>1</sup>Prof. S.B.Bele, <sup>2</sup>Prasad Katyarmal, <sup>3</sup>Swaraj Gangane, <sup>4</sup>Komal Thakare, <sup>5</sup>Tasmeeya Sheikh

<sup>1</sup>Professor, Department of MCA, Vidya Bharati Mahavidyalaya, Amravati, India

<sup>2,3,4,5</sup>Student, Department of MCA, Vidya Bharati Mahavidyalaya, Amravati, India

**Abstract - The Robot Operating System (ROS) comprises a collection of software libraries and tools utilized for constructing robotic systems, distinguished by its distributed and modular design. Within the context of ROS, task planning pertains to the arrangement of actions into a structured sequence aimed at achieving predefined objectives, all while striving to minimize associated costs, whether in terms of time or energy consumption. Task planning assumes critical importance when guiding the actions of a robotic agent, particularly in scenarios where a causal sequence could potentially lead the agent into a deadlock situation. Furthermore, task planning finds utility in less restrictive environments, contributing to the delivery of more intelligent and adaptive robotic behavior. This paper introduces the ROSPLAN framework, an architectural solution designed to seamlessly integrate task planning into ROS-based systems. It presents a comprehensive overview of this framework.**

**Keywords:** Robotic Operating Systems (ROS), Simulation, Unity3D, SLAM, Real-time Robotics Operating Systems, Robotics Development Platforms.

## 1. Introduction

Developing software for robots is a complex task due to the varying hardware of different robots and the overwhelming amount of code required. Robotics software architectures must facilitate large-scale software integration efforts. The integration of task planning and robotics presents several challenges, including generating an initial state that aligns with current environmental conditions, transforming actions planned by task planners into concrete actions, and developing and executing plans with a strategic approach that accommodates action failures, plan failures resulting from uncertainty or dynamic environmental changes, and evolving mission requirements.

This paper presents a framework that establishes a connection between generic task planning and an execution interface seamlessly provided by the Robot Operating System (ROS). This approach bridges two established standards: PDDL2.1, the planning domain description language encompassing temporal and numeric aspects, and the Robot Operating System (ROS). The primary objective is to create a modular architecture that readily accommodates various

temporal planners, ensuring the effectiveness of plan execution frameworks like T-REX.

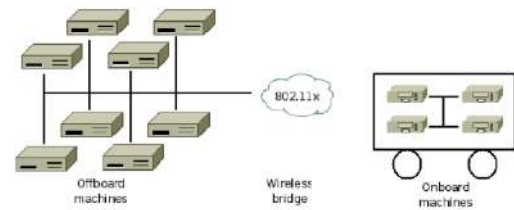


Figure 1: A typical ROS network configuration

## ROS 1:

ROS 1 is a collection of libraries used to build various types of robots, including tools for monitoring processes, inspecting communications, and receiving time-series transformations. It has a thriving ecosystem of sensor, control, and algorithmic packages, enabling even small teams to build sophisticated robotics applications. However, ROS 1 struggles to deliver data consistently over lossy connections, has a single point of failure and lacks built-in security features. ROS 2 has been developed to address these issues but has faced numerous challenges due to architectural and engineering limitations. For example, the SROS project was introduced to enhance ROS 1's security but required consistent maintenance and further development to keep up with security trends.

Category	ROS 1	ROS 2
Network Transport	Bespoke protocol built on TCP/UDP	Existing standard (DDS), with abstraction supporting addition of others
Network Architecture	Central name server ( <code>roscore</code> )	Peer-to-peer discovery
Platform Support	Linux	Linux, Windows, macOS
Client Libraries	Written independently in each language	Sharing a common underlying C library ( <code>rcl</code> )
Node vs. Process	Single node per process	Multiple nodes per process
Threading Model	Callback queues and handlers	Swappable executor
Node State Management	None	Lifecycle nodes
Embedded Systems	Minimal experimental support ( <code>rosserial</code> )	Commercially supported implementation (micro-ROS)
Parameter Access	Auxiliary protocol built on XMLRPC	Implemented using service calls
Parameter Types	Type inferred when assigned	Type declared and enforced

Figure 2: Summary of ROS 2 features compared to ROS 1

**ROS 2:**

ROS 2 is an open software platform that allows the development of robotic applications. Also known as Robotics Software Development Kit (SDK). ROS 2 is distributed under the Apache 2.0 License, which allows users to modify, implement, and redistribute the software without obligation to return it. ROS 2 is built on a government ecosystem that encourages partners to develop and publish their own software. Most plugin packages also use the Apache 2.0 license or a similar license. ROS 2 aims to increase mass adoption by making the code freely available, allowing users to use and distribute their applications without restrictions.

1. Middleware: This is also called ROS 2's pipeline. It manages communication between different components of the platform, from the network API to the language parser.
2. Algorithms: ROS 2 provides many algorithms frequently used in robotic applications. These include perception, SLAM, planning, etc. takes place.
3. Developer tools: ROS 2 has a command line and graphical tools that developers can use to configure, initialize, understand, visualize, debug, simulate, and log. There are also many tools for site management, design processes, and deployment.

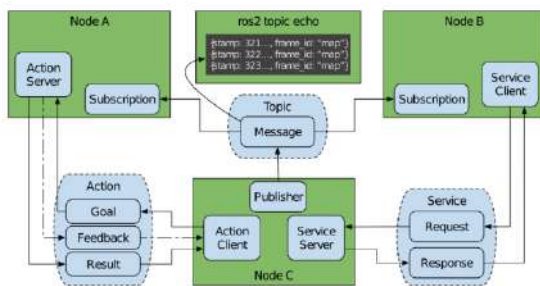


Figure 3: ROS 2 node interfaces: topics, services, and actions

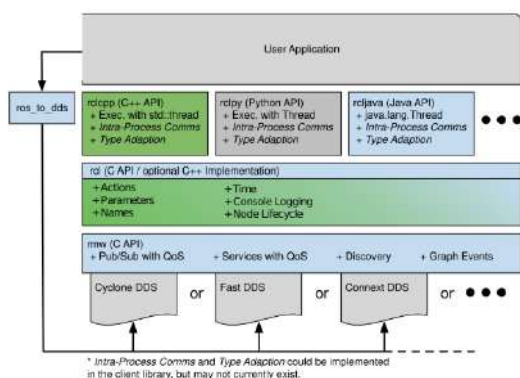


Figure 4: ROS 2 Client Library API Stack

**2. Case studies**

Five case studies were conducted to showcase the material acceleration provided by ROS 2. Each study presents a qualitative analysis of the impact of ROS 2 on the respective

organization, based on interviews, customer experiences, and codebases analyzed during the study. The various use cases and scales demonstrate the significance of ROS 2 across the robotics sector.

**A) Land: Ghost Robotics**

Ghost Robotics, a Philadelphia-based company, specializes in quadruped robots for defense, enterprise, and research. These robots can navigate difficult environments like caves, mines, forests, and deserts. They have partnerships with the US military for base security and experimental applications. Ghost uses ROS 2 on its main computing platform, a Nvidia Jetson Xavier, for mission execution, high-level gait planning, terrain mapping, and localization. Their software architecture is heavily integrated with ROS 2, allowing for parallel development without disrupting other teams.

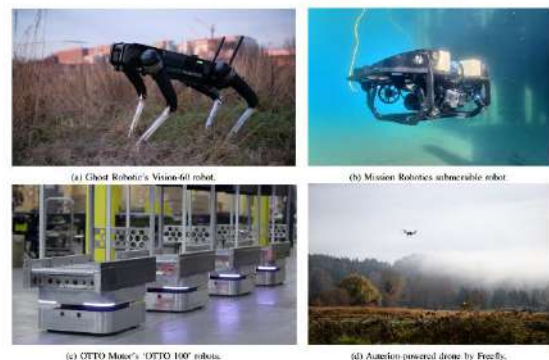


Figure 4: Case-study robot systems deployed on land, air, and sea

**B) Sea: Mission Robotics**

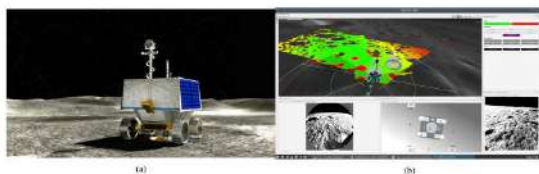
Mission Robotics, a San Francisco-based company, specializes in building marine robots for tasks such as structure inspection, environmental survey, salvage, and security. Their robots are designed to be flexible, allowing customers to customize their platform for their specific application. Mission's robots are equipped with sensors that gather data about the surface and underwater environment, allowing for more frequent, longer, and less risky underwater tasks. The mission uses ROS 2 as a common data bus to facilitate data streams and enable seamless integration of new hardware. The company's on-robot software is built on Cyclone and Connex DDS, which are more flexible and easier to customize. Mission Robotics uses ROS 2 as a common interface, allowing customers to create their own extensions and share a common infrastructure. For example, Mission collaborated with Aqua link to add depth sensing to an autonomous surface vessel using a Zed stereo camera, creating a starting point for developing new computer vision and autonomy capabilities for marine applications.

### C) Large Scale: OTTO Motors

OTTO Motors, a Canadian company, offers autonomous robots for material handling services in warehouses and factories, replacing manually controlled equipment at scale. With thousands of robots deployed worldwide, OTTO operates fleets of over 100 robots in a single facility. Customers like Toyota and General Electric have adopted OTTO's technology. Initially developed on ROS 1, OTTO found it could not test more than 25 robots on the same shared network due to a custom multi-master system. To address this, they decided to use DDS, a flexible and efficient data exchange protocol widely used in robotics. As an early adopter of ROS 2, OTTO could scale up to 100+ robots in customer facilities, thanks to ROS 2's fine-grained network topology management and better support for bandwidth management through QoS on shared network links.

### D) Air: Auterion Systems

Auterion, a Swiss aerial drone startup, aims to develop commercial autopilots based on the open-source PX4 Autopilot project. The company supports various types of airframes and aims to extend drone operations into unstructured spaces with hazards while enhancing autonomy. Auterion uses ROS 2 to integrate higher-level functionality into its drone systems, focusing on logging and introspection capabilities. ROS 2's logging capabilities collect runtime events, metadata, and raw data streams from all layers of the system, making it crucial for effective development, debugging, and validation processes. Auterion also uses rviz2, a 3-dimensional renderer, to visualize drones and sensor data in an interactive environment. These capabilities enable Auterion to focus on core flight control capabilities and customer requirements, allowing them to focus on building foundational tooling instead of building foundational tools. The company's focus on open standards and open standards has led to improved efficiency in its development process.



(a) VIPER on Lunar Surface (rendering), (b) Command and Operations Software

### E) Space: NASA VIPER

NASA's Volatiles Investigating Polar Exploration Rover (VIPER) mission is set to launch in November 2023 to explore the southern polar region of the Moon. The rover will spend 100 days searching for water ice and other resources using

various instruments. It will communicate with Earth using the X-band link to the Deep Space Network and use Earth-based computer resources to map terrain and compute stereo solutions. Earth-based operation tools, compute modules and high-fidelity simulations are based on ROS 2 and Gazebo.

The VIPER team is focused on producing highly reliable software and is extensively utilizing Gazebo for high-fidelity testing of all their components and systems. The project developed new plugins to model mission-specifics, such as camera lens flare, lunar lighting conditions, gravity, and terrain on the lunar surface. The VIPER team used Gazebo to test and validate almost all of their rover's software prior to launch.

VIPER reused 284,500 significant lines of code (SLOC) without modification from Gazebo, modifying <1% to pass validation. This code reuse accelerated development, allowing them to produce a simulation in just 266 work months focused on VIPER-specific elements. A combination of Gazebo and ROS 2 is used to train the rover's operators.

## 3. Research Methodology

"Comparative Analysis of Robotic Operating Systems" would require a structured methodology to systematically compare different robotic operating systems (ROS) and provide meaningful insights. To conduct a comparison of robotic operating systems, it is important to first define the research problem. Which is followed by an explanation of the significance and relevance of the study. The research then states its objectives and hypotheses. A brief overview of robotic operating systems is provided, including their history and evolution. Some existing literature on ROS is reviewed to identify gaps and areas of comparison. The key features, characteristics, and components of ROS that are relevant for comparison have been discussed. A set of ROS packages is compared and identified, based on relevance, popularity, and diversity. Data sources and collection methods are described, including documentation, user feedback, technical specifications, and community support. Criteria and parameters for comparison are defined, such as hardware compatibility, real-time capabilities, middleware architecture, community support and ecosystem, security features, scalability, and performance metrics. Each ROS package is evaluated based on the defined criteria, using quantitative and qualitative analysis methods, such as surveys, interviews, or experimental data, depending on the criteria. The results are presented in tables, charts, and visual aids, with explanations and interpretations for each comparison point. Later the strengths and weaknesses of each ROS package are highlighted, and the results' implications are discussed. The

findings are compared with the literature and existing knowledge, and potential future research directions in the field of ROS are suggested. Finally, the key findings are summarized, and the significance of the study is done.

#### 4. Future Scope

The future scope of research papers in comparative analysis of Robotics operating systems (ROS) is vast and exciting. ROS is a middleware platform that provides a set of tools and libraries for developing robotic applications. It has become the de facto standard for ROS development and is used by researchers and developers all over the world.

One area of future research is in the development of new ROS-based applications for a variety of industries, such as healthcare, manufacturing, and logistics. For example, ROS could be used to develop new surgical robots, autonomous assembly line robots, and self-driving delivery trucks.

Another area of future research is developing new ROS-based tools and libraries to make it easier and more efficient to develop robotic applications. For example, researchers could develop new ROS-based tools for planning, navigation, and control.

Finally, researchers could also focus on improving the performance and reliability of ROS. For example, they could develop new ROS-based tools for real-time task scheduling and fault tolerance.

#### 5. Conclusion

ROS 2 has been completely redesigned to meet the challenges of modern robotics. It was created with a thoughtful set of principles and modern robotics requirements in mind, allowing for extensive customization. Built on top of DDS, ROS 2 is a reliable and high-quality robotics framework that can support a wide range of applications. It continues to accelerate the deployment of robots and drive the next wave of the robotics revolution.

Through a series of case studies, we have shown that ROS 2 is significantly accelerating companies and institutions toward useful deployment in various environments and scales. ROS 2 is an enabler, equalizer, and accelerator. Standardization around ROS 2 in multiple industries is creating opportunities for new collaborations, faster development, and propelling newly developed technologies forward. This trend is expected to continue to manifest in the coming years as ROS 2 reaches peak maturity.

#### REFERENCES

- [1] Morgan Quigley, Brian Gerkey, Ken Conley, Josh Faust, Tully Foote, Jeremy Leib, Eric Berger, Rob Wheeler, and Andrew Ng. ROS: an open-source Robot Operating System. In IEEE International Conference on Robotics and Automation Workshop on Open Source Software, 2009.
- [2] Sachin Chitta, Eitan Marder-Eppstein, Wim Meeussen, Vijay Pradeep, Adolfo Rodriguez Tsouroukdissian, Jonathan Bohren, David Coleman, Bence Magyar, Gennaro Raiola, Mathias Ludtke, and Enrique Fernandez Perdomo. ROS control: A generic and simple control framework for ROS. *Journal of Open-Source Software*, 2(20):456, 2017.
- [3] Eitan Marder-Eppstein, Eric Berger, Tully Foote, Brian Gerkey, and Kurt Konolige. The Office Marathon: Robust navigation in an indoor office environment. In IEEE International Conference on Robotics and Automation, pages 300–307, 2010.
- [4] David Coleman, Ioan Sucan, Sachin Chitta, and Nikolaus Correll. Reducing the Barrier to Entry of Complex Robotic Software: a MoveIt! Case Study. *Journal of Software Engineering for Robotics*, 5(1):3–16, 2014.
- [5] Brian Cairl (Fetch Robotics Inc.). Deterministic, asynchronous message-driven task execution with ROS. In ROSCon Madrid 2018. Open Robotics, September 2018.
- [6] Steve Macenski, Francisco Martin, Ruffin White, and Jonatan Gines Clavero. The Marathon 2: A Navigation System. In IEEE/RSJ International Conference on Intelligent Robots and Systems, 2020.
- [7] G. Pardo-Castellote. OMG Data-Distribution Service: architectural overview. In the International Conference on Distributed Computing Systems Workshops, pages 200–206, 2003.
- [8] William Woodall. ROS on DDS. [https://design.ros2.org/articles/ros\\_on\\_dds.html](https://design.ros2.org/articles/ros_on_dds.html), accessed February 11, 2022.
- [9] Benjamin Kuipers, Edward A. Feigenbaum, Peter E. Hart, and Nils J. Nilsson. Shakey: From Conception to History. *AI Magazine*, pages 88–103, 2017.
- [10] Richard E Fikes and Nils J Nilsson. Strips: A new approach to applying theorem proving to problem-solving. *Artificial intelligence*, 2(3-4):189–208, 1971.

**Citation of this Article:**

Prof. S.B.Bele, Prasad Katyarmal, Swaraj Gangane, Komal Thakare, Tasmeeya Sheikh, “Comparative Analysis of Robotic Operating Systems” Published in *International Research Journal of Innovations in Engineering and Technology - IRJIET*, Volume 7, Issue 10, pp 371-375, October 2023. Article DOI <https://doi.org/10.47001/IRJIET/2023.710050>

\*\*\*\*\*



ISSN(online): 2581-3048

Impact Factor : 5.95

## CERTIFICATE OF PUBLICATION

# INTERNATIONAL RESEARCH JOURNAL OF INNOVATIONS IN ENGINEERING AND TECHNOLOGY

*Is Hereby Awarding this Certificate to*

**Prof. S.B.Bele**

**Professor, Department of MCA, Vidya Bharati Mahavidyalaya,  
Amravati, India**

*In Recognition of the Publication of Manuscript Entitled*

## **Comparative Analysis of Robotic Operating Systems**

*Published in International Research Journal of Innovations in  
Engineering and Technology (IRJIET)*

**Volume 7, Issue 10, pp 371-375, October-2023**

<https://doi.org/10.47001/IRJIET/2023.710050>

**Manuscript ID : IRJIET710050**

**Date of Issue : November 02, 2023**



*S. B. Bele*  
Editor-In-Chief  
IRJIET

*S. S. Suresh*  
Managing Editor  
IRJIET

Mail us at: [editor@irjiet.com](mailto:editor@irjiet.com) / [irjietjournal@gmail.com](mailto:irjietjournal@gmail.com)

Journal Website : [www.irjiet.com](http://www.irjiet.com)

# Data Mining Techniques: A Review of Literature

Prof. S. B. Bele, Vaishnavi G. Shinde, Yash S. Kalaskar, Dipali V. Mendhe

Department of MCA

Vidya Bharati Mahavidyalaya, Amaravati, India

**Abstract– Data mining is very important and useful. It involves using various algorithms to extract valuable knowledge and insights. It allows us to obtain diverse information from datasets and use it to perform various tasks.**

**Keywords- Data Mining Techniques, Classification, Predication, Knowledge base.**

## I. INTRODUCTION

Information and knowledge from complex engineering design to scientific research can be quickly and effectively applied. Human life has become increasingly characterized by data, which is essential in creating data-driven solutions. The collection of data from numerous sources, stored in large and diverse warehouses, forms the basis of this process. The data collection thus exceeds the human aptitude for analysis without a powerful analysis tool, as an effect these warehouses become ‘data vaults’, that are not often visited. Data mining is simple process of sorting the large amount of data sets to identify patterns and relationship that can help solve our problems through data analysis. Data mining is the process of analysing and extracting valuable insights and meaningful interpretations from large amounts of data, such as customer feedback and product reviews. By using techniques like natural language processing and sentiment analysis, businesses can gain valuable insights into customer preferences and improve their products.

## II. REVIEW OF LITERATURE

Based on your messages, the optimization technique specifically applied to cancer patients and supports treatment decisions using cluster analysis. This approach can help strengthen validity. To put it simply, the technique involves using a method on the first tap and creating a new configuration by finding differences in the existing rules. The K-means algorithm is then used to improve the visualizations of the results. These various social media platforms have made complex tasks easier. Social media data itself is vast in quantity, dynamic, and intricate. It particularly creates a rich and dynamic set for social media communication data and meta-data, which has not been systematically treated in the literature on data and text mining. Literary review refers to the survey of various scholarly sources (such as books, journal articles, and research papers) related to a specific topic or research question. It is often written as part of a thesis, dissertation, or research paper to contextualize your work within existing knowledge.

## III. WHAT IS DATA MINING

Data mining is a process of extracting valuable insights from data. Analysing samples from a large dataset that incorporates methods from machine learning, statistics, and database systems. This is a field of computer science, and has various applications in different industries. Data science that aims to retrieve information from data (using intelligent methods) for specific purposes and transform the information into a usable structure for further applications. Data mining is very important! By using it, you can explore your data to uncover hidden insights and improve your business relationships, customer behaviour, and performance. Data mining can help your business and decision-making. This is a multi-disciplinary skill that uses machine learning, statistics, and AI to gather information for evaluating the likelihood of future events.

### Types Of Data Mining Techniques

#### 1. Tracking patterns

Tracking patterns is a fundamental data mining technique. It involves identifying to extract trends or patterns from data, we can use data mining techniques intelligent conclusions about business outcomes and testing them. When historical data doesn't provide insights, businesses can recommend products to customers based on that information. These recommendations can lead to profitable deals and satisfied customers.

#### 2. Decision Tree

In this system, the decision tree is a division of the original dataset. Each data in the partition is compared with the estimated information. The root node of the tree is taken as the initial point and the appropriate class label is estimated for each data entry, which is used to classify the data until further classification is not possible.

#### 3. Prediction

In this data mining framework, historical data and the sequence of events are used to understand patterns and estimate future event outcomes. One widely used application of prediction is to forecast sales and determine the profitability for businesses. Prediction is a use of data

mining techniques, such as sequential patterns, trends, clustering, and classification. They decode past events or examples in a suitable order to estimate future events.

#### 4. Association

Association or relationship mining is related to data analysis. Using this data mining technique, data scientists and analysts can discover associations or correlations between two or more data attributes. It informs about the frequency events of objects in behaviour dataset. One benefit of this system is that it passes through the database with fewer numbers. This makes it suitable for solving problems like analysing customer behaviour.

#### 5. Neural networks

Neural networks, or artificial neural networks, are computational models inspired by biological neural networks. They are extensively used for data mining tasks, such as artificial intelligence and machine learning, which involve significant utilization of computational power and extensive data analysis neural networks, there is a notable ability to extract meaning from complex or noisy data and to be used for cleaning impure data and for trend analysis, which can be quite intricate. They are similar to a human or another computer system.

#### 6. Sequential Patterns

Association mining helps discover relationships between events and actions. For example, let's say there is a customer who makes more purchases than usual in the first quarter of the year. There is a possibility that they will make at least one purchase in the second quarter as well.

### IV. ADVANTAGES

- Direct mail, online marketing, and other new marketing initiatives can elicit responses from targeted customers, resulting in profitable sales.
- Data mining can help businesses automate processes and identify inefficiencies in their operations, thereby aiding in recognizing patterns and improving productivity.
- Each customer in the market is unique in their behaviour and characteristics. Understanding their fundamental traits and preferences is essential.
- Data mining can help businesses identify market differences and assist in developing new products or services to fill those gaps.
- It is also useful for creating algorithms for machine learning and is suitable for designing specific AI applications and programs.

### V. DISADVANTAGES

- To extract more accurate and efficient information, a large database, storage space, and processing power are necessary.
- The previous bullet point mentioned that data mining requires investment in database, storage, and processing power.

#### Future Scope

By incorporating various specified algorithms in our future work, we can increase accuracy, resulting in more precise outcomes. Data sets that identify hidden patterns will be utilized, primarily focusing on research and analysis to benefit from those insights. The system is very relevant. It can help users in various ways, such as researching substances and providing valuable treatment options. It can also assist in preserving the value of human life. Data mining is widely used and popular for extracting necessary information. Data mining also helps banks understand their customers' online behaviour and preferences in a better way, which is very helpful for creating new marketing campaigns.

### VI. RESULT

According to the results of the analysis, there is an increasing focus on performance in educational data mining. With the improvement in our studies, it has been concluded that data mining is generally centered around the estimation of student performance. Selecting the right curriculum and providing timely warnings about students' education is an important task in SPP, but a significant component for achieving meaningful outcomes in educational practices is to identify the major factors influencing academic performance through research.

### VII. CONCLUSION

The Internet of Things (IoT) has emerged to manage, automate, and explore all devices, tools, and sensors in the world. It has been brought together with data mining for supporting decision-making for people and things in IoT, and for system optimization's the application view, we review data mining applications in e-commerce, industry, healthcare, and public services. The discussion includes technical views, knowledge views, and application views.

### REFERENCE

1. [https://www.researchgate.net/publication/49616224\\_Data\\_mining\\_techniques\\_and\\_applications](https://www.researchgate.net/publication/49616224_Data_mining_techniques_and_applications)
2. [https://www.academia.edu/45618032/Top\\_10\\_Data\\_mining\\_Papers](https://www.academia.edu/45618032/Top_10_Data_mining_Papers)
3. [https://www.worldwidejournals.com/paripex/recent\\_issues\\_pdf/2013/Je/review-of-data-mining-techniques-applications](https://www.worldwidejournals.com/paripex/recent_issues_pdf/2013/Je/review-of-data-mining-techniques-applications)



4. <https://arxiv.org/ftp/arxiv/papers/1211/1211.5723.pdf>
5. <https://www.slidare.net/ernancy/a-review-on-data-mining>
6. <https://www.enceirect.com/science/article/pii/S1877050915023479>
7. <https://www.tetarget.com/searchbusinessanalytics/definition/data-mining>
8. <https://www.taau.com/learn/articles/what-is-data-mining>



# **International Journal of Scientific Research and Engineering Trends (IJSRET)**

**This is to certify that  
Prof. S. B. Bele  
has published a paper entitled  
“Data Mining Techniques: A Review of Literature”  
in International Journal of Scientific Research  
and Engineering Trends, in Volume 09, Issue 05,  
Sept-Oct-2023, Page 1457-1459**



[www.ijsret.com](http://www.ijsret.com)  
ISSN : 2395-566X

# Mobile Broadband Networking

<sup>1</sup>Prof. S. B. Bele, <sup>2</sup>Akash L. Chonde, <sup>3</sup>Sumit S. Jawanjal

<sup>1</sup>Professor, Department of MCA, Vidya Bharati Mahavidyalaya, Amravati, Maharashtra, India

<sup>2,3</sup>Student, Department of MCA, Vidya Bharati Mahavidyalaya, Amravati, Maharashtra, India

**Abstract - Broadband networking has become an integral part of modern communication infrastructure, enabling high-speed data transmission, seamless connectivity, and transformative technological applications. This research paper presents a comprehensive analysis of recent advancements in broadband networking technologies, with a focus on fiber-optic, DSL, cable, and wireless broadband solutions. We investigate the technical innovations, performance improvements, and emerging trends in these technologies, assessing their impact on internet access, business communication, and the digital divide. The study incorporates an evaluation of the challenges posed by expanding broadband access in rural and underserved areas, alongside the economic and social benefits it brings to developed regions. Furthermore, this research explores the security and privacy concerns associated with broadband networking, emphasizing the importance of safeguarding data in an era of increasing digital connectivity. Through a synthesis of both qualitative and quantitative research methods, this paper provides insights into the evolution of broadband networking and its implications for the future of global connectivity.**

**Keywords:** Mobile Broadband, 4G and 5G, LTE, Newtork Operators, SIM Card, Roaming, Coverage, Data Plans, Mobile Hotspot, Network Architecture, Mobile Broadband Standards, VoLTE, Mobile Broadband Security.

## 1. Introduction

In an increasingly interconnected world, the role of broadband networking technologies has never been more significant. Broadband networking, encompassing various high-speed data transmission methods, underpins the fabric of modern communication systems, facilitating the exchange of information, supporting technological innovations, and influencing socioeconomic development. The advent of broadband technologies has transformed how we work, communicate, and access information. As our reliance on digital connectivity grows, it becomes imperative to critically examine the advancements and challenges inherent in this domain.

The motivation behind this research stems from the pivotal role broadband networking plays in our daily lives, from powering our homes and businesses to enabling

emerging technologies such as the Internet of Things (IoT) and 5G wireless communications. This paper seeks to provide a comprehensive exploration of broadband networking, shedding light on its evolution, contemporary developments, and future prospects. We will delve into the key broadband technologies, including fiber-optic, DSL, cable, and wireless broadband, assessing their technical underpinnings, performance characteristics, and practical applications.

Moreover, the digital divide, a persistent concern in the broadband landscape, will be addressed within this research. As technology continues to advance at a rapid pace, ensuring equitable access to broadband services remains a critical challenge. We will investigate the disparities in broadband deployment between urban and rural areas, as well as the implications for economic and social equity.

Security and privacy are also paramount in the age of ubiquitous connectivity. The digital infrastructure that underlies broadband networking is not without vulnerabilities, and the protection of sensitive data remains a pressing issue. This paper will scrutinize the security concerns associated with broadband technologies and outline strategies for safeguarding data in an interconnected world.

To accomplish these objectives, a multifaceted research approach will be employed, drawing upon both qualitative and quantitative methods. Through this study, we aim to provide a comprehensive understanding of the current state of broadband networking and the implications for future advancements in technology, business, and society.

As we embark on this journey through the world of broadband networking, it is our hope that this research will contribute to a more informed and enlightened discourse surrounding the pivotal role of high-speed internet access in our lives.

## 2. Related Work

### 1. Type of Mobile Broadband Networks

Broadband networking is a high-speed internet connection that allows for the efficient transfer of data, enabling various applications like streaming, online gaming, telecommuting, and more. Here is a more detailed explanation of broadband networking.

### **Fiber-Optic Broadband:**

Fiber-optic broadband uses optical fibers made of glass or plastic to transmit data as pulses of light. These pulses are encoded with digital information.

It is known for its high data transfer speeds and low latency, making it ideal for demanding applications.

Fiber networks can provide both residential and business users with symmetrical, high-speed connections, often exceeding 1 Gbps.

### **DSL (Digital Subscriber Line):**

DSL utilizes the existing copper telephone lines in most homes. It employs different frequency bands for data and voice, allowing simultaneous voice calls and internet access.

Speeds can range from 1 Mbps to 100 Mbps, depending on the type of DSL and the distance from the telephone exchange.

DSL is widely available and cost-effective, and it doesn't require significant infrastructure changes.

### **Cable Broadband:**

Cable broadband uses the same coaxial cable infrastructure as cable television. Data is transmitted over separate frequency channels, allowing for simultaneous TV and internet access.

Cable broadband speeds can range from 25 Mbps to over 1 Gbps, depending on the network and service provider.

It's prevalent in urban and suburban areas and can offer high-speed internet bundled with TV services.

### **Satellite Broadband:**

Satellite broadband connects users to the internet via geostationary satellites. Data signals are sent to and received from a satellite dish at the user's location.

Speeds typically range from 12 Mbps to 100 Mbps, making it suitable for remote and rural areas with limited terrestrial options.

Satellite broadband provides wide geographic coverage but may have higher latency due to the distance signals travel to and from satellites.

### **Wireless Broadband (4G LTE and 5G):**

Wireless broadband, including 4G LTE and 5G, uses wireless radio signals for internet connectivity. These technologies are commonly used for mobile devices and home internet.

4G LTE offers speeds from 10 Mbps to 100 Mbps, while 5G is designed for even faster speeds and lower latency.

Wireless broadband is highly mobile and supports various devices, including smartphones, tablets, and IoT devices.

### **Broadband over Power Lines (BPL):**

Broadband over Power Lines (BPL) delivers internet access through existing electrical power lines. Data signals travel alongside electricity.

Speeds can range from 1 Mbps to over 100 Mbps, depending on the BPL technology and infrastructure quality.

BPL can be an alternative in areas with limited broadband options and utilizes the existing power grid.

## **2. Advantages of Broadband Networking:**

**High-Speed Internet Access:** Broadband networks provide fast and efficient internet access, enabling high-quality video streaming, online gaming, video conferencing, and other bandwidth-intensive activities.

**Reliability:** Broadband networks are generally more reliable than traditional dial-up connections, offering consistent and stable internet access.

**Widespread Availability:** Different broadband types cater to various geographic areas, ensuring that both urban and rural regions can access high-speed internet.

**Support for Multiple Devices:** Broadband networks can connect numerous devices in homes and businesses simultaneously, accommodating the needs of modern households and organizations.

**Enabler of Emerging Technologies:** Broadband networking supports technologies like the Internet of Things (IoT), 5G, and smart cities, facilitating technological advancements.

## **3. Limitations and Considerations:**

**Cost:** High-speed broadband technologies like fiber-optic can be expensive to deploy, which can affect access in some areas.

**Distance:** DSL and cable broadband can experience speed degradation over longer distances from the network's central point.

**Latency:** Satellite broadband typically has higher latency due to the distance signals travel to and from satellites.

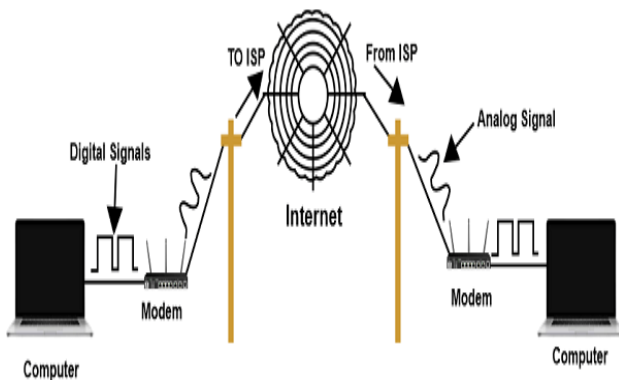
**Infrastructure:** The choice of broadband type depends on the existing infrastructure in a given area, which may limit the options available to users.

**Security:** As broadband networking increases connectivity, there are concerns about security and privacy. Protecting sensitive data is crucial.

In conclusion, broadband networking is a crucial component of modern communication infrastructure, with various types catering to different needs and regions. Choosing the right broadband type depends on factors like location, speed requirements, infrastructure, and cost considerations.

establish a connection every time they want to go online. This provides continuous and immediate access to the internet.

**Improved Multimedia Experiences:** Broadband is essential for streaming high-quality video and audio content. It has revolutionized entertainment, allowing for services like Netflix, YouTube, and online gaming. Certainly, broadband networking refers to high-speed data transmission technologies and communication methods that provide fast and efficient internet access. It is a critical component of modern communication infrastructure, enabling individuals and businesses to access the internet, exchange data, and utilize various online services.



#### 4. Key features and aspects of broadband networking include:

**High Data Transfer Rates:** Broadband networks offer significantly higher data transfer rates compared to traditional dial-up connections. This allows for faster downloads, smoother streaming, and better overall internet performance.

**Multiple Access Technologies:** Broadband can be delivered through various access technologies, including fiber optics, DSL (Digital Subscriber Line), cable, and wireless methods (such as Wi-Fi, 4G/5G mobile networks, and satellite).

**Always-On Connectivity:** Unlike dial-up connections, broadband connections are "always-on," meaning users don't need to dial in or establish a connection each time they want to access the internet. This constant connectivity is ideal for applications like VoIP (Voice over Internet Protocol) and online gaming.

**Support for Multiple Users:** Broadband connections are typically designed to support multiple users and devices simultaneously. This is crucial for households or businesses with multiple internet-connected devices.

**Applications and Services:** Broadband enables a wide range of online services, including video streaming, cloud computing, telecommuting, and real-time communication.

Broadband networking refers to high-speed internet access that provides users with faster data transmission compared to traditional dial-up connections. It allows for the quick and efficient exchange of digital information, enabling various online activities such as web browsing, streaming video, online gaming, and data sharing.

#### 3. Here are some key aspects of broadband networking:

**High Speed:** Broadband connections offer significantly faster data transfer rates than dial-up connections. This enables users to access data and content more quickly and efficiently.

**Multiple Technologies:** Broadband can be delivered through various technologies, including fiber-optic, DSL (Digital Subscriber Line), cable, satellite, and wireless. Each technology has its advantages and limitations.

**Always-On Connection:** Unlike dial-up, broadband connections are "always on," meaning users don't need to

These services depend on high-speed connections to function effectively.

**Reduced Latency:** Broadband networks generally have lower latency, meaning there is less delay in data transmission. This is essential for applications like online gaming and video conferencing.

**Digital Divide:** While broadband networking offers numerous advantages, there are disparities in access. Rural and underserved areas often lack broadband infrastructure, leading to a "digital divide" where some communities have limited access to high-speed internet.

**Security and Privacy:** As broadband networks facilitate a broad range of online activities, security and privacy concerns are paramount. Protecting personal and sensitive data is a major focus of broadband networking.

**Future Developments:** Broadband networking continues to evolve with advancements such as 5G wireless technology and the expansion of fiber-optic networks. These developments have the potential to further transform the way we connect and communicate.



**Economic and Social Impact:** Broadband access is linked to economic growth and social development. It can improve educational opportunities, healthcare access, and business productivity, making it an important driver of progress.

Broadband networking is a dynamic field that intersects with various aspects of technology, business, and society. As technology continues to advance, it plays a central role in shaping our digital future.

**Business and Communication:** Broadband is crucial for businesses as it enables video conferencing, cloud-based services, and efficient data transfer. It has also transformed communication through email, instant messaging, and social media.

**Digital Divide:** Access to broadband is not uniform, leading to a "digital divide" where some areas or communities

have limited or no access to high-speed internet. Bridging this divide is a significant challenge.

**Security Concerns:** Broadband networks can be vulnerable to cyberattacks and breaches. Ensuring the security and privacy of data transmitted over these networks is a critical consideration.

**Economic and Social Impact:** Broadband access has economic implications, as it enables e-commerce, remote work, and digital entrepreneurship. It also has social implications, influencing education, healthcare, and civic participation.

**Future Technologies:** Broadband networking continues to evolve with the introduction of technologies like 5G and the expansion of fiber-optic networks. These advancements promise even faster and more reliable internet access.

Broadband networking plays a fundamental role in the modern digital landscape, impacting how people live, work, and communicate. The development and accessibility of broadband networks continue to be a topic of significant interest and research as technology evolves and societies become increasingly connected.

## 5. Uses

Broadband networking is a critical technology with a wide range of applications that affect various aspects of our lives. Here are some key uses of broadband networking in detail:

### 1. Internet Access:

**Residential:** Broadband networking provides high-speed internet access to households, enabling users to browse the web, stream video and audio content, and engage in online gaming with ease.

**Business:** Businesses rely on broadband connections for tasks like email, web conferencing, cloud-based services, and e-commerce. Broadband networking facilitates the efficient exchange of data, enhancing productivity and communication.

### 2. Telecommuting and Remote Work:

Broadband connections have become indispensable for remote work, enabling employees to access company networks, collaborate on projects, and attend virtual meetings from home or remote locations. The COVID-19 pandemic further highlighted the importance of broadband for remote work.



### 3. Education:

Broadband networking plays a crucial role in online education, providing students and teachers with access to e-learning platforms, digital resources, and interactive online classes. This is particularly significant for remote or distance learning.

### 4. Healthcare (Telemedicine):

Telemedicine relies on broadband networking to connect patients with healthcare professionals remotely. Video consultations, remote monitoring of health data, and telehealth services are made possible through high-speed internet connections.

### 5. Entertainment:

Video streaming services like Netflix, Hulu, and YouTube, as well as online gaming platforms, require high-bandwidth broadband connections to deliver high-definition and 4K content seamlessly. This enhances the entertainment experience for users.

### 6. Smart Home Technology:

Broadband networking supports the growing ecosystem of smart home devices, including smart thermostats, security cameras, and voice-activated assistants. These devices depend on internet connectivity to communicate and function.

### 7. IoT (Internet of Things):

IoT devices, from smart appliances to industrial sensors, rely on broadband networking to transmit data to central servers for analysis and control. Broadband provides the necessary connectivity to enable IoT applications in various domains.

### 8. E-Government and Public Services:

Many government services are now accessible online, from paying taxes to renewing driver's licenses. Broadband networking allows citizens to interact with government agencies conveniently, reducing the need for in-person visits.

### 9. E-commerce:

E-commerce businesses rely on broadband connections to provide an efficient and responsive online shopping experience. Customers expect quick loading times, secure transactions, and reliable access to e-commerce websites.

### 10. Research and Development:

In the academic and research sectors, broadband networking is crucial for data sharing, collaboration, and accessing vast online repositories of knowledge. High-speed internet connections facilitate global research efforts.

### 11. Telecommunications and VoIP (Voice over Internet Protocol):

Voice and video calls are increasingly made over broadband networks using VoIP services such as Skype and Zoom. This technology has revolutionized communication by enabling low-cost international calls and video conferencing.

### 12. Cloud Computing:

Cloud services, including storage, infrastructure, and software as a service (SaaS), rely on broadband networking to provide on-demand access to computing resources. This technology is fundamental to modern business operations and data storage.

In summary, broadband networking has become an integral part of modern life, affecting various sectors, from communication and entertainment to education and healthcare. Its high-speed, reliable connectivity is foundational for supporting the digital transformation that is reshaping industries and the way we live and work.

Broadband networking refers to high-speed internet connections that have revolutionized how we communicate and access information in today's digital age. These networks utilize different technologies to transmit data quickly and efficiently, catering to a wide range of applications and user needs.

One prevalent broadband technology is fiber-optic broadband, which relies on thin strands of glass or plastic fibers to transmit data as pulses of light. The result is extremely high data transfer speeds and low latency, making it

ideal for data-intensive activities such as streaming, online gaming, and telecommuting. Fiber-optic networks often provide symmetric upload and download speeds, exceeding 1 Gbps, ensuring users can send and receive data rapidly.

Another common broadband type is DSL (Digital Subscriber Line), which capitalizes on existing copper telephone lines to deliver internet access. DSL employs different frequency bands for data and voice, allowing for simultaneous voice calls and internet usage. While DSL's speeds can vary based on the distance from the telephone exchange, it is widely available and cost-effective for many users. However, the upload speed may be slower than the download speed.

Cable broadband, which uses coaxial cable infrastructure like that of cable television, is widely deployed in urban and suburban areas. It provides high-speed internet access, with speeds ranging from 25 Mbps to over 1 Gbps, depending on the network and service provider. This technology offers convenience by bundling TV and internet services but can experience speed reductions during peak usage times.

In remote and rural areas, satellite broadband often comes to the rescue. It connects users to the internet through geostationary satellites, ensuring wide geographic coverage. However, it does have higher latency due to the considerable distance signals travel to and from satellites. Speeds typically range from 12 Mbps to 100 Mbps, making it suitable for areas with limited terrestrial options.

Wireless broadband, including 4G LTE and 5G, relies on wireless radio signals for internet connectivity. It is highly mobile and supports various devices, including smartphones, tablets, and IoT devices. 4G LTE offers speeds from 10 Mbps to 100 Mbps, while 5G is designed for even faster speeds and lower latency. These technologies have transformed mobile connectivity and enable on-the-go internet access.

Broadband over Power Lines (BPL) is another, though less common, broadband technology. It delivers internet access through existing electrical power lines, enabling speeds ranging from 1 Mbps to over 100 Mbps. It can be an alternative in areas with limited broadband options and utilizes the existing power grid infrastructure.

In summary, broadband networking has become an essential component of modern communication infrastructure. It offers high-speed internet access, reliability, and widespread availability, supporting a multitude of applications and emerging technologies. However, the choice of broadband type depends on factors such as location, speed requirements, existing infrastructure, and cost considerations. As the digital world continues to evolve, ensuring access to high-speed

broadband is essential to keep pace with technological advancements and the changing demands of our interconnected society.

Broadband networking is a high-speed internet connection that has revolutionized the way we access and share data, transforming how we work, communicate, and entertain ourselves. This advanced networking technology encompasses a variety of options, each with its unique features and advantages.

Fiber-optic broadband, for instance, employs thin strands of glass or plastic fibers to transmit data as pulses of light. This technology offers exceptionally high data transfer speeds and low latency, making it ideal for data-intensive applications, such as high-definition video streaming and online gaming. Fiber-optic broadband often provides symmetrical upload and download speeds, and in many cases, it exceeds 1 Gbps, making it a top choice for those who demand the utmost in internet performance.

DSL (Digital Subscriber Line) utilizes existing copper telephone lines to deliver broadband internet access. It achieves this by using different frequency bands to separate data from voice signals. While DSL speeds can vary based on proximity to the telephone exchange, it typically offers users speeds ranging from 1 Mbps to 100 Mbps. DSL is widely available, cost-effective, and does not require significant infrastructure changes, making it a popular choice for many households and small businesses. Cable broadband, on the other hand, leverages the same coaxial cable infrastructure used for cable television. Data is transmitted over separate frequency channels, enabling simultaneous access to television and the internet. Cable broadband provides speeds ranging from 25 Mbps to over 1 Gbps, depending on the network and service provider. It's widely available in urban and suburban areas, often bundled with TV services, making it a convenient choice for many consumers.

Satellite broadband takes a different approach by connecting users to the internet through geostationary satellites in Earth's orbit. While it provides an essential lifeline for remote and rural areas, it often comes with higher latency due to the extended distance that signals travel to and from satellites. Speeds generally range from 12 Mbps to 100 Mbps, ensuring that users in underserved areas can access high-speed internet.

In the realm of wireless broadband, 4G LTE and 5G technologies shine. They use wireless radio signals to deliver internet access and have become prevalent options for mobile devices and home internet connectivity. 4G LTE typically offers speeds from 10 Mbps to 100 Mbps, while 5G is engineered for even faster speeds and reduced latency,



heralding the advent of transformative technologies like autonomous vehicles and augmented reality.

Finally, Broadband over Power Lines (BPL) delivers internet access through existing electrical power lines. Data signals travel alongside electricity, providing speeds that can range from 1 Mbps to over 100 Mbps. BPL has the advantage of utilizing the existing power grid, offering an alternative in areas with limited broadband options.

The choice of broadband networking type depends on various factors, including location, infrastructure availability, speed requirements, and cost considerations. In an interconnected world, the right broadband network can unlock a world of opportunities, from high-quality video streaming to advanced telecommuting and the seamless integration of emerging technologies. However, it's important to be aware of the limitations and considerations associated with each broadband type, as these factors can influence the quality and availability of high-speed internet access.

## 6. Conclusion

In conclusion, mobile broadband networking has become an integral part of our modern digital lives, providing wireless internet access through cellular networks. It has evolved through different generations, with 4G and 5G being the most prominent, offering faster speeds, lower latency, and improved network capabilities.

Mobile broadband relies on network operators that offer various data plans to cater to the diverse needs of users. The technology utilizes SIM cards for user identification and authentication, and roaming services allow users to stay connected while traveling.

Coverage and network quality are critical factors, as they determine the availability and performance of mobile broadband services. Bandwidth, ping, and latency measurements help assess network responsiveness and speed. Users often employ modems, routers, or mobile hotspots to distribute mobile broadband within homes and businesses.

Data caps and quality of service (QoS) measures play a role in managing and prioritizing network traffic. Users can also use speed tests to monitor the performance of their mobile broadband connections.

Mobile broadband technology has a wide range of applications, from mobile phones and tablets to IoT devices and smart homes. It enables various services, including streaming, online gaming, and real-time communication.

Mobile broadband networks have gone through different standards and architectures, each improving upon the previous

generation's limitations. VoLTE has made it possible to make voice calls over 4G or 5G networks, adding versatility to the technology.

Security is a critical aspect of mobile broadband networking, as it involves the transmission of sensitive data. Various security measures, such as encryption and authentication, are in place to protect user information.

In summary, mobile broadband networking has revolutionized the way we access the internet, providing flexibility, mobility, and connectivity on the go. It continues to evolve and expand, offering faster speeds and more services, making it an essential part of the modern digital landscape.

## REFERENCES

- [1] "Mobile Broadband: Including WiMAX and LTE" by Mustafa Ergen.
- [2] "Wireless and Mobile Network Architectures" by Yi-Bing Lin and Imrich Chlamtac.
- [3] "LTE, WiMAX and WLAN Network Design, Optimization and Performance Analysis" by Leonhard Korowajczuk.
- [4] "4G: LTE/LTE-Advanced for Mobile Broadband" by Erik Dahlman, Stefan Parkvall, and Johan Skold.
- [5] "Wireless Communications and Networking" by Jon W. Mark and Weihua Zhuang.
- [6] IEEE Xplore Digital Library (<https://ieeexplore.ieee.org/>)
- [7] ACM Digital Library (<https://dl.acm.org/>)
- [8] Mobile World Live (<https://www.mobileworldlive.com/>)
- [9] 3GPP (3rd Generation Partnership Project) Official Website (<https://www.3gpp.org/>)
- [10] 5G.co.uk (<https://5g.co.uk/>)



**Citation of this Article:**

Prof. S. B. Bele, Akash L. Chonde, Sumit S. Jawanjal, “Mobile Broadband Networking” Published in *International Research Journal of Innovations in Engineering and Technology - IRJIET*, Volume 7, Issue 10, pp 676-683, October 2023. Article DOI <https://doi.org/10.47001/IRJIET/2023.710088>

\*\*\*\*\*



ISSN(online): 2581-3048

Impact Factor : 5.95

## CERTIFICATE OF PUBLICATION

### INTERNATIONAL RESEARCH JOURNAL OF INNOVATIONS IN ENGINEERING AND TECHNOLOGY

*Is Hereby Awarding this Certificate to*

**Prof. S. B. Bele**

Professor, Department of MCA, Vidya Bharati Mahavidyalaya, Amravati,  
Maharashtra, India

*In Recognition of the Publication of Manuscript Entitled*

### **Mobile Broadband Networking**

*Published in International Research Journal of Innovations in  
Engineering and Technology (IRJIET)*

**Volume 7, Issue 10, pp 676-683, October-2023**

<https://doi.org/10.47001/IRJIET/2023.710088>

Manuscript ID : IRJIET710088

Date of Issue : November 08, 2023



*S. B. Bele*  
Editor-In-Chief  
IRJIET

*S. M. ...*  
Managing Editor  
IRJIET

Mail us at: [editor@irjiet.com](mailto:editor@irjiet.com) / [irjietjournal@gmail.com](mailto:irjietjournal@gmail.com)  
Journal Website : [www.irjiet.com](http://www.irjiet.com)

# Methods in Cryptography

<sup>1</sup>Prof. Sunita K. Totade, <sup>2</sup>Prathmesh R. Kathe, <sup>3</sup>Chandrakant R. Chavan, <sup>4</sup>Akshay S. Borkar

<sup>1</sup>Professor, Department of MCA, Vidya Bharati Mahavidyalaya, Amravati, Maharashtra, India

<sup>2,3,4</sup>Student, Department of MCA, Vidya Bharati Mahavidyalaya, Amravati, Maharashtra, India

**Abstract - Cryptography, the science and art of secure communication, has evolved into a cornerstone of the digital age. This abstract delves into the core principles, historical development, and contemporary significance of cryptography in the context of data protection, privacy, and cybersecurity.**

**Historical Foundations:** It was initially used for military and diplomatic purposes. From rudimentary ciphers to complex code-breaking machines during World War II, the historical progression of cryptography reflects humanity's quest for secure communication.

**Fundamental Principles:** Modern cryptography relies on mathematical and computational principles. It encompasses symmetric and asymmetric encryption. Symmetric encryption employs a shared secret key for both encryption and decryption, while asymmetric encryption uses a public-private key pair. Algorithms such as AES and RSA exemplify the robust mathematical foundations of cryptography.

**Applications in the Digital Era:** In the contemporary digital landscape, cryptography plays a pivotal role in safeguarding sensitive data. It enables secure online transactions, protects information during transmission, and ensures the integrity of data. Beyond communication security, cryptography is vital in diverse fields like blockchain technology, digital signatures, and privacy-preserving protocols.

**Keywords:** Cryptography, Information Security, Encryption, Decryption, Digital Privacy, Digital Signatures, Blockchain, Quantum Computing, Cybersecurity.

## 1. Introduction

Cryptography, the science and art of secure communication, has evolved into a cornerstone of the digital age. This abstract delves into the core principles, historical development, and contemporary significance of cryptography in the context of data protection, privacy, and cybersecurity. It was initially used for military and diplomatic purposes. From rudimentary ciphers to complex code-breaking machines during World War II, the historical progression of cryptography reflects humanity's quest for secure

communication. Modern cryptography relies on mathematical and computational principles. It encompasses symmetric and asymmetric encryption. Symmetric encryption employs a shared secret key for both encryption and decryption, while asymmetric encryption uses a public-private key pair. Algorithms such as AES and RSA exemplify the robust mathematical foundations of cryptography. In the contemporary digital landscape, cryptography plays a pivotal role in safeguarding sensitive data. It enables secure online transactions, protects information during transmission, and ensures the integrity of data. Beyond communication security, cryptography is vital in diverse fields like blockchain technology, digital signatures, and privacy-preserving protocols.

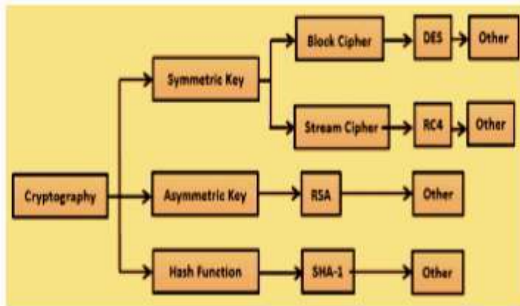


Cryptography faces ongoing challenges, including the looming threat of quantum computing, which could compromise current encryption standards. Researchers are actively developing post-quantum cryptographic solutions. Additionally, the pursuit of privacy has given rise to advanced techniques like homomorphic encryption and zero-knowledge proofs.

## 2. Methods of Cryptography

### Symmetric-key cryptography:

Symmetric-key cryptography, also known as secret-key cryptography or private-key cryptography, is a fundamental branch of cryptography that involves using the same secret key for both the encryption and decryption of data. In this cryptographic system, the security of the communication relies on keeping the key itself secret, as anyone with access to the key can both encrypt and decrypt the data. Symmetric-key cryptography is characterized by the following key principles:



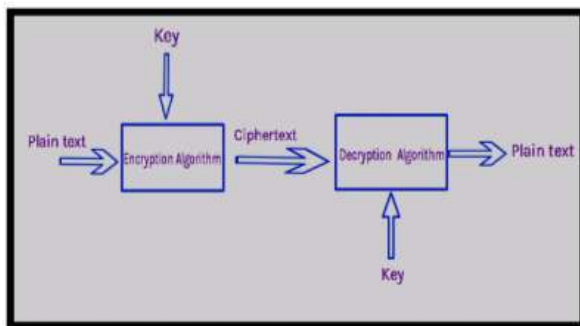
**Single Key:** Both the sender and the recipient use a single shared secret key for encryption and decryption. This key is typically a random string of bits, and the security of the system relies on the secrecy and strength of this key.

**Efficiency:** Symmetric-key algorithms are typically much faster than their asymmetric (public-key) counterparts. This makes them ideal for encrypting large amounts of data, such as data storage and streaming media.

**Examples:** Common symmetric-key encryption algorithms include the Advanced Encryption Standard (AES), Data Encryption Standard (DES), and Triple DES. These algorithms employ mathematical operations and the secret key to transform plaintext into ciphertext and vice versa.

**Key Distribution:** A major challenge with symmetric-key cryptography is key distribution. To securely share the secret key between the sender and receiver, secure key exchange protocols are often used. This can be a vulnerable point if not handled carefully.

**Security:** The security of symmetric-key systems is dependent on the key length and the quality of the encryption algorithm. Modern symmetric-key algorithms, such as AES, are considered highly secure when used with sufficiently long keys.



**Asymmetric-key cryptography**

Asymmetric-key cryptography, also known as public-key cryptography, is a fundamental branch of cryptography that employs a pair of distinct keys for secure communication and

data protection. In this system, each participant has both a public key and a private key, and they perform different functions in the encryption and decryption processes. Asymmetric-key cryptography provides several key advantages, and its applications extend to various aspects of digital security and authentication. Here is an overview of asymmetric-key cryptography:

**Key Concepts:**

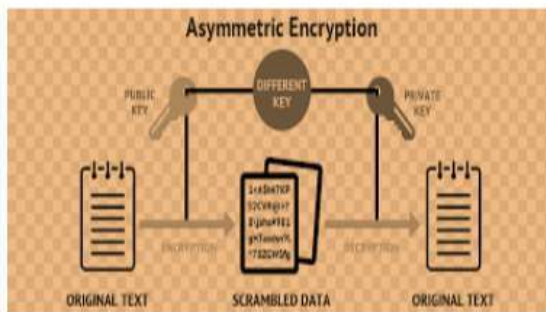
- 1. Public Key:** This key is widely distributed and known to anyone who wants to communicate with the key's owner. It is used for encrypting data that only the owner of the corresponding private key can decrypt.
- 2. Private Key:** This key is kept secret and is only known to the owner.
- 3. Encryption:** To send an encrypted message to someone, you use their public key to encrypt the message.
- 4. Digital Signatures:** Asymmetric cryptography is used to create digital signatures. The private key is used to sign a message, and the recipient can verify the signature using the sender's public key. This ensures the message's authenticity and integrity.
- 5. Key Pairs:** A user or entity generates a pair of keys, typically using mathematical algorithms.

**3. Applications**

- Secure Communication Asymmetric cryptography is often used in secure email communication, securing data transmission over the internet, and protecting sensitive information. Protocols like SSL/TLS are used to secure web traffic by employing asymmetric encryption for key exchange.
- Digital Signatures: It is essential in verifying the authenticity and integrity of documents, messages, and software updates. Digital signatures are commonly used in e-commerce, legal contracts, and software distribution.
- Public Key Infrastructure (PKI): PKI systems are built on asymmetric cryptography to manage digital certificates, which are used to verify the identity of individuals and entities in online interactions.
- Cryptocurrency: Blockchain technology, which underlies cryptocurrencies like Bitcoin, uses asymmetric cryptography to secure transactions and control the transfer of digital assets.
- Secure Authentication: Asymmetric keys are often used in secure authentication protocols, providing secure access to networks, systems, and data.

#### 4. Advantages

1. **Key Distribution:** Asymmetric cryptography eliminates the need for secure key distribution because public keys can be openly shared, while private keys remain secret.
2. **Non-Repudiation:** The use of digital signatures provides non-repudiation, making it difficult for parties to deny their involvement in a transaction or the authenticity of a document.
3. **Scalability:** Asymmetric cryptography can be used in scenarios involving multiple parties without the need for shared secret keys for each pair of participants.
4. **Security:** When properly implemented, asymmetric cryptography offers a high level of security, particularly against brute-force attacks.



#### 5. Algorithms

Cryptography relies on various algorithms to provide secure encryption, decryption, and other cryptographic operations. These algorithms are designed to protect sensitive information from unauthorized access and ensure the confidentiality, integrity, and authenticity of data. Here are some of the most commonly used cryptographic algorithms:

##### 1. Symmetric Key Algorithms:

**Advanced Encryption Standard (AES):** AES is one of the most widely used symmetric encryption algorithms. It supports key lengths of 128, 192, and 256 bits and is known for its speed and security.

**Data Encryption Standard (DES):** Although DES is now considered outdated and insecure for many applications, it was one of the first widely adopted symmetric encryption algorithms.

**Triple Data Encryption Standard (3DES):** 3DES is a more secure variant of DES that applies the DES algorithm three times with different keys.

**Blowfish:** Blowfish is a symmetric block cipher known for its speed and simplicity.

**Twofish:** Twofish is a symmetric key block cipher designed as an alternative to AES.

##### 2. Asymmetric (Public Key) Algorithms:

**Rivest-Shamir-Adleman (RSA):** RSA is a widely used asymmetric algorithm for secure key exchange, digital signatures, and encryption. It is based on the mathematical properties of large prime numbers.

**Elliptic Curve Cryptography (ECC):** ECC is a type of asymmetric cryptography that uses the algebraic structure of elliptic curves to provide strong security with shorter key lengths, making it efficient for resource-constrained devices.

**Diffie-Hellman (DH):** Diffie-Hellman is a key exchange algorithm used to securely exchange keys over an untrusted network.

**Digital Signature Algorithm (DSA):** DSA is an asymmetric algorithm designed for creating digital signatures.

**Elliptic Curve Digital Signature Algorithm (ECDSA):** ECDSA is an elliptic curve-based digital signature algorithm used for cryptographic authentication and data integrity.

##### 3. Asymmetric key algorithms:

Common asymmetric encryption algorithms include:

**RSA (Rivest-Shamir-Adleman):** One of the oldest and widely used asymmetric encryption algorithms, it's used for encryption, digital signatures, and key exchange.

**DSA (Digital Signature Algorithm):** Primarily used for digital signatures, DSA is part of the Digital Signature Standard (DSS).

**ECC (Elliptic Curve Cryptography):** ECC provides strong security with shorter key lengths compared to RSA, making it more efficient for many applications.

Common asymmetric key exchange protocols include:

**Diffie-Hellman (DH):** Used to securely exchange keys over an untrusted network.

**ECDH (Elliptic Curve Diffie-Hellman):** A variant of Diffie-Hellman that uses elliptic curve cryptography for key exchange.

Asymmetric cryptography is essential for securing communications, data, and digital transactions in various applications, including secure web browsing (HTTPS), email encryption, secure chat applications, and more. It offers a way

to protect data confidentiality, integrity, and authenticity in a public and interconnected world.

#### 4. Hash Functions:

SHA-2 (Secure Hash Algorithm 2): SHA-2 includes several hash functions, such as SHA-256 and SHA-512, and is widely used for data integrity and digital signatures.

SHA-3: SHA-3 is the latest member of the Secure Hash Algorithm family, designed for improved security and performance.

MD5 (Message Digest Algorithm 5): MD5 was widely used in the past for data integrity and checksums but is now considered weak and unsuitable for security-critical applications.

SHA-1 (Secure Hash Algorithm 1): SHA-1 was commonly used for data integrity but is now considered insecure due to vulnerabilities.

#### 5. Key Exchange Algorithms:

Diffie-Hellman Key Exchange (DHE): This algorithm allows two parties to securely exchange encryption keys over an untrusted network.

Elliptic Curve Diffie-Hellman (ECDH): ECDH is a variant of Diffie-Hellman that uses elliptic curve cryptography for key exchange.

RSA Key Exchange: RSA can also be used for key exchange, though it is typically slower than the aforementioned methods.

These are just a few examples of cryptographic algorithms used in the field of cryptography. The choice of which algorithm to use depends on the specific requirements of the cryptographic application, including factors such as security, performance, and compatibility with existing systems. Cryptographers and security experts continually evaluate and update these algorithms to address emerging threats and vulnerabilities.

#### 6. Homomorphic Encryption:

Partially Homomorphic Encryption Schemes:

These schemes support one type of homomorphic operation, either addition (homomorphic under addition) or multiplication (homomorphic under multiplication), but not both.

Paillier Cryptosystem: A partially homomorphic encryption scheme that is homomorphic under addition. It's used for secure aggregation of data without revealing individual values.

Fully Homomorphic Encryption (FHE) Schemes: These schemes support both addition and multiplication operations on encrypted data, making them more versatile but also more complex.

RSA-based Fully Homomorphic Encryption: Builds on the RSA cryptosystem to achieve fully homomorphic encryption. It's computationally intensive and typically used for proof-of-concept rather than practical applications due to its inefficiency.

Gentry's Fully Homomorphic Encryption: Proposed by Craig Gentry, this was the first practical FHE scheme. It uses lattice-based cryptography and has since evolved to become more efficient and secure. Some popular implementations include the BFV (Brakerski-Vaikuntanathan) and CKKS (Cheon-Kim-Kim-Song) schemes.

LWE-based Fully Homomorphic Encryption: Several modern FHE schemes are based on the Learning with Errors (LWE) problem, a hard mathematical problem. These schemes are known for their security and efficiency.

Ring-LWE-based Fully Homomorphic Encryption: This is an extension of LWE-based schemes that leverages the Ring-LWE problem. It offers certain advantages in terms of efficiency and security.

#### 6. Conclusion

Cryptography is a continuously evolving field, with new algorithms and methods being developed to address emerging security challenges. The choice of cryptographic method depends on the specific use case, security requirements, and the threat model. It's essential to stay updated with the latest developments and best practices in cryptography to ensure the security of digital information and communications.

#### REFERENCES

- [1] J. SEBERRY AND J. PIEPRZYK, *Cryptography: An Introduction to Computer Security*, Prentice-Hall, Upper Saddle River, New Jersey, 1989.
- [2] C. E. SHANNON, "Communication Theory of Secrecy Systems", *Bell Systems Technical Journal*, 28, 656–715 (1949).
- [3] *The Code Book: The Science of Secrecy from Ancient Egypt to Quantum Cryptography*.
- [4] Ivan Ristic *Bulletproof SSL and TLS: Understanding and Deploying SSL/TLS and PKI to Secure Servers and Web Applications*.
- [5] I.Blake, G. Seroussi, N. Smart: *Elliptic Curves in Cryptography*.
- [6] R. Churchhouse: *Codes and Ciphers*.

[7] R. Lidl, H. Niederreiter: Finite Fields (2nd Edition).

[8] M. A. Nielsen, I. L. Chuang: Quantum Computation and Quantum Information.

[9] M. Obaidat, N. Boudriga: Security of e-Systems and Computer Networks.

**Citation of this Article:**

Prof. Sunita K. Totade, Prathmesh R. Kathe, Chandrakant R. Chavan, Akshay S. Borkar, "Methods in Cryptography" Published in *International Research Journal of Innovations in Engineering and Technology - IRJIET*, Volume 7, Issue 10, pp 668-672, October 2023. Article DOI <https://doi.org/10.47001/IRJIET/2023.710086>

\*\*\*\*\*







ISSN(online): 2581-3048  
Impact Factor : 5.95

## CERTIFICATE OF PUBLICATION

### INTERNATIONAL RESEARCH JOURNAL OF INNOVATIONS IN ENGINEERING AND TECHNOLOGY

*Is Hereby Awarding this Certificate to*

**Prof. Sunita K. Totade**

Professor, Department of MCA, Vidya Bharati Mahavidyalaya, Amravati,  
Maharashtra, India

*In Recognition of the Publication of Manuscript Entitled*

### **Methods in Cryptography**

*Published in International Research Journal of Innovations in  
Engineering and Technology (IRJIET)*

**Volume 7, Issue 10, pp 668-672, October-2023**

<https://doi.org/10.47001/IRJIET/2023.710086>

**Manuscript ID :** IRJIET710086

**Date of Issue :** November 08, 2023



*[Signature]*  
Editor-In-Chief  
IRJIET

*[Signature]*  
Managing Editor  
IRJIET

Mail us at: [editor@irjiet.com](mailto:editor@irjiet.com) / [irjietjournal@gmail.com](mailto:irjietjournal@gmail.com)  
Journal Website : [www.irjiet.com](http://www.irjiet.com)

# Challenges of Digital Forensic in Cloud Computing

<sup>1</sup>Prof. Sunita K. Totade, <sup>2</sup>Tushar R. Salphale, <sup>3</sup>Shweta V. Tungar, <sup>4</sup>Prashik V. Waghmare, <sup>5</sup>Mohit D. Joshi

<sup>1</sup>Assistant Professor, Department of MCA, Vidya Bharati Mahavidyalaya, Amravati, India

<sup>2,3,4,5</sup>Student, Department of MCA, Vidya Bharati Mahavidyalaya, Amravati, India

**Abstract** - Cloud services are becoming the most promising technology of recent days. It provides scalable, flexible services to many users at the same time and it helps to quickly access resources from the cloud service provider. Digital forensics is part of the computer forensic science. Various cloud issues block the cloud forensics process, so there is no standard framework for cloud forensics can be drawn. This article summarizes the challenges, various challenges are also discussed in this article at each stage of cloud forensics in cloud computing.

**Keywords:** Cloud Computing System, Cloud Forensics, Digital Forensics Process.

## 1. Introduction

Cloud technology enables convenient use when needed use of computing resources with minimal management work and communication with the service provider. Virtualization and the nature of multithreading the cloud offers better utilization of resources and exists basic cloud computing functions, but they do the main problems of the cloud. But with any new technology, security comes into play about whether the technology in question has good protection and privacy The implementation of this technique is very simple, but some techniques such as cloud computing, digital forensics and the cloud forensics is more useful in today's world, but less so it takes a lot of time to implement the security of these technologies. Digital forensics is a part of computer forensics. The identification, collection, analysis and presentation digital evidence called digital forensics. In this paper we discuss the challenges of each stage for digital forensics in a cloud computing environment.

## 2. Challenges of Cloud Forensics

This section presents the challenges in every phase of cloud forensics.

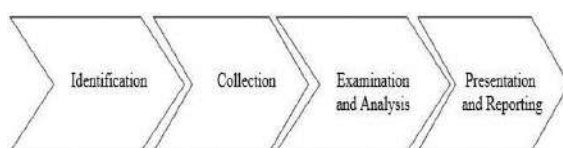


Figure 1: Cloud forensic process flow

### 1) Identification

The identification phase mainly defines the goal and the research process. Crime detection is an initial step in the digital research process model. Detecting malicious activity is easy the recognition phase. The most important thing here is how we say it is it a crime traditionally in digital forensics investigators detect crime in the following ways:

- If someone has made a complaint.
- Due to anomalies detected by the intrusion detection system.
- During the computer system audit.

### Challenges:

#### i) Using evidence in logs:

Decentralized nature the cloud makes it difficult to identify the data. Availability of log files depends on maintenance cloud model. In SaaS, there is more to identify PaaS difficult due to limited access, detection is better in IaaS but not full access.

#### ii) Persistent data:

Cloud is essentially volatile, volatile data means that when the device is turned off, all data will be lost deleted in the same way in the cloud when the VM is completely powered off data is lost if it is not saved somewhere. RAM may contain valuable evidence such as username, passwords and encryption keys. Because RAM capacity increases and RAM memory increases use of data encryption.

#### iii) Lack of cloud management:

This is a subscription network connection to a common set of resources and resources are virtual in nature, namely physical no cloud ever knows the location of the resource user.

#### iv) Lack of customer awareness:

Everything is down in the cloud there is little control over the CSP and cloud user interaction with CSP is sometimes absent. CSP lack of transparency and little international regulation leads to the loss of important terms in relation to forensic investigations at the service level agreement (SLA). This problem affects all three service models.

## 2) Collection and preservation of evidence

Evidence gathering collects evidence of what has been identified sources of evidence. The evidence collected must be maintained Data Retention is the maintenance of data integrity raw data should not be changed until the study is completed. In the traditional system, the research process starts by grabbing and taking the system hard drive a bit clever copy to keep the same integrity system but, in the cloud, it is practically impossible because evidence is intrinsically intact and changeable.

### Challenges:

#### i) Data Integrity:

Researchers must maintain integrity of evidence maintains integrity raw data is very difficult for a cloud researcher. Data integrity is a complex part of the entire cloud process forensic data, as there is no need to change the original data the evidence is presented to the law.

#### ii) Cloud Situation isolation:

When a criminal incident occurs in the cloud, in the cloud case, and in collected evidence the cloud instance must be isolated for digital research. Isolation prevents possible corruption and contamination of collected evidence. Isolated cloud the example helps maintain the integrity of the evidence collected from the cloud case.

#### iii) Digital provenance:

This is an important feature of forensic science digital history descriptive studies object A secure origin system was proposed which performs reliable evidence of digital forensics in a cloud environment. This formula proves this cloud the evidence is admissible in court.

#### iv) Chain of Custody:

In the traditional research process scientists must create and preserve supply chain. The chain of descent is documentation from the testimonies collected, as who collects evidence, when and how evidence is preserved and by whom. Researcher required maintaining a proper chain of custody beforehand it documents.

## 3) Examination and Analysis

Once in a digital imaging process (DIP) model. Information is collected and stored using various research techniques and there are several software tools to help researchers FTK (Forensic Toolkit). All these tools are available to filter and search for pattern matching content or

files or file types. Using these tools, one deleted or modified data can be restored. During the analysis stage, the evidence must be evaluated. The evidence obtained in the analysis phase is confirmed compare with alternative evidence confirm that evidence has not been changed. Research and the analysis phase of cloud expertise is similar digital forensics phase of investigation and analysis.

### Challenges:

#### i) Lack of cloud forensics tools:

Cloud Forensics is cloud driven, Currently, there are mostly no cloud forensics tools cloud researchers use digital forensics and the web forensic tools in one cloud, but they are not adequate cloud expertise differs from digital and online in criminology never study these tools in the cloud is not enough. Many cloud researchers beginning to explore cloud-based forensics technology and some tools are already in place use, but we need better tools.

#### ii) Correlation of evidence from multiple sources:

In the cloud one resource is shared between cloud users. Evidence also comes from several sources that bring various problems to researchers.

### Presentation:

The gathered evidence in the digital investigation process is needed to be submitted in the court of law to prove the crime. At the end of investigation, the investigator needs to present a report and it must be useful for cross- examination. The result report should be used by an organization to improve their security policy and must be documented for future investigation.

## 3. Research Methodology

Cloud Forensics is the process of analysing and gathering evidence from cloud-based systems and infrastructure for a legal investigation or security breach. As the use of cloud technology increases, so does the need for cloud-based forensic tools and techniques.

It is a complex and challenging field due to the dynamic and distributed nature of cloud computing. By developing new techniques, researchers can help investigators collect and analyse evidence from cloud environments more effectively.

It is important to note that cloud forensics investigation process can vary depending on the specific investigation.

#### 4. Conclusion

In this paper, we discussed the technical challenges of implementation digital forensics in the cloud environment and presented requirements for forensic data from the cloud. There are many things that can be done to improve cloud computing for digital forensics. The collection is reliable proving the cloud is difficult because we have very little control clouds compared to traditional computer systems. This paper presents different challenges of digital forensic in cloud computing with the help of cloud forensic process flow. With each phase it describes the challenges in cloud. Digital forensic refers to investigations that are focused on challenges that occur primarily involving in cloud.

#### REFERENCES

- [1] Zargari S, Benford D. Cloud forensics: concepts, issues, and challenges. 2012 Third International Conference on Emerging Intelligent Data and Web Technologies; 2012. IEEE. pp. 236–43.
- [2] K. Ruan, J. Carthy, T. Kechadi, and M. Crosbie, “Cloud forensics: An overview,” in proceedings of the 7th IFIP International Conference on Digital Forensics, 2011.
- [3] [https://www.researchgate.net/publication/351049927\\_Recent\\_Challenges\\_in\\_Digital\\_Forensics](https://www.researchgate.net/publication/351049927_Recent_Challenges_in_Digital_Forensics)
- [4] <https://www.intechopen.com/chapters/64377>
- [5] <https://www.mailxaminer.com/blog/current-challenges-in-digital-forensics-investigations/>

#### Citation of this Article:

Prof. Sunita K. Totade, Tushar R. Salphale, Shweta V. Tungar, Prashik V. Waghmare, Mohit D. Joshi, “Challenges of Digital Forensic in Cloud Computing” Published in *International Research Journal of Innovations in Engineering and Technology - IRJIET*, Volume 7, Issue 10, pp 312-314, October 2023. Article DOI <https://doi.org/10.47001/IRJIET/2023.710041>

\*\*\*\*\*



ISSN(online): 2581-3048  
Impact Factor : 5.95

## CERTIFICATE OF PUBLICATION

### INTERNATIONAL RESEARCH JOURNAL OF INNOVATIONS IN ENGINEERING AND TECHNOLOGY

*Is Hereby Awarding this Certificate to*

**Prof. Sunita K. Totade**

Assistant Professor, Department of MCA, Vidya Bharati Mahavidyalaya, Amravati, India

*In Recognition of the Publication of Manuscript Entitled*

### **Challenges of Digital Forensic in Cloud Computing**

*Published in International Research Journal of Innovations in  
Engineering and Technology (IRJIET)*

**Volume 7, Issue 10, pp 312-314, October-2023**

<https://doi.org/10.47001/IRJIET/2023.710041>

**Manuscript ID :** IRJIET710041

**Date of Issue :** October 31, 2023



*[Signature]*  
Editor-In-Chief  
IRJIET

*[Signature]*  
Managing Editor  
IRJIET

Mail us at: [editor@irjiet.com](mailto:editor@irjiet.com) / [irjietjournal@gmail.com](mailto:irjietjournal@gmail.com)

Journal Website : [www.irjiet.com](http://www.irjiet.com)

# Cloud Computing Security

<sup>1</sup>Prof. S.K.Totade, <sup>2</sup>Priyanka Bhumbar, <sup>3</sup>Vaishnavi Samudre, <sup>4</sup>Lalita Darsimbe

<sup>1</sup>Assistant Professor, Department of MCA, Vidya Bharati Mahavidyalaya, Amaravati, India

<sup>2,3,4</sup>Student, Department of MCA, Vidya Bharati Mahavidyalaya, Amaravati, India

**Abstract - Cloud computing refers to the management of data and servers and the provision of technology services using cloud computing technology. It is commonly used to store large amounts of data on cloud platforms. As a result, it is essential to safeguard data in various formats such as text, audio, video, and others. This paper presents a research study on cloud security, focusing on AWS, the most trusted cloud computing provider. AWS offers not only cloud security but also cloud storage services. The document addresses several key security challenges, including virtualization security, data storage in the cloud, and risk tolerance assessment in cloud computing. As the cloud grows, it is increasingly important to understand and implement effective security measures to protect sensitive information and maintain trust in cloud-based services.**

**Keywords:** Cyber Security, Virtualization, Scalability, Cloud Service provider, Storage security, Data integrity and Data confidentiality.

## 1. Introduction

Cloud computing refers to the practice of storing and accessing data and programs on remote servers hosted on the internet, rather than on a computer's hard drive or local server. The term "cloud" simply means the servers that are accessed over the internet. Cloud providers usually offer a "pay-as-you-go" model, which may result in unexpected operating expenses if administrators are not familiar with cloud pricing models. Essentially, cloud computing allows users to access data and applications from anywhere, at any time, as long as they have an internet connection. This technology has become increasingly popular due to its flexibility, scalability, and cost-effectiveness.

### Service providers:

- Google Cloud
- AWS(Amazon web server)
- Microsoft Azur
- IBM Cloud
- Alibaba Cloud

### Cloud providers offer types of services:

- 1) **Infrastructure as a Service (IaaS):** Which provides hardware-related services through cloud computing.
- 2) **Platform as a Service (PaaS):** Which provides a cloud development platform. However, different vendors offer incompatible platforms.
- 3) **Software as a Service (SaaS):** Which offers complete software services in the cloud.

Cloud computing security concerns include sensitive data access, sharing, privacy, authentication, hacking, recovery, accountability, and account control.

## 2. Security Analysis

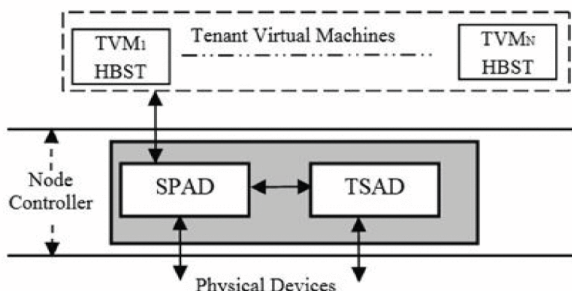
ECC encryption efficiently encrypts messages by utilizing varying points on an elliptic curve. This method uses a short key size of 256 bits which makes it difficult for algorithms to attack the encryption system as the computing complexity of attacking algorithms is  $O(2^{128})$ . Cloud clients' IDs and private keys are stored in their smart cards to prevent illegal users from generating a valid digital signature.

## 3. Security Architecture

When designing cloud security architecture, it is crucial to define the objectives. The architecture must address three key factors: the attack surface that represents external access interfaces, the protected asset set that contains the information being safeguarded, and vectors intended to perform indirect attacks, including those in the cloud and attacks on the system.

To achieve the goal of cloud security architecture, a set of functional elements must be implemented. These elements are often treated as separate entities rather than being part of a coordinated architectural plan. They include access control, network security, application security, contractual security, and monitoring, also called service security. Additionally, data protection measures are implemented at the protected asset level.

A comprehensive cloud security architecture brings together the functional elements to achieve the objectives.



#### 4. Security

Cloud security is crucial to protecting data that is either stored or moving in and out of the cloud. It is designed to protect your data from various security threats like unauthorized access, theft, and corruption. The concept of cloud security relies on physical security, technology tools, access management and controls, and organizational policies. These pillars form the basis of any organization's security program.

The three key concepts of cloud security are as follows:

- **Data confidentiality:** It ensures that data can only be accessed or modified by authorized people or processes. The organization must take measures to keep its data private.
- **Data integrity:** This concept ensures that data is trustworthy, accurate, authentic, and reliable. To maintain data integrity, organizations must implement policies or measures that prevent the data from being tampered with or deleted.
- **Data availability:** While unauthorized access must be stopped, data must still be available and accessible to authorized people and processes when required. Therefore, the organization must ensure continuous uptime and keep systems, networks, and devices running smoothly to ensure data availability.

#### 5. Security Issues In Cloud Computing

##### Data Loss

Cloud computing faces a significant challenge - data loss, commonly referred to as a data leak. Insiders, such as employees and business partners, who have access to sensitive data, can enable hackers to compromise the security of a cloud service and gain access to private and confidential information.

##### Malware injection

Malware injections are scripts or code fragments inserted into cloud services, operating as Software as a Service from cloud servers, and mimicking "genuine instances". This

implies that malicious code can infiltrate cloud services and appear to be part of the program or service running on cloud servers themselves.

##### Insider Threat

Insider threats in companies are a real possibility, even though they may seem unlikely. Authorized employees who have access to a company's cloud-based services can exploit or obtain sensitive data such as client accounts, financial forms, and other vital information. Furthermore, insiders do not necessarily have to be malicious to pose a threat.



#### 6. Cloud Security Solution

Cloud Workload Protection Platforms are tools used to reduce security risks by identifying vulnerabilities in static code, performing system hardening, and detecting workload misconfigurations. These agent-based tools use a variety of tactics such as network segmentation and system integrity protection to provide security at a workload level.

It is important to note that CWPPs do not provide coverage at the data or application layer. Furthermore, they exclude runtime security when it comes to defending containers, which is a critical component of advanced threat detection and response.

#### 7. Network Detection And Response

Network Detection and Response tools are a security approach that uses network data to defend against cloud threats and to secure containers. These tools are very effective in detecting post-compromise behaviors within the perimeter and are an essential component of defense-in-depth strategies. Since all workloads communicate through the network, network data is important for security analysts, incident responders, and forensic investigators.

While on-premises security has been using network-based tools for years, collecting network data in cloud environments has been challenging in the past. However, with network taps from major cloud service providers and third-

party packet brokers, much of the complexity and friction that came with NDR in the cloud has been eliminated.

### 8. Cloud Access Security Brokers

Breaches can happen due to misconfigured cloud settings, weak access controls, or insider threats. When confidential data is stored in the cloud, it becomes vulnerable to cybercriminals. Therefore, it is of utmost importance to ensure that only authorized individuals have access by managing user identities, permissions, and access controls across a dynamic cloud environment. Proper management of these controls is essential to mitigate the risk of unauthorized access and data breaches.

When it comes to securing applications, Static Application Security Testing (SAST) is an essential measure. While encrypting data in transit and at rest is crucial, managing encryption keys can become challenging, especially in multi-cloud or hybrid environments. Misconfigurations in cloud services can create vulnerabilities, making it critical to configure security measures properly.

Cloud resources often lack visibility into their security posture, but CSPM tools can help in complex environments.

#### Cloud Infrastructure Entitlement Management

It is crucial to implement DDoS protection measures. Developing and testing an effective incident response plan specific to cloud environments is also important.

### 9. Cloud Security Challenges

Data breaches can occur due to misconfigured cloud settings, weak access controls, or insider threats. When sensitive information is stored in the cloud, it becomes a target for cybercriminals. Therefore, it is crucial to ensure that authorized individuals have access by managing user identities, permissions, and access controls across a dynamic cloud environment. It is important to understand the shared responsibility model, where the cloud provider secures the infrastructure, but users are responsible for securing their data and applications. Encrypting data both in transit and at rest is essential, but key management can be challenging, especially in multi-cloud or hybrid environments. Misconfigurations in cloud services can cause vulnerabilities, making it critical to configure security groups, firewalls, and access controls correctly. Maintaining visibility into the security of cloud resources can be challenging without the right tools, especially in large and complex cloud environments. Cloud services are also prone to Distributed Denial of Service (DDoS) attacks, which can disrupt operations. Therefore, it is crucial to implement DDoS protection measures. Finally, developing

and testing an effective incident response plan specific to cloud environments is crucial to minimize the impact of security incidents.

### 10. Cloud Vendor's Growth

Global spending on cloud infrastructure services increased by 16% to reach \$72 billion in the second quarter of 2023. Although this growth rate represents a slowdown from the previous quarter's 19%, it can be attributed to market pressures. Additionally, slower growth is also due to the market's larger size.



In the same quarter, AWS, Microsoft Azure, and Google Cloud, the top three vendors, collectively grew by 20%, accounting for 65% of total spending. While AWS and Microsoft both experienced a deceleration in growth, Google Cloud's growth rate remained steady from the previous quarter at 31%.

### 11. Conclusion

Cloud security is a sophisticated technology that provides computing and access to high-performance computing, storage, and infrastructure through the Internet. Cloud computing has significantly impacted the computer industry, including software companies and internet service providers. It is an ever-growing part of the IT industry and is provided by cloud service providers (CSPs). The key technology used to develop cloud security is virtualization.

In the future, work on data science, artificial intelligence, and machine learning services should be prioritized inside cloud providers to protect customer-sensitive data such as login credentials through encryption techniques and other password protection techniques inside the security group. This will increase efficiency and accuracy and make the data more secure. Multi-factor authentication should be practiced to protect the data. Frequent clearing of cache and cookies is recommended, and passwords should never be auto-saved in the browser.

### REFERENCES

- [1] <https://www.javatpoint.com/what-is-cloud-security>
- [2] <https://www.geeksforgeeks.org/cloud-computing-security/>



[3] [https://www.geeksforgeeks.org/security-issues-in-cloud-computing/amp/#amp\\_tf=From%20%251%24s&aoh=16972181138706&referrer=https%3A%2F%2Fwww.google.com](https://www.geeksforgeeks.org/security-issues-in-cloud-computing/amp/#amp_tf=From%20%251%24s&aoh=16972181138706&referrer=https%3A%2F%2Fwww.google.com)

[4] <https://www.tutorialspoint.com/cloud-computing/cloud-computing-11.htm>

[5] <https://www.educba.com/>

**Citation of this Article:**

Prof. S.K.Totade, Priyanka Bhumbar, Vaishnavi Samudre, Lalita Darsimbe, “Cloud Computing Security” Published in *International Research Journal of Innovations in Engineering and Technology - IRJIET*, Volume 7, Issue 10, pp 579-582, October 2023. Article DOI <https://doi.org/10.47001/IRJIET/2023.710076>

\*\*\*\*\*



ISSN(online): 2581-3048  
Impact Factor : 5.95

## CERTIFICATE OF PUBLICATION

# INTERNATIONAL RESEARCH JOURNAL OF INNOVATIONS IN ENGINEERING AND TECHNOLOGY

*Is Hereby Awarding this Certificate to*

**Prof. S.K.Totade**

**Assistant Professor, Department of MCA, Vidya Bharati Mahavidyalaya,  
Amaravati, India**

*In Recognition of the Publication of Manuscript Entitled*

**Cloud Computing Security**

*Published in International Research Journal of Innovations in  
Engineering and Technology (IRJIET)*

**Volume 7, Issue 10, pp 579-582, October-2023**

<https://doi.org/10.47001/IRJIET/2023.710076>

**Manuscript ID : IRJIET710076**

**Date of Issue : November 04, 2023**



*S.K. Totade*  
Editor-In-Chief  
IRJIET

*S. S. Suman*  
Managing Editor  
IRJIET

Mail us at: [editor@irjiet.com](mailto:editor@irjiet.com) / [irjietjournal@gmail.com](mailto:irjietjournal@gmail.com)  
Journal Website : [www.irjiet.com](http://www.irjiet.com)

# Natural Language Processing (NLP): A Review

<sup>1</sup>Prof. S.K.Totade, <sup>2</sup>Pooja Bhombre, <sup>3</sup>Mohini Bagde

<sup>1</sup>Professor, Department of MCA, Vidya Bharati Mahavidyalaya, Amravati, India

<sup>2,3</sup>Student, Department of MCA, Vidya Bharati Mahavidyalaya, Amravati, India

**Abstract - The field of natural language processing (NLP) has evolved and influenced recent advances in the fields of artificial intelligence (AI) and computing technologies that open up new applications and novel interactions with people. NLP is a constantly evolving field that constantly pushes the boundaries of what is possible. Natural Language Processing (NLP) has become a dynamic and transformative field at the intersection of linguistics, computer science, and artificial intelligence. This research paper provides a comprehensive overview of recent advances in NLP, highlighting key developments, challenges, and promising future directions. Modern NLP involves the interaction of machines with human languages to study patterns and obtain important information. Reading comprehension, with real-world performance constantly improving. Natural Language Processing (NLP) is the study of mathematical and computational modeling of various aspects of language and the development of various systems. This includes spoken language systems that integrate speech and natural language.**

**Keywords:** Natural Language Processing, Machine learning, Deep models, Word vectors, Emotion analysis, text extraction, Named entity discovery, Part of sentence labeling.

## 1. Introduction

Natural language processing (NLP) is a machine-learning technology that allows computers to interpret, manipulate, and understand human language. Natural language processing (commonly known as NLP) is a subset of artificial intelligence research that deals with machine learning modeling tasks that aim to give computer programs the ability to understand both written and spoken human language.

Natural language processing is not just about processing, as recent developments in this area, such as the introduction of large language models (LLM) and GPT3, are also targeting speech generation.

**The five phases of natural language processing are:**

### A) Lexical or morphological analysis

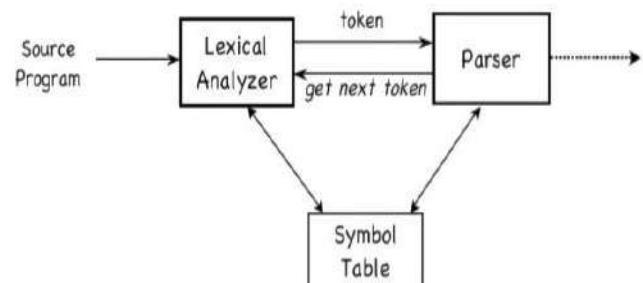
The first phase of NLP is the analysis of the structure of words, which is called lexical or morphological analysis. A lexicon is defined as a collection of words and phrases in a

particular language, where the analysis of this collection is the process of dividing the lexicon into components based on what the user sets as parameters: paragraphs, phrases, words, or characters.

The lexicon describes the understandable vocabulary that makes up a language. Lexical analysis is the process of deciphering language and dividing it into units, or lexemes, such as paragraphs, sentences, phrases, and words. NLP algorithms classify words into parts of the sentence (POS) and divide lexemes into morphemes, significant linguistic units that cannot be further subdivided. There are two categories of morphemes:

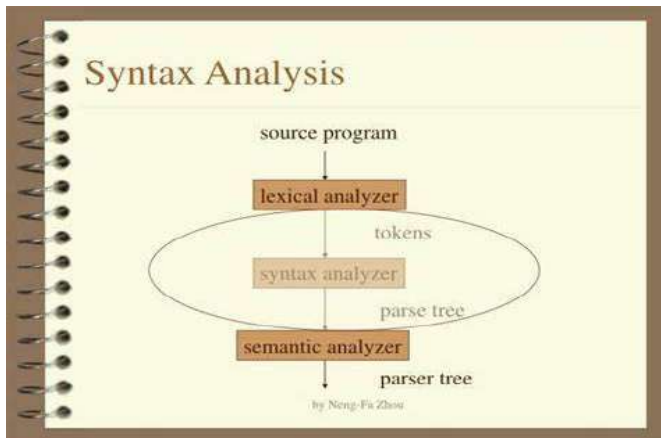
- Free morphemes function independently as words (such as "cow" and "house")
- Linked morphemes form larger words. The word "inconceivable" contains the morphemes "un-" (a linked morpheme denoting a negative context), "imagine" (the free root of the morpheme of the whole word), and "-able" (a linked morpheme denoting the ability of the root morpheme to terminate).

## Lexical Analysis



### B) Syntactic analysis (Syntax Analysis)

Syntactic analysis is the second phase of natural language processing. Syntactic analysis, or syntactic analysis, is the process of checking grammar, and word order, and generally identifying relationships between words and whether they make sense. The process consisted of examining all the words and phrases in a sentence and the structures between them.



**E) Pragmatic analysis**

Pragmatic analysis is the fifth and final stage of natural language processing. As a final stage, pragmatic analysis extrapolates and integrates findings from all other previous phases of NLP. Pragmatic analysis all about understands or extracting meaning from how language is put into action& translating a text, using the accumulated knowledge of all the other steps of NLP previously performed.

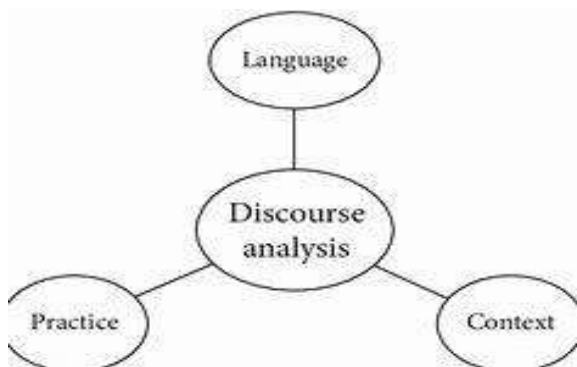
**C) Semantic Analysis**

Semantic analysis is the third stage of NLP in which an analysis is performed to understand the meaning of a statement. This type of analysis focuses on discovering the definitions of words, phrases, and sentences and determining whether the way words are organized in a sentence makes semantic sense. This task is performed by mapping the syntactic structure and checking the logic in the relationships presented between entities, words, phrases, and sentences in the text.

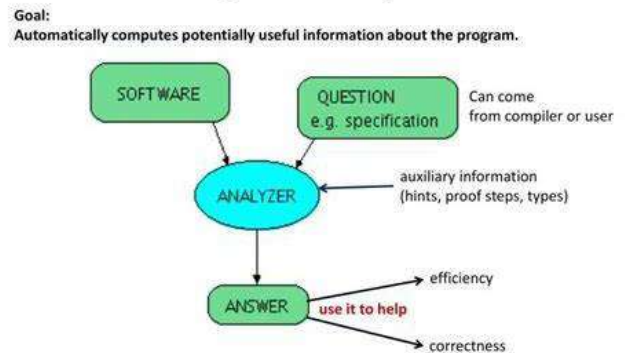
**D) Discourse Integration**

Discourse integration is the fourth phase of NLP, and it simply means contextualization. Discourse integration is the analysis and identification of the broader context for any smaller part of the natural language structure (e.g., a phrase, a word, or a sentence). At this stage, it is important to ensure that each phrase, word, and entity mentioned is mentioned in the appropriate context. Not only the structure and semantics of the sentence are taken into account, but also the composition of the sentence and the meaning of the text as a whole.

When analyzing the structure of texts, sentences are broken down and analyzed and are also considered in the context of the preceding and subsequent sentences and the impact they have on the structure of the text.



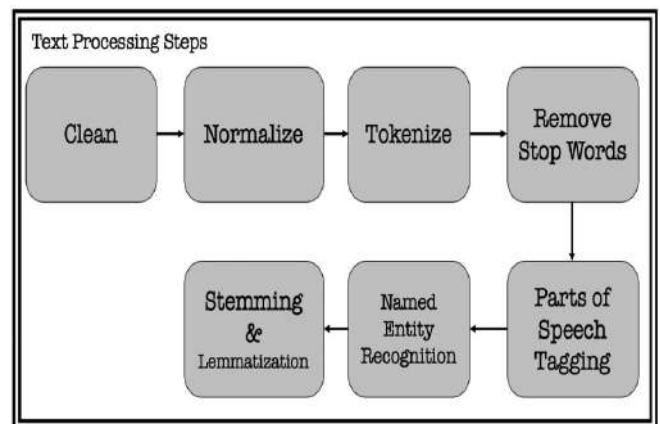
**Program Analysis**



**3. Methods of NLP**

**Text preprocessing:**

The raw text data is cleaned and processed. Tasks include tokenization (breaking text into smaller words or units), lowercase letters, punctuation removal, and handling special characters.



**Word segmentation:** Word segmentation is the process of breaking down text into individual words or tokens. It is a fundamental step in many NLP tasks, as it allows the computer to understand and work with individual language units.

**Stop word removal:** Common words like "and", "the", "in", etc. are often removed because they have no meaningful meaning and can represent noise in some NLP applications.

**Stemming and lemmatization:** These techniques reduce words to their root or root form. Lemmatization is more aggressive and does not always result in valid words, while lemmatization guarantees valid words, but is generally slower.

**Text vectorization:** It consists of converting text data into numerical vectors or matrices with which machine learning algorithms can work. Techniques such as Word Bag, TF-IDF (Term Frequency-Reverse Document Frequency), and Word Embeddings are commonly used.

**Text classification:** In the text classification phase, processed text is categorized into predefined tags or categories. This technique is useful in sentiment analysis, spam detection, and topic categorization.

**Named Entity Recognition (NER):** NER identifies and classifies entities in the text, such as names of people, organizations, places, dates, etc.

**Parts of Speech Tagging (POS):** POS tagging is the process of assigning grammatical parts of the sentence (e.g., noun, verb, adjective) to every phrase in a sentence

**Machine translation:** At this stage, text is translated from one language to another using models and algorithms developed for translation tasks.

**Questions to answer:** NLP models can be used to answer questions based on a specific text, which often involves understanding and reasoning.

**Text generation:** In some cases, NLP models can generate human-like text, such as in chatbots, content creation, and speech generation.

#### 4. Aim

The goal of Natural Language Processing (NLP) is to develop computer-aided methods for understanding and processing human language. This can be used to improve the quality and efficiency of research in a variety of ways, such as:

Extracting information from text: NLP can be used to extract important information from research, such as key findings, methods used, and conclusions reached. This can help researchers quickly and easily identify relevant work and keep up with the latest research in their field.

#### 5. Objective

The goal of natural language processing (NLP) is to enable computers to understand, interpret, and generate human language in a valuable way. This field of artificial intelligence

focuses on the development of algorithms, models, and techniques that enable machines to:

**Language comprehension:** NLP aims to allow computers to understand text or speech and extract meaning from them. This includes tasks such as text classification, sentiment analysis, and named entity recognition.

**Generate language:** NLP also involves the generation of human-like speech, either in the form of text or speech. This can include chatbots, language translations, and text summaries.

**Enable human-machine communication:** NLP enables more natural and effective human-computer communication, which is especially important for voice assistants, virtual agents, and other interactive systems.

### 6. Application

Application NLP has a wide range of real-world applications, including:

**Automated translation:** language is flexible and there are many ways to express the same idea. This is used by a variety of services, including Google Translate and Bing Translate.

**Speech-to-text conversion:** NLP is amazing at transforming spoken language into written text. Services like Siri and Google Assistant use this.

**Text summary:** NLP can be used to condense long sections of text into shorter, more concise versions. This is used in a variety of applications, such as news articles and search engine results.

**Sentiment analysis or emotion detection:** NLP can be used to identify the sentiment of a text, for example, whether it is positive, negative, or neutral. This is used in a variety of applications, such as social media monitoring and product reviews.

**AI-generated creative content:** NLP is used to generate creative content such as poems, code, scripts, and musical pieces.

**Real-time language translation:** NLP is used to develop real-time language translation systems that can translate voice and text instantly.

**Multilingual search:** NLP is used to develop search engines that can understand and search for information in multiple languages.

**Chatbot:** They use NLP techniques to understand and interpret human language, allowing them to have interactive

conversations with users. NLP allows chatbots to understand users' intentions, extract relevant information, and provide accurate answers.

### 7. Advantages

Its ability to generate creative text formats such as poems, code, scripts, musical pieces, emails, letters, etc. This is due to the development of large language models (LLMs) such as GPT-3 and LAMDA, which have been trained on huge text and code data sets. These LLMs can be used to generate text that is creative and informative and can be used to perform a variety of tasks, such as writing articles, generating marketing copy, and even creating code.

**Large-scale analysis:** NLP can analyze large amounts of text data quickly and efficiently. This can be useful for tasks such as market research, customer sentiment analysis, and fraud detection.

**Improved accuracy:** NLP can help improve the accuracy of tasks such as machine translation, text summarization, and answering questions.

### 8. Future Scope

Natural Language Processing (NLP) has a bright future with numerous possibilities and applications. In the coming years, advances can be expected in areas such as speech recognition, machine translation, sentiment analysis, and chatbots, to name a few. NLP will be further integrated with other innovative technologies such as artificial intelligence (AI), the Internet of Things (IoT), and blockchain.

These integrations will enable greater automation and optimization of numerous processes, as well as more secure and efficient communication between devices and systems. In addition to these specific areas, NLP is also expected to have a wider impact on society in the coming years. For example, NLP could be used to develop new educational tools that can personalize each student's learning.

### 9. Conclusion

Natural language processing (NLP) is a dynamic and rapidly evolving field at the intersection of computer science, linguistics, and artificial intelligence. By the time of my last knowledge refresh in September 2021, NLP had made significant strides in several areas, including machine translation, sentiment analysis, chatbots, and text generation. It is important to note that NLP continued to face challenges related to understanding context, handling languages with limited data, and handling issues of bias and fairness in linguistic models. NLP researchers and practitioners actively

worked to improve the robustness of the models and address these ethical issues.

### REFERENCES

- [1] "Natural Language Understanding" Author: James Allen.
- [2] "Natural language processing, Sentiment Analysis" Author: Adil Rajput.
- [3] Natural Language Processing Journal Journal Homepage: [www.elsevier.com/locate/nlp](http://www.elsevier.com/locate/nlp).
- [4] "Speech & Language Processing" Author: Daniel Jurafsky & James H. Martin.
- [5] Stanford NLP Group: <https://nlp.stanford.edu/>
- [6] E.D. Liddy, Natural Language Processing, 2001.
- [7] P. Jackson and I. Moulinier, "Natural Language Processing for Online Applications": Cambridge University press, New York. 2012, page 7-9.
- [8] J. Eisner. Current and future NLP research.
- [9] J. Weizenbaum, "ELIZA-A Computer Program For the Study of Natural Language Communication Between Man And Machine", Communications of the ACM Vol.9., No.1pp:36- 45, January 1966), doi:10.1145/365153.365168.
- [10] R. Bose. "Natural language processing: Current state and future directions". International Journal of the Computer, the Internet and Management.
- [11] R. J Bobrow and R.M. Weischedel, "Challenges in Natural Language Processing," Cambridge University press.
- [12] Y. Wilks, Preference Semantics".
- [13] G. Chowdhury, "Natural language processing", Annual Review of Information Science and Technology.
- [14] Handbook of Natural Language Processing. By Nitin Indurkha, Fred J. Damaerau.
- [15] Natural Language Processing and Information Retrieval. By Tanveer Siddiqui, U.S. Tiwari.

**Citation of this Article:**

Prof. S.K.Totade, Pooja Bhombre, Mohini Bagde, "Natural Language Processing (NLP): A Review" Published in *International Research Journal of Innovations in Engineering and Technology - IRJIET*, Volume 7, Issue 10, pp 589-593, October 2023. Article DOI <https://doi.org/10.47001/IRJIET/2023.710078>

\*\*\*\*\*



ISSN(online): 2581-3048  
Impact Factor : 5.95

## CERTIFICATE OF PUBLICATION

# INTERNATIONAL RESEARCH JOURNAL OF INNOVATIONS IN ENGINEERING AND TECHNOLOGY

*Is Hereby Awarding this Certificate to*

**Prof. S.K.Totade**

**Professor, Department of MCA, Vidya Bharati Mahavidyalaya,  
Amravati, India**

*In Recognition of the Publication of Manuscript Entitled*

**Natural Language Processing (NLP): A Review**

*Published in International Research Journal of Innovations in  
Engineering and Technology (IRJIET)*

**Volume 7, Issue 10, pp 589-593, October-2023**

<https://doi.org/10.47001/IRJIET/2023.710078>

**Manuscript ID :** IRJIET710078

**Date of Issue :** November 05, 2023



*S.K. Totade*  
Editor-In-Chief  
IRJIET

*S. S. ...*  
Managing Editor  
IRJIET

Mail us at: [editor@irjiet.com](mailto:editor@irjiet.com) / [irjietjournal@gmail.com](mailto:irjietjournal@gmail.com)  
Journal Website : [www.irjiet.com](http://www.irjiet.com)



# Advancements in 5G and Beyond Networks: Enabling the Fourth and Sixth Industrial Revolutions

<sup>1</sup>Prof. Kunal. P. Raghuvanshi, <sup>2</sup>Umesh. R. Tambatkar, <sup>3</sup>Sanket. V. Sawarkar, <sup>4</sup>Manisha. B. Kapate

<sup>1</sup>Professor, Department of MCA, Vidyabharati Mahavidyalaya, Amravati, India

<sup>2,3,4</sup>Student, Department of MCA, Vidyabharati Mahavidyalaya, Amravati, India

**Abstract** - This paper explores the evolution from 5G to 6G cellular communication technologies and their integration into the Fourth Industrial Revolution (Industry 4.0). It assesses 5G transmission techniques and anticipates advancements like NOMA with SC-FDE for spectral efficiency. Key 5G features include mm-wave, microwave, and m-MIMO. 5G enables IoT, V2V communication, and transformative technologies like autonomous driving and smart cities. The study offers insights into 6G, highlighting VR, AR, holography, advanced IoT, AI applications, wireless BCI, and high-speed mobility. It emphasizes 5G and 6G integration in Industry 4.0, shaping future industries and economies. The paper also examines post-5G trends, indicating reliance on new MIMO techniques and terahertz bands for emerging applications.

**Keywords:** 5G; 6G; NOMA; Industry 4.0; massive MIMO; mm-wave; IoT.

## 1. Introduction

The advent of the Fourth Industrial Revolution signifies a profound era marked by the fusion of human capabilities with machine integration and advanced AI development. This transformative epoch extends well beyond the realms of robotics and AI, encompassing a complex network of technological dimensions. A pivotal aspect of this paradigm shift is the need for efficient machine communication and perception, facilitated by cutting-edge sensor technologies and robust communication protocols. At its core lies the Internet of Things (IoT), an expansive network interconnecting devices across the Internet Protocol (IP) spectrum, generating copious amounts of data, often referred to as "big data." Artificial intelligence processes this data, transforming it into actionable knowledge, valuable for human decision-making and the autonomous decision-making of machines.

These innovations, with far-reaching implications, extend beyond industry and commerce, shaping society and disrupting traditional employment landscapes. They manifest as more efficient mobility solutions, including autonomous vehicles, smart cities, home automation, intelligent industrial processes, precision agriculture, streamlined logistics, AI-driven medical and legal services, and the proliferation of

intelligent drones. The future of mobility, particularly autonomous driving, hinges on the interactions between robotic entities and their environment, generating vast amounts of data processed by AI for informed decision-making. Fifth-generation (5G) communications play a pivotal role, offering ultra-reliable low-latency communications (URLLC), vital for services like remote surgery and autonomous vehicle operations.

This is comprehensively explores the evolution of 5G, delving into current transmission techniques, with a particular focus on non-orthogonal multiple access (NOMA) technology for its potential to enhance spectral efficiency. It also looks ahead to the sixth generation (6G) of communications and contextualizes both 5G and 6G within the overarching framework of the Fourth Industrial Revolution. The following sections provide in-depth analysis of 5G, NOMA technology, potential 6G trajectories, and conclude by summarizing key insights.

## 2. Varied Applications in 5G Communications

5G technology brings a plethora of use cases:

**Enhanced Mobile Broadband (eMBB):** This ushers in an era of high-speed connectivity, promising significantly higher peak data rates, enabling applications like virtual reality (VR) to thrive.

**Massive Machine-Type Communications (mMTC):** 5G is designed to support a large number of connected devices, essential for the Internet of Things (IoT).

**Ultra-Reliable Low-Latency Communications (URLLC):** URLLC facilitates large-scale sensor networks with minimal human intervention and ultra-low latency demands, necessitating flexible multiple access methods.

## 3. 5G Standardization and Progression

The road to 5G standards started with the appearance of the first study item related to 5G in 3GPP Release 14. However, formal standardization began after 3GPP Release 15. This process involved two phases, one focusing on

broadband wireless cellular services and the other addressing specific 5G use cases such as mMTC and URLLC.

#### 4. Scalable Subcarrier Spacing and Numerology

5G NR introduces scalable subcarrier spacing, a departure from the fixed subcarrier spacing in 4G. The subcarrier frequency in 5G is adaptable, spanning a range from  $\mu = 0$  to  $\mu = 5$ , allowing adjustments of transmitted waveforms based on channel conditions. This adaptability, referred to as 5G numerology, is vital given the diverse carrier frequencies in 5G, ranging from microwave to mm-wave spectrums.

The capability to tailor subcarrier spacing accommodates varying channel conditions, such as multipath environments and phase noise common in mm-wave communications. This adaptability supports applications with stringent latency requirements, such as URLLC, by adjusting the duration of OFDMA symbols.

#### 5. Enhancing Spectral Efficiency with NOMA

As 5G advances, the pursuit of improved spectral efficiencies is paramount. One avenue to achieve this objective is through the adoption of Non-Orthogonal Multiple Access (NOMA). NOMA is a promising multiple access technique in 5G and beyond. It utilizes power allocation strategies to serve multiple users simultaneously on the same time and frequency resources, significantly enhancing spectral efficiency. NOMA can be categorized into conventional and cooperative NOMA, with the latter offering superior performance in mitigating the near-far problem.

#### 6. Non-Orthogonal Multiple Access (NOMA)

Non-Orthogonal Multiple Access, or NOMA, is a pivotal advancement in multiple access techniques within the realm of 5G and beyond. It leverages power allocation strategies to serve multiple users simultaneously on the same time and frequency resources, offering enhanced spectral efficiency compared to conventional Orthogonal Frequency Division Multiple Access (OFDMA). NOMA is often integrated with multiple-input multiple-output (MIMO) systems, particularly massive MIMO.

##### 6.1 Enhanced Spectral Efficiency

NOMA's primary advantage is its capacity to serve a larger number of users without requiring a spectrum expansion. This results in a substantial increase in channel capacity, especially valuable in scenarios with a high density of mobile devices, such as massive Machine-Type Communications (mMTC) or Ultra-Reliable Low-Latency Communications (URLLC) in 5G.

##### 6.2 Addressing the Near-Far Problem

NOMA addresses a significant challenge known as the near-far problem, caused by varying transmission power levels among users. To mitigate this, NOMA employs Successive Interference Cancellation (SIC), enabling the receiver to detect user signals in descending order of received power. This approach cancels users with higher power levels first, enabling interference-free detection of weaker signals.

##### 6.3 Two Types of NOMA

NOMA can be categorized into two primary categories: conventional NOMA and cooperative NOMA. In the conventional NOMA scenario, the SIC receiver of a reference user cancels signals with powers exceeding that of the reference user. However, signals from users closer to the base station, which have lower power levels due to power control, are not canceled, potentially causing interference.

Cooperative NOMA provides a solution to this challenge by enabling the cancellation of all interfering users' signals, introducing diversity. This approach allows users closer to the base station to detect and subtract signals from more powerful, distant users. Users closer to the base station can also transmit copies of signals from more distant users, resulting in interference-free detection and improved performance, especially for users farther from the base station.

##### 6.4 Performance Comparison

Performance simulations demonstrate the effectiveness of cooperative NOMA over conventional NOMA. Cooperative NOMA shows significant improvements, closely approaching the Matched Filter Bound (MFB) performance. These simulations consider various factors such as channel modeling, signal power levels, and the use of efficient algorithms.

#### 7. Evolution toward 6G: Meeting Emerging Needs

The landscape of cellular communications is in a constant state of evolution to meet the expanding demands of modern society and emerging technologies. As we look toward the digital society of 2030 and beyond, it's clear that the trajectory of progress will only intensify. The proliferation of connected devices, including the Internet of Things (IoT), sensors, vehicles, drones, and data-driven applications, necessitates a paradigm shift in our communication networks.

##### 7.1 Enhanced Services for 6G

The forthcoming 6G networks are expected to usher in a new era of connectivity, unlocking capabilities that transcend the boundaries of previous generations, such as:

- Augmented Reality (AR) and Extended Reality (XR): AR and XR applications, infused with immersive experiences, will rely on the lightning-fast data transmission and ultra-low latencies of 6G networks to deliver seamless interactions with the virtual world.
- Artificial Intelligence (AI)-Infused Applications: 6G will be the breeding ground for AI-driven innovations, enabling applications that harness the power of machine learning and deep learning in real-time.
- Wireless Brain-Computer Interactions (BCI): The convergence of wireless communication and neuroscience will open up possibilities for direct interactions between the human brain and digital interfaces.
- Holographic Services: Holography, once confined to science fiction, will become a reality in 6G, revolutionizing telepresence and communication.
- Integration with Localization, Mapping, and Remote Control: 6G will bridge the gap between communication and spatial awareness, facilitating precise localization, mapping, and remote control of devices and assets.
- Emerging eHealth Applications: Healthcare will witness a transformation, with 6G supporting advanced eHealth applications, remote diagnostics, and telemedicine.
- Improved Autonomous Vehicles: The automotive industry will experience a leap forward with enhanced communication capabilities that ensure the reliability and safety of autonomous vehicles.
- Efficient Support for IoT: Smart cities and smart homes will become even smarter, accommodating a vast array of low-power IoT devices efficiently.
- Support for Flying Vehicles and High Mobility: The advent of flying vehicles and the need for ultra-high mobility support will require a three-dimensional network architecture with widespread 3D coverage.

### 8. Literature Review

Sr. No.	Model	Author	Techniques	Conference/Journal and Year	Conclusion
1.	Network Slicing and Service Differentiation	Andrews et al	Network Slicing	IEEE Communications Magazine 2014	Network slicing, introduced by Andrews et al., has revolutionized 5G by enabling dedicated network segments for distinct applications. This approach, encompassing enhanced mobile broadband (eMBB), massive machine-type communications (mMTC), and ultra-reliable low-latency communications (URLLC), provides unparalleled flexibility, allowing 5G to cater to a wide array of services and requirements.
2.	mmWave Technology	Rappaport et al.	Millimeter-Wave Technology Small Cells, Advanced Beamforming	IEEE Transactions on Wireless Communications 2013	The pioneering work of Rappaport and team on millimeter-wave (mmWave) technology has been instrumental in unleashing the potential of 5G. Operating at higher frequencies, mmWave technology has paved the way for higher data rates and increased network capacity. Through the utilization of small cells and advanced beamforming techniques, it has transformed wireless communication, redefining our expectations for speed and efficiency..
3.	Small Cells in 5G Networks	S. M. Alam et al.	Small cell deployment, HetNets, Network capacity.	IEEE Access 2017	Small cell deployment in heterogeneous networks (HetNets) is vital for increasing network capacity, improving coverage, and managing the data explosion in 5G networks
4.	Network Security in 5G	R. Roman et al.	5G security, Threats, Security mechanisms	IEEE Communications Magazine 2018	Ensuring robust network security is paramount in 5G due to increased vulnerabilities. Effective security mechanisms are crucial to protect against emerging threats in 5G networks
5.	Massive MIMO	Larsson et	Massive	IEEE Journal on	Larsson and colleagues' work on massive

		al.	multiple-Input, Multiple-Output (MIMO)	Selected Areas in Communications 2014	multiple-input, multiple-output (MIMO) technology has established it as a cornerstone of 5G networks. By harnessing a multitude of antennas, this technology has significantly enhanced spectral efficiency and network coverage. The result is improved network performance, which is crucial in meeting the ever-growing demand for wireless connectivity and data.
6.	Infrastructure Requirements	Andrews et al.	Small Cells, Fiber-Optic backhaul, Edge Computing	IEEE Communications Magazine 2014	The deployment of 5G networks, as discussed by Andrews et al., demands a substantial investment in infrastructure. This encompasses the deployment of small cells, the establishment of robust fiber-optic backhaul networks, and the construction of edge computing facilities. While these requirements are essential for realizing the full potential of 5G, they present both cost and logistical challenges.
7.	Spectrum Allocation	Al-Turjman	Spectrum Allocation Regulatory Coordination	IEEE Wireless Communications 2019	Spectrum allocation, as explored by Al-Turjman in 2019, remains a substantial challenge in 5G deployment. It necessitates coordinated efforts from regulatory bodies and network operators to ensure the allocation of sufficient spectrum in desirable frequency bands, including the critical mmWave frequencies. Overcoming this challenge is vital for 5G to deliver on its promises.
8.	Terahertz (THz) Communication	Jornet et al.	Terahertz (THz) Frequencies High Data Rates, Propagation Challenges	IEEE Transactions on Terahertz Science and Technology 2018	The concept of terahertz (THz) communication, introduced by Jornet and collaborators in 2018, holds tremendous promise for beyond-5G and 6G networks. THz frequencies offer vast bandwidth and the potential for exceptionally high data rates. However, the propagation challenges associated with THz frequencies must be addressed to fully exploit their potential. THz communication is poised to transform the landscape of future wireless communication.
9.	Quantum Communication	Diamanti et al.	Quantum Key Distribution (QKD).	Nature Photonics 2016	Quantum communication, as explored by Diamanti and team, represents a futuristic and highly secure approach to data transmission for beyond-5G and 6G networks. Quantum key distribution (QKD) promises unbreakable encryption, ensuring the utmost security for sensitive data. This technology holds the potential to redefine the standards for secure communication in an increasingly interconnected digital world.
10.	AI-Enabled Networking	Zhao et al.	Artificial Intelligence (AI)	IEEE Network Magazine 2021	Zhao et al.'s work underscores the pivotal role of artificial intelligence (AI) in optimizing and managing beyond-5G and 6G networks. AI-driven network orchestration, predictive maintenance, and resource allocation are poised to significantly enhance network performance and efficiency. These advancements will render future networks more adaptive and intelligent, meeting the

					evolving demands of a highly interconnected world.
11.	Software-Defined Networking (SDN)	N. M. Khan et al.	SDN, Network management, Virtualization	IEEE Communications Magazine 2015	SDN enhances network management and agility in 5G networks, enabling dynamic resource allocation and efficient virtualization.
12.	mobile Edge Computing (MEC)	K. Zhang et al.	Mobile Edge Computing, Low latency, Edge services.	IEEE Transactions on Wireless Communications 2018	MEC, offering low-latency processing at the network edge, plays a pivotal role in supporting real-time applications in 5G networks, improving user experiences.
13.	AI-Enabled Networking	M. Aazam et al.	Fog computing, IoT, Edge analytics.	IEEE Access 2018	Fog computing, acting as an intermediary between the cloud and IoT devices, enhances 5G network performance by enabling low-latency, localized data processing and analytics.
14.	Massive Machine- Type Communications (mMTC)	M. Bennis et al.	mMTC, IoT, Low-power devices.	IEEE Communications Magazine 2018	mMTC in 5G is vital for connecting massive low-power IoT devices, enabling applications in smart cities, agriculture, and healthcare.
15.	Cloud RAN (C-RAN)	G. Wu et al.	Cloud RAN, Centralized processing, Network capacity.	IEEE Network 2015	C-RAN centralizes processing to improve network capacity and efficiency, reducing costs and enhancing the performance of 5G networks.

### 9. Conclusion

The review paper concludes by summarizing the key findings and underscoring the significance of the transition from 5G to B6G networks, setting the stage for unprecedented advancements in wireless communications.

By providing a structured and precise summary of the research paper, readers can easily grasp the key insights and advancements in cellular communication technologies, from 5G to the anticipated B6G networks, and their implications for various applications and services.

### 10. Future scope

The future scope in 5G and beyond networks research encompasses several critical domains. It includes autonomous network management through AI, sustainable practices for reduced environmental impact, dynamic spectrum optimization, and integration of edge computing and security enhancements. Heterogeneous network integration, cross-layer optimization, and user-centric services aim to enhance user experiences. Research in developing regions is essential for inclusive deployment. Furthermore, exploration of network slicing in various industries, quantum communication for security, and the advent of 6G networks are key focus areas.

Ethical considerations related to data privacy, surveillance, and digital equity also feature prominently. These research directions promise to drive innovation and address emerging challenges.

### REFERENCES

- [1] Andrews, J.G., Buzzi, S., Choi, W., Hanly, S.V., Lozano, A., Soong, A.C.K., Zhang, J.C. (2014). What Will 5G Be? IEEE Journal on Selected Areas in Communications, 32(6), 1065-1082.
- [2] Rappaport, T.S., Sun, S., Mayzus, R., Zhao, H., Azar, Y., Wang, K., Wong, G.N., Schulz, J.K., Samimi, M., Gutierrez, F. (2013). Millimeter Wave Mobile Communications for 5G Cellular: It Will Work! IEEE Access, 1, 335-349.
- [3] Larsson, E.G., Edfors, O., Tufvesson, F., Marzetta, T.L. (2014). Massive MIMO for Next Generation Wireless Systems. IEEE Communications Magazine, 52(2), 186-195.
- [4] Al-Turjman, F. (2019). Spectrum Allocation and Challenges in 5G. IEEE Access, 7, 137665-137673.
- [5] Jornet, J.M., Akyildiz, I.F. (2018). Terahertz Band: Next Frontier for Wireless Communications. Physical Communication, 30, 1-17.
- [6] Zhao, Y., Yu, F.R., Li, Y., Ji, H., Wang, T., Leung, V.C.M. (2021). A Survey of Artificial Intelligence-

- Enabled Wireless Communication for 6G and Beyond. IEEE Transactions on Network Science and Engineering, 9(1), 94-115.
- [7] Diamanti, E., Lo Piparo, N., Lombardi, P., Mancini, M., Ottaviani, C., Spagnolo, N., Cald, A., Suraci, V., Bianchi, A., Detti, A., Di Pietro, R., Cuomo, F., Prati, M., Andreani, P. (2016). Quantum Communication for Future Smart Grids. IEEE Transactions on Industrial Informatics, 12(6), 2642-2652.
- [8] Giordani, M., De Domenico, A., Benassi, G., Zanella, A. (2020). Towards 6G Networks: Use Cases and Technologies. IEEE Access, 8, 25967-25975.
- [9] Wan, J., Tang, S., Shu, L., Li, D. (2018). Vehicle-Assisted Data Delivery in Vehicular Ad Hoc Networks with Network Slicing. IEEE Communications Magazine.
- [10] Alam, S.M., Rehman, S.U., Kalsoom, U., Rehman, A., Saleh, A.H. (2017). A Survey of 5G Network: Architecture and Emerging Technologies. IEEE Access.
- [11] Roman, R., Zhou, J., Lopez, J. (2018). On the features and challenges of security and privacy in distributed Internet of Things. IEEE Communications Magazine.
- [12] Shi, M., Yu, X., Yao, Y. (2016). Edge Computing: Vision and Challenges. IEEE Internet of Things Journal.
- [13] Aazam, M., Huh, E.N., Foo, S. (2018). Fog Computing: A Survey of Trends, Architectures, Requirements, and Research Directions. IEEE Access.
- [14] Ahmed, E., Yaqoob, I., Gani, A., Imran, M., Guizani, M. (2020). A Survey of Network Slicing in 5G Networks: Architecture, Scenarios, and Challenges. IEEE Internet of Things Journal.
- [15] Liu, S., Li, K., Hui, L., Deng, L., Chen, H. (2015). Software-Defined Networking (SDN) and Network Function Virtualization (NFV) for Future Internet: A Survey. IEEE Xplo.
- [16] Simeone, O., & Spasojevic, P. (2017). Device-to-Device Communications with Massive MIMO: A New Approach to Enhance Spectral Efficiency. IEEE Communications Letters, 21(7), 1493-1496.
- [17] Farooq, M. O., Gani, A., He, W., Ahmed, E., & Anisi, M. H. (2016). Toward energy-efficient Vehicular Cloud Computing: Understanding the challenges and approaches. IEEE Access, 4, 8157-8171.
- [18] Lu, X., Wang, P., Niyato, D., Kim, D. I., & Han, Z. (2015). Wireless networks with RF energy harvesting: A contemporary survey. IEEE Communications Surveys & Tutorials, 17(2), 757-789.
- [19] Park, J., Kim, H., Kim, S., & Qaraqe, K. (2016). Wireless Network Slicing for Diverse Services. IEEE Access, 4, 875-884.

**Citation of this Article:**

Prof. Kunal. P. Raghuvanshi, Umesh. R. Tambatkar, Sanket. V. Sawarkar, Manisha. B. Kapate, "Advancements in 5G and Beyond Networks: Enabling the Fourth and Sixth Industrial Revolutions" Published in *International Research Journal of Innovations in Engineering and Technology - IRJIET*, Volume 7, Issue 10, pp 583-588, October 2023. Article DOI <https://doi.org/10.47001/IRJIET/2023.710077>

\*\*\*\*\*



ISSN(online): 2581-3048

Impact Factor : 5.95

## CERTIFICATE OF PUBLICATION

### INTERNATIONAL RESEARCH JOURNAL OF INNOVATIONS IN ENGINEERING AND TECHNOLOGY

*Is Hereby Awarding this Certificate to*

**Prof. Kunal. P. Raghuvanshi**

**Professor, Department of MCA, Vidya Bharati Mahavidyalaya,  
Amaravati, India**

*In Recognition of the Publication of Manuscript Entitled*

**Advancements in 5G and Beyond Networks: Enabling the  
Fourth and Sixth Industrial Revolutions**

*Published in International Research Journal of Innovations in  
Engineering and Technology (IRJIET)*

**Volume 7, Issue 10, pp 583-588, October-2023**

<https://doi.org/10.47001/IRJIET/2023.710077>

**Manuscript ID :** IRJIET710077

**Date of Issue :** November 04, 2023



*K. Raghuvanshi*  
Editor-In-Chief  
IRJIET

*S. S. S. S.*  
Managing Editor  
IRJIET

Mail us at: [editor@irjiet.com](mailto:editor@irjiet.com) / [irjietjournal@gmail.com](mailto:irjietjournal@gmail.com)

Journal Website : [www.irjiet.com](http://www.irjiet.com)

# AI in Healthcare

<sup>1</sup>Prof. K.P.Raghuvanshi, <sup>2</sup>Vaishnavi Kakde, <sup>3</sup>Vaishnavi Bhonde, <sup>4</sup>Sakshi Jawarkar

<sup>1</sup>Professor, Department of MCA, Vidya Bharati Mahavidyalaya, Amravati, India

<sup>2,3,4</sup>Student, Department of MCA, Vidya Bharati Mahavidyalaya, Amravati, India

**Abstract - Artificial intelligence (AI) is a technology that helps to make tasks easier for humans, especially in healthcare. This transformation is driven by the increasing availability of healthcare data and the rapid advancements in analytical techniques. In this article, we aim to provide an overview of the current status of AI applications in healthcare and explore its potential future uses, considering it as one of the most revolutionary technologies of the 21st century. Healthcare is identified as an early candidate for a significant transformation through AI technologies, and our goal is to contribute to the discussion on how AI can enhance decision-making capabilities in this sector. Our aim will assess whether the current structures are adequately equipped to handle the challenges posed by AI in healthcare. Artificial intelligence, machine learning, and deep learning have the potential to greatly assist in proactive patient care, mitigate future health risks, and streamline healthcare workflows. The future of healthcare, driven by AI, holds promise for more efficient and effective healthcare delivery.**

**Keywords:** Artificial intelligence, Machine learning, Clinical decision support, Healthcare.

## 1. Introduction

Artificial intelligence (AI) technology is quite distinct from traditional healthcare methods because it can gather information, process it, and provide clear results to users. AI achieves this through machine learning algorithms. In healthcare, AI is used to tackle complex problems by analyzing intricate medical data. It enables computer algorithms to make conclusions without direct human input, recognizing patterns and creating logical pathways. However, to minimize errors, AI outputs need to be repeatedly tested.

Unlike humans, AI algorithms are quite literal; they can't adapt or understand context beyond what's explicitly provided. Understanding the future of healthcare requires a good grasp of AI's role. Although AI research began in 1956, it had a limited impact on medical practice for many years. However, the recent hype surrounding machine learning is becoming a reality.

AI is particularly well-suited for healthcare delivery, and its use in clinical settings has grown exponentially. Modern medicine faces the challenge of managing vast amounts of structured and unstructured data to treat and manage diseases. AI systems, with their data-mining and pattern-recognition abilities, come to the rescue. Medical AI is helpful for the prediction, diagnosis, and treatment of diseases. It uses symbolic models of diseases and analyzes their connections with patient signs and symptoms. Diagnostic AI applications collect and synthesize clinical data, compare it with predefined disease categories, and aid in diagnosis and treatment. Furthermore, AI is involved in developing treatment protocols, drug research, and patient monitoring.

## 2. Technologies of Artificial Intelligence

Many technologies are directly concerned with healthcare, each supporting particular mechanisms and tasks. A few important AI technologies in healthcare are detailed as follows:

### 1) Machine learning

Machine learning is a specific area within the broader field of artificial intelligence (AI). It relies on algorithm models to implement AI concepts. What sets machine learning apart is its ability to adapt and improve over time when exposed to new data. It's as if the machines are actually learning as they process information. Neural Networks and Deep Learning One of the biggest prevailing types of AI is machine learning which is a statistical method. For the healthcare industry, machine learning plays an important role because it can help us to make sense of the large amount of healthcare data that is generated every day within electronic health records. The use of machine learning in healthcare is automating medical billing, clinical decision support, and the development of clinical practice guidelines within health systems. Machine learning algorithms can help us to find patterns and insights in medical data that would be impossible to find manually. The neural network is an intricate technology that became feasible after the 1960s. It is used to find out whether a patient will develop a specific disease. It works similarly to a neuron's function in processing signals but it is not as functional when compared to the brain's functions. Deep learning is progressively utilized for speech



recognition and fundamentally is a type of natural language processing (NLP).

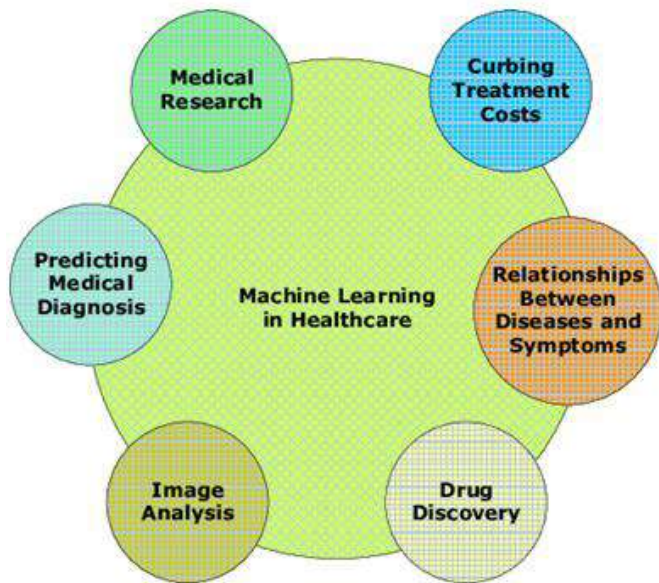


Figure 1: Application of Machine Learning

## 2) Natural Language Processing (NLP)

In the medical dataset, data is categorized as structured and unstructured. NLP techniques are used to extract insights from unstructured clinical text, such as doctor’s notes and patient records. This helps in identifying patterns, trends, and important information within textual data. NLP is utilized for converting data into a usable and analyzable form. Doctors can use speech-to-text conversion tools with built-in NLP capabilities to transcribe their notes and enter them into the corresponding patents in Electronic Health Record (EHR) fields and also medical staff can use the NLP tools to extract relevant data from EHRs.

## 3) Artificial neural networks

Artificial neural networks (ANNs) are a fundamental component of AI and machine learning in healthcare. Artificial neural networks are data processing models inspired by the structure and functioning of the human brain, consisting of interconnected nodes (neurons) that process and transmit data and make predictions or decisions based on that learning. The main objectives of artificial neural networks are to reflect the activities of human brain nerve cells utilizing neural networks of algorithms and maintaining information. In healthcare, artificial neural networks are used for a wide range of applications, leveraging their ability to learn.

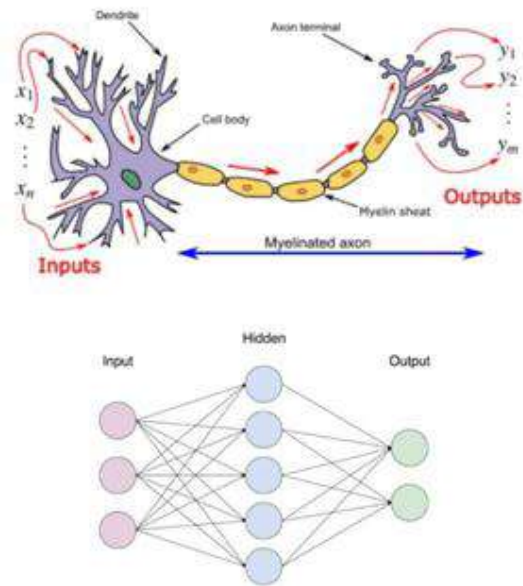


Figure 2: Process of Artificial neural networks

## 4) Robotic Process Automation

Robotic Process Automation (RPA) is a technology that uses software robots to automate repetitive, rule-based tasks in various industries, including healthcare. While RPA is not a form of artificial intelligence, it is often used with AI to improve process efficiency and accuracy. Robotic Process Automation helps many areas in healthcare, including appointment scheduling, billing, and claims processing, reducing operational costs and human errors. Robotic surgery, also known as robot- assisted surgery, revolutionizes the field of medicine by empowering surgeons to perform various types of surgical procedures with unmatched precision and flexibility. Some benefits of RAS are increased accessibility and better decision-making, less tissue damage, and faster recovery.

During the recent COVID-19 crisis, healthcare facilities harnessed the potential of robots in the operating room and clinical settings to address pressing challenges. Robots were employed to reduce the risk of pathogen exposure and provide vital support to healthcare workers, thereby helping to ensure the safety of both patients and medical professionals.



Figure 3: Robotic surgery

### 3. Advantages of AI in Healthcare

#### Ability to analyze data and improve diagnosis:

AI technology is great at quickly and accurately viewing medical records and data. It's faster and more precise than humans, helping doctors make quicker and better diagnoses, which means patients get better care.

#### Better patient care:

When AI is used well in healthcare, it makes patient care better. It makes medical research faster, helps doctors make better decisions, and reduces mistakes in treatment plans.

#### Reduced cost of care:

AI can help save money in healthcare. It can do tasks like paperwork faster and with fewer mistakes than people. This saves money and helps us use resources better.

#### Quick and Accurate data:

In medicine, it's important to have information that is both quick and right. AI gives real-time data that helps doctors make decisions faster and can prevent problems from getting worse.

#### Reduced staffs stress:

Jobs in healthcare can be very stressful, and there aren't always enough people to do the work. AI can help by doing some tasks, making it easier on the staff, and making sure that patients get good care even when things are busy.

#### Support with administrative tasks:

AI can do things like keeping records, analyzing scans, and entering data. This means doctors and nurses have more time to take care of patients and do other important parts of their jobs.

### 4. Future Scope

The future scope of AI in healthcare research is highly hopeful. Future studies can explore the integration of AI into remote patient monitoring, enhancing healthcare accessibility and reducing geographical barriers. Additionally, there is potential to develop AI algorithms for predicting disease outbreaks and optimizing resource allocation during health crises. As AI continues to evolve, research can focus on creating user-friendly AI interfaces for healthcare professionals and patients, facilitating seamless adoption. The future of AI in healthcare research is assured to revolutionize healthcare delivery, diagnostics, and patient outcomes.

### 5. Conclusion

Artificial intelligence technology is rapidly advancing and holds tremendous potential to improve various aspects of healthcare, ultimately leading to better and quicker patient outcomes. Healthcare organizations must be agile in adapting to these evolving technologies, changing regulations, and the expectations of consumers. Artificial intelligence, along with machine learning and deep learning, plays a vital role in enabling proactive patient care, reducing future health risks, and streamlining healthcare processes. It has proven particularly valuable in robot-assisted surgeries and early disease diagnosis, such as detecting cancer in its initial stages. Another advantage of AI is its capacity to handle data storage, apply advanced data analysis, and perform complex tasks at high speeds and low costs. AI is also employed in roles like virtual nursing assistants, clinical judgment or diagnosis support, image analysis, as well as managing workflows and administrative tasks.

### REFERENCES

- [1] S Gaikwad, K Hingol, S Kapadi, S Renuke and M Gaonkar, "Smart Assistant for Doctors", Journal of Computational and Theoretical Nanoscience, vol. 15, no. 11-12, pp. 3324-3327.
- [2] A Martín-Campillo, C. Martínez-García, J. Cucurull, R. Martí, S. Robles and J. Borrell, "Mobile Agents in Healthcare a Distributed Intelligence Approach", Computational Intelligence in Healthcare 4. Studies in Computational Intelligence, vol. 309, 2010.
- [3] Arnold, M. H. (2021). Teasing out artificial intelligence in medicine: An ethical critique of artificial intelligence and machine learning in medicine. Journal of Bioethical Inquiry, 18(1), 121-139. <https://doi.org/10.1007/s11673-020-10080-1>.
- [4] Davenport, T., & Kalakota, R. (2019). The potential for artificial intelligence in healthcare. Future Healthcare Journal, 6(2), 94-98. <https://doi.org/10.7861/futurehosp.6-2-94>
- [5] Guan. (2019). Artificial intelligence in healthcare and medicine: Promises, ethical challenges, and governance. Chinese Medical Sciences Journal, 0(0), 99. <https://doi.org/10.24920/003611>
- [6] Khanna, D. (2020). Use of artificial intelligence in healthcare and medicine. <https://doi.org/10.31221/osf.io/eshm9>
- [7] Kiener, M. (2020). Artificial intelligence in medicine and the disclosure of risks. AI & Kaur, et al Page 12 SOCIETY, 36(3), 705-713. <https://doi.org/10.1007/s00146-020-01085-w>
- [8] N.M.J. Augusstine and S.R.N. Samy, "Smart Healthcare Monitoring System using Support Vector

- Machine", Australian Journal of Science and Technology, vol. 2, no. 3, pp. 1-8, 2018.
- [9] Price, W. N., & Cohen, I. G. (2019). Privacy in the age of medical big data. *Nature Medicine*, 25(1), 37-43. <https://doi.org/10.1038/s41591-018-0272-7>.
- [10] Reddy, S., Fox, J., & Purohit, M. P. (2018). Artificial intelligence-enabled healthcare delivery. *Journal of the Royal Society of Medicine*, 112(1), 22-28. <https://doi.org/10.1177/0141076818815510>.
- [11] Artificial intelligence in healthcare: past, present and future <https://svn.bmj.com/content/2/4/230>
- [12] Artificial intelligence in healthcare [https://en.wikipedia.org/wiki/Artificial\\_intelligence\\_in\\_healthcare](https://en.wikipedia.org/wiki/Artificial_intelligence_in_healthcare)
- [13] Role of artificial intelligence in healthcare in the future <http://rx4group.com/what-role-is-artificial-intelligence-likely-to-play-in-healthcare-in-the-future/>
- [14] Use of Artificial intelligence in healthcare delivery, Sandeep Reddy, page 8/19.
- [15] Artificial intelligence in healthcare, eHealth initiatives, November 2018, 2 of 7.

**Citation of this Article:**

Prof. K.P.Raghuvanshi, Vaishnavi Kakde, Vaishnavi Bhonde, Sakshi Jawarkar, "AI in Healthcare" Published in *International Research Journal of Innovations in Engineering and Technology - IRJIET*, Volume 7, Issue 10, pp 308-311, October 2023. Article DOI <https://doi.org/10.47001/IRJIET/2023.710040>

\*\*\*\*\*



ISSN(online): 2581-3048  
Impact Factor : 5.95

## CERTIFICATE OF PUBLICATION

# INTERNATIONAL RESEARCH JOURNAL OF INNOVATIONS IN ENGINEERING AND TECHNOLOGY

*Is Hereby Awarding this Certificate to*

**Prof. K.P.Raghuvanshi**

Professor, Department of MCA, Vidyabharati Mahavidyalaya, Amravati, India

*In Recognition of the Publication of Manuscript Entitled*

**AI in Healthcare**

*Published in International Research Journal of Innovations in  
Engineering and Technology (IRJIET)*

**Volume 7, Issue 10, pp 308-311, October-2023**

<https://doi.org/10.47001/IRJIET/2023.710040>

Manuscript ID : IRJIET710040

Date of Issue : October 31, 2023



*K. P. Raghuvanshi*  
Editor-In-Chief  
IRJIET

*S. S. Suman*  
Managing Editor  
IRJIET

Mail us at: [editor@irjiet.com](mailto:editor@irjiet.com) / [irjietjournal@gmail.com](mailto:irjietjournal@gmail.com)  
Journal Website : [www.irjiet.com](http://www.irjiet.com)

# Cloud Computing for Big Data Analytics: A Comparative Evaluation

<sup>1</sup>Prof. K.P.Raghuvanshi, <sup>2</sup>Pranali Ganjare, <sup>3</sup>Gauri Wakekar, <sup>4</sup>Rutuja Bambal

<sup>1</sup>Professor, Department of MCA, Vidyabharati Mahavidyalaya, Amravati, India

<sup>2,3,4</sup>Student, Department of MCA, Vidyabharati Mahavidyalaya, Amravati, India

**Abstract** - The fusion of cloud computing with big data analytics has emerged as a catalyst for transformative insights and operational efficiency in a data-driven environment. The study investigates the function of cloud computing in the context of big data analytics, outlining its importance, potential, and constraints. It demonstrates the development of cloud computing platforms and the services they provide for storing, processing, and analyzing data. In addition, it explores the broad spectrum of big data analytics tools, platforms, and methodologies, highlighting the scalability and adaptability they accomplish in cloud contexts.

This study explores the distinct benefits and difficulties that arise as firms progressively move their analytical workloads to the cloud, examining crucial factors including security, compliance, and cost-effectiveness. The article examines the transformative effects of cloud-based big data analytics on several industries, from healthcare to finance, revealing creative solutions and predictive capabilities. It does this by drawing conclusions from real-world case studies.

**Keywords:** Cloud Analytics, Big Data Cloud, Platform Comparison, Data-driven Decisions, Security Assessment, Cloud Services, Business, Insights, Performance Evaluation.

## 1. Introduction

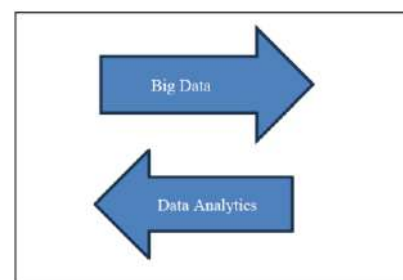
"Big Data" describes data volumes of one exabyte or more. According to Wikipedia, "big data" is a collection of datasets that are so large and complicated that they are difficult to process using database management tools or conventional data processing software. The issues involved in handling big data include gathering, storing, searching, sharing, transferring, analyzing, and visualizing it.

Volume, Velocity, and Variety are the three traits that must accompany the data to be deemed "big data" according to industry analyst Doug Laney from Gartner in 2001. Data size is determined by a quality or attributes called volume, which is typically expressed in Terabytes or Petabytes. Social media sites like Facebook, for instance, retain user images in addition to other things. Facebook is thought to hold over 250 billion

photos and more than 2.5 trillion posts from its users due to the vast number of users. The amount of data that needs to be processed and stored is tremendously large. 'Big data's' most illustrative characteristic is volume.

Velocity is the second quality or attribute. This is a reference to how much data is created or how quickly it needs to be processed and examined. For instance, Facebook members post more than 900 million images every day, or 104 photos per second. As a result, Facebook must analyze, store, and retrieve this data in real time for its users. As can be seen, the Internet of Things (IoT) and social media are the biggest data generators, and both are on the rise.

Variety, which refers to various data types that are produced from various sources, is the third attribute. Structured data (transactional data, spreadsheets, relational databases, etc.), semi-structured data (Extensible Markup Language, web server logs, etc.), and unstructured data (social media postings, audio, photos, and video, etc.) are the three main categories into which "Big Data" is typically divided. Meta-data, or data about data, is referred to in the literature as a fourth category.



## 2. Aim

The main goal of this research is to examine the interaction between big data and cloud computing, with a particular emphasis on how doing so can enable organizations to effectively manage, process, and gain useful insights from massive and complex datasets. This study aims to examine the core ideas behind big data and cloud computing, to highlight the benefits and drawbacks of its intersection, and to offer useful advice on how to deploy cloud-based big data analytics solutions. The ultimate objective is to arm enterprises with the

information and tactics required to capitalize on the promise of big data and cloud computing together, empowering them to make data-driven decisions, promote innovation, and keep a competitive edge in a data-centric environment.

### 3. Objective

The first step is to give a thorough evaluation of the fundamental ideas and supporting technology for both big data and cloud computing. This requires a thorough investigation of the fundamental elements and skills present in these two transforming realms.

Second, to examine the benefits and difficulties brought about by the combination of big data and cloud computing. The focus of this inquiry will be on crucial factors such data processing, scalability, cost-effectiveness, and cost-effective data storage. By doing this, we hope to present a complete view of the complexities related to this integration.

The third goal is to examine actual use cases and applications where cloud computing has been applied to big data analytics. We look to demonstrate the transformative impact on creativity and competitive advantage through in-depth assessments of how expands across many industries have used this integration.

The convergence of machine learning, artificial intelligence, and serverless computing will be highlighted, emphasizing their importance in data processing and analytics. This analysis will provide an opportunity into this field's evolving future.

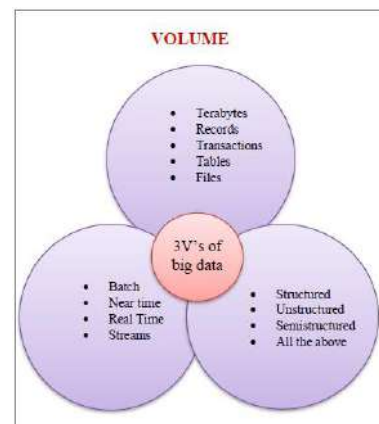
### 4. Opportunities

- Flexibility and scalability: To adapt to a business's changing demands, cloud computing platforms may be simply scaled up or down. Big data analytics, which frequently calls for the processing of enormous and intricate datasets, depend on this.

- Cost-effectiveness: Because cloud computing operates on a pay-as-you-go model, you only pay for the resources you really utilize. This can help you save a lot of money, especially if your big data demands are unpredictable.
- Quickness: Cloud computing platforms provide high-performance computing resources that may be leveraged to rapidly and efficiently execute big data workloads.
- Accessibility: Platforms for cloud computing are reachable from any location with an internet connection. This makes it simple for groups to work together on big data analytics projects, regardless of where they are in the world.

### 5. Research Methodology

This study's research technique uses a mixed-methods approach to thoroughly examine the point at which big data and cloud computing converge. Through focus groups, focus interviews, and content analysis of case studies and pertinent industry literature, qualitative data will also be acquired concurrently. These in-depth qualitative analyses seek to learn more about the struggles, successes, and experiences of businesses that have embraced this technological convergence.



### 6. Literature Review

Sr. No	Prediction Model	Authors	Techniques	Conference/Journal And Year	Year	Conclusion
1	Application of Cloud Computing for the Development of Big Data	Lam Ying Xian; Muhamad Ehsan Rana	Big Data processing, Big data Analytics	International Conference on Data Analytics for Business and Industry	2021	The application of cloud computing in the development of big data solutions has revolutionized the way organizations harness data for insights and innovation. The synergy between cloud and big data opens new opportunities for organizations to remain competitive in a data-driven world.
2	The Rise of Big Data and Cloud Computing	MohaiminUllam, Shamim Reza	Big Data Technologies, Big Data and Cloud Computing	Internet of Things and Cloud Computing	2019	Big data has become a new phenomenon in recent years Paradigm that offers abundant data and possibilities Improve and/or enable research and decision support. Applications with unprecedented value for the digital and Applications including business, science and technology.

3	Challenges and Benefits of Deploying Big Data Analytics in the Cloud for Business Intelligence	Data Integration and Management, Cost-Efficiency	Bala M. Balachandran, Shivika Prasad	International Conference on Knowledge Based and Intelligent Information and Engineering Systems	2017	In the ever-evolving landscape of data-driven decision making, the adoption of big data analytics in the cloud has emerged as a transformative force, challenging and empowering organizations seeking to leverage their data assets for business intelligence
4	Regression Analysis	M.Smithetal.	Statistical Modeling	Big Data Research	2019	This paper explores regression analysis as a predictive model for cloud-based big data analytics, highlighting its significance in comprehending data link ages and forecasting the future.
5	Challenges of Cloud Computing & Big Data Analytics	Anita Gupta; Abhay Mehrotra; P. M. Khan	Challenges in Big Data Analytics	International Conference on Computing for Sustainable Global Development	2015	We've delved into the diverse landscape of cloud computing and big data analytics, shedding light on the myriad challenges faced by practitioners and researchers in these interconnected fields.
6	Cloud Platform	Duan, Y., & Huang, J.	Comparative Analysis	IEEE International Congress on Big Data	2017	In order to shed light on the unique methodologies and strategies used on various cloud services, this study gives a thorough comparative analysis of big data management on several cloud platforms.
7	Big data Analytics tools	Verma,P., Ahuja,S., Sharma,M.	Comparative Analysis	Procedia Computer Science	2014	This study offers insights into the unique features and methodologies of numerous big data analytics tools through a detailed comparison examination.
8	Review Paper on Big Data Analytics in Cloud Computing	Saneh Lata Yadav , Asha Sohal	Map Reduce and Hadoop, Data Preprocessing	International Journal of Computer Trends and Technology	2017	This article describes a systematic process Exploring big data in the cloud environment Calculate. Big data is large and complex data sets and is created from various sources such as social networks.
9	Model for Big Data Analytics in Cloud Environment	Anupama M. Pande and Sunita A. Khaparde	Distributed Clustering, Map Reduce, K-Means	International Journal of Computer Applications	2013	Propose a distributed clustering model for big data analytics in the cloud using the K-Means and Map Reduce algorithm, which improves efficiency and scalability.
10	Service Performance and Analysis in Cloud Computing	Kaiqi Xiong	Security Considerations, Cloud Cost Analysis	IEEE	2019	By understanding the challenges and opportunities associated with service performance and analytics in cloud computing, cloud providers and customers can improve the quality of service provided to customers.
11	Cloud Computing: A Review	Abhishek Gautam	Services, Deployment Model	Journal For Research in Applied Science and Engineering Technology	2017	This article concluded the Introduction to Cloud Computing part, about its development and the purpose of development. And three types of services, Saas, Paas, Iaas.
12	Big Data Analytic Using Cloud Computing	Vinay kumarjain,Shi shirkumar	Big Data Processing, Real-time Data Analytics	IEEE International Conference on Spatial Data Mining and Geographical Knowledge Services	2015	The fusion of big data analytics and cloud computing offers businesses the opportunity to thrive in an era of data-driven competition. As the digital realm expands, the tools and techniques described in this document serve as a guide for those embarking on the journey to realize the potential of big data analytics in the cloud.
13	Cloud Computing-based Big Data mining Connotation and Solution	Yuan jjugen,xingruo nan	Data mining, Cloud computing	IEEE Second International Conference on Advances in Computing and Communication Engineering	2015	The convergence of cloud computing and big data mining has ushered in a new era of data-driven decision making and advanced analytics.

14	Cloud Based Big Data Analytics a Review	Amit Kumar Manekar, G. Pradeepini	Data management, Distributed Computing	International Conference on Computational Intelligence and Communication Networks	2015	We explore the dynamic and evolving landscape of cloud-based big data analytics. The convergence of big data and cloud computing has opened up a host of new possibilities.
----	---	-----------------------------------	--	---	------	---

### 7. Future Scope

- Integration of advanced analytics and AI: As machine learning and artificial intelligence (AI) technologies continue to advance, it will become more crucial to include big data and cloud computing into AI-driven analytics. Research can concentrate on improving real-time data analysis for predictive and prescriptive insights as well as optimizing AI algorithms in cloud environments.
- Edge computing and IoT: As Internet of Things (IoT) devices proliferate, so do the potential and difficulties associated with managing and analyzing data closer to its source. Future studies can explore the effective processing and analysis of data from edge devices and sensors using cloud computing.
- Hybrid and Multi-Cloud Environments: For flexibility and redundancy, businesses are increasingly implementing hybrid and multi- cloud strategies. Future research might examine the most effective methods for controlling and maximizing data and analytics workloads across various on-premises and cloud service providers.
- Data Privacy and Security: Research on effective data protection methods within the context of big data and cloud computing will remain vital as data privacy legislation grow and cybersecurity threats endure. This includes adhering to international data privacy standards, access control, and encryption.
- Cost Optimization: Future research on cloud- based big data analytics can concentrate on cost optimization measures, such as effective resource allocation, auto-scaling mechanisms, and picking the appropriate pricing models to limit costs.

### 8. Conclusion

Big data analytics and cloud computing together have a transformational power that improves the scalability and effectiveness of data-driven decision-making. Applications in the real world highlight its potential. However, it is crucial to handle security, compliance, and cost management. The relationship between cloud computing and big data analytics is a catalyst for innovation in this constantly changing digital age. The scope of data-driven opportunities grows tremendously as technology, from machine learning to artificial intelligence, continues to progress. The difficulties we encounter, such as those involving data security, moral

issues, and cost reduction, simply serve to highlight how important and fundamental this collaboration.

### REFERENCES

- Big Data Analytics and Cloud Computing by Richard Hill.
- Arpita, S., & Singh, R. K. (2018). Big Data Analytics in Cloud Computing: Opportunities, Issues and Future Trends. *Procedia Computer Science*, 132, 991-997.
- Duan, Y., & Huang, J. (2017). Comparative Study of Big Data Management on Different Cloud Platforms. In *2017 IEEE International Congress on Big Data (BigData Congress)* (pp. 311-318). IEEE.
- Lin, Y., Lee, W. C., & Lin, C. T. (2015). A Comparative Analysis for Big Data and Cloud Computing. *Procedia Computer Science*, 55, 993-1000.
- Verma, P., Ahuja, S., Sharma, M., & Kaur, A. (2014). Comparative Analysis of Big Data Analytics Tools. *Procedia Computer Science*, 50, 643-648.
- Zhang, Q., Cheng, L., & Boutaba, R. (2016). Cloud computing: state-of-the-art and research challenges. *Journal of Internet Services and Applications*, 7(1), 41.
- Subashini, S., & Kavitha, V. (2011). A survey on security issues in service delivery models of cloud computing. *Journal of network and computer applications*, 34(1), 1-11.
- Marz, N., & Warren, J. (2015). *Big Data: Principles and best practices of scalable real- time data systems*. Manning Publications.
- Han Hu, Yongyang Nen, Tat Seng Chua, Xuelong Li, "Towards Scalable System for Big Data Analytics: A Technology Tutorial", *IEEE Access*, Volume 2, June 2014.
- S.Vikram Phaneendra & E. Madhusudhan Reddy "Big Data solutions for RDBMS problems- A survey" In *12th IEEE/IFIP*.
- Anita Gupta; Abhay Mehrotra; P. M. Khan, Challenges of Cloud Computing & Big Data Analytics, *2015 2nd International Conference on Computing for Sustainable Global Development*.
- Neelay Jagani, Parthil Jagani, Big Data in cloud computing: A Literature Review *International Journal of Engineering Applied Sciences and Technology*, 2021, Vol 5.
- Blend Berisha, Endrit meizu, Ishak Shabani, Big data analytics in Cloud computing: an overview, *Journal of*





Cloud Computing volume 11, Article number: 24  
(2022).

**Citation of this Article:**

Prof. K.P.Raghuvanshi, Pranali Ganjare, Gauri Wakekar, Rutuja Bambal, “Cloud Computing for Big Data Analytics: A Comparative Evaluation” Published in *International Research Journal of Innovations in Engineering and Technology - IRJIET*, Volume 7, Issue 10, pp 366-370, October 2023. Article DOI <https://doi.org/10.47001/IRJIET/2023.710049>

\*\*\*\*\*



ISSN(online): 2581-3048

Impact Factor : 5.95

## CERTIFICATE OF PUBLICATION

### INTERNATIONAL RESEARCH JOURNAL OF INNOVATIONS IN ENGINEERING AND TECHNOLOGY

*Is Hereby Awarding this Certificate to*

**Prof. K.P.Raghuvanshi**

Professor, Department of MCA, Vidyabharati Mahavidyalaya,  
Amravati, India

*In Recognition of the Publication of Manuscript Entitled*

**Cloud Computing for Big Data Analytics: A Comparative  
Evaluation**

*Published in International Research Journal of Innovations in  
Engineering and Technology (IRJIET)*

**Volume 7, Issue 10, pp 366-370, October-2023**

<https://doi.org/10.47001/IRJIET/2023.710049>

**Manuscript ID :** IRJIET710049

**Date of Issue :** November 02, 2023



Editor-In-Chief  
IRJIET

Managing Editor  
IRJIET

Mail us at: [editor@irjiet.com](mailto:editor@irjiet.com) / [irjietjournal@gmail.com](mailto:irjietjournal@gmail.com)

Journal Website : [www.irjiet.com](http://www.irjiet.com)

# Generalization of Data Mining with Cloud Computing

<sup>1</sup>Prof. Kunal P. Raghuvanshi, <sup>2</sup>Anirudha S. Wankhede, <sup>3</sup>Chaitanya B. Karemore, <sup>4</sup>Yashavant G. Mundwaik, <sup>5</sup>Gaurav M. Chopade

<sup>1</sup>Professor, Department of MCA, Vidyabharati Mahavidyalaya, Amravati, India  
<sup>2,3,4,5</sup>Student, Department of MCA, Vidyabharati Mahavidyalaya, Amravati, India

**Abstract - Data mining with cloud computing is the process of extracting knowledge and ideas from large data sets using the resources and capabilities of cloud computing platforms. Cloud computing provides a scalable and cost-effective way to store, process and analyze large data sets. Cloud mining refers to the combination of dynamic, distributed real-time data management technology and data mining technology to achieve dynamic, distributed and efficient real-time processing, extraction and analysis of large amounts of data. In this paper, we present a data-mining platform based on cloud computing.**

**Keywords:** Data mining, Cloud computing, Data storage, Data Security, Data Management.

## 1. Introduction

Data mining is the process of obtaining valuable information from large amounts of data. Various techniques are used to identify patterns, trends, and anomalies in data. This information can then be used to improve business operations, make better decisions, and develop new products and services. At the same time, cloud computing has become an innovative technology that provides scalable and on-demand computing resources over the Internet. Combining the power of data mining with the flexibility of cloud computing offers a powerful synergy that is revolutionizing the way companies manage and derive value from their data.

Cloud computing is a general term for anything that involves providing hosted services over the Internet. These services are broadly divided into three categories: infrastructure as a service (IaaS), Platform as a Service (PaaS) and Software as a Service (SaaS). The name was cloud computing inspired by the cloud symbol commonly used to represent the Internet in flowcharts and diagrams.

## 2. Cloud Service Model and Models of its Implementation

There are three types of cloud service infrastructure Service, platform as a service, software as a service. In which SaaS is the king of all services.

### IaaS:

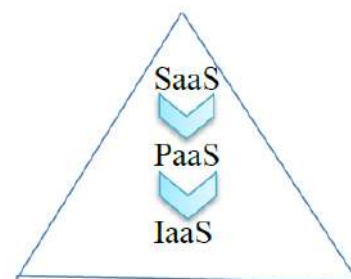
- Provides computing infrastructure as a utility Service, typically in a virtualized environment.
- Offers huge potential for extensibility and Scale.

### PaaS:

- Provides a platform or stack of solutions in a cloud Infrastructure.
- It is on top of IaaS architecture and Integrates with development and middleware Functions as well as database, messaging and Queue functions.

### SaaS:

- Deliver the application over the Internet or Intranet via a cloud infrastructure.
- Built on top of the underlying IaaS and PaaS layer.



Regardless of the type of service delivery model (SaaS, PaaS or IaaS), there are Three basic models of Implementation of cloud computing services, including:

### 1) Public Cloud:

A public cloud is a model of cloud computing in which resources, such as servers, storage, and networking, are owned and operated by a third-party cloud provider. Public clouds are available to everyone over the internet and are usually paid for as needed.

### 2) Private cloud:

A private cloud is a cloud computing environment intended for a single company. It is usually hosted on-

premises, but can also be hosted in a colocation facility or with a managed cloud service provider.

**3) Community cloud:**

Give more organizations the opportunity to share the same Cloud computing structure. Infrastructure supports special Communities that share common interests, needs and security Requirements.

**4) Hybrid Cloud:**

Hybrid cloud is a composition of two or more clouds (private, community or public), which remain independent entities, are interconnected and offer the benefits of multiple deployments Models. Hybrid cloud can also mean the ability to connect colocation, managed and/or dedicated services to the cloud Resource.

**3. Data Mining in Cloud**

Data Mining technique and application are very much needed in the cloud computing. Cloud computing infrastructure and resources play a critical role in supporting data mining tasks by providing scalable, flexible, accessibility and cost-effective solutions to handle large and complex data sets. And also make the good choice for business of all sizes.

Below are some examples of how cloud computing is used for data mining in the real world:

- Netflix: Netflix uses data mining to recommend movies and TV shows to its users based on their viewing history.
- Amazon: Amazon uses data mining to recommend products to its customers based on their purchasing history.

- Banks: Banks use data mining to detect fraudulent transactions.

**4. Cloud-Based Data Storage and Management**

Cloud-based data storage and management is the process of storing and managing data in the cloud. Cloud-based data storage solutions are a popular method of storing data as they offer a number of advantages over traditional on-premises storage solutions. The most popular cloud-based data storage solutions include:

- Amazon Simple Storage Service
- Microsoft Azure Blob Storage
- Google Cloud Storage



These services offer a variety of features and pricing options so you can choose the solution that best suits your needs. Here are some of the benefits of using cloud-based data storage solutions:

- Reduced costs
- Improved Scalability
- Increased Accessibility
- Enhanced Security

**5. Literature Review**

Sr. No.	Prediction Model	Authors	Techniques	Conference/Journal and Year	Conclusion
1	Cloud-Based Data Mining for Enhanced IoT Analytics	Saad Alahmari, Ekram Khan, and Saeed Anwar	Decision Trees, AWS IoT, Lambda	IEEE Internet of Things Journal, 2019	Developed an IoT analytics framework using AWS services that facilitates real-time data extraction and decision making in IoT applications.
2	Developed an IoT analytics framework using AWS services that facilitates real-time data extraction and decision making in IoT applications.	Charu Aggarwal	Scalability, Cloud Data Mining Challenges	Data Mining and Knowledge Discovery, 2013	It explored the challenges and opportunities in scalable data mining in cloud environments and highlighted the need for efficient algorithms and data preprocessing techniques.

3	Secure Data Mining in Cloud Computing Environments	Saeed Anwar, Shyam S. Chakraborty, and Zubair Baig	Homomorphic Encryption, Privacy-Preserving Mining	EEE Transactions on Industrial Informatics, 2017	Investigated secure data mining techniques in cloud computing environments, focusing on privacy-preserving mining using homomorphic encryption.
4	Scalable Data Mining in Cloud: Challenges and Opportunities	Charu Aggarwal	Scalability, Cloud Data Mining Challenges	Data Mining and Knowledge Discovery, 2013	Explored the challenges and opportunities in scalable data mining in cloud environments and highlighted the need for efficient algorithms and data pre-processing techniques.
5	Model for Big Data Analytics in Cloud Environment	Anupama M. Pande and Sunita A. Khaparde	Distributed Clustering, MapReduce, K-Means	International Journal of Computer Applications, 2013	Propose a distributed clustering model for big data analytics in the cloud using the K-Means and MapReduce algorithm, which improves efficiency and scalability.
6	Integration of Data Mining in Cloud Computing	Chetna Kaushal, Aashima Arya, Shikha Pathania	Scalable Cloud Resources	Advances in Computer Science and Information Technology (ACSIT),2015	Data mining integrated with cloud computing is very important Business characteristics to make effective decisions in order to Predict future trends and behaviors
7	Data Mining Based on Cloud-Computing Technology	Ying Ren, Hong Lv, Hua-wei Li, Li-jun Zhou	Parallel processing, data warehouse	MATEC web of Conference, January 2016	Through the analysis of data mining and cloud computing technology, this article proposes the architecture of data mining platform based on cloud computing, so that the data mining task of enterprises and users Individuals provide a good solution.
8	Data mining in Cloud Computing	Ruxandra-Stefania Petre	Data Security,Real time data mining	Database Systems Journal,2012	This document provides and overview of the Need and benefits of cloud data mining Computer science. Such as the need for data mining tools every day grows, the capacity of the Integration with Cloud Computing It is becoming stricter.
9	Data Mining and Cloud Computing	Robert Vrbic	Map Reduce, Parallel and Distributed Data Mining	Journal of Information Technology and Applications, 2012	The convergence of data mining and cloud computing has resulted in a transformative synergy that enables organizations to derive valuable insights from vast and complex data sets with unprecedented efficiency and scalability.
10	Implementation of Data Mining on a Secure Cloud Computing over a Web API using Supervised Machine Learning Algorithm	Tosin Ige, Sikiru Adewale	Web API Development, Data Preprocessing	International Journal of Advanced Computer Science and Applications,2022	We are able to implement data mining in a secure cloud Ninety-four accurate computing environment percentage after optimization in our decision tree algorithm through Web API. They are all AI engineers, data scientists, or machines. Learning engineer requirements are just the endpoint of the API
11	Study of Data Mining algorithm in cloud computing using MapReduce Framework	Viki Patil, V. B. Nikam	Handling Big Data, MapReduce Framework	Journal of Engineering, Computers & Applied Sciences ,2012	There are many new technologies emerging at a rapid rate, each with technological advancements and with the potential of making ease in use of technology.
12	Cloud Computing Concepts	M. Malathi	Service model,Load balancing	IEEE,2011	Cloud computing is a powerful tool that can help businesses of all sizes improve their efficiency and productivity. If you are considering using cloud computing, you should carefully consider your needs and requirements
13	Service Performance and Analysis in Cloud Computing	Kaiqi Xiong	Security Considerations, Cloud Cost Analysis	IEEE, 2009	By understanding the challenges and opportunities associated with service performance and analytics in cloud computing, cloud providers and customers can improve the quality of service provided to customers.
14	Cloud Computing: A Review	Abhishek Gautam	Services, Deployment Model	Journal For Research in Applied Science and Engineering Technology	This article concluded the Introduction to Cloud Computing part, about its development and the purpose of development. And three types of services, Saas, Paas, Iaas.

## 6. Conclusion

Data mining technologies provided by Cloud computing is absolutely necessary Characteristic of today's companies proactive and knowledge-based decisions, there helps them develop future tendencies and behaviours predicted. In cloud computing, integrated data mining is very important feature in companies to make effective decisions and predict future trends and behaviors.

Cloud computing is increasingly a part of IT and many large companies will implement cloud computing. Some of them offer IaaS, PaaS and others SaaS. Amazon.com and IBM offer storage services, while Google Apps provides software as a service. In the near future, we will be working on data science, artificial intelligence and machine learning services within the cloud provider to protect sensitive customer data such as login information using encryption techniques and other passwords Protection engineering within the security group so that we can increase efficiency and accuracy and make the data more secure.

## REFERENCES

- [1] Data Mining: Concept and Technique by Jiawei Han and Micheline Kamber.
- [2] Cloud Computing: Concepts, Technology & Architecture by Thomas Erl, Ricardo Puttini & Zaigham Mahmood.
- [3] Data Mining in Cloud Computing By Ruxandra Stefania Petre Database Systems Journal vol.III, no 3/2012.
- [4] Big Data with Cloud Computing: Discussions and Challenges by Amanpreet Kaur Sandu, Big Data Mining and Analytics Volume 5, Number 1, March 2022.
- [5] Kaiqi Xiong, "Service Performance and Analysis in Cloud Computing", IEEE, 2009.
- [6] Integration of Data Mining In Cloud Computing, Chetna Kaushal, Aashima Arya, Shikha Pathania,

- Advance in Computer Science and Information Technology, Volume 2, Number 7 , June 2015.
- [7] Data Mining in Cloud Computing, Xia Geng , Zhi Yang, International Conference on Information Science and Computer Applications, 2013.
  - [8] Review Of Data Mining Technique in Cloud Computing Database, Astha Pareek, Manish Gupta, International Journal Of Advance Computer Research, Volume 2, Number 2, 2012.
  - [9] Intelligent Cloud Resource Management with Deep Reinforcement Learning IEEE, cloud computing, Volume 4, December 2017.
  - [10] A Review Paper on Cloud Computing, Abhiraj Apurav, International Journal Of Scientific Research In Engineering And Management, August 2023.
  - [11] A Study on Cloud Computing Services, Dr. CH. V. Raghavendran, Dr. G. Naga Satish, Dr. P. Suresh Varma Dr. G. Jose Moses , International Journal of Engineering Research & Technology, 2016.
  - [12] M. Malathi, "Cloud Computing Concepts", IEEE, 2011.
  - [13] N. Sadashiv and S. D. Kumar, "Cluster, grid and cloud computing: A detailed comparison," 2011 IEEE 6th International Conference on Computer Science & Education (ICCSE), pp. 477–482, 2011.
  - [14] Data mining in cloud computing: Survey, Medara Rambabu, Swati Gupta, Advance in Intelligent System and Computing.
  - [15] [https://www.researchgate.net/publication/344353852\\_Data\\_Mining\\_in\\_Cloud\\_Computing\\_Survey](https://www.researchgate.net/publication/344353852_Data_Mining_in_Cloud_Computing_Survey).
  - [16] Research paper on security issues in cloud Computing, International Journal of Creative Research Thoughts, Volume 9, April 2021.
  - [17] Research Analysis Of Cloud Computing, G. Vijay Baskar, N. Sathees Kumar, N. Karthick, International Journal of computer Science and Mobile Computing, volume 2, May 2013.

### Citation of this Article:

Prof. Kunal P. Raghuvanshi, Anirudha S. Wankhede, Chaitanya B. Karemore, Yashavant G. Mundwaik, Gaurav M. Chopade, "Generalization of Data Mining with Cloud Computing" Published in *International Research Journal of Innovations in Engineering and Technology - IRJIET*, Volume 7, Issue 10, pp 304-307, October 2023. Article DOI <https://doi.org/10.47001/IRJIET/2023.710039>

\*\*\*\*\*



ISSN(online): 2581-3048  
Impact Factor : 5.95

## CERTIFICATE OF PUBLICATION

### INTERNATIONAL RESEARCH JOURNAL OF INNOVATIONS IN ENGINEERING AND TECHNOLOGY

*Is Hereby Awarding this Certificate to*

**Prof. Kunal P. Raghuvanshi**

Professor, Department of MCA, Vidyabharati Mahavidyalaya, Amravati, India

*In Recognition of the Publication of Manuscript Entitled*

### **Generalization of Data Mining with Cloud Computing**

*Published in International Research Journal of Innovations in  
Engineering and Technology (IRJIET)*

**Volume 7, Issue 10, pp 304-307, October-2023**

<https://doi.org/10.47001/IRJIET/2023.710039>

**Manuscript ID :** IRJIET710039

**Date of Issue :** October 31, 2023



*K. Raghuvanshi*  
Editor-In-Chief  
IRJIET

*S. S. S. S.*  
Managing Editor  
IRJIET

Mail us at: [editor@irjiet.com](mailto:editor@irjiet.com) / [irjietjournal@gmail.com](mailto:irjietjournal@gmail.com)

Journal Website : [www.irjiet.com](http://www.irjiet.com)

# Transparent Supply Chains with Blockchain

<sup>1</sup>Prof. S.R.Thakare, <sup>2</sup>Shubhangi Raut, <sup>3</sup>Vaishavi Ingale

<sup>1</sup>Head of MCA Department, Vidya Bharati Mahavidyalaya, Amaravati, India

<sup>2,3</sup>Student, Department of MCA, Vidya Bharati Mahavidyalaya, Amaravati, India

**Abstract** - Supply chain operation (SCM) is a core commercial exertion responsible for moving goods and services from one point to another through colorful stakeholders. The traditional SCM is grounded on a centralized approach managed at the central headquarter, and all other sub-offices get instructions from the main office. Some major issues with present SCM systems are security, transactional translucency, traceability, stakeholder involvement, product counterfeiting, fresh detainments, fraud, and precariousness. The traditional SCM is grounded on a centralized approach. A single business headquarters and a single storehouse full of departmental directors in different areas like logistics, distribution, and procurement, and these directors are responsible for overseeing their specific position during the complete force chain. They keep track of the information in a centralized database stored hard. When the data on the record isn't salutary to the company's growth, it may be misrepresented intimately. As a result, distrust between a ventures has precipitously conspicuous, performing in advanced communication charges. Also, there's no pricing translucency in the force chain because of the mediators. Likewise, because of the high threat of data manipulation inside the adventure, the data across force chain realities is inharmonious; as a result, the product tracing procedure has been delayed. In moment's force chain, there's no translated medium to store consumers' private information. Cyber-attacks will be suitable to pierce this data, revealing important public and particular information.

Another crucial issue is that goods only travel in one direction in moment's force chain operation. As a result, if a product is defective, the client is responsible for the consequences. SCM is a core commercial exertion responsible for moving goods and services from one point to another through a variety of stakeholders. Different groups, coffers, actions, and associations are concerned with converting raw accoutrements into completed products and satisfying consumer orders, which are appertained to as force chains. It's an connected network of pots, individualities, conditioning, information, and coffers that are included in fabricating and transferring a product or service from the dealer to the customer via a planned inflow of information, physical dispersion, and

payment. It starts with the delivery of raw accoutrements to a manufacturer and stops with the delivery of the completed product or service to the consumer. Control of the sluice of products and services to maintain the quality of sensitive goods throughout the payload, exclude gratuitous charges, and more satisfy client prospects is known as force chain operation.

**Keywords:** Transparent, Supply Chains, Blockchain, SCM.

## 1. Introduction

Transparency is viewed as a supporting pillar of supply chain management (SCM). A lack of transparency involving supply chain partners and practices can contribute to corporate and government scandals. As a result, improving supply chain transparency offers potential benefits to firms across the supply chain network. Globalization of supply chains, moreover, increases the complexity of these networks and thereby also increases the need for transparency to better manage processes, product flows, financial transactions, and information exchange. Maintaining secure supply chain information networks is another key feature of supply chain strategy. The critical purpose of information security is to protect user data from being modified or compromised. Yet, transparency requires disclosing potentially sensitive information to other participants in the supply chain. This raises the issue as to whether both transparency and security can be achieved simultaneously in SCM. Blockchain applications are currently evolving from pilot trials to real world applications. According to the International Data Corporation (IDC), worldwide spending on blockchain solutions will reach \$11.7 billion in 2022. This is particularly relevant to SCM, as supply chain blockchains represent one of the most promising opportunities for the implementation of the distributed ledger technology.

## 2. Supply chain transparency

Supply Chain Transparency and Security Transparency involve sharing information among different participants across the supply chain network. As more partners engage within that network, information availability increases resulting in greater transparency, which boosts both traceability and visibility. Traceability in a supply chain is generally the ability of the system to identify and verify



individual components including the historical state of activities. This involves tracking a product's flow and its attributes throughout the entire supply network. Traceability applies not only to the physical movement of a product but also to the information related to product quality and safety.

### 3. Blockchain in supply managements

**Blockchain in Supply Chain** The creation of blockchains has been called one of the most revolutionary innovations to emerge in recent years. Several studies reported that blockchain SCM integration is still in its infancy. Researchers typically suggest that blockchains can bring specific benefits to SCM.

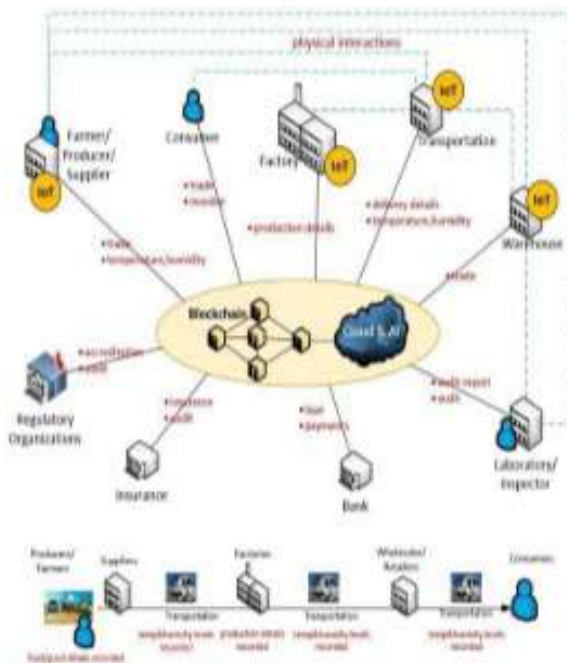


Figure 1: Participants and their roles in a typical blockchain integrated supply chain flow

### 4. Blockchain technology background

Original idea and building blocks of blockchain technology are coming from crypto money and date back to 1980s. Most recently, in 2008 December the article by an author nicknamed Satoshi Nakamoto titled as "Bitcoin: A Peer-to-peer Electronic Cash System" popularized the blockchain technology. The blockchain concept consists of a combination of mathematics, crypto, computer and monetary science.

Blockchain technology, in fact, is a type of parallel and distributed computing architecture. It allows to eliminate central servers or trusted authority in digital interactions of partners. Thus it is classified as a disruptive technology which has potential to transform radically most of the processes in

our daily life. Simply, copies of the data, called ledger, are stored on thousands of computers working together, and all changes to the data are provided by consensus of partners. The parties of the system are according to consensus protocols used to ensure trust are Proof of Work (PoW), Byzantine Fault Tolerance (BFT), Proof of Stake (PoS) and Proof of Elapsed Time (PoET). The main purpose of the consensus mechanism is to ensure that proposed change requests are compatible with existing status of data and rules. Blockchain computers, called nodes, perform these validations. Cryptography is mainly used to ensure the authenticity of change requests on data and the immutability of data in the ledger by organizing modification history as blocks cryptographically connected each other. Privacy is another important issue in blockchain. Crypto is also used to ensure the privacy of the participant. High availability of the ledger is provided by keeping the entire ledger at the nodes, not at the center.

The main consensus protocols used to ensure trust are Proof of Work (PoW), Byzantine Fault Tolerance (BFT), Proof of Stake (PoS) and Proof of Elapsed Time (PoET). The main purpose of the consensus mechanism is to ensure that proposed change requests are compatible with existing status of data and rules. Blockchain computers, called nodes, perform these validations. Cryptography is mainly used to ensure the authenticity of change requests on data and the immutability of data in the ledger by organizing modification history as blocks cryptographically connected each other. Privacy is another important issue in blockchain. Crypto is also used to ensure the privacy of the participant. High availability of the ledger is provided by keeping the entire ledger at the nodes, not at the center.

There are mainly two types of blockchain platform namely, public and private. In public blockchain anyone can send change requests to the network and can operate a node. In private blockchain, also called permissioned blockchain, both sending requests to the network and having a node is restricted to a set of actors.

### 5. Problems of Supply Chain and Opportunities with Blockchain

The main objectives of the supply chain are listed as cost, quality, speed, dependability, risk reduction, sustainability, and flexibility (Kshetri, 2018). Manufacturing has been globalized, leads well defined supply chain management more crucial and valuable. In today's supply chain systems, it is difficult for customers to know exactly the value of a product due to lack of transparency. In addition, investigating supply chains mostly is not feasible in case of suspicion of illegal or unethical activities.

Heavy paperwork, process costs, and slow processes are other main challenges of the supply chain. A literature survey on the research focuses on blockchain for supply chain domain shows that the supply chain domain already benefits from blockchain technology because of its four main features.

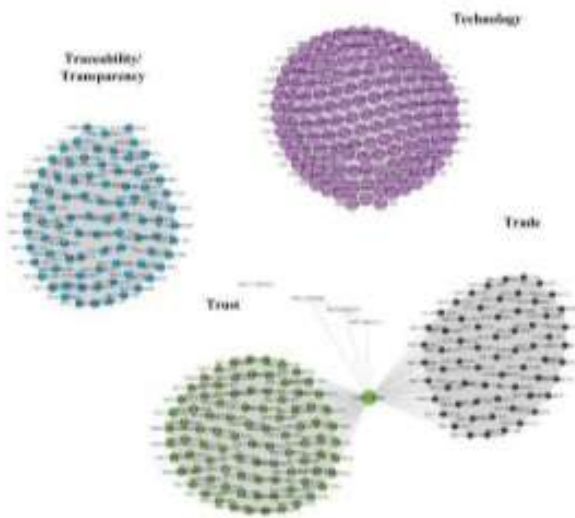


Figure 2: Research focuses in literature for deployment of blockchain for supply chain

Supply chain participants	Current limitations	Blockchain impact
Producer	Lack of ability to prove the origin and quality metrics of products transparently	Benefits from increased trust of keep track of the production raw material and value chain from producer to consumer
Manufacturer	Limited ability to monitor the product to the final destination. Limited capabilities of checking quality measured from raw material.	Added value from shared information system with raw material suppliers and distribution networks
Distributor	Custom tracking systems with poor collaboration capabilities. Limited certification identity and trust issues.	Ability to have proof-of-location and conditions certifications registered in the ledger.
Wholesaler	Lack of trust and verification of the products' path.	Ability to check the origin of the goods and the transformation/transportation conditions.
Retailer	Lack of trust and certification of the products' path. Tracking of products between consumers and wholesalers.	Ability to handle effectively the return of malfunctioning products.
Consumer	Lack of trust regarding the compliance of the product with respect to origin, quality and compliance of the product to the specified standards and origin.	Full and transparent view on the product origin and its whole journey from raw material to final purchased product.

Table 1: How blockchain can improve the existing limitations of supply chains

In order to give an idea how blockchain might impact the needs of supply chain actors, we quoted Table 1 from literature. It presents Litke (2019)'s summary on how blockchain responds to the limitations that the actors of supply chains encounter today, other application areas. Employing blockchain in supply chain processes provides transparent, decentralized, secure, faster and low cost transactions. By eliminating unnecessary third parties and covering more daily life processes in digital systems minimizes paperwork. Blockchain establishes trust among trading partners. Making more detailed data available in blockchain, improves supply chain monitoring ability and safety. This reduces insurance risks. Smart contracts and automated payments are game changer. They add efficiency and remove bureaucracy especially in insurance, and traceability. They also allow escrowed payment by keeping money until terms of the deal are met and agreed, and then releasing automatically.

Blockchain technology, in fact, provides missing infrastructure the cutting edge technologies need. Thus, increasing focus on providing integration and cooperation with technologies such as Artificial Intelligence, Big Data Analytic, Cloud Computing and IoT will help to realize advanced supply chain systems.

Now, there has been a considerable increase in the need for SC's fairness, security, and efficiency. The stakeholders have begun to demand a more transparent SCM process. End users want to know the complete information on the provenance of the items. To address such a problem, a tamper resistant tracking method must be created. Infrastructure decentralization and the development of a trust layer for business logic may be revolutionized using BC technology. BC is an immutable, permanent record system created by covering encrypted information in chronological order. Decentralization, traceability, tamper-proofing, and cryptographic security are all important elements of the BC system. Besides, smart contracts can be created, permitting transactions to be done safely between commonly un-trusted parties. Smart contracts are a type of digital contract or agreement. When a certain goal is fulfilled, a smart contract can be configured to do a task without the participation of a third party. BC can also support automatic payments, quality control, and stakeholder trust, among other things. Real-time data handling with monitoring and regulating data in a virtual environment, less paperwork, increased efficiency with faster response times, increased supply chain visibility, and reduced geographic limits are several advantages of adopting BC in supply chains. It also reduces the risk of SCM attacks.

## 6. Comparisons with the Existing Surveys

Several industries outside of finance, such as the supply chain, are among the most extensively discussed BC applications. BC technology is ideal for addressing supply chain concerns. The possibility of adopting BC technology in SCM has been a topic of investigation, and several reviews have been published so far that gives an overview of the current situation and a research path forward. Motivated by these facts, we have reviewed various supply chains in the proposed survey. This section compares state-of-the-art works that focus on the BC and SCM and their integration.

### 1) Conclusions

Blockchain is widely regarded as one of the important technology in many industries. It improves trust, transparency, traceability and security in the supply chain. The purpose of this literature is to focus on the usage of the blockchain in the supply chain.

## 2) Contributions

This paper investigates the current status of BC technology implementation in various supply chain network areas. We comprehensively surveyed the application of BC in Food and Health supply chain networks. This study makes several significant contributions, including theoretical advances related to the adoption of BC in the supply chain.

## REFERENCES

- [1] News articles  
<https://www.cryptopolitan.com/blockchain-technology-boost-business-growth/>
- [2] [https://www.meity.gov.in/writereaddata/files/National\\_BCT\\_Strategy.pdf](https://www.meity.gov.in/writereaddata/files/National_BCT_Strategy.pdf)
- [3] <https://blockchain.gov.in/>
- [4] [https://www2.deloitte.com/content/dam/insights/us/articles/2019-global-blockchain-survey/DI\\_2019-global-blockchain-survey.pdf](https://www2.deloitte.com/content/dam/insights/us/articles/2019-global-blockchain-survey/DI_2019-global-blockchain-survey.pdf)
- [5] [https://www.researchgate.net/publication/353764416\\_Blockchain\\_Technology\\_for\\_Supply\\_Chain\\_Management](https://www.researchgate.net/publication/353764416_Blockchain_Technology_for_Supply_Chain_Management)

### Citation of this Article:

Prof. S.R.Thakare, Shubhangi Raut, Vaishavi Ingale, "Transparent Supply Chains with Blockchain" Published in *International Research Journal of Innovations in Engineering and Technology - IRJIET*, Volume 7, Issue 10, pp 696-699, October 2023. Article DOI <https://doi.org/10.47001/IRJIET/2023.710092>

\*\*\*\*\*





ISSN(online): 2581-3048

Impact Factor : 5.95

## CERTIFICATE OF PUBLICATION

### INTERNATIONAL RESEARCH JOURNAL OF INNOVATIONS IN ENGINEERING AND TECHNOLOGY

*Is Hereby Awarding this Certificate to*

**Prof. S.R.Thakare**

**Head of MCA Department, Vidya Bharati Mahavidyalaya, Amaravati, India**

*In Recognition of the Publication of Manuscript Entitled*

### **Transparent Supply Chains with Blockchain**

*Published in International Research Journal of Innovations in  
Engineering and Technology (IRJIET)*

**Volume 7, Issue 10, pp 696-699, October-2023**

<https://doi.org/10.47001/IRJIET/2023.710092>

**Manuscript ID : IRJIET710092**

**Date of Issue : November 13, 2023**



  
Editor-In-Chief  
IRJIET

  
Managing Editor  
IRJIET

Mail us at: [editor@irjiet.com](mailto:editor@irjiet.com) / [irjietjournal@gmail.com](mailto:irjietjournal@gmail.com)  
Journal Website : [www.irjiet.com](http://www.irjiet.com)

# Impact of Machine Learning in Natural Language Processing (NLP)

<sup>1</sup>Prof. S.R.Thakare, <sup>2</sup>Darshana Bhatti, <sup>3</sup>Shubhangi Shende

<sup>1</sup>Professor, Department of MCA, Vidya Bharti Mahavidyalaya, Amravati, India

<sup>2,3</sup>Student, Department of MCA, Vidya Bharti Mahavidyalaya, Amravati, India

**Abstract** - Natural Language Processing (NLP) has witnessed unprecedented growth and innovation in recent years, largely propelled by advancements in machine learning techniques. This research paper provides a detailed exploration of the pivotal role that machine learning plays in the field of NLP, highlighting its profound impact on various aspects of language understanding, generation, and analysis. The paper begins by tracing the historical evolution of NLP, from rule-based approaches to the current era dominated by data-driven machine-learning methods. It elucidates how machine learning, with its ability to extract patterns and meaning from vast amounts of textual data, has revolutionized the NLP landscape. Furthermore, the paper delves into the core components of NLP where machine learning has made significant contributions. It discusses the pivotal role of supervised learning in tasks such as sentiment analysis, text classification, and named entity recognition. Additionally, It explores the emergence of unsupervised learning and its applications in topics like word embeddings, topic modeling, and document clustering.

**Keywords:** Natural Language Processing, Machine Learning, Deep Learning, Sentiment Analysis, Neural Networks, pre-trained Language Models, Ethical Considerations, Multimodal learning.

## I. Introduction

Machine Learning and Natural Language Processing are super important subfields of Artificial Intelligence that have gained prominence in recent times. The goal of NLP is to build systems that can make sense of the text and automatically perform tasks like translation, spell check, or topic classification.

Machine Learning and Natural Language Processing play an awfully important part in making a synthetic agent into an artificial 'intelligent' agent. An Artificial Intelligence system can accept better information from the environment and might act on the environment in a user-friendly manner because of the advancement of Language Processing.

Similarly, artificial intelligent systems can process information and make more accurate forecasts for their actions. It's like they've become supercharged with intelligence.

Example Traditional algorithms follow a predefined set of instructions and struggle to handle unknown problems with multiple variables. However, machine learning algorithms excel in such situations by leveraging past examples and adapting to new challenges. Machine learning algorithms can learn from data and make informed predictions, making them much more effective when dealing with unknown variables in real-world problems.

Deep learning, which encompasses the use of artificial neural networks, is a specialized branch of machine learning. Lately, deep learning techniques have gained significant popularity and have achieved remarkable results. One key reason behind their success is the flexibility they offer in designing the network architecture. This adaptability has proven crucial in various applications, including natural language processing research. Deep learning techniques have truly revolutionized the field of machine learning and continue to push boundaries. Natural language processing empowers machines to understand and process human languages. Natural Language Processing gave the system the ability to understand English or the Hind language.

Natural language processing has gained widespread adoption due to its incredible user-friendliness. It allows us to do so much with just our voice, from selecting music to controlling various electronic appliances like air conditioners, ovens, and even ceiling fans and light bulbs. This technology has truly transformed these devices into smart gadgets that respond to our commands. All this is possible because of Natural Language Processing.

## II. Impact of Machine Learning in Natural Language Processing

Processing natural language involves multiple steps to enable machines to understand and interpret human language. These steps include Morphological Analysis, Semantic Analysis, Semantic Analysis, Discourse Analysis, and pragmatic Analysis, generally, these analysis tasks are applied

serially. Machine learning plays a crucial role in enhancing various natural language processing processes. It adds value by enabling systems to learn patterns and make predictions based on vast amounts of data.



### 1. Morphological Analysis:

It is the study of word structure and forms in NLP. It helps understand word meaning and grammar.

### 2. Syntactic Analysis:

It is study of sentence structure and grammar in NLP. It helps understand how words are combined to form meaningful sentences.

### 3. Semantic Analysis:

It is the study of meaning in NLP. It helps understand the interpretation and representation of words and sentences.

### 4. Discourse Analysis:

It is the study of how language is used in communication and conversation. It helps understand the structure, coherence, and meaning of extended texts or conversations.

### 5. Pragmatic Analysis:

It is the study of how language is used in context to convey meaning beyond the literal interpretation of words. It helps understand the intentions, implicatures, and social aspects of communication.

## III. Role of Machine Learning In The Application Of Natural Language Processing

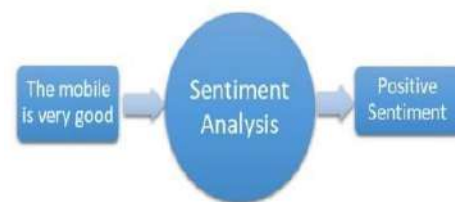
NLP applications heavily rely on natural language machine learning and deep learning algorithms to process tasks. These algorithms play a crucial role across a wide range of NLP applications, making them an integral part of the field.

Various deep learning techniques, such as Deep Neural Networks, Autoencoders, Restricted Boltzmann Machines, Recurrent Neural Networks, and Convolutional Neural Networks, have been extensively explored and implemented in different applications of natural language processing

Recurrent Neural Networks (RNNs) and their variants, such as Long Short-Term Memory (LSTM) and Gated Recurrent Unit (GRU), along with Convolutional Neural Networks (CNNs) and their variants like Recurrent Convolutional Neural Networks (RCNN) and Regional Convolutional Neural Networks (R-CNN), have been extensively studied and applied in natural language processing applications.

### 1. Sentiment Analysis:

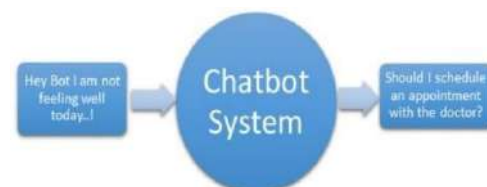
Sentiment analysis plays a crucial role in understanding user opinions and sentiments towards a particular product or service. It has become increasingly important in customer relationship management, as even a single negative opinion can have a significant impact on the product's reputation. In recent times, deep learning techniques have gained popularity and have been extensively utilized in sentiment analysis.



### 2. Chatbot Systems:

Chatbot systems are conversational agents or dialog systems that try to engage the user in conversation. Conversation can be continued through voice or text. Personal assistants like Amazon's Alexa and Google Assistant have made the chatbot system more popular and have shown the convenience they offer. However, developing a fully capable chatbot that can replace a human agent is indeed a challenging task, which requires Natural Language Understanding and Natural Language Generation.

Recent frameworks like Google's, IBM's Watson AI, and Amazon's Alexa AI provide an easy way of developing a chatbot system. And, all these frameworks employ complex and proprietary deep-learning architectures.



### 3. Question and Answering Systems:

Nowadays, there is a blurring line between dialogue systems and question-answering systems. Chatbot systems often perform question-answering tasks, and vice versa. So, research efforts focused on developing a chatbot system will likely involve developing a question-answering system as well.

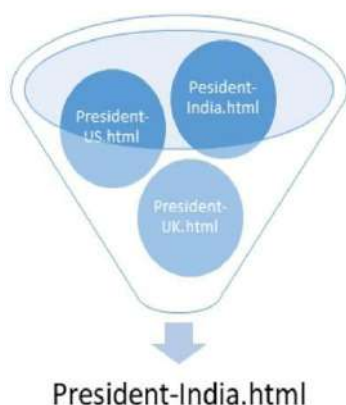
A question-answering system consists of three key components: question processing, information retrieval, and answer processing. Machine learning and deep learning techniques have been instrumental in advancing all three components.

Question processing, in particular, has received significant research attention. The goal is to understand the question to improve answer retrieval effectively. Researchers have approached question processing as a classification problem and explored various deep-learning techniques for better question classification.



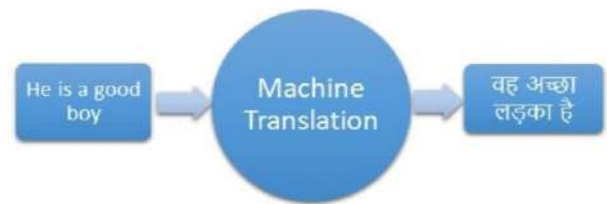
### 4. Information Retrieval Systems:

Information Retrieval is another important application of NLP that tries to retrieve relevant information. Information retrieval systems act as the backbone of systems like chatbot systems and question-answering systems. The basic way to retrieve information is by analyzing keyword frequency. However, advanced systems process a vast amount of data to extract only the relevant information. This alternative method allows for more efficient and accurate retrieval of data. This process is carried out using deep learning techniques.



### 5. Machine Translation

A machine translation system aims to translate a text from one language to another with minimal or no human intervention. Applications like Google Translate are prime examples of machine translation systems. Simply translating word-for-word is not sufficient, as sentence structure can vary across languages. Machine translation systems use advanced algorithms and artificial intelligence to analyze and understand the structural and linguistic differences between languages.



### IV. The Relationship between Machine Learning and Natural Language Processing

Machine learning and natural language processing are closely related. Machine Learning techniques, such as deep learning and neural networks, are used in natural language processing to train models that can understand, interpret, and generate human language. These models learn from large amounts of text data to recognize patterns, extract meaning, and make predictions. Machine learning empowers natural language processing systems to perform tasks like sentiment analysis, text classification, machine translation, and more. It's an exciting field that continues to advance our ability to interact with computers using human language.

#### 1. Supervised Machine Learning for NLP:



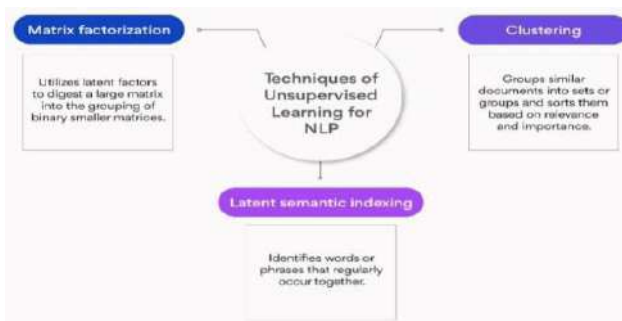
In supervised learning, models are trained using labeled data to find the mapping function between input variable X and output variable Y.  $Y=f(X)$  Supervised learning needs supervision to train the model, which is similar to how a student learns things in the presence of a teacher. Supervised learning can be applied to regression problems (predicting

continuous values) and classification problems (predicting categorical values). In this form of NLP machine learning, statistical models are employed to enhance its understanding and performance. It becomes precise over time and data scientists can broaden the textual data the machine interprets as it continually learns.



## 2. Unsupervised Machine learning for NLP:

Unsupervised learning is a different type of machine learning where patterns are discovered in unlabeled data. It aims to find hidden structures and patterns without any guidance or supervision. Instead, the algorithm learns on its own by analyzing the data.



## V. Conclusion

In conclusion, the research paper underscores the pivotal role that machine learning plays in advancing the capabilities of natural language processing, it emphasizes the need for ongoing research to address challenges and maximize the potential of these technologies in revolutionizing communication understanding, and interaction with human language.

In conclusion, we can say using machine learning makes our life easy for example if we are searching for something it helps to make it easy by machine learning keep learning from history so it helps us in it. All our grammatical mistakes it automatically corrected and gives us accurate results of our search. Through this research paper, we can easily understand the processes of processing. How it converts our language to computer language make it easy and by using natural language processing computer can easily understand our language. Machines make it easy to use computers in our comfort zone and without any problem of understanding.

Throughout the paper, it becomes evident that the utilization of machine learning methods significantly enhances the performance of NLP applications. The accuracy and efficiency of tasks like language translation, sentiment analysis, and speech recognition have improved due to the power of machine learning algorithms.

## REFERENCES

- [1] Natural Language Processing and Information Retrieval. By Tanveer Siddiqui, U.S. Tiwari.
- [2] Handbook of Natural Language Processing. By Nitin Indurkha, Fred J. Damaerau.
- [3] Machine Learning (Master Supervised and Unsupervised Learning Algorithms with Real Example) By Dr. Ruchi Doshi, Dr. Kamal Kant Hiran.
- [4] Google.

### Citation of this Article:

Prof. S.R.Thakare, Darshana Bhatti, Shubhangi Shende, "Impact of Machine Learning in Natural Language Processing (NLP)" Published in *International Research Journal of Innovations in Engineering and Technology - IRJIET*, Volume 7, Issue 10, pp 315-318, October 2023. Article DOI <https://doi.org/10.47001/IRJIET/2023.710042>

\*\*\*\*\*





ISSN(online): 2581-3048

Impact Factor : 5.95

## CERTIFICATE OF PUBLICATION

### INTERNATIONAL RESEARCH JOURNAL OF INNOVATIONS IN ENGINEERING AND TECHNOLOGY

*Is Hereby Awarding this Certificate to*

**Prof. S.R.Thakare**

Professor, Department of MCA, Vidya Bharti Mahavidyalaya,  
Amravati, India

*In Recognition of the Publication of Manuscript Entitled*

**Impact of Machine Learning in Natural Language Processing  
(NLP)**

*Published in International Research Journal of Innovations in  
Engineering and Technology (IRJIET)*

**Volume 7, Issue 10, pp 315-318, October-2023**

<https://doi.org/10.47001/IRJIET/2023.710042>

**Manuscript ID :** IRJIET710042

**Date of Issue :** November 02, 2023



*S.R. Thakare*  
Editor-In-Chief  
IRJIET

*S. S. ...*  
Managing Editor  
IRJIET

Mail us at: [editor@irjiet.com](mailto:editor@irjiet.com) / [irjietjournal@gmail.com](mailto:irjietjournal@gmail.com)

Journal Website : [www.irjiet.com](http://www.irjiet.com)



# Artificial Intelligence in E-commerce

<sup>1</sup>Prof. Rana Afreen Sheikh, <sup>2</sup>Miss Mahima H. Sawarkar ,

<sup>3</sup>Mr. Arshad A. Khan, <sup>4</sup>MR. Shiva V. Kadu

<sup>1</sup> Professor, Department of MCA, Vidyabharti Mahavidyalaya, Amravati

<sup>2,3,4</sup> Student ,Department of MCA, Vidyabharti Mahavidyalaya, Amravati

## Abstract

Day by day artificial intelligence is becoming increasingly popular and the main aim of companies in today's e-commerce world is to influence customer behavior in favor of certain brands and products. The paper focuses on the impact of artificial intelligence in e-commerce. And also, on the description of the essence of e-commerce and artificial intelligence and their benefits. The E-commerce industry has seen a high degree of digitization and automation simultaneously, and both these aspects have allowed the industry as a whole to increase productivity, performance, and persistence. Focusing on the micro-levels of the E-commerce industry we can observe the highest rate of adoption by leaders such as Amazon, Walmart, Flipkart (Walmart-Flipkart), eBay etc.

## Keywords: -

Artificial intelligence · AI · Machine learning · E-commerce · Electronic commerce , buying and selling of goods ,NLP - Natural Language Processing , ML -Machine Learning

## Introduction

The main aim of companies in today's e-commerce world is to influence customer behavior in favor of certain products and brands. The application of artificial intelligence as an innovative tool in the field of e-commerce may seem as a positive step forward.

Artificial Intelligence (AI) has emerged as a transformative force in the realm of e-commerce, reshaping how businesses engage with customers, streamline operations, and optimize decision-making. By harnessing advanced algorithms and computational power, AI empowers machines to replicate human-like cognitive functions, enabling them to perform tasks that traditionally required human intervention.

In the context of e-commerce, AI is a driving force behind a multitude of applications that enhance customer experiences, bolster sales strategies, and improve operational efficiency. Through sophisticated data analysis and machine learning, AI algorithms adapt and respond in real-time to customer behavior, preferences, and market trends. This results in a more personalized, efficient, and ultimately profitable e-commerce ecosystem.

This introduction will delve into the key applications of AI in e-commerce, illustrating how it is revolutionizing everything from customer engagement to inventory management. The application of artificial intelligence as an innovative tool in the field of e-commerce may seem as a positive step forward as businesses increasingly rely on data-driven insights to stay competitive in a fast-paced digital landscape, the role of AI in e-commerce is more crucial than ever before. Let's explore the innovative ways in which AI is shaping the future of online commerce.

### What is AI?

AI, or Artificial Intelligence, refers to the simulation of human intelligence in machines that are programmed to think and learn like humans. It involves the development of algorithms and computer systems that can perform tasks that typically require human intelligence. AI can be categorized into **two main types**:

#### 1. Narrow or Weak AI:

- This form of AI is designed and trained for a specific task. It excels at that /particular task but lacks the broad cognitive abilities of a human. Examples include virtual personal assistants like Siri and Alexa, as well as image recognition software.

#### 2. General or Strong AI:

- This represents a level of AI that can understand, learn, and apply knowledge across different domains, similar to human intelligence. Achieving general AI is an aspirational goal and is not yet realized.

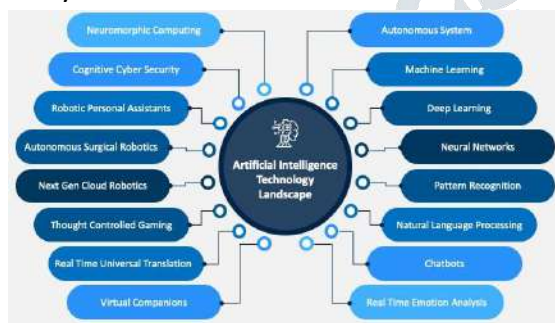


Fig1:- Artificial Intelligence Dimension

Key components and techniques within AI include:-

**Machine Learning (ML):** A subset of AI that focuses on enabling machines to learn from data without explicit programming

**Natural Language Processing (NLP):** NLP enables machines to understand, interpret, and generate human-like language.

**Robotics:** Integrating AI with robotics allows machines to perform physical tasks in various environments.

**Speech Recognition:** AI systems can be trained to recognize and understand human speech

### What is E-commerce?

E-commerce, short for electronic commerce, refers to the buying and selling of goods and services over the internet. It encompasses a wide range of online business activities, including online shopping, electronic payments, online auctions, and internet banking.

E-commerce enables businesses and consumers to conduct transactions without the need for physical presence in a brick-and-mortar store. It has become an integral part of the global economy and has revolutionized the way people shop and do business.

There are several types of e-commerce models:

**Consumer to Consumer (C2C):** This model involves consumers selling directly to other consumers. Online marketplaces like eBay or classified ads platforms like Craigslist are examples of C2C e-commerce.

**Consumer to Business (C2B):** This is when individual consumers offer products or services to businesses. For instance, freelance platforms where individuals offer services like graphic design or writing to companies.

**Business to Government (B2G):** This type of e-commerce involves businesses providing products or services to governments or government agencies. This can include services like procurement platforms for government organizations.

**Mobile Commerce (m-commerce):** This refers to e-commerce transactions that occur through mobile devices like smartphones and tablets. Mobile apps and mobile-optimized websites play a crucial role in m-commerce.

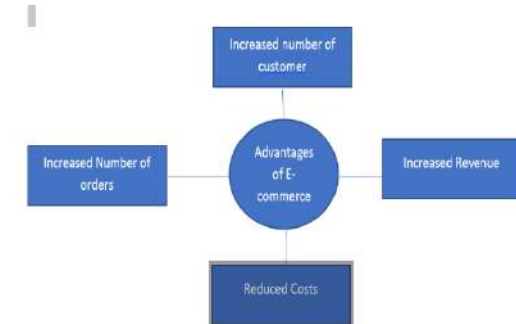


Fig 2:-Advantage of E-commerce

## Use of Ai in E-Commerce

Artificial Intelligence (AI) is revolutionizing the e-commerce industry in a multitude of ways. Here are some key applications of AI in e-commerce:

- **Personalized Recommendations:** AI analyzes customer behavior, preferences, and purchase history to provide tailored product recommendations. This increases the likelihood of conversion and enhances the shopping experience.
- **Chatbots and Virtual Assistants:** AI-powered chatbots offer instant customer support, answering queries, providing product information, and assisting with transactions 24/7. This improves customer satisfaction and reduces response times.
- **Predictive Analytics:** AI algorithms analyze large volumes of data to predict trends, customer behaviors, and inventory needs. This allows businesses to optimize their supply chain, stock levels, and marketing strategies.
- **Visual Search and Image Recognition:** AI enables customers to search for products using images rather than text. This feature enhances the search experience and facilitates quicker and more accurate product discovery.
- **Fraud Detection and Security:** AI algorithms can identify suspicious activities and potential fraud in real-time, safeguarding both the business and its customers.
- **Dynamic Pricing and Revenue Optimization:** AI algorithms adjust prices in real-time based on various factors like demand, competition, and customer behavior. This ensures optimal pricing strategies that maximize revenue.
- **Natural Language Processing (NLP):** AI-powered NLP enables businesses to analyze and understand customer feedback, reviews, and social media

interactions. This valuable insight can be used to improve products and services.

- **Inventory Management and Demand Forecasting:** AI helps businesses optimize their inventory levels by accurately predicting demand, reducing overstocking, and minimizing out-of-stock situations.
- **Customer Segmentation and Targeting:** AI identifies customer segments based on various criteria, allowing businesses to tailor marketing campaigns and promotions for specific demographics.
- **Augmented Reality (AR) and Virtual Reality (VR):** AI-driven AR and VR applications enable customers to visualize products in their real-world environment, enhancing the online shopping experience.
- **Content Generation and Optimization:** AI-powered tools can generate product descriptions, blog posts, and marketing content. They can also optimize content for search engines, improving visibility.
- **Voice Commerce:** AI-driven voice assistants like Amazon's Alexa and Google Assistant facilitate voice-based shopping, allowing customers to make purchases using voice commands.

### Conclusion: -

The aim of the paper is to describe the essence of e-commerce and artificial intelligence and their benefits. It concludes that artificial intelligence has helped e-commerce websites in providing with better user experience. The application of artificial intelligence in e-commerce has become the subject of interest of many business scientists and experts. It is possible to expect that artificial intelligence in the conditions of electronic commerce will be used more and more often and will become an integral part of all companies of this type. This research paper explores the multifaceted integration of artificial intelligence (AI) in the realm of e-commerce, aiming to elucidate the transformative impact on operational processes and user experience.

## Reference

1. Artificial Intelligence by Puntambekar  
Author: Puntambekar, A. M.  
Publication: Tech- Max Publication
2. Pallathadka H, Ramirez-Asis EH, Loli-Poma TP, Kaliyaperumal K, Ventayen RJM, Naved M(2022)
3. Applications of artificial intelligence in business management, e-commerce and finance.
4. Mater Today: Proc, (Article in Press  
Sterne J Artificial intelligence for marketing: practical applications. Wiley, USA
5. "E - Commerce: Strategy, Technologies and Applications" by David Whiteley
6. Zhang C, Yang L (2021) Study on artificial intelligence: the state of the art and future prospects.





# Journal of Emerging Technologies and Innovative Research

An International Open Access Journal Peer-reviewed, Refereed Journal

www.jetir.org | editor@jetir.org **An International Scholarly Indexed Journal**

## Certificate of Publication

The Board of

Journal of Emerging Technologies and Innovative Research (ISSN : 2349-5162)

Is hereby awarding this certificate to

**Rana Afreen Sheikh**

In recognition of the publication of the paper entitled

**Artificial Intelligence in E-commerce**

Published In JETIR ( www.jetir.org ) ISSN UGC Approved (Journal No: 63975) & 7.95 Impact Factor

Published in Volume 10 Issue 10 , October-2023 | Date of Publication: 2023-10-31

*Parisa P*

EDITOR

JETIR2310620

*[Signature]*

EDITOR IN CHIEF

Research Paper Weblink <http://www.jetir.org/view?paper=JETIR2310620>

Registration ID : 526975





## BLOCKCHAIN & CRYPTOCURRENCY

<sup>1</sup> Prof. Rana Afreen Sheikh, <sup>2</sup> Miss. Sanjana Deshmukh, <sup>3</sup> Miss. Shreya Sonar, <sup>4</sup> Mr. Pranay Rayke

<sup>1</sup> Professor, Department Of MCA, Vidya Bharati Mahavidyalaya, Amravati, Maharashtra, India.

<sup>2,3,4</sup> Students, Department Of MCA, Vidya Bharati Mahavidyalaya, Amravati, Maharashtra, India

### ABSTRACT

The document's acknowledgment of the emerging phenomenon of cryptocurrencies. The increase in the value of cryptocurrencies available in the market and the increasing recognition in the arena are opening up some demanding situations and concerns for businesses and the business economy. The studies were carried out through the description of the technique, the evaluation of the literature and the research carried out. This article discusses the main developments in academic studies related to the current cryptocurrency scenario, a brief overview of cryptocurrency, cryptocurrencies across market capitalization, cryptocurrency trends in Asia, Cryptocurrency in India, Cryptocurrency Exchanges, cryptocurrency rules internationally. Cryptocurrency inside the surroundings, and Cryptocurrency Security. The dossier also covers the responses of governments and imperative banks to this phenomenon and the modern nation's legal definitions of cryptocurrencies in the chosen countries.

**Keywords:** Cryptocurrency, Bitcoin, Ethereum, Ripple, Virtual Currency, Blockchain, Cybersecurity, Blockchain Wallets, Distributed Ledger.

### INTRODUCTION

As a growing decentralized structure and distributed computing paradigm underlying Bitcoin and different cryptocurrencies, blockchain has attracted attention in every study and application in recent years. Cryptocurrencies have transpired as one of the trending economic software structures. (Raju, 2018) Cryptocurrencies and their entire technical infrastructure are still sort of unknown to most people Cryptocurrency refers to a form of virtual asset that uses disbursed ledger, or blockchain, generation to permit a comfy transaction. [3] Blockchain, the center concept or the electricity behind the fulfillment of Bitcoin is one of the maximum trending and not unusual subjects for virtual forex in recent times.

Blockchain offers a number of features such as decentralization, verifiable record keeping,

persistent garage, performance, and security. Blockchain and its use are not best restricted to cryptocurrency however in numerous different fields as well. [1]

### LITERATURE REVIEW

At the center of the economic common sense of cryptocurrencies lies the hassle of surmounting the double-spending hassle, which poses accounting and duty challenges that effective cryptocurrencies have sought to conquer. This discussion paper evaluates the salient literature to be able to better inform academic and practitioner inquiries on the double-spending issues in cryptocurrencies.

The U.S. Has approximately 1,600 cryptocurrencies. No cryptocurrency is certified as being known as silver due to the fact that none have been specified via the United States. Government as being felony tender. Cryptocurrencies are called virtual currencies because they possess some of the traits of cash. In this text, three issues related to cryptocurrencies are analyzed. First, bitcoins are considered, because they are the primary cryptocurrency. Secondly, an assessment of the processes by which the Federal Reserve and Sweden's main financial institution are evaluating the possibility of issuing some new forms of electronic forex, which are no longer but fully described. Third, an examination of the viability of blockchain, which has become an internal aspect of bitcoin, as a successful autonomous technology.

this paper is prompted by using a speculation that the lengthy-time period value of a cryptocurrency is determined with the aid of its future use as cash. For a cryptocurrency to be used as a medium of price, it has to fulfill three impartial functions: medium of change, a unit of account, and store of value. Currently, cryptocurrencies are held for funding purposes in place of being used for transactions and for that reason as a medium of change. For cryptocurrency to emerge as extensively adopted as a method of price, it first needs to go through a very volatile duration due to the fact speculative investors see long-run destiny cost within the cryptocurrency.[6] Cryptocurrencies, along with Bitcoin, were an essential component in some monetary activities. For example, Bitcoin is the primary payment approach for ransomware attackers and retailers on the Darknet. So, it is beneficial to understand the functions of cryptocurrencies and their monetary implications. In this studies, we use bitcoin, Ether, and XRP, the three cryptocurrencies with the highest marketplace values as of this writing, in addition to Libra, that is impending and topical, as examples to investigate their functions. Specifically, we argue that these cryptocurrencies are basically extraordinary due to variations in the following elements: the identity management of their ledger writers, their consensus algorithms, and their coin supply. We discuss how these elements determine cryptocurrency performance, which include safety, privacy, and economic influence.

We also talk capacity studies subjects round those cryptocurrencies that can be still open. this paper researches the position of technological complication in original Coin Offering( ICO) successes and valuations. Using different system learning ways, we construct technology indicators from ICO whitepapers to seize technological sophistication for all cryptocurrencies. We discover that cryptocurrencies with high technology indicators are more likely to succeed and less likely to be excluded eventually. also, the period indicators explosively and really are awaiting the lengthy-run performances of the ICOs. Overall, the goods propose that technological complication is an essential determinant of cryptocurrency valuations.( 12) A popular form of Govt. Is constantly defined as “ by using the Public, for the Public and to the Public. ” The primary specific of a government is to supply public services to its citizens for which it calls for means to finance its expenditure. Among others, taxation works as a primary force to fund public expenditure. Developments and Advancements in technologies, has enabled the Govt. To perceive new ways and opened new systems to collect levies. Among them, comes the curious state of affairs of taxation of Cryptocurrency. Unlike the edict foreign plutocrat, Cryptocurrencies are decentralized, counting on a peer- to- peer community that operates with none third- festivity intervention just like the Central Bank. 25) the effect of the creation of cryptocurrencies in all husbandry is bandied right then. The benefits of the operation of cryptocurrencies as well as the downsides of conventional digital payments are included. Cryptocurrency pretensions to revise the virtual bills business; but, it does supply upward push to numerous questions as to its figure, trust ability, and fortune opposition amongst the cryptocurrencies as nicely. In this paper, I try to answer the simple questions springing up because of the preface of cryptocurrencies, in addition to the profitable troubles it offers.( 6) Using specific records from a medium- sized cryptocurrency trade in Asia, we establish 10 data about cryptocurrency exchanges and cryptocurrency buying and selling. 1) individualities keep cryptocurrency



portfolios of a small cost, 2) they trade veritably many cryptocurrencies, 3) their trading patterns are veritably concentrated, and 4) their buying and dealing horizon may be veritably short. Five) Cryptocurrency characteristics explain how a lot they're traded and the way long they're held in buyers' portfolios. 6) utmost of the trades do between individual investors and institutional investors and business makers play a minor function within the exchange. 7) It's hard to standard portfolio returns because buyers' portfolios aren't different sufficient, still eight) institutional buyers don't outperform person investors. 9) Individual buyers make duly buying and dealing opinions; within the sense that the cryptocurrencies they buy outperform those they vend. 10) The same is not genuine for institutional dealers.

## OBJECTIVES OF THE STUDY

To understand the conception of cryptocurrency, To study the advantages and downsides of cryptocurrency To dissect the legal status, challenges and openings of cryptocurrency.

## RESEARCH METHODOLOGY

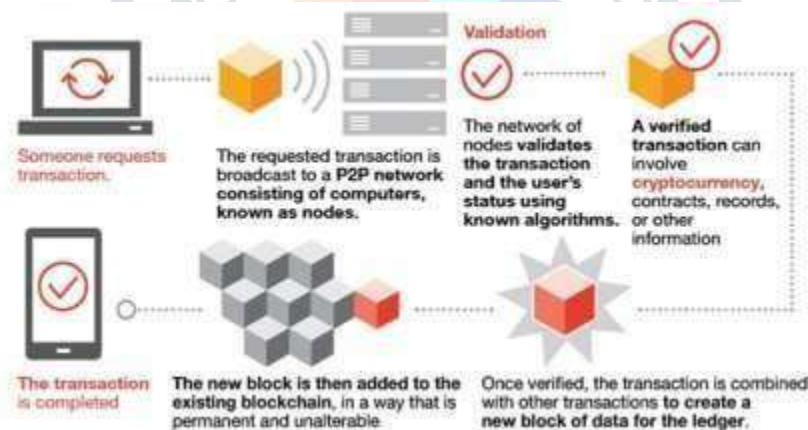
This paper uses the handiest secondary data that has been accumulated from Web of Science Core Collection( WOS), Science Citation Index Expanded( SCI- EXPANDED), Social lores Citation Index( SSCI), Arising Sources Citation Index( ESCI) and pertaining to colorful sources similar as review papers, websites, finance reports and World Bank report.

## CRYPTO CURRENCY: A BRIEF OVERVIEW

### Blockchain

The blockchain is the decentralized distributed tally machine used to report statistics deals throughout a multiple computers. In other expressions, it's long hauls an translated chain of data held over a distributed network with an incommutable timestamp. It won recognition due to its capability to keep any virtual asset or sale no matter the enterprise.

Figure 1: Blockchain Works



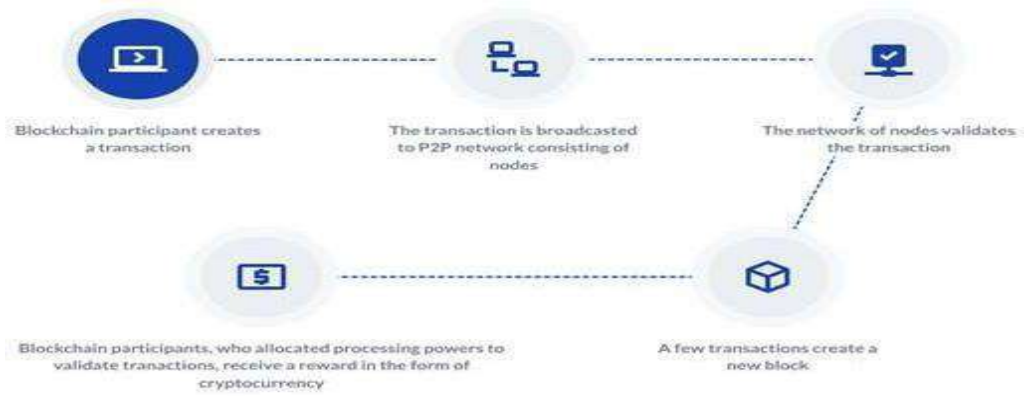
Source: <https://themarketblogs.wordpress.com/>

### Cryptocurrency

Cryptocurrency is decentralized digital cash, based on blockchain technology. You may be familiar with the most popular versions, Bitcoin and Ethereum, but there are greater than 5,000 different cryptocurrencies in movement, in keeping with Coin Lore. You can use crypto to

shop for ordinary goods and services, although many humans put money into cryptocurrencies as they could in different belongings, like shares or precious metals. While cryptocurrency is a singular and interesting asset elegance, buying it may be volatile as you must take on an honest amount of studies to absolutely recognize how every system works

Figure 2: Cryptocurrency Works



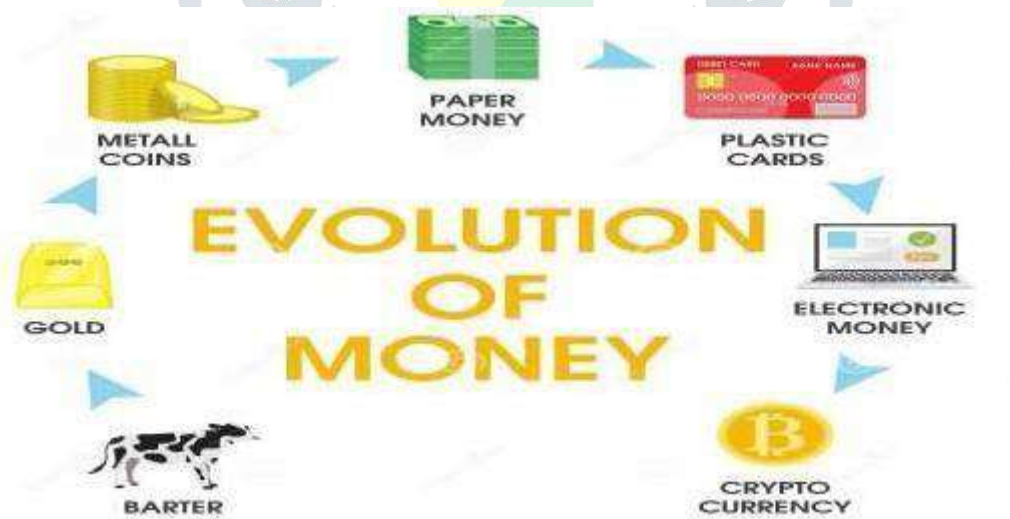
Source: <https://mlsdev.com>

Cryptocurrency is a critical part of the blockchain. Distributed tally period is erected at the agreement algorithms regulating the arrival of new blocks. All actors in the P2P community ought to take delivery of a block for it to be registered within the blockchain. There are multitudinous forms of agreement with PoW (evidence- of- work), PoS (evidence- of- stake), DPoS (delegated evidence- of- stake), and PoA (evidence- of- authority) a many of the maximum popular.

**Types of Cryptocurrencies**

There are three big types of cryptocurrencies- Bitcoin, altcoins, and commemoratives. Bitcoin is tone- explicatory- it's the crypto coin that everyone generally talks about. Altcoins are generally derivations of Bitcoin, but there are lots of standalone coins, too. Eventually, commemoratives are astronomically speaking used for dApps.[26]

Figure 3: The Evolution of Cryptocurrency



Source: <https://www.dreamstime.com/>



Dogecoin	\$24.9 billion
Polkadot	\$12.5 billion
Binance USD	\$11.5 billion

Source: <https://www.nerdwallet.com/>

Data current as of July 23, 2021.

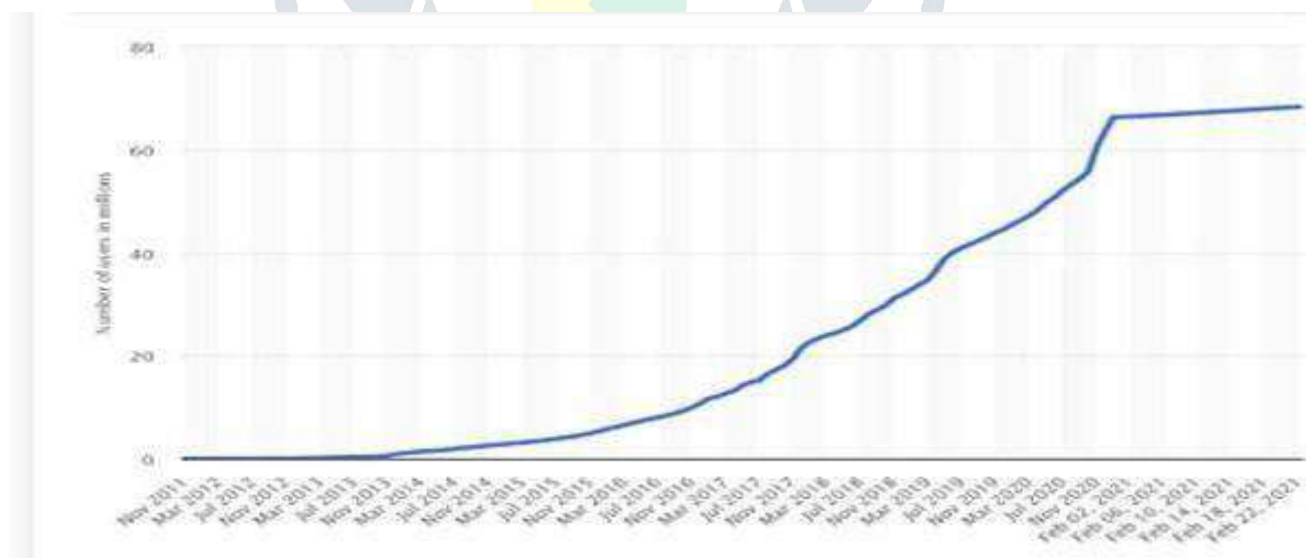
**Top 5 Cryptocurrencies of 2021, From Bitcoin to Dogecoin, cryptocurrencies have seen a significant jump in popularity and adoption in 2021.**

The cryptocurrency request started 2021 on the reverse of substantial earnings in December 2020. The overall request cap of cryptocurrencies jumped from roughly\$ 500 billion to\$ 752 billion in the last month of2020.2021 started as a ‘ game- changing ’ time for the cryptocurrency request as a dramatic swell in demand for cryptocurrencies led to a substantial jump in the value of digital means. The overall request cap of digital currencies jumped from\$ 750 billion in January to a record high of roughly\$2.5 trillion in May 2021. Despite the rearmost dip, the total request cap of cryptocurrencies is swimming near\$1.4 trillion, which is over by further than 85 in the last six months.( 4)

**Cryptocurrency Users Statistics and Cryptocurrency Demographics**

A blockchain portmanteau, or cryptocurrency portmanteau, is a device, medium, or other operation or service that can protect your cryptocurrency. This portmanteau not handiest stores your cryptocurrency statistics but also encrypts the information and utmost effective lets in you to log in together with your credentials to grease a clever agreement, crypto sale, or other fairly binding sale. nearly 70 million people use a blockchain portmanteau transnational. About a third of Nigerians use a cryptocurrency, while 1 in 5 in Vietnam and the Philippines do

**Figure 5: Number of Blockchain wallet users worldwide from November 2011 to February 22, 2021. (In millions)**



Source: Statista

**TOP 10 CRYPTOCURRENCIES TRENDING IN ASIA**

Asia is arising as considered one of the biggest crypto requests inside the international.

With it being the house to India and China, the most vibrant transnational locales. It's primed to grow to be the chief within the crypto transnational. Asia has been the primary business for numerous cryptos and exchanges. Coin Market Cap, the largest destination online for crypto costs, in a tweet gave an overview of the top 10 cryptos in Asia.

1. Xenon Pay II (X2P)
2. Moonstar (MOONSTAR)
3. IRON Titanium Token (TITAN)
4. SHIBA INU (SHIB)
5. Mozart Finance (MELODY)
6. Bitcoin (BTC)
7. Safe Energy (ENERGYX)
8. Keep Network (KEEP)
9. SafeMoon (SAFEMOON)
10. Baby Doge Coin (BabyDoge)

### CRYPTOCURRENCY IN INDIA

Cryptocurrency is a recent and significant invention in the financial assiduity. The purpose is to give forex that is not tied, created, or patronized by using a central authority. Cryptocurrency uses blockchain generation as a financial platform. The cryptocurrency relinquishment degree has bettered, and the request has grown dramatically( 2) Though India becomes regularly buying and dealing bitcoin as early as 2015, the cryptocurrency made its real debut as edict cash in November 2016 whilst the Modi- led government demonetized 86 percent of paper foreign plutocrat.(5) As in line with data from blockchain analytics company Chain analysis, Indian investments in the cryptocurrency have surged to USD 6.6 billion in 2021, driven by a shift inside the considering youthful dealers – stirring far down from gold and other precious essences. Another motive is the

safety and translucency handed by using this technology. According to a record, over 10 million crypto dealers have been added by means of India in 2021. This is noteworthy in mild enterprise that the civil authorities plan to put a ban on using cryptocurrency. still, nothing may be stated conclusively except the law regulating digital forex is passed. 9) Cryptocurrencies continue to draw a variety of attention from investors, entrepreneurs, controllers, and utmost people. numerous current public conversations of cryptocurrencies were brought on with the aid of the substantial adaptations of their charges, claims that the request for cryptocurrencies is a bubble with no abecedarian value, and also worries roughly delusion of nonsupervisory and criminal oversight [11]

### CRYPTOCURRENCY REGULATIONS ACROSS THE WORLD

Cryptocurrency has been around for a long time now. still, its mainstream relinquishment has boosted recently with 2020 being a remarkable time to add to its significance. But 2021 is a major drive as countries across the globe have tried accepting cryptocurrency in some form or the other. also, these countries have also been working on cryptocurrency regulations to govern the process of swapping through crypto. We still are yet to witness transnational regulations on cryptocurrency. still, looking at the evolving geography of crypto, it's relatively apparent that we may witness it soon. moment, we will know about different countries that have managed to set government regulations on cryptocurrency

#### Cryptocurrency Regulations in India

While there have been signs and symptoms in 2017 and 2018 that India were allowing about much lower prohibitive cryptocurrency programs, the rearmost reviews suggest a trade of course. In July 2019, an inter-ministerial commission supported a mask ban on cryptocurrencies except for proposed dependable digital foreign plutocrats. The blurled, contended draft tab counseled captivity time for folks who “ mine, induce, save, vend, deal in, difficulty, transfer, dispose of, or use cryptocurrency inside

the home of India. ” Although that draft bill didn't make it to the congress bottom, India's aversion to cryptocurrency maintains and, in overdue 2020, leaks suggested that the government was drafting a new tab to ban cryptocurrency buying and selling. While it has come down tough on cryptocurrency from a nonsupervisory station, India's authorities has stated that it's open to exploring the capability of blockchain generation to enhance its financial services assiduity [8]

**CRYPTOCURRENCY EXCHANGES**

Still, you 'll need to apply a cryptocurrency trade, If you 're searching to buy or vend cryptocurrencies. These online immolations frequently oils also to a stockbroker, furnishing you with the gear to buy and vend digital currencies like bitcoin, ethereum, and dogecoin. The stylish crypto exchanges make it clean to protect for and vend the currencies you need with low freights and sturdy protection functions. [24]

**Table 2: Comparison Between Centralized, Decentralized and P2P Cryptocurrency Exchanges**

Features	Centralized	DEX	P2P
Fiat to Crypto Trading	Supported	Not Supported	Supported
Crypto to Crypto Trading	Supported	Supported	Supported
Smart Contract	No	Yes	No
Escrow Protection	Optional	No	Must
Trade matching Engine	Yes	No	Yes
Atomic Swap	No	Yes	No
Splitted Trading	Yes	No	No

Source: <https://www.bitdeal.net>

**THE BENEFITS THAT CRYPTOCURRENCIES OFFER OVER FIAT MONEY ARE SEVERAL**

A cryptocurrency or crypto virtual asset is truly a digital form of cash that exists only digitally. The foremost difference between crypto and the virtual cash that we formerly use on each day foundation( credit score/ disbenefit cards, e-banking, etc.) is that a cryptocurrency isn't issued by way of any government or bank, is specifically decentralized and is primarily grounded on blockchain technology

**CRYPTOCURRENCY SECURITY**

While nevertheless no longer completely understood through the general public the world over, it's long hauls important to fete that numerous banks, governments, and global businesses are privy to cryptocurrencies, and they are assaying and assessing their use and emergence as a doable currency on an ongoing

recognize the bitcoin we fete currently turned into built-on the substantiation- of- work principle that deals may be securely reused on a decentralized peer- to- peer network, without the want for a primary series group, the mining and transaction strategies aren't completely cozy. In verity, conspiring actors can put upon the issues discovered within the process. Then are five crucial protection enterprises that can affect in presumably dangerous assaults and pitfalls with using cryptocurrencies Selfish Mining

- Double Spending
- Wallet Software/Distributed Denials of Service Attacks
- Acquiring Greater Than 50% Computing Power
- Time jacking

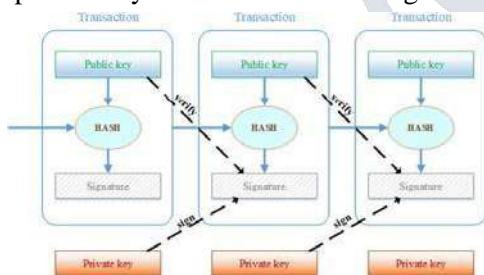
**Table 3: Benefits of Cryptocurrencies**

Traits of money	Gold	Fiat (US Dollar)	Crypto
Fungible (Interchangeable)	High	High	High
Non-Consumable	High	High	High
Portability	Moderate	High	High
Durable	High	Moderate	High
Highly Divisible	Moderate	Moderate	High
Secure (Cannot be counterfeited)	Moderate	Moderate	High
Easily Transactable	Low	High	High
Scarce (Predictable Supply)	Moderate	Low	High
Sovereign (Government issued)	Low	High	Low
Decentralized	Low	Low	High
Smart (Programmable)	Low	Low	High

Source: <https://panos.writeas.com/cryptocurrencies-the-evolution-of-money>

**A. Bitcoin essentials**

Bitcoin rudiments In his now notorious work, Satoshi Nakamoto showed a result to the problems that the perpetration and usability of digital currency faced, especially the double- spending problem( 14). While the true identity of Nakamoto is a point of speculations, what's known is that until 2010 he remained active on the Bitcoin design, and also he stepped back and gave the design to the community for farther development( 13). He proposed a system with P2P distributed timestamp garçon that serves as a creator of the computational evidence of the chronological orders of deals( 12). An electronic coin is defined as a chain of digital autographs. Each transaction is defined as a set of digitally inked hash of the former sale and the public key of the coming proprietor. The private key is used for subscribing the sale,



and the public key is used for verification of the transaction, as shown in Fig. The public key is kept in the portmanteau, which can be enforced in software, tackle, or online.

The Bitcoin tally is defined as a state transition system, conforming of a state that shows the power status of all existing Bitcoins and a state transition function, in the form of a sale. The affair of the state transition function is a new state ( 15). The results of this process are state changes of the sender and philanthropist if the sender has enough bitcoins to make a sale or an error,else.

**Bitcoin transactions**

Each Bitcoin deal Each sale is determined with its hash value representing a sale identifier and a set of inputs and labors. Each affair of the sale can only be used once as an input in the entire blockchain( 13). The attempt to represent the same affair doubly leads to the double-spending problem and is interdicted in the network. However, it's called an unspent sale affair( UTXO), and if it has been substantiated, If the affair of the sale hasn't been substantiated ahead. A sale can have multiple inputs and only over to two laborers. Multiple inputs can be used to combine lower quantities of coins being transferred, and labor can be either a quantum transferred to the other party or the change that's transferred back to the sender( 14). Bitcoin distributed tally describes all deals and hands in the network. Every knot in this P2P network keeps a dupe of the tally record( 15). still, he can do that by intimately publicizing this sale and it's over to the network to corroborate its correctness, If one stoner wants to send some quantum of coins to another. still, a stoner can try to manipulate the network and issue further than one sale of the same coin to the different druggies(double-spending problem). also, the same stoner can set up several cases to confirm his original intent and therefore perform a Sybil attack.

**B. Proof-of-work and blockchain**

These situations are averted( or at least minimized) in the Bitcoin network by demanding evidence- of- work from each node that verifies the sale. The bumps have to do some heavy calculations to prove that they're valid members of the network. As long as the total computational power of the honest bumps is lesser than the computational power of the bushwhacker, the system will remain harmonious and all legal deals will do.

A set of deals, together with the hash of the previous block and a nonce, declares a block. A timestamp garçon makes a hash of a block and intimately announces it,

therefore proving that the data inside the block must have been at the time of mining. The timestamp generated has to corroborate that the timestamp of the block is lesser than the timestamp of the former block in the chain and lower than two hours into the future. The important property of the blockchain is that the deals can be traced back at any time in history.

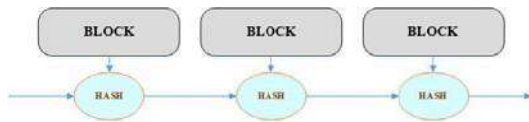


Figure 2. The blockchain scheme

The evidence-of-work mining scheme Bitcoin uses is analogous to Hash cash (16) and grounded on the SHA-256 hash function (17). The evidence-of-work is done by incrementing a nonce in the block until the value is produced that has the needed number of zero bits on the morning of the block hash. Once it's done, it can not be undone without repeating the calculations still, also all the following blocks would have invalid hashes if it is somehow changed by a vicious bushwhacker. The rule is that the longest chain that has the maturity agreement in the network is the correct one, so if the bushwhacker wishes to change a block, he needs to have enough computational power to overcome the voting of the maturity of honest bumps, therefore entering the race problem. The deals within a block are mined in Merkle tree (19), (20). A Merkle tree is a type of double tree with numerous leaf nodes, and a root of the splint bumps is a hash of its children. Fig. 4 shows a Bitcoin block composed of a Merkle tree of sale hashes. Any inconsistency in the tree will reflect nearly in the chain, so the Merkle tree is vital for long-term maintainability (15). This is done to free up the storehouse space demanded to store the blockchain on the bumps. The current size of the Bitcoin blockchain is about 144.8 GB (21). After the transactions are incorporated in a block and this block is vindicated, the network discards all hashes in a tree except the root hash included in the block title. Bitcoin introduced a Simplified Payment Verification (SPV), which doesn't require the bumps to keep a full record of deals, but only the dupe of the blockheads of the longest chain (14).

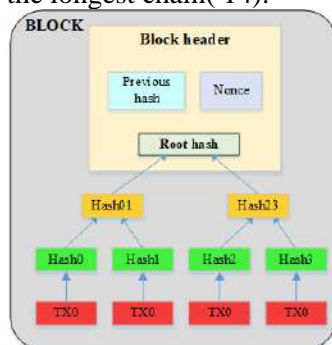


Figure 3. A Bitcoin block with hashed transactions into a Merkle tree

### C. Bitcoin scalability problem

With a block size of 1 MB, Bitcoin has severe scalability issues. The quantum of deals that can be supported with this block size is lower than seven deals per second (tps) (21). In comparison, the payment network Visa achieved 47,000 tps during the 2013 leave and presently pars with hundreds of millions per day (22). To achieve a similar rate on the Bitcoin network with 1 MB block size, assuming that the sale is 300 bytes in size, it would bear an outturn of 8 GB per Bitcoin block every ten twinkles, which would lead to over 400 TB of data per time (19). This would largely polarize the Bitcoin network to support only those bumps with such storehouse capacities, and this is veritably contrary of what Bitcoin and blockchain are intended for. Several results were suggested in order to attack this issue efficiently. As a result, a number of soft and hard spoons of Bitcoin passed. A soft chopstick is any change that's backward compatible, i.e. enabling the old software to fete recently created blocks as valid. A hard chopstick, on the other hand, is a software update introducing a new rule to the network, therefore rendering the old software unfit to fete new blocks [23].

### CONCLUSION

The emergence of Bitcoin has sparked a debate roughly its unborn and that of other cryptocurrencies. Despite Bitcoin's rearmost problems, its fulfillment for the reason that its 2009 release has inspired the creation of occasion cryptocurrencies including Ethereum, Litecoin, and Ripple. A cryptocurrency that aspires to crop as part of the mainstream fiscal device could have to fulfill veritably divergent criteria. While that possibility seems far out, there is little question that Bitcoin's success or failure in managing the demanding situations it faces may also determine the fortunes of different cryptocurrencies within the times in advance. (3) Cryptocurrency continues to be loaded in its early ranges and many people are nonetheless skeptical about it but it's long hauls right then to live and has been acclimatized into our lives and will be currency employed by everybody that is stylish a count of time. With the acceptance and how extensively talked about it is, the future of Cryptocurrency is sure to be bright.



## Reference:

- [1] Härdle, W. K., Harvey, C. R., & Reule, R.C. (2019, April 29). Understanding Cryptocurrencies. Retrieved from [https://papers.ssrn.com/sol3/papers.cfm?a\\_bstract\\_id=3360304](https://papers.ssrn.com/sol3/papers.cfm?a_bstract_id=3360304).
- [2] AdamBaron(2019)<https://www.investopedia.com/articles/forex/091013/future-cryptocurrency.asp>
- [3] BilalJafar(2021)<https://www.financemagnates.com/cryptocurrency/news/top-5-cryptocurrencies-of-2021/>
- [4] Bradley Dunseith (2017) <https://www.india-briefing.com/news/cryptocurrency-bitcoin-india-usage-regulation-15343.html/>
- [5] Li, X., & Whinston, A. B. (2019, December 30). Analyzing Cryptocurrencies. Retrieved from [https://papers.ssrn.com/sol3/papers.cfm?a\\_bstract\\_id=3500276](https://papers.ssrn.com/sol3/papers.cfm?a_bstract_id=3500276)
- [6] Chohan, U. W. (2017, December 23). The Double Spending Problem and Cryptocurrencies. Retrieved from [https://papers.ssrn.com/sol3/papers.cfm?a\\_bstract\\_id=3090174](https://papers.ssrn.com/sol3/papers.cfm?a_bstract_id=3090174)
- [7] Crypto Regulations in India. (2021, March 25). Retrieved from <https://complyadvantage.com/knowledgebase/crypto-regulations/cryptocurrency-regulations-india/>
- [8] Does Cryptocurrency Attract Tax in India? Here's What We Know. (2021, July 20). Retrieved from <https://www.india-briefing.com/news/what-are-the-tax-implications-for-cryptocurrency-assets-in-india-22610.html/>
- [9] Francis, J. C. (2019, April 12). Bitcoins, Cryptocurrencies and BlockChains. Retrieved from [https://papers.ssrn.com/sol3/papers.cfm?abstract\\_id=3371051](https://papers.ssrn.com/sol3/papers.cfm?abstract_id=3371051)
- [10] Giudici, G., Milne, A., & Vinogradov, D. (2019, September 17). Cryptocurrencies: Market analysis and perspectives. Retrieved from <https://link.springer.com/article/10.1007/s40812-019-00138->
- [11] S. Nakamoto, "Bitcoin: a peer-to-peer electronic cash system," 2008, available at: <https://bitcoin.org/bitcoin.pdf>
- [12] Ethereum Community, "A next-generation smart contract and decentralized application platform," WhitePaper, available at: <https://github.com/ethereum/wiki/wiki/White-Paper>
- [13] A. Back, "Hashcash – a denial of service counter-measure," 2002, available at: <http://www.hashcash.org/papers/hashcash.pdf>
- [14] Bitcoin Blockchain Size, <https://charts.bitcoin.com/chart/blockchain-size>
- [15] J. Poon and T. Dryja, "The bitcoin lightning network: scalable off-chain instant payments," 2016, available at: <https://lightning.network/lightning-network-paper.pdf>
- [16] Luke Conway (2021) <https://www.investopedia.com/best-crypto-exchanges-5071855>
- [17] Kishore Jain, D. (2020, August 03). The Economics of Cryptocurrencies - Why Does It Work? Retrieved from [https://papers.ssrn.com/sol3/papers.cfm?a\\_bstract\\_id=3644159](https://papers.ssrn.com/sol3/papers.cfm?a_bstract_id=3644159)
- [18] Laura M (2021) <https://www.bitdegree.org/crypto/tutorial/types-of-cryptocurrency#:~:text=In%20total%2C%20there%20are%20three,are%20mostly%20used%20for%20dApps.>



# Journal of Emerging Technologies and Innovative Research

An International Open Access Journal Peer-reviewed, Refereed Journal

www.jetir.org | editor@jetir.org An International Scholarly Indexed Journal

## Certificate of Publication

The Board of

Journal of Emerging Technologies and Innovative Research (ISSN : 2349-5162)

Is hereby awarding this certificate to

**Rana Afreen Sheikh**

In recognition of the publication of the paper entitled

**BLOCKCHAIN & CRYPTOCURRENCY**

Published In JETIR ( www.jetir.org ) ISSN UGC Approved (Journal No: 63975) & 7.95 Impact Factor

Published in Volume 10 Issue 10 , October-2023 | Date of Publication: 2023-10-25

*Parisa P*

EDITOR

*[Signature]*

EDITOR IN CHIEF

JETIR2310479

Research Paper Weblink <http://www.jetir.org/view?paper=JETIR2310479>

Registration ID : 526748



# Chat GPT Curse or Blessings

<sup>1</sup>Prof. Rana Afreen Sheikh, <sup>2</sup>Sakshi Gunavant Pawar, <sup>3</sup>Aishwarya Sunil Lakras, <sup>4</sup>Gauri Rajesh Kasture

<sup>1</sup>Professor, Department of MCA, Vidyabharati Mahavidyalaya, Amravati, India

<sup>2,3,4</sup>Student, Department of MCA, Vidyabharati Mahavidyalaya, Amravati, India

**Abstract** - Chat GPT is an AI language model developed by open AI that can understand and generate human-like text. It can be used for a variety of use cases such as language generation, question, question answering, text summarization, chat bot development, language translation. Chat GPT is a large language model that uses queues and millions of data points to mimic human responses. This form of mimicry is why Chat GPT will answer questions even when it doesn't output the correct answer. So, make sure you're not using any information from Chat GPT without fact-checking it.

**Keywords:** Chat GPT; Chat GPT Curse; Chat GPT Blessings; Chatbot; OpenAI; AI.

## 1. Introduction

Chat GPT is an artificial intelligence (AI) chatbot that uses natural language processing to create humanlike conversational dialogue. The language model can respond to questions and compose various written content, including articles, social media posts, essays, code and emails. The journey began with the introduction of the GPT-1 model in 2018. GPT-1 was a groundbreaking language. It was pre-trained on a massive corpus of text from the internet.

## 2. History of Chat GPT

Chat GPT was developed by OpenAI, an artificial intelligence research lab founded in December 2015. The team behind OpenAI consisted of prominent individuals such as Elon Musk, Sam Altman, Greg Brockman, Ilya Sutskever, Wojciech Zaremba, and John Schulman. Chat GPT was launched on November 30, 2022, by San Francisco-based open AI (the creator of the initial GPT series of large language models; DALL.E2, a diffusion model used to generate images; and whisper, a speech transcription model).



Figure 1: History of Chat GPT

Description of Chat GPT- ChatGPT, which stands for chat generative pre-trained Transformer, is a large language model-based chat bot developed by Open AI and launched on November 30, 2022, which enables users to refine and steer a conversation towards a desired length, format, style, level of detail, and language. Chat GPT is an AI-powered language model developed by OpenAI. It's designed to engage in natural language conversations with users like you. It uses a deep learning architecture called GPT-3.5 to generate text-based responses. Chat GPT can provide information, assist with tasks, and have discussions on a wide range of topics. It's trained on a diverse dataset, but its knowledge is up to date only until September 2021.



Figure 2: What is Chat GPT?

## 3. Chat GPT Curse and Blessings

Chat GPT can be both blessings and curse, depending on how they are used. While they are offering numerous benefits, such as quick access to information and automation of repetitive tasks, they also have the potential to spread misinformation and perpetuate harmful biases. In the researching and writing that students will learn, and there is a real very danger that Chat GPT will be detrimental to their education simply because it is so good at what it does. I imagine in the not too distant future there will be software written to detect whether a piece of writing has been composed by a human, or Chat GPT – but all this doing is pitting one form of AI against another, and Chat GPT most likely only ever produce inconclusive results.



Figure 3: Chat GPT Curse or Blessings

#### 4. Chat GPT architecture

Chat GPT is built upon either GPT-3.5 or GPT-4 - members of open-AI's proprietary series of generative pre-trained transformer (GPT) models based on the transformer architecture developed by Google and is fine tuned for conversational applications using a combination of supervised and reinforcement learning techniques. There is the main part of transformer, Transformer Model, Layer Stacking, Attention Mechanism, Parameter Size, Pre-training, Fine-tuning, Decoding Strategies, Context Windows, Prompt Engineering, API Integration. It's very important to implementation of version.

ChatGPT's Neural Network Architecture

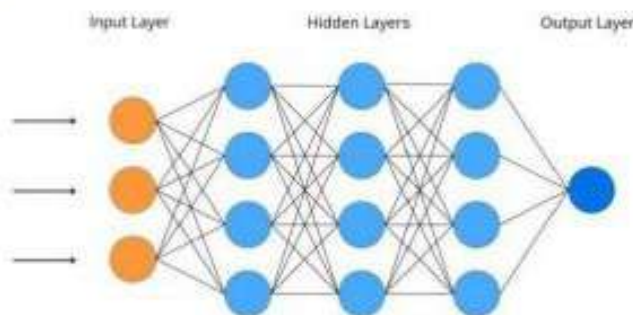


Figure 4: Chat GPT Neural Network Architecture

#### 5. Application of Chat GPT

Chat GPT is an artificial intelligence program that generates dialogue. Created by Open AI, this high capable chat bot uses machine learning algorithms to process and analyze large amounts of data to generate responses to user inquiries. Some applications of Chat GPT, Customer Support and Service, Content Generation, Virtual Assistants, Language

Translation, Education and Tutoring, Healthcare, Information Retrieval, E-commerce, Legal and Financial Services, Entertainment, Language Learning, Creative Writing and Storytelling, Accessibility, Market Research and Surveys, etc.



Figure 5: Application of Chat GPT

#### 6. Chat-GPT Design Model

Table 1: Chat-GPT Design Model

Model name	Technical name	Max Tokens
GPT-3.5 16K	gpt-3.5 turbo16k	16384
GPT-3.5	gpt-3.5-turbo	4084
Davinci	text-davinci-003	4096
Curie	text-curie-001	2049

#### 7. Conclusion

Chat GPT is a powerful language model that can generate human-like text in a variety of scenarios. Its potential applications are vast and can revolutionize many industries. Chat GPT can be employed in customer support, content generation, virtual assistance education, healthcare, and many other domains. Its extensive pre-training on large text corpora, coupled with fine-tuning for specific tasks, allows it to provide contextually relevant and coherent responses to user queries. As technology continues to advance, Chat GPT and similar models hold significant potential for improving user experiences, automating tasks, and enhancing communication in various industries and applications.

#### REFERENCES

- [1] [https://www.researchgate.net/publication/Research-On-ChatGPT-Curse-And-Blessings\\_Riview-Trend-And-perspectives](https://www.researchgate.net/publication/Research-On-ChatGPT-Curse-And-Blessings_Riview-Trend-And-perspectives).
- [2] <https://www.greeksforgreeks.org/What-is-ChatGPT-Curse-And-Blessings/>.

- [3] <https://www.tutorhunt.com/blog/post/chatgpt-a-blessing-or-a-curse-for-today's-students/>
- [4] <https://www.ihs.ac.at/publications-hub/blog/chat-gpt/>
- [5] <https://www.google.com/>
- [6] <https://www.bogotobogo.com/>
- [7] <https://www.technologyreview.com/>
- [8] <https://towardsdatascience.com>
- [9] <https://futurism.com/>
- [10] <https://www.immersiveauthority.com/>

**Citation of this Article:**

Prof. Rana Afreen Sheikh, Sakshi Gunavant Pawar, Aishwarya Sunil Lakras, Gauri Rajesh Kasture, "Chat GPT Curse or Blessings" Published in *International Research Journal of Innovations in Engineering and Technology - IRJIET*, Volume 7, Issue 9, pp 150-152, September 2023. Article DOI <https://doi.org/10.47001/IRJIET/2023.709018>

\*\*\*\*\*



ISSN(online): 2581-3048  
Impact Factor : 5.95

## CERTIFICATE OF PUBLICATION

### INTERNATIONAL RESEARCH JOURNAL OF INNOVATIONS IN ENGINEERING AND TECHNOLOGY

*Is Hereby Awarding this Certificate to*

**Prof. Rana Afreen Sheikh**

**Professor, Department of MCA, Vidyabharati Mahavidyalaya, Amravati, India**

*In Recognition of the Publication of Manuscript Entitled*

**Chat GPT Curse or Blessings**

*Published in International Research Journal of Innovations in  
Engineering and Technology (IRJIET)*

**Volume 7, Issue 9, pp 150-152, September-2023**

<https://doi.org/10.47001/IRJIET/2023.709018>

**Manuscript ID :** IRJIET709018

**Date of Issue :** October 30, 2023



Editor-In-Chief  
IRJIET

Managing Editor  
IRJIET

Mail us at: [editor@irjiet.com](mailto:editor@irjiet.com) / [irjietjournal@gmail.com](mailto:irjietjournal@gmail.com)  
Journal Website : [www.irjiet.com](http://www.irjiet.com)

# Cloud Computing & It's Security

<sup>1</sup>Prof. Rana Afreen Sheikh, <sup>2</sup>Chetan V. Sonwal, <sup>3</sup>Vaishnavi S. Deshmukh, <sup>4</sup>Chinmay U. Shirkhedkar

<sup>1</sup>Professor, Department of MCA, Vidya Bharati Mahavidyalaya, Amravati, Maharashtra, India

<sup>2,3,4</sup>Student, Department of MCA, Vidya Bharati Mahavidyalaya, Amravati, Maharashtra, India

**Abstract** – It is particularly relevant to Hong Kong because of the tremendous amounts of data that are being processed here daily in various sectors, research. There cent establishment of a major cloud R&D center in Hong Kong by Lenovo (January 2015) attests to this fact. The results will also benefit Hong Kong as the reliance on cloud computing services is rapidly increasing.

**Keywords:** Scalability, flexibility, data storage, software development, website hosting, bigdata analytics, virtual desktops, and Internet of Things (IoT).

## 1. Introduction

With cloud computing, you can store your data on remote servers and access it anytime, anywhere. It's super convenient and saves you from worrying about hardware or software maintenance. Plus, it's scalable, so you can easily adjust your storage and computing needs.

Cloud computing is like having your own virtual storage and computing power. You can access your files and software from anywhere, anytime. It's super convenient and saves you from worrying about hardware or software maintenance. Plus, it's scalable, so you can easily adjust your storage and computing needs.

Another cool thing about cloud computing is that it allows for easy collaboration. Multiple users can work on the same files and projects in real-time, regardless of their physical location. It's like having a virtual team working together seamlessly. Plus, cloud computing also enhances data security by providing backup and disaster recovery options.

Did you know that cloud computing also offers cost savings? Instead of investing in expensive hardware and infrastructure, you can pay for cloud services on a subscription basis. This means you only pay for what you use, which can be more cost-effective for businesses and individuals. Plus, cloud providers handle the maintenance and updates, saving you time and resources. It's a win-win situation!

Example, Let's say you have a bunch of photos on your phone, but you're running out of storage. With cloud computing, you can upload those photos to a cloud storage service like Google Drive or iCloud. Once they're in the cloud, you can access them from any device with an internet

connection. It's like having your own personal photo album in the virtual sky!

Cloud computing offers different types of services? There's Infrastructure as a Service (IaaS), where you can rent virtualized hardware resources. Then there's Platform as a Service (PaaS), which provides a platform for developing and deploying applications. Lastly, there's Software as a Service (SaaS), where you can access software applications over the internet.

## 2. Roles of Cloud Computing

Cloud computing has various roles, It serves as a platform for storing and accessing data, hosting applications, and providing computing resources on-demand. It also enables collaboration, data backup, and disaster recovery. In simpler terms, cloud computing plays the role of a flexible and convenient technology partner that helps you with storage, computing.

And it doesn't stop there; Cloud computing also plays a crucial role in enabling scalability, cost-efficiency, and global accessibility. It allows businesses to easily scale their resources up or down based on demand, saving costs on hardware and infrastructure. Additionally, it provides users with the ability to access their data and applications from anywhere in the world, as long as they have an internet connection. It's like having a virtual powerhouse at your service!

The diagram for cloud computing includes four main components:

1. Cloud Storage: This is where you can store your data virtually, like files, documents, and media. It provides a secure and accessible space for your information.
2. Cloud Computing: This component offers on-demand computing resources, like servers and processing power, that can be accessed remotely. It allows you to run applications and perform tasks without needing to have physical hardware or software installed on your own device.
3. Cloud Security: This aspect focuses on keeping your data safe and protected in the cloud. It includes measures like

encryption, access controls, and regular backups to ensure the confidentiality and integrity of your information.

4. Cloud Accessibility: With cloud computing, you can access your data and applications from anywhere with an internet connection. This means you're not limited to a specific device or location, giving you more flexibility and convenience.

### 3. The Applications of Cloud Computing

Cloud computing has a wide range of applications; It can be used for data storage, software development, website hosting, big data analytics, and even running virtual machines. The flexibility and scalability of cloud computing make it suitable for various industries and purposes. Let me know if you'd like more details about any specific application!

Cloud computing has a wide range of applications; It can be used for data storage, software development, website hosting, big data analytics, and even running virtual machines. The flexibility and scalability of cloud computing make it suitable for various industries and purposes.

And the applications of cloud computing are vast, some common examples include:

1. Data Storage and Backup: Cloud storage services like Google Drive and Dropbox allow you to store and access your files from anywhere with an internet connection.
2. Software Development and Testing: Cloud platforms like AWS and Microsoft Azure provide developers with the infrastructure and tools to build, test, and deploy applications without the need for physical servers.
3. Website Hosting: Cloud hosting services like Amazon Web Services (AWS) and Google Cloud Platform (GCP) offer scalable and reliable hosting solutions for websites and web applications.
4. Big Data Analytics: Cloud-based platforms like Google BigQuery and Amazon Redshift enable businesses to process and analyze large volumes of data quickly and cost-effectively.
5. Virtual Desktops: Cloud-based virtual desktop infrastructure (VDI) solutions like Amazon WorkSpaces and Microsoft Azure Virtual Desktop allow users to access their desktop environments from any device.
6. Internet of Things (IoT): Cloud computing provides the necessary infrastructure to collect, store, and analyze data from IoT devices, enabling smart and connected solutions.

These are just a few examples, but cloud computing has applications in various industries and sectors.

### 4. Cloud Computing Model

There are three main models of cloud computing:

1. Infrastructure as a Service (IaaS): In this model, cloud providers offer virtualized computing resources such as virtual machines, storage, and networks.
2. Platform as a Service (PaaS): PaaS provides a platform for users to develop, test, and deploy applications without worrying about underlying infrastructure. Cloud providers manage the infrastructure, and users focus on building and running their applications.
3. Software as a Service (SaaS): SaaS allows users to access and use software applications over the internet. Each model offers different levels of control and management, catering to different user needs.

### Data Security in Cloud Computing

When it comes to data security in cloud computing, it's important to choose a reputable cloud provider that prioritizes security measures. Cloud providers implement various security measures like encryption, access controls, and regular security audits to protect data from unauthorized access. Additionally, users can also take steps to enhance data security by implementing strong passwords, using multi-factor authentication, and regularly backing up data. It's always a good idea to stay informed about the security practices of your chosen cloud provider and take necessary precautions to ensure the safety of your data.

#### • Data in Rest

When data is at rest in cloud computing, it is securely stored in encrypted form on the cloud provider's servers. This helps protect the data from unauthorized access and ensures its confidentiality and integrity. Cloud providers implement robust security measures to safeguard data, giving users peace of mind about the security of their information.

#### • Data in Transit

When data is in transit in cloud computing, it is encrypted and securely transmitted over the internet. This ensures that the data remains protected from interception and unauthorized access during its journey from the user's device to the cloud provider's servers. Cloud providers use encryption protocols



and secure communication channels to maintain the confidentiality and integrity of the data in transit.

### 5. Conclusion

In conclusion, the research paper underscores the pivotal role that cloud computing plays in modern business operations. Let's dive a bit deeper into the benefits of cloud computing. One of the key advantages is the ability to access your files and software from anywhere, anytime. Whether you're on your phone, tablet, or computer, as long as you have an internet connection, you can easily retrieve and work on your data.

Another great aspect is the scalability of cloud computing. You can easily adjust your storage and computing needs based on your requirements. If you need more storage space or computing power, you can easily upgrade your plan without having to invest in additional hardware.

Collaboration is another major perk. With cloud computing, multiple users can work on the same files and projects simultaneously, regardless of their physical location. This makes it incredibly convenient for teams to collaborate in real-time, increasing productivity and efficiency.

Data security is also a top priority with cloud computing. Cloud providers offer backup and disaster recovery options, ensuring that your data is protected and can be easily restored in case of any unforeseen events. This gives you peace of mind knowing that your important files are safe and secure.

Lastly, let's not forget about the cost savings. Instead of investing in expensive hardware and infrastructure, you can pay for cloud services on a subscription basis. This means you

only pay for what you use, making it a more cost-effective option for businesses and individuals alike. Plus, cloud providers handle the maintenance and updates, saving you time and resources.

Overall, cloud computing offers a wide range of benefits, from convenience and scalability to collaboration and cost savings. It's definitely worth considering if you're looking for a flexible and efficient way to store and manage your data.

### REFERENCES

- [1] Cloud computing. (2015). Retrieved from <https://med.stanford.edu/irt/security/cloud.html>
- [2] GCFLearnFree.org. (Producer). (2012, March 08). Computer Basics: What is the Cloud? [WebVideo]. Retrieved from <https://www.youtube.com/watch?v=gu4FYsFeWag>
- [3] Passary, S. (2015, June 15). Cloud computing is the future but not if security problems persist. Retrieved from <http://www.techtimes.com/articles/8449/20140615/cloud-computing-is-the-future-but-not-if-security-problems-persist.htm>
- [4] M.A. Vouk, "cloud computing" issue, research and implementations, proc. Int. conf, inf, technol. interfaces, ITI, pp.31-40,2008.
- [5] Spector, L. (2011, August 22). Is cloud-based backup safe?. Retrieved from [http://www.pcworld.com/article/238503/cloud\\_backup\\_safe.html](http://www.pcworld.com/article/238503/cloud_backup_safe.html)
- [6] Bradford, C. (2019). 7 most infamous cloud security breaches –storagecraft. Retrieve from <http://blog.storagecraft.com/7-infamous-cloud-security-breches>.

#### Citation of this Article:

Prof. Rana Afreen Sheikh, Chetan V. Sonwal, Vaishnavi S. Deshmukh, Chinmay U. Shirkhedkar, "Cloud Computing & It's Security" Published in *International Research Journal of Innovations in Engineering and Technology - IRJIET*, Volume 7, Issue 10, pp 673-675, October 2023. Article DOI <https://doi.org/10.47001/IRJIET/2023.710087>

\*\*\*\*\*



ISSN(online): 2581-3048  
Impact Factor : 5.95

## CERTIFICATE OF PUBLICATION

### INTERNATIONAL RESEARCH JOURNAL OF INNOVATIONS IN ENGINEERING AND TECHNOLOGY

*Is Hereby Awarding this Certificate to*

**Prof. Rana Afreen Sheikh**

**Professor, Department of MCA, Vidya Bharati Mahavidyalaya, Amravati,  
Maharashtra, India**

*In Recognition of the Publication of Manuscript Entitled*

**Cloud Computing & It's Security**

*Published in International Research Journal of Innovations in  
Engineering and Technology (IRJIET)*

**Volume 7, Issue 10, pp 673-675, October-2023**

<https://doi.org/10.47001/IRJIET/2023.710087>

**Manuscript ID : IRJIET710087**

**Date of Issue : November 08, 2023**



*h. Thakur*  
Editor-In-Chief  
IRJIET

*S. S. S. S.*  
Managing Editor  
IRJIET

Mail us at: [editor@irjiet.com](mailto:editor@irjiet.com) / [irjietjournal@gmail.com](mailto:irjietjournal@gmail.com)  
Journal Website : [www.irjiet.com](http://www.irjiet.com)

# Impact of Garlic (*Allium sativum*) on Glycogen Level of Fresh Water Fish *Channa Striatus* (Bloch, 1793)

Thorat N.R. Thorat, S. H. Rathod

Department of Zoology, Vidyabharti Mahavidyalaya, Camp, Amravati, Maharashtra, India

## ABSTRACT

The present work was conducted to study the effect of garlic (*Allium sativum*) on glycogen content of fresh water fish *Channa striatus*. Live specimens of *Channa striatus* were collected from local market of Amravati city. The controlled fishes were fed with normal diet and experimental fishes were fed with garlic pellets. Fishes were randomly selected from each control and experimental tanks, anesthetized, sacrificed after day 7, 14 and 21 days and muscle tissue were taken for glycogen estimation. The glycogen levels in the muscle of the controlled and experimental fishes were estimated by Nelson-somogy's method. The glycogen level of controlled and experimental was compared. The present investigation indicated that the glycogen contents in muscle of experimental fish decreased  $29.07 \pm 0.833$ ,  $26.18 \pm 0.904$ ,  $23.78 \pm 1.784$  as compared to control  $30.45 \pm 1.18$ ,  $28.73 \pm 0.591$  and  $30.33 \pm 0.498$ . Thus, *Allium sativum* fed to *Channa striatus* showed significant decreased in the glycogen level of muscle tissue.

**Keywords:** *Channa striatus*, *Allium sativum*, glycogen

## Article Info

Volume 9, Issue 6

Page Number : 498-502

## Publication Issue

November-December-2022

## Article History

Accepted : 01 Nov 2022

Published : 12 Dec 2022

## I. INTRODUCTION

Plants have been used as medical practice since prehistoric times. Modern approaches to determine the medical properties of plant involve collaborative efforts that can include ethnobotanist, anthropologists, pharmaceutical chemists and physicians. Many antibiotics are commonly used to promote growth and health in carp, trout and Nile tilapia (Essa et al., 1995). Also artificial feeds supplemented with antibiotic were used to prevent the spread of disease and

improve food conversion ratio (FCR) by Reilly and Kaferstein (1997).

Approximately 25% of the prescribed drugs sold in United States are plant based. Medicines that come from plants include willow bark (*Salix* species) and foxglove (*Digitalis purpurea*). Garlic (*Allium sativum*) is one of the most commonly used plants, both for medicinal and culinary purposes as providing flavour and taste to the final product. However, whole garlic as well as its components/fractions are used in medicines since long time and depict its presence in the Chinese medicines 3000 years ago. Garlic based

medications were also famous in India about 5000 years ago.

Garlic contains at least 33 sulphur compounds, several enzymes and minerals like germanium, calcium, copper, iron, potassium, magnesium, selenium, and zinc; vitamins A, B1 and C, fiber and water. It also contains 17 amino acids; lysine, histidine, arginine, aspartic acid, threonine, serine, glutamine, proline, glycine, alanine, cysteine, valine, methionine, isoleucine, leucine, tryptophan and phenylalanine (Josling, 2005). The most abundant sulphur compound in garlic is alliin (s-allylcysteine sulfoxide), which is present at 10 and 30 mg/g in fresh and dry garlic, respectively (Lawson, 1994).

Fishes are one of the most important dietary animal protein sources in human nutritional status. Fish is the excellent substitute for the meat and is the excellent source of protein. *Channa striatus* is commonly called as “spotted murrel” and distributed throughout South East Asia and also known for its taste, high nutritive value and medicinal value. It is naturally distributed in India and other neighbouring countries.

Liver is the main store of carbohydrates that are the biggest source of blood glucose. The ratio of the carbohydrates utilization in fish varies according to feeding habits of fish. The basic energy reserve glycogens consists 1% of total body weight. This source is sufficient to provide the energy need for a short time, but not for a long time. The glycogen amount stored in liver depends on the physical, chemical and biological factors faced by the fish rapid movement, stress factors or environmental hypoxia causes carbohydrates reserves to diminish (first glycogen in liver and muscles). The glycogen level in muscles may reflect the glycogen level in liver which is the main storage place for glycogen. The glycogen stocks in striated muscles of fish have an important role. After physical activity, the glycogen in muscle is

converted into lactic acid and causes the pH of the muscles to decrease.

Kumar and Reddy (1999), studied that feeding mice with garlic, induce significant decrease in serum glucose levels. Lower levels of plasma glucose in fish have also been reported in the assessment of biochemical effects of *Allium sativum*. Sheela and Augusti (1992) studied that glucose concentration significantly decreased in fish fed on diets containing the *Allium Sativum*.

Similarly Gupta et al., (2009) studied that the garlic decreases plasma glucose and increases serum insulin in diabetic rat. They also studied that the effect of garlic extract on nickel or chromium induced alteration of plasma glucose and hepatic glycogen levels and anti oxidant status in rats.. Metwally (2009) showed that the effect of garlic on weight gain and growth performance of *O. niloticus* significantly increased in all groups fed on garlic with lower mortality rate and increases the antioxidant activity in fish. Total protein in blood serum significantly increased in the groups fed on garlic, while blood glucose, triglycerides and cholesterol levels were significantly decreased in the same treated groups.

Amin Farahi et.al., (2010) studied effect of garlic on growth factors, some haematological parameters and body compositions in rainbow trout (*Oncorhynchus mykiss*) which showed that weight gain and growth performance of *O. mykiss* significantly increased in all groups fed on garlic. Megbowon et al., (2013) observed that effects of garlic on the growth performance and nutrient utilization of fingerlings of an ecotype cichlid commonly called “wesafu” in Nigeria. Results showed significant increase in weight and growth performance of the ecotype cichlid in all groups fed on garlic.

Agatha A. et.al., (2012) studied the effect of different concentrations of garlic supplement in fish diet on growth and haematological parameters of *Clarias*

gariepinus fingerlings. They observed that increase in total length of garlic treated fish and white blood cell (WBC), red blood cell(RBC), packed cell volume (PCV), haemoglobin(HB) were observed to be significantly higher than the initial counts in the treatment groups as compared to the controls. AL-Salahy and Mahmoud (2003) studied that the effect of garlic administration on the carnivorous fish *Chrysichthys auratus* showed a hypoglycaemia, hypolipidaemia, hypocholesterolaemia, hypotriglyceridaemia and a drop in serum trifluoroacetic acid (TFAA) in response to repeated doses of garlic. Thus the objective of this experiment trails is to assess the influence of supplementary feeding of the garlic on total glycogen level of muscle tissue.

## II. METHODS AND MATERIAL

The fishes selected for the experimental study was *Channa striatus*. Fishes were collected from the local fish market of Amravati. The average length of the fish was 16-18 cm and the weight was 17-45gm respectively. They were kept in glass aquarium, having tap water and added 1% KMnO4 solution for disinfection. The fishes were acclimated for 8-10 days in the laboratory condition by APHA (1998) method. During acclimatization they were feed with prawns as a natural food. After two weeks the fishes were separated into two groups. First group was considered as control and second group was considered as experimental. The first group of fishes considered as controlled were daily feed twice by prawns and the second group considered as experimental were feed with garlic pellets. The second group were given garlic pellets as dose two times a day after 7, 14, 21 days. Garlic was brought from the market and then it was converted to paste with the help of mixer and dried to form powder. This powder form of garlic was converted to small pellets and soybeans oil was used. These garlic pellets was given as dose for the fishes and it is 12 gm given as 1/3 of the total fish weight.

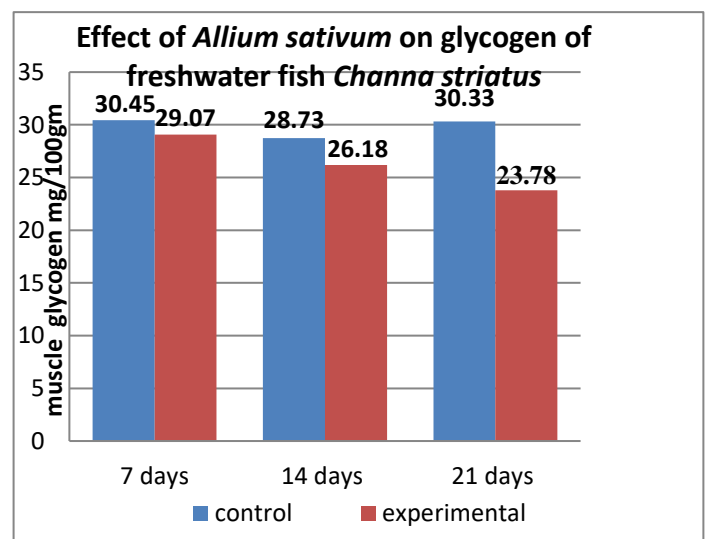
On the desire day the fishes were sacrificed and then dissected to collect the muscle tissue to study the effect of garlic on glycogen in the muscle tissue. Glycogen was estimated by Nelson-Somogy's (1944) or DNS method. Glucose was taken as standard solution.

## III. RESULTS AND DISCUSSION

In the present study the impact of garlic on glycogen level in muscle tissue of fresh water fish *Channa striatus* was found to be in experimental treated fishes as  $29.07 \pm 0.833$ ,  $26.18 \pm 0.904$ ,  $23.78 \pm 1.784$ , and control fishes  $30.45 \pm 1.18$ ,  $28.73 \pm 0.591$  and  $30.33 \pm 0.498$ , it is observed that glycogen level in the muscle tissue of fish was significantly decreased in the groups fed on garlic as compared to the control.

Table no 1:- Effect of garlic on glycogen in muscle of fresh water fish *Channa striatus*.

Days	Concentration of glycogen mg/100gm	
	Control	Experimental
7	$30.45 \pm 1.18$	$29.07 \pm 0.833$
14	$28.73 \pm 0.591$	$26.18 \pm 0.904$
21	$30.33 \pm 0.498$	$23.78 \pm 1.784$



#### IV. DISCUSSION AND CONCLUSION

Garlic is one of the most commonly used plants, both for medicinal and culinary purposes as providing flavor and taste to the final product. It is believed to be originated from central Asia over 6,000 years ago and has been extended towards west, south and east. The current experiment aimed to study the effects of garlic (*Allium sativum*) on the concentration of glycogen in the muscle tissue of the fresh water fish *Channa striatus*.

Glycogen level in muscles tissue reduced significantly in fish feed on diets containing garlic (*Allium sativum*). This condition was attributed to improving of the antioxidant system in cell of pancreas to produce insulin. These results agree with those of Kumar and Reddy (1999), who found that feeding mice with garlic induced significant decrease of serum glucose levels. Lower levels of plasma glucose in fish have also been reported in the assessment of biochemical effects of *allium sativum* by Sheela and Augusti (1992). The present study demonstrated that administration of garlic induced glycogen concentration to reduce significantly in muscles of *Channa striatus* feed on diets containing garlic (*Allium sativum*). These results agree with those of Thomson and Ali (2003) and Shalaby et al., (2006). The effect of garlic on growth factors, some hematological parameters and body compositions in rainbow trout (*Oncorhynchus mykiss*) was studied by Amin Farahi et al., (2010) and their result showed that the weight gain and growth performance of *Oncorhynchus mykiss* significantly increased in all groups feed on garlic. There was a significant decrease of glycogen level in the fish feed on diets containing garlic as compared to the control group, this favors our study and the result observed, according to which the concentration of glycogen decreases after the fish feeds on garlic (*allium sativum*).

In the present study it was observed that the garlic decreases glycogen level in the muscle tissue of *Channa striatus*. All the above benefits of garlic are very helpful in aquaculture. At the end, from the obtained results it could be recommended that garlic may be used to decrease glycogen level. Also garlic can be used as antibiotic for the treatment or prevention of disease and for enhancing fish tolerance to environmental stressors (Sivam, 2001), so addition of garlic to the diets of fish would be beneficial for the health of fishes.

#### V. REFERENCES

- [1]. Agatha, A. N. (2012). Effect of garlic (*Allium sativum*) on growth and haematological parameters of *Clarias gariepinus*. Sustainable agriculture research; Vol 1, No.2; Pp 222-228.
- [2]. AL Salahy, M. B., Mahmoud, AAB, (2003). Metabolic and histological studies on the effect of garlic administration on carnivorous fish *Chrysichthys auratus*. EGYPT J. BIO 5:94-107.
- [3]. Amin Farahi, Kasiri, M., Mohammad, S., Mohsen S. Iraei and D. Morteza Shah Kolaei (2010): Effect of garlic on growth factors, some haematological parameters and body composition in rainbow trout *Oncorhynchus mykiss*, Aquaculture, Aquarium, Conservation and Legislation International Journal of the Bioflux Society 3(4), 317-323
- [4]. APHA/AWWA (1998). Standard for examination of toxicity of cypermethrin on fishes, 20th Edn. APHA.
- [5]. Chakrabarti, R. and Vasudeva Rao, (2006). *Achyranthes aspera* stimulate the immunity and enhances the antigen clearance in fish *Catla catla*, International Immuno Pharmacol, 6(5):782-790
- [6]. Essa a. A., Hady a. M., Maha M. and M. S. Marzouk (1995). Effect of virginniamycin on performance and susceptibility of *Oreochromis niloticus* to *A. Hydrophila* infection J. Egypt Vet. Med. Ass. 55, 109-21

- [7]. Gupta, A. D., Prakash, C. D., Salim A. Dhundasi and Kusal K. Das (2009). Effect of garlic (*Allium sativum*) on nickel II or chromium VI induced alterations of glucose homeostatis and hepatic antioxidant status under sub-chronic exposure conditions. *J. Basic Clin. Physiol Pharmacol.* 20(1):1-14.
- [8]. Josling, P. (2005). *The heart of garlic Nature's aid to healing the human body*, HEC Publishing, Chicago Illinois. Pp20.
- [9]. Kumar, G.R. and K.P. Reddy, (1999). Reduced nociceptive responses in mice with alloxan induced hyperglycemia after garlic (*Allium sativum*) treatment. *Indian J. Exper. Biol.*, 37:662-666.
- [10]. Lawson LD (1994). Human medical agents from plants in bioactive organo sulphur compounds of garlic and garlic products. American Chemical Society, Washington, DC, pp.306-330.
- [11]. Megbowon, Adejonwo, O., Adeyemi YB, Kolade OY., Adetoye, AAACA., Edah, B., Okunade, O.A. and Adedji, AK (2013). Effect of garlic on growth performance, nutrient utilization and survival of an ecotype Cichlid, 'Wesafu' IQSR *Journal of agriculture and veterinary Sciences* 6(3) pp 10-13.
- [12]. Mitwally, M.A.A. (2009). Effects of garlic on some antioxidant activities in *Tilapia nilotica* (*Oreochromis niloticus*) world *J. of fish and marine sciences* 1 (1):56-64.
- [13]. Naylor, R. and Burke, M. (2005): *Aquaculture and ocean resources-raising tigers of the sea. Annual review of environmental resources*, 30:185-218.
- [14]. Nelson N. Photometric adaptation of Somogy's method for estimation of glucose (1944): *J. Biol. Chem.*153:357
- [15]. Reilly and Kaferstein, F. (1997): Food safety hazard and the application of the hazard analysis and critical control point (HACCP) for their control in aqua culture production. *Aqua Res.*28:735-752
- [16]. Sheela, C. G. and K. T. Augusti (1992): Antidiabetic effects of S-allyl cysteine sulphoxide isolated from garlic, *allium sativum* linn. *Indian J. Exper. Bio.* 30: 523.
- [17]. Sivam G. P., (2011): Recent advances on the nutritional effects associated with the use of garlic as supplement. *AM. SOC. Nutr. Sci.* 2001: pp 1106-1108.
- [18]. Tacon, A. G. J. (1994): Feed ingredients for carnivorous fish species alternation to fish meal and other fishery resources. *Fish Res. Environ. Div. Fish department Rome*, PP 89-114.
- [19]. Thompson, M. and M. Ali (2003): Garlic *allium sativum* a review of its potential use as an anticancer agent. *Curr. Cancer drug targets* 3:67-81.

**Cite this article as :**

Thorat N.R. Thorat, S. H. Rathod, "Impact of Garlic (*Allium sativum*) on Glycogen Level of Fresh Water Fish *Channa Striatus* (Bloch, 1793)", *International Journal of Scientific Research in Science and Technology (IJSRST)*, Online ISSN : 2395-602X, Print ISSN : 2395-6011, Volume 9 Issue 6, pp. 498-502, November-December 2022. Available at doi : <https://doi.org/10.32628/IJSRST229172>  
Journal URL : <https://ijsrst.com/IJSRST229172>

## Toxic effects of *Parthenium hysterophorus* on Muscles of freshwater fish *Labeo rohita*.

(Vikhar) Khedkar A.P.

Department of Zoology, Vidya Bharati Mahavidyalaya, Camp, Amravati, Maharashtra, India

### ABSTRACT

#### Article Info

#### Publication Issue

Volume 9, Issue 6

January-February-2023

#### Page Number

28-32

#### Article History

Accepted: 01 Jan 2023

Published: 05 Jan 2023

The present study is conducted and assessed the toxicity of *Parthenium hysterophorus* is on locally available fresh water fish. The present study deals with to determine histological effects on fresh water fish, *Labeo rohita*. The fishes were collected from nearby water body and brought to the laboratory for determination of histological parameters up to 96hr. period. The muscles of fish exposed lethal concentration for different time exposure (24hrs. 48hrs. 72hrs. and 96hrs.) showed lesion, inflammation, pigment and necrosis of primary and secondary gill lamellae during low concentration while, increasing concentration for different time exposure showed necrosis, malignancy and cellular degeneration were seen at later time of exposure.

**Keywords:** *Parthenium hysterophorus*, Muscles, Histology, *Labeo rohita*

### I. INTRODUCTION

Water pollution, has been increasing at an alarming rate due to rapid industrialization, civilization and green revolution. Urban, agricultural and industrial activities release xenobiotic compounds that may pollute the aquatic habitat. Industrialization and growth of human population have led to a progressive deterioration in the quality of the earth's environment. India is a country having great cultural diversity associated with all kinds of climates, rich flora and fauna, and supporting an estimated total of eight percentages of the globally documented species. It is experiencing increasing pressure on its bio-resource and ecosystem services due to high demand of food (Kannupandi et al., 2003; Varadharajan et al.,

2009). The higher concentration of toxicants brings the adverse effects on aquatic organisms, at cellular level or molecular level and ultimately lead to disorder in biochemical composition which is useful in determining different toxicants and protective mechanism of the body to resist the toxic effects of the substances (Jain and Kulshreshta, 2000). Rohu is the natural inhabitant of freshwater sections of the rivers. Rohu thrives well in all fresh waters below an altitude of approximately 549 m. Rohu is a bottom feeder and prefers to feed on plant matter including decaying vegetation. Rohu attains maturity towards the end of the second year in ponds. The spawning season of rohu generally coincides with the southwest monsoon. Spawning takes place in flooded rivers. The fecundity of rohu varies from 226,000 to 2,794,000,



depending upon the length and weight of the fish and weight of the ovary. The spawn of this fish is collected from rivers during monsoon and reared in tanks and lakes (Talwar and Jhingran 1991). Rohu is very commonly eaten in Bangladesh and the Indian states of Bihar, West Bengal, Odisha, Assam, and Uttar Pradesh. The Maithil Brahmins and the Kayastha community of Nepal, Bihar and Uttar Pradesh treats it as one of their most sacred foods, to be eaten on all auspicious occasions. Rohu is the most commonly used fish in Pakistan and is usually eaten fried, or in a sauce with spices.

*Parthenium hysterophorus* is an aggressive ubiquitous annual herbaceous weed. This erect, ephemeral herb known for its vigorous growth and high fecundity especially in warmer climates is a native of north-east Mexico and is endemic in America. It is commonly known as 'altamisa', carrot grass, star weed, white top, wild feverfew, the "Scourge of India" and congress grass. *Parthenium hysterophorus* is a prolific weed belonging to Asteraceae family, producing thousands of small white capitula each yielding five seeds on reaching maturity. In the past century it has found its way to Africa, Australia, Asia and Pacific Islands and has now become one of the world's seven most devastating and hazardous weeds. Exposure to *P. hysterophorus* also causes systemic toxicity in livestock. *Parthenium hysterophorus* is a serious invasive weed of pasture systems, reducing pasture productivity 90%. (*Parthenium hysterophorus* L.) Congress grass is an exotic weed comes under Asteraceae family, accidentally introduced in India, 1955 in Pune through the imported food grains (Dhawan and Dhawan, 1996). It has become naturalized and is spreading at an alarming rate all over India (Sivakumar et al. 2009) and can adopt any climate very easily. Adewoye and Fawole, (2002; 2005) studied the concentration of metals in the tissue of *Clarias gariepinus* fingerlings exposed to lethal concentration of cassava Waste water. The histopathological examination of the gill, liver, and

muscle of the exposed fish indicated that the gill and liver were the organs most affected. This is similar to the observation of (Rahman et al., 2002; Aguiw, 2002; Omitoyin et al., 2006; Ayoola, 2008).

## II. MATERIALS & METHODS

*Labeo rohita* fish were collected from Nal Damayanti Dam, local fish market Amravati washed with 10% solution of Potassium Permanganate to free any fungal infections. Then acclimatized to the laboratory condition for fifteen days in large aquarium. The fish size 15 to 20 cm in length and weight 150 to 200 gm. Fishes maintained in well water and its physico-chemical characteristics analyzed following the method given in APHA (2005). Fishes fed with ad libitum food, oil cake and rice bran to keep them more or less in the same state of metabolic requirement.

A group contain ten fishes were taken in both container experimental and control respectively. The dose starting from 10 ml in 10 lit. Well water. The dose increased daily by 10 ml. Their behavioral changes recorded daily and throughout the exposure period.

Everyday water changes to maintain the concentration of *Parthenium hysterophorus* extract and histological changes were recorded.

## III. RESULT AND DISCUSSION

For lethal concentration at control there are no lesion, no necrosis, no pigments, no malignancy, no inflammation and cellular degradation seen for the 24hrs, 48hrs, 72hrs, and 96hrs.

At 6.00ml/l lesion occurs on muscle bundle and nucleus for 24hrs, for 48hrs lesion, inflammation on muscle bundle, nucleus and muscle striation while, for 72hrs necrosis occurs in muscle bundle and

nucleus, for 96hrs necrosis, cellular degradation occurs on muscle bundle, nucleus and muscle striation.

Muscle (Section) of *Labeo rohita* exposed to lethal concentration (control) of root water extract of *Parthenium hysterophorus*

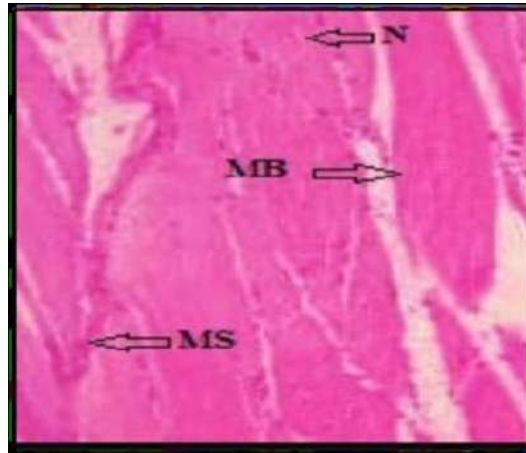


Fig.: Muscle of *Labeo rohita* (Control).

MB: Muscle bundles, N: nucleus, MS: muscle striation, M: microfilament. No lesion (L), inflammation (I), pigment (P), necrosis (N), malignancy (M) and cellular degeneration(C).

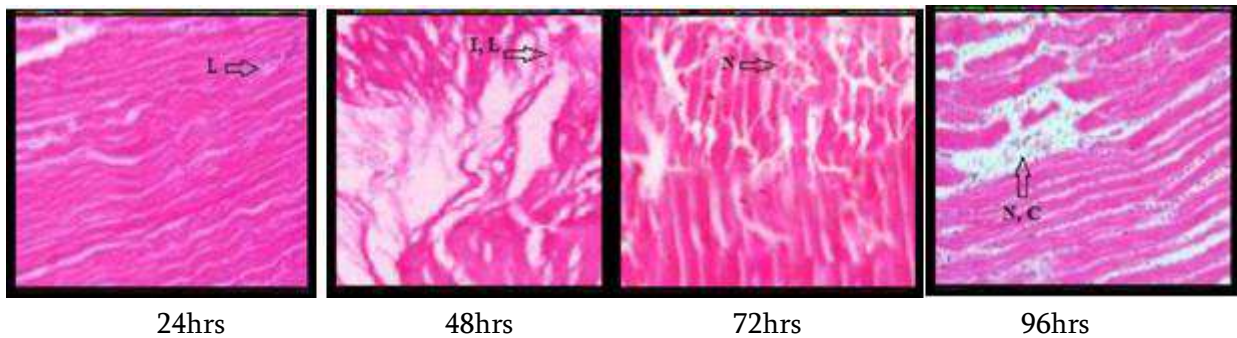


Fig.: Muscle (Section) of *Labeo rohita* exposed to lethal concentration (6.00 ml/l) of root water extract of *Parthenium hysterophorus* showing lesion (L), inflammation (I), necrosis (N) and cellular degeneration(C).

The muscle of fish exposed to lethal concentration for different time exposure (24hrs. 48hrs. 72hrs. and 96hrs.) showed lesion, inflammation and necrosis of muscle bundle, nucleus and muscle striation during low concentration while, increasing concentration for different time exposure showed necrosis and cellular degeneration and muscle bundle, nucleus and muscle striation were seen at later time of exposure.

In the present work, severe damage of muscle bundles, shortening of muscle bundles, thickening of muscle bundles, severe intra muscular oedema and necrosis of muscle bundle. This similar finding was observed by

(Bharat Bhusan Patnaik et al., 2011). All these changes indicate the fish under the highly stressful

conditions. Mohamed, 2009 observed the degeneration of muscle bundles with aggregation of inflammatory cells between them and focal areas of necrosis. Similar result is observed in present work. A focal area of myolysis was seen in the muscles of *O. spilurus* exposed to contra / insect 500/50E.C. observed by (Elnemaki and Abuzinadah, 2003). Abbas and Ali (2007) observed destruction and vaculation of the muscle cells in *Oreochromis* spp. exposed to chromium. The histological alteration in the fish muscle was reported by many investigators who have

studied the effect of different pollutants on fish muscle (Rakhi et al., 2013; Jeheshadevi et al., 2014).

#### IV. CONCLUSION

The muscle of fish exposed to lethal concentration for different time exposure (24hrs. 48hrs. 72hrs. and 96hrs.) showed lesion, inflammation and necrosis of muscle bundle, nucleus and muscle striation during low concentration while, increasing concentration for different time exposure showed necrosis and cellular degeneration and muscle bundle, nucleus and muscle striation were seen at later time of exposure.

#### V. REFERENCES

- [1]. Abbas, H.H. and Ali F.K. (2007): Study the effect of hexavalent chromium on some biochemical, citotoxicological and histopathological aspects of the Oreochromis spp. Pak. J. Biol. Sci., 10:3973-3982.
- [2]. Adewoye, S.O. and O.O. Fawole, (2002): Bioconcentration of metals in the tissue of Clarias gariepinus fingerlings exposed to lethal concentration of cassava Waste water. World J. Biotechnol., 3: 465-468.
- [3]. Aguiwo, J.N. (2002): The Toxic Effect of Cymbush Pesticide on growth and survival of African catfish, Clarias gariepinus (Burchell, 1822). J. Aquat. Sci. 17(2): 81-84.
- [4]. APHA, (2005): Standard method for the examination of IBERUS, water and waste water. American Public Health Association, Washington, D.C. Ayoola, S.O. (2008): Toxicity of Glyphosate Herbicide on Nile tilapia (Oreochromis niloticus) juvenile. Afr. J. Agric. Res. 3(12), 825-834.
- [5]. Bharat Bhusan Patnaik, J. Hongray Howrelia, Theresia Mathews and M. Selvanayagam, (2011): Histopathology of gill, liver, muscle and brain of Cyprinus carpio communis L. exposed to sublethal concentration of lead and cadmium. African J. of Biotech. Vol. 10(57), pp, 12218-12223.
- [6]. Dhawan, S. R. and Dhawan, P. (1996): Regeneration in Parthenium hysterophorus L. World Weeds, 2: 244-249.
- [7]. Elnemaki, F. and Abuzinadah, O. (2003): Effect of contra/insect 500/50 E.C. on the histopathology of Oreochromis spilurus fish. Egypt. J. Aquat. Res. Fish. 29: 221-253.
- [8]. Jain, M. and K. Kulshreshtha (2000): Effect of pesticides on fishes. A review of recent studies in India. J. Nation. 7 (2): 14-18.
- [9]. Jeheshadevi, A.K, Ramya T.M, Mr. S. Sridhar and J. Helan Chandra. (2014): Histological Alterations on the Muscle and Intestinal Tissues of Catla Catla Exposed to Lethal Concentrations of Naphthalene. International Journal of Applied Engineering Research. 9( 2) 159-164.
- [10]. Kannupandi, T., Vijayakumar G. And Soundarapandian P. (2003): Yolkutilization in a mangrove crab Sesarma brockii (deman). Indian Journal of Fisheries, 50: 199-202.
- [11]. Mohamed, F.A.S. (2009): Histopathological Studies on Tilapia zillii and Solea vulgaris from Lake Qarun, Egypt. World Journal of Fish and Marine Sciences, 1 (1): 29-39.
- [12]. Omitoyin, B.O., Ajani E.K., Adesina B.T. and Okuagu C.N.F. (2006): Toxicity of Lindane (gamma-hexachloro- cyclohexane) to Clarias gariepinus (Burchell, 1822). World Journal of Zoology 1(1): 57-63.
- [13]. Rahman MZ, Hossain Z, Mellah MFA, Ahmed GU (2002). Effect of diazinon 60EC on Anabus testudineus, Channa punctatus and Barbades gomnotus Naga. The ICLARM Quart., 25: 8-11.
- [14]. Rakhi, S.F., AHMM, Reza M.S., Hossen Z, Hossain, (2013): Alterations in histopathological features and brain acetylcholinesterase activity in stinging catfish Heteropneustes fossilis exposed to polluted river water. Int Aqua Resea., 2013, 5 (7): 1-18.

- [15]. Sivakumar, S., Kasthuri, H., Prabha, D., Senthilkumar, P., Subbhuraam, C.V. and Song, Y.C. (2009): Efficiency of composting parthenium plant and Neem leaves in the presence and absence of an oligochaete, *Eisenia fetida*. Iran. J. Environ. Health. Sci. Eng. 6 (3) :201-208.
- [16]. Talwar, P. K. and A. K. Jhingran. (1992): Inland fishes of India and adjacent countries. A. A. Balkema / Rotterdam, 1:1177.
- [17]. Varadharajan D., Soundarapandian P., Dinakaran G. K., et al., (2009): Crab Fishery Resources from Arukkattuthurai to Aiyampattinam, South East Coast of India. Current Research Journal of Biological Sciences, 1(3): 118-122.

**Cite this article as :**

(Vikhar) Khedkar A.P., "Toxic effects of *Parthenium hysterophorus* on Muscles of freshwater fish *Labeo rohita*", International Journal of Scientific Research in Science and Technology (IJSRST), Online ISSN : 2395-602X, Print ISSN : 2395-6011, Volume 10 Issue 1, pp. 28-32, January-February 2023. Available at doi : <https://doi.org/10.32628/IJSRST2296113>  
Journal URL : <https://ijsrst.com/IJSRST2296113>

# Effect of *Zingiber officinale* and *Tinospora cordifolia* on Freshwater Fish *Ophocephalus striatus* (Bloch 1973)

S. H. RATHOD\*<sup>1</sup>

<sup>1</sup>Department of Zoology, Vidya Bharati Mahavidyalaya, Amravati - 444 602, Maharashtra, India

Received: 07 Oct 2023; Revised accepted: 26 Nov 2023; Published online: 15 Dec 2023

**Key words:** *Zingiber officinale*, *Tinospora cordifolia*, *Ophocephalus striatus*, Fish, Freshwater

Aquaculture also known as fish farming, is an important sector in the Indian economy and plays an essential role in the country's food security. Aquaculture is the fastest food production sector in the world due to the demand and scarcity of other sources of food production and also due to the health benefits of fish consumption the demand for fishes as a source of food widely throughout the world. The additional demand for fish consumption must be achieved only through aquaculture [1]. Aquaculture farming in India has spot tremendous growth over the last few decades, with significant offering to employment, export earnings, and rural development. As the world population increases the demand of the aquaculture industry increases [2]. Aquaculture become an important resource for humans worldwide, in addition; it is one of the cheapest sources of easily digestible animal protein.

Fishes play a vital role in food security and poverty alleviation in both rural and urban areas often referred to as "rich food for people". Fish provide essential nourishment more ever quality proteins, vitamins, and minerals [3]. Due to high protein content, low fat, and abundant amount of omega-3 fatty acid present in the fish which is an important part of the human diet. Freshwater fish food is essential for the nutrition of famed fish. Fishes require a balanced diet to grow and develop properly, lack of essential nutrients can lead to stunted growth, reduced immunity, and increased mortality. Freshwater fish food typically contains a combination of plant and animal ingredients including soybean meal, corn, wheat, vitamins, and minerals. Fish meal is considered as the major source of dietary protein and lipid supplement in the diets of carnivore fishes. Herbs are more compatible with the body because of their normal nature and having medicine homologous components together and lack of unwanted side effects, therefore they are most suitable [4]. This sustainable and successful freshwater fish culture on a scientific basis principally depends upon the use of adequate, economically valuable, and environmentally artificial food as well as the use of ayurvedic plants to improve the yield of fish culture.

*Zingiber officinale* is a versatile root that has been used for centuries for its medicinal and culinary properties. It is highly valued for its many health benefits, which include reducing inflammation, improving digestion, boosting the immune system, and reducing nausea [5].

*Tinospora cordifolia* commonly known as giloy or heart-leaved moonseed is a popular medicinal plant that has been used in Ayurveda as a medicine for centuries. *Tinospora cordifolia* has a rich source of antioxidants, including alkaloids, glycosides, and steroids which have been shown to have anti-inflammatory and immune-boosting properties [6]. In the present investigation, the effect of *Zingiber officinale* and *Tinospora cordifolia* on freshwater fish *Ophocephalus striatus* was observed.

The basal experimental diet was formulated with the commonly available ingredients. The formula and analyzed proximate composition of basal the diet is shown in (Table 1).

Table 1 Analyzed proximate composition of basal the diet

Ingredients (gm/ dry weight)	Control diet (100gm)	Experimental (100gm)
Prawns	60	60
Fish meal powder	40	35
<i>Zingiber officinale</i>	00	2.5
<i>Tinospora cordifolia</i>	00	2.5

The freshwater fishes were collected from a local fish market measuring about 7.8-11.5 cm in length and weighing ranges from 4.60-14.95gm for the experimental study. The fishes were brought to the laboratory and acclimatized for seven days by feeding them with prawns.

After acclimatization, the two groups of fishes were made:

- Group I) Control
- Group II) Experimental

During Experiment, fishes were fed with a prepared formulated diet twice a day. After 7, 14, 21, and 28 days from each group, the fishes were taken out and tissue of the liver and muscle was removed for the further investigation of total protein [7] ash content [8], and moisture [9].

## Total protein

The present study (Table 2, Fig 1) showed that the total protein of muscle and liver of experimental fishes were found to increase in trend 71.87±1.85, 78.83±0.69, 79.90±0.78, 81.90±1.06 and 37.98±1.01, 39.90±1.15, 43.76±1.80,

\*Correspondence to: Rathod S. H., E-mail: [siddhartrathod86@gmail.com](mailto:siddhartrathod86@gmail.com); Tel: +91 9834665076

45.78±0.93 from 7, 14, 21, 28, days as compared with control group of fishes total protein 58.50±1.8, 62.56±2.2, 68.90±1.5,

72.76±2.6 and 34.44±1.81, 36.76±2.66, 36.79±1.62, 37.90±1.11 respectively.

Table 2 Total protein (gm/100gm) of *Ophiocephalus striatus* fed with *Zingerber officinale* and *Tinospora cordifolia*

Days	Control(gm/100gm)		Experiment (gm/100gm)	
	Muscle	Liver	Muscle	Liver
7 days	58.50 ± 1.8	34.44 ± 1.81	71.87 ± 1.85	37.98 ± 1.01
14 days	62.56 ± 2.2	36.76 ± 2.66	78.83 ± 0.69	39.90 ± 1.15
21 days	68.90 ± 1.5	36.79 ± 1.62	79.90 ± 0.78	43.76 ± 1.80
28 days	72.76 ± 2.6	37.90 ± 1.11	81.90 ± 1.06	45.78 ± 0.93

\*Values are mean ± SD

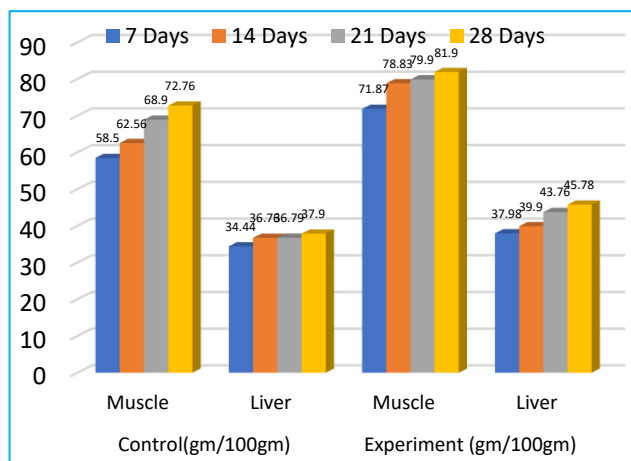


Fig 1 Total protein (gm/100gm) of *Ophiocephalus striatus* fed with *Zingerber officinale* and *Tinospora cordifolia*

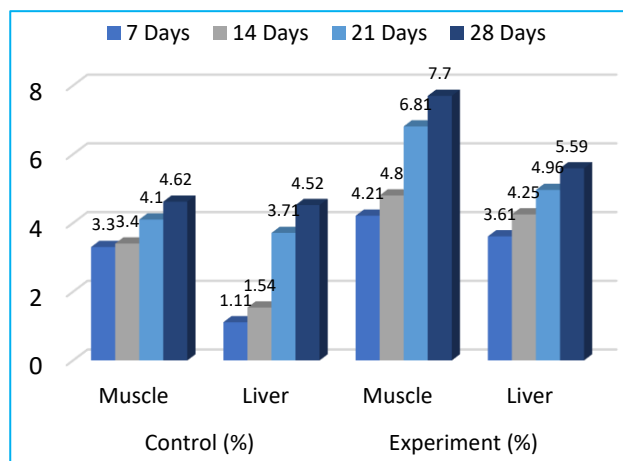


Fig 2 Ash content (%) of *Ophiocephalus striatus* fed with *Zingerber officinale* and *Tinospora cordifolia*

**Ash content**

The ash content (Table 3, Fig 2) showed increasing in trend in the experimental group of fishes fed with *Zingerber officinale* and *Tinospora cordifolia* in muscle tissue 4.21%, 4.80%, 6.81%, 7.70% and 3.61%, 4.25%, 4.96%, 5.59% in liver tissue as compared with control group of fishes 3.30%, 3.40%, 4.10%, 4.62% and 1.11%, 1.54%, 3.71%, 4.52% from 7, 14, 21, 28 days respectively.

**Moisture content**

The moisture content (Table 4, Fig 3) showed increasing in trend in the experimental group of fishes fed with *Zingerber officinale* and *Tinospora cordifolia* in muscle tissue 76.1%, 82.2%, 88.9%, 96.2% and 80.6%, 84.8%, 88.4%, 89.6% in liver tissue as compared with control group of fishes 80.6%, 84.8%, 88.4%, 89.6% from 7, 14, 21, 28 days respectively.

Table 3 Ash content (%) of *Ophiocephalus striatus* fed with *Zingerber officinale* and *Tinospora cordifolia*

Days	Control (%)		Experiment (%)	
	Muscle	Liver	Muscle	Liver
7 days	3.30	1.11	4.21	3.61
14 days	3.40	1.54	4.80	4.25
21 days	4.10	3.71	6.81	4.96
28 days	4.62	4.52	7.70	5.59

Table 4 Moisture content (%) of *Ophiocephalus striatus* fed with *Zingerber officinale* and *Tinospora cordifolia*

Days	Control (%)		Experiment (%)	
	Muscle	Liver	Muscle	Liver
7 days	76.1	88	80.6	78.1
14 days	82.2	89	84.8	79.5
21 days	88.9	92.1	88.4	82.41
28 days	96.2	94.1	89.6	88.6

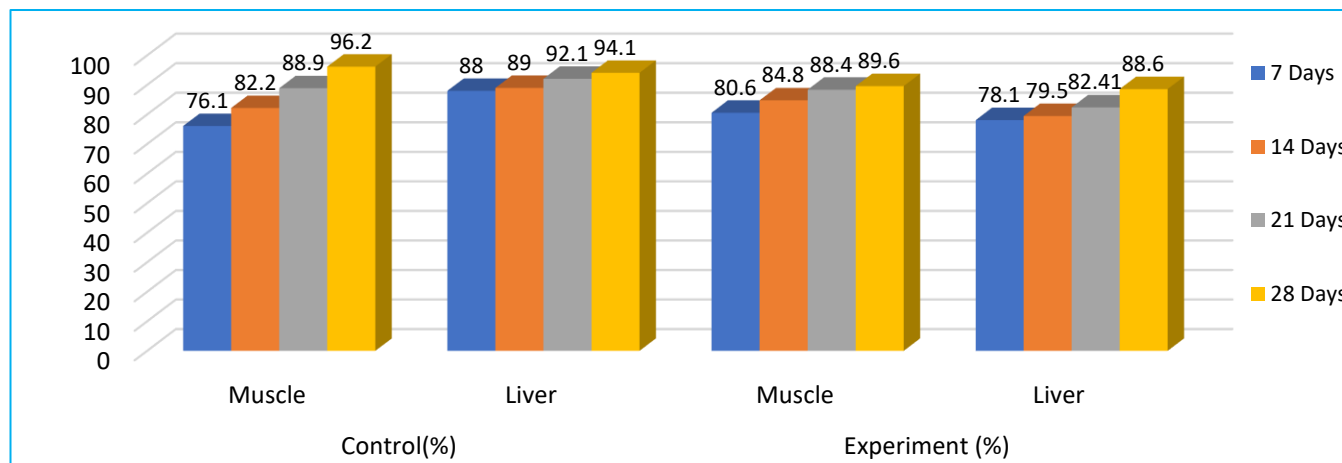


Fig 3 Moisture content (%) of *Ophiocephalus striatus* fed with *Zingerber officinale* and *Tinospora cordifolia*

The obtained results fed with *Zingiber officinale* and *Tinospora cordifolia* to freshwater fish *Ophicephalus striatus* showed major improvement in body weight as compared to control groups. Furthermore, dietary *Zingiber officinale* and *Tinospora cordifolia* enhance metabolic activities and enhance the level of protein. Moreover, the study provided a new dimension for the use of medicinal plants as supplementation to fishes. Kobeisy and Hussain [10], studied *Oreochromis niloticus* and found that dietary food was given to the fishes showed a significant increase in protein level and body weight of fish. Among three carps *Catla catla*, showed maximum average body weight (1256 g), followed by *Labeo rohita* (1215.0g) and *Cyprinus carpio* (1119.01g) in a supplemented diet. Mansour *et al.* [11] studied that ginger has been purported to have anti-inflammatory, anti-hypertensive, and glucose-sensitizing effects as well as stimulatory effects on the gastrointestinal tract by increasing gastric secretions. Also, Singh and Gaur [12], stated that weight gain is maximum when various dietary protein levels and carcass composition are given to *Labeo rohita* fingerlings. Finally, in the present investigation, it was suggested that the *Zingiber officinale* and *Tinospora*

*cordifolia* as feed alternative solutions in aquaculture feed as growth promoters. Distinctly it showed a significant increase in growth performance, feed utilization, and increase in metabolic activity.

## SUMMARY

The study aimed to observe the effect of *Zingiber officinale* and *Tinospora cordifolia* on freshwater fish *Ophicephalus striatus*. The experimental diet was formulated to contain *Zingiber officinale* (2.5gm/100gm diet), and *Tinospora cordifolia* (2.5gm/100gm diet) prepared in the pellet form and fed to the experimental fishes to observe the total protein, ash content, and moisture of the freshwater fish *Ophicephalus striatus* for 7<sup>th</sup>, 14<sup>th</sup>, 21<sup>st</sup>, 28<sup>th</sup> days. The results showed that significant increase in total protein, ash content, and moisture of the experimental group of fishes. The results of this study show that the addition of *Zingiber officinale* and *Tinospora cordifolia* to a fish diet can promote the health benefit and growth of fish.

## LITERATURE CITED

1. Swain S, Ferosekhan S. 2022. Present status and future scope of freshwater aquaculture sector in India. Souvenir of 1<sup>st</sup> Indian fisheries outlook. ICA-CIFRI, Kolkata. pp 84-99.
2. Shalaby AM, Khattab YM, Abdel Rahman AM. 2006. Effects of garlic (*Allium sativum*) and chloramphenicol on growth performance, physiological parameters and survival of Nile Tilapia (*Oreochromis niloticus*). *Jr. Venom. Anim. Toxins Incl. Trop. Dis.* 12: 172-20.
3. Mohanty BP, Mahanty A, Ganguly S, Mitra T, Karunakaran D, Anandan R. 2019. Nutritional composition of food fishes and their importance in providing food and nutritional security. *Food Chemistry* 293: 561-570.
4. Borimnejad V. 2008. Niche markets in the agricultural sector: Case study: Iran. *American –Eurasian Jr. Agric. Environ. Science* 3: 893-899.
5. Marcquin CI. 2013. Effect of ginger extract on stability and sensorial quality of smoked mackerel (*Scomber scombrus*) fish. *Jr. Nutr. Food Science* 3: 3. 1000199.
6. Anita MK, Khati DA, Kanyal PA. 2015. Study of haematological profile of *Labeo rohita* (Rohu) fed with *Tinospora cordifolia* (Giloy) as Nutraceutical. *Jr. Env. Bio-Science* 29(2): 319-322.
7. Lowry OM, Rosebrough NJ, Farr AC, Randall RF. 1951. Protein estimation with folin phenol reagent. *Journal of Biol. Chemistry* 193: 265-275.
8. AOAC. 1990. *Official Methods of Analysis*. Association of Official Analytical Chemists, Washington D.C.
9. APHA. 1998. Standard Method for Examination of Water and Wastewater, 2540D.
10. Kobaeisy MA, Hussein SY. 1995. Influence of dietary live yeast on growth performance and some blood constituents in *Oreochromis niloticus*. *Animal Nutrition* 12-13 *Ismailia Egypt* pp 417-425.
11. Mansour Muhammad S, Yu-Ming Ni, Amy L, Roberts, Kellerman M, Choudhury AR, d Marie-Pierre St-Onge. 2012. Ginger consumption enhances the thermic effect of food and promotes feelings of satiety without affecting metabolic and hormonal parameters in overweight men: A pilot study. *Metabolism* 61(10): 1347-1352.
12. Singh PK, Gaur SR. 2005. Effect of various dietary protein levels on growth Food utilization and carcass composition of *Labeo rohita* fingerlings. *Environment and Ecology* 235(3): 492-496.

### Behaviour of Bianchi Type-V Dark Energy Model in $f(R, T)$ Gravity with a Specific Form of Hubble Parameter

**Pramod P. Khade**

*Vidya Bharati Mahavidyalaya, Amravati-444402, India.*

**Doi:** <https://doi.org/10.47011/16.1.5>

*Received on: 30/04/2021;*

*Accepted on: 04/08/2021*

---

**Abstract:** In this paper, we have constructed a Bianchi type V cosmological model, in the presence of bulk viscous fluid and within the framework of  $f(R, T)$  theory of gravity with an appropriate choice of the functional  $f(R, T)$  in the form  $f(R, T) = R + 2f(T)$ , where  $R$  and  $T$  are respectively Ricci scalar and trace of energy momentum tensor. In order to obtain a deterministic solution, we have considered two general forms of hyperbolic scale factors. The different forms of scale factors considered here produce time-varying deceleration parameters in all the cases that simulate the cosmic transition. The state finder diagnostic pair is found to be in the acceptable range. The physical parameters are constrained from different representative values to build up a realistic cosmological model aligned with the observational behaviour.

**Keywords:** Bianchi type V, Dark energy,  $f(R, T)$  gravity, Variable deceleration parameter.

## 1. Introduction

In recent years, several modified gravity theories, like  $f(R)$  gravity,  $f(G)$  gravity,  $f(T)$  gravity and so on, were investigated by many researchers. A large class of cosmological models has explained the acceleration of the universe in terms of a component with negative pressure, the so-called dark energy (DE). The limitations of general relativity in providing a satisfactory explanation of this phase of evolution have led cosmologists to adopt hypotheses and study their implications in this context. The hypotheses include those assigning (I) the time-dependence of the gravitational constant and cosmological term (II) some other geometries or physical fields associated with the universe and (III) modified or alternative theories of gravity. Modified gravity theories certainly provide a way of understanding the problem of DE and the possibility to reconstruct the gravitational field theories that would be capable to reproduce the late-time acceleration of the universe. In an effort to address the

cosmic speed-up issue, Harko et al. [1] introduced a modified gravity theory known as  $f(R, T)$  gravity. Several studies were made in this theory addressing different contexts, such as energy conditions (Alvarenga et al. [2]; Kiani & Nozari [3]), wormhole solution (Azizi [4]; Moraes et al. [5]), anisotropy cosmology (Sharif & Zubair [6]; Mishra et al. [7-8]), higher dimensions (Troisi [9]) and non-interacting Chaplygin gas (Shabani [10]; Shabani & Farhoudi [11]). Sharma and Singh [12] have studied the string cosmological model with magnetic field in Bianchi Type II space-time. With a rescaled functional of  $f(R, T)$  gravity, extensive investigations were carried out in Bianchi type VIIh space-time to understand the dynamical behaviour of the anisotropic universe (Mishra et al. [13-14]). Zubair et al. [15] have investigated the anisotropy source with the dynamical analysis of cylindrically symmetric space-time, whereas Mishra and Vadrevu [16] have constructed a cylindrically symmetric



model with the exact solution. Aktas and Aygun [17] have shown that magnetized field vanishes in FRW universe for  $f(R, T)$  gravity. Many more Bianchi type cosmological models have been developed in recent past (Shamir [18]; Chaubey & Shukla [19]; Pawar [20-23]; Samanta [24]; Reddy et al. [25-27]; Shri Ram [28]; Nasr Ahmed [29]). The extraordinary phenomena of  $f(R, T)$  gravity may provide some significant signatures and effects which could distinguish and discriminate between various gravitational models. Therefore, this theory has attracted many researchers to explore different aspects of cosmology and astrophysics in isotropic and in anisotropic space-times (See for example Khade and Wasnik [30]; Chakraborty [31]; Houndjo et al. [32]; Pasqua et al. [33]; Singh and Singh [34]; Baffou et al. [35]; Santos and Ferst [36]; Noreen et al. [37]; Shamir [38]; Singh and Singh [39]; Alhamzawi and Alhamzawi [40]; Yousaf et al. [41]; Alves et al. [42]; Zubair et al. [43]; Sofuoglu [44]; Momeni et al. [45]; Das et al. [46]; Salehi and Aftabi [47]; Singh and Beesham [48]; Srivastava and Singh [49]; Sharif and Anwar [50]; Tiwari and Beesham [51]; Shabani et al. [52]; Rajabi and Nozari [53]; Baffou et al. [54]; Lobato et al. [55]; Tretyakov [56]; Elizalde and Khurshudyan [57]; Ordines and Carlson [58]; Maurya and Tello-Ortiz [59]; Esmaeili [60] and references therein).

Bulk viscosity is the only dissipative phenomenon occurring in FRW models and is significant in causing the accelerated expansion of the universe known as inflationary phase as discussed by Setaren et al. [61]. Several cosmologists have discussed the role of bulk viscosity in the early evolution of the universe in different physical contexts. The cosmological and astrophysical implications of  $f(R, T)$  gravity theory in the presence of perfect fluids and bulk viscous fluids have been studied by several cosmologists. Shri Ram et al. [62] investigated Bianchi type-I and -V bulk viscous fluid cosmological models. Sahu et al. [63] discussed cosmic transits and anisotropic models of Bianchi type-III. Further, Sahoo et al. [64-69] studied cosmological models in  $f(R, T)$  theory with variable deceleration parameters. This motivates the theorists to construct various models of different Bianchi space-times in different contexts.

Spatially homogeneous and anisotropic Bianchi models have been widely studied in the

framework of general relativity to describe the early stage of evolution of the universe. The theoretical studies and observational data of cosmic microwave background (CMB) and the large structure have stimulated the study of anisotropic models. The study of anisotropic models has also been extended to modified gravitational theories. Pradhan et al. [70], Aktas et al. [71], Yilmaz et al. [72] and Sharif and Zubair [73, 74] are some of the authors who have investigated several aspects of anisotropic Bianchi models in  $f(R, T)$  gravity.

Recently, the dark energy models, which are inspiring many astrophysicists, are the holographic dark-energy models. According to the holographic principle, the number of degrees of freedom in a bounded system should be finite.

In this paper, we have investigated the physical behaviour of the cosmological model obtained with Bianchi type-V space-time in the presence of hyperbolic scale factor in two different cases. The present paper is organized as follows. The field equations of  $f(R, T)$  gravity have been derived in Section 2. The model and basic framework have been presented in Section 3. In Sections 4, 6, the derivation and analysis of parameters have been derived for cases I, II. In Sections 5, 7, the physical properties of the model have been discussed for cases I, II, respectively. Finally, the conclusion is given in Section 8.

## 2. Field Equations

We assume that the cosmic matter may be represented by the energy-momentum tensor of an imperfect bulk viscous fluid as:

$$T_{ij} = (\rho + \bar{p})u_i u_j - \bar{p}g_{ij} \quad (1)$$

where  $\bar{p}$  is the bulk viscous pressure given by:

$$\bar{p} = p - \zeta u^i{}_{;i} \quad (2)$$

satisfying a linear equation of state:

$$p = \epsilon\rho, 0 \leq \epsilon \leq 1. \quad (3)$$

Here,  $p$  is the equilibrium pressure,  $\rho$  is the energy density of matter,  $\zeta$  is the coefficient of bulk viscosity and  $u^i$  is the flow vector of the fluid satisfying  $u_i u^i = 1$ . The semicolon stands for covariant differentiation. On thermodynamic grounds, bulk viscosity coefficient  $\zeta$  is positive, assuring that the viscosity pushes the dissipative pressure  $\bar{p}$  towards negative values. However,

the correction applied to the thermodynamical pressure  $p$  due to bulk viscous pressure is very small. Therefore, the dynamics of cosmic evolution is not fundamentally influenced by the inclusion of the viscous term in the energy-momentum tensor.

For the field equations in  $f(R, T)$  modified gravity model, we assume that the function  $f(R, T)$  is given by:

$$f(R, T) = R + 2f(T) \quad (4)$$

where  $f(T)$  is an arbitrary function of the trace of the stress-energy tensor of matter. The gravitational field equation is immediately given by:

$$R_{ij} - \frac{1}{2}Rg_{ij} = 8\pi T_{ij} + 2f'(T)T_{ij} + [2\bar{p}f'(T) + f(T)]g_{ij} \quad (5)$$

where the prime denotes a derivative with respect to the argument.

The simplest cosmological model can be obtained by choosing the function  $f(T)$ , so that  $f(T) = \lambda T$ , where  $\lambda$  is a constant.

### 3. The Model and Basic Framework

The diagonal form of the metric of Bianchi type-V cosmological model is given by:

$$ds^2 = dt^2 - A^2 dx^2 - e^{2\beta x} [B^2 dy^2 + C^2 dz^2]. \quad (6)$$

Here,  $A = A(t)$ ,  $B = B(t)$  and  $C = C(t)$  are cosmic scale factors and  $\beta$  is an arbitrary constant.

The spatial volume  $V$  and the average Hubble's parameter  $H$  are defined as:

$$V = a^3 = ABC, \quad (7)$$

$$3H = \frac{\dot{V}}{V} = \frac{\dot{A}}{A} + \frac{\dot{B}}{B} + \frac{\dot{C}}{C}, \quad (8)$$

where a dot denotes differentiation with respect to cosmic time  $t$ .

The shear scalar  $\sigma$  and anisotropy parameter  $Am$  are defined as follows:

$$\sigma^2 = \frac{1}{2} \left[ \left( \frac{\dot{A}}{A} \right)^2 + \left( \frac{\dot{B}}{B} \right)^2 + \left( \frac{\dot{C}}{C} \right)^2 \right] - \frac{1}{6} \theta^2 \quad (9)$$

$$Am = \frac{1}{3} \sum_{i=1}^3 \left( \frac{\Delta H_i}{H} \right)^2 \quad (10)$$

where  $\Delta H_i = H_i - H$ , ( $i = 1, 2, 3$ ) and  $H_1 = \frac{\dot{A}}{A}$ ,  $H_2 = \frac{\dot{B}}{B}$  and  $H_3 = \frac{\dot{C}}{C}$  are the directional Hubble parameters.

For the metric (6), Eqs. (1), (4) and (5) in comoving coordinates lead to the following set of equations:

$$\frac{A\dot{B}}{AB} + \frac{\dot{B}C}{BC} + \frac{A\dot{C}}{AC} - \frac{3\beta^2}{A^2} = (8\pi + 3\lambda)\rho - \lambda\bar{p} \quad (11)$$

$$\frac{\dot{B}}{B} + \frac{\dot{C}}{C} + \frac{\dot{B}C}{BC} - \frac{\beta^2}{A^2} = \lambda\rho - (8\pi + 3\lambda)\bar{p} \quad (12)$$

$$\frac{\dot{A}}{A} + \frac{\dot{C}}{C} + \frac{A\dot{C}}{AC} - \frac{\beta^2}{A^2} = \lambda\rho - (8\pi + 3\lambda)\bar{p} \quad (13)$$

$$\frac{\dot{A}}{A} + \frac{\dot{B}}{B} + \frac{A\dot{B}}{AB} - \frac{\beta^2}{A^2} = \lambda\rho - (8\pi + 3\lambda)\bar{p} \quad (14)$$

$$\frac{2\dot{A}}{A} - \frac{\dot{B}}{B} - \frac{\dot{C}}{C} = 0. \quad (15)$$

After integrating Eq. (15) and absorbing integration constant into  $B$  or  $C$ , we get:

$$A^2 = BC. \quad (16)$$

We have five highly non-linear differential equations with six unknowns; namely,  $A, B, C, \rho, \bar{p}, \zeta$ . Therefore, to find a consistent solution to these equations, subtracting Eq. (13) from Eq. (12), Eq. (14) from Eq. (13), Eq. (14) from Eq. (12) and integrating the resulting equations, we obtain the following three relations (Saha and Rikhvitsky [75,76]), respectively:

$$\frac{A}{B} = m_1 \exp \left[ k_1 \int \frac{dt}{a^3} \right] \quad (17)$$

$$\frac{A}{C} = m_2 \exp \left[ k_2 \int \frac{dt}{a^3} \right] \quad (18)$$

$$\frac{B}{C} = m_3 \exp \left[ k_3 \int \frac{dt}{a^3} \right] \quad (19)$$

where  $m_1, m_2, m_3, k_1, k_2, k_3$  are constants of integration.

Using Eq. (7), we write the metric functions from (17)-(19) in explicit form as:

$$A = ad_1 \exp \left[ \alpha_1 \int \frac{dt}{a^3} \right] \quad (20)$$

$$B = ad_2 \exp \left[ \alpha_2 \int \frac{dt}{a^3} \right] \quad (21)$$

$$C = ad_3 \exp \left[ \alpha_3 \int \frac{dt}{a^3} \right] \quad (22)$$

where:

$$d_1 = \sqrt[3]{m_1 m_2}, d_2 = \sqrt[3]{m_1^{-1} m_3}, d_3 = \sqrt[3]{(m_2 m_3)^{-1}}, \quad (23)$$

and

$$\alpha_1 = \frac{k_1 + k_2}{3}, \alpha_2 = \frac{k_3 - k_1}{3}, \alpha_3 = \frac{-(k_2 + k_3)}{3}. \quad (24)$$

The constants  $d_1, d_2, d_3$  and  $\alpha_1, \alpha_2, \alpha_3$  satisfy the following two relations:

$$\alpha_1 + \alpha_2 + \alpha_3 = 0; d_1 d_2 d_3 = 1. \quad (25)$$

Substituting Eq. (16) in Eqs. (20)-(22), we obtain:

$$A = a \quad (26)$$

$$B = a \exp\left[\alpha \int \frac{dt}{a^3}\right], \quad (27)$$

$$C = a d^{-1} \exp\left[-\alpha \int \frac{dt}{a^3}\right] \quad (28)$$

where:

$$d_1 = 1, d_2 = d_3^{-1} = d, \alpha_1 = 0, \alpha_2 = -\alpha_3 = \alpha.$$

#### 4. Derivation and Analysis of Parameters

**Case (i):** For  $H = \eta \tanh(\eta t)$

For the explicit determination of the cosmic parameters, we need one more condition. Recently, Pacif and Mishra [77] as well as Esmaeili and Mishra [78] have obtained cosmological model in Bianchi types geometry with a specific variation of the Hubble parameter in general relativity, which is a good approximation concerning the current late-time

acceleration of the universe. Following the same here, we consider that:

$$H = \eta \tanh(\eta t). \quad (29)$$

With the form of H given by Eq. (29), we obtain the average scale factor as:

$$a = \delta \cosh(\eta t). \quad (30)$$

Using Eqs. (26)-(28) with the help of (30), we obtain the metric functions as:

$$A = \delta \cosh(\eta t). \quad (31)$$

$$B = \delta \cosh(\eta t) \exp\left[\frac{\alpha}{2\eta\delta^3} (\operatorname{sech}(\eta t) \tanh(\eta t) + 2 \arctan e^{\eta t})\right]. \quad (32)$$

$$C = \delta^{-1} \delta \cosh(\eta t) \exp\left[\frac{-\alpha}{2\eta\delta^3} (\operatorname{sech}(\eta t) \tanh(\eta t) + 2 \arctan e^{\eta t})\right]. \quad (33)$$

$$\rho = \frac{1}{(8\pi+2\lambda)(8\pi+4\lambda)} \left\{ 6\eta^2 (4\pi + \lambda) \tanh^2(\eta t) - 2\lambda\eta^2 \operatorname{sech}^2(\eta t) - \frac{\alpha^2}{\delta^6} (2\pi + \lambda) \left[ 2\operatorname{sech}^3(\eta t) - \operatorname{sech}(\eta t) + \frac{2e^{\eta t}}{1+e^{2\eta t}} \right]^2 - \frac{8(3\pi+\lambda)\beta^2}{\delta^2 \cosh^2(\eta t)} \right\}. \quad (34)$$

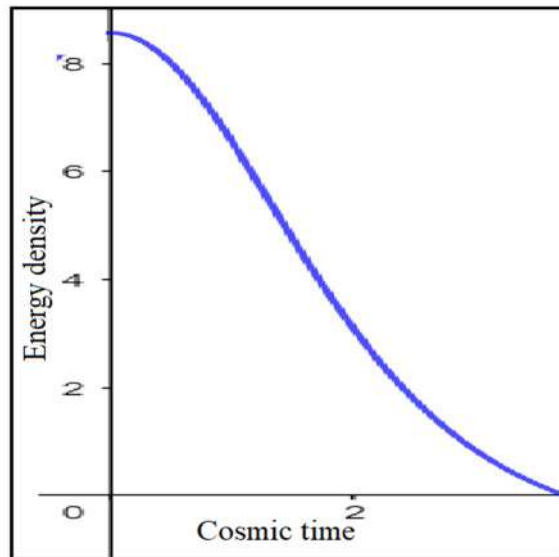
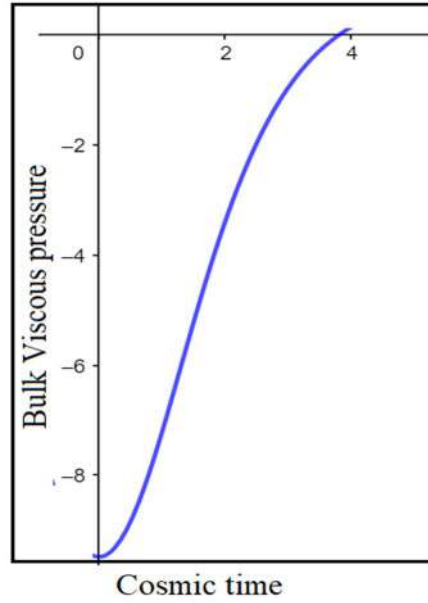


FIG. 1. Energy density vs. time for  $\eta = 0.5, \alpha = 2, \lambda = -6.5, \delta = 1, \beta = 2$ .

The energy density in Fig. 1 lies in the positive domain. It has been observed that the energy density is high in the early time of the universe and then gradually decreases to null. It may be noted here that since  $\rho$  needs to be positive, the first term of (34) should dominate the second. Therefore, the behaviours of the parameters are constrained accordingly within the admissible limits.

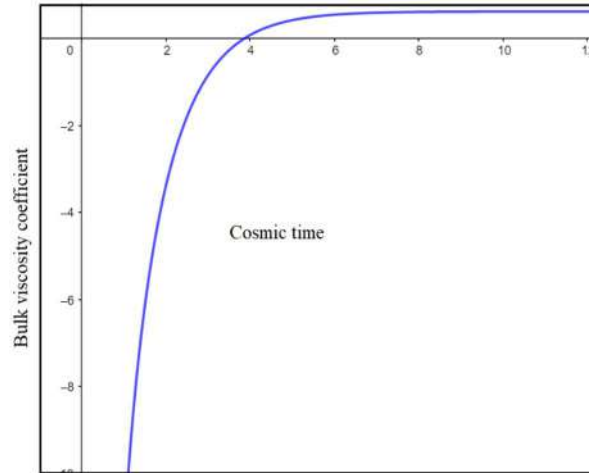
$$\bar{\rho} = \frac{1}{(8\pi+2\lambda)(8\pi+4\lambda)} \left\{ -6\eta^2 (4\pi + \lambda) \tanh^2(\eta t) - 2(8\pi + 3\lambda)\eta^2 \operatorname{sech}^2(\eta t) - \frac{\alpha^2}{\delta^6} (2\pi + \lambda) \left[ 2\operatorname{sech}^3(\eta t) - \operatorname{sech}(\eta t) + \frac{2e^{\eta t}}{1+e^{2\eta t}} \right]^2 + \frac{8\pi\beta^2}{\delta^2 \cosh^2(\eta t)} \right\}. \quad (35)$$


 FIG. 2. Bulk viscous pressure  $\bar{p}$  vs. time for  $\eta = 0.5, \alpha = 2, \lambda = -6.5, \delta = 1, \beta = 2$ .

From Fig. 2, we observe that bulk viscous pressure  $\bar{p}$  lies in the negative range to suffice the acceleration of the universe. The bulk viscous pressure of the universe is an increasing function of cosmic time  $t$ , which begins from a negative value and tends to zero at a present epoch. The accelerated expansion of the universe, as per the recent cosmological observations, is due to dark energy which is nothing but negative pressure. Thus, the derived

model is in good agreement with the observation.

$$\zeta = \frac{1}{3(8\pi+2\lambda)(8\pi+4\lambda)\eta \tanh(\eta t)} \left\{ 6\eta^2(4\pi + \lambda)(\varepsilon + 1)\tanh^2(\eta t) + 2(8\pi + 3\lambda - \varepsilon\lambda)\eta^2 \operatorname{sech}^2(\eta t) - \frac{\alpha^2}{\delta^6}(1 - \varepsilon)(2\pi + \lambda) \left[ 2\operatorname{sech}^3(\eta t) - \operatorname{sech}(\eta t) + \frac{2e^{\eta t}}{1+e^{2\eta t}} \right]^2 - \frac{8[(3\pi+\lambda)\varepsilon+\pi]\beta^2}{\delta^2 \cosh^2(\eta t)} \right\}. \quad (36)$$


 FIG. 3. Bulk viscosity coefficient vs. time for  $\eta = 0.5, \alpha = 2, \lambda = -6.5, \delta = 1, \beta = 2, \varepsilon = 0.1$ .

The barotropic equation of state parameter is used to obtain the coefficient of bulk viscosity. It can be observed that the bulk viscosity is negative at higher redshift (early time) and positive at lower redshift (late time) in the present model with bulk viscosity shown in Fig. 3. This means that the rate of entropy production is negative in the early epoch and positive in the

later epoch. Thus, the model does not violate the law of entropy. It also shows the transition from negative to positive in due course of evolution, which indicates the earlier decelerating phase of the universe with positive pressure (suitable for structure formation) and present accelerating phase of the evolution with negative pressure.

## 5. Physical Properties of the Model

The spatial volume ( $V$ ), the directional Hubble parameter ( $H_i$ ), the expansion scalar ( $\theta$ ), the shear scalar ( $\sigma^2$ ), the deceleration parameter ( $q$ ) and the anisotropy parameter ( $Am$ ) are, respectively, given by:

$$V = a^3 = \delta^3 \cosh^3(\eta t). \quad (37)$$

$$H_1 = \frac{\dot{A}}{A} = \eta \tanh(\eta t). \quad (38)$$

$$H_2 = \frac{\dot{B}}{B} = \frac{\alpha}{2\delta^3} \left[ 2\operatorname{sech}^3(\eta t) - \operatorname{sech}(\eta t) + \frac{2e^{\eta t}}{1+e^{2\eta t}} \right] + \eta \tanh(\eta t). \quad (39)$$

$$H_3 = \frac{\dot{C}}{C} = \frac{-\alpha}{2\delta^3} \left[ 2\operatorname{sech}^3(\eta t) - \operatorname{sech}(\eta t) + \frac{2e^{\eta t}}{1+e^{2\eta t}} \right] + \eta \tanh(\eta t). \quad (40)$$

$$\theta = 3\eta \tanh(\eta t). \quad (41)$$

$$\sigma^2 = \frac{\alpha^2}{4\delta^6} \left[ 2\operatorname{sech}^3(\eta t) - \operatorname{sech}(\eta t) + \frac{2e^{\eta t}}{1+e^{2\eta t}} \right]^2. \quad (42)$$

$$q = -\coth^2(\eta t). \quad (43)$$

$$Am = \frac{1}{3} \left\{ 4 + \frac{\alpha^2}{2\eta^2 \delta^6 \tanh^2(\eta t)} \left[ 2\operatorname{sech}^3(\eta t) - \operatorname{sech}(\eta t) + \frac{2e^{\eta t}}{1+e^{2\eta t}} \right]^2 \right\}. \quad (44)$$

The above results are useful to discuss the behavior of the model.

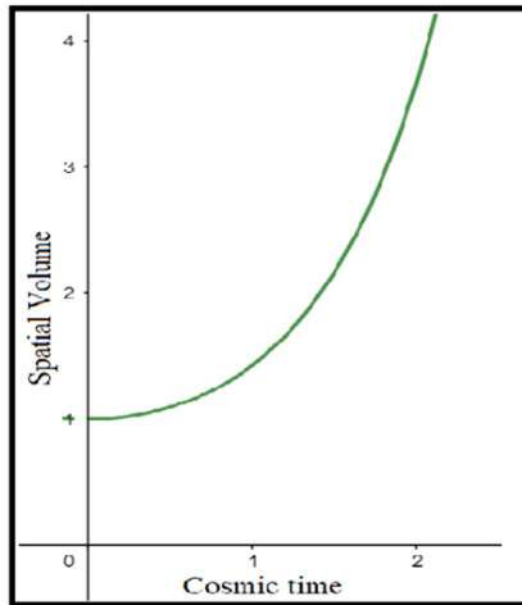


FIG. 4. Spatial volume vs. time for  $\delta = 1, \eta = 0.5$ .

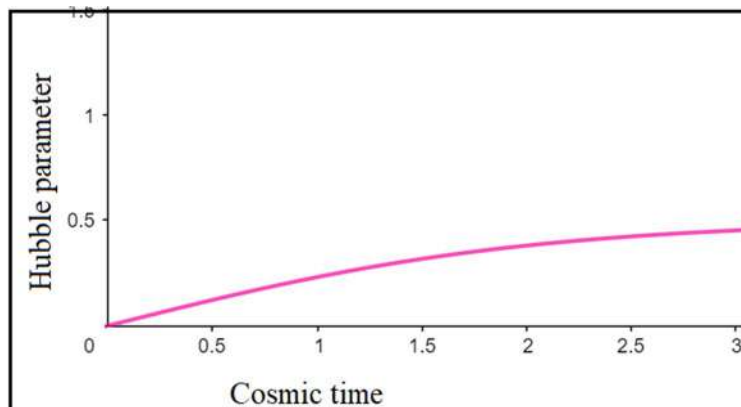
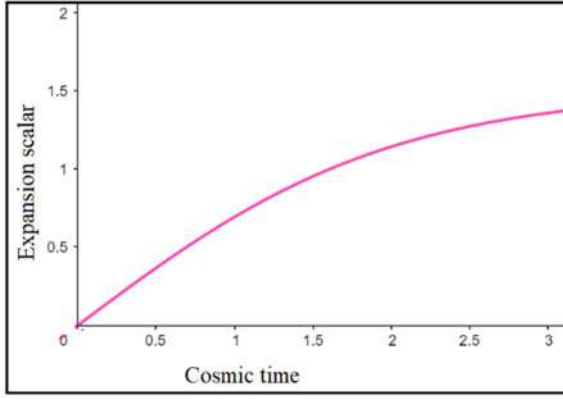
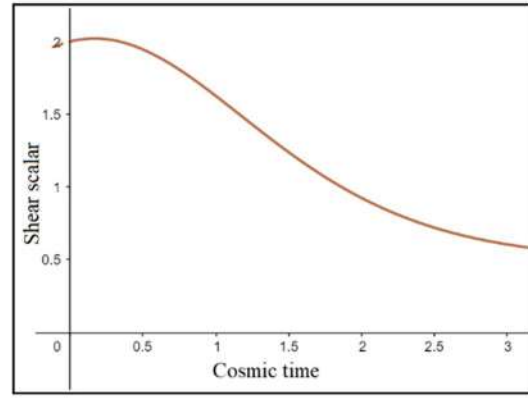
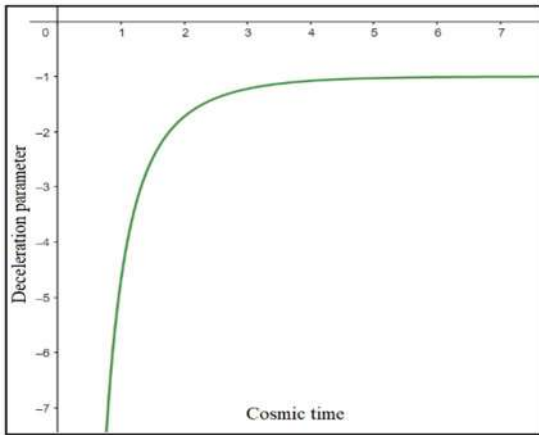
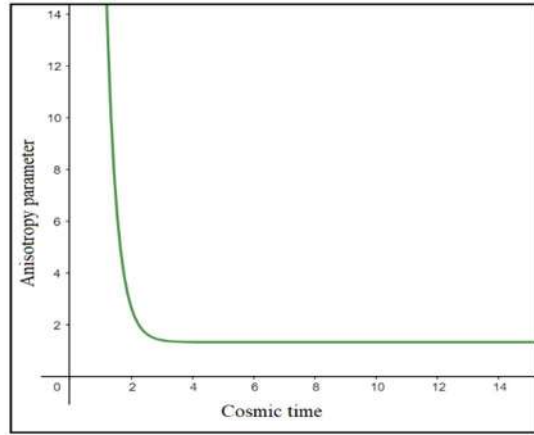


FIG. 5. Hubble parameter vs. time for  $\delta = 1, \eta = 0.5$ .


 FIG. 6. Expansion scalar vs. time for  $\delta = 1, \eta = 0.5$ .

 FIG. 7. Shear scalar vs. time for  $\delta = 1, \eta = 0.5, \alpha = 2$ .

 FIG. 8. Deceleration parameter vs. time for  $\delta = 1, \eta = 0.5$ .

 FIG. 9. Anisotropic parameter vs. time for  $\delta = 1, \eta = 0.5, \alpha = 2$ .

We have the following observations:

From Eq. (37), it can be observed that the volume scale factor is finite at the initial epoch and positive throughout the evolution. It increases gradually with the increase in time as shown in (Fig 4). The graphical representation of the Hubble parameter is shown in Fig. 5. The parameter is governed by the constant  $\eta$  and the cosmic time. Since we have already assumed a positive constant  $\eta$  to obtain a model that fits observationally, the parameter is now totally controlled by the cosmic time. Hubble parameter increases with the increase in time. Shear scalar decreases with the increase in time (Fig 7). Fig.6 depicts that the expansion scalar increases with the increase in time.

The deceleration parameter is found to be  $q = -\coth^2(\eta t)$ . It indicates that the parameter always remains negative throughout the cosmic evolution for  $\eta = 0.5$ . Since the scale factor is hyperbolic and can never be negative, this confirms that the deceleration parameter will always remain in the negative domain. It is also observed from Fig. 8 that the accelerated expansion occurs in a reasonable time period,

which can be termed as the transition period. The mean anisotropic parameter decreases exponentially and approaches null with an increase in time (Fig. 9).

## 6. Derivation and Analysis of Parameters

**Case (ii):** For  $H = \eta \coth(\eta t)$

$$H = \eta \coth(\eta t). \quad (45)$$

With the form of H given by Eq. (45), we obtain the average scale factor as:

$$a = \delta \sinh(\eta t). \quad (46)$$

Using Eqs. (26)-(28) with the help of (30), we obtain the metric functions as:

$$A = \delta \sinh(\eta t). \quad (47)$$

$$B = \delta \delta \sinh(\eta t) \exp \left[ \frac{-\alpha}{2\eta \delta^3} \left( \operatorname{cosech}(\eta t) \coth(\eta t) + \log \tanh\left(\frac{\eta t}{2}\right) \right) \right]. \quad (48)$$

$$C = d^{-1} \delta \sinh(\eta t) \exp \left[ \frac{\alpha}{2\eta\delta^3} \left( \operatorname{cosech}(\eta t) \coth(\eta t) + \log \tanh\left(\frac{\eta t}{2}\right) \right) \right]. \quad (49)$$

$$\rho = \frac{1}{(8\pi+2\lambda)(8\pi+4\lambda)} \left\{ 6\eta^2(4\pi+\lambda) \coth^2(\eta t) + 2\lambda\eta^2 \operatorname{cosech}^2(\eta t) - \frac{\alpha^2}{\delta^6} (2\pi+\lambda) \left[ \operatorname{cosech}(\eta t) \left( \operatorname{cosech}^2(\eta t) + \coth^2(\eta t) - \frac{1}{2} \operatorname{cosech}\left(\frac{\eta t}{2}\right) \coth\left(\frac{\eta t}{2}\right) \right) \right]^2 - \frac{8(3\pi+\lambda)\beta^2}{\delta^2 \sinh^2(\eta t)} \right\}. \quad (50)$$

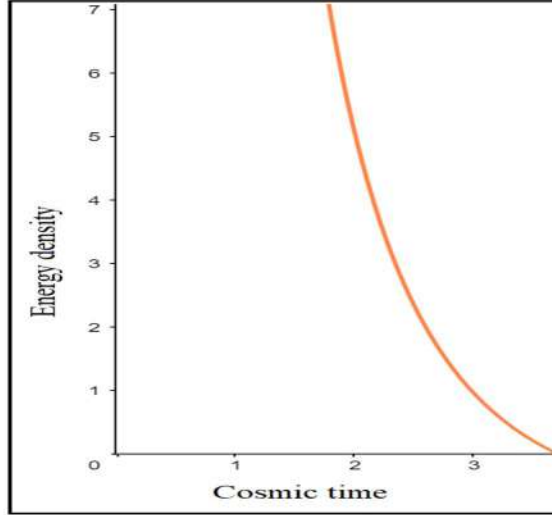


FIG. 10. Energy density vs. time for  $\eta = 0.5, \alpha = 2, \lambda = -6.5, \delta = 1, \beta = 2$ .

The energy density in Fig. 10 lies in the positive domain. It has been observed that the energy density decreases with the increase in time, but it is infinite at the initial epoch.

$$\bar{p} = \frac{1}{(8\pi+2\lambda)(8\pi+4\lambda)} \left\{ -6\eta^2(4\pi+\lambda) \coth^2(\eta t) + 2(8\pi+3\lambda)\eta^2 \operatorname{cosech}^2(\eta t) - \frac{\alpha^2}{\delta^6} (2\pi+\lambda) \left[ \operatorname{cosech}(\eta t) \left( \operatorname{cosech}^2(\eta t) + \coth^2(\eta t) - \frac{1}{2} \operatorname{cosech}\left(\frac{\eta t}{2}\right) \coth\left(\frac{\eta t}{2}\right) \right) \right]^2 + \frac{8\pi\beta^2}{\delta^2 \sinh^2(\eta t)} \right\}. \quad (51)$$

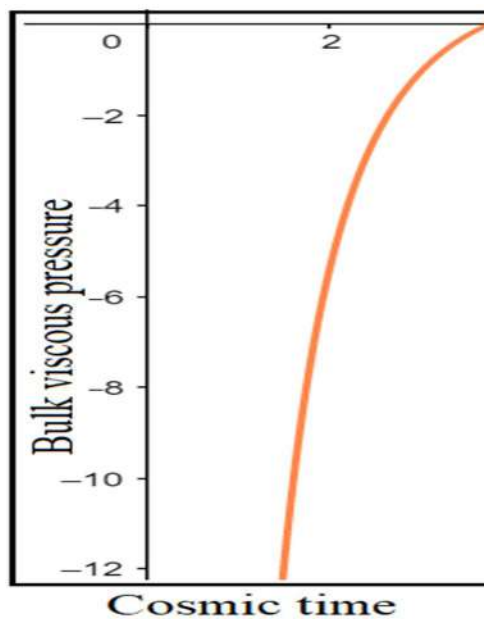


FIG. 11. Bulk viscous pressure  $\bar{p}$  vs. time for  $\eta = 0.5, \alpha = 2, \lambda = -6.5, \delta = 1, \beta = 2$ .

From Fig. 11, we observe that bulk viscous pressure  $\bar{p}$  is increasing as a function of time. It begins from a large negative value and tends to zero at the present epoch. The present study demonstrates the expanding behaviour of the universe and on the other hand, negative pressure indicates the cosmic accelerated expansion of the universe.

$$\zeta = \frac{1}{3(8\pi+2\lambda)(8\pi+4\lambda)\eta \coth(\eta t)} \times \left\{ \begin{aligned} &6\eta^2(4\pi+\lambda)(\varepsilon+1)\coth^2(\eta t) \\ &+2(8\pi+3\lambda-\varepsilon)\eta^2\operatorname{cosech}^2(\eta t) - \frac{\alpha^2}{\delta^6}(1-\varepsilon)(2\pi+\lambda) \\ &\left[ \operatorname{cosech}(\eta t) \left( \operatorname{cosech}^2(\eta t) + \coth^2(\eta t) \right) \right]^2 \\ &\quad - \frac{8[(3\pi+\lambda)\varepsilon+\pi]\beta^2}{\delta^2\sinh^2(\eta t)} \end{aligned} \right\} \quad (52)$$

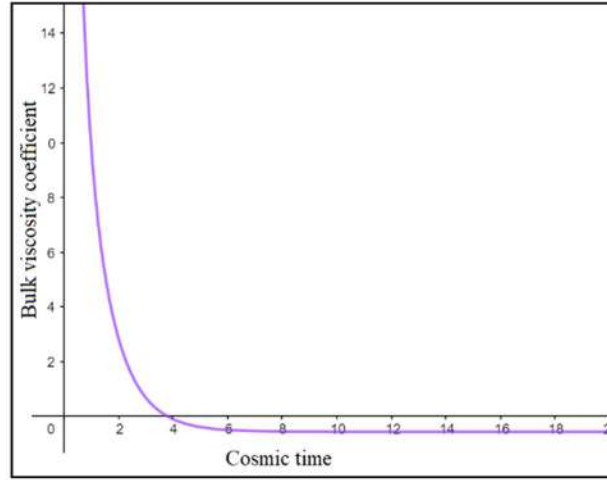


FIG. 12. Bulk viscosity coefficient vs. time for  $\eta = 0.5, \alpha = 2, \lambda = -6.5, \delta = 1, \beta = 2, \varepsilon = 0.1$ .

Using the equation of state parameter, the bulk viscosity coefficient is shown in Fig. 12. Bulk viscosity coefficient is infinite at the initial epoch and has a transition from positive to negative. It also shows the transition from positive to negative in due course of evolution, which indicates the earlier accelerating phase of the universe with negative pressure (suitable for structure formation) and the present decelerating phase of the evolution with positive pressure.

## 7. Physical Properties of the Model

The spatial volume ( $V$ ), the directional Hubble parameter ( $H_i$ ), the expansion scalar ( $\theta$ ), the shear scalar ( $\sigma^2$ ), the deceleration parameter ( $q$ ) and the anisotropy parameter ( $Am$ ) are, respectively, given by:

$$V = a^3 = \delta^3 \sinh^3(\eta t). \quad (53)$$

$$H_1 = \frac{\dot{A}}{A} = \eta \coth(\eta t). \quad (54)$$

$$H_2 = \frac{\dot{B}}{B} = \frac{\alpha}{2\delta^3} \left[ \operatorname{cosech}(\eta t) \left( \operatorname{cosech}^2(\eta t) + \coth^2(\eta t) - \frac{1}{2} \operatorname{cosech}\left(\frac{\eta t}{2}\right) \coth\left(\frac{\eta t}{2}\right) \right) \right] + \eta \coth(\eta t). \quad (55)$$

$$H_3 = \frac{\dot{C}}{C} = \frac{-\alpha}{2\delta^3} \left[ \operatorname{cosech}(\eta t) \left( \operatorname{cosech}^2(\eta t) + \coth^2(\eta t) - \frac{1}{2} \operatorname{cosech}\left(\frac{\eta t}{2}\right) \coth\left(\frac{\eta t}{2}\right) \right) \right] + \eta \coth(\eta t). \quad (56)$$

$$\theta = 3\eta \coth(\eta t). \quad (57)$$

$$\sigma^2 = \frac{\alpha^2}{4\delta^6} \left[ \operatorname{cosech}(\eta t) \left( \operatorname{cosech}^2(\eta t) + \coth^2(\eta t) - \frac{1}{2} \operatorname{cosech}\left(\frac{\eta t}{2}\right) \coth\left(\frac{\eta t}{2}\right) \right) \right]^2. \quad (58)$$

$$q = -1 + \operatorname{sech}^2(\eta t). \quad (59)$$

$$Am = \frac{1}{3} \left\{ 4 + \frac{\alpha^2}{2\eta^2\delta^6\coth^2(\eta t)} \left[ \operatorname{cosech}(\eta t) \left( \operatorname{cosech}^2(\eta t) + \coth^2(\eta t) - \frac{1}{2} \operatorname{cosech}\left(\frac{\eta t}{2}\right) \coth\left(\frac{\eta t}{2}\right) \right) \right]^2 \right\}. \quad (60)$$



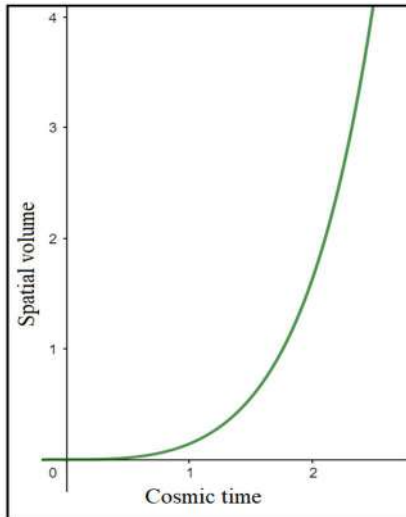


FIG. 13. Spatial volume vs. time for  $\delta = 1, \eta = 0.5$ .

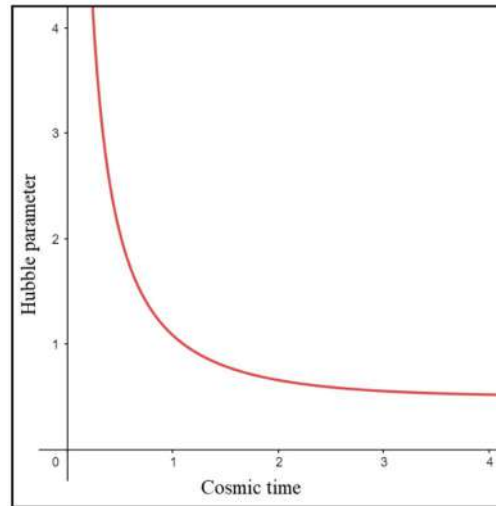


FIG.14. Hubble parameter vs. time for  $\delta = 1, \eta = 0.5$ .

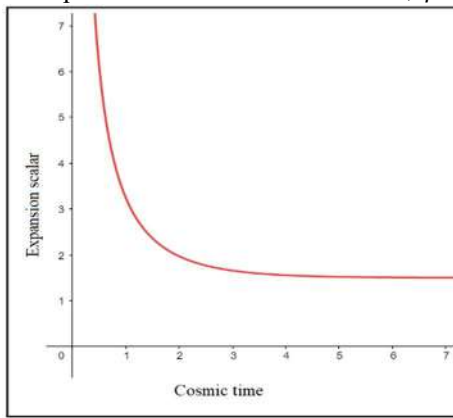


FIG. 15. Expansion scalar vs. time for  $\delta = 1, \eta = 0.5$ .

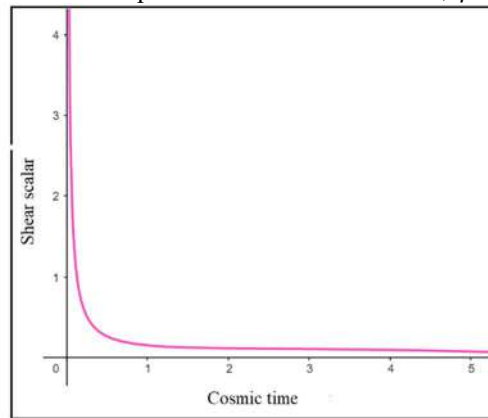


FIG. 16. Shear scalar vs. time for  $\delta = 1, \eta = 0.5, \alpha = 2$ .

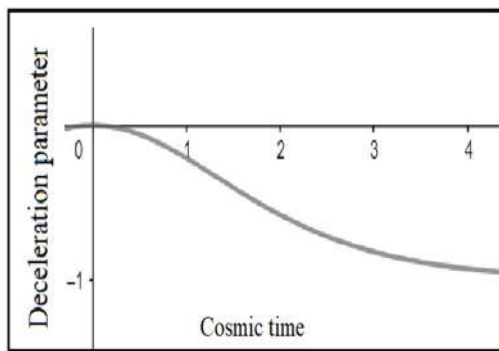


FIG. 17. Deceleration parameter vs. time for  $\delta = 1, \eta = 0.5$ .

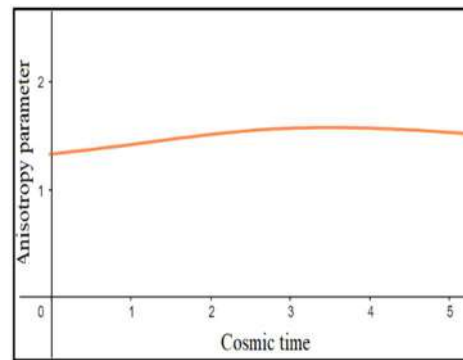


FIG. 18. Anisotropic parameter vs. time for  $\delta = 1, \eta = 0.5, \alpha = 2$ .

We have the following observations:

Spatial volume is zero when  $t = 0$  and it increases as time increases. This means that the expansion of the universe starts with finite volume and it is expanding as  $t$  increases (Fig. 13). The average Hubble parameter ( $H$ ), expansion scalar ( $\theta$ ) and shear scalar ( $\sigma$ ) are functions of time  $t$ , have a singularity at  $t = 0$  and

tend to zero for large  $t$ . The expansion scalar and shear scalar diverge at an early stage of the universe and tend to zero for infinitely large values. It is observed that the universe initially evolves with an infinite expansion rate and shows a constant expansion at a later epoch. Also,  $H$  decreases as  $t$  increases (Fig. 14). The Hubble parameter  $H$  approaches zero for infinitely large time. Expansion scalar ( $\theta$ ) also

decreases as  $t$  increases (Fig. 15), but the positive values of Hubble parameter and expansion scalar throughout the evolution show that the universe is expanding gradually. Here, the anisotropy parameter is finite at initial time and is uniform throughout the evolution of the universe.

## 8. Conclusion

We have considered two different hyperbolic forms of Hubble parameter to construct some DE cosmological models of the universe in the framework of  $f(R, T)$  gravity. The space-time considered is the spatially homogeneous anisotropic Bianchi V metric. With the help of the forms of Hubble parameter and Hubble expansion rate along different directions, the anisotropic behaviour of the dark energy-driven cosmological model has been simulated. For case I, energy density is finite, whereas in case II, energy density is infinite for  $t = 0$ . In both cases, energy density is a decreasing function of time and lies in the positive domain. For the first case, the bulk viscous pressure of the universe is an increasing function of cosmic time  $t$ , which begins from a negative value and tends to zero at the present epoch, whereas in the second case, bulk viscous pressure  $\bar{p}$  is an increasing function of time. It begins from a large negative value and tends to zero at the present epoch. In both cases, the model provides an accelerating behaviour of the universe at late time of the evolution. More

or less, the physical behaviour of both models appears to be the same at least at late times. In both cases, the model represents an expanding, shearing and accelerating universe. In both cases, the model has no initial singularity. Since the metric potential of the universe  $A(t)$  and  $B(t)$  are constant at  $t = 0$ , we observed that in both cases, the positive value of the Hubble parameter and the deceleration parameter  $q \rightarrow -1$  for infinite time throughout the evolution show that the universe is expanding and accelerating exponentially. In the first case, there is no initial singularity, whereas in the second case, we have infinite energy density, infinite internal pressure for initial time. This means that our universe has an initial singularity for case II. In the present work, we observed that different DE anisotropic models depend on Hubble parameter. It is concluded that the bulk viscous pressure anisotropy in DE fluid plays a very important and interesting role, so that bulk viscous pressure anisotropy needs to be investigated for further better understanding of the accelerated expansion of the universe.

## Acknowledgements

The author is grateful to the honourable referees and the editor for the illuminating suggestions that have significantly improved this work in terms of research quality and presentation.

## References

- [1] Harko, T., Lobo, F.S.N., Nojiri, S. and Odintsov, S.D., Phys. Rev. D, 84 (2011) 024020.
- [2] Alvarenga, F.G., Houndjo, M.J.S., Monwanou, A.V. and Chabi, J.B., J. Mod. Phys., 04 (2013) 130.
- [3] Kiani, F. and Nozari, K., Phys. Lett. B, 728 (2014) 554.
- [4] Azizi, T., Int. J. Theor. Phys., 52 (2013) 3486.
- [5] Moraes, P.H.R.S., Correa, R.A.C. and Lobato, R.V., JCAP, 2017 (2017) 029.
- [6] Sharif, M. and Zubair, M., Astrophys. Space Sci., 349 (2014) 457.
- [7] Mishra, B., Tarai, S. and Pacif, S.K.J., Int. J. Geom. Mod. Phys., 15 (2018a) 1850036.
- [8] Mishra, B., Tarai, S. and Tripathy, S.K., Ind. J. Phys., 92 (2018b) 1199.
- [9] Troisi, A., Eur. Phys. J. C., 77 (2017) 171.
- [10] Shabani, H., arXiv:1604.04616 [gr-qc] (2016).
- [11] Shabani, H. and Farhoudi, M., Phys. Rev. D., 90 (2014) 044031.
- [12] Zubair, M., Azmat, H. and Noureen, I., Eur. Phys. J. C., 77 (2017) 169.
- [13] Mishra, B. and Vadrevu, S., Astrophys. Space Sci., 362 (2017) 26.
- [14] Mishra, B., Tarai, S. and Tripathy, S.K., Adv. High. Energy Phys., 8543560 (2016) 1.
- [15] Zubair, M. and Hassan, S.M.A., Astrophys. Space Sci., 361 (2016) 149.

- [16] Mishra, B., Tripathy, S.K. and Tarai, S., *Mod. Phys. Lett. A*, 33 (2018)1850052.
- [17] Aktas, C. and Aygun, S., *Chinese J. Phys.*, 55 (2017) 71.
- [18] Shamir, F.M., *Eur. Phys. J. C.*, 75 (2015) 354.
- [19] Chaubey, R. and Shukla, A.K., *Pramana - J. Phys.*, 88 (2017) 65.
- [20] Pawar, D.D., Dagwal, V. and Agrawal, P., *Malaya J. Mat.*, 4 (2016) 111.
- [21] Agrawal, P.K. and Pawar, D.D., *New Astron.*, 54 (2017) 56.
- [22] Agrawal, P.K. and Pawar, D.D., *J. Astrophys. Astron.*, 38 (2017) 2.
- [23] Pawar, D.D., *J. Astrophys. Astr.*, 40 (2019) 13.
- [24] Samanta, G.C., *Int. J. Theor. Phys.*, 52 (2013) 2303.
- [25] Reddy, D.R.K., Santikumar, R. and Naidu, R.L., *Astrophys. Space Sci.*, 342 (2012) 249.
- [26] Reddy, D.R.K., Naidu, R.L. and Satyanarayana, B., *Int. J. Theor. Phys.*, 51 (2012) 3222.
- [27] Reddy, D.R.K., Kumar, R.S. and Kumar, T.V.P., *Int. J. Theor. Phys.*, 52 (2013) 239.
- [28] Ram, S. and Priyanka, *Astrophys. Space Sci.*, 347 (2013) 389.
- [29] Ahmed, N. and Pradhan, A., *IJTP*, 53 (2014) 289.
- [30] Khade, P. and Wasnik, A.P., *IJMER*, 9 (2020) 2277.
- [31] Chakraborty, S., *Gen. Rel. Grav.*, 45 (2013) 2039.
- [32] Houndjo, M.J.S., Batista, C.E.M., Campos, J.P. and Piattella, O.F., *Can. J. Phys.*, 91 (2013) 548.
- [33] Pasqua, A., Chattopadhyay, S. and Khomenkoc, I., *Can. J. Phys.*, 91 (2013) 632.
- [34] Singh, V. and Singh, C.P., *Int. J. Theor. Phys.*, 55 (2016) 1257.
- [35] Baffou, E.H., Kpadonou, A.V., Rodrigues, M.E., Houndjo, M.J.S. and Tossa, J., *Astrophys. Space Sci.*, 356 (2015) 173.
- [36] Santos, A.F. and Ferst, C.J., *Mod. Phys. Lett. A*, 30 (2015) 1550214.
- [37] Noureen, I., Zubair, M., Bhatti, A.A. and Abbas, G., *Eur. Phys. J. C.*, 75 (2015) 323.
- [38] Shamir, M.F., *Eur. Phys. J. C.*, 75 (2015) 354.
- [39] Singh, C.P. and Singh, V., *Gen. Relativ. Grav.*, 46 (2014) 1696.
- [40] Alhamzawi, A. and Alhamzawi, R., *Int. J. Mod. Phys. D*, 35 (2016) 1650020.
- [41] Yousaf, Z., Bamba, K. and Bhatti, M.Z., *Phys. Rev. D*, 93 (2016) 124048.
- [42] Alves, M.E.S., Moraes, P.H.R.S., de Araujo, J.C.N. and Malheiro, M., *Phys. Rev. D*, 94 (2016) 024032.
- [43] Zubair, M., Waheed, S. and Ahmad, Y., *Eur. Phys. J. C.*, 76 (2016) 444.
- [44] Sofuoglu, D., *Astrophys. Space Sci.*, 361 (2016) 12.
- [45] Momeni, D., Moraes, P.H.R.S. and Myrzakulov, R., *Astrophys. Space Sci.*, 361 (2016) 228.
- [46] Das, A., Rahaman, F., Guha, B.K. and Ray, S., *Eur. Phys. J. C.*, 76 (2016) 654.
- [47] Salehi, A. and Aftabi, S., *J. High Energ. Phys.*, 09 (2016) 140.
- [48] Singh, V. and Beesham, A., *Eur. Phys. J. C.*, 78 (2018) 564.
- [49] Srivastava, M. and Singh, C.P., *Astrophys. Space Sci.*, 363 (2018) 117.
- [50] Sharif, M. and Anwar, A., *Astrophys. Space Sci.*, 363 (2018) 123.
- [51] Tiwari, R.K. and Beesham, A., *Astrophys. Space Sci.*, 363 (2018) 234.
- [52] Shabani, H. and Farhoudi, M., *Phys. Rev. D*, 88 (2013) 044048.
- [53] Rajabi, F. and Nozari, K., *Phys. Rev. D*, 96 (2017) 084061.
- [54] Baffou, E.H., Houndjo, M.J.S., Kanfon, D.A. and Salako, I.G., *Phys. Rev. D*, 98 (2018) 124037.
- [55] Lobato, R.V., Carvalho, G.A., Martins, A.G. and Moraes, P.H.R.S., *Eur. Phys. J. Plus*, 134 (2019) 132.
- [56] Tretyakov, P.V., *Eur. Phys. J. C.*, 78 (2018) 896.

- [57] Elizalde, E. and Khurshudyan, M., Phys. Rev. D, 98 (2018) 123525.
- [58] Ordines, T.M. and Carlson, E.D., Phys. Rev. D, 99 (2019) 104052.
- [59] Maurya, S.K. and Tello-Ortiz, F., J. Cosmol. Astropart. Phys., 28 (2019) 1950056.
- [60] Esmaeili, F.M., J. of High Energ. Phys., Gravit. and Cosmo., 4 (2018) 716.
- [61] Setaren, M.R. and Sheyki, A., Int. J. Mod. Phys. D, 19 (2010) 171.
- [62] Ram, S. and Priyanka, K., Cent. Eur. J. Phys., 12 (2014) 744.
- [63] Sahu, S.K., Chin. J. Phys., 55 (2017) 862.
- [64] Sahoo, P.K., Int. J. Geometric Methods in Modern Phys., 4 (2017) 1750097.
- [65] Sahoo, P.K. and Sivakumar, M., Astrophys. Space Sci., 357 (2015) 60.
- [66] Sahoo, P.K., Sahoo, P., Bishi, B.K. and Aygun, S. et al., Mod. Phys. Letter, 32 (2017) 1750105.
- [67] Sahoo, P.K., Can. J. Phys., 2 (2014) 1062.
- [68] Sahoo, P.K., Mishra, B, Sahoo, P. et al., Eur. Phys. J. Puls, 131 (2016) 333.
- [69] Sahoo, P.K., Fortschr. Phys., 64 (2018) 414.
- [70] Pradhan, A., Ahmed, N. and Saha, B., Candian Journal of Physics, 6 (2015) 93.
- [71] Aktas, C. et al., Phys. Lett. B, 707 (2012) 237.
- [72] Yilmaz, I. et al., Gen. Relativ. Gravit., 44 (2012) 9.
- [73] Sharif, M. and Zubair, M., J. Phys. Soc. Jpn., 81 (2012) 114005.
- [74] Sharif, M. and Zubair, M., Astrophys. Space Sci., 349 (2014) 457.
- [75] Saha, B. and Rikhvitsky, V., Physica D, 2 (2006) 219.
- [76] Saha, B. and Rikhvitsky, V., Physica D, 219 (2006) 168.
- [77] Pacif, S.K.J. and Mishra, B., Astrophys. Space Sci., 360 (2015) 48.
- [78] Esmaeili, F. and Mishra, B., J. Astrophys. Astr., 39 (2018) 59.

# Electrical Response of PVC-PMMA Thin Films: A Comprehensive Investigation into the Effects of Frequency, Temperature, and Salicylic Acid Dopant<sup>1</sup>

A.B.More, G.T.Lamdhade, K.B. Raulkar

Department of Physics, Vidya Bharati Mahavidyalaya, C.K Naidu Road, Camp Amravati, M.S. India 444602

DOI: 10.37648/ijps.v16i01.003

Received: 05 July 2023; Accepted: 12 September 2023; Published: 20 September 2023

---

## ABSTRACT

This research delves into the electrical properties of Polyvinyl Chloride (PVC) - Polymethyl Methacrylate (PMMA) Polyblend thin films with a 1:1 weight ratio, investigating the impact of varying salicylic acid (SA) dopant percentages (0%, 2%, 4%, 6%, 8%). Film fabrication employed the isothermal evaporation technique, and AC conductivity measurements were conducted across a frequency range of 25 Hz to 1 MHz at temperatures of 313 K, 323 K, 333 K, 343 K, and 353 K. The primary focus of this study is on the variations in dielectric constant and AC conductivity concerning temperature, frequency, and dopant percentage.

**Keywords:** PVC-PMMA; AC conductivity; Dielectric constant; frequency; salicylic acid

## INTRODUCTION

Polyvinyl Chloride (PVC) and Polymethyl Methacrylate (PMMA) Polyblend thin films have emerged as a subject of considerable interest in materials science due to their versatile properties and potential applications in various fields. The combination of PVC and PMMA, two distinct polymers with contrasting characteristics, offers a unique platform for tailoring the properties of thin films to meet specific requirements. In the realm of polymer blending, the addition of dopants further expands the scope for manipulating the physical and electrical characteristics of these films. This study focuses on PVC-PMMA Polyblend thin films, with particular emphasis on the incorporation of salicylic acid (SA) as a dopant. Salicylic acid is chosen for its potential influence on the electrical properties of the Polyblend, and its incorporation into the polymer matrix is facilitated through the use of Tetrahydrofuran (THF) as a solvent during the thin film preparation process. THF, a common and versatile solvent, plays a crucial role in ensuring the uniform dispersion of the polymers and dopant, leading to well-defined thin films with controlled morphologies. The fabrication of these thin films using the isothermal evaporation technique allows for precise control over the film composition, enabling a systematic exploration of the effects of varying SA dopant concentrations. The electrical properties, particularly the AC conductivity and dielectric constant, are investigated across a range of temperatures and frequencies. Understanding the interplay between temperature, frequency, and dopant concentration is essential for optimizing the performance of these polyblend thin films for potential applications in electronic devices, sensors, and other advanced technologies.

---

<sup>1</sup> How to cite the article:

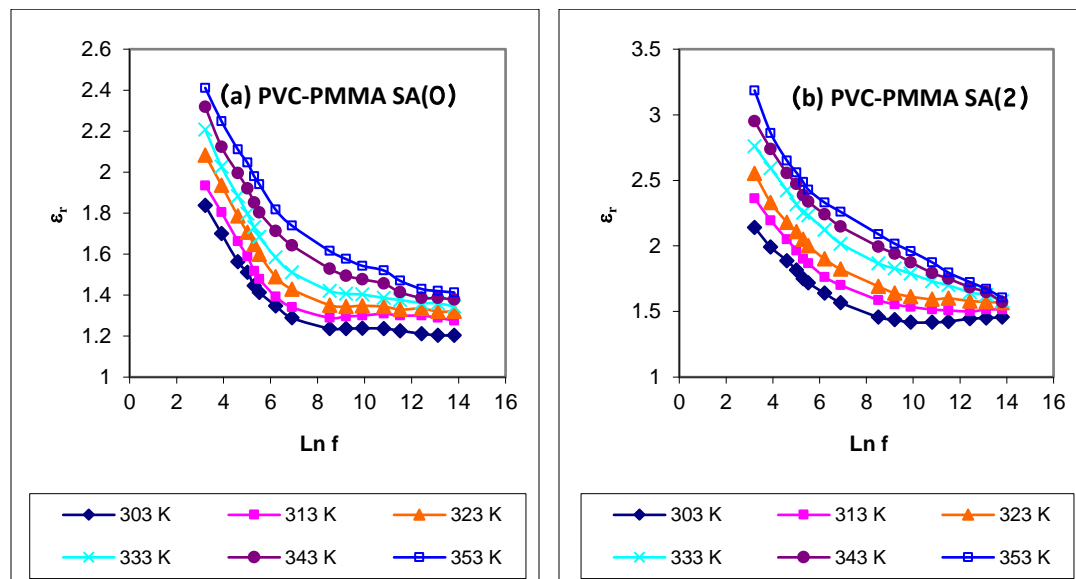
More A.B. Lamdhade G.T.; Jul-Dec 2023; Electrical Response of PVC-PMMA Thin Films: A Comprehensive Investigation into the Effects of Frequency, Temperature, and Salicylic Acid Dopant; *International Journal of Professional Studies*; Vol 16, 40-46; DOI: <http://doi.org/10.37648/ijps.v16i01.003>

Polymer blends and composite materials are widely used in various industrial applications due to their unique properties. Polyvinyl Chloride (PVC) and Polymethyl Methacrylate (PMMA) are two common polymers known for their versatility and widespread applications. In this study, we investigate the effect of salicylic acid (SA) as a dopant on the structural and chemical properties of PVC-PMMA thin films. SA is a compound with a phenolic structure, and its introduction into the polymer matrix may lead to changes in film properties, making it an interesting area of study.

**EXPERIMENTAL**

Thin films of PVC-PMMA with different dopant concentrations were prepared using the isothermal evaporation technique. Preparation of a Polyblend thin film of PVC-PMMA in 1:1 weight proportional, the dopant and the polymer mixture were dissolved in a solvent (THF) were mixed in solution form .for a complete Homogeneous solution was kept for two or three days. after two or three days solution are in a homogeneous form then the solution mixture was poured onto a perfectly planed glass plate floating freely in a pool of mercury for perfect levelling .it was thereafter allowed to evaporate at room temperature further, and it was dried for 2 days to remove any traces of solvent. the dry film removes from the glass plate and cuts into pieces of desired size then measure the thickness of the thin film by DIGMATIC micrometer, which was then coated on two sides with silver paint then by using the multimeter check whether the two electrodes working or not .then investigate the conductivity .Two sets of films were fabricated: one without salicylic acid (0% dopant) and the other with 2%,4%,6%, 8% salicylic acid as the dopant. AC conductivity measurements were performed using an LCR meter, covering a frequency range of 20 Hz to 1 MHz. The measurements were carried out at five different temperatures 313 K, 323 K, 333 K, 343 K, and 353 K.

**GRAPH RELATED FOR DIELECTRIC CONSTANT AND AC CONDUCTIVITY**



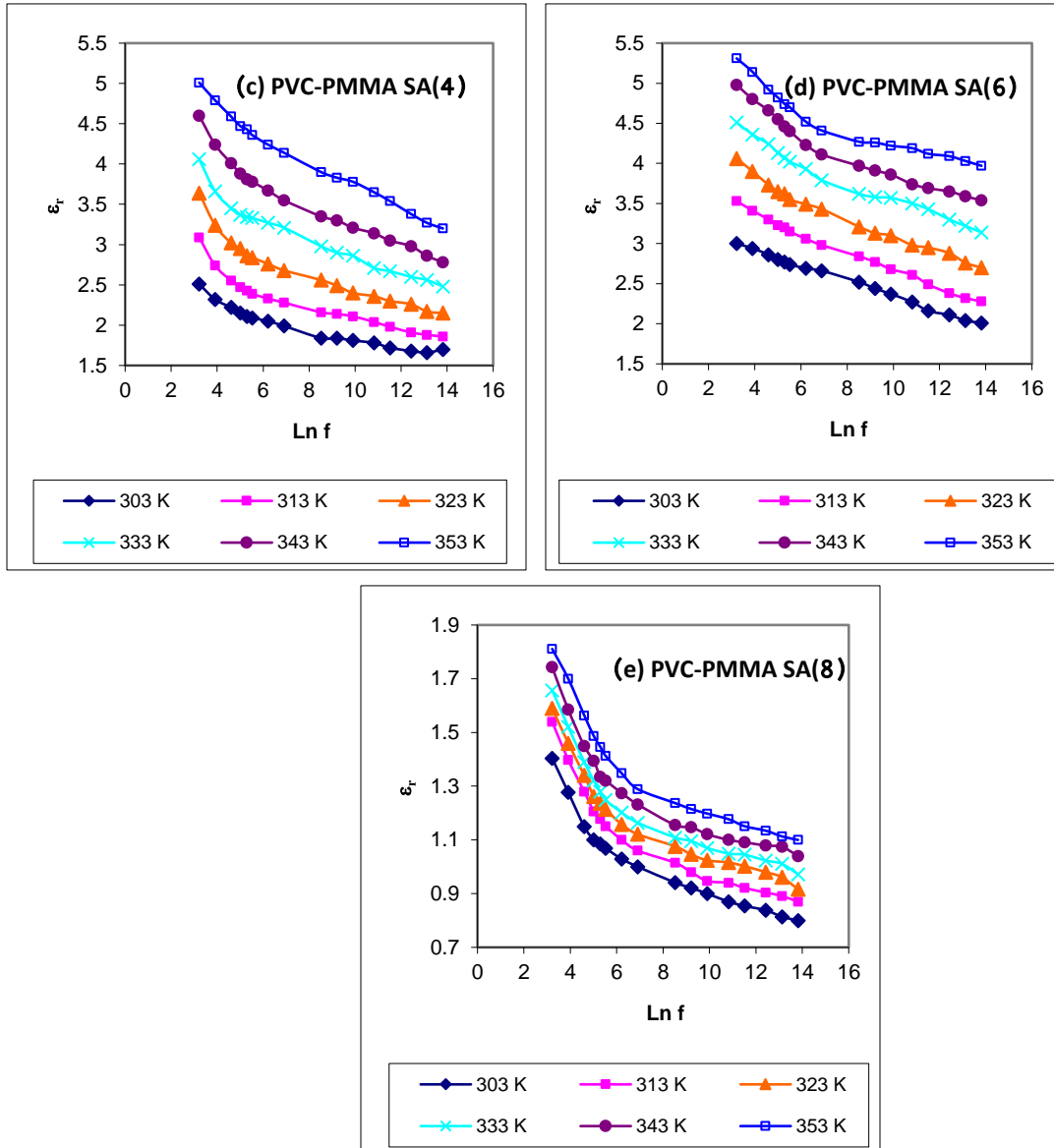
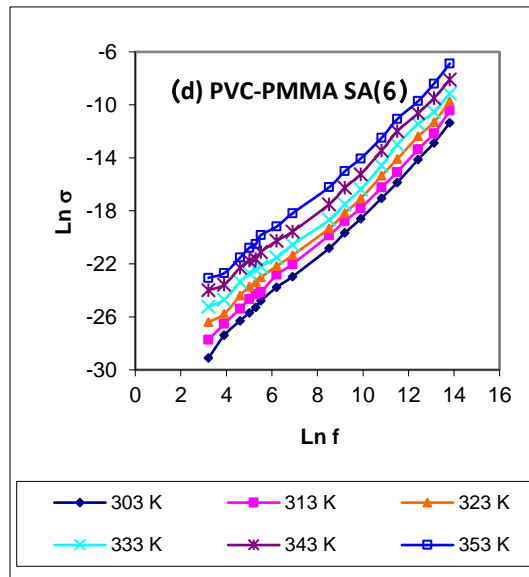
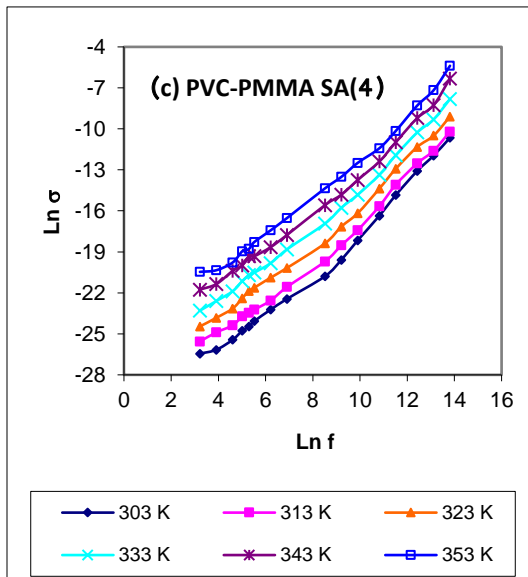
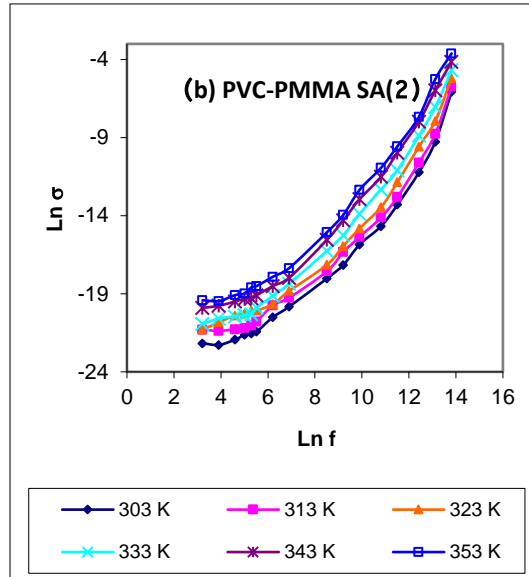
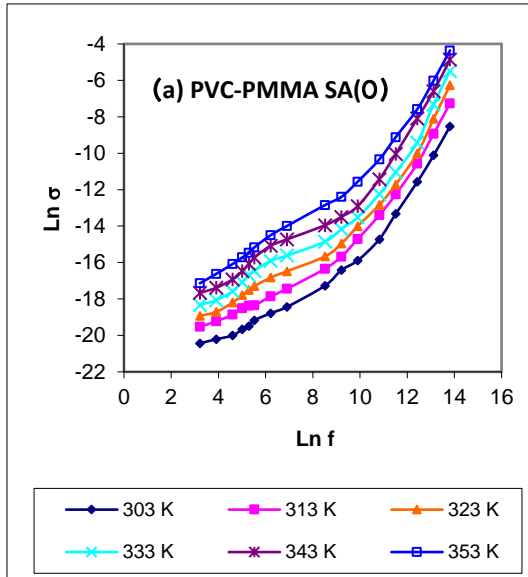
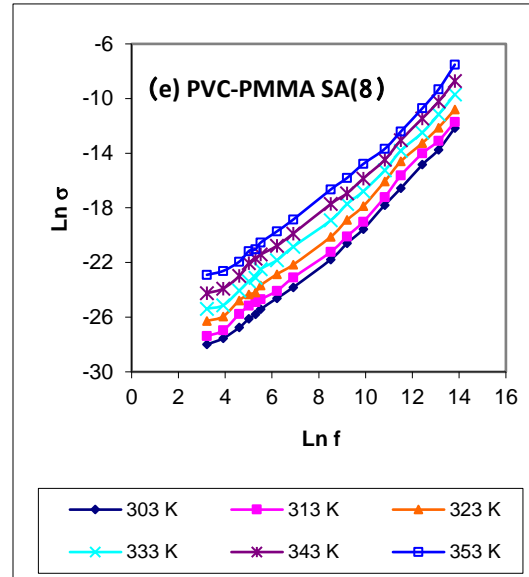


Figure 1.1 (a-e): Variation of  $\epsilon''$  with  $\ln f$  at different temperatures for 1:1 PVC-PMMA doped with different wt% of SA







**Figure 1.2 (a-e): Variation of  $\text{Ln } \sigma$  with  $\text{Ln } f$  at different temperatures for 1:1 PVC-PMMA doped with different wt% of SA**

## RESULTS AND DISCUSSION

In this section, we examine the behavior of PVC-PMMA thin films with and without a dopant (Salicylic Acid) with respect to alternating current (AC) conductivity and dielectric constant. We observe how these properties are influenced by frequency, temperature and dopant.

At constant temperature, Dielectric Constant decreases the increase of frequency

At constant temperature, Dielectric constant increases with the percentage of dopant and then decreases

At constant temperature, AC conductivity ( $\sigma_{ac}$ ) increases with increase in frequency

At constant frequency, AC Conductivity ( $\sigma_{ac}$ ) very marginally increases with the increase of temperature

At constant frequency, AC conductivity ( $\sigma_{ac}$ ) gradually decreases with the increase in the dopant percentage

In our study, we observed a decrease in the dielectric constant of our samples as the frequency increased Fig 1.1(a-e) this can be explained by considering the polarization and polarizability of the dielectric samples. In practical scenarios, a dielectric faces an alternating current (AC) field, changing its direction over time. The ability of dipoles to align with the field during each alternation affects the total polarization. The relative permittivity, measuring polarization, behaves differently at various frequencies. When a dielectric is placed in an electric field between capacitor plates, polarization occurs. This polarization aligns polar species with the applied field and alters the distribution of electric charges in the dielectric. Under a static or low-frequency AC field, the net polarization involves electronic, atomic, and orientation polarization. However, at higher frequencies, the orientation polarization struggles to keep up with field variations, causing a decrease in dielectric constant.

**Effect of Frequency on AC Conductivity** We observed an increase in AC conductivity ( $\sigma_{ac}$ ) with higher frequencies at various constant temperatures in Fig 1.2(a-e). Let's break down why this happens: Imagine you have a capacitor with a dielectric material. When this capacitor is charged under an alternating current (AC) voltage or electric field described by  $E = E \cos \omega t$ , certain phenomena come into play. These include ohmic resistance, impedance, heat absorption, and the Debye relaxation process, all contributing to the frictional resistance within the system. In simpler terms, as the AC voltage is applied, a loss current occurs due to these factors. This loss current is essentially the movement of charge carriers experiencing resistance and undergoing processes like Debye relaxation, resulting in a

conversion of electrical energy into heat. In summary, the increase in AC conductivity with frequency is a consequence of the capacitor's response to the changing electric field, leading to higher loss currents and enhanced conductivity.

Effect of Dopant (SA) on Dielectric Constant The dielectric constant of samples gets increased with increase in dopant percentage. If we again increase dopant percentage then dielectric constant decreases. Effect of Dopant (SA) on AC Conductivity AC conductivity gets decreased with increase in dopant percentage. As the salicylic acid is least interested in making any kind of association with PVC-PMMA blend, its presence becomes unnecessary. This stranger particle may exert its overshadowing impact on the functional sites of the poly-blends. This may be the reason for decrease in conductivity with increase in dopant percentage.

## CONCLUSION

The observed trends highlight the complex interplay of frequency, temperature, and dopant concentration on the electrical properties of PVC-PMMA thin films. These findings contribute valuable insights for applications involving dielectric materials, providing a foundation for further exploration and optimization of these materials in various technological contexts. Understanding these behaviors is crucial for the development of advanced electronic devices and materials with tailored electrical characteristics.

## REFERENCES

1. Deshmukh, S. H., Burghate, D. K., Akhare, V. P., Deogaonkar, V. S., Deshmukh, P. T., & Deshmukh, M. S. (2007). *Bull. Mater. Sci.*, 30(1), 51–56. doi.org/10.1007/s12034-007-0009-6
2. Belsare, N. G., Wadatkar, A. S., Joat, R. V., Wasnik, T. S., Raghuvanshi, F. C., Raulkar, K. B., & Lamdhade, G. T. (2011). *Journal of Electron Devices*, 11, 583-587.
3. Fahmy, T., & Elzanaty, H. (2019). *Bull. Mater. Sci.*, 42, 220. doi.org/10.1007/s12034-019-1906-1
4. Dakre, A. B., & Lamdhade, G. T. (2014). *International Journal of Science and Research (IJSR)*, 3(6).
5. Ojha, P., Siddaiah, T., Gopal, N. O., & Ramu, Ch. (2018). *International Journal of Scientific Research in Physics 022222222 and Applied Sciences*, 6(6), 80-87. doi.org/10.26438/ijrps/v6i6.8087
6. Tanwar, A., Gupta, K. K., Singh, P. J., & Vijay, Y. K. (2006). *Bull. Mater. Sci.*, 29(4), 397–401. doi.org/10.1007/bf02704142
7. Vidhale S.G., Belsare N.G., A.S.Wadatkar, September-(2013), *International Journal of Scientific & Engineering Research*, Volume 4, Issue 9.
8. Vdhale, S.G., N. G. Belsare, November(2013), *International Journal of Scientific & Engineering Research*, Volume4, Issue11, 1253, doi.org/10.14299/ijser.2013.11
9. R. V. Waghmare, Belsare N.G, Raghuvanshi F C and Shilaskar S N, April (2007), *Bull. Mater. Sci.*, Vol. 30, No. 2, pp. 167–172., doi.org/10.1007/s12034-007-0030-9
10. R Padma Suvarna, K Raghavendra Rao and K Subbarangaiah, (2002), *Bull. Mater. Sci.*, Vol. 25, No. 7, pp. 647–651.
11. Shukla, J. P., & Gupta, M. (1987). *Indian Journal Pure and Applied Physics*, 25, 242-244.
12. Dandel, R. M., Belsare, N. G., & Raghuvanshi, F. C. (2011). *International Journal of Polymers and Technologies*, 3(2).
13. Ramesh, S., & Liew, C. W. (2013). *Measurement*, 46(5), 1650-1656. doi.org/10.1016/j.measurement.2013.01.003.
14. Wadatkar, A. S., Wasnik, T. S., Vidhale, S. G., & Belsare, N. G. (2014). *International Journal of Basic and Applied Research*, 4, 196-200.
15. Ahmad, A. H. (2014). *International Journal of Computer Science*, 2, 20-23.
16. Bushra, A. H., Ahmad, A. H., & Duaa, A. U. (2013). *International Journal of Application or Innovation in Engineering & Management*, 2(11), 86.
17. Khaled, M. A., Elwa, Y. A., Hussein, A. M., & Abdullah, K. (2003). *Egypt Journal*, 26(1), 83-91.
18. Sharma, D., & Tripathi, D. (2018). *AIP Conference Proceedings*, 1953(1), 050056. doi.org/10.1063/1.5032711
19. V. P. Akhare, (2013), *Acta Ciencia Indica*, Vol. XXXIX P, No. 2, 79
20. Patil Shatala. D. (2007) *Mater Sc.*, 2, 89-92
21. Joseph Jenifer, Deshmukh, Kalim, Chidambaram, K., Faisal, Muhammad, Selvarajan, E. Sadasivuni, Kishor Kumar, Ahamed, M. Basheer, Pasha, S. K. Khadheer, (2018), *Journal of Materials Science: Materials in Electronics* 29:20172–20188, doi.org/10.1007/s10854-018-0150-6
22. Adel M. El Sayed, (2020), *Results in Physics*, doi.org/10.1016/j.rinp.2020.103025

23. Suresh S.S Mohanty. S., Nayak. S.K. (2017) J. Clean. Product. 149 863-873.
24. Alghunaim N.S., Results in Physics, 2015,vol 5,331-336,doi.org/10.1016/j.rin p.2015.11.003
25. Mohammad Saleem , Raina Aman Qazi and Mian Said Wahid , (2008), African Journal of Pure and Applied Chemistry Vol. 2 (4), pp. 041-045
26. S.K. Mahto, S. Das, A. Ranjan, S.K. Singh, P. Roy, N. Misra, (2015),RSC Adv. 5, 45231–45238
27. Vijayakumaria .G., Selvakumara .N., Jeyasubramaniana .K. , Malab. R., ( 2013 ) , Physics Procedia ,49 67 – 78
28. S. Ramesh, Leen K.H., Kumutha .K, Arof A.K., (2007), Spectrochim. Acta Part A Mol. Biomol. Spectrosc. 66, 1237–1242
29. Fahmy T and Elzanaty Hesham, Sci. (2019), Bull. Mater. 42:220,1-7, <https://doi.org/10.1007/s12034-019-1906-1>
30. Rajendran S and T Uma, (2000), J.Power Sources 88,282
31. Rajendran S and T Uma, (2000),Matter Lett.44,242-248
32. Cyprian yameso Abasi, Donbebe wankasi and Ezekiel Dixon Dikio, (2018), Asian journal of chemistry, vol 30(4),859-867,doi.org/10.14233/ajchem.201821112.
33. Yongseok Kim, Sangdo Park, Young-Soo Seo, Naesung Lee and Yongho Seo., (2009), Journal of the Korean Physical Society, Vol. 54, No. 2, 749-753
34. S Rajendran., Prabhu M.R., Rani M.U., (2008), Int. J. Electrochem. Sci., 3, 282- 290
35. Rao Vijayalakshmi, Ashogkan P V and Shridhar M H, (2000), Mater Sci. and Engg. Elsevier A 281, 213-220,
36. Akram Muhammad, Athar Javed and Tasneem Zaher Rizvi, (2005), Turk J. Phys. 29, 355-62.
37. Reda S M, Dyes and Pigments (2006), Elsevier, 75, 526-532.
38. Ranga Raja MR, Choudhary RN P and Ram S, (2003),Phys Status Solid B 239, 2, 480.

# Nanocrystalline Titanium Dioxide Dipped with $AlCl_3$ as a Humidity Sensors<sup>1</sup>

**R B Butley, R V Joat, G T Lamdhade, K B Raulkar, A O Chauhan**

*Department of Physics, Vidya Bharati Mahavidyalaya, Amravati(M.S.), India*

DOI:10.37648/ijrst.v13i01.004

Received: 31 December 2022; Accepted: 07 February 2023; Published: 17 February 2023

## ABSTRACT

Titanium dioxide and  $AlCl_3$  was mixed in different stoichiometry in mol wt. % for the study. By using the screen printing technique, the thick films of humidity sensors are prepared. All of the humidity sensor devices are tested and finally concluded that the sample T-1 at constant temperature 400C to 700C exhibited high sensitivity and fast response time to humidity sensing at room temperature. In the case of conductivity, curves are frequently crowded and mixed together. The conductivity of Sample films linearly responds to Relative Humidity. The resistance of thick films decreases by increasing the humidity of sensors at room temperatures due to surface oxygen vacancies of  $TiO_2$  acting as electron donors.

**Keywords:** *Thick films;  $TiO_2-AlCl_3$ ; Sensitivity; Humidity sensors*

## INTRODUCTION

These humidity chambers are designed to maintain temperature and relative humidity at set points controllable by the operator at the front panel.[1-4] Air is constantly being circulated through the chamber, scheduled for comparison to set points. Heat is produced by electric resistance heaters that turn off and on for temperature control. On units with cooling there is a refrigeration unit continuously on. Chamber humidification is reached by means of a low-pressure vapor generator injecting water vapor into the chamber through a small orifice. The water vapor is reached into the chamber at the blower discharge. Chambers were programmable, and networked or Web- enabled test chambers are also available. In the present study is to synthesize and structural characterization of  $TiO_2$  nanoparticles by using liquid phase method with effectively more surface area in short reaction time at room temperature and this method is the simplest, cost effective, eco-friendly method. It is also probed for its effect on nanocrystalline size structure via XRD studies of  $TiO_2$  nanoparticles.[5-9]

## EXPERIMENTAL METHOS:

All the chemicals used in this present work were of GR grade purchased from Sd-fine chemicals, India having purity 99.99%. $TiO_2$  nanoparticles are synthesised by sol-gel method. The synthesis of  $TiO_2$  nanoparticles is divided into various steps, such as mixing, stirring, filtering, drying and calcination. Finally by the calcinating the powder at 400 °C for 3 hours, the  $TiO_2$  is obtained in the nanoparticles form.

Screen printing is a technique in which a mesh is used to transfer ink onto a substrate, except in areas made impermeable to the ink by a blocking stencil. A material or gel which is formed is moved across the screen to fill the open mesh apertures with ink, and vice versa then causes the screen to touch the substrate momentarily along a line of contact. This causes the material to wet the substrate and be pulled out of the mesh apertures as the screen springs back after the blade has passed. In the similar way, instead of ink we use paste of nanomaterial and glass slides as substrate.

<sup>1</sup> How to cite the article: Butley R.B., Joat R.V., Lamdhade G.T., Raulkar K.B., Chauhan A.O., Nanocrystalline Titanium Dioxide Dipped with  $AlCl_3$  as a Humidity Sensors, IJRST, Jan-Mar 2023, Vol 13, Issue 1, 23-31, DOI: <http://doi.org/10.37648/ijrst.v13i01.004>

So, we have use here mesh which has permeable stencil area smaller in area than glass slide which we are used. Firstly we take nanomaterial (90%) and in order to make its paste mix with solid binder (10%) known as Ethyl cellulose. When we make a well grind mixture of nanomaterial and solid binder then we add drop by drop liquid binder. We should careful about that liquid binder is added in appropriate quantity. So the perfect thick paste of nanomaterial is prepared. Then we follow the procedure that with the help of squeegee spread paste of permeable mesh for well layered nanomaterial on substrate (Glass slides). As these Titanium dioxide Nanoparticle thick films are prepared, firstly we allow them to dry in the atmosphere. Then they are subjected to the vacuum oven at 80°C for 1 hour. Then we put these thick films at Muffle furnace at 250°C for 3 hours. Now these Thick films are dip in Aluminium Chloride with different dipping time [10-12].

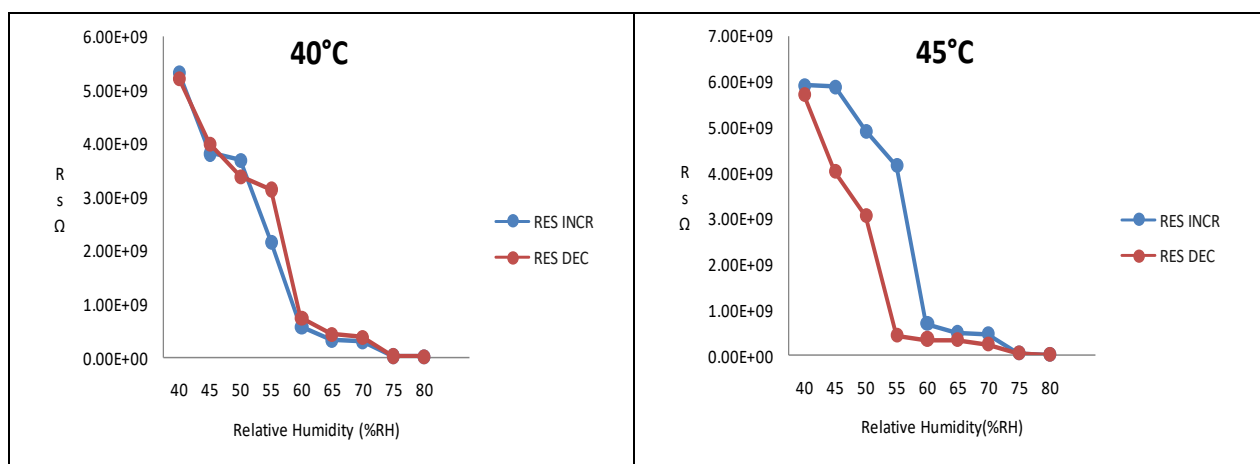
The main compound of aluminium chloride (AlCl<sub>3</sub>) is aluminium and chlorine. The compound is regularly cited as a Lewis acid. In the dipping method, we have used Aluminium chloride for the dipping method. As we prepared solution of AlCl<sub>3</sub> then we dipped the thick film of Titanium dioxide for different time parameters. We take 1, 2, 3 minutes dipping and after firing these slides for 1 hour at 250°C finally the three thick films slides for different dipping time is prepared and one thick film taken for pure.

Humidity is a quantity representing the amount of water vapour in the atmosphere or in a gas. The level of comfort is determined by a combination of two factors namely relative humidity and ambient temperature. Humidity measurement is an important factor for operating certain equipment. A rule of thumb is to assure a relative humidity near 50% RH at normal room temperature (20–25°C). This may vary from a low as 40% RH for the clean rooms to 60% RH in hospital operating rooms. By the use of hygrometers humidity can be measured. The first hygrometer was invented by Sir John Leslie. Humidity measurement is an important quantity for predicting the climate outdoors as well as controlling the climate indoors. [13-18]

**RESULTS AND DISCUSSION:**

**Hysteresis:**

The phenomenon in which the value of a physical property lags behind changes in effect causing is known as Hysteresis. In our present work, humidity sensing with TiO<sub>2</sub> nonmaterial thick films shows the hysteresis plot of sample T-1, T-2,T-3,T-0 at constant temperature 40°C. Hysteresis plot shows variation between resistance of sample with respect to relative humidity in increasing and decreasing order of 40 to 80 % RH and 80 to 40 %RH in steps of 5 % RH. The resistance measurement was done with Keithley 2400 source meter at different constant temperature 40°C to 70°C in steps of 10<sup>0</sup>C.



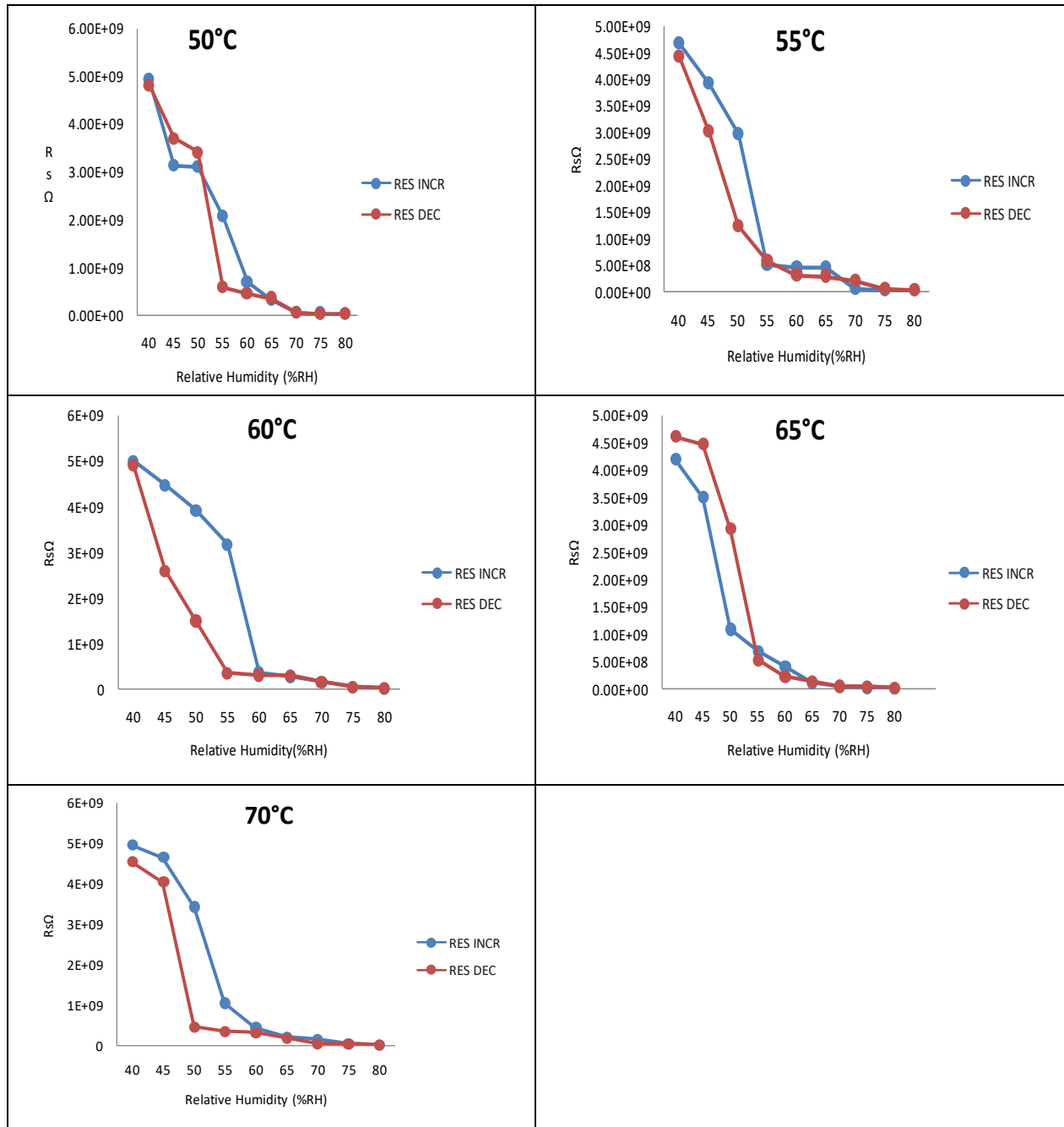


Figure 1.1 T-1 Metal oxide Thick Film (1-minute) hysteresis plot

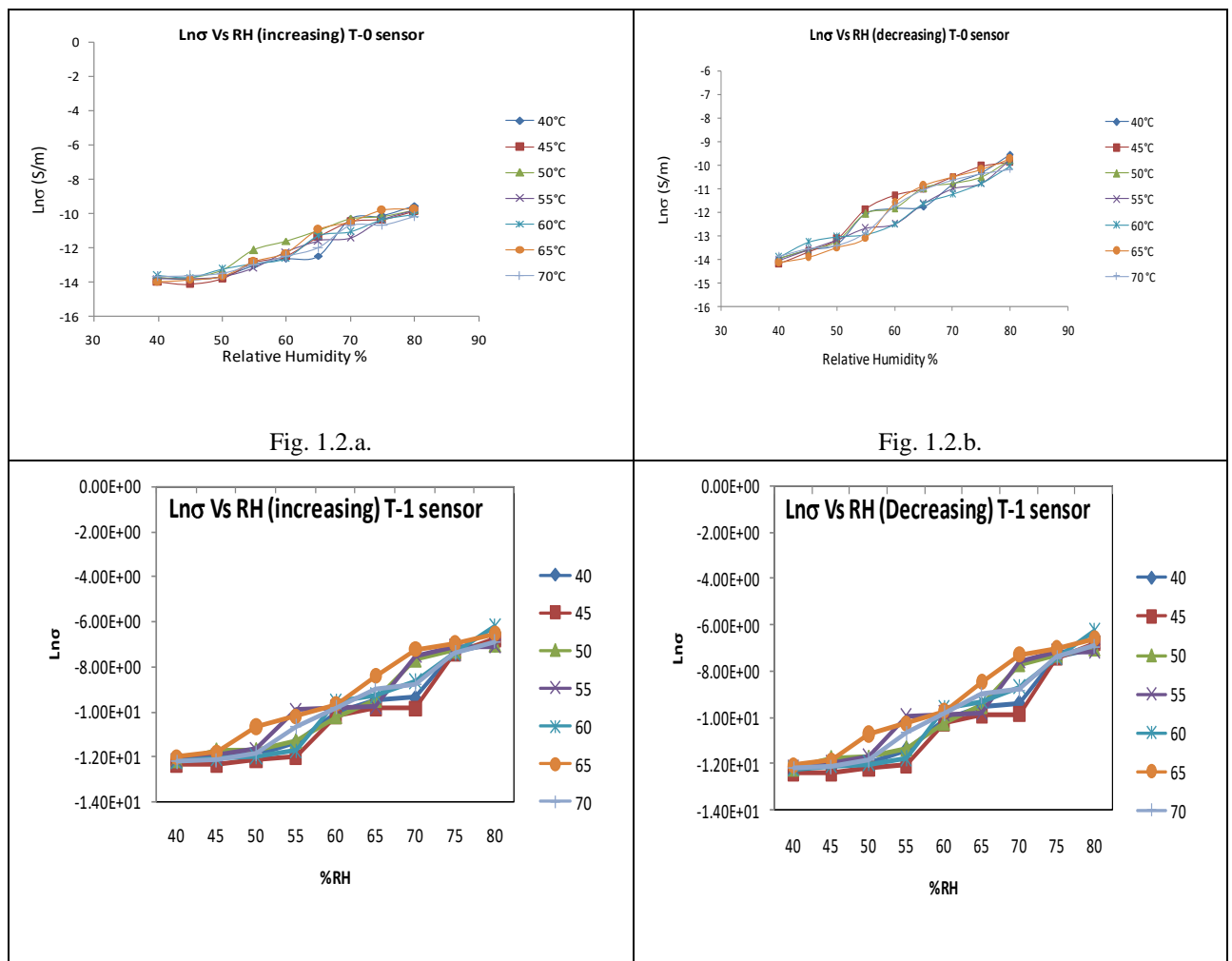
Similarly, we can plot the graphs for remaining samples. In present work it is observed that from hysteresis plot series of a sample which is TiO<sub>2</sub> nanomaterial film T-1, T-2, T-3 dipped in Aluminium Chloride for different dipping time i.e. for 1, 2 and 3 minutes respectively and hysteresis plot of pure sample of TiO<sub>2</sub> nanoparticle film at respective constant temperature. From hysteresis plot, it is clearly seen that there is very small hysteresis is present during forward (increasing) and reverse (decreasing) cycle of RH. It is observed that there is very significant average change was observed in value of resistance of sample in the range of 10<sup>10</sup> to 10<sup>8</sup>Ω.m. From 40 to 80 % RH except in the sample T-1 (1 minutes) change in the value of resistance from 10<sup>9</sup> to 10<sup>7</sup>Ω.m. There is a noticeable change in the value of resistance of sample T-1 at constant temperature 40°C to 70°C.

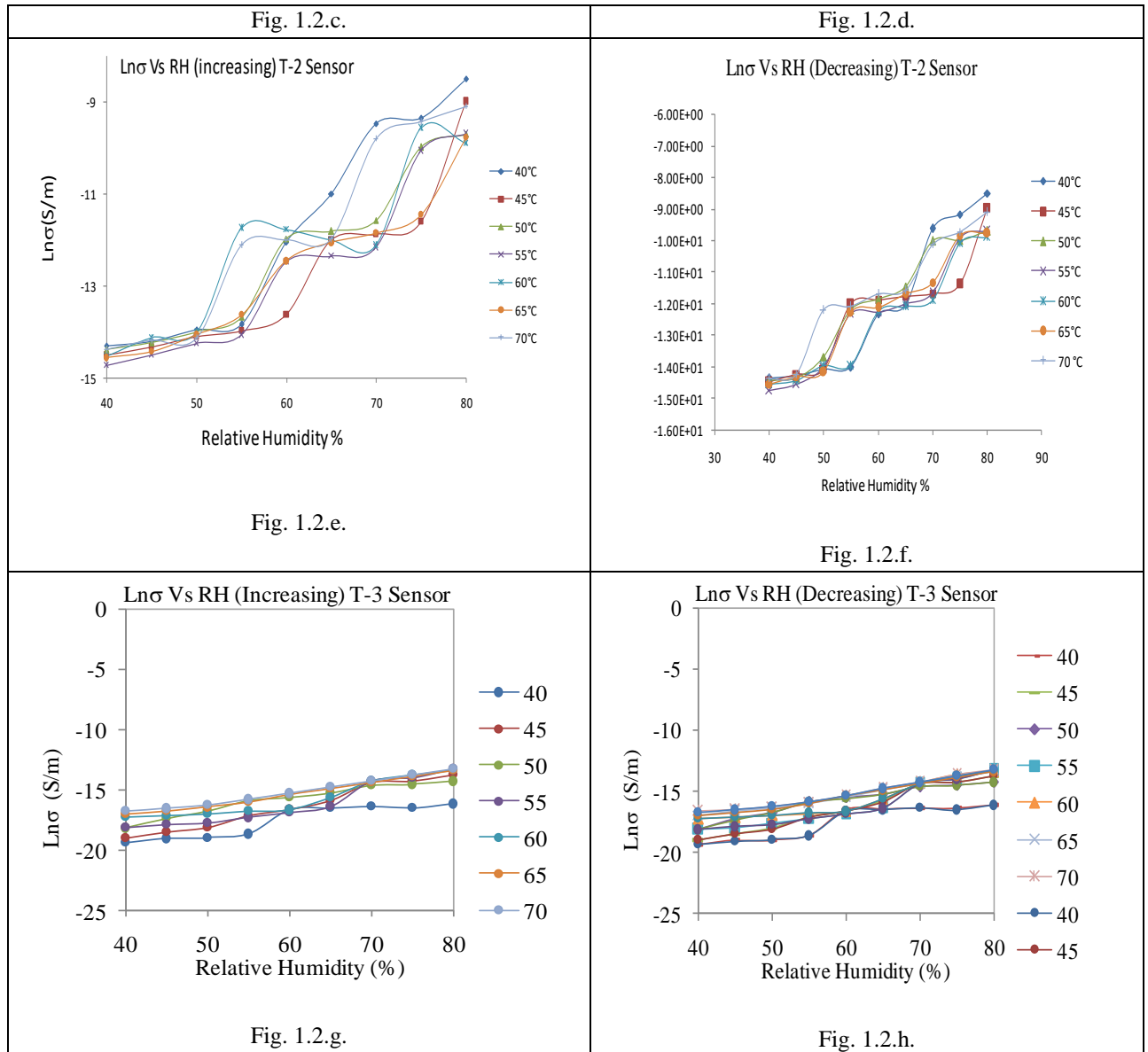
Table 1.1 Sample Codes

Sr. No.	Sample	Thickness $\times 10^{-6}$ m	Material
1.	T-0	24	Pure $\text{TiO}_2$
2.	T-1	18	$\text{TiO}_2$ +Dipped with $\text{AlCl}_3$ for 1 minutes dipping and after firing these slides for 1 hour at $250^\circ\text{C}$ .
3.	T-2	19	$\text{TiO}_2$ +Dipped with $\text{AlCl}_3$ for 2 minutes dipping and after firing these slides for 1 hour at $250^\circ\text{C}$ .
4.	T-3	20	$\text{TiO}_2$ +Dipped with $\text{AlCl}_3$ for 3 minutes dipping and after firing these slides for 1 hour at $250^\circ\text{C}$ .

The hysteresis was observed because of the process of adsorption and de-adsorption are not so faster at particular humidity. As the adsorption would not be efficient which causes small change in the value of resistance, the physisorbed water molecules is converted into chemisorbed by donating the surface electron at the constant temperature and for de-adsorption it requires large activation energy. As we observed that on the other hand sample shows the comparable decrease in resistance with increase in % RH which indicates that conduction occurs grain surface by release of electron from water molecule. Hence, the sample as shows the noticeable change in resistance between the values in between humidity range 40 -80 % RH. [19-20]

DC Conductivity



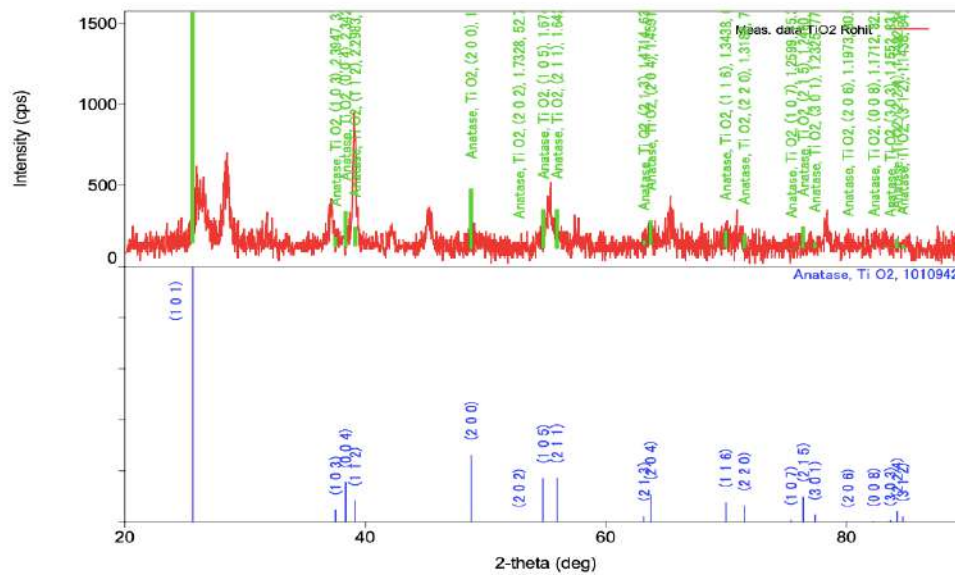


**Fig. 1.2** Variation (a-d)  $\text{Ln}\sigma$  Vs RH at different constant temperature (40°C to 80°C)

The variation of  $\text{Ln}\sigma$  with increasing and decreasing (40 to 80 % RH and 80 to 40 % RH) of the series sample. Respectively at constant temperature 40°C to 70°C. It is observed that the conductivity increases partially linearly with relative humidity from 40 to 80 % RH and vice-versa. When the temperature of sample T-1 increases, the conductivity also increases. In all the series of sample, the conductivity found to be lowest at temperature 40°C, while it is highest at high temperatures.[21-22]



**XRD OF TITANIUM DIOXIDE**



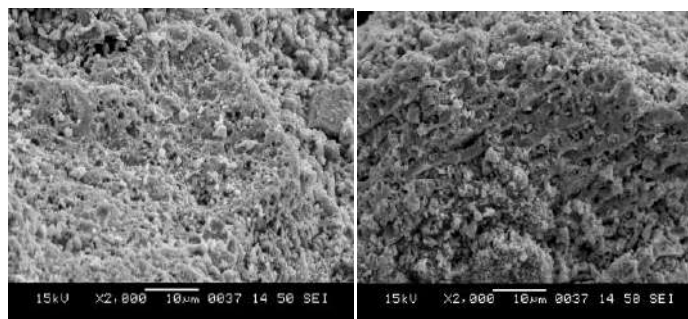
**Fig. 1.3 XRD pattern of Periclase Titanium dioxide (TiO<sub>2</sub>)**

The XRD pattern of Periclase Titanium dioxide (TiO<sub>2</sub>) nanostructure synthesized by liquid phase via co-precipitation method calcinated at 300°C. It is clearly observed that the highest intensity peak is obtained at (200) crystal planes and other peaks lying at (101), (004), (200), (105) and (211) of TiO<sub>2</sub>.The (200) is observed as intense and sharp peak. Periclase phase in diffraction pattern exactly matches with JCPDS card no. 21-1272. All the peaks are perfectly match with Pericles TiO<sub>2</sub> nanostructure, which indicates that Periclase TiO<sub>2</sub> nanoparticles obtained. The average crystalline size was found to be 39.69 nm calculated by using Debye-Scherer formula. Debye Scherer formula as follows,

$$D = K\lambda / \beta \cdot \text{Cos}\theta$$

Where, D is crystalline size, λ is wavelength of X-ray, β is Full Width Half Maxima, θ is Diffraction angle, K is constant closed to unity.[23]

**SEM PICTURES:**



SEM pictures of TiO<sub>2</sub> at 2000 magnification

The FE-SEM morphology of nanocomposites shows the particles are nanoporous, small size, like spherical shape. One can see that nanocrystalline and porous TiO<sub>2</sub>, is formed on the surface. The Prepared sample shows agglomerated in nature. Grains exhibit a variety of sizes and forms, as well as a nanometer-scale order and a nanoporous structure. Because of the nano capillary pore and the structure's huge surface area, the adsorption and condensation of water molecules are anticipated to be made easier. Due to this porosity, humidity can be responded to and recovered from effectively.

## CONCLUSIONS

The study of humidity sensors has led to novel sensing mechanism that can exploited in a different condition. It is observed that there is very significant average change was observed in value of resistance of the sample in the range of 10<sup>10</sup> to 10<sup>8</sup> ohm. There is noticeable change in the value of resistance of sample T-1 at constant temperature 40°C to 70°C. In the case of conductivity, curves are frequently crowded and mixed together. Conductivity of Sample films linearly responds to Relative Humidity. The Sample films shows the appreciable results regarded with Humidity Sensing. All the peaks are perfectly match with Periclase TiO<sub>2</sub> nanostructure, which indicates that Periclase TiO<sub>2</sub> nanoparticles obtained. No other peaks were detected in spectrum within detection limit of XRD instrument, indicating the pure periclase TiO<sub>2</sub> Nanomaterial is synthesized [19-25].

## ACKNOWLEDGEMENT:

One of the authors Rohit B Butley is very much thankful to Vidya Bharati Mahavidyalaya Amravati, India for providing the XRD facility.

**Financial support and sponsorship:** Nil

**Conflict of Interest:** None

## REFERENCES

1. Sarita Sharma, (2016) Synthesis and characterization of ZnO based nanomaterials, *Shodhganga*, <http://hdl.handle.net/10603/293636>.
2. Carlo Cantalini and Mario Pelino, Dipartimento di Chimica, Ingegneria Chimica e Materiali, (1992) Universit; de L'Aquila, L'Aquila, *Italy J. Am. Ceram. Soc.*, 75 [3] 546-51. doi : 10.1111/j.1151-2916.1992.tb07840.x .
3. Richa Srivastava and B. C. Yadav (2012) Nanostructured ZnO, ZnO-TiO<sub>2</sub> And ZnO-Nb<sub>2</sub>O<sub>5</sub> As Solid State Humidity Sensor, *Advanced Materials Letters*, Vol.3, Issue3, doi: 10.5185/amlett.2012.4330.
4. N. K. Pandey, Karunesh Tiwari, and Akash Roy, (2011) Moisture Sensing Application of Cu<sub>2</sub>O Doped ZnO Nanocomposites *IEEE Sensors Journal*, VOL. 11, NO. 9, doi: 10.1109/JSEN.2011.2112764, SEPTEMBER.
5. Y Shimizu, H Arai and T Seiyama (1985) Theoretical studies on the impedance-humidity characteristics of ceramic humidity sensors, *Elsevier*, Volume 7, Issue 1, March 1985, Pages 11-22 doi.: 1016/0250-6874(85)87002-5
6. B.C. Yadav, Richa Srivastava & C.D. Dwivedi (2008) Synthesis and characterization of ZnO–TiO<sub>2</sub> nanocomposite and its application as a humidity sensor, *Philosophical magazine*, Vol.88, 2008 Issue 7, doi. /10.1080/14786430802064642.
7. D.G. Yarkin, (2003) Impedance of humidity sensitive metal/porous silicon/n-Si structures Sensors and Actuators, *Elsevier*, Volume 107, Issue 1, 1 October 2003, Pages 1-6 ,doi:10.1016/S0924-4247(03)00231-0.

8. Vijay K. Tomer, Ritu Malik, Vandna Chaudhary Arabinda Baruah and Lorenz Kienle, (2019) Noble Metals Metal Oxide Mesoporous Nano hybrids in Humidity and Gas Sensing Applications doi. /10.1016/B978-0-12-814134-2.00014-0 .
9. Hamid Farahani, Rahman WagiranandMohd Nizar Hamidon (2014) Humidity Sensors Principle, Mechanism, and Fabrication Technologies: A Comprehensive Review *Sensors*, 14, 7881-7939; doi:10.3390/s140507881 .
10. Raid A. Ismail,\*Ala Al-Naimi, and Alaa A. Al-Ani , (2006) Preparation and characteristics study of ZnO: (Al, Cu, I) thin films by chemical spray pyrolysis *e-J. Surf. Sci. Nanotech.* Vol. 4 636-639 doi:10.1380/ejsnt.2006.636.
11. Wensheng Wang, Anil V. Virkar , (2004) A conductimetric humidity sensor based on proton conducting perovskite oxides, *sensors and Actuators, B* 98, 282–290, doi:10.1016/j.snb.2003.10.035.
12. Vijay K. Tomer, Surender Duhan, Parag V. Adhyapak, and Imtiaz S. Mulla (2014) Mn-Loaded Mesoporous Silica Nanocomposite: A Highly Efficient Humidity Sensor *J. Am. Ceram. Soc.*, 1–7 ,doi: 10.1111/jace.13383.
13. Nor Diyana Md Sin, Mohd Firdaus Malek, Mohamad Hafiz Mamat, Mohamad Rusop Bin Mahmood, (2014) *International Journal of Materials Engineering Innovation*, Volume 5, Issue 2, doi: 10.1504/IJMATEI.2014.060343.
14. Macagnano, V. Perri, E. Zampetti, A. Bearzotti, F. De Cesare,( 2016) Humidity effects on a novel eco-friendly chemosensor based on electrospun PANi/PHB nanofibres *Sensors and Actuators B: Chemical*, Volume 232, 16-27, doi.10.1016/j.snb.2016.03.055 .
15. Yuan Liu, Hui Huang, Lingling Wang, Daoping Cai, Bin Liu, Dandan Wang, Qihong Li, Taihong Wang, (2016) *Sensors and Actuators B: Chemical*, Volume 223 , 730-737. doi.10.1016/j.snb.2015.09.148.
16. Mohamad Izzat Azmer, Zubair Ahmad, Khaulah Sulaiman, Abdullah G. Al-Sehemi, (2015) Humidity dependent electrical properties of an organic material DMBHPET *Sensors and Actuators B: Chemical* 61 , 180-184, doi.10.1016/j.measurement.2014.10.048 .
17. Kyung Hyun Choi, Memoon Sajid, Shahid Aziz, Bong-Su Yang, (2015) *Sensors and Actuators A: Physical*, Volume 228, 40-49, doi. 10.1016/j.sna.2015.03.003 .
18. Yang Li, Kaicheng Fan, Huitao Ban, Mujie Yang, (2016) *Sensors and Actuators B: Chemical*, Volume 222, 151-15, doi. 10.1016/j.sna.2015.03.003.
19. Yuan Liu, Hui Huang, Lingling Wang, Daoping Cai, Bin Liu, Dandan Wang, Qihong Li, Taihong Wang, ,(2016) *Sensors and Actuators B: Chemical*, Volume 223, 2016, 730-737, doi. 10.1016/j.snb.2015.09.148.
20. Xiuping Han, Binghua Yao, Keying Li Wenjing Zhu, and Xuyuan Zhang (2020) Preparation and Photocatalytic Performances of WO<sub>3</sub>/TiO<sub>2</sub> Composite Nanofibers |Article ID 2390486 | doi.10.1155/2020/2390486.
21. Hao Cheng, Wenkang Zhang, Xinmei Liu, Tingfan Tang, and Jianhua Xiong (2021) Fabrication of Titanium Dioxide/Carbon Fiber (TiO<sub>2</sub>/CF) Composites for Removal of Methylene Blue (MB) from Aqueous Solution with Enhanced Photocatalytic Activity *Research Article*, Article ID 9986158 | doi./10.1155/2021/9986158.
22. Jing Yan, Xiaojuan Li, Bo Jin , Min Zeng, and Rufang Peng, (2020) Synthesis of TiO<sub>2</sub>/Pd and TiO<sub>2</sub>/PdO Hollow Spheres and Their Visible Light Photocatalytic Activity *International Journal of Photoenergy*, Article ID 4539472, 9 pages <https://doi.org/10.1155/2020/4539472> .
23. Tan Lam Nguyen, Viet Dinh Quoc, Thi Lan Nguyen, Thi Thanh Thuy Le, Thanh Khan Dinh, Van Thang Nguyen, and Phi Hung Nguyen, (2021) Visible-Light-Driven SO<sub>4</sub><sup>2-</sup>/TiO<sub>2</sub> Photocatalyst Synthesized from BinhDinh

(Vietnam) Ilmenite Ore for Rhodamine B Degradation Article ID 8873181, <https://doi.org/10.1155/2021/8873181>

24. Buzuayehu Abebe , H. C. Ananda Murthy, and Enyew Amare Zereffa, (2020), Synthesis and Characterization of PVA-Assisted Metal Oxide Nanomaterials: Surface Area, Porosity, and Electrochemical Property Improvement Article ID 6532835, <https://doi.org/10.1155/2020/6532835>.

# Preparation and Characterization of 4:1 (EC-PVC) Ethyl Cellulose - Polyvinyl Chloride Polyblends Thin Films<sup>1</sup>

Welekar N.R., Wasnik T.S., Lamdhade G. T.

*Department of Physics, Vidya Bharati Mahavidyalaya, C.K. Naidu Road, Camp, Amravati.-444602*

DOI:10.37648/ijrst.v13i01.010

Received: 10 February 2023; Accepted: 16 March 2023; Published: 25 March 2023

---

## ABSTRACT

The present study is focused on preparation and characterization of 4:1 (EC-PVC) Ethyl Cellulose - Polyvinyl Chloride polyblends thin films of pure and doping with different weight ratio of Salicylic Acid (SA) and the isothermal evaporation technique used for its preparation. In order to investigate properties of the prepared samples were characterized by Fourier Transform Infrared Spectroscopy (FTIR) techniques.

**Keywords:** 4:1 (EC-PVC); Ethyl Cellulose; Polyvinyl Chloride; FTIR .

---

## INTRODUCTION:

In recent years, considerable progress has been made to enhance the electrical conductivity, electrochemical and mechanical stability of these polymer electrolyte materials to be utilized for various applications like solid state batteries, fuel cells, sensors, super capacitors, electro chromic display devices, photo electrochemical solar cells etc. [1-4]. The conducting polymer composites and blends have attracted the attention of material researchers, with increase in interest in obtaining properties that are intermediate between those of homo polymers [5,6]. Generally polyvinyl chloride (PVC) is being used for the consumer products like cables, pipes, window frames, packaging bottles, Hit cards and audio recording. It is also used in car interiors and in hospital as medical disposables. The presence of chlorine in the PVC structure is the reason of its better properties like fire resistance and durability. Dielectric properties and surface morphology of proton irradiated ferric oxalate dispersed PVC films has been studied [7]. A lightweight, rigid plastic in its pure form, it is also manufactured in a flexible "plasticized". Polyvinyl chloride (PVC) is one of the most important commercial polymer that have wide range of applications [8].

Due to accessibility to basic raw materials and to its properties incorporating plasticisers, the rigid PVC makes the soft PVC products and it has been used in cable and wire covers, children toys and medical devices. [9] PVC's relatively low cost, biological and chemical resistance and workability have resulted in it being used for a wide variety of applications. It is used for sewerage pipes and other pipe applications where cost or vulnerability to corrosion limits the use of metal. With the addition of impact modifiers and stabilizers, PVC scrap has become a popular material for

---

<sup>1</sup> How to cite the article: Welekar N.R., Wasnik T.S., Lamdhade G. T Preparation and Characterization of 4:1 (EC-PVC) Ethyl Cellulose - Polyvinyl Chloride Polyblends Thin Films; *International Journal of Research in Science and Technology*, Jan-Mar 2023, Vol 13, Issue 1, 87-96, DOI: <http://doi.org/10.37648/ijrst.v13i01.010>

# To Study the Effect of Solvent on AC Conductivity and Dielectric Constant on Blend Formation of Poly (Styrene): Poly (Vinyl Acetate)<sup>1</sup>

H.G. Pande, G. T. Lamdhade

*Department of Physics, Vidya Bharati Mahavidyalaya, Camp, C.K. Naidu Road, Amravati, Maharashtra, India*

DOI:10.37648/ijrst.v13i01.006

Received: 02 February 2023; Accepted: 17 March 2023; Published: 18 March 2023

---

## ABSTRACT

The main objective of this work is to illustrate miscibility, when formation of poly blends occurred in different solvents. Isothermal evaporation method was used to achieve poly blends of poly styrene and poly vinyl acetate (PS: PVAc). The FTIR spectroscopy results reveal that there are miscibility exists. For these blends with different solvents, electrical conductivity and dielectric constant were measured at different temperatures (313K, 323K, 333K and 343K) and at the different frequencies (1 KHz to 10MHz) using 4284 LCR meter. It is found that ac conductivity of polyblends thin film varies with temperature for all values of frequencies and it varies with increase in frequencies at constant temperature. The dielectric constant also varies with the increasing of the temperature of polyblends.

**Keywords:** *Solvents; Polystyrene (PS); Polyvinyl acetate (PVAc); Miscibility; AC Conductivity; Dielectric Constants.*

---

## INTRODUCTION

Polymers and their blends are significant materials, growing with a lot of potential applications in various areas. In recent era, the scientists have focused toward the synthesis and development of new efficient polyblends materials derived monomer polymers like Poly-vinyl acetate (PVAc), Polystyrene (PS), Polymethyl methacrylate (PMMA) etc. So many methods were developing to synthesis polyblends. One most used method is isothermal evaporation method because its ease and low costing. In this method different solvents were used such as Acetone, Methyl-ethyl ketone (MEK), Tetra hydro furan (THF), Toluene and pure distilled Water etc [1-5] to dissolve polymeric materials to form homogenous solution. During this procedure, several improvements in physical and chemical properties like dielectric properties, mechanical and thermal durability and process ability rather than development of new polymers are also observed.

## EXPERIMENTAL

Poly-styrene (PS) and Poly-vinyl acetate (PVAc) were supplied by Sigma –Aldrich, Co., 3050 spruce street, St. Louis. MO 63103 USA 314-771-5765. Methyl-ethyl ketone (MEK), Tetra hydro furan (THF) and Toluene used as organic media, (E-Merck India Ltd., Mumbai) are being used as a solvent for poly-blending process. All chemicals

---

<sup>1</sup> How to cite the article: Pande H.G., Lamdhade G.T., To Study the Effect of Solvent on AC Conductivity and Dielectric Constant on Blend Formation of Poly (Styrene): Poly (Vinyl Acetate), IJRST, Jan-Mar 2023, Vol 13, Issue 1, 40-47, DOI: <http://doi.org/10.37648/ijrst.v13i01.006>

were of analytical grade used. In the present work, thin films were prepared by Isothermal Evaporation Technique (IET) [3, 6].

### Preparation of Polyblends

Polystyrene and Poly-vinyl acetate were dissolved in Methyl-ethyl ketone, Tetra hydro furan and Toluene in three different beakers. Stirring was continued for one hour before deposition of film. Total concentration of the polymeric mixture in solvent was kept 5%. So, films of polymer blends were prepared by IET [2-3, 5-6].

### Measurements

FTIR measurements were carried out using the single beam FTIR [Agilent Technologies, Singapore]. The FTIR spectra of all samples are in the range of 700-3800  $\text{cm}^{-1}$ . The ac frequencies were applied (in the range 1 KHz –10 MHz) across the sample by using the 4284 A precision LCR meter [Agilent Technologies, Singapore].

## RESULTS AND DISCUSSION

### FTIR Spectroscopic Analysis

Fourier transform infrared (FTIR) spectroscopy is one of the widely used optical methods to study the interaction of electromagnetic radiation in the infrared region with chemical compounds.

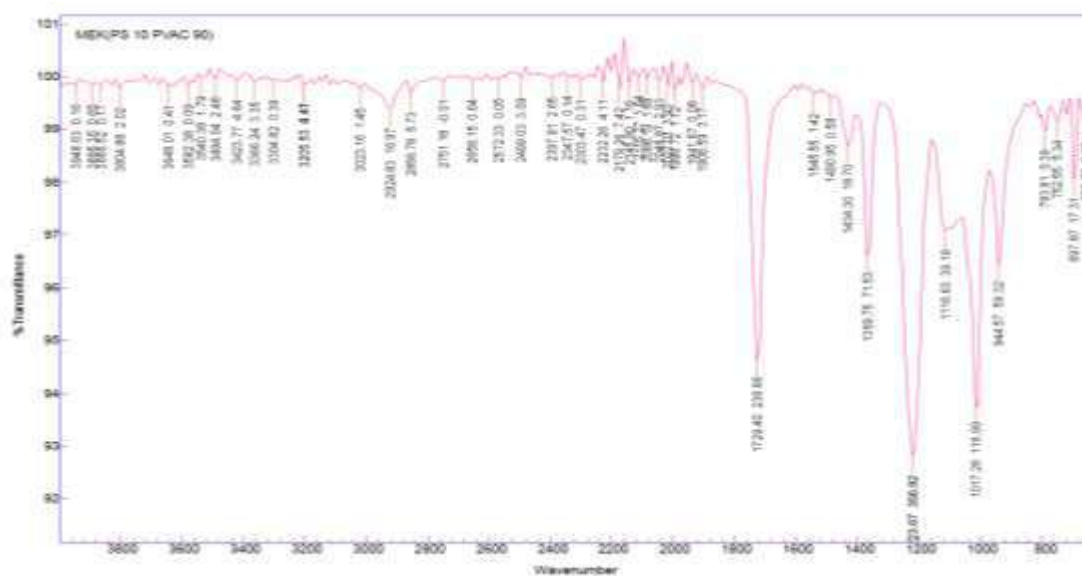


Fig.1 (a): FTIR PS (10) + PVAc (90) (MEK)

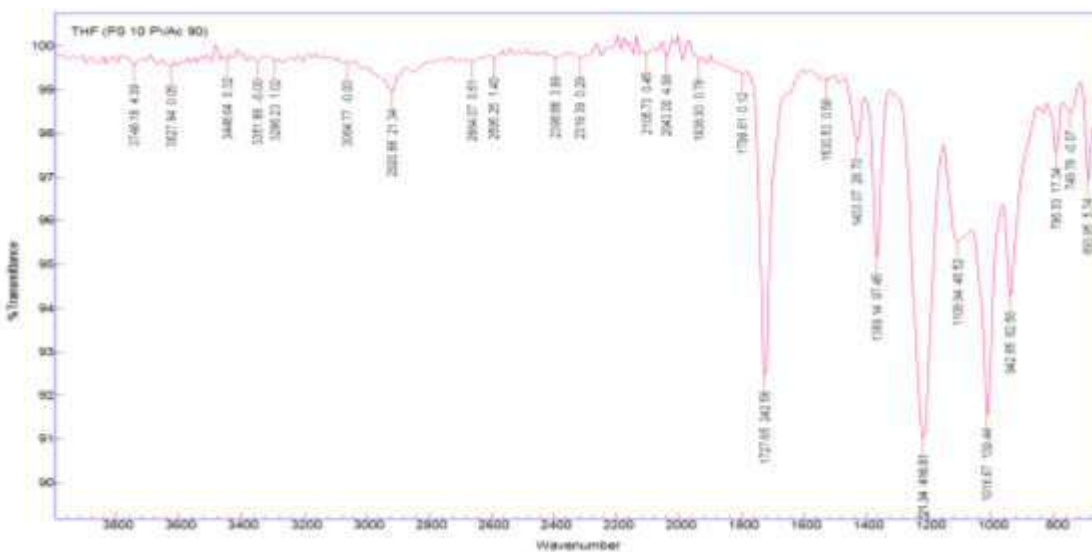


Fig.1 (b): FTIR PS (10) +PVAc (90) (THF)

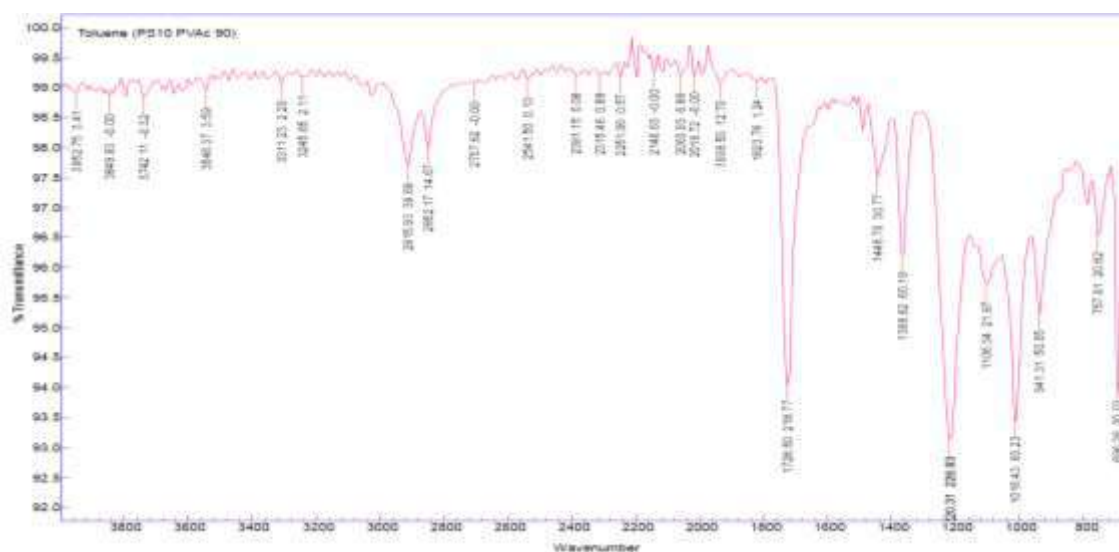


Fig.1 (b): FTIR PS (10) +PVAc (90) (Toluene)

Figure 1(a), (b) and (c) depicts the FTIR spectra of PS: PVAc blend dissolved in MEK, THF and Toluene respectively in the wave number range 700 – 3800  $\text{cm}^{-1}$ . From figures it is observed that the vibrational bands at (2924 and 2856), (3064 and 2920) and (2915 and 2852)  $\text{cm}^{-1}$  are ascribed to O–CH<sub>3</sub> (ester group) asymmetric stretching and symmetric stretching vibrations, respectively. The intense band at around (1729.40, 1727.65, 1728.50)  $\text{cm}^{-1}$  represents the C=O stretching band of an un-conjugated ester. At (1369.75, 1369.14, 1368.92)  $\text{cm}^{-1}$ , a prominent band is evident, here the CH<sub>3</sub> (C=O) group strongly absorbs acetate esters. The strong band at (1223.67, 1221.34, 1220.31)  $\text{cm}^{-1}$  and the band at (1116.63, 1109.94, 1106.34)  $\text{cm}^{-1}$  are ascribed to C–O–C symmetric stretching and C–O stretching vibrations, respectively. Also the peak at (944, 942, 941)  $\text{cm}^{-1}$  is ascribed to CH bending vibrations. This all show the evidences for PVAc [1]. However, each repeat unit in PS contains a pendant benzene ring. Mainly PS characterizing bands are observed. The methylene (CH<sub>2</sub>) asymmetric stretching bands are observed at 3023.16  $\text{cm}^{-1}$ . There is a C=O stretching



at  $1729.40\text{ cm}^{-1}$ . The out-of-plane C–H bending mode of the aromatic ring is shown at  $944.57\text{ cm}^{-1}$  and the ring-bending vibrational band appears at  $693\text{ cm}^{-1}$  [7-9].

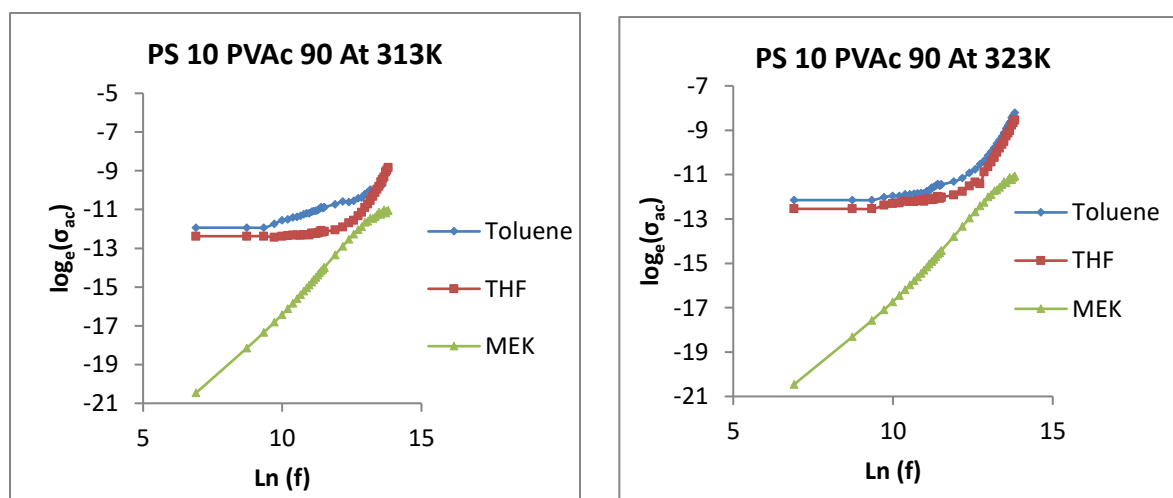
From FTIR spectrum of PS: PVAc polyblends it is also observed that spectrum that C=O stretching at  $1727\text{ cm}^{-1}$  and C–C stretching in aromatic ring found at  $1433\text{ cm}^{-1}$  and typical C–H bend being usually present as band at  $1369\text{ cm}^{-1}$ . Some bands are disappeared in the blends and the intensity of some bands was changed. All results data suggest that homogeneous polymer composites are formed over all the blend compositions.

Further the FTIR spectrum recorded on PS: PVAc blend did not indicate the existence of any interaction between the components. There is no change in the position of either peak of aromatic ring of PVAc or the ether lone pair peak of PS, which means that neither ether linkage is interacting nor the aromatic ring is affected by blending these two polymers. Furthermore it is to be pointed here that the Sun's formula seems to be well applicable in describing the miscibility of PS: PVAc blend system [10].

### AC Electrical Conductivity and Dielectric Constant Studies

**Figure 2 (a)** shows the relation between frequency and ac conductivity for (PS: PVAc) blends in MEK, Toluene and THF at constant temperature 313K, 323K, 333K and 343K. Plot shows rise in conductivity with increasing frequencies from 1 KHz to 10 MHz. The rise of conductivity on increasing the frequency and temperature is a common respond for polymeric thin films samples. It is due to the tremendous increase of the mobility of charge carriers in the blend films i.e. at higher frequencies blends of molecules starts vibrating with large amplitude within the polymeric chains hence the effect of increase in conductivity of blends [8,11].

It also shows that conductivity shifted above the frequency axis for blend dissolve in Toluene, THF and MEK solvent respectively. Further table 1 illustrates that Frequency their corresponding ac conductivities values for PS (10): PVAc (90). From table it's clear that PS: PVAc (THF as Solvent) shows maximum ac conductivity among other solvent samples. In observed that in same poly-blend film  $\sigma_{ac}$  increases with frequency which is the common characteristic of disordered materials. Hence an increase in frequency leads to increase in ac conductivity [12]. Furthermore, almost all the prepared PS: PVAc films show similar behaviour up to 10 MHz, which is typical for hopping conduction.



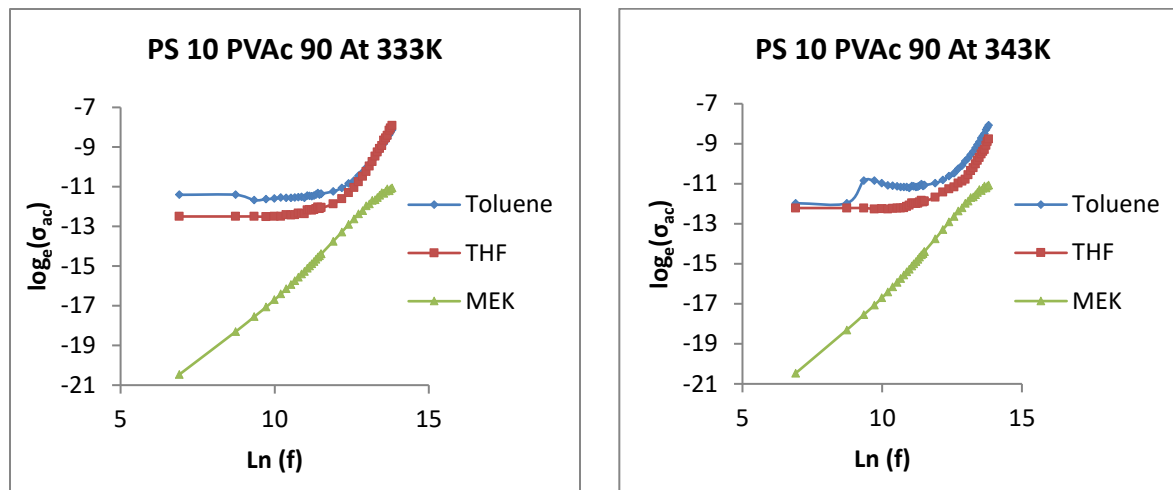


Fig. 2 (a): Variation between frequency and a.c. conductivity for blend in different solvent at constant temperatures.

Table 1: Frequency their corresponding a.c. conductivities values for PS (10): PVAc (90)

Constant Temperature	Values	Solvent					
		Toluene		THF		MEK	
313K	Frequency	1kHz	10MHz	1kHz	10MHz	1kHz	10MHz
	A.C. Conductivity ln[S/m]	1.6639	4.8380	1.09	8.88	0.5264	0.1263
323K	Frequency	1kHz	10MHz	1kHz	10MHz	1kHz	10MHz
	A.C. Conductivity ln[S/m]	0.2221	7.6013	1.34	5.91	0.5314	0.1037
333K	Frequency	1kHz	10MHz	1kHz	10MHz	1kHz	10MHz
	A.C. Conductivity ln[S/m]	0.2501	7.9442	1.09	8.88	0.5355	0.1072
343K	Frequency	1kHz	10MHz	1kHz	10MHz	1kHz	10MHz
	A.C. Conductivity ln[S/m]	1.3705	8.5226	1.18	5.50	0.6217	0.1771

Figure 2 (b) shows the relation between frequency and dielectric constant for (PS:PVAc) blends in different solvent i.e. Toluene, THF and MEK at constant temperatures 313K, 323K, 333K and 343K. Plot shows rise in dielectric constant with increasing frequencies from 1 KHz to 15MHz. The rise of dielectric constant upon increasing the frequency and temperature is a common respond for all blends samples [11, 13-14]. Table 2 illustrates that Frequency their corresponding dielectric constant values for PS (10): PVAc (90). From table it's observed that PS: PVAc (THF as

Solvent) shows maximum dielectric constant among other solvent samples. For the future research scope THF dissolve polyblends samples will used.

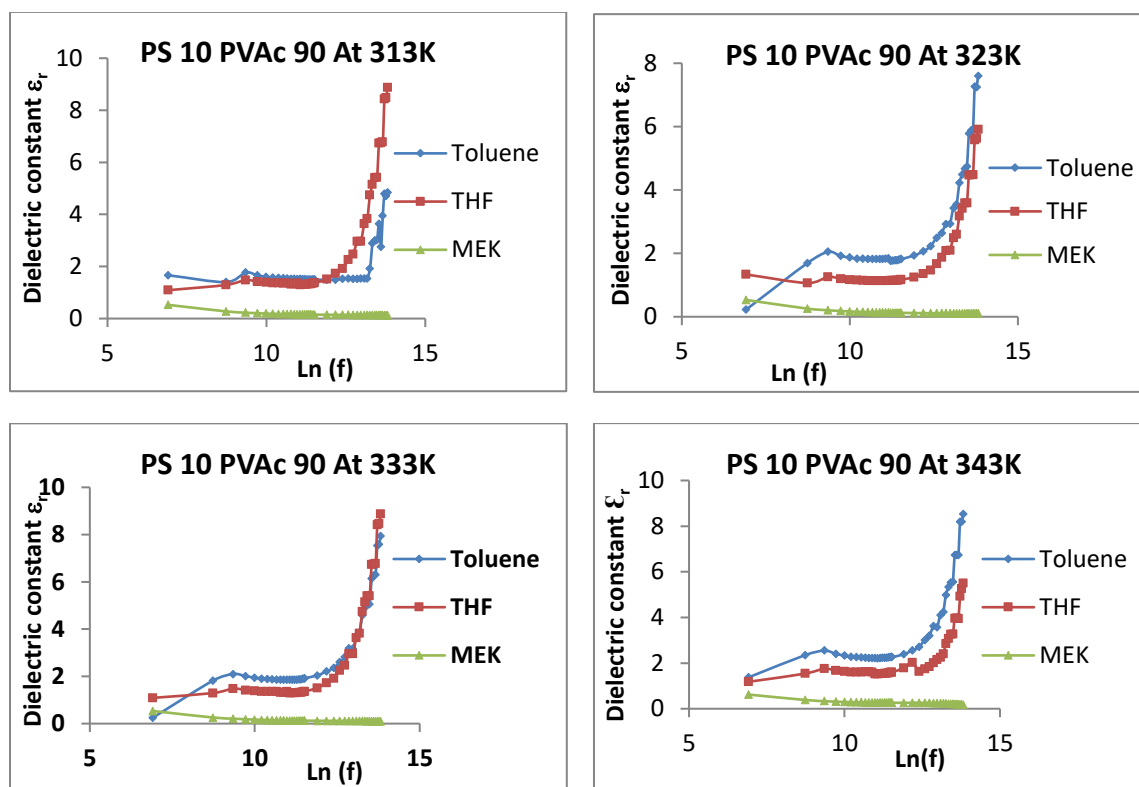


Fig. 2 (b): Variation between frequency and dielectric constant for blends in different solvent at constant temperatures.

Table 2: Frequency their corresponding dielectric constant for PS (10): PVAc (90)

Constant Temperature	Values	Solvent					
		Toluene		THF		MEK	
313K	Frequency	1 kHz	10MHz	1 kHz	10MHz	1kHz	10 MHz
	Dielectric Constant	1.6639	4.8380	1.09	8.88	0.5264	0.1263
323K	Frequency	1 kHz	10MHz	1 kHz	10MHz	1kHz	10 MHz
	Dielectric Constant	0.2221	7.6013	1.34	5.91	0.5314	0.1037
333K	Frequency	1 kHz	10MHz	1 kHz	10MHz	1kHz	10 MHz
	Dielectric Constant	0.2501	7.9442	1.09	8.88	0.5355	0.1072
343K	Frequency	1 kHz	10MHz	1 kHz	10MHz	1kHz	10 MHz
	Dielectric Constant	1.3705	8.5226	1.18	5.50	0.6217	0.1771

## CONCLUSIONS

FTIR results concludes that miscibility of PS (10): PVAc (90) polymer blends were maximum in Toluene, moderate in THF and minimum in MEK solvents. Hence all samples show the miscibility existence.

The ac electrical conductivity and dielectric constants have been measured for (PS:PVAc) blends in different solvent i.e. MEK, THF and Toluene at constant temperature 313K, 323K, 333K at the different frequencies. It is found that ac conductivity of blends thin film increases with increase in frequencies at constant temperature and also the dielectric constant increases with the increasing frequencies of blends. Further graphs reveals that Toluene dissolve blend shows maximum ac conductivity at different constant temperature, THF dissolve blend shows moderate ac conductivity range while MEK dissolve blend shows minimum ac conductivity. Furthermore in case of dielectric constant similar consequence follows all blend samples.

## ACKNOWLEDGEMENT

Financial support and characterization facility sanctioned by UGC-DAE Consortium for Scientific Research Indore Centre under Collaborative Research Project (2017-18) for this work is gratefully acknowledged by authors.

**Conflict of Interest:** None

## REFERENCES

1. Cristovan, F. H., Paula, D. F. R., Lemos, S. G., De Oliveira, A. J. A., & Pereira, E. C. (2009). DC conductivity study of polyaniline and poly (acrylonitrile-butadiene-styrene) blends. *Synthetic Metals*, 159(21), 2188-2190. DOI: <https://doi.org/10.1016/j.synthmet.2009.08.042>
2. I.S. Elashmawi, N.A. Hakeem, and E.M. Abdelrazek, (Oct 2008), Spectroscopic and thermal studies of PS/PVAc Blends; *Physica B: Condensed Matter* volume 403 issue 19-20, 3547 - 3552, <https://doi.org/10.1016/j.physb.2008.05.024>
3. H. Rawal and S. Devi, (Dec 1993), Compatibility of Poly(styrene)/Poly(vinyl acetate) Blends; *Polymer Journal*, volume 25 issue 12, 1215 to 1221 <https://doi.org/10.1295/polymj.25.1215>
4. S.G. Vidhale and N.G. Belsare, (2013), Effect of IR Radiation on the Dielectric Properties of Salicylic Acid Doped Poly- blend Thin Films of PS and PMMA; *International Journal of Scientific & Engineering Research*, Vol.4 [09].
5. P.A.P. Mamza and B.T. Nwifo, (22 Jan 2010), Density and Morphological Properties of Some Reinforced Polymers; *Nigerian Journal of Basic and Applied Sciences* volume 17 issue 2, <https://doi.org/10.4314/njbas.v17i2.49888>.
6. M. M. Kummali, G. A. Schwartz, Angel Alegría, Richard Arinero, Juan Colmenero, (15 Sep 2011), Compatibility studies of polystyrene and poly(vinyl acetate) blends using electrostatic force microscopy; *Journal of Polymer Science Part B: Polymer Physics* volume 49 issue 18 pages 1332 - 1338, <https://doi.org/10.1002/polb.22301>.
7. P.P. Raut, G.T. Lamdhade, F. C. Raghuvanshi, T. Shripathi, (2016) *National Conference on Material Science and Renewable Energy Sources (NCMSRES) Proceeding*, 200-202.
8. N. G. Belsare, A.S. Wadkatkar, R. V. Joat, T. S. Wasnik, F. C. Raghuvanshi, K. B. Raulkar, and G.T. Lamdhade, (2011), Polyvinyl chloride–polymethyl methacrylate micro-composite polymers: miscibility; *Journal of Electron Devices*, 11, 583-587.
9. V.Rao, P.V Ashokan, M.H Shridhar, (April 2000), Studies of Dielectric Relaxation and A C Conductivity on Cellulose Acetate Hyderogen Phthalate-Poly(Methyl Methacrylate) Blends); *Materials Science and Engineering: A*; volume 281 issue 1-2, pages 213 to 220, [https://doi.org/10.1016/s0921-5093\(99\)00723-6](https://doi.org/10.1016/s0921-5093(99)00723-6).
10. Mohammad Saleem Khan, Raina Aman Qazi and Mian Said Wahid, (April, 2008), Miscibility studies of PVC/PMMA and PS/PMMA blends by dilute solution viscometry and FTIR; *African Journal of Pure and Applied Chemistry*, Vol. 2 (4), pages 041-045.
11. H. Kaczmarek, (Nov 1995), Photodegradation of polystyrene and poly(vinyl acetate) blends—I. Irradiation of PS/PVAc blends by polychromatic light; *European Polymer Journal* volume 31 issue 11, 1037 - 1042, [https://doi.org/10.1016/0014-3057\(95\)00094-1](https://doi.org/10.1016/0014-3057(95)00094-1)

12. K. Prabha, H. S. Jayanna, (2015), Study the Frequency Dependence of Dielectric Properties of Gamma Irradiated PVA(1-x)PSx Polymer Blends; *Open Journal of Polymer Chemistry* volume 05 issue 04 , 47 - 54, <https://doi.org/10.4236/ojpchem.2015.54006>
13. P. Dutta, S. Biswas, M. Ghosh, S. K. De and S. Chatterjee, (Jun 2001) The dc and ac conductivity of polyaniline–polyvinyl alcohol blends; *Synthetic Metals* volume 122 issue 2, 455 - 461, [https://doi.org/10.1016/s0379-6779\(00\)00588-9](https://doi.org/10.1016/s0379-6779(00)00588-9).
14. I.C. McNeill, (May 1997), Thermal degradation mechanisms of some addition polymers and copolymers; *Journal of Analytical and Applied Pyrolysis*; volume 40-41, 21- 41, [https://doi.org/10.1016/s0165-2370\(97\)00006-5](https://doi.org/10.1016/s0165-2370(97)00006-5)

# Nonlinear I–V Characteristics and Thermal Stability of Nanocrystalline Titanium Oxide<sup>1</sup>

\*Balkhande V.M., \*\*Lamdhade G.T.

\*Dept. of Physics, Prof. Ram Meghe Institute of Tech. & Research, Badnera-Amravati M.S. India

\*\*Dept. of Physics, Vidya Bharati Mahavidyalaya, Amravati M.S. India

DOI:10.37648/ijrst.v12i04.005

Received: 03 September 2022; Accepted: 08 November 2022; Published: 08 December 2022

---

## ABSTRACT

Current versus voltage characteristics (I-V) of nanocrystalline Titanium oxide (TiO<sub>2</sub>) has been investigated at various temperatures (from 50°C to 350°C) in air, measured by using a data acquisition system consisting of Keithley 6487 voltage source cum picoammeter. The nanocrystalline powder of TiO<sub>2</sub> was prepared by the liquid phase method and samples were prepared via spray pyrolysis technique in the form of thin films on an optically plane and clean glass surface. X-ray diffraction studies showed a , mostly as rutile and anatase phases which both of them have the tetragonal structures of TiO<sub>2</sub>. Surface morphological studies were performed with scanning electron microscopy. The nanocrystalline Titanium oxide exhibited nonlinear I-V characteristics of the negative resistance type with thermal stability.

**Keywords:** Nanocrystalline Titanium oxide; XRD; FE-SEM; I-V characteristics; thermal stability

---

## INTRODUCTION

Titanium dioxide is a cheap, chemically stable, and non-toxic material. However, its electrical properties are unstable and it is a modest semiconductor and a mediocre insulator. For several applications, it would be interesting to make it either more insulating or more conducting. Titanium dioxide (TiO<sub>2</sub>) is a material used in a wide range of common and high-tech applications. It is cheap, chemically stable, non-toxic, and last but not least bio-compatible. Titanium is successfully used as an implant material for dental, orthopedic and osteosynthesis applications, and its native oxide is mostly constituted of titanium dioxide [1]. TiO<sub>2</sub> powder is used as a white pigment in paint [2], replacing lead oxide which is toxic, and in toothpaste. Transparent single crystals or thin films have a high refractive index that makes TiO<sub>2</sub> suitable for optical applications [3-5]. Thus, research in many different fields is devoted to titanium dioxide under various forms such as single crystals, ceramics, and thin films. The goal of this work was to study the I-V characteristics, and structural, morphological properties of nano-crystalline TiO<sub>2</sub> thin films deposited by the spray pyrolysis technique.

## EXPERIMENTAL

The methods of synthesis of nanoparticles can be broadly classified into three categories namely, liquid-phase synthesis, gas-phase synthesis, and vapor-phase synthesis. In the present work of the thesis, we have used the sol-gel method (which is under liquid phase synthesis) for the synthesis of pristine nanoparticles of TiO<sub>2</sub> [6-8].

### Synthesis of TiO<sub>2</sub>

Titanium tetra iso propoxide [Ti(OCH(CH<sub>3</sub>)<sub>2</sub>)<sub>4</sub>], iso-propanol [(CH<sub>3</sub>)<sub>2</sub>CHOH] and nitric acid [HNO<sub>3</sub>] were used as received without any further purification. A 20 ml of solution of Titanium tetra isopropoxide was added drop by drop into the 22 ml of a solution containing 10 ml of iso-propanol and 12 ml deionised water under constant stirring at 80°C into the round bottom beaker. After 1 hour, concentrated HNO<sub>3</sub> (.8 ml) mixed with deionised water was added into the TTIP

---

<sup>1</sup> How to cite the article: Balkhande V.M., Lamdhade G.T., Nonlinear I-V Characteristics and Thermal Stability of Nanocrystalline Titanium Oxide, IJRST, Oct-Dec 2022, Vol 12, Issue 4, 25-30, DOI: <http://doi.org/10.37648/ijrst.v12i04.005>

solution and keep it under constant stirring at 60 °C for 6 hours highly viscous sol-gel was obtained. The prepared sol-gel was heated at 300 °C for 2 hours in the open atmosphere. After annealing, the TiO<sub>2</sub> nanocrystalline 2 g powder was obtained. In further preparation of TiO<sub>2</sub> film, the prepared powder was added in the ratio of 1:10 to the solution of isopropanol. The obtained powder is kept in a vacuum oven at 70 °C for 24 hours so as to get completely dried powder.

### Preparation of Samples

After the synthesis, obtained fine nanopowder of TiO<sub>2</sub> was calcinated at 800 °C up to 5 hours in the auto-controlled muffle furnace, so that the impurities from product will be completely removed. The obtained product of fine nanopowder is further used for the preparations of samples. The obtained product of fine nanopowder of TiO<sub>2</sub> used for the fabrication samples was prepared via spray pyrolysis technique using Thin-film equipment: (Holmarc USA Make) in the form of thin films on an optically plane and clean glass surface [9-10].

### Data Acquisition System

The data acquisition system consists of a Keithley 6487 source meter, GPIB cable, temperature controller, and computer as shown in fig. 1.1.

The picoammeter is controlled by the installation of GPIB (General Purpose Interface Bus) card. This GPIB card has an IEEE-488.2 bus, which is common to the testing meter. Communication with the temperature controller is done using Rs-232 port.

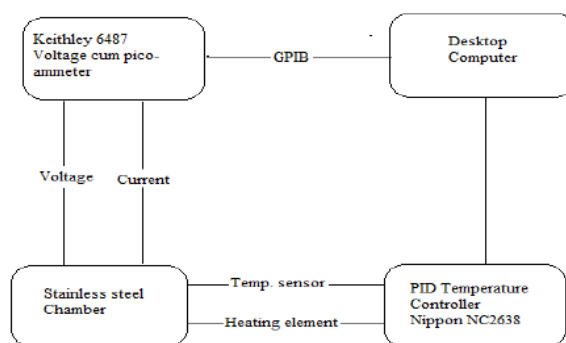


Fig.1.1 Flow Chart of Data Acquisition System

The language used for controlling the source meter and temperature controller is lab view graphical programming language, which can provide a friendly user interface. To study the VI characteristics of the sample element, special software was designed.

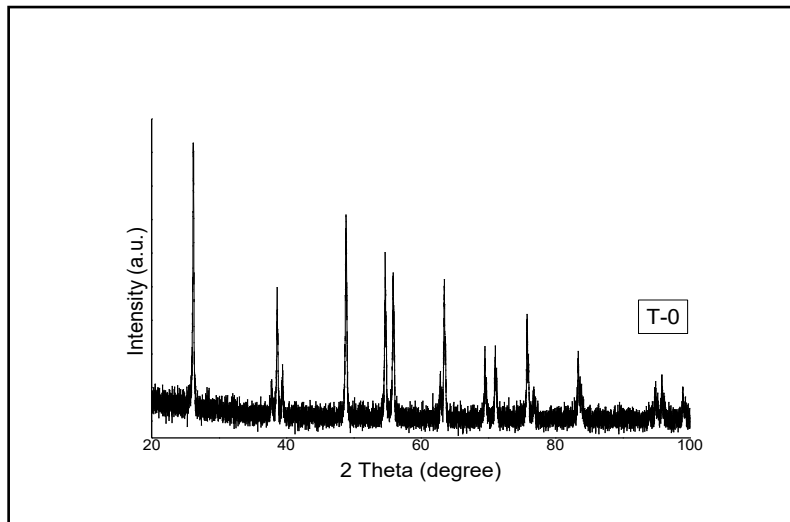
## RESULTS AND DISCUSSION

### X-Ray Diffraction : Nanocrystalline TiO<sub>2</sub>

Titanium dioxide or Titania (TiO<sub>2</sub>) is widely nominated for three main phases of rutile, anatase and brookite . Among them, the TiO<sub>2</sub> exists mostly as rutile and anatase phases which both of them have the tetragonal structures. However, rutile is a high-temperature stable phase and anatase is formed at a lower temperature .

Figure 1.2 shows the XRD pattern of pure Titanium Dioxide (TiO<sub>2</sub>) which is calcinated at temperature 800°C, which shows crystalline annealed with 2θ peaks lying at planes (1 0 1), (1 0 3), (0 0 4), (1 1 2), (2 0 0), (1 0 5), (2 1 1), (2 1 3), (2 0 4), (1 1 6), (2 2 0), (1 0 7), (2 1 5), (3 0 1), (0 0 8), (3 0 3), (2 2 4) and (3 1 2) respectively. The sharp diffraction peaks were clearly seen and they perfectly match with crystal structure of TiO<sub>2</sub> therefore, we get perfectly crystallinity of TiO<sub>2</sub> particles in Anatase phase. The calculated crystallographic parameters are a = 3.7300 (Å), b = 3.7300 (Å) and c = 9.3700 (Å) [Crystal system: Tetragonal ; Space group: I41/amd ; Space group number: 141, Reference Code: 01-075-1537] . All the peaks match well with the standard tetragonal type structures of titanium dioxide (TiO<sub>2</sub>) in the Anatase phase and well agree with the JCPDS card No. 21-1272 . The average crystalline size was calculated by using the Scherrer formula found to **82.75** nm. The stick pattern of crystalline TiO<sub>2</sub> is as shown in fig. 1.2. It was found

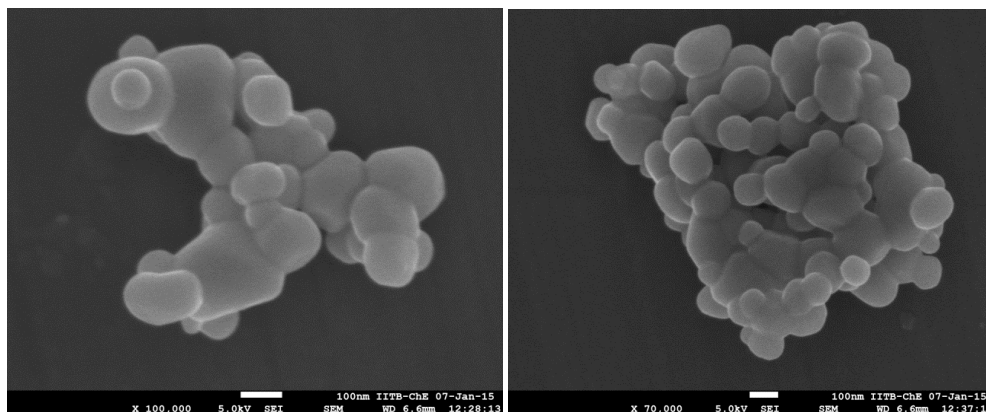
that the thick films consisted only of the tetragonal structure  $\text{TiO}_2$  with no structural change and they were well crystallized during deposition [11-12].



**Fig. 1.2** XRD of crystalline pristine  $\text{TiO}_2$

### Field Emission - Scanning Electron Microscope

The surface morphology and the nanocrystalline particle size of titanium oxide ( $\text{TiO}_2$ ) were examined by using Field Emission Scanning Electron Microscope. Figure 1.3 show the FE-SEM micrograph of pristine  $\text{TiO}_2$ , thin films. To verify the morphology scheme data obtained from the scanning electron microscopy will confirm the structural analysis obtained by the X-ray diffraction pattern [13-14].



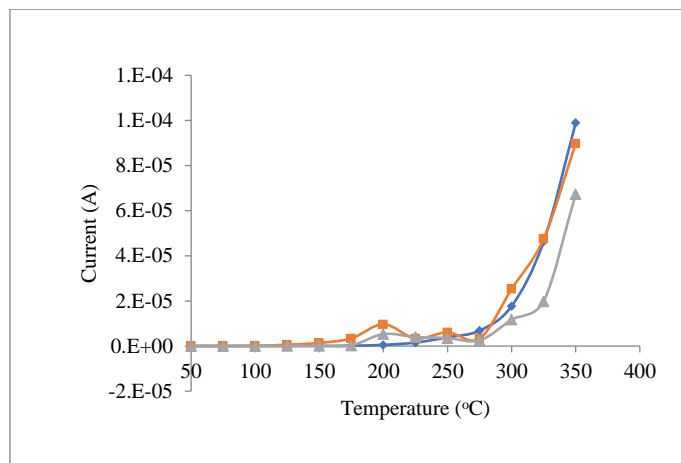
**Fig. 1.3** FESEM of Nano-crystalline pristine  $\text{TiO}_2$

Figure 1.3. shows the micrograph of sample pure  $\text{TiO}_2$  thick films.  $\text{TiO}_2$  particles are found to be tetragonal and semi spherical shape with the average size in the range of 85-94 nm. The average particle size observed in FE-SEM is in good agreement with the calculated value from XRD analysis [15].

### Thermal Stability of $\text{TiO}_2$ thin films

Figure 1.4 shows the variation of current Vs. temperature from  $50^\circ\text{C}$  to  $350^\circ\text{C}$  at constant source voltage (10 V DC) by using Keithley (6487) voltage source cum picoammeter. i.e. thermal stability for different samples of pristine  $\text{TiO}_2$





**Fig. 1.4** Thermal Stability Curves of pristine TiO<sub>2</sub> Samples.

When samples are kept to a thermal treatment in an inert atmosphere (N<sub>2</sub>), from 50°C to 350°C under the small interval of time, there occurs also a mass loss on heating in air atmosphere but it happens at higher temperature, around 500°C and in a smaller temperature interval (the mass loss begins in the neighborhood of 430°C and considerably slower down around 550°C). It is noteworthy that the temperature at which we observe oxidation in as-grown films is significantly lower than temperatures mentioned in for samples deposited by screen printing technique, a fact that seems to confirm the sensitivity of oxidation temperature on sample texture. In present study, thermal treatment of samples is less than temperature 500°C, so there is no problem of mass loss of thick film samples. Generally, the grain size of nanocrystalline materials increases by increasing annealing temperature. This could be attributed to the effects of evaporation of absorbed water and reorganization of the grain. Uniform distribution of the grain is also observable. This is important to note that, due to thermal treatment to the films, which show better and excellent sensitivity and stability results without any further mechanical deformations obtained or seen in the films [16-17].

#### **Current-Voltage (I–V) Characteristics :**

The current-voltage (I–V) characteristics of the sample of pristine TiO<sub>2</sub> and their temperature dependence have been investigated in the air by using a data acquisition system consisting of a Keithley 6487 source meter, GPIB cable, temperature controller, and computer. Fig. 1.4 shows the current-voltage (I–V) characteristics sample of pristine TiO<sub>2</sub> measured at different temperatures (50°C, 100°C, 150°C, 200°C, 250°C, 300°C and 350°C). All the samples show semiconducting behavior as the resistance of samples is decreasing with an increase in the I-V measurement temperature. The nature of the plot is initially linear and then it becomes nonlinear beyond threshold voltage, said to be exponential in nature. The resistance is drastically falling at temperature 350°C and is found to be in the range of 5-15 MΩ. The nanocrystalline titanium oxide exhibited nonlinear I-V characteristics of the current-controlled negative resistance type [18].

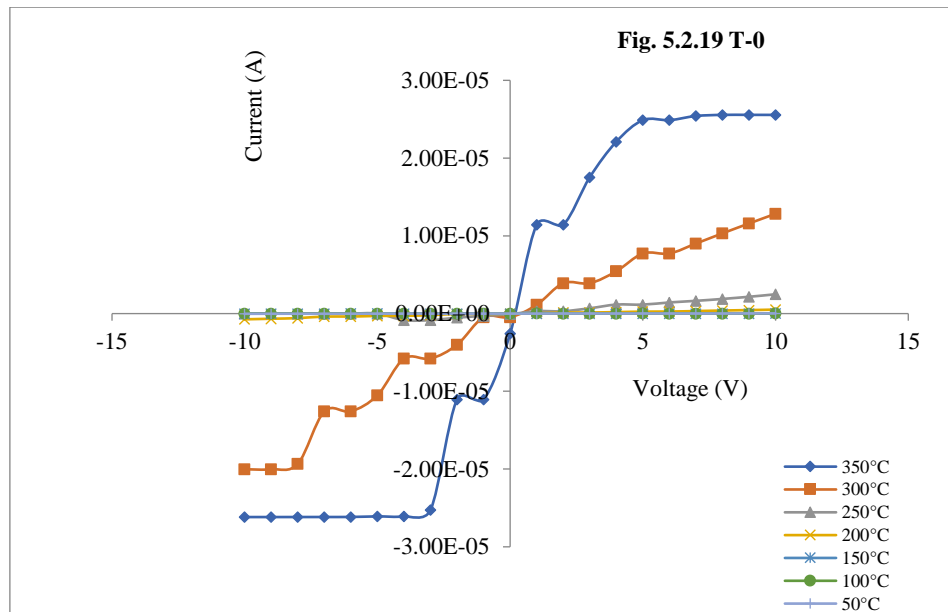


Fig. 1.4 Current–Voltage (I–V) Characteristic of pristine TiO<sub>2</sub>

## CONCLUSIONS

Current versus voltage characteristics (I-V) of nanocrystalline TiO<sub>2</sub> has been investigated at various temperatures (from 50°C to 350°C) in air and characteristic curves are generally used as a tool to determine and understand the basic parameters of a component or device and can also be used to mathematically model its nonlinear behaviour within an electronic circuit.

## REFERENCES :

1. C. E. Sittig: “Charakterisierung der Oxidschichten auf Titan und Titanlegierungen sowie deren Reaktionen in Kontakt mit biologisch relevanten Modellösungen”, Dissertation ETH Nr. 12657, Zürich (1998).
2. W. Clark and P. Broadhead, *Journal of Physics C* 3 (1970), 1047.
3. R. R. Willey: “Practical design and production of optical thin films”, Marcel Dekker, New York (1996).
4. M. Radecka, K. Zahrzewska, H. Czternastek, and T. Stapinski, *Applied Surface Science* 65/66 (1993), 227.
5. S. Lee, B. Hun Park, and S.-G. Oh, *Journal of the Korean Physical Society* 31 (1997), 352
6. Eucken and A. Büchner, *Zeitschrift für physikalische Chemie B* 27 (1935), 321.
7. H. L. Hartnagel, A. L. Dawar, A. K. Jain, and C. Jagadish: “Semiconducting transparent thin films”, Institute of Physics Publishing, Bristol (1995).
8. M. Ohring: “The materials Science of Thin Films”, Academic Press, San diego (1992).
9. G Korotcenkov, V Brinzari, J Schwank, M DiBattista and A Vasiliev, (2001) *Sensors and Actuators B: Chemical*, Volume 77, Issue 1-2, pp: 244- 252
10. G. Gordillo, L.C. Moreno, W. de la Cruz and P. Teheran, (1994 ), *Thin Solid Films*, Volume 252, Issue 1, pp: 61 - 66
11. T.K. Kim, M.N. Lee, S.H. Lee, Y.C. Park, C.K. Jung and J.-H. Boo, “ *Thin Solid Films*, Volume 475, Issue 1-2, pp: 171-177, Mar (2005), DOI: 10.1016/j.tsf.2004.07.021
12. Brady, G.S. 1971. *Materials Handbook* . New York: McGraw-Hill.
13. Parker, R.L., *Z. Kristallogr., Kristallgeom., Kristallphys., Kristallchem.*, 59, 1, (1924)
14. Zeljka Antic, Radenka M. Krsmanovic, Marko G. Nikolic, Milena Marinovic-Cincovic, Miodrag Mitric, Stefano Polizzi and Miroslav D. Dramicanin, “*Materials Chemistry and Physics*, Volume 135, Issue 2-3, pp: 1064–1069, Aug (2012) DOI: 10.1016/j.matchemphys.2012.06.016
15. Liqiang Jing, Zili Xu, Xiaojun Sun, Jing Shang and Weimin Cai, “*Applied Surface Science*, Volume 180, Issue 3-4, pp: 308–314, Aug (2001) DOI: 10.1016/s0169-4332(01)00365-8

16. Zili Xu, Jing Shang, Chunming Liu, Chunli Kang, Haichen Guo and Yaoguo Du, *Materials Science and Engineering: B*, Volume 63, Issue 3, pp: 211–214, Aug (1999) DOI: 10.1016/s0921-5107(99)00084-7
17. Agbo P.E, Pelagia Research Library, *Advances in Applied Science Research*, Volume 2 (6), pp393-399, (2011)
18. Xiaofei Han, Run Liu, Weixiang Chen and Zhude Xu, *Thin Solid Films*, 516(12):4025-4029 · April (2008), DOI: 10.1016/j.tsf.2007.08.006
19. M. Di Giulio, G. Micocci, R. Rella, P. Siciliano and A. Tepore, *Physica Status Solidi (a)* Volume 136, Issue 2, pp K101 to K104, Apr (1993) DOI: 10.1002/pssa.2211360236

# Synthesis and Characterisation of Cupric Oxide (CuO) Doped Tungsten Oxide (WO<sub>3</sub>) Multilayer Thick Films<sup>1</sup>

\*Mankar S.S., \*\*Lamdhade G.T., \*\*Raulkar K.B

\*Department of Physics, Shivramji Moghe Arts, Commerce and Science College, Kelapur, Pandharkawada, Dist. Yavatmal, M.S. India

\*\*Department of Physics, Vidya Bharati Mahavidyalaya, CK Naidu Road, Amravati, M.S. 444602 India

---

## ABSTRACT

This paper is focused on preparation of cupric oxide doped tungsten oxide multilayer thick film by screen printing method on alumina substrates. XRD and SEM are used to study structural and morphological properties of CuO-WO<sub>3</sub>. The XRD pattern of (CuO-WO<sub>3</sub>) system samples show nanocrystalline form and found the desired peaks of composites. FESEM study reveals that the grain size of nanometer order and shows nano-porous structure, which leads to exhibit large surface area, stability and highest response to gas. In present study B5 sensor (25CuO:75WO<sub>3</sub>) is found to optimized multilayer thick film.

**Keywords:** Sol-Gel Method; (CuO-WO<sub>3</sub>); multilayer thick films; XRD; FESEM

## INTRODUCTION

Due to interesting properties and promising applications Cupric oxide (CuO) nanostructures gain interest in many applications. Nanoparticles CuO and its composite oxides have potential applications as gas sensor. As compared to bulk materials, nanoparticles of Copper oxide (CuO) show high catalytic activity and selectivity due to their large surface to volume ratio. The sensitivity and response time of CuO based sensors strongly depend on the particle size of the material [1]. With introducing changes into the procedure of its chemical synthesis, physical and micro structural properties of metal oxide can be modified. Different nanostructures of CuO like nanowire, nanorod, nanoneedle, nano-flower and nanoparticles are synthesized by using various approaches such as; Sol-Gel Combustion Route [1], Microwave Assisted Co-Precipitation Method [2], Chemical Precipitation Method [3], Simple Precipitation Method [4], Sono-chemical Method [5-7] and etc.

WO<sub>3</sub> films are more attractive due to their high catalytic behavior on the surface of the film. The resistance of the WO<sub>3</sub> increases & decreases in the presence of oxidizing and reducing gases respectively. WO<sub>3</sub> can be obtained in various morphological forms such as nano-wires, nano-plates, nano-sheets, nano-flowers, nano-sphere and, sub-micron porous balls. The WO<sub>3</sub> nano-particles or nano-crystallites have been synthesized by various techniques given below; Acid Precipitation Method [8], Hydrothermal Method [9], Reverse Micro-Emulsion-Mediated Synthesis Method [10], Sol-Gel Method [11], Calcinations Method [12] and etc.

Yu Il et al. 2010 [13] studied for gas sensing properties of CuO doped and undoped WO<sub>3</sub> thick films. CuO doped and undoped WO<sub>3</sub> thick films gas sensors were prepared using screen-printing method on alumina substrates. A structural properties of WO<sub>3</sub>:CuO thick films had monoclinic phase and triclinic phase of WO<sub>3</sub> together. Artur Rydosz et al. 2014 [14] investigated results on nanocrystalline CuO and WO<sub>3</sub> thin films by magnetron sputtering technology. XRD, GIR, SEM and AFM methods were used to study the films phase composition, microstructure and surface topography and found to be useful in portable gas sensor applications. Nirmal Kumar et al 2018 [15] was used to deposit tungsten oxide (WO<sub>3</sub>) thin films Cupric oxide (CuO) thin films were deposited by RF magnetron sputtering. Fuchao Yang et al 2018 [16] worked on acetone odor detection. With the formation of the interfacial heterojunction, the WO<sub>3</sub>@CuO

---

<sup>1</sup> How to cite the article: Mankar S.S., Lamdhade G.T., Raulkar K.B., (2023); Synthesis and Characterisation of Cupric Oxide (CuO) Doped Tungsten Oxide (WO<sub>3</sub>) Multilayer Thick Films; *Multidisciplinary International Journal*; Vol 9 (Special Issue), 323-333

shows the best sensing performance. Soo-Yeon Cho et al. 2019 [17] fabricated 10 nm scale p-n heterojunction nanochannel with ultrasmall grained  $\text{WO}_3/\text{CuO}$  nanopatterns to study ethanol sensing.  $\text{WO}_3/\text{CuO}$  nanopattern was also used to study for dynamic sensing behavior for various toxic analytes such as toluene, ethanol, acetone, and ammonia. In the present work of this paper focused on synthesis of pristine nano-particles of  $\text{CuO}$ ,  $\text{WO}_3$  and  $\text{Al}_2\text{O}_3$ , and also ( $\text{CuO}-\text{WO}_3$ ) mixed oxide multilayer thick films.

## EXPERIMENTAL

In the present work, we have used sol-gel method (which is under liquid phase synthesis) for the synthesis of pristine nano-particles of  $\text{CuO}$ ,  $\text{WO}_3$  and  $\text{Al}_2\text{O}_3$  [18-20]. All the chemicals used in this study were of GR grade purchase from Sd-fine, India (purity 99.99%). The chemicals are used without any further purification.

### Synthesis of Cupric Oxide ( $\text{CuO}$ )

In a cleaned round bottom flask, the aqueous solution of  $\text{CuCl}_2 \cdot 6\text{H}_2\text{O}$  (0.2 M) was prepared. After addition of 1 ml of glacial acetic acid to above aqueous solution it was heated to  $100^\circ\text{C}$  with constant stirring. 8 M  $\text{NaOH}$  was added to above heated solution till its pH attains a value of 7. After this process immediately the color of the solution turned from blue to black and the large amount of black precipitate was obtained. The obtained precipitate was centrifuged and washed 3-4 times with de ionized water. The obtained powder was kept in vacuum oven at  $70^\circ\text{C}$  for 24 hours so as to get completely dried powder of  $\text{CuO}$ .

### Synthesis of Tungsten Oxide ( $\text{WO}_3$ )

For Synthesis of  $\text{WO}_3$  particles were simply precipitation method was used. Firstly, Sodium tungstate ( $\text{Na}_2\text{WO}_4$ ) salt (6.59 gm) was dissolved in (200 ml) de-ionized water. Then in to the sodium tungstate solution 10 ml of hydrochloric acid (HCL) was added dropwise with continuous stirring. After the stirring for 5 hours of this mixed solution, the precipitates were allowed to settle for 1 day at room temperature. The precipitate was filtered using a filter paper. Then precipitate was washed many times by de-ionized water until pH reached to 7. The washed precipitate was dried at  $100^\circ\text{C}$  in an oven for 1 hour and further the precipitates were passed from calcination processes in muffle furnace at  $500^\circ\text{C}$  for 4 hours to get  $\text{WO}_3$  powder.

### Synthesis of Alumina ( $\text{Al}_2\text{O}_3$ )

All chemicals used were analytical grade. Aluminium chloride,  $\text{AlCl}_3$  (MOLYCHEM), 25%  $\text{NH}_3$  solution (QUALIGEN Fine Chemicals) and polyvinyl alcohol (PVA) were used as raw materials for the synthesis of aluminium oxide nanoparticles. 1M alcoholic  $\text{AlCl}_3$  solution was prepared, followed by addition of 25% ammonia solution. The resulting solution turned to a white sol. This was followed by the addition of PVA (0.5M). The solution was stirred continuously using a magnetic stirrer until it became a transparent sticky gel. The gel was allowed to mature for 24 hours at room temperature. The resultant gel was heat treated at  $100^\circ\text{C}$  for 24 hours which led to the formation of light weight porous materials due to the enormous gas evolution. The dried gel was, then calcined at  $1000^\circ\text{C}$  for 4 hours and finally, the calcined powders were crushed using mortar and pestle to get the fine homogeneous dense powder of Alumina ( $\text{Al}_2\text{O}_3$ ).

### Fabrication of Sensors

Three series of the samples prepared were  $\text{CuO}:\text{WO}_3$  with  $\text{Al}_2\text{O}_3$  base of multilayer sensors. The different combinations are shown in tables 1.

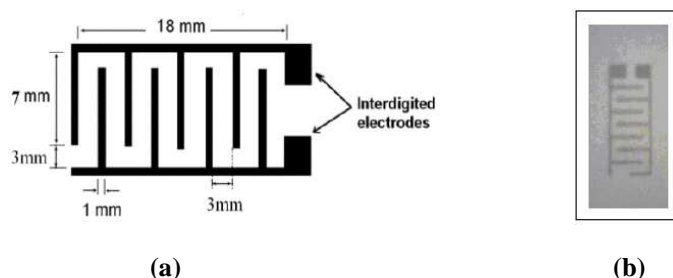
**Table 1** Samples Codes of Series: CuO: WO<sub>3</sub>/Al<sub>2</sub>O<sub>3</sub>/GP

Sample Code	Composition of CuO (mole %)	Composition of WO <sub>3</sub> (mole %)
B1	5	95
B2	10	90
B3	15	85
B4	20	80
B5	25	75
B6	30	70
PC	100	0
PW	0	100

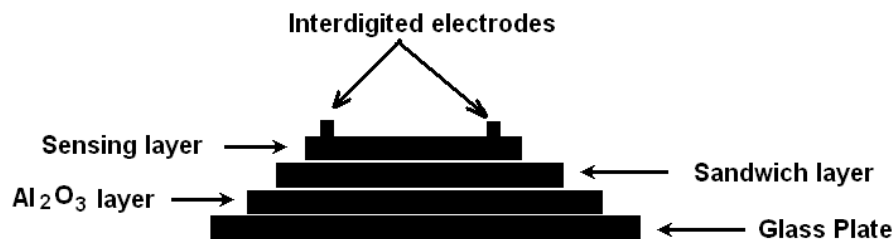
Out of various methods of sensors preparation, the screen-printing (thick film technology) is most widely used. Screen-printing is the transfer of pastes through a fabric screen onto a substrate.

**Multilayer preparation**

Fig. 1 (a), and 1(b) show fabrication of interdigitated electrodes, actual photographs of interdigitated electrodes respectively.



**Fig. 1** (a) Fabrication of interdigitated Electrodes (b) Actual photograph of interdigitated electrodes



**Fig.2** Design of multilayer Sensor

On clean glass plate, Al<sub>2</sub>O<sub>3</sub> was deposited by using screen-printing technique and it was used as base of the sensor. On Al<sub>2</sub>O<sub>3</sub>, the sample layers were prepared. Finally on the top, Interdigitated electrodes were fabricated [21] using conducting silver paste as shown in the Fig. 1(b). Design of multilayer sensor is shown in Fig. 2.

### Preparation of Samples of Series: CuO: WO<sub>3</sub> / Al<sub>2</sub>O<sub>3</sub>/GP

The obtained product of fine nanopowder of CuO and WO<sub>3</sub> are used for fabrication of thick films sensors by using screen-printing technique. For this, the different X mole% CuO powder (X = 05, 10, 15, 20, 25, 30) was mixed thoroughly with different X mole% of WO<sub>3</sub> (X = 95, 90, 85, 80, 75, 70) along with Al<sub>2</sub>O<sub>3</sub> base on glass plate (GP) substrate the aid of acetone by using the mortar and pestle. The sample codes, mole% of powder, and thickness are listed in the Table 2.. The mixed powder of CuO : WO<sub>3</sub> system was further calcinated at temperature 800°C for 5hrs. in the autocontrolled muffle furnace (*Gayatri Scientific, Mumbai, India.*) After, the calcinations again uniformly mixed the powder using the grinder.

**Table 2** Thickness of Multi-layers for Series: CuO: WO<sub>3</sub> / Al<sub>2</sub>O<sub>3</sub>/GP Gas Sensors.

Sample Code	Composition	Thickness (x 10 <sup>-4</sup> cm)		
	Layers:----	Upper Layer(1)	Al <sub>2</sub> O <sub>3</sub> Layer(2)	Total (1+2)
	Upper /Al <sub>2</sub> O <sub>3</sub> /Glass plate (GP)			
B1	05CuO:95 WO <sub>3</sub> / Al <sub>2</sub> O <sub>3</sub> /GP	4.1	29.3	33.4
B2	10CuO:90 WO <sub>3</sub> / Al <sub>2</sub> O <sub>3</sub> /GP	3.8	28.5	32.3
B3	15CuO:85 WO <sub>3</sub> / Al <sub>2</sub> O <sub>3</sub> /GP	2.6	29.7	32.3
B4	20CuO:80 WO <sub>3</sub> / Al <sub>2</sub> O <sub>3</sub> /GP	3.9	28.8	32.7
B5	25CuO:75 WO <sub>3</sub> / Al <sub>2</sub> O <sub>3</sub> /GP	4.9	28.1	33
B6	30CuO:70 WO <sub>3</sub> / Al <sub>2</sub> O <sub>3</sub> /GP	4.1	30.2	34.3

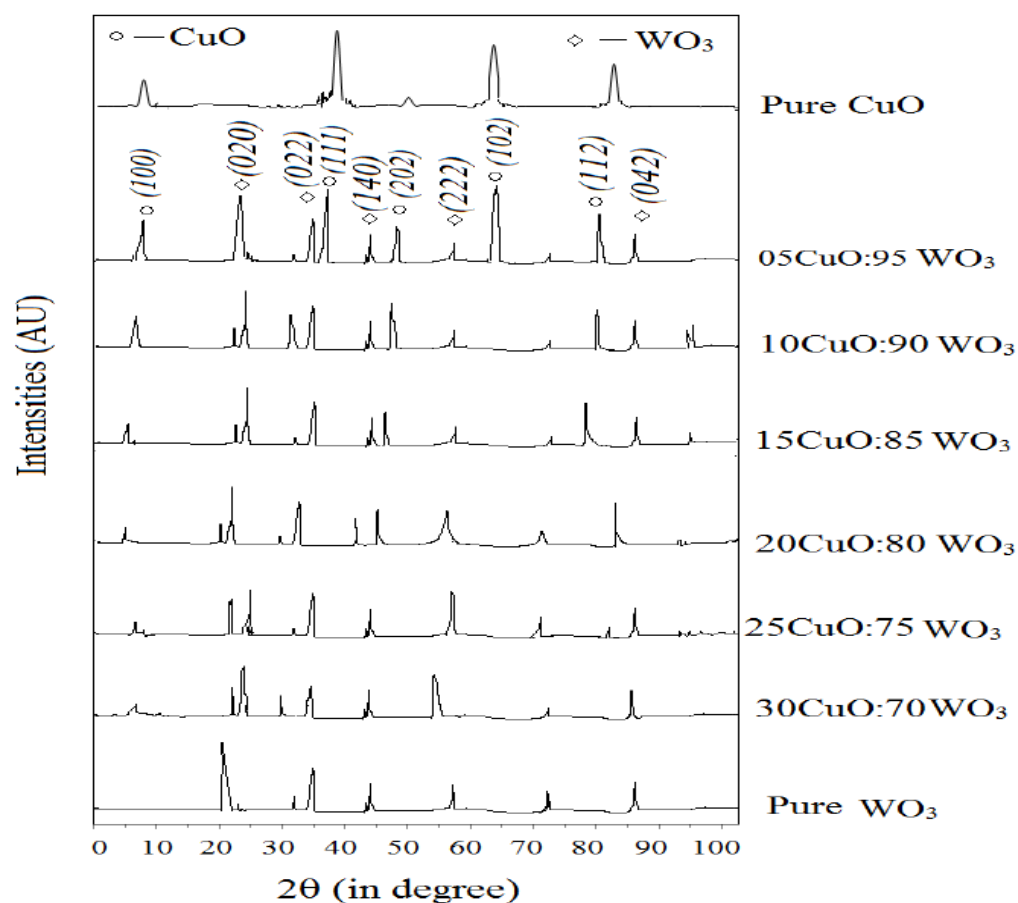
## RESULTS AND DISCUSSION

### XRD of CuO & WO<sub>3</sub> Nanomaterial and their dopings

The average crystallite size was calculated by Debye-Scherrer's equation with the help of XRD patterns as shown in figure 3. The strong and sharp peak of CuO observed at 37° position with (1 1 1) indicates that the sample is having high crystalline quality, and it is in the structure of monoclinic with lattice parameters a = 0.4685 nm, b = 0.3532 nm, and c = 0.5121 nm, which is good agreement with JCPDS card number 88-2341. The average crystalline size was obtained 27 nm from Debye-Scherrer's equation,  $D = \frac{K\lambda}{\beta \cos\theta}$

Where, D = nanoparticles crystalline size, K = Scherrer constant (0.98),  $\lambda$  = wavelength and  $\beta$  denotes the full width at half maximum (FWHM).

As shown in figure 3. spectra, main peak, in case of pure WO<sub>3</sub>, is observed at 23.21° and this peak corresponds to the plane (0 2 0) of WO<sub>3</sub> in monoclinic structure (JCPDS Card No.3-1124) with 100% intensity. The other peaks of WO<sub>3</sub> mainly correspond to the crystalline planes (0 2 2), (1 4 0), (2 2 2), (0 4 2), matching well with the monoclinic structure of WO<sub>3</sub>. This manifested that the WO<sub>3</sub> is well crystallized. As compared with diffraction peaks of WO<sub>3</sub>, those of CuO are wide and weak due to small grain sizes [22]. From table 3., it is seen that the sample 25CuO:75 WO<sub>3</sub> has small crystalline size.



**Fig.3.** XRD spectra of Pure CuO, Pure WO<sub>3</sub> and CuO doped with WO<sub>3</sub> Nanomaterial

The crystallite size (D) of WO<sub>3</sub> and CuO doped WO<sub>3</sub> was calculated from Scherer's formula using FWHM and it is listed in the table 3, as below.

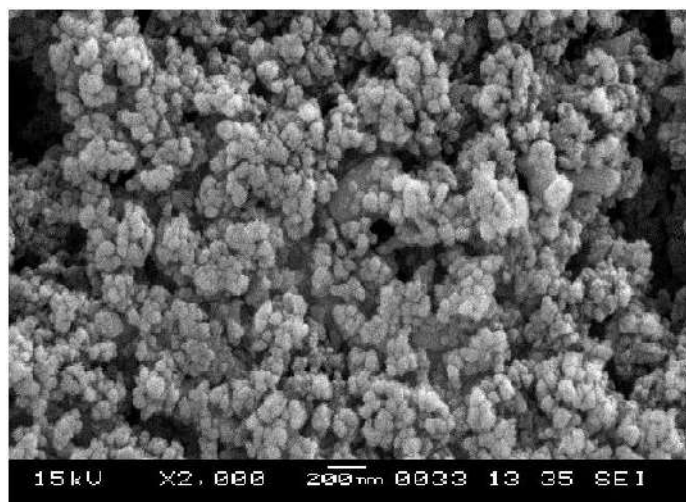
**Table 3.** Average crystallite size of WO<sub>3</sub> and CuO doped WO<sub>3</sub>

Chemical Composition of CuO:WO <sub>3</sub> (mole %)	Maximum Intensity Peak Position (2θ) degree	FWHM (2θ) degree	Average Crystallite Size (D) in nm
05CuO:95 WO <sub>3</sub>	28.34	0.2634	112.51
10CuO:90 WO <sub>3</sub>	29.23	0.2112	126.67
15CuO:85 WO <sub>3</sub>	30.65	0.2217	118.23
20CuO:80 WO <sub>3</sub>	31.45	0.1934	109.83
<b>25CuO:75 WO<sub>3</sub></b>	<b>57.12</b>	<b>0.1732</b>	<b>87.72</b>
30CuO:70 WO <sub>3</sub>	53.89	0.1994	105.45
Pure WO <sub>3</sub>	23.04	0.3214	143.22

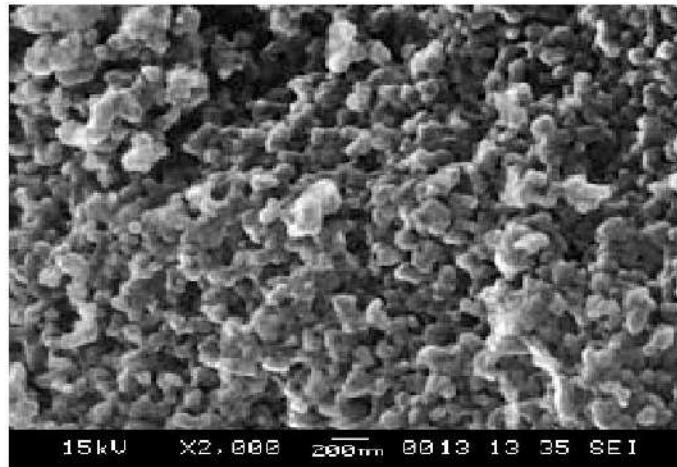


**Scanning electron microscopy (SEM) Analysis**

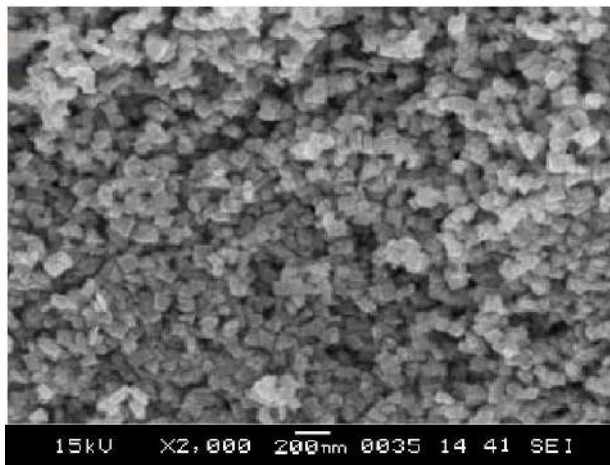
From SEM picture (figure 4 (a) to (c)), it is observed that all the samples viz.  $\text{Al}_2\text{O}_3$ ,  $\text{CuO}$ ,  $\text{WO}_3$  are porous in nature. Porosity varies with sample to sample and among these material,  $\text{SnO}_2$  showed more porosity (small size ~ 60 to 80 nm). Due to small pores size, its surface area is more [22-23] and it shows more sensing nature. Some portion of SEM picture shows some rods with fine voids over them which helps to increase sensing properties. The surface morphology of pure  $\text{Al}_2\text{O}_3$ ,  $\text{CuO}$ , and  $\text{WO}_3$ , nano materials were studied by SEM and its picture is shown in the Fig. 4.



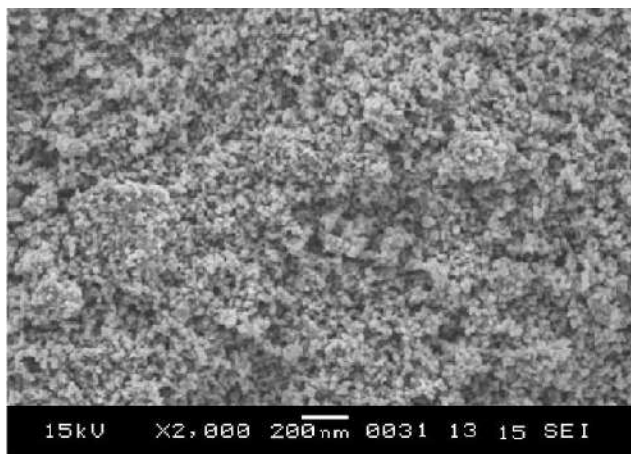
*Fig. 4 (a) SEM picture of  $\text{Al}_2\text{O}_3$*



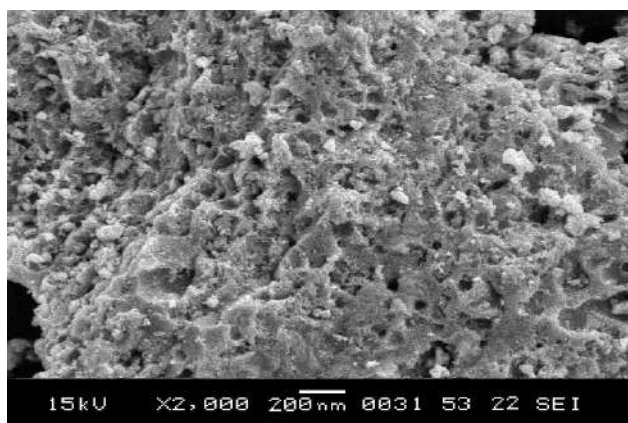
*Fig. 4 (b) SEM picture of  $\text{CuO}$*



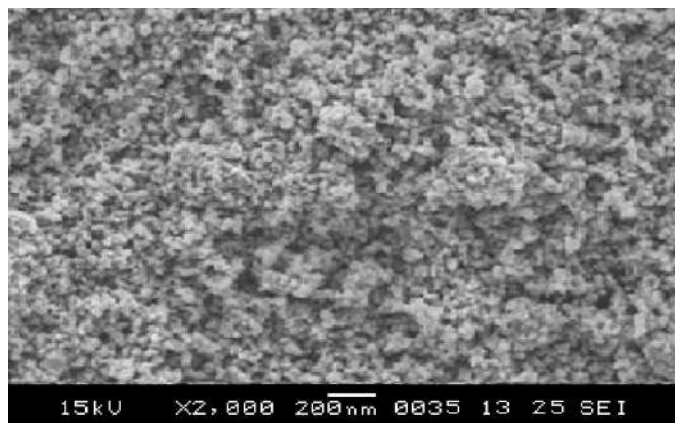
*Fig. 4 (c) SEM picture of WO<sub>3</sub>*



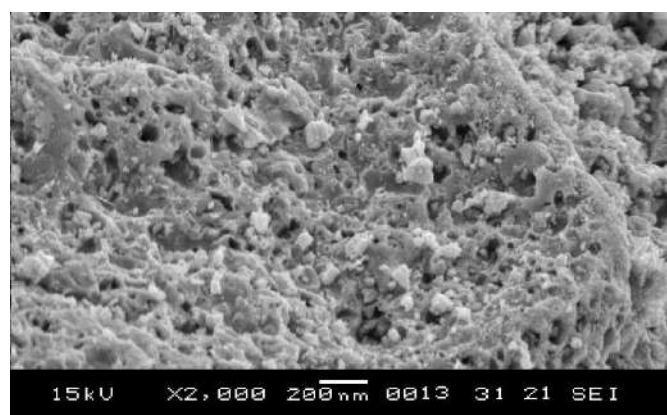
*Fig. 4 (d) SEM picture of 05CuO:95WO<sub>3</sub>*



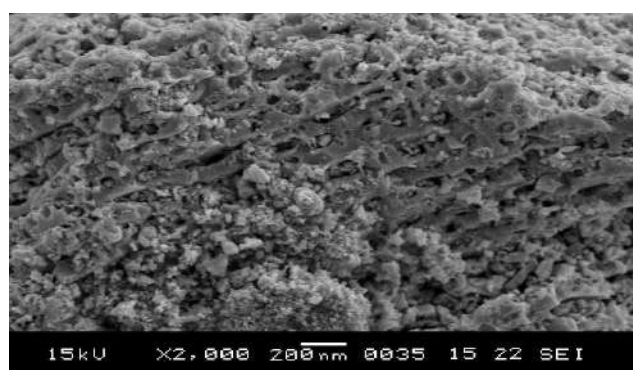
*Fig. 4. (e) SEM picture of 10CuO:90WO<sub>3</sub>*



*Fig. 4. (f) SEM picture of 15CuO:85WO<sub>3</sub>*



*Fig. 4. (g) SEM picture of 20CuO:80WO<sub>3</sub>*



*Fig. 4. (h) SEM picture of 25CuO:75WO<sub>3</sub>*

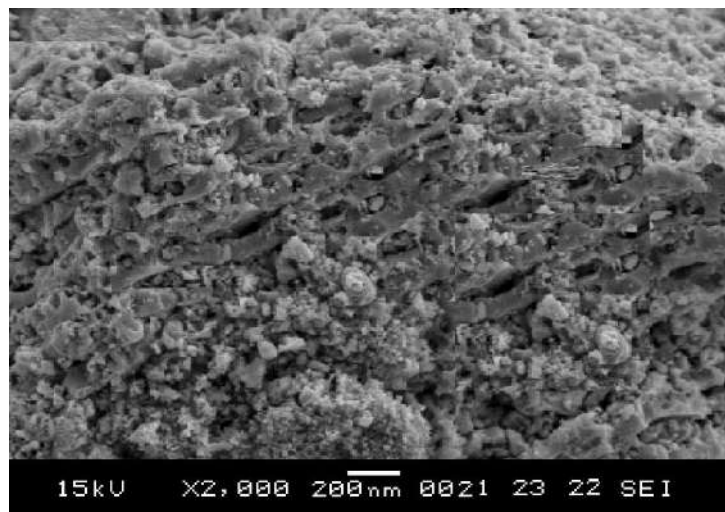


Fig. 4. (i) SEM picture of 30CuO:70WO<sub>3</sub>

#### Fig. 4. SEM picture of Samples of Series CuO:WO<sub>3</sub>

The surface morphologies of pure Al<sub>2</sub>O<sub>3</sub>, CuO, WO<sub>3</sub>, and their dopings materials were studied by SEM and its picture are shown in the figures 4. As shown in the SEM pictures, some pores are in the form of rods, some are the form of circles and some are in conical shapes [24].

Table 4. shows the average diameter and number of pores per inch of pure Al<sub>2</sub>O<sub>3</sub>, CuO, WO<sub>3</sub> and their dopings.

Table 4. Average diameter of pore and number of pores per inch of pure samples and their dopings.

Sample Code	Pure sample and their dopings (mole %)	Average diameter of pore (nm)	Number of pores per inch (in x 2000 magnification)
PA	Al <sub>2</sub> O <sub>3</sub>	95	154
PC	CuO	80	172
PW	WO <sub>3</sub>	98	145
B1	05CuO:95WO <sub>3</sub>	73	155
B2	10CuO:90WO <sub>3</sub>	82	143
B3	15CuO:85WO <sub>3</sub>	79	158
B4	20CuO:80WO <sub>3</sub>	83	138
B5	<b>25CuO:75WO<sub>3</sub></b>	<b>52</b>	<b>218</b>
B6	30CuO:70WO <sub>3</sub>	71	177

From the SEM pictures (table 4), it is observed that, Sample Code B5 i.e. (**25CuO:75WO<sub>3</sub>**), have more pores per inch (calculated for x 2,000 magnification for each composition) than other sensors. Thus, these sensors have more active surface areas and exhibit more sensing nature [24-25]. It is also found that average diameter of pore in case of Sample Code B5 i.e. (**25CuO:75WO<sub>3</sub>**) are small as compared to other doping. This also tends to exhibit large surface area and exhibited high response of the samples.

## CONCLUSIONS

The XRD pattern of (CuO-WO<sub>3</sub>) system samples show nanocrystalline form and found the desired peaks of composites. FESEM study reveals that the grain size of nanometer order and shows nano-porous structure, which leads to exhibit large surface area, stability and highest response. Therefore the B5 sensor (**25CuO:75WO<sub>3</sub>**) is found to optimized multilayer thick film sensor.

## REFERENCES

1. Sanjay Srivastava, Mahendra kumar, Arvind Agrawal and Sudhanshu Kumar Dwivedi, Synthesis and Characterisation of Copper Oxide nanoparticles, 2013, IOSR Journal of Applied Physics (IOSR-JAP) Volume 5, Issue 4 PP 61-65.
2. S. M. Sathiya, G. S. Okram, M. A. Jothi Rajan, 2017, Structural, optical and electrical properties of copper oxide nanoparticles prepared through microwave assistance, *Advanced Materials Proceedings*, 2(6), 371-377, DOI: 10.5185/amp.2017/605
3. R. Chopra, N. Kashyap, Amit Kumar, D. Banerjee, 2020 Chemical synthesis of copper oxide nanoparticles study of its optical and electrical properties, *International Journal of Engineering Research & Technology (IJERT)* ISSN: 2278-0181, Vol. 9 Issue 01, IJERTV9IS010160
4. S. Thamaraiselvi, G. Thenmozhi, 2022, Synthesis of CuO Nanoparticles by using Simple Precipitation Method, *International Journal of Science and Research (IJSR)* ISSN: 2319-7064, Volume 11 Issue 4, DOI: 10.21275/SR22425202059
5. Nataly Silva, Sara Ramírez, Isaac Díaz, Andreina Garcia and Natalia Hassan, 2019, Easy, Quick, and Reproducible Sonochemical Synthesis of CuO Nanoparticles, *Materials*, 12, 804; doi:10.3390/ma12050804
6. Kailash R. Nemade and Sandeep A. Waghuley, 2014, Optical and Gas Sensing Properties of CuO Nanoparticles Grown by Spray Pyrolysis of Cupric Nitrate Solution, *International Journal of Materials Science and Engineering* Vol. 2, No. 1, doi: 10.12720/ijmse.2.1.63-66
7. Panya Khaenamkaew, Dhonluck Manop, Chaileok Tanghengjaroen and Worasit Palakawong Na Ayuthaya, 2020 Crystal structure, lattice strain, morphology, and Electrical Properties of SnO<sub>2</sub> nanoparticles induced by low calcination temperature, *Advances in Materials Science and Engineering*, Article ID 3852421, <https://doi.org/10.1155/2020/3852421>
8. Sitthisuntorn Supothina, Panpailin Seeharaj, Sorachon Yoriya, Mana Sriyudthsak, 2007, Synthesis of tungsten oxide nanoparticles by acid precipitation method, *Ceramics International* 33, 931–936, doi:10.1016/j.ceramint.2006.02.007
9. X.C. Song, Y.F. Zheng, E. Yang and Y. Wang, 2007, Large-scale hydrothermal synthesis of WO<sub>3</sub> nanowires in the presence of K<sub>2</sub>SO<sub>4</sub>, *Mater. Lett.* 61, 3904–3908. <https://doi.org/10.1016/j.matlet.2006.12.055>.
10. L. Xiong, T. He, 2006, Synthesis and characterization of ultrafine tungsten and tungsten oxide nanoparticles by a reverse microemulsion-mediated method, *Chem. Mater.* 18, 2211–2218. <https://doi.org/10.1021/cm052320t>
11. M. Jamali, F and Shariatmadar Tehrani, 2020, Effect of synthesis route on the structural and morphological properties of WO<sub>3</sub> nanostructures, *Mater. Sci. Semicond. Process.* 107, 104829. <https://doi.org/10.1016/j.mssp.2019.104829>
12. P. Gibot, M. Comet, L. Vidal, F. Moitrier, F. Lacroix, Y. Suma, F. Schnell and D. Spitzer, 2011, Synthesis of WO<sub>3</sub> nanoparticles for superthermites by the template method from silica spheres, *Solid State Sci.* 13, 908–914. <https://doi.org/10.1016/j.solidstatesciences.2011.02.018>
13. Yu Il, Lee, Don-Kyu, Shin, Deuck-Jin, Yu, Yoon-Sik, 2010, Characteristics of CuO doped WO<sub>3</sub> Thick Film for Gas Sensors, *The Transactions of The Korean Institute of Electrical Engineers* Volume 59 Issue 9 / Pages.1621-1625 /1975-8359 (pISSN) / 2287-4364 (eISSN) <https://doi.org/10.5370/KIEE.2010.59.9.1621>
14. Artur Rydosz, Wojciech Maziarz, Tadeusz Pisarkiewicz, Krzysztof Wincza, Sławomir Gruszczyński, *Deposition of Nanocrystalline WO<sub>3</sub> and CuO Thin Film in View of Gas Sensor Applications*, ISBN: 978-0-9891305-4-7 ©2014 SDIWC
15. Nirmal Kumar, Stanislav Haviar, Jiri Capek, Sarka Batkova, Pavel Baroch, 2018, Nanostructured Metal-Oxide Based Hydrogen Gas Sensor Prepared by Magnetron Sputtering, *StudenskaVedecka Konference*

16. Fuchao Yang a, Fengyi Wang a, Zhiguang Guo, 2018, Characteristics of binary WO<sub>3</sub>@CuO and ternary WO<sub>3</sub>@PDA@CuO based on impressive sensing acetone odor, *Journal of Colloid and Interface Science* 524, 32–41, <https://doi.org/10.1016/j.jcis.2018.04.013>
17. Soo-Yeon Cho, Doohyung Jang, Hohyung Kang, Hyeong-Jun Koh, Junghoon Choi, and Hee-Tae Jung, 2019, Ten Nanometer Scale WO<sub>3</sub>/CuO Heterojunction Nanochannel for an Ultrasensitive Chemical Sensor, *Anal. Chem.*, 91, 6850–6858, DOI: 10.1021/acs.analchem.9b01089
18. K. B. Raulkar, (2019), Study on sensitivity of nano SnO<sub>2</sub>-ZnO composites with and without PPy layer for sensing CO<sub>2</sub> gas, 2019, *Materials Today: Proceedings* 15, 604–610.
19. Dmitry Bokov, Abduladheem Turki Jalil, Supat Chupradit, Wanich Suksatan, Mohammad Javed Ansari, 6 Iman H. Shewael, Gabdrakhman H. Valiev, and Ehsan Kianfar, (2021), Review Article, *Nanomaterial by Sol-Gel Method: Synthesis and Application, Advances in Materials Science and Engineering Volume 2021*, <https://doi.org/10.1155/2021/5102014>
20. Zahrah Alhalili, (2023), Review Metal Oxides Nanoparticles: General Structural Description, Chemical, Physical, and Biological Synthesis Methods, Role in Pesticides and Heavy Metal Removal through Wastewater Treatment, *Molecules*, 28, 3086. <https://doi.org/10.3390/molecules28073086>
21. Khaled Tawfik Alali, Jingyuan Liu, Kassem Aljebawi, Peili Liu, Rongrong Chen, Rumin Li, Hongquan Zhang, Limin Zhou, Jun Wang, 2019, Electrospun n-p WO<sub>3</sub>/CuO heterostructure nanofibers as an efficient sar in nerve agent sensing material at room temperature, *Journal of Alloys and Compounds* 793, 31e41, <https://doi.org/10.1016/j.jallcom.2019.04.157>
22. Fang Peng, Yan Sun, Weiwei Yu, Yue Lu, Jiaming Hao, Rui Cong Jichao Shi, Meiyong Ge and Ning Dai, 2020, ‘Gas Sensing Performance and Mechanism of CuO(p)-WO<sub>3</sub>(n) Composites to H<sub>2</sub>S Gas.’ *Nanomaterials*, 10, 1162; doi:10.3390/nano10061162
23. Quentin Simon, Davide Barreca, Alberto Gasparotto, Chiara Maccato, Eugenio Tondello, Cinzia Sada, Elisabetta Comini, Giorgio Sberveglieri, Manish Banerjee, Ke Xu, Anjana Devi, and Roland A. Fischer, CuO/ZnO Nanocomposite Gas Sensors Developed by a Plasma-Assisted Route, *ChemPhysChem* 0000, 00, 1 – 8, DOI:10.1002/cphc.201101062
24. Yalu Chen, Zhurui Shen, Qianqian Jia, Jiang Zhao, Zhe Zhao, Huiming Ji, 2013, A CuO-ZnO Nanostructured p-n Junction Sensor for Enhanced N-butanol Detection, *The Royal Society of Chemistry*, DOI: 10.1039/x0xx00000x
25. Raulkar K.B, Wasnik T.S, Joat R.V., Wadtkar A.S. Agrawal, R.M. and Lamdhade G.T., (2019). Study on DC Conductivity of PPy-ZnO Nanocomposites, *Materials today Proceedings*, 15(3), 595-603.

# Investigation of Dielectric Constant of PVC-PMMA Thin Films Doped with Salicylic Acid at Different Frequency, Dopant and Temperature<sup>1</sup>

A.B.More, G.T. Lamdhade, K.B.Raulkar

*Department of physics, Vidya Bharati Mahavidyalaya, C.K Naidu Road, Camp, Amravati, M.S. India 444602*

---

## ABSTRACT

This research study examines the influence of frequency and salicylic acid dopant and temperature on the dielectric constant of PVC-PMMA thin films. The thin films were prepared using the isothermal evaporation technique, and their dielectric constants were measured using an LCR meter over a frequency range of 20 Hz to 200 KHz at 303 k and 323 k. The  $\ln f$  vs dielectric constant plots were analyzed to investigate the effects of frequency and salicylic acid dopant concentration and temperature on the dielectric properties of the films.

**Keyword:** PVC; PMMA; Salicylic Acid; Dielectric Constant.

## INTRODUCTION

Dielectric materials find extensive applications in various electronic devices and capacitors due to their ability to store and transmit electrical energy. Polymer blends, such as PVC-PMMA, have gained significant attention for their potential in dielectric applications. The dielectric properties of such blends can be modified by incorporating dopants, offering opportunities for enhanced electrical performance.

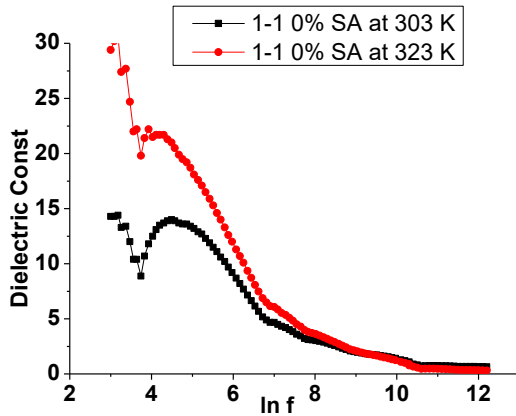
## EXPERIMENTAL PROCEDURE

The PVC-PMMA thin films were prepared by the isothermal evaporation technique. Two sets of films were fabricated: one with a 6% salicylic acid dopant and the other without any dopant. The dielectric constants of the films were measured using an LCR meter over a frequency range of 20 Hz to 200 kHz at 303 k and 323 k. The natural logarithm of frequency ( $\ln f$ ) and dielectric constant values were recorded and tabulated for further analysis.

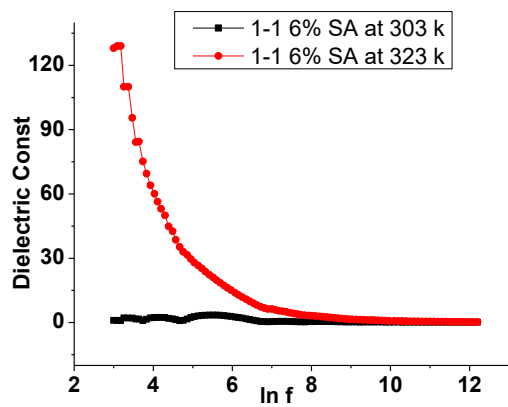
---

<sup>1</sup> How to cite the article: More A.B., Lamdhade G.T., Raulkar K.B., (2023); Investigation of Dielectric Constant of PVC-PMMA Thin Films Doped with Salicylic Acid at Different Frequency, Dopant and Temperature; *Multidisciplinary International Journal*; Vol 9 (Special Issue), 318-322

**GRAPH RELATED FOR DIELECTRIC CONSTANT**



**Fig 1.1 Variation of  $\ln f$  vs Dielectric constant**



**Fig 1.2 Variation of  $\ln f$  vs Dielectric constant**



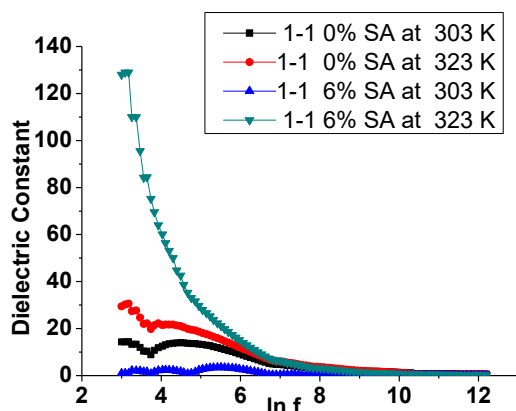


Fig 1.3 Variation of  $\ln f$  vs. Dielectric constant doped and undoped SA

## RESULTS AND DISCUSSION

The  $\ln f$  vs. dielectric constant (fig1.1, 1.2, 1.3) plots were examined to analyze the effects of frequency and salicylic acid dopant on the dielectric properties of the PVC-PMMA thin films.

### Effect of Frequency

The dielectric constant of the PVC-PMMA films exhibited a frequency-dependent behavior. As the frequency increased, the dielectric constant decreased for both the film with 6% salicylic acid dopant and the film without any dopant. This behavior is consistent with the characteristics of dielectric materials, where the dielectric constant decreases with increasing frequency.

The behavior of the dielectric constant of a material in response to varying frequencies of an electric field provides valuable insights into its electrical and structural properties. The observed trends in the dielectric constant of the PVC-PMMA thin film can be explained through the interaction of the polymer matrix with the electric field, as well as the inherent characteristics of the system.

#### 1. High Dielectric Constant at Lower Frequencies:

In the lower frequency range, it is observed that the dielectric constant of the PVC-PMMA thin film is relatively high. The high dielectric constant can be attributed to the presence of charges that are able to respond to the electric field. In the case of the PVC-PMMA thin film, the presence of localized charge carriers, such as polarons, might contribute to this behavior. These charges can align and respond to the field, leading to an enhanced dielectric constant.

#### 2. Decrease in Dielectric Constant at Higher Frequencies:

As the frequency of the applied electric field increases beyond 100 Hz, the dielectric constant of the PVC-PMMA thin film is observed to decrease. This decrease can be attributed to the interplay between the ordered structure of the material and the mobility of ions within the polymer matrix. At higher frequencies, the mobility of ions becomes significant, allowing them to move and oppose the effect of the applied electric field.

The decrease in dielectric constant could be explained by considering the following factors:

##### i. Ordered Material Characteristics:

In materials with an ordered structure, such as crystalline regions within the PVC-PMMA thin film, the alignment of charges in response to the electric field can be hindered by the organized arrangement of molecules. This leads to a lower dielectric constant as the material becomes less responsive to the field.

**ii. Ionic Mobility:**

As the frequency increases, the mobility of ions within the polymer matrix becomes more pronounced. These ions are not tightly bound to the polymer chains and can move in response to the field, counteracting its effect. This ion movement contributes to a decrease in the overall dielectric constant.

The findings presented in Migahed et al.'s work (reference [24]) further support the observed trend of decreasing dielectric constant with increasing frequency in ordered materials.

**Influence of Temperature on Dielectric Constant in PVC-PMMA Films**

The dielectric constant of the PVC-PMMA films was also affected by temperature. As the temperature increased from 303 K to 323 K, the dielectric constant values for both the film with 6% salicylic acid dopant and the film without any dopant generally increased. This temperature-dependent behavior indicates that the dielectric constant of the films is influenced by thermal effects.

Temperature is a critical parameter that can significantly impact the electrical properties of materials, including the dielectric constant. In this study, the effect of temperature on the dielectric constant of PVC-PMMA films was investigated. The dielectric constant was analyzed across a temperature range, and the results reveal a clear correlation between temperature and dielectric constant values.

**Influence of Salicylic Acid Dopant on Dielectric Constant in PVC-PMMA Films**

The presence of salicylic acid dopant influenced the dielectric constant behavior of the PVC-PMMA films. Comparing the two sets of films, it was observed that the film with 6% salicylic acid dopant consistently exhibited higher dielectric constant values compared to the film without any dopant at all frequencies and temperatures. This suggests that the addition of salicylic acid as a dopant increases the dielectric constant of the PVC-PMMA films.

The dielectric constant of a material is a key parameter that characterizes its electrical response to an applied electric field. In this study, the impact of salicylic acid as a dopant on the dielectric constant behavior of PVC-PMMA films was investigated. The dielectric constant was examined across a range of frequencies and temperatures to elucidate the effects of the dopant on the electrical properties of the films.

**CONCLUSION**

In conclusion, the observed frequency-dependent behavior of the dielectric constant in the PVC-PMMA thin film is a result of the interplay between the presence of charges, the ordered or disordered nature of the material, and the mobility of ions within the polymer matrix. The high dielectric constant at lower frequencies can be attributed to the response of charges to the electric field, while the decrease in dielectric constant at higher frequencies is influenced by the ordered structure of the material and the mobility of ions. These insights contribute to a deeper understanding of the electrical properties of the PVC-PMMA thin film.

The presence of 6% salicylic acid dopant in the PVC-PMMA films leads to a consistent increase in the dielectric constant values across frequencies and temperatures. This effect can be attributed to enhanced polarization, dipole alignment, and possibly improved charge carrier mobility within the polymer matrix due to the presence of the dopant. These findings underscore the potential of salicylic acid as a dopant to tailor the dielectric properties of PVC-PMMA films for specific applications requiring higher dielectric constants. Further investigations could delve into the underlying molecular interactions that drive this enhanced dielectric behavior.

**REFERENCES**

1. Vdhale. S.G., Belsare N. G., November(2013), International Journal of Scientific & Engineering Research, Volume4, Issue11, 1253, <https://doi.org/10.14299/ijser.2013.11>
2. Dakre, A. B., & Lamdhade, G. T. (2014). International Journal of Science and Research (IJSR), 3(6).
3. Ojha. P., Siddaiah. T., Gopal, N. O., & Ramu, Ch. (2018). International Journal of Scientific Research in Physics and Applied Sciences, 6(6), 80-87. <https://doi.org/10.26438/ijsrpas/v6i6.8087>

4. Tanwar, A., Gupta, K. K., Singh, P. J., & Vijay, Y. K. (2006). *Bull. Mater. Sci.*, 29(4), 397–401. <https://doi.org/10.1007/bf02704142>
5. Vidhale S.G., Belsare N.G., A.S.Wadatar, September-(2013), *International Journal of Scientific & Engineering Research*, Volume 4, Issue 9.
6. Renukappa, N. M., Sudhakar, S. R. D., Siddaramaiah, R., Rajan, J. S., & Vishvanathan. (2007). *ICPMPE*.
7. Abraham, R., Issac, J., Varughese, K., & Thomas, S. (2007). *ICPMPE*.
8. Mamza, P. A., & Folaranmi, F. M. (1996). *European Polymer Journal*, 32(7), 909-912.
9. Dandel, R. M., Belsare, N. G., & Raghuvanshi, F. C. (2011). *International Journal of Polymers and Technologies*, 3(2).
10. Ramesh, S., & Liew, C. W. (2013). *Measurement*, 46(5), 1650-1656. <https://doi.org/10.1016/j.measurement.2013.01.003>.
11. Wadatar, A. S., Wasnik, T. S., Vidhale, S. G., & Belsare, N. G. (2014). *International Journal of Basic and Applied Research*, 4, 196-200.
12. Ahmad, A. H. (2014). *International Journal of Computer Science*, 2, 20-23.
13. Bushra, A. H., Ahmad, A. H., & Duaa, A. U. (2013). *International Journal of Application or Innovation in Engineering & Management*, 2(11), 86.
14. Khaled, M. A., Elwa, Y. A., Hussein, A. M., & Abdullah, K. (2003). *Egypt Journal*, 26(1), 83-91.
15. Sharma, D., & Tripathi, D. (2018). *AIP Conference Proceedings*, 1953(1), 050056. <https://doi.org/10.1063/1.5032711>
16. Rajendran, S., & Uma, T. (2000). *Materials Letters*, 44, 242-247.
17. Raja, V., Sharma, A. K., & Narasimha Rao, V. V. R. (2004). *Materials Letters*, 58, 3242-3247. <https://doi.org/10.1016/j.matlet.2004.05.061>
18. Elizabeth, R. N., Kalyanasundaram, S., Gopalan, A., & Saito, Y. (2004). *Polímeros: Ciencia e Tecnologia*, 14(1), 1-7.
19. Suvarna, R. P., Raghavendra Rao, K., & Subbarangaiah, K. (2002). *Bull. Mater. Sci.*, 25(7), 647-651.
20. Roaramadan, E., Ahmad Abass Hasan (2014), *PASJ International Journal of Computer Science (IIJCS)*, 2(3).
21. Khan, M. S., Gul, R., & Wahid, M. S. (2013). *J Polym Eng*, 33(7), 633-638. <https://doi.org/10.1515/polyeng-2013-0028>
22. El Sayed, A. M. (2020). *Results in Physics*, 17, 103025. <https://doi.org/10.1016/j.rinp.2020.103025>
23. Kyritsis A., Pissi P., Grammatikakis I., (1995). *J. Polymer Sci. Part B*.33 173-77.
24. Migahed, M.D., Ishra, M., Fahmy, T., Basakat, (2004). *A., J. of Phys. and Chem. of Solids* 65, 1121-1125
25. Devikala S., Kamaraj P. and Arthanareeswarl M., *Chem Sci Trans.*, 2013, 2(S1), S129-S134 DOI:10.7598/cst2013.26

# Cupric Oxide (CuO) Doped Tin Oxide (SnO<sub>2</sub>) MOS Multilayer CO<sub>2</sub> Gas Sensor

\*Mankar S.S., \*\*Lamdhade G.T., \*\*Raulkar K.B

\*Department of Physics, Shivramji Moghe Arts, Commerce and Science College, Kelapur, Pandharkawada, Dist. Yavatmal, M.S. India

\*\*Department of Physics, Vidya Bharati Mahavidyalaya, CK Naidu Road, Amravati, M.S. 444 602 India

DOI:10.37648/ijrst.v13i03.013

<sup>1</sup>Received: 14 August 2023; Accepted: 18 September 2023; Published: 23 September 2023

---

## ABSTRACT

Nanoparticles of cupric oxide and tin oxide are synthesized via liquid-phase method. The samples are prepared in the form of multilayer thick films by screen printing technique having based of alumina, samples having different mol % of tin oxide and copper oxide.

CO<sub>2</sub> gas concentration increases from 600 ppm to 1500 ppm, there is little increase of sensitivity, from 600 ppm to 1100 ppm, sensitivity increases linearly and becomes maximum at 1100 ppm. With further increase in CO<sub>2</sub> gas concentration, sensitivity increases by little amount. The XRD pattern of (CuO-SnO<sub>2</sub>) system samples show nanocrystalline form and found the desired peaks of composites. FESEM study reveals that the grain size of nanometer order and shows nano- porous structure, which leads to exhibit large surface area, stability and highest response to CO<sub>2</sub> gas. The response time is faster than recovery time. The sample A3 sensor (15CuO:85SnO<sub>2</sub>) offers high sensitivity, rapid response and recovery to CO<sub>2</sub> gas.

**Keywords:** Nanoparticles; CuO-SnO<sub>2</sub>; multilayer thick films; CO<sub>2</sub> Gas Sensors

## INTRODUCTION

Semiconductor gas sensor is known as metal oxide semiconductor gas sensors. Metal oxide Semiconductor sensors (MOS) are also known as chemiresistive gas sensors and have been considered as solid-state gas-sensing materials [1-3]. Khanidtha Jantasom et al. 2013 [4] studied gas sensing properties of SnO<sub>2</sub>-CuO Nanocomposites for CO<sub>2</sub> gas. XRD and SEM shows that SnO<sub>2</sub>-CuO nanocomposites have a tetragonal and monoclinic structure respectively. It was observed that the nanocomposite products were highly sensitivity to CO<sub>2</sub> gas at room temperature. Satyendra Singh et al. 2014 [5] prepared CuO-SnO<sub>2</sub> nanocomposite by sol-gel route as a sensor by using screen printing methods are used to fabricate thin and thick film samples respectively. For CuO-SnO<sub>2</sub> thick and thin films maximum response. Shrivanti Joshi et al. 2015 [6] used simple hydrothermal route method to form heterojunction nanocomposites between p-type CuO and n-type SnO<sub>2</sub>, which nanocomposite exhibited superior sensitivity with short response/recovery times. Fumin Ren et al. 2015 [7] for selectively sensing BTEX (benzene, toluene, ethylbenzene, and xylol) CuO/SnO<sub>2</sub> composites were prepared by a facile microwave-assisted approach. Gas sensing results shows that the sensor based on 3 mol% CuO/SnO<sub>2</sub> composite has the best selectivity and sensitivity. Arindam Das and

---

<sup>1</sup> How to cite the article: Mankar S.S., Lamdhade G.T., Raulkar K.B. (September 2023); Cupric Oxide (CuO) Doped Tin Oxide (SnO<sub>2</sub>) MOS Multilayer CO<sub>2</sub> Gas Sensor; *International Journal of Research in Science and Technology*, Vol 13, Issue 3, 123-133, DOI: <http://doi.org/10.37648/ijrst.v13i03.013>

Dipankar Panda 2019 [8] prepared functional metal oxide of SnO<sub>2</sub> tailored by CuO via a coprecipitation chemical route followed by annealing in air.

Many metal oxides are suitable for detecting combustible, reducing, or oxidizing gases by conductive measurements. Composite metal oxides usually show better gas response than the single component if the catalytic actions of the components complement each other [9-10]. The main purpose of this work was to develop CuO doped SnO<sub>2</sub>, nano-crystalline composites sensors which operate at relatively low temperature and sensitive in low possible detection limit with better selectivity.

## EXPERIMENTAL

In the present work of paper, we have used sol-gel method (which is under liquid phase synthesis) for the synthesis of pristine nano-particles of CuO, SnO<sub>2</sub> and Al<sub>2</sub>O<sub>3</sub> [11-13]. All the chemicals used in this study were of GR grade purchase from Sd-fine, India (purity 99.99%). The chemicals are used without any further purification.

### Synthesis of Cupric Oxide (CuO)

In a cleaned round bottom flask, the aqueous solution of CuCl<sub>2</sub>·6H<sub>2</sub>O (0.2 M) was prepared. After addition of 1 ml of glacial acetic acid to above aqueous solution it was heated to 100°C with constant stirring. 8 M NaOH was added to above heated solution till its pH attains a value of 7. After this process immediately the color of the solution turned from blue to black and the large amount of black precipitate was obtained. The obtained precipitate was centrifuged and washed 3-4 times with de ionized water. The obtained powder was kept in vacuum oven at 70°C for 24 hours so as to get completely dried powder of CuO.

### Synthesis of Tin Oxide (SnO<sub>2</sub>)

For Synthesis of SnO<sub>2</sub> Stannous chloride dehydrate (SnCl<sub>2</sub>·2H<sub>2</sub>O), Ammonia Solution and de ionised water were used during reaction. All the chemicals used in this study were of GR grades are used without any further purification. 2 g (0.1 M) of stannous chloride dehydrate (SnCl<sub>2</sub>·2H<sub>2</sub>O) was dissolved in 100 ml water. When the complete dissolution occurs about 4 ml ammonia solution was added to this aqueous solution with continuous magnetic stirring. After the 20 minutes of stirring white gel precipitate was formed. This precipitate was allowed to settle for 12 hours. After this it was filtered and by using de-ionised water washed 2-3 times. The obtained precipitate were mixed with 0.27 g activated charcoal (carbon black powder). Then the powder was kept in vacuum oven at 70°C for 24 hours so as to get completely dried SnO<sub>2</sub> powder.

### Synthesis of Alumina (Al<sub>2</sub>O<sub>3</sub>)

All chemicals used were analytical grade. Aluminium chloride, AlCl<sub>3</sub> (MOLYCHEM), 25% NH<sub>3</sub> solution (QUALIGEN Fine Chemicals) and polyvinyl alcohol (PVA) were used as raw materials for the synthesis of aluminium oxide nanoparticles. 1M alcoholic AlCl<sub>3</sub> solution was prepared, followed by addition of 25% ammonia solution. The resulting solution turned to a white sol. This was followed by the addition of PVA (0.5M). The solution was stirred continuously using a magnetic stirrer until it became a transparent sticky gel. The gel was allowed to mature for 24 hours at room temperature. The resultant gel was heat treated at 100°C for 24 hours which led to the formation of light weight porous materials due to the enormous gas evolution. The dried gel was, then calcined at 1000°C for 4 hours and finally, the calcined powders were crushed using mortar and pestle to get the fine homogeneous dense powder of Alumina (Al<sub>2</sub>O<sub>3</sub>).

### Fabrication of Sensors

Three series of the samples prepared were CuO:SnO<sub>2</sub> with Al<sub>2</sub>O<sub>3</sub> base of multilayer sensors. The different combinations are shown in tables 1.

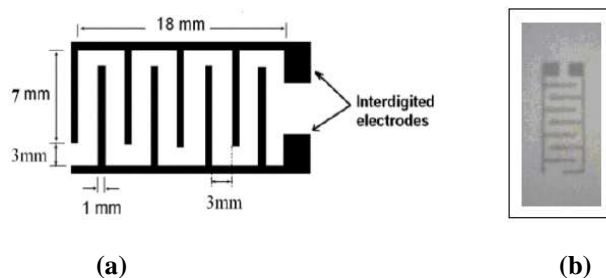
**Table 1** Samples Codes of Series: CuO: SnO<sub>2</sub>/Al<sub>2</sub>O<sub>3</sub>/GP

Sr. No.	Sample Codes	Composition of CuO (mole %)	Composition of SnO <sub>2</sub> (mole %)
1	A1	5	95
2	A2	10	90
3	A3	15	85
4	A4	20	80
5	A5	25	75
6	A6	30	70
7	PC	100	0
8	PS	0	100

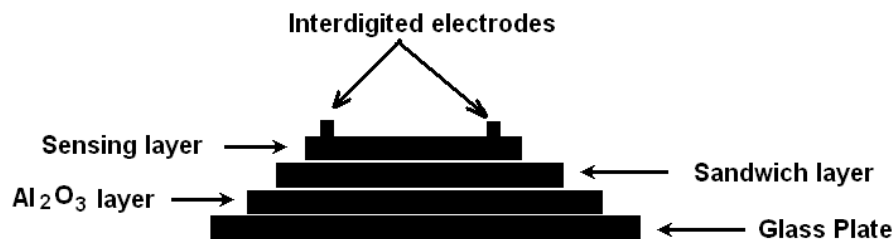
Out of various methods of sensors preparation, the screen-printing (thick film technology) is most widely used. Screen-printing is the transfer of pastes through a fabric screen onto a substrate.

### Multilayer preparation

Fig. 1 (a), and 1(b) show fabrication of interdigitated electrodes, actual photographs of interdigitated electrodes respectively.



**Fig. 1** (a) Fabrication of interdigitated Electrodes (b) Actual photograph of interdigitated electrodes



**Fig.2** Design of multilayer Sensor

On clean glass plate, Al<sub>2</sub>O<sub>3</sub> was deposited by using screen-printing technique and it was used as base of the sensor. On Al<sub>2</sub>O<sub>3</sub>, the sample layers were prepared. Finally on the top, Interdigitated electrodes were fabricated using conducting silver paste as shown in the Fig. 1(b). Design of multilayer sensor is shown in Fig. 2.

**Preparation of Samples of Series: CuO: SnO<sub>2</sub> / Al<sub>2</sub>O<sub>3</sub>/GP**

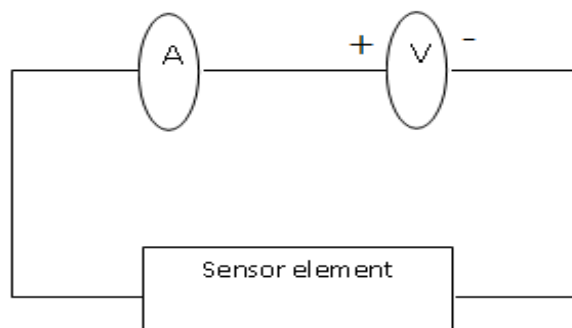
The obtained product of fine nanopowder of CuO and SnO<sub>2</sub> are used for fabrication of thick films sensors by using screen-printing technique. For this, the different X mole% CuO powder (X = 05, 10, 15, 20, 25, 30) was mixed thoroughly with different X mole% of SnO<sub>2</sub> (X = 95, 90, 85, 80, 75, 70) along with Al<sub>2</sub>O<sub>3</sub> base on glass plate (GP) substrate the aid of acetone by using the mortar and pestle. The sample codes, mole% of powder, and thickness are listed in the Table 2.. The mixed powder of CuO : SnO<sub>2</sub> system was further calcinated at temperature 800°C for 5hrs. in the auto-controlled muffle furnace (*Gayatri Scientific, Mumbai, India.*) After, the calcinations again uniformly mixed the powder using the grinder.

**Table 2** Thickness of Multi-layers for Series: CuO: SnO<sub>2</sub> / Al<sub>2</sub>O<sub>3</sub>/GP Gas Sensors.

Sample Code	Composition Layers:--- Upper /Al <sub>2</sub> O <sub>3</sub> /Glass plate (GP)	Thickness (x 10 <sup>-4</sup> cm)		
		Upper Layer(1)	Al <sub>2</sub> O <sub>3</sub> Layer(2)	Total (1+2)
		A1	05CuO:95SnO <sub>2</sub> / Al <sub>2</sub> O <sub>3</sub> /GP	4.1
A2	10CuO:90SnO <sub>2</sub> / Al <sub>2</sub> O <sub>3</sub> /GP	3.8	28.5	32.3
A3	15CuO:85SnO <sub>2</sub> / Al <sub>2</sub> O <sub>3</sub> /GP	2.6	29.7	32.3
A4	20CuO:80SnO <sub>2</sub> / Al <sub>2</sub> O <sub>3</sub> /GP	3.9	28.8	32.7
A5	25CuO:75SnO <sub>2</sub> / Al <sub>2</sub> O <sub>3</sub> /GP	4.9	28.1	33
A6	30CuO:70SnO <sub>2</sub> / Al <sub>2</sub> O <sub>3</sub> /GP	4.1	30.2	34.3

**Electrical Measurements**

Electrical measurements were performed with a Keithley 6487 voltages source cum picoammeter using setup shown in fig. 3. A constant voltage source in the range 1 to 10V is supplied to the sensor electrodes and the current through the sensor measured. The sensor resistance can be calculated by using Ohm's law. The range of voltage used is between  $\pm 10$  V, in increment of 1V.

**Fig.3** Circuit Configuration of Electrical Measurement**RESULTS AND DISCUSSION****XRD of CuO & SnO<sub>2</sub> Nanomaterial and their dopings**

The average crystallite size was calculated by Debye-Scherrer's equation with the help of XRD patterns as shown in figure 4. The strong and sharp peak of CuO observed at 37° position with (1 1 1) indicates that the sample is having high crystalline quality, and it is in the structure of monoclinic with lattice parameters a = 0.4685 nm, b = 0.3532 nm,

and  $c = 0.5121$  nm, which is good agreement with JCPDS card number 88-2341. The average crystalline size was obtained 27 nm from Debye-Scherrer's equation,  $D = \frac{K\lambda}{\beta \cos\theta}$

Where,  $D$  = nanoparticles crystalline size,  $K$  = Scherrer constant (0.98),  $\lambda$  = wavelength and  $\beta$  denotes the full width at half maximum (FWHM).

All the peaks are showing very sharp; it observed that there is no impurities means the prepared sample is having high purity. The peaks position and (h k l) values mentioned, some of the (h k l) values shows bar on the top, it means that the negative direction of the corresponding (h k l). From table 3, it is exhibited that the A3 sample 15CuO:85SnO<sub>2</sub> has small crystalline size [14].

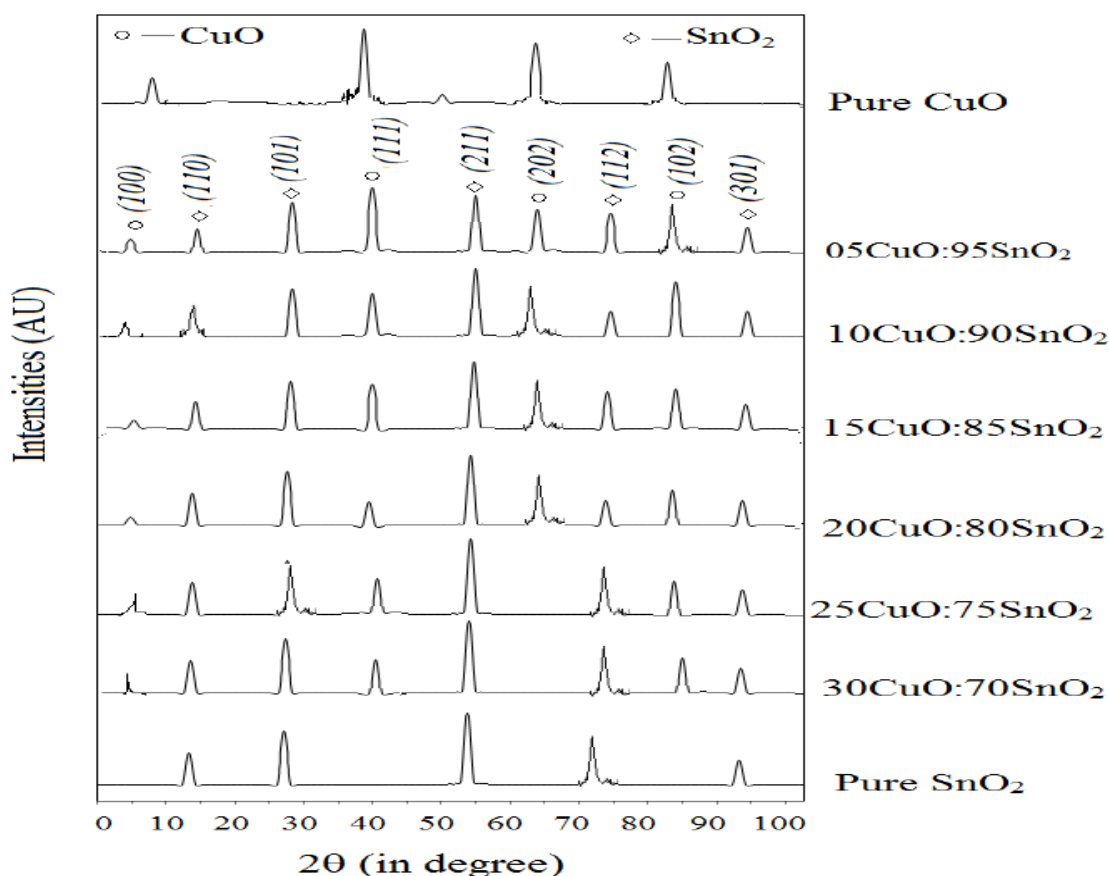


Fig.4. XRD spectra of Pure CuO, Pure SnO<sub>2</sub> and CuO doped with SnO<sub>2</sub> Nanomaterial

Table 3. Average crystallite size of CuO, SnO<sub>2</sub> and doping

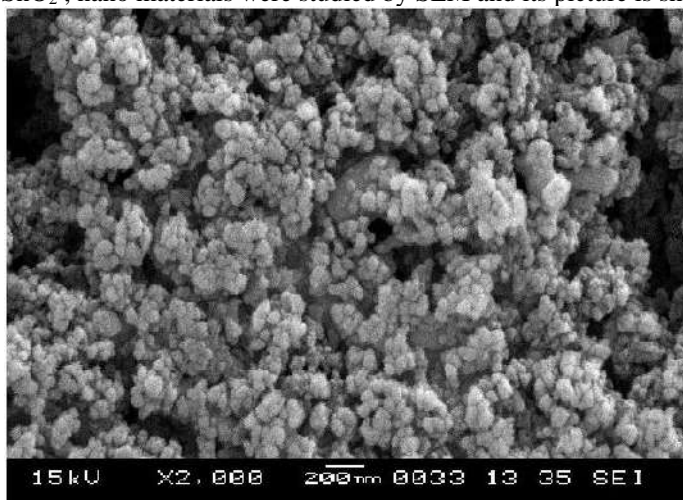
Sample Code	Chemical Composition of CuO:SnO <sub>2</sub> (mole %)	Maximum Intensity Peak Position (2θ) degree	FWHM (2θ) degree	Average Crystallite Size (D) in nm
PC	Pure CuO	43.32	0.1865	162.22
A1	05CuO:95SnO <sub>2</sub>	49.11	0.2522	122.45



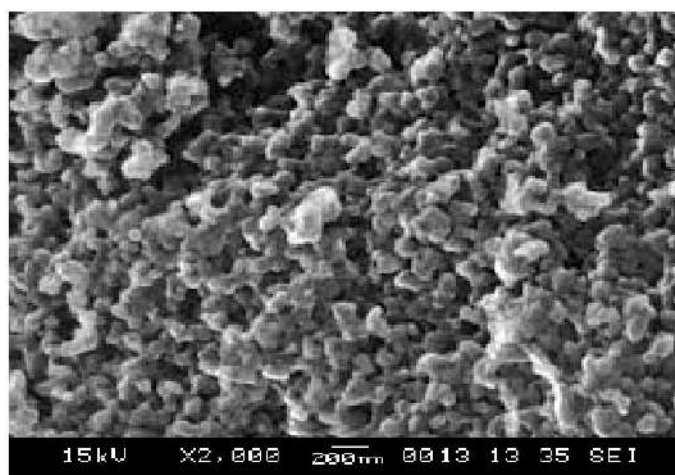
A2	10CuO:90SnO <sub>2</sub>	54.65	0.1934	153.31
A3	<b>15CuO:85SnO<sub>2</sub></b>	<b>55.71</b>	<b>0.2312</b>	<b>89.65</b>
A4	20CuO:80SnO <sub>2</sub>	55.02	0.1832	113.43
A5	25CuO:75SnO <sub>2</sub>	54.12	0.2433	154.18
A6	30CuO:70SnO <sub>2</sub>	54.44	0.2132	167.87
PS	Pure SnO <sub>2</sub>	53.04	0.2823	132.34

### Scanning electron microscopy (SEM) Analysis

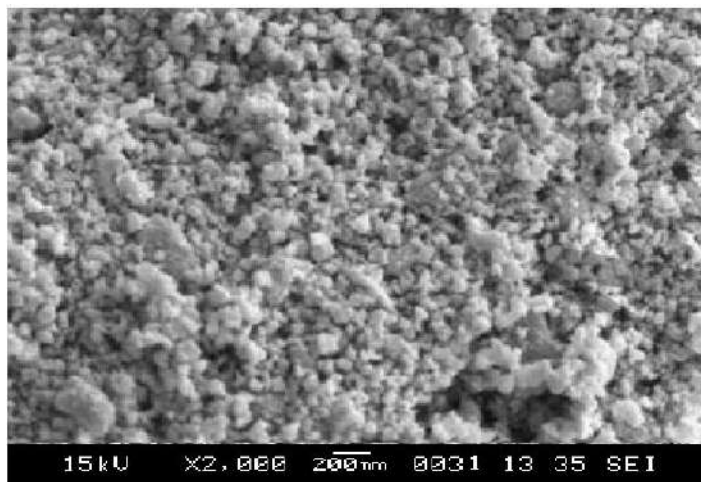
From SEM picture (figure 5 (a) to (c)), it is observed that all the samples viz. Al<sub>2</sub>O<sub>3</sub>, CuO, SnO<sub>2</sub> are porous in nature. Porosity varies with sample to sample and among these material, SnO<sub>2</sub> showed more porosity (small size ~ 60 to 80 nm). Due to small pores size, its surface area is more [11-14] and it shows more sensing nature. Some portion of SEM picture shows some rods with fine voids over them which helps to increase sensing properties. The surface morphology of pure Al<sub>2</sub>O<sub>3</sub>, CuO, and SnO<sub>2</sub>, nano materials were studied by SEM and its picture is shown in the Fig. 5



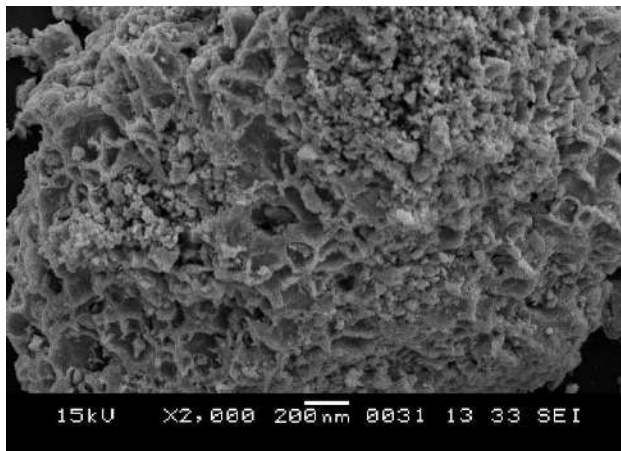
*Fig. 5 (a) SEM picture of Al<sub>2</sub>O<sub>3</sub>*



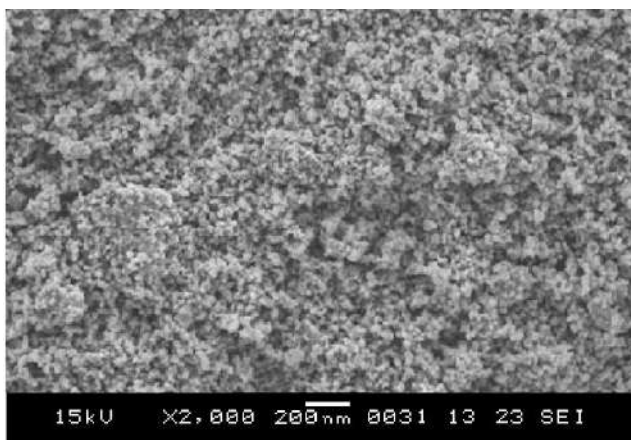
*Fig. 5 (b) SEM picture of CuO*



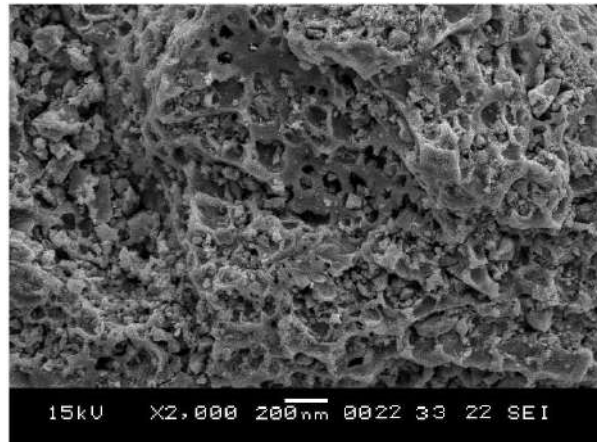
*Fig. 5 (c) SEM picture of SnO<sub>2</sub>*



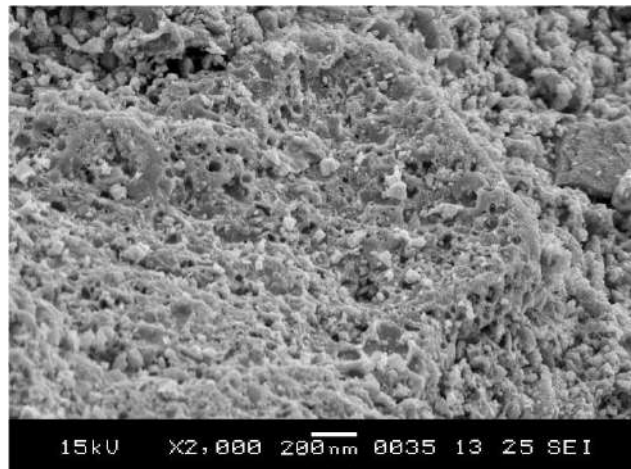
*Fig. 6 (a) SEM picture of 05CuO:95SnO<sub>2</sub>*



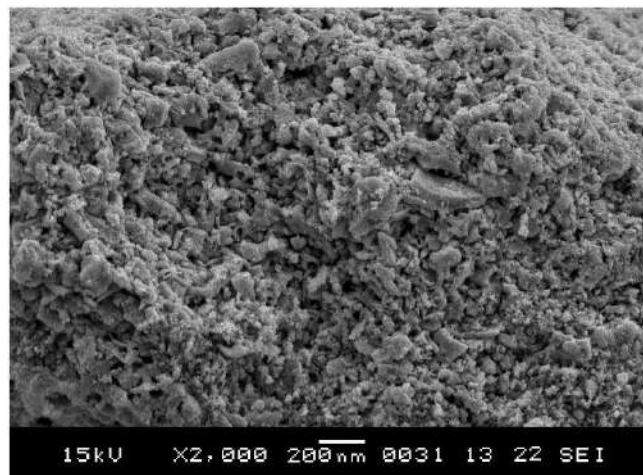
*Fig. 6 (b) SEM picture of 10CuO:90SnO<sub>2</sub>*



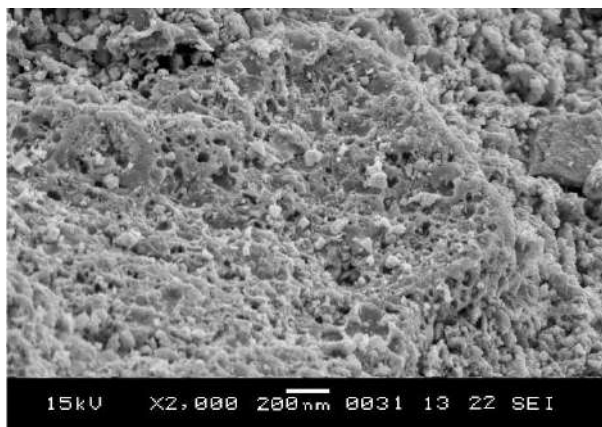
*Fig. 6 (c) SEM picture of 15CuO:85SnO<sub>2</sub>*



*Fig. 6 (d) SEM picture of 20CuO:80SnO<sub>2</sub>*



*Fig. 6 (e) SEM picture of 25CuO:75SnO<sub>2</sub>*



**Fig. 6 (f)** SEM picture of 30CuO:70SnO<sub>2</sub>

The surface morphologies of pure Al<sub>2</sub>O<sub>3</sub>, CuO, SnO<sub>2</sub>, and their dopings materials were studied by SEM and its picture are shown in the figures 5 to 6. As shown in the SEM pictures, some pores are in the form of rods, some are the form of circles and some are in conical shapes [14].

Table 4. shows the average diameter and number of pores per inch of pure Al<sub>2</sub>O<sub>3</sub>, CuO, SnO<sub>2</sub>, and their dopings.

**Table 4. Average diameter of pore and number of pores per inch of pure samples and their dopings.**

Sample Code	Pure sample and their dopings (mole %)	Average diameter of pore (nm)	Number of pores per inch (in x 2000 magnification)
PA	Al <sub>2</sub> O <sub>3</sub>	95	154
PC	CuO	80	172
PS	SnO <sub>2</sub>	87	160
A1	05CuO:95SnO <sub>2</sub>	72	183
A2	10CuO:90SnO <sub>2</sub>	78	171
A3	<b>15CuO:85SnO<sub>2</sub></b>	<b>59</b>	<b>206</b>
A4	20CuO:80SnO <sub>2</sub>	69	192
A5	25CuO:75SnO <sub>2</sub>	65	195
A6	30CuO:70SnO <sub>2</sub>	75	157

From the SEM pictures (table 4), it is observed that 15CuO:85SnO<sub>2</sub>, have more pores per inch (calculated for x 2,000 magnification for each composition) than other sensors. Thus, these sensors have more active surface areas and exhibit more sensing nature [14-15]. It is also found that average diameter of pore in case of 15CuO:85SnO<sub>2</sub> are small as compared to other doping. This also tends to exhibit large surface area and exhibited high response of the samples.

#### Detection of CO<sub>2</sub> gas: Gas Sensing Properties

CO<sub>2</sub> acts as an oxidizing agent in some chemical reactions, such as the production of carbonates. It can also participate in redox reactions, where it can accept electrons and become reduced and hence its resistance increases with increase of CO<sub>2</sub> gas concentration [16]. The sensitivity of the sensor is given by,

$$S = \left( \frac{R_{\text{gas}} - R_{\text{air}}}{R_{\text{air}}} \right) = \left( \frac{\Delta R}{R_{\text{air}}} \right)$$

Where,  $R_{gas}$  = resistance of the sensor in presence of gas and  
 $R_{air}$  = resistance of the sensor in air

The variations of sensitivities and sensors with concentration of CO<sub>2</sub> gas at room temperature are shown below.

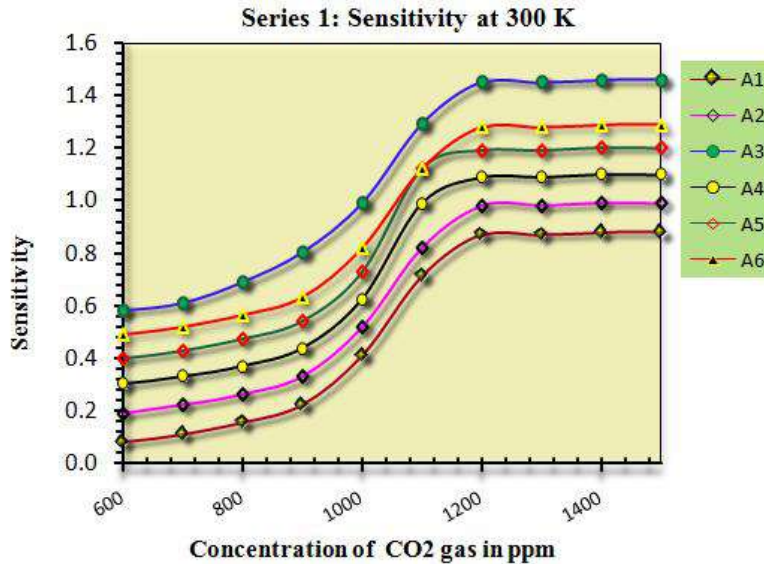


Fig. 7: The variations of sensitivity with CO<sub>2</sub> gas concentration

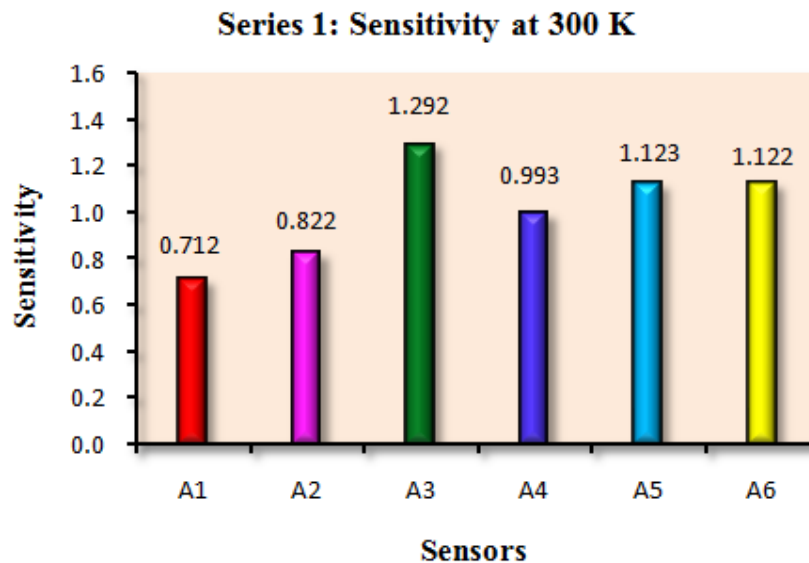


Fig. 8: Sensitivity of different sensors at 1100 ppm

From CO<sub>2</sub> gas detection [17-18] graphs (Fig. 7 and 8) it is observed and manifested that: As CO<sub>2</sub> gas concentration increases from 600 ppm to 1500 ppm, there is little increase of sensitivity, from 600 ppm to 1100 ppm, sensitivity increases linearly and becomes maximum at 1100 ppm. With further increase in CO<sub>2</sub> gas concentration, sensitivity increases by little amount. From Fig. 8, sensitivity was found to be 1.292 (maximum) for A3 sensor (15CuO:85SnO<sub>2</sub>) amongst the prepared sensors.

## CONCLUSIONS

The XRD pattern of (CuO-SnO<sub>2</sub>) system samples shows nanocrystalline form and found the desired peaks of composites. FESEM study reveals that the grain size of nanometer order and shows nano-porous structure, which leads to exhibit large surface area, stability and highest response to CO<sub>2</sub> gas. The response time is faster than recovery time therefore the A3 sensor (15CuO:85SnO<sub>2</sub>) is found to optimized sensor for CO<sub>2</sub> gas.

## REFERENCES

1. Chengxiang Wang, Longwei Yin, Luyuan Zhang, Dong Xiang and Rui Gao, 2010, Review Metal Oxide Gas Sensors: Sensitivity and Influencing Factors, *Sensors*, 10, 2088-2106; doi:10.3390/s100302088
2. G. Korotcenkov, (2014), Handbook of Gas Sensor Materials, doi:10.1007/978-1-4614-7165-3.
3. Nithya Sureshkumar and Atanu Dutta,(2023) Environmental Gas Sensors Based on Nanostructured Thin Films, *Multilayer Thin Films - Versatile Applications for Materials Engineering*, doi.org/10.5772/intechopen. 89745
4. Khanidtha Jantasom, Suttinart Noothongkaew and Supakorn Pukird, (2013), Synthesis and Gas Sensing Properties of SnO<sub>2</sub>-CuO Nanocomposites, *Advanced Materials Research Vol. 645*, pp 129-132 doi:10.4028/www.scientific.net/AMR.645.129
5. Satyendra Singh, Nidhi Verma, Archana Singh, B.C.Yadav, (2014), Synthesis and characterization of CuO-SnO<sub>2</sub> nanocomposite and its application as liquefied petroleum gas sensor, *Materials Science in Semiconductor Processing* 18(2014)88-96, <http://dx.doi.org/10.1016/j.mssp.2013.11.002>
6. Shravanti Joshi ,L.Satyanarayana , P.Manjula , Manorama V. Sunkara, (2015), Chemo - Resistive CO<sub>2</sub> Gas Sensor Based on CuO-SnO<sub>2</sub> Heterojunction Nanocomposite Material, *Proceedings of the 2015 2nd International Symposium on Physics and Technology of Sensors*, Pune,
7. Fumin Ren, Liping Gao, Yongwei Yuan, Yuan Zhang, Ahmed Alqrni, Omar M. Al-Dossary, Jiaqiang Xu, (2015), Enhanced BTEX gas-sensing performance of CuO/SnO<sub>2</sub> Composite, *Sensors and Actuators B*, <http://dx.doi.org/doi:10.1016/j.snb.2015.09.140>
8. Arindam Das and Dipankar Panda ,(2019), SnO<sub>2</sub> Tailored by CuO for Improved CH<sub>4</sub> Sensing at Low Temperature, *Advanced Science News, Phys. Status Solidi B*, 1800296, DOI: 10.1002/pssb.201800296
9. Chengxiang Wang, Longwei Yin , Luyuan Zhang, Dong Xiang and Rui Gao, (2010), Metal Oxide Gas Sensors: Sensitivity and Influencing Factors *Sensors*, 10, 2088-2106; doi:10.3390/s100302088
10. Ali Mirzaei, Hamid Reza Ansari, Mehrdad Shahbaz, Jin-Young Kim, Hyoun Woo Kim and Sang Sub Kim, (2022), Metal Oxide Semiconductor Nanostructure Gas Sensors with Different Morphologies, *Chemosensors*, 10, 289. doi.org/10.3390/chemosensors10070289
11. K. B. Raulkar, (2019), Study on sensitivity of nano SnO<sub>2</sub> -ZnO composites with and without PPy layer for sensing CO<sub>2</sub> gas, 2019, *Materials Today: Proceedings* 15, 604-610.
12. Dmitry Bokov, Abduladheem Turki Jalil, Supat Chupradit, Wanich Suksatan, Mohammad Javed Ansari, 6 Iman H. Shewael, Gabdrakhman H. Valiev, and Ehsan Kianfar, (2021), Review Article, Nanomaterial by Sol-Gel Method: Synthesis and Application, *Advances in Materials Science and Engineering Volume 2021*, <https://doi.org/10.1155/2021/5102014>
13. Zahrah Alhalili, (2023), Review Metal Oxides Nanoparticles: General Structural Description, Chemical, Physical, and Biological Synthesis Methods, Role in Pesticides and Heavy Metal Removal through Wastewater Treatment, *Molecules*, 28, 3086. <https://doi.org/10.3390/molecules28073086>
14. Tai H., Wang S., Duan Z. and Jiang Y., (2020). Evolution of breath analysis based on humidity and gas sensors: Potential and challenges, *Sens. Actuators B Chem.*, 318, 128104.
15. Nakhleh, M.K., Amal H., Jeries R., Broza Y.Y., Aboud M., Gharra A., Ivgi H., Khatib S., Badarneh S. and Har-Shai, L., (2017). Diagnosis and Classification of 17 Diseases from 1404 Subjects via Pattern Analysis of Exhaled Molecules, *ACS Nano*, 11, 112-125.
16. Hua B. and Gaoquan S., (2007). Gas Sensors Based on Conducting Polymers, *Sensors*, 7, 267-307
17. Capone S., Forleo A., Francioso L., Rella R., Siciliano P., Spada- vecchia J., Presicce D.S. and Taurino A.M. (2003), Solid state gas sensors: state of the art and future activities, *Journal of Optoelectronics and Advanced Materials* 5, 5, 1335 - 1348.
18. Garg R., Kumar V., Kumar D., and Chakarvarti S.K., (2015). Polypyrrole Microwires as Toxic Gas Sensors for Ammonia and Hydrogen Sulphide, *Columbia International Publishing Journal of Sensors and Instrumentation*, 3, 1-13.

# Exploitation of Nano-Crystalline Cupric Oxide (CuO) Doped Zinc Oxide (ZnO) Multilayer Thick Film as a CO<sub>2</sub> Gas Sensor

\*Mankar S.S., \*\*Lamdhade G.T., \*\*Raulkar K.B

\*Department of Physics, Shivramji Moghe Arts, Commerce and Science College, Kelapur, Pandharkawada, Dist. Yavatmal, M.S., India

\*\*Department of Physics, Vidya Bharati Mahavidyalaya, CK Naidu Road, Amravati, M.S., India

DOI:10.37648/ijrst.v13i04.008

<sup>1</sup>Received: 17 August 2023; Accepted: 12 October 2023; Published: 27 December 2023

---

## ABSTRACT

Cupric oxide and Zinc oxide nano-crystalline powder were synthesized via liquid-phase method. The samples are prepared in the form of multilayer thick films. The XRD pattern of (CuO-ZnO) system samples show nanocrystalline form and found the desired peaks of composites. FESEM study reveals that the grain size of nanometer order and shows nano-porous structure, which leads to exhibit large surface area, stability and highest response to CO<sub>2</sub> gas. The response time is faster than recovery time. The sample C3 sensor (15CuO:85ZnO) offers high sensitivity, rapid response and recovery to CO<sub>2</sub> gas.

**Keywords:** *Nanoparticles; CuO-ZnO; multilayer thick films; CO<sub>2</sub> Gas Sensors*

## INTRODUCTION

Nanoparticles CuO and its composite oxides have potential applications as gas sensor. As compared to bulk materials, nanoparticles of Copper oxide (CuO) show high catalytic activity and selectivity due to their large surface to volume ratio. [1-3]. Quentin Simon et al. 2012 [4] synthesized CuO/ZnO nanocomposites on Al<sub>2</sub>O<sub>3</sub> substrates by a hybrid plasma-assisted approach. Various oxidizing and reducing gases such as O<sub>3</sub>, CH<sub>3</sub>CH<sub>2</sub>OH, and H<sub>2</sub> are studied for gas sensing properties of CuO/ZnO nanocomposites. Yalu Chen et al. 2013 [5] prepared CuO-ZnO nanostructured p-n junction composite via the hydrothermal method. The gas sensing performance of pure ZnO and CuO-ZnO composite toward n-butanol was studied. They show that porous structure allows the target gas molecules diffuse rapidly making chemisorption and the chemical reactions on the p-n junctions more easily. At 220 °C 2.7 times higher sensitivity was obtained for CuO-ZnO composite than that of pure ZnO. Ryan Dula Corpuza and Jason Rayala Albiab 2014 [6] fabricated ZnO and ZnO-CuO composites on a graphite electrode via electrophoretic deposition. Greater surface area, smaller particle sizes and thicker deposits exhibit high gas sensitivity. The addition of CuO in the deposition gives compact and dense surface structure resulted to decrease in sensitivity. The expected increase in sensitivity in the presence of CuO was not attained. Madhavrao K. Deore et al. 2016 [7] prepared CuO-doped ZnO thick films by the screen printing technique. These films were studied for different gases such as CO, Cl<sub>2</sub>, NH<sub>3</sub>, Ethanol, H<sub>2</sub>S and LPG and observed that CuO doped films were more selective to H<sub>2</sub>S gas against the other test gases showing rapid response and recovery time. The main purpose of this work was to develop CuO doped ZnO, nano-crystalline composites sensors which operate at relatively low temperature and sensitive in low possible detection limit with better sensitivity.

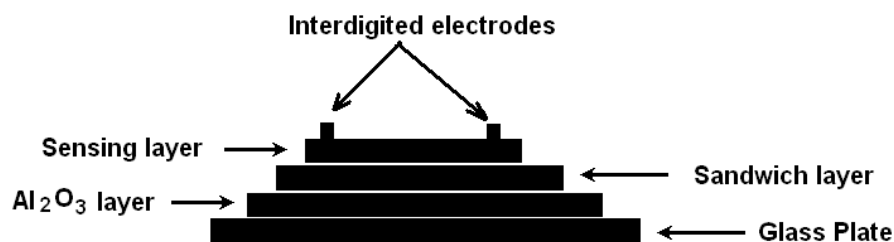
---

<sup>1</sup> How to cite the article: Mankar S.S., Lamdhade G.T., Raulkar K.B.; December 2023; M Exploitation of Nano-Crystalline Cupric Oxide (CuO) Doped Zinc Oxide (ZnO) Multilayer Thick Film as a CO<sub>2</sub> Gas Sensor; *International Journal of Research in Science and Technology*, Vol 13, Issue 4, 56-64, DOI: <http://doi.org/10.37648/ijrst.v13i04.008>

## EXPERIMENTAL

In the present work of thesis, we have used liquid phase synthesis method for the synthesis of pristine nano-particles of CuO, ZnO and Al<sub>2</sub>O<sub>3</sub> [8-10]. All the chemicals used in this study were of GR grade purchase from Sd-fine, India (purity 99.99%). The chemicals are used without any further purification.

### Fabrication of Sensors : Multilayer preparation



**Fig.1** Design of multilayer Sensor

On clean glass plate, Al<sub>2</sub>O<sub>3</sub> was deposited by using screen-printing technique and it was used as base of the sensor. On Al<sub>2</sub>O<sub>3</sub>, the sample layers were prepared. Finally on the top, Inter-digited electrodes were fabricated using conducting silver paste and design of multilayer sensor is shown in Fig. 1.

### Preparation of Samples of Series: CuO: ZnO / Al<sub>2</sub>O<sub>3</sub>/GP

The obtained product of fine nanopowder of CuO and ZnO are used for fabrication of thick films sensors by using screen-printing technique. For this, the different X mole% CuO powder (X = 05, 10, 15, 20, 25, 30) was mixed thoroughly with different X mole% of ZnO (X = 95, 90, 85, 80, 75, 70) along with Al<sub>2</sub>O<sub>3</sub> base on glass plate (GP) substrate the aid of acetone by using the mortar and pestle. The sample codes, mole% of powder, and thickness are listed in the Table 2.. The mixed powder of CuO : ZnO system was further calcinated at temperature 800°C for 5hrs. in the auto-controlled muffle furnace (*Gayatri Scientific, Mumbai, India.*) After, the calcinations again uniformly mixed the powder using the grinder.

**Table 1** Thickness of Multi-layers for Series: CuO: ZnO / Al<sub>2</sub>O<sub>3</sub>/GP Gas Sensors.

Sample Code	Composition Layers:----	Thickness (x 10 <sup>-4</sup> cm)		
		Upper Layer(1)	Al <sub>2</sub> O <sub>3</sub> Layer(2)	Total (1+2)
		Upper /Al <sub>2</sub> O <sub>3</sub> /Glass plate (GP)		
C1	05CuO:95ZnO/ Al <sub>2</sub> O <sub>3</sub> /GP	2.8	27.1	29.9
C2	10CuO:90 ZnO / Al <sub>2</sub> O <sub>3</sub> /GP	3.4	28.7	32.1
C3	15CuO:85 ZnO / Al <sub>2</sub> O <sub>3</sub> /GP	2.2	29.4	31.6
C4	20CuO:80 ZnO / Al <sub>2</sub> O <sub>3</sub> /GP	3.9	28.8	32.7
C5	25CuO:75 ZnO / Al <sub>2</sub> O <sub>3</sub> /GP	2.8	28.9	31.7
C6	30CuO:70 ZnO / Al <sub>2</sub> O <sub>3</sub> /GP	2.9	30.2	33.1

## RESULTS AND DISCUSSION

### XRD of CuO & ZnO Nanomaterial and their dopings

The average crystallite size was calculated by Debye-Scherrer's equation with the help of XRD patterns as shown in figure 4. The strong and sharp peak of CuO observed at 37° position with (1 1 1) indicates that the sample is having high crystalline quality, and it is in the structure of monoclinic with lattice parameters a = 0.4685 nm, b = 0.3532 nm,



and  $c = 0.5121$  nm, which is good agreement with JCPDS card number 88-2341. The average crystalline size was obtained 27 nm from Debye-Scherrer's equation,  $D = \frac{K\lambda}{\beta \cos\theta}$

Where,  $D$  = nanoparticles crystalline size,  $K$  = Scherrer constant (0.98),  $\lambda$  = wavelength and  $\beta$  denotes the full width at half maximum (FWHM).

As shown in figure 2, the XRD pattern peak for CuO doped ZnO exhibits hexagonal and monoclinic crystalline phases at  $2\theta$  values of  $8.25^\circ$ ,  $26.56^\circ$ ,  $38.45^\circ$ ,  $44.21^\circ$ ,  $53.56^\circ$ ,  $62.55^\circ$ ,  $73.12^\circ$  and  $82.67^\circ$  (JCPDS Card No.5-3242), with the corresponding planes of (1 0 0), (1 1 0), (1 1 1), (2 2 0), (1 0 2), (2 0 2), (1 0 3), and (1 0 2), respectively. As shown in table 2, Sample Code C3 i.e. (15CuO:85ZnO) sample shows small crystalline size. The average crystalline size was found to be smaller in case of C3 sample and hence its active surface is more [11].

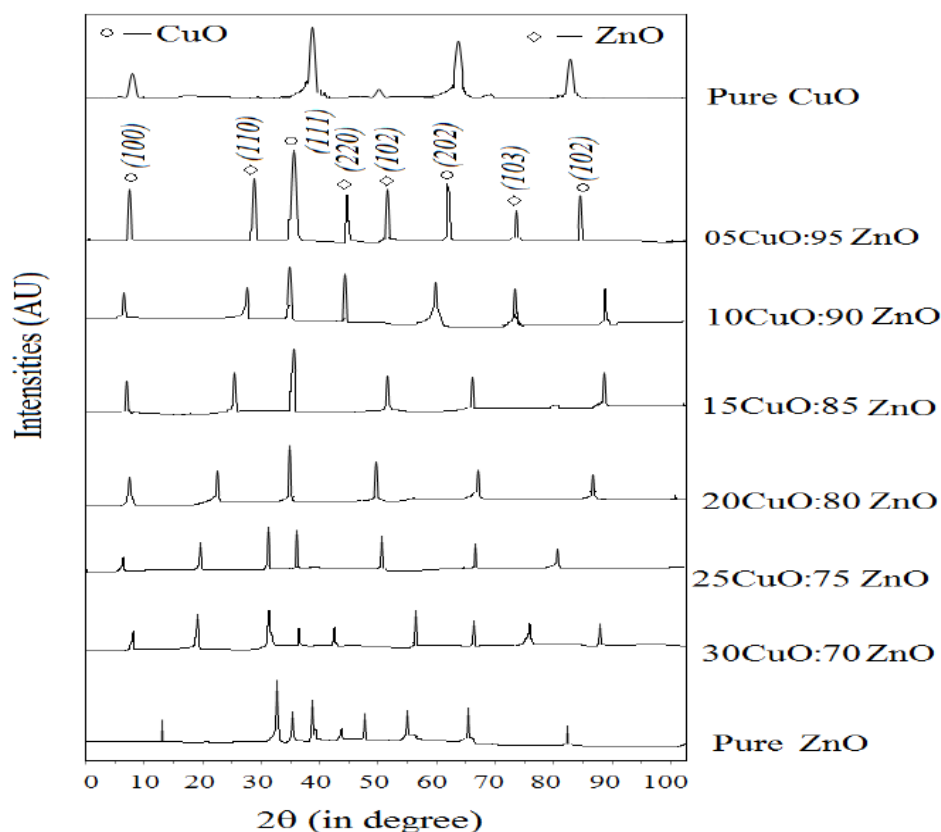


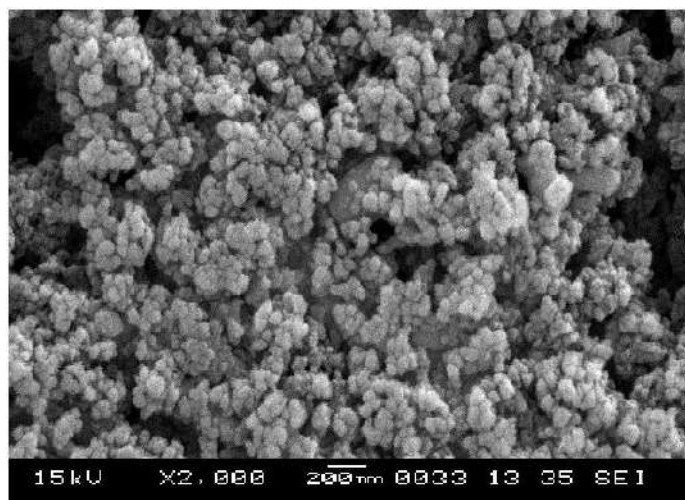
Fig.2. XRD spectra of Pure CuO, Pure ZnO and CuO doped with ZnO Nanomaterial

**Table 2** Average crystallite size of ZnO and CuO doped ZnO

Sample Code	Chemical Composition of CuO:ZnO (mole %)	Maximum Intensity Peak Position ( $2\theta$ ) degree	FWHM ( $2\theta$ ) degree	Average Crystallite Size (D) in nm
PC	Pure CuO	43.32	0.1865	162.22
C1	05CuO:95 ZnO	26.45	0.1786	102.33
C2	10CuO:90 ZnO	28.44	0.1862	98.22
<b>C3</b>	<b>15CuO:85 ZnO</b>	<b>29.34</b>	<b>0.1372</b>	<b>78.33</b>
C4	20CuO:80 ZnO	32.45	0.1672	93.23
C5	25CuO:75 ZnO	38.33	0.1932	105.22
C6	30CuO:70 ZnO	48.34	0.2122	112.44
PZ	Pure ZnO	57.33	0.2344	117.87

### Scanning electron microscopy (SEM) Analysis

From SEM picture (figure 3 (a) to (d)), it is observed that all the samples viz.  $Al_2O_3$ , CuO, ZnO and Sample Code C3 i.e. (15CuO:85ZnO) (optimize sample shown only) are porous in nature. Porosity varies with sample to sample and among these material, Sample Code C3 i.e. (15CuO:85ZnO) showed more porosity (small size ~ 60 to 80 nm). Due to small pores size, its surface area is more [12-14] and it shows more sensing nature. Some portion of SEM picture shows some rods with fine voids over them which helps to increase sensing properties.



*Fig. 3 (a)* SEM picture of  $Al_2O_3$

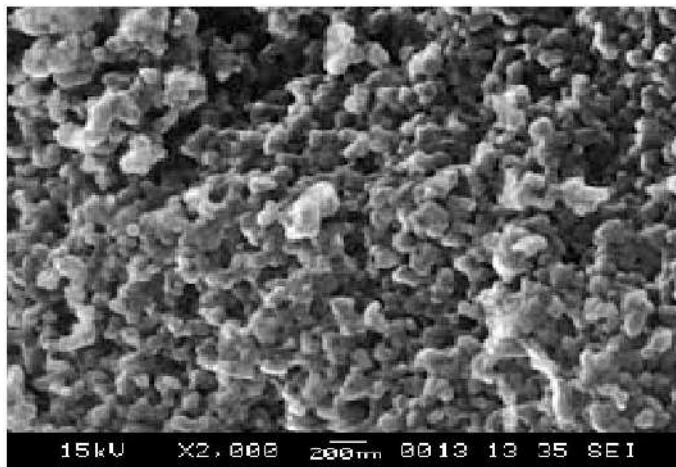


Fig. 3 (b) SEM picture of CuO

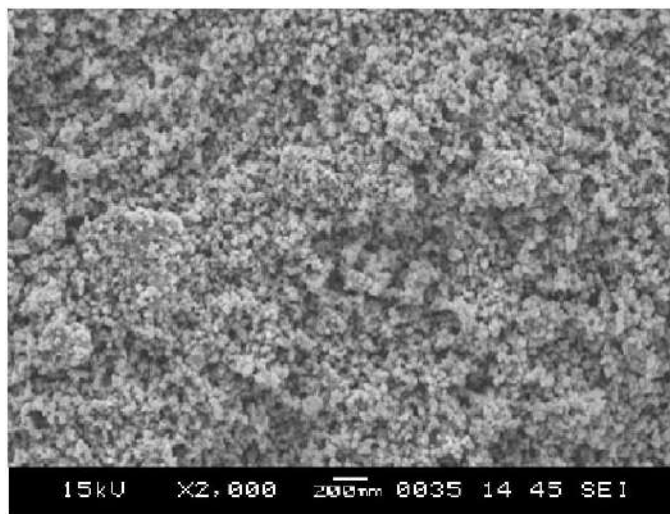


Fig. 3(c) SEM picture of ZnO

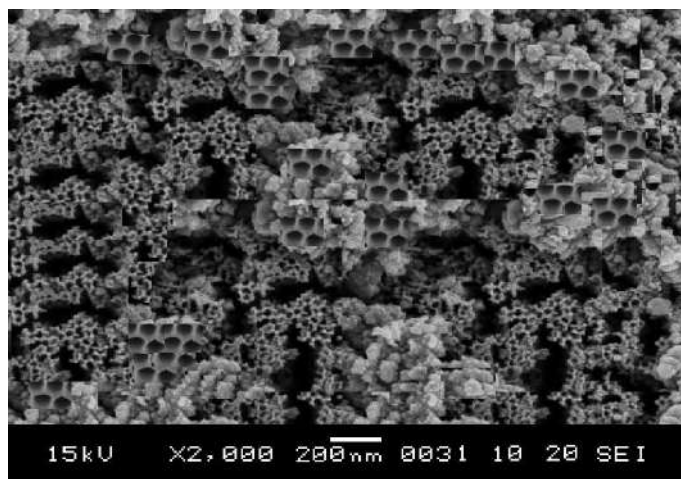


Fig. 3 (d) SEM picture of 15CuO:85ZnO

Table 3. shows the average diameter and number of pores per inch of pure Al<sub>2</sub>O<sub>3</sub>, CuO, and ZnO and their dopings.

**Table 3. Average diameter of pore and number of pores per inch of pure samples and their dopings.**

Sample Code	Pure sample and their dopings (mole %)	Average diameter of pore (nm)	Number of pores per inch (in x 2000 magnification)
PA	Al <sub>2</sub> O <sub>3</sub>	95	154
PC	CuO	80	172
PZ	ZnO	87	160
C1	05CuO:95ZnO	79	165
C2	10CuO:90ZnO	81	161
C3	<b>15CuO:85ZnO</b>	<b>45</b>	<b>245</b>
C4	20CuO:80ZnO	67	187
C5	25CuO:75ZnO	74	176
C6	30CuO:70 ZnO	69	183

From the SEM pictures (table 3), it is observed that Sample Code C3 i.e. (15CuO:85ZnO), have more pores per inch (calculated for x 2,000 magnification for each composition) than other sensors. Thus these sensors have more active surface areas and exhibit more sensing nature [14-15]. It is also found that average diameter of pore in case of (15CuO:85ZnO) are small as compared to other doping. This also tends to exhibit large surface area and exhibited high response of the samples.

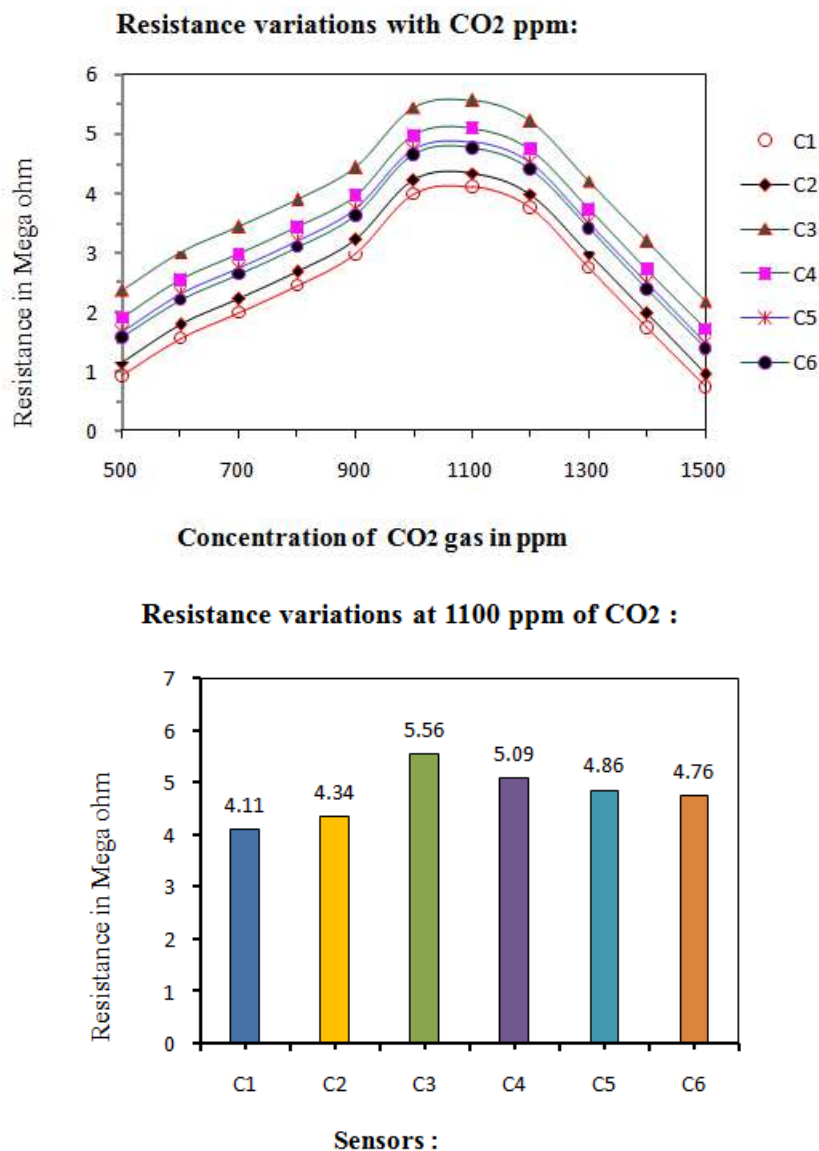
#### Detection of CO<sub>2</sub> gas: Gas Sensing Properties

CO<sub>2</sub> acts as an oxidizing agent in some chemical reactions, such as the production of carbonates. It can also participate in redox reactions, where it can accept electrons and become reduced and hence its resistance increases with increase of CO<sub>2</sub> gas concentration [16]. The sensitivity of the sensor is given by,

$$S = \left( \frac{R_{\text{gas}} - R_{\text{air}}}{R_{\text{air}}} \right) = \left( \frac{\Delta R}{R_{\text{air}}} \right)$$

Where,  $R_{\text{gas}}$  = resistance of the sensor in presence of gas and  
 $R_{\text{air}}$  = resistance of the sensor in air

The variations of sensitivities and sensors with concentration of CO<sub>2</sub> gas at room temperature are shown below.

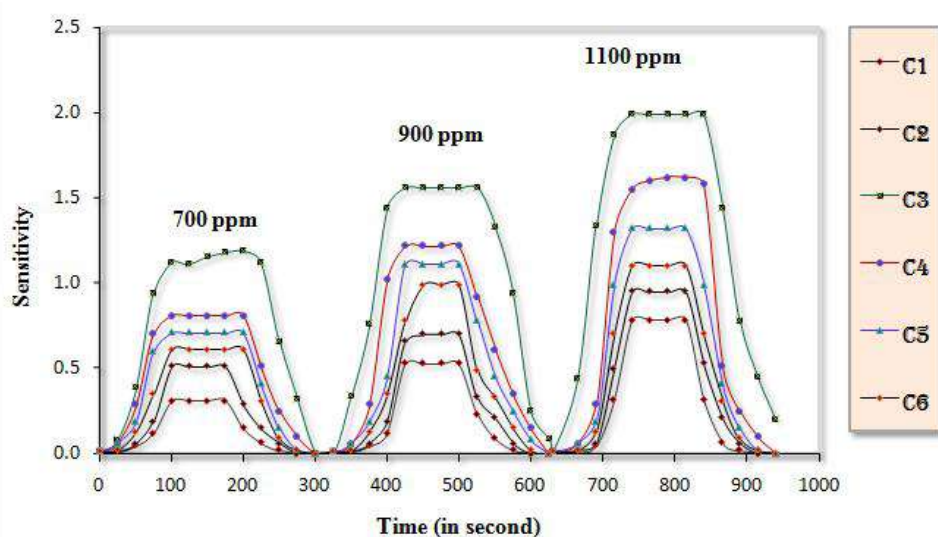


**Fig. 4 :** variations of resistance with CO<sub>2</sub> gas concentration

For CO<sub>2</sub> gas concentration variation from 500 ppm to 1500 ppm, variation of resistance for C1 to C6 sensors is shown in Fig. 4. As carbon-dioxide concentration increases, Cu ions interact with Zn ions by absorbing CO<sub>2</sub> gas and resistance increases. It is exhibited that, initially resistance increases with increases of concentration of gas, becomes maximum at 1100 ppm and then with further increase of gas concentration, it decreases. It is recorded maximum resistance for C3 sensor (15CuO:85ZnO) to be 5.56 MΩ at 1100 ppm CO<sub>2</sub> gas concentration [17-19].

**Static Responses of sensors:**

Static responses [20-21] of samples Fig. 5. of (CuO:ZnO/Al<sub>2</sub>O<sub>3</sub>/GP) were studied at 700, 900 and 1100 ppm of CO<sub>2</sub> gas concentration as a function of time and from the manifested variations, response and recovery times were calculated.



**Fig. 5:** Static response (response and recovery times)

**Table 4.** Response and Recovery times of Samples

Sr. No.	Sample Compositions	Sensor	Response time (s) for 1100 ppm	Recovery time (s) for 1100 ppm
1	05CuO:95 ZnO /Al <sub>2</sub> O <sub>3</sub> /GP	C1	93	95
2	10CuO:90 ZnO /Al <sub>2</sub> O <sub>3</sub> /GP	C2	87	89
3	15CuO:85 ZnO /Al <sub>2</sub> O <sub>3</sub> /GP	C3	56	61
4	20CuO:80 ZnO /Al <sub>2</sub> O <sub>3</sub> /GP	C4	69	76
5	25CuO:75 ZnO /Al <sub>2</sub> O <sub>3</sub> /GP	C5	72	79
6	30CuO:70 ZnO /Al <sub>2</sub> O <sub>3</sub> /GP	C6	82	91

At 100 ppm CO<sub>2</sub> gas concentration, from table 4, sensor C3 manifested fast response (response time 56 s and recovery time 61 s) among the fabricated sensors. Also, it is observed that response time less than that of recovery time.

## CONCLUSIONS

The XRD pattern of (CuO-ZnO) system samples shows nanocrystalline form and found the desired peaks of composites. FESEM study reveals that the grain size of nanometer order and shows nano-porous structure, which leads to exhibit large surface area, stability and highest response to CO<sub>2</sub> gas. The response time is faster than recovery time therefore the Sample C3 i.e. (15CuO:85ZnO) is found to optimized sensor for CO<sub>2</sub> gas.

## REFERENCES

1. Chengxiang Wang, Longwei Yin , Luyuan Zhang, Dong Xiang and Rui Gao, (2010),Review Metal Oxide Gas Sensors: Sensitivity and Influencing Factors, *Sensors*, 10, 2088-2106; doi:10.3390/s100302088
2. G. Korotcenkov, (2014), Handbook of Gas Sensor Materials, doi:10.1007/978-1-4614-7165-3.

3. Nithya Sureshkumar and Atanu Dutta,(2023) Environmental Gas Sensors Based on Nanostructured Thin Films, Multilayer Thin Films - Versatile Applications for Materials Engineering, doi.org/10.5772/intechopen. 89745
4. Quentin Simon, Davide Barreca, Alberto Gasparotto, Chiara Maccato, Eugenio Tondello, Cinzia Sada, Elisabetta Comini, Giorgio Sberveglieri, Manish Banerjee, Ke Xu, Anjana Devi, and Roland A. Fischer, CuO/ZnO Nanocomposite Gas Sensors Developed by a Plasma-Assisted Route, ChemPhysChem 0000, 00, 1 – 8, DOI: 10.1002/cphc.201101062
5. Yalu Chen, Zhurui Shen, Qianqian Jia, Jiang Zhao, Zhe Zhao, Huiming Ji, 2013, A CuO-ZnO Nanostructured p-n Junction Sensor for Enhanced N- butanol Detection, The Royal Society of Chemistry, DOI: 10.1039/x0xx00000x
6. Ryan Dula Corpuza, Jason Rayala Albiab,2014, Electrophoretic Fabrication of ZnO/ZnO-CuO Composite for Ammonia Gas Sensing, Materials Research. 2014; 17(4): 851-856 DOI: <http://dx.doi.org/10.1590/S1516-14392014005000097>
7. Madhavrao K. Deore, Vishwas B. Gaikwad and Gotan H. Jain, 2016, Role of CuO-ZnO Heterojunctions in Gas Sensing Response of CuO-ZnO Thick Films, Journal of Physical Science and Application 6 (2), 51-60, doi: 10.17265/2159-5348/2016.02.008
8. K. B. Raulkar, (2019), Study on sensitivity of nano SnO<sub>2</sub> -ZnO composites with and without PPy layer for sensing CO<sub>2</sub> gas, 2019, Materials Today: Proceedings 15, 604–610.
9. Dmitry Bokov, Abduladheem Turki Jalil, Supat Chupradit, Wanich Suksatan, Mohammad Javed Ansari, 6 Iman H. Shewael, Gabdrakhman H. Valiev, and Ehsan Kianfar, (2021), Review Article, Nanomaterial by Sol-Gel Method: Synthesis and Application, Advances in Materials Science and Engineering Volume 2021, <https://doi.org/10.1155/2021/5102014>
10. Zahrah Alhalili, (2023), Review Metal Oxides Nanoparticles: General Structural Description, Chemical, Physical, and Biological Synthesis Methods, Role in Pesticides and Heavy Metal Removal through Wastewater Treatment, Molecules, 28, 3086. <https://doi.org/10.3390/molecules28073086>
11. Tai H., Wang S., Duan Z. and Jiang Y., (2020). Evolution of breath analysis based on humidity and gas sensors: Potential and challenges, Sens. Actuators B Chem., 318, 128104.
12. Nakhleh, M.K., Amal H., Jeries R., Broza Y.Y., About M., Gharra A., Ivgi H., Khatib S., Badarneh S. and Har-Shai, L., (2017). Diagnosis and Classification of 17 Diseases from 1404 Subjects via Pattern Analysis of Exhaled Molecules, ACS Nano, 11, 112–125.
13. Hua B. and Gaoquan S., (2007). Gas Sensors Based on Conducting Polymers, Sensors, 7, 267-307
14. Capone S., Forleo A., Francioso L., Rella R., Siciliano P., Spada- vecchia J., Presicce D.S. and Taurino A.M. (2003), Solid state gas sensors: state of the art and future activities, Journal of Optoelectronics and Advanced Materials 5, 5, 1335 – 1348.
15. Garg R., Kumar V., Kumar D., and Chakarvarti S.K., (2015). Polypyrrole Microwires as Toxic Gas Sensors for Ammonia and Hydrogen Sulphide, Columbia International Publishing Journal of Sensors and Instrumentation, 3, 1-13.
16. Arindam Das and Dipankar Panda ,(2019), SnO<sub>2</sub> Tailored by CuO for Improved CH<sub>4</sub> Sensing at Low Temperature, Advanced Science News, Phys. Status Solidi B, 1800296, DOI: 10.1002/pssb.201800296
17. Capone S., Forleo A., Francioso L., Rella R., Siciliano P., Spada- vecchia J., Presicce D.S. and Taurino A.M. (2003), Solid state gas sensors: state of the art and future activities, Journal of Optoelectronics and Advanced Materials 5, 5, 1335 – 1348.
18. Garg R., Kumar V., Kumar D., and Chakarvarti S.K., (2015). Polypyrrole Microwires as Toxic Gas Sensors for Ammonia and Hydrogen Sulphide, Columbia International Publishing Journal of Sensors and Instrumentation, 3, 1-13.
19. Lin C.W., Chen H.I., Chen T.Y., Huang C.C., Hsu C.S., Liu R.C. and Liu W.C. (2011), Ammonia Gas Sensing Performance of an Indium Tin Oxide (ITO) Based Device with an Underlying Au-Nanodot Layer, Sens Actuators B 160:1481.
20. Shang Y., Wang X., Xu E., Tong C. and Wu J. (2015), Porous Silicon Structures as Optical Gas Sensors, Anal Chim Acta, 15(8), 19968–19991.
21. Wang Y., Jia W., Strout T., Schempf A., Zhang H., Li B., Cui J. and Lei Y., (2009), Preparation, Characterization and Sensitive Gas Sensing of Conductive Core-sheath TiO<sub>2</sub>-PEDOT Nanocables, Sensors (Basel), 9(9), 6752–6763.

# Exploitation of PANI based Metal Oxide (ZnO-SnO<sub>2</sub>) Thick Films Humidity Sensor<sup>1</sup>

T.R. Ingle, G.T. Lamdhade

*Department of Physics, Vidya Bharati Mahavidyalaya, Camp, C.K. Naidu Road, Amravati (M.S.) India*

DOI:10.37648/ijrst.v13i01.003

Received: 29<sup>th</sup> December 2022; Accepted: 05 February 2023; Published: 08 February 2023

---

## ABSTRACT

Polyaniline (PANI) based Metal oxide nanocomposite thick films were prepared by using the screen printing technique. The films were fired and optimized temperature of 60°C for 30 minutes in an air atmosphere. In the present work, Polyaniline is prepared by polymerization of aniline under acidic conditions. Zinc Oxide (ZnO) nanoparticles and Tin Oxide (SnO<sub>2</sub>) prepared by the Precipitation method at room temperature. The films were showing a decrease in resistance with an increase in temperature indicating semiconducting behavior. It is observed that PANI doped Metal oxide nanocomposite sensor shows a high response and sensitivity with good repeatability as compared to that of pure PANI and Metal oxide nanoparticle. The crystallinity and the crystallite size were examined by X-Ray Diffraction technique (XRD), and Scanning Electron Microscopy (SEM). Also confirms that the properties of pure polyaniline can be improved by the synthesis of Polyaniline - Metal oxide nanocomposites

**Keywords:** *Polyaniline; Metal Oxides Nanocomposites; Humidity sensor; XRD; SEM*

---

## INTRODUCTION

There is a growing demand for a sensing system that has high sensitivity, wide dynamic range, good stability, quick response, good reproducibility, simple structure and minimal cost. Metal oxide films sensitive to humidity have been reported earlier where sensing has been done using optical means. However, metal oxide humidity sensors depending upon measurements of electrical parameters require high temperature operation and consume significant amount of power. Humidity control and monitoring are of great interest to a wide area; these include moisture sensitive products, fresh and pack-age food, drug storage and environmental control for valuable Antiques or paintings etc. [1, 2]. Humidity sensors that are available in the market include dew point, infrared, catalytic and tin oxide-based sensors, which may be expensive, or require high temperature operation and consume significant amount of power and high cost of maintenance [3]. Much research has been focused on the development of humidity sensitive material [4–6]. Among these are the investigation of using conducting polymers such as polyaniline, polypyrrole, and polythiophene for humidity and gas sensing [7–9]. Advantages with polymers as sensing materials are light weight, flexible, low cost and simple fabrication process [10]. Pure polymer, polymer blends and polymer–inorganic composites have also been studied for the purposes, resulting in different degree of advancements in this area [11–16].

---

<sup>1</sup> How to cite the article: Ingle T.R., Lamdhade G.T., Exploitation of PANI Based Metal Oxide(ZnO-SnO<sub>2</sub>) Thick Films Humidity Sensor, IJRST, Jan-Mar 2023, Vol 13, Issue 1, 16-22, DOI: <http://doi.org/10.37648/ijrst.v13i01.003>



# Investigation of Frequency and Temperature Dependent Electrical and Structural Characterization of PVC-PMMA Thin Films with Salicylic Acid Doping

A.B.More, G.T.Lamdhade

*Department of Physics, Vidya Bharati Mahavidyalaya, C.K Naidu Road, Camp Amravati, M.S. India 444602*

DOI:10.37648/ijrst.v13i03.012

*<sup>1</sup>Received: 14 August 2023; Accepted: 12 September 2023; Published: 20 September 2023*

---

## ABSTRACT

This research explores the electrical, molecular, and structural characteristics of PVC: PMMA Polyblend (1:2) doped with 8% salicylic acid. AC conductivities and dielectric constants were measured over a temperature range of 303 K to 353 K using a Precision LCR meter, revealing nuanced with dopant concentration, temperature, and frequency. FTIR spectroscopy highlighted distinct peak differences in PVC-PMMA films with and without the dopant, emphasizing the impact of salicylic acid on molecular interactions. XRD analysis demonstrated an amorphous nature in both doped and undoped thin films, while SEM and EDX revealed heterogeneous structures with varying dopant percentages. The study provides valuable insights into the intricate interplay between temperature, frequency, and dopant concentration in the electrical and structural properties of PVC: PMMA blends. These findings contribute to the understanding of material behavior for potential applications in diverse fields such as materials science and pharmaceuticals.

**Keywords:** *PVC-PMMA; AC conductivity; dielectric constant; frequency; salicylic acid; FTIR; XRD; SEM; EDX*

## INTRODUCTION

Polymer composites have garnered significant attention for their diverse applications in the field of electronics, owing to their tunable electrical properties and flexibility. Among these materials, Polyvinyl Chloride (PVC) and Poly(methyl methacrylate) (PMMA) blends have gained prominence as potential candidates for various electronic and optoelectronic devices due to their intriguing characteristics, such as high dielectric strength, thermal stability, and ease of processing. To further enhance their electrical performance, the introduction of dopants has emerged as a promising strategy.

## EXPERIMENTAL

Thin films of PVC-PMMA with different dopant concentrations were prepared using the isothermal evaporation technique. Preparation of a Polyblend thin film of PVC-PMMA in 1:2 weight proportional, the dopant and the polymer mixture were dissolved in a solvent (THF) were mixed in solution form .for a complete Homogeneous solution was kept for two or three days. after two or three days solution are in a homogeneous form then the solution mixture was poured onto a perfectly planed glass plate floating freely in a pool of mercury for perfect leveling. it was thereafter allowed to evaporate at room temperature further, and it was dried for two days to remove any traces of solvent. the

---

<sup>1</sup> How to cite the article: More A.B., Lamdhade G.T. (September 2023); Investigation of Frequency and Temperature Dependent Electrical and Structural Characterization of PVC-PMMA Thin Films with Salicylic Acid Doping; *International Journal of Research in Science and Technology*, Vol 13, Issue 3, 114-122, DOI: <http://doi.org/10.37648/ijrst.v13i03.012>

dry film removes from the glass plate and cuts into pieces of desired size then measure the thickness of the thin film by DIGMATIC micrometer, which was then coated on two sides with silver paint then by using the multimeter check whether the two electrodes working or not .then investigate the conductivity .Two sets of films were fabricated: one without salicylic acid (0% dopant) and the other with 8% salicylic acid as the dopant. AC conductivity measurements were performed using 4284 A precision LCR meter (Agilent Make), covering a frequency range of 20 Hz to 1MHz. The measurements were carried out at two different temperatures: 303 K to 353 K. The ln f and ln AC conductivity and dielectric values were recorded for further analysis.

Graph related to Dielectric constant of PVC-PMMA 1:2 with 0% SA and 8% SA

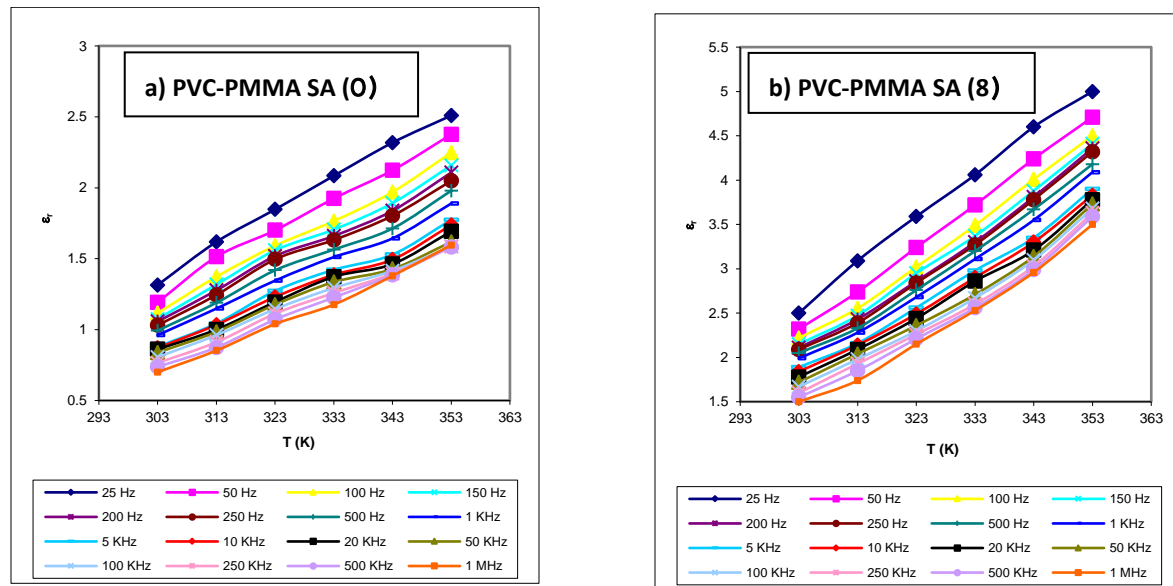


Fig 1.1. (a-b)Variation of  $\epsilon_r$  with T(K) at different frequencies for 1:2 PVC-PMMA System

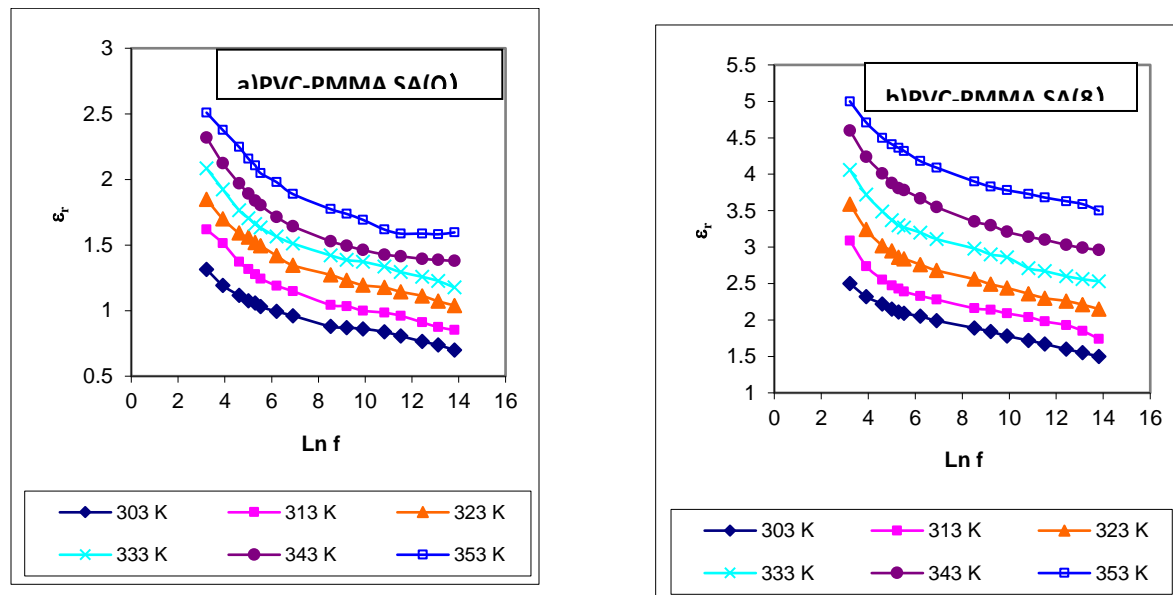


Fig 1.2.(a-b)Variation of  $\epsilon_r$  with Ln f at different temperatures for 1:2 PVC-PMMA System

Graph related to AC Conductivity of PVC-PMMA 1:2 with 0% SA and 8% SA

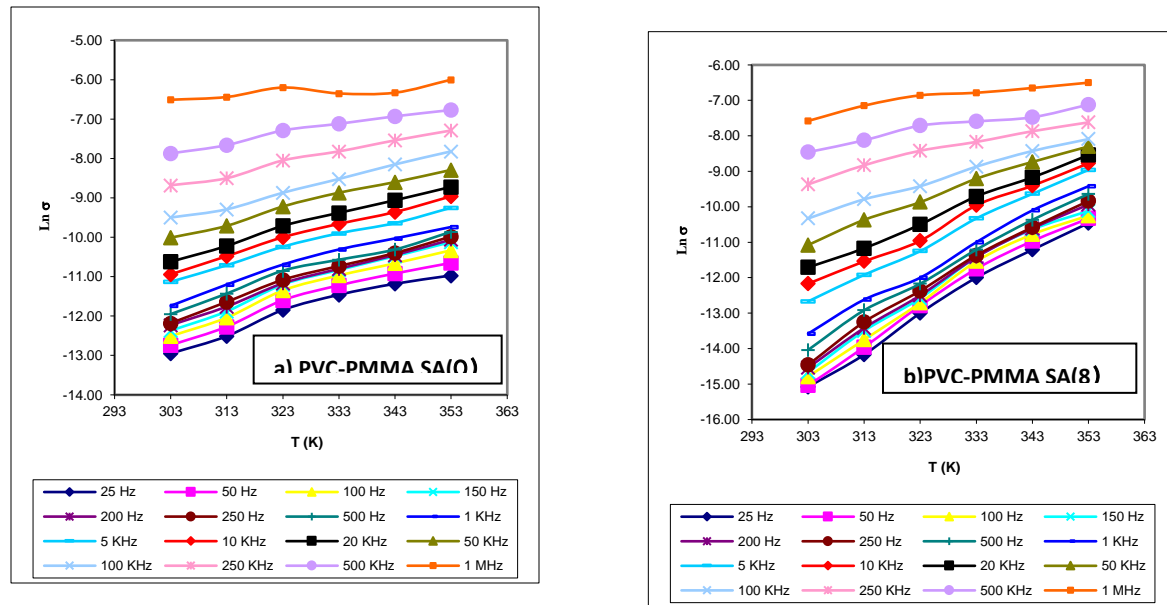


Fig 1.3. (a-b)Variation of  $\ln \sigma$  with  $T$  (K) at different frequencies for 1:2 PVC-PMMA System

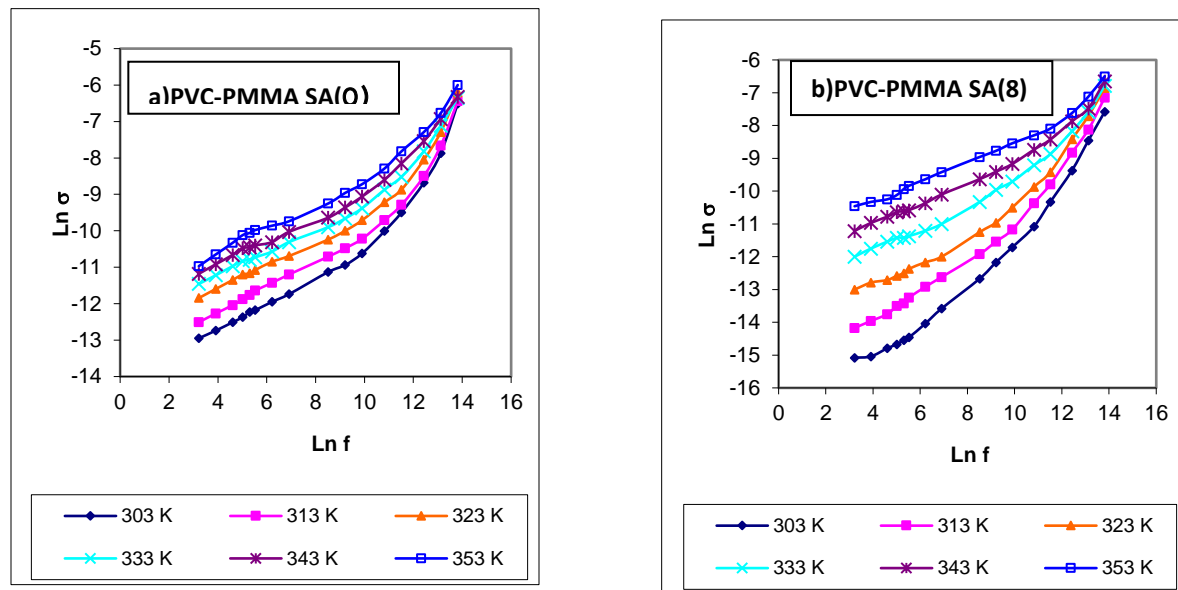


Fig 1.4. Variation of  $\ln \sigma$  with  $\ln f$  at different temperatures for 1:2 PVC-PMMA System

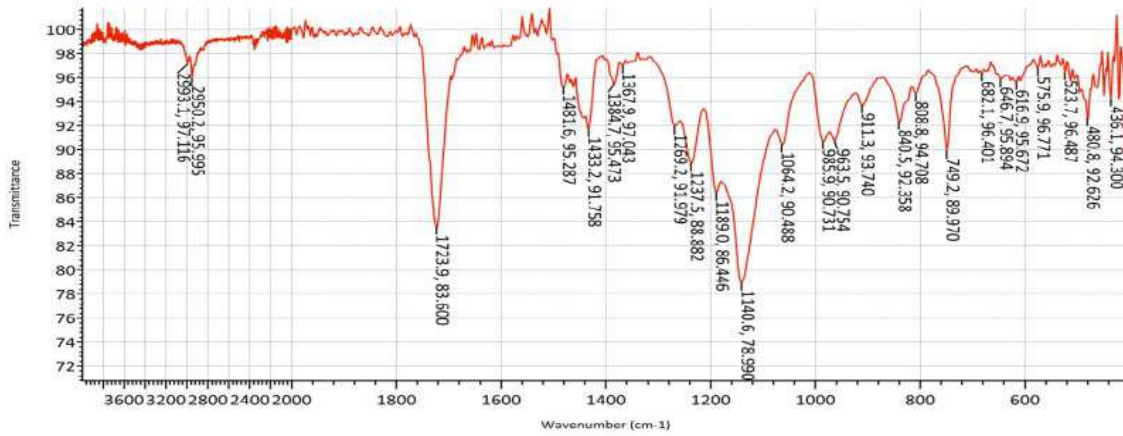


Fig 1.5 FTIR of 1:2 (PVC-PMMA) SA (0)

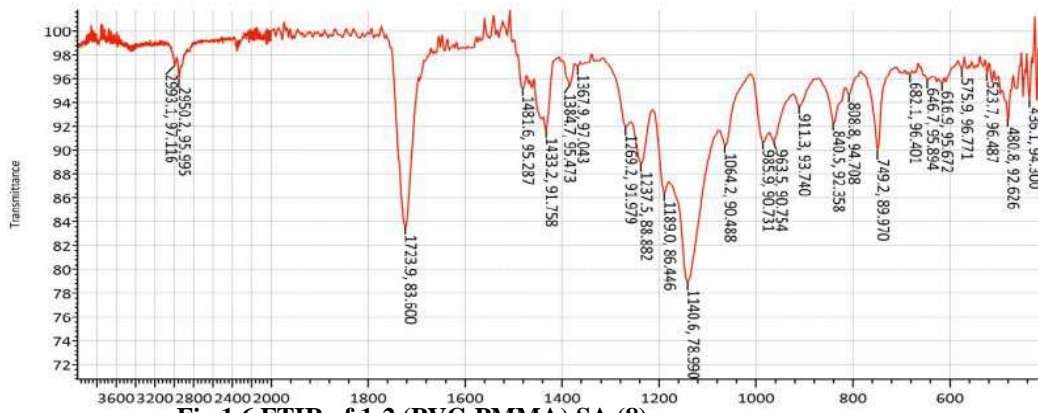


Fig 1.6 FTIR of 1:2 (PVC-PMMA) SA (8)

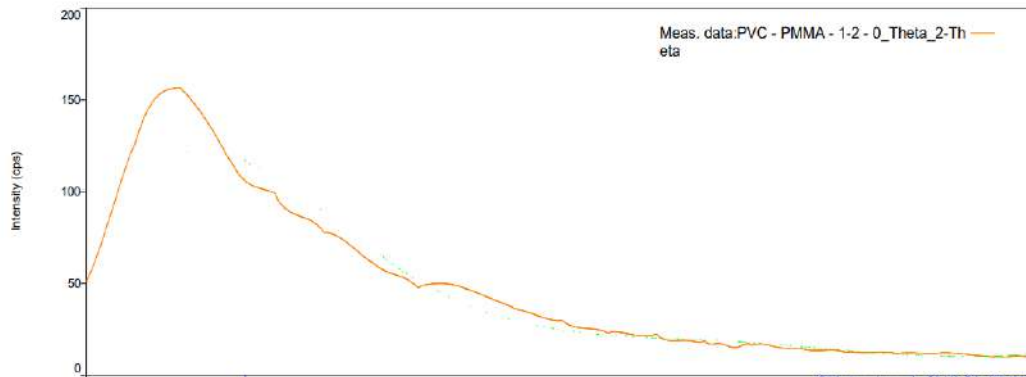


Fig 1.7 XRD Spectra of 1:2 PVC-PMMA 0% SA

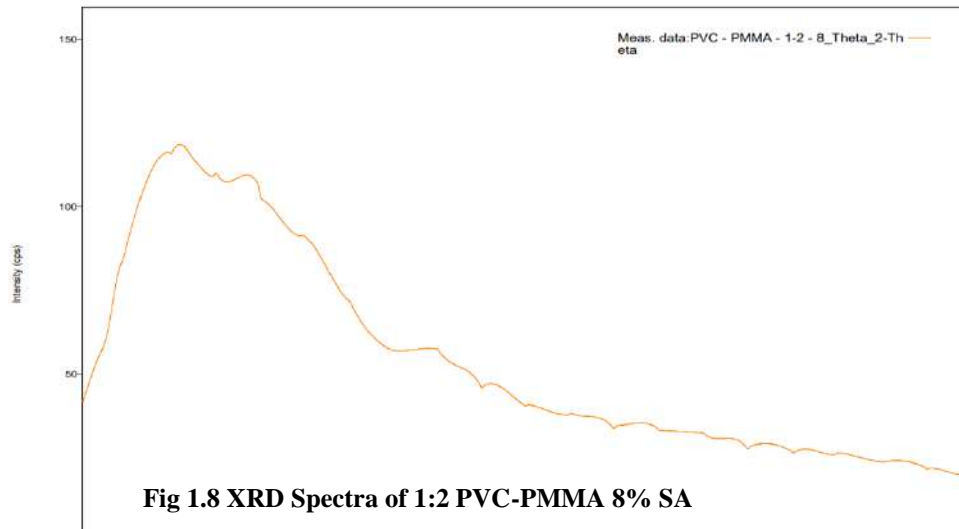


Fig 1.8 XRD Spectra of 1:2 PVC-PMMA 8% SA

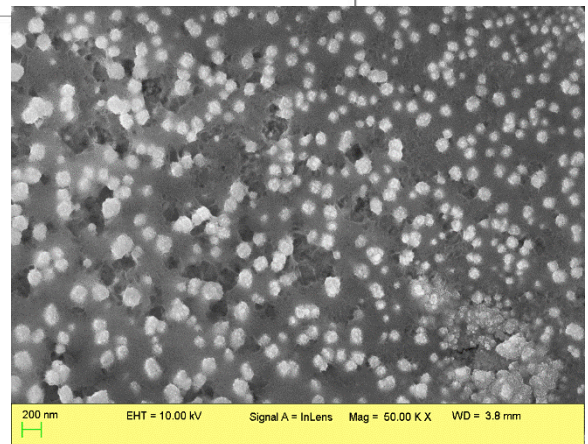
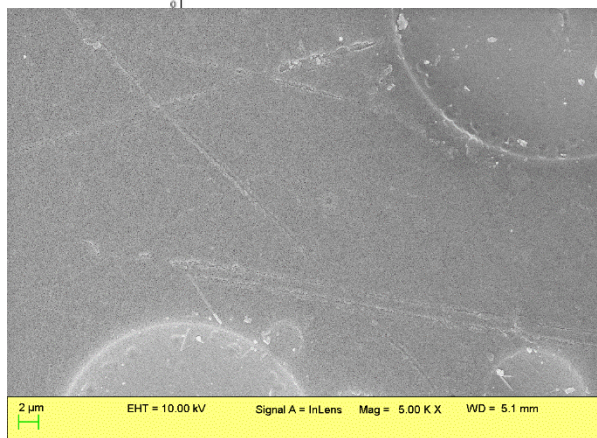


Fig 1.10 SEM of 1:2 PVC-PMMA 8% SA

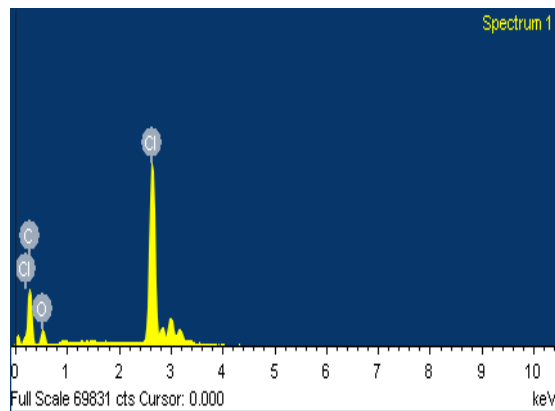


Fig 1.11 SEM of 1:2 PVC-PMMA 0% SA

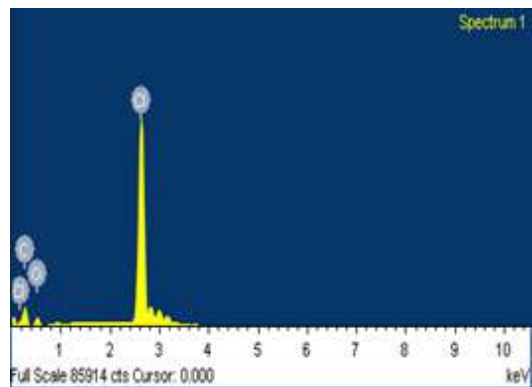


Fig 1.12 SEM of 1:2 PVC-PMMA 8% SA

## RESULTS AND DISCUSSION

### AC conductivities and dielectric constant:

The AC conductivities and dielectric constant, XRD, SEM, EDAX of PVC:PMMA blends (1:2)doped with 8% percentages of Salicylic acid were examined in this study. Measurements were taken using a 4284 A precision LCR meter (Agilent Make) with a frequency range of 20 Hz to 1 MHz. The tests were conducted over a temperature range of 303 K to 353 K.

Here's a summary of the key findings:

1. Variation of dielectric constant with temperature at different frequencies with and without dopant
2. Variation of dielectric constant with frequency at different temperatures with and without dopant
3. Variation of AC conductivity with frequency at different constant temperatures with and without dopant
4. Variation of AC conductivity with temperature at different constant frequencies with and without dopant
5. Variation of dielectric constant with concentration of dopant at various temperatures.
6. AC conductivity with concentration of dopant at various temperatures

The study explored PVC: PMMA blends (1:2) doped with 8% salicylic acid, examining various properties using a Precision LCR meter. Dielectric constant increased with temperature due to enhanced dipole flexibility, particularly notable in the polar PVC: PMMA blend. Conversely, dielectric constant decreased with increasing frequency, attributed to orientation polarization struggling to match field variations at higher frequencies. AC conductivity rose with frequency, indicating higher loss currents in response to changing electric fields. Notably, the dielectric constant increased with dopant percentage but decreased in AC conductivity, suggesting the salicylic acid's impact on the blend's functional sites. This sheds light on the nuanced interplay between temperature, frequency, and dopant concentration in the electrical and structural properties of the PVC: PMMA blends.

### FTIR:

The FTIR spectroscopy is a very useful technique to elucidate the intermolecular interaction between PVC, PMMA and Salicylic Acid. FTIR spectra were collected using an Agilent Micro Lab instrument. The spectra were recorded in the range of 4000-400  $\text{cm}^{-1}$  each sample was scanned 64 times, and background scans were taken 32 times to ensure accuracy and reliability. The FTIR spectra of PVC/PMMA/SA films were depicted in Fig. 1.5 demonstrates the FTIR spectrum of PVC-PMMA thin film without doping and Fig 1.6. Demonstrates the FTIR spectrum of PVC-PMMA thin film with doping. PVC-PMMA with SA. The FTIR spectra of PVC-PMMA thin films with and without an 8% SA dopant reveal notable differences in peak wavenumbers and intensities. The prominent peaks and their implications are discussed below In Fig 1.5. FTIR of PVC-PMMA 0% SA the peak 1062-1064.2  $\text{cm}^{-1}$  rocking vibration of  $\text{CH}_2$  group of PVC. The Peak 2950.2 In both film with and without SA which shows C- $\text{CH}_3$ , C-H Stretching in PMMA (Rajendra and Uma (2000)). The Peak 1481.6 C-H Stretching in PMMA. The Peak 1481.6 C-H Stretching in PMMA. The peaks at 2993.1  $\text{cm}^{-1}$  and 2951-2950.2  $\text{cm}^{-1}$  corresponds to the stretching of  $-\text{CH}_3$  and  $-\text{CH}_2-$  groups of PMMA. The band 616.9-617  $\text{cm}^{-1}$  demonstrate the C-Cl bond of the isotactic and syndiotactic structure of PVC. Broader and stronger bands in the region 1300-1000  $\text{cm}^{-1}$  correspond to C-O stretching vibrations which usually consists of two asymmetric coupled vibrations. i.e. C-C(=O)-O and O-C-C. The Peak at 749.2  $\text{cm}^{-1}$  corresponds to out of plane C-H bending in PVC. A sharp band located at 1723.9  $\text{cm}^{-1}$  was ascribed to the carbonyl group (C=O) in the film, which is typically attributed to PMMA. Similarity Peak at 840.5  $\text{cm}^{-1}$  PVC-PMMA without SA: Intensity of 94.708 and PVC-PMMA with 8% SA: Intensity of 92.801 This peak is associated with  $\text{CH}_2$  rocking vibrations in PVC. In Both Film the band at 1433-1433.2  $\text{cm}^{-1}$  is due to the wagging of methylene groups in PVC and/or owing to the asymmetric stretching of O- $\text{CH}_3$  group of PMMA. FTIR analysis highlights the presence of both PVC and PMMA components in the film. The intensity of various peaks provides information about the relative composition and structural aspects of the film. The reduction in intensity for specific PVC-related peaks suggests a decrease in the PVC content and potential structural changes. Fig 1.6 .FTIR of PVC-PMMA 8% SA which shows the stretching vibrations of C-H bonds 2849.5  $\text{cm}^{-1}$  [21]. The bands at 1328.8  $\text{cm}^{-1}$  represents the deformation of  $-\text{CH}_2$  in PVC and attributed

the overlapping CH<sub>2</sub> wagging in PMMA, 1249 cm<sup>-1</sup>, The peaks at 609 cm<sup>-1</sup> demonstrate the C-Cl bond of an isotactic and syndiotactic structure of PVC. 609.4 cm<sup>-1</sup> signifies C-Cl bonding. The characteristic peak at 1722-1723.9 cm<sup>-1</sup> can be attributed to the C=O stretching vibration of acrylate carboxyl group of PMMA and Both Film the asymmetric stretching of CH<sub>3</sub> group was observed at 1433.2-1435 cm<sup>-1</sup>. The bands at 1140.6- 1141 cm<sup>-1</sup> and 1237.5- 1238 cm<sup>-1</sup> are because of the C-O-C absorption and the stretching vibration of -OCH<sub>3</sub> group of PMMA. The characteristic absorption bands of PMMA occur at 1189.6-1190 cm<sup>-1</sup>, 1064-1064.2 cm<sup>-1</sup>, 985-985.9 cm<sup>-1</sup> and 840-840.5 cm<sup>-1</sup> [26, 28]. In PVC-PMMA doped SA thin film The 1727.6 cm<sup>-1</sup> characteristic peak is attributed to the C=O stretching vibration of the acrylate. The band located at 1148-1146.2 cm<sup>-1</sup> was attributed to the C-O group carboxyl group of PMMA and. In Both Film The bands at 961-963.5 cm<sup>-1</sup> are of CH<sub>2</sub> rocking vibration. The bands at 688-689.6 cm<sup>-1</sup> and Peak at 436.1 cm<sup>-1</sup> PVC-PMMA without SA: Intensity of 94.300 and PVC-PMMA with 8% SA: Intensity of 93.656. This peak is attributed to C-Cl stretching in PVC. The decrease in intensity in the doped film suggests a reduction in the PVC component. The decrease in intensity indicates changes in the polymer structure due to the presence of SA. Peak at 1384.7 cm<sup>-1</sup> PVC-PMMA without SA: Intensity of 95.473. PVC-PMMA with 8% SA: Intensity of 95.505. This peak represents the CH<sub>3</sub> symmetric deformation in PVC. The marginal difference in intensity suggests minor changes in the polymer structure. Peak at 1587.8 cm<sup>-1</sup> PVC-PMMA without SA: Absent. PVC-PMMA with 8% SA: Intensity of 98.436. This strong peak corresponds to the CO stretching in SA, confirming the successful incorporation of SA into the doped film. Peak at 2950.2 cm<sup>-1</sup> PVC-PMMA without SA: Intensity of 95.995. PVC-PMMA with 8% SA: Intensity of 95.158. This peak is linked to CH<sub>3</sub> stretching in PMMA. The similar intensities suggest that SA has a limited effect on PMMA. Peak 1587.8 cm<sup>-1</sup> corresponds to CO stretching in SA, confirming the successful incorporation of SA into the film. Peak 23 at 1727.6 cm<sup>-1</sup> indicates the presence of C=O stretching vibration of the acrylate carboxyl group of PMMA and is attributed to the SA dopant. In the film doped with 8% SA, several new peaks emerge, suggesting successful incorporation of SA: The presence of SA is evident with a strong peak at 1587.8 cm<sup>-1</sup>, representing CO stretching in SA. Other peaks related to PVC and PMMA, including C-Cl stretching and CH<sub>2</sub> rocking vibrations, are also present. The FTIR analysis indicates that SA has a limited effect on the characteristic peaks of PMMA, as the peak related to CH<sub>3</sub> stretching remains similar in intensity.

The introduction of Salicylic Acid into the PVC-PMMA thin film is confirmed by the appearance of SA-specific peaks. The decrease in the intensity of PVC-related peaks in the doped film suggests a reduction in the PVC component, indicating a change in the polymer structure due to SA doping. SA has a limited impact on PMMA, as indicated by the consistent intensity of PMMA-related peaks. This FTIR analysis underscores the importance of studying the molecular interactions and structural changes when incorporating SA into PVC-PMMA films, which has implications for various applications, including materials science and pharmaceuticals. The FTIR analysis confirms the presence of SA in the film, as evidenced by the SA-specific peaks. The peaks related to PVC and PMMA are still present in the film, indicating the coexistence of these components with SA. The similar intensity of PMMA-related peaks suggests that SA has a limited effect on PMMA. This analysis provides essential information about the molecular interactions and structural changes occurring when SA is introduced into the PVC-PMMA thin film, highlighting the impact of the dopant on the film's chemical composition and structure.

### Result from XRD Spectra and SEM and EDX analysis:

XRD of undoped and doped thin film show almost amorphous Nature. There are no sharp peaks in all the X-RD patterns. It is well known that the absence of peaks in intensity versus 2θ curve indicates that the (thin films) samples are amorphous in nature. Energy dispersive X-ray (EDX) was engaged for elemental analysis of the PVC-PMMA Polyblend without and with SA thin film. The EDX spectrum presented in Fig. 1.11-1.12. Confirmed sharp peaks due to the following elements: fig 1.11 shows C (67.84%), O (13.21%) and Cl(18.94 %) and fig 1.12 shows C (56.81%), O (11.07%) and Cl (32.12 %) in addition to hydrogen. The occurrence of these elements will generate charges on the surface of the polymer and create electrostatic forces of attraction between the samples

Explanation from SEM Photography Scanning electron microscope images of the 1:2 PVC-PMMA blend without SA and with SA. The images exhibit heterogeneous structure in both blends. Fig 1.9 shows the morphology of blends show a phase separated region. The PVC domains are visualized as the holes from which the material was pulled out. Systems the phase separations were observed. This is in agreement with result reported by (Yongseok Kim et al., 2008), (Rajendran S. et al, 2008). fig 1.10. Shows as dopant percentage increases. That is due to the increase in amorphousity. This is in agreement with XRD results.

## CONCLUSIONS

In conclusion, the study investigated (1:2) PVC:PMMA blends doped with 8% salicylic acid. AC conductivity and dielectric constant variations were studied at different temperatures and frequencies, revealing nuanced interactions. FTIR analysis confirmed the successful incorporation of salicylic acid, impacting PVC but having a limited effect on PMMA. XRD patterns indicated an amorphous nature in both doped and undoped thin films. SEM images showed a heterogeneous structure, with increasing dopant percentages leading to higher amorphousness. Overall, the findings highlight the complex interplay of temperature, frequency, and dopant concentration on the electrical and structural properties of PVC:PMMA blends.

## REFERENCES

1. Belsare, N. G., Wadtkar, A. S., Joat, R. V., Wasnik, T. S., Raghuvanshi, F. C., Raulkar, K. B., & Lamdhade, G. T. (2011). *Journal of Electron Devices*, 11, 583-587
2. Deshmukh, S. H., Burghate, D. K., Akhare, V. P., Deogaonkar, V. S., Deshmukh, P. T., & Deshmukh, M. S. (2007). *Bull. Mater. Sci.*, 30(1), 51–56. <https://doi.org/10.1007/s12034-007-0009-6>
3. Fahmy, T., & Elzanaty, H. (2019). *Bull. Mater. Sci.*, 42, 220. <https://doi.org/10.1007/s12034-019-1906-1>
4. Dakre, A. B., & Lamdhade, G. T. (2014). *International Journal of Science and Research (IJSR)*, 3(6).
5. Ojha, P., Siddaiah, T., Gopal, N. O., & Ramu, Ch. (2018). *International Journal of Scientific Research in Physics and Applied Sciences*, 6(6), 80-87. <https://doi.org/10.26438/ijrps/v6i6.8087>
6. Tanwar, A., Gupta, K. K., Singh, P. J., & Vijay, Y. K. (2006). *Bull. Mater. Sci.*, 29(4), 397–401. <https://doi.org/10.1007/bf02704142>
7. Vidhale S.G., Belsare N.G., A.S.Wadtkar, September-(2013), *International Journal of Scientific & Engineering Research*, Volume 4, Issue 9.
8. Vdhale, S.G., N. G. Belsare, November(2013), *International Journal of Scientific & Engineering Research*, Volume4, Issue11, 1253, <https://doi.org/10.14299/ijser.2013.11>
9. R. V. Waghmare, Belsare N.G, Raghuvanshi F C and Shilaskar S N, April (2007), *Bull. Mater. Sci.*, Vol. 30, No. 2, pp. 167–172., <https://doi.org/10.1007/s12034-007-0030-9>
10. R Padma Suvarna, K Raghavendra Rao and K Subbarangaiah, (2002), *Bull. Mater. Sci.*, Vol. 25, No. 7, pp. 647–651.
11. Shukla, J. P., & Gupta, M. (1987). *Indian Journal Pure and Applied Physics*, 25, 242-244.
12. Dandel, R. M., Belsare, N. G., & Raghuvanshi, F. C. (2011). *International Journal of Polymers and Technologies*, 3(2).
13. Wadtkar, A. S., Wasnik, T. S., Vidhale, S. G., & Belsare, N. G. (2014). *International Journal of Basic and Applied Research*, 4, 196-200.
14. Ramesh,S.,&Liew,C.W.(2013).*Measurement*,46(5),1650-1656, <http://doi.org/10.1016/j.measurement.2013.01.003>.
15. Ahmad, A. H. (2014). *International Journal of Computer Science*, 2, 20-23.
16. Bushra, A. H., Ahmad, A. H., & Duaa, A. U. (2013). *International Journal of Application or Innovation in Engineering & Management*, 2(11), 86.
17. Khaled, M. A., Elwa, Y. A., Hussein, A. M., & Abdullah, K. (2003). *Egypt Journal*, 26(1), 83-91.
18. Sharma, D., & Tripathi, D. (2018). *AIP Conference Proceedings*, 1953(1), 050056. <https://doi.org/10.1063/1.5032711>
19. V. P. Akhare, (2013), *Acta Ciencia Indica*, Vol. XXXIX P, No. 2, 79
20. Patil Shatala. D. (2007) *Mater Sc.*, 2, 89-92
21. Joseph Jenifer, Deshmukh, Kalim,Chidambaram, K.,Faisal, Muhammad,Selvarajan, E. Sadasivuni, Kishor Kumar, Ahamed, M. Basheer,Pasha, S. K. Khadheer, (2018) ,*Journal of Materials Science: Materials in Electronics* 29:20172–20188, <https://doi.org/10.1007/s10854-018-0150-6>
22. Adel M. El Sayed, (2020), *Results in Physics*,<https://doi.org/10.1016/j.rinp.2020.103025>
23. Suresh S.SMohanty.S.,Nayak. S.K. (2017) *J. Clean. Product*. 149 863-873.
24. Alghunaim.N.S., *Results in Physics*,2015,(5),331-336,[doi.org/10.1016/j.rinp.2015.11.003](https://doi.org/10.1016/j.rinp.2015.11.003)
25. Mohammad Saleem , Raina Aman Qazi and Mian Said Wahid , (2008), *African Journal of Pure and Applied Chemistry* Vol. 2 (4), pp. 041-045
26. S.K. Mahto, S. Das, A. Ranjan, S.K. Singh, P. Roy, N. Misra, (2015),*RSC Adv.* 5, 45231–45238



27. Vijayakumaria .G., Selvakumara .N. , Jeyasubramaniana .K. , Malab. R., ( 2013 ) , Physics Procedia ,49 67 – 78
28. S. Ramesh, Leen K.H., Kumutha .K, Arof A.K., (2007),Spectrochim. Acta Part A Mol. Biomol. Spectrosc. 66, 1237–1242
29. Rajendran S and T Uma, (2000),J.Power Sources 88,282
30. Fahmy T and Elzanaty Hesham, Sci. (2019), Bull. Mater. 42:220,1-7 <https://doi.org/10.1007/s12034-019-1906-1>
31. Rajendran S and T Uma, (2000),Matter Lett.44,242-248
32. Cyprian yameso Abasi,Donbebe wankasi and Ezekiel Dixon Dikio,(2018),Asian journal of chemistry,vol 30(4),859-867,doi.org/10.14233/ajchem.201821112.
33. Yongseok Kim, Sangdo Park, Young-Soo Seo, Naesung Lee and Yongho Seo., (2009); Journal of the Korean Physical Society, Vol. 54, No. 2, 749-753
34. S Rajendran., Prabhu M.R., Rani M.U., (2008); Int.J.Electrochem. Sci., 3, 282- 290.

# Sol-Gel Synthesis and Characterization of SnO<sub>2</sub>- PPy Multilayer Thick Films<sup>1</sup>

\*Bhuyar R.S., Raulkar K.B, Lamdhade G.T.

Department of Physics, Vidya Bharati Mahavidyalaya, CK Naidu Road, Amravati, M.S., India

DOI:10.37648/ijrst.v13i02.010

Received: 10 June 2023; Accepted: 24 June 2023; Published: 29 June 2023

---

## ABSTRACT

The aim of this study is focused on preparation of tin oxide doped with polypyrrole multilayer thick film by using base as a alumina substrates. The structural and morphological properties reported, XRD patterns show nanocrystalline form with desired peaks of composites and SEM study reveals that the grain size of nanometer order and shows nano- porous structure, which leads to exhibit large surface area, stability and highest response to gas and found (92SnO<sub>2</sub>:8 PPy) sensor multilayer thick film as optimised sensors

**Keywords:** Tin oxide; polypyrrole; multilayer thick films; XRD; SEM

## INTRODUCTION

Tin oxide (SnO<sub>2</sub>) is the most used sensing material in commercially sensor devices for toxic gases detection [1]. It is well known that the sensing properties of SnO<sub>2</sub>-based material depend on its chemical and physical characteristics, which are strongly dependent on the preparation conditions, dopant and grain size. This implies that the synthesis of the sensing material is a key step in the preparation of high-performance MOS gas sensors. SnO<sub>2</sub> powders and films can be prepared by a variety of synthesis methods [2-5]. This paper focused on synthesis of pristine nano-particles of SnO<sub>2</sub>, ppy and Al<sub>2</sub>O<sub>3</sub> and also (SnO<sub>2</sub>- ppy) multilayer thick films with Al<sub>2</sub>O<sub>3</sub>, as base material.

## EXPERIMENTAL: PREPARATION OF MATERIALS

The methods of synthesis of nano-particles can be broadly classified in the three categories namely, liquid phase synthesis, gas-phase synthesis and vapour-phase synthesis . In the present work, we have used sol-gel method for the synthesis of pristine nano-particles of SnO<sub>2</sub>, Al<sub>2</sub>O<sub>3</sub> and PPy [6].

### Preparation of Tin Oxide (SnO<sub>2</sub>)

All the chemicals used in this study were of GR grade purchase from Sd-fine, India (purity 99.99%). The chemicals are used without any further purification. Stannous chloride dehydrates (SnCl<sub>2</sub>.2H<sub>2</sub>O), Ammonia solution and deionized water were used during reaction. The conducting silver paint (Sigma Aldrich Chemical, USA) is used to form electrodes.

---

<sup>1</sup> How to cite the article: Bhuyar R.S., Raulkar K.B., Lamdhade G.T.; Apr-Jun 2023; Sol-Gel Synthesis and Characterization of SnO<sub>2</sub>- PPy Multilayer Thick Films; *International Journal of Research in Science and Technology*, Vol 13, Issue 2, 67-77, DOI: <http://doi.org/10.37648/ijrst.v13i02.010>

In preparation of SnO<sub>2</sub>, 2g (0.1 M) of stannous chloride dehydrate (SnCl<sub>2</sub>.2H<sub>2</sub>O) is dissolved in 100 ml water. After complete dissolution, about 4 ml ammonia solution is added to above aqueous solution with magnetic stirring. Stirring is continued for 20 minutes. White gel precipitate is immediately formed. It is allowed to settle for 12 hrs. Then it is filtered and washed with water 2-3 times by using deionized water. The obtained precipitate were mixed with 0.27 g carbon black powder (charcoal activated). The obtained mixer is kept in vacuum oven at 70 °C for 24 hours so that the mixer gets completely in to dried powder. Then this dry product was crushed into a fine powder by grinder. Now obtained product of fine nanopowder of SnO<sub>2</sub> was calcinated at 700°C up to 6 hours in the auto controlled muffle furnace (GAYATRI Scientific, Mumbai, India.) so that the impurities from product will be completely removed.

### Preparation of Polypyrrole (PPy)

The method used for the preparation of polypyrrole is chemical polymerization. Powder polypyrrole was prepared with 4.290 (high) weight ratio of pyrrole (Py) monomer/oxidant (FeCl<sub>3</sub>). During the synthesis, concentration of FeCl<sub>3</sub> was kept constant and methanol was used as a solvent.

The Py monomer, anhydrous iron (III) chloride (FeCl<sub>3</sub>) and methanol were used as received for synthesis of PPy. The solution of 7 ml methanol and 1.892 g FeCl<sub>3</sub> was first prepared in round bottom flask. Then 8.4 ml Py monomer was added to (FeCl<sub>3</sub> + methanol) solution with constant stirring in absence of light. The amount of Py monomer added to the solution (1/2.33 times of FeCl<sub>3</sub>) was in such a way to get maximum yield [7].

The polymerization of Py, which was suppressed in a solution, progressed rapidly due to an increase of oxidation potential caused by evaporation of solvent. In the polymerization reaction of Py, it was observed that as soon as the Py monomer was added to the solution, the colour changed to dark green/black. There was an increase in temperature of the solution during the start of reaction, which showed that it is an exothermic reaction [8]. The reaction was carried out at room temperature for 4 hrs. The final precipitated polymer was filtered by a conventional method. The polymer was washed with distilled water several times till the filtrate obtained was colourless. To remove last traces of unreacted pyrrole and remaining ferric and ferrous chloride formed due to polymerization, it was then washed with methanol.

The polymer, obtained in powder form was dried first at room temperature for a few hours and then finally dried in an oven kept at 80°C for 5-6 hrs. This polypyrrole is then used for active layers of Semiconductor Gas Sensors.

### Preparation of Alumina (Al<sub>2</sub>O<sub>3</sub>)

1M alcoholic AlCl<sub>3</sub> solution was prepared, followed by addition of 25% ammonia solution. The resulting solution turned to a white sol. This was followed by the addition of PVA (0.5M). The solution was stirred continuously using a magnetic stirrer until it became a transparent sticky gel. The gel was allowed to mature for 24 hours at room temperature. The resultant gel was heat treated at 100°C for 24 hours which led to the formation of light weight porous materials due to the enormous gas evolution. The dried gel was, then calcined at 1000°C for 4 hours and finally, the calcined powders were crushed using mortar and pestle to get the fine homogeneous dense powder of Alumina.

### Fabrication of Sensors

Three series of the samples prepared were SnO<sub>2</sub>: PPy with Al<sub>2</sub>O<sub>3</sub> base of multilayer sensors. The different combinations are shown in tables 1.

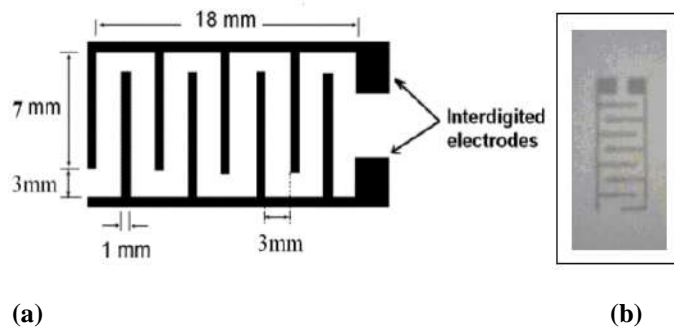
**Table 1 Samples codes of series : SnO<sub>2</sub>: PPy**

Sr. No.	Sample codes	SnO <sub>2</sub> (mole %)	PPy (mole %)
1	F1	100	00
2	F2	98	02
3	F3	96	04
4	F4	94	06
5	F5	92	08
6	F6	90	10

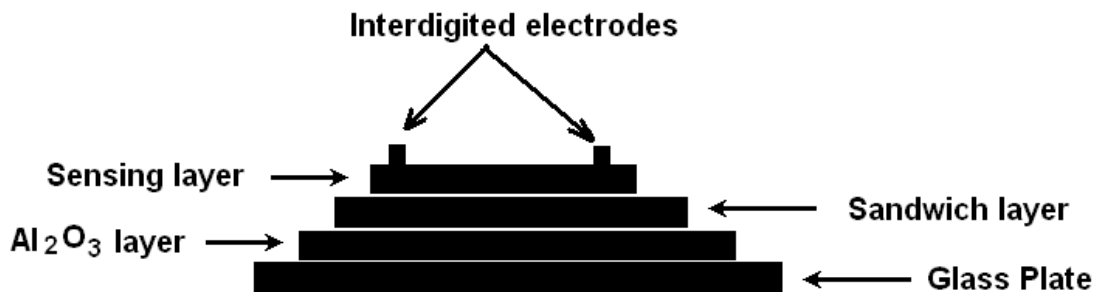
Out of various methods of sensors preparation, the screen-printing (thick film technology) is most widely used. Screen-printing is the transfer of pastes through a fabric screen onto a substrate.

**Multilayer preparation**

Fig. 1 (a), and 1(b) show fabrication of interdigitated electrodes, actual photographs of interdigitated electrodes respectively.



**Fig. 1** (a) Fabrication of interdigitated Electrodes (b) Actual photograph of interdigitated electrodes



**Fig.2** Design of multilayer Sensor

On clean glass plate, Al<sub>2</sub>O<sub>3</sub> was deposited by using screen-printing technique and it was used as base of the sensor. On Al<sub>2</sub>O<sub>3</sub>, the sample layers were prepared. Finally on the top, Interdigitated electrodes were fabricated using conducting silver paste as shown in the Fig. 1(b). Design of multilayer sensor is shown in Fig. 2.

**Preparation of Samples of Series SnO<sub>2</sub>: PPy/Al<sub>2</sub>O<sub>3</sub>/GP**

The obtained product of fine nano-powder of SnO<sub>2</sub> and PPy are used for fabrication of thick films sensors by using screen-printing technique. For this, the SnO<sub>2</sub> powder was mixed thoroughly with different X mole% of PPy (X = 2, 4, 6, 8,10) along with Al<sub>2</sub>O<sub>3</sub> base on glass plate (GP) substrate the aid of acetone by using the mortar and pestle. The sample codes, mole% of powder, and thickness are listed in the Table 2. The mixed powder of SnO<sub>2</sub>:PPy system was further calcinated at temperature 800°C for 5hrs. in the auto controlled muffle furnace (Gayatri Scientific, Mumbai, India.) After, the calcinations again uniformly mixed the powder using the grinder

Table 2: Length, Width and Thickness of Multi-layers in SnO<sub>2</sub>: PPy/Al<sub>2</sub>O<sub>3</sub>/GP gas sensor

Sample Code	Doping mole %	Upper layer length (cm)	Upper layer width (cm)	Thickness (x 10 <sup>-4</sup> cm)		
	Layers:			Upper Layer (1)	Al <sub>2</sub> O <sub>3</sub> L ayer (2)	Total (1+2)
	Upper/ /Al <sub>2</sub> O <sub>3</sub> / Glass plate (GP)					
F1	SnO <sub>2</sub> / Al <sub>2</sub> O <sub>3</sub> /GP	3	1.5	5.1	26.4	31.5
F2	98 SnO <sub>2</sub> :2 PPy/ Al <sub>2</sub> O <sub>3</sub> /GP	3	1.5	3.1	34.2	37.3
F3	96 SnO <sub>2</sub> :4 PPy/ Al <sub>2</sub> O <sub>3</sub> /GP	3	1.5	2.8	35.1	37.9
F4	94 SnO <sub>2</sub> :6 PPy/ Al <sub>2</sub> O <sub>3</sub> /GP	3	1.5	3.4	32.6	36.0
F5	92 SnO <sub>2</sub> :8 PPy/ Al <sub>2</sub> O <sub>3</sub> /GP	3	1.5	3.0	35.5	38.5
F6	90 SnO <sub>2</sub> :10 PPy/ Al <sub>2</sub> O <sub>3</sub> /GP	3	1.5	3.6	32.3	35.9
F7	PPy/ Al <sub>2</sub> O <sub>3</sub> /GP	3	1.5	1.9	48.4	50.3

**RESULTS AND DISCUSSION**

X-Ray diffraction pattern of polypyrrole [9] showed that, it is amorphous in nature. In Fig. 3 XRD pattern of polypyrrole was recorded in terms of  $2\theta$  in the range 5 to 100°. As shown in XRD pattern broad peak occurs at 29° and it is characteristics of amorphous nature of polypyrrole. The broad peak occurs due to the scattering of X-rays from polymer chains at the interplaner spacing. The position of maximum intensity of amorphous halos depends on monomer to oxidant ratio. The average crystallite size of polypyrrole is about 119 nm. Abroad peak is observed at about  $2\theta = 29.36$  which is characteristics peak of amorphous PPy. However, the peak obtained at 29 degree matches with the value of (3.040 Å) FeCl<sub>3</sub>. The average green size determines from XRD pattern using Scherrer formula of these material is about 119 nm for PPy.

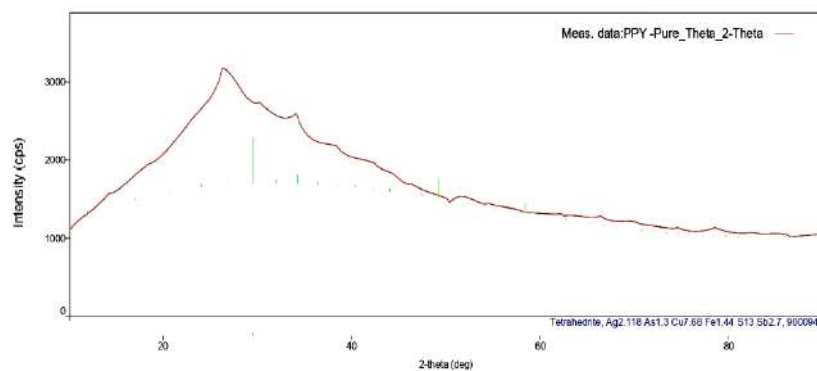


Fig. 3 XRD of Spectra of Polypyrrole

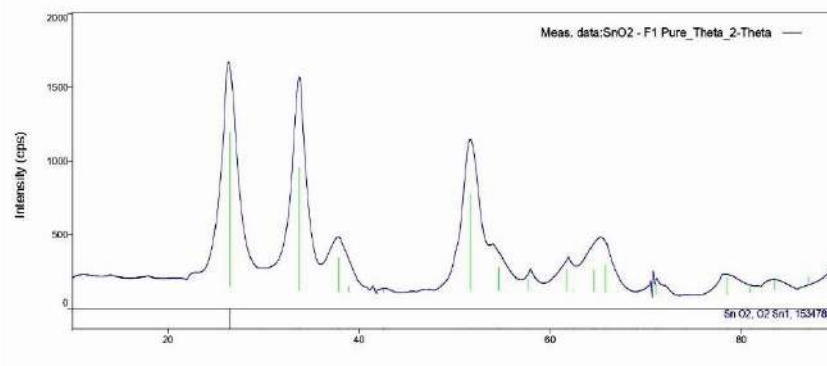
Fig. 4 XRD Pattern of SnO<sub>2</sub>

Figure 4 shows the X-ray diffraction pattern of pure SnO<sub>2</sub>, calcinated at 800°C for 4-5 hours. It is recorded in terms of  $2\theta$  in the 10 to 100°.

In case of pure SnO<sub>2</sub> a main pic is observed at 26.54°. This peak corresponding to the plane (110) of SnO<sub>2</sub> in tetragonal structure (JCPDS card No.1534785) with 100% intensity. The other Peak of SnO<sub>2</sub> mainly correspondent to the planes (101), (200), (211), (220), (310), (301) and (321).

These planes correspond to the cassiterite phase of SnO<sub>2</sub>. Tin (IV) dioxide (II) i.e. SnO<sub>2</sub> has only one stable phase the so called cassiterite (mineral form) or rutile (material structure). It crystallizes in the tetragonal rutile structure with space group  $D^{14}_{4h}$  ( $P_{42/mnm}$ ), which correspondence to the number 136 in the standard listening with cell parameter  $a=b=4.7456$  Å,  $C=3.1930$  Å and  $\alpha = \beta = \gamma = 90^\circ$  with  $c/a$  ratio of 0.6728.

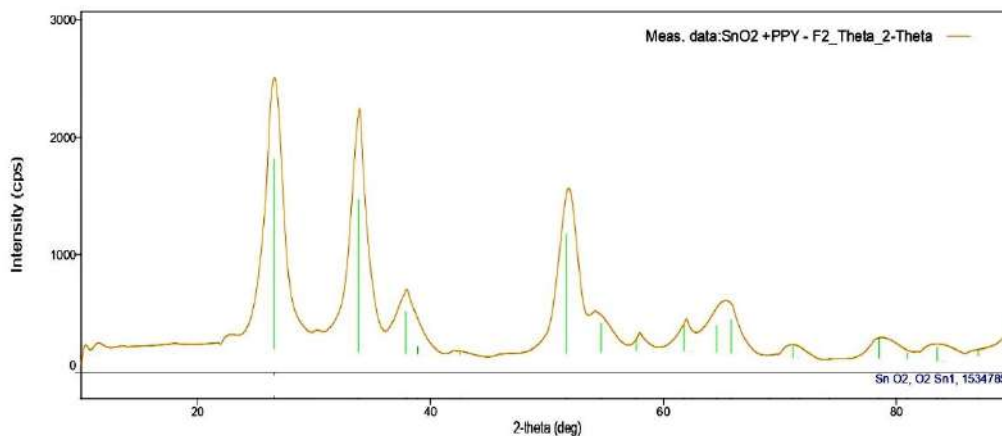
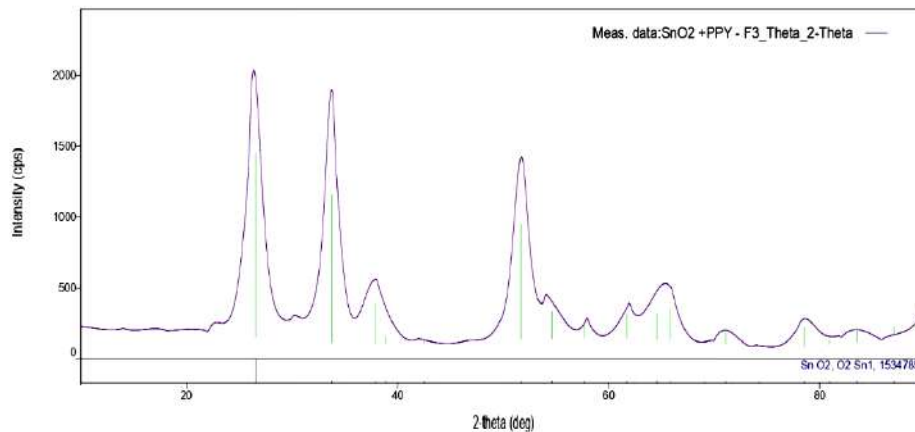
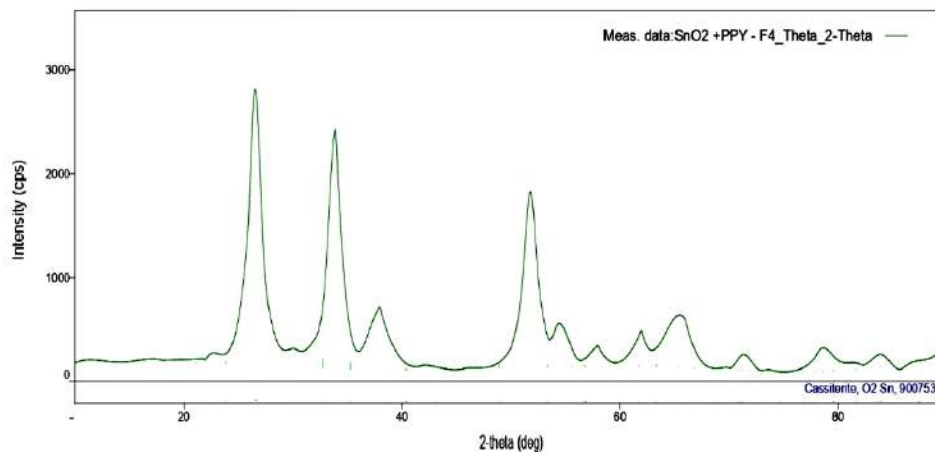
Fig. 5 XRD Pattern of 98SnO<sub>2</sub>:2PPy

Fig. 5. shows that the X-ray diffraction pattern of 98SnO<sub>2</sub>:2PPy calcinated at 800°C for 4 to 5 hours. It is recorded in terms of  $2\theta$  in the range of 10 to 100 degree. It is observed as the doping of PPy increases, the intensity of corresponding peak increases. This peak correspondence to the plane of 96SnO<sub>2</sub>:4PPy (JCPDS Card no.1534785) with 100% intensity. The other peaks of 98SnO<sub>2</sub>:2PPy correspondence to the plane (101), (200), (211), (220), (310), (301), (321).

Fig. 6 XRD Pattern of 96SnO<sub>2</sub>:4PPy

As shown in above spectra fig.6. 96SnO<sub>2</sub>:4PPy main peak in case of pure SnO<sub>2</sub> is observe at 26.54 degree and his correspondence to the plane (110) of SnO<sub>2</sub> in tetragonal structure(JCPDS Card no.1534785) with 100% intensity the other pic of SnO<sub>2</sub> mainly correspondence to the plane (101), (200), (111) and (301).

Fig. 7. XRD Pattern of 94SnO<sub>2</sub>:6PPy

As shown in above fig.7. 94SnO<sub>2</sub>:6PPy main peak [10], in case of pure SnO<sub>2</sub>, is observed at 26.58 and this peak corresponds to the plane(110) of SnO<sub>2</sub> in tetragonal structure(JCPDS Card no.9007533) with 100% intensity the other peaks of SnO<sub>2</sub> mainly corresponds to the Planes (101), (200), (111), (211) and (301). These planes corresponds to the cassiterite phase of SnO<sub>2</sub>.SnO<sub>2</sub> has only one stable phase, the so called (mineral form) or rutile (material structure) JCPDS Card no.9007533. It crystallizes in the tetragonal rutile structure with space group which corresponds to the number 136 in the standard listing with cell parameter  $a = b = 4.7380\text{\AA}$ ,  $c = 3.1865\text{\AA}$  and  $\gamma = \beta = \alpha = 90$  degree with  $c/a$  ratio of 0.6725.

From table 3. it is observed that average crystallite size of 94SnO<sub>2</sub>:6PPy doping is list as compared to the other compositions and pure materials and hence 94SnO<sub>2</sub>:6PPy compositions has large active surface area for sensing the gas.

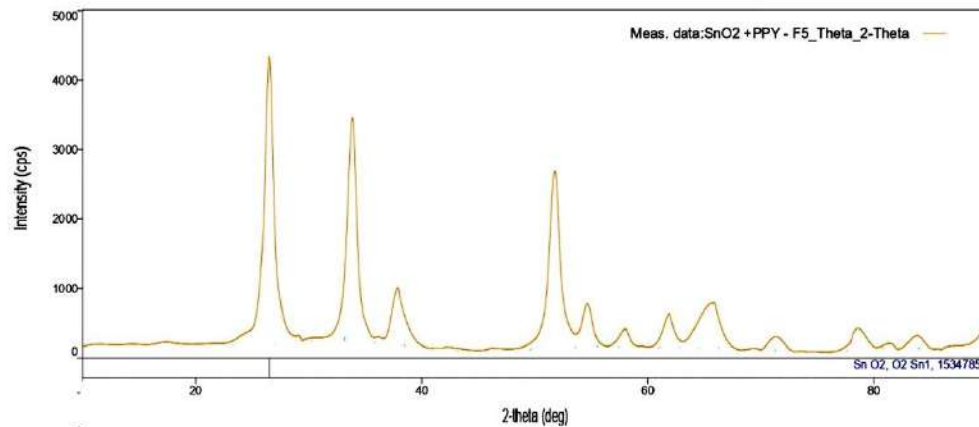
Fig. 8. XRD Pattern of 92SnO<sub>2</sub>:8PPy

Fig 8. 92SnO<sub>2</sub>:8PPy XRD spectra of doping of SnO<sub>2</sub>:PPy, incase of pure SnO<sub>2</sub> is observed at 26.54 degree and this peak corresponds to the plane (110) of SnO<sub>2</sub> and PPy in bixbyite phase (JCPDS Card No. 1011264) with  $2\theta=33.16$ , d-value is 2.699 with 100% intensity peak of SnO<sub>2</sub> and PPy mainly correspond to the Planes (220), (310) and (301).

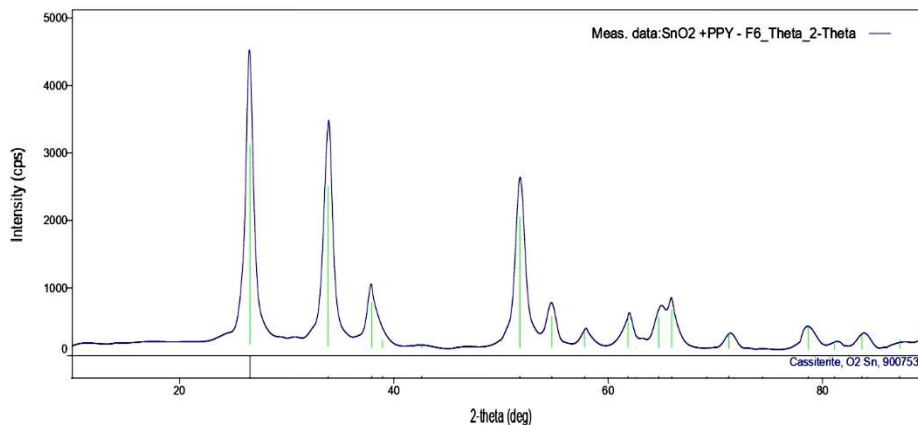
Fig. 9. XRD Pattern of 90SnO<sub>2</sub>:10PPy

Fig. 9. as shown in above spectra of doping of SnO<sub>2</sub> and PPy main peak is observed at 26.58° and this corresponds to the plane (110) of SnO<sub>2</sub> in tetragonal structure (JCPDS Card No. 9007533) with 100% intensity. The other peak of SnO<sub>2</sub> and PPy Mainly correspond to the planes (110), (101), (112) and (301). These planes correspondence to the cassiterites phase of SnO<sub>2</sub> (JCPDS Card No. 9007533). In fig 9. it is observed that XRD pattern contains 8-10 peaks. These are prominent peak of SnO<sub>2</sub>. The (hkl) values are obtained by using  $2\theta$  and d- values from XRD pattern.



The crystallite size (D) was calculated from Scherer's formula using FWHM and it is listed in the table 3. as below,

Table 3. Average crystallite size of SnO<sub>2</sub>, PPy and their compositions

Sr. No.	Chemical Composition of SnO <sub>2</sub> :TiO <sub>2</sub> (mole %)	Maximum Intensity Peak Position ( $2\theta$ ) in degree	FWHM ( $2\theta$ ) degree	Average Crystallite Size (D) in nm
01	Pure SnO <sub>2</sub>	26.5414	0.1338	120.68
02	98SnO <sub>2</sub> :2PPy/Al <sub>2</sub> O <sub>3</sub> /GP	26.6424	0.2165	102.62
03	96SnO <sub>2</sub> :4 PPy/Al <sub>2</sub> O <sub>3</sub> /GP	26.7123	0.2168	103.68
04	94SnO <sub>2</sub> :6 PPy/Al <sub>2</sub> O <sub>3</sub> /GP	26.6821	0.2178	105.24
05	92SnO <sub>2</sub> :8 PPy/Al <sub>2</sub> O <sub>3</sub> /GP	26.6531	0.2175	98.23
06	90SnO <sub>2</sub> :10PPy/Al <sub>2</sub> O <sub>3</sub> /GP	26.7512	0.2040	110.58
07	Pure PPy	27.8710	0.1991	146.09

### SEM Analysis

The surface morphology of polypyrrole [11-13] material was studied by SEM and its picture is shown in the Fig. 10.

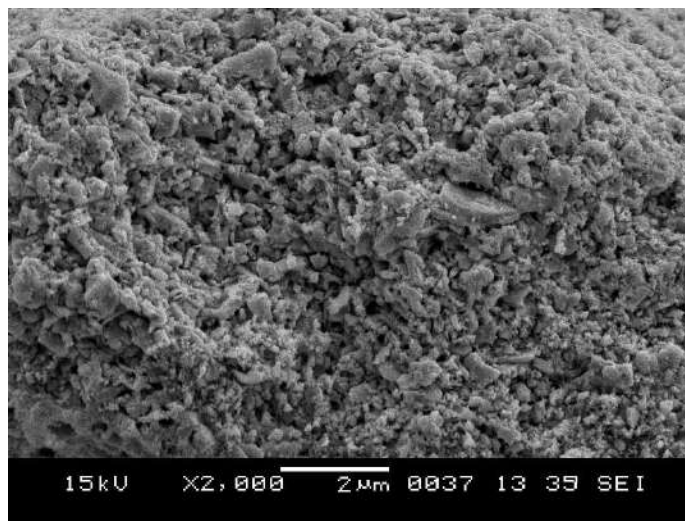


Fig. 10. SEM picture of polypyrrole

From SEM picture, it is observed that PPy is porous in nature and pore size varies from ~ 0.5 to 3  $\mu\text{m}$ . Due to small pores size, its surface area is more and it shows more sensing nature. Some portion of SEM picture shows some rods with fine voids over them which helps to increase sensing properties.

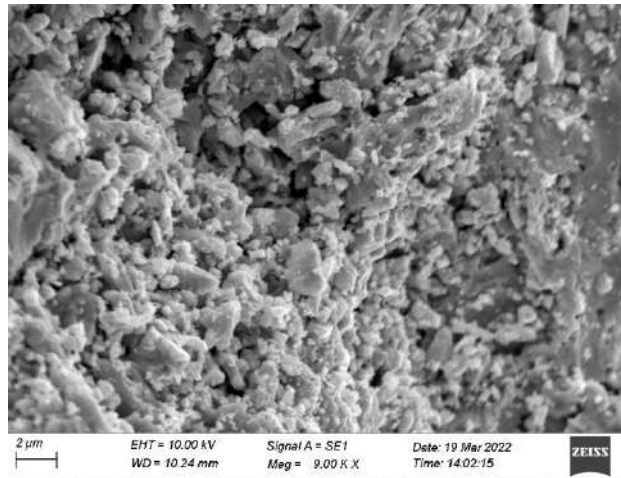
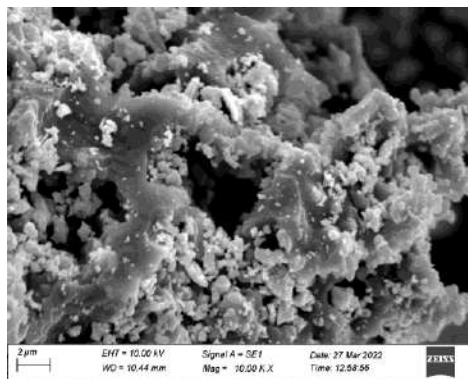
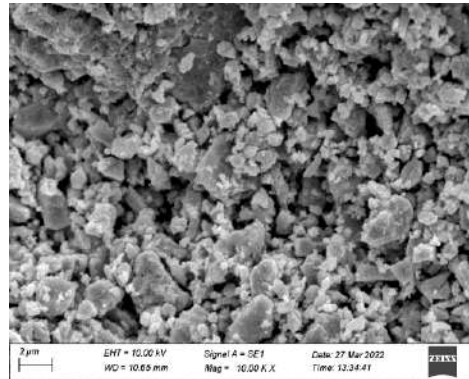


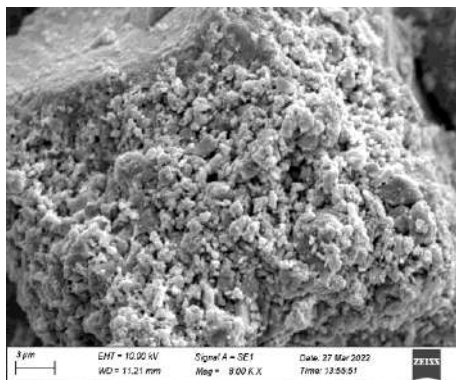
Fig. 11. SEM picture of Pure SnO<sub>2</sub>



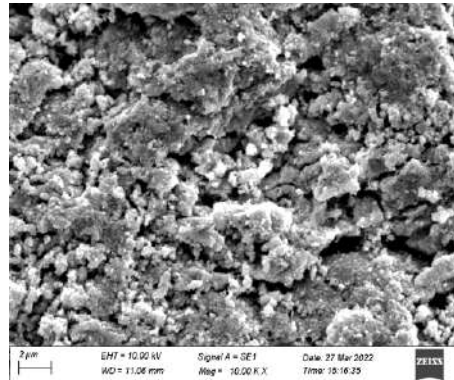
(a) SEM Picture of 98SnO<sub>2</sub>:2PPy



(b) SEM Picture of 96SnO<sub>2</sub>:4PPy



(c) SEM Picture of 94SnO<sub>2</sub>:6PPy



(d) SEM Picture of 92SnO<sub>2</sub>:8PPy

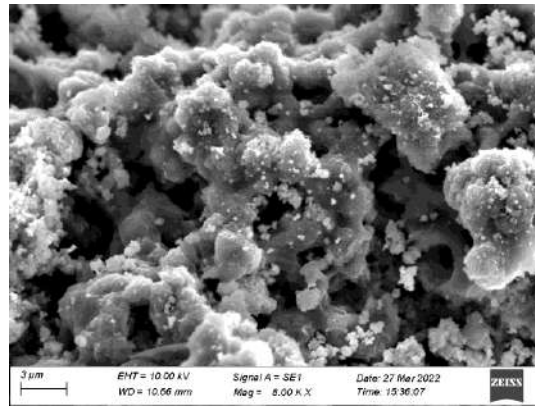
(e) SEM Picture of 90SnO<sub>2</sub>:10PPyFig. 12. SEM Picture of SnO<sub>2</sub>:PPy Series

Table 4 Average diameters of pore and number of pores per inch of pure samples and their dopings.

Serial No.	Pure sample and their dopings (mole %)	Codes	Average diameter of pore (nm)	No. of pores per inch
1	Pure SnO <sub>2</sub>	F1	335	93
2	98SnO <sub>2</sub> :2 PPy/ Al <sub>2</sub> O <sub>3</sub> /GP	F2	387	83
3	96SnO <sub>2</sub> :4 PPy/ Al <sub>2</sub> O <sub>3</sub> /GP	F3	310	112
4	94SnO <sub>2</sub> :6 PPy/ Al <sub>2</sub> O <sub>3</sub> /GP	F4	289	134
5	92SnO <sub>2</sub> :8 PPy/ Al <sub>2</sub> O <sub>3</sub> /GP	F5	215	154
6	90SnO <sub>2</sub> :10 PPy/ Al <sub>2</sub> O <sub>3</sub> /GP	F6	323	95

From table 4 the SEM pictures showed that 92SnO<sub>2</sub>:8PPy, compositions have more pores per inch than other compositions. Thus these three compositions have more active surface areas and exhibit more sensing nature. It is also found that average diameter of pore in case of 92SnO<sub>2</sub>:8PPy compositions are small as compared to other compositions. This also tends to exhibit large surface area and exhibited high response of the samples [14,15].

## CONCLUSIONS

All samples show nanocrystalline form and found the desired peaks of composites and also the grain size of nano-meter order and shows nano-porous structure, which leads to exhibit large surface area, stability and highest response particularly from this study (92SnO<sub>2</sub>:8 PPy) sensor was found to optimized for gas sensing applications.

## REFERENCES

1. Han Z., Guo N., Li F., Zhang W., Zhao H. and Qian Y., (2001). Materials Letters, 48(2), 99-103. [https://doi.org/10.1016/S0167-577X\(00\)00286-X](https://doi.org/10.1016/S0167-577X(00)00286-X)
2. Song K. C. and Kim J. H., (2000). Powder Technology, 107(3), 268-272. [https://doi.org/10.1016/S0032-5910\(99\)00255-7](https://doi.org/10.1016/S0032-5910(99)00255-7)
3. Shek C. H., Lai J. K. L. and Lin G. M., (1999). Nanostructured Materials, 11(7), 887-893. [https://doi.org/10.1016/S0965-9773\(99\)00387-6](https://doi.org/10.1016/S0965-9773(99)00387-6)

4. Briand D., Labcau M., Currie J. F. and Delabouglise G., (1998). Pd-doped SnO<sub>2</sub> thin film deposited by assisted ultrasonic CVD for gas sensing : selectivity and effect of annealing, *Sensors and Actuators B*, 48(1-3), 395- 402. [https://doi.org/10.1016/S0925-4005\(98\)00102-6](https://doi.org/10.1016/S0925-4005(98)00102-6)
5. Pinna N. and Niederberger M., (2008). Surfactant-free nonaqueous synthesis of metal oxide nanostructures, *Angewandte Chemie International Edition*, 47 (29), 5292-5304. <https://doi.org/10.1002/anie.200704541>
6. Lamdhade G. T., Raghuvanshi F. C., Agrawal R. M., Balkhande V. M. and Shripathi T., (2015). SnO<sub>2</sub> Nanoparticles Synthesis via Liquid-phase Co- precipitation Technique, *Advanced Materials Letters*, 6 (8), 738-742. <https://doi.org/10.5185/amlett.2015.5877>
7. Xiaobo Chen, Samuel S. Mao (2007). Titanium dioxide Nanomaterials: Synthesis, properties, modifications and applications, *Chem. Rev.*, 107 (7), 2891-2959. <https://doi.org/10.1021/cr0500535>
8. Lamdhade G. T., Raulkar K. B., Yawale S. S. and Yawale S. P., (2015). Fabrication of multilayer SnO<sub>2</sub>– ZnO–PPy sensor for ammonia gas detection, *Indian Jour. of Phys.*, 89 (10), 1025-1030. <https://doi.org/10.1007/s12648-015-0676-x>
9. Sachan, A., Castro, M., Choudhary V. and Feller J.F., (2018). Influence of Water Molecules on the Detection of Volatile Organic Compounds (VOC) Cancer Biomarkers by Nanocomposite Quantum Resistive Vapor Sensors vQRS, *Chemosensors*, 6, 64. <https://doi.org/10.3390/chemosensors6040064>
10. Tang X., Raskin J.P., Kryvutsa N., Hermans S., Slobodian O., Nazarov A.N. and Debliquy M. (2020). An ammonia sensor composed of PPy synthesized on reduced graphene oxide by electropolymerization, *Sens. Actuators B Chem.*, 305, 127423. <https://doi.org/10.1016/j.snb.2019.127423>
11. Capone S., Forleo A., Francioso L., Rella R., Siciliano P., Spada- vecchia J., Presicce D.S. and Taurino A.M. (2003), Solid state gas sensors: state of the art and future activities, *Journal of Optoelectronics and Advanced Materials* 5, 5, 1335 – 1348.
12. Garg R., Kumar V., Kumar D., and Chakarvarti S.K., (2015). Polypyrrole Microwires as Toxic Gas Sensors for Ammonia and Hydrogen Sulphide, *Columbia International Publishing Journal of Sensors and Instrumentation*, 3, 1-13. <https://doi.org/10.7726/jsi.2015.1001>
13. Raulkar K.B, Wasnik T.S, Joat R.V., Wadatkarkar A.S. Agrawal, R.M. and Lamdhade G.T., (2019). Study on DC Conductivity of PPy-ZnO Nanocomposites, *Materials today Proceedings*, 15(3), 595-603. <https://doi.org/10.1016/j.matpr.2019.04.126>
14. Ly A., Luo Y., Cavailles G., Olivier M.G., Debliquy M. and Lahem D., (2020). Ammonia Sensor Based on Vapor Phase Polymerized Polypyrrole, *Chemosensors*, 8, 30. <https://doi.org/10.3390/chemosensors8020038>
15. X.C. Song, Y.F. Zheng, E. Yang and Y. Wang, 2007, *Mater. Lett.* 61, 3904–3908. <https://doi.org/10.1016/j.matlet.2006.12.055>

# Tin Oxide (SnO<sub>2</sub>) Doped with Polypyrrole (PPy) Screen-printed Multilayer CO<sub>2</sub> Gas Sensor<sup>1</sup>

\*Bhuyar R.S., Raulkar K.B., Lamdhade G.T.

Department of Physics, Vidya Bharati Mahavidyalaya, CK Naidu Road, Amravati, M.S., India

DOI:10.37648/ijrst.v13i02.011

Received: 10 June 2023; Accepted: 24 June 2023; Published: 29 June 2023

---

## ABSTRACT

The multilayer thick films series of sensors (SnO<sub>2</sub>-PPy) tested for CO<sub>2</sub> gas sensing application in the concentration range from 200 ppm to 2000 ppm, sensitivity increases is very small upto 1200ppm but beyond 1400 ppm of CO<sub>2</sub> gas concentration, sensitivity becomes maximum. With further increase in CO<sub>2</sub> gas concentration, sensitivity decreases. Static responses of the series of (SnO<sub>2</sub>:PPy) system also studied at 1000, 1200 and 1400 ppm of CO<sub>2</sub> gas concentration. sensor shows less response time and less recovery time, F5 sensor is faster in operation that other prepared sensors. F5 sensor (92SnO<sub>2</sub>:8 PPy) offers high sensitivity, rapid response and recovery to CO<sub>2</sub> gas.

**Keywords:** SnO<sub>2</sub>-PPy; multilayer thick films; CO<sub>2</sub> Gas Sensors

## INTRODUCTION

Gas sensors consisting of metal oxides like SnO<sub>2</sub>, TiO<sub>2</sub>, ZnO and others employ a variation of electrical conductance by ambient gases such as ethanol, carbon monoxide, methane, hydrogen sulfide, nitrogen oxide, and oxygen [1]. The effects of additive of various metals and metal oxides on SnO<sub>2</sub>, TiO<sub>2</sub>, ZnO and others sensors are examined by Yamazoe *et al.* [2]. They found that gas sensitivity usually goes through a maximum with increasing nature. The effects of additives can be appropriately compared in terms of the temperature at the maximum of gas sensitivity. A new type of CO<sub>2</sub> gas sensor was developed by Masayuki *et al.* [3] using porous hydroxyapatite ceramics, both DC and AC conductivities measurement were earned out in various atmospheres including air, CO<sub>2</sub> and air containing different amount of CO<sub>2</sub>. Thick films of SnO<sub>2</sub>, ZnO, TiO<sub>2</sub> were prepared by screen printing technique and studied by Mude *et al.* [4] result the semiconducting metal oxide gas sensor extensively used in the gas sensing. The chemical used for the designing of gas sensor was first calcinated at 650°C for 6 hrs. Thick films of SnO<sub>2</sub>, ZnO, TiO<sub>2</sub> were prepared using screen printing technique with Al<sub>2</sub>O<sub>3</sub> as substrate on glass plate. Sensitivity was found to be more for SnO<sub>2</sub> than other metal oxides. It was observed that stability is found better in SnO<sub>2</sub> as compare with other metal oxides, sensitivity is also more as compare to other metal oxides. This paper focused on CO<sub>2</sub> gas sensing application of (SnO<sub>2</sub>-ppy) multilayer thick films system with Al<sub>2</sub>O<sub>3</sub> as base material.

## EXPERIMENTAL

The methods of synthesis of nano-particles can be broadly classified in the three categories namely, liquid phase synthesis, gas-phase synthesis and vapour-phase synthesis. In the present work, we have used sol-gel method for the synthesis of pristine nano-particles of SnO<sub>2</sub>, Al<sub>2</sub>O<sub>3</sub> and PPy [5].

---

<sup>1</sup> How to cite the article: Bhuyar R.S., Raulkar K.B., Lamdhade G.T.; Apr-Jun 2023; Tin Oxide (SnO<sub>2</sub>) Doped with Polypyrrole (PPy) Screen-printed Multilayer CO<sub>2</sub> Gas Sensor; *International Journal of Research in Science and Technology*, Vol 13, Issue 2, 78-83, DOI: <http://doi.org/10.37648/ijrst.v13i02.011>

**Preparation of Samples of Series : SnO<sub>2</sub>: PPy/Al<sub>2</sub>O<sub>3</sub>/GP**

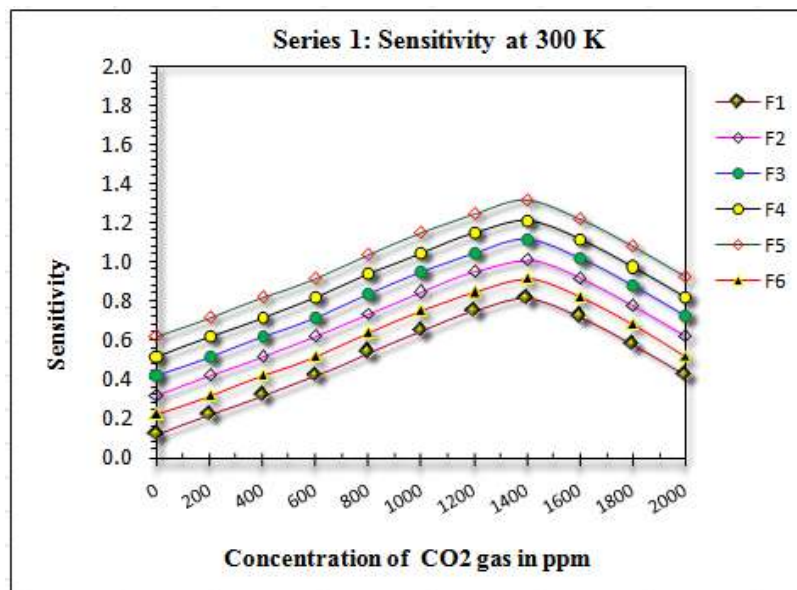
The obtained product of fine nanopowder of SnO<sub>2</sub> and PPy are used for fabrication of thick films sensors by using screen-printing technique. For this, the SnO<sub>2</sub> powder was mixed thoroughly with different X mole% of PPy (X = 2, 4, 6, 8,10) along with Al<sub>2</sub>O<sub>3</sub> base on glass plate (GP) substrate the aid of acetone by using the mortar and pestle. The sample codes, mole% of powder, and thickness are listed in the Table 1. The mixed powder of SnO<sub>2</sub>:PPy system was further calcinated at temperature 800°C for 5hrs. in the auto controlled muffle furnace (Gayatri Scientific, Mumbai, India.) After, the calcinations again uniformly mixed the powder using the grinder

**Table 1 Length, Width and Thickness of Multi-layers in SnO<sub>2</sub>: PPy/Al<sub>2</sub>O<sub>3</sub>/GP gas sensor**

Sample Code	Doping mole %	Upper layer length (cm)	Upper layer width (cm)	Thickness (x 10 <sup>-4</sup> cm)		
	Layers:			Upper Layer (1)	Al <sub>2</sub> O <sub>3</sub> Layer (2)	Total (1+2)
	Upper/ /Al <sub>2</sub> O <sub>3</sub> / Glass plate (GP)					
F1	SnO <sub>2</sub> /Al <sub>2</sub> O <sub>3</sub> /GP	3	1.5	5.1	26.4	31.5
F2	98 SnO <sub>2</sub> :2 PPy/ Al <sub>2</sub> O <sub>3</sub> /GP	3	1.5	3.1	34.2	37.3
F3	96 SnO <sub>2</sub> :4 PPy/ Al <sub>2</sub> O <sub>3</sub> /GP	3	1.5	2.8	35.1	37.9
F4	94 SnO <sub>2</sub> :6 PPy/ Al <sub>2</sub> O <sub>3</sub> /GP	3	1.5	3.4	32.6	36.0
F5	92 SnO <sub>2</sub> :8 PPy/ Al <sub>2</sub> O <sub>3</sub> /GP	3	1.5	3.0	35.5	38.5
F6	90 SnO <sub>2</sub> :10 PPy/ Al <sub>2</sub> O <sub>3</sub> /GP	3	1.5	3.6	32.3	35.9
F7	PPy/ Al <sub>2</sub> O <sub>3</sub> /GP	3	1.5	1.9	48.4	50.3

**RESULTS AND DISCUSSION****CO<sub>2</sub> Gas Sensing Properties at room temperature (300 K) & at (330 K)**

The variations of sensitivities and sensors with concentration of CO<sub>2</sub> gas at 300K and 330K temperature are shown below;



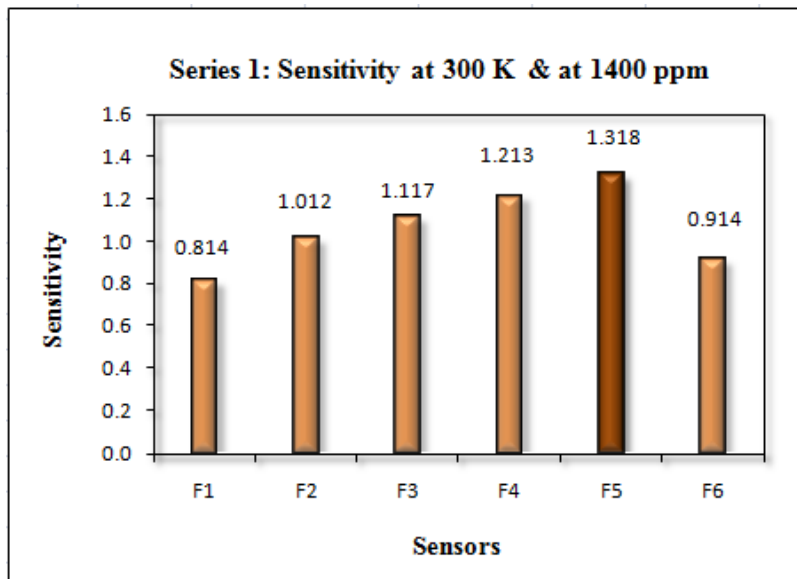
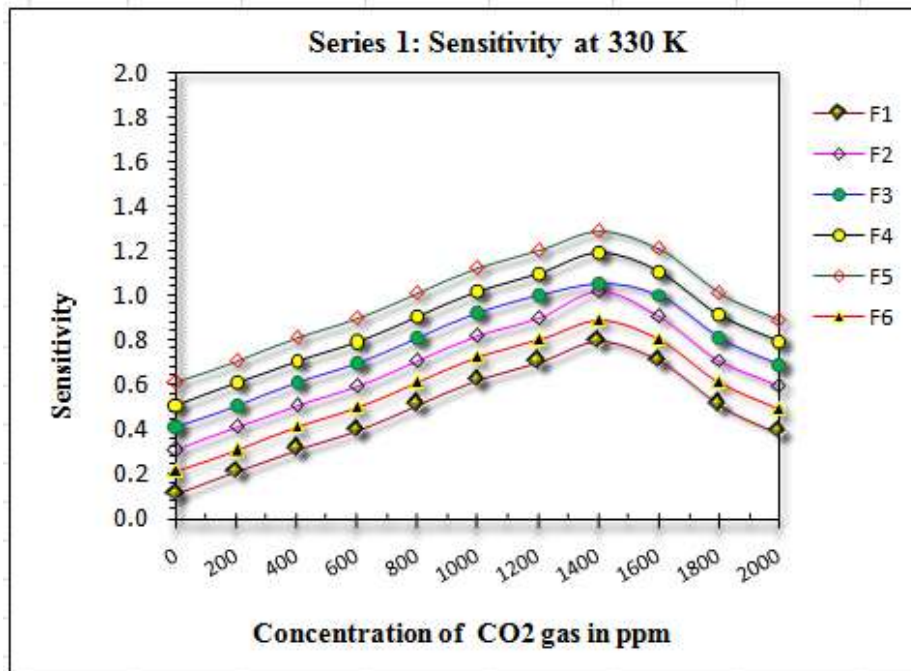
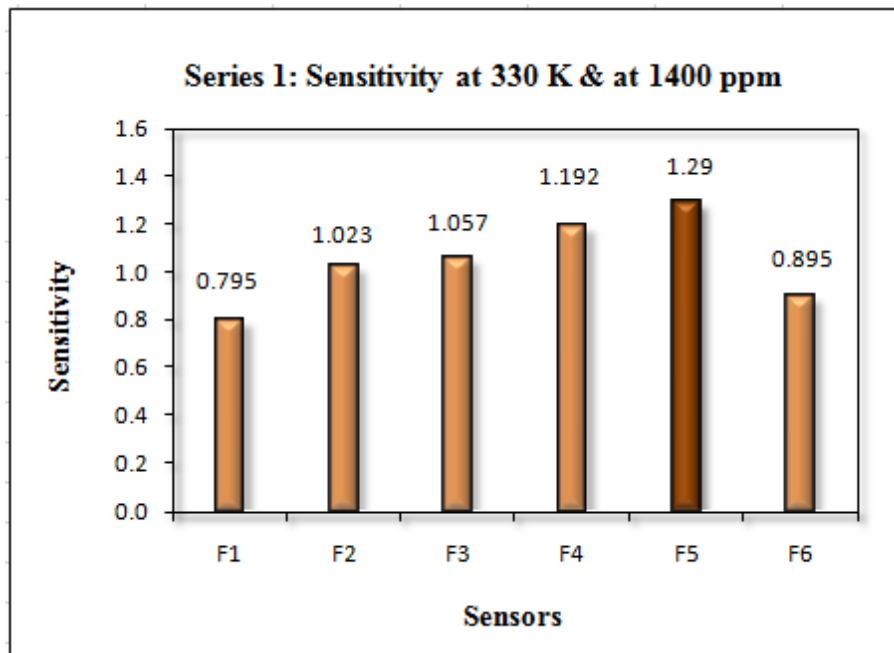


Fig. 1: variations of sensitivity with CO<sub>2</sub> gas concentration at 300 K





**Fig. 2: variations of sensitivity with CO<sub>2</sub> gas concentration at 330 K**

From Fig. 1 and 2 for the CO<sub>2</sub> gas detection and sensing at room temperature (300 K) and at temperature 330 K respectively, exhibited that,

As CO<sub>2</sub> gas concentration increases up-to 1200 ppm, sensitivity increases by small amount. At about 1400 ppm of CO<sub>2</sub> gas concentration, sensitivity becomes maximum. With further increase in CO<sub>2</sub> gas concentration, sensitivity decreases. From Fig. 2 (Bar Graph), sensitivity was found to be 1.318 (maximum) for F5 sensor, amongst the prepared all sensors. From figures, it is manifested that, as temperature increases, sensitivity decreases because size of porosity increases and therefore number of pores in given area decreases. This means that the prepared sensors work better at room temperature (300 K). In brief, among the prepared sensors, F5 sensor showed optimum sensitivity at 1400 ppm of CO<sub>2</sub> gas concentration [6,7].

### Static Responses of sensors

Static responses of the series of (SnO<sub>2</sub>:PPy) system, was studied at 1000, 1200 and 1400 ppm of CO<sub>2</sub> gas concentration [8-10]. The variation in sensitivity was plotted as a function of time in second. From the variations, response and recovery times were calculated and listed in the following tables, separately for each series. Static response of this series at 1000, 1200 and 1400 ppm of CO<sub>2</sub> gas concentration is shown Fig. 3.



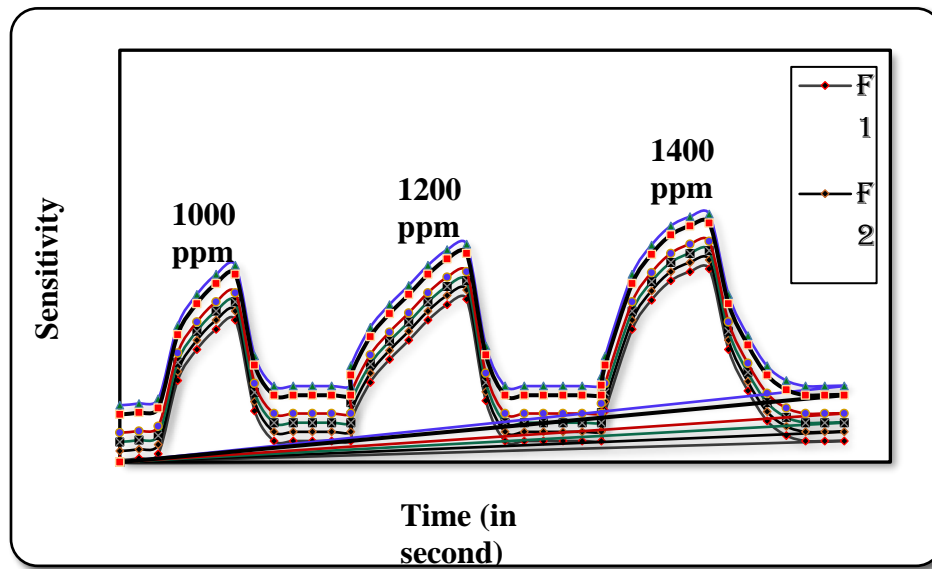


Fig. 3.: Static response (response and recovery times) of series of (SnO<sub>2</sub>:PPy) system

Table 2. Response and Recovery times of series of (SnO<sub>2</sub>:PPy) system

Sr. No.	Sample Compositions	Sensor	Response time (s) for 1400 ppm	Recovery time (s) for 1400 ppm
1	100SnO <sub>2</sub> :0 PPy/Al <sub>2</sub> O <sub>3</sub> /GP	F1	118	152
2	98SnO <sub>2</sub> :2 PPy/ Al <sub>2</sub> O <sub>3</sub> /GP	F2	103	149
3	96SnO <sub>2</sub> :4 PPy/ Al <sub>2</sub> O <sub>3</sub> /GP	F3	97	143
4	94SnO <sub>2</sub> :6 PPy/ Al <sub>2</sub> O <sub>3</sub> /GP	F4	91	139
5	92SnO <sub>2</sub> :8 PPy/ Al <sub>2</sub> O <sub>3</sub> /GP	F5	81	129
6	90SnO <sub>2</sub> :10 PPy/ Al <sub>2</sub> O <sub>3</sub> /GP	F6	89	134

From table 2, it is clear that, F5 sensor shows less response time (81 s) and less recovery time (129 s), i.e. F5 sensor is faster in operation that other prepared sensors from series (SnO<sub>2</sub>:PPy) .

## CONCLUSIONS

F5 sensor shows less response time and less recovery time, therefore F5 sensor is faster in operation that other prepared sensors from series (SnO<sub>2</sub>:PPy). The sample F5 sensor (92SnO<sub>2</sub>:8 PPy/ Al<sub>2</sub>O<sub>3</sub>/GP) offers high sensitivity, rapid response and recovery to CO<sub>2</sub> gas.

## REFERENCES

1. Heiland G. (1981). Homogeneous semiconducting gas sensors. *Sensors and Actuators*, 2, 343-361. [https://doi.org/10.1016/0250-6874\(81\)80055-8](https://doi.org/10.1016/0250-6874(81)80055-8)
2. Yamazoe N., Fuchigami J., Kishikawa M., and Seiyama T., (1979). Interactions of tin oxide surface with O<sub>2</sub>, H<sub>2</sub>O and H<sub>2</sub>, *Surface Science*, 86 (2) 335-344. [https://doi.org/10.1016/0039-6028\(79\)90411-4](https://doi.org/10.1016/0039-6028(79)90411-4)
3. Nagai M., Nishino T. and Saeti T., (1988). A new type of CO<sub>2</sub> gas sensor comprising porous hydroxyapatite ceramics. *Sensors and Actuators*, 15,145-151. [https://doi.org/10.1016/0250-6874\(88\)87004-5](https://doi.org/10.1016/0250-6874(88)87004-5)
4. Mude M. B., Mude M. K., Zade N. R., Yenorkar M. S. and Yawale S. P., (2018). Study of sensitivity and stability of metal oxides in gas sensing properties, *Journal of Emerging Technologies and Innovative Research*, 5 (11), 2349-5162.
5. Nithya Sureshkumar and Atanu Dutta,(2023) Environmental Gas Sensors Based on Nanostructured Thin Films, Multilayer Thin Films- Versatile Applications for Materials Engineering, <http://doi.org/10.5772/intechopen.89745>
6. K. B. Raulkar, (2019), Study on sensitivity of nano SnO<sub>2</sub> -ZnO composites with and without PPy layer for sensing CO<sub>2</sub> gas, 2019, *Materials Today: Proceedings* 15, 604–610. <https://doi.org/10.1016/j.matpr.2019.04.127>
7. Chartuprayoon N., Hangarter C.M., Rheem Y., Jung H. and Myung N.V. (2010), Wafer- scale fabrication of single PPy nanoribbon-based ammonia sensor, *J. Phys. Chem.*, 114, 11103–11108. <https://doi.org/10.1021/jp102858w>
8. Capone S., Forleo A., Francioso L., Rella R., Siciliano P., Spada- vecchia J., Presicce D.S. and Taurino A.M. (2003), Solid state gas sensors: state of the art and future activities, *Journal of Optoelectronics and Advanced Materials* 5, 5, 1335 – 1348.
9. Garg R., Kumar V., Kumar D., and Chakarvarti S.K., (2015). Polypyrrole Microwires as Toxic Gas Sensors for Ammonia and Hydrogen Sulphide, *Columbia International Publishing Journal of Sensors and Instrumentation*, 3, 1-13. <https://doi.org/10.7726/jsi.2015.1001>
10. Shao Q., Chen W., Wang Z., Qie L., Yuan L., Zhang W., Hu X., Huang Y., (2011). SnO<sub>2</sub>-based composite coaxial nanocables with multi-walled carbon nanotube and polypyrrole as anode materials for lithium-ion batteries, *Electrochem. Commun.* 13, 1431-1434. <https://doi.org/10.1016/j.elecom.2011.09.014>



DR. DNYANESHWARI  
S. WANKHADE

Associate Professor  
Vidya Bharati  
Mahavidyalaya, Amravati

One Day International Multi-Disciplinary Conference  
**RESEARCH, INNOVATION, CHALLENGES & OPPORTUNITIES  
IN HIGHER EDUCATION**

On 13<sup>th</sup> January, 2023 @  
Smt Salunkabai Raut Arts & Commerce College, Wanoja,  
*In collaboration with*  
Saraswati Kala Mahavidyalaya, Dahihanda  
Arts And Science College, Kurha,  
Physical Education Foundation of India, New Delhi.

**RESEARCH INNOVATION IN HIGHER EDUCATION IN INDIA  
AND WORLD WIDE**

**ANSTRACT**

*Advancement in education urges educators and understudies to investigate, examination and utilize every one of the devices to uncover a genuinely new thing. It includes an alternate perspective on and tackling them. The reasoning system that goes into it will assist understudies with fostering their inventiveness and their critical thinking abilities. Research on opportune and significant themes stands out, which thus prompts more noteworthy institutional perceivability and notoriety. As a college becomes known for its exploration in specific fields, they become magnets for understudies, workforce, awards, media inclusion, and even magnanimity. The world has understood that the financial outcome of the states not entirely settled by their school systems. Instruction is a Country's Solidarity. A created country is definitely an informed country. Indian higher education framework is the third biggest on the planet, close to the US and China. Since freedom, India as a non-industrial country is petulantly advancing in the education field. In spite of the fact that there have been part of difficulties to higher education arrangement of India however similarly have parcel of chances to conquer these difficulties and to make higher education framework much better. It needs more noteworthy straightforwardness and responsibility, the job of schools and colleges in the new thousand years, and arising logical examination on how individuals learn is of most extreme significant. India need well talented and profoundly instructed individuals who can drive our economy forward. India gives profoundly gifted individuals to different nations in this way; it is exceptionally simple for India to move our country from an agricultural country to a created country. The ongoing review plans to feature the difficulties and to call attention to the open doors in higher education framework in India.*

**Keywords:** *Instruction, Open doors, Difficulties, Schools, Colleges*

India's higher education framework is the world's third biggest with regards to understudies, close to China and the US. In future, India will be one of the biggest training centers. India's Higher education area has seen an enormous expansion in the quantity of Colleges/College level Establishments and Schools since freedom. The 'Right to Training Act' which specifies mandatory and free education to all youngsters inside the age gatherings of 6-14 years, has achieved an upset in the education system of the country with measurements uncovering a stunning enrolment in schools throughout the course of recent years. The contribution of private area in higher education has seen extreme changes in the field. Today more than 60% of higher education establishments in India are higher

by the confidential area. This has sped up foundation of organizations which have started over the course of the past ten years making India home to the biggest number of Higher education establishments on the planet, with understudy enrolments at the second most noteworthy (Shaguri, 2013). The number of Colleges has expanded multiple times from 20 out of 1950 to 677 of every 2014. Regardless of these numbers, global education rating organizations have not set a considerable lot of these establishments inside the best of the world positioning. Likewise, India has neglected to deliver a-list colleges. Today, Information is power. The more information one has, the more engaged one is. Be that as it may, India keeps on confronting harsh difficulties. In spite of developing interest in training,

25% of its populace is as yet unskilled; just 15% of Indian understudies arrive at secondary school, and only 7% alumni .

The nature of training in India whether at essential or higher education is altogether poor when contrasted with significant emerging countries of the world. Starting around 2008, India's post-optimal foundations offer just an adequate number of seats for 7% of India's school age populace, 25% of showing positions cross country are empty, and 57 percent of school teachers need either an expert's or PhD degree. Starting around 2011, there are 1522 certification giving designing universities in India with a yearly understudy admission of 582,000 in addition to 1,244 polytechnics with a yearly admission of 265,000. Nonetheless, these organizations face lack of personnel and concerns have been raised over the nature of instruction. Regardless of these difficulties higher education arrangement of India similarly have parcel of chances to beat these moves and have the capacity to make its personality at global level. Notwithstanding, it needs more prominent straightforwardness and responsibility, the job of colleges and universities in the new thousand years, and arising logical exploration on how individuals learn is of most extreme significant. India gives exceptionally talented individuals to different nations hence; it is extremely simple for India to move our country from an emerging country to a created country.

#### **Evolution of Higher education:**

The custom of higher education framework India is old and acquired an age which has produced information and advancing right from the outset of the Indian civilization. To think about the time of Guptas they supported higher advancing by belittling place for higher education at Nalanda, Takshila, Ujjain, vikramshila and vallabhi. Every college as referenced had practical experience in a specific gathering of study. These colleges have become well known in seventh and eighth hundreds of years A.D. After the coming of Buddhism individuals rushed to saranath college to concentrate on Buddhist religion and to Ajanta to have practical experience in craftsmanship, design and painting. These establishments principally subsidized by awards of land and gifts. Such awards came from rulers as well as princely individuals existing in the then-society. Truth be told the verifiable information sorts out a deeply grounded framework, what worked in India as soon as 1000 B.C. In that framework the development of information, the convictions on which the information is based, essential ideas of the hierarchical gaining were altogether different from the European practice. Perceiving that understudies are ideally serviced by a flipped study hall where they watch addresses at home and complete tasks in the study hall. Presenting more innovation in the homeroom

to make a mixed homeroom where understudies experience innovation as they would in reality.

Upgrade and further develop the understudy insight. Make new academic encounters using new advancements and computerized administrations. Give potential open doors to development and extension. Empower efficiencies and make learning and showing processes more powerful. Examination and advancement (R&I) assumes a fundamental part in setting off savvy and feasible development and occupation creation. By delivering new information, research is vital to growing new and inventive items, cycles and administrations, which empower higher efficiency, modern seriousness, and at last success. Advancement and instructive innovation is fundamentally worried about utilizing present day and logical educating learning techniques and educational procedures in the arrangement of education. Four year college educations. Higher Public Endorsements and Higher Public Certificates Establishment degree courses, endorsements and other scholastic honors conceded by a college or higher education school (yet not privileged degrees and higher doctorates).

#### **Significance of Innovative Research in education**

The exploration capability of the scholarly community stays a superb wellspring of information and development at public, territorial and global levels. Behind the homeroom entryway the vital consider the progress of an example, in deciding if the understudies really learn something that is important, is the imaginative capacity of the educators — their capacity to consolidate hypothesis and commonsense study hall experience. Viable educating and advancing in this way includes the useful utilization of new examination/hypothesis in a study hall climate. The examination is important to build comprehension of arrangements and techniques, educational methodologies, program educational programs and content, and partner inclusion that add to students living up to their scholarly potential. Through the creative examination, we will distinguish instructive program parts that effectively animate high level scholastic information and abilities.

#### **Growth of Higher Education Sector in India**

As higher education frameworks develop and enhance, society is progressively worried about the nature of projects, public appraisals and worldwide rankings of higher education establishments. Anyway these correlations will generally overemphasize research, involving research execution as a measuring stick of institutional worth. Assuming these cycles neglect to address the nature of educating, it is to some degree since estimating showing quality is testing. Lego has been changing the materials of its renowned blocks to biodegradable oil-based plastics. The principal

electric vehicles presented in the vehicle's market were likewise a development, and new batteries with longer ranges that continue to come out are additionally an illustration of advancement. The course of advancement is research and the end-product of it is development. The study of development could be alluded to as Exploration; while, advancement alludes to the compelling utilization of this information. While expounding on the Development and Inventiveness of your exploration, you really want to zero in on HOW your methodology is NEW and Unique. Consider these components in organizing your reaction to this part: Obviously state, at the earliest reference point of this segment, why is your proposed research NEW or Unique. Instructive examination can be extensively ordered into 3 which are clear exploration, correlational examination, and exploratory examination. Each of these has particular and covering highlights.

#### **Innovations in educational research**

Among late advancements in the education system, the presentation of PCs in study halls is frequently alluded to as the main development. While the actual appearance of homerooms has not changed much since blackboards were presented in study halls in the late eighteenth 100 years, the appearance of PCs, tablets, and the Web has prompted the reexamining of numerous customary showing rehearses and is for the most part seen as a chance for development. Various researchers have shifting understandings of the thought "Inventive examination". Advancement is much of the time saw as the use of improved arrangements that meet new prerequisites, implied needs, or existing cultural necessities. Imaginative examination includes finding new methods and expanding working arrangement of an instructive foundation It could include mechanical development or enhancements in HR. Following are sure instructive regions which require imaginative exploration:

- What sort of academic information and abilities are key to educators' viability?
- How does learning explore, new assumptions with respect to understudies' acquiring results and abilities, and changing worth and conviction frameworks shape the scope of conduct mediations of educators? (Pramodini and Sophia, 2012)
- How could educators all the more really organize the learning climate to make ideal circumstances for figuring out how to appear, both intellectually and inwardly? Geeta Ramanujan, pioneer head of Institute of narrating explored different avenues regarding "narrating as an instructing tehnogue" to talk imagination and the soul of request inside youngsters (EducationWorld, 2015).
- In our mechanical society where each sex is supposed to satisfy numerous jobs, we should have more

examination studies to help education in defeating sex job generalizing and in fostering a climate that will sustain the ideal of female equity and advance objective of equivalent appropriate for improvement of self idea

#### **The need of research in education**

Research in education has empowered huge headway to be made in educational plan advancement and change, teaching students with troubles, grasping the singular distinctions and inclinations and in adjusting techniques for guidance to the requirements of individual students. Scholarly examination works with learning, features central questions in the public arena and can advance the development of organizations. It's in this manner vital that each piece of exploration is perused by however many closely involved individuals as possible. Institutions in higher education, examination and development assume a focal part in the headway of social orders and economies. They cultivate monetary development, reinforce mechanical advancement, and improve work creation. Moreover, higher education establishments add to the self-awareness of people and assist with teaching proactive residents in social orders. To accomplish the most ideal outcomes, these foundations require current and compelling administration.

Expert's Program in Exploration and Advancement in Higher education - MARIHE (Erasmus Mundus Joint Degree) centers around the administration of higher education, examination and development. It gives understudies capabilities to go about as change specialists ready to play the main job in institutional turn of events. Simultaneously, MARIHE graduates are ready to partake in the cycles that produce plans and approaches for the headway of examination, advancement and business. They are prepared to function as directors, advancement specialists, strategy producers, experts, analysts and advisors in HE, exploration and development establishments, as well as in privately owned businesses, policy management, global associations, and NGOs. They can likewise proceed to doctoral examinations and seek after a scholarly vocation.

#### **Technology and innovation in higher education**

Dataquest Higher education Meeting and Grants coordinated an entire day conceptualizing with the top personalities in Training fragment on The meeting with the subject "Enabling The Cutting edge" was centered around the key advancements that are reshaping the training area today.

- Shift from disconnected to on the web.
- Half and half instructing.
- Innovation molding the eventual fate of education.
- Higher learning and ability holes.

- Learning and advancement for Industry 4.0.

The meeting on Innovation Development in Higher education comprised of a heavenly board from the scholarly community and industry: Dr J.V. Desai, Bad habit Chancellor, MVN College; Mr Raunak Singh, Organizer University18; Rajesh Kumar, Innovation Head, Undertaking and Government, India and SAARC, Juniper Organizations; Nitesh Rohatgi, COO, ImaginXP and Narayan Mahadevan, Pioneer, BridgeLabz.

Dr. Desai, who has spent as many as 30 years of his work life in mission learning and man-made intelligence in his introductory statements recognized that innovation advancement had sneaked in unexpectedly because of the pandemic. Online classes, classes and live showing made a ton of difficulties since it was another experience. Colleges were associated on rented lines, however most understudies didn't have high velocity access gadgets. Obviously, the country distant framework actually stays a test.

Simultaneously there were numerous open doors that emerged. "We created content for YouTube educating," he said. This was another thing for the scholarly world - particularly the conventional grounds. What's more, it had its own arrangement of difficulties - content in English introduced an issue, so many moved to vernacular classes. Shockingly there were more than 5000 endorsers in a brief time frame - an unfathomable number in the college. Dr. Desai subsequently felt for development to truly have an effect, a key necessity is to welcome on more neighborhood/vernacular instructors for online courses.

Rajesh Kumar said Juniper Organizations has fabricated the foundation across numerous instructive establishments and furthermore collaborated with networks for conveying content to Understudies. "As an OEM and tech supplier to the Instructive area, we observe that understudies are presently really quick to return to the grounds, yet they need that learning ought to be independent and they ought to have the option to get a similar internet based insight," he said. Seamless mixture training is a vital result of this, where an Information Organization will permit all colleges to connect on the organization, maybe alluding to the Public Information Organization that is as of now a work underway.

Dr Raunak Singh, a veteran in scholarly community and organizer behind his college repeated the contemplations of Dr Desai, "There isn't sufficient substance accessible in vernacular. In any case, our creativity and extraordinary workforce will actually want to improve and adjust to this test." The goal has forever been to give access, associate, and enable. "Our nation has forever been ahead in creating and taking on innovation. From ISRO to Bhabha Nuclear Exploration Place and from the most recent telecom organizations

(fiber and portable) to the fast development of online stages like Swayam."

Educators are conveying addresses from anyplace on the planet. What's more, understudies can get to courses from anyplace on the planet. "This is the Meta Training

structure." It is basic to grow the skylines and empower understudies from various colleges to go to talks of incredible instructors from different colleges. What's more, credits, grades and so forth need to integrate this into their system. One more repeating subject in the conversation spun around — How to guarantee understudies were more employable (prepared for industry with the most recent necessary abilities). Step by step instructions to use innovation and development to guarantee a model where the scholarly community and industry shake hands.

ImaginXP is assuming a basic part in shutting this hole and Nitesh Rohatgi felt that the educational program should be planned in organization with industry. All specialists concurred with this idea. ImaginXP is arranging programs that empowers upgradation of abilities of understudies in a state of harmony with Industry specialists (be it blockchain or UI/UX creators) and works with virtual labs and stages for offering understudies equivalent admittance to these courses in all colleges the nation over.

#### Challenges in Higher Education in India

It is our 69th year of freedom still our education system has not been grown completely. We can't list a solitary college in top 100 colleges of the world. Different legislatures changed during these sixty years. They attempted to help the education system and carried out different training arrangements however they were not adequate to put a model for the universe. UGC is persistently working and zeroing in on quality education in higher education area. Still we are confronting part of issues and difficulties in our school system. A portion of the fundamental difficulties in higher education framework in India are examined beneath:

**Enrolment:** The Gross Enrolment Proportion (GER) of India in higher education is just 15% which is very low when contrasted with the created as well as, other non-industrial nations. With the increment of enrolments at school level, the stockpile of higher education foundations is lacking to satisfy the developing need in the country.

**Equity:** There is no value in GER among various organizations of the general public. As per past examinations the GER in higher education in India among male and female fluctuates positively. There are local varieties too a few states have high GER while as some is very behind the public GER which mirror a critical lopsided characteristics inside the higher education framework.

**Quality:** Quality in higher education is a multi-layered, staggered, and a powerful idea. Guaranteeing quality in higher education is among the first difficulties being looked in India today. Nonetheless, Government is persistently zeroing in on the quality education. Still Enormous number of schools and colleges in India can't meet the base prerequisites

set somewhere near the UGC and our colleges are not in that frame of mind to check its place among the top colleges of the world.

**Political interference:** The vast majority of the instructive Organizations are claimed by the political pioneers, who are assuming key part in administering collections of the Colleges. They are involving the guiltless understudies for their narrow minded implies. Understudies sort out crusades, fail to remember their own goals and start to foster their vocations in governmental issues.

**Faculty:** Workforce deficiencies and the powerlessness of the state school system to draw in and hold wellqualified educators have been presenting difficulties to quality training for a long time. Huge quantities of NET/PhD competitors are jobless even there are part of opportunities in higher education, these meriting up-and-comers are then applying in different divisions which is a greatest disaster for the higher education framework.

**Accreditation:** According to the information given by the NAAC, as of June 2010, "not even 25% of the complete higher education establishments in the nation were licensed. Furthermore, among those certify, just 30% of the colleges and 45% of the universities were viewed as of value to be positioned at 'A' level"

**Research and Innovation:** there are exceptionally ostensible researchers in our country whose composing is referred to by renowned western creators. There is lacking spotlight on research in higher education establishments. There are inadequate assets and offices, as well as, restricted quantities of value workforce to exhortation understudies. A large portion of the exploration researchers are without cooperations or not getting their partnerships on time which straightforwardly or by implication influences their examination. In addition, Indian Higher education organizations are inadequately associated with research focuses. Thus, this is one more area of challenge to the higher education in India.

### Opportunities in Higher Education

India is a huge country, with an expected populace of youngsters matured between 18 to 23 years to be around 150 millions. The sheer size of the market offers enormous open doors for improvement of the higher education area in India. India presently gloats of having in excess of 33,000 schools and 659 colleges, which has been a seriously noteworthy development

during the most recent sixty years. The year 2012 saw 21.4 million enlistments, which makes India the third biggest education system on the planet. Tragically, the instructive foundation of India is lacking to deal with such colossal volumes. In demonstrate hatred for all the public authority spending in the instructive area, meeting the developing requirements is simply excessively deficient. Subsequently, higher education area has now been recognized as one of the promising regions for private and unfamiliar speculations. It offers tremendous speculation open doors in both non-endlessly directed fragments Indian higher education framework is becoming extremely quick regardless of different difficulties yet there is no great explanation that these Difficulties can't be survived. With the assistance of trendy learning devices, it is simple for country like India to defeat these issues and bring a change in perspective in the country's higher education area. With such a lively country with tremendous populace appropriately instructed, the conceivable outcomes are unfathomable. On the off chance that information is granted utilizing progressed computerized educating and learning apparatuses, and society is made mindful of where we are right now falling behind, our nation can without much of a stretch arise as perhaps of the most evolved country on the planet. There are amazing open doors for vital commitment and limit working in higher education administration and the board at the state level. There are open doors for India to joint effort at public and global level on areas of fundamental change, including quality affirmation, worldwide credit acknowledgment, and bound together public capabilities structure. Equity of instructive open door in higher education is viewed as fundamental in light of the fact that higher education is a useful asset for diminishing or taking out pay and abundance variations. Leveling instructive open doors additionally lies in the way that "the capacity to benefit by higher education is spread among all classes of individuals. There are extraordinary stores of undiscovered capacity in the general public; in the event that offered the opportunity they can ascend to the top. A lot of ability of the greatest level is, truth be told, lost by an inequalitarian arrangement of education".

### Suggestions Improving the System of Higher Education:

- There is a need to carry out inventive and groundbreaking methodology structure essential to higher education level to make Indian school system worldwide more pertinent and cutthroat.
- Higher instructive organizations need to work on quality and notoriety.
- There ought to be a decent foundation of schools and colleges which might draw in the understudies. Government should advance joint effort

between Indian higher education foundations and top Global organizations and furthermore creates linkage between public exploration labs and examination focuses of top establishments for better quality and cooperative exploration.

□ There is a need to zero in on the alumni understudies by giving them such courses in which they can accomplish greatness, gain further information on subject so they will land positions after enlistment in the organizations which would lessen pointless hurry to the higher education.

□ Colleges and schools in both public private should be away from the political affiliations, Bias, lucrative cycle ought to be out of school system and so forth.

□ There ought to be a multidisciplinary approach in higher education so understudies information may not be limited just upto his own subjects.

#### Some Examples Of Innovation In Education?

- Capability Based Learning. ...
- Video Real time/Flipped Study hall/eLearning Patterns. ...
- Open Educational program. ...
- Changing nature of staff. ...
- Changing income hotspots for organization subsidizing. ...
- Higher course readings. ...
- 3D Printing. ...
- Utilization of information examination.

#### Conclusion

Instruction is a cycle by which an individual's body, psyche and character are shaped and fortified. It is bringing of head, heart and brain together and subsequently empowering an individual to foster an overall character recognizing the best in that person. Higher education in India has extended quickly over the most recent sixty years after autonomy yet it isn't similarly open to all. India is today one of the quickest agricultural nations of the world with the yearly development rate going above 9%. Still a huge segment of the populace stays uneducated and an enormous number of youngsters' don't get even essential instruction. This isn't just rejected an enormous part of the populace from adding to the improvement of the nation completely yet it has likewise kept them from using the advantages of anything improvement have occurred to support individuals. Presumably India is confronting different difficulties in higher education yet to handle these difficulties and to support higher education is most extreme significant. India is a nation of immense human asset potential, to use this potential

appropriately is the issue which expected to examine. Valuable open doors are accessible yet how to get benefits from these potential open doors and how to make them available to others is the question of concern. To support that pace of development, there is need to build the quantity of establishments and furthermore the nature of higher education in India.

To reach and accomplish the future prerequisites there is a pressing need to relook at the Monetary Assets, Access and Value, Quality Norms, Pertinence, framework and toward the end the Responsiveness.

Training for Supportable Improvement has turned into a significant issue in the public eye. The Assembled Countries Ten years for ESD has supported creative methodologies in training to add to the cultural change towards manageability through both the conventional school system and non-formal and casual learning settings Generally speaking, it isn't really to be expected that exploration on development has acquired significance. It has become fundamental to comprehend the reason why and how certain empowering conditions energize development and assist with advancing its different advantages. In addition to other things, exploration can distinguish how information converts into creative activity and how variety can drive positive change.

#### References

1. "India Country Summary of Higher Education" (PDF). World Bank.
2. India 2009: A Reference Annual "Higher Education, National Informatics Centre, Government of India". Education.nic.in. Archived from the original on 18 July 2011.
3. Rukmini S. "Only 8.15% of Indians are graduates, Census data show". The Hindu.
4. "Latest Statistics on Indian Higher Education". DrEducation.com. 17 July 2012.
5. "Statistics – Ministry of Human Resource Development" (PDF). mhrd.gov.in.
6. "Central Universities". ugc.ac.in.
7. "List of State Universities" (PDF). 27 May 2011. Archived from the original
8. "Deemed University – University Grants Commission". ugc.ac.in. 23 June 2008.
9. "Private Universities – University Grants Commission". ugc.ac.in.
10. "The Institutes of National Importance" (PDF). Archived from the original (PDF)



Online ISSN : 2395-602X

Print ISSN : 2395-6011

[www.ijrst.com](http://www.ijrst.com)



**Conference  
Proceedings**

**National Multidisciplinary Conference  
on  
Emerging Trends, Opportunities and  
Challenges in Higher Education**

**Date : 28th January, 2023**

**Organized By**

Janata Shikshan Prasarak Mandal's  
Smt. Vatsalabai Naik Mahila Mahavidyalaya Pusad,  
Department of Home Science and IQAC  
NAAC RE-ACCREDITED -B GRADE

affiliated to

Sant Gadge Baba Amravati University, Amravati, Maharashtra, India

**VOLUME 10, ISSUE 7, JANUARY-FEBRUARY-2023**

**INTERNATIONAL JOURNAL OF SCIENTIFIC  
RESEARCH IN SCIENCE AND TECHNOLOGY**

PEER REVIEWED AND REFEREED INTERNATIONAL SCIENTIFIC RESEARCH JOURNAL

Scientific Journal Impact Factor : 8.014

Email : [editor@ijrst.com](mailto:editor@ijrst.com) Website : <http://ijrst.com>



18	<b>Role of Academic Libraries in Higher Education</b> Dr. Chhaya B. Jatkar	87-89
19	<b>Contribution of Indian Women Writers in English Literature</b> Dr. Vijay Baburao Pande	90-93
20	<b>Innovation In Teaching and Learning</b> Dr. Dnyaneshwari S. Wankhade	94-99
21	<b>Contribution of Indian Women in Literature: Special Reference to Kamala Markanadaya's Novel 'Nectar in A Sieve' : A Study</b> Dr. Anand Y. Bhaik	100-102
22	<b>Impact of Governance, Leadership and Management on Enhancement of Quality of Education and Institution Grading</b> Prof. Dr. D. R. Bambole	103-109
23	<b>Impact of Interactive Technology and Smart Education on Academic Achievement of Students</b> Ravisha R. Ambekar, Dr. Anuradha S. Deshmukh	110-115
24	<b>Education of Creativity Development Is a New Thought Stream in Modern Education</b> Prof. Mayur R. Chaudhari	116-121
25	<b>National Education Policy Challenges and Opportunities in Higher Education System</b> Dr. Premlata P. Kurhekar	122-123
26	<b>Indian Women Writers in English Literature</b> Rinku Vaijanath Rukke	124-127
27	<b>Conservation of Natural Resources and Waste Management : A Future Approach</b> Dr. Sandeep Rambhau Nimbhorkar	128-131
28	<b>Google Classroom : An Important Tool for Assessment</b> Sneha Shende	132-137
29	<b>Higher Education in Women Empowerment</b> Prof. Dr. Nida P. Raut	138-140
30	<b>A Review on Rust Dyeing and Ayurveda Dyeing on Silk with Onion Peel and Harad</b> Harleen Kaur, Dr. Harpreet Kaur	141-147
31	<b>A Study on Traditional Costumes and Accessories of Punjabi Female Folk Dances in Youth Festivals of GNDU since Last Five Years</b> Ms. Randeep Kaur, Dr. Simerjeet Kaur, Dr. Harpreet Kaur	149-167
32	<b>National Education Policy 2020 &amp; New Approach towards Mathematics Teaching and Learning with New Challenges and Opportunities</b> Rupesh R Atram	168-172
33	<b>Online Learning : Challenges for Education in Rural and Remote Areas</b> Sandip. B. Rathod, Dr. Ganesh.T. Patil	173-180



## Innovation In Teaching and Learning

Dr. Dnyaneshwari S. Wankhade

Director, Department of Physical Education, Vidya Bharati Mahavidyalaya, Amravati, Maharashtra, India

### ABSTRACT

incorporating more technology into the classroom to create a blended environment in which students are exposed to technology in a manner comparable to that of the real world. Using powerful video tools to make communication between parents of school districts easier and more clear, innovation in education has the potential to improve overall school outcomes. Students in innovative classrooms are improving their capacity for peer engagement and improving their communication skills. One of our nation's most important basic rights is access to education. After India gained independence, literacy rates have consistently increased. Indians are employable all over the world due to their excellent English skills. Over the years, Indians have made some wonderful discoveries. Innovation is essential to the advancement of our nation and the entire world. Additionally, education benefits greatly from innovation. The application of technology is encouraged by our educational system.

**Keywords:** Elementary education, computerization, holistic growth, and balance in education

### I. INTRODUCTION

to There is a widespread misconception that technological advancements are the only source of educational innovation. Innovation in education, on the other hand, transcends technical expertise. Human nature and tendency are synonymous with the terms "innovation" and "learning." These two words are incredibly dependent on one another. Although there cannot be a greater emphasis on innovation, it is well-established that learning drives innovation. Innovative learning serves as the foundation for the future generation of Creative Leaders. Let us examine the teaching innovation in this article. Design innovation and creative thinking are applied in a variety of industries and sectors, including education. Students are able to develop skills and expand their minds outside of the classroom as a result of the introduction of innovation in education. The true mark of intelligence is imagination, as Albert Einstein so eloquently put it. As a result, it is essential that we adapt our educational and teaching practices to the shifting dynamics of society. To channel innovative education, innovative teaching methods are required to assist students in comprehending and resolving contemporary challenges, breaking social constructs that are pointless, and developing toward a sustainable future.

Computerization, manual labor, and superior matter are all given equal weight in our balanced educational system. Education should be stress-free at least until the primary level, but healthy competition should also be

encouraged. Students' holistic development must be guaranteed by education. Students should be praised for their work and encouraged to learn from their mistakes.

## II. INNOVATIVE TEACHING

The room's spirit and character are developed by teachers. The foundation of innovative education is innovative teaching concepts that encourage learning, inquiry, exploration, and risk-taking. Giving students responsibility, for instance, is a great way to learn. Experimentally, when a primary school teacher let students choose their chapter to study and asked them to create real-world use cases and connections to the subject they had just learned in the lesson. Another educator asked students to self-evaluate their work and identify errors or incorrect assumptions. The students embraced innovative education in an open and curious manner because they loved these methods, became excited about them, and enjoyed being treated as adults and given responsibility. Another name for this is the "Flipped Classroom Model."

The instructor employed an immediate feedback system and required her students to submit a second response based on the feedback she provided in another innovative teaching strategy. This introduced a novel approach to rewarding risks and took away the pressure to achieve high grades in order to excel. She said that students preferred innovative teaching and were excited about the chance to explore. The traditional rule of avoiding and ignoring mistakes at school is harshly criticized in Janet Metcalfe's "Learning from Errors" paper. She puts a lot of emphasis on her argument that labeling failure as a bad thing hinders not only the growth of individual students but also the education system as a whole. A teacher twisted the concept of finding a solution to problems in yet another innovative teaching method. Similar to problem discovery, problem-finding entails looking for missing parts or additional layers that can be added to make something better. Making products that have an impact on the lives of others is similar to this. He gave his students the chance to think deeply, ask tough questions, and come up with innovative solutions to problems by employing this method.

They will be inspired to think creatively and outside the box as a result of this. The students must be encouraged to develop their ideas and make a list of potential solutions after investigating all of the available information. This is a great innovative educational strategy that requires students to interpret their knowledge. The instructor should then encourage the students to see the problem as an opportunity and produce something using their potential solutions. A lot of questioning, self-reflection, teamwork, peer learning, and curiosity will be required throughout this process. The instructor is obligated to provide the students with feedback and prompt them to consider ways in which it could enhance their final solution.

## III. INNOVATION

Indians have discovered extraordinary things like zero. While the value that is placed behind another integer is miraculous, there is no value for a single zero. Amazing, isn't it? This is innovation's power. Innovation does not always require extraordinary effort or a lot of money; On the other hand, the spirit of innovation is maximizing value with as few scarce resources as possible. This is necessary for inclusive and sustainable innovation. The need for quick, inclusive, and effective innovation has been prioritized by a combination of unstable and compound factors, such as the rapid exhaustion of the world's natural resources, growing hopes, income gaps, and the significance of raising the standard of living for millions of poor and deprived communities worldwide. Climable innovation has emerged as a means of overcoming social and economic

obstacles all over the world, but particularly in large nations like India. When progress is slow, the problems must be balancedly solved. Humanity's success depends on how people use their creative potential.

#### **IV. SCOPE OF INNOVATION IN EDUCATION**

India's education system is undergoing transformation, with many schools adopting world-class teaching and learning methods. The goal of education is essentially the same, regardless of whether it involves continuous advancements or complete overhaul: creating a bright future through modern methods. Today, students and their parents seek an educational experience that not only meets their individual requirements but also prepares them for the future. It should also be made certain that students receive up-to-date information about global developments. Visionary teaching and learning practices seem like a prerequisite for meeting these requirements. Every educational establishment must create an engaging, challenging, but productive learning environment. Students' world of imagination is bursting with countless concepts and versatility when they look at the situations that are prevalent in large centers. They can achieve world-class knowledge through controlled exposure to knowledge tailored to their needs, enabling them to compete globally. It can be said that education needs to incorporate information and communication technology (ICT) in ways that support and complement students' worldviews. Therefore, it is not just a matter of improving the methods used to impart education. Ideally, all education stakeholders must have a greater desire to transform the education sector. We can now create learning forums where families and the community can also participate in the education of young students thanks to technology. Nowadays, technology can be used in more creative ways. Learning is liberated from the confines of the classroom and innovative learning strategies are laid out. The applied innovative methods ought to be distinctive. It could be advancing existing practices or altering the method by which the objectives are accomplished. Using audiovisual illustrations to learn Indian history and participate in advanced STEM programs requires inventiveness in the education sector.

#### **V. ROLE OF TECHNOLOGY IN EDUCATION**

Technology is encouraged by our educational system. We not only make sure that students are familiar with and understand technology, but we also encourage them to use it. The majority of schools today have 1:1 computer labs and incorporate technology into their curriculum. Parents and students alike are becoming more technologically savvy.

Thus, the children and their parents are aware of the most recent situation. As soon as possible, all schools will be online. Computerization, manual labor, and superior matter are all given equal weight in our balanced educational system. Children are receiving up-to-date textbooks from numerous State boards and the Central Board. The textbooks now include inspirational stories. Respect and acceptance of one another's shortcomings are essential for children. The human element of education must be preserved through technology.

#### **VI. INNOVATIVE IDEAS OF EDUCATION**

Attracting each student's attention and successfully imparting beliefs in order to leave a lasting impression are the most difficult tasks for any teacher to complete. To successfully complete this task, you as a teacher should incorporate novel ideas to make learning enjoyable for your students. As a result, we've compiled a list of fresh

ideas that will help you rethink your teaching methods and increase student interest. Innovation can be encouraged with the assistance of tools. Include fun games or visual exercises that will captivate young minds and keep them interested. This is a tried-and-true method for inspiring young people to be creative and discovering their creative potential. All of your subjects should include aspects of creativity. Examine the methods they use to develop inventive concepts. Help different ideas; Allow students to testify on their own. During your classes, you should use audiovisual materials to supplement the textbooks. Prototypes, filmstrips, motion pictures, images, visual representations, and other brain-exploring equipment are examples of audio-visual materials. These tools will push students' intellects to new heights. These methods will not only improve students' listening skills but also help them better comprehend concepts. There are a lot of clever toddler applications that you can use to create stunning presentations if you enjoy technology. Teaching will be fresher and students will learn more if you incorporate real-world events into your lessons. When learning materials are connected to and illustrated with real-world examples, they will be more effective. It will pique the interest of students and boost their enthusiasm and attachment to their studies. Teaching should incorporate idea sharing on a regular basis. Students' creativity is boosted when they share their ideas. When a large number of people deliberate over a single idea, everyone is guaranteed to participate and learning becomes more enjoyable for everyone. Students can freely express their opinions at these idea sharing assemblies without worrying about being graded or assessed. You should establish guidelines for the idea sharing assembly. It should be decided in advance what kind of idea sharing is used for a particular topic. An off-site location should be used for idea sharing assemblies in order to maximize learning on certain subjects. Some subjects may be better understood through industrial or recreational trips, while others may only require a trip to the school playground. The students' involvement will rise as a result, and outcomes will be significantly improved. Another important new method of teaching is role play because it helps students connect with the subject and develop their personalities. Teaching about literature, recent happenings, or historical events can all benefit greatly from this method.

Students will become aware of the material's practical application through this method. Role playing is beneficial for students of all ages. For each age group, a little bit of conditioning is needed. This method works well for teaching toddlers as well. Another popular method of teaching subjects where visualization enhances learning is through portrayal. It's a common method for teaching history.

## VII. BENEFITS OF INNOVATION IN EDUCATION

There are numerous indications that, when utilized appropriately, technology is extremely beneficial to students' learning. Technology is very helpful for learning; Additionally, it aids communication. To communicate with parents and students, educators and management use electronic devices. Because it enables students to consult online term papers and other educational applications, technology enhances learning and aids students in their homework. The following are significant advantages of using technology in the classroom: For young students who are familiar with the most recent technology, it makes learning exciting and participatory. It enables a faster and more effective method of teaching at home and in the classroom. It reduces the need for textbooks and other printed materials, saving money in the teaching-learning process. It makes cooperation easier. Students, teachers, and parents can all work together effectively and communicate clearly. It raises students' experimental skills, enables them to learn quickly, and enables them to take full advantage of the tools that technology provides.

## VIII. INNOVATIVE LEARNING

The process of creating an environment where students regularly learn about new things, question them, and come up with new ideas on their own is called innovative learning. It could involve allowing students to explore and comprehend something by utilizing technology like augmented reality, deep learning, or something as common and necessary as the Internet. It could include more practicals and do-it-yourself projects to allow students to take chances and learn by doing. As a Creative Leader, it can also facilitate group explorations that aid in the development of skills like learning from others, growing, and fostering harmony among themselves. These skills will later be useful when managing a large team. One fundamental question is at the heart of the concept of educational innovations: "What do you mean by education?" The current curriculum ought to be more adaptable if it is the art of learning things. In addition, it must include encouraging students to explore and use technology. Risks and failures should be rewarded, and grades should be used to provide less validation. We should learn from education innovation to look ahead of our current methods and make room for better ones.

In today's world, there is a wealth of information available for use in MOOCs, blogs, and other resources to create endless opportunities and spread educational innovation. In the EduTech industry, there are a lot of startups using Augmented Reality and Neural Networks to make learning more fun and engaging, which can encourage curiosity and innovation in education. There are also growing numbers of open source communities where anyone, regardless of age, can join and participate in discussions about novel concepts.

## IX. CONCLUSION

"The value of an idea lies in the use of it," was a quote by the great scientist Thomas Edison. As a result, our educational system needs to maintain its effectiveness while also remaining relevant to the advancements we are making and the challenges our world is currently facing. It's time to encourage new ways of learning so that students learn more than just what is in a textbook. Check out Jigsaw Academy's Post Graduate Certificate Program in Design Innovation & Strategy, a 5.5-month online instructor-led program that enables students to Design Innovation and Creativity-led Entrepreneurship, if you are interested in learning more about Design Innovation & Thinking and its application across domains. For improved outcomes, some educators have also combined textbook learning with technology. Stories told through videos, graphic novels, robots, etc., is rooted in the concept of an innovation school. For instance, introducing graphic novels and storybooks to history lessons increases a student's likelihood of retention over oral instruction. Alternately, utilizing the Design Thinking method for educational innovation in teaching is a comprehensive strategy. A methodical approach known as the "Design Thinking Process" is one that focuses on problem-solving, information gathering, idea generation, idea refinement, and solution testing. Discovery, Interpretation, Ideation, Experimentation, and Evolution are the five phases of this process. The teacher can begin by challenging the students with a problem by dividing them into groups in innovative schools and teaching methods.

## X. REFERENCES

- [1]. Schumpeter, Joseph A., 1883–1950 (1983). The theory of economic development : an inquiry into profits, capital, credit, interest, and the business cycle.

- [2]. "ISO 56000:2020(en)Innovation management — Fundamentals and vocabulary.
- [3]. Lijster, Thijs, ed. (2018). The Future of the New: Artistic Innovation in Times of Social Acceleration.
- [4]. Bhasin, Kim (2 April 2012). "This Is The Difference Between 'Invention' And 'Innovation.
- [5]. "What's the Difference Between Invention and Innovation?", Forbes,
- [6]. Edison, H., Ali, N.B., & Torkar, R. (2014). Towards innovation measurement in the software industry.
- [7]. Baregheh, Anahita; Rowley, Jennifer; Sambrook, Sally (4 September 2009). "Towards a multidisciplinary definition of innovation"





|| Yoga Karmashu Kaushalam ||



**Shree Hanuman Vyayam Prasarak Mandal, Amravati (M.S.) INDIA**

## **2<sup>nd</sup> INTERNATIONAL CONFERENCE ON YOGA FOR GLOBAL WELL-BEING**

**Bridging the Gap Between Yogic Sciences and Diverse Communities**

**Workshop**

**3<sup>rd</sup> Feb 2023 to 4<sup>th</sup> Feb 2023**

**Conference and Yogasana Competition**

**5<sup>th</sup> Feb 2023 to 6<sup>th</sup> Feb 2023**

**Venue:- Business Centre, Dubai**

### **HOST ORGANIZATIONS**

**Shree Hanuman Vyayam Prasarak Mandal,  
Amravati, (MS) India**

**Degree College of Physical Education, Amravati, (MS) India**

### **PARTNERS ORGANIZATIONS:**

**Burhan Maharashtra Yoga Parisad  
Nehru Mahavidyalaya, Nerparsopant, Distt. Yavatmal**

### ***Introduction:***

*Yoga is an ancient physical, mental and spiritual practice that originated in India. The word 'yoga' derives from Sanskrit and means to join or to unite, symbolizing the union of body and consciousness. Today, more than ever the world needs to be in harmony and peace not just with the outer environment but also internally for a wholesome well-being of body, mind and soul. Hence experts from diverse communities representing physical education, elite sports, sport for all, management, social sciences, Medical Sciences and Neuro engineering are invited to discuss dimensions of Yogic Sciences and its applicability via research papers and symposiums at the international conference in the divinely scenic 'Pearl Nation'.*

### ***Shree H. V. P Mandal, Amravati (M.S.), India***

*Established in 1914 - promotes traditional sports, games and physical culture of India. A voluntary, social, non-political and secular institute; managed with democratic principles. Recognized NGO by UNESCO ICH NGO- Forum, a member of ICSSPE and TAFISA among other national & international organizations. Proudly celebrating golden jubilee of its premier Degree College of Physical Education, Amravati in 2017-18. Also, focusing on Engineering, Technology and Sports Management through its College of Engineering & Technology, Amravati.*

## INDEX

Sr. No	Title	Page No
1	EFFECTS OF YOGA PRACTICES ON DEVELOPMENT OF IMMUNITY - SARITA S. NIMGARE	1-3
2	ANALYSIS OF YOGIC PRACTICES: IMPACT ON MENTAL AND PHYSICAL HEALTH - DR. JYOTI JUNGARE	4-8
3	ANALYSIS ON LUNG CAPACITY OF SENIOR CITIZEN: IMPACT OF YOGA AND PRANAYAM - KIRAN VISHWAKARMA	9-12
4	EFFECT OF TEN WEEKS YOGA PROGRAMME ON SELECTED PSYCHOLOGICAL VARIABLES OF COLLEGE STUDENTS - DR. AJAY S. BONDE	13-19
5	RECENT ADVANCES IN YOGIC THERAPY AND PRACTICES - DR. VASISTHA A. KHODASKAR	20-24
6	YOGA AS THERAPEUTIC MODALITY: MENTAL AND PHYSICAL WELLNESS - DR. RAVINDRA D. SAWARKAR	25-27
7	IMPORTANTE OF YOGIC JAL-NETI KRIYA: IMPROVE RESPIRATORY FUNCTIONS - PROF. SUBHANGI RAWALE	28-30
8	A COMPARATIVE STUDY OF SELF CONCEPT BETWEEN THE YOGA AND BALLGAME PLAYERS - SUMIT AMLEKAR, RAHUL SARSWAT, PUSHPAK KHONDE	31-32
9	IMPACT OF YOGA AND PRANAYAM ON SENIOR CITIZENS: AN ANALYSIS ON LUNG CAPACITY - DR. AJIT J. BHISE	33-36
10	YOGA FOR PREVENTING INJURIES, HEALTH AND WELLBEING - DR. ATUL R. PATIL	37-39
11	ROLE OF YOGA IN REDUCTION OF CRIMES AND DE- ADDICTION - DR. DNYANESHWARI S. WANKHADE	40-46
12	IMPACT OF YOGIC PRACTICES: MENTAL AND PHYSICAL HEALTH - PROF. DR. NANASAHEB SAPKAL	47-49
13	AN EXPERIMENTAL INVESTIGATION OF USE OF YOGA AND NUTRITION FOR IMPROVING PHYSICAL HEALTH OF TRIBAL STUDENTS - TEJSIHA LAXMANRAO JAGDALE	50-53
14	EFFECT OF YOGA PRACTISES ON SELECTED PHYSIOLOGICAL PARAMETERS OF B.ED. STUDENTS OF AMRAVATI - DR. KAVITA N. WATANE	54-56
15	YOGA AND MEDITATION: MENTAL AND PHYSICAL WELLNESS - ASST. PROF DR. KIRAN GAYAKWAD (RAHANE)	57-58



## ROLE OF YOGA IN REDUCTION OF CRIMES AND DE- ADDICTION

**DR. DNYANESHWARI S. WANKHADE**

DIRECTOR, DEPARTMENT OF PHYSICAL EDUCATION, VIDYA BHARATI  
MAHAVIDYALAYA, AMRAVATI, MAHARASHTRA, INDIA-444603

### ABSTRACT:

The term "yoga" refers to various forms of bodywork. Yoga and trans-dental meditation therefore emphasize the human child's spiritual development today. Yoga builds mental fortitude and self-control. Yoga has the potential to enhance children's learning and achievement. Children with special needs, people who break the law, people who are violent and in disciplined, and people who are aggressive can all benefit greatly from being calmed down. Yoga is essential for the full development of one's personality, and it can help one realize most aspects of Indian spirituality. Yoga was once emphasized by Vedic sages as a way to cultivate psychological and psychic discipline in one's personality, which led to the highest form of spirituality. Spiritual growth is impossible without yoga, and holistic growth of a person becomes challenging without spiritual growth. However, with the western influence.

### KEYWORDS:

**QUALITY OF LIFE, AGGRESSION, SUDARSHAN KRIYA YOGA, AND YOGA TECHNIQUES.**

### INTRODUCTION:

As a result, the "Art of Living" movement in India, which places an emphasis on yoga, meditation, and living a disciplined life, is increasingly taking centre stage. Yoga, a variety of exercises, and good habits for self-discipline and mental purity are all part of Art of Living. Today, the average person is very fond of it. Yoga has been incorporated into the curriculum of many schools and colleges because of its significance. Yoga is now taught to children as a form of physical and mental exercise in schools by yoga teachers. Television regularly features demonstrations of yoga and other physical activities. Parents and teachers are encouraging their children and students to practise yoga to restore a positive attitude toward spiritual growth. In India, yoga and meditation schools are becoming increasingly popular. Yoga and meditation are attracting visitors from all over the world to India in search of inner tranquillity. Everyone in society knows that practising yoga is necessary for mental and physical well-being as well as peace and happiness. Every day, people go to Meditation Halls in big cities to practise meditation.

The mind and body benefit from concentration and relaxation through meditation. Everyone, regardless of age or physical condition, should begin practising yoga and meditation because of the importance of the practice to easing tension, improving physical and mental health, and maintaining physical and mental fitness. Yoga and meditation have been shown to not only improve a person's mental and physical health, help them relax, and relieve stress, but they also help cure a lot of diseases. When practising yoga, a person must be guided through their nature in accordance with their capacity. A man can also learn to be disciplined and not aggressive through

yoga.

Yoga of love, work, and knowledge, yoga of Bhakti, and yoga of self-exceeding through physical beings are among the many types of yoga, according to legend. Additionally, yoga is necessary for self-discipline, which is crucial for developing non-aggressive, reasonable, emotional intelligence, and mental health.

Yoga enables a person to exhibit nonviolent behaviour that is conducive to a peaceful, law-abiding society by reducing their violent tendencies. Yoga and trans-dental meditation are essential for spiritual growth in accordance with our extensive cultural heritage.

Maharishi Mahesh Yogi and a number of other Indian saints have opened massive yoga studios in Western nations to promote yoga and encourage spiritual growth in materialistic nations. In this world of anxiety and stress, yoga centres all over the world are getting a lot of interest. In order to alleviate stress, Sri Ravi Sankarjee is preaching the Art of Living in various nations. People from all walks of life have benefited physically, mentally, emotionally, and spiritually from his preaching, words, and even his very presence. Parents should encourage their children to meditate from the beginning. Keeping in mind the number of students, every school ought to have a meditation hall. Yoga and meditation should be done every day. Physical education is more important than formal education because it cleans the mind and body at the same time. To begin, children should be allowed to meditate for a brief period of time, which can be extended as they get older. Yoga, meditation, and other forms of physical activity should be practised by parents as well. A person's holistic and all-round development, including his physical, mental, emotional, and cognitive development, is aided by his

spiritual development. From an early age, spiritual growth aids in the proper development of morality and conscience. Moral growth and spiritual growth are strongly correlated. For a peaceful, non-aggressive society, both of these developments are necessary.

### DEFINITION OF YOGA

Patanjali defines "Yogashchittavritti nirodhah" Yoga is a process of gaining control over the mind. By so controlling the mind we reach our original state; "Tada Drashtuh Svarupe avasthanam" Then the Seer establishes himself in his causal state. This is the technique of 'mind control' prescribed by Patanjali. Control involves two aspects – a power to concentrate on any desired subject or object and a capacity to remain quiet any time. Rarely, the second capacity of man, to remain calm and silent, has been harnessed. Hence, Yoga mainly emphasises, this second aspect. Yoga is thus a skilful, subtle process and not a brutal, mechanical gross effort to stop the thoughts in the mind and thereby becomes a process for elevating oneself through calming of mind

### THE INFLUENCE OF SPIRITUALITY

Today, spirituality is regarded as one of the most effective methods for personal transformation. It has the capacity to profoundly alter one's perceptions, values, and actions as well as to sustain those transformations. When it comes to overcoming physical, emotional, or environmental stress, it can be a personal source of strength. Science has been baffled by the numerous advantages of being "spiritual" and the miraculous transformations that spirituality may bring about in individuals.

Koenig and others According to Larson, Sawyers, and McCullough (1997), spirituality has a "sacred core" that consists of "feelings, thoughts, experiences, and behaviours that arise from a search for the sacred that involves attempts to identify, to articulate, to maintain or to transform." They define spirituality as "the personal quest for understanding the answers to ultimate questions about life, about meaning, and about relationship to the sacred or transcendent, which may (or may not) lead to or arise from the development

Spirituality, according to Burkhardt (1989), is "harmonious interconnectedness with self, others, a higher power, and environment." Beliefs, values, actions, and experiences all play a role in spirituality. It is a relationship in which beliefs give rise to values, which change our actions and have an effect on the spiritual belief system through experience. A spiritual person is on a quest for meaning and purpose and believes that his or her life has meaning and a purpose (Elkins et al., 1988).

### SPIRITUALITY IN PRISONS

Globally, there has been a significant shift to view criminals as individuals who require reform and transformation rather than as dangerous, hardcore, and alienated individuals in the past. Prison should no longer be viewed as a place for punishment but rather as one for education, personal development, and advancement. It is a

haven for change. The ultimate goal of the prison term is the offender's transformation into a better person. One of the jail authorities' most important goals has become the rehabilitation of criminals. In the United States, the Department of Correction has replaced the Department of Jails. As a result, modern educational, vocational, recreational, and spiritual programs are increasingly being offered to inmates.

The situation in India is also favourable, with numerous reforms implemented throughout the country. According to the article "Reformation of Prisoners" on the website of the Department of Prison, Tamil Nadu Government, "the administration of prisons is accorded utmost priority by the Government." A coordinated effort is made to enhance the overall welfare of prisoners as well as basic infrastructure facilities. Correctional facilities are undergoing administrative changes as well as improvements to their safety and security. The prison department adheres to the principles of correctional administration in order to facilitate reformation and rehabilitation throughout the system. Dr. Kiran Bedi, better known as the architect of Tihar Jail's reforms, believes that prison reforms require a holistic approach and that isolated programs for inmate development, which were used in jails all over the country and the world, would not produce the desired outcomes. She has proposed the straightforward and efficient "3 Cs model" for prison management: collective, corrective, and community-based prison management.

### HEALTH CARE

The human race has entered the 21st century. In order to provide better healthcare, men are collaborating with numerous superior technologists in medical science. The World Health Organization is conducting assessments of global health conditions and taking the necessary steps to improve health conditions. Although high-tech medical facilities and fascinating advancements in spare-part surgeries have made life easier, the expected quality of life of peace and harmony appears far from reality, despite the fact that life expectancy has increased to more than seventy years. There is an exponential increase in stress-related issues, stress-related illnesses, unrest, and family breakups. Because of the pressing need of the time, health care providers, who initially provided relief to their ill patients through surgeries and medications, are now confronted with such novel inquiries. The majority of prevalent social and health issues cannot be resolved through germ theory, antibiotics, or surgical procedures. The influence of mind on matter has begun to be highlighted by the development of fascinating diagnostic tools. Psycho-neurophysiological, immunological, and biochemical researchers are all recognizing the role of the mind, lifestyle, suppressed emotions, stress, and other factors. In the genesis of numerous of the millennium's challenges. Despite opposition from hard core matter-based pharmaceutical and surgery-oriented researchers, several research publications on the value of positive thinking, prayer, spiritual healing, mind-body

medicine, yoga, acupuncture, and energy medicine are being poured into medical journals.

## YOGA

Swami Satyananda Saraswati referred to yoga as "a complete science of consciousness." It grants control over every stage of consciousness. In the Rig Veda, specifically the Atharva Veda, where there is a lengthy discussion of the individual's psyche and well-being, yoga is mentioned. However, Patanjali's Yoga Sutras contain the most comprehensive explanation of yoga. Beginning at the turn of the 20th century, psychologists, medical researchers, and therapists working in other fields, including psychology, began verifying the yogic principles and utilising its methods for human adjustment and health promotion. The practices of yoga, particularly raja yoga and hatha yoga, have stood up to scientific scrutiny and been found to be helpful in the treatment of many chronic diseases (Bhushan, 1998) (Sengupta and Banerjee, 1994). The effects of yoga on one's physical and mental well-being have been extensively studied. According to Behera and Jindal (1990), yoga has positive effects on health conditions like bronchial asthma. Chronic tinnitus (Kroner, Hebing, and Van Rijn, 1995), back pain (Nespor, 1989), hypertension (Brownstein and Dembert, 1989), migraines and tension headaches (Latha and Kaliappan, 1987), and A lot of research shows that yoga can help people with mental disabilities get better (Uma, Nagendra, Nagarathna, et al., anxiety (Singh and Madhu, 1987; 1989); Depression (Khumar, Kaur, and Kaur, 1993; Sahasi, Mohan, and Kacker, 1989)

In his 1998 article *Yoga, Bhushan: The following is written in An Instrument of Psychological Transformation: Psychosomatic disorders are the result of mental stress-induced imbalances in the neurophysiological and endocrinal systems. DIAFS (Disease Induced Anxiety and Fear Syndrome) is a term used to describe the psychological symptoms and anxiety brought on by these disorders once more. As a result, psychosomatic and somatopsychic symptoms are caused by the mind-body interaction in a chain of cause-and-effect relationships. Somatic or psychological management alone is not sufficient for their proper treatment. Because of its psycho-somato-spiritual approach, yoga practices are effective.*

Aminabhai (1996) claims that yoga training significantly improves subjects' mental health. According to Selvamurthy (1993), a number of studies have shown that yoga has numerous positive effects on stress management. The cognitive processes of perception, subjective well-being, quality of life, and criminal propensity can all benefit from yoga and meditation. According to Venkatesh, Pal, Negi, Verma, Sapru, and Verma (1994), the yoga group had significantly higher social desirability scores. Additionally, it was discovered that yoga practitioners had significantly lower life event scores for the preceding year.

## MEDITATION

According to Odanjeny (1988), meditation teaches a

"focused attention that leads to increased self-awareness of mental and emotional states, mastery over instinctive, compulsive reactions, insight into one's true nature and into reality, exploration of religious themes, images, and feelings, and expansion of ego consciousness into a more universal consciousness." [Citation needed] [Citation needed] [Citation needed] According to Bogart (1991), meditation has the potential to have therapeutic benefits and suggests that it is more than just a relaxation, behavioural, or cognitive technique. It also causes changes in physiological, behavioural, and cognitive processes.

According to Bogart (1991), many require a state of inner and outer stillness in which attention is diverted from the external world and from conventional patterns of perceptual, cognitive, emotional, and motor activity. Music, movement, visual or auditory

Contemplation of physical objects or processes, such as staring at a candle flame or listening to a stream of water or ocean waves, are all used in some forms of meditation. According to Deikman (1982), meditative practices raise awareness of the self that is being observed and alter established patterns of perception and thought, thereby bringing about change. According to Kornfield, Dass, and Miyuki (1983), meditation is a tool for more than just seeking safety and security. It can also be used to deal with inner turmoil and undergo profound transformation.

According to Bogart (1991), a number of studies have suggested that meditation may be an effective preventative or rehabilitative strategy for treating conditions such as hypertension, asthma, addictions, fears, phobias, insomnia, and stress. According to Brooks and Scarano (1985), meditation works to treat post-traumatic stress disorder. According to Seeman, Nidich, and Banta's 1972 study, subjects who meditate also change more than those in control groups in positive mental health, positive personality change, self-actualization, increased spontaneity, self-regard, inner directedness, and self-perceived increased capacity for intimate contact. 1974, Hjelle; Otis, 1974). Delmonte (1984) looked at how self-esteem and self-concept, depression, psychosomatic symptomatology, self-actualization, locus of control, and introversion/extroversion were related to meditation and personality scores. He discovered that meditation does appear to be associated with increases in self-actualization and decreases in depression, but he found no compelling evidence to suggest that meditation alters psychometric scores. According to Childs (1976), the use of TM with juvenile offenders was linked to self-actualization, a decrease in anxiety and drug use, improvements in behaviour and interpersonal relationships, and lessening of anxiety.

Researchers have demonstrated that meditative practices have a beneficial effect on prisoners (Alexander, 1982; Dhar and Khurana, 2000). Meditation requires a person to focus on a single aspect (such as a dot, mantra, image, etc.) and block out all unnecessary thoughts from immediate awareness. Being able to meditate necessitates the meditator's normal state, if not a higher level of

consciousness. The seventh step in Patanjali's Yoga Sutras is meditation, or dhyana. Even though there is no hierarchy in the eight-fold path, achieving the dhyana states necessitates satisfying other prerequisites. The yama and niyamas, or moral behaviour, are very important for entering the meditation state. It is necessary to perform additional internal and external purification, either through pranayama, kriyas, or surrendering to God. When the person cultivates a spiritual outlook, this becomes possible.

TM was used by some researchers as a treatment for juvenile offenders and as a method of rehabilitation (Anklesaria, 1992). According to Childs (1976) and Bleick and Abrams (1987), the TM program has led to reoffending in California. However, as the majority of prisoners will be depressed and experiencing negative emotions, using only meditation may not be very effective. Using other methods like yoga and spiritual counselling to live with depression would be the first step in the process. Different outcomes from those promoted by the TM movement have been documented by a number of studies. In a ten-year study of TM participants, Desiraju (1990) found that they were drowsier than participants in other forms of meditation; Compared to other methods of meditation, their EEGs revealed weaker alpha and theta waves. TM showed a lot of variation from session to session, and physiological correlates were always erratic.

### KNOWING OF YOGA

It is referred to as the union of jivatma and paramatma—the individual self with the universal self—in conventional terminology. It is a transformation of the confined, narrow, and egotistic personality into an all-encompassing, eternal, and blissful state of reality. One of the six Indian philosophical systems known as "Shad Darshanas" is Patanjali Yoga. Nearly 5000 years ago, one of the great seers Patanjali made a significant contribution to the field of yoga by compiling the essential features and principles of yoga in the form of "Sutras," or aphorisms. As a result, yoga is a deliberate effort to control one's thoughts. Man, endowed with discriminative power, the buddhic faculty, and well-developed voluntary control systems, wants to grow faster. Yoga is a methodical conscious practice that can significantly accelerate man's growth. As a result, yoga is a methodical approach to accelerating a man's complete development. Man learns to live in higher states of consciousness as a result of this development. The cultivation of the mind is essential to this holistic development and growth of the personality.

### VIPASSANA MEDITATION

Under the direction of Shri S. N. Goenka, the guru of vipassana, an ancient meditation technique known as vipassana, is currently being taught in India and a number of other nations. "Insight" in Vipassana means seeing things as they really are. A ten-day residential course with a qualified instructor is required to learn this method. First and foremost, one must swear to uphold certain moral principles (sila). They are: avoiding the killing of any living

thing, stealing, engaging in sexual misconduct, lying, or taking any drug. Anapana, or awareness of one's breathing, is the second part of this training. This requires constant "observation" of the natural flow of breath in and out. The third step, development of panna— also known as wisdom—entails mind purification through increased awareness. The individual tries to cultivate an attitude of non-judgment and non-reaction by engaging in choiceless and effortless observation of body sensations (Khurana and Dhar, 2000).

Students are confined to the course site throughout the retreat and have no contact with the outside world. Writing and reading are not something they do. They adhere to a rigorous daily routine that includes sitting meditation for approximately ten hours. Additionally, they remain silent and refrain from interacting with other students. Several times a day, students are given systematic meditation instructions, and Shri Goenka gives an evening video-taped speech about the day's progress. For the first nine days, there is no talking. Students resume speaking on day ten, transitioning back to a more outgoing lifestyle. On the morning of the eleventh day, the course comes to an end.

In a number of Indian prisons, vipassana meditation has become the most widely used method of rehabilitation. Goenkaji conducted the first such experiment in Indian penal history in 1975 with 120 inmates at the Central Jail in Jaipur. A second class was offered at the Jaipur Central Jail in 1977. The University of Rajasthan carried out a number of sociological studies on these classes. Another course was held in the Jaipur Central Jail in 1990, with positive outcomes for forty life-term inmates and ten jail staff members. On these early courses, there was no systematic research done. The prisoners, the majority of whom were life criminals or had committed serious offences, were evaluated before and after the course by the Department of Sociology at the University of Rajasthan. In an interview that was published in Yoga Magazine in 1975, Dr. Chokhani, Director of Research at Igatpuri Vipassana Meditation Center, stated that "unfortunately there was no long term follow-up due to the transient political leadership."

In 1991, the Department of Education, Gujarat Vidyapeeth, conducted a research project on a course offered to life-sentenced inmates at the Sabarmati Central Jail in Ahmedabad. According to Hurana and Dhar (2000), the studies in Rajasthan and Gujarat demonstrated that vipassana is a beneficial reform measure that enables criminals to become wholesome members of society and that the participants' attitudes and behaviours changed in a clear and positive way. Numerous questions have been raised by studies on vipassana meditation due to a lack of appropriate scientific methods. In Tihar Jail, Vipassana was first taught in 1993, and AIIMS carried out two studies in 1994. In 1994, 120 people participated in the initial study. Well-being, hostility, hope, helplessness, personality, psychopathy, and, in the case of psychiatric disorders, anxiety and depression, were the studied dimensions. A

second study with 150 subjects followed. There were two groups in the sample: a control group of 65 people and a group of 85 people who took a 10- day vipassna course. Anomie, attitude toward the law, personality, and psychiatric illness were the investigated dimensions. According to Vipassana Research Institute (1990), the subjects reported feeling less helpless and less hostile toward their surroundings immediately following the course.

Quantitative evaluation of the positive effects of vipassana in Tihar Jail inmates was the primary goal of another study. With the assistance of two experts, a structured questionnaire was created: Dr. Adarsh Sharma of NIPCID and Prof. Purnima Mathur of IIT. A week before the camp, they were given the questionnaire to find out about their personal and family history, the kind of crime they committed, how they felt about other people, how their imprisonment affected them, and other things. After the camp, a second questionnaire was given to see how the meditation had affected them. Seventy-four of the ninety-six inmates completed both questionnaires, and their responses form the basis of the analysis provided below. The majority of prisoners suffer from tension, as expected; 73% of respondents stated that they were overly concerned about the future; 39% stated that they were frequently reflecting on the past; and 47% said that their thoughts were not at all peaceful. In fact, 16% of respondents admitted that they constantly considered taking vengeance on the people who were to blame for their imprisonment. The most missed area was family (61%) This study did not employ a rigorous scientific methodology or standard questionnaires. Additionally, the volunteers who collected the data were primarily vipassana trainees.

Vipassana meditation (VM) was studied by Khurana and Dhar (2000) to see how it affected the criminal propensity (CP), subjective well-being (SWB), and quality of life (QOL) of Tihar Jail, Delhi, inmates. 262 inmates (232 males and 30 females) were the subjects of five studies that utilised both pre- and post- and control-group experimental designs. Meditation through vipassana was the independent variable. These were the dependent variables: subjective well-being (SWB), quality of life (QOL), and criminal propensity (CP). The variables were measured using the Life Satisfaction Scale, Subjective Well-Being Scale (Nagpal and Sell, 1985), and Criminal Propensity Scale (Sanyal and Kathpalia, 1999). According to the findings, vipassana meditation significantly reduced criminal propensity and improved subjective well-being. Due to improper methodology, these studies have numerous flaws. In addition, the majority of prisoners lack the integrity necessary to withstand the rigorous procedures of vipassana meditation, so practising only this form of meditation could have many negative effects on them.

Long-term studies on the effects of Yoga on inmates in jail are uncommon, despite the fact that numerous studies have been carried out to ascertain the effects of Yogic

practice on the mental health of populations of various ages, genders, occupations, health and disease categories. In light of this background, the purpose of the current study was to determine how six months of yoga training affected the mental health of inmates at Tihar Jail, Delhi. The study was part of a project called "Sanjeevan" that Morarji Desai National Institute of Yoga, New Delhi, and Prison Headquarters, Central Jail, Tihar, New Delhi, were working on to train inmates of Tihar Jail to teach yoga. Aggression, anxiety, depression, stress, physical health, psychological health, and general well-being were all used in this study to determine how yoga training affected the mental health of jail inmates. Mental health is linked to every parameter. Negative correlations exist between aggression, anxiety, depression, and stress, whereas positive correlations exist between mental health and physical, psychological, and general well-being. The hypothesis that regular yoga practice will lessen aggression, anxiety, depression, and stress was the basis for the study. and improve the mental, physical, and overall well-being of inmates in jail. As a result, the jail inmates' aggression, anxiety, depression, stress, psychological health, and general well- being will all improve as a result of the yogic practices.

## YOGA, MEDITATION, AND BREATHING TECHNIQUE

The union of one's own self and the divine is the definition of yoga, an ancient Indian practice. It is a mind-body system that incorporates spiritual, mental, and physical practices. Yoga has been practised as a healthy way to live since ancient times and has also been used in alternative medicine. Pranayama, a type of breathing exercise that improves respiratory function, deep relaxation techniques that cultivate the ability to physically and mentally release tension and stress, and meditation to enhance mind-body awareness and improve attention and emotional regulation skills are all common components of yoga. The spine, muscles, and joints become healthy and flexible through asana practice. It is hypothesised that practising breathing exercises helps to maintain the equilibrium of the autonomic nervous system, which has an impact on psychological and stress-related disorders and helps to prevent the negative effects of stress. Sudarshan Kriya Yoga (SKY) is one of the many breathing exercises out there. The mind-body system benefits from this particular type of breathing exercise. The Art of Living Foundation teaches this renowned method. Millions of people in 155 nations have benefited from it. 67% and 71% of study participants experienced relief from depression and anxiety following regular use of SKY. It improved hormones related to well-being and deep sleep, as well as decreased cortisol production in response to stress. It was discovered that the impact of SKY on youth in the United States significantly reduced impulsive behaviour and enhanced mental health. There is increasing evidence to suggest that SKY can be a useful, low-risk, and inexpensive addition to the treatment of stress, anxiety, post-traumatic stress disorder, depression, and other stress-related

medical conditions. As a result, it can help criminal offenders get back on their feet.

Although SKY's efficacy in a variety of medical conditions and population subsets has been demonstrated, little is known about its effects on people who exhibit aggression and violence. As a result, the purpose of this study was to add to the existing body of research on the effects of SKY and meditation on the behaviour and well-being of people who have spread extreme violence and aggression or participated in it. The United Liberation Front of Assam (ULFA) militants' aggression, life satisfaction, and quality of life after surrendering their arms were specifically measured in this study.

### COMPREHENSIVE YOGA WORKSHOP

The Art of Living International Centre in Bengaluru, India, served as the venue for the intensive 40-day workshop, which was led by certified instructors. The sessions (morning hatha yoga, seva/service sessions after breakfast, meditation, seva/service sessions after lunch, meditation, nature walk to connect with nature, satsang/singing songs together, and knowledge sessions after dinner) were held all day from 06:00 a.m. to 10:00 p.m. The Art of Living Happily Program taught everyone the SKY, and then an advanced program of deep meditation, personal transformation, and empowerment followed. Participants in this specialised program were given the tools they needed to become community leaders, allowing them to be agents of change once they reached their communities. All participants attended evening "satsangs" and participated in daily SKY and meditation practices for 40 days.

### YOGA AND DE- ADDICTION

One of the best yoga poses for treating addiction is the yoga butterfly pose, also known as Baddha Konasana. Learning this pose will teach you how to deal with cravings while relaxing and having a clear mind. Yoga is a mindful exercise that helps people deal with stress and is especially important for addicts and people in recovery. Yoga helps curb drug cravings by employing mental and physical techniques that target the brain region affected by substance abuse. For those in recovery from addiction or alcoholism, yoga can be a powerful tool. The practice of yoga aids in the healing and reconnection of the mind, body, and soul due to its emphasis on mindfulness, slow movements, and deep breathing.

The incorporation of meditation and breathing into yoga can contribute to an improvement in mental health. Mindfulness and tranquillity are cultivated through regular yoga practice; enhances body consciousness; reduces patterns of long-term stress; soothes the mind; focuses on one thing; Yoga is a great active recovery workout for the body and mind, improves concentration, and can help you become a better athlete. You are not the only one who considers yoga to be stretching; in fact, some fitness professionals and athletes share your opinion. Low-intensity yoga's gentle movements aid in blood flow. The body has an easier time getting nutrients to muscle

cells because of this. Better muscle damage repair is possible with the help of these nutrients. The amount of soreness you may experience is also affected by this. Because of the positive effects it has on the nervous system, restorative yoga can be used to help trauma survivors heal. Five or six poses are common in sequences. It gives you the chance to feel and accept every sensation when combined with stillness, deep breathing, and meditation. Physical and behavioural addictions of all kinds can be effectively treated by professionals. Addicts can manage withdrawal and learn to live without their addictions thanks to individualised treatment plans.

### CONCLUSION

The current study demonstrates that a comprehensive yoga program, which includes SKY and meditation, can transform a person in a short amount of time by reducing aggression and enhancing life satisfaction and quality of life. All of these are necessary for harmony and peace. A calm mind is better able to respond to and deal with life's challenges in a productive way. Techniques like SKY and meditation make people happier, less aggressive, and more at ease. When they have more awareness, they are better able to make decisions about how to get through difficult situations. It is a potent instrument for enhancing mental and physical well-being and may be useful as a rehabilitation measure for people who want to reintegrate into society.

Policymaking is also affected by the findings. Psychological and psychosocial treatments have dominated prior research and policy on mental health interventions in prisons. An effective option is yoga-based interventions like SKY and meditation, which merit further investigation. This research has some limitations. During their 40-day stay at the Art of Living International Centre, participants not only participated in daily SKY and meditation practices, but they also attended evening satsangs (singing and knowledge sessions) and followed a predetermined routine in a serene setting. The participants' alterations may also have been influenced by these variables. As a result, determining which aspects of the intervention contributed to the change is challenging. Second, the study did not include a control group, despite the fact that the feasibility of such a study may make it challenging. Thirdly, whether or not the Yoga program actually helped these surrendered militants integrate back into the community will be revealed by their lack of follow-up.

### REFERENCES

1. "yoga, n." OED Online. Oxford University Press. September 2015.
2. Denise Lardner Carmody, John Carmody (1996), Serene Compassion. Oxford University Press.



3. "Yoga: How did it conquer the world and what's changed?". BBC News.

4. Karel Werner (1977), Yoga and the R̥g Veda: An Interpretation of the Keśin Hymn (RV 10, 136), Religious Studies.

5. Andrew J. Nicholson (2013). Unifying Hinduism: Philosophy and Identity in Indian Intellectual History

6. Rajghatta, Chidanand (28 September 2014). "Narendra

Modi calls for International Yoga Day"

7. Yoga joins Unesco world heritage list". The Guardian. 1 December 2016.

8. Ross, Alyson; Thomas, Sue (2010). "The Health Benefits of Yoga and Exercise: A Review of Comparison Studies

# Tourism Planning and Regional Development

**Dr. Dnyaneshwari S. Wankhade**

Director, Department of Physical Education

Vidya Bharati Mahavidyalaya, Amravati.

[dnyaneshwariingle18@gmail.com](mailto:dnyaneshwariingle18@gmail.com)

Mob. No. 9359220717

## ABSTRACT :

Since the second half of the last century, academics and governments in various parts of the world, particularly in the Less Developed Countries (LDCs), have developed and implemented numerous strategies for regional development. The degree and nature of the success or failure of various strategies varies from nation to nation.

**KEYWORDS :** *Industrialization, Tourism Planning, Regional Development, Less Developed Countries (LDCs).*

## INTRODUCTION :

Industrialization, mineral resource exploration, primary product exportation, and the concentration of investments in major urban centers at the expense of the regions were some of these strategies. The "Growth pole theory," developed by Perroux in 1950, was modified by Myrdal (1957), Hirschmann (1958), and Boulderville (1966) into the "Growth Centre Theory" that serves as the foundation for these kinds of development strategies.

The search for an alternative development paradigm was fueled by the growing disparity in development levels and the growth center models' inability to achieve the desired equitable balance. In contrast to the growth center model, which is referred to as the "Center-down approach," researchers have developed the "Bottom-up Theory" of regional development over the past three decades.

The modernization approach was one of several strategies associated with the bottom-up approach; fundamentals of strategy; unified strategy for rural development; agribusiness strategy and agropolitan strategy, to name a few (see Adeyinka et al., 2002). The various bottom-up paradigm strategies typically concentrate on distinct aspects of regional development.

Regional development, as defined by the World Bank in 1975, is a process of growth, transformation, and progress. The ability to retain and absorb a young, progressive, and productive population demonstrates the growth. It also implies reorganizing the economy to meet the material

requirements and aspirations of the populace, particularly the rural masses, who make up the majority of the population.

It must also encourage incentives for individuals and groups to participate in development. The transformation of rural residents' monotonous and stale existence into a dynamic and exciting one is the "progress" aspect of regional development.

According to Lele (1979), development is defined as raising the standard of living of the majority of low-income rural residents and making their development self-sustaining. She says that this straightforward definition has three important characteristics that have significant repercussions for the design and implementation of regional development programs: namely-

1. Mobilization and the creation of conditions that encourage people to increase their income-generating capabilities are necessary for raising the standard of living of the subsistence population,
2. People must be involved in the formulation and design of developmental programs in order for mass participation to occur, and
3. Thus, self-sufficiency entails involving the populace in the implementation and administration of development programs with the ultimate objective of enhancing the populace's social and economic well-being.

Given the circumstances described above, various governments in LDCs have taken a sectoral approach to regional development, focusing on various economic facets, in order to fulfill these three requirements. Tourism is a neglected part of the economy in many LDCs, especially in sub-Saharan Africa. Cole (1981) asserts that a nation's level of technology and its endowment of natural resources are among the factors that influence development. The potential for rapid socio-economic development, as well as the ability to generate foreign exchange, reduce unemployment, and raise people's standard of living, was not fully appreciated by many less developed nations.

As a result, the various characteristics of tourism resources and their adaptation as a strategy for regional planning are examined in this paper.

There are sections to the paper. The definition of tourism, as well as its potential and benefits, follow immediately after the introduction; The treasures for tourism development came next; ecotourism as a strategy for growing tourism; criteria for the growth

### **1.0 TOURISM: -DEFINITION, POTENTIALS AND BENEFITS**

The leisure industry, according to the definition, "operates within capabilities for regeneration and future productivity of natural resources," is referred to as tourism. recognizes the role that costumes, communities, and lifestyles play in the tourism experience; accept that these individuals must receive an equitable share of the tourism industry's economic benefits and be guided by the wishes of the host community As a result, the tourism environment consists of both physical and human components.

The physical part includes things like weather and climate, water, and natural plant and animal biodiversity; Even though the history, culture, and tradition of the people make up the human component, all of these things provide people with challenges and adventures.

Less Developed Countries (LDCs) in dire need of an alternative source of foreign exchange earnings have turned to tourism as an appealing and sustainable strategy for economic development. Tourism is the global net foreign exchange earner, second only to oil. It is the largest and second-largest employer of labor in the tertiary sector of the global economy, after agriculture. The transportation, manufacturing, food processing and packaging, construction, trade and commerce, and other ancillary services sectors are just a few of the many areas where tourism could have an impact on the economy. Because it is a commodity that is sold all over the world, it has a global market from which it gets its customers and no age limit for them.

Numerous advantages of tourism have been identified by the United Nations Environmental Programme (UNEP, 2000). Among these are the following:

- It engenders the development of public infrastructures (transport, electricity, water, and health),
- It engenders the generation of foreign exchange and income for the government and individuals,
- It engenders the generation of direct and indirect employment opportunities with greater multiplier effects,
- It encourages people to participate at all levels,
- It has the potential to increase public appreciation of the environment and to spread awareness of environmental problems when it

of eco-tourism; a few instances from Nigeria; Ecotourism treasures in Ethiopia's Amhara region and conclusion.

brings people into closer contact with nature.

- It contributes significantly to environmental protection, the conservation and restoration of biological diversity (including plant and animal species), and the sustainable use of natural resources. This confrontation may make people more aware of how important nature is and inspire environmentally conscious actions and behaviors to protect the fragile environment.

### **2.0 THE TREASURE FOR TOURISM DEVELOPMENT**

There is nothing on Earth that does not have one or more things that draw tourists there. The way tourist facilities are packaged for local and international consumption is what sets them apart. Despite the fact that there are resorts and recreation centers in cities, any nation's greatest tourist potential is found in its countryside. There are three types of tourism development treasure:

1. Geological or topographic features of particular interest, rare plants and animals, water bodies (oceans, seas, lakes, and waterfalls), ecological features that should be preserved, and areas with special scenic appeal are all examples of natural treasures.
2. Prehistoric sites (camps, artifacts, etc.), ancient monuments (precious stones, monoliths, historical buildings and ruins, and memorials), and features of industrial archaeological interest are examples of man-made treasures.
3. Places with historical, biographical, artistic, and literary treasures, as well as cultural, traditional, and lifestyle treasures, are allusive treasures.

All of these are part of the world's natural heritage. The majority of them are in the countryside and offer visitors from all over the world great challenges and adventures.

#### **2.1 The demand and uses of tourism facilities can also be grouped in to five as:**

1. the short-term vacationers' need for peace and quiet as well as mental and physical refreshment in nature. The stresses of modern life, which can be eased by tranquility, necessitate rest and recuperation in order to get away from the crowd, get back to sanity, and recharge in a quiet environment.
2. traveling to far-flung parts of the countryside to take in the unspoiled view of the natural

- environment and engaging in exercise to find contentment and relaxation.
- Engaging in permissible rural outdoor activities like hunting, shooting, fishing, sailing or canoeing, swimming, mountain climbing, etc. Most of these are sports in rural areas with both natural and artificial facilities on which people are willing to spend their leisure time and extra

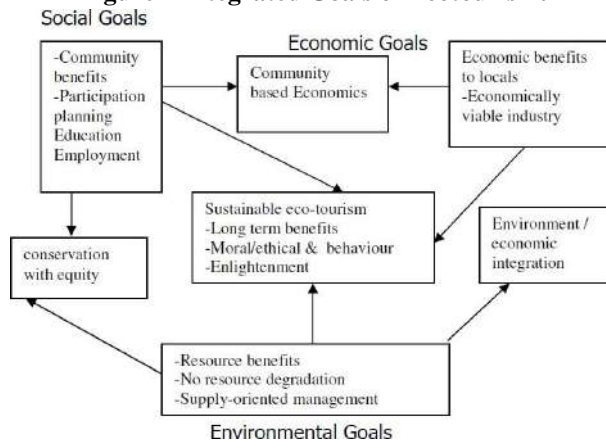
money.

- Educational use: tourist facilities serve as both a research tool and an object of study in and of themselves.
- The use of the countryside as a "second home," either permanently or for a short period of time, with country home cottages apart.

### 3.0 ECO-TOURISM AS AN APPROACH TO TOURISM DEVELOPMENT

The adaptation of tourism as a strategy in regional planning and development was given a new boost by the concept of "eco-tourism," which was developed a few decades ago. This had a noticeable multiplier effect. As shown in figure 1, eco-tourism is a holistic approach to tourism development because it incorporates the three fundamental development goals of economic goals, social goals, and environmental goals into its operations.

**Figure 1 Integrated Goals of Ecotourism.**



Ecotourism outlines management strategies and introduces the environment as a resource for tourism and recreation. Because of its connection to conservation, sustainability, and biological diversity, it is particularly intriguing. Ecotourism has the potential to advance the following three fundamental objectives as a development tool:

- Enhance the value of healthy ecosystems and strengthen public or private protected area management systems to preserve biological and cultural diversity.
- Create income, jobs, and business opportunities in eco-tourism and related business networks to support the sustainable use of biodiversity.
- Obtain the informed consent and full participation of indigenous communities and local communities in the planning and management of ecotourism businesses to fairly share the benefits of ecotourism developments. Ecotourism examines negative cultural and environmental impacts, outlines strategies for managing recreational pressures on the environment, and introduces new economies based on leisure resources.

### 4.0 ECO-TOURISM ENCOMPASSES THE FOLLOWING FIVE CRITERIA:

- Conservation:** Private reserves, native tree reforestation, or supporting established reserve areas are all examples of conservation practices. It is essential to understand that the purpose of a protected area is to preserve habitat for flora and fauna, allowing species to exist and thrive without human interference, despite the fact that protected areas are extremely appealing to tourists. It is best to make your visit to a protected area as minimally disruptive as possible.
- Green and low-impact efforts:** Ecotourism—also known as "green hotels" or "Ecotels"—follows ecofriendly management practices like water recycling, composting, and energy conservation.
- Sustainability:** A well-balanced lifestyle that can be easily maintained in the future is considered sustainable. This is especially critical when traveling to environmentally sensitive locations. Sustainable practices include building with local materials and techniques and growing food in organic gardens.
- Community Participation:** Community involvement is one of ecotourism's most crucial components. Whether or not the establishment is sensitive to its impact on the community and whether or not tourism is benefiting the region are two of the considerations taken into account.

Tourism must benefit the local culture and population. In an ideal world, the business would be owned by the community; however, in the event that this is not the case, the locals who work there should have jobs that aren't mundane. The community ought to reap the benefits of the resources it is willing to share with visitors.

#### 4.5 Interpretation and environmental education:

As a result of environmental education and interpretation, guests can return to the Eco-Facility with new recycling techniques or knowledge of the local culture. Clear and pertinent dissemination of information is critical. development).

While the idea of sustainable tourism varies from country to country, it is still a development strategy for tourism

. However, it does not limit the availability of natural capital or prevent visitors from enjoying the same experiences. Ecological, sociocultural, and economic sustainability capabilities are the three components that make up sustainable tourism. Ecological sustainability, according to Puczko (1998), ensures that the development is compatible with the site's environmental process, economic sustainability emphasizes continuous benefit for all generations, and socio-cultural sustainability ensures that tourism development preserves community identity. Therefore, eco-tourism is relevant to tourism advancements and falls under the umbrella of sustainable development. Traditional cultures and wilderness environments face pressure from population growth, resource exploitation, poor management, debt, and issues with recreation development (external development pressures) in many developing countries.

The environment has a limited capacity to withstand the effects of human activity without losing the characteristics that initially attracted tourists and recreationists to it.

#### CONCLUSION

Since the 1950s, academics and governments in various parts of the world have developed and implemented regional development strategies. Industrialization, mineral resource exploration, primary product exportation, and the

Education programs that assist the community in preserving their environment and growing as a whole are also very important.

#### 4.6 Growth of Sustainable Tourism

Tourism and recreation ought to be sustainable, just like other land and water resources. Linking ecological principles to economic processes to reduce environmental stress and meet the needs of the populace is necessary for the long-term integrity of ecosystems and preservation of the environment's regenerative capacity (sustainable

concentration of investments in major urban centers were some of these strategies. The degree and nature of the success or failure of various strategies varies from nation to nation.

#### REFERENCES:

- 1) Hirschmann, A.O.(1958) .The strategy of economic development. Yale university press.
- 2) Ishida L. (1999) "Eco-tourism through participatory action research : A case study of a community based project in Hugotulco, Mexico." Michigan State University, USA.
- 3) Adeyinka S.A. Ajala O.A. and Sanni L. (2002) Process of Rural Development: A Theoretical and Empirical Analysis of Alternative Methods- in Ibitoye O.A. (edit.) Rural Environment and sustainable Development in Nigeria. Pp 32-38
- 4) Kurian Joseph and R.Nagendran (2005) Essentials of Environmental Studies. Pearson Education, Singapore.
- 5) Lele U. (1979) The Design of Rural Development, Lessons from Africa. Baltimore Johns Hopkins University.
- 6) Renard Y. (2001) " Practical Strategies for Pro-Poor Tourism: A case study of the St. Lucia Heritage Tourism Programme" PPT Working Paper No. 7.

\*\*\*\*\*

I have completed My Bachelor's Degree in Arts in the year 1992, Bachelor of Physical Education in the year 1994, Master of Physical Education in the year 1994, Master of Philosophy in the year 1999 and I have completed by Ph. D. in the year 2008 I have been working in Vidya Bharati Mahavidyalaya since 1995 and I have published 9 Research Papers in Journal 3 Research Paper in Conferences and 1 book (Sharirik Swastha eva Yog Shiksha) from 2014-15 to 2019-20. I have been awarded with Best Program officer award in the year 1998, Virangana Savitribai Fule National Award in the year 2010 and Guru Gaurav Award in the year 2019.

Impact Factor-8.575 (SJIF)

ISSN-2278-9308

# *B.Aadhar*

Single Blind Peer-Reviewed & Refreed Indexed  
Multidisciplinary International Research Journal

FEBRUARY 2023

New Directions in Humanities



VOLUME -B



Chief Editor  
Prof. Virag S. Gawande  
Director  
Aadhar Social  
Research & Development  
Training Institute Amravati

Editor  
Dr. Pradnya S. Yenkar  
Principal,  
Vidya Bharati Mahavidyalaya,  
Camp, Amravati



This Journal is indexed in :

- Scientific Journal Impact Factor (SJIF)
- Cosmos Impact Factor (CIF)
- International Impact Factor Services (IIFS)

For Details Visit To : [www.aadharsocial.com](http://www.aadharsocial.com)

Aadhar PUBLICATIONS



# B.Aadhar

Single Blind Peer-Reviewed & Refereed Indexed

Multidisciplinary International Research Journal

**FEBRUARY 2023**

ISSUE No - 390 -B

**Sciences, Social Sciences, Commerce,  
Education, Language & Law**

**Prof. Virag.S.Gawande**

Chief Editor

Director

Aadhar Social Research &, Development Training Institute, Amravati.

**Dr. Pradnya S. Yenkar**

Editor

Principal,

Vidya Bharati Mahavidyalaya,

Camp, Amravati

**Aadhar International Publication**

For Details Visit To : [www.aadharsocial.com](http://www.aadharsocial.com)

© All rights reserved with the authors & publisher

**New challenges in psycho-physical health pandemic Stress****Dr. Dnyaneshwari S. Wankhade**

Director, Department of Physical Education

Vidya Bharati Mahavidyalaya, Amravati.

[dnyaneshwariingle18@gmail.com](mailto:dnyaneshwariingle18@gmail.com) Mob. No. 9359220717**ABSTRACT:-**

The COVID-19 pandemic has caused young people to experience stress like never before. There have been no systematic efforts to measure this, despite recent speculation that young people in India have had worse mental health since the pandemic began. In addition to reporting on the effects that the corona virus has had on the lives of Indian adolescents, we also identify subgroups of young people who may be particularly susceptible to negative emotions. Three hundred and ten young people from North India (51 percent of who were male and between the ages of 12 and 18) shared their personal experiences with the corona virus, as well as their top concerns, social restrictions, and levels of negative affect and anhedonia. The majority of respondents agreed that COVID-19 had a moderate to severe impact on their academic, social, and professional lives, despite not having any personal experience with the virus or knowing anyone who did. These effects, in turn, have a negative effect. Academic achievement, social and recreational activities, and physical health were the top concerns of the participants. Males were more concerned about social and recreational activities, while females were more concerned about academic achievement and physical health. As a result, adolescents in India report that the pandemic has had a significant impact on many aspects of their lives, particularly their academic performance, social and recreational activities, and physical health. Digital education and medical care must be made available and accessible as a result of these findings.

**Keywords:** *Psycho-Physical, health pandemic Stress, COVID-19 pandemic***Introduction :**

The COVID-19 pandemic has had far-reaching effects not only on individuals' physical and mental health but also on the health of economies around the world. As emotional symptoms in adolescence can become associated with many serious mental health outcomes including suicide, long-term physical health consequences, and significant healthcare burden, the effect of COVID-19 on young people's mental health could be more damaging in the long run than the infection itself. Therefore, measuring early signs of mental health challenges such as worries and negative emotions in young people is an urgent priority for researchers as well as policymakers, including identifying those who are most susceptible to mental health difficulties. Young people may be less susceptible to severe forms. Even though countries with high and low incomes need this information, those with fewer resources dedicated to mental health may gain more from early forecasts of these needs.

With over 2.5 million confirmed cases and an increasing death toll, India has one of the highest COVID-19 infection rates in the world. The first case of the disease was found on January 30, 2020, in Kerala, in a student who had recently returned from Wuhan, China. However, the spread of the disease has increased since March 2020. In response, the government put in place a nationwide lockdown to stop the infection from spreading to other communities. Based on the total number of COVID-19 cases in that region, all educational and training institutions in India have been closed, despite some regional differences in the extent of lockdown restrictions; restaurants and lodgings; cinemas, sports centers, malls; and religious institutions. Patra and Patro's most recent correspondence article emphasized the urgent need to address mental health issues among Indian adolescents and speculated that school closures in particular may have been particularly detrimental to young people. To our knowledge, however, no such coordinated efforts have been made. New information from a small group of Indian youth is presented here. We talk about how they felt about the COVID-19 pandemic and how it affected their day-to-day lives. Along with quantitative measures of current negative and (absence of) positive emotions—symptom-markers of common mental health issues like anxiety and depression—we describe the content of the most common concerns that young people report. Then, we look at young people's gender, age, and socioeconomic status to determine which ones are more likely to report more negative emotions and fewer positive ones. Our data can thus point out emerging, potentially costly





mental health issues following the pandemic in India, where public awareness of mental health issues affecting young people had been rising prior to the outbreak.

For children to reach developmental milestones, good mental health is just as important as good physical health. It enhances children's social and emotional well-being. In addition, children who are mentally healthy are more likely to have happy and successful lives and to perform well at home, in school, and in their communities. On the other hand, having poor mental health as a child can have a significant impact on how children learn, act, or handle their emotions. The COVID-19 pandemic brought a diverse set of difficulties that affected everyone's mental health, including children and adolescents. The mental health of children has been negatively impacted by grief, fear, uncertainty, social isolation, an increase in screen time, and parental exhaustion. Children benefit greatly from the stability provided by friendships and family support, but the COVID-19 pandemic has also disrupted these relationships.

#### Method

##### Participants and General Procedures

The Institutional Ethics Committee of the Institute of Medical Sciences at Banaras Hindu University gave their blessing to this study (Ref No.: Dean/2020/EC/1975) and the Research Ethics Committee at King's College London (Ref: HR-19/20-18250). Between the dates of June 5, 2020 and July 12, 2020, participants were sought out. By disseminating information about the study, including the eligibility criteria (aged 12–18 years; New Delhi, West Bengal, Madhya Pradesh, and Gujrat), prospective participants and their parents were identified. Currently residing in India) via Face book and WhatsApp and other social media platforms. Information sheets in two languages—Hindi and English—were sent to interested and eligible participants—one for young people and one for parents of participants aged 12 to 17 years. After reading the information sheet, those who agreed to participate received a link to the survey in both English and Hindi, and they were asked to choose which version to complete. The age of the participants was the first question in the survey link. If the participant was over the age of 18, they read and signed a consent form that included their contact information for future assessments and an electronic signature. An assent form and a consent form for parents or guardians were provided to any participant between the ages of 12 and 17. Using the provided contact information, a follow-up phone call was made to the parent or guardian to confirm the authenticity of the consents. For consent/assent forms that were not completed, additional survey questions were not presented.

The software called Qualtrics (Qualtrics, Provo, UT) was used to create the online survey. The demographics, personal experiences and knowledge of others who had been infected with the corona virus, extent of social restrictions and social contact, and the impact of the viral outbreak on various life domains were the topics covered in the first third of the survey. Measures of poor mental health included negative affect, anhedonia (absence of positive affect), and the nature of worries in the second third of the survey. Measures of well-being (positive aspects of mental health), more specific negative emotional experiences (such as loneliness and boredom), and a cognitive measure (positive and negative future imagery) were included in the final third. The translation-back translation approach was utilized in all Hindi translations. The initial set of translations, which were completed by MS and back translated by TS. The back-translations were checked by JL. MS retranslated where there were definitional inconsistencies with the original scale. RP and VK discussed these in detail. The survey was completed by participants in 20 minutes on average.

##### Personal Experiences of and Knowledge of Close Others With COVID-19

The extent to which participants had been infected was assessed using five yes/no responses: Do you currently have a confirmed diagnosis of corona virus infection, are you currently suspected of having a diagnosis of corona virus infection, have you had a past confirmed diagnosis of corona virus infection but have now recovered, have you had a past suspected diagnosis of corona virus infection but have now recovered? Have you ever been affected or suspected of having the corona virus infection at any time? Participants' knowledge of others who had contracted the infection was assessed using five yes/no responses: a relative, friend, another acquaintance (such as a classmate), or another person who is known indirectly (such as an acquaintance of a relative, friend, or acquaintance) but does not know anyone who is afflicted with the disease. If one of the first four items was agreed upon, participants were asked whether the affected person had recovered, was still recovering, was in the hospital, or had passed away

**Social Restrictions Associated With COVID-19**

Participants indicated the total number of days they spent in self-isolation (i.e., not leaving the house), the number of days they spent 15 minutes or more outside the house, the number of days they had face-to-face contact with another person for 15 minutes or more, and the number of days they had a phone or video call with another person for 15 minutes or more to describe the extent of reduced social contact.

**Impact of COVID-19**

Mitigating the global COVID-19 pandemic threat is essential for human life and reducing livelihood distortion. More than 200 countries have been affected by the COVID-19 pandemic, which has resulted in a significant number of confirmed cases and deaths, public panic, and mental health stress (Huang & Zhao, 2020). To break the transmission chain, most nations have implemented complete lockdowns with stringent social distancing measures. The global health and mental health are severely impacted by the current COVID-19 outbreak. Additional global strategies are required to address the related mental health issues, despite the use of all available resources to stop the virus from spreading (Torales et al., 2020). It is essential that public mental health paradigms and measures are used to protect people and prevent the spread of this outbreak. On January 30, 2020, India reported the first case of COVID-19, and the numbers have risen steadily since then, albeit at an alarming rate in the final days of March. These health problems include stress, anxiety, depressive symptoms, insomnia, denial, anger, and fear worldwide. The world's largest democracy has imposed the world's largest nationwide lockdown since March 24, 2020, with the goal of limiting community transmission. The country remains vulnerable to COVID-19 due to its high population density, socioeconomic fabric, and overstretched health care infrastructure.

The only immediate, ideal, and best way to control the COVID-19 pandemic in India was a total lockdown. At multiple levels, the Indian government has responded appropriately, appropriately, and quickly to the COVID-19 pandemic. India has been able to buy crucial time with the lockdown: time for extensive contact tracing, time to increase testing, and most importantly, time to prepare our health system so that it doesn't become overwhelmed like it did in Italy, the United States, and Spain. The lockdown is a good way to stop the infection from spreading. However, this is extremely difficult, and it is even more difficult for larger segments of society. In India, social isolation is extremely challenging for many households, particularly in slum areas; The family must be supported by the daily wage earner, and individuals with mental health conditions face severe challenges. For vulnerable populations, a prolonged lockdown may result in psychosocial difficulties, stress, anxiety, frustration, boredom, depression, and even suicidal thoughts and attempts. In addition, the mental health requirements of vulnerable groups, such as those with severe mental illness, learning difficulties, and neurodevelopment disorders, as well as socially excluded groups like prisoners, the homeless, and refugees, were brought to the attention of The Lancet Psychiatry (2020). Despite the fact that it may pose a challenge to patients, the general public, policymakers, and health organizations and teams, the infection's burden on global mental health is currently ignored. Lockdown was a difficult measure for the less fortunate in India due to health inequalities, widening economic and social disparities, and distinct cultural values. The nationwide lockdown has increased economic losses, rendered the country's large number of daily wage earners and migrant laborers helpless, and developed into a significant mental health issue. The nation's vulnerable population may be isolated and stigmatized as a result of the emerging mental health issues brought on by this global event.

**Mental Health Infrastructure and Challenges Ahead**

Common mental disorders affect 10% of the population in India, while severe mental disorders affect 1.9% of the population. Mental illnesses like schizophrenia, bipolar affective disorder (BPAD), depression, anxiety disorders, psychoses, phobias, suicidal ideation, mood disorders, neurotic or stress-related disorders, post-traumatic stress disorder, marital disharmony, sleep disorders, alcohol dependence, substance abuse, and dementia are becoming more common in the general population. The main problems the Indian mental health system has to deal with are a lack of knowledge about mental illnesses and a lack of mental health services that are sufficient. The inadequacy exists in both areas, such as infrastructure and human resources. India devotes significantly less than many other nations' annual health budgets to mental health. In their examination of the Indian mental health system, Mahajan et al. came to the conclusion that effective information, education, and communication (IEC) efforts are necessary for effective utilization of health care. They did, however, point out that IEC activities were not population-centric, targeted at local circumstances, uniform in coverage, highly



visible, or ongoing over time; rather, they were merely limited to the preparation of posters and the distribution of pamphlets. Stigma is observed as a result of a lack of awareness, which results in inadequate utilization of the available services and problems that continue to escalate. Effective community involvement in the prevention and promotion of mental health among populations is required. In light of the current COVID-19 situation, in which communities may experience serious mental health issues, the nation's task will be difficult given the obstacles it faces.

#### **Solutions against COVID-19**

Pandemic while discussing the factors that contributed to the problem, it may be possible to immediately discuss the factors that protected the population's mental health. Due to the virus's spread, physical health is a top priority right now, so secondary issues and concerns must be monitored and prevention must be implemented at the individual, family, and community levels. Galea and others (2020) offered three primary preventative measures for improved mental health in populations: planning for loneliness, having ways to monitor, report, and help people who are at risk of abuse, and last but not least, strengthening the mental health system and getting ready for the challenges that COVID-19 has brought with it. In order to help people around the world maintain mental health during this unprecedented global health crisis, the WHO (2020b) has also shared strategies. In summary, it urges people to engage in routine activities, remain calm, indulge in hobbies, maintain social media connections, talk to friends or counselors if they experience unmanaged anxiety or fear, exercise, and avoid using drugs or alcohol to deal with emotional issues.

Additionally, at the national level, government agencies are directing institutions to operate dedicated psychosocial and mental health help lines in order to resolve any issues that individuals may be experiencing during the lockdowns. Numerous of these help lines are now operational and accessible through the country's top educational institutions. Active citizen groups, civil society organizations, and government agencies are disseminating the positive messages on social media to raise awareness and share methods for monitoring individuals' mental health. India is a land of spirituality and yoga; it carries a significant legacy of traditional mindfulness and meditative practices. It has been demonstrated that such practices can lessen mental anguish. Incorporating meditation into our daily routine can be extremely beneficial for improving our mental and physical health.

While treatment-needy individuals should have access to sufficient services, prevention and promotion should also be prioritized. People with mental illnesses need follow-up sessions because the situation might make their illness worse and they might need counseling and monitoring all the time. Along with curricular resources, educational institutions must reach out to their students to offer guidance and support for maintaining composure during this crisis. Through effective messages and media awareness campaigns, the community must awaken its collective conscience toward the economically disadvantaged, disabled, elderly, or anyone else they know would require physical or mental support.

In this crisis, the victorious Corona Warriors have emerged as highly sought-after and significant healthcare human resources. They have worked extremely hard and put their own lives at risk while treating corona virus patients in an extremely stressful environment. Police, providers of essential services, and government officials who are confronting the challenge are also important frontline workers. Instead of stigmatizing them, governments and communities must show compassion for them and praise their efforts, dedication, and diligence. Because of their unwavering courage and dedication to service, they require physical, mental, legal, and financial protection. In conclusion, the current global pandemic requires a multifaceted strategy for providing healthcare. It requires a holistic delivery model that takes into account the patients' and communities' multifaceted physical, mental, social, and spiritual health. To incorporate these aspects of health care delivery, the public health systems must be strengthened by making their workforce more responsive and prepared to handle the pandemic's burden. The most vulnerable groups and populations may have uninterrupted access to essential services organized and provided by the governments.

#### **Statistical Analyses**

Independent sample t-tests were used to examine gender differences in age and income following the presentation of the sample's demographics. The next section provided descriptions of the young people's personal experiences with the infection, their knowledge of others who were infected, the impact of the lockdown on social isolation and contact with others, and other life domains. The data were examined to see if they satisfied the normality assumptions prior to any statistical analysis (23).



With the exception of a slight positive skew for anhedonia, the histogram plots revealed no significant deviations from normality in the data. The data's skewness and kurtosis values were also within the acceptable range of 2 (24, 25), with the exception of anhedonia, which was greater than 1. With the exception of anhedonia, which was investigated using non-parametric tests, we therefore utilized parametric analyses for all of the variables. Using an independent samples t-test and bivariate correlations, we examined how gender, age, and family income levels affected the overall impact of COVID-19 across life domains. For each of the top three worries (first, second, and third), the percentage of people who agreed with each worry category was calculated for the data on worries. However, in the end, we collapsed all three of the participants' top three concerns to generate an overall percentage of participants who endorsed that concern as one of their top three concerns. This meant, for instance, that each participant was only represented once if they rated the same concern across all three of their top concerns. The final percentage of young people who agreed with the worry categories was compared by gender and categorical age group for interpretability (younger adolescents = 12–15 years; older adolescents (defined as those aged 16 to 18) In conclusion, we presented data on negative affect and anhedonia, or the absence of positive affect; Using multiple linear regression models, we examined how these variables varied by gender, age, and per capita monthly income: We also looked into whether interaction terms significantly increased variance explanation. During the regression analysis, we log-transformed this variable due to anhedonia's slight positive skew. We also ran a series of parametric and non-parametric t-tests and correlations for negative affect and anhedonia, respectively, to determine the extent to which gender, age, and family income levels were individually associated with these variables. This was done in addition to the multiple regression analysis of demographic predictors and their interactions. The degree to which negative affect and anhedonia were associated with the overall impact of COVID-19 was also evaluated using correlations.

#### Discussion

This paper provides a description of the baseline data for a group of Indian adolescents who were recruited into a study that aimed to examine the long-term effects of COVID-19 on anxious thoughts, negative emotions, and emotional management strategies. During the period of (baseline) data collection, participants were recruited when the total number of corona virus-infected individuals in India was 236,184. However, even during this period of rising infections, personal experiences and knowledge of others who had been exposed to the corona virus infection were uncommon for the majority of our participants. However, participants reported moderate to severe COVID-19 effects. Academic studies were highlighted as a prominent area of concern for the majority of young people in this cohort, a likely result of social distancing measures preventing school attendance and educational progress, according to the impact data and qualitative data on their top concerns. The absence of age-typical social and recreational activities, as well as concerns regarding the health and safety of oneself and loved ones, were also prominent concerns for young people. Again, these concerns were anticipated to arise as a result of the pandemic itself and the lockdown measures that were associated with it. Interestingly, young people frequently expressed concerns regarding their own finances, the Indian and global economies, and society as a whole. Adolescence is a time of emerging independence (taking on more responsibilities for their own future) but also of interdependence, where self-construal becomes linked to roles and commitments to other groups in society. Identifying the content of these stressors and worries can help governments decide where to propose subsequent policy changes and facilitate society-wide measures. A significantly higher percentage of older adolescents (16–18 years) than younger adolescents (12–15 years) were worried about their academics, physical health and safety, global and societal concerns Our data specifically highlight the need to invest resources into the safe opening of schools, changes to the curriculum, and/or the provision of digital education to all young people, in addition to the requirement for dedicated mental health services (help lines, centers) outlined in earlier papers. A second priority is reassurance regarding access to high-quality medical care. Gender differences were present in these effects and concerns. Males reported a greater impact of COVID-19 on physical health in quantitative ratings; however, this gender difference was not replicated in the quantitative impact ratings. Indian adolescent females have been reported to be "more sincere" toward studies than Indian adolescent males, possibly indicating that they are more committed and motivated to academic achievement. Male adolescents in India are more likely than female adolescents to participate in outdoor sports and face fewer sociocultural barriers to outdoor physical activity. This difference between the sexes, in which men spent more time out of the house than women did, may also



have been caused by the fact that men prioritized social and recreational activities; Females, on the other hand, reported spending more time alone, on phone or video calls, and following COVID restrictions. Perhaps relatedly, female participants were more concerned than male participants about their physical fitness, health, and the risk of contracting the virus. The lockdown may lead to sedentary lifestyles, which can have a significant impact not only on the mental health of adolescents but also on childhood obesity. The participants' socio-economic status (SES), as measured by the family's monthly per capita income also revealed some interesting trends. COVID had a greater impact across all life domains, but particularly on family and physical health, when SES was lower. Participants with lower SES were more likely to spend more time away from home, which may explain the reported negative impact on physical health. In addition to experiencing parental stress as a result of the economic crisis, adolescents with lower SES may be forced to navigate more complicated family dynamics in crowded living situations. The fact that participants with higher SES have greater access to laptops, smart phones, and/or tablets than those with lower SES is likely the reason why participants with higher SES were found to spend more time on phone and video calls on a daily basis.

Self-reported negative affect did not correlate with age, SES, or gender, but it was greater among those who reported more impact of COVID-19 across life domains. The means reported in our sample using translated versions of standardized questionnaires were comparable to those reported in general youth population samples in the west. Anhedonia was more common in men and people with lower SES. If we examine these results over a longer period of time, we may be able to identify individuals who exhibit a tendency toward anxiety or depression over time, thereby indicating a need for mental health services. Even though there was a weak link between anhedonia and how COVID-19 affected the participants' study and social lives, the link was not strong. There are a few limitations to the study. First, the sample was obtained through social media-based convenience sampling, and respondents came only from a few North Indian states. As a result, it's hard to say how representative it is of Indian adolescents between the ages of 12 and 18. In addition, the study sample composition was skewed due to the survey requirements requiring only Internet access and a registered phone number (to verify parental consent). However, the sample reflected the entire continuum of SES classes in India using the Modified BG Prasad Socio-economic Classification 2019, despite some missing data. According to this, SES classes appeared to be adequately represented. Second, because the data were collected online, qualitative responses were not probed, and singleword responses frequently required coding, affecting the data's reliability. Nonetheless, this coding scheme produced high inter-rater reliability. Thirdly, because participants did not specify whether they resided in urban or rural areas of their respective cities, our data cannot address differences in adolescents' worries, positive and negative emotions, between urban and rural areas. The impact of rural and urban populations on these indices of poor mental health should be measured and compared in subsequent research. Last but not least, many of the scales used were not uniform. However, this study adds potential new measures for future studies of young people in the Indian context because internal consistency was acceptable.

#### Conclusion:-

All of our participants reported a significant impact of the pandemic on various aspects of their lives, which was linked to higher negative affectivity, despite the fact that a small number of them had personal experiences with the COVID-19 pandemic or knew someone who had been infected with the virus. This was the finding of our study. With some gender differences, adolescents also expressed concerns regarding their studies, physical health and safety, as well as social and recreational activities. Despite the fact that our findings do not demonstrate a causal relationship between the effects of these COVID19-related changes on anxiety, negative affect, and anhedonia, they emphasize the urgent need for government policymakers to take concrete steps to mitigate the potential negative effects of the pandemic on Indian adolescents' mental health. Due to their diverse sociodemographic backgrounds, a variety of healthcare workers are experiencing mental health issues. Policies and tailored and personalized care may assist in alleviating their issues. The psychological distress experienced by these frontline workers during and after the ongoing pandemic crisis merits additional study.



**References:**

- ❖ CDC (11 February 2020). "Corona virus Disease 2019 (COVID-19)". Centers for Disease Control and Prevention
- ❖ Stix G. "Pandemic Year 1 Saw a Dramatic Global Rise in Anxiety and Depression". Scientific American.
- ❖ Luo Y, Chua CR, Xiong Z, Ho RC, Ho CS (23 November 2020). "A Systematic Review of the Impact of Viral Respiratory Epidemics on Mental Health: An Implication on the Corona virus Disease 2019 Pandemic"
- ❖ Santomauro DF, Herrera AM, Shadid J, Zheng P, Ashbaugh C, Pigott DM, et al. (November 2021). "
- ❖ "COVID-19: Depression, anxiety soared 25 per cent in a year"
- ❖ "Nearly one billion people have a mental disorder: WHO".
- ❖ Jemberie WB, Stewart Williams J, Eriksson M, Grönlund AS, Ng N, Blom Nilsson M, et al. (21 July 2020). "
- ❖ Larsen J (29 November 2021). "7 Remote Working from Home Techniques To Protect Mental Health".
- ❖ Labrague LJ (October 2021). "Pandemic fatigue and clinical nurses' mental health, sleep quality and job contentment during the covid-19 pandemic:

Impact Factor-8.632 (SJIF)

ISSN-2278-9308

# *B.Aadhar*

Single Blind Peer-Reviewed & Refereed Indexed

Multidisciplinary International Research Journal

**March-2023**

ISSUE No - (CCCXCVIII) 398 (A)

**A Journey of Indian women**



**Chief Editor**

**Prof. Virag S. Gawande**

**Director**

Aadhar Social  
Research & Development  
Training Institute Amravati

**Editor**

**Dr.V.R.Kodape**

**Principal**

Shri Kisanlal Nathmal Goenka Arts & Com,  
College Karanja (LAD) Dist. Washim

**The Journal is indexed in:**

**Scientific Journal Impact Factor (SJIF)**

**Cosmos Impact Factor (CIF)**

**International Impact Factor Services (IIFS)**

For Details Visit To : [www.aadharsocial.com](http://www.aadharsocial.com)

**Aadhar PUBLICATIONS**



Impact Factor – (SJIF) –8.632

ISSN – 2278-9308

# B.Aadhar

**Single Blind Peer-Reviewed & Refereed Indexed**

**Multidisciplinary International Research Journal**

**March- 2023**

ISSUE No - 398 -A

## A Journey of Indian women

**Prof. Virag.S.Gawande**

Chief Editor

Director

Aadhar Social Research &, Development Training Institute, Amravati.

**Dr.V.R.Kodape**

Editor,

Principal,

Shri Kisanlal Nathmal Goenka Arts & Com,  
College Karanja (LAD) Dist. Washim

**Aadhar International Publication**

For Details Visit To : [www.aadharsocial.com](http://www.aadharsocial.com)

© All rights reserved with the authors & publisher





23	Women And Atmanirbar Bharat	<b>Dr. Vandana K. Mishra</b>	73
24	Improved Overall Health Of Women Through Sports	<b>Gajanan V. Patil</b>	78
25	Significance Of Nutrients: Women's Health And Wellness	<b>Dr. Kamini M. Mamarde</b>	81
26	A Study of Social Reforms of Indian Women's	<b>Dr. N.M.Gutte</b>	84
27	Women And Sports	<b>Dr. Dnyaneshwari S. Wankhade</b>	87
28	Women sports activities participation in India	<b>Ulhas V. Bramhe</b>	92
29	Socio- Psychological Aspects Of Women Athlete For Less Participation In Sports	<b>Dr. Savita M. Kene</b>	94
30	Issues of Otherness and Displacement in Manju Kapur's 'The Immigrant'	<b>Dr. Bharati S. Patnaik</b>	98
31	Women and Domestic violence in India	<b>Dr. Shantarm Chavan</b>	101
32	Ladies Coupe" As A Voice Of Suffering Women	<b>Dr.Varsha E. Gawande</b>	105
33	Women and sports	<b>Dr Jayawant Mane</b>	107
34	The Indian Women Writers and their Contributions to Indian Literature	<b>Porf.O.S.Pawar</b>	110
35	Women In Vedic Period	<b>Dr. Pradip P. Yeole</b>	112
36	A Comparative study of Attitude about Life Skill of Household workers and Factory Workers Working in Unorganised Sector for Women Empowerment.	<b>Snehal A. Ganar , Dr. S. S. Satturwar</b>	113
37	Impact of Social Media on Woman	<b>Ku.J.M.Bhagat</b>	116
38	Women's Health Issue and Government Schemes in Kolam Tribe (Special Reference to Yavatmal District)	<b>Rutvika Deepak Koturwar</b>	119
39	Comparative study of Mental Health between Morning Walker and Yoga Practitioner Women's of Amravati	<b>Dr. Pushpalata M Deshmukh</b>	121
40	Empowering Women through Education	<b>Julie Kukreja</b>	124
41	Women & Sports - A New Vistas	<b>Dr. Alka Karanwal</b>	127
42	The Role Of Woman In Indian Economy And Across The World	<b>Abhinav Raosaheb Pundkar</b>	129
43	Women's Participation In Sports And Leadership In India	<b>Akshay S. Gohad</b>	132
44	Marginalization of Women in Githa Hariharan's The Thousand Faces of Night	<b>Dr. Ajay R. Patalbansi</b>	136
45	Depiction of Pathetic Images of Women in The Select Novelof Mulk Raj Anand.	<b>Mangesh N. Wankhade ,Prof. Dr.Ashalata M.V.P. Raman</b>	139



## Women And Sports

**Dr. Dnyaneshwari S. Wankhade**

Director, Department of Physical Education Vidya Bharati Mahavidyalaya, Amravati.

dnyaneshwariingle18@gmail.com

### ABSTRACT:

Women's sports, according to many sports fans, are less interesting than men's sports. Moreover, women's sports are less frequently covered in the media than men's sports. Therefore, by not covering women's sports as much, could the media be giving the impression to sports fans that they are less desirable? An intervention was created with the help of Agenda-Setting Theory, Framing Theory, and the Mere Exposure Effect to promote women's sports to sports fans. Over the course of four weeks, half of the participants watched highlight films of women's sports. After three weeks, the intervention decreased prejudice against female athletes but did not affect interest in women's sports. Instead of using highlight videos, participants should be immersed in live women's sports action in future studies.

In the sport industry, the statement "women are the weaker sex" is not accurate. Women, like men, have the ability to be competitive and aggressive without sacrificing their inherent beauty and charm. Women's sports participation is, after all, a worthwhile objective. The perception of women's sports participation and its correlation with the type and degree of participation are the focus of this study. It also determined the moderating variables' contributing factors, such as; the family's income, educational attainment, and institutional setting of the father and mother. The study was carried out on the 973 female Physical Education students from the three institutions who were selected at random; Marawi City, Mindanao State University; Iligan City's Mindanao State University-Iligan Institute of Technology; and Capitol University in the city of Cagayan de Oro. The Perception on Women's Sports Participation Inventory (PWSPI) served as the primary instrument for data collection in the descriptive-correlation method of the study. According to the findings, there was a significant correlation between the perception of women's sports participation and the variables of father and mother's educational attainment and family income, but there was no significant correlation between the variables and the location of the institution. In addition, a significant correlation was found between the father's and mother's educational attainment and the institution's location with regard to the sports participation type variable. However, there was no significant relationship found between the type of sports played and family income. It was also discovered that there was no significant correlation between the level of sports participation and the mother's educational attainment, family income, or institutional location. However, a significant correlation was found between father's level of sports participation and educational attainment. It was discovered that perceptions of women's sports participation were significantly correlated with the type and level of participation. Further, it was concluded that the positive perception of women's sports participation was significantly influenced by the variables' relationships.

**KEY WORDS :** *Gender, perception, sports participation type and level.*

### INTRODUCTION :

Sports participation has largely been male-dominated in most societies. However, advocates for women in sports have demonstrated over the past few decades that women are also competent and deserve a place in the sporting world. Sportswomen have taken their sports experiences to heart ever since the first female ball player circled the bases at Vassar College in 1866 (Sandoz & Winans, 1999). Indeed, even areas of strength for without of accomplishments ladies needed to demonstrate that they were capable in sports. Nowadays, a lot of women participate in sports that aren't just considered "minor" but also "major" in terms of skill and ability.



The modern Olympic Games' gradual but persistent expansion of women's events is the best indicator of the development of women's sports (Bennette, Howell, and Simri, 1983). Women, on the other hand, faced a lot of opposition when they first tried to enter sportsworld. According to Lutter & Jaffee (1996), the acceptance of women in sports has not progressed steadily over time; rather, it has experienced numerous peaks and valleys, including periods in which female sports figures were portrayed as more popular heroines and periods in which women were regarded as unfit mothers. According to Klafs & Lyon (1978), the sentimental thesis that women are delicate in nature and dainty in appearance has been the foundation for the majority of subjective goals aimed at encouraging women to participate in sports over the years. It is also related to the Victorian ideal of femininity, which discouraged women from participating in vigorous sports because it was believed that doing so could compromise a woman's modesty, put her emotional control in jeopardy, and cause injury that could impede or prevent childbearing and mate conflict (Eitzer & Sage, 1978). When it comes to sports, women are an exceptional group. Unfortunately, sport has always been seen as a male activity, and women's access to sports has been seen as unusual to the point where it is discouraged and, in some cases, illegal (Coakley, 2001). The real reason why women's active participation in sports received so much attention was the fear of losing one's femininity. Miller & Levy (1996) also came to the conclusion that "sports participation by women routinely carries a negative stigma" because traditional sports images are viewed as incompatible with traditional female roles (Goldberg & Chandler, 1991). Because society is still more comfortable with women who participate in sports that emphasize traditional feminine characteristics like grace and beauty, Nixon, Maresca, and Silverman (1979) state that women athletes have been hypothesized to experience gender role conflict, particularly if they participate in sports that are traditionally regarded as being more masculine. Therefore, it is proposed that the dissonance caused by the women athletes' need to identify with two roles is the source of gender role conflict: the athletic role for girls and women, which is undervalued and even stigmatized (Adler, Kless, 1992). According to Hall (1996), the real reason why an athlete's femininity received so much attention was the fear that she might be a lesbian. She went on to say that sports researchers were quick to pick up on this idea, and their studies typically revealed that female athletes were more androgynous, more masculine, or less of a sex type. On the other hand, the study by Metheny (1965) provides a positive perception of women athletes, indicating that they are respected and viewed as feminine by men and women, athletes and non-athletes alike, despite the existence of negative stereotypes regarding the femininity of women athletes.



In addition, according to Fasting (1996), the global women's movement has emphasized that women are better human beings when they develop their intellectual and physical abilities over the past thirty years. Women of all ages have been inspired to pursue their passions for sports by this idea, which has also sparked new interests in people who would never have considered playing sports in the past. Coakley (2001) went on to say that the women's movement helped women rethink their roles in the workplace and at home, which has given more women the time and resources they need to play sports. More women are choosing to participate in sports as a result of the waning of male dominance over women's lives and bodies and the growing acceptance of the feminist ideals. The importance of determining other impressions and perceptions regarding women's sports participation has been underscored by these and other issues. As a result, the students' perceptions of women's sports participation may be influenced by their past and current participation in sports and physical activities.

#### **PURPOSE OF THE STUDY**

The study's objective is to ascertain how the 973 randomly selected female Physical Education students at the three institutions feel about women's sports participation; Marawi City, Mindanao State University; Iligan City's Mindanao State University-Iligan Institute of Technology; and Capitol University in the city of Cagayan de Oro. In addition, it sought to ascertain the relationships between the dependent variables of sports participation type and degree and the moderating variables of father and mother's educational attainment, family income, and institutional location.

This study aims to increase women's participation and involvement in sports management, administration, and leadership in addition to playing sports. The study is also important for women in developing and promoting more sports programs that will improve positive perceptions and influence those who have a fair perception of women's sports participation. Women should also be made aware of the health benefits, healthy lifestyle, and social benefits of sports in order to encourage them to participate.

Additionally, this study's findings provide coaches, administrators, trainers, and sports program organizers with empirically based information that can be used to expand opportunities for women to participate in sports. Finally, it will serve as a foundation for subsequent studies on women in sports.

#### **METHODOLOGY**

##### **Research Design**

A descriptive–correlation type of research design was utilized in this particular study to ascertain the respondents' perceptions of women's sports participation. The objective was to ascertain the connection between the dependent variables of type and degree of sports participation and the independent variable of perception regarding sports participation. It also sought to determine whether the independent and dependent variables are affected by the selected moderating variables of parents' educational attainment, family income, and institutional location. A questionnaire designed by the researcher on women's perceptions of sports participation was used to collect and evaluate the data.

##### **Samples and Sampling Procedures**

The female Physical Education 1 to 4 students from the three universities were the subjects of the study: Capitol University (CU) in Cagayan de Oro City, Mindanao State University–Main Campus (MSU–Main) in Marawi City, Mindanao State University–Iligan Institute of Technology (MSU–IIT) in



Iligan City, and Mindanao State University Using the stratified random sampling method, the following distribution was used to determine the number of respondents from each university: MSU-Marawi, 484; 307 MSU-IIT; and CU, 182 out of 973 total samples.

### **Instrumentation**

The review utilized a specialist mentioned survey created in light of objective facts, interviews, writing survey and with the assistance of specialists. There are two main parts to the questionnaire: the respondents' demographic profile, which includes the following: location of the institution, parents' educational attainment, family income, sports participation type and degree. The primary instrument used to determine respondents' perceptions of women's sports participation is the Perception on Women's Sports Participation Inventory (PWSPI) in the second section. It has fifteen (15) questions, including both positive and negative ones; Depending on respondents' perceptions of women's active involvement and participation in sports, both have five options to choose from. The research adviser and a few experts verified the questionnaire that the researcher created. With a reliability of .703, it was pilot tested at the Princess Lawan Bae Hall Dormitory with 50 selected tenants.

### **RESULTS AND DISCUSSION**

The five categories of the respondents' parents' educational attainment were shown in the data. Both the father and mother had high percentages of 46.8% and 49.7%, respectively, of respondents who were able to graduate from college. The respondents' awareness of the significance of sports and other related physical activities was significantly influenced by the parents' intellectual capacity. The responses ranged from "Below P10,000.00" to "Above P15,000.00" in terms of the family's monthly income. 360 of the 973 respondents have a monthly family income between P10,000 and P15,000, while 375 of the respondents have a monthly family income below P10,000.00. Only 238 respondents reported earning more than P15,000.00 per month as a family. With a frequency distribution of 486, the majority of respondents belonged to MSU-Marawi. With a percentage of 54.4 percent (529), the majority of respondents participate in individual and dual sports, while 43.4 percent (422) participate in team sports. 22 respondents indicated that they had not played at all. The majority of the respondents, 620, participate in sports occasionally, while 20.6% (200) do so regularly and 15.7% (153) do not participate at all. The findings revealed that 919 out of 973 respondents perceive female sports participation as "positive" or "strongly positive."

There was a significant correlation between father and mother's educational attainment and family income and perceptions of sports participation, but there was no significant correlation between institutional location and perceptions of sports participation. The father and mother's educational attainment, institutional location, and sports participation were all found to have significant correlations.

However, there was no significant correlation between the type of sports played and family income. The level of sports participation did not significantly correlate with the mother's educational attainment, family income, or institutional location. However, a significant relationship was discovered between the father's level of sports participation and educational attainment.

It was discovered that the level and type of sports participation were significantly correlated with perceptions of sports participation. Further, it was concluded that the relationships between the variables significantly contributed to the favorable perception of women's sports participation.

### **CONCLUSION**

Sports participation has largely been reserved for men in most societies. However, advocates for women in sport have demonstrated over the past decade that women are also competent and deserve a place in sports. It is interesting to note that women who participate in sports are thought to be more self-assured and self-aware, to have better leadership skills, and to lead healthier lifestyles. As a result, women's active participation in sports does not diminish their femininity but rather enhances them as individuals. To encourage more certain discernment on ladies' games cooperation, advocates accordingly on ladies in sports ought to proceed and grow the promotion on engaging ladies' value in sports.

### **REFERENCES**

- Klafs, C. E., & Lyon, M. J. (1978). *The female athlete: A coach's guide to conditioning and training*. Saint Louis, Missouri: The C.V. Mosby Company.
- Lutter, J. M., & Jaffee, L. (1996). *The bodywise woman*. 2<sup>nd</sup> Ed. USA: Human Kinetics.
- Sandoz, J., & Winans, J. (1999). *Whatever it takes: Women on women's sport*. Published



by Farrar, Strans & Giroux.

- Webster's. (1976). The New International Dictionary. Springfield, Massachusetts, USA Gand C Meriam Company.
- Metheny, E. (1965). Symbolic forms of movement: The feminine image in sports. Connotations of Movement in Sport, and Dance, 43-56.

ISSN No 2347-7075  
Impact Factor- 7.328  
Volume-4 Issue-36

**INTERNATIONAL  
JOURNAL of  
ADVANCE and  
APPLIED  
RESEARCH**



**Publisher: P. R. Talekar**  
Secretary,  
Young Researcher Association  
Kolhapur(M.S), India

Young Researcher Association



**CONTENTS**

<b>Sr No</b>	<b>Paper Title</b>	<b>Page No.</b>
1	Empowering Women's Health through Nutrients and Physical Activities <b>Dr. Anjali digambar barde</b>	1-3
2	Recent Trends in Research & Innovation Technology in Arts, Humanities and Culture In Connection with Indian Classical Music <b>Pravin R. Alshi</b>	4-9
3	Historical Significance of Nagar Parishad School in Khamgaon Town in pre-independence period <b>Dr. Pramod Rameshwar Chavan</b>	10-12
4	Rereading Annihilation of Caste <b>Dr. Manohar A. Wasnik</b>	13-15
5	Changing Scenario of Guru Shishya Tradition in Indian Classical Music <b>Dr. Ajaykumar G. Solanke</b>	16-19
6	The Evolution of Music Production: Midi Technology's Ascendancy over Acoustic Instruments <b>Mr. Tanmoy Mani</b>	20-25
7	Feminism Theory and Gender Equality <b>Prof. N.J. Shende</b>	26-28
8	Changing Nature of Indirect Tax Structure in India <b>Prarthana Kasbe, Dr. Gadekar B.P</b>	29-32
9	Diasporic Elements in V. S. Naipaul's Novel A Bend in the River <b>Dr. B. W. Somatkar</b>	33-35
10	Women Empowerment Is Necessary For Over All Development. <b>Dr. Dnyaneshwari S. Wankhade</b>	36-42
11	Patriarchal Dominance in Laxman Mane's An Outsider <b>Dr. D. R. Khanderao</b>	43-46
12	Gender Discrimination is the prominent theme of some Indian Women Novelist <b>Mr. Pravin Sopan Shimbre</b>	47-50
13	Comparative Study on Social and Mental Health between Team and Individual Game Female Player with Reference to their Sports Participation <b>Dr. Pushpalata M. Deshmukh</b>	51-54
14	Challenges before Translating a Marathi Dalit Text into English in Lexical View Points: With Special Reference to 'The Prisons We Broke' <b>Dr Rajendra Vithal Waghmare</b>	55-57
15	Upliftment of Women in Sports: A Way towards Women Empowerment <b>Dr. Sangita N. Lohakpure</b>	58-60
16	Empowering Women and Girls through Sports, Health And nutrition <b>Dr. Sangita M. Khadse</b>	61-64
17	Women and Enrichment: Empowerment through Sports <b>Dr. Seema V. Deshmukh</b>	65-67
18	Bhon : The Golden Era of history of Berar <b>Dr Shyam Prakash Deokar</b>	68-70
19	A Literary Study of Dalit Feminism in India <b>Dr. Sidhartha B. Sawant</b>	71-73
20	A Study of Self-Esteem among College Students With Reference To Selection Criteria of Kabaddi Team <b>Umesh S. Vyas, Dr. Shirish V. Topre</b>	74-76
21	Need of Electronic Indian Musical Instruments in Present Scenario <b>Dr. Vivek Santoshrao Chapke</b>	77-81
22	Music Therapy for healthy body and peaceful mind. <b>Mr. Vishal Vijay Korde</b>	82-83
23	The Interplay of Humanity and The Natural World: Ecological Sensitivity in Toru Dutt's Poem "Our Casuarina Tree" <b>Dr. Sanjay T. Vite</b>	84-85
24	Physical Education and Games as a tool to empower girls and women in India <b>Dr. Kamini Mohan Mamarde</b>	86-88
25	An In-depth Study of Intra-racial Struggle: A Special Reference to Paule Marshall's The Fisher King <b>Dr. Vaijanath Gangaram Hangarge</b>	89-91
26	Effect of Visual Training on Throwing and Kicking Skill of School Going Children <b>Saurav Tripathy, Dr. Tanuja S. Raut</b>	92-95





## Women Empowerment Is Necessary For Over All Development

**Dr. Dnyaneshwari S. Wankhade**

Director Department of Physical Education, Vidya Bharati Mahavidyalaya, Amravati

**Corresponding Author- Dr. Dnyaneshwari S. Wankhade**

**Email:** [dnyaneshwarriingle18@gmail.com](mailto:dnyaneshwarriingle18@gmail.com)

**DOI-** 10.5281/zenodo.10334923

### Abstract

Being a conventional male centric culture, ladies have been given an optional status which is reflected in the monetary, social and political circles. Notwithstanding, ladies uniformity and strengthening has consistently stayed a need region and has been taken absolute attention to detail by partners. The paper fundamentally explores the Indian status among different nations and attempts to figure out readiness to accomplish Economical improvement Objective - 5 of the Unified Countries. The paper creates contention based on auxiliary sources as survey of existing writing distributed in diary, books, reports of different, NGOs, Government and worldwide associations and sites. The paper fundamentally looks at ladies strengthening in India, different models and aspects. The paper talks about protected safe watchmen as well as plans and projects by the public authority and their execution, signs of ladies strengthening. Be that as it may, the nation positions low while contrasting and different nations. Ladies Strengthening assists with making the general public and world a superior spot to live in and walk forward on way to comprehensive support. It implies increment bliss for the family and the associations where ladies have an effect. Allow us to move to one more article on Ladies strengthening with 600 words. In any case, it is feasible to assist ladies shield themselves against these shameful acts with various types of strengthening, like social, financial, instructive, political, and mental.

**Keywords:** Ladies Strengthening; Orientation Fairness; Government; Social; Rights

### Introduction

Engaging ladies is fundamental for the wellbeing and social advancement of families, networks and nations. At the point when ladies are living protected, satisfied and useful lives, they can arrive at their maximum capacity. contributing their abilities to the labor force and can bring up more joyful and better kids. Engaging ladies assists with making an all the more and impartial society for everybody. Wellbeing and Prosperity: Ladies' strengthening is additionally significant for advancing wellbeing and prosperity. At the point when ladies approach training and medical services, they can all the more likely deal with themselves and their families Strengthening of ladies is a critical calculate encouraging wellbeing and prosperity, which is another justification for why it is essential. Ladies are better ready to deal with themselves as well as their youngsters when they approach schooling and medical care. Advancing female strengthening is profoundly vital to lay out equity in the public arena. Ladies comprise approx half of the absolute populace. Subsequently, to engage them means to foster society in different ways, for

example, financially, socially, strategically, and so on. There are valid justifications to accept that enabling ladies helps monetary turn of events. Diminishing segregation in admittance to schooling and the work market would utilize ladies' abilities and capacities. Ladies' strengthening has five parts: ladies' healthy identity worth; their entitlement to have and to decide decisions; their entitlement to approach open doors and assets; their entitlement to have ability to control their own lives, both inside and outside the home; also, their capacity to impact the heading of social

### Women's Empowerment in India and its Importance

Ladies strengthening alludes to empowering ladies to have command over their lives, decide and choices, and have equivalent admittance to assets and amazing open doors. It includes establishing a climate where ladies can partake in the public eye and the economy on neutral ground with men, and where their voices are heard and their privileges are safeguarded. Ladies' strengthening can take many structures, including schooling, monetary, political, and social.

Eventually, ladies' strengthening means to make a reality where ladies have the power and opportunity to carry on with their lives, without segregation or impediments in view of orientation. **Types of Women's Empowerment:**

There are various ways of arranging ladies' strengthening, however the following are five normal sorts:

- ❖ **Monetary Strengthening:** This alludes to ladies' capacity to partake in financial exercises on an equivalent premise with men. It incorporates admittance to schooling, preparing, business, and business open doors, as well as fair wages, equivalent compensation, and admittance to credit and monetary administrations.
- ❖ **Social Strengthening:** This kind of strengthening alludes to ladies' capacity to partake completely in friendly and social life, liberated from separation and viciousness. It incorporates admittance to training, medical care, and lawful administrations, as well as the capacity to practice their privileges and opportunities.
- ❖ **Political Strengthening:** This sort of strengthening alludes to ladies' capacity to take part in political life and dynamic on an equivalent premise with men. It incorporates the capacity to cast a ballot and campaign for office, as well as admittance to administrative roles and support in strategy making processes.
- ❖ **Instructive Strengthening:** This alludes to ladies' capacity to get to schooling and foster abilities and information that empower them to go with informed choices, seek after their objectives, and add to society. It incorporates admittance to quality training at all levels and amazing open doors for deep rooted learning.
- ❖ **Wellbeing Strengthening:** This alludes to ladies' capacity to get to medical services and arrive at conclusions about their wellbeing and prosperity. It incorporates admittance to data, administrations, and assets that advance conceptive wellbeing, maternal wellbeing, and generally prosperity.

In general, these kinds of strengthening are interconnected and corresponding, and enabling ladies in a single region can have positive gradually expanding influences in different regions.

**Importance of Women's Empowerment:**

Ladies' strengthening is significant because of multiple factors, including

- ❖ **Orientation Fairness:** Ladies' strengthening is fundamental for accomplishing orientation correspondence, which is a basic common liberty. Orientation equity implies that ladies and men have equivalent freedoms, open doors, and assets, and can take part similarly in all parts of life.
- ❖ **Monetary Development:** Ladies' strengthening is likewise significant for financial development and improvement. At the point when ladies have equivalent admittance to instruction, business, and different open doors, they are better ready to add to the economy and society all in all.
- ❖ **Civil rights:** Ladies' strengthening is likewise fundamental for accomplishing civil rights. Ladies and young ladies are in many cases subject to segregation, savagery, and different types of mistreatment just as a result of their orientation. Engaging ladies assists with making an all the more and impartial society for everybody.
- ❖ **Wellbeing and Prosperity:** Ladies' strengthening is additionally significant for advancing wellbeing and prosperity. At the point when ladies approach training and medical services, they can more readily deal with themselves and their families.
- ❖ **Manageable Turn of events:** Ladies' strengthening is basic for accomplishing practical turn of events. At the point when ladies are engaged, they are better ready to add to endeavors to address natural difficulties, decrease destitution, and advance civil rights.

To put it plainly, ladies' strengthening is critical for accomplishing a fair, impartial, and maintainable world.

**Women's Empowerment through education**

Ladies strengthening through training alludes to the most common way of furnishing young ladies and ladies with the information, abilities, and certainty to take part completely in the public eye and settle on informed conclusions about their lives. Schooling is one of the most incredible assets for enabling ladies, as it can assist them with acquiring information, abilities, and certainty that can assist them with working on their daily routines and the existences of their families and networks. Monetary strengthening, Wellbeing and prosperity, Political interest, and Social strengthening are a few different ways that training can assist with enabling ladies. Generally speaking, ladies' schooling is

fundamental for accomplishing orientation balance and enabling ladies to understand their maximum capacity. By putting resources into young ladies' schooling, we can make an all the more and evenhanded world for all.

### **The Women empowerment in India and its Importance**

Ladies strengthening in India is the best apparatus for advancement as nowadays; ladies across the world are effectively functioning as a pioneer and outperforming others in every one of the circles of life. As the whole world is fastening its breath and imploring each and every day for an extraordinary departure from the Coronavirus Pandemic, it is the ladies lead representatives and countries directed by these astounding figures who are assuming control over the obligation and walking ahead in the fight alone any place required. Ladies strengthening in India is reliant up by and large on various factors that envelop geological setting (metropolitan/country), economic wellbeing (standing and class), instructive status, and age factor. Activities on the ladies strengthening exist at the state, nearby (panchayat), and public levels. Notwithstanding, ladies experience separation in many areas like training, monetary open doors, wellbeing and clinical help, and political support, which exhibits that there are significant holes between methodology progressions and genuine activity at the local area level.

### **Women Empowerment in India: An Introduction**

The term ladies strengthening is about power, or the power set out on ladies sharing unclear privileges. The term alludes to the freedom of ladies from financial restrictions of dependence. Ladies involve around half of the nation's populace, and a heft of them remains monetarily subject to one another without business. In the time of woman's rights, a little part of ladies in India are liberated and can utilize their freedom of thought and are allowed to cut out their lives the manner in which they need. Be that as it may, there is a significant division of the ladies in this country who need hopeful help. In most Indian towns and semi-metropolitan urban communities, ladies are as yet denied principal schooling and are never approved to proceed with advanced education regardless of hoarding the comprehension required. Ladies are known for conveying various jobs easily each day, and in this manner, they are viewed as the foundation of each and every general public. Living in male-overwhelming social orders, ladies play a large

**Dr. Dnyaneshwari S. Wankhade**

number of jobs, like caring moms, cherishing little girls, and able partners. Best of all, they fit the bill totally in each job. In any case, they've likewise remained as an ignored bundle of society in various regions of the planet. Thusly, it has brought about ladies enduring the brunt of lopsidedness, monetary reliability, mistreatment, and particular social wrongs. Ladies have been living under the shackles of subjugation throughout recent centuries that obstructs them from achieving proficient as well as private highs. Being a NGO for ladies strengthening in India, Hindrise Establishment has planned our dynamic and change situated programs in such a way that the preparing of ruined little kids will elevate the state of the country.

### **Need for Women Empowerment**

For days of yore ladies overall been compelled to possess an optional spot corresponding to men. Ladies have been consigned to the edges notwithstanding the way that they are mathematically 50% of the total populace. This has brought about ladies being not able to have a spot of human nobility as free and autonomous elements related with men on a scholarly and proficient equivalent frequency. In the antiquated period ladies were known to participate in numerous useful exercises yet throughout the time proliferation and difficulties of pregnancy and labor bit by bit made her ward on people for security and food. When humankind arrived at more settled presence man controlled society was completely settled. The men were to compose the codes of the general public and administration where ladies were given subordinate job. The men extended the prevailing perspective as well known fact. However even in the periods of severe predominance by guys society has hurled ladies of type who could match even outperform the abilities of men. The noticeable accomplishments of ladies as instructors, specialists, pilots, lawmakers and wayfarers and so forth. have crushed the male centric ideas of binding ladies' job to home and hearth. However, these accomplishments have been made generally at individual levels now and again when ladies confronted separation and analysis at all levels. It is more straightforward to perceive how inconvenient to advance it is to confine ladies to determined jobs and subordinate them to men. Indeed, even to bring youngsters up in the present climate to make them fit to confront the difficulties of a cutthroat future a lady should be completely mindful of her decisions and direction.

The requirement for ladies' strengthening is felt in view of the status they have in the public arena starting from the start. There is a need to rethink the situation with ladies in the general public. A change can be brought through the constitution and steady regulations. The Constitution of India gives a ladies status equivalent to men. There have been endeavors to hold seats for ladies in political bodies. This is no question a positive development. Ladies can decide for them and take right choices. Anyway only considering reservation of ladies in Panchayat and administrative bodies without engaging ladies separately misses the mark concerning genuine liberation. Ladies have been prohibited from focuses of force because of precise connivance by man centric idea most normal in India Khap Panchayat that has consigned ladies to an assigned and restricted space. A reorientation of our perspectives towards ladies must be painstakingly directed for their genuine liberation from the man centric mastery. The ruined and unskilled status of most ladies in the public eye is because of their failure to achieve adequate degrees of monetary power. To support any degree of strengthening ladies must be taught to know about their freedoms and honors in a cutting edge society. It is just when they become mindful of their status in the public eye that they will actually want to make the most of the concessions proposed to them as a remedial measure. Ladies strengthening needs regardless ladies' dynamic support. Except if ladies lose the shackles that overlook their ability, expertise and soul ladies through schooling and monetary independence, can't be engaged. Except if they are engaged to take a definitive part in the social, political and monetary existence of the country the actual improvement of the nation will be trim sided.

### **Women Empowerment: Need, Steps , And Impact**

Ladies' freedoms backing, orientation correspondence, and assurance that ladies have equivalent open door in all parts of life are the objectives of the overall development known as Ladies strengthening. It incorporates the method involved with giving ladies the instruments, data, and organization they need to assume responsibility for their own lives and use sound judgment. Ladies' strengthening is fundamental for social headway and harmless to the ecosystem improvement as well as being an issue of equity and common freedoms. In this article, we will look at the possibility of ladies'

**Dr. Dnyaneshwari S. Wankhade**

strengthening, consider its significance, discuss the hardships ladies experience, and feature the main plans and projects for advancing ladies' strengthening across the globe.

### **Understanding Women Empowerment**

The most common way of fortifying ladies' ability to completely participate in the public eye, practice their freedoms, as well as access amazing open doors on an equivalent premise with men is known as "ladies strengthening." It involves going up against and adjusting the accepted practices, social practices, and power structures that help orientation disparity and segregation. Ladies' strengthening recognizes the innate worth and capability of ladies, including attempting to eliminate the deterrents that substitute the approach to accomplishing their objectives and making a positive commitment to society. It covers points including schooling, business, prosperity, savagery against ladies, and partaking in dynamic activities, as well as monetary, political, social, and individual parts.

### **Need for Women Empowerment**

Ladies' strengthening isn't just a stylish thought; it is fundamental in the present society. In spite of impressive progressions in ladies' privileges as well as orientation correspondence, there are as yet numerous snags and issues that keep ladies from contributing completely to society and arriving at their maximum capacity. Coming up next are a few in number contentions for ladies' strengthening:

**Gender Equality:** The strengthening of ladies is important to accomplish orientation correspondence. Social shows, social practices, as well as biased mentalities that confine ladies' possibilities and undermined their privileges are at the core of orientation difference. By enabling ladies, we question these assumptions and attempt to make a general public where people are managed the cost of similar freedoms, potential open doors, and commitments.

**Economic Development:** Monetary development and the strengthening of ladies are personally related. A big part of the total populace is comprised of ladies, and financial maintainability relies upon their dynamic commitment. Whenever ladies have a similar chance for schooling, work, and business, they make a significant commitment to financial creation, the destruction of destitution, and general turn of events.

**Education and Knowledge:** A strong technique for changing civilizations is instructing and engaging

ladies. Ladies who have gotten a schooling are more taught, more skilled, and more confident, which enables them to address orientation standards and effectively take part in friendly, financial, and political domains. Training builds a lady's penchant to make interests in her family's government assistance, particularly the wellbeing and schooling of her youngsters, which helps people in the future and breaks the pattern of neediness.

**Health and Well-being:** Ladies' prosperity and actual wellbeing are personally connected with ladies' strengthening. Ladies' strengthening requires approaching great medical services, the right to an early termination, and command over one's own body. Ladies who are engaged are better ready to take satisfactory consideration of their wellbeing, look for clinical consideration when essential, and settle on choices that will further develop their prosperity.

**Violence and Discrimination:** To conquer brutality and bias against ladies, ladies should be enabled. Homegrown maltreatment, lewd behavior, as well as illegal exploitation are only a couple of the fierce wrongdoings against ladies that they actually need to manage. Difficulties to these unsafe practices, more secure settings, and the progression of a culture of equity and regard are made conceivable by the strengthening of ladies by means of training, mindfulness, and lawful insurance.

**Leadership and Decision-making:** To make powerful approaches, methodologies, as well as dynamic cycles, ladies' voices and perspectives are essential. For comprehensive administration to be elevated and to satisfy the many requests and targets of society, orientation equality in positions of authority should be achieved in the private as well as open areas. Ladies' strengthening guarantees that they have an equivalent voice in choices that influence their networks and lifestyle.

**Social and Cultural Change:** To challenge cultural and social shows that help orientation disparity, ladies' strengthening is critical. By engaging ladies, we dissipate bias, eliminate obstructions, and advance a culture that distinctions as well as regards ladies' commitments beyond the bounds of traditional orientation jobs. This outcomes in social change and fabricates a really inviting and enhanced society that is useful to everyone.

Today both young fellows and young women go to classes. Today guidance is the right of both young fellows and young women; no matter what that, 50 % of young women get tutoring. India has

**Dr. Dnyaneshwari S. Wankhade**

measurements as expected which includes the quantity of occupants in the country. This information is used to measure things like schooling, sex extent, etc. Numerous SC and ST kids leave school at an early age. The 2014 insights even show the expense of preparing and the uninterested attitude of instructors and gatekeepers are liable for the imprudence of guidance.

### **Women Empowerment in India**

India is an extremely confounded country. Throughout the span of numerous hundreds of years, we have gathered a wide range of practices, customs, and customs. These ceremonies and practices, both the positive and negative parts of them, are currently imbued in the aggregate mind of our general public. We honor female divinities as gods deserving of love, and we likewise put a high worth on the connections we have with our own moms, little girls, sisters, life partners, and some other female family members or companions. Then again, Indian men are infamous for their unfortunate treatment of their spouses and lady friends, both inside and beyond the house. There are people in Indian culture who stick to pretty much every possible sort of strict conviction. In all of the world's religions, ladies are given a remarkable position, and we are told to treat them with the highest level of love and responsiveness. Be that as it may, for reasons unknown, the improvement of civilization has prompted it being satisfactory for different destructive practices, both physical and mental, to be completed against ladies. This has been the situation for a really long time. For example, the sati pratha, the custom of endowment, the Parda pratha, female child murder, spouse burning, sexual mischief, lewd behavior at the area of work, aggressive behavior at home, as well as different kinds of segregating rehearses all have both a psychological and an actual part. Moreover, there is a huge issue with abusive behavior at home in India. Since the guys accept that ladies are their property, they treat their spouses harmfully and beat them. Considerably more so since most ladies are excessively tentative to communicate their psyches. Along these lines, ladies who take care of business are paid not exactly their male partners who do similar errands. At the point when somebody gets compensated less for a similar measure of work due to their orientation, this conduct must be depicted as chauvinist and totally unreasonable. Subsequently, obviously engaging ladies is an unquestionable necessity nowadays. We have an obligation to give

these ladies the instruments they need to advocate for them and guarantee that they are never the survivors of shamefulness.

### **Steps For Women Empowerment**

Strengthening of ladies should be possible in different ways, through both government plans and individual levels. The public authority has thought of different plans like Beti Bachao Beti Padhao Yojana, Mahila-E-Haat, Sukanya Samridhhi Yojana, and so on., to engage ladies. Aside from this, exclusively, we can work by nullifying social wrongs like share and youngster marriage. Regarding ladies and giving equivalent open doors should be possible independently.

### **Women's Movements**

Ladies have only and, with everything taken into account, endeavored to accomplish changes is known as the Ladies' Development. Different systems have been used to spread care, fight partition, and search for value. These advancements are associated with fighting, uncovering issues, contradicting, and showing strength. Individuals in the public eye are seen as playing unequivocal direction occupations. Ladies have been standing up to inconsistencies at each step since the times from past times. Apparently, their circumstance and status have improved with the distinction in time; in any case, they wait behind men in basically every field.

### **Breaking Stereotypes and Developments**

In this male-managed society, they disregard to benefit identical distinctions and entryways. It has additionally been seen that a few callings are viewed as more fitting for men than for ladies. It implies ladies are reasonable just for a couple of occupations. Numerous people acknowledge that women further develop chaperons since they are all the more tranquil and sensitive. It is similarly acknowledged that women don't bear particular personalities, and along these lines, they are not prepared to oversee specific things. Thusly, they have been summed up as extraordinary specialists, incredible teachers, etc. They are never seen as equipped power authorities, pilots, railroad engine drivers, etc. A bigger piece of Indians confides in these speculations. It is, thus, that young women don't get the very support that young fellows do to study and plan to become subject matter experts and modelers. Ladies are planned to abuse these generalizations by succeeding in fields that were assumed male jam till now. We presently have ladies pilots, engineers, cops, researchers, etc. Bit by

**Dr. Dnyaneshwari S. Wankhade**

bit there came a steadily expanding number of positive changes. The social class that never gotten examining and making started sending their children to school. Before all else, there was a lot of protection from showing young women.

Nonetheless, there were also women and men who set forth endeavors to open schools for young women.

### **Some Examples of Women's Empowerment**

Ladies endeavored to sort out some way to seek after work and make. Here, the experience of Rashundari Devi (1800-1890) merits zeroing in on. She was a housewife of a rich landowner's friends and family. Around then, at that point, it was trusted that assuming a woman sorted out some way to scrutinize and form, she would transform into a widow. Despite this, she told herself the best way to seek after and compose clandestinely after her marriage. She thought about her self-representation in Bangla named Amar Jiban. Rokeya Sakhawat Hossain was another model who did an incredible arrangement for women's tutoring. She knew how to examine and make Urdu, yet she was stopped from learning Bangla and English. Back then, simply young fellows were taught in English. Anyway, she sorted out some way to parse and make Bangla and English. From there on, she transformed into a writer and formed an uncommon story named Sultana's Fantasy in 1905. She did an incredible arrangement to help different young women with going to class and building their own dreams. In 1910, she began a school for young women in Kolkata which is yet to work.

In all likelihood, an always expanding number of young women have begun going to class, yet, they drop behind young fellows. As per the most recent measurements of 2001, 76% of young fellows and men are taught, yet the figure is generally outstandingly low in case of young women. Only 54% of young women and women are taught in India. As needs be, the level of the male social event is higher than the female get-together. Young ladies who are from Dalit and Adivasi establishments are less disposed to remain in school. One of the many reasons is that couple of families are unnecessarily poor and unequipped for bearing the cost of showing all of their young people. Young fellows get tendencies in such circumstances. The position and status of women have, beyond question, further fostered a ton which is a result of the total undertakings of the women of the country. The Ladies' Development similarly gets the

assistance of men. They used different techniques to spread care, fight partition, and search for value. For example, they coordinate missions to fight isolation and brutality against women. They furthermore challenge women to happen. The women's Development moreover shows courage with various women and causes.

#### References

1. Kabeer, Naila. "Gender equality and women'empoverment: A critical analysis o the third millennium development goal 1."
2. Mosedale, Sarah (March 1, 2005). "Assessing women's empowerment: towards a conceptual framework". Journal of International Development.
3. Bayeh, Endalcachew (January 2016). "The role of empowering women and achieving gender equality to the sustainable development of Ethiopia".
4. Oxfam (Forthcoming), "Women's Economic Empowerment Conceptual Framework" □ Baden, Sally; Goet, Anne Marie (July 1997). "Who Needs [Sex] When You Can Have [Gender]? Conflicting Discourses on Gender at Beijing".
5. Lopez, Alvarez (2013). "From unheard screams to powerful voices: a case study of Women's political empowerment in the Philippines".
6. "Innovation for women's empowerment and gender equality". ICRW | PASSION . PROOF. POWER. Archived from the original on May 20, 2021.
7. Deneulin, Séverine; Lila Shahani, eds. (2009). "An Introduction to the Human Development and Capability Approach: Freedom and Agency" (PDF). Sterling,
8. Gupta, Kamla; Yesudian, P. Princy (2006). "Evidence of women's empowerment in India: a study of socio-spatial disparities".
9. Kabeer, Naila. "Contextualising the Economic Pathways of Women's Empowerment: